รายงานวิจัยฉบับสมบูรณ์

โครงการ

การสังเคราะห์ สมบัติ และการประยุกต์ใช้เบต้าพิโรลิดินิลเพปไทด์นิวคลีอิกแอซิดที่มีคอนฟอร์เมชันถูกจำกัด

โดย **ธีรยุทธ วิไลวัลย์ และคณะ**

เดือน-ปี ที่เสร็จโครงการ มกราคม 2556

สัญญาเลขที่ RTA5280002

รายงานวิจัยฉบับสมบูรณ์

โครงการ การสังเคราะห์ สมบัติ และการประยุกต์ใช้เบต้าพิโรลิดินิลเพปไทด์
นิวคลีอิกแอซิดที่มีคอนฟอร์เมชันถูกจำกัด

คณะผู้วิจัย

1. รศ.ดร.ธีรยุทธ วิไลวัลย์	ภาควิชาเคมี คณะวิทยาศาสตร์ จุฬาลงกรณ์มหาวิทยาลัย
2. อ.ดร.จตุรงค์ สุภาพพร้อม	ภาควิชาเคมี คณะวิทยาศาสตร์ มหาวิทยาลัยนเรศวร
3. อ.ดร.ช่อลัดดา ศรีสุวรรณเกศ	ภาควิชาเคมี คณะวิทยาศาสตร์ มหาวิทยาลัยพระจอมเกล้าธนบุรี
4. รศ.ดร.มงคล สุขวัฒนาสินิทธิ์	ภาควิชาเคมี คณะวิทยาศาสตร์ จุฬาลงกรณ์มหาวิทยาลัย
5. รศ.ดร.วรวีร์ โฮเว่น	ภาควิชาเคมี คณะวิทยาศาสตร์ จุฬาลงกรณ์มหาวิทยาลัย
6. รศ.ดร.เมธา รัตนากรพิทักษ์	ภาควิชาเคมี คณะวิทยาศาสตร์ มหาวิทยาลัยนเรศวร
7. ผศ.ดร.บุญจิรา บุญทา	ภาควิชาเคมี คณะวิทยาศาสตร์ มหาวิทยาลัยนเรศวร
8. อ.ดร.อุทัย วิชัย	ภาควิชาเคมี คณะวิทยาศาสตร์ มหาวิทยาลัยนเรศวร
9. รศ.ดร.ปณต ถาวรังกูร	ภาควิชาฟิสิกส์ คณะวิทยาศาสตร์ มหาวิทยาลัยสงขลานครินทร์
10. รศ.ดร.เพริศพิชญ์ คณาธารณา	ภาควิชาเคมี คณะวิทยาศาสตร์ มหาวิทยาลัยสงขลานครินทร์
11. อ.ดร.วรากร ลิ่มบุตร	ภาควิชาวิทยาศาสตร์ประยุกต์ คณะวิทยาศาสตร์ มหาวิทยาลัยสงขลานครินทร์
12. อ.ดร.อาภรณ์ นุ่มน่วม	ภาควิชาเคมี คณะวิทยาศาสตร์ มหาวิทยาลัยสงขลานครินทร์
13. ผศ.ดร.ปิยะศักดิ์ ชอุ่มพฤกษ์	ภาควิชาพฤกษศาสตร์ คณะวิทยาศาสตร์ จุฬาลงกรณ์มหาวิทยาลัย
14. รศ.พญ.ดร.ณัฏฐิยา หิรัญกาญจน์	ภาควิชาจุลชีววิทยา คณะแพทยศาสตร์ จุฬาลงกรณ์มหาวิทยาลัย
15. อ.นพ.ดร.อมรพันธ์ เสรีมาศพันธ์	ภาควิชากายวิภาคศาสตร์ คณะแพทยศาสตร์ จุฬาลงกรณ์มหาวิทยาลัย
16. ผศ.ดร.ไพฑูรย์ รัชตะสาคร	ภาควิชาเคมี คณะวิทยาศาสตร์ จุฬาลงกรณ์มหาวิทยาลัย

สนับสนุนโดยสำนักงานกองทุนสนับสนุนการวิจัย
(ความเห็นในรายงานนี้เป็นของผู้วิจัย สกว.ไม่จำเป็นต้องเห็นด้วยเสมอไป)

กิตติกรรมประกาศ

งานวิจัยเรื่องการสังเคราะห์การสังเคราะห์ สมบัติ และการประยุกต์ใช้เบต้าพิโรลิดินิลเพปไทด์นิวคลีอิกแอซิดที่มีคอนฟอร์เมชันถูกจำกัดได้ดำเนินการไปจนสำเร็จลุล่วงไปได้ด้วยความร่วมมือของหลายฝ่าย กระผมในฐานะหัวหน้าโครงการขอขอบคุณ แหล่งเงินทุนสนับสนุน ได้แก่ ทุนส่งเสริมกลุ่มวิจัย (เมธีวิจัยอาวุโส) จากสำนักงานกองทุนสนับสนุนการวิจัย ประจำปี พ.ศ. 2552 (RTA5280002) และแหล่งทุนอื่นที่มีส่วนเกี่ยวข้องได้แก่ Alexander von Humboldt Foundation กองทุนรัชดาภิเษกสมโภช จุฬาลงกรณ์มหาวิทยาลัยร่วมกับสำนักงานคณะกรรมการการอุดมศึกษา ผ่านโครงการมหาวิทยาลัยแห่งชาติ ทุนวิจัยของผู้ร่วมโครงการ และทุนอื่นๆ ที่ให้แก่นิสิต-นักศึกษา ได้แก่ทุนปริญญาเอกกาญจนาภิเษก (คปก.) ทุนพัฒนาและส่งเสริมผู้มีความสามารถพิเศษทางวิทยาศาสตร์และเทคโนโลยี (พสวท.) ทุนโครงการพัฒนากำลังคนด้านวิทยาศาสตร์ (ทุนเรียนดีวิทยาศาสตร์แห่งประเทศไทย) ทุนโครงการพัฒนาอัจฉริยภาพทางวิทยาศาสตร์สำหรับเด็กและเยาวชน (JSTP) และทุนจากศูนย์ความเป็นเลิศด้านนวัตกรรมทางเคมี (PERCH-CIC) ขอขอบคุณสถาบันต้นสังกัดของหัวหน้าโครงการและคณะผู้วิจัยทุกท่านที่ให้ความอนุเคราะห์สถานที่ เครื่องมือ ระบบสาธารณูปโภค และการสนับสนุนอื่นๆ ที่จำเป็น โดยเฉพาะอย่างยิ่ง คณะวิทยาศาสตร์ มหาวิทยาลัยนเรศวร และ คณะวิทยาศาสตร์ร่วมกับสถานวิจัยการวิเคราะห์สารปริมาณน้อยและไบโอเซนเซอร์ (TAB-RC) มหาวิทยาลัยสงขลานครินทร์ ที่ได้รับเป็นเจ้าภาพดูแลเรื่องสถานที่ในการจัดประชุมวิชาการประจำปีของกลุ่มวิจัยครั้งที่ 2 และ 3 สุดท้ายต้องขอขอบคุณคณะผู้วิจัยทุกท่าน ทั้งอาจารย์ผู้ร่วมโครงการ และนิสิต นักศึกษา และผู้ช่วยวิจัยรวมกว่า 30 คน รวมทั้งผู้ร่วมวิจัยที่ไม่ได้อยู่ในโครงการอีกหลายท่านที่ไม่สามารถกล่าวนามได้ทั้งหมด หากปราศจากท่านเหล่านี้แล้วงานคงจะดำเนินไปไม่ได้ สุดท้ายขอขอบคุณคุณโชติมา วิไลวัลย์ เจ้าหน้าที่โครงการที่ช่วยประสานงานและอำนวยความสะดวกในโครงการตั้งแต่การจัดซื้อ ทำบัญชี งานเอกสาร ดูแลห้องปฏิบัติการ รวมถึงการสังเคราะห์พีเอ็นเอ

บทคัดย่อ

รหัสโครงการ: RTA5280002

ชื่อโครงการ: การสังเคราะห์ สมบัติ และการประยุกต์ใช้เบต้าพิโรลิดินิลเพปไทด์นิวคลีอิกแอซิดที่มีคอนฟอร์เมชันถูกจำกัด

ชื่อนักวิจัย: ธีรยุทธ วิไลวัลย์และคณะ

E-mail address: vtirayut@chula.ac.th

ระยะเวลาของโครงการ: 3 ปี (1 สิงหาคม 2552 - 31 กรกฎาคม 2555 ขยายระยะเวลาเพิ่มเติมถึง 31 มกราคม 2556)

เพปไทด์นิวคลีอิกแอซิดหรือพีเอ็นเอเป็นสารสังเคราะห์เลียนแบบดีเอ็นเอที่มีโครงหลักคล้ายเพปไทด์ซึ่งมีความเป็นกลางทางไฟฟ้า และสามารถจับยึดกับดีเอ็นเอและอาร์เอ็นเอเป้าหมายได้อย่างจำเพาะเจาะจงตามกฎการเข้าคู่เบสของวัตสัน-คริก จากความสำเร็จที่ผ่านมาในการพัฒนาเพปไทด์นิวคลีอิกแอซิดชนิดใหม่ที่มีคอนฟอร์เมชันที่ถูกจำกัดโดยมีโครงหลักเป็นกรดแอลฟ่าและเบต้าอะมิโนเรียงสลับกันที่ได้มาจากโพรลีนและกรดเบต้าอะมิโนที่เป็นวงแหวน เช่น(2*R*,4*R*)-โพรลิล/(1*S*,2*S*)-2-อะมิโนไซโคลเพนเทนคาร์บอกซิลิก แอซิด (เอซีพีซีพีเอ็นเอ) ในงานวิจัยนี้จะมุ่งเน้นไปที่การออกแบบ สังเคราะห์ ศึกษาสมบัติ และการนำไปประยุกต์ใช้ของพีเอ็นเอระบบใหม่ในกลุ่มนี้ การปรับเปลี่ยนโครงสร้างและสเตอริโอเคมีของส่วนโครงหลักอย่างเป็นระบบทำให้พบระบบพิร์โรลิดินิลพีเอ็นเอใหม่ๆ ที่บางชนิดแสดงสมบัติการเข้าคู่เบสที่เป็นเอกลักษณ์เฉพาะตัว และแตกต่างไปจากเอซีพีซีพีเอ็นเอ นอกจากนี้ ยังได้พัฒนาวิธีการใหม่ในการดัดแปลงเอซีพีซีพีเอ็นเอด้วยเบสที่ไม่พบในธรรมชาติ และฉลากเรืองแสงในลักษณะที่ควบคุมตำแหน่งของการติดฉลากได้ และได้แสดงตัวอย่างการนำไปใช้เป็นโพรบเรืองแสงที่สามารถตอบสนองต่อการเกิดไฮบริดกับดีเอ็นเอเป้าหมาย และยังได้นำเอซีพีซีพีเอ็นเอไปประยุกต์ใช้เป็นโพรบสำหรับตรวจสอบลำดับเบสของดีเอ็นเอที่มีความไวและความจำเพาะเจาะจงสูงโดยใช้ร่วมกับเด็นดริเมอร์เรืองแสง กระดาษกรองที่เคลือบด้วยพอลิเมอร์ที่มีประจุบวก อนุภาคแม่เหล็กขนาดนาโนที่เคลือบด้วยพอลิเมอร์ที่มีประจุบวก และระบบคาพาซิทีฟ อย่างไรก็ตาม แม้ว่าการตรวจสอบลำดับเบสที่พัฒนาขึ้นจะให้ผลดีเป็นที่น่าพอใจกับตัวอย่างที่เป็นโอลิโกดีออกซีนิวคลีโอไทด์สังเคราะห์เป็นส่วนใหญ่ แต่ก็ยังต้องมีการพัฒนาต่อไปในการนำไปใช้กับตัวอย่างดีเอ็นเอจริงซึ่งอยู่ในสภาพที่เป็นสายคู่ และมักจะมีความยาวมากกว่าตัวโพรบค่อนข้างมาก

คำสำคัญ: DNA, PNA, fluorescence, genotyping, diagnostic

Abstract

Project Code : RTA5280002

Project Title : Synthesis, properties and applications of conformationally constrained beta-pyrrolidinyl peptide nucleic acids

Investigators : Tirayut Vilaivan and co-workers

E-mail Address : vtirayut@chula.ac.th

Project Period : 3 years (1 August 2009 - 31 July 2012 extended to 31 January 2013)

Peptide nucleic acid or PNA is a type of DNA mimic with electrostatically neutral peptide-like backbone that can bind strongly and specifically to DNA and RNA targets following Watson-Crick base paring rules. Based on our previous success in developing a new class of conformationally-constrained peptide nucleic acid bearing alternating alpha-/beta-peptide backbone derived from proline and cyclic beta-amino acids such as (2*R*,4*R*)-prolyl/(1*S*,2*S*)-2-aminocyclopentanecarboxylic acid (acpcPNA), this research focuses on designing, synthesis, properties studies and applications of these new PNA systems. Systematic variation of the structure and stereochemistry of the backbone lead to several other new pyrrolidinyl PNA systems, many of which exhibit unique pairing properties that are different from acpcPNA. In addition, new chemistries have been develop to incorporate artificial nucleobases and fluorescence labels to acpcPNA in a site specific fashion and their applications as hybridization-responsive fluorescence probes have been demonstrated. Applications of acpcPNA as a probe in combination with fluorescence dendrimers, cationic polymer-coated filter papers, cationic polymer-coated magnetic nanoparticles and capacitive system for DNA sequence determination with high sensitivity and specificity have also been demonstrated. Although excellent results were obtained with synthetic oligodeoxyribonucleotide in most cases, improvements are still required with respect to applications to real DNA samples which are double-stranded and usually much longer than the probes.

Keywords: DNA, PNA, fluorescence, genotyping, diagnostic

บทสรุปสำหรับผู้บริหาร (Executive Summary)
ทุนส่งเสริมกลุ่มวิจัย

1. ชื่อโครงการ

ภาษาไทย การสังเคราะห์ สมบัติ และการประยุกต์ใช้เบต้าพิโรลิดินิลเพปไทด์นิวคลีอิกแอซิด ที่มีคอนฟอร์เมชันถูกจำกัด

ภาษาอังกฤษ Synthesis, properties and applications of conformationally constrained beta-pyrrolidinyl peptide nucleic acids

2. ชื่อหัวหน้าโครงการ หน่วยงานที่สังกัด ที่อยู่ หมายเลขโทรศัพท์ โทรสาร และ e-mail

รศ.ดร.ธีรยุทธ วิไลวัลย์
ภาควิชาเคมี คณะวิทยาศาสตร์ จุฬาลงกรณ์มหาวิทยาลัย
ถนนพญาไท เขตปทุมวัน กรุงเทพฯ 10330
โทรศัพท์: 022187627 ต่อ 101
โทรศัพท์เคลื่อนที่: 0839868772
โทรสาร: 022187598
อีเมล์: vtirayut@chula.ac.th

3. สาขาวิชาที่ทำการวิจัย เคมีอินทรีย์, เคมีวิเคราะห์

5. ระยะเวลาดำเนินงาน 3 ปี

6. ได้เสนอโครงการนี้ หรือโครงการที่มีส่วนเหมือนกับเรื่องนี้บางส่วน เพื่อขอทุนต่อแหล่งทุนอื่นที่ใดบ้าง

☑ ไม่ได้เสนอต่อแหล่งทุนอื่น
☐ เสนอต่อ_____
ชื่อโครงการที่เสนอ _____
กำหนดทราบผล(หรือสถานภาพเท่าที่ทราบ) _____

หมายเหตุ:

1. บางส่วนของโครงการย่อยที่ 1 (คิดเป็นเนื้องานประมาณ 20% ของโครงการย่อย) หัวหน้าโครงการได้รับการสนับสนุนจาก Alexander von Humboldt Foundation ภายใต้ชื่อโครงการ "New conformationally constrained beta-pyrrolidinyl peptide nucleic acids: synthesis and applications in DNA sequence determination" ซึ่งเป็นความร่วมมือกับ University of Regensburg, Germany (Mar 2009 – May 2011) ในรูปค่าตอบแทนเฉพาะบางช่วงเวลา โดยไม่มีค่าวัสดุ

7. ปัญหาที่ทำการวิจัย และความสำคัญของปัญหา

เพปไทด์นิวคลีอิกแอซิดหรือพีเอ็นเอเป็นโมเลกุลสังเคราะห์ที่ได้จากการแทนที่หมู่(ดีออกซี)ไรโบสฟอสเฟตที่เป็นแกนหลักของดีเอ็นเอ/อาร์เอ็นเอด้วยแกนหลักของเพปไทด์ พีเอ็นเอบางระบบสามารถจับยึดกับดีเอ็นเอและอาร์เอ็นเอได้อย่างแข็งแรงและจำเพาะเจาะจง การที่พีเอ็นเอปราศจากประจุลบเนื่องจากหมู่ไรโบสฟอสเฟตทำให้มันมีสมบัติที่เป็นเอกลักษณ์เฉพาะตัว เช่น ความสามารถในการจับกับดีเอ็นเอ/อาร์เอ็นเอที่แข็งแรงและจำเพาะเจาะจง แม้ภายใต้ภาวะที่มีความเข้มข้นของเกลือต่ำ และไม่เป็นสับสเตรตของเอนไซม์ที่ทำงานกับกรดนิวคลีอิก สมบัติเหล่านี้ประกอบกับความง่ายในการสังเคราะห์พีเอ็นเอทำให้มันเป็นตัวเลือกที่มีศักยภาพในการศึกษาการจดจำระดับโมเลกุล และในการประยุกต์ใช้ทางชีวภาพเช่น การพัฒนาระบบสำหรับตรวจสอบลำดับเบสของสารพันธุกรรม เป็นแอนติเซนส์เอเจนต์ และเป็นเครื่องมือในทางชีววิทยาระดับโมเลกุล

เมื่อไม่นานมานี้กลุ่มของผู้วิจัยได้พัฒนาระบบพีเอ็นเอชนิดใหม่ที่มีคอนฟอร์เมชันถูกจำกัด เรียกว่าเบต้าพิโรลิดินิลเพปไทด์นิวคลีอิกแอซิด ซึ่งประกอบด้วยหน่วยซ้ำๆ กันของไดเพปไดท์โพรลิล-อะมิโนไซโคลเพนเทนคาร์บอกซิลิกแอซิดในรูปแบบที่มีคอนฟิกกิวเรชันจำเพาะ โดยเรียกย่อๆ ว่า SS-ACPC PNA

เมื่อเปรียบเทียบกับระบบพีเอ็นเอที่มีผู้เคยศึกษามาก่อน SS-ACPC PNA แสดงความจำเพาะเจาะจงในการจับยึดกับดีเอ็นเอที่ดีเยี่ยมและความแข็งแรงของการจับยึดใกล้เคียงกัน แต่มีความแข็งแรงของการจับยึดกับอาร์เอ็นเอที่ต่ำกว่ามาก ความเสถียรของไฮบริดระหว่าง SS-ACPC PNA·DNA ไม่ขึ้นกับลำดับเบสมากเท่ากับดีเอ็นเอหรือพีเอ็นเอต้นแบบ ทำให้มันมีศักยภาพในการประยุกต์ใช้งานที่ต้องการโพรบซึ่งมีความสามารถในการจับยึดใกล้เคียงกัน เช่น ในการวิเคราะห์ลำดับเบสของดีเอ็นเอแบบมัลติเพล็กซ์ และในไมโครแอเรย์ ซึ่งจำเป็นต้องใช้โพรบหลายตัวเข้าจับกับดีเอ็นเอเป้าหมายพร้อมๆ กัน การจับยึดระหว่างพีเอ็นเอระบบใหม่นี้กับดีเอ็นเอเกิดในทิศทางแอนติพาราเรลเท่านั้น นอกจากนี้ยังมีสมบัติอื่นที่แตกต่างจากพีเอ็นเอต้นแบบได้แก่การไม่สามารถเกิดไฮบริดแบบทริเพล็กซ์ในระบบที่มีเฉพาะเบสไทมีน ซึ่งคาดว่าน่าจะเกิดจากปัจจัยด้านสเตอริก และการที่พีเอ็นเอชนิดใหม่นี้ไม่สามารถเกิดไฮบริดกับตัวเองได้

เป็นที่น่าสนใจว่าพีเอ็นเอชนิดใหม่นี้มีสมบัติที่เป็นเอกลักษณ์เฉพาะตัวหลายประการ มันจึงมีความสำคัญที่จะเข้าใจปัจจัยทางโครงสร้างที่มีผลต่อสมบัติเหล่านี้ เช่น ทำไม SS-ACPC PNA ถึงจับกับดีเอ็นเอได้ดีกว่าอาร์เอ็นเอ และทำไมถึงไม่สามารถจับกันเองได้ การตอบคำถามเหล่านี้ต้องใช้ความเชี่ยวชาญนอกเหนือจากที่กลุ่มของผู้วิจัยมีอยู่ ซึ่งนำไปสู่การร่วมมือของต่างสาขาวิชา และผลงานวิจัยที่มีผลกระทบสูง ความเข้าใจนี้อาจนำไปสู่การออกแบบพีเอ็นเอชนิดใหม่ที่สามารถควบคุมสมบัติได้ตามต้องการ เช่น การเลือกจับกับอาร์เอ็นเอได้ดีกว่าดีเอ็นเอ ซึ่งสามารถนำไปประยุกต์ใช้ในงานวิจัยด้านแอนติเซนส์ได้ แม้ว่าในปัจจุบันจะยังไม่มีความเข้าใจปัจจัยทางโครงสร้างที่มีผลต่อสมบัติการจับยึดของพีเอ็นเอชนิดใหม่นี้อย่างสมบูรณ์ แต่ก็เป็นที่ชัดเจนว่าพีเอ็นเอดังกล่าวน่าจะมีศักยภาพอย่างยิ่งในการนำไปประยุกต์ใช้ในด้านต่างๆ โดยเฉพาะอย่างยิ่งการตรวจสอบลำดับเบสของสารพันธุกรรม ซึ่งจะเป็นหัวข้อวิจัยที่เน้นในงานวิจัยนี้ แม้ว่าในปัจจุบันจะมีระบบตรวจสอบลำดับเบสโดยอาศัยดีเอ็นเอหรือพีเอ็นเออยู่มากมาย แต่ก็ยังคงมีความต้องการระบบที่ทำได้ง่าย ไม่แพง แต่ให้ความแม่นยำสูง ว่องไว และสามารถตรวจวัดตัวอย่างจำนวนมากได้โดยใช้เวลาจำกัด วิธีการดังกล่าวย่อมมีประโยชน์ทั้งในด้านการแพทย์ อาหาร การเกษตร และนิติเวช งานวิจัยในลักษณะนี้ต้องการความเชี่ยวชาญจากหลายสาขา ซึ่งถ้าสำเร็จก็จะเป็นตัวอย่างของการพัฒนางานวิจัยพื้นฐานจากโมเลกุลสังเคราะห์ที่สร้างขึ้นเพื่อตอบคำถามบางอย่างทางทฤษฎีไปสู่การประยุกต์ใช้จริงโดยผู้ร่วมงานคนไทยเป็นส่วนใหญ่ ผลที่ได้สามารถตีพิมพ์ในวารสารวิชาการที่มีผลกระทบสูง และอาจมีศักยภาพในเชิงพาณิชย์ นอกจากนี้ การร่วมมือจากหลากหลายสาขาวิชาดังกล่าวยังนำไปสู่การสร้างเครือข่ายนักวิจัยทั้งในระดับปริญญาโทและเอกอย่างน้อย 15-20 คน ที่จะเป็นทรัพยากรบุคคลที่สำคัญของสังคมวิจัยไทยต่อไปในอนาคต

8. วัตถุประสงค์

1. เพื่อออกแบบและสังเคราะห์เพปไทด์นิวคลีอิกแอซิด (พีเอ็นเอ) ชนิดใหม่ที่มีคอนฟอร์เมชันที่ถูกจำกัด
2. เพื่อศึกษาสมบัติการจับยึดกับดีเอ็นเอ/อาร์เอ็นเอ และการจับยึดกับตัวเองของพีเอ็นเอที่สังเคราะห์ได้
3. เพื่อทำความเข้าใจปัจจัยทางโครงสร้างที่ส่งผลต่อสมบัติการจับยึดของพีเอ็นเอ
4. เพื่อหาวิธีใหม่สำหรับการตรวจสอบลำดับเบสของดีเอ็นเอโดยใช้พีเอ็นเอเป็นโพรบ
5. เพื่อประยุกต์ใช้วิธีการตรวจสอบลำดับเบสของดีเอ็นเอด้วยพีเอ็นเอ ในทางการแพทย์ อาหาร และการเกษตร
6. เพื่อผลิตผลงานตีพิมพ์ในวารสารที่มีผลกระทบสูงและผลิตบุคคลากรที่มีความเชี่ยวชาญในสาขาวิจัยด้านนี้
7. เพื่อสร้างเครือข่ายวิจัยที่ยั่งยืนทั้งในระดับชาติและนานาชาติโดยใช้ระบบพีเอ็นเอเป็นจุดสนใจร่วม

9. ระเบียบวิธีวิจัย

โครงการวิจัยนี้แบ่งเป็นหกโครงการย่อย ซึ่งครอบคลุมงานวิจัยเกี่ยวกับการสังเคราะห์และศึกษาสมบัติการจับยึดกับกรดนิวคลีอิกของพีเอ็นเอชนิดใหม่ที่มีคอนฟอร์เมชันจำกัด และการพัฒนาระบบตรวจสอบลำดับเบสของสารพันธุกรรมโดยอาศัยพีเอ็นเอชนิด SS-ACPC ได้แก่

โครงการย่อยที่ 1 : Conformationally restricted PNA: synthesis and binding properties

สังเคราะห์และประเมินสมบัติการจับยึดกรดนิวคลีอิกของพีเอ็นเอที่ประกอบด้วยโพรลีนและเบต้าอะมิโนแอซิด ได้แก่ 2-aminocyclopentanecarboxylic acids และอนุพันธ์เอซาของมัน, 2-aminocyclopropanecarboxylic acids และ 2-aminocyclohexanecarboxylic acids พร้อมทั้งศึกษาการจับยึดของ SS-ACPC PNA กับกรดนิวคลีอิก และปัจจัยทางโครงสร้างที่มีผลต่อสมบัติการจับยึดโดยอาศัยการทดลองประกอบกับการคำนวณทางทฤษฎี

โครงการย่อยที่ 2: Dendritic fluorophores for detection of DNA/PNA hybridization

สังเคราะห์ฟลูออโรฟอร์เด็นดริเมอร์ที่มีประจุบวก (dendritic polycationic fluorophores, DPFs) ที่มีจำนวนประจุแตกต่างกัน และประเมินการเปลี่ยนแปลงการเรืองแสงเมื่อจับกับดีเอ็นเอและพีเอ็นเอในสภาวะต่างๆ เพื่อพัฒนาเป็นระบบตรวจวัดความแตกต่างระหว่างพีเอ็นเอในสภาพที่เป็นอิสระและเมื่อจับยึดกับดีเอ็นเอ

โครงการย่อยที่ 3: Development of positively charged polymeric support for high throughput DNA sequence analysis using PNA probes

ส่วนที่ 1 เป็นการเตรียมอนุภาคไคโตซานที่ดัดแปลงให้เป็นหมู่ควอเทอร์นารีแอมโมเนียมโดยใช้ปฏิกิริยาเมทิลเลชันของไคโตซานหรืออนุพันธ์เอ็น-อัลคิลที่ได้จากการทำรีดักทีฟแอลคิลเลชันของไคโตซานด้วยแอลดีไฮด์ และเตรียมอนุภาคไคโตซานแบบแอมฟิฟิลิกจากไคโตซานที่ผ่านการดัดแปลงด้วยหมู่ชอบน้ำได้แก่พอลิเอทิลีนไกลคอลที่มีความยาวต่างๆ กัน หรือควอเทอร์นารีแอมโมเนียม และหมู่ไฮโดรโฟบิกเช่นไฮโดรคาร์บอนสายยาวหรือฟลูออโรคาร์บอน จากนั้นจึงประเมินความสามารถในการดูดซับดีเอ็นเอของอนุภาคที่ได้ในแต่ละวิธี และนำไปทดลองใช้งานในการตรวจสอบลำดับเบสของดีเอ็นเอร่วมกับพีเอ็นเอโพรบและมัลดิทอฟแมสสเปกโทรเมตรี

ส่วนที่ 2 เป็นการเตรียมพื้นผิวเมมเบรนที่มีประจุบวกโดยวิธี surface-initited polymerization ของ 2-(dimethylamino)ethyl methacrylate) (DMAEMA) บนกระดาษกรองผ่านกระบวนการ ARGET ATRP ตามด้วยการทำเมทิลเลชัน การตรวจสอบดีเอ็นเอทำโดยอาศัยพีเอ็นเอโพรบที่ติดฉลากด้วยไบโอติน ซึ่งจะจับกับดีเอ็นเอที่ตรึงอยู่บนพื้นผิวนี้อย่างจำเพาะเจาะจง จากนั้นจึงให้ทำปฏิกิริยาต่อกับ horse radish peroxidase-streptavidin conjugate และสาร

สร้างสี โดยจะมีการ optimize ภาวะในการเตรียมพื้นผิวให้มีความหนาแน่นของประจุที่เหมาะสม และภาวะของการตรวจสอบเพื่อให้ได้ความแม่นยำและความว่องไวสูงสุด

ในทั้งสองส่วนจะมีการทดสอบการวิเคราะห์กับตัวอย่างดีเอ็นเอสังเคราะห์และดีเอ็นเอจริง

โครงการย่อยที่ 4: Surface-functionalized magnetic nanoparticles for immobilization of PNA and DNA

สังเคราะห์และดัดแปลงพื้นผิวของอนุภาคแมกนีไทต์ขนาดนาโนเพื่อให้มีประจุบวกโดยอาศัยการเคลือบด้วยแคตไอออนิกพอลิเมอร์ร่วมกับพอลิเมอร์ที่ชอบน้ำ โดยจะมีการปรับอัตราส่วนของแคตไอออนิกพอลิเมอร์ต่อพอลิเมอร์ที่ชอบน้ำเพื่อให้ได้อนุภาคที่สามารถจับยึดกับดีเอ็นเอซึ่งมีประจุลบได้ดีที่สุด และมีการจับยึดแบบไม่จำเพาะเจาะจงกับพีเอ็นเอซึ่งไม่มีประจุได้น้อยที่สุด และศึกษาการประยุกต์ใช้ระบบดังกล่าวในการตรวจวิเคราะห์ลำดับเบสของดีเอ็นเอ

โครงการย่อยที่ 5: Development of label-free electrochemical DNA biosensor based on immobilized PNA probes

เปรียบเทียบภาวะที่เหมาะสมในการตรึงพีเอ็นเอบนผิวอิเล็กโทรดที่เป็นทองโดยใช้อาศัย self-assembled monolayers (SAMs) และการตรึงผ่านชั้นของพอลิเมอร์ เพื่อสร้างอุปกรณ์สำหรับตรวจลำดับเบสของดีเอ็นเอที่มีความว่องไวและความจำเพาะเจาะจงสูงโดยใช้เทคนิค capacitive และ/หรือ impedimetric และใช้อุปกรณ์ดังกล่าวในการตรวจสอบลำดับเบสของดีเอ็นเอจากตัวอย่างจริง

Project 6: Applications of PNA based diagnostics in medical, food and agricultural sciences

งานวิจัยจะแบ่งเป็นสองส่วน ซึ่งจะมีขั้นตอนแรกเหมือนกัน คือการเลือกลำดับเบสของดีเอ็นเอเป้าหมายเพื่อนำมาใช้ในการออกแบบพีเอ็นเอโพรบ ขั้นตอนต่อมาในงานวิจัยส่วนแรกเป็นการพัฒนาระบบพีเอ็นเอเรืองแสงที่มีสมบัติการเรืองแสงเปลี่ยนไปตามสถานะการเกิดไฮบริดกับดีเอ็นเอ และนำระบบพีเอ็นเอเรืองแสงนี้ไปประยุกต์ใช้ร่วมกับเทคนิคการเตรียมตัวอย่างดีเอ็นเอที่มีประสิทธิภาพสูง เพื่อตรวจสอบสายพันธุ์เชื้อที่ก่อให้เกิดโรค และการปนเปื้อนของสารก่อภูมิแพ้ในอาหารและผลิตภัณฑ์ทางการเกษตร สำหรับงานวิจัยในส่วนที่สองเป็นการพัฒนาระบบพีเอ็นเอร่วมกับเทคนิค MALDI-TOF เพื่อนำไปประยุกต์ใช้ในทางการแพทย์ได้แก่ การศึกษาการเกิดเมทิลเลชันของดีเอ็นเอ และการทำ HLA typing ซึ่งงานทั้งสองส่วนต้องมีการเปรียบเทียบผลที่ได้กับเทคนิคมาตรฐานอื่นๆ เช่น pyrosequencing เพื่อตรวจสอบความแม่นยำของการวิเคราะห์

10. ผลการดำเนินงาน

ผลการดำเนินการในส่วนที่เป็นงานวิจัยทั้ง 6 โครงการย่อยเป็นไปได้ตามแผนงานที่วางไว้ โดยภาพรวมตัวงานเสร็จสมบูรณ์ตามข้อเสนอโครงการแล้ว ได้องค์ความรู้ใหม่ที่เกี่ยวข้องกับระบบพีเอ็นเอที่มีคอนฟอร์เมชันจำกัดชนิดใหม่ที่แสดงสมบัติการจับยึดกับดีเอ็นเอที่น่าสนใจ และได้ศึกษาสมบัติของระบบพีเอ็นเอชนิด acpcPNA ในด้านการจับยึดกับดีเอ็นเอและอาร์เอ็นเออย่างละเอียด อีกทั้งยังได้พัฒนาวิธีการติดฉลากเรืองแสงแก่ acpcPNA ที่ตำแหน่งใดๆ ของโมเลกุลตามต้องการ และได้นำ acpcPNA ไปใช้เป็นโพรบสำหรับตรวจสอบลำดับเบสของดีเอ็นเอโดยอาศัยเทคนิคฟลูออเรสเซนส์ (ใช้พีเอ็นเอที่ติดฉลากเรืองแสงโดยตัวของมันเอง หรือใช้ร่วมกับพอลิเมอร์เรืองแสง) การเกิดสีที่เร่งด้วยเอนไซม์ (ใช้ร่วมกับกระดาษกรองที่ดัดแปรพื้นผิวด้วยพอลิเมอร์ที่มีประจุบวก) แมสสปกโตรเมตรี (ใช้ร่วมกับอนุภาคไคโทซาน และอนุภาคแม่เหล็กที่มีประจุบวก) เทคนิคคาพาซิทีฟ (ใช้พีเอ็นเอที่ไม่ต้องติดฉลาก) และยังได้นำระบบดังกล่าวไปประยุกต์ใช้ในการตรวจวินิจฉัยทางการแพทย์และทางการเกษตร เช่น การตรวจเชื้อไวรัสไข้หวัดใหญ่สายพันธุ์ใหม่ โรคไวรัสในกุ้งและสับปะรด การทำ HLA genotyping เป็นต้น ปัญหาสำคัญที่พบคือระบบตรวจวัดดังกล่าวข้างต้นส่วนใหญ่สามารถทำงานได้กับดีเอ็นเอตัวอย่างที่ได้มาจากการสังเคราะห์ โดยให้ความจำเพาะเจาะจงและความไวของการตรวจวัดสูงตามที่คาดหมายไว้ แต่เมื่อนำไปตรวจวิเคราะห์กับดีเอ็นเอตัวอย่างจริงยังพบปัญหาด้านประสิทธิภาพของการ

จับยึดระหว่างพีเอ็นเอกับดีเอ็นเอเป้าหมาย คาดว่าความแตกต่างที่สำคัญคือการที่ดีเอ็นเอจากตัวอย่างจริงมักจะอยู่ในรูปของ duplex ไม่ใช่ single stranded DNA เหมือนที่ได้จากการสังเคราะห์ และมี matrix ที่ซับซ้อนกว่าตัวอย่างสังเคราะห์ จึงยังต้องศึกษารายละเอียดต่อไปเพื่อพัฒนาการตรวจสอบดีเอ็นเอจากตัวอย่างจริงให้มีประสิทธิภาพมากขึ้นถึงระดับที่จะนำไปใช้งานได้จริงในทางปฏิบัติ นับถึงวันที่รายงานมีผลงานที่ตีพิมพ์และได้รับการตอบรับให้ตีพิมพ์ถึงวันที่รายงาน จำนวนรวม 20 บทความ เป็นผลงานจากโครงการย่อยที่ 1 จำนวน 11 บทความ โครงการย่อยที่ 2 จำนวน 3 บทความ โครงการย่อยที่ 3 จำนวน 1 บทความ โครงการย่อยที่ 4 จำนวน 2 บทความ โครงการย่อยที่ 5 จำนวน 2 บทความ โครงการย่อยที่ 6 จำนวน 1 บทความ และมีบทความที่กำลังเตรียมต้นฉบับอยู่อีกจำนวนหนึ่ง ในแง่ของคุณภาพ มีบทความที่ได้ลงตีพิมพ์ในวารสารที่มี IF2011 > 5 จำนวน 4 บทความ, IF2011 อยู่ระหว่าง 4–5 จำนวน 3 บทความ, IF2011 อยู่ระหว่าง 3–4 จำนวน 7 บทความ, IF2011 อยู่ระหว่าง 2–3 จำนวน 3 บทความ, และ IF2001 อยู่ระหว่าง 0.5–1 จำนวน 1 บทความ และมีอีก 2 บทความที่ลงตีพิมพ์ในวารสารใหม่ จึงยังไม่มีข้อมูลในฐานข้อมูล ISI ข้อมูลสรุป output ในด้านอื่นๆ เป็นดังแสดงในตาราง

ตารางสรุปผลงานที่ได้ตลอดโครงการ (ตัวเลขในวงเล็บคือเป้าหมายที่ตั้งไว้ในข้อเสนอโครงการ)

ผลงาน	ปีที่ 1	ปีที่ 2	ปีที่ 3	ช่วงขยายโครงการ	รวม
1 จำนวนนักวิจัยที่สร้างจากโครงการ					
1.1 สถาบันเดียวกัน	7 (6)	-	-	-	7 (6)
1.2 ต่างสถาบัน	9 (8)	0 (1)	-	-	9 (9)
1.3 นักศึกษาระดับปริญญาเอก*	-	2 (3)	2 (2)	-	4 (5)
1.4 นักศึกษาระดับปริญญาโท**	2 (2)	3 (3)	3 (3)	-	8 (8)
2. จำนวนผลงานตีพิมพ์ในวารสารวิชาการนานาชาติ	3 (3)	2 (8)	9 (7)	6 (-)	20 (18)
3. จำนวนผลงานการจดสิทธิบัตร***	-	-	1 (1)	-	1 (1)

*นับเฉพาะผู้ที่รับทุนผู้ช่วยวิจัยจากโครงการ หากนับนักศึกษาที่ทำงานเป็นส่วนหนึ่งของโครงการแต่รับทุนจากแหล่งอื่นจะมีจำนวนมากกว่านี้อย่างน้อย 1 เท่าตัว

**นับเฉพาะผู้ที่รับทุนผู้ช่วยวิจัยจากโครงการ หากนับนักศึกษาที่ทำงานเป็นส่วนหนึ่งของโครงการแต่รับทุนจากแหล่งอื่นจะมีจำนวนมากกว่านี้

***ยื่นจดในประเทศ

สัญญาเลขที่ RTA5280002

โครงการ การสังเคราะห์ สมบัติ และการประยุกต์ใช้เบต้าพิโรลิดินิลเพปไทด์นิวคลีอิกแอซิด ที่มีคอนฟอร์เมชันถูกจำกัด

รายงานฉบับสมบูรณ์

ชื่อหัวหน้าโครงการวิจัยผู้รับทุน นายธีรยุทธ วิไลวัลย์

รายงานในช่วงตั้งแต่วันที่ 1 สิงหาคม 2552 - 31 มกราคม 2556

1. กิจกรรมที่ได้ดำเนินการ

โครงการวิจัยนี้แบ่งเป็นหกโครงการย่อย ซึ่งครอบคลุมงานวิจัยเกี่ยวกับการสังเคราะห์และศึกษาสมบัติการจับยึดกับกรดนิวคลีอิกของพีเอ็นเอชนิดใหม่ที่มีคอนฟอร์เมชันจำกัด และการพัฒนาระบบตรวจสอบลำดับเบสของสารพันธุกรรมโดยอาศัยพิร์โรลิดินิลพีเอ็นเอชนิด *RR*-Pro/*SS*-ACPC (ต่อไปจะเรียกย่อว่า acpcPNA) ที่คณะผู้วิจัยได้พัฒนาขึ้น ได้แก่

โครงการย่อยที่ 1 : Conformationally restricted PNA: synthesis and binding properties

แผนงานตลอดโครงการ

สังเคราะห์และประเมินสมบัติการจับยึดกรดนิวคลีอิกของพีเอ็นเอที่ประกอบด้วยโพรลีนและเบต้าอะมิโนแอซิด ได้แก่ 2-aminocyclopentanecarboxylic acids และอนุพันธ์เอซาของมัน, 2-aminocyclopropanecarboxylic acids และ 2-aminocyclohexanecarboxylic acids พร้อมทั้งศึกษาการจับยึดของ acpcPNA กับกรดนิวคลีอิก และปัจจัยทางโครงสร้างที่มีผลต่อสมบัติการจับยึดโดยอาศัยการทดลองประกอบกับการคำนวณทางทฤษฎี

สรุปกิจกรรมที่ได้ทำจริงตลอดโครงการ

งานวิจัยที่ได้ดำเนินการภายใต้โครงการย่อยนี้แบ่งออกเป็น 3 ส่วนหลักๆ คือ 1) การสังเคราะห์และศึกษาสมบัติจับยึดของ acpcPNA 2) การสังเคราะห์และศึกษาสมบัติจับยึดของการสังเคราะห์และศึกษาสมบัติจับยึดของ acpcPNA ที่มี modified base และ 3) การสังเคราะห์และศึกษาสมบัติจับยึดของพีเอ็นเอที่มี modified backbone รายละเอียดของงานวิจัยโดยสรุปมีดังนี้

1.1 การสังเคราะห์และศึกษาสมบัติจับยึดของ acpcPNA

ได้สังเคราะห์ acpcPNA ที่มีความยาวเท่ากันคือ 10 เบส แต่มีสัดส่วนของเบส AT และ CG แตกต่างกันจำนวนทั้งสิ้น 9 ลำดับเบส และศึกษาสมบัติการจับยึดกับดีเอ็นเอ เปรียบเทียบกับอาร์เอ็นเอ และการจับยึดกับตัวเอง ผลการทดลองทั้งหมดยืนยันสมบัติที่เป็นเอกลักษณ์เฉพาะตัวของ acpcPNA 3 ประการ คือ 1. ความสามารถในการเลือกจับกับดีเอ็นเอได้ดีกว่าอาร์เอ็นเอ 2. ความเสถียรของโมเลกุลลูกผสมระหว่างพีเอ็นเอกับดีเอ็นเอที่ไม่ขึ้นกับสัดส่วนของเบสที่เป็นองค์ประกอบ และ 3. ไม่เกิดโมเลกุลลูกผสมกับตัวเองในทิศทางแอนติพาราเรล สมบัติประการแรกเป็นการบ่งชี้ข้อจำกัดของ acpcPNA ว่าน่าจะเหมาะกับงานที่เกี่ยวข้องกับเป้าหมายของการจับยึดที่เป็นดีเอ็นเอมากกว่าอาร์เอ็นเอ เช่นงานทางด้าน DNA-based diagnostics และ antigene therapeutics ส่วนสมบัติประการที่สองน่าจะเป็นประโยชน์ในการนำไปใช้เป็นโพรบสำหรับตรวจวินิจฉัยแบบ high throughput เช่นในการทำไมโครแอเรย์ เนื่องจากสามารถออกแบบพีเอ็นเอโพรบหลายๆ ชนิดเพื่อให้จับกับดีเอ็นเอเป้าหมายได้หลายๆ ตำแหน่งพร้อมกัน และสมบัติประการที่สามอาจนำไปประยุกต์ใช้ประโยชน์ได้ในการออกแบบพีเอ็นเอสองสายเพื่อให้จับกับดีเอ็นเอเป้าหมายที่เป็นโมเลกุลแบบเกลียวคู่โดยการเกิด double duplex invasion ซึ่งน่าจะช่วยเพิ่มประสิทธิภาพของการจับยึดระหว่างพีเอ็นเอกับดีเอ็นเอแบบเกลียวคู่(ซึ่งจะพบในสถานการณ์ของการใช้งานจริง)

1.2 การสังเคราะห์และศึกษาสมบัติจับยึดของ acpcPNA ที่มี modified base

ได้ศึกษา acpcPNA ที่มี modified base อยู่ 3 กลุ่ม กลุ่มแรกคือเบส hypoxanthine (H) ซึ่งพบว่า เบส H ใน acpcPNA แสดงการจับยึดอย่างจำเพาะเจาะจงกับเบส C ในดีเอ็นเอ การค้นพบนี้ได้เสนอแนะว่าสามารถแทนที่เบส G ใน acpcPNA ด้วยเบส H ได้โดยไม่มีผลกระทบต่อ specificity ในการจดจำเบส C ซึ่งมีความสำคัญอย่างยิ่งต่อการนำ acpcPNA ไปประยุกต์ใช้ประโยชน์ในด้านต่าง ๆ เนื่องจากโมโนเมอร์ของเบส H สามารถสังเคราะห์ได้ง่ายกว่าโมโนเมอร์ของ G นอกจากนี้ยังไม่มีปัญหาเรื่อง oxidation, quenching และการเกิด secondary structure เหมือนเบส G

งานในกลุ่มที่สองเป็นการพัฒนาวิธีการสังเคราะห์และศึกษาสมบัติการจับยึดกับดีเอ็นเอและสมบัติการเรืองแสงของ acpcPNA ที่มีฉลากเรืองแสง pyrene ติดอยู่ที่ตำแหน่ง 5 ของนิวคลีโอเบสยูเรซิล (U^{Py}) โดยพบว่าเบส U^{Py} ใน acpcPNA สามารถจดจำเบส A ในดีเอ็นเอได้อย่างจำเพาะเจาะจง และแสดงสมบัติ base discriminative fluorescence กล่าวคือการเรืองแสงจะเพิ่มขึ้นอย่างมากเมื่อมีการเข้าคู่ระหว่างเบส U^{Py} ใน acpcPNA กับเบส A ใน DNA ทำให้ acpcPNA ที่มีเบส UPy ทำตัวเป็น quencher free molecular beacon ได้ งานในกลุ่มที่ 3 เกี่ยวข้องกับการแทนที่นิวคลีโอเบสใน acpcPNA ด้วย polycyclic aromatic hydrocarbon เช่น pyrene และ anthracene ที่ต่อกับวงแหวนไตรอะโซล (Tz^{Py} และ Tz^{Ant}) โดยอาศัยปฏิกิริยาคลิกกับพีเอ็นเอที่มีหมู่เอไซด์ โดยพบว่าเบส Tz^{Py} ทำหน้าที่เป็น universal base กล่าวคือสามารถเข้าคู่กับเบสธรรมชาติได้ทุกตัวโดยมีความเสถียรไม่แตกต่างกันมากนัก จากนั้นจึงได้ศึกษาสมบัติการเรืองแสงของพีเอ็นเอที่ได้ในสภาพที่เป็นสายเดี่ยวเปรียบเทียบกับเมื่อเข้าคู่กับดีเอ็นเอ พบว่าพีเอ็นเอที่มีเบส Tz^{Py} เมื่อเข้าคู่กับดีเอ็นเอจะมีการเปลี่ยนแปลงการเรืองแสงจากพีเอ็นเอสายเดี่ยวอย่างชัดเจน กล่าวคือการเรืองแสงที่ 460 nm จะลดลง และการเรืองแสงที่ช่วง 390–430 nm จะเพิ่มขึ้น

1.3 การสังเคราะห์และศึกษาสมบัติจับยึดของพีเอ็นเอที่มี modified backbone

งานวิจัยที่ได้ดำเนินการไปแบ่งเป็น 3 ส่วน คือ 1. การสังเคราะห์และศึกษาสมบัติการจับยึดของพีเอ็นเอที่มีสเตอริเอเคมีของวงแหวนโพรลีนเป็น (2*R*′,4′*R*) 2. การสังเคราะห์และศึกษาสมบัติการจับยึดของพีเอ็นเอที่มีกรดเบต้าอะมิโนชนิดอื่นนอกเหนือจาก ACPC เป็นตัวเชื่อม และ 3. การสังเคราะห์ สมบัติการจับยึด และสมบัติการเรืองแสงของพีเอ็นเอที่ติดฉลากเรืองแสงผ่านตัวเชื่อม 3-aminopyrrolidine-4-carboxylic acid (APC)

งานวิจัยส่วนแรกเป็นการสังเคราะห์ acpcPNA ที่มีสเตอริโอเคมีของวงแหวนโพรลีนและ ACPC ที่ต่างไปจาก *RR*-Pro/*SS*-ACPC โดยแยกศึกษาแต่ละส่วนในพีเอ็นเอที่มีลำดับเบสเป็น T_5 พบว่าจากพีเอ็นเอทั้ง 7 ไดอะสเตอริโอเมอร์นั้น มีเพียงระบบ acpcPNA เดิม [(2′*R*,4′*R*)-Pro/(1*S*,2*S*)-ACPC] และอีพิเมอร์ของมันที่มีสเตอริโอเคมีของตำแหน่ง 4′ บนวงแหวนโพรลีนเปลี่ยนแปลงไป [(2′*R*,4′*S*)-Pro/(1*S*,2*S*)-ACPC] เท่านั้นที่แสดงการจับยึดกับดีเอ็นเอได้ จึงได้ศึกษาระบบใหม่ที่เรียกชื่อว่า *epi*-acpcPNA นี้ต่ออย่างละเอียดในพีเอ็นเอที่มีลำดับเบสที่ซับซ้อนขึ้น ผลการทดลองแสดงให้เห็นว่า *epi*-acpcPNA แสดงการจดจำดีเอ็นเอและอาร์เอ็นเอที่คล้ายคลึงกับ acpcPNA แต่ระบบ *epi*-acpcPNA สามารถเกิดไฮบริดที่ค่อนข้างเสถียรกับตัวเองได้ได้ในทิศทางแอนติพาราเรล ซึ่งแตกต่างจาก acpcPNA อย่างชัดเจน และอาจนำไปสู่การประยุกต์ใช้ที่แตกต่างกันของพีเอ็นเอทั้งสองระบบ โดย acpcPNA น่าจะเหมาะสำหรับ applications ที่เกี่ยวกับ DNA ที่ไม่ต้องการการเกิด self hybrid เช่น การ target cellular DNA ด้วย double duplex invasion mechanism ในขณะที่ *epi*-acpcPNA น่าจะเหมาะสมกับการนำไปใช้ทางด้านนาโนเทคโนโลยี/เครื่องมือระดับโมเลกุลที่อาศัยการจดจำระหว่างพีเอ็นเอสองสาย

งานวิจัยในส่วนที่สองเป็นการสังเคราะห์และศึกษาสมบัติการจับยึดของพีเอ็นเอที่มีการแทนที่ตัวเชื่อมที่เป็นกรดเบต้าอะมิโน 2-aminocyclopentancecarboxylic acid (ACPC) ซึ่งเป็น 5-membered ring ใน acpcPNA ด้วยไซคลิกเบต้าอะมิโนแอซิดที่มีวงแหวนขนาดเล็กลงและใหญ่ขึ้น ได้แก่ aminocyclopropanecarboxylic acid (ACC) (3-membered) /2-aminocyclobutanecarboxylic acid (ACBC) (4-membered) และ 2-aminocyclohexanecarboxylic acid (ACHC) (5-membered) ทำให้ได้พีเอ็นเอชนิดใหม่คือ accPNA, acbcPNA และ achcPNA ผลการศึกษาการจับยึดของ acbcPNA กับ DNA และ RNA พบว่า acbcPNA เกิดไฮบริดกับ DNA และ RNA เฉพาะในทิศทางแอนติพาราเรล โดยไฮบริดที่เกิดขึ้นมีความเสถียรมากกว่าของ acpcPNA อยู่ประมาณ 9–15 °C สำหรับดีเอ็นเอ และ 15–18 °C

สำหรับอาร์เอ็นเอ โดยที่ความจำเพาะเจาะจงของการจับยึดยังสูงอยู่ ในขณะที่ accPNA และ achcPNA ไม่แสดงการจับยึดกับดีเอ็นเอและอาร์เอ็นเอที่มีลำดับเบสคู่สม ซึ่งสามารถอธิบายได้จากค่า torsional angle (θ) ของไซคลิกเบต้าอะมิโนแอซิดที่เกี่ยวข้อง (ได้จากการคำนวณทางทฤษฎีและข้อมูลจากเอกสารอ้างอิง) โดย acbcPNA จะมีค่าใกล้เคียงกับค่าที่เหมาะสม (99 º)มากที่สุด ในขณะที่ accPNA และ achcPNA มีค่าต่างออกไปมากที่สุด ข้อมูลที่ได้จะนำไปสู่การออกแบบพีเอ็นเอระบบใหม่ที่มีความสามารถในการจับยึดกับดีเอ็นเอและ/หรืออาร์เอ็นเอที่ดีขึ้น

งานวิจัยในส่วนที่ 3 เป็นการสังเคราะห์ acpcPNA ที่มีการแทนที่ตัวเชื่อม ACPC ด้วย 3-aminopyrrolidine-4-carboxylic acid (APC) เพื่อให้มีหมู่อะมิโนที่สามารถดัดแปลงเพิ่มเติมได้ด้วยฉลากเรืองแสงที่บริเวณใดๆ ตามต้องการบนสายของพีเอ็นเอ โดยอาศัยการสร้างพันธะเอไมด์ ปฏิกิริยารีดักทีฟแอลคิลเลชัน หรือปฏิกิริยารีดักทีฟแอลคิลเลชัน-คลิก ได้ใช้วิธีการใหม่เหล่านี้ในการสังเคราะห์พีเอ็นเอที่ติดฉลากเรืองแสงที่สามารถเปลี่ยนแปลงการเรืองแสงได้ตามสภาพแวดล้อม ได้แก่ไพรีน และไทอะโซลออเรนจ์ และได้แสดงให้เห็นว่าพีเอ็นเอที่ติดฉลากเหล่านี้มีการเรืองแสงเพิ่มขึ้นเมื่อมีการเข้าคู่กับดีเอ็นเอ โดยพีเอ็นเอที่ติดฉลากไพรีนจะให้การเปลี่ยนแปลงการเรืองแสงประมาณ 4-14 เท่า ในขณะที่พีเอ็นเอที่ติดฉลากไทอะโซลออเรนจ์จะให้การเปลี่ยนแปลงการเรืองแสงที่ชัดเจนกว่า (10–50 เท่า) พีเอ็นเอที่ติดฉลากเหล่านี้แสดงการเรืองแสงที่เพิ่มขึ้นด้วยเมื่อมีดีเอ็นเอที่ไม่เป็นคู่สม อย่างไรก็ตาม สามารถใช้การย่อยด้วยเอนไซม์ nuclease S1 เพื่อช่วยเพิ่มความจำเพาะเจาะจงได้ โดยในทุกกรณีหลังการย่อย สัญญาณของไฮบริดคู่สมจะคงเดิม แต่สัญญาณของไฮบริดที่ไม่เป็นคู่สมจะลดลงเหลือเท่าสัญญาณของพีเอ็นเอสายเดี่ยว พีเอ็นเอที่ติดฉลากเหล่านี้จึงมีศักยภาพสูงในการนำไปใช้เป็น quencher free molecular beacon สำหรับการตรวจสอบลำดับเบสของดีเอ็นเอ

สรุปกิจกรรมที่ได้ทำเพิ่มเติมในช่วงขยายระยะเวลาโครงการ (1 สิงหาคม 2555 - 31 มกราคม 2556)

งานที่ได้ทำในช่วงขยายระยะเวลาโครงการเป็นการเก็บข้อมูลเพิ่มเติมของงานวิจัยเพิ่มเติมและร่างต้นฉบับบทความเพื่อตีพิมพ์ของงานวิจัยหัวข้อ 1.2 ในส่วนของ acpcPNA ที่มี modified base เบสเป็น hypoxanthine (ต้นฉบับได้รับการตอบรับให้ตีพิมพ์ในวารสาร Organic & Biomolecular Chemistry เรียบร้อยแล้ว) และหัวข้อ 1.3 ในส่วนของการสังเคราะห์พีเอ็นเอที่ติดฉลากไทอะโซลออเรนจ์ที่สามารถเปลี่ยนแปลงการเรืองแสงได้ตามสภาพแวดล้อมโดยอาศัยปฏิกิริยารีดักทีฟแอลคิลเลชัน-คลิก (ต้นฉบับเตรียมเสร็จแล้วและ submit ไปแล้ว กำลังอยู่ระหว่างรอผลการพิจารณา) และปฏิกิริยาการสร้างพันธะเอไมด์กับฉลากไพรีน (กำลังอยู่ระหว่างเตรียมต้นฉบับ) นอกจากนี้ยังได้มีการสังเคราะห์ acpcPNA ที่มีเบสเรืองแสงเพิ่มเติมอีก 1 ชนิดคือ 8-((pyren-1-yl)ethynyl)adenine (A^{PyE}) และ acpcPNA ที่มีตัวเชื่อมที่ดัดแปรด้วยหมู่ชอบน้ำได้แก่พอลิเอทิลีนไกลคอล รวมทั้ง acpcPNA ที่ติดฉลากชนิดอื่นๆ ได้แก่ฉลากเรืองแสง Nile Red, Nile Blue และฉลากที่ว่องไวทางเคมีไฟฟ้า เช่น anthraquinone, methylene blue และ acpcPNA ที่ติดฉลากเรืองแสงคู่ (doubly-labeled) ในทุกกรณีมีผลการทดลองเบื้องต้นเป็นที่น่าพอใจ แต่งานยังไม่เสร็จสมบูรณ์พอที่จะเขียนบทความได้ ยังต้องมีการคาดว่าน่าจะได้อีกอย่างน้อย 2–3 บทความในระยะเวลาประมาณ 1 ปีนับจากนี้

โครงการย่อยที่ 2 : Dendritic fluorophores for detection of DNA/PNA hybridization

แผนงานตลอดโครงการ

สังเคราะห์ฟลูออโรฟอร์เด็นดริเมอร์ที่มีประจุบวก (dendritic polycationic fluorophores, DPFs) ที่มีจำนวนประจุแตกต่างกัน และประเมินการเปลี่ยนแปลงการเรืองแสงเมื่อจับกับดีเอ็นเอและพีเอ็นเอในสภาวะต่างๆ เพื่อพัฒนาเป็นระบบตรวจวัดความแตกต่างระหว่างพีเอ็นเอในสภาพที่เป็นอิสระและเมื่อจับยึดกับดีเอ็นเอ

สรุปกิจกรรมที่ได้ทำจริงตลอดโครงการ

กิจกรรมที่ได้ดำเนินการตลอดโครงการแบ่งเป็น 1. การสังเคราะห์เดนดริติกพอลิแคทไอออนฟลูออโรฟอร์ในกลุ่ม ethynyltriphenylamine ที่ละลายน้ำได้ 2. การศึกษาสมบัติเชิงแสงของฟลูออโรฟอร์โดยเทคนิค UV-Vis และ Fluorescence 3. การศึกษาอันตรกิริยาของฟลูออโรฟอร์ที่สังเคราะห์ได้กับดีเอ็นเอ และสารอื่นๆ ได้แก่โปรตีน สารลดแรงตึงผิว ไซโคลเดกซ์ทริน และพอลิเมอร์ที่มีประจุลบ (PVSK) โดยพบว่าโมเลกุลเหล่านี้สามารถทำให้ฟลูออโรฟอร์มี

การเรืองแสงที่เพิ่มขึ้นและเกิด bathochromic shift ของ fluorescence emission และ 4. การนำฟลูออโรฟอร์ดังกล่าวมาประยุกต์ใช้ในการตรวจสอบลำดับเบสของดีเอ็นเอ อย่างไรก็ตาม พบว่าฟลูออโรฟอร์สามารถจับกับดีเอ็นเอทั้งสายเดี่ยวและสายคู่ด้วยแรงกระทำทางไฟฟ้าสถิต โดยการจับกับดีเอ็นเอสายคู่ทำให้เกิดการเพิ่มขึ้นของการเรืองแสง แต่การจับกับดีเอ็นเอสายเดี่ยวอาจทำให้การเรืองแสงลดลง หรือเพิ่มขึ้นก็ได้โดยขึ้นกับลำดับเบส ดังนั้นจึงไม่สามารถนำฟลูออโรฟอร์ดังกล่าวมาใช้ในการตรวจสอบลำดับเบสของดีเอ็นเอโดยตรงได้ จึงได้พัฒนาวิธีตรวจสอบลำดับเบสของดีเอ็นเอโดยอาศัยหลักการ FRET โดยใช้เดนดริติกฟลูออโรฟอร์เป็น donor และสีย้อมอีกตัวหนึ่งเป็น acceptor ผลการทดลองเบื้องต้นแสดงให้เห็นว่าสามารถเกิด energy transfer จากเดนดริติกฟลูออโรฟอร์ไปยัง SYBR Green II ได้เมื่อมีดีเอ็นเออยู่ด้วย นอกจากนี้ยังได้พัฒนาระบบตรวจสอบลำดับเบสของดีเอ็นเอโดยอาศัยเดนดริติกฟลูออโรฟอร์นี้ร่วมกับพีเอ็นเอที่ติดฉลากด้วย Fluorescein โดยมีหลักการคือแคทไอออนิกเดนดริติกฟลูออโรฟอร์จะไม่จับกับพีเอ็นเอซึ่งเป็นกลาง ดังนั้นจึงไม่ควรจะเกิดการถ่ายเทพลังงาน แต่ถ้ามีดีเอ็นเอที่มีลำดับเบสคู่สมกับพีเอ็นเออยู่ด้วยจะทำให้เกิดการจับกันระหว่างเดนดริติกฟลูออโรฟอร์(ที่มีประจุบวก) กับดีเอ็นเอ (ที่มีประจุลบ) และระหว่างดีเอ็นเอ กับพีเอ็นเอที่ติดฉลากด้วย fluorescein ด้วยการเข้าคู่เบสตามกฎของวัตสัน-คริก ทำให้เดนดริติกฟลูออโรฟอร์ที่จับกับดีเอ็นเอสามารถถ่ายเทพลังงานไปยัง Fluorescein ที่อยู่บนพีเอ็นเอได้

ผลการทดลองได้ยืนยันสมมติฐานดังกล่าวข้างต้น แต่พบปัญหาว่ามีการจับยึดกันแบบไม่จำเพาะเจาะจงระหว่างฟลูออโรฟอร์กับพีเอ็นเอด้วย ซึ่งสามารถแก้ปัญหาได้โดยการเติมตัวทำละลายอินทรีย์ลงไปเพื่อทำลายแรงกระทำแบบไม่จำเพาะเจาะจงนี้ โดยพบว่าการเติม N-methylpyrrolidinone (NMP) ที่ความเข้มข้น 10% ให้ FRET ratio ที่ดีที่สุด จากนั้นจึงได้ทดสอบความจำเพาะเจาะจงกับดีเอ็นเอที่เป็น mismatched เปรียบเทียบกับที่เป็นคู่สม พบว่าในทุกกรณี FRET ratio จะมีค่าสูงกว่า 1 เมื่อมีดีเอ็นเอคู่สม และจะต่ำกว่า 1 เมื่อมีดีเอ็นเอที่ไม่เป็นคู่สม โดยในสภาวะที่ดีที่สุดจะได้ FRET ratio สูงถึง 1.42 เมื่อเทียบกับ single mismatched และ non-complementary DNA ที่ให้ค่า FRET ratio เพียง 0.51 และ 0.26 โดยมี detection limit ของการตรวจวัดดีเอ็นเอเป้าหมายที่ต่ำกว่า 1 nM

นอกจากนี้ยังได้นำแคทไอออนิกเดนดริติกฟลูออโรฟอร์ที่สังเคราะห์ในงานวิจัยนี้ร่วมกับดีเอ็นเอสายเดี่ยวที่ออกแบบมาให้จับกับโพแทสเซียมไอออน (โพแทสเซียมแอปตาเมอร์) ไปประยุกต์ใช้ในการตรวจวัดโพแทสเซียมไอออนโดยเทคนิคฟลูออเรสเซนส์ โดยอาศัยหลักการที่ทราบมาก่อนหน้านี้แล้วว่าเดนดริติกฟลูออโรฟอร์สามารถจับกับดีเอ็นเอได้ ซึ่งแต่สิ่งที่ค้นพบใหม่คือการเรืองแสงของฟลูออโรฟอร์ที่จับกับดีเอ็นเอที่เป็นโพแทสเซียมแอปตาเมอร์จะขึ้นอยู่กับความเข้มข้นของโพแทสเซียมไอออน กล่าวคือ เมื่อไม่มีโพแทสเซียมไอออน ดีเอ็นเอจะอยู่ในสภาพสายเดี่ยวอิสระ ซึ่งเมื่อจับกับฟลูออโรฟอร์จะทำให้การเรืองแสงเพิ่มขึ้น และเมื่อมีโพแทสเซียมไอออนอยู่ด้วย ดีเอ็นเอจะเปลี่ยนคอนฟอร์เมชันเป็นโครงสร้างแบบ G-quadruplex และส่งผลให้การเรืองแสงลดลง ซึ่งยืนยันโดยใช้เทคนิค CD spectroscopy จากนั้นจึงได้ศึกษาหาภาวะที่เหมาะสม ได้แก่(ความเข้มข้น ชนิดความยาวของดีเอ็นเอ อัตราส่วนของดีเอ็นเอต่อฟลูออโรฟอร์) โดยประเมินจากการเปลี่ยนแปลงสัญญาณฟลูออเรสเซนส์ และการเลือกจำเพาะระหว่างโพแทสเซียมไอออนกับแคทไอออนชนิดอื่นๆ เมื่อได้ภาวะที่ดีที่สุดแล้วจึงนำมาศึกษาช่วงการตรวจวัดที่เป็นเส้นตรง ซึ่งพบว่ามีอยู่สองช่วงคือระหว่าง 4–1000 μM และ 2–6 μM โดยมีขีดจำกัดการตรวจวัดอยู่ที่ 0.9 μM และได้นำไปทดสอบการตรวจวัดความเข้มข้นของโพแทสเซียมในตัวอย่างปัสสาวะ ซึ่งได้ผลสอดคล้องกับการตรวจวัดโดยเทคนิค ICP-MS

สรุปกิจกรรมที่ได้ทำเพิ่มเติมในช่วงขยายระยะเวลาโครงการ (1 สิงหาคม 2555 - 31 มกราคม 2556)

เนื่องจากรูปแบบการจับกันระหว่างไซโคลเด็กซ์ตริน (cyclodextrin, CyD) กับโมเลกุลสารอินทรีย์ชนิดต่างๆ ในสภาพสารละลายมีความสำคัญสำหรับการออกแบบและอธิบายอันตรกิริยาแบบโฮสต์-เกสต์ (host-guest chemistry) ที่เกิดขึ้นในการรับรู้ (sensing) หรือระบบการควบคุมการปลดปล่อย คณะผู้วิจัยจึงได้ศึกษาเพิ่มเติมกับแอมฟิฟิลิก (amphiphilic) ฟลูออเรสเซนต์โพรบที่เป็นแคทไอออนิกเดนไดรติกฟลูออโรฟอร์ (**3N$^+$**) และฟลูออโรฟอร์อื่นที่คล้ายคลึงกันแต่มีการปรับเปลี่ยนประจุของโมเลกุลให้แตกต่างออกไป คือ **N^{0}N$^+$**, **N$^+$** และ **2N$^+$** พบว่าอันตรกิริยาเชิงซุปราโมเลกุล

กับไซโคลเด็กซ์ตรินในกรณีของ **3N**$^+$/γ-CyD และ **2N**$^+$/γ-CyD ได้มีการขยายสัญญาณฟลูออเรสเซนต์อย่างมาก และมีการเหนี่ยวนำสัญญาณ circular dichroism (CD) ซึ่ง ^{1}H NMR แสดงชัดเจนถึงการเกิดอินคลูชันคอมเพล็กซ์ (inclusion complex) แบบ 1:1 โดยที่การจับกันของ **3N**$^+$ กับ γ-CyD ให้ค่าคงที่ของการจับกัน (binding constant) ที่สูงถึง 3.0×10^4 ในขณะที่ β-CyD แสดงการขยายสัญญาณฟลูออเรสเซนซ์ของฟลูออโรฟอร์ในระดับปานกลางเท่านั้น และมีการเหนี่ยวนำสัญญาณ CD เพียงเล็กน้อย เช่นเดียวกับสัญญาณ ^{1}H NMR ที่เปลี่ยนไปเพียงเล็กน้อย บ่งบอกถึงการเกิดสารประกอบเชิงซ้อนแบบ fast exchange โดยไม่มีการเกิดอินคลูชั่นคอมเพล็กซ์ระหว่าง β-CyD กับฟลูออโรฟอร์ ส่วน α-CyD แสดงการขยายสัญญาณฟลูออเรสเซนซ์ที่ชัดเจนกับฟลูออโรฟอร์ **N^{0}N**$^+$ ที่มีโครงสร้างเป็นแท่งตรงเท่านั้น โดยไม่พบการแยกของสัญญาณ ^{1}H NMR หรือการเหนี่ยวนำสัญญาณ CD การจับกันจึงไม่น่าจะใช่การเกิดอินคลูชัน และการเปรียบเทียบโครงสร้างฟลูออดรฟอร์ที่สามารถเกิดอินคลูชันกับ γ-CyD บ่งชี้ว่าการเกิดสารเชิงซ้อนแบบอินคลูชัน ต้องอาศัยทั้งแรง hydrophobic และแรง dipole-dipole ซึ่งข้อมูลทาง spectroscopy ที่ได้จากงานวิจัยนี้จะเป็นประโยชน์ต่อการอธิบายอันตรกิริยาและการเปลี่ยนแปลงสัญญาณฟลูออเรสเซนซ์ของฟลูออโรฟอร์โดยไซโคลเดกซ์ทริน ดีเอ็นเอ และโปรตีนต่อไป

โครงการย่อยที่ 3: Development of positively charged polymeric support for high throughput DNA sequence analysis using PNA probes

แผนงานตลอดโครงการ

ส่วนที่ 1 เป็นการเตรียมอนุภาคไคโทซานที่ดัดแปลงให้เป็นหมู่ควอเทอร์นารีแอมโมเนียมโดยใช้ปฏิกิริยาเมทิลเลชันของไคโทซานหรืออนุพันธ์เอ็น-อัลคิลที่ได้จากการทำรีดักทีฟแอลคิลเลชันของไคโทซานด้วยแอลดีไฮด์ และเตรียมอนุภาคไคโทซานแบบแอมฟิฟิลิกจากไคโตซานที่ผ่านการดัดแปลงด้วยหมู่ชอบน้ำได้แก่ พอลิเอทิลีนไกลคอล หรือควอเทอร์นารีแอมโมเนียม และหมู่ไฮโดรโฟบิกเช่นไฮโดรคาร์บอนสายยาวหรือเบนซิล จากนั้นจึงประเมินความสามารถในการดูดซับดีเอ็นเอของอนุภาคที่ได้ในแต่ละวิธี และนำไปทดลองใช้งานในการตรวจสอบลำดับเบสของดีเอ็นเอร่วมกับพีเอ็นเอโพรบและ MALDI-TOF mass spectrometry

ส่วนที่ 2 เป็นการเตรียมพื้นผิวเมมเบรนที่มีประจุบวกเพื่อนำไปใช้ในการตรวจสอบลำดับเบสของดีเอ็นเอโดยเทคนิค Dot blot โดยสามารถเตรียมพื้นผิวดังกล่าวได้โดยวิธี surface-initiated polymerization ของ 2-(dimethylamino)ethyl methacrylate) (DMAEMA) บนกระดาษกรองผ่านกระบวนการ ARGET ATRP ตามด้วยการทำเมทิลเลชัน การตรวจสอบดีเอ็นเอทำโดยอาศัยพีเอ็นเอโพรบที่ติดฉลากด้วยไบโอติน ซึ่งจะจับกับดีเอ็นเอที่ตรึงอยู่บนพื้นผิวนี้อย่างจำเพาะเจาะจง จากนั้นจึงให้ทำปฏิกิริยาต่อกับ horse radish peroxidase-streptavidin conjugate และสารสร้างสี โดยจะมีการ optimize ภาวะในการเตรียมพื้นผิวให้มีความหนาแน่นของประจุที่เหมาะสม และภาวะของการตรวจสอบเพื่อให้ได้ความแม่นยำและความว่องไวสูงสุด

ในทั้งสองส่วนจะมีการทดสอบการวิเคราะห์กับตัวอย่างดีเอ็นเอสังเคราะห์และดีเอ็นเอจริง

สรุปกิจกรรมที่ได้ทำจริงตลอดโครงการ

โครงการนี้จะเน้นการพัฒนาเทคนิคสำหรับตรวจสอบลำดับเบสของสารพันธุกรรมในรูปแบบที่มีประสิทธิภาพสูงโดยใช้พีเอ็นเอโพรบร่วมกันวัสดุชนิดใหม่ๆ ที่ทางกลุ่มวิจัยได้พัฒนาขึ้น โดยงานที่ได้ทำทั้งหมดแบ่งเป็น

3.1 การตรวจลำดับเบสของดีเอ็นเอโดยใช้พีเอ็นเอร่วมกับอนุภาคไคโทซานด้วยมัลติทอฟแมสสเปกโตรเมตรี

งานวิจัยนี้ได้เตรียมอนุภาคไคโทซานที่มีพื้นผิวภายนอกเป็นประจุบวกสองวิธี วิธีแรกเป็นการสังเคราะห์อนุภาคไคโตซานที่ผ่านการดัดแปลงหมู่อะมิโนที่ตำแหน่ง 2 ให้เป็นหมู่ควอเทอร์นารีแอมโมเนียมชนิดต่างๆ (trimethylammonium – TMC และ *N*-[(2-hydroxyl-3-trimethylammonium)propyl] – HTACC) โดยอาศัยการตกตะกอนไคโตซานที่ผ่านการดัดแปลงด้วยการเชื่อมขวางด้วยไตรพอลิฟอสเฟต (TMC และ HTACC) หรือโดยการดัดแปลงอนุภาคไคโตซานด้วยเมทิลไอโอไดด์ (MC) พบว่าได้อนุภาคทรงกลม ขนาดอยู่ในช่วง 0.13–0.40 ไมโครเมตร

และมีประจุที่พื้นผิวเป็นบวก (ค่าศักย์เซต้าอยู่ในช่วง 24.3–39.8 mV) และได้ทดลองใช้อนุภาคที่ผ่านการดัดแปลงนี้ร่วมกับ acpcPNA ที่มีความยาว 14 เบส เพื่อตรวจสอบลำดับเบสของดีเอ็นเอเป้าหมาย (*K-ras* gene) ในตัวอย่างดีเอ็นเอสังเคราะห์ได้โดยอาศัยเทคนิค MALDI-TOF mass spectrometry โดยอนุภาคเหล่านี้ให้ประสิทธิภาพในการวิเคราะห์ที่ดีกว่าอนุภาคไคโตซานที่ไม่ได้ผ่านการดัดแปลง โดยสามารถเห็นสัญญาณได้ชัดเจนในกรณีที่มีดีเอ็นเอเป้าหมายอยู่ด้วย และไม่พบสัญญาณในกรณีที่ไม่มีดีเอ็นเอ นอกจากนี้ยังได้พิสูจน์ความจำเพาะเจาะจงกับดีเอ็นเอเป้าหมายที่มีลำดับเบสตรงกันกับโพรบ เปรียบเทียบกับดีเอ็นเอเป้าหมายที่มีลำดับเบสผิดไปหนึ่งตำแหน่ง โดย HTACC ให้ประสิทธิภาพสูงที่สุดในแง่ของความจำเพาะเจาะจง กล่าวคือสามารถบอกความแตกต่างได้อย่างชัดเจน แต่ข้อเสียคืออนุภาคนี้ให้สัญญาณที่ต่ำมากในกรณีที่พีเอ็นเอและดีเอ็นเอเป็นคู่สมกัน เมื่อทำการทดลองภายใต้ภาวะที่มี 20% ฟอร์มาไมด์อยู่ด้วย จะสามารถกำจัด non-specific signal จากอนุภาค MC และ TMC ได้โดยไม่รบกวนต่อสัญญาณของพีเอ็นเอในกรณีที่เป็นคู่สมกันมากนัก ดังนั้นอนุภาคสองชนิดหลังนี้จึงมีประสิทธิภาพโดยรวมดีกว่า

วิธีข้างต้นมีข้อจำกัดในแง่ของการเตรียมอนุภาคที่อาศัยการตกตะกอนอนุภาคด้วยการเชื่อมขวางยังมีประสิทธิภาพต่ำ ไม่สามารถใช้เตรียมอนุภาคในปริมาณมากๆ ได้ จึงได้พัฒนาวิธีเตรียมอนุภาคไคโตซานอีกวิธีหนึ่งโดยอาศัยการประกอบตัวเองของแอมฟิฟิลิกไคโตซานที่มีหมู่ไม่ชอบน้ำเป็นพทาโลอิล เฮกซิลและโดเดกซิล และมีหมู่ชอบน้ำเป็น $mPEG_{5000}$ และ *N*-[(2-hydroxyl-3-trimethylammonium)propyl] (HTAP) และให้ชื่อว่า PgH, DgH และ HgH ตามลำดับ ผลการศึกษาค่าศักย์เซต้าพบว่าอนุภาคสองชนิดหลังแสดงประจุพื้นผิวเป็นบวกในขณะที่อนุภาคชนิดแรกแสดงประจุพื้นผิวเป็นลบ จากนั้นจึงใช้อนุภาค PgH และ HgH ร่วมกับพีเอ็นเอโพรบในการตรวจสอบลำดับเบสของดีเอ็นเอ โดยเทคนิคมัลดิทอฟแมสสเปกโตรเมตรี พบว่าอนุภาคทั้งสองชนิดไม่แสดงการดูดจับพีเอ็นเอ(ซึ่งไม่มีประจุ) แต่เมื่อเติม DNA ซึ่งมีลำดับเบสคู่สมเข้าไป ซึ่งตามหลักการน่าจะพบสัญญาณของพีเอ็นเอ กลับพบสัญญาณที่ต่ำมาก แสดงให้เห็นว่าอนุภาคเหล่านี้ไม่สามารถนำมาใช้เป็นตัวแลกเปลี่ยนแอนไอออนในการวิเคราะห์ลำดับเบสของดีเอ็นเอได้ ซึ่งอาจเกิดจากการผลักกันของประจุลบของอนุภาค PgH กับดีเอ็นเอ หรือการที่อนุภาคเหล่านี้ไปรบกวนการตกผลึกของ CCA เมทริกซ์ที่ใช้ในการวิเคราะห์โดยเทคนิคมัลดิทอฟ

งานส่วนขยายเพิ่มเติมจากนี้คือการสังเคราะห์อนุภาคแอมฟิฟิลิกไคโตซานที่ติดฉลากเรืองแสง (Pyr-CS-HTAP) โดยได้เตรียมอนุภาคควอเทอร์ไนซ์ไคโตซานจากการตรึงหมู่ไพรีน เพื่อใช้เป็นทั้งฉลากเรืองแสงและหมู่ไฮโดรโฟบิกบนโซ่หลักของไคโตซานผ่านปฏิกิริยาคลิก (click reaction) ระหว่าง 1-ethynylpyrene กับพทาโลอิลไคโตซานที่ผ่านการดัดแปลงหมู่ 5'-CH_2OH ให้เป็นหมู่เอไซด์ จากนั้นจึงกำจัดหมู่พทาโลอิลและต่อส่วนของ HTAP เข้าไปที่ตรงส่วนของหมู่ 2'-NH_2 ผ่านปฏิกิริยาการเปิดวงของอิพอกไซด์ โดยใช้เทคนิค IR ในการยืนยันการเกิดปฏิกิริยาในแต่ละขั้นตอน ไคโตซานที่ผ่านการดัดแปลงแล้วนี้ในภาวะที่มีตัวทำละลายที่เป็นน้ำจะทำให้เกิดอนุภาคขึ้น การวิเคราะห์ด้วยเทคนิค SEM แสดงว่าอนุภาคที่สังเคราะห์ได้เกิดจากการเกาะกลุ่มกันของอนุภาคขนาดเล็กกว่าเกิดเป็นโครงสร้างที่มีลักษณะคล้ายลูกแบล็คเบอร์รี่ (blackberry-like) มีเส้นผ่าศูนย์กลางขนาด 1.17±0.46 ไมโครเมตร และจากการวิเคราะห์ด้วยเทคนิค photon correlation spectroscopy พบว่าอนุภาคมีประจุเป็นบวก มีค่าศักย์เซต้าเท่ากับ +49.6 mV และพบการเรืองแสงสีเขียวเมื่อส่องผ่านกล้องฟลูออเรสเซนต์ไมโครสโกป อนุภาคดังกล่าวมีความเสถียรในช่วงอุณหภูมิและพีเอชที่กว้าง (T 0–100 ºC, pH 1–12) แต่จะแตกตัวออกในตัวทำละลายที่ไม่มีขั้วเช่นเฮกเซน โดยอนุภาคที่แตกออกแล้วนี้สามารถกลับมารวมตัวกันอีกครั้งในน้ำ อนุภาค Pyr-CS-HTAP นี้ไม่เป็นพิษต่อเซลล์ของหนู (MTT assay) และสามารถเข้าสู่เซลได้ แสดงให้เห็นถึงศักยภาพในการนำไปประยุกต์ใช้เป็นวัสดุในการนำส่งยาหรือสารออกฤทธิ์ทางชีวภาพที่สามารถตรวจติดตามการเข้าสู่เซลล์เป้าหมายได้โดยเทคนิคฟลูออเรสเซนส์

3.2 การตรวจลำดับเบสของดีเอ็นเอโดยใช้กระดาษกรองที่ตรึงด้วยพอลิเมอร์บรัชที่มีประจุบวกร่วมกับเพปไทด์นิวคลีอิกแอซิดโดยอาศัยหลักการของ "Dot blot"

ในงานวิจัยนี้ได้เตรียมเมมเบรนที่มีประจุบวกจากกระดาษกรองเพื่อใช้ในการตรึง DNA และตรวจสอบลำดับเบสของดีเอ็นเอด้วยพีเอ็นเอโพรบในรูปแบบ "Dot blot" โดยมีจุดมุ่งหมายที่จะพัฒนาระบบสำหรับตรวจสอบลำดับเบส

ของดีเอ็นเอที่มีราคาถูก ความไวสูง และสามารถทำได้หลายตัวอย่างพร้อมกัน เมมเบรนที่มีประจุบวกดังกล่าวสามารถทำได้จากปฏิกิริยา surface initiated polymerization ของ DMAEMA (2-dimethylaminoethyl methacrylate) บนผิวของกระดาษกรองที่ติดด้วยตัวริเริ่มปฏิกิริยา (bromoisobutyryl group) ตามด้วยการควอเทอร์ไนซ์ด้วยเมทิลไอโอไดด์และแลกเปลี่ยนเคาน์เตอร์ไอออนเป็นคลอไรด์ และได้นำกระดาษกรองที่ผ่านการดัดแปลงดังกล่าวมาใช้ในการตรวจสอบลำดับเบสของดีเอ็นเอในรูปแบบ Dot blot โดยอาศัยพีเอ็นเอโพรบที่ติดฉลากด้วยไบโอตินร่วมกับปฏิกิริยาการเกิดสีที่เร่งด้วยเอนไซม์ HRP ในงานวิจัยได้ศึกษาอิทธิพลของตัวแปรต่างๆ เพื่อหาภาวะที่เหมาะสมในการตรวจสอบการเกิดการจับยึดระหว่างพีเอ็นเอกับดีเอ็นเออย่างจำเพาะเจาะจง พบว่าแผ่นเมมเบรนที่พัฒนาขึ้นนี้มีประสิทธิภาพดีกว่าไนลอนหรือไนโตรเซลลูโลสเมมเบรนในการใช้งานร่วมกับพีเอ็นเอโพรบเพื่อตรวจวัดดีเอ็นเอในรูปแบบ Dot blot โดยสามารถบอกความแตกต่างของ complementary จาก single mismatched และ non-complementary DNA ได้อย่างชัดเจนภายใต้ non-stringent conditions โดยสามารถตรวจวัดได้ต่ำถึง 10 fmol เมื่อใช้ synthetic DNA เป็นตัวทดสอบ และได้เริ่มนำเทคนิคที่ได้ไปประยุกต์ใช้ในการตรวจสอบดีเอ็นเอที่มาจากตัวอย่างจริง (SNP ของ human *IL-10* promoter และ Interferon gamma gene) ผลที่ได้ยังไม่เป็นที่น่าพอใจนัก เนื่องจากต้องใช้ตัวอย่างในปริมาณมาก ซึ่งอาจเป็นเพราะตัวอย่างจริงอยู่ในสภาพที่เป็นดีเอ็นเอสายคู่ และมีความยาวมากกว่า synthetic oligonucleotide มาก การจับกับพีเอ็นเออาจไม่มีประสิทธิภาพมากนัก จึงอาจต้องหาทางเพิ่มความไวของการตรวจวัดต่อไป เช่นโดยการใช้ปฏิกิริยาพอลิเมอไรเซชันของมอนอเมอร์มีสี เป็นต้น

สรุปกิจกรรมที่ได้ทำเพิ่มเติมในช่วงขยายระยะเวลาโครงการ (1 สิงหาคม 2555 - 31 มกราคม 2556)

กิจกรรมที่ได้ดำเนินการเพิ่มเติมจากที่เคยรายงานมาแล้วคือ การศึกษาการตรวจวัดดีเอ็นเอในรูปแบบ Dot blot โดยใช้พอลิเมอร์ที่มีประจุบวกของ poly(quaternized 2-dimethylaminoethyl methacrylate) ตรึงบน screen printed gold electrode ร่วมกับพีเอ็นเอโพรบที่ติดฉลากด้วยไบโอตินร่วมกับการตรวจวัดการเกิดปฏิกิริยาไฟฟ้าเคมีของไฮโดรควิโนนที่เร่งโดยเอนไซม์ HRP โดยคาดว่าแนวทางนี้จะช่วยเพิ่มขีดจำกัดในการตรวจวัดดีเอ็นเอให้มีประสิทธิภาพกว่าการสังเกตการเกิดสีที่เร่งด้วยเอนไซม์บนแผ่นกระดาษดังที่ได้รายงานไว้แล้วก่อนหน้านี้

โครงการย่อยที่ 4: Surface-functionalized magnetic nanoparticles for immobilization of PNA and DNA

แผนงานตลอดโครงการ

สังเคราะห์และดัดแปลงพื้นผิวของอนุภาคแมกนีไทต์ขนาดนาโนเพื่อให้มีประจุบวกโดยอาศัยการเคลือบด้วยแคตไอออนิกพอลิเมอร์ร่วมกับพอลิเมอร์ที่ชอบน้ำ โดยจะมีการปรับอัตราส่วนของแคตไอออนิกพอลิเมอร์ต่อพอลิเมอร์ที่ชอบน้ำเพื่อให้ได้อนุภาคที่สามารถจับยึดกับดีเอ็นเอซึ่งมีประจุลบได้ดีที่สุด และมีการจับยึดแบบไม่จำเพาะเจาะจงกับพีเอ็นเอซึ่งไม่มีประจุได้น้อยที่สุด และศึกษาการประยุกต์ใช้ระบบดังกล่าวในการตรวจวิเคราะห์ลำดับเบสของดีเอ็นเอ

สรุปกิจกรรมที่ได้ทำจริงตลอดโครงการ

ได้สังเคราะห์สังเคราะห์อนุภาคนาโนแมกนีไทต์จากปฏิกิริยาแตกสลาย $Fe(acac)_3$ ด้วยความร้อน แล้วนำอนุภาคที่ได้มาดัดแปรพื้นผิวให้มีประจุบวกโดยอาศัยปฏิกิริยา ATRP ที่ริเริ่มด้วยหมู่ bromoisobutyryl ที่ตรึงบนพื้นผิวของอนุภาค เพื่อให้เกิดเป็นพอลิเมอร์ร่วมระหว่าง PEGMA และ DEAEMA ที่อัตราส่วนต่างๆ กัน โดยได้ยืนยันการเกิดปฏิกิริยาโดย IR spectroscopy ผลการวิเคราะห์ด้วย TEM แสดงว่าอนุภาคที่ได้มีขนาดประมาณ 6.5 ไมครอน แต่มีการเกาะกลุ่มกันอยู่ค่อนข้างมาก ซึ่งยืนยันโดยการวัดเส้นผ่านศูนย์กลางไฮโดรไดนามิก ได้ค่าอยู่ในช่วง 219 ถึง 457 nm และได้พิสูจน์ว่าอนุภาคที่ได้มีค่าความต่างศักย์พื้นผิวเป็นบวก โดยความเป็นบวกเพิ่มขึ้นตามอัตราส่วนของ DEAEMA ที่เพิ่มขึ้น และสามารถเพิ่มความเป็นบวกได้อีกโดยการทำควอเทอร์ไนซ์ด้วยเมทิลไอโอไดด์ ซึ่งจะส่งผลให้อนุภาคมีการเกาะกลุ่มลดลง โดยอนุภาคที่มีความเป็นบวกมากที่สุดคือที่มีอัตราส่วนโมลระหว่าง PEGMA:DEAEMA เป็น 0:100 ที่ผ่านการควอเตอร์ไนซ์แล้ว ซึ่งมีค่าความต่างศักย์พื้นผิวอยู่ที่ +32 mV และได้ศึกษาความเป็นไปได้เบื้องต้นในการนำอนุภาคที่สังเคราะห์ได้สามารถนำมาใช้เป็นวัสดุดูดซับที่มีประจุบวกสำหรับใช้ร่วมกับ acpcPNA และ

เทคนิคแมสสเปกโตรเมตรีในการตรวจสอบลำดับเบสของดีเอ็นเอ โดยอาศัยหลักการ ion-exchange capture พบว่าอนุภาคที่มีอัตราส่วนของ PEGMA:DEAEMA เป็น 0:100 และ 50:50 ที่ผ่านการควอเทอร์ไนซ์แล้ว ให้ผลใกล้เคียงกันและดีกว่าอนุภาคที่ไม่ได้ผ่านการควอเทอร์ไนซ์ กล่าวคือสามารถบอกความแตกต่างของดีเอ็นเอเป้าหมายที่มีลำดับเบสต่างกันเพียงตำแหน่งเดียวได้ โดยอาศัยเทคนิค ion exchange capture ร่วมกับ MALDI-TOF mass spectrometry อย่างไรก็ตาม วิธีนี้ยังต้องการปริมาณพีเอ็นเอและดีเอ็นเออย่างน้อย 70 pmol ซึ่งยังถือว่าค่อนข้างสูงเมื่อเทียบกับการใช้อนุภาคที่มีประจุบวกทางการค้าเช่น Q-sepharose ที่ใช้ปริมาณดีเอ็นเอได้ต่ำถึง 1 pmol โดยคาดว่าอาจเนื่องมาจากการกระจายตัวของอนุภาคที่ยังไม่ดีนัก และความต่างศักย์พื้นผิวที่ยังเป็นบวกน้อย ผลการศึกษาความสามารถในการดูดจับ DNA ของอนุภาคที่มีอัตราส่วนของ PEGMA:DEAEMA เป็น 0:100 และ 50:50 โดยอาศัยเทคนิคฟลูออเรสเซนส์ได้ค่าเป็น 171 และ 88 pmol ของนิวคลีโอไทด์ต่ออนุภาค 1 mg

สรุปกิจกรรมที่ได้ทำเพิ่มเติมในช่วงขยายระยะเวลาโครงการ (1 สิงหาคม 2555 - 31 มกราคม 2556)

กิจกรรมที่ได้ทำเพิ่มเติมในช่วงเวลาดังกล่าวคือการตรวจสอบลำดับเบสของ DNA ที่เกี่ยวข้องกับการเกิดโรคคือ *K-ras* gene โดยอนุภาคนาโนแมกนีไทท์ที่มีประจุบวก ร่วมกับ acpcPNA 2 ชนิดที่มีลำดับเบสที่สอดคล้องกับ *K-ras* gene แบบ wild type และ mutant เป็นโพรบในการตรวจสอบโดยเทคนิค MALDI-TOF mass spectrometry ผลการทดลองพบว่าการใช้พีเอ็นเอสองโพรบสามารถแยกแยะความแตกต่างระหว่าง wild type และ single-mismatched mutant DNA target ที่เป็นดีเอ็นเอสังเคราะห์ ที่ปริมาณ 70 pmol ได้อย่างชัดเจน

โครงการย่อยที่ 5: Development of label-free electrochemical DNA biosensor based on immobilized PNA probes

แผนงานตลอดโครงการ

เปรียบเทียบภาวะที่เหมาะสมในการตรึงพีเอ็นเอบนผิวอิเล็กโทรดที่เป็นทองโดยใช้อาศัย self-assembled monolayers (SAMs) และการตรึงผ่านชั้นของพอลิเมอร์ เพื่อสร้างอุปกรณ์สำหรับตรวจลำดับเบสของดีเอ็นเอที่มีความว่องไวและความจำเพาะเจาะจงสูงโดยใช้เทคนิค capacitive และ/หรือ impedimetric และใช้อุปกรณ์ดังกล่าวในการตรวจสอบลำดับเบสของดีเอ็นเอจากตัวอย่างจริง

สรุปกิจกรรมที่ได้ทำจริงตลอดโครงการ

โครงการนี้ประกอบด้วยงานวิจัย 2 ส่วน ได้แก่

5.1 ศึกษาการตรึงเพปไทด์นิวคลีอิกแอซิดบนผิวหน้าอิเล็กโทรด

งานวิจัยส่วนแรกนี้เกี่ยวข้องกับการพัฒนาวิธีการตรึงพีเอ็นเอบนผิวหน้าอิเล็กโทรดเพื่อนำมาใช้เป็นดีเอ็นเอไบโอเซ็นเซอร์ผ่านชั้นของ SAM โดยเปรียบเทียบประสิทธิภาพของการตรึง acpcPNA ที่มีลำดับเบสเป็น T9 และเบสผสม 12mer ที่มี Lys ต่ออยู่ตรงปลายด้าน C บน SAM ที่เตรียมจากสารประกอบไทออล 4 ชนิด คือ 3-mercaptopropionic acid (3-MPA), mercaptosuccinic acid (MSA), thioctic acid (TA) และ thiourea (TU) ผ่านการสร้างพันธะเอไมด์ (MPA, MSA และ TA) หรือการเชื่อมขวางด้วยกลูทารัลดีไฮด์ (TU) และได้ศึกษาความยาวและหมู่ฟังก์ชันของ thiol blocking reagent ที่เหมาะสมสำหรับการดัดแปลงผิวอิเล็กโทรดแต่ละชนิด การนำกลับมาใช้ใหม่ได้ของอิเล็กโทรดและความจำเพาะเจาะจงและความว่องไวในการตรวจวัดดีเอ็นเอเป้าหมาย โดยอาศัยเทคนิคคาพาซิทีฟ โดยพบว่าการใช้ blocking thiol ที่มีความยาวเท่ากับ spacer ของสารประกอบไทออลที่ใช้ในการสร้าง SAM รวมกับ Lysine และมีหมู่ฟังก์ชันที่ปลายเป็น OH จะให้ความไวของการวิเคราะห์สูงสุด เซนเซอร์ที่พัฒนาขึ้นมีความเลือกจำเพาะสูงกับดีเอ็นเอเป้าหมาย โดยให้สัญญาณลดลง 75–79%, 76–83% และ 99–100% ในกรณีที่เป็น single mismatched, double mismatched และ non-complementary DNA target ตามลำดับ (perfect discrimination คือ 100%) มีช่วงความเป็นเส้นตรงสูงตั้งแต่ 10^{-8} – 10^{-11} M โดยมีขีดจำกัดของการตรวจวัดอยู่ในระดับ 6─10 pM และอิเล็กโทรดที่เตรียมได้สามารถนำมาใช้ใหม่ได้ไม่ต่ำกว่า 50 ครั้ง ไม่ว่าจะผ่านการตรึงแบบใด

นอกจากนี้ยังได้พัฒนาวิธีการตรึงพีเอ็นเอโพรบ T9 ลงบนผิวหน้าอิเล็กโทรดอีกแบบหนึ่งโดยผ่านชั้นของพอลิเมอร์ที่ไม่นำไฟฟ้า ซึ่งได้จากการทำอิเล็กโตรพอลิเมอไรเซชันของ *o*-phenylenediamine (*o*PD), *p*-phenylenediamine (*p*PD) หรือ tyramine (Ty) ก่อน โดยได้ศึกษาภาวะที่เหมาะสมในการสร้างชั้นของพอลิเมอร์ แล้วจึงตรึงพีเอ็นเอโพรบลงไปโดยใช้กลูทารัลดีไฮด์เป็นตัวเชื่อมขวางระหว่างหมู่อะมิโนของพีเอ็นเอ กับหมู่อะมิโนบนผิวของพอลิเมอร์ ตามด้วยการปิดช่องว่างบนผิวอิเล็กโทรดด้วย blocking thiol พบว่าพีเอ็นเอที่ตรึงบนชั้นของ P*o*PD ให้ช่วงการตอบสนองที่เป็นเส้นตรงตั้งแต่ 10^{-8} – 10^{-11} M และมีขีดจำกัดการตรวจวัด 10 pM ซึ่งใกล้เคียงกับการตรึงผ่าน SAM ส่วนพีเอ็นเอที่ตรึงบนชั้นของ P*p*PD และ Pty ให้ช่วงการตอบสนองที่เป็นเส้นตรงตั้งแต่ 10^{-8} – 10^{-12} M และมีขีดจำกัดการตรวจวัดต่ำถึง 0.2-0.8 pM ซึ่งดีกว่าการตรึงผ่าน SAM และยังสามารถตรึงพีเอ็นเอได้เร็วกว่า (8 นาที เทียบกับ 12–24 ชั่วโมงในวิธีตรึงผ่าน SAM) ความสามารถในการเลือกจำเพาะและการใช้ซ้ำของอิเล็กโทรดที่เตรียมโดยวิธีนี้ใกล้เคียงกับที่เตรียมโดยวิธี SAM

5.2 การพัฒนาอิเล็กโตรเคมิคัลไบโอเซนเซอร์สำหรับตรวจวัดดีเอ็นเอ

งานวิจัยในส่วนที่ 2 เป็นการพัฒนาอิเล็กโทรเคมิคัลไบโอเซนเซอร์สำหรับตรวจวัด DNA โดยอาศัยการตรึงพีเอ็นเอโพรบบนชั้นของพอลิเมอร์ PpPD ที่พัฒนาขึ้นในส่วนที่ 1 โดยเลือกตรึง 11-mer mix base PNA probe Ac-GCTCCGTCCTC-LysNH_2 ที่มีลำดับเบสจำเพาะกับยีน HLA-B* 5801 ซึ่งเกี่ยวข้องกับการแพ้ยาบางชนิด ผลการศึกษาเบื้องต้นกับ synthetic oligonucleotide โดยระบบคาพาซิทิฟแอฟฟินิตีไบโอเซนเซอร์ ให้ที่น่าพอใจ กล่าวคือไบโอเซนเซอร์ที่ได้มีค่าการตอบสนองที่ดีในช่วง 10^{-11} ถึง 10^{-8} M โดยความสามารถในการเลือกจับกับดีเอ็นเอเป้าหมายอย่างจำเพาะเจาะจง กล่าวคือ single และ double mismatched DNA ให้สัญญาณลดลง 53─68% และ 60─73% ตามลำดับ มีความสามารถในการทำซ้ำได้ สามารถเก็บไว้ได้ไม่ต่ำว่า 3 เดือน และใช้ซ้ำได้ไม่ต่ำกว่า 80 ครั้ง ขณะนี้กำลังอยู่ระหว่างการศึกษาสภาวะที่เหมาะสมในการนำไปวิเคราะห์ดีเอ็นเอจากตัวอย่างจริงต่อไป (เป็นความร่วมมือกับรศ.พญ.ณัฏฐิยา หิรัญกาญจน์ หัวหน้าโครงการย่อย 6b)

สรุปกิจกรรมที่ได้ทำเพิ่มเติมในช่วงขยายระยะเวลาโครงการ (1 สิงหาคม 2555 - 31 มกราคม 2556)

สำหรับงานวิจัยส่วนที่ 2 การพัฒนาอิเล็กโตรเคมิคัลไบโอเซนเซอร์สำหรับตรวจวัดดีเอ็นเอโดยอาศัยการตรึงพีเอ็นเอโพรบบนชั้นของพอลิเมอร์ P*p*PD ได้ศึกษาเพิ่มเติมโดยใช้ synthetic DNA ที่มีความยาวมากกว่าโพรบ ซึ่งจะเป็นสถานการณ์ที่สอดคล้องกับการวิเคราะห์ตัวอย่างจริง พบว่าความยาวของส่วน overhang มีผลให้ความไววิเคราะห์ของระบบสูงขึ้นเมื่อส่วน overhang อยู่บนผิวอิเล็กโทรด และได้ศึกษาความจำเพาะเจาะจงของเซนเซอร์กับตัวอย่างจริงคือ HLA-B* 5801 ที่มีลำดับเบสจำเพาะกับโพรบและ HLA-B* 5701 ซึ่งเป็น double-mismatched DNA พบว่าความสามารถในการแยกระหว่างตัวอย่างจริงทั้งสองค่อนข้างต่ำ (%SS ต่ำกว่า 40 %) คาดว่าน่าจะเป็นผลมาจากส่วน overhang ของ double mismatched DNA ที่ทำให้สัญญาณที่วัดได้มีค่าสูง จึงได้ทดลองเติมสารลดความเสถียรของไฮบริด พบว่า acetamide สามารถทำให้เซนเซอร์มีความจำเพาะเจาะจงเพิ่มขึ้นโดยมีค่า % SS สูงขึ้น (49–74 %) งานที่จะทำต่อไปคือการตรวจวิเคราะห์ตัวอย่างจริงจำนวนมากขึ้นเพื่อทดสอบความจำเพาะเจาะจง (specificity) และความไว (sensitivity) ของการตรวจวัดในสถานการณ์จริง ปัญหาที่พบในขณะนี้คือจำเป็นต้องทราบความเข้มข้นของดีเอ็นเอตัวอย่าง ซึ่งอาจไม่สะดวกในทางปฏิบัติ แนวทางแก้ปัญหาคือการใช้พีเอ็นเอสองโพรบ (B*5801 และ B*5701) ร่วมกันในการวิเคราะห์ตัวอย่างเดียวกันเพื่อช่วยแยกแยะความแตกต่างระหว่าง complementary กับ mismatched DNA target คาดว่าเมื่องานเสร็จสมบูรณ์น่าจะได้ผลงานตีพิมพ์เพิ่มอีก 1 เรื่อง

Project 6: Applications of PNA based diagnostics in medical, food and agricultural sciences

แผนงานตลอดโครงการ

งานวิจัยจะแบ่งเป็นสองส่วน ซึ่งจะมีขั้นตอนแรกเหมือนกัน คือการเลือกลำดับเบสของดีเอ็นเอเป้าหมายเพื่อนำมาใช้ในการออกแบบพีเอ็นเอโพรบ ขั้นตอนต่อมาในงานวิจัยส่วนแรกเป็นการพัฒนาระบบพีเอ็นเอเรืองแสงที่มีสมบัติ

การเรืองแสงเปลี่ยนไปตามสถานะการเกิดไฮบริดกับดีเอ็นเอ และนำระบบพีเอ็นเอเรืองแสงนี้ไปประยุกต์ใช้ร่วมกับเทคนิคการเตรียมตัวอย่างดีเอ็นเอที่มีประสิทธิภาพสูง เพื่อตรวจสอบสายพันธุ์ของเชื้อที่ก่อให้เกิดโรค และการปนเปื้อนของสารก่อภูมิแพ้ในอาหารและผลิตภัณฑ์ทางการเกษตร สำหรับงานวิจัยในส่วนที่สองเป็นการพัฒนาระบบพีเอ็นเอร่วมกับเทคนิค MALDI-TOF เพื่อนำไปประยุกต์ใช้ในทางการแพทย์ได้แก่ การศึกษาการเกิดเมทิลเลชันของดีเอ็นเอ และการทำ HLA typing ซึ่งงานทั้งสองส่วนต้องมีการเปรียบเทียบผลที่ได้กับเทคนิคมาตรฐานอื่นๆ เช่น pyrosequencing เพื่อตรวจสอบความแม่นยำของการวิเคราะห์

สรุปกิจกรรมที่ได้ทำจริงตลอดโครงการ

โครงการนี้ได้แยกการดำเนินการออกเป็น 3 ส่วนคือ

6.1 การประยุกต์ใช้พีเอ็นเอในการตรวจวินิจฉัยทางการแพทย์ เกษตร และอาหาร

โครงการนี้มุ่งเน้นการพัฒนาระบบตรวจวิเคราะห์ DNA โดยอาศัยเทคนิค Loop-mediated isothermal amplification (LAMP) เพื่อเพิ่มปริมาณดีเอ็นเอ ร่วมกับพีเอ็นเอโพรบ เพื่อการตรวจหาลำดับเบสของดีเอ็นเอที่เป็นเครื่องหมายของโรค หรือสิ่งบ่งชี้ของลักษณะทางพันธุกรรมที่สนใจจะศึกษา การใช้เทคนิคเพิ่มปริมาณดีเอ็นเอแบบ LAMP มีข้อได้เปรียบเทคนิค PCR คือสามารถทำได้ที่อุณหภูมิเดียว โดยไม่ต้องใช้เครื่อง thermal cycler ที่มีราคาแพง อีกทั้งยังมีอัตราการเพิ่มปริมาณสารพันธุกรรมที่สูงกว่า PCR และมีความจำเพาะเจาะจงสูงกว่าเนื่องจากใช้ไพรเมอร์ที่จำเพาะถึง 6 ตำแหน่ง และการใช้งานร่วมกับพีเอ็นเอน่าจะช่วยเพิ่มความจำเพาะเจาะจงมากขึ้นอีก โดยได้พัฒนาวิธีการขึ้นมาสองรูปแบบคือ 1) การแทนที่แบบ competitive hybridization ของพีเอ็นเอโพรบที่ติดฉลากด้วยสารเรืองแสง และไฮบริไดซ์อยู่กับดีเอ็นเอสายสั้นๆ ที่ติดฉลากด้วยตัวดับแสง (quencher) หรือ 2) การตกตะกอนของอนุภาคขนาดนาโนของโลหะเงินหรือทองที่ขึ้นกับการเกิดไฮบริดระหว่างพีเอ็นเอกับดีเอ็นเอ โดยได้นำไปประยุกต์ใช้กับการตรวจวินิจฉัยดีเอ็นเอทางด้านการแพทย์ เกษตร และอาหาร ได้แก่ 1) การตรวจสอบเชื้อไวรัสไข้หวัดใหญ่สายพันธุ์ใหม่ 2009 (H1N1) ทั้งชนิดธรรมดาและชนิดดื้อต่อยา oseltamivir ซึ่งเกิดจากการกลายพันธุ์ของยีน neuraminidase 2) การตรวจสอบไวรัส Pineapple mealybug wilt-associated virus (PMWaV1 และ PMWaV2) ที่ทำให้เกิดโรคเหี่ยวในสับปะรด 3) การตรวจโรค Chikunkunya 4) การตรวจการสุกแก่ทางสรีระวิทยาผ่านการแสดงออกของยีน AcSUT1 ในสับปะรด และ 5) การตรวจสอบไวรัสที่ทำให้เกิดโรคในกุ้ง ได้แก่ White Spot Syndrome Virus (WSSV), Infectious Hypodermal and Hematopoietic Necrosis Virus (IHHNV), Taura Syndrome Virus (TSV) และ Yellow Head Virus (YHV) ซึ่งในทุกปัญหามีขั้นตอนศึกษาเหมือนกันคือการออกแบบไพรเมอร์ การ optimize และ validate การเพิ่มปริมาณ DNA โดยเทคนิค LAMP ซึ่งถ้าเป็นกรณีของการตรวจสารพันธุกรรมที่มาจากอาร์เอ็นเอ (ปัญหาที่ 3 และ 4) จะมีขั้นตอนการทำ reverse transcription เพิ่มขึ้นมาเพื่อเปลี่ยนอาร์เอ็นเอให้เป็นดีเอ็นเอก่อนการเพิ่มปริมาณด้วย LAMP จากนั้นจึงไฮบริไดซ์กับพีเอ็นเอโพรบที่จำเพาะกับบริเวณใดบริเวณหนึ่งในดีเอ็นเอที่ได้จากการเพิ่มปริมาณโดยเทคนิค LAMP ซึ่งทำได้สองรูปแบบคือการใช้ฉลากเรืองแสง และการตกตะกอนของอนุภาคเงินหรือทองดังที่ได้กล่าวไปแล้ว โดยการตกตะกอนของอนุภาคเงินจะมีต้นทุนต่ำกว่า เนื่องจากใช้ปริมาณโพรบน้อยกว่าและไม่ต้องมีการติดฉลากเรืองแสง และไม่ต้องใช้ร่วมกับดีเอ็นเอโพรบที่ติดตัวดับแสง ซึ่งมีราคาแพง ผลการทดลองเบื้องต้นที่ได้แสดงให้เห็นถึงศักยภาพของการใช้เทคนิค LAMP ร่วมกับพีเอ็นเอโพรบในการตรวจวินิจฉัยลำดับเบสของดีเอ็นเอในลักษณะ point of care service โดยไม่ต้องอาศัยเครื่องมือที่ซับซ้อนและบุคลากรที่มีความชำนาญสูง

6.2 การพัฒนาวิธีการตรวจยีน HLA โดยใช้พีเอ็นเอโพรบ

งานที่วางแผนไว้แต่ต้นคือการใช้พีเอ็นเอในการตรวจสอบชนิดของยีน HLA (Human Leukocyte Antigen) เพื่อแยกความแตกต่างของยีน HLA B*1502 และ HLA B*5801 จากยีน HLA ชนิดอื่นๆ โดย HLA ทั้งสอง type พบมากในคนเอเชียและมีส่วนเกี่ยวข้องกับการแพ้ยาบางชนิด เช่น carbamazepine (B*1502) และ allopurinol (B*5801) โดยในช่วงแรกได้พัฒนาระบบ nested PCR เพื่อเพิ่มปริมาณ DNA ซึ่งพบว่ามีความจำเพาะเจาะจงที่ดี และได้ตีพิมพ์ผลงานวิจัยในส่วนนี้ไปแล้ว และได้นำไปให้บริการแก่คนไข้ ณ โรงพยาบาลจุฬาลงกรณ์ แต่การทำ PCR ดังกล่าวยังมี

ขั้นตอนที่ซับซ้อน ไม่สามารถนำไปใช้งานในภาคสนามได้ จึงมีแนวคิดที่จะเพิ่มปริมาณดีเอ็นเอโดยใช้ PCR ธรรมดา หรือ LAMP แล้วใช้พีเอ็นเอโพรบเพื่อเพิ่มความจำเพาะเจาะจงของการตรวจสอบดีเอ็นเอ โดยเทคนิคฟลูออเรสเซนส์ที่พัฒนาขึ้นในโครงการย่อย 6.1 แต่ก็พบปัญหาว่าไม่สามารถตรวจสอบกับตัวอย่างจริงได้ โดยมีสมมติฐานว่าปัญหาอาจจะเกิดจากการที่ตัวอย่างที่ได้จาก PCR หรือ LAMP เป็น double stranded DNA ซึ่งแตกต่างจาก synthetic oligonucleotide ที่เป็น single stranded DNA จึงได้มีการศึกษาภาวะในการแยกสายดีเอ็นเอใน LAMP หรือ PCR product ออกจากกันก่อนเพื่อให้เกิดการจับกับ PNA ได้อย่างมีประสิทธิภาพ โดยอาศัยเทคนิคเจลอิเล็กโตรโฟรีซิสเพื่อติดตามการจับกันระหว่างพีเอ็นเอโพรบที่ติดฉลากเรืองแสงฟลูออเรสซีนกับดีเอ็นเอที่ได้จากการทำ PCR โดยใช้ยีน intereferon gamma (IFN-g) เป็นกรณีศึกษา และเปรียบเทียบผลระหว่าง single stranded synthetic oligonucleotide และ PCR product โดยได้ศึกษาตัวแปรต่างๆ ได้แก่ อุณหภูมิที่ใช้ในการแยกสายดีเอ็นเอ ลำดับการเติมพีเอ็นเอ เวลาในการทำปฏิกิริยา และการใช้ pseudocomplementary PNA สองสาย เพื่อช่วยในการแยกสายดีเอ็นเอออกจากกัน ผลการทดลองแสดงให้เห็นว่าพีเอ็นเอสามารถจับยึดกับ PCR product ได้ โดยสังเกตได้จากแถบเรืองแสงที่ไม่ตรงกับแถบของพีเอ็นเอในเจล จากความเข้มของแถบนี้สามารถประเมินประสิทธิภาพของการเกิดไฮบริดได้ โดยพบว่าอุณหภูมิ 99 $^{\circ}$C จะมีประสิทธิภาพในการแยกสายดีเอ็นเอได้ดีกว่า 95 $^{\circ}$C และเวลาของการทำไฮบริไดเซชันมีความสำคัญอย่างยิ่ง โดยหากปล่อยพีเอ็นเอที่ไฮบริไดซ์กับดีเอ็นเอที่ผ่านการแยกสายเป็นเวลานานขึ้นจะทำให้ความเข้มของแถบของไฮบริดลดลง คาดว่าเกิดจากการที่ดีเอ็นเอกลับมาเข้าคู่กัน แล้วไล่พีเอ็นเอที่จับอยู่แต่แรกออกไป และการใช้พีเอ็นเอที่เป็น pseudocomplementary กันสองสายเพื่อให้จับที่บริเวณเดียวกันของ PCR product แต่เป็นบนดีเอ็นเอคนละเส้น จะสามารถยับยั้งกระบวนการไล่พีเอ็นเอนี้ได้ แต่ในทุกกรณีพบว่าไม่สามารถทำให้เกิดการเกิดไฮบริไดซ์อย่างสมบูรณ์ได้ แม้จะมีพีเอ็นเอมากเกินพอ และได้พบเพิ่มเติมว่าการทำ asymmetric PCR จะช่วยให้พีเอ็นเอสามารถเข้าจับอย่างสมบูรณ์ และเสถียรอยู่ได้มากกว่า 2 ชั่วโมง โดยใช้พีเอ็นเอเพียงสายเดียว (ไม่ต้องมี pseudocomplementary PNA strand) จากนั้นจึงได้พยายามนำเทคนิคดังกล่าวไปใช้ในการตรวจยีน HLA B*1502 แต่ก็ยังพบปัญหาคือพีเอ็นเอไม่สามารถเข้าจับได้อย่างสมบูรณ์ และไม่พบความแตกต่างระหว่างการทำ PCR แบบปกติและ asymmetric PCR ซึ่งแตกต่างจากในกรณีของยีน IFN-g แสดงว่าประสิทธิภาพของการจับยึดระหว่างพีเอ็นเอกับดีเอ็นเอเป้าหมาย (รวมถึงประสิทธิภาพของการทำ asymmetric PCR ด้วย) น่าจะขึ้นกับลำดับเบสด้วย จึงยังต้องมีการศึกษาในรายละเอียดต่อไป อย่างไรก็ตาม การจับยึดระหว่างพีเอ็นเอกับยีนเป้าหมายเป็นไปอย่างอย่างจำเพาะเจาะจง โดยสามารถบอกความแตกต่างระหว่าง HLA B*1502 กับ HLA ชนิดอื่น ยกเว้น B*1525 ซึ่งมีลำดับเบสตรงกันทุกประการในบริเวณที่มีการจับยึดกับพีเอ็นเอ โดยแผนที่จะทำต่อไปคือการใช้เทคนิค PCR clamping มาช่วยเพิ่มความจำเพาะเจาะจงของการตรวจวัด ซึ่งผลเบื้องต้นแสดงให้เห็นว่าพีเอ็นเอสามารถหยุดการเกิด PCR ได้จริง แต่ประสิทธิภาพของการยับยั้งยังขึ้นกับลำดับเบส จึงต้องมีการ optimize กันเป็นกรณีๆ ไป

6.3 การพัฒนาชุดตรวจกรอง Hemoglobin E โดยอาศัยเทคนิคทางนาโนเทคโนโลยีร่วมกับตัวตรวจจับที่เป็นพีเอ็นเอ

ในงานนี้เป็นการพัฒนาชุดตรวจกรองชนิด strip test โดยอาศัยอนุภาคทองคำขนาดนาโนร่วมกับพีเอ็นเอโพรบในการตรวจวินิจฉัยทางการแพทย์ โดยปัญหาที่เลือกมาเป็นกรณีศึกษาคือการตรวจ Hemoglobin E อันเป็นความผิดปกติของยีนที่ทำให้เกิดสร้างเม็ดเลือดแดงที่ผิดปกติ ทำให้เกิดโรคเบต้าทาลัสซีเมีย ซึ่งพบได้บ่อยในประชากรไทย ซึ่งวิธีการตรวจมาตรฐานคือการใช้สีย้อม DCIP ซึ่งมีโอกาสผิดพลาด และมีขั้นตอนที่ยุ่งยาก มีค่าใช้จ่ายสูง จึงมีแนวคิดที่จะพัฒนาชุดตรวจที่ทำงานในระดับดีเอ็นเอ ตัวงานจะเกี่ยวข้องกับการตรึงพีเอ็นเอโพรบที่จำเพาะกับยีนของ HbE และ Hb ปกติ ซึ่งมีเบสต่างกันเพียงตำแหน่งเดียว โดยอาศัยอันตรกิริยาระหว่างไบโอติน(บนพีเอ็นเอ)กับสเตรปตาวิดินที่เคลือบอยู่บนกระดาษไนโตรเซลลูโลส แล้วนำมาประกอบกับส่วนที่เรียกว่า conjugate pad ซึ่งเป็นตัวดูดซับที่เคลือบด้วยอนุภาคทองคำขนาดนาโนที่ดัดแปรพื้นผิวด้วยดีเอ็นเอโพรบอีกตัวหนึ่งที่จับกับดีเอ็นเอเป้าหมายในอีกบริเวณหนึ่งที่ไม่ใช่บริเวณที่จับกับโพรบ โดยอนุภาคทองคำนี้จะทำหน้าที่เป็นตัวบ่งชี้ว่ามีดีเอ็นเอที่สนใจอยู่ในตัวอย่างหรือไม่ ในการใช้งานจะนำทั้งสองส่วนนี้มาประกอบกัน แล้วหยดตัวอย่างที่เป็นดีเอ็นเอลงไป จากนั้นนำไปแช่ในบัฟเฟอร์ ซึ่งจะพา

ตัวอย่างไปติดกับอนุภาคทองคำ และเคลื่อนที่ไปด้วยกัน จนถึงบริเวณที่ตรึงพีเอ็นเอไว้ หากตัวอย่างมีลำดับเบสที่ตรงกับพีเอ็นเอโพรบ ดีเอ็นเอตัวอย่าง(ที่อยู่บนอนุภาคทองคำ)ก็จะถูกดูดซับไว้ตรงตำแหน่งที่มีการตรึงพีเอ็นเอ และทำให้เกิดแถบสีม่วงที่มองเห็นด้วยตาเปล่า โดยต้องมีการใส่ control ที่เหมาะสมเพื่อควบคุมว่าส่วนของอนุภาคทองคำทำงานได้ถูกต้อง ซึ่งเป็นหลักการเดียวกับที่ใช้ในชุดตรวจการตั้งครรภ์ แต่เป็นการตรวจวัดดีเอ็นเอแทนที่จะเป็นโปรตีน

งานวิจัยเกี่ยวข้องกับการออกแบบพีเอ็นเอและดีเอ็นเอโพรบ การสังเคราะห์อนุภาคทองคำขนาดนาโนและการเชื่อมต่อเข้ากับดีเอ็นเอโพรบ การศึกษาภาวะที่เหมาะสมในการตรวจวัดดีเอ็นเอโดยหลักการดังกล่าว โดยในเบื้องต้นได้ทดสอบกับดีเอ็นเอสังเคราะห์ ซึ่งพบว่ามีการเกิดแถบสีแบบไม่จำเพาะเจาะจง ผู้วิจัยมีสมมติฐานว่าน่าจะเกิดจากการจับยึดระหว่างพีเอ็นเอกับอนุภาคทองคำแบบไม่จำเพาะเจาะจง และสามารถแก้ปัญหาได้โดยการเพิ่มขั้นตอนการเคลือบผิวอนุภาคทองคำด้วย BSA และการเพิ่มฟอร์มาไมด์ลงในบัฟเฟอร์ ซึ่งภายใต้ภาวะดังกล่าวสามารถตรวจสอบดีเอ็นเอสังเคราะห์ได้ผลเป็นที่น่าพอใจ โดยสามารถตรวจวัดได้ต่ำสุดถึง 10 nM โดยมีความจำเพาะเจาะจงที่สูง แต่เมื่อนำไปใช้กับตัวอย่างจริงยังให้ผลไม่แน่นอน และการปรับเปลี่ยนภาวะ เช่น การนำ PCR product ไป purify ก่อน การทำ asymmetric PCR ไม่ทำให้ได้ผลดีขึ้น และยังพบปัญหาแถบสีที่เกิดขึ้นมีความเข้มลดลงเมื่อเวลาผ่านไป จึงยังจำเป็นต้องมีการพัฒนาต่อไปถึงจะสามารถนำไปใช้งานจริงได้

สรุปกิจกรรมที่ได้ทำเพิ่มเติมในช่วงขยายระยะเวลาโครงการ (1 สิงหาคม 2555 - 31 มกราคม 2556)

งานที่ได้มีการดำเนินการเพิ่มเติมในส่วนของการประยุกต์ใช้พีเอ็นเอในการตรวจวินิจฉัยทางการแพทย์ เกษตร และอาหารคือการศึกษาปัจจัยที่เกี่ยวข้องในการออกแบบ fluorescence displacement probe ที่มาจาก acpcPNA รวมถึงความยาวและลำดับเบสของ quencher probe โพรบ และลำดับเบสของ fluorphore labeled PNA probe ที่มีต่ออัตราเร็วของการแทนที่และความจำเพาะเจาะจงต่อดีเอ็นเอเป้าหมาย ผลที่ได้ยังแสดงให้เห็นข้อจำกัดของการออกแบบดังกล่าว กล่าวคือมีอัตราเร็วที่ค่อนข้างช้า และความจำเพาะเจาะจงยังไม่เป็นที่น่าพอใจนัก ขณะนี้กำลังอยู่ระหว่างการศึกษาตัวแปรต่างๆ เพิ่มเติมเพื่อจะปรับปรุงประสิทธิภาพของโพรบดังกล่าวให้ดีกว่าที่เป็นอยู่ นอกจากนี้ยังได้พัฒนาอุปกรณ์ตรวจสอบลำดับเบสของดีเอ็นเออย่างง่ายจากกระดาษกรองโดยใช้พีเอ็นเอโพรบร่วมกับอนุภาคเงินขนาดนาโน และนำไปประยุกต์ในการตรวจสอบ hemeagglutinin (HA) gene จากตัวอย่างที่ได้จากการเพิ่มปริมาณดีเอ็นเอโดยเทคนิค LAMP ผลการทดสอบเบื้องต้นพบว่าอุปกรณ์ดังกล่าวมีความไวของการตรวจสอบเป็น 100% และความจำเพาะเป็น 92.3% (N=29) ซึ่งควรมีการพัฒนาต่อไปอีก

งานในส่วนของการพัฒนาวิธีการตรวจยีน HLA โดยใช้พีเอ็นเอโพรบนั้นได้ปรับปรุงภาวะในการทำไฮบริไดเซชันระหว่างพีเอ็นเอกับดีเอ็นเอตัวอย่างที่ได้จากการทำ PCR โดยการติดตามด้วยเทคนิค gel electrophoresis จนได้ภาวะที่เหมาะสมแล้ว งานที่จะทำต่อไปคือการทดสอบกับตัวอย่างจริง โดยได้เลือกใช้เทคนิคคาพาซิทีฟของโครงการย่อยที่ 5 เนื่องจากเป็นเทคนิคที่ให้ความไวสูงกว่างานอื่นๆ ขณะนี้กำลังอยู่ระหว่างการ optimize ตัวแปรต่างๆ ก่อนที่จะทดสอบกับตัวอย่างจริงต่อไป

งานในส่วนสุดท้ายเป็นการพัฒนาระบบ lateral flow สำหรับตรวจสอบยีนฮีโมโกลบิน E โดยใช้พีเอ็นเอโพรบร่วมกับอนุภาคทองคำขนาดนาโน ซึ่งยังไม่มีความคืบหน้าไปจากเดิมมากนักเนื่องจากปัญหาของการให้สีที่ยังไม่แน่นอน อย่างไรก็ตาม โดยหลักการแล้วสามารถพิสูจน์ว่าระบบดังกล่าวสามารถทำงานได้จริง อย่างน้อยก็กับตัวอย่างที่เป็นดีเอ็นเอสังเคราะห์ ขณะนี้กำลังอยู่ระหว่างการเตรียมเอกสารเพื่อยื่นจดสิทธิบัตร

2. ผลงาน

2.1 ผลงานตีพิมพ์ในวารสารวิชาการนานาชาติ/หนังสือ/สิทธิบัตร

ผลงานได้รับการตีพิมพ์หรือตอบรับให้ตีพิมพ์แล้วจำนวน 20 เรื่อง

(เดือนที่ 1-18)

2.1.1 Taechalertpaisarn, J.; Sriwarom, P.; Boonlua, C.; Yotapan, N.; Vilaivan, C.; Vilaivan, T.

"DNA-, RNA- and self-pairing properties of pyrrolidinyl peptide nucleic acids with (2'*R*,4'*S*)-prolyl-(1*S*,2*S*)-aminocyclopentanecarboxylic acid backbone" *Tetrahedron Lett.* **2010**, *51*, 5822–5826. (IF2011 = 2.652) (เป็น output จากโครงการย่อย 1)

2.1.2 Ananthanawat, C.; Hoven, V. P.; Vilaivan, T.; Su, X. D. “Surface Plasmon Resonance Study of PNA Interactions with Double Stranded DNA” *Biosens. Bioelectron.* **2011**, *26*, 1918–1923. (IF2011 = 5.602) (เป็น output จากโครงการย่อย 1)

2.1.3 Ngamwiriyawong, P.; Vilaivan, T. "Synthesis and nucleic acids binding properties of diasteromeric aminoethylprolyl peptide nucleic acids (aepPNA)" *Nucleosides Nucleotides and Nucleic Acids* **2011**, 30, 97–112. (IF2011 = 0.899) (เป็น output จากโครงการย่อย 1)

(เดือนที่ 19-24)

2.1.4 Vilaivan, C.; Srisuwannaket, C.; Ananthanawat, C.; Suparpprom, C.; Kawakami, J.; Yamaguchi, Y.; Tanaka, Y.; Vilaivan, T. "Pyrrolidinyl peptide nucleic acid with α/β-peptide backbone: A conformationally constrained PNA with unusual hybridization properties" *Artificial DNA: PNA and XNA* **2011**, 2, 50–59. (IF2011 = ยังไม่มี เนื่องจากเป็นวารสารใหม่) (เป็น output จากโครงการย่อย 1)

2.1.5 Boonlua, C.; Vilaivan, C.; Wagenknecht, H.-A.; Vilaivan, T. "5-Pyren-1-yl uracil as a base discriminating fluorophore in pyrrolidinyl peptide nucleic acids" *Chem. Asian J.* **2011**, 6, 3251–3259. (IF2011 = 4.500) (เป็น output จากโครงการย่อย 1)

(เดือนที่ 25-30)

2.1.6 Reenabthue, N.; Boonlua, C.; Vilaivan, C.; Vilaivan, T.; Suparpprom, C. "3-Aminopyrrolidine-4-carboxylic acid as versatile handle for internal labeling of pyrrolidinyl PNA" *Bioorganic Med. Chem. Lett.* **2011**, *21*, 6465–6469. (IF2011 = 2.554) (เป็น output จากโครงการย่อย 1 ร่วมกับผลงานจากทุนวิจัยหลังปริญญาเอกของ ดร.จตุรงค์ สุภาพพร้อม)

2.1.7 Rutnakornpituk, B.; Wichai, U.; Vilaivan, T.; Rutnakornpituk, M. "Surface-initiated atom transfer radical polymerization of poly(4-vinylpyridine) from magnetite nanoparticle" *J. Nanopart. Res.* **2011**, *13*, 6847–6857. (IF2011 = 3.287) (เป็น output จากโครงการย่อย 4)

2.1.8 Rashatasakhon, P.; Vongnam, K.; Siripornnoppakhun, W.; Vilaivan, T.; Sukwattanasinitt, M. "FRET Detection of DNA sequence via electrostatic interaction of polycationic phenylene-ethynylene dendrimer with DNA/PNA hybrid" *Talanta*, **2012**, *88*, 593–598. (IF2011 = 3.794) (เป็น output จากโครงการย่อย 2)

2.1.9 Yuanboonlim, W.; Siripornnoppakhun, W.; Rashatasakhon, P.; Vilaivan, T.; Sukwattanasinitt, M. "Phenylene-ethynylene trication as an efficient fluorescent signal transducer in an aptasensor for potassium ion" *Biosens. Bioelectron.* **2012**, *12*, 17–22. (IF2011 = 5.602) (เป็น output จากโครงการย่อย 2)

2.1.10 Virakul, S.; Kupatawintu, P.; Nakkuntod, J.; Kangwanshiratada, O.; Vilaivan, T.; Hirankarn, N. "A nested sequence specific primer-polymerase chain reaction for the detection of HLA-B*15:02" *Tissue Antigens* **2012**, *79*, 295–301. (IF2011 = 2.588) (เป็น output จากโครงการย่อย 6)

(เดือนที่ 30-36)

2.1.11 Mansawat, W.; Vilaivan, C.; Balázs, A.; Aitken, D.; Vilaivan, T. "Pyrrolidinyl peptide nucleic acid homologues: Effect of ring size on hybridization properties" *Org. Lett.* **2012**, *14*, 1440–1443. (IF2011 = 5.862) (เป็น output จากโครงการย่อย 1)

2.1.12 Mansawat, W.; Boonlua, C.; Siriwong, K.; Vilaivan, T. "Clicked polycyclic aromatic hydrocarbon as a hybridization-responsive fluorescent artificial nucleobase in pyrrolidinyl peptide nucleic acids" *Tetrahedron.* **2012**, *68*, 3988–3995. (IF2011 = 3.025) (เป็น output จากโครงการย่อย 1)

2.1.13 Thipmanee, O.; Samanman, S.; Sankoh, S.; Numnuam, A.; Limbut, W.; Kanatharana, P.; Vilaivan, T.; Thavarungkul, P. "Label-free capacitive DNA sensor using immobilized PNA probe: Effect of the length and terminated head group of blocking thiols" *Biosens. Bioelectron.* **2012**, *38*, 430–435. (IF2011 = 5.602) (เป็น output จากโครงการย่อย 5)

2.1.14 Sezi, S.; Varghese, R.; Vilaivan, T.; Wagenknecht, H.-A. "Conformational control of dual emission by pyrrolidinyl PNA–DNA hybrids" *ChemistryOpen* **2012**, *1*, 173–176. (IF2011 = ยังไม่มี เนื่องจากเป็นวารสารใหม่) (เป็น output จากโครงการย่อย 1)

(เดือนที่ 37-42)

2.1.15 Siripornnoppakhun, W.; Niamnont, N.; Krumsri, A.; Tumcharern, G.; Vilaivan, T.; Rashatasakhon, P.; Thayumanavan, S.; Sukwattanasinitt, M. "Inclusion complexes between amphiphilic phenyleneethynylene fluorophores and cyclodextrins in aqueous media" *J. Phys. Chem. B* **2012**, *116*, 12268–12274. (IF2011 = 3.696) (เป็น output จากโครงการย่อย 2)

2.1.16 Laopa, P.S.; Vilaivan, T.; Hoven, V. P. "Positively charged polymer brushes-functionalized filter paper for DNA sequence determination following Dot Blot hybridization employing pyrrolidinyl peptide nucleic acid probe" *Analyst* **2013**, *138*, 269–277. (IF2011 = 4.230) (เป็น output จากโครงการย่อย 3)

2.1.17 Janrungroatsakul, W.; Vilaivan, T.; Vilaivan, C.; Watchasit, S.; Suksai, C.; Ngeontae, W.; Aeungmaitrepirom, W.; Tuntulani, T. "New calix[4]arene derivatives as ionophores in polymeric membrane electrodes for Ag(I): Comparative selectivity studies and detection of DNA hybridization" *Talanta* **2013**, *105*, 1–7. (IF2011 = 3.794) (เป็น output จากโครงการย่อย 1 ร่วมกับทุนเมธีวิจัยอาวุโสของ ศ.ดร.ธวัชชัย ตันฑุลานิ รหัสโครงการ RTA5380003)

2.1.18 Sankoh, S.; Samanman, S.; Thipmanee, O.; Numnuam, A.; Limbut, W.; Kanatharana, P.; Vilaivan, T.; Thavarungkul, P. “A comparative study of a label-free DNA capacitive sensor using a pyrrolidinyl peptide nucleic acid probe immobilized through polyphenylenediamine and polytyramine non-conducting polymers” *Sens. Actuator B.* **2013**, *177*, 543–554. (IF2011 = 3.898) (เป็น output จากโครงการย่อย 5)

2.1.19 Vilaivan, C.; Srinarang, W.; Yotapan, N.; Mansawat, W.; Boonlua, C.; Kawakami, J.; Vilaivan, T. "Specific recognition of cytosine by hypoxanthine in pyrrolidinyl peptide nucleic acids" *Org. Biomol. Chem.* **2013**, DOI: 10.1039/C3OB27129C (IF2011 = 3.696) (เป็น output จากโครงการย่อย 1)

2.1.20 Theppaleak, T.; Rutnakornpituk, B.; Wichai, U.; Vilaivan, T.; Rutnakornpituk, M. "Magnetite nanoparticle with positively charged surface for immobilization of PNA and DNA" *J. Biomed. Nanotechnol.* **2013**, accepted (IF2011 = 4.216) (เป็น output จากโครงการย่อย 4)

ผลงานที่ submit ไปแล้วอยู่ระหว่างรอผล 1 เรื่อง

2.1.21 Ditmangklo, B.; Boonlua, C.; Suparpprom, C.; Vilaivan, T. "Sequential reductive alkylation-click chemistry for on-solid-support modification of pyrrolidinyl peptide nucleic acid" (เป็น output จากโครงการย่อย 1)

ผลงานที่กำลังอยู่ระหว่างร่างต้นฉบับเพื่อส่งตีพิมพ์จำนวน 3 เรื่อง

2.1.22 Meebungpraw, J.; Vilaivan, T.; Kiatkamjornwong, S.; Hoven, V.P. "Determination of DNA sequences using peptide nucleic acid in combination with chitosan particles by MALDI-TOF mass spectrometry" (เป็น output จากโครงการย่อย 3 ร่วมกับโครงการ Novel Research and Development in Green Polymer Materials and Their Applications – RTA5080004 ของ ศ.ดร.สุดา เกียรติกำจรวงศ์)

2.1.23 Taboonpong, K.; Vilaivan, T.; Hoven, V. P. "Blackberry-like particles assembled from fluorescent-labeled amphiphilic chitosan: Preparation and their potential for bioimaging" (เป็น output จากโครงการย่อย 3)

2.1.24 Theppaleak, T.; Rutnakornpituk, M.;, Wichai, U.; Vilaivan, T.; Rutnakornpituk, B. “The use of anion exchanged nanosolid support of magnetic nanoparticle in combination with PNA probe for DNA sequence analysis” (เป็น output จากโครงการย่อย 4)

2.2 ผลงานตีพิมพ์ในวารสารวิชาการในประเทศ

ไม่มี

2.3 หนังสือ/สิทธิบัตร

(ยื่นจด)

2.3.1 ปิยะศักดิ์ ชอุ่มพฤกษ์, ธีรยุทธ วิไลวัลย์ “อนาล็อกดีเอ็นเอสังเคราะห์และโอลิโกนิวคลีโอไทด์สังเคราะห์เพื่อการตรวจสารพันธุกรรมของไวรัสโรคเหี่ยวสับปะรดชนิดพีอ็มดับเบิลยูเอวี (PMWaV)1 และ 2 และวิธีตรวจสอบสารพันธุกรรม“ คำขอรับสิทธิบัตรการประดิษฐ์ เลขที่ 1201004109 ยื่นเมื่อ 14 สิงหาคม 2555 (เป็น output จากโครงการย่อย 6)

(อยู่ระหว่างดำเนินการ)

2.3.2 ธีระเดช ขมหวาน, อมรพันธุ์ เสรีมาศพันธุ์, ธีรยุทธ วิไลวัลย์, ณัฏฐิยา หิรัญกาญจน์ “ชุดตรวจคัดกรองโรคธาลัสซีเมียชนิด Hemoglobin E ที่ใช้ตัวตรวจจับที่เป็น PNA ในชุดตรวจวินิจฉัยโรค“ กำลังอยู่ระหว่างดำเนินการ (เป็น output จากโครงการย่อย 6)

2.4 ความก้าวหน้าในการสร้างทีมวิจัย

ได้สร้างทีมนักวิจัยระดับปริญญาเอกที่เป็นอาจารย์ในสถาบันอุดมศึกษาจานวน 16 คนที่มีความสนใจร่วมกันในการพัฒนาและใช้ประโยชน์จากพีเอ็นเอ โดยหัวหน้าโครงการได้พบปะเพื่อสอบถามความก้าวหน้าของโครงการวิจัยและปัญหา-อุปสรรคอย่างสม่าเสมอ ทั้งในรูปแบบตัวต่อตัวและการใช้อีเมล์ รายนามของนักวิจัยผู้ร่วมโครงการมีดังนี้

1. รศ.ดร.ธีรยุทธ วิไลวัลย์ (Assoc. Prof. Dr. Tirayut Vilaivan) หัวหน้าโครงการ
   สังกัด ภาควิชาเคมี คณะวิทยาศาสตร์ จุฬาลงกรณ์มหาวิทยาลัย
   โทรศัพท์ 022187627 ext 101 E-mail vtirayut@chula.ac.th
2. อ.ดร.จตุรงค์ สุภาพพร้อม (Dr. Chaturong Suparpprom) ผู้ร่วมวิจัย
   สังกัด ภาควิชาเคมี คณะวิทยาศาสตร์ มหาวิทยาลัยนเรศวร โครงการย่อยที่ 1
   โทรศัพท์ 055963462 E-mail chaturongs@nu.ac.th
3. อ.ดร.ช่อลัดดา ศรีสุวรรณเกศ (Dr. Choladda Srisuwannaket) ผู้ร่วมวิจัย
   สังกัด ภาควิชาเคมี คณะวิทยาศาสตร์ มหาวิทยาลัยพระจอมเกล้าธนบุรี โครงการย่อยที่ 1
   โทรศัพท์ 024709556 E-mail choladda.sri@kmutt.ac.th
4. รศ.ดร.มงคล สุขวัฒนาสินิทธิ์ (Assoc. Prof. Dr. Mongkol Sukwattanasinitt) ผู้ร่วมวิจัย
   สังกัด ภาควิชาเคมี คณะวิทยาศาสตร์ จุฬาลงกรณ์มหาวิทยาลัย โครงการย่อยที่ 2

โทรศัพท์ 022187620 E-mail smongkol@chula.ac.th

5. รศ.ดร.วรวีร์ โฮเว่น (Assoc. Prof. Dr. Voravee Hoven) ผู้ร่วมวิจัย
สังกัด ภาควิชาเคมี คณะวิทยาศาสตร์ จุฬาลงกรณ์มหาวิทยาลัย โครงการย่อยที่ 3
โทรศัพท์ 022187627 ext 102 E-mail vipavee.p@chula.ac.th

6. รศ.ดร.เมธา รัตนากรพิทักษ์ (Assoc. Prof. Dr. Metha Rutnakornpituk) ผู้ร่วมวิจัย
สังกัด ภาควิชาเคมี คณะวิทยาศาสตร์ มหาวิทยาลัยนเรศวร โครงการย่อยที่ 4
โทรศัพท์ 055963464 E-mail methar@nu.ac.th

7. อ.ดร.บุญจิรา บุญทา (Dr. Boonjira Boontha) ผู้ร่วมวิจัย
สังกัด ภาควิชาเคมี คณะวิทยาศาสตร์ มหาวิทยาลัยนเรศวร โครงการย่อยที่ 4
โทรศัพท์ 055963466 E-mail b_boonjira@hotmail.com

8. อ.ดร.อุทัย วิชัย (Dr. Uthai Wichai) ผู้ร่วมวิจัย
สังกัด ภาควิชาเคมี คณะวิทยาศาสตร์ มหาวิทยาลัยนเรศวร โครงการย่อยที่ 4
โทรศัพท์ 055963466 E-mail uthaiw@nu.ac.th

9. รศ.ดร.ปณต ถาวรังกูร (Assoc. Prof. Dr. Panote Thavarungkul) ผู้ร่วมวิจัย
สังกัด ภาควิชาฟิสิกส์ คณะวิทยาศาสตร์ มหาวิทยาลัยสงขลานครินทร์ โครงการย่อยที่ 5
โทรศัพท์ 074288753 E-mail panote.t@psu.ac.th

10. รศ.ดร.เพริศพิชญ์ คณาธารณา (Assoc. Prof. Dr. Proespichaya Kanatharana) ผู้ร่วมวิจัย
สังกัด ภาควิชาเคมี คณะวิทยาศาสตร์ มหาวิทยาลัยสงขลานครินทร์ โครงการย่อยที่ 5
โทรศัพท์ 074288420 E-mail proespichaya.k@psu.ac.th

11. อ.ดร.วรากร ลิ่มบุตร (Dr. Warakorn Limbut) ผู้ร่วมวิจัย
สังกัด ภาควิชาวิทยาศาสตร์ประยุกต์ คณะวิทยาศาสตร์ มหาวิทยาลัยสงขลานครินทร์ โครงการย่อยที่ 5
โทรศัพท์ 074288563 E-mail warakorn.l@psu.ac.th

12. อ.ดร.อาภรณ์ นุมน่วม (Dr. Apon Numnuam) ผู้ร่วมวิจัย
สังกัด ภาควิชาเคมี คณะวิทยาศาสตร์ มหาวิทยาลัยสงขลานครินทร์ โครงการย่อยที่ 5
โทรศัพท์ 074288457 E-mail apon.n@psu.ac.th

13. ผศ.ดร.ปิยะศักดิ์ ชะอุ่มพฤกษ์ (Assist. Prof. Dr. Piyasak Chaumpluk) ผู้ร่วมวิจัย
สังกัด ภาควิชาพฤกษศาสตร์ คณะวิทยาศาสตร์ จุฬาลงกรณ์มหาวิทยาลัย โครงการย่อยที่ 6
โทรศัพท์ 022185494 E-mail piyasakcha@gmail.com

14. รศ.พญ.ดร.ณัฏฐิยา หิรัญกาญจน์ (Assoc. Prof. Dr. Nattiya Hirankarn) ผู้ร่วมวิจัย
สังกัด ภาควิชาจุลชีววิทยา คณะแพทยศาสตร์ จุฬาลงกรณ์มหาวิทยาลัย โครงการย่อยที่ 6
โทรศัพท์ 022564132 E-mail fmednpt@md.chula.ac.th

15. อ.นพ.ดร.อมรพันธ์ เสรีมาศพันธ์ (Dr. Amornpun Sereemaspun) ผู้ร่วมวิจัย
สังกัด ภาควิชากายวิภาคศาสตร์ คณะแพทยศาสตร์ จุฬาลงกรณ์มหาวิทยาลัย โครงการย่อยที่ 6
โทรศัพท์ 022564281 E-mail amornpun.s@chula.ac.th

16. ผศ.ดร.ไพฑูรย์ รัชตะสาคร (Assist. Prof. Dr. Paitoon Rashtaskon) ผู้ร่วมวิจัย
สังกัด ภาควิชาเคมี คณะวิทยาศาสตร์ จุฬาลงกรณ์มหาวิทยาลัย โครงการย่อยที่ 2
โทรศัพท์ 022187620 E-mail paitoon.r@chula.ac.th

2.5 การนำผลจากโครงการไปใช้ประโยชน์

2.5.1 มีการนำวิธี A Nested Sequence Specific Primer-Polymerase Chain Reaction for the detection of HLA-B*15:02 ที่รายงานใน Tissue Antigens 2012 (ผลงานลำดับที่ 2.1.10) มาใช้ให้บริการที่โรงพยาบาลจุฬา โดยอยู่ในแบบฟอร์มใบส่งตรวจของโรงพยาบาล รหัส MI149 (HLA-B*1502) ในปี 2554 มีส่งตรวจทั้งหมด 169 ราย

3. กิจกรรมอื่นที่เกี่ยวข้อง ได้แก่

3.1 ผลงานอื่นๆ เช่นการไปเสนอผลงาน การได้รับเชิญไปเป็นวิทยากร การได้รับรางวัล

3.1a การเสนอผลงานระดับนานาชาติ

(เดือนที่ 1-6)

3.1a.1 Ananthanawat, C.; Boontha, B.; Korkaew, P.; Hoven, V.; Vilaivan, T. "Pyrrolidinyl peptide nucleic acids as probes for DNA sensor applications", The 4th International Conference on Cutting-Edge Organic Chemistry in Asia, November 29 - December 3, 2009, Chulabhorn Research Institute Conference Center, Bangkok, Thailand. (oral, invited lecture)

3.1a.2 Vilaivan, T. "β-Pyrrolidinyl peptide nucleic acids: Synthesis and applications as probes for DNA sequence analysis" The 5th Mathematics and Physical Sciences Graduate Congress, December 7-9, 2009, Bangkok, Thailand. (oral, invited lecture)

3.1a.3 Vilaivan, T. "Pyrrolidinyl peptide nucleic acids with unusual pairing properties as potential antigene agents" The Second China-Thailand Joint Workshop on Natural Products and Drug Discovery, November 25-29, 2009, Cape Panwa Hotel, Phuket, Thailand. (oral, invited lecture)

3.1a.4 Vilaivan, T. "Synthesis and pairing properties of pyrrolidinyl peptide nucleic acid: Beyond PNA.DNA duplexes", Pure and Applied Chemistry International Conference 2010 (PACCON 2010), January 21-23, 2010, Sunee Grand Hotel, Ubon Ratchathani, Thailand. (oral, invited lecture)

3.1a.5 Taechalertpaisarn, J.; Sriwarom, P.; Vilaivan, C.; Vilaivan T. "Synthesis and DNA binding properties of (2R,4S) pyrrolidinyl peptide nucleic acid", Pure and Applied Chemistry International Conference 2010 (PACCON 2010), January 21-23, 2010, Sunee Grand Hotel, Ubon Ratchathani, Thailand. (poster)

3.1a.6 Donraman, N., Ekgasit, S., Vilaivan, T., Poovorawan, Y., Chaumpluk, P. "Rapid detection of oseltamivir resistant mutation at amino acid residue 274 of novel 2009 Human Influenza A Virus (H1N1) based on blue silver nanoparticle", Pure and Applied Chemistry International Conference 2010 (PACCON 2010), January 21-23, 2010, Sunee Grand Hotel, Ubon Ratchathani, Thailand. (oral)

(เดือนที่ 7-12)

3.1a.7 Meebungpraw, J.; Vilaivan, T.; Kiatkamjornwong, S.; Hoven, V. P. "Determination of DNA sequences using peptide nucleic acid in combination with chitosan particles by MALDI-TOF mass spectrometry" The 11th Pacific Polymer Conference, December 6-10, 2009, Cairns, Australia (poster). (เป็นผลงานร่วมกับโครงการ Novel Research and Development in Green Polymer Materials and Their Applications – RTA5080004 ของ ศ.ดร.สุดา เกียรติกำจรวงศ์)

3.1a.8 Ananthanawat, C.; Hoven, V. P; Vilaivan, T.; Su, X. D. "Studying PNA interactions with duplex DNA using surface plasmon resonance technique" Biosensors 2010, May 26-28, 2010, Glasgow, United Kingdom, (oral)

3.1a.9 Srikaenjan, P.; Vilaivan, T.; Hoven, V. P. "Enzymatic amplified colorimetric detection of DNA following “Dot Blot” format employing filter paper functionalized with quaternized polymer brushes and peptide nucleic acid probe" Biosensors 2010, May 26-28, 2010, Glasgow, United Kingdom (poster)
(เดือนที่ 12-18)
3.1a.10 Reenabthue, N.; Vilaivan, T.; Suparpprom, C. "Synthesis and nucleic acid binding properties of novel pyrrolidinyl peptide nucleic acid carrying 3-aminopyrrolidine-4-carboxylic acid spacer" Pure and Applied Chemistry International Conference 2011 (PACCON 2011), January 5-7, 2011, Miracle Grand Hotel, Bangkok, Thailand. (poster)
3.1a.11 Vongnam, K.; Vilaivan, T.; Sukwattanasinitt, M.; Rashtasakhon, P. "Anionic water soluble terphynylene diethynylene fluorophores" Pure and Applied Chemistry International Conference 2011 (PACCON 2011), January 5-7, 2011, Miracle Grand Hotel, Bangkok, Thailand. (poster)
3.1a.12 Rutnakornpituk, M.; Inpotha, T.; Rutnakornpituk, B.; Wichai, U.; Vilaivan, T. "Synthesis of poly(4-vinylpyridine) via atom transfer radical polymerization (ATRP) from surface of magnetite nanoparticle" Pure and Applied Chemistry International Conference 2011 (PACCON 2011), January 5-7, 2011, Miracle Grand Hotel, Bangkok, Thailand. (poster).
3.1a.13 Akkahat, P.; Mekboonsonglarp, W.; Vilaivan, T.; Kiatkamjornwong, S.; Hoven, V. P. "Using poly(acrylic acid) brushes as SPR precursor layer for DNA sensor" The 59th SPSJ Symposium on Macromolecules, September 15-17, 2010, Sapporo, Japan, Poster.
3.1a.14 Hoven, V. P.; Akkahat, P.; Srikaenjan, P.; Vilaivan, T.; Kiatkamjornwong, S. "The power of polymer brushes in biosensing applications" The 7th International Symposium on Advanced Materials in Asia-Pacific (7th ISAMAP) and JAIST International Symposium on NanoTechnology 2010 (NT2010), September 30 – October 1, 2010, Ishikawa High Tech Center, Ishikawa, Japan, Invited presentation.
3.1a.15 Booranabunyat, N.; Hoven, V. P. "Quaternized chitosan particles prepared by self assembly of amphiphilic chitosan" The 7th International Symposium on Advanced Materials in Asia-Pacific (7th ISAMAP) and JAIST International Symposium on NanoTechnology 2010 (NT2010), September 30 – October 1, 2010, Ishikawa High Tech Center, Ishikawa, Japan, Poster.
3.1a.16 Sae-ung, P.; Meebungpraw, J.; Tumcharern, G.; Vilaivan, V.; Kiatkamjornwong, S.; Hoven, V. P. "Featuring biosensing applications of chitosan" Pure and Applied Chemistry International Conference 2011 (PACCON 2011), January 5-7, 2011, Miracle Grand Hotel, Bangkok, Thailand. (oral, invited presentation)
(เป็นผลงานร่วมกับโครงการ Novel Research and Development in Green Polymer Materials and Their Applications – RTA5080004 ของศ.ดร.สุดา เกียรติกำจรวงศ์)
3.1a.17 Virakul, S.; Kupatawintu, P.; Reantragoon, R.; Nakkuntod, J.; Kangwanshiratada, O.; Hirankarn, N. "A simple nested sequence specific primer-polymerase chain reaction for HLA-B*1502" The 14th International Congress of Immunology, August 12, 2010, Kobe, Japan. (poster)
(เดือนที่ 19-24)
ไม่มี
(เดือนที่ 25-30)

3.1a.18 Mansawat, W.; Boonlua, C.; Vilaivan, C.; Vilaivan, T. "Polycyclic aromatic hydrocarbons as fluorescent universal bases in pyrrolidinyl peptide nucleic acids", 14th Asian Chemical Congress 2011 (14ACC), 5 – 8 September 2011, QSNCC, Bangkok, Thailand. (poster)

3.1a.19 Siripornnoppakhun, W.; Niamnonth, N.; Rashtasakhon, P.; Vilaivan, T.; Sukwattanasinitt, M. "Water soluble polycationic dendritic fluorophores for CMC determination and DNA detection", 14th Asian Chemical Congress 2011 (14ACC), 5 – 8 September 2011, QSNCC, Bangkok, Thailand. (oral)

3.1a.20. Laopa, P.S.; Vilaivan, T.; Hoven, V. P. "Detection of DNA following “Dot Blot” format employing filter paper functionalized with quaternized polymer brushes and peptide nucleic acid probe", 14th Asian Chemical Congress 2011 (14ACC), 5 – 8 September 2011, QSNCC, Bangkok, Thailand. (oral)

3.1a.21 Booranabanyat, N.; Vilaivan, T.; Hoven, V.P. "Quaternized chitosan particles prepared by self assembly of amphiphilic chitosan", 14th Asian Chemical Congress 2011 (14ACC), 5 – 8 September 2011, QSNCC, Bangkok, Thailand. (oral)

3.1a.22. Thipmanee, O.; Samanman, S.; Sankoh, S.; Numnuam, A.; Limbut, W.; Kanatharana, P.; Vilaivan, T.; Thavarangkul, P. "Effect of blocking reagents on the capacitive detection of PNA-DNA hybridization", 14th Asian Chemical Congress 2011 (14ACC), 5 – 8 September 2011, QSNCC, Bangkok, Thailand. (poster)

3.1a.23 Ditmangklo, B.; Suparpprom, C.; Vilaivan, T. "Synthesis and optical properties of internally thiazole orange-labeled pyrrolidinyl peptide nucleic acid" The 6th Pure and Applied Chemistry International Conference 2012 (PACCON2012), 11th-13th January 2012, The Empress Convention Center, Chiang Mai, Thailand. (poster)

3.1a.24 Yuanboonlim, W.; Siripornnoppakhun, W.; Rashatasakhon, P.; Vilaivan, T.; Sukwattanasinitt, M. "A polycationic phenylene-ethynylene as a fluorescent transducer in an aptasensor for potassium ion" The 6th Pure and Applied Chemistry International Conference 2012 (PACCON2012), 11th-13th January 2012, The Empress Convention Center, Chiang Mai, Thailand. (poster)

3.1a.25 Taboonpong, K.; Vilaivan, T.; Hoven, V. P. "Blackberry-like particles assembled from fluorescent-labeled quaternized amphiphilic chitosan" The 6th Pure and Applied Chemistry International Conference 2012 (PACCON2012), 11th-13th January 2012, The Empress Convention Center, Chiang Mai, Thailand. (oral)

3.1a.26 Laopa, P.; Vilaivan, T.; Hoven, V. P. "Development of signal amplification method assisted by polymerization for dna detection" The 6th Pure and Applied Chemistry International Conference 2012 (PACCON2012), 11th-13th January 2012, The Empress Convention Center, Chiang Mai, Thailand. (poster)

3.1a.27 Theppaleak, T.; Rutnakornpituk, B.; Wichai, U.; Vilaivan, T.; Rutnakornpituk, M. "Surface functionalization of magnetite nanoparticle with polycation and its bioconjugation" The 6th Pure and Applied Chemistry International Conference 2012 (PACCON2012), 11th–13th January 2012, The Empress Convention Center, Chiang Mai, Thailand. (oral)

3.1a.28. Sankoh, S.; Thipmanee, O.; Samanman, S.; Limbut, W.; Numnuam, A.;Kanatharana, P.; Vilaivan, T.; Thavarungkul, P. "The chain length effect of blocking reagent on the capacitive detection of pna-dna hybridization" The 6th Pure and Applied Chemistry International Conference 2012 (PACCON2012), 11th-13th January 2012, The Empress Convention Center, Chiang Mai, Thailand. (poster)

(เดือนที่ 31-36)

3.1a.29 Aitken, D.J.; Balás, A.; Mansawat, W.; Vilaivan, C.; Vilaivan, T. "Cyclobutane β-amino-acid–proline PNA: A ring size effect?" Bordeaux 2012 Symposium on Foldamers, 30th January–2nd February 2012, European Institute of Chemistry and Biology Bordeaux-Pessac, France. (poster)

3.1a.30 Virakul, S.; Kupatawintu, P.; Chaumpluk, P.; Vilaivan, T.; Hirankarn, N. "Loop-mediated isothermal amplification as a screening test for HLA-b*57:01 and 58:01 in drug hypersensitivity prediction" The Joint 16th International HLA and Immunogenetics Workshop, 26th European Federation for Immunogenetics Conference and 23rd British Society of Histocompatibility and Immunogenetics Conference, 31st May-3rd June, 2012 Liverpool, U.K. (Abstract published as: Virakul, S.; Kupatawintu, P.; Chaumpluk, P.; Vilaivan, T.; Hirankarn, N. "Loop-mediated isothermal amplification as a screening test for HLA-b*57:01 and 58:01 in drug hypersensitivity prediction" *Tissue Antigens* **2012**, *79*, 569-570.)

3.1a.31 Taboonpong, K.; Vilaivan, T.; Hoven, V. P. "Blackberry-like particles assembled from fluorescent-labeled quaternized amphiphilic chitosan: Preparation and their potential for bioimaging" The 44th International Symposium on Macromolecules-IUPAC World Polymer Congress (MACRO 2012), 24th–29th June 2012, Virginia Polytechnic Institute and State University, Blacksburg, Virginia, USA (Oral).

3.1a.32 Chaumpluk, P.; Chaiprasart, P.; Vilaivan, T. "Postharvest non-destructive determination of fruits: A model on fruit maturity assay via biosensor based on colorimetric change of gold nanoparticles" *Acta Horticulturae* **2012**, *945*, 205-212. (proceedings)

(เดือนที่ 37-42)

3.1a.33 Siripornnoppakhun, W.; Rashatasakhon, P.; Sukwattanasinitt, M. “Cyclodextrins discrimination by tricationic phenylene-ethynylene fluorophore” The 6th Pure and Applied Chemistry International Conference 2012 (PACCON2012), 11th-13th January 2012, The Empress Convention Center, Chiang Mai, Thailand. (oral)

3.1a.34 Taboonpong, K.; Sangpech, N.; Palaga, T.; Vilaivan, T.; Hoven, V. P. “Cytocompatibility and cellular uptake of blackberry-like particles assembled from fluorescent-labeled quaternized chitosan” The 8th Mathematics and Physical Science Graduate Congress, 8th–10th December 2012, Faculty of Science, Chulalongkorn University, Thailand. (poster)

3.1a.35 Sae-ung, P.; Tumcharern, G.; Vilaivan, T.; Hoven, V. P. “Functional polymer-stabilized gold nanoparticles: Preparation and peptide nucleic acid immobilization” The 8th Mathematics and Physical Science Graduate Congress, 8th–10th December 2012, Faculty of Science, Chulalongkorn University, Thailand. (poster)

3.1a.36 Vilaivan, T.; Ditmangklo, B.; Boonlua, C. "Internally-labeled pyrrolidinyl peptide nucleic acids as hybridization responsive fluorescence probes for DNA sequence detection" The 7th International Conference on Cutting-Edge Organic Chemistry in Asia (ICCEOCA-7), 11-14 Dec 2012, Nanyang Technological University, SINGAPORE. (oral)

3.1a.37 Jampasa, S.; Wonsawat, W.; Vilaivan, T.; Chailapakul, O. "Peptide nucleic acid probe for electrochemical detection of human papiloma virus DNA type 16" The 7th Pure and Applied Chemistry International Conference 2013 (PACCON2013), 23rd-25th January 2013, The Tide Resort, Bangsaen Beach, Thailand. (oral)

3.1b การเสนอผลงานระดับชาติ

(เดือนที่ 1-6)

3.1b.1 Srinarang, W.; Boonlua, C.; Yothapan, N.; Vilaivan, C.; Vilaivan, T. "Synthesis of pyrrolidinyl peptide nucleic acid (PNA) carrying universal base" The 35th Congress on Science and Technology of Thailand (STT35), Oct 15-17, 2009, Bangsaen, Chonburi. (poster)

3.1b.2 Boontha, B.; Reiser, O.; Vilaivan, T. "Synthesis of novel peptide nucleic acids bearing beta-2-aminocyclopropane carboxylic acid spacer" The 35th Congress on Science and Technology of Thailand (STT35), Oct 15-17, 2009, Bangsaen, Chonburi. (poster)

(เดือนที่ 7-12)

ไม่มี

(เดือนที่ 12-18)

3.1b.3 Boonlua, C.; Vilaivan, C.; Vilaivan, T. "Hybridization responsive fluorescent pyrrolidinyl peptide nucleic acid probes" The 36th Congress on Science and Technology of Thailand (STT36), Oct 26-28, 2010, BITEC, Bangkok. (oral)

3.1b.4 Booranabunyat, N.; Hoven, V. P. "Quaternized chitosan particles prepared by self- assembly of amphiphilic chitosan" The 5th National Chitin-Chitosan Conference, August 26-27, 2010, Miracle Grand Hotel, Bangkok. (oral)

3.1b.5 Virakul, S.; Nakkuntod, J.; Kupatawintu, P.; Kangwanshiratada, O.; Paiboonkasarp, S.; Hirankarn, N. "Detection of HLA-B*5801 by in-house PCR-SSP" The 11th Graduate Research Conference, Feb 12, 2010, Khon Kaen University, Khon Kaen. (poster)

(เดือนที่ 19-24)

3.1b.6 Sankoh, S.; Thipmanee, O.; Samanman, S.; Limbut, W.; Numnuam, A.; Kanatharana, P.; Vilaivan, T.; Thavarungkul, P. "Capacitive DNA sensor using immobilized PNA" The International Congress for Innovation in Chemistry" (PERCH-CIC Congrss VII), May 4-7, 2011, Jomtien Palm Beach Hotel and Resort, Pattaya. (poster)

3.1b.7 Reenabthue, N.; Vilaivan, T.; Suparpprom, C. " Synthesis and nucleic acid binding properties of novel pyrrolidinyl peptide nucleic acid carrying 3-aminopyrrolidine-4-carboxylic acid spacer " The International Congress for Innovation in Chemistry" (PERCH-CIC Congrss VII), May 4-7, 2011, Jomtien Palm Beach Hotel and Resort, Pattaya. (poster)

(เดือนที่ 25-30)

3.1b.8 Maneelun, N.; Boonlua, C.; Vilaivan, T. "Dual-pyrene-labeled pyrrolidinyl peptide nucleic acid probes" The 37th Congress on Science and Technology (STT37), Oct 10–12, 2011, Centara Grand & Bangkok Convention Centre at CentralWorld, Bangkok. (poster)

3.1b.9 Ditmangklo, B.; Suparpprom, C.; Vilaivan, T. "A new strategy for on-solid-support labeling of pyrrolidinyl peptide nucleic acid by reductive alkylation and click chemistry" The 37th Congress on Science and Technology (STT37), Oct 10–12, 2011, Centara Grand & Bangkok Convention Centre at CentralWorld, Bangkok. (oral)

(เดือนที่ 31-36)

ไม่มี

(เดือนที่ 37-42)

3.1b.10 Maneethamwong, C.; Ditmangklo, B.; Suparpprom, C.; Vilaivan, T. “Pyrrolidinyl peptide nucleic acid terminally-labeled with thiazole orange as a fluorescent DNA probe” The 38th Congress on Science and Technology (STT38), Oct 17–19, 2012, Empress Convention Centre, Chiang Mai. (poster)
3.1b.11 Yotapan, N.; Vilaivan, T. “Orthogonally-protected 3-aminopyrrolidine-4-carboxylic acids for syntheses of doubly-labeled pyrrolidinyl peptide nucleic acids” The 38th Congress on Science and Technology (STT38), Oct 17–19, 2012, Empress Convention Centre, Chiang Mai. (poster)
3.1b.12 Boonlua, C.; Ditmangklo, B.; Suparpprom, C.; Vilaivan, C.; Vilaivan, T. “Highly specific DNA sequence determination by pyrene-labeled pyrrolidinyl peptide nucleic acid probes in combination with enzymatic digestion” The 38th Congress on Science and Technology (STT38), Oct 17–19, 2012, Empress Convention Centre, Chiang Mai. (poster)

3.1c วิทยากรรับเชิญ
3.1c.1 รศ.ดร.ธีรยุทธ วิไลวัลย์ หัวหน้าโครงการ ได้รับเชิญให้เป็นวิทยากรบรรยายหลัก (Keynote speaker) เรื่อง “β-Pyrrolidinyl peptide nucleic acids: Synthesis and applications as probes for DNA sequence analysis” ในงานประชุมวิชาการ The 5th Mathematics and Physical Sciences Graduate Congress ซึ่งจัดขึ้นที่ คณะวิทยาศาสตร์ จุฬาลงกรณ์มหาวิทยาลัย ระหว่างวันที่ 7–9 ธันวาคม 2552
3.1c.2 รศ.ดร.ธีรยุทธ วิไลวัลย์ หัวหน้าโครงการ ได้รับเชิญให้เป็นวิทยากรบรรยาย (Invited speaker) เรื่อง “Pyrrolidinyl peptide nucleic acids with unusual pairing properties as potential antigene agents” ในงานประชุมวิชาการ The Second China-Thailand Joint Workshop on Natural Products and Drug Discovery ซึ่งจัดขึ้นที่โรงแรมเคปพันวา จังหวัดภูเก็ต ระหว่างวันที่ 25–29 พฤศจิกายน 2552
3.1c.3 รศ.ดร.ธีรยุทธ วิไลวัลย์ หัวหน้าโครงการ ได้รับเชิญให้เป็นวิทยากรบรรยาย (Invited speaker) เรื่อง “Synthesis and pairing properties of pyrrolidinyl peptide nucleic acid: Beyond PNA•DNA duplexes” ในงานประชุมวิชาการ Pure and Applied Chemistry International Conference 2010 (PACCON 2010) ซึ่งจัดขึ้นที่โรงแรม Sunee Grand Hotel จังหวัดอุบลราชธานี ระหว่างวันที่ 21–23 มกราคม 2553
3.1c.4 รศ.ดร.ธีรยุทธ วิไลวัลย์ หัวหน้าโครงการ ได้รับเชิญให้เป็นวิทยากรสัมมนาเรื่อง “β-Pyrrolidinyl peptide nucleic acid: A new PNA with unusual binding properties” ณ Uppsala University, Sweden (Host: Prof. Pher G. Andersson) เมื่อวันที่ 14 กันยายน 2552
3.1c.5 รศ.ดร.ธีรยุทธ วิไลวัลย์ หัวหน้าโครงการ ได้รับเชิญให้เป็นวิทยากรสัมมนาเรื่อง “Synthesis, Properties and Applications of conformationally constrained β-pyrrolidinyl peptide nucleic acids” ณ Ruhr University of Bochum, Germany (Host: Prof. Chiara Cabrele) เมื่อวันที่ 29 มีนาคม 2554
3.1c.6 รศ.ดร.ธีรยุทธ วิไลวัลย์ หัวหน้าโครงการ ได้รับเชิญให้เป็นวิทยากรสัมมนา เรื่อง “Hybridization-responsive fluorescence pyrrolidinyl peptide nucleic acids probes for DNA sequence analysis” ณ Karlsruhe Institute of Technology, Germany (Host: Prof. Hans-Achim Wagenknecht) เมื่อวันที่ 26 เมษายน 2554
3.1c.7 รศ.ดร.ธีรยุทธ วิไลวัลย์ หัวหน้าโครงการ ได้รับเชิญให้เป็นวิทยากรสัมมนา เรื่อง “Pyrrolidinyl peptide nucleic acid with α/β-peptide backbone: Synthesis, properties and applications” ณ Nanyang Technological University, Singapore (Host: Prof. Roderick W. Bates) เมื่อวันที่ 29 กรกฎาคม 2554
3.1c.8 รศ.ดร.วรวีร์ โฮเว่น หัวหน้าโครงการย่อยที่ 3 ได้รับเชิญให้เป็นวิทยากรบรรยายเรื่อง “The power of polymer brushes in biosensing applications” ในงานประชุม The 7th International Symposium on Advanced

Materials in Asia-Pacific (7th ISAMAP) and JAIST International Symposium on NanoTechnology 2010 (NT2010) ณ Ishikawa High Tech Center, Ishikawa, Japan ระหว่างวันที่ 30 กันยายน–1 ตุลาคม 2553

3.1c.9 รศ.ดร.วรวีร์ โฮเว่น หัวหน้าโครงการย่อยที่ 3 ได้รับเชิญให้เป็นวิทยากรบรรยายเรื่อง “Featuring biosensing applications of chitosan” ในงานประชุม Pure and Applied Chemistry International Conference 2011 (PACCON 2011) ณ Miracle Grand Hotel กรุงเทพฯ ระหว่างวันที่ 5–7 มกราคม 2554

3.1c.10 รศ.ดร.วรวีร์ โฮเว่น หัวหน้าโครงการย่อยที่ 3 ได้รับเชิญให้เป็นวิทยากรบรรยายเรื่อง “Chemistry for Material Research: Opportunity and Serendipity” ในรายวิชาสัมมนา บัณฑิตศึกษา สาขาวิชาเคมีประยุกต์ ภาควิชาเคมี คณะวิทยาศาสตร์ มหาวิทยาลัยรามคำแหง เมื่อวันที่ 14 มีนาคม 2555

3.1c.11 รศ.ดร.ธีรยุทธ วิไลวัลย์ หัวหน้าโครงการ ได้รับเชิญให้เป็นวิทยากรสัมมนา เรื่อง “Internally-labeled pyrrolidinyl peptide nucleic acids as a quencher-free molecular beacon” ณ Pohang University of Science and Technology (POSTECH) (Host: Prof. Byeang-Hyean Kim), Kyangpook National University (Host: Prof. Gil-Tae Hwang) และ Sungkyunkwan University (Host: Prof. Changsik Song) ระหว่างวันที่ 30 พฤษภาคม–1 มิถุนายน 2555

3.1c.12 รศ.ดร.เมธา รัตนากรพิทักษ์ หัวหน้าโครงการย่อยที่ 4 ได้รับเชิญให้เป็นวิทยากรบรรยายเรื่อง “Azlactone functionalization of magnetite nanoparticles using ATRP and their bioconjugation” ในการประชุม The 44th International Symposium on Macromolecules-IUPAC World Polymer Congress (MACRO 2012), 24th—29th June 2012, Virginia Polytechnic Institute and State University, Blacksburg, Virginia, USA (Invited Oral).

3.1c.13 รศ.ดร.เมธา รัตนากรพิทักษ์ หัวหน้าโครงการย่อยที่ 4 ได้รับเชิญให้เป็นวิทยากรบรรยายเรื่อง “Surface modification of magnetite nanoparticle with functional polymers” ในการประชุมวิชาการ วทท. ครั้งที่ 38 ณ จังหวัดเชียงใหม่ ระหว่างวันที่ 17-19 ตุลาคม 2555

3.1c.14 รศ.ดร.เมธา รัตนากรพิทักษ์ หัวหน้าโครงการย่อยที่ 4 ได้รับเชิญให้เป็นวิทยากรบรรยายเรื่อง “Surface modification of magnetite nanoparticle with functional polymers” ณ งานประชุม The 2nd Taiwan-Thailand Bilateral Mini-Symposium: Chemistry for Creative Economy ระหว่างวันที่ 17–18 มกราคม 2556 ณ มหาวิทยาลัยมหิดล

3.1c.15 รศ.ดร.เมธา รัตนากรพิทักษ์ หัวหน้าโครงการย่อยที่ 4 ได้รับเชิญให้เป็นวิทยากรบรรยายเรื่อง “Surface modification of magnetite nanoparticle with functional polymers” ณ งานประชุม 1st Thai-Taiwan Colloquium on “Frontier Research in Science and Technology วันที่ 30 พฤศจิกายน 2555 ณ มหาวิทยาลัยนเรศวร

3.1c.16 รศ.ดร.เมธา รัตนากรพิทักษ์ หัวหน้าโครงการย่อยที่ 4 ได้รับเชิญให้เป็นวิทยากรบรรยายเรื่อง “Immobilization of bioentities on surface of magnetic nanoparticle” ณ งานประชุมวิชาการระหว่างสถาบัน Academia Sinica ไต้หวันและมหาวิทยาลัยนเรศวร วันที่ 25 มกราคม 2556 ณ มหาวิทยาลัยนเรศวร

3.1d รางวัล-ทุนวิจัยที่ได้รับระหว่างรับทุนส่งเสริมกลุ่มวิจัย

3.1d.1 รศ.ดร.ธีรยุทธ วิไลวัลย์ หัวหน้าโครงการ ได้รับรางวัล CST Citation Award 2009 จากสมาคมเคมี (มกราคม 2553)

3.1d.2 รศ.ดร.ธีรยุทธ วิไลวัลย์ หัวหน้าโครงการ ได้รับรางวัลนักวิจัยดีเด่นแห่งชาติ สาขาวิทยาศาสตร์เคมีและเภสัช ประจำปี 2553 จากสำนักงานคณะกรรมการวิจัยแห่งชาติ (กุมภาพันธ์ 2554)
3.1d.3 รศ.ดร.เพริศพิชญ์ คณาธารณา (ผู้ร่วมโครงการย่อยที่ 5) ได้รับรางวัลนักวิจัยดีเด่นแห่งชาติ สาขาวิทยาศาสตร์เคมีและเภสัช ประจำปี 2554 จากสำนักงานคณะกรรมการวิจัยแห่งชาติ (กุมภาพันธ์ 2555)
3.1d.4 รศ.ดร.เพริศพิชญ์ คณาธารณา, รศ.ดร.ปณต ถาวรังกูร, ดร.จงดี ธรรมเขต และนายศักดิ์ชัยบดี สังข์แก้ว (ผู้ร่วมโครงการย่อยที่ 5) ได้รับรางวัลประกาศเกียรติคุณ ผลงานประดิษฐ์คิดค้นประจำปี 2553 สาขาวิชาวิทยาศาสตร์เคมีและเภสัช ผลงานเรื่อง “อุปกรณ์สกัดสารแบบไมโครที่เป็นมิตรกับสิ่งแวดล้อม” จากสำนักงานคณะกรรมการวิจัยแห่งชาติ (กุมภาพันธ์ 2553)
3.1d.5 รศ.ดร.เพริศพิชญ์ คณาธารณา , รศ.ดร.ปณต ถาวรังกูร, ดร.วรากร ลิ่มบุตร, ดร.จงดี ธรรมเขต และ ดร.ชิตนนท์ บูรณชัย (ผู้ร่วมโครงการย่อยที่ 5) ได้รับทุนวิจัยโครงการวิจัยเรื่อง Synthesis of polymer nanowire for sorbent in sample preparation step and modified electrode on detection of organic compound จาก NANOTEC, NSTDA ระยะเวลา พฤศจิกายน 2552-ตุลาคม 2554
3.1d.6 ดร.วรากร ลิ่มบุตร (ผู้ร่วมโครงการย่อยที่ 5) ได้รับทุนพัฒนาศักยภาพในการทำงานของอาจารย์รุ่นใหม่ ในฐานะหัวหน้าโครงการวิจัยเรื่อง Design and application of a simple hybrid batch-flow cell for capacitive affinity biosensor จากสำนักงานกองทุนสนับสนุนการวิจัยร่วมกับสำนักงานคณะกรรมการอุดมศึกษา และคณะวิทยาศาสตร์ มหาวิทยาลัยสงขลานครินทร์ ระยะเวลา มิถุนายน 2553-มิถุนายน 2555
3.1d.7 ดร.อาภรณ์ นุ่มน่วม (ผู้ร่วมโครงการย่อยที่ 5) ได้รับทุนพัฒนาศักยภาพในการทำงานของอาจารย์รุ่นใหม่ ในฐานะหัวหน้าโครงการวิจัยเรื่อง การปรับปรุงผิวอิเล็กโทรดด้วยฟิล์มเส้นใยนาโนพอลิเมอร์โดยเทคนิคอิเล็กโทรสปินนิงสำหรับการประยุกต์ใช้ทางไบโอเซนเซอร์ จากสำนักงานกองทุนสนับสนุนการวิจัยร่วมกับสำนักงานคณะกรรมการอุดมศึกษา และคณะวิทยาศาสตร์ มหาวิทยาลัยสงขลานครินทร์ ระยะเวลา มิถุนายน 2553-มิถุนายน 2555
3.1d.8 รศ.ดร.ปณต ถาวรังกูร, รศ.ดร.เพริศพิชญ์ คณาธารณา, ดร.วรากร ลิ่มบุตร, รศ.บุญเจริญ วงศ์กิตติศึกษา, ดร.อาภรณ์ นุ่มน่วม, ผศ.พรรณี อัศวตรีรัตนกุล ดร.จงดี ธรรมเขต และ รศ.ดร.ชูศักดิ์ ลิ่มสกุล ได้รับทุนวิจัยโครงการวิจัยเรื่อง การพัฒนาเซนเซอร์ความไวสูง จากโครงการพัฒนามหาวิทยาลัยวิจัยแห่งชาติ สำนักงานคณะกรรมการการอุดมศึกษา ระยะเวลา ตุลาคม 2553 ถึง กันยายน 2556
3.1d.9 รศ.ดร.เพริศพิชญ์ คณาธารณา, รศ.ดร.ปณต ถาวรังกูร, ดร.จงดี ธรรมเขต ดร.อารีย์ ชูดำ ดร.วรากร ลิ่มบุตร ดร.อาภรณ์ นุ่มน่วม ดร.ชิตนนท์ บูรณชัย ดร.ชุตินธร พันธ์วงศ์ และ ดร.สุรีรัตน์ หอมหวล ได้รับทุนวิจัยโครงการวิจัยเรื่อง เทคโนโลยีวัสดุกับการพัฒนาเทคนิคการเตรียมตัวอย่าง และเทคนิควิเคราะห์สำหรับการวิเคราะห์สาร จากโครงการพัฒนามหาวิทยาลัยวิจัยแห่งชาติ สำนักงานคณะกรรมการการอุดมศึกษา ระยะเวลา ตุลาคม 2553 ถึง กันยายน 2556
3.1d.10 รศ.ดร.วรวีร์ โฮเว่น, รศ.ดร.ธีรยุทธ วิไลวัลย์ ได้รับทุนวิจัยโครงการวิจัยเรื่อง การวิเคราะห์ลำดับเบสของดีเอ็นเอด้วยพิโรลิดินิลเพปไทด์นิวคลีอิกแอซิดโพรบโดยใช้พอลิเมอไรเซชันริเริ่มจากพื้นผิวสำหรับการขยายสัญญาณ จากโครงการพัฒนามหาวิทยาลัยวิจัยแห่งชาติ สำนักงานคณะกรรมการการอุดมศึกษา และกองทุนรัชดาภิเษกสมโภช จุฬาลงกรณ์มหาวิทยาลัย ระยะเวลา 1 ตุลาคม 2553 ถึง 30 กันยายน 2556
3.1d.11 รศ.ดร.วรวีร์ โฮเว่น, น.ส.นัดดา บูรณะบัญญัติ ได้รับทุนวิจัยโครงการวิจัยเรื่อง อนุภาคควอเทอไนซ์ไคโทซานเตรียมโดยการประกอบตัวเองของแอมฟิฟิลิกไคโทซาน จากทุนวิจัยมหาบัณฑิต สาขาวิทยาศาสตร์และ

เทคโนโลยี จากสำนักงานกองทุนสนับสนุนการวิจัย และ ทุน 90 ปี จุฬาลงกรณ์มหาวิทยาลัย กองทุนรัชดาภิเษกสมโภช จุฬาลงกรณ์มหาวิทยาลัย ระยะเวลา 1 ธันวาคม 2553 – 29 กุมภาพันธ์ 2555

3.1d.12 รศ.ดร.แพทย์หญิงณัฏฐิยา หิรัญกาญจน์ (ผู้ร่วมโครงการย่อยที่ 6) และคณะ ได้รับรางวัลผลงานวิจัยดีมาก เรื่อง “ปัจจัยทางพันธุกรรมของโรคเอสแอลอี (Genetics of Systemic Lupus Erythematosus)” จาก กองทุนรัชดาภิเษกสมโภช จุฬาลงกรณ์มหาวิทยาลัย ประจำปี 2553

3.1d.13 รศ.ดร.มงคล สุขวัฒนาสินิทธ์ (หัวหน้าโครงการย่อยที่ 2) และคณะ ได้รับรางวัลผลงานวิจัยระดับดีเด่น สาขาวิทยาศาสตร์เคมีและเภสัช จากผลงานเรื่อง “เซนเซอร์จากพาย-คอนจูเกตอะเซทิลีน” ประจำปี 2553 จากสำนักงานคณะกรรมการวิจัยแห่งชาติ (กุมภาพันธ์ 2554)

3.1d.14 รศ.ดร.ธีรยุทธ วิไลวัลย์ หัวหน้าโครงการ ได้รับรางวัล Asian CORE Program Lectureship Award 2012 (Japan) ในงานประชุม The 7th International Conference on Cutting-Edge Organic Chemistry in Asia (ICCEOCA-7), 11-14 Dec 2012, Nanyang Technological University, SINGAPORE (ธันวาคม 2555)

3.1d.15 รศ.ดร.เมธา รัตนากรพิทักษ์ (หัวหน้าโครงการย่อยที่ 4) ได้รับรางวัลผลงานวิจัยระดับดี สาขาวิทยาศาสตร์เคมีและเภสัช จากผลงานเรื่อง “การสังเคราะห์และการดัดแปรพื้นผิวอนุภาคนาโนแมกนีไทท์ด้วยพอลิเมอร์” ประจำปี 2555 จากสำนักงานคณะกรรมการวิจัยแห่งชาติ (มกราคม 2556)

3.1d.16 รศ.ดร.เพริศพิชญ์ คณาธารณา (ผู้ร่วมโครงการย่อยที่ 5) ได้รับโล่เกียรติยศ รางวัลอาจารย์ผู้มีผลงานดีเด่นสาขาการวิจัย ในงานวันสงขลานครินทร์ จากผลงานเรื่อง “การพัฒนาเทคนิคการวิเคราะห์สารปริมาณน้อย” จากมหาวิทยาลัยสงขลานครินทร์ (ตุลาคม 2555)

3.1d.17 รศ.ดร.เพริศพิชญ์ คณาธารณา, รศ.ดร. ปณต ถาวรังกูร, ดร. จงดี ธรรมเขต และ ดร. โอภาส บุญเกิด (ผู้ร่วมโครงการย่อยที่ 5) ได้รับ Gold Prize จากผลงานเรื่อง “Cost-effective Formaldehyde Test Kit” จาก Seoul International Invention Fair 2012 (29 November – 2 December 2012)

3.1d.18 รศ.ดร.เพริศพิชญ์ คณาธารณา, รศ.ดร. ปณต ถาวรังกูร, ดร. จงดี ธรรมเขต และ ดร. โอภาส บุญเกิด (ผู้ร่วมโครงการย่อยที่ 5) ได้รับ Bronze Prize จากผลงานเรื่อง “Environmental Friendly Solid Phase Microextractor” จาก Seoul International Invention Fair 2012 (29 November – 2 December 2012)

3.1d.19 รศ.ดร.เพริศพิชญ์ คณาธารณา, รศ.ดร.ปณต ถาวรังกูร, ดร.จงดี ธรรมเขต และดร.ภมรรัตน์ เกื้อเส้ง (ผู้ร่วมโครงการย่อยที่ 5) ได้รับรางวัลประกาศเกียรติคุณ ผลงานประดิษฐ์คิดค้นประจำปี 2556 สาขาวิชาวิทยาศาสตร์เคมีและเภสัช ผลงานเรื่อง “วัสดุคอมโพสิทของท่อนาโนคาร์บอนและครัยโอเจล : ตัวดูดซับราคาประหยัดชนิดใหม่สาหรับการวิเคราะห์สารพิษ”

3.2 กิจกรรมที่เกี่ยวข้องกับการนำผลจากโครงการไปใช้ประโยชน์

ยังไม่มี

3.3 การเชื่อมโยงทางวิชาการกับนักวิชาการอื่นๆ ทั้งในและต่างประเทศ

(เดือนที่ 1-18)

3.3.1 Professor Dr. Oliver Reiser, Institute for Organic Chemistry, University of Regensburg, Germany มีโครงการวิจัยร่วมกันภายใต้การสนับสนุนจากทุน Alexander von Humboldt ของเยอรมนี (มีนาคม 2552 - พฤษภาคม 2554) โดย Prof. Reiser มีความเชี่ยวชาญในการสังเคราะห์กรดเบต้าอะมิโนที่เป็น three-membered ring และได้ร่วมมือกันโดยคณะผู้วิจัยได้สังเคราะห์พีเอ็นเอที่มีกรดเบต้าอะมิโนเหล่านี้เป็นส่วนของโครงสร้างหลัก มีการแลกเปลี่ยน

บุคลากรด้านวิจัยแล้ว 1 ครั้ง คือ นส.บุญจิรา บุญทา ได้เดินทางไปทำงานวิจัยที่ University of Regensburg ระหว่าง กุมภาพันธ์ 2552 - สิงหาคม 2552 ภายใต้หัวข้อเรื่อง "Synthesis of PNA with prolyl-beta-ACC dipeptide backbone" และได้วางแผนโครงการความร่วมมือในการศึกษาโครงสร้างสามมิติของ RR-Pro/SS-ACPC PNA และสารประกอบเชิงซ้อนของมันกับดีเอ็นเอ โดยเทคนิค NMR

3.3.2 Professor Dr. Hans-Achim Wagenknecht , Institute for Organic Chemistry, University of Regensburg, Germany (ข้อมูลเพิ่มเติมเมื่อ ก.ค. 2554: ปัจจุบัน Prof. Wagenknecht ย้ายไปอยู่ที่ Institute for Organic Chemistry, Karlsruhe Institute of Technology ประเทศเยอรมนี) มีโครงการวิจัยร่วมกันภายใต้การสนับสนุนจากทุน Alexander von Humboldt ของเยอรมนี (มีนาคม 2552 - พฤษภาคม 2554) โดย Prof. Wagenknecht มีความเชี่ยวชาญในการศึกษาอันตรกิริยาระหว่างฟลูออโรฟอร์ที่ต่ออยู่กับนิวคลีโอเบสในดีเอ็นเอ และมีความสนใจที่จะสังเคราะห์พีเอ็นเอที่มีโครโมฟอร์อยู่ในส่วนของนิวคลีโอเบส โดยมีผลงานวิจัยตีพิมพ์ร่วมกันภายใต้โครงการนี้แล้ว 1 เรื่อง และเดิมได้วางแผนไว้ว่าจะมีนักศึกษาจากประเทศเยอรมนีมาทำวิจัยที่ประเทศไทยภายใต้ความร่วมมือดังกล่าวในช่วงระหว่าง มิถุนายน 2553 - สิงหาคม 2553 แต่เนื่องจากเหตุการณ์ความไม่สงบในกรุงเทพมหานครในช่วงเดือนเมษายน-พฤษภาคมที่ผ่านมาทำให้คณะผู้วิจัยตัดสินใจร่วมกันว่าจะชะลอการเดินทางครั้งนี้ไปก่อน คาดว่าจะสามารถร่วมมือกันได้ใหม่ในปี 2554-2555

ข้อมูลเพิ่มเติม ก.ค. 2554: ขณะนี้นักศึกษาปริญญาเอกจากกลุ่มวิจัยของ Prof. Wagenknecht คนหนึ่งกำลังอยู่ระหว่างสมัครขอทุนวิจัย DAAD เพื่อมาทำวิจัยระยะสั้นที่ห้องปฏิบัติการของหัวหน้าโครงการวิจัยในช่วงปลายปี 2554

ข้อมูลเพิ่มเติม ม.ค. 2555: ขณะนี้ Miss Claudia Stubinitzky นักศึกษาปริญญาเอกจากกลุ่มวิจัยของ Prof. Wagenknecht ได้รับทุนอุดหนุนของ KIT เพื่อมาทำวิจัยระยะสั้นที่ห้องปฏิบัติการของหัวหน้าโครงการวิจัยเป็นเวลา 3 เดือน โดยเริ่มต้นตั้งแต่เดือนตุลาคม 2554 แต่ติดน้ำท่วม จึงกลับไปเยอรมนีก่อน และได้กลับมาทำงานวิจัยต่ออีกในช่วง12 มกราคม– 16 มีนาคม 2555

ข้อมูลเพิ่มเติม ม.ค. 2556: ปัจจุบันมีผลงานวิจัยตีพิมพ์ร่วมกันภายใต้โครงการนี้แล้ว 2 เรื่อง

3.3.3 Professor Peter E. Nielsen, The Panum Institute, University of Copenhagen, Denmark เป็นผู้บุกเบิกพีเอ็นเอเป็นคนแรก และปัจจุบันก็ยังเป็นแนวหน้าของงานวิจัยทางด้านนี้ หัวหน้าโครงการได้เดินทางไปพบปะปรึกษาหารือกับ Prof. Nielsen ถึงความเป็นไปได้ในการร่วมมือกันทางด้านวิจัย ในช่วงเดือนกันยายน 2553 ด้วยทุนส่วนตัว ซึ่ง Prof. Nielsen ก็ให้ความสนใจ และได้นำตัวอย่างพีเอ็นเอของกลุ่มผู้วิจัยซึ่งมีสมบัติบางประการแตกต่างจากพีเอ็นเอของ Prof. Nielsen ไปศึกษาความสามารถในการจับกับ double-stranded DNA

3.3.4 ศ.ดร.สุพจน์ หารหนองบัว เมธีวิจัยอาวุโส ภาควิชาเคมี คณะวิทยาศาสตร์ จุฬาลงกรณ์มหาวิทยาลัย มีโครงการวิจัยร่วมกันในการพัฒนาแบบจำลองโมเลกุลเพื่ออธิบายความสัมพันธ์ระหว่างโครงสร้างและสมบัติของพีเอ็นเอ

3.3.5 Prof. Junji Kawakami, Department of Nanobiochemistry, Konan University, Japan มีโครงการวิจัยร่วมกันในการวิเคราะห์ค่า Thermodynamics parameters ของ acpcPNA เพื่อใช้อธิบายสมบัติการจับยึดกับกรดนิวคลีอิกที่ไม่ธรรมดาของมัน มีผลงานวิจัยตีพิมพ์ร่วมกันภายใต้โครงการนี้แล้ว 2 เรื่อง

(เดือนที่ 19-24)

3.3.6 Professor David J. Aitken จาก Laboratoire de Synthèse Organique & Méthodologie, ICMMO (CNRS UMR 8182), Université Paris-Sud XI ประเทศฝรั่งเศส มีความร่วมมือในการพัฒนาระบบพีเอ็นเอที่มีตัวเชื่อมที่เป็นกรดเบต้าอะมิโนชนิดใหม่คือ 2-aminocyclobutanecarboxylic acid ซึ่งกลุ่มวิจัยของ Prof. Aitken จะสังเคราะห์โมโนเมอร์ของตัวเชื่อมนี้ที่ประเทศฝรั่งเศส และกลุ่มของหัวหน้าโครงการจะนำมาสังเคราะห์เป็นพีเอ็นเอและศึกษาสมบัติการจับยึดกับดีเอ็นเอและอาร์เอ็นเอที่ประเทศไทย มีผลงานวิจัยตีพิมพ์ร่วมกันภายใต้โครงการนี้แล้ว 1 เรื่อง และกำลังเขียนโครงการขอทุนวิจัยร่วมกันอีก 1 เรื่อง

(เดือนที่ 25-30)

3.3.7 Professor Byeang Hyean Kim จาก Department of Chemsitry, Pohang University of Science and Technology (POSTECH) ประเทศเกาหลี Prof. Kim ซึ่งเป็นผู้เชี่ยวชาญด้านเคมีของกรดนิวคลีอิกที่ติดฉลากเรืองแสง ต้องการสร้างความร่วมมือในการวิจัยทางเคมีของกรดนิวคลีอิกในระดับภูมิภาค โดยติดต่อประสานงานผ่านหัวหน้าโครงการฯ และได้เดินทางมาประเทศไทยระหว่างวันที่ 3 – 9 มกราคม 2555 ด้วยทุนวิจัยของ Prof. Kim เอง และได้มาบรรยายเรื่องอ “Fluorescent nucleic acid systems: Design, construction and evaluation” ที่จุฬาลงกรณ์มหาวิทยาลัย มหาวิทยาลัยนเรศวร และมหาวิทยาลัยพระจอมเกล้าธนบุรี และได้เจรจาสร้างความร่วมมือด้านการวิจัยระยะยาวต่อไป โดยเบื้องต้น Prof. Kim ได้เสนอว่าจะมีการแลกเปลี่ยนนักศึกษา รวมทั้งอาจารย์เพื่อไปทำวิจัยระยะสั้น โดยหัวหน้าโครงการได้ส่งนิสิตปริญญาโท คือนายณัฐพล มณีลุน ไปทำวิจัยระยะสั้น ตั้งแต่เดือนเมษายน – สิงหาคม 2555 และได้ไปเยี่ยมชมและให้บรรยายที่ POSTECH และที่มหาวิทยาลัยอื่นอีก 2 แห่งในเกาหลี โดยได้รับการสนับสนุนค่าใช้จ่ายในประเทศเกาหลีจาก Prof. Kim

(เดือนที่ 31-36)

3.3.9 ผศ.ดร.ศัชรินทร์ ศิริวงศ์ ภาควิชาเคมี คณะวิทยาศาสตร์ จุฬาลงกรณ์มหาวิทยาลัย มีโครงการวิจัยร่วมกันในการพัฒนาแบบจำลองโมเลกุลเพื่ออธิบายความสัมพันธ์ระหว่างโครงสร้างและสมบัติของพีเอ็นเอ (รับช่วงต่อมาจากโครงการวิจัยร่วมกับ ศ.ดร. สุพจน์ หารหนองบัว) มีผลงานวิจัยตีพิมพ์ร่วมกันภายใต้โครงการนี้แล้ว 1 เรื่อง

3.3.8 ศ.ดร.ธวัชชัย ตันฑุลานิ เมธีวิจัยอาวุโส ภาควิชาเคมี คณะวิทยาศาสตร์ จุฬาลงกรณ์มหาวิทยาลัย มีโครงการวิจัยร่วมกันในการพัฒนาดีเอ็นเอไบโอเซ็นเซอร์โดยอาศัยพีเอ็นเอเป็นโพรบ มีผลงานวิจัยตีพิมพ์ร่วมกันภายใต้โครงการนี้แล้ว 1 เรื่อง

3.3.10 ศ.ดร.อรวรรณ ชัยลภากุล ภาควิชาเคมี คณะวิทยาศาสตร์ จุฬาลงกรณ์มหาวิทยาลัย มีโครงการวิจัยร่วมกันในการพัฒนาอิเล็กโทรเคมิคัลดีเอ็นเอไบโอเซ็นเซอร์โดยอาศัยพีเอ็นเอเป็นโพรบ

3.4 การจัดประชุมวิชาการ

(เดือนที่ 1-18)

3.4.1 ตามเงื่อนไขในสัญญารับทุนจาก สกว. หัวหน้าโครงการจะต้องจัดการประชุมวิชาการประจำทุกปี ประกอบกับขณะนี้งานได้ดำเนินการมาเป็นระยะเวลา 18 เดือนแล้ว จึงได้มีการงานประชุมประจำปีของกลุ่มวิจัยขึ้นเพื่อให้ผู้ร่วมโครงการได้มีโอกาสนำเสนอความก้าวหน้าของโครงการวิจัยร่วมกัน และแลกเปลี่ยนความรู้ระหว่างกลุ่มวิจัย-สาขา และรับฟังข้อเสนอแนะจากผู้ทรงคุณวุฒิ อันจะทำให้เกิดการพัฒนางานวิจัยไปในทิศทางที่ดีขึ้น โดยการประชุมได้จัดขึ้นที่ภาควิชาเคมี คณะวิทยาศาสตร์ จุฬาลงกรณ์มหาวิทยาลัยเมื่อวันที่ 21 มกราคม 2554 มี ศ.ดร.สุพจน์ หารหนองบัว คณบดีคณะวิทยาศาสตร์เป็นประธานเปิดงานประชุม ดร.บงกช ธารชมพู (ศูนย์พันธุวิศวกรรมและเทคโนโลยีชีวภาพแห่งชาติ) เป็นผู้ทรงคุณวุฒิ มีหัวหน้าโครงการย่อยและผู้ร่วมโครงการ และผู้สนใจทั่วไปเข้าร่วมประชุมจำนวน 40 คน มีผลงานนำเสนอในรูปบรรยาย 7 เรื่อง และโปสเตอร์อีก 10 เรื่อง

(เดือนที่ 19-24)

3.4.2 ได้จัดประชุมวิชาการครั้งที่ 2 ในวันที่ 9 ธันวาคม 2554 ณ คณะวิทยาศาสตร์ มหาวิทยาลัยนเรศวร จังหวัดพิษณุโลก โดยมี ศ.ดร.สุจินต์ จินายน อธิการบดีมหาวิทยาลัยนเรศวรเป็นประธานเปิดงานประชุม ผศ.พญ. ดร. สุธาทิพย์ พงษ์เจริญ ภาควิชาอายุรศาสตร์ คณะแพทยศาสตร์ มหาวิทยาลัยนเรศวร เป็นผู้ทรงคุณวุฒิ มีหัวหน้าโครงการและผู้ร่วมโครงการ 36 คน และผู้สนใจทั่วไปอีกจำนวน 30 คน เข้าร่วมประชุม มีผลงานนำเสนอในรูปบรรยาย 6 เรื่อง และโปสเตอร์อีก 8 เรื่อง

(เดือนที่ 25-36)

-

(เดือนที่ 37-42)

3.4.3 ได้จัดประชุมวิชาการครั้งที่ 3 ในวันที่ 11 มกราคม 2556 ธันวาคม 2554 ณ คณะวิทยาศาสตร์ มหาวิทยาลัยสงขลานครินทร์ จังหวัดสงขลา โดยมี รศ.ดร.วิไลวรรณ โชติเกียรติ คณบดีคณะวิทยาศาสตร์ และอาจารย์ประจำภาควิชาเทคโนโลยีชีวภาพโมเลกุลและชีวสารสนเทศ คณะวิทยาศาสตร์ มหาวิทยาลัยสงขลานครินทร์ ให้เกียรติเป็นประธานเปิดงานประชุม และเป็นผู้ทรงคุณวุฒิด้วย มีหัวหน้าโครงการและผู้ร่วมโครงการและผู้สนใจทั่วไป เข้าร่วมประชุมจำนวน 55 คน เข้าร่วมประชุม มีผลงานนำเสนอในรูปบรรยาย 6 เรื่อง และโปสเตอร์อีก 9 เรื่อง

4. ความเห็นของผู้วิจัย

ผลการดำเนินการในส่วนที่เป็นงานวิจัยทั้ง 6 โครงการย่อยเป็นไปได้ตามแผนงานที่วางไว้ โดยภาพรวมตัวงานเสร็จสมบูรณ์ตามข้อเสนอโครงการแล้ว ได้องค์ความรู้ใหม่ที่เกี่ยวข้องกับระบบพีเอ็นเอที่มีคอนฟอร์เมชันจำกัดชนิดใหม่ที่แสดงสมบัติการจับยึดกับดีเอ็นเอที่น่าสนใจ และได้ศึกษาสมบัติของระบบพีเอ็นเอชนิด acpcPNA ในด้านการจับยึดกับดีเอ็นเอและอาร์เอ็นเออย่างละเอียด อีกทั้งยังได้พัฒนาวิธีการติดฉลากเรืองแสงแก่ acpcPNA ที่ตำแหน่งใดๆ ของโมเลกุลตามต้องการ และได้นำ acpcPNA ไปใช้เป็นโพรบสำหรับตรวจสอบลำดับเบสของดีเอ็นเอโดยอาศัยเทคนิคฟลูออเรสเซนส์ (ใช้พีเอ็นเอที่ติดฉลากเรืองแสงโดยตัวของมันเอง หรือใช้ร่วมกับพอลิเมอร์เรืองแสง) การเกิดสีที่เร่งด้วยเอนไซม์ (ใช้ร่วมกับกระดาษกรองที่ดัดแปรพื้นผิวด้วยพอลิเมอร์ที่มีประจุบวก) แมสสปกโตรเมตรี (ใช้ร่วมกับอนุภาคไคโทซาน และอนุภาคแม่เหล็กที่มีประจุบวก) เทคนิคคาพาซิทีฟ (ใช้พีเอ็นเอที่ไม่ต้องติดฉลาก) และยังได้นำระบบดังกล่าวไปประยุกต์ใช้ในการตรวจวินิจฉัยทางการแพทย์และทางการเกษตร เช่น การตรวจเชื้อไวรัสไข้หวัดใหญ่สายพันธุ์ใหม่ โรคไวรัสในกุ้งและสับปะรด การทำ HLA genotyping เป็นต้น ปัญหาสำคัญที่พบคือระบบตรวจวัดดังกล่าวข้างต้นส่วนใหญ่สามารถทำงานได้กับดีเอ็นเอตัวอย่างที่ได้มาจากการสังเคราะห์ โดยให้ความจำเพาะเจาะจงและความไวของการตรวจวัดสูงตามที่คาดหมายไว้ แต่เมื่อนำไปตรวจวิเคราะห์กับดีเอ็นเอตัวอย่างจริงยังพบปัญหาด้านประสิทธิภาพของการจับยึดระหว่างพีเอ็นเอกับดีเอ็นเอเป้าหมาย คาดว่าความแตกต่างที่สำคัญคือการที่ดีเอ็นเอจากตัวอย่างจริงมักจะอยู่ในรูปของ duplex ไม่ใช่ single stranded DNA เหมือนที่ได้จากการสังเคราะห์ และมี matrix ที่ซับซ้อนกว่าตัวอย่างสังเคราะห์ จึงยังต้องศึกษารายละเอียดต่อไปเพื่อพัฒนาการตรวจสอบดีเอ็นเอจากตัวอย่างจริงให้มีประสิทธิภาพมากขึ้นถึงระดับที่จะนำไปใช้งานได้จริงในทางปฏิบัติ นับถึงวันที่รายงานมีผลงานที่ตีพิมพ์และได้รับการตอบรับให้ตีพิมพ์ถึงวันที่รายงานจำนวนรวม 20 บทความ เป็นผลงานจากโครงการย่อยที่ 1 จำนวน 11 บทความ โครงการย่อยที่ 2 จำนวน 3 บทความ โครงการย่อยที่ 3 จำนวน 1 บทความ โครงการย่อยที่ 4 จำนวน 2 บทความ โครงการย่อยที่ 5 จำนวน 2 บทความ โครงการย่อยที่ 6 จำนวน 1 บทความ และมีบทความที่กำลังเตรียมต้นฉบับอยู่อีกจำนวนหนึ่ง ในแง่ของคุณภาพ มีบทความที่ได้ลงตีพิมพ์ในวารสารที่มี IF2011 > 5 จำนวน 4 บทความ, IF2011 อยู่ระหว่าง 4–5 จำนวน 3 บทความ, IF2011 อยู่ระหว่าง 3–4 จำนวน 7 บทความ, IF2011 อยู่ระหว่าง 2–3 จำนวน 3 บทความ, และ IF2001 อยู่ระหว่าง 0.5–1 จำนวน 1 บทความ และมีอีก 2 บทความที่ลงตีพิมพ์ในวารสารใหม่ จึงยังไม่มีข้อมูลในฐานข้อมูล ISI

ตารางสรุปผลงานที่ได้ตลอดโครงการ (ตัวเลขในวงเล็บคือเป้าหมายที่ตั้งไว้ในข้อเสนอโครงการ)

ผลงาน	ปีที่ 1	ปีที่ 2	ปีที่ 3	ช่วงขยายโครงการ	รวม
1 จำนวนนักวิจัยที่สร้างจากโครงการ					
1.1 สถาบันเดียวกัน	7 (6)	-	-	-	7 (6)
1.2 ต่างสถาบัน	9 (8)	0 (1)	-	-	9 (9)
1.3 นักศึกษาระดับ	-	2 (3)	2 (2)	-	4 (5)

ปริญญาเอก* 1.4 นักศึกษาระดับปริญญาโท**	2 (2)	3 (3)	3 (3)	-	8 (8)
2. จำนวนผลงานตีพิมพ์ในวารสารวิชาการนานาชาติ	3 (3)	2 (8)	9 (7)	6 (-)	20 (18)
3. จำนวนผลงานการจดสิทธิบัตร***	-	-	1 (1)	-	1 (1)

*นับเฉพาะผู้ที่รับทุนผู้ช่วยวิจัยจากโครงการ หากนับนักศึกษาที่ทำงานเป็นส่วนหนึ่งของโครงการแต่รับทุนจากแหล่งอื่นจะมีจำนวนมากกว่านี้อย่างน้อย 1 เท่าตัว

**นับเฉพาะผู้ที่รับทุนผู้ช่วยวิจัยจากโครงการ หากนับนักศึกษาที่ทำงานเป็นส่วนหนึ่งของโครงการแต่รับทุนจากแหล่งอื่นจะมีจำนวนมากกว่านี้

***ยื่นจดในประเทศ

5. เอกสารแนบ

5.1 reprint หรือ manuscript

(เฉพาะที่มีเลขหน้าแล้ว เป็นเอกสารแนบในภาคผนวก 1)

5.2 ข้อมูลและประวัติย่อของผู้ได้รับทุนวิจัยระดับปริญญาโท/เอกจากโครงการ

โครงการย่อย	ชื่อ	ระดับ	สาขา	สังกัด	สถานภาพ
2	น.ส.กรรณิการ์ วงษ์นาม	ปริญญาโท	ปิโตรเคมีและวิทยาศาสตร์พอลิเมอร์	จุฬาลงกรณ์มหาวิทยาลัย	สำเร็จการศึกษา
2	น.ส.วราทิพย์ ศิริพรนพคุณ	ปริญญาเอก	ภาควิชาเคมี คณะวิทยาศาสตร์ จุฬาลงกรณ์มหาวิทยาลัย	จุฬาลงกรณ์มหาวิทยาลัย	สำเร็จการศึกษา (ต.ค. 2555)
3	น.ส. แพรทอง เหลาภา (ศรีแก่นจันทร์)	ปริญญาเอก	ปิโตรเคมีและวิทยาศาสตร์พอลิเมอร์	จุฬาลงกรณ์มหาวิทยาลัย	สำเร็จการศึกษา (เม.ย. 2555)
3	น.ส.นัดดา บูรณะบัญญัติ	ปริญญาโท	ปิโตรเคมีและวิทยาศาสตร์พอลิเมอร์	จุฬาลงกรณ์มหาวิทยาลัย	สำเร็จการศึกษา เม.ย. 2554
3	น.ส. จิตติมา มีบึงพร้าว	ปริญญาโท	สาขาปิโตรเคมีและวิทยาศาสตร์พอลิเมอร์	จุฬาลงกรณ์มหาวิทยาลัย	สำเร็จการศึกษา เม.ย. 2553
3	น.ส. กัญญา ตะบูนพงศ์	ปริญญาโท	ปิโตรเคมีและวิทยาศาสตร์พอลิเมอร์	จุฬาลงกรณ์มหาวิทยาลัย	สำเร็จการศึกษา เม.ย. 2555

					และศึกษาต่อในระดับปริญญาเอก
4	น.ส. ศิรประภา มีรอด	ปริญญาเอก	เคมี	มหาวิทยาลัยนเรศวร	กำลังศึกษา
5	น.ส.กนกรัตน์ เจริญพรภักดี	ปริญญาโท	เคมีวิเคราะห์	มหาวิทยาลัยสงขลานครินทร์	ออกจากโครงก แล้ว (รับทุนอื่น)
5	น.ส.ศุภมาศ ยอดบุตร	ปริญญาโท	เคมีวิเคราะห์	มหาวิทยาลัยสงขลานครินทร์	ออกจากโครงการแล้ว
5	น.ส.จินดาพร แซ่ลิ่ม	ปริญญาโท	เคมีวิเคราะห์	มหาวิทยาลัยสงขลานครินทร์	สำเร็จการศึกษา เม.ย. 2554
5	น.ส. อังคณา มีชัยชนะ	ปริญญาโท	นิติวิทยาศาสตร์	มหาวิทยาลัยสงขลานครินทร์	กำลังศึกษา

5.3 บทคัดย่อ หรือบทสรุปของบทความวิชาการ หรือเอกสารในลักษณะอื่น ๆ ตลอดจนสื่อประเภทต่าง ๆ ที่โครงการได้จัดทำขึ้น

1. บทคัดย่องานประชุมวิชาการ (เป็นเอกสารแนบในภาคผนวก 2 ในแผ่น CD)
2. เอกสารรวมคัดย่องานประชุมประจำปีกลุ่มวิจัยครั้งที่ 1–3 (เป็นเอกสารแนบในภาคผนวก 3 ในแผ่น CD)

5.4 ผลงานอื่น ๆ ที่เกี่ยวข้อง

รายละเอียดทางวิชาการของโครงการย่อย 1–6 (เป็นเอกสารแนบในภาคผนวก 4 ในแผ่น CD)

ลงนาม .....
(หัวหน้าโครงการวิจัยผู้รับทุน)

ภาคผนวก 1

ผลงานตีพิมพ์และสิทธิบัตร

Provided for non-commercial research and education use.
Not for reproduction, distribution or commercial use.

This article appeared in a journal published by Elsevier. The attached copy is furnished to the author for internal non-commercial research and education use, including for instruction at the authors institution and sharing with colleagues.

Other uses, including reproduction and distribution, or selling or licensing copies, or posting to personal, institutional or third party websites are prohibited.

In most cases authors are permitted to post their version of the article (e.g. in Word or Tex form) to their personal website or institutional repository. Authors requiring further information regarding Elsevier's archiving and manuscript policies are encouraged to visit:

http://www.elsevier.com/copyright

Author's personal copy

Tetrahedron Letters 51 (2010) 5822–5826

Contents lists available at ScienceDirect

Tetrahedron Letters

journal homepage: www.elsevier.com/locate/tetlet

DNA-, RNA- and self-pairing properties of a pyrrolidinyl peptide nucleic acid with a (2′*R*,4′*S*)-prolyl-(1*S*,2*S*)-2-aminocyclopentanecarboxylic acid backbone

Jaru Taechalertpaisarn, Pitchanun Sriwarom, Chalotorn Boonlua, Nattawut Yotapan, Chotima Vilaivan, Tirayut Vilaivan *

Organic Synthesis Research Unit, Department of Chemistry, Faculty of Science, Chulalongkorn University, Phayathai Road, Patumwan, Bangkok 10330, Thailand

ARTICLE INFO

Article history:
Received 13 May 2010
Revised 6 August 2010
Accepted 31 August 2010
Available online 6 September 2010

Keywords:
β-Amino acid
DNA
PNA
Diastereomer
Epimer
Foldamer
α-DNA

ABSTRACT

A new pyrrolidinyl peptide nucleic acid (PNA) comprising of an alternate sequence of 4′-nucleobase-modified proline with (2′*R*,4′*S*) configuration and a (1*S*,2*S*)-2-aminocyclopentanecarboxylic acid [(2′*R*,4′*S*)-acpcPNA] backbone was synthesized and its DNA-, RNA- and self-pairing properties studied. T_m and CD studies suggested that the (2′*R*,4′*S*)-acpcPNA forms antiparallel hybrids to DNA and RNA with high sequence and direction specificity. The stability of these hybrids is comparable to those of the (2′*R*,4′*R*)-acpcPNA hybrids previously reported by our group. On the other hand, experiments with a self-complementary sequence indicated that the new (2′*R*,4′*S*)-acpcPNA forms a more stable antiparallel self-hybrid than (2′*R*,4′*R*)-acpcPNA.

© 2010 Elsevier Ltd. All rights reserved.

A peptide nucleic acid (PNA) is a DNA analogue that binds with single- and double-stranded nucleic acids with high affinity and sequence specificity.[1] In addition to their stronger binding affinity, they are chemically and physiologically more stable than DNA/RNA. These properties lead to a number of applications in the field of diagnostics, therapeutics and biotechnology.[2] After almost two decades since the first peptide nucleic acid (PNA) was introduced by Nielsen et al.[3] this original PNA system (also known as aegPNA) is still perhaps the only PNA system to have found widespread use. Many attempts have been made to improve current PNA technology by incorporating rigidity to the flexible aegPNA backbone in such a way that the PNA backbone is pre-organized for nucleic acid binding.[4,5] Inspired by the concept of foldamers,[6] we recently introduced a series of novel, conformationally rigid PNA analogues with a pyrrolidine core structure in combination with β-amino acid spacers.[7] Preliminary screening based on the (2′*R*,4′*R*) stereoisomer of the nucleobase-modified proline at the 4′ position, which corresponded to the configuration of natural nucleosides, revealed only certain allowable β-amino acid spacers. In particular, the PNA carrying D-aminopyrrolidinecarboxylic acid (DAPC)[7a,b] or (1*S*,2*S*)-2-aminocyclopentanecarboxylic acid (ssACPC)[7c,d] spacers, for example, (2′*R*,4′*R*)-acpcPNA (Scheme 1), can form particularly stable antiparallel hybrids with DNA and less so with RNA.[7d] On the other hand, the effect of changing the configuration of the pyrrolidine in these β-amino acid-containing PNAs has not been systemically investigated.

It is well known that α-anomeric DNA and its backbone-modified analogues can bind to normal β-DNA, albeit with polarity reversal (the two strands must be parallel to each other).[8–10] We therefore proposed that the pyrrolidinyl PNA epimer with a (2′*R*,4′*S*)-prolyl-(1*S*,2*S*)-2-aminocyclopentanecarboxylic acid backbone, that is, (2′*R*,4′*S*)-acpcPNA (Scheme 1), should retain the ability to bind to the target DNA. Furthermore, this epimeric acpcPNA might exhibit different directional specificity (parallel vs antiparallel) and preference for binding to different types of nucleic acid targets (DNA vs RNA) as observed with α-anomeric DNA.[11] Preliminary UV-melting experiments with the remaining three diastereomeric pyrrolidinyl PNAs with the same T_5 sequence and (2′*S*,4′*S*), (2′*S*,4′*R*) and (2′*R*,4′*S*) configurations of the proline moiety revealed that only the (2′*R*,4′*S*) diastereomer binds to poly(dA). To investigate the binding behaviour of this particular epimeric PNA in detail, studies of more complex sequences are required.

The four nucleobase-modified pyrrolidine monomers (A, T, C and G) were prepared starting from the known intermediate **1**[12] according to the method outlined in Scheme 2. In brief, the nucleobases were installed on the pyrrolidine ring, with inversion of

* Corresponding author. Tel.: +66 2 2187627; fax: +66 2 2187598.
E-mail address: vtirayut@chula.ac.th (T. Vilaivan).

0040-4039/$ - see front matter © 2010 Elsevier Ltd. All rights reserved.
doi:10.1016/j.tetlet.2010.08.102

Author's personal copy

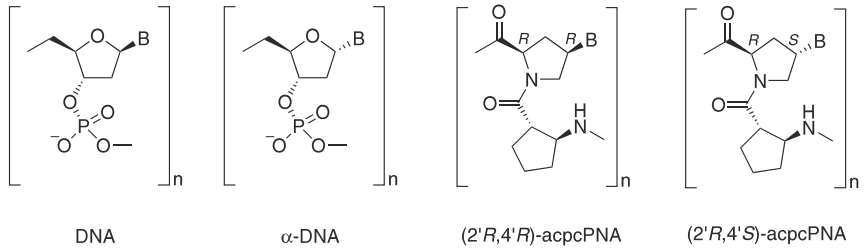

Scheme 1.

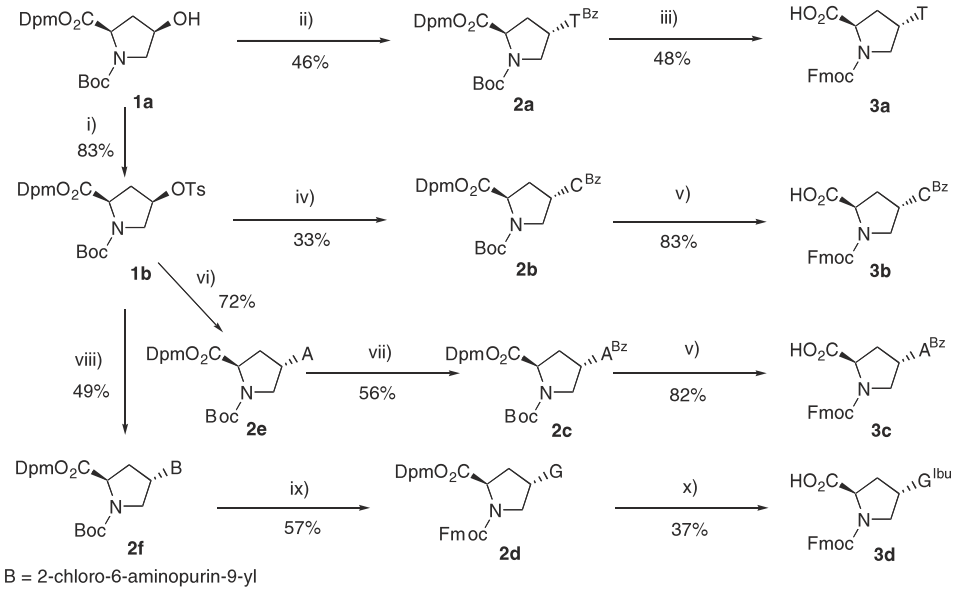

i) TsCl, Et_3N, cat. DMAP, CH_2Cl_2, rt, 4 h
ii) N^3-BzT, Ph_3P, DIAD, THF, 0 °C-rt, O/N
iii) a) TsOH, MeCN, rt, 3 h b) FmocCl, DIEA, rt, 1 h c) TFA, anisole, rt, O/N
iv) N^4-BzC, K_2CO_3, DMF, 80 °C, 8 h
v) a) TFA, anisole, rt, 3 h b) FmocOSu, $NaHCO_3$, aq. MeCN, O/N
vi) adenine, K_2CO_3, DMF, 80 °C, 6 h
vii) a) BzCl, pyridine, 0 °C, 2 h b) aq. NH_3, MeOH, rt
viii) 2-amino-6-chloropurine, K_2CO_3, DMF, 80 °C, 2 h
ix) a) TFA, rt, 2 h b) 2M HCl, reflux, 2 h c) FmocOSu, $NaHCO_3$, aq. MeCN, rt, O/N d) Ph_2CHN_2, EtOAc-MeOH, rt, 2 h
x) a) $(CH_3)_2CHCOCl$, pyridine, 0 °C-rt, O/N b) TFA, 1 h

Scheme 2.

configuration, via Misunobu reaction on **1a** (T monomer) or S_N2 substitution of the corresponding tosylate **1b** (C^{Bz}, A^{Bz} and G^{Ibu} monomers; Bz = benzoyl and Ibu = isobutyryl).[12] Due to the poor yield and regioselectivity associated with direct tosyl displacement with A^{Bz} and G^{Ibu}, the displacements were carried out with adenine and 2-amino-6-chloropurine instead. The initial products, **2e** and **2f**, were subsequently transformed into the desired protected monomers by standard nucleoside chemistry. Protecting group exchange from *N*-Boc to *N*-Fmoc afforded the Fmoc-protected monomers **3a–d** for the synthesis of the PNA by Fmoc-SPPS.[13] These monomers, together with Fmoc-(1*S*,2*S*)-2-aminocyclopentanecarboxylic acid[14] were coupled on Tentagel resin equipped with an acid-labile Rink amide linker via their pentafluorophenyl esters,[15] as previously described for similar PNAs.[7,16] One homopyrimidine (**P1**) and two mixed-base PNAs (non self-complementary **P2** and self-complementary **P3**) were synthesized. The identities of all the synthesized PNAs were confirmed by MALDI-TOF mass spectrometry (Table 1, see also Fig. S19–S21, Supplementary data) after cleavage from the resin using trifluoroacetic acid (TFA) and reverse phase HPLC purification.

Table 1
Sequences and characterization data of (2′*R*,4′*S*)-acpcPNA **P1–P3**

PNA	Sequence[a] (N → C)	Length (bases)	*m*/*z* (calcd)[b]	*m*/*z* (found)[c]
P1	TTTTTTTTT	9	3266.153	3265.575
P2	GTAGATCACT	10	3620.907	3618.854
P3	CGCGAATTCGCG	12	4233.184	4234.538

[a] All PNAs were modified with lysinamide at the C-termini and end-capped by acetylation (**P3**), benzoylation (**P2**) or with lysine (**P1**).
[b] Average mass, calculated for $M{\cdot}H^+$
[c] MALDI-TOF, linear mode, α-cyano-4-hydroxycinnamic acid (CCA) matrix

The interaction of the 9mer homothymine (2′*R*,4′*S*)-acpcPNA **P1** with its complementary DNA (dA_9) was first studied by UV-melting experiments. A single-transition melting curve was observed with a T_m of 67.8 °C.[17] Although this T_m value was ~5 °C lower than

Author's personal copy

Table 2
Tm values of hybrids between **P2** and DNA/RNA

Entry	DNA/RNA sequence (5′→3′)	T_m[a] (°C) (2′*R*,4′*R*)	T_m[a] (°C) (2′*R*,4′*S*)	Note
1	dAGTGATCTAC	53.3	50.8	Antiparallel, perfect matched
2	dAGTGCTCTAC	23.8	26.5	Antiparallel, single mismatched
3	dAGTGTTCTAC	29.4	27.4	Antiparallel, single mismatched
4	dAGTGGTCTAC	23.9	28.1	Antiparallel, single mismatched
5	dCATCTAGTGA	<20	<20	Parallel, perfect matched
6	rAGUGAUCUAC	42.3	40.7	Antiparallel, perfect matched
7	rCAUCUAGUGA	<20	<20	Parallel, perfect matched

[a] Conditions: 10 mM sodium phosphate buffer, pH 7.0, 100 mM NaCl; concentration of PNA = DNA = 1 μM, heating rate 1 °C/min. The T_m figures are accurate to within ±0.5 °C.

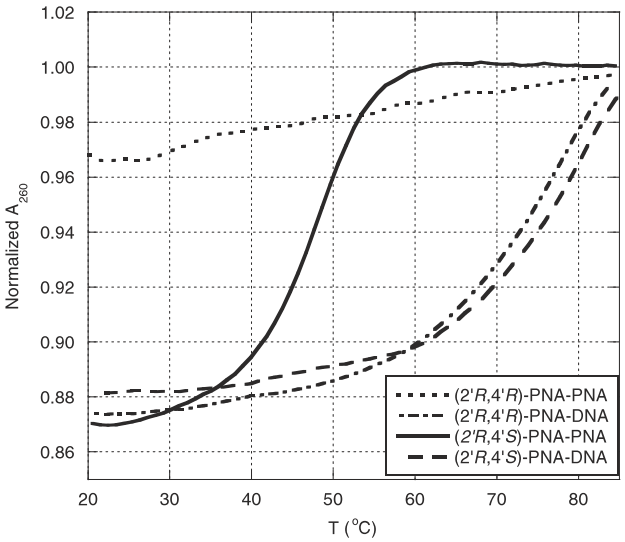

Figure 1. Melting curves of self-complementary PNA P3 in the absence and presence of complementary DNA. The experiments were carried out at a concentration of PNA strand = 2 μM (without DNA target) or 1 μM (with DNA target at 1 μM) in 10 mM sodium phosphate buffer (pH 7.0) containing 100 mM of NaCl, heating rate = 1 °C/min.

that of diastereomeric (2′*R*,4′*R*)-acpcPNA under similar conditions (72.9 °C), we were pleased to find that the (2′*R*,4′*S*)-acpcPNA could indeed retain strong binding to DNA. The T_m values of the hybrids of the mixed-base 10mer (2′*R*,4′*S*)-acpcPNA **P2** and DNA were also measured, and the data compared with (2′*R*,4′*R*)-acpcPNA with the same sequence (Table 2, see also Fig. S22). In this particular sequence, the thermal stability of the complementary antiparallel (2′*R*,4′*S*)-acpcPNA·DNA hybrid was only slightly lower (~2.5 °C) than that of the corresponding (2′*R*,4′*R*)-acpcPNA·DNA hybrid (Table 2, entry 1). No melting could be observed for the corresponding complementary parallel hybrids in both cases, suggesting a strong preference of both PNA diastereomers to bind to their DNA targets in an antiparallel fashion (Table 2, entry 5). When a mismatched base was introduced to the DNA strand, the stabilities of the mismatched PNA–DNA hybrids decreased sharply (Table 2, entries 2–4). The T_m decrease for each (2′*R*,4′*S*)- and (2′*R*,4′*R*)-acpcPNA mismatched hybrid was >20 °C, indicating the high specificity in DNA recognition of both PNA systems. As previously observed with the (2′*R*,4′*R*)-acpcPNA system,[7d] (2′*R*,4′*S*)-PNA also binds with its complementary RNA, selectively, in antiparallel fashion, and with a lower affinity compared to the corresponding DNA hybrids (Table 2, entries 6 and 7).

Finally, the two epimeric PNAs were compared in terms of the ability to self-hybridize. It was established from our previous work that two complementary strands of (2′*R*,4′*R*)-acpcPNA cannot form a hybrid with each other.[7d] The absence of any melting upon heating (2′*R*,4′*R*)-PNA with the same sequence as **P3**, without its DNA target, supported our earlier findings. On the other hand, the self-complementary (2′*R*,4′*S*)-acpcPNA **P3** showed a well-defined melting curve with a T_m value of 47.8 °C suggesting the formation of a PNA·PNA homoduplex (Fig. 1).[18] In the presence of complementary DNA, both PNAs form very stable PNA·DNA heteroduplexes with T_m values of 77.0 °C (2′*R*,4′*R*) and 78.6 °C (2′*R*,4′*S*), respectively. CD spectra (Fig. 2) of the self-complementary PNAs also revealed that the self-complementary (2′*R*,4′*S*)-acpcPNA was more structurally organized than (2′*R*,4′*R*)-acpcPNA with the same sequence, which was consistent with the T_m results. In the presence of the DNA strand, both PNAs become more ordered as shown by the increase in magnitude of the negative CD bands at 208 and 250 nm. The CD spectra also suggested that the helical senses of PNA·DNA hybrids derived from both epimeric PNAs should be similar.

Although only a few other workers have described the syntheses and compared DNA-pairing properties of related diastereomeric pyrrolidinyl PNA systems,[19] these comparisons were limited to homopurine/pyrimidine sequences or chimeric backbones consisting of different type of PNA monomers. The present work is the first example of critical evaluation on mixed sequences with homogeneous, non-chimeric backbones. The exclusive antiparallel binding mode of (2′*R*,4′*S*)-acpcPNA to its complementary DNA is similar to (2′*R*,4′*R*)-acpcPNA,[7d] and is in sharp contrast with the DNA counterparts. In addition, while normal DNA and α-anomeric DNA bind more strongly to RNA than DNA,[11] the corresponding epimeric (2′*R*,4′*S*)-acpcPNA exhibited stronger binding to DNA over RNA being similar to (2′*R*,4′*R*)-acpcPNA.[7d] These, together with the relatively strong, yet highly sequence specific, binding of the new (2′*R*,4′*S*)-acpcPNA to DNA and RNA indicates that the configuration of the proline ring in the pyrrolidinyl PNA can tolerate modification to some extent, without significantly altering the DNA-binding properties. From this study, the only significant difference between the two epimeric PNA systems is that (2′*R*,4′*S*)-acpcPNA can form a relatively stable antiparallel self-complementary hybrid while (2′*R*,4′*R*)-acpcPNA cannot. This emphasizes the delicate effect of stereochemistry on the self-pairing properties of these pyrrolidinyl PNAs. Although the structural basis of this difference is not clear at present, the explanation for the inability of (2′*R*,4′*R*)-acpcPNA to self-hybridize based on steric effects alone may not be sufficient.

This work suggests that the more easily synthesized (2′*R*,4′*S*)-acpcPNA could substitute (2′*R*,4′*R*)-acpcPNA as probes for nucleic acid detection[20] due to their similar DNA- and RNA-binding properties. The unexpected possibility to modulate the self-pairing behaviour of pyrrolidinyl PNA by changing the configuration of the pyrrolidine ring should further expand the potential scope of applications of these pyrrolidinyl PNAs. Although the inability to form a self-pairing hybrid of the original (2′*R*,4′*R*)-acpcPNA system is highly desirable for certain applications such as DNA targeting

Author's personal copy

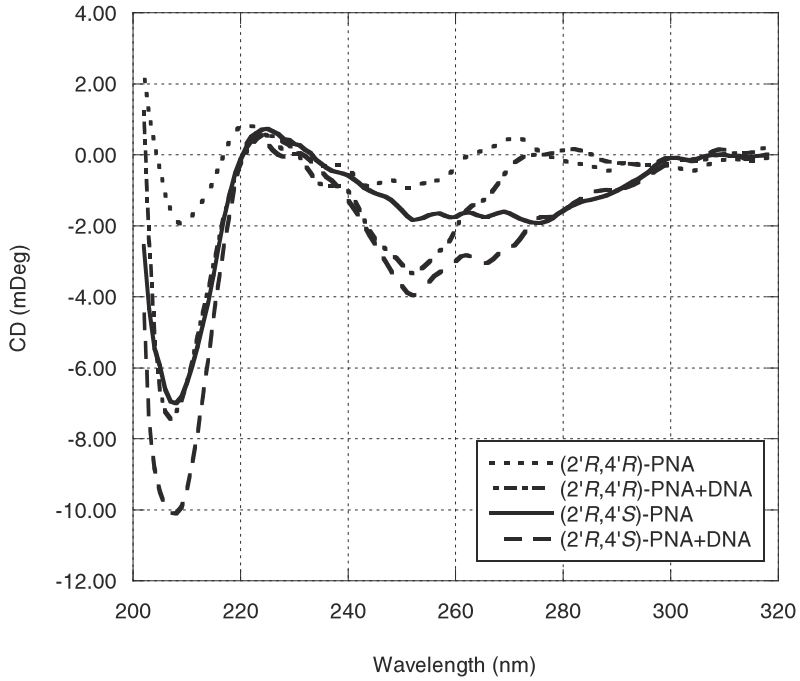

Figure 2. CD spectra of self-complementary (2′*R*,4′*R*)- and (2′*R*,4′*S*)-acpcPNA **P3** in the absence and presence of complementary DNA. The spectra were measured at a fixed concentration of PNA strand = 1 μM and DNA strand = 1 μM in 10 mM sodium phosphate buffer (pH 7.0) containing 100 mM of NaCl at 20 °C.

by double duplex invasion,[21] the self-pairing may also be useful for applications including the construction of PNA-based nanomaterials.[22]

Acknowledgements

Financial support from the Thailand Research Fund (RTA5280002 to T.V.), the Development and Promotion of Science and Technology Talents Project (DPST) (to J.T. and C.B.) and the National Center of Excellence for Petroleum, Petrochemicals and Advanced Materials (NCE-PPAM) is acknowledged.

Supplementary data

Supplementary data (experimental details, copies of ^{1}H and ^{13}C NMR spectra of compounds **1b**, **2a–f** and **3a–d**, mass spectra of (2′*R*,4′*R*)-acpcPNA **P1–P3** and T_m curves of **P2** hybrids) associated with this article can be found, in the online version, at doi:10.1016/j.tetlet.2010.08.102.

References and notes

1. (a) Nielsen, P. E.; Haaima, G. *Chem. Soc. Rev.* **1997**, *26*, 73–78; (b) Uhlmann, E.; Peyman, A.; Breipohl, G.; Will, D. W. *Angew. Chem., Int. Ed.* **1998**, *37*, 2797–2823.
2. (a) Demidov, V. V. *Drug Discovery Today* **2002**, *7*, 153–154; (b) Nielsen, P. E. *Curr. Opin. Biotechnol.* **2001**, *12*, 16–20; (c) Ray, A.; Nordén, B. *FASEB J.* **2000**, *14*, 1041–1060.
3. (a) Nielsen, P. E.; Egholm, M.; Berg, R. H.; Buchardt, O. *Science* **1991**, *254*, 1497–1500; (b) Egholm, M.; Buchardt, O.; Nielsen, P. E.; Berg, R. H. *J. Am. Chem. Soc.* **1992**, *114*, 1895–1897.
4. (a) Kumar, V. A. *Eur. J. Org. Chem.* **2002**, 2021–2032; (b) Kumar, V. A.; Ganesh, K. N. *Acc. Chem. Res.* **2005**, *38*, 404–412.
5. Selected examples: (a) Govindaraju, T.; Kumar, V. A.; Ganesh, K. N. *J. Am. Chem. Soc.* **2005**, *127*, 4144–4145; (b) Pokorski, J. K.; Witschi, M. A.; Purnell, B. L.; Appella, D. H. *J. Am. Chem. Soc.* **2004**, *126*, 15067–15073; (c) Dragulescu-Andrasi, A.; Rapireddy, S.; Frezza, B. M.; Gayathri, C.; Gil, R. R.; Ly, D. H. *J. Am. Chem. Soc.* **2006**, *128*, 10258–10267; (d) Gogoi, K.; Kumar, V. A. *Chem. Commun.* **2008**, 706–708; (e) Worthington, R. J.; Bell, N. M.; Wong, R.; Micklefield, J. *Org. Biomol. Chem.* **2008**, *6*, 92–103.
6. Review: Cheng, R. P.; Gellman, S. H.; DeGrado, W. F. *Chem. Rev.* **2001**, *101*, 3219–3232.
7. (a) Vilaivan, T.; Suparpprom, C.; Harnyuttanakorn, P.; Lowe, G. *Tetrahedron Lett.* **2001**, *42*, 5533–5536; (b) Vilaivan, T.; Lowe, G. *J. Am. Chem. Soc.* **2002**, *124*, 9326–9327; (c) Suparpprom, C.; Srisuwannaket, C.; Sangvanich, P.; Vilaivan, T. *Tetrahedron Lett.* **2005**, *46*, 2833–2837; (d) Vilaivan, T.; Srisuwannaket, C. *Org. Lett.* **2006**, *8*, 1897–1900; (e) Vilaivan, T.; Suparpprom, C.; Duanglaor, P.; Harnyuttanakorn, P.; Lowe, G. *Tetrahedron Lett.* **2003**, *44*, 1663–1666.
8. Séquin, U. *Experientia* **1973**, *29*, 1059–1062.
9. Morvan, F.; Rayner, B.; Imbach, J. L.; Lee, M.; Hartley, J. A.; Chang, D. K.; Lown, J. W. *Nucleic Acids Res.* **1987**, *15*, 7027–7044.
10. (a) Nielsen, P.; Christensen, N. K.; Dalskov, J. K. *Chem. Eur. J.* **2002**, *8*, 712–722; (b) Laurent, A.; Naval, M.; Debart, F.; Vasseur, J.-J.; Rayner, B. *Nucleic Acids Res.* **1999**, *27*, 4151–4159.
11. Thuong, N. T.; Asseline, U.; Roig, V.; Takasugi, M.; Hélène, C. *Proc. Natl. Acad. Sci. U.S.A.* **1987**, *84*, 5129–5133.
12. Lowe, G.; Vilaivan, T. *J. Chem. Soc., Perkin Trans. 1* **1997**, 547–554.
13. Spectroscopic data of PNA monomers:
Compound **3a** (T monomer): $[\alpha]_D^{25}$ −2.90 (*c* 1.0, DMF); ^{1}H NMR (400 MHz, DMSO-d_6) (ratio minor/major isomer ~1:1.38) δ_H 1.80 (s, 3H, CH_3 thymine), 2.20–2.32 and 2.58–2.75 [br m, 2H, CH_2(3′) rotamers], 3.44–3.49 and 3.73–3.82 [m, 2H, CH_2(5′) rotamers], 4.18–4.33 (m, 3H, CH Fmoc and CH_2 Fmoc), 4.40–4.43 and 4.53–4.57 [m, 1H, CH(2′) rotamers], 5.03–5.11 [m, 1H, CH(4′)], 7.31–7.35 [m, 3H, CH(6) thymine and CH Ar Fmoc], 7.40–7.45 (m, 2H, CH Ar Fmoc), 7.59 and 7.62 (2 × s, 1H, NH thymine), 7.64–7.66 (m, 2H, CH Ar Fmoc), 7.89–7.91 (m, 2H, CH Ar Fmoc), 11.32 and 11.35 (2 × s, 1H, COOH); ^{13}C NMR (100 MHz, DMSO-d_6) δ_C 12.6 (CH_3 thymine), 32.7 and 33.8 [CH_2(3′) rotamers], 47.0 and 47.1 (CH Fmoc), 49.3 and 49.5 [CH(5′) rotamers], 52.3 and 53.3 [CH(4′) rotamers], 57.9 and 58.1 [CH(2′) rotamers], 67.4 and 67.7 (CH_2 Fmoc rotamers), 110.0 [C(5) thymine], 120.6 (CH Ar Fmoc), 125.6 (CH Ar Fmoc), 127.6 (CH Ar Fmoc), 128.2 (CH Ar Fmoc), 138.1 [C(6)H thymine], 141.1 (C Ar Fmoc), 144.1 (C Ar Fmoc), 151.4 [C(2) thymine], 154.0 and 154.3 (CO Fmoc rotamers), 164.2 [C(4) thymine], 173.5 and 173.8 (COOH rotamers); HRMS (ESI) calcd for $C_{25}H_{23}N_3O_6{\cdot}H^+$ 462.1665, found 462.1654.
Compound **3b** (C^{Bz} monomer): $[\alpha]_D^{24}$ −15.1 (*c* 1.0, DMF); ^{1}H NMR (400 MHz, DMSO-d_6) (ratio minor/major isomer ~1:1.37) δ_H 2.34–2.47 and 2.71–2.86 [br m, 2H, CH_2(3′) rotamers], 3.59–3.63 and 3.85–3.94 [m, 2H, CH_2(5′) rotamers], 4.19–4.38 (m, 3H, CH_2 and CH Fmoc rotamers), 4.49 (dd *J* = 8.8, 3.3 Hz) and 4.63 (m) [1H, CH(2′) rotamers], 5.14 [m, 1H, CH(4′)], 7.30–7.38 [m, 3H, CH Ar Fmoc and CH(5) cytosine], 7.33–7.45 (m, 2H, CH Ar Fmoc), 7.51–7.55 (m, 2H, CH Ar Fmoc), 7.62–7.69 (m, 3H, CH Bz), 7.88–7.91 (m, 2H, CH Ar Fmoc), 8.00–8.05 (m, 2H, CH Bz), 8.14 (d *J* = 7.5 Hz) and 8.19 (d *J* = 7.5 Hz) [1H, CH(6) cytosine rotamers], 11.28 (br s, 1H, COOH); ^{13}C NMR (100 MHz, DMSO-d_6) δ_C 32.9 and 34.1 [CH_2(3′) rotamers], 47.0 and 47.1 (CH Fmoc rotamers), 50.1 and 50.5 [CH_2(5′) rotamers], 55.4 and 56.4 [CH(4′) rotamers], 57.9 and 58.1 [CH(2′) rotamers], 67.3 and 67.7 (CH_2 Fmoc rotamers), 96.9 [C(5)H cytosine], 120.6 (CH Ar Fmoc), 125.6 (CH Ar Fmoc), 127.6 (CH Ar Fmoc), 128.2 (CH Ar Fmoc), 128.9

Author's personal copy

(CH Bz), 133.2 (CH Bz), 133.6 (C Bz), 141.1 (C Ar Fmoc), 144.1 (C Ar Fmoc), 147.6 [C(6)H cytosine], 154.1 and 154.2 (CO Fmoc rotamers), 155.4 [C(2) cytosine], 163.2 [C(4) cytosine], 168.0 (CO Bz), 173.5 and 173.8 (COOH rotamers); HRMS (ESI+) calcd for $C_{31}H_{26}N_4O_6{\cdot}H^+$ 551.1931, found 551.1873.

Compound **3c** (A^{Bz} monomer): $[\alpha]_D^{24}$ +7.70 (*c* 1.0, DMF); ^{1}H NMR (400 MHz, DMSO-d_6) (ratio minor/major isomer ~1:1.36) δ_H 2.54–2.68 and 3.01–3.18 [m, 2H, CH_2(3′) rotamers], 3.87–3.98 and 4.03–4.07 [m, 2H, CH_2(5′) rotamers], 4.20–4.38 (m, 3H, CH_2 Fmoc and CH Fmoc rotamers), 4.60 (dd *J* = 8.9, 3.8 Hz) and 4.76 (dd *J* = 9.0, 3.1 Hz) [1H, CH(2′) rotamers], 5.37 [m, 1H, CH(4′)], 7.21–7.45 (m, 4H, CH Ar Fmoc), 7.55–7.70 (m, 5H, CH Ar Fmoc and Bz), 7.82–7.91 (m, 2H, CH Ar Fmoc), 8.06 (m, 2H, CH Bz), 8.59 and 8.62 [2 × s, 1H, CH(8) adenine rotamers], 8.75 and 8.78 [2 × s, 1H, CH(2) adenine rotamers], 11.22 (br s, 1H, COOH); ^{13}C NMR (100 MHz, DMSO-d_6) δ_C 33.5 and 34.7 [CH_2(3′) rotamers], 46.5 and 46.6 (CH Fmoc rotamers), 50.2 and 50.6 [CH_2(5′) rotamers], 52.2 and 53.0 [CH(4′) rotamers], 57.5 and 57.7 [CH(2′) rotamers], 66.9 and 67.3 (CH_2 Fmoc rotamers), 120.1 (CH Ar Fmoc), 125.0 and 125.2 (CH Ar Fmoc), 125.6 [C(5) adenine], 127.1 and 127.7 (CH Ar Fmoc), 128.5 (CH Bz), 132.4 (CH Bz), 133.4 (C Bz), 140.6 (C Ar Fmoc), 143.3 and 143.4 [C(8)H adenine rotamers], 143.6 (C Ar Fmoc), 150.3 [C(4) adenine], 151.3 [C(2)H adenine], 152.2 [C(6) adenine], 153.8 (CO Fmoc), 165.8 (CO Bz), 173.0 and 173.3 (COOH rotamers); HRMS (ESI+) calcd for $C_{32}H_{26}N_6O_5{\cdot}H^+$ 575.2043, found 575.2095.

Compound **3d** (G^{Ibu} monomer): $[\alpha]_D^{23}$ −3.43 (*c* 0.5, DMF); ^{1}H NMR (400 MHz, DMSO-d_6) (ratio minor/major isomer ~1:1.32) δ_H 1.13 (d, *J* = 6.0 Hz) and 1.14 (d, *J* = 6.5 Hz) (6H, CH_3 Ibu rotamers), 2.45–2.61 and 2.89–3.04 [m, 2H, CH_2(3′) rotamers], 2.78 (m, 1H, *CH* Ibu), 3.69–3.78 and 3.94–4.02 [m, 2H, CH_2(5′) rotamers], 4.19–4.38 (m, 3H, CH_2 Fmoc and CH Fmoc rotamers), 4.51 (dd *J* = 8.7, 2.9 Hz) and 4.65 (dd *J* = 8.8, 2.2 Hz) [1H, CH(2′) rotamers], 5.06–5.14 [m, 1H, CH(4′)], 7.23–7.45 (m, 4H, CH Ar Fmoc rotamers), 7.59–7.68 (m, 2H, CH Ar Fmoc rotamers), 7.84–7.91 (m, 2H, CH Ar Fmoc rotamers), 8.14 and 8.18 [2 × s, 1H, CH(8) guanine rotamers], 11.73 and 11.76 (2 × s, 1H, NH/OH rotamers), 12.10 and 12.12 (2 × s, 1H, NH/OH rotamers); ^{13}C NMR (100 MHz, DMSO-d_6) δ_C 19.3 (CH_3 Ibu), 34.1 and 35.3 [CH_2(3′) rotamers], 35.2 (CH Ibu), 47.0 and 47.1 (CH Fmoc rotamers), 50.9 and 51.3 [CH_2(5′) rotamers], 51.7 and 52.7 [CH(4′) rotamers], 57.8 and 58.1 [CH(2′) rotamers], 67.3 and 67.7 (CH_2 Fmoc rotamers), 120.6 (CH Ar Fmoc), 120.7 [C(5)H guanine], 125.5 and 125.7 (CH Ar Fmoc rotamers), 127.5 and 127.6 (CH Ar Fmoc rotamers), 128.1 and 128.2 (CH Ar Fmoc rotamers), 138.3 [C(8)H guanine], 141.2 (C Ar Fmoc), 144.1 (C Ar Fmoc), 148.4 and 149.0/149.1 [C(6) and C(2) guanine], 154.0 and 154.2 (CO Fmoc rotamers), 155.3 [C(4) guanine], 173.4 and 173.7 (COOH rotamers), 180.7 (CO Ibu); HRMS (ESI+) calcd for $C_{29}H_{28}N_6O_6{\cdot}H^+$ 557.2149, found 557.2100.

14. LePlae, P. R.; Umezawa, N.; Lee, H. S.; Gellman, S. H. *J. Org. Chem.* **2001**, *66*, 5629–5632.
15. The pentafluorophenyl esters were generated from the corresponding Fmoc free acids by treatment with pentafluorophenyl trifluoroacetate/DIEA. The unstable active esters were used following an acid-base extraction to remove DIEA salts without further purification.
16. Lowe, G.; Vilaivan, T. *J. Chem. Soc., Perkin Trans. 1* **1997**, 555–560.
17. In contrast to homopyrimidine aegPNA which readily forms $(PNA)_2{\cdot}DNA$ hybrids, it was established from our previous titration experiments (Refs. 7a–d) that homothymine pyrrolidinyl PNA forms only 1:1 hybrids with DNA.
18. Heating of single-stranded (2′*R*,4′*S*)-acpcPNA with a non-self-complementary sequence such as **P1** resulted in no melting curve. This rules out the possibilities of intramolecular folding or non-specific aggregate formation such as those observed in aegPNA.
19. (a) Kitamatsu, M.; Shigeyasu, M.; Okada, T.; Sisido, M. *Chem. Commun.* **2004**, 1208–1209; (b) Kitamatsu, M.; Shigeyasu, M.; Saitoh, M.; Sisido, M. *Biopolymers* **2006**, *84*, 267–273; (c) Lonkar, P. S.; Ganesh, K. N.; Kumar, V. A. *Org. Biomol. Chem.* **2004**, *2*, 2604–2611.
20. (a) Boontha, B.; Nakkuntod, J.; Hirankarn, N.; Chaumpluk, P.; Vilaivan, T. *Anal. Chem.* **2008**, *80*, 8178–8186; (b) Ananthanawat, C.; Vilaivan, T.; Hoven, V. P.; Su, X. *Biosens. Bioelectron.* **2010**, *25*, 1064–1069.
21. (a) Lohse, J.; Dahl, O.; Nielsen, P. E. *Proc. Natl. Acad. Sci. U.S.A.* **1999**, *96*, 11804–11808; (b) Ishizuka, T.; Yoshida, J.; Yamamoto, Y.; Sumaoka, J.; Tedeschi, T.; Corradini, R.; Sforza, S.; Komiyama, M. *Nucleic Acids Res.* **2008**, *36*, 1464–1471.
22. (a) Gothelf, K. V.; LaBean, T. H. *Org. Biomol. Chem.* **2005**, *3*, 4023–4037; (b) Ito, Y.; Fukusaki, E. *J. Mol. Catal. B: Enzym.* **2004**, *128*, 155–166.

Provided for non-commercial research and education use.
Not for reproduction, distribution or commercial use.

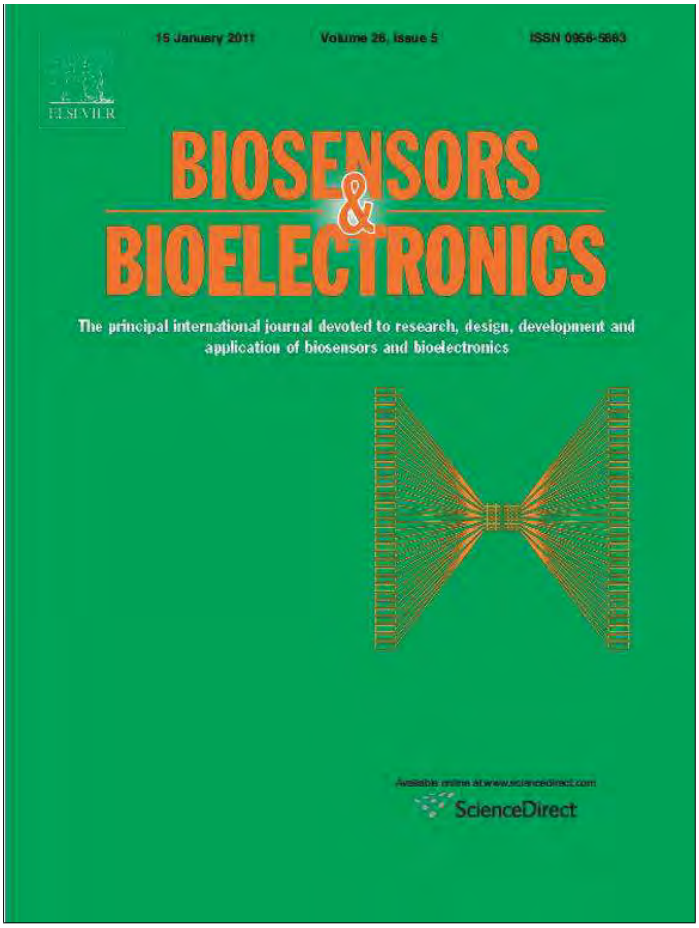

This article appeared in a journal published by Elsevier. The attached copy is furnished to the author for internal non-commercial research and education use, including for instruction at the authors institution and sharing with colleagues.

Other uses, including reproduction and distribution, or selling or licensing copies, or posting to personal, institutional or third party websites are prohibited.

In most cases authors are permitted to post their version of the article (e.g. in Word or Tex form) to their personal website or institutional repository. Authors requiring further information regarding Elsevier's archiving and manuscript policies are encouraged to visit:

http://www.elsevier.com/copyright

Author's personal copy

Biosensors and Bioelectronics 26 (2011) 1918–1923

Contents lists available at ScienceDirect

Biosensors and Bioelectronics

journal homepage: www.elsevier.com/locate/bios

Surface plasmon resonance study of PNA interactions with double-stranded DNA

Cheeraporn Ananthanawat[a], Voravee P. Hoven[b], Tirayut Vilaivan[b,*], Xiaodi Su[c,**]

[a] Program of Macromolecular Science, Faculty of Science, Chulalongkorn University, Bangkok 10330, Thailand
[b] Organic Synthesis Research Unit, Department of Chemistry, Faculty of Science, Chulalongkorn University, Bangkok 10330, Thailand
[c] Institute of Materials Research and Engineering, A*STAR (Agency for Science, Technology and Research), 3 Research Link, Singapore 117602, Singapore

ARTICLE INFO

Article history:
Received 23 March 2010
Received in revised form 19 May 2010
Accepted 21 May 2010
Available online 8 June 2010

Keywords:
Peptide nucleic acid
Higher-order complex
Triplex formation
Duplex invasion
SPR

ABSTRACT

Peptide nucleic acid (PNA) is a well known DNA analogue bearing a *N*-(2-aminoethyl)glycine backbone (aegPNA). This molecule is able to not only form a duplex with single stranded (ss) nucleic acids but also higher-order (i.e., three- and four-stranded) complexes with double-stranded (ds) DNA in a sequence specific manner. Here, the application of surface plasmon resonance (SPR) to study the binding of PNA to dsDNA is reported for the first time. SPR protocols were developed to verify the sequence rules and conditions for binding (pH and ionic strength) of homopyrimidine and homopurine aegPNAs to dsDNA, for which the solution phase behaviors are known, allowing a direct comparison. Then, using real-time SPR measurements, the hybridization efficiency, binding direction (antiparallel and parallel direction), sequence-dependent binding modes of the PNA to dsDNA (triplex formation and duplex invasion) and the binding kinetics associated with the binding mode were all ascertained. These SPR protocols were then further applied to study the dsDNA binding properties of a new conformationally rigid PNA bearing a *D*-prolyl-2-aminocyclopentanecarboxylic acid (ACPC) backbone (acpcPNA), which revealed that acpcPNA cannot form higher-order complexes with dsDNA through either triplex formation or duplex invasion. The SPR technique is thus shown to be a powerful technique for studying higher-order nucleic acid complexes. The binding behaviors of aegPNA obtained from the SPR analysis in the solid–liquid phase measurement correlate well with those in the literature derived from solution phase measurements.

© 2010 Elsevier B.V. All rights reserved.

1. Introduction

Triplex-forming oligonucleotides (TFOs), that is oligonucleotide strands that can bind in the major groove of double-stranded DNA (dsDNA), were first reported in 1957 (Felsenfeld and Rich, 1957). Binding of the third strand takes place with high specificity *via* Hoogsteen pairing, differing from the Watson–Crick base pairing found in normal DNA·DNA duplexes. Because of their potential in gene-targeted therapeutic and biotechnological applications, the binding behaviors of TFOs with dsDNA have been extensively studied (Frank-Kamenetskii and Mirkin, 1995). For example, TFOs can inhibit gene expression, or induce targeted mutagenesis and recombination (Chin and Glazer, 2008).

Peptide nucleic acid (PNA) is an uncharged DNA analogue (Nielsen et al., 1991; Egholm et al., 1992) with a *N*-(2-aminoethyl) glycine linkages (also known as aegPNA) that can form duplexes with its complementary DNA, following the Watson–Crick base pairing rules, with a higher stability and sequence-specificity than its DNA counterpart (Egholm et al., 1993). One of the most important applications of aegPNA, which relies on its duplex formation properties, is in biosensors for DNA detection, whereby the aegPNA is often immobilized as a sensing probe. Many studies have evaluated the performance of aegPNA probes in comparison to their DNA counterparts (Burgener et al., 2000; Wittung-Stafshede et al., 2000; Höök et al., 2001; Arlinghaus et al., 2003, 2004; Feldner et al., 2003; Xu et al., 2008; Lao et al., 2009). In addition to the ability to form aegPNA·DNA duplexes, aegPNAs have been found to form higher-order complexes with dsDNA or single stranded DNA (ssDNA). A number of sequence rules for higher-order complex formation have been discovered, including that: (1) thymine-rich homopyrimidine aegPNAs can invade dsDNA to form an aegPNA·DNA × aegPNA triplex with a looped out polypyrimidine region (Nielsen et al., 1994; Wittung et al., 1996, 1997); (2) cytosine-rich pyrimidine aegPNAs can bind to dsDNA to form DNA·DNA × aegPNA triplexes (Wittung et al., 1997); (3) purine-rich aegPNAs can invade dsDNA and form a new DNA·aegPNA duplex with its complementary DNA strand, causing the unpaired DNA strand to loop out (Nielsen and Christensen, 1996; Wittung et al., 1997); and (4) mixed pyrimidine-purine (T and G) aegPNAs can invade dsDNA to form a new DNA·aegPNA duplex (Wittung et al., 1997) and can also form aegPNA·DNA × aegPNA triplexes with ssDNA (Nielsen and Egholm, 2001). The ability of aegPNA to form

* Corresponding author. Tel.: +66 2218 7627x101; fax: +66 2218 7598.
** Corresponding author. Tel.: +65 6874 8420; fax: +65 6872 0785.
E-mail addresses: vtirayut@chula.ac.th (T. Vilaivan), xd-su@imre.a-star.edu.sg (X. Su).

0956-5663/$ – see front matter © 2010 Elsevier B.V. All rights reserved.
doi:10.1016/j.bios.2010.05.027

Author's personal copy

higher-order complexes is potentially useful for gene targeting and gene regulation (Mollegaard et al., 1994; Wang et al., 1999; Wang and Xu, 2004). Hence, an insight into the binding behaviors of aegPNA to dsDNA has potentially important clinical implications in the treatment of human diseases.

Previous studies on the formation of DNA- and aegPNA-related higher-order nucleic acid complexes have largely relied on traditional techniques, including thermal denaturation (T_m) measurement (Egholm et al., 1992; Nielsen and Christensen, 1996; Nielsen and Egholm, 2001), Job plot analysis or UV titration (Egholm et al., 1992; Nielsen and Christensen, 1996; Nielsen and Egholm, 2001), circular dichroism (CD) (Wittung et al., 1996, 1997), linear dichroism (LD) (Wittung et al., 1997), chemical probing (Nielsen et al., 1994) and electrophoretic mobility shift assays (EMSA) (Demidov et al., 1995; Demidov and Frank-Kamenetskii, 2001). These methods can confirm the specificity of binding and the formation of higher-order complexes. However, most of these techniques cannot be used alone to differentiate among the different binding modes. For example, EMSA cannot differentiate the stoichiometric composition of the higher-order complexes that have similar migration rates (e.g. between DNA·DNA × aegPNA triplexes and duplex invasion complexes). Furthermore, some of them have their own limitations. For example, T_m measurements are only suitable over a limited temperature range of 20–95 °C. Consequently, if the T_m of the complex is above 95 °C, it cannot simply be tested by heating.

Surface plasmon resonance (SPR) is a powerful technique that measures molecular interactions on the solid–liquid interface in real-time. The technique has been widely used to detect DNA·DNA (Peterlinz et al., 1997; Peterson et al., 2002; Mannelli et al., 2005; Su et al., 2005; Nakamura et al., 2006) and PNA·DNA hybridizations (Jensen et al., 1997; Burgener et al., 2000; Wittung-Stafshede et al., 2000; Höök et al., 2001; Arlinghaus et al., 2003, 2004; Feldner et al., 2003; Xu et al., 2008; Lao et al., 2009), but these studies have mostly been focused upon duplex formation only. In contrast, only a few studies have reported on the higher-order complexes between ssDNA and dsDNA (Bates et al., 1995; Asensio et al., 1998; Sugimoto et al., 2001), and the guanine (G) quadruplex structures of PNA and DNA using SPR (Lusvarghi et al., 2009).

Here, the use of the SPR technique to study the binding of PNA to dsDNA to form triplexes or duplex invasion complexes is reported for the first time. To establish the SPR assay protocols, and to validate the suitability of the solid–liquid phase measurement mode, we first used aegPNA and DNA sequences with known binding modes from their corresponding solution phase studies. Specifically, the homopyrimidine aegPNA [$(CT)_5$] and the homopurine aegPNA [$(GA)_5$] plus their respective target dsDNAs were chosen. The cytosine-rich homopyrimidine aegPNA is known to bind to dsDNA to form a DNA·DNA × aegPNA triplex, whilst the purine-rich aegPNA can invade dsDNA and hybridize with the complementary DNA strand to form a new DNA·aegPNA duplex, causing the unpaired DNA strand to form a displacement loop (D-loop) (Nielsen and Christensen, 1996; Wittung et al., 1997). Having established the SPR protocols to study triplex formation and the duplex invasion, the effects of pH and ionic strength on the complex formation and the direction of the PNA binding (parallel or antiparallel) were also evaluated. The correlation of the SPR results obtained here, with the published solution phase results in the literature, were used to validate the utility of the solid–liquid phase SPR assays.

PNA bearing a conformationally rigid D-prolyl-2-aminocyclopentane-carboxylic acid (ACPC) backbone (acpcPNA or pyrrolidinyl PNA) is a relatively new PNA system (Suparpprom et al., 2005; Vilaivan and Srisuwannaket, 2006) (Fig. 1), that has been shown to have at least a comparable, and in some cases a higher, binding affinity and sequence-specificity towards DNA than that of aegPNA (Ananthanawat et al., 2010). The high binding affinity and the powerful discrimination for single-mismatched DNA, together with the high directional specificity of acpcPNA render it a potential candidate for the development of highly effective DNA biosensors. The application of acpcPNA as a sensing probe for the detection of DNA hybridization and for highly specific SNP analysis have recently been demonstrated (Boontha et al., 2008; Korkaew and Vilaivan, 2008; Ananthanawat et al., 2009a,b; 2010). However, there are no studies on the higher-order complex formation of acpcPNA with dsDNA. Thus, the SPR protocols developed for aegPNAs were used to study the dsDNA binding properties of acpcPNA with the same sequences. This revealed the different abilities of aegPNA and acpcPNA to form higher-order complexes that may be attributable to their distinct backbone properties.

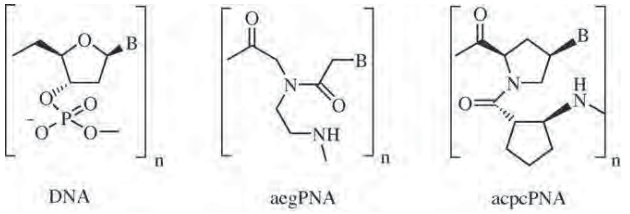

Fig. 1. Schematic representation of the structures of DNA, aegPNA, and acpcPNA (B = nucleobase A, T, C or G).

2. Materials and methods

2.1. Materials

Two 5′-biotinylated DNA (30 mer) sequences (**b-DNA1** and **b-DNA3**) and their complementary DNA (30 mer, unmodified) sequences (**DNA2** and **DNA4**) were purchased from Singapore-Proligo (Singapore), and used as received. The biotinylated strand **b-DNA1** (Biotin-5′-CGATTCGACT**$(AG)_5$**TACCGAGCTC-3′) and its fully complementary **DNA2** (5′-GAGCTCGGTA**$(CT)_5$**AGTCGAATCG-3′) were annealed to form a perfectly matched DNA duplex that carries a 10 bp target region in the middle for the PNA-$(CT)_5$ to bind and form a triplex in an antiparallel fashion. The biotinylated **b-DNA3** (Biotin-5′-GAGCTCGGTA**$(TC)_5$**AGTCGAATCG-3′) and its fully complementary **DNA4** (5′-CGATTCGACT**$(GA)_5$**TACCGAGCTC-3′) were annealed for studying the triplex formation in a parallel fashion with the PNA-$(CT)_5$ and also for studying the duplex invasion by the PNA-$(GA)_5$. The unmodified aegPNAs, i.e. $(GA)_5$ and $(CT)_5$, were obtained from Bio-Synthesis, Inc. (USA) and used without further purification. Streptavidin was purchased from Sigma. The acpcPNA-$(CT)_5$ and acpcPNA-$(GA)_5$ were synthesized at Chulalongkorn University (Thailand) following the reported protocol (Suparpprom et al., 2005; Vilaivan and Srisuwannaket, 2006).

2.2. Methods

2.2.1. SPR apparatus and surface preparation

SPR measurements were conducted using a double channel AutoLab ESPR (Eco Chemie, The Netherlands) at room temperature (25 °C). The gold SPR disk was first treated with UV/ozone plasma for 15 min followed by rinsing with ethanol and drying under a nitrogen stream prior to use. A mixture of 10% biotin–thiol and 90% hydroxyl–thiol at a net concentration of 1 mM, in water was then placed on the top of the freshly cleaned disks and incubated for 18 h (Su et al., 2004, 2005, 2008; Park et al., 2007; Ananthanawat et al., 2010). After rinsing with MilliQ water and drying with a gentle stream of nitrogen gas, the disk was seated in the SPR cell. After a stable baseline was recorded in 10 mM phosphate buffer (pH 7.4) containing 150 mM NaCl, streptavidin (0.1 mg/mL) was applied for 15 min for immobilization.

Author's personal copy

2.2.2. SPR measurement of PNA binding to dsDNA

The two DNA duplexes **b-DNA1·DNA2** or **b-DNA3·DNA4** were pre-annealed at a 1:3 molar ratio of biotinylated: unmodified DNA in 10 mM phosphate buffer, so as to ensure all b-DNA, and thus streptavidin bound DNA was dsDNA with little to no ssb-DNA. After annealing each DNA duplex, at 0.5 μM with respect to the biotinylated probes, was injected over the respective streptavidin immobilized surface for 10 min. After rinsing the surface to remove unbound ssDNA and dsDNA, the third PNA strand (1 μM) was applied and allowed to bind for 5 min. Phosphate buffer solutions (10 mM, pH 7.4 or 5.0) containing 50, 100 or 150 mM NaCl, as indicated, were used as the PNA binding or wash buffer, as indicated, to determine the effects of the pH and salt concentration on the complex formation. The SPR angle shifts, caused by dsDNA immobilization and the third PNA strand hybridization, were converted to the surface density of the dsDNA and the bound PNA using the mass conversion factor of 122 mDegrees per 100 ng/cm^2 (Su et al., 2005), and the MW of the dsDNA (in Da). The hybridization efficiency (% HE) was further calculated according to Eq. (1):

$$\%\mathrm{HE} = \left(\frac{\text{PNA density}}{\text{dsDNA density}}\right) \times 100 \quad (1)$$

3. Results and discussion

3.1. Detection of DNA·DNA × PNA triplex formation

Fig. 2 shows the schematic binding schemes of the higher-order complexes through either triplex formation (antiparallel and parallel fashions) or duplex invasion. To study the ability of aegPNA-$(CT)_5$ to form a DNA·DNA × aegPNA triplex in an antiparallel fashion (with respect to the central purine strand), the ds(**b-DNA1·DNA2**) was first immobilized on a streptavidin-modified surface. The use of a 1:3 molar ratio excess of the nonbiotinylated **DNA2** to the biotinylated **b-DNA1** in the annealing was to ensure that there was no remaining free **b-DNA1** in the solution, and hence all immobilized DNAs were in the form of dsDNA. Fig. 3 depicts a typical SPR sensorgram showing the immobilization of dsDNA of **b-DNA1·DNA2**, followed by aegPNA-$(CT)_5$ binding in phosphate buffer solutions of pH 7.4 and 5.0, containing 150 mM NaCl. The immobilization of the dsDNA over the surface yielded an SPR angle shift of 121.6 mDegrees (Fig. 3, Part I), which corresponds to a surface density of 3.19×10^{12} dsDNA molecules/cm^2 (molecular weight of the dsDNA is 18,821 Da). The subsequent injection of aegPNA-$(CT)_5$ in the pH 7.4 buffer solution yielded no significant SPR angle shift, indicating that no binding of the aegPNA strand to the dsDNA occurred. Previous studies using circular dichroism (CD) have indicated that binding of a cytosine-rich pyrimidine aegPNA to a dsDNA to form a triplex requires a lower pH (Wittung et al., 1997). To confirm this binding rule, in the successive experiment, the aegPNA-$(CT)_5$ was allowed to interact with the ds(**b-DNA1·DNA2**) at pH 5.0. Five minutes after the interaction, an increase in the SPR angle of 20.4 mDegrees was obtained, indicating the successful binding of the PNA, presumably through triplex formation in an antiparallel fashion (i.e. 5′- or *N*-terminus of the aegPNA binds to the 3′-terminus of its complementary homopurine DNA strand). It has been reported for solution phase complex formation that cytosine-rich pyrimidine PNAs (T–C sequences) containing triplexes consist entirely of T·A × T and C·G × C$^+$ triplexes, where the T·A and C·G pair *via* Watson–Crick base pairing and the A × T and G × C$^+$ interact *via* Hoogsteen base pairing. A lower pH of 5.0 is required to stabilize the C·G × C$^+$ triplexes because the Hoogsteen base pairing involves protonated cytosine bases (Egholm et al., 1992; Wittung et al., 1997). The confirmation of the pH dependence of the triplex formation using SPR analysis (Fig. 3) validates our SPR protocol and

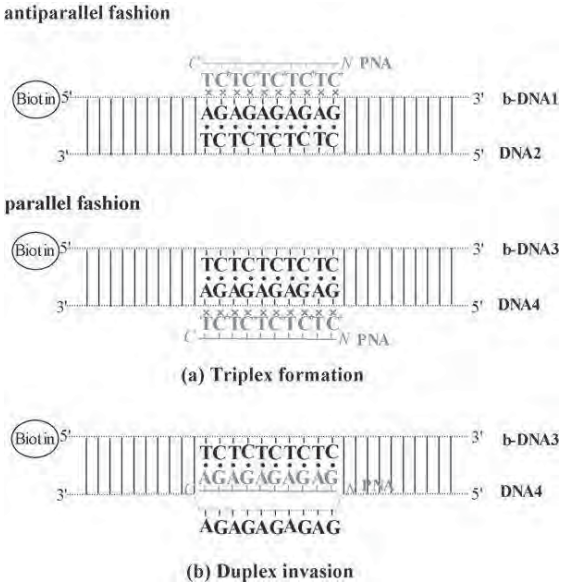

Fig. 2. Schematic illustration of PNA binding modes to dsDNA. (a) Triplex formation of ds(**b-DNA1·DNA2**) × [PNA-$(CT)_5$] (antiparallel fashion) and ds(**b-DNA3·DNA4**) × [PNA-$(CT)_5$] (parallel fashion). (b) Duplex invasion of ds(**b-DNA3·DNA4**) by PNA-$(GA)_5$.

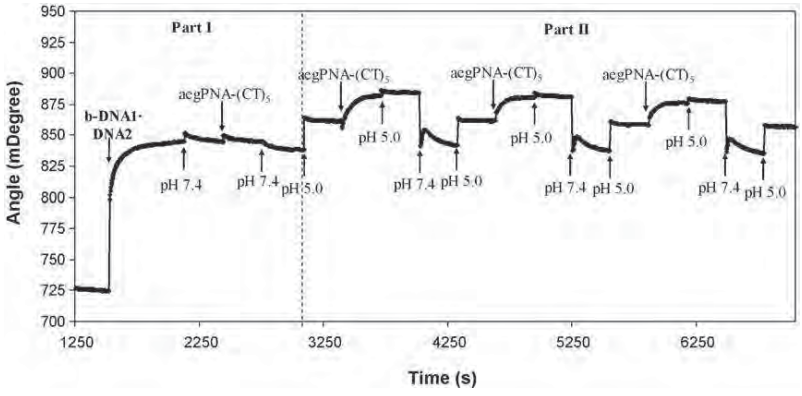

Fig. 3. Triplex formation in an antiparallel fashion: representative SPR responses to the sequential reaction steps of (Part I) ds(**b-DNA1·DNA2**) immobilization over the streptavidin-immobilized surface and addition of 1 μM aegPNA-$(CT)_5$ in pH 7.4 phosphate buffer with 150 mM NaCl to attempt the hybridization with the immobilized ds(**b-DNA1·DNA2**), and (Part II) three consecutive hybridizations in pH 5.0/dehybridizations in pH 7.4 cycles of 1 μM aegPNA-$(CT)_5$ with ds(**b-DNA1·DNA2**).

Author's personal copy

supports the potential utility of the solid–liquid phase measurement method.

Since the triplex formation is pH sensitive with an acidic pH (5.0) being required to form the Hoogsteen pairing bonds, we anticipated that raising the pH may affect the stability of the preformed triplex. To confirm our speculation, the SPR surface carrying the DNA·DNA × aegPNA triplex formed at pH 5.0 was rinsed with phosphate buffer containing 150 mM NaCl at pH 5.0 or pH 7.4, as indicated, for 5 min. As expected, washing in pH 7.4, but not pH 5.0, buffer essentially returned the SPR signal to the original baseline before the injection of the aegPNA-$(CT)_5$ (Fig. 3, Part II), which indicates the complete dissociation of the PNA strand from the dsDNA-immobilized surface. The dissociation of the PNA strand could be explained by the deprotonation of the cytosine base ($pK_a = 6.2$) back to its neutral form at pH 7.4 (Ahmed et al., 1994). The pH controlled triplex hybridization/dehybridization cycle was repeated to confirm the pH dependence of the triplex formation and also to assess the reproducibility of the SPR measurement and/or the reusability of the immobilized dsDNA. As can be seen from the repeated measurement cycles (Fig. 3, Part II) the hybridization/dehybridization of the aegPNA-$(CT)_5$ with surface-immobilized dsDNA occurred reversibly upon switching of the buffer solutions between pH 5.0 and 7.4. After three consecutive cycles, the PNA binding signal strength had only marginally if at all decreased indicating a good potential reproducibility of the triplex formation on the SPR surface. The average SPR angle shift of the PNA binding over the three cycles was 19.4 ± 0.7 mDegrees, corresponding to a PNA surface density of 3.50×10^{12} molecules/cm^2. Referring to the surface density of the immobilized dsDNA of 3.19×10^{12} molecules/cm^2, a ~100% HE (calculated according to Eq. (1)) was obtained. This strongly supports that the stoichiometric molar ratio of the aegPNA-$(CT)_5$ to dsDNA was 1:1 and that the immobilized dsDNA is completely hybridized with the aegPNA strands. Thus, the SPR measurement appears to offer convenient opportunities for studying the conditions required for triplex formation and the efficiency and/or the stoichiometry of the triplex formation, at least under these conditions.

To further validate the reliability of the SPR based measurement of triplex formation, a negative control PNA sequence (aegPNA-TTCTTCTTTT) that is non complementary to the ds(**b-DNA1·DNA2**) was tested. In addition, to further extend the triplex binding study to our synthetic acpcPNA, the binding of acpcPNA-$(CT)_5$ was also tested. In between each cycle of PNA injection, pH 7.4 buffer solution was used to rinse the surface to dissociate the bound PNA (if there was any). The sequential injection of aegPNA-$(CT)_5$ (positive control), acpcPNA-$(CT)_5$ and aegPNA-TTCTTCTTTT (negative control) over the immobilized dsDNA at pH 5.0 resulted in no significant SPR angle shift being detected for both for the acpcPNA-$(CT)_5$ and the negative control, aegPNA-TTCTTCTTTT (Fig. 4). These results indicate that, unlike the aegPNA-$(CT)_5$, the acpcPNA-$(CT)_5$ showed very little binding to its complementary dsDNA, supporting the notion that the triplex formation between aegPNA-$(CT)_5$ and dsDNA is sequence–structure specific.

In addition to the antiparallel fashion formation of triplex DNA illustrated above, triplex formation in a parallel fashion (i.e. 5′- or *N*-terminus of PNA facing the 5′-terminus of the purine DNA strand), was also tested. In this parallel hybridization experiment, the DNA duplex ds(**b-DNA3·DNA4**) was immobilized on the streptavidin layer instead of the ds(**b-DNA1·DNA2**). A typical SPR sensorgram obtained from the sequential injections of aegPNA-$(CT)_5$, acpcPNA-$(CT)_5$ and aegPNA-TTCTTCTTTT (negative control) over the immobilized ds(**b-DNA3·DNA4**) at pH 5.0 followed by rinsing with pH 7.4 buffer is shown in Fig. S1. The hybridization of aegPNA-$(CT)_5$ in a parallel fashion resulted in a nearly 100% hybridization efficiency, the same as that observed in the antiparallel fashion. This means that aegPNA can bind to its complementary dsDNA strand in both an antiparallel and a parallel fashion. In contrast, no significant SPR angle shift was detected for both acpcPNA-$(CT)_5$ and the negative control, aegPNA-TTCTTCTTTT. Again, unlike the aegPNA-$(CT)_5$, acpcPNA-$(CT)_5$ failed to bind to its complementary dsDNA in a parallel fashion, but rather the triplex formation in parallel fashion of aegPNA-$(CT)_5$ is also sequence–structure specific.

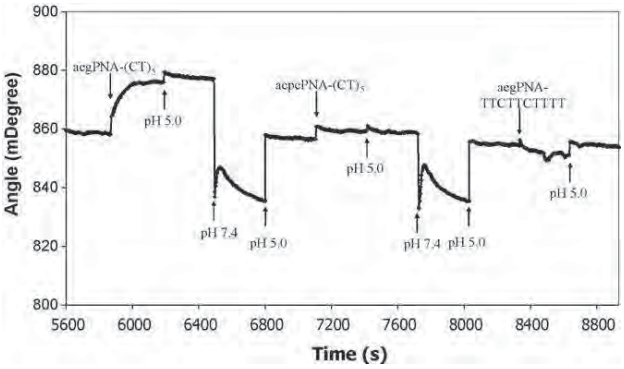

Fig. 4. Triplex formation in an antiparallel fashion: representative SPR responses obtained from three consecutive hybridization/dehybridization cycles of aegPNA-$(CT)_5$, acpcPNA$(CT)_5$ or aegPNA-TTCTTCTTTT (all at 1 μM) with the streptavidin immobilized ds(**b-DNA1·DNA2**) by switching the phosphate buffer pH between 5.0 and 7.4.

3.2. Detection of DNA duplex invasion by PNA

To study the duplex invasion of dsDNA by homopurine $(GA)_5$ PNAs (see Fig. 2b for schematic illustration), the pre-annealed dsDNA (**b-DNA3·DNA4**) was immobilized on the SPR surface with streptavidin as described above. An increase in the SPR angle shift of 136.4 mDegrees was obtained after the immobilization of the ds(**b-DNA3·DNA4**) (SPR curves not shown), corresponding to a surface coverage of 3.58×10^{12} dsDNA molecules/cm^2. Successive injections of the aegPNA-$(GA)_5$ or acpcPNA-$(GA)_5$ in the 10 mM phosphate buffer (pH 7.4) containing 150 mM NaCl, resulted in no significant SPR angle shift, indicating no detectable binding of the PNA to the dsDNA. This result is not surprising since it is well known that the strand invasion of PNA (particularly aegPNA) to its complementary dsDNA is inhibited at high salt concentrations (Wittung et al., 1996; Bentin et al., 2002; Abibi et al., 2004). To determine the effect of NaCl concentration on the occurrence of duplex invasion, 10 mM phosphate buffer (pH 7.4) supplemented with NaCl at 50, 100 or 150 mM were evaluated as the binding buffer. With the target ds(**b-DNA3·DNA4**), no hybridization was detectable for the aegPNA-$(GA)_5$ at 150 mM NaCl, as mentioned earlier, but when the NaCl concentration was decreased to 100 mM, a steady SPR angle shift of 6.2 ± 0.6 mDegrees was obtained, corresponding to a PNA density of 1.03×10^{12} molecules/cm^2, or a hybridization efficiency of 29% (Fig. 5). Decreasing the NaCl concentration further to 50 mM increased the SPR angle shift to 22.9 ± 1.9 mDegrees (PNA surface density 3.79×10^{12} molecules/cm^2), representing a hybridization efficiency of ~100% and suggesting a 1:1 stoichiometric binding of aegPNA-$(GA)_5$ to the dsDNA. From the above results, it can be concluded that a low salt concentration is essential for the invasion of homopurine aegPNA to its complementary dsDNA. This observation derived here from the SPR technique is consistent with that already reported using circular dichroism (CD) (Wittung et al., 1997). Indeed, it is well known that duplex invasion occurs when the PNA breaks the Watson–Crick pairs between the dsDNA and then pairs to the complementary DNA strand, whereas the non complementary DNA strand forms a stable displacement loop (D-loop). These processes can be facilitated at low ionic strength conditions when the DNA duplex has a weaker binding affinity and

Author's personal copy

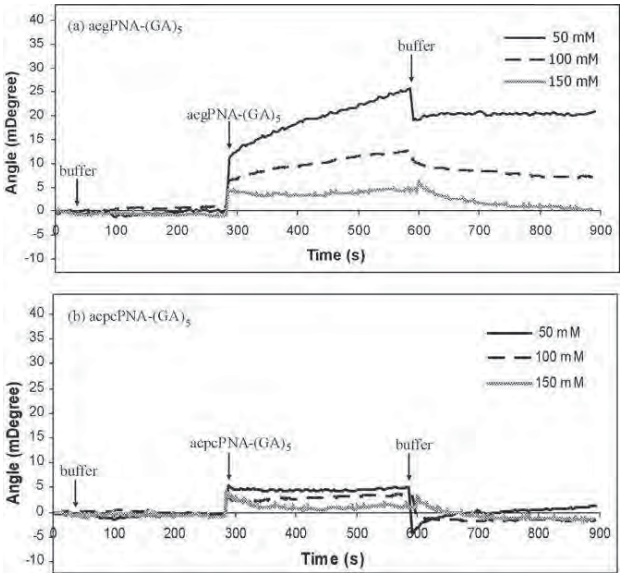

Fig. 5. Duplex invasion: a representative overlay plot of the SPR responses obtained from the hybridization of (a) aegPNA-$(GA)_5$ and (b) acpcPNA-$(GA)_5$ with ds(**b-DNA3**·**DNA4**) -immobilized surface in 10 mM phosphate buffer of pH 7.4 containing different amount of NaCl (50, 100 and 150 mM).

so the displacement of the non complementary strand can occur more easily.

The higher-order complexes formed from the triplex binding and duplex invasion have the same stoichiometry (1:1 molar ratio) and chemical composition (aegPNA and not acpcPNA). The measurement of the binding kinetics (Wittung et al., 1997) using CD and the evaluation of the activation energies (E_a) have been used to differentiate the two binding modes. The E_a for the binding reaction of A–G sequences by duplex invasion is higher than that of T–C sequences for triplex formation, which supports the hypothesis that the opening of the dsDNA is a critical step in, and affecting the rate of, duplex invasion. Taking advantage of the real-time measurement ability of the SPR technique, an assessment of the binding kinetics of the aegPNA-$(GA)_5$ to the ds(**b-DNA3**·**DNA4**) (through double strand invasion), compared to that with the single stranded **b-DNA3** (through direct duplex formation) as a reference was performed (Fig. S2). Both aegPNA-$(GA)_5$ and acpcPNA-$(GA)_5$ could bind to the single stranded (**b-DNA3**) over a wide range of salt concentrations (the example shown in Fig. S2 is in 150 mM NaCl); and the binding which involved direct duplex formation was much faster than the binding to ds(**b-DNA3**·**DNA4**). This strongly supports that in the strand invasion mode there is an additional energy barrier to be overcome in order to break the Watson–Crick bonds that, as a consequence, leads to a slower binding of PNA.

To further confirm that the aegPNA-$(GA)_5$ binding to ds(**b-DNA3**·**DNA4**) is through double strand invasion, rather than triplex formation, we treated the preformed complex with phosphate buffer pH 7.4 containing 150 mM NaCl (the solution that was used to dissociate the pyrimidine aegPNA-$(CT)_5$ from the DNA·DNA × aegPNA triplex). However, at the end of the 5 min treatment period, no obvious loss of the third strand was observed (Fig. 6). This is in contrast to the DNA·DNA × PNA triplex formed by the PNA-$(CT)_5$, where this near-neutral pH wash readily dissociated the PNA strand bound through Hoogsteen base pairing (Fig. 3, part II and Fig. 4). The retention of the aegPNA-$(GA)_5$ in this case strongly supports the assumption that the PNA-$(GA)_5$ binds the dsDNA through duplex invasion *via* Watson–Crick pairing, which is stable in pH 7.4 buffer solution. Combining the results for the pyrimidine PNA-$(CT)_5$ and the purine PNA-$(GA)_5$, we conclude that comparison of the SPR sensorgrams from the two different buffers (pH 5 and 7.4) can be used to distinguish duplex invasion from triplex formation of PNA with the corresponding dsDNA.

Next, the ability of the synthetic acpcPNA-$(GA)_5$ to invade dsDNA was investigated. It was found that the acpcPNA-$(GA)_5$ failed to invade into the dsDNA under all three NaCl concentrations tested in 10 mM phosphate buffer pH 7.4 (Fig. 5b). The inability of the homopyrimidine acpcPNA to form a triplex is not totally unexpected considering the relative bulkiness of the backbone. Unlike homopyrimidine aegPNA, which readily forms very stable triplexes with ssDNA and dsDNA in solutions, the analogous triplexes consisting of acpcPNA have not been observed (Suparpprom et al., 2005; Vilaivan and Srisuwannaket, 2006). On the other hand, in view of the high affinity of the acpcPNA towards ssDNA relative to aegPNA (Ananthanawat et al., 2010), it was quite surprising to observe that the invasion of acpcPNA was unsuccessful. This may imply the slow kinetics of duplex invasion by acpcPNA, perhaps due to the lower conformational flexibility of the acpcPNA backbone that may deplete its ability to find the complementary region that is in the center of the immobilized dsDNA.

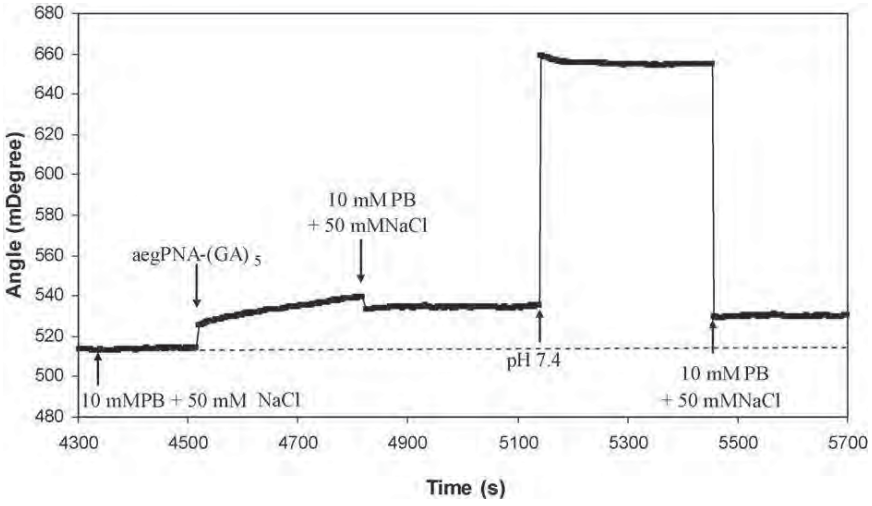

Fig. 6. Duplex invasion: representative SPR responses obtained from the hybridization of aegPNA-$(GA)_5$ with ds(**b-DNA3**·**DNA4**)-immobilized surface in 10 mM phosphate buffer of pH 7.4 containing 50 mM NaCl. The as-formed complex is successively treated by the pH 7.4 phosphate buffer containing 150 mM NaCl to test the stability of the bound PNA, so as to verify the aegPNA-$(GA)_5$ binding mode.

Author's personal copy

4. Conclusions

We have developed SPR assay based protocols for studying the binding of PNAs to dsDNA. The solid–liquid phase binding characteristics of the conventional aegPNA (i.e., sequence rule, directionality, and binding modes under different conditions.) correlate well with those obtained from the solution phase studies. Particularly, with the real-time SPR quantification, the sequence specificity, direction of PNA binding, and the hybridization efficiency of the aegPNA as a third strand can be evaluated. With an appropriate treatment of the preformed higher-order complexes with selected buffer solutions, and thereafter an observation of the stability of the bound aegPNA, we can distinguish the binding modes, in terms of triplex formation and duplex invasion, which is difficult to achieve using traditional techniques, such as EMSA. While having many advantages for studying PNA-dsDNA bindings, as demonstrated using aegPNA (real-time, rapid measurements of sequence-dependent formation of high order complexes of different models, possibilities of direct quantification of binding strength and kinetics), the solid–liquid phase measurement nature may render the SPR results for PNA′s with a more rigid backbone less straightforward when compared to traditional liquid phase methods. Indeed, we observed that, unlike the conventional aegPNA, the conformationally rigid acpcPNA was not capable of binding to its complementary dsDNA by either triplex formation or duplex invasion in the SPR measurement. Whether this is due to the spatial constraint of the immobilized dsDNA, and how this result correlates with the liquid phase binding when both PNA and dsDNA are freely accessible, will be the subject of further studies.

Acknowledgements

Financial support for this work is acknowledged from the Thailand Research Fund through the Royal Golden Jubilee Ph.D. Program (Grant No. PHD/0192/2550) (awarded to CA and VPH), the TRF Senior Research Scholar Grant (RTA5280002 to TV and VPH), and the Institute of Materials Research and Engineering (to XS). We also thank Dr. Robert Butcher of Publication Counselling Unit (PCU), Faculty of Science, Chulalongkorn University, for language editing.

Appendix A. Supplementary data

Supplementary data associated with this article can be found, in the online version, at doi:10.1016/j.bios.2010.05.027.

References

Abibi, A., Protozanova, E., Demidov, V.V., Frank-Kamenetskii, M.D., 2004. Biophys. J. 86, 3070–3078.
Ahmed, S., Kintanar, A., Henderson, E., 1994. Nat. Struct. Biol. 1, 83–88.
Ananthanawat, C., Vilaivan, T., Hoven, V.P., 2009a. Sens. Actuators B: Chem. 137, 215–221.
Ananthanawat, C., Vilaivan, T., Mekboonsonglarp, W., Hoven, V.P., 2009b. Biosens. Bioelectron. 24, 3544–3549.
Ananthanawat, C., Vilaivan, T., Hoven, V.P., Su, X.D., 2010. Biosens. Bioelectron. 25, 1064–1069.
Arlinghaus, H.F., Ostrop, M., Friedrichs, O., Feldner, J.C., 2003. Appl. Surf. Sci. 203–204, 689–692.
Arlinghaus, H.F., SchrÖder, M., Feldner, J.C., Brandt, O., Hoheisel, J.D., Lipinsky, D., 2004. Appl. Surf. Sci. 231–232, 392–396.
Asensio, J.L., Dosanjh, H.S., Jenkins, T.C., Lane, A.N., 1998. Biochemistry 37, 15188–15198.
Bates, P.J., Dosanjh, H.S., Kumar, S., Jenkins, T.C., Laughton, C.A., Neidle, S., 1995. Nucleic Acids Res. 23, 3627–3632.
Bentin, T., Hansen, G.I., Nielsen, P.E., 2002. Methods Mol. Biol. 208, 91–107.
Boontha, B., Nakkuntod, J., Hirankarn, N., Chaumpluk, P., Vilaivan, T., 2008. Anal. Chem. 80, 8178–8186.
Burgener, M., Sanger, M., Candrian, U., 2000. Bioconj. Chem. 11, 749–754.
Chin, J.Y., Glazer, P.M., 2008. Mol. Carcinog. 48, 389–399.
Demidov, V.V., Yavnilovich, M.V., Belotserkovskii, B.P., Frank-Kamenetskii, M.D., Nielsen, P.E., 1995. Proc. Natl. Acad. Sci. U.S.A. 92, 2637–2641.
Demidov, V.V., Frank-Kamenetskii, M.D., 2001. Methods 23, 108–122.
Egholm, M., Nielsen, P.E., Buchardt, O., Berg, R.H., 1992. J. Am. Chem. Soc. 114, 1895–1897.
Egholm, M., Buchardt, O., Christensen, L., Behrens, C., Freier, S.M., Driver, D.A., Berg, R.H., Kim, S.K., Nordén, B., Nielsen, P.E., 1993. Nature 365, 566–568.
Feldner, J.C., Ostrop, M., Friedrichs, O., Sohn, S., Lipinsky, D., 2003. Appl. Surf. Sci. 203–204, 722–725.
Felsenfeld, G., Rich, A., 1957. Biochim. Biophys. Acta 26, 457–468.
Frank-Kamenetskii, M.D., Mirkin, S.M., 1995. Annu. Rev. Biochem. 64, 65–95.
Höök, F., Ray, A., Nordén, B., Kasemo, B., 2001. Langmuir 17, 8305–8312.
Jensen, K.K., Örum, H., Nielsen, P.E., Nordén, B., 1997. Biochemistry 36, 5072–5077.
Korkaew, P., Vilaivan, T., 2008. Nucleic Acids Symp. Ser. 52, 251–252.
Lao, A.I.K., Su, X.D., Aung, K.M.M., 2009. Biosens. Bioelectron. 24, 1717–1722.
Lusvarghi, S., Murphy, C.T., Roy, S., Tanious, F.A., Sacui, I., Wilson, W.D., Ly, D.H., Armitage, B.A., 2009. J. Am. Chem. Soc. 131, 18415–18424.
Mannelli, I., Minunni, M., Tombelli, S., Wang, R., Spiriti, M.M., Mascini, M., 2005. Bioelectrochemistry 66, 129–138.
Mollegaard, N.E., Buchardt, O., Egholm, M., Nielsen, P.E., 1994. Proc. Natl. Acad. Sci. U.S.A. 91, 3892–3895.
Nakamura, F., Ito, E., Hayashi, T., Hara, M., 2006. Colloids Surf. A 284–285, 495–498.
Nielsen, P.E., Egholm, M., Berg, R.H., Buchardt, O., 1991. Science 254, 1497–1500.
Nielsen, P.E., Egholm, M., Buchardt, O., 1994. J. Mol. Recognit. 7, 165–170.
Nielsen, P.E., Christensen, L., 1996. J. Am. Chem. Soc. 118, 2287–2288.
Nielsen, P.E., Egholm, M., 2001. Bioorg. Med. Chem. 9, 2429–2434.
Park, H., Germini, A., Sforza, S., Corradini, R., Marchelli, R., Knoll, W., 2007. Biointerphases 2, 80–88.
Peterlinz, K.A., Georgiadis, R.M., Herne, T.M., Tarlov, M.J., 1997. J. Am. Chem. Soc. 119, 3401–3402.
Peterson, A.W., Wolf, L.K., Georgiadis, R.M., 2002. J. Am. Chem. Soc. 124, 14601–14607.
Su, X.D., Robelek, R., Wu, Y., Wang, G., Knoll, W., 2004. Anal. Chem. 76, 489–494.
Su, X.D., Wu, Y.J., Knoll, W., 2005. Biosens. Bioelectron. 21, 719–726.
Su, X.D., Teh, H.F., Aung, K.M.M., Zong, Y., Gao, Z., 2008. Biosens. Bioelectron. 23, 1715–1720.
Sugimoto, N., Wu, P., Hara, H., Kawamoto, Y., 2001. Biochemistry 40, 9396–9405.
Suparpprom, C., Srisuwannaket, C., Sangvanich, P., Vilaivan, T., 2005. Tetrahedron Lett. 46, 2833–2837.
Vilaivan, T., Srisuwannaket, C., 2006. Org. Lett. 8, 1897–1900.
Wang, G., Xu, X., Pace, B., Dean, D.A., Glazer, P.M., Chan, P., Goodman, S.R., Shokolenko, I., 1999. Nucleic Acids Res. 27, 2806–2813.
Wang, G., Xu, X.S., 2004. Cell Res. 14, 111–116.
Wittung, P., Nielsen, P., Nordén, B., 1996. J. Am. Chem. Soc. 118, 7049–7054.
Wittung, P., Nielsen, P., Nordén, B., 1997. Biochemistry 36, 7973–7979.
Wittung-Stafshede, P., Rodahl, M., Kasemo, B., Nielsen, P., Norden, B., 2000. Colloids Surf. A. 174, 269–273.
Xu, F., Pellino, A.M., Knoll, W., 2008. Thin Solid Films 516, 8634–8639.

This article was downloaded by: *[2007 - 2008-2009 Chulalongkorn University]*
On: *14 March 2011*
Access details: *Access Details: [subscription number 780894003]*
Publisher *Taylor & Francis*
Informa Ltd Registered in England and Wales Registered Number: 1072954 Registered office: Mortimer House, 37-41 Mortimer Street, London W1T 3JH, UK

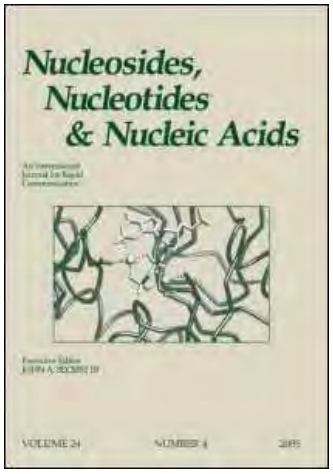

Nucleosides, Nucleotides and Nucleic Acids
Publication details, including instructions for authors and subscription information:
http://www.informaworld.com/smpp/title~content=t713597286

Synthesis and Nucleic Acids Binding Properties of Diastereomeric Aminoethylprolyl Peptide Nucleic Acids (*aep*PNA)

Patcharee Ngamwiriyawong[a]; Tirayut Vilaivan[a]
[a] Organic Synthesis Research Unit, Department of Chemistry, Faculty of Science, Chulalongkorn University, Bangkok, Thailand

Online publication date: 24 February 2011

To cite this Article Ngamwiriyawong, Patcharee and Vilaivan, Tirayut(2011) 'Synthesis and Nucleic Acids Binding Properties of Diastereomeric Aminoethylprolyl Peptide Nucleic Acids (*aep*PNA)', Nucleosides, Nucleotides and Nucleic Acids, 30: 2, 97 — 112
To link to this Article: DOI: 10.1080/15257770.2010.547839
URL: http://dx.doi.org/10.1080/15257770.2010.547839

PLEASE SCROLL DOWN FOR ARTICLE

Full terms and conditions of use: http://www.informaworld.com/terms-and-conditions-of-access.pdf

This article may be used for research, teaching and private study purposes. Any substantial or systematic reproduction, re-distribution, re-selling, loan or sub-licensing, systematic supply or distribution in any form to anyone is expressly forbidden.

The publisher does not give any warranty express or implied or make any representation that the contents will be complete or accurate or up to date. The accuracy of any instructions, formulae and drug doses should be independently verified with primary sources. The publisher shall not be liable for any loss, actions, claims, proceedings, demand or costs or damages whatsoever or howsoever caused arising directly or indirectly in connection with or arising out of the use of this material.

Nucleosides, Nucleotides and Nucleic Acids, 30:97–112, 2011
Copyright © Taylor and Francis Group, LLC
ISSN: 1525-7770 print / 1532-2335 online
DOI: 10.1080/15257770.2010.547839

Downloaded By: [2007 - 2008-2009 Chulalongkorn University] At: 11:09 14 March 2011

SYNTHESIS AND NUCLEIC ACIDS BINDING PROPERTIES OF DIASTEREOMERIC AMINOETHYLPROLYL PEPTIDE NUCLEIC ACIDS (*aep*PNA)

Patcharee Ngamwiriyawong and Tirayut Vilaivan
Organic Synthesis Research Unit, Department of Chemistry, Faculty of Science, Chulalongkorn University, Bangkok, Thailand

□ *A general synthetic method for Fmoc-protected monomers of all four diastereomeric aminoethyl peptide nucleic acid (*aep*PNA) has been developed. The key reaction is the coupling of nucleobase-modified proline derivatives and Fmoc-protected aminoacetaldehyde by reductive alkylation. Oligomerization of the* aep*PNAs up to 10mer was achieved by Fmoc-solid phase peptide synthesis methodology. Preliminary binding studies of these* aep*PNA oligomers with nucleic acids suggested that the "*cis*-" homothymine* aep*PNA decamers with (2′*R*,4′*R*) and (2′*S*,4′*S*) configurations can bind, albeit with slow kinetics, to their complementary RNA [poly(adenylic acid)] but not to the complementary DNA [poly(deoxyadenylic acid)]. On the other hand, the* trans *homothymine* aep*PNA decamers with (2′*R*,4′*S*) and (2′*S*,4′*R*) configurations failed to form stable hybrid with poly(adenylic acid) and poly(deoxyadenylic acid). No hybrid formation could be observed between a mixed-base (2′*R*,4′*R*)-*aep*PNA decamer with DNA and RNA in both antiparallel and parallel orientations.*

Keywords PNA; RNA; hybridization; triplex forming oligonucleotides

INTRODUCTION

Peptide nucleic acid is a structural mimic of DNA that exhibits interesting base-pairing properties.[1] Since the first introduction of aminoethylglycyl (*aeg*) PNA in 1991,[2] a number of modifications of the original *aeg*PNA backbone have been proposed with the aim to improve certain properties such as binding affinity, solubility and cell penetration. A considerable success has been made by restriction of the original *aeg*PNA conformations by incorporating one or more ring structures in the backbone.[3,4] Some of these conformationally restricted PNA exhibited comparable or even

Received 12 October 2010; accepted 10 December 2010.
Financial support for this work comes from the Thailand Research Fund (RTA5280002) and Chulalongkorn University (Rachadapisek Sompoj Endowment to OSRU).
Address correepondence to Tirayut Vilaivan, Organic Synthesis Research Unit, Department of Chemistry, Faculty of Science, Chulalongkorn University, Phayathai Road, Patumwan, Bangkok 10330, Thailand. E-mail: vtirayut@chula.ac.th

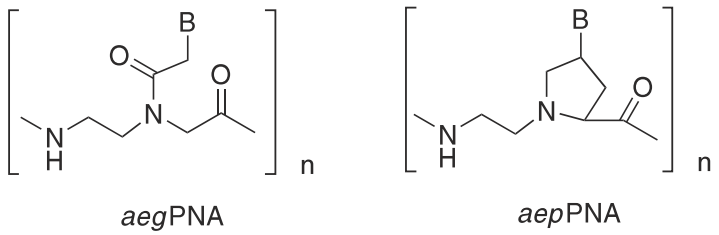

*aeg*PNA *aep*PNA

FIGURE 1 Structures of *aeg*PNA and *aep*PNA (stereochemistry not shown).

Downloaded By: [2007 - 2008-2009 Chulalongkorn University] At: 11:09 14 March 2011

stronger affinity to DNA and/or RNA, while the high specificity of the base-pairing was still retained. Furthermore, few modified PNA even possess extra features not present in the original Nielsen's *aeg*PNA such as preference for binding to DNA in one specific direction and preferential binding to specific types of nucleic acids (DNA or RNA)[5–7].

Since 1999, at least three research groups have independently reported syntheses and hybridization studies of a new conformationally constrained and positively charged PNA known as aminoethylprolyl PNA (*aep*PNA, Figure 1). The presence of a positive charge on the non-acylated pyrrolidine nitrogen atom ($pK_a \sim 6.5$)[8] in the PNA backbone could potentially improve the solubility and binding affinity to DNA, which is negatively charged. D'Costa and coworkers have studied two of the four possible stereoisomers of *aep*PNA. They reported that the homothymine *aep*PNA octamer with (2′*S*,4′*S*) and (2′*R*,4′*S*) stereochemistry formed very stable $(PNA)_2$·DNA triplexes with their complementary DNA ($T_m > 80°C$).[8] They also reported a site-specific incorporation of *aep*PNA monomers into Nielsen's *aeg*PNA oligomers by solid phase synthesis. These chimeric *aeg*-*aep*PNAs were shown to have improved antiparallel *vs* parallel directional selectivity toward DNA compared to the unmodified *aeg*PNA, while the binding affinity and specificity was retained.[9,10] Liu and coworkers reported the synthesis of nonchimeric *aep*PNA oligomers with (2′*S*,4′*S*) stereochemistry.[11] In contrast to earlier findings,[8] The non-chimeric homothymine and mixed-sequence *aep*PNA showed no detectable binding with complementary DNA according to UV melting and titration.[11] Our study on *aep*PNA oligomer with a different stereochemistry, namely (2′*R*,4′*R*), revealed that the homothymine *aep*PNA decamer forms a fairly stable hybrid with complementary RNA, whereas no binding to the complementary DNA could be observed.[12]

The hybridization properties of *aep*PNA oligomers reported so far showed some discrepancies, which may be sequence and stereochemistry dependent. None of these research groups has yet synthesized all four possible stereoisomers and perform a systematic comparison under identical conditions. In addition, work from other groups involving *aep*PNA mostly emphasized on its DNA binding properties. In view of our previous success in developing a PNA that binds preferentially to DNA,[5,6] it would be desirable to have an alternative PNA system that binds favorably, or at least

equally well, to RNA. These RNA binding PNAs would have a great potential in antisense applications.[1] Toward this goal, a general synthetic route toward the PNA momomers and oligomers first needs to be developed. In this paper, we report a successful synthesis of all four stereoiosomers of Fmoc-protected *aep*PNA monomers employing a new reductive alkylation strategy. We also report a synthesis of the *aep*PNA up to 10mer from these monomers as well as a preliminary binding study between these diastereomeric *aep*PNA oligomers and DNA/RNA.

Downloaded By: [2007 - 2008-2009 Chulalongkorn University] At: 11:09 14 March 2011

RESULTS AND DISCUSSION

Synthesis of Monomers

Ganesh[8,9] and Lui[11] had previously developed a method for the synthesis of Boc-protected *aep*PNA monomers. *N*-alkylation of 4-hydroxyproline esters with *N*-Boc-bromoethylamine afforded *N*-(*N*-Boc-aminoethyl)hydroxyproline intermediates in 60–68% yield. These hydroxyl compounds were activated by mesylation and then displaced with an appropriately protected nucleobase to give the *N*-Boc protected *aep*PNA monomers in moderate yields. In our previous report, a different approach had been taken whereby a nucleobase-modified proline was *N*-alkylated with *N*-nosylaziridine.[12] Exchanging the *N*-protecting groups from nosyl to Fmoc via the Boc-protected intermediate provided the expected monomers. These methods, however, suffer from providing low yield and require many steps.

Reductive alkylation of amino acids by *N*-protected aminoaldehydes in the presence of $NaBH_3CN$ had been widely used in the synthesis of *N*-aminoethylated amino acids, including *aeg*PNA monomers.[13–16] We proposed that the reductive alkylation of nucleobase-substituted proline with *N*-Fmoc-aminoacetaldehyde should directly provide the Fmoc-protected *aep*PNA monomers without the need for protecting group conversion (Scheme 1).

N-Fmoc-aminoacetaldehyde (**1**) was easily prepared in two steps with 90% overall yield from $NaIO_4$ oxidation of 3-amino-1,2-propanediol.[16,17] The Boc group in the *N*-Boc thymine-modified proline derivative (**2a**) was selectively removed in the presence of the diphenylmethyl ester by treatment with 3 equivalents of *p*-toluenesulfonic acid (*p*-TsOH) in acetonitrile at ambient temperature.[18] The reductive alkylation of the free amine with **1** took place in the presence of $NaBH_3CN$ as a reductant and NaOAc as a buffering agent. The desired product (**3a**) was obtained as a white foam in 76% overall yield (two steps from **2a** and **1**). Spectroscopic data of the product were identical to those of the same compound obtained *via* alkylation with aziridine followed by protecting group conversion.[12] Other Boc-protected

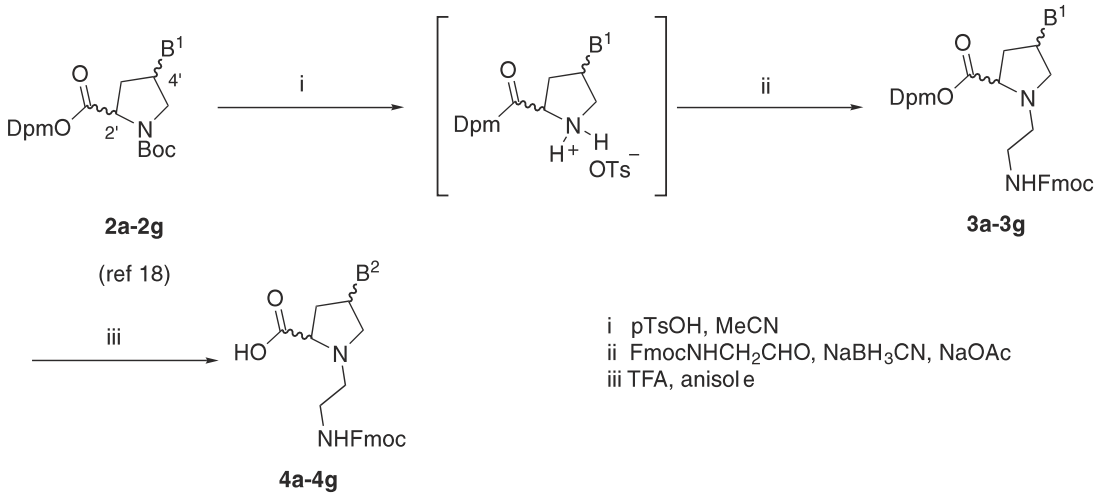

SCHEME 1 Synthesis of *aep*PNA monomers via reductive alkylation.

nucleobase-modified proline derivatives (**2b–2g**)[18] were then subjected to the same reductive alkylation with **1** under similar conditions. In all cases the expected products **3b–3g** were obtained in moderate to good yields (Table 1). Although no satisfactory explanation could be offered, it is interesting to note that the reductive alkylation of the "*trans*" (2′*R*,4′*S*) and (2′*S*,4′*R*) isomers consistently gave poorer yield compared to the "*cis*" (2′*R*,4′*R*) and (2′*S*,4′*S*) isomers (Table 1, compare entries 3, 4, and 1, 2).

To obtain the Fmoc-protected free acids **4**, the diphenylmethyl ester group in **3a–3g** was next removed by treatment with trifluoroacetic acid in the presence of anisole at ambient temperature. The free acids **4a–4g** were obtained in 72–85% yield (Table 1). In case of the thymine monomers **4a–4d**, the N^3-benzoyl group on the thymine was simultaneously cleaved under these conditions. As protection of the thymine-N^3 was not generally required during the PNA synthesis, this premature cleavage would not be considered as a serious problem.

TABLE 1 Synthesis of protected PNA monomers by reductive alkylation with *N*-Fmoc-aminoacetaldehyde

Entry	Starting material	Config.	Product	B^1	Yield (%)	Product	B^2	Yield (%)
1	**2a**	(2′*R*,4′*R*)	**3a**	T^{Bz}	76	**4a**	T	85
2	**2b**	(2′*S*,4′*S*)	**3b**	T^{Bz}	87	**4b**	T	72
3	**2c**	(2′*R*,4′*S*)	**3c**	T^{Bz}	40	**4c**	T	72
4	**2d**	(2′*S*,4′*R*)	**3d**	T^{Bz}	43	**4d**	T	75
5	**2e**	(2′*R*,4′*R*)	**3e**	G^{Ibu}	69	**4e**	G^{Ibu}	77
6	**2f**	(2′*R*,4′*R*)	**3f**	A^{Bz}	60	**4f**	A^{Bz}	75
7	**2g**	(2′*R*,4′*R*)	**3g**	C^{Bz}	89	**4g**	C^{Bz}	74

Downloaded By: [2007 - 2008-2009 Chulalongkorn University] At: 11:09 14 March 2011

Epimerization at the position 2′ in the proline ring *via* the enamine intermediate resulting from iminium-enamine tautomerization would have been considered as a plausible side reaction of the present reductive alkylation strategy. If this had taken place, a diastereomeric mixture consisting of the (2′*R*,4′*R*) and (2′*S*,4′*R*) products would have formed. ^{1}H and ^{13}C NMR spectra of the compounds **3** and **4** suggested the presence of only one diastereomer in all cases. Furthermore, HPLC analysis of the compound **4a**, which possesses (2′*R*,4′*R*) stereochemistry, revealed no detectable contamination by the (2′*S*,4′*R*) diastereomer **4d** (<0.5%, verified by co-injection t_R *RR* = 46.4 minutes, t_R *SR* = 47.2 minutes). This confirmed that no significant epimerization had occurred during the reductive alkylation and deprotection steps.

The present reductive alkylation of nucleobase-derivatized proline proved to be a more efficient route for the synthesis of *aep*PNA monomers than the previously reported methods. It provided the Fmoc-protected intermediates **4a–4g** directly without the need for protecting group conversion. The Fmoc-protected intermediate **3a** ($B^1 = T^{Bz}$) has previously been obtained in 22% overall yield (6 steps) starting from **2a**,[12] while the present method gave the desired products in 40–89% overall yield (two steps) depending on the nucleobases.

Synthesis of *aep*PNA Oligomers

Oligomerization of the activated *aep*PNA monomers was performed by manual Fmoc-solid phase peptide synthesis methodology.[19] The sequences synthesized included four homothymine *aep*PNA decamers with different configurations at the proline moiety (denoted ***RR*-$\mathbf{T_{10}}$**, ***SS*-$\mathbf{T_{10}}$**, ***RS*-$\mathbf{T_{10}}$** and ***SR*-$\mathbf{T_{10}}$** in Table 2), and a mixed base decamer with (2′*R*,4′*R*) configurations (denoted ***RR*-mix** in Table 2). All sequences were capped with acetyl and lysine amide at the N- and C-termini respectively. Generally, the average coupling yields of 95–99% for each step were achieved according to UV absorbance measurement of the dibenzofulvene-piperidine adduct released during deprotection step. In cases of sequences containing nucleobases

TABLE 2 Sequences and characterization details of the *aep*PNA synthesized

Entry	Code	Config.	Sequence[a]	M·H$^+$ (calcd.)	M·H$^+$ (found)[b]
1	***RR*-$\mathbf{T_{10}}$**	(2′*R*,4′*R*)	TTTTTTTTTT	2830.05	2830.04
2	***SS*-$\mathbf{T_{10}}$**	(2′*S*,4′*S*)	TTTTTTTTTT	2830.05	2830.27
3	***SR*-$\mathbf{T_{10}}$**	(2′*S*,4′*R*)	TTTTTTTTTT	2830.05	2830.31
4	***RS*-$\mathbf{T_{10}}$**	(2′*R*,4′*S*)	TTTTTTTTTT	2830.05	2830.24
5	***RR*-mix**	(2′*R*,4′*R*)	GTAGATCACT	2877.09	2877.57

[a]*N*-Ac, *C*-LysNH_2 capped.
[b]MALDI-TOF, α-cyano-4-hydroxy cinnamic acid (CCA) matrix.

Downloaded By: [2007 - 2008-2009 Chulalongkorn University] At: 11:09 14 March 2011

other than thymine, the nucleobase protecting groups (Bz, Ibu) were removed after completion of the synthesis by treatment of the support-bound PNA with aqueous ammonia/dioxane 1:1 at 60°C for 6 hours prior to the usual TFA cleavage. The decamer *aep*PNAs were obtained after reverse phase HPLC purification and were characterized by MALDI-TOF mass spectrometry. In all cases quasi-molecular ions were observed with m/z within ±0.5 Da to the calculated values, thus confirming the identities of all PNA synthesized (Table 2).

DNA and RNA Binding Properties of *aep*PNA

Interactions between the decamer *aep*PNA with complementary DNA and RNA were investigated by T_m measurement. The thermal transition curves were recorded at 260 nm over 20–90°C range and the T_m values are shown in Table 3.

The binding experiments clearly indicate that the homothymine *aep*PNA decamers with *cis*-configurations (***RR*-T$_{10}$** and ***SS*-T$_{10}$**) could form reasonably stable hybrids with poly(rA) (T_m = 43 and 42°C) but not poly(dA). On the other hand, the homothymine *aep*PNA decamers with *trans*-configurations (***RS*-T$_{10}$** and ***SR*-T$_{10}$**) failed to form stable hybrids with both poly(rA) and poly(dA), although an apparent melting was observed between ***RS*-T$_{10}$** and poly(dA) at a rather low temperature (24°C). CD spectra of the *aep*PNA and their mixture with their complementary DNA/RNA were in good agreement with T_m data. Significant differences between the observed and sum of the individual component CD spectra, which indicate hybrid formation, were observed only for the pairs ***RR*-T$_{10}$**/poly(rA) and ***SS*-T$_{10}$**/poly(rA) (Figure 2). Disappointingly, no hybridization of the mixed base *aep*PNA decamer (***RR*-mix**) to complementary DNA and RNA could be observed in both parallel

TABLE 3 T_m values of hybrids between decamer *aep*PNA and polynucleotides

Entry	*aep*PNA	polynucleotide	T_m (°C)[a]
1	***RR*-T$_{10}$**	poly(rA)	43
2	***SS*-T$_{10}$**	poly(rA)	42
3	***SR*-T$_{10}$**	poly(rA)	<20
4	***RS*-T$_{10}$**	poly(rA)	<20
5	***RR*-T$_{10}$**	poly(dA)	<20
6	***SS*-T$_{10}$**	poly(dA)	<20
7	***SR*-T$_{10}$**	poly(dA)	<20
8	***RS*-T$_{10}$**	poly(dA)	24
9	***RR*-mix**	d(CATCTAGTGA)	<20
10	***RR*-mix**	d(AGTGATCTAC)	<20
11	***RR*-mix**	r(CAUCUAGUGA)	<20
12	***RR*-mix**	r(AGUGAUCUAC)	<20

[a] T_m were measured at [PNA] = [DNA] = 1 μM, 10 mM sodium phosphate pH 7.0, heating rate 1°C/min.

Downloaded By: [2007 - 2008-2009 Chulalongkorn University] At: 11:09 14 March 2011

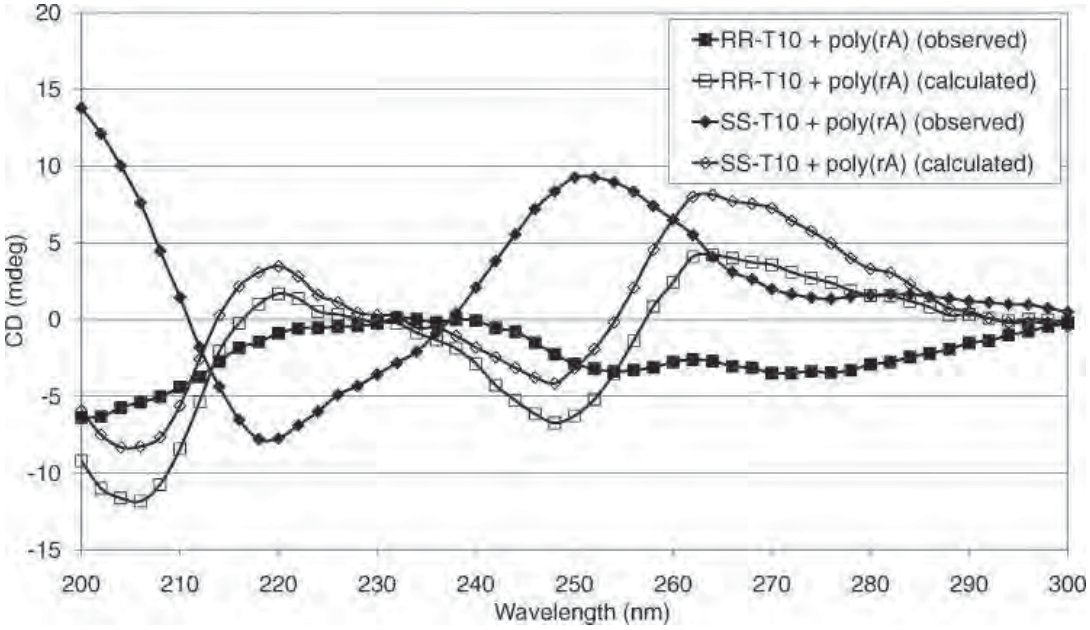

FIGURE 2 CD spectra of PNA-DNA or RNA hybrids. Conditions: [PNA] = [DNA or RNA] = 1 μM, 10 mM sodium phosphate pH 7.0, 25°C.

(Table 3, entries 9 and 11) and antiparallel orientations (Table 3, entries 10 and 12). The duplex structures formed between the mixed base *aep*PNA with (2′*R*,4′*R*) configuration is therefore likely to be less stable than the corresponding DNA·DNA or DNA·RNA hybrids.[20] The unusually high stability of the homothymine *aep*PNA hybrids compared to the mixed sequence in this case could be explained by the formation of triplex structures, which was confirmed by ultraviolet (UV) titration experiments. It had been previously observed in other PNA systems with homopyrimidine sequences that these triplexes could form exclusively even when the stoichiometry was not correct because the triplex was more stable than the intermediate duplex.[1] Our results with the (2′*S*,4′*S*) isomer is in accordance with the observation by Liu that no stable hybrid was formed between homothymine *aep*PNA and its complementary DNA.[11] Preliminary time-dependent UV experiments indicated that the binding between the *aep*PNA (***RR*-$\mathbf{T_{10}}$** and ***SS*-$\mathbf{T_{10}}$**) and RNA are kinetically slow. More than 30 minutes are required for the maximum hypochromism to be established (Figure 3). The significant hysteresis observed in the cooling curves of both *aep*PNA-RNA hybrids also confirmed the slow kinetics of the hybridization, which may suggest that there was substantial reorganization of the single stranded counterparts upon hybridization. No hypochromism was observed in the corresponding DNA experiments, confirming that both *aep*PNAs could not bind to their complementary DNA under these conditions. Whether the preferential binding of the *aep*PNA to RNA, and the failure of the mixed base *aep*PNA to bind to both DNA and

Downloaded By: [2007 - 2008-2009 Chulalongkorn University] At: 11:09 14 March 2011

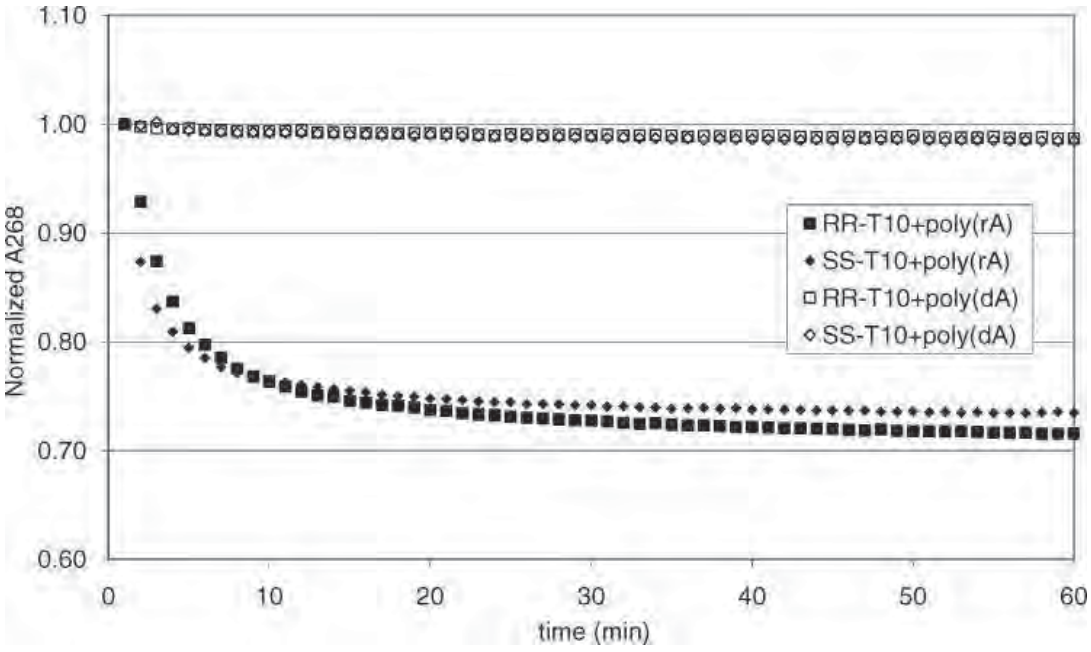

FIGURE 3 Time-dependent normalized UV absorbance at 268 nm of *aep*PNA-DNA/RNA hybridization reactions. Conditions: [PNA] = [DNA or RNA] = 1 μM, 10 mM sodium phosphate pH 7.0, 25°C.

RNA are due to thermodynamic or kinetic factors, and the structural basis of this selectivity, remains to be further investigated.

CONCLUSION

The reductive alkylation of nucleobase-modified proline derivative with Fmoc-aminoacetaldehyde (**1**) was found to be an efficient method for the synthesis of *aep*PNA monomers. Deprotection of the C-terminal protecting group gave the (2′*R*,4′*R*)-*aep*PNA monomers containing all four nucleobase (A^{Bz}, T, C^{Bz}, and G^{Ibu}) and the thymine monomers with different configuration (2′*R*,4′*R*, 2′*S*,4′*S*, 2′*R*,4′*S*, 2′*S*,4′*R*). Oligomerization of the PNA monomers was carried out employing Fmoc SPPS. Five *aep*PNA decamers were successfully synthesized. The hybridization properties of the *aep*PNA were investigated by UV and circular dichroism (CD) spectroscopy. The results suggested that the stereochemistry on the pyrrolidine ring and the nucleobase sequence can have a dramatic effect on the binding characteristics of the *aep*PNA. Only the *cis*-stereoisomers with a homothymine sequence can form stable triplexes with RNA, but not DNA. The hybrid formation in these cases is kinetically slow. No hybrid formation could be observed between a mixed-base sequence (2′*R*,4′*R*)-*aep*PNA with DNA and RNA in both antiparallel and parallel orientations.

Downloaded By: [2007 - 2008-2009 Chulalongkorn University] At: 11:09 14 March 2011

Downloaded By: [2007 - 2008-2009 Chulalongkorn University] At: 11:09 14 March 2011

EXPERIMENTAL

Materials and Methods

^{1}H and ^{13}C spectra were recorded on a Varian Mercury-400 plus NMR spectrometer operating at 400 MHz. MALDI-TOF mass spectra were obtained in reflectron mode on an Omniflex MALDI-TOF mass spectrometer (Bruker Daltonics, Germany) using α-cyano-4-hydroxy cinnamic acid (CCA) as matrix employing 0.1% trifluoroacetic acid in acetonitrile:water (1:2) as diluents for samples preparation. CD experiments were performed on a JASCO Model J-810 Spectropolarimeter, Japan. The CD spectra were recorded at 25°C from 300 to 200 nm and averaged four times then subtracted from a spectrum of the buffer under the same conditions. All chemicals were purchased from Fluka (Switzerland), Merck (Germany), or Aldrich (USA), and were purified as appropriate. The *N-tert*-butoxycarbonyl (Boc)/diphenylmethyl (Dpm) ester protected nucleobase-modified proline derivatives **2a–2d** were synthesized from *trans*-4-hydroxy-L-proline according to our previously published procedure.[18]

N-Fluoren-9-ylmethoxycarbonylaminoacetaldehyde (1)

A mixture of *rac*-3-amino-1,2-propanediol (0.4556 g, 5 mmol), FmocCl (1.2935 g, 5 mmol) and $NaHCO_3$ (0.4201 g, 5 mmol) were dissolved in 1:1 dioxane:H_2O (10 mL). The reaction mixture was stirred at ambient temperature overnight. The solvent was removed by rotary evaporation under reduced pressure. The residue was diluted with 20 mL of water and extracted with dichloromethane (3 × 30 mL) The combined organic extract was dried over magnesium sulfate and evaporated under reduced pressure to give *N*-Fmoc-3-amino-1,2-propanediol as a white solid (1.3935 g, 90%). A mixture of this intermediate (1.2534 g, 4 mmol) and $NaIO_4$ (1.0233 g, 4.8 mmol) were dissolved in 1:1 MeCN:H_2O (8 mL) and allowed to stir at 30°C for 3 hours. The solvents were removed by rotary evaporation and the residue was diluted with 20 mL of water and extracted with dichloromethane (3 × 30 mL). The combined organic extract was dried over magnesium sulfate and evaporated to give the product as a white fluffy solid; yield: 1.1224 g (99%); m.p. 141.0–143.0°C; ^{1}H NMR (400 MHz, $CDCl_3$) δ 4.21 (d $J = 5.0$ Hz, 2H), 4.27 (t $J = 6.8$ Hz, 1H), 4.47 (d $J = 6.8$ Hz, 2H), 5.48 (br m, 1H), 7.36 (m, 2H), 7.45 (m, 2H), 7.64 (d $J = 7.5$ Hz, 2H), 7.81 (d $J = 7.5$ Hz, 2H), 9.71 (s, 1H); ^{13}C NMR (100 MHz, $CDCl_3$) δ 47.1, 51.7, 67.2, 120.0, 125.1, 127.1, 127.8, 141.3, 143.7, 156.3, 196.5.

A Representative Procedure for the Reductive Alkylation

The protected proline derivative **2** (1 mmol) was treated with *p*-toluenesulfonic acid (3 mmol) in MeCN (5 mL). The solvent was removed by

rotary evaporation at 30°C. The residue was dissolved in MeOH (2 mL) followed by successive addition of **1** (1.2 mmol), NaOAc (0.41 g) and $NaBH_3CN$ (1.2 mmol). The solution was stirred at ambient temperature (30°C) for one hour then the solvent was removed by rotary evaporation, diluted with ethyl acetate, and extracted with 10% HCl. The organic layer was washed with aq. $NaHCO_3$ and combined organic phase was dried over magnesium sulfate and evaporated under reduced pressure. The residue was purified by flash column chromatography eluting with hexanes:ethyl acetate (1:1) on silica gel to afford **3**.

Downloaded By: [2007 - 2008-2009 Chulalongkorn University] At: 11:09 14 March 2011

A Representative Procedure for Deprotection of the Dpm Ester 3

A mixture of the protected intermediate **3** (0.3–0.5 mmol), anisole (1 mL) and trifluoroacetic acid (3 mL) was stirred at ambient temperature (30°C) overnight. The volatiles were removed under a gentle N_2 stream. Diethyl ether (20 mL) was added to the residue to precipitate the product **4**, which was collected by filtration and dried under vacuum.

Spectroscopic Data of Compounds 3a–3g and 4a–4g

N-2-(N-Fluoren-9-ylmethoxycarbonylamino)ethyl-(4′R)-(N^3-benzoylthymin-1-yl)- (2′R)-proline diphenylmethyl ester (3a)

White foam; yield: 0.6052 g (76%); ^{1}H NMR (400 MHz, $CDCl_3$) δ 1.87 (s, 3H), 2.01 (m, 1H), 2.65 (m, 1H), 2.78–2.88 (m, 2H), 2.93 (dt, J = 14.4, 9.2 Hz, 1H), 3.18 (m, 1H), 3.31 (m, 1H), 3.39 (m, 1H), 3.49 (m, 1H), 4.26 (t J = 6.8 Hz, 1H), 4.35 (dd J = 9.9, 7.4 Hz, 1H), 4.52 (dd, J = 10.2, 7.3 Hz, 1H), 5.28 (m, 1H), 5.58 (m,1H), 7.03 (s, 1H), 7.32–7.49 (m, 14H), 7.51 (t J = 7.7 Hz, 2H), 7.64–7.73 (m, 3H), 7.82 (d J = 7.4 Hz, 2H), 7.94–8.02 (m, 3H); ^{13}C NMR (100 MHz, $CDCl_3$) δ 12.7, 36.6, 39.5, 47.3, 52.7, 53.3, 58.2, 65.0, 66.8, 78.2, 111.4, 120.1, 125.3, 127.0, 127.3, 127.9, 128.5, 128.8, 129.3, 130.5, 131.7, 135.2, 138.0, 139.4, 139.5, 141.4, 144.0, 150.0, 156.6, 162.9, 169.5, 172.5; MS (MALDI-TOF) *m/z* 797.64 [M+Na^+]; HRMS (FAB+) *m/z* calcd for $C_{47}H_{42}N_4O_7 \cdot H^+$: 775.3132, found: 775.3154.

N-2-(N-Fluoren-9-ylmethoxycarbonylamino)ethyl-(4′S)-(N^3-benzoylthymin-1-yl)-(2′S)-proline diphenylmethyl ester (3b)

White foam; yield: 0.6840 g (87%); ^{1}H NMR (400 MHz, $CDCl_3$) δ 1.87 (s, 3H), 2.01 (m, 1H), 2.66 (m, 1H), 2.77–2.86 (m, 2H), 2.93 (dt, J = 14.9, 9.6 Hz, 1H), 3.18 (m, 1H), 3.31 (d J = 10.7 Hz, 1H), 3.40 (m, 1H), 3.49 (m, 1H), 4.26 (t J = 6.8 Hz, 1H), 4.36 (dd J = 10.1, 7.1 Hz, 1H), 4.53 (dd, J = 10.5, 7.3 Hz, 1H), 5.29 (m, 1H), 5.58 (m,1H), 7.04 (s, 1H), 7.33–7.47 (m, 14H), 7.52 (t J = 7.8 Hz, 2H), 7.64–7.70 (m, 3H), 7.83 (d J = 7.5 Hz, 2H), 7.95–8.00 (m, 3H); ^{13}C NMR (100 MHz, $CDCl_3$) δ 12.6, 36.6, 39.4, 47.3, 52.5, 53.3, 58.3, 65.0, 66.8, 78.2, 111.5, 120.1, 125.1, 126.9, 127.2, 127.8, 128.4,

128.8, 129.2, 130.5, 131.7, 135.0, 137.6, 139.3, 139.4, 141.4, 144.0, 150.0, 156.6, 162.7, 169.2, 172.5; MS (MALDI-TOF) *m/z* 797.67 [M+Na^+]; HRMS (FAB+) *m/z* calcd for $C_{47}H_{42}N_4O_7 \cdot H^+$: 775.3132, found: 775.3122.

N-2-(N-Fluoren-9-ylmethoxycarbonylamino)ethyl-(4′S)-(N^3-benzoylthymin-1-yl)-(2′R)-proline diphenylmethyl ester (3c)

White foam; yield: 0.3185 g (40%); ^{1}H NMR (400 MHz, $CDCl_3$) δ 2.06 (s, 3H), 2.25 (m, 1H), 2.53 (m, 1H), 2.72 (m, 2H), 2.96 (m, 1H), 3.27 (m, 2H), 3.40 (m, 1H), 4.04 (dd J = 8.2, 2.8 Hz, 1H), 4.23 (t J = 6.9 Hz, 1H), 4.43 (m, 2H), 5.25 (m, 1H), 5.48 (m, 1H), 6.95 (s, 1H), 7.27–7.46 (m, 15H), 7.49 (t J = 7.9 Hz, 2H), 7.61–7.66 (m,3H), 7.79 (d J = 7.5 Hz, 2H), 7.97 (d J = 7.4 Hz, 2H), ^{13}C NMR (100 MHz, $CDCl_3$) δ 12.6, 35.4, 39.3, 47.3, 51.2, 54.3, 56.0, 63.9, 66.6, 77.6, 111.6, 120.1, 125.1, 127.0, 127.1, 127.8, 128.3, 128.7, 129.3, 130.5, 131.6, 135.1, 137.7, 139.5, 139.6, 141.3, 143.9, 149.7, 156.7, 162.9, 169.3, 171.5; MS (MALDI-TOF) *m/z* 797.68 [M+Na^+]; HRMS (FAB+) *m/z* calcd for $C_{47}H_{42}N_4O_7 \cdot H^+$: 775.3132, found: 775.3144.

N-2-(N-Fluoren-9-ylmethoxycarbonylamino)ethyl-(4′R)-(N^3-benzoylthymin-1-yl)- (2′S)-proline diphenylmethyl ester (3d)

White foam; yield: 0.1652 g (43%); ^{1}H NMR (400 MHz, $CDCl_3$) δ 2.08 (s, 3H), 2.28 (m, 1H), 2.56 (m, 1H), 2.74 (m, 2H), 2.98 (m, 1H), 3.29 (m, 2H), 3.44 (m, 1H), 4.04 (dd J = 8.2, 2.8 Hz, 1H), 4.24 (t J = 6.7 Hz, 1H), 4.44 (d J = 6.8 Hz, 2H), 5.25 (m, 1H), 6.95 (s, 1H), 7.27–7.44 (m, 14H), 7.51 (t J = 7.8 Hz, 2H), 7.61–7.69 (m,3H), 7.80 (d J = 7.5 Hz, 2H), 7.96 (d J = 7.4 Hz, 2H), ^{13}C NMR (100 MHz, $CDCl_3$) δ 12.6, 35.5, 39.3, 47.3, 51.2, 54.3, 56.0, 63.9, 66.6, 77.6, 111.7, 120.1, 125.0, 127.1, 127.2, 127.8, 128.3, 128.7, 129.3, 130.5, 131.5, 135.2, 137.5, 139.5, 139.6, 141.3, 143.9, 149.7, 156.6, 162.8, 169.2, 171.5; MS (MALDI-TOF) *m/z* 797.80 [M+Na^+]; HRMS (FAB+) *m/z* calcd for $C_{47}H_{42}N_4O_7 \cdot H^+$: 775.3132, found: 775.3138.

N-2-(N-Fluoren-9-ylmethoxycarbonylamino)ethyl-(4′R)-(N^2-isobutyrylguanin-9-yl)-(2′R)-proline diphenylmethyl ester (3e)

White foam; yield: 0.2654 g (69%); ^{1}H NMR (400 MHz, $CDCl_3$) δ 1.24 (d J = 6.0 Hz, 6H), 2.10–2.22 (m, 1H), 2.55–2.92 (m, 5H), 3.20 (m, 1H), 3.26–3.40 (m, 1H), 3.52 (m, 1H), 4.23 (t J = 6.8 Hz, 1H), 4.35 (d J = 6.8 Hz, 2H), 5.00 (m, 1H), 5.78 and 6.20 (2 × m, 1H), 6.92 (s, 1H), 7.21–7.44 (m, 15H), 7.62 (d J = 7.2 Hz, 2H), 7.75 (d J = 7.2 Hz, 2H), 7.83 and 8.14 (2 × s, 1H), 9.82 and 10.53 (2 × s, 1H), 12.12 and 12.46 (2 × s, 1H); ^{13}C NMR (100 MHz, $CDCl_3$) δ 19.1, 19.2, 36.0, 36.9, 39.6, 47.2, 51.9, 53.5, 59.1, 64.7, 66.9, 77.9, 119.9, 120.2, 125.2, 126.9, 127.1, 127.7, 128.3, 128.7, 138.2, 139.4, 141.2, 144.0, 147.9, 148.5, 156.0, 156.8, 172.4, 180.0; MS (MALDI–TOF) *m/z* 766.86 [M+H^+]; HRMS (FAB+) *m/z* calcd for $C_{44}H_{43}N_7O_6 \cdot H^+$: 766.3353, found: 766.3378.

Downloaded By: [2007 - 2008-2009 Chulalongkorn University] At: 11:09 14 March 2011

N-2-(N-Fluoren-9-ylmethoxycarbonylamino)ethyl-(4′R)-4′-(N^6-benzoyladenin-9-yl)-(2′R)-proline diphenylmethyl ester (3f)

White foam; yield: 0.3499 g (60%); ^{1}H NMR (400 MHz, $CDCl_3$) δ 2.25 (m, 1H), 2.80 (m, 1H), 2.89 (m, 1H), 3.02 (m, 2H), 3.16 (m, 1H), 3.39 (m, 1H), 3.47 (m, 1H), 3.62 (m, 1H), 4.29 (t J = 7.2 Hz, 1H), 4.39 (m, 2H), 5.37 (m, 1H), 5.61 (m, 1H), 6.97 (s, 1H), 7.22–7.41 (m, 14H), 7.50 (t J = 7.6 Hz, 2H), 7.58–7.70 (m, 3H), 7.77 (d J = 7.2 Hz, 2H), 8.02 (d J = 7.6 Hz, 2H), 8.65 (s, 1H), 8.82 (s, 1H), 9.36 (s, 1H); ^{13}C NMR (100 MHz, $CDCl_3$) δ 37.2, 39.5, 47.3, 52.1, 53.6, 59.1, 64.5, 66.9, 78.1, 119.9, 122.4, 125.3, 126.9, 127.1, 127.7, 127.9, 128.3, 128.7, 128.8, 132.7, 133.8, 139.3, 141.3, 142.2, 144.1, 149.4, 151.5, 152.4, 156.6, 164.7, 172.5; MS (MALDI–TOF) m/z 784.53 [M+H$^+$]; HRMS (FAB+) m/z calcd for $C_{47}H_{41}N_7O_5 \cdot H^+$: 784.3247, found: 784.3271.

N-2-(N-Fluoren-9-ylmethoxycarbonylamino)ethyl-(4′R)-(N^4-benzoylcytosin-1-yl)-(2′R)-proline diphenylmethyl ester (3g)

White foam; yield: 0.3231 g (89%); ^{1}H NMR (400 MHz, $CDCl_3$) δ 2.05 (m, 1H), 2.67 (m, 1H), 2.86 (m, 2H), 2.98 (m, 1H), 3.15 (m, 1H), 3.34 (m, 1H), 3.41 (m, 1H), 3.51 (m, 1H), 4.28 (t J = 7.2 Hz, 1H), 4.42 (t J = 6.8 Hz, 2H), 5.43 (m, 1H), 6.96 (s, 1H), 7.18–7.72 (m, 14H), 7.42 (m, 2H), 7.53 (m, 2H), 7.61–7.72 (m, 2H), 7.79 (d J = 7.2 Hz, 2H), 7.93 (m, 2H), 8.43 (d J = 6.4 Hz, 1H); ^{13}C NMR (400 MHz, $CDCl_3$) δ 36.6, 39.4, 47.2, 53.7, 54.3, 58.6, 65.2, 66.8, 78.1, 97.5, 119.9, 125.3, 127.7, 128.3, 126.9, 127.1, 127.7, 127.8, 128.4, 128.8, 128.9, 133.1, 139.3, 141.3, 144.1, 146.8, 156.0, 156.6, 161.9, 166.5, 172.4; HRMS (FAB+) m/z calcd for $C_{46}H_{41}N_5O_6 \cdot H^+$: 760.3135, found: 760.3137.

N-2-(N-Fluoren-9-ylmethoxycarbonylamino)ethyl-(4′R)-(thymin-1-yl)-(2′R)-proline (4a)

White solid; yield: 0.2545 g (85%); ^{1}H NMR (400 MHz, DMSO–d_6 + 1 drop TFA) δ 1.77 (s, 3H), 2.35 (m, 1H), 2.83 (m, 1H), 3.20 (m, 1H), 3.37 (m, 2H), 3.51 (m, 1H), 3.69 (m, 1H), 3.94 (m, 1H), 4.26 (t J = 6.8 Hz, 1H), 4.40 (m, 2H), 4.54 (m, 1H), 5.14 (m, 1H), 7.33 (t J = 7.2 Hz, 2H), 7.41 (t J = 7.2 Hz, 2H), 7.57 (s, 1H), 7.69 (d J = 7.2 Hz, 2H), 7.89 (d J = 7.2 Hz, 2H); ^{13}C NMR (100 MHz, DMSO–d_6 + 1 drop TFA) δ 12.7, 34.4, 38.3, 47.2, 53.3, 54.2, 57.5, 66.0, 66.2, 109.7, 120.6, 125.6, 127.6, 128.1, 139.3, 141.2, 144.3, 151.6, 156.7, 164.2, 171.5; MS (MALDI–TOF) m/z 505.13 [M+H$^+$]; HRMS (FAB+) m/z calcd for $C_{27}H_{28}N_4O_6 \cdot H^+$: 505.2087, found: 505.2102.

N-2-(N-Fluoren-9-ylmethoxycarbonylamino)ethyl-(4′S)-(thymin-1-yl)-(2′S)-proline (4b)

White solid; yield: 0.3711 g (72%); ^{1}H NMR (400 MHz, DMSO–d_6 + 1 drop TFA) δ 1.76 (s, 3H), 2.37 (m, 1H), 2.83 (m, 1H), 3.20 (m, 1H), 3.37 (m, 2H), 3.52 (m, 1H), 3.69 (dd J = 12.5, 10.1 Hz, 1H), 3.95 (dd J = 12.6,

Downloaded By: [2007 - 2008-2009 Chulalongkorn University] At: 11:09 14 March 2011

3.9 Hz, 1H), 4.25 (t J = 6.4 Hz, 1H), 4.36–4.44 (m, 2H), 4.54 (m, 1H), 5.15 (m, 1H), 7.32 (t J = 7.3 Hz, 2H), 7.40 (t J = 7.3 Hz, 2H), 7.56 (s, 1H), 7.68 (d J = 7.5 Hz, 2H), 7.87 (d J = 7.5 Hz, 2H); ^{13}C NMR (100 MHz, DMSO–d_6 + 1 drop TFA) δ 12.7, 34.2, 38.1, 47.2, 53.4, 54.3, 57.4, 66.0, 66.3, 109.8, 120.6, 125.6, 127.6, 128.1, 139.2, 141.2, 144.3, 151.6, 156.7, 164.3, 171.1; MS (MALDI–TOF) m/z 505.13 [M+H$^+$]; HRMS (FAB+) m/z calcd for $C_{27}H_{28}N_4O_6 \cdot H^+$: 505.2087, found: 505.2088.

N-2-(N-Fluoren-9-ylmethoxycarbonylamino)ethyl-(4′S)-(thymin-1-yl)-(2′R)-proline (4c)

White solid; yield: 0.1201 g (72%); ^{1}H NMR (400 MHz, DMSO–d_6 + 1 drop TFA) δ 1.78 (s, 3H), 2.49 (m, 1H), 2.66 (m, 1H), 3.25 (m, 1H), 3.38 (m, 2H), 3.47 (m, 1H), 3.58 (m, 1H), 4.00 (dd J = 11.3, 8.8 Hz, 1H), 4.25 (t J = 6.3 Hz, 1H), 4.40 (d J = 6.6 Hz, 2H), 4.77 (t J = 9.5 Hz, 1H), 4.98 (m, 1H), 7.33 (t J = 7.3 Hz, 2H), 7.42 (t J = 7.4 Hz, 2H), 7.54 (br m, 1H), 7.62 (s, 1H), 7.70 (d J = 7.4 Hz, 2H), 7.90 (d J = 7.5 Hz, 2H); ^{13}C NMR (100 MHz, DMSO–d_6 + 1 drop TFA) δ 12.6, 33.6, 38.6, 47.2, 52.9, 53.0, 55.6, 65.1, 65.9, 110.0, 120.6, 125.6, 127.5, 128.1, 138.8, 141.2, 144.3, 151.3, 156.7, 164.3, 172.3; MS (MALDI–TOF) m/z 505.12 [M+H$^+$]; HRMS (FAB+) m/z calcd for $C_{27}H_{28}N_4O_6 \cdot H^+$: 505.2087, found: 505.2062.

N-2-(N-Fluoren-9-ylmethoxycarbonylamino)ethyl-(4′R)-(thymin-1-yl)-(2′S)-proline (4d)

White solid; yield: 0.1201 g (72%); ^{1}H NMR (400 MHz, DMSO–d_6 + 1 drop TFA) δ 1.78 (s, 3H), 2.46 (m, 1H), 2.67 (m, 1H), 3.26 (m, 1H), 3.38 (m, 2H), 3.48 (m, 1H), 3.58 (m, 1H), 4.01 (dd J = 10.8, 8.9 Hz, 1H), 4.25 (t J = 6.4 Hz, 1H), 4.40 (d J = 6.7 Hz, 2H), 4.78 (t J = 9.3 Hz, 1H), 4.98 (m, 1H), 7.33 (t J = 7.3 Hz, 2H), 7.41 (t J = 7.4 Hz, 2H), 7.61 (br s, 1H), 7.52 (br m, 1H), 7.69 (d J = 7.3 Hz, 2H), 7.89 (d J = 7.5 Hz, 2H); ^{13}C NMR (100 MHz, DMSO–d_6 + 1 drop TFA) δ 12.6, 33.8, 38.7, 47.2, 52.8, 53.0, 55.7, 65.0, 65.9, 110.0, 120.6, 125.6, 127.5, 128.1, 138.7, 141.2, 144.3, 151.3, 156.7, 164.3, 172.7; MS (MALDI–TOF) m/z 505.00 [M+H$^+$]; HRMS (FAB+) m/z calcd for $C_{27}H_{28}N_4O_6 \cdot H^+$: 505.2087, found: 505.2063.

N-2-(N-Fluoren-9-ylmethoxycarbonylamino)ethyl-(4′R)-(N^2-isobutyrylguanin-9-yl)-(2′R)-proline (4e)

White solid; yield: 0.1565 g (77%); ^{1}H NMR (400 MHz, DMSO–d_6 + 1 drop TFA) δ 1.14 (d, J = 6.8 Hz, 6H), 2.20 (m, 1H), 2.70 (m, 1H), 2.79 (sept J = 6.8 Hz, 1H), 2.90 (m, 1H), 2.98–3.13 (m, 2H), 3.17–3.29 (m, 2H), 3.50–3.67 (m, 2H), 4.20–4.43 (m, 3H), 5.04 (s, 1H), 7.34 (m, 2H), 7.42 (m, 2H), 7.70 (d J = 7.2 Hz, 2H), 7.89 (d J = 7.2 Hz, 2H), 8.26 (s, 1H), 11.67 (s, 1H), 12.08 (s, 1H); ^{13}C NMR (100 MHz, DMSO–d_6 + 1 drop TFA) δ 19.3, 35.2, 36.2, 39.1, 47.2, 52.1, 54.0, 58.7, 65.4, 65.9, 120.1, 120.6,

Downloaded By: [2007 - 2008-2009 Chulalongkorn University] At: 11:09 14 March 2011

125.6, 127.6, 128.1, 138.5, 141.2, 144.4, 148.2, 148.7, 155.4, 156.6, 173.5, 180.5; MS (MALDI–TOF) *m/z* 600.19 [M+H$^+$]; HRMS (FAB+) *m/z* calcd for $C_{31}H_{33}N_7O_6 \cdot H^+$: 600.2571, found: 600.2568.

N-2-(N-Fluoren-9-ylmethoxycarbonylamino)ethyl-(4′R)-(N^6-benzoyladenin-9-yl)- (2′R)-proline (4f)

White solid; yield: 0.1431 g (75%); ^{1}H NMR (400 MHz, DMSO–d_6 + 1 drop TFA) δ 2.34 (m, 1H), 2.84 (m, 1H), 2.90–3.08 (m, 2H), 3.17–3.39 (m, 3H), 3.75 (m, 1H), 3.88 (m, 1H), 4.21–4.30 (m, 3H), 5.46 (m, 1H), 7.22–7.41 (m, 4H), 7.46 (br m, 1H), 7.57 (t J = 7.6 Hz, 2H), 7.52–7.74 (m, 3H), 7.89 (d J = 7.6 Hz, 2H), 8.08 (d J = 7.6 Hz, 2H), 8.72 (s, 1H), 8.75 (s, 1H); ^{13}C NMR (100 MHz, DMSO–d_6 + 1 drop TFA) δ 35.7, 38.7, 47.1, 52.2, 54.1, 58.4, 65.7, 66.0, 120.6, 125.6, 125.7, 127.6, 128.1, 128.9, 129.0, 133.0, 133.8, 141.2, 143.7, 144.3, 150.7, 151.6, 152.3, 156.7, 166.2, 172.5; MS (MALDI–TOF) *m/z* 618.19 [M+H$^+$]; HRMS (FAB+) *m/z* calcd for $C_{34}H_{31}N_7O_5 \cdot H^+$: 618.2465, found: 618.2466.

N-2-(N-Fluoren-9-ylmethoxycarbonylamino)ethyl-(4′R)-(N^4-benzoylcytosin-1-yl)- (2′R)-proline (4g)

White solid; yield: 0.2226 g (74%); ^{1}H NMR (400 MHz, DMSO–d_6 + 1 drop TFA) δ 2.47 (m, 1H), 2.98 (m, 1H), 3.24 (m, 1H), 3.41 (m, 2H), 3.57 (m, 1H), 3.77 (m, 1H), 4.14 (m, 1H), 4.28 (m, 1H), 4.36 (m, 2H), 4.60 (m, 1H), 5.13 (m, 1H), 7.32 (m, 2H), 7.42 (m, 2H), 7.54 (m, 2H), 7.58–7.74 (m, 4H), 7.90 (d J = 6.4 Hz, 2H), 8.00 (d J = 7.6 Hz, 2H), 8.20 (d J = 5.6 Hz, 1H); ^{13}C NMR (400 MHz, DMSO–d_6) δ 35.6, 39.0, 47.2, 53.9, 55.8, 58.0, 65.9, 66.0, 96.8, 120.6, 125.6, 127.5, 128.1, 128.9, 129.5, 133.2, 133.7, 141.2, 144.3, 148.6, 155.7, 156.7, 163.2, 167.9, 173.0; MS (MALDI–TOF) *m/z* 594.11 [M+H$^+$]; HRMS (FAB+) *m/z* calcd for $C_{33}H_{31}N_5O_6 \cdot H^+$: 594.2353, found: 594.2334.

Solid Phase Synthesis of *aep*PNA Oligomers

The Fmoc-protected PNA monomers **4a–4g** were activated just before use as pentafluorophenyl esters by treatment with 1 equiv of pentafluorophenyl trifluoroacetate and DIEA. The products obtained following acid-base extraction to remove DIEA salts were unstable upon prolonged storage and thus were used without further purification. All peptide syntheses were carried out manually in a custom-made glass column with a fritted glass tip (i.d. = 5 mm). The reaction column was filled with TentaGel S RAM Fmoc resin (0.24 meq/g loading, 6.3 mg, 1.5 μmol). The resin, after swollen in DMF, was deprotected by treating with 20% piperidine in DMF (500 μL) for 15 minutes at room temperature with occasional agitation. After washing, the deprotected resin was treated with Fmoc-L-Lys(Boc)-OPfp (9.5 mg, 15 μmol) and HOAt (2.0 mg, 15 μmol) dissolved in anhydrous DMF (35 μL).

Downloaded By: [2007 - 2008-2009 Chulalongkorn University] At: 11:09 14 March 2011

After 2 hours at room temperature, the resin was washed exhaustively with DMF and capped with acetic anhydride/DIEA mixture (Ac_2O 10 μL, DIEA 10 μL and DMF 80 μL). Next the Fmoc deprotection was repeated and the resin was treated with an appropriate activated PNA monomer (6.0 μmol) and 7-aza-1-hydroxybenzotriazole (HOAt) (0.8 mg, 6.0 μmol) dissolved in 35 μL DMF for 2 hours. After capping, the deprotection-coupling-capping steps were repeated until the desired sequence was obtained. After final cleavage of the Fmoc protecting group, the PNA was end-capped by acetylation with 10% Ac_2O/DIEA in DMF. With the exception of homothymine sequence, the resin-bound *aep*PNA was treated with 1:1 concentrated aqueous ammonia-dioxane at 60°C overnight to remove the exocyclic amino protecting groups. The crude *aep*PNA was released from the resin by treatment with trifluoroacetic acid (1 mL) at room temperature for 1 hour with occasional agitation. The trifluoroacetic acid was removed by a nitrogen stream (fume hood). The procedure was repeated two more times to ensure a complete cleavage of the peptide from the resin. The crude *aep*PNA was centrifugally washed with diethyl ether (3 times) and was air-dried at room temperature. Analysis and purification was performed by reverse phase HPLC on a Water 600^{TM} system equipped with gradient pump and Water 996 photodiode array detector. A Hypersil C_{18} HPLC column (4.6 × 250 mm, 5 μ particle size) was used for both analytical and preparative purposes. Elution was carried out with a gradient system of 0.1% TFA in acetonitrile/water and monitored at 260 nm. The purity and identity of the products were confirmed by MALDI-TOF mass spectrometry.

T_m Experiments

T_m experiments were performed on a CARY 100 Bio UV-Visible spectrophotometer (Varian Ltd., Australia) equipped with a thermal melt system. The sample for T_m measurement was prepared by mixing calculated amounts of stock oligonucleotide and *aep*PNA solutions together to give final concentration of nucleotides and sodium phosphate buffer (pH 7.0) and the final volumes were adjusted to 3.0 mL by addition of deionized water. The samples were transferred to a 10 mm quartz cell with a Teflon stopper and equilibrated at the starting temperature for 10 minutes. The A_{260} was recorded in steps from 20–90°C (block temperature) with a temperature increment of 1°C/min. The temperature was corrected by applying a linear equation obtained from temperature probe read out. The results were normalized by dividing the absorbance at each temperature by the initial absorbance. T_m values were obtained from first derivative plots.

REFERENCES

1. Uhlmann, E.; Peyman, A.; Breipohl, G.; Will, D. W. PNA: Synthetic polyamide nucleic acids with unusual binding properties. *Angew. Chem. Int. Ed.* **1998**, 37, 2796–2823.

Downloaded By: [2007 - 2008-2009 Chulalongkorn University] At: 11:09 14 March 2011

2. Nielsen, P. E.; Egholm, M.; Berg, R. H.; Buchardt, O. Sequence-selective recognition of DNA by strand displacement with a thymine-substituted polyamide. *Science* **1991**, 254, 1497–1500.
3. Kumar, V. A. Structural preorganization of peptide nucleic acids: Chiral cationic analogues with five- or six-membered ring structures. *Eur. J. Org. Chem.* **2002**, 2021–2032.
4. Kumar, V. A.; Ganesh, K. N. Conformationally constrained PNA analogues: Structural evolution toward DNA/RNA binding selectivity. *Acc. Chem. Res.* **2005**, 38, 404–412.
5. Vilaivan, T.; Lowe, G. A novel pyrrolidinyl PNA showing high sequence specificity and preferential binding to DNA over RNA. *J. Am. Chem. Soc.* **2002**, 124, 9326–9327.
6. Vilaivan, T.; Srisuwannaket, C. Hybridization of pyrrolidinyl peptide nucleic acids and DNA: Selectivity, base-pairing specificity, and direction of binding. *Org. Lett.* **2006**, 8, 1897–1900.
7. Govindaraju, T.; Kumar, V. A.; Ganesh, K. N. (*SR*/*RS*)-Cyclohexanyl PNAs: Conformationally preorganized PNA analogues with unprecedented preference for duplex formation with RNA. *J. Am. Chem. Soc.* **2005**, 127, 4144–4145.
8. D'Costa, M.; Kumar, V. A.; Ganesh, K. N. Aminoethylprolyl peptide nucleic acids (aepPNA): Chiral PNA analogues that form highly stable DNA:aepPNA$_2$ triplexes. *Org. Lett.* **1999**, 1, 1513–1516.
9. D'Costa, M.; Kumar, V.; Ganesh, K. N. Aminoethylprolyl (aep) PNA: Mixed purine/pyrimidine oligomers and binding orientation preferences for PNA:DNA duplex formation. *Org. Lett.* **2001**, 3, 1281–1284.
10. D'Costa, M.; Kumar, V. A.; Ganesh, K. N. N^7-Guanine as a C mimic in hairpin aeg/aep PNA-DNA triplex: Probing binding selectivity by UV-T_m and kinetics by fluorescence-based strand-invasion assay. *J. Org. Chem.* **2003**, 68, 4439–4445.
11. Li, Y.; Jin, T.; Liu, K. Synthesis and binding affinity of a chiral PNA analogue. *Nucleosides Nucleotides Nucleic Acids* **2001**, 20, 1705–1721.
12. Vilaivan, T.; Khongdeesameor, C.; Harnyuttanakorn, P.; Westwell, M. S.; Lowe, G. Synthesis and properties of chiral peptide nucleic acids with a *N*-aminoethyl-D-proline backbone. *Bioorg. Med. Chem. Lett.* **2000**, 10, 2541–2545.
13. Porcheddu, A.; Giacomelli, G.; Piredda, I.; Carta, M.; Nieddu, G. A practical and efficient approach to PNA monomers compatible with Fmoc-mediated solid-phase synthesis protocols. *Eur. J. Org. Chem.* **2008**, 5786–5797.
14. Lee, J.Y.; Chung, Y. J.; Bae, Y.S.; Ryu, S.H.; Kim, B.H. Synthesis of hexapeptide and tetrapeptide analogues of the immunomodulating peptides. *J. Chem. Soc., Perkin Trans. 1* **1998**, 359–365.
15. Khan, N. M.; Arumugam, V.; Balasubramanian, S. Solid phase reductive alkylation of secondary amines. *Tetrahedron Lett.* **1996**, 37, 4819–4822.
16. Finn, P. J.; Gibson, N. J.; Fallon, R.; Hamilton, A.; Brown, T. Synthesis and properties of DNA–PNA chimeric oligomers. *Nucleic Acids Res.* **1996**, 24, 3357–3363.
17. Hamzavi, R.; Dolle, F.; Tavitian, B.; Dahl, O.; Nielsen, P.E. Modulation of the pharmacokinetic properties of PNA: Preparation of galactosyl, mannosyl, fucosyl, *N*-acetylgalactosaminyl, and *N*-acetylglucosaminyl derivatives of aminoethylglycine peptide nucleic acid monomers and their incorporation into PNA oligomers. *Bioconjugate Chem.* **2003**, 14, 941–954.
18. Lowe, G.; Vilaivan, T. Dipeptides bearing nucleobases for the synthesis of novel peptide nucleic acids. *J. Chem. Soc., Perkin Trans. 1* **1997**, 547–554.
19. Lowe, G.; Vilaivan, T. Solid-phase synthesis of novel peptide nucleic acids. *J. Chem. Soc., Perkin Trans. 1* **1997**, 555–560.
20. The T_m of the corresponding DNA·DNA hybrid was ~33.5°C (see: Egholm, M.; Buchardt, O.; Christensen, L.; Behrens, C.; Freier, S. M.; Driver, D. A.; Berg, R. H.; Kim, S. K.; Norden, B.; Nielsen, P. E. PNA hybridizes to complementary oligonucleotides obeying the Watson-Crick hydrogen-bonding rules. *Nature* **1993**, 365, 566–568.

Downloaded By: [2007 - 2008-2009 Chulalongkorn University] At: 11:09 14 March 2011

Artificial DNA: PNA & XNA 2:2, 50-59; April/May/June 2011; © 2011 Landes Bioscience

Pyrrolidinyl peptide nucleic acid with α/β-peptide backbone

A conformationally constrained PNA with unusual hybridization properties

Chotima Vilaivan,[1] Choladda Srisuwannaket,[2] Cheeraporn Ananthanawat,[1] Chaturong Suparpprom,[3] Junji Kawakami,[4,5] Yoshie Yamaguchi,[4,5] Yuko Tanaka[4,5] and Tirayut Vilaivan[1,*]

[1]Organic Synthesis Research Unit; Department of Chemistry; Faculty of Science; Chulalongkorn University; Patumwan, Bangkok, Thailand; [2]Department of Chemistry; Faculty of Science;
King Mongkut's University of Technology Thonburi; Thungkru, Bangkok, Thailand; [3]Department of Chemistry and Center of Excellence for Innovation in Chemistry; Faculty of Science; Naresuan University; Muang, Phitsanulok Thailand; [4]Department of Nanobiochemistry; FIRST; Konan University
[5]Frontier Institute for Biomolecular Engineering Research (FIBER); Konan University; Chuo-ku, Kobe, Japan

Key words: peptide nucleic acid, nucleic acid, DNA recognition, RNA recognition, pre-organization, foldamer, α/β-peptide

We describe herein a new conformationally constrained analog of PNA carrying an alternating α/β amino acid backbone consisting of (2'*R*,4'*R*)-nucleobase-subtituted proline and (1*S*,2*S*)-2-aminocyclopentanecarboxylic acid (acpcPNA). The acpcPNA has been synthesized and evaluated for DNA, RNA and self-pairing properties by thermal denaturation experiments. It can form antiparallel hybrids with complementary DNA with high affinity and sequence specificity. Unlike other PNA systems, the thermal stability of acpcPNA·DNA hybrid is largely independent of G+C contents, and is generally higher than that of acpcPNA·RNA hybrid with the same sequence. Thermodynamic parameters analysis suggest that the A·T base pairs in the acpcPNA·DNA hybrids are enthalpically stabilized over G·C pairs. The acpcPNA also shows a hitherto unreported behavior, namely the inability to form self-pairing hybrids. These unusual properties should make the new acpcPNA a potentially useful candidate for various applications including microarray probes and antigene agents.

Do not distribute.

Introduction

Almost 20 years ago, Nielsen et al. demonstrated an unusually high affinity as well as sequence specificity in recognition of DNA and RNA by a new class of DNA analog called peptide nucleic acid (PNA).[1-3] In many aspects, PNA behaves just like a structural mimic of natural nucleic acids.[4] However, PNA also displays many unique characteristics not found in DNA/RNA or analogs that derived from partial modification of the natural sugar-phosphate backbone.[5] The electrostatically neutral backbone of PNA contributes to the enhanced stability of PNA·DNA hybrids, which is also relatively independent of salt concentrations In addition to binding to single stranded nucleic acid targets, PNA can bind, either by a triplex formation or strand invasion, to double stranded DNA[7,8] as well as RNA targets.[9] The unnatural backbone of PNA makes it stable towards degradation by nucleases and proteases.[10] These properties make PNA a potential candidate for many applications ranging from nucleic acid detection probes[11,12] to therapeutic agents via antisense or antigene applications.[13,14]

Until recently, the original PNA system derived from an achiral backbone of *N*-2-aminoethylglycine (now generally referred to as aegPNA) has been the most widely studied. Although a number of new PNA systems have been developed in the past decades, few of them offer comparable or better hybridization properties found in the original aegPNA.[15-21] It has been argued that the binding properties should be improved if one could restrict the conformational flexibility of the PNA backbone, for example, by locking the PNA backbone into cyclic structures[15-18] or by adding one or more substituents at a specific position of the aegPNA backbone.[19-21] In addition to improving binding affinity and specificity, conformational restriction should offer a possibility to selectively recognize different types of nucleic acids. While aegPNA has been shown to bind marginally more strongly to RNA over DNA, the selectivity towards RNA has been improved by incorporating one or more cyclohexane rings into the PNA backbone.[16,17] Kinetic selectivity in RNA recognition over DNA has been observed in some pyrrolidinyl PNA variants,[22,23] although this behavior seems to be highly sequence-dependent.[24,25] In a much fewer instances, preference for DNA binding over RNA has also been reported.[26]

Recently, oligomers with α/β peptide backbone were recognized as a potential foldamer system due to their well defined helical conformation.[27-29] We have recently developed a new class of pyrrolidinyl PNA consisting of an alternate sequence

*Correspondence to: Tirayut Vilaivan; Email: vtirayut@chula.ac.th
Submitted: 04/30/11; Revised: 06/09/11; Accepted: 06/10/11
DOI: 10.4161/adna.2.2.16340

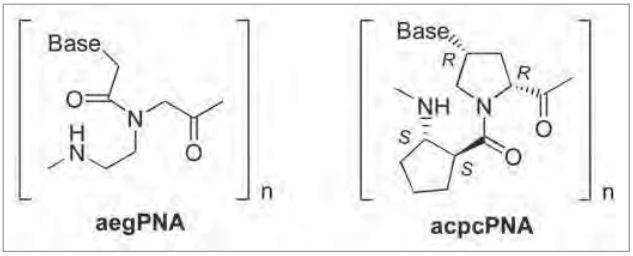

Figure 1. Structures of aegPNA and the pyrrolidinyl PNA carrying 2-aminocyclopen-tanecarboxylic acid spacer (acpcPNA); B = nucleobase (A, C, G or T).

of nucleobase-modified proline and five-membered ring cyclic β-amino acids.[30-33] These pyrrolidinyl PNA retained the basic property of nucleic acid mimics, i.e., the ability to bind to their complementary nucleic acid targets in a sequence-specific fashion. The specificity towards DNA target is in fact considerably better than the original aegPNA system.[34] Applications of these pyrrolidinyl PNA as probes for DNA sequence determination have been successfully demonstrated Furthermore, our preliminary studies in a few representative sequences revealed additional unique features of these pyrrolidinyl PNA including the high directional specificity (parallel/antiparallel), the preference for binding to DNA over RNA, and the inability of two complementary PNA sequences to self-hybridize.[33] Nevertheless, from the limited data available, it is difficult to conclude whether these properties are general or limited to certain sequences as observed in many other cases.[24,25] Herein we describe a comprehensive study of DNA, RNA and self-pairing properties of the pyrrolidinyl PNA system with a backbone consisting of alternating nucleobase-modified proline with a (2'*R*,4'*R*)-configuration and (1*S*,2*S*)-2-aminocyclopentanecarboxylic acid (acpcPNA) (**Fig. 1**). The results clearly indicate that the high antiparallel selectivity, the lack of self-pairing, and the preference for binding to DNA over RNA are general properties of acpcPNA over a range of sequences with different G+C contents. They also further revealed an important new observation that the thermal stability of the acpcPNA·DNA hybrid is much less dependent on the G+C content than the corresponding acpcPNA·RNA hybrid.

Results and Discussion

Effect of stereochemistry on DNA binding. The backbone of the pyrrolidinyl PNA described in this study consists of an alternating nucleobase-modified proline and 2-aminocyclopentanecarboxylic acid, each of which carries two stereogenic centers. As a result, there are 16 possible stereoisomers of the pyrrolidinyl PNA. It is highly probable that the configuration of the monomers will exert significant influences on the ability of the PNA backbone to adopt the correct geometry required for binding with the nucleic acid targets. To systematically determine the effect of stereochemistry on the DNA binding properties, the spacer and the proline parts were optimized separately. Firstly, four diastereomers of pentathymidine (T_5) pyrrolidinyl PNA with different stereochemistry at the 2-aminocyclopentanecarboxylic acid (acpc) part, namely (1*S*,2*S*)-, (1*S*,2*R*)-, (1*R*,2*R*)- and (1*R*,2*S*)-, but with the same (2'*R*,4'*R*)-configuration of the pyrrolidine part were synthesized. This particular configuration of the pyrrolidine part was chosen as the starting point because of its stereochemical similarity to natural nucleosides (assuming that the 2' and 4' positions in the pyrrolidine ring are equivalent to the 4' and 1' positions in natural nucleosides, respectively). Our previous results have also shown that conformationally restricted PNA derived from the (2'*R*,4'*R*)-pyrrolidine monomer can exhibit DNA and RNA binding properties.[30,31] Melting experiments of the hybrid formed between each of the four T_5 pyrrolidinyl PNA diastereomers and poly(dA) at 1:1 ratio of T and A nucleotides were carried out to evaluate the effect of the stereochemistry on the aminocyclopentanecarboxylic acid moiety to DNA binding. The thermal denaturation experiment (**Fig. 2A**) revealed that only the pyrrolidinyl PNA with a combination of (1*S*,2*S*)-acpc and (2'*R*,4'*R*)-pyrrolidine can form hybrids that are sufficiently stable to exhibit observable melting behavior above room temperature (T_m = 35.5°C). Accordingly, the (1*S*,2*S*)-acpc spacer was chosen for studying the effect of the pyrrolidine part. Three additional pyrrolidinyl PNAs with the same T_5 sequence but different stereochemistry at the pyrrolidine ring, i.e., (2'*S*,4'*S*), (2'*R*,4'*S*) and (2'*S*,4'*R*), all of which carry the same (1*S*,2*S*)-acpc spacer, were synthesized. The UV melting results suggested that the acpcPNA with (2'*R*,4'*S*) configurations on the proline ring could also form a stable hybrid with poly(dA) (T_m = 36.5°C) (**Fig. 2B**). These results, together with our earlier reported UV titration data[32] indicate that only the combination of (1*S*,2*S*)-acpc and (2'*R*,4'*R*)- or (2'*R*,4'*S*)-pyrrolidine could allow optimal binding with DNA. This paper will focus on the binding properties of the pyrrolidinyl PNA with (2'*R*,4'*R*)-proline and (1*S*,2*S*)-acpc backbone (**Fig. 1**), which will be simply referred as acpcPNA from this point onward. Synthesis and hybridization properties of the other pyrrolidinyl PNA diastereomer with (2'*R*,4'*S*)-pyrrolidine/(1*S*,2*S*)-acpc backbone that also exhibits DNA binding properties are the subject of a separated investigation.

Hybridization studies of homothymine and homoadenine acpcPNA. Thermal denaturation experiments of the hybrids formed between the homothymine acpcPNA (**T5**, **T7**, **T9** and **T10**) and their complementary DNA (dA_5, dA_7, dA_9 and dA_{10}, respectively) were then carried out (**Fig. 3**). While the relatively short acpcPNA **T5** binds to poly(dA) giving a hybrid with a T_m value of 35.5°C (**Fig. 2A**), it does not show any melting when hybridized with dA_5. Evidently the hybrid formed between the short acpcPNA and DNA was too unstable. However, as observed with aegPNA, the thermal stability of the hybrid increased with the number of base pairs (T_m for 5-, 7-, 9- and 10-mer were <20, 55.5, 77.0 and >85°C, respectively). The T_m of the hybrid between the acpcPNA **T10** and DNA was so high that the melting was not yet complete at 90°C. These T_m figures are considerably higher than the $(PNA)_2$·DNA triplexes formed from homothymine aegPNA with comparable length (T_m for 6-, 8- and 10-mer were 31, 52 and 72°C, respectively).[37] This dramatic increase in the melting temperature as the number of the base increases was further confirmed by variable temperature CD experiments (**Sup. Figs. 34 and 35**). In all cases the CD melting

©2011 Landes Bioscience. Do not distribute.

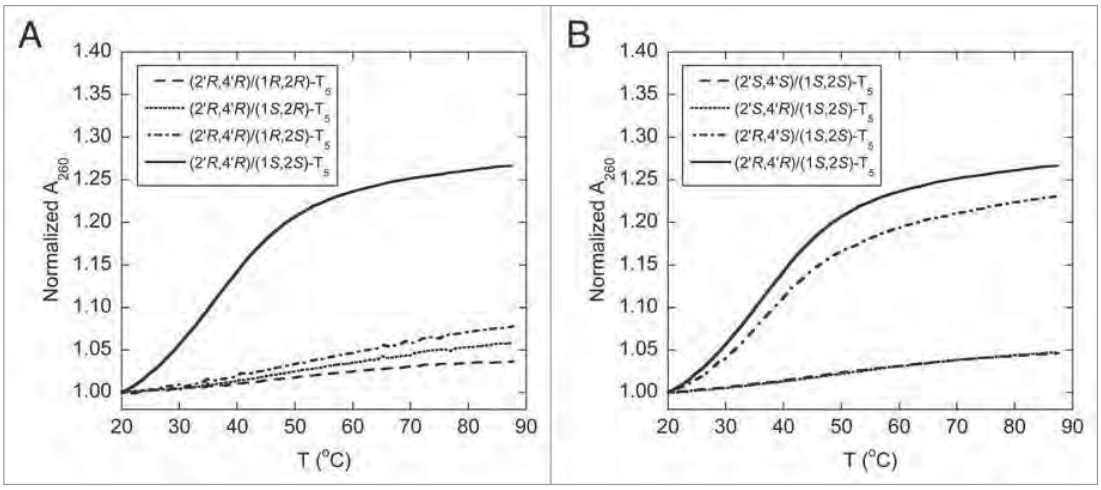

Figure 2. T_m curves of the hybrids between poly(dA) and T_5 pyrrolidinyl PNA with different stereochemistry on the aminocyclopentanecarboxylic acid part (A) and the proline part (B). Conditions: 10.0 μM PNA (by nucleotides), 10.0 μM DNA (by nucleotides), 10 mM sodium phosphate buffer pH 7.0, 0 mM NaCl, heating rate 1.0°C/min.

profiles were in good agreement with those obtained from UV melting studies. The melting process is completely reversible and shows very little hysteresis (**Sup. Fig. 36**), suggesting fast kinetics of the hybridization. The single transition observed in the melting curves, together with the data from CD and UV titration experiments (**Sup. Figs. 37 and 39**) suggested that 1:1 hybrids were formed between these homothymine acpcPNA and DNA. The formation of only acpcPNA·DNA duplexes with homopyrimidine sequences is in sharp contrast to the behavior of aegPNA and many other PNA systems whereby the formation of $(PNA)_2$·DNA triplexes was usually observed.[8,37,38] Steric bulkiness of the present acpcPNA backbone could be one important factor that make the binding of the third PNA strand to the PNA·DNA duplex initially formed difficult.

The melting behavior of the hybrid between homoadenine acpcPNA **A9** and its complementary DNA is somewhat more complex than the corresponding homothymine sequence. When the DNA component (dT_9) was present in excess, the melting proceeded in two steps (**Fig. 4A**). The first transition took place just above room temperature (~34°C) whereas the other appeared at a much higher temperature (>80°C). Such double-transition melting curve is explained by the formation of a $(DNA)_2$·PNA triplex. The triplex could form by Hoogsteen base pairing between the T base of the second strand of DNA to the originally formed Watson-Crick pA·dT pair. When the acpcPNA was present in excess, only the transition at the higher temperature remained, suggesting the presence of only the acpcPNA·DNA duplex in the solution (**Fig. 4A**). The triplex and duplex melting showed an interesting opposite salt-dependency. When the salt concentration was increased, the T_m of the triplex melting increased markedly. This could be explained by the screening effect of salt on the electrostatically repulsive interaction between the duplex and the third DNA strand. On the other hand, the T_m of the duplex melting slightly decreased at high salt concentrations, which is in accordance with the results observed in aegPNA·DNA hybrids,

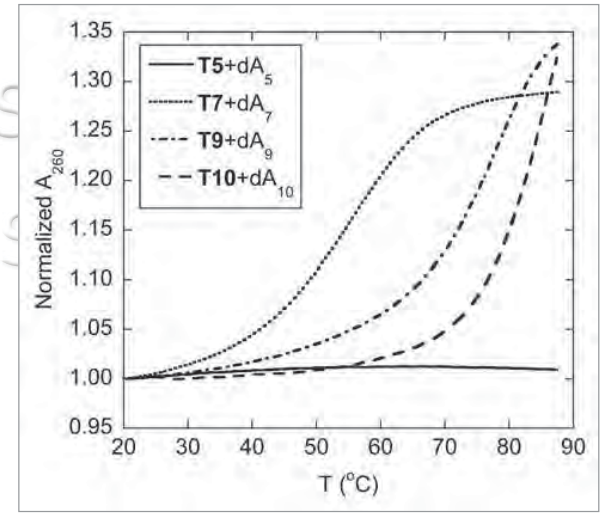

Figure 3. T_m curves of homothymine acpcPNA·DNA hybrids with different length. Conditions: 1.0 μM PNA, 1.0 μM DNA, 10 mM sodium phosphate buffer pH 7.0, 0 mM NaCl, heating rate 1.0°C/min.

and a similar explanation based on counterion release upon duplex formation should be applicable here.[6] At sufficiently high salt concentrations (~500 mM or higher), the two transitions merged to give just one melting curve, indicating a simultaneous dissociation of the triplex to the three single strand components at the same temperature.

The formation of a triplex structure between **A9** and dT_9 was also confirmed by UV titration and circular dichroism (CD) spectroscopy. The UV titration revealed two inflection points at acpcPNA:DNA ratio of 1:1 and 1:2 respectively (**Sup. Fig. 38**). The CD spectrum of single-stranded acpcPNA **A9** (**Fig. 4B**) shows strong signals in the region of nucleobase absorption around 265 nm. This suggests that the single stranded

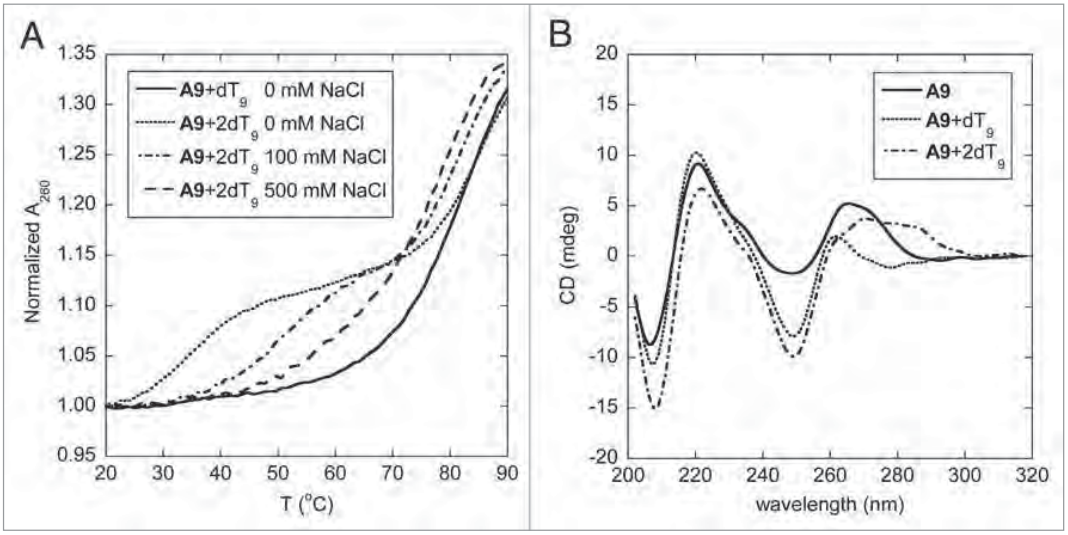

Figure 4. T_m curves (A) and CD spectra (B) of homoadenine acpcPNA·DNA hybrids at different ratio. Conditions: (A) 1.0 μM acpcPNA, 10 mM sodium phosphate buffer pH 7.0, 0–500 mM NaCl, heating rate 1.0°C/min; (B) 2.0 μM acpcPNA, 10 mM sodium phosphate buffer pH 7.0, 0 mM NaCl, 25°C.

homoadenine acpcPNA exists in a well-defined helical conformation, allowing effective stacking of the nucleobases. Addition of one equivalent of dT_9 to this acpcPNA solution caused a substantial spectral change in both position and magnitude of the CD bands in the nucleobase absorption region. The positive CD bands at 265 nm in the original single stranded acpcPNA shifted to a shorter wavelength of 260 nm in the duplex. This is also accompanied by an increase in the intensity of the negative CD band at 250 nm. The CD spectrum of this **A9**·dT_9 is remarkably similar to the CD spectrum of the **T9**·dA_9 duplex reported earlier.[32] Upon addition of the second equivalent of the DNA, a distinctive change was again observed in the nucleobase absorption region. The measured CD spectrum is clearly different from the sum of the CD spectra of each component, therefore it can be concluded that yet another species—most likely to be the triplex—is formed at 2:1 DNA:PNA ratio. In all cases, very little changes of the CD signal were observed in the peptide backbone region suggesting that there is little conformational change of the acpcPNA backbone upon hybrid formation.

Despite the extremely high stability of the homothymine and homoadenine acpcPNA hybrids with their complementary DNA, T_m data of mismatched acpcPNA·DNA hybrids (**Table 2**) revealed that the specificity is not compromised. It can be clearly seen that the base T in the acpcPNA **T9** can recognize only the base A in DNA, and the base A in the acpcPNA **A9** can recognize only the base T in DNA. Introduction of a mismatched base in the DNA strand caused a significant destabilization of the mismatched duplex as shown by the large decrease of T_m (ΔT_m) ranging from -23.4 to -37.8°C. The T_m decreases per mismatch in these cases are considerably larger than those typically observed in aegPNA (~10–15°C per mismatched base).[4]

Hybridization studies of mixed-base acpcPNA—directional preference and base pairing specificity. We have previously shown that the mixed sequence PNA decamer **M10a** preferred hybridization with DNA in antiparallel orientation.[33] To ascertain that the antiparallel directional preference is a general behavior of the present acpcPNA system, additional T_m experiments were performed with nine different 10mer mixed-base PNA sequences (**Table 3**). Although the stability of acpcPNA·DNA hybrids is not expected to be very much dependent to the ionic strength as in the case of DNA·DNA hybrids, the melting studies were performed in 10 mM sodium phosphate buffer both in the absence and presence of NaCl (100 mM) conditions. All antiparallel hybrids showed single-transition melting curves with T_m in the range of 57.0–65.5°C (at 0 mM NaCl) and 52.8–61.0°C (at 100 mM NaCl). The slightly lower T_m values at high salt conditions compared to the low salt conditions (~4–5°C) are consistent with the behavior of aegPNA.[6] On the other hand, no sigmoidal transtitions could be observed when parallel DNA were present under both low salt and high salt conditions in all cases. This indicates that the parallel hybrids would have T_m values of less than 20°C for all nine sequences tested. The T_m difference by more than 30°C suggests that the antiparallel PNA·DNA hybrids are much more stable than the corresponding parallel hybrids. This property is in sharp contrast to the original aegPNA which could form both antiparallel and parallel hybrids with DNA, although the antiparallel hybrid was slightly more stable (ΔT_m antiparallel vs. parallel hybrids ~13°C for a 10mer mixed base aegPNA with the same sequence as **M10a**).[4] It has been observed that a modification of the aegPNA backbone with a short stretch of chiral monomer ("chiral box") could greatly enhance the antiparallel preference by destabilization of the parallel hybrid.[39] It appears that the presence of stereoregular backbone in these chiral PNAs allows binding to DNA in only one direction, thus enhancing the orientation selectivity relative to the achiral backbone of aegPNA.

The T_m of the complementary hybrid formed between the acpcPNA **M10a** and its complementary DNA was 53.3°C at

©2011 Landes Bioscience.
Do not distribute.

100 mM NaCl and 10 mM sodium phosphate. This figure is slightly higher than the corresponding aegPNA system with identical sequence (48.9°C) under comparable conditions.[15] To determine the base pairing specificity, the acpcPNA **M10a** was hybridized, one by one, with twelve other DNA probes carrying a mismatched base between the positions 4 to 7 of the sequence. The results, which are summarized in **Table 4**, indicated that the acpcPNA·DNA hybridization strictly follows the Watson-Crick base pairing rules and is highly specific. As observed in the case of homothymine or homoadenine acpcPNA hybrids with DNA, the presence of one mismatched base in the DNA part caused a substantial decrease in T_m values (-22.3 to -29.5°C) of the mixed sequence acpcPNA·DNA hybrids. With few exceptions, the pyrimidine-pyrimidine mismatched pairs tend to be more stable than the purine-purine mismatched pairs. The potentially wobble G·T pairs[40] showed a similar drop in T_m to other mismatched pairs. It is important to note that the T_m values of all single mismatched hybrids of acpcPNA are smaller than the corresponding mismatched hybrids of aegPNA. As a result, the differences in thermal stability between complementary and mismatched hybrids of the present acpcPNA system are significantly greater than those of the original aegPNA system (ΔT_m = -12.9 to -16.9°C for aegPNA/DNA with the same sequences).[15] The enhanced directional selectivity and discrimination of single base mismatched target of acpcPNA over aegPNA have also been independently verified by surface plasmon resonance (SPR) experiments in a different sequence.[34] Thus it can be concluded that the more rigid acpcPNA backbone improves both the binding affinity and the specificity for single base mismatches discrimination towards DNA targets.

Hybridization studies of mixed-base PNA—comparison between DNA and RNA. We have previously noted that the acpcPNA·DNA hybrids are more thermally stable than the corresponding acpcPNA·RNA hybrids in a few representative sequences.[33] In the present study, a larger pool of acpcPNA and RNA sequences were included to obtain a clearer picture. Comparison between the results shown in **Table 5** and **Table 3** confirmed our previous observation that the acpcPNA·DNA hybrids are more stable than acpcPNA·RNA hybrids with identical sequences in all cases. The results also unexpectedly revealed an interesting relationship between T_m and G+C content, which can be observed more clearly in **Figure 5**. The T_m values of the antiparallel acpcPNA·RNA hybrids appears to show relationships to the %G+C content in the same way as normal DNA/RNA duplexes, i.e., duplexes with greater %G+C content possess higher T_m values. The nine antiparallel acpcPNA·RNA hybrids included in this study showed T_m values between 32.6 and 51.2°C (T_m difference = 18.6°C). On the other hand, the T_m values for the corresponding antiparallel acpcPNA·DNA hybrids span a much smaller temperature range between 52.8 and 61.0°C (T_m difference = 8.2°C) and do not show obvious correlations with %G+C content. It has been earlier noted that aegPNA·DNA duplexes derived from purine-rich aegPNA were much more stable than those derived from pyrimidine-rich aegPNA with identical G+C content.[41] Such purine-stabilizing effect should be minimal here since all acpcPNA sequences used in this study contain a similar purine content of 40–60%. Furthermore, no correlation could be observed between thermal stability and purine content of the acpcPNA·DNA and acpcPNA·RNA hybrids used in this study and in other additional sequences.[42] As shown in **Figure 5**, the difference in the stability between acpcPNA·DNA and acpcPNA·RNA hybrids is more pronounced at lower G+C contents than at higher ones. It is also interesting to note that the formation of parallel acpcPNA·RNA hybrids could be observed, especially when the G+C content is high. Nevertheless, the T_m values of these parallel acpcPNA·RNA hybrids are much lower than the corresponding antiparallel hybrids. Hence it can be concluded that (1) the acpcPNA binds more strongly to DNA over RNA, but the difference in thermal stability is dependent on the G+C content and (2) although the antiparallel binding mode is preferred in acpcPNA·RNA hybrids, the selectivity between the antiparallel/parallel binding modes is lower than the corresponding acpcPNA·DNA hybrids.

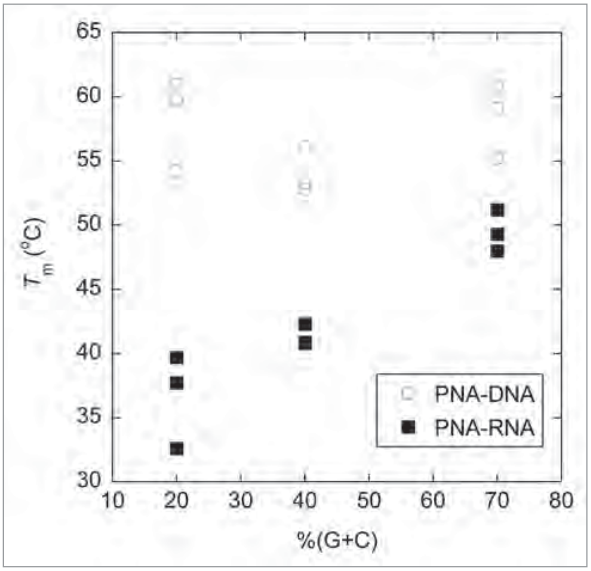

Figure 5. A plot showing relationship between G+C content and thermal stability of acpcPNA·DNA and acpcPNA·RNA hybrids. Conditions: 1.0 μM acpcPNA, 1.0 μM DNA, 10 mM sodium phosphate buffer pH 7.0, 100 mM NaCl, heating rate 1.0°C/min. T_m values are accurate to within ±0.5°C.

Most other PNA systems reported to date bind more strongly to RNA than DNA, and many attempts have been made to further enhance the RNA binding with a view to antisense and other applications involving RNA targets.[16,17,22,23] It is interesting to note that while the original aegPNA showed a preference for binding to RNA over DNA, substitution at the γ-position of the PNA backbone by a methyl group increased the stability of the DNA hybrids considerably more than the corresponding RNA hybrid, leading to a lower discrimination between DNA and RNA.[19] The present acpcPNA system and its aza-analog described previously by our group,[31] as well as a chimeric (aeg-pyrrolidine)PNA developed by Kumar,[26] are among a few examples of PNA that show a preference for DNA binding.[23] Although the structural basis

Landes Bioscience. Do not distribute.

Table 1. Sequences and characterization data of acpcPNA used in this study

Entry	PNA	PNA sequence[a] (N → C)	*m/z* (calcd for $[M+H]^+$)	*m/z* (found)
1	**T5**	TTT TT	1848.9	1848.8
2	**T7**	TTT TTT T	2513.2	2513.5
3	**T9**	TTT TTT TTT	3177.5	3177.6
4	**T10**	TTT TTT TTT T	3467.6	3468.8
5	**A9**	AAA AAA AAA	3258.6	3258.7
6	**M10a**	GTA GAT CAC T	3556.7	3555.9
7	**M10b**	GCT ACG TCG C	3533.7	3533.9
8	**M10c**	TAT GTA CTA T	3546.7	3546.9
9	**M10d**	AGT GAT CTA C	3556.7	3556.0
10	**M10e**	CAT CTA GTG A	3556.7	3556.5
11	**M10f**	GCG ACG TAG C	3582.7	3582.6
12	**M10g**	CGA TGC AGC G	3582.7	3582.6
13	**M10h**	ATA GTA CAT A	3564.7	3564.6
14	**M10i**	ATA CAT GAT A	3564.7	3564.5

[a]All sequences carried a *C*-terminal lysinamide and were *N*-acetylated. [b]MALDI-TOF, linear mode, CCA matrix.

Table 2. T_m data for the hybrids between acpcPNA **T9** and **A9** with complementary and single mismatched DNA

Entry	PNA	DNA		T_m (°C)[a,b]	ΔT_m (°C)[c]
1	**T9**	dAAAAXAAAA	X = A	76.8	-
2			X = T	47.6	-29.2
3			X = C	47.7	-29.1
4			X = G	39.0	-37.8
5	**A9**	dTTTTYTTTT	Y = A	54.6	-25.3
6			Y = T	79.9	-
7			Y = C	56.5	-23.4
8			Y = G	52.7	-27.2

[a]Conditions: 1.0 μM acpcPNA, 1.0 μM DNA, 10 mM sodium phosphate buffer pH 7.0, 0 mM NaCl, heating rate 1.0°C/min. T_m values are accurate to within ±0.5°C. [b]Data for **T9** (entries 1–4) were taken from reference 33. [c]T_m (mismatched) - T_m (complementary).

Table 3. T_m data for the binding between mixed base acpcPNA and DNA in antiparallel and parallel directions[a]

Entry	PNA	T_m (antiparallel DNA) (°C)		T_m (parallel DNA) (°C)	
		0 mM NaCl	100 mM NaCl	0 mM NaCl	100 mM NaCl
1	**M10a**	57.0[b]	53.3[c]	<20[b]	<20[c]
2	**M10b**	60.4	54.5	<20	<20
3	**M10c**	59.6	54.2	<20	<20
4	**M10d**	57.2	52.8	<20	<20
5	**M10e**	60.6	56.1	<20	<20
6	**M10f**	65.2	60.8	<20	<20
7	**M10g**	65.1	59.1	<20	<20
8	**M10h**	65.5	61.0	<20	<20
9	**M10i**	65.3	59.8	<20	<20

[a]Conditions: 1.0 μM acpcPNA, 1.0 μM DNA, 10 mM sodium phosphate buffer pH 7.0 at 0 or 100 mM NaCl concentrations, heating rate 1.0°C/min. T_m values are accurate to within ±0.5°C. [b]Data taken from reference 33. [c]Data taken from reference 36.

of this preference is not available at present, it can be speculated that the preferential binding to DNA over RNA may be due to the more limited conformations space available in RNA duplexes compared to DNA duplexes as a result of the additional 2'-OH group present in RNA. Upon binding to RNA, it is likely that the acpcPNA could not adopt the same conformation as when it is bound to DNA. Works in this area, including molecular dynamics simulations[43] and NMR spectroscopic studies are in progress.

Thermodynamic parameters of acpcPNA·DNA and acpcPNA·RNA hybridization. The extremely high stability of homoadenine/homothymine acpcPNA·DNA hybrids compared to the mixed base acpcPNA·DNA of comparable length, as well as the sequence-independent stability of acpcPNA·DNA, but not acpcPNA·RNA, hybrids are quite unexpected. In an attempt to understand this unusual behavior, the melting curves of DNA and RNA hybrids of the acpcPNA **M10a**–**M10c** having different G+C contents between 20–70% were analyzed by nonlinear curve fitting[44] and by van't Hoff analysis[45] to extract the thermodynamic parameters (**Table 6**). The data suggested that despite the large enthalpy gain for G·C rich acpcPNA hybrids compared to A·T rich ones, the entropy terms are more negative (less favorable). This is true for both acpcPNA·DNA (entry 2) and acpcPNA·RNA hybrids (entry 5). In order to achieve the required geometry for the usual three hydrogen bonding pattern and/or maximum stacking of the G·C pairs, the structure of the base pairs must be distorted to some extent, resulting in a large entropy loss. On the other hand, the enthalpy term of the A·T rich acpcPNA·DNA hybrids (entry 3) were relatively large compared to the corresponding acpcPNA·RNA hybrid (entry 6), while the entropy terms were similar. Since Watson-Crick A·T pairs can form only two hydrogen bonds compared to three in G·C pairs, hydrogen bonding cannot be the main contributor to the enthalpy term. We propose that base stacking must be the main factor to stabilize the A·T pair relative to the G·C pairs in the acpcPNA·DNA hybrids. The stacking-hydrogen bonding compensation[46-48] might explain why the difference of the enthalpy change between G·C and A·T pairs is rather small. The same stabilization effects of A·T pair are absent in acpcPNA·RNA hybrids, perhaps due to the more limited conformation space available in acpcPNA·RNA hybrids, which may keep the spatial geometry from achieving maximum stacking. Additional structural studies, e.g., by X-ray or NMR are required to understand this behavior in details.

Evidences for the absence of self-hybridization in acpcPNA. In addition to the preference for binding to DNA over RNA, the acpcPNA system also displayed another rather unusual property, namely the inability of two complementary PNA strands to form self-pairing hybrids. This behavior has been previously demonstrated for acpcPNA with the sequence **M10a** and its antiparallel and parallel complementary acpcPNA sequences

©2011 Landes Bioscience. Do not distribute

Table 4. Comparison of T_m data to show specificity of binding between mixed base acpcPNA **M10a** and complementary/single base mismatched DNA

Entry	DNA sequence (5' → 3')	T_m (°C)[a]	ΔT_m (°C)[b]	Note
1	AGT GAT CTA C	53.3[c]	-	complementary
2	AGT AAT CTA C	26.4	-26.9	pC·dA mismatch
3	AGT TAT CTA C	27.8	-25.5	pC·dT mismatch
4	AGT CAT CTA C	31.0	-22.3	pC·dC mismatch
5	AGT GGT CTA C	23.9[c]	-29.4	pT·dG mismatch
6	AGT GTT CTA C	29.4[c]	-23.9	pT·dT mismatch
7	AGT GCT CTA C	23.8[c]	-29.5	pT·dC mismatch
8	AGT GAG CTA C	26.5	-26.8	pA·dG mismatch
9	AGT GAA CTA C	28.4	-24.9	pA·dA mismatch
10	AGT GAC CTA C	28.8	-24.5	pA·dC mismatch
11	AGT GAT GTA C	26.4	-26.9	pG·dG mismatch
12	AGT GAT ATA C	24.2	-29.1	pG·dA mismatch
13	AGT GAT TTA C	28.5	-24.8	pG·dT mismatch

[a]Conditions: 1.0 μM acpcPNA, 1.0 μM DNA, 10 mM sodium phosphate buffer pH 7.0, 100 mM NaCl, heating rate 1.0°C/min. T_m values are accurate to within ±0.5°C. [b]T_m (mismatched) - T_m (complementary). [c]Data taken from reference 36.

Table 5. T_m data for the binding between mixed base acpcPNA and RNA in antiparallel and parallel directions[a]

Entry	PNA	%G+C	T_m (antiparallel RNA) (°C)	T_m (parallel RNA) (°C)
1	**M10a**	40	42.3[b]	<20[b]
2	**M10b**	70	48.0	32.9
3	**M10c**	20	32.6	<20
4	**M10d**	40	40.8	not determined
5	**M10e**	40	40.9	not determined
6	**M10f**	70	49.3	30.2
7	**M10g**	70	51.2	28.5
8	**M10h**	20	39.7	not determined
9	**M10i**	20	37.7	not determined

[a]Conditions: 1.0 μM acpcPNA, 1.0 μM DNA, 10 mM sodium phosphate buffer pH 7.0, 100 mM NaCl, heating rate 1.0°C/min. T_m values are accurate to within ±0.5°C. [b]Data taken from reference 36.

M10d and **M10e**.[33] In this work, we extend the study to four other acpcPNA·acpcPNA pairs to demonstrate that the non-self pairing behavior is general over a range of sequences with different G+C contents (**Table 7**). Indeed, no melting could be observed in all of the antiparallel hybrids indicating that these hybrids were not stable above 20°C. On the other hand, some rather unstable parallel hybrids could be observed for sequences with ≥40% G+C content (entries 2 and 4). The low stability of both the antiparallel and parallel acpcPNA·acpcPNA hybrids is in sharp contrast to the situation of aegPNA, whereby the PNA·PNA hybrids are very stable. In fact, the stability of aegPNA·aegPNA antiparallel hybrids is generally much higher than the corresponding aegPNA·DNA and aegPNA·RNA hybrids.[6] To the best of our knowledge this absence of self-pairing, despite the ability to cross-pair with both DNA and RNA, has not been reported in other PNA systems. Interestingly, our recent investigation revealed that the epimeric acpcPNA with the (2'*R*,4'*S*)-configuration on the proline ring could form an antiparallel self-pairing hybrid.[36] Nevertheless, the self-pairing hybrid is considerably less stable than the corresponding acpcPNA·DNA hybrid. Although more studies are required to understand its structural basis, this unusual property is a highly desirable one. For example, the non-self-pairing acpcPNA may be useful for targeting dsDNA via a "double duplex invasion" mechanism whereby the two PNA strands designed to target two opposite DNA strands in the same region of the dsDNA target. The original aegPNA is not suitable for this purpose as the two complementary PNA strands binds to each other much more strongly than with their respective DNA targets.[49,50] Current strategies to use aegPNA for double duplex invasion involve modification of the aegPNA by modifying the nucleobases[49] and incorporation of multiple positive charges into the PNA backbone[50] to provide a so-called pseudocomplementary PNA that binds more strongly to DNA than to itself. The present acpcPNA system does not require any modification to achieve this property. The absence of self-pairing in acpcPNA also means that there is a low propensity for secondary structure formation by intra- or inter-strand self-pairing, which are often problematic in designing DNA and aegPNA sequences for various applications such as probes for DNA sequence determination. On the other hand, this property restricts the use of acpcPNA in applications that require self-organization of the PNA strand such as molecular beacons with the classical stem-loop design.[51]

In conclusion, we have developed new conformationally constrained pyrrolidinyl PNA systems based on an alternating nucleobase-subtituted proline and 2-aminocyclopentanecarboxylic acid backbone. The specific stereochemical requirements of both the proline and the 2-aminocyclopentanecarboxylic acid parts that allow effective binding to DNA have been identified. The PNA system with (2'*R*,4'*R*)-proline/(1*S*,2*S*)-2-aminocyclopentanecarboxylic acid backbone, which is named acpcPNA, binds to DNA only in antiparallel orientation with exceptionally high affinity and sequence specificity following the Watson-Crick base pairing rules. In addition, the stability of the acpcPNA·DNA hybrids is largely independent of the base

©2011 Landes Bioscience

Table 6. Thermodynamic parameters of hybrids of acpcPNA with DNA and RNA[a]

Entry	PNA	Counterstrand[b]	%G+C	T_m (°C)[c]	$\Delta H°$ (kcal/mol)[c]	$\Delta S°$ (cal/mol·K)[c]	$\Delta G°_{298}$ (kcal/mol)[c]
1	**M10a**	DNA	40	53.1	-64.1 ± 1.0 (-64.1 ± 0.7)	-168 ± 3 (-167 ± 2)	-14.1 ± 0.1 (-14.1 ± 0.0)
2	**M10b**	DNA	70	56.4	-68.9 ± 1.9 (-69.0 ± 3)	-180 ± 6 (-180 ± 10)	-15.2 ± 0.3 (-15.2 ± 0.4)
3	**M10c**	DNA	20	53.8	-60.9 ± 1.0 (-61.7 ± 1.0)	-157 ± 3 (-160 ± 3)	-14.0 ± 0.0 (-14.1 ± 0.0)
4	**M10a**	RNA	40	42.8	-60.0 ± 0.2 (-60.1 ± 0.9)	-161 ± 0.5 (-161 ± 3)	-12.0 ± 0.1 (-12.0 ± 0.0)
5	**M10b**	RNA	70	48.1	-68.0 ± 2.6 (-67.9 ± 2.8)	-183 ± 8 (-183 ± 8)	-13.5 ± 0.3 (-13.5 ± 0.3)
6	**M10c**	RNA	20	33.1	-54.9 ± 3.1 (-54.3 ± 1.4)	-151 ± 10 (-148 ± 4)	-10.1 ± 0.3 (-10.0 ± 0.2)

[a]Conditions: 1.0 μM of each acpcPNA and DNA or RNA strand, 10 mM sodium phosphate buffer pH 7.0, 150 mM NaCl, heating rate 1.0°C/min. [b]Antiparallel complementary DNA or RNA. [c]T_m and thermodynamic parameters are obtained from curve fitting.[44] Those obtained from van't Hoff analysis[45] are shown in parentheses. All figures are average of at least three independent analyses. Errors are calculated based on standard deviation.

Table 7. T_m data for the binding between two complementary strands of acpcPNA in antiparallel and parallel directions

Entry	PNA pairs	%G+C	T_m (°C)[a]	Note
1	**M10a·M10d**	40	<20	antiparallel
2	**M10a·M10e**	40	24.2	parallel
3	**M10b·M10f**	70	<20	antiparallel
4	**M10b·M10g**	70	35.1	parallel
5	**M10c·M10h**	20	<20	antiparallel
6	**M10c·M10i**	20	<20	parallel

[a]Conditions: 1.0 μM of each acpcPNA strand, 10 mM sodium phosphate buffer pH 7.0, 100 mM NaCl, heating rate 1.0°C/min. T_m values are accurate to within ±0.5°C.

©2011 Landes Bioscience. Do not distribute

sequence. This particular property should render the acpcPNA system highly useful as probes in multiplex SNP analysis and microarray applications whereby several DNA targets are to be analyzed simultaneously.[35,49] The acpcPNA also binds to complementary RNA, albeit with lower hybrid stability and directional specificity compared to DNA. Consequently, the present acpcPNA system may be less useful for applications that require targeting RNA such as RNA detection or antisense applications. The difference in stability between acpcPNA·DNA and acpcPNA·RNA hybrids is more pronounced in A·T rich than G·C rich sequences, which could be explained by enthalpic stabilization of A·T pairs over G·C pairs in acpcPNA·DNA hybrids. Finally, the unique absence of self-pairing between two complementary strands of acpcPNA suggests that it should be a potential candidate for targeting double stranded DNA by double duplex invasion, which could be useful for antigene applications.

Materials and Methods

Materials and reagents. Oligonucleotides were obtained from Biodesign (Pathumthani, Thailand) and were used as received. The concentration of oligonucleotides and acpcPNAs was determined from the absorbance at 260 nm using the reported molar extinction coefficients at 260 nm (ε_{260}) for DNA monomers.[53]

PNA synthesis. Synthesis and characterization data of acpcPNA monomers have either been previously described [(2'*R*,4'*R*) and (2'*R*,4'*S*) diastereomers][33,36] or can be found in the supporting information [(2'*S*,4'*S*) and (2'*S*,4'*R*) diastereomers]. All acpcPNAs were synthesized manually from the corresponding Fmoc-protected acpcPNA monomers and β-amino acids spacers by Fmoc-solid phase peptide synthesis on a Tentagel resin carrying the acid-labile Rink amide linker as described previously.[33] L-Lysinamide was incorporated at the C-termini of the acpcPNAs to improve water solubility and the PNA was end-capped by acetylation. The acpcPNAs were purified by reverse-phase HPLC and characterized by MALDI-TOF mass spectrometry. The sequences and MALDI-TOF analysis data of the synthesized PNA are shown in **Table 1**.

UV melting experiments. UV melting experiments were performed on a CARY 100 UV Spectrophotometer (Varian Inc., Australia) equipped with a Peltier temperature controller and a thermal analysis software. The sample for thermal denaturation measurement was prepared by mixing calculated amounts of stock oligonucleotide, PNA and buffer solutions together to give the final concentration of PNA = 1.0 μM and DNA = 1.0 μM, sodium phosphate buffer pH 7.0 (10 mM) and sodium chloride (0 or 100 mM). The final volumes were adjusted to 1.0 mL by addition of deionized water. The samples were transferred to a 10 mm quartz cell with Teflon stopper and equilibrated at the starting temperature for 10 min. The A_{260} was recorded in steps from 20 to 90°C in two heating and one cooling cycles (20-90-20-90) with a temperature increment of 1.0°C/min and a hold time of 10 min at the end of each cycle. The recorded temperature was corrected by a linear equation obtained from the relationship between the recorded temperature and actual temperature measured by a built-in temperature probe. Only the result taken from the last heating cycle was used. This was normalized by dividing the absorbance at each temperature by the initial absorbance. Thermodynamic parameters were obtained from melting curves by non-linear curve fitting[44] and by van't Hoff analysis.[45] The data obtained are average of at least three melting curves for each PNA samples at a concentration of PNA = DNA = 1.0 μM (c_t = 2.0 μM) in sodium phosphate buffer, pH 7.0 and 150 mM NaCl. The $\Delta G°$ at 298 K and T_m were calculated from the $\Delta H°$ and $\Delta S°$ values.

CD experiments. CD measurements were performed on a JASCO Model J-715 or J-815 Spectropolarimeter (JASCO,

Japan). The samples were prepared by mixing the calculated amounts of stock oligonucleotide and PNA solutions in an appropriate buffer in a quartz cell (path length = 10 mm). The spectra were measured at 25°C from 320 to 200 nm and averaged 4 times then subtracted from a spectrum of the buffer under the same conditions.

Acknowledgments

Financial support to this work from the Thailand Research Fund (RTA5280002), the Thai government stimulus package 2 (TKK2555, SP2) under the Project for Establishment of Comprehensive Center for Innovative Food, Health Products and Agriculture,and the National Research University of CHE and the Ratchadaphiseksomphot Endowment Fund (AM1006A).

Note

Supplementary information for this article can be found at http://www.landesbioscience.com/journals/artificialdna/article/16340/

References

1. Nielsen PE. Peptide nucleic acid. A molecule with two identities. Acc Chem Res 1999; 32:624-30.
2. Uhlman E, Peyman A, Breipohl G, Will DW. PNA: Synthetic polyamide nucleic acids with unusual binding properties. Angew Chem Int Ed 1998; 37:2796-823.
3. Nielsen PE, Haaima G. Peptide nucleic acid (PNA). A DNA mimic with a pseudopeptide backbone. Chem Soc Rev 1997; 26:73-8.
4. Egholm M, Buchardt O, Christensen L, Behrens C, Freier SM, Driver DA, et al. PNA hybridizes to complementary oligonucleotides obeying the Watson-Crick hydrogen-bonding rules. Nature 1993; 365:566-8.
5. Leumann CJ. DNA analogues: From supramolecular principles to biological properties. Bioorg Med Chem 2002; 10:841-54.
6. Tomac S, Sarkar M, Ratilainen T, Wittung P, Nielsen PE, Nordén B, Gräslund A. Ionic effects on the stability and conformation of peptide nucleic acid complexes. J Am Chem Soc 1996; 118:5544-52.
7. Bentin T, Hansen GI, Nielsen PE. Structural diversity of target-specific homopyrimidine peptide nucleic acid-dsDNA complexes. Nucl Acids Res 2006; 34:5790-9.
8. Nielsen PE, Egholm M, Berg RH, Buchardt O. Sequence-selective recognition of DNA by strand displacement with a thymine-substituted polyamide. Science 1991; 254:1497-500.
9. Li M, Zengeya T, Rozners E. Short peptide nucleic acids bind strongly to homopurine tract of double helical RNA at pH 5.5. J Am Chem Soc 2010; 132:8676-81.
10. Demidov VV, Potaman VN, Frank-Kamenetskii MD, Egholm M, Buchardt O, Sönnichsen SH, Nielsen PE. Stability of peptide nucleic acids in human serum and cellular extracts. Biochemical Pharmacology 1994; 48:1310-3.
11. Brandt O, Hoheisel JD. Peptide nucleic acids on microarrays and other biosensors. Trends Biotechnol 2004; 22:617-22.
12. Pellestor F, Paulasova P, Hamamah S. Peptide nucleic acids (PNAs) as diagnostic devices for genetic and cytogenetic analysis. Curr Pharm Des 2008; 14:2439-44.
13. Braasch DA, Corey DR. Novel antisense and peptide nucleic acid strategies for controlling gene expression. Biochemistry 2002; 41:4503-10.
14. Ray A, Nordén B. Peptide nucleic acid (PNA): its medical and biotechnical applications and promise for the future. FASEB J 2000; 14:1041-60.
15. Pokorski JK, Witschi MA, Purnell BL, Appella DH. (S,S)-trans-Cyclopentane-constrained peptide nucleic acids. A general backbone modification that improves binding affinity and sequence specificity. J Am Chem Soc 2004; 126:15067-73.
16. Govindaraju T, Kumar VA, Ganesh KN. (SR/RS)-Cyclohexanyl PNAs: Conformationally preorganized PNA analogues with unprecedented preference for duplex formation with RNA. J Am Chem Soc 2005; 127:4144-5.
17. Govindaraju T, Madhuri V, Kumar VA, Ganesh KN. Cyclohexanyl peptide nucleic acids (chPNAs) for preferential RNA binding: Effective tuning of dihedral angle β in PNAs for DNA/RNA discrimination. J Org Chem 2006; 71:14-21.
18. Kumar VA, Ganesh KN. Conformationally constrained PNA analogues: Structural evolution toward DNA/RNA binding selectivity. Acc Chem Res 2005; 38:404-12.
19. Dragulescu-Andrasi A, Rapireddy S, Frezza BM, Gayathri C, Gil RR, Ly DH. A simple γ-backbone modification preorganizes peptide nucleic acid into a helical structure. J Am Chem Soc 2006; 128:10258-67.
20. Yeh JI, Shivachev B, Rapireddy S, Crawford MJ, Gil RR, Du SC, et al. Crystal structure of chiral γPNA with complementary DNA strand: Insights into the stability and specificity of recognition and conformational preorganization. J Am Chem Soc 2010; 132:10717-27.
21. Englund EA, Appella DH. γ-Substituted peptide nucleic acids constructed from L-Lysine are a versatile scaffold for multifunctional display. Angew Chem Int Ed 2007; 46:1414-8.
22. Ngamwiriyawong P, Vilaivan T. Synthesis and nucleic acids binding properties of diastereomeric aminoethylprolyl peptide nucleic acids (aepPNA). Nucleosides Nucleotides and Nucleic Acids 2011; 30:97-112.
23. Tan THS, Hickman DT, Morral J, Beadham IG, Micklefield J. Nucleic acid binding properties of thyminyl and adeninyl pyrrolidine-amide oligonucleotide mimics (POM). Chem Comm 2004; 516-7.
24. Tan THS, Worthington RJ, Pritchard RG, Morral J, Micklefield J. Homopolymeric pyrrolidine-amide oligonucleotide mimics: Fmoc-synthesis and DNA/RNA binding properties. Org Biomol Chem 2007; 5:239-48.
25. Worthington RJ, O'Rourke AP, Morral J, Tan THS, Micklefield J. Mixed sequence pyrrolidine-amide oligonucleotide mimics: Boc(Z) synthesis and DNA/RNA binding properties. Org Biomol Chem 2007; 5:249-59.
26. Lonkar PS, Ganesh KN, Kumar VA. Chimeric (aegpyrrolidine)PNAs: synthesis and stereodiscriminative duplex binding with DNA/RNA. Org Biomol Chem 2004; 2:2604-11.
27. Choi SH, Guzei IA, Spencer LC, Gellman SH. Crystallographic characterization of helical secondary structures in α/β-peptides with 1:1 residue alternation. J Am Chem Soc 2008; 130:6544-50.
28. Hayen A, Schmitt MA, Ngassa FN, Thomasson KA, Gellman SH. Two helical conformations from a single foldamer backbone: "Split personality" in short α/β-peptides. Angew Chem Int Ed 2004; 43:505-10.
29. Gogoi K, Kumar VA. Chimeric (α-amino acid + nucleoside-β-amino acid)$_n$ peptide oligomers show sequence specific DNA/RNA recognition. Chem Commun 2008; 706-8.
30. Vilaivan T, Suparpprom C, Harnyuttanakorn P, Lowe G. Synthesis and properties of novel pyrrolidinyl PNA carrying β-amino acid spacers. Tetrahedron Lett 2001; 42:5533-6.
31. Vilaivan T, Lowe G. A novel pyrrolidinyl PNA showing high sequence specificity and preferential binding to DNA over RNA. J Am Chem Soc 2002; 124:9326-7.
32. Suparpprom C, Srisuwannaket C, Sangvanich P, Vilaivan T. Synthesis and oligodeoxynucleotide binding properties of pyrrolidinyl peptide nucleic acids bearing prolyl-2-aminocyclopentanecarboxylic acid (ACPC) backbones. Tetrahedron Lett 2005; 46:2833-7.
33. Vilaivan T, Srisuwannaket C. Hybridization of pyrrolidinyl peptide nucleic acids and DNA: Selectivity, base-pairing specificity and direction of binding. Org Lett 2006; 8:1897-900.
34. Ananthanawat C, Vilaivan T, Hoven VP, Su X. Comparison of DNA, aminoethylglycyl PNA and pyrrolidinyl PNA as probes for detection of DNA hybridization using surface plasmon resonance technique. Biosens Bioelectron 2010; 25:1064-9.
35. Boontha B, Nakkuntod J, Hirankarn N, Chaumpluk P, Vilaivan T. Multiplex mass spectrometric genotyping of single nucleotide polymorphisms employing pyrrolidinyl peptide nucleic acid in combination with ion-exchange capture. Anal Chem 2008; 80:8178-86.
36. Taechalertpaisarn J, Sriwarom P, Boonlua C, Yotapan N, Vilaivan C, Vilaivan T. DNA-, RNA- and self-pairing properties of a pyrrolidinyl peptide nucleic acid with a (2'R,4'S)-prolyl-(1S,2S)-2-aminocyclopentanecarboxylic acid backbone. Tetrahedron Lett 2010; 51:5822-6.
37. Egholm M, Buchardt O, Nielsen PE, Berg RH. Peptide nucleic acids (PNA). Oligonucleotide analogues with an achiral peptide backbone. J Am Chem Soc 1992; 114:1895-7.
38. Kim SK, Nielsen PE, Egholm M, Buchardt O, Berg RH, Nordén B. Right-handed triplex formed between peptide nucleic acid PNA-T$_8$ and poly(dA) shown by linear and circular dichroism spectroscopy. J Am Chem Soc 1993; 115:6477-81.
39. Sforza S, Corradini R, Ghirardi S, Dossena A, Marchelli R. DNA binding of a D-lysine-based chiral PNA: Direction control and mismatch recognition. Eur J Org Chem 2000; 2905-13.
40. Igloi GL. Variability in the stability of DNA-peptide nucleic acid (PNA) single-base mismatched duplexes: Real-time hybridization during affinity electrophoresis in PNA-containing gels. Proc Natl Acad Sci USA 1998; 95:8562-7.
41. Sen A, Nielsen PE. Unique properties of purine/pyrimidine asymmetric PNA·DNA duplexes: Differential stabilization of PNA·DNA duplexes by purines in the PNA strand. Biophys J 2006; 90:1329-37.
42. In an extreme case, the T_m difference between two complementary acpcPNA·DNA hybrids with purine rich (AGG TAA CGA G) and pyrimidine rich (CTC GTT ACC T) sequences is only 8.4°C compared to a difference of 26.0°C for the corresponding aegPNA·DNA hybrids under identical conditions (data extracted from reference 41).
43. Siriwong K, Chuichay P, Saen-oon S, Suparpprom C, Vilaivan T, Hannongbua S. Insight into why pyrrolidinyl peptide nucleic acid binding to DNA is more stable than the DNA·DNA duplex. Biochem Biophys Res Commun 2008; 372:765-71.

©2011 Landes Bioscience. Do not distribute

44. Kawakami J, Tanaka Y, Kishimoto K. Accurate curve fitting procedure for UV melting analysis of highly thermostable RNA hairpins. Nucleic Acids Symp Series 2009; 53:227-8.
45. Marky LA, Breslauer KJ. Calculating thermodynamic data for transitions of any molecularity from equilibrium melting curves. Biopolymers 1987; 26:1601-20.
46. Guckian KM, Schweitzer BA, Ren RXF, Sheils CJ, Tahmassebi DC, Kool ET. Factors contributing to aromatic stacking in water: Evaluation in the context of DNA. J Am Chem Soc 2000; 122:2213-22.
47. Bommarito S, Peyret N, SantaLucia J Jr. Thermodynamic parameters for DNA sequences with dangling ends. Nucl Acids Res 2000; 28:1929-34.
48. Sugimoto N, Kierzek R, Turner DH. Sequence dependence for the energetics of dangling ends and terminal base pairs in ribonucleic acid. Biochemistry 1987; 26:4554-8.
49. Demidov VV, Protozanova E, Izvolsky KI, Price C, Nielsen PE, Frank-Kamenetskii MD. Kinetics and mechanism of the DNA double helix invasion by pseudocomplementary peptide nucleic acids. Proc Natl Acad Sci USA 2002; 99:5953-8.
50. Ishizuka T, Yoshida J, Yamamoto Y, Sumaoka J, Tedeschi T, Corradini R, et al. Chiral introduction of positive charges to PNA for double-duplex invasion to versatile sequences. Nucleic Acids Res 2008; 36:1464-71.
51. Tyagi S, Kramer FR. Molecular beacons: Probes that fluoresce upon hybridization. Nat Biotechnol 1996; 14:303-8.
52. Ahlborn C, Siegmund K, Richert C. Isostable DNA. J Am Chem Soc 2007; 129:15218-32.
53. Egholm M, Nielsen PE, Buchardt O, Berg RH. Recognition of guanine and adenine in DNA by cytosine and thymine containing peptide nucleic acids (PNA). J Am Chem Soc 1992; 114:9677-8.

©2011 Landes Bioscience.
Do not distribute.

CHEMISTRY
AN ASIAN JOURNAL

DOI: 10.1002/asia.201100490

5-(Pyren-1-yl)uracil as a Base-Discriminating Fluorescent Nucleobase in Pyrrolidinyl Peptide Nucleic Acids

Chalothorn Boonlua,[a] Chotima Vilaivan,[a] Hans-Achim Wagenknecht,*[b] and Tirayut Vilaivan*[a]

Abstract: A pyrene-labeled uridine (U^{Py}) monomer for a pyrrolidinyl peptide nucleic acid with an alternating proline/2-aminocyclopentanecarboxylic acid backbone (acpcPNA) was synthesized and incorporated into the PNA. The U^{Py} base in acpcPNA could specifically recognize the base A in its complementary DNA strand as determined by thermal denaturation (T_m) experiments. The fluorescence of the U^{Py}-containing single-stranded acpcPNA was very weak in aqueous buffer. In the presence of a complementary DNA target, the fluorescence was enhanced significantly (2.7–41.9 folds, depending on sequences). The fluorescence enhancement was specific to the pairing between U^{Py} and dA, making the U^{Py}-modified acpcPNA useful as a hybridization-responsive fluorescence probe for DNA-sequence determination.

Keywords: electron transfer · fluorescence · molecular beacons · oligonucleotides · peptide nucleic acids

Introduction

Fluorescent DNA-base analogues are potentially useful as probes for DNA-sequence determination as well as physicochemical studies of DNA, such as electron transport. Although a number of such fluorescent bases have been reported,[1] not all of them show a significant fluorescence change upon pairing with their complementary nucleobases. The term base discriminating fluorescent (BDF) nucleosides/nucleobases was introduced by Saito and co-workers to describe such behavior.[2,3] BDF nucleobases can be an entirely re-designed nucleobase surrogate or a canonical nucleobase that is modified with a fluorophore. The latter category is more attractive since the pairing behavior of these nucleobases is, at least in principle, more easily predicted. The nature of the fluorophore itself as well as the linker joining the fluorophore and the nucleobase is very important in determining the fluorescence properties. In DNA, nucleobases that are modified by a fluorophore, such as pyrene through a flexible linker, are usually quenched upon duplex formation as a result of intercalation.[4–7] On the other hand, the fluorescence of the pyrene-modified nucleobase through a rigid linker often increases under similar situations, thus generating a more-desirable turn-on signal.[8–11] In addition to pyrene, other fluorophores that have been successfully incorporated into a DNA nucleobases and yield turn-on signals upon duplex formation include perylene,[12] anthracene,[13,14] and fluorene.[15,16] In all cases, there are one or more of the following limitations: the fluorescence enhancement was modest, the fluorescence change was highly dependent on the flanking bases, and the degree of mismatch discrimination was far from perfect.

The optical properties of 5-(pyren-1-yl)uracil (U^{Py}) deoxyriboside have been extensively studied, both as the monomer[17–19] and when incorporated into DNA.[20,21] The indifferences of the T_m and fluorescence among DNA duplexes carrying different nucleobases opposite to the U^{Py} suggest that this strongly electronically coupled fluorophore-nucleobase does not form typical Watson–Crick-type base-pairing

[a] C. Boonlua, C. Vilaivan, Dr. T. Vilaivan
Organic Synthesis Research Unit
Department of Chemistry, Faculty of Science
Chulalongkorn University
Phayathai Road, Patumwan, Bangkok 10330 (Thailand)
Fax: (+662)2187598
E-mail: vtirayut@chula.ac.th

[b] Prof. Dr. H.-A. Wagenknecht
Institute for Organic Chemistry
Karlsruhe Institute of Technology
76131 Karlsruhe (Germany)
Old address: Institute for Organic Chemistry
University of Regensburg
93040 Regensburg (Germany)
Fax: (+662)2187598
E-mail: hans-achim.wagenknecht@kit.edu

Supporting information for this article is available on the WWW under http://dx.doi.org/10.1002/asia.201100490.

 © 2011 Wiley-VCH Verlag GmbH & Co. KGaA, Weinheim

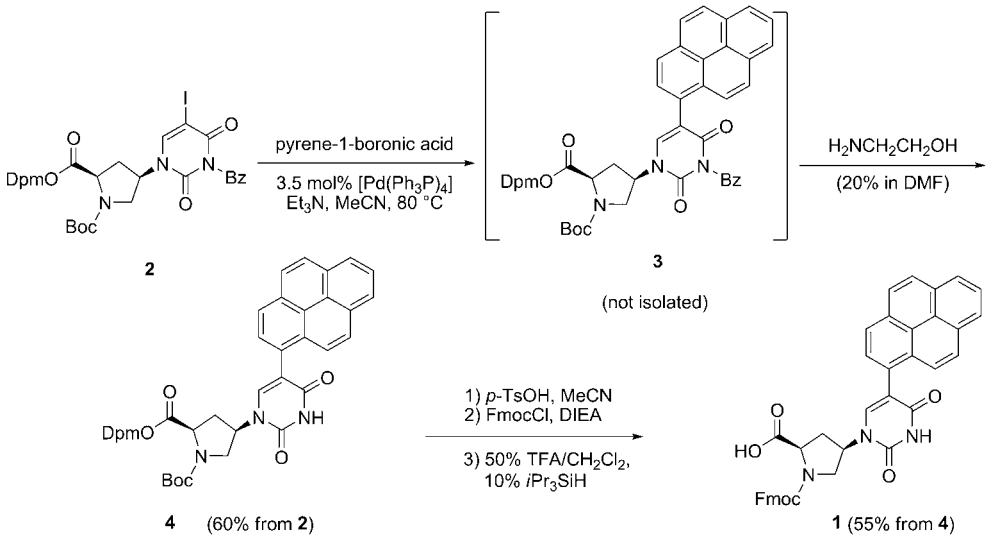

Scheme 1. Synthesis of the Fmoc-protected U^{Py} acpcPNA monomer (**1**). DMF = *N*,*N*-dimethylformamide, Fmoc = fluorenylmethyloxycarbonyl.

with adenine. Accordingly, its application as a BDF in DNA system is limited. On the other hand, there is no report on the pairing and optical properties of this particular U^{Py} base in other DNA analogues, including peptide nucleic acid (PNA). We became interested in designing a quencher-free, singly-labeled PNA beacon[22] using the BDF concept based on our new pyrrolidinyl PNA with a proline/2-aminocyclopentanecarboxylic acid backbone (acpcPNA).[23,24] Herein, we report the synthesis of U^{Py}-modified acpcPNA and demonstrate that the U^{Py} base in acpcPNA can specifically recognize adenine in DNA targets. Most importantly, the fluorescence of the U^{Py}-modified acpcPNA increased significantly in response to the specific base pairing event between U^{Py} and dA.

Abstract in Thai:

ในงานวิจัยนี้ได้สังเคราะห์ยูริดีนโมโนเมอร์ดัดแปลงด้วยไพรีน (U^{Py}) ของพิร์โรลิดินิลเพปไทด์นิวคลีอิกแอซิด (พีเอ็นเอ) ที่ประกอบด้วยโพรลีน/2-อะมิโนไซโคลเพนเทนคาร์บอกซิลิกแอซิด เป็นโครงสร้างหลัก (acpcPNA) และได้สังเคราะห์พีเอ็นเอที่มีโมโนเมอร์ดังกล่าว การวิเคราะห์อุณหภูมิของการหลอมเหลว (T_m) แสดงให้เห็นว่าเบส U^{Py} ใน acpcPNA มีความสามารถในการจดจำเบสอะดีนีนในดีเอ็นเอได้อย่างจำเพาะเจาะจง การเรืองแสงของ acpcPNA สายเดี่ยวซึ่งมี U^{Py} อยู่ด้วยมีค่าต่ำในสารละลายบัฟเฟอร์ แต่เมื่อเกิดไฮบริดกับดีเอ็นเอเป้าหมายที่มีลำดับเบสคู่สมจะมีการเรืองแสงเพิ่มขึ้นอย่างมาก (2.7–41.9 เท่า, ขึ้นกับลำดับเบส) การเพิ่มขึ้นของการเรืองแสงนี้จำเพาะเจาะจงต่อการเข้าคู่กันระหว่างเบส U^{Py} กับเบสอะดีนีน ดังนั้น acpcPNA ที่ผ่านการดัดแปลงด้วย U^{Py} นี้จึงเป็นโพรบเรืองแสงที่ตอบสนองต่อการเกิดไฮบริดที่มีประโยชน์สำหรับการตรวจสอบลำดับเบสของดีเอ็นเอ

Results and Discussion

Synthesis of the U^{Py} Monomer and U^{Py}-Containing PNA

The U^{Py} acpcPNA monomer (**1**) was synthesized in an analogous way to the corresponding DNA nucleoside, as outlined in Scheme 1.[19,25,26] Suzuki–Miyaura cross-coupling between the commercially available pyren-1-boronic acid and the protected iodouracil acpcPNA monomer (**2**) gave the Boc-protected intermediate (**4**; Boc = *tert*-butoxycarbonyl), which, after protecting-group exchange, afforded the desired Fmoc-protected U^{Py} acpcPNA monomer **1**. Compound **2** was obtained from a Mitsunobu reaction between N^3-benzoyl-5-iodouracil and the known Boc/diphenylmethyl-protected *trans*-hydroxy-D-proline intermediate.[27] The U^{Py} acpcPNA monomer **1** was successfully incorporated into internal positions of various acpcPNA sequences (**PNA1**–**PNA8**) through standard O-(7-azabenzotriazol-1-yl)-N,N,N′,N′-tetramethyluronium hexafluorophosphate (HATU) coupling.[23] The identity of all U^{Py}-modified acpcPNA was confirmed by MALDI-TOF mass spectrometry (see the Supporting Information, Table S1).The sequences of all acpcPNA and DNA used in this study are shown in Scheme 2.

Thermal Stabilities and Optical Properties of DNA Hybrids with Homothymine acpcPNA Carrying U^{Py} Modification

Initially, the ability of the U^{Py} residue in acpcPNA to recognize adenine was evaluated in homothymine acpcPNA. One thymine residue in acpcPNA with a T_9 sequence was replaced by a U^{Py} base to give **PNA1**. Thermal stability and fluorescence properties data of **PNA1** and its DNA hybrids are summarized in Table 1. Thermal denaturation experiment of hybrids between **PNA1** and **DNA1a**-**DNA1d** (dA_4XA_4, X = A, T, C, and G, respectively) clearly indicated that the U^{Py} base could specifically recognize the adenine base. The melting temperature (T_m) of the **PNA1**·**DNA1a**

 © 2011 Wiley-VCH Verlag GmbH & Co. KGaA, Weinheim

(N) T–T–T–X–U^{Py}–X–T–T–T (C) — **PNA1**: X = T; **PNA2**: X = A; **PNA3**: X = G; **PNA4**: X = C

(3') A–A–A–Y– Z –Y–A–A–A (5') — **DNA1a**: Y = A; Z = A; **DNA1b**: Y = A; Z = T
DNA1c: Y = A; Z = C; **DNA1d**: Y = A; Z = G
DNA2: Y = T; Z = A; **DNA3**: Y = C; Z = A **DNA4**: Y = G; Z = A

(N) T–T–T–T–T–C–U^{Py}–C–T–T–T–T–T (C) — **PNA5**

(3') A–A–A–A–A–G– T –G–A–A–A–A–A (5') — **DNA5**

acpcPNA =

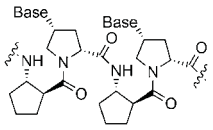

(N) A–G–T–T–A–U^{Py}–C–C–C–T–G–C (C) — **PNA6**

(3') T–C–A–A–T– X – Y –G–G–A–C–G (5') — **DNA6a**: X = A; Y = G (complementary)
DNA6b: X = C; Y = G (C mismatch)
DNA6c: X = G; Y = G (G mismatch)
DNA6d: X = T; Y = G (T mismatch)
DNA6e: X = A; Y = A (indirect mismatched)
DNA6f: X = G; Y = A (double mismatched)

(N) C–T–A–A–X–U^{Py}–T–C–A–G–A (C) — **PNA7**: X = A; **PNA8**: X = T

(3') G–A–T–T–Y– A – A –G–T–C–T (5') — **DNA7**: Y = T; **DNA8**: Y = A

Scheme 2. Structure of acpcPNA and sequences of PNA/DNA used in this study.

Table 1. Melting temperatures, quantum yields, and fluorescence intensity ratios of **PNA1**–**PNA5** and their hybrids with DNA.

Entry	System[a]	T_m [°C]	Φ_F[b]	$\frac{I_{465}}{I_{465}(ss)}$[c]	$\frac{I_{465}(comp)}{I_{465}}$[d]	Notes
1	**PNA1**	–	0.006	1.0	41.9	ss, $TU^{Py}T$
2	**PNA1+DNA1a**	65.8	0.131	41.9	1.0	ds, complementary
3	**PNA1+DNA1b**	25.7	0.022	5.3	7.9	ds, pU^{Py}·dT mismatched
4	**PNA1+DNA1c**	27.3	0.039	8.7	4.8	ds, pU^{Py}·dC mismatched
5	**PNA1+DNA1d**	<20	0.013	3.0	14.0	ds, pU^{Py}·dG mismatched
6	**PNA2**	–	0.011	1.0	6.2	ss, $AU^{Py}A$
7	**PNA2+DNA2**	60.2	0.051	6.2	1.0	ds, complementary
8	**PNA3**	–	0.006	1.0	8.3	ss, $GU^{Py}G$
9	**PNA3+DNA3**	54.1	0.032	8.3	1.0	ds, complementary
10	**PNA4**	–	0.006	1.0	2.0	ss, $CU^{Py}C$
11	**PNA4+DNA4**	<20	0.010	2.0	1.0	ds, complementary
12	**PNA5**	–	0.009	1.0	6.8	ss, $CU^{Py}C$
13	**PNA5+DNA5**	72.7	0.048	6.8	1.0	ds, complementary

[a] Conditions: [PNA] = 2.5 μM; [DNA] = 3.0 μM, 10 mM sodium phosphate buffer, pH 7.0, λ_{ex} 350 nm. [b] Measured using quinine sulfate as a standard. [c] Ratio of fluorescence intensity at 465 nm to single-stranded PNA. [d] Ratio of fluorescence intensity at 465 nm to complementary hybrids.

pair (pU^{Py}·dA) was 65.8 °C. This value is considerably smaller than the corresponding unmodified T_9 acpcPNA·**DNA1a** pair under identical conditions (T_m = 82.0 °C), probably owing to the unfavorable steric effects of the bulky pyrene group. However, the remaining three **PNA1**·**DNA** pairs carrying a single base mismatch yielded either much-lower T_m values (25.7 and 27.3 °C for pU^{Py}·dT, pU^{Py}·dC) or no sigmoidal transition at all (pU^{Py}·dG). This result suggests a remarkable difference in the thermal stabilities between the complementary and mismatched hybrids of more than 35 °C.

The absorption spectrum of **PNA1** (Figure 1) showed a broad pyrene absorption band with a λ_{max} of 345 nm in addition to the normal nucleobase absorption in the region of 260 nm. The pyrene absorption band showed no fine structure, except for a shoulder at ca. 340 nm which was consistent in shape with the absorption spectra of DNA carrying a U^{Py} base reported previously.[17,18,21] The shape and magnitude of the pyrene absorption band changed noticeably upon addition of the complementary DNA target (**DNA1a**). The absorption maxima was broadened and shifted slightly to a longer wavelength (350 nm). This shift was also accompanied by a small hyperchromism. No significant change in

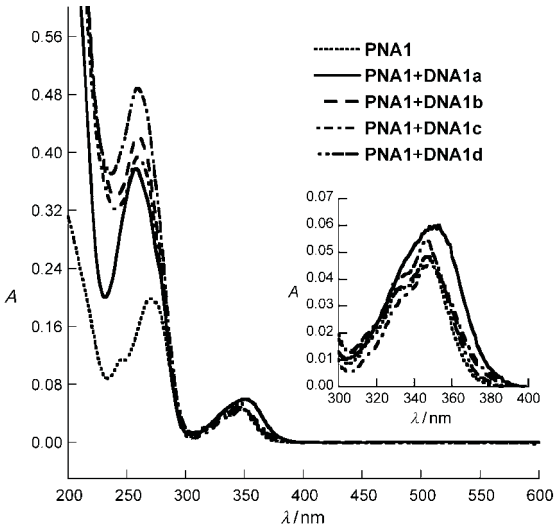

Figure 1. UV/Vis spectra of **PNA1** (2.5 μM)+**DNA1a**–**DNA1d** (3.0 μM) in 10 mM sodium phosphate buffer pH 7.0.

 © 2011 Wiley-VCH Verlag GmbH & Co. KGaA, Weinheim

the absorption spectra in the pyrene absorption region could be observed with the three remaining mismatched hybrids. The change in the absorption spectra indicated a ground-state interaction between the U^{Py} unit and the surrounding nucleobases, which took place only when the perfect base-pairing between the PNA and the DNA was formed. The change in the absorption spectra of **PNA1** upon hybridization with DNA is fully reversible (Figure 2). At temperatures above the T_m, the absorption spectra in the pyrene chromophore region of **PNA1·DNA1a** was similar to that of the single-stranded **PNA1** and, after cooling, the absorption spectra changed again.

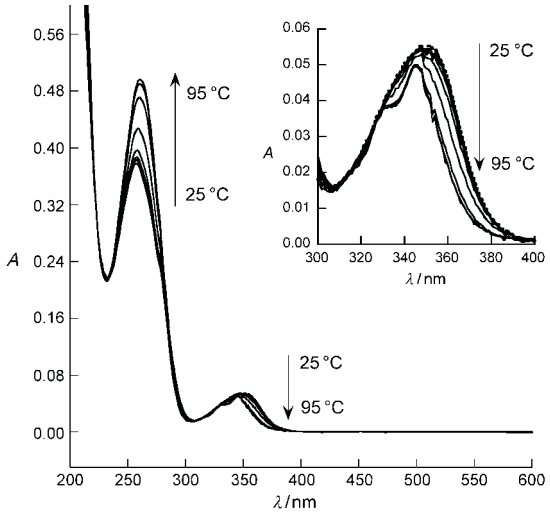

Figure 2. Temperature-dependent UV/Vis spectra of **PNA1** (2.5 μM)+**DNA1a** (3.0 uM) in 10 mM sodium phosphate buffer pH 7.0, from 25 to 95 °C (solid line) and back to 25 °C (dotted line), temperature step = 10 °C.

Most interestingly, the fluorescence of the U^{Py}-containing acpcPNA is highly sensitive to its hybridization state (Figure 3). The single-stranded **PNA1** exhibited a broad and unstructured fluorescence peak owing to the U^{Py} base that is forming an exciplex state when excited at 350 nm, thereby indicating strong electronic coupling between the pyrene chromophore and the U base as observed in DNA cases.[21] The maximum emission wavelength in aqueous phosphate buffer appeared at 465 nm with a rather low quantum yield ($\Phi_F = 0.006$). When hybridized with **DNA1a** with a complementary sequence, the fluorescence intensity of the duplex at 465 nm was enhanced by a factor of 42 relative to the single-stranded **PNA1**, and the quantum yield was increased to 0.131 without change in the maximum emission wavelength. The increases in the fluorescence intensity were also observed in other mismatched PNA·DNA hybrids, but to a much-lesser degree ranging from 3.0 (in the **PNA1·DNA1d** carrying a pU^{Py}·dG mismatch) to 8.7 fold (in the **PNA1·DNA1c** carrying a pU^{Py}·dC mismatch). This range translates to a discrimination factor between complementary and single-mismatched hybrids of between 4.8 and 14 fold. The

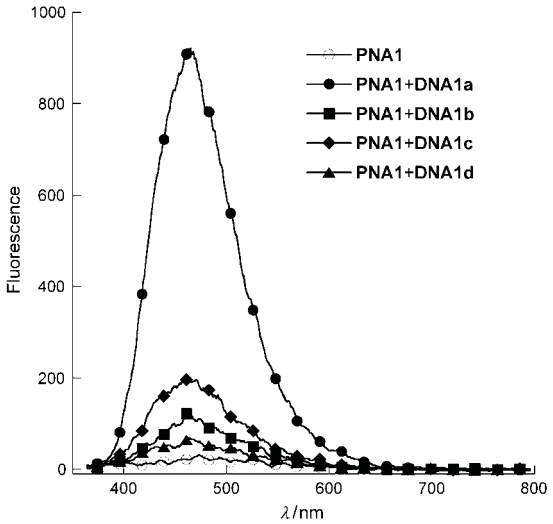

Figure 3. Steady-state fluorescence spectra of **PNA1** (2.5 μM)+**DNA1a**–**DNA1d** (3.0 μM) in 10 mM sodium phosphate buffer pH 7.0, λ_{ex} 350 nm.

difference between the fluorescence of the complementary and non-complementary hybrids of **PNA1**, as well as the single-stranded **PNA1**, could be visualized by the naked eye under UV light irradiation (365 nm; Figure S17).

Effect of Neighboring Bases on the Fluorescence of DNA Hybrids with Homothymine acpcPNA Carrying U^{Py} Modification

The fluorescence of BDF nucleobases is often strongly influenced by neighboring bases. To investigate the effect of neighboring bases on the fluorescence properties of acpcPNA carrying U^{Py} modification, **PNA2**–**PNA5** which had different bases adjacent to U^{Py} were used as models. The data on thermal stabilities and fluorescence properties are summarized in Table 1 and Figure 4. As with **PNA1**, in all cases the fluorescence of the single-stranded PNAs was very low ($\Phi_F = 0.006$–0.011). **PNA2**, which had a A/A neighboring base, was the brightest, with a fluorescence approximately 2 fold stronger than **PNA3** and **PNA4**. Not unexpectedly, the fluorescence of the hybrids with corresponding complementary DNAs is quite sensitive to the nature of the neighboring bases. Nevertheless, the increase in fluorescence of the U^{Py} upon hybrid formation could be observed with A/A and G/G as neighboring bases (**PNA2** and **PNA3**). The seeming absence of fluorescence increase with C/C neighboring bases in **PNA4** was attributed to the low stability of acpcPNA hybrids containing multiple TC/CT steps, as revealed by the absence of a sigmoidal thermal denaturation curve (see the Supporting Information, Figure S13). To circumvent this problem, the fluorescence experiment was repeated with the 13 mer hybrid **PNA5·DNA5** having two pT·dA pairs extended from both termini to increase the stability. This hybrid had a T_m of 72.7 °C and displayed a 6.8-fold increase in fluo-

 © 2011 Wiley-VCH Verlag GmbH & Co. KGaA, Weinheim

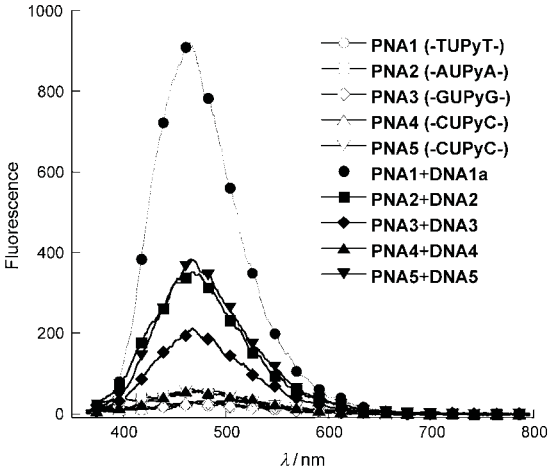

Figure 4. Steady-state fluorescence spectra of **PNA1**–**PNA5** (2.5 μM) and **PNA1**–**PNA5+DNA1a**–**DNA5** (3.0 μM) in 10 mM sodium phosphate buffer pH 7.0, λ_{ex} 350 nm.

rescence relative to single-stranded **PNA5**. The order of the fluorescence change as a function of neighboring base was T/T > A/A ~ C/C > G/G. Despite these variations, there is a general trend that the single-stranded U^{Py}-labeled acpcPNA is weakly fluorescent, and upon hybridization the fluorescence intensity at 465 nm increased consistently within the range 6.2–41.9 fold. This result suggests that the U^{Py} can function as a base-discriminating fluorescent nucleobase in acpcPNA system. The general increase in fluorescence signal upon hybridization to complementary DNA regardless of the nature of neighboring bases suggests that the U^{Py}-modified acpcPNA should be useful as a quencher-free beacon probe that yield turn-on signals in the presence of the correct DNA target. Although many fluorophore-labeled nucleobases have been proposed as BDF in both DNA and aegPNA systems, many of them do not give turn-on signals.[3,7,28,29] In addition, the signal change is often highly dependent on the nature of the flanking bases to the extent that little or no discrimination could be observed for some sequences.[16]

Thermal Stabilities and Optical Properties of DNA Hybrids with Mixed Sequence acpcPNA Carrying U^{Py} Modification

Next, the thermal stabilities and optical properties of U^{Py} containing a mixed-sequence acpcPNA **PNA6** were investigated. The data are summarized in Table 2. As shown by T_m analysis, the hybrid between **PNA6** and complementary DNA (**DNA6a**) was more thermally stable than the mismatched hybrids. The T_m values of hybrids between **PNA6** and **DNA6a** (complementary) and **DNA6b**–**DNA6d** (single mismatched) were 66.3 and 54.2–54.5 °C, respectively. The decrease in the T_m values of the single mismatched hybrid from the complementary hybrid by ca. 12 °C suggested that the U^{Py} base in mixed sequence acpcPNA can still specifically recognize A in the complementary DNA strand. Interestingly, the T_m decrease in the mismatched hybrids is much smaller than would be expected from acpcPNA (a T_m decrease of ca. 20–25 °C is typical for single mismatched acpcPNA·DNA hybrids of this length). For example, T_m values of the unmodified acpcPNA with the same sequence as **PNA6**, but carrying T instead of U^{Py}, with **DNA6a** (complementary) and **DNA6b** (single mismatched) were 75.0 and 51.8 °C, respectively under similar conditions (T_m decrease = 23.2 °C). Despite this, the ability of U^{Py} in acpcPNA to differentiate A from other bases is in sharp contrast to the behavior of the same U^{Py} base in DNA whereby there was essentially no T_m difference in the duplexes having the four bases located opposite to the U^{Py}.[21] We propose that the mismatched PNA·DNA and DNA·DNA hybrids could be stabilized by rotation of the U^{Py} base to allow "pairing" between the pyrene and the mismatched base, which would result in an intercalation of the pyrene unit between the base stack.[30] This intercalation might also partially take place in the complementary DNA·DNA hybrid with a relatively weak pairing between U^{Py} and T, but would be more difficult in complementary PNA·DNA hybrids whereby the pairing is much stronger. UV/Vis spectra support this hypothesis as shown by the significant red-shifted absorption maxima to ca. 360 nm with a pronounced broadening and hypochromism of the pyrene absorption in all mismatched hybrids of **PNA6** compared to the single-stranded **PNA6** (Figure 5). This spectral characteristic is remarkably similar to that of complementary and mismatched DNA duplexes carrying U^{Py} reported in the literature.[21] In addition, CD spectra of **PNA6** with **DNA6a** (complementary) and **DNA6b–d** (mismatched) (Figure S14) also support this in-

Table 2. Melting temperatures, quantum yields, and fluorescence intensity ratios of **PNA6**–**PNA8** and their hybrids with DNA.

Entry	System[a]	T_m [°C]	Φ_F[b]	$\frac{I_{465}}{I_{465}(ss)}$[c]	$\frac{I_{465}(comp)}{I_{465}}$[d]	Notes
1	**PNA6**	–	0.009	1.0	6.5	ss, $AU^{Py}C$
2	**PNA6+ DNA6a**	66.3	0.052	6.5	1.0	ds, complementary
3	**PNA6+ DNA6b**	54.3	0.018	1.1	5.9	ds, pU^{Py}·dC mismatch
4	**PNA6+ DNA6c**	54.2	0.025	1.6	4.1	ds, pU^{Py}·dG mismatch
5	**PNA6+ DNA6d**	54.5	0.014	1.0	6.5	ds, pU^{Py}·dT mismatch
6	**PNA6+ DNA6e**	46.1	0.029	3.1	2.1	ds, indirect mismatched
7	**PNA6+ DNA6f**	40.0	0.011	0.8	8.1	ds, double mismatched
8	**PNA7**	–	0.030	1.0	2.7	ss, $AU^{Py}T$
9	**PNA7+ DNA7**	–[e]	0.066	2.7	1.0	ds, complementary
10	**PNA8**	–	0.027	1.0	4.0	ss, $TU^{Py}T$
11	**PNA8+ DNA8**	–[e]	0.084	4.0	1.0	ds, complementary

[a] Conditions: [PNA] = 2.5 μM; [DNA] = 3.0 μM, 10 mM sodium phosphate buffer, pH 7.0, λ_{ex} 350 nm. [b] Measured using quinine sulfate as a standard. [c] Ratio of fluorescence intensity at 465 nm to single-stranded PNA. [d] Ratio of fluorescence intensity at 465 nm to complementary hybrids. [e] non-two-state melting curve.

 © 2011 Wiley-VCH Verlag GmbH & Co. KGaA, Weinheim

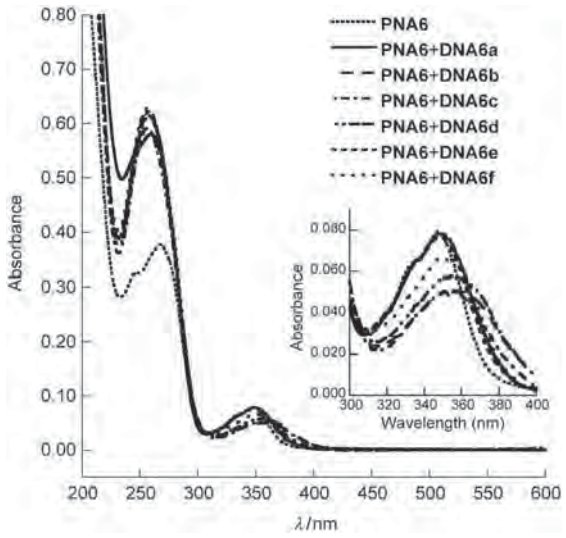

Figure 5. UV/Vis spectra of **PNA6** (2.5 μM)+**DNA6a**–**DNA6f** (3.0 μM) in 10 mM sodium phosphate buffer pH 7.0.

tercalation model. The difference in the pyrene absorption region (ca. 360 nm) suggests that the pyrene chromophore is differently organized in the complementary and mismatched duplexes. Among all mismatched hybrids of **PNA6** studied, only the **PNA6·DNA6e** pair carrying a mismatch base not directly opposite to the U^{Py} base shows a similar absorption spectrum to the complementary hybrid, thus indicating the absence of intercalation of the pyrene moiety. Interestingly, this particular indirect mismatch hybrid is also much-less thermally stable (T_m = 46.1 °C) than the other mismatch pairs (T_m = 54.3–54.5 °C). These results are completely consistent with the proposed model above since in the indirect mismatched hybrid **PNA6·DNA6e**, the U^{Py} still forms hydrogen bonds with A; therefore, no intercalation is possible.

It is important to note that the absorption spectra of the DNA hybrids of **PNA6** are quite different from those of **PNA1**. In the case of complementary hybrids, the change in the UV absorption spectra of the pyrene chromophore of **PNA6** was much-smaller than that of **PNA1**, thereby suggesting that the two duplexes might adopt different structures. The unusual structure of homothymine/homopyrimidine sequence is well recognized in the DNA field, which is also supported here by the unusually high thermal stability and the very large increase in fluorescence change of the **PNA1·DNA1a** hybrid compared to the **PNA6·DNA6a** hybrid. In the case of mismatched duplexes of **PNA6**, significant bathochromic shifts were observed in the absorption spectra. However, these shifts are not the same as that observed in the complementary **PNA1·DNA1a** duplex because the magnitude of the shifts was much-larger (15 nm vs 5 nm) and the shape of the absorption spectra were different. We attribute the spectral change in this case to the intercalation of the pyrene into the base stack of the mismatched duplex. No similar change was observed in the mismatched hybrids of **PNA1**. This may be due to the poor ability of AT pairs to accommodate pyrene intercalation, which results in very unstable mismatched duplexes.

Fluorescence spectra of the single stranded **PNA6** showed a weak and broad emission band similar to **PNA1** with a fluorescence quantum yield of 0.009 (Figure 6). In the presence of the complementary **DNA6a**, the intensity of the

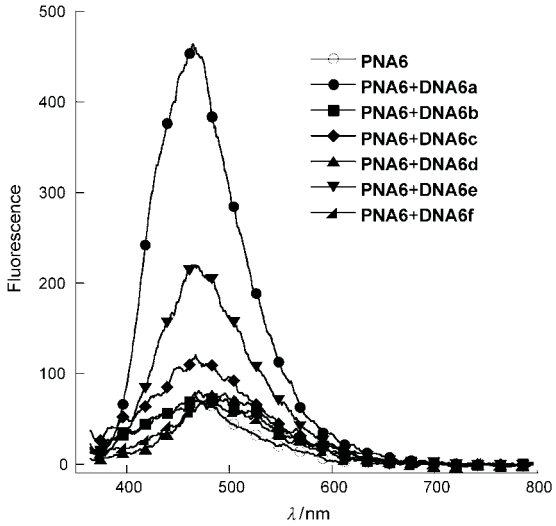

Figure 6. Steady-state fluorescence spectra of **PNA6** (2.5 μM)+**DNA6a**–**DNA6f** (3.0 μM) in 10 mM sodium phosphate buffer pH 7.0, λ_{ex} 350 nm.

emission at 465 nm increased ca. 6.5 fold. This increase was accompanied by an increase in the quantum yield to 0.052. The presence of single mismatched targets **DNA6b**–**DNA6d** resulted in little or almost no change in the fluorescence intensity, although the fluorescence quantum yields increased a little because of the hypochromism of the pyrene chromophore in the absorption spectra. The pU^{Py}·dG mismatch hybrid (**PNA6·DNA6c**) exhibited the highest fluorescence among all mismatched hybrids (1.6 fold enhancement relative to the single-stranded **PNA6**). Nevertheless, the signal is still much lower than that of the complementary hybrid, allowing unambiguous differentiation between complementary and single mismatched DNA targets. On the other hand, when the mismatched base in the DNA strand was located in a position that is not directly opposite to the U^{Py} as in **DNA6e**, a significant fluorescence enhancement relative to the single-stranded **PNA6** (3.1 folds) was observed even though this single mismatched hybrid was less thermally stable than the other mismatched hybrids studied earlier (see the T_m figures in Table 2). When a second base mismatch was introduced to the DNA strand at the position opposite to the U^{Py} base as in **DNA6f**, the fluorescence becomes indifferent from the single-stranded **PNA6**.

These results indicate that the fluorescence enhancement of the U^{Py} is directly associated to the base pairing event between the U^{Py} and A. The same fluorescence enhancement upon hybridization was also observed in **PNA7** and **PNA8**, which carry different flanking bases ($AU^{Py}T$ and $TU^{Py}T$).

 © 2011 Wiley-VCH Verlag GmbH & Co. KGaA, Weinheim

CHEMISTRY
AN ASIAN JOURNAL

The fluorescence enhancements in these cases are considerably smaller than in the case of **PNA6** owing to a relatively high fluorescence background of the single stranded **PNA7** and **PNA8**. Nevertheless, the fluorescence enhancement still reached 2.7 fold in the worst case (**PNA7**), which could still be readily distinguished by the naked eye (Figure 7; also see the Supporting Information, Figure S20). These results con-

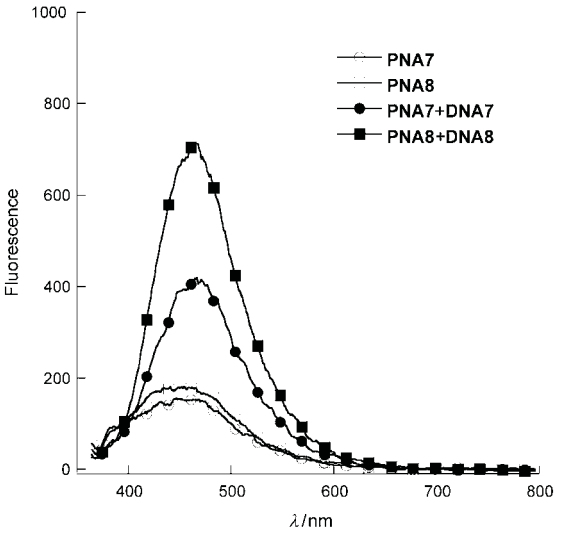

Figure 7. Steady-state fluorescence spectra of **PNA7** and **PNA8** (2.5 μM), and with addition of **DNA7** and **DNA8** (3.0 μM), respectively. 10 mM Sodium phosphate buffer pH 7.0, λ_{ex} 350 nm.

firms the above conclusion based on experiments with homothymine sequences that the U^{Py} is a versatile BDF in acpcPNA system that produce a turn-on signal upon pairing with the base A, irrespective of the nature of the flanking base sequences.

On the Origin of the Fluorescence Enhancement

In the single-stranded acpcPNA, the U^{Py} base should be quenched by photoinduced electron transfer because of interactions with neighboring nucleobases. The fluorescence spectra of the monomer (one acpcPNA dipeptide unit with U^{Py} as a base, capped with acetyl and lysinamide at the N- and C-termini) showed an emission band at ca. 400 nm typical of free pyrene in aqueous buffer, possibly as a result of the non-coplanarity between the pyrene and uracil chromophores. In the same buffer, the **PNA1** showed a weak emission band at 465 nm, which should arise from the internal exciplex $Py^{\cdot+}$-$U^{\cdot-}$.[17] Addition of an organic co-solvent, especially dimethyl sulfoxide, which is known to disrupt base stacking increased the emission intensities of the monomer without changing the emission maxima (Figure S15). On the other hand, a hypsochromic shift of the emission spectrum with an increased in intensity was observed for **PNA1** in the presence of dimethyl sulfoxide (Figure S16). In pure dimethyl sulfoxide, the emission maxima of the monomer and **PNA1** were almost identical. This is interpreted as an evidence for the interaction of the U^{Py} with the neighboring T bases, which is disrupted in the presence of dimethyl sulfoxide. From the variation in the fluorescence quantum yield of the single stranded **PNA1**–**PNA8** (ranging from 0.006 in **PNA1** to 0.030 in **PNA7**), it is clear that the base sequence is an important factor to determine the "darkness" of the single-stranded probe. The homo-T sequence **PNA1** was the darkest, which seem to be reasonable based on the knowledge that T is an effective quencher for pyrene.[31] In general, single-stranded T-rich sequences appear to be darker than the mixed sequences, even when the flanking bases of the U^{Py} are not T. On the other hand, the mixed sequence **PNA7** and **PNA8** carrying one and two flanking T bases, respectively, are relatively bright in the single-stranded state. These results suggest that the quenching effect must also, at least additionally, take place by non-nearest neighboring bases. This is not unexpected because the hydrophobic backbone of the single-stranded PNA can fold into a compact shape in an aqueous environment,[32] thus leading to possible interactions between the U^{Py} and non-proximal nucleobases. When the base pairing between the U^{Py} and A takes place, the rigidly-linked pyrene must be forced into a more pronounced coplanar situation with the U moiety and to point into the major groove direction, away from the helix center and interacting with the aqueous environment.[8,22] The change in the local environment of the U^{Py} chromophore, as well as the twisting between the pyrene and uracil aromatic planes along the connecting C–C bond which controls the charge-transfer contribution leads to the observed fluorescence enhancement.[33,34] The described differences in the UV/Vis absorption spectra support this interpretation. Since the pyrene unit is electronically coupled to the uracil base and in the duplex state this base can only directly interact with the two neighboring base pairs, the brightness of the fluorescence should now be mainly determined by the nature of the flanking bases. The observed brightness with different neighboring bases is decreasing from T/T > A/A ~ C/C > G/G. Nevertheless, in all cases the expected fluorescence enhancement was observed upon duplex formation, indicating that the system should be widely applicable to a variety of sequences. When hybridized to a mismatched DNA target carrying a mismatched base opposite to the U^{Py}, the duplex is stabilized by intercalation of the pyrene substituent of the U^{Py} into the duplex, as suggested by the red shift of the UV spectra. Fortunately, this event does not lead to a significant fluorescence change from the single strand PNA as compared to the complementary hybrid, therefore the U^{Py} in acpcPNA can behave as a BDF which yields a turn-on signal only when paired with adenine.

Conclusions

In conclusion, we have demonstrated the suitability of 5-(pyren-1-yl)uracil (U^{Py}) as a base-discriminating fluorescent (BDF) nucleobase in the conformationally rigid acpcPNA

 © 2011 Wiley-VCH Verlag GmbH & Co. KGaA, Weinheim

system. In contrast to the analogous study in DNA, the U^{Py} base in acpcPNA exhibits a strict Watson–Crick base-pairing-specificity towards A. Most importantly, the fluorescence of the U^{Py} base is significantly enhanced when the acpcPNA is hybridized to its DNA target, irrespective of the nature of the flanking bases. The high specificity of the acpcPNA system allows discrimination between the complementary and single-mismatched DNA targets. Experiments with mismatched DNA targets revealed that the fluorescence enhancement was specific to the pairing between U^{Py} and dA. As a result, the U^{Py}-modified acpcPNA is potentially useful as a hybridization-responsive fluorescent probe for DNA sequence determination.

Experimental Section

General

Chemicals and solvents were purchased from commercial suppliers and used without further purification. Oligonucleotides were purchased from Biodesign (Bangkok, Thailand). RP-HPLC experiments were performed on a Water Delta 600 HPLC system. ^{1}H and ^{13}C NMR spectra were recorded on a Bruker Avance 400 NMR spectrometer operating at 400 MHz for ^{1}H nuclei and 100 MHz for ^{13}C nuclei. MALDI-TOF mass spectra were obtained on a Microflex MALDI-TOF mass spectrometry (Bruker Daltonics) using α-cyano-4-hydroxycinnamic acid (CCA) as the matrix. High resolution mass spectra were recorded in positive ESI mode on a Bruker Daltonics micrOTOF. IR spectra were recorded on Nicolet iS10 FT-IR spectrometer. The acpcPNAs were synthesized according to the previously published solid-phase peptide synthesis procedure[23] (0.5 μmol scale) and were purified by reverse-phase HPLC. Spectroscopic measurements were carried out in sodium phosphate buffer solution (10 mM, pH 7.0) using 10 mm quartz glass cuvettes. Absorption spectra and the melting temperatures (2.5 μM PNA, 3.0 μM DNA, 20–90 °C, 1.0 °C min^{-1}) were recorded on a Varian Cary 100 UV/Vis spectrophotometer. Fluorescence spectra were measured on a Varian Eclipse spectrofluorimeter.

*N-tert-Butoxycarbonyl-(4′R)-[3-benzoyl-5-iodouracil-1-yl]-(2′R)-proline diphenylmethyl ester (**2**)*

N-tert-Butoxycarbonyl-*trans*-4-hydroxy-D-proline diphenylmethyl ester[27] (0.9938 g, 2.5 mmol), triphenylphosphine (0.7213 g, 2.75 mmol) and N^3-benzoyl-5-iodouracil (0.9407 g, 2.75 mmol) were dissolved in dry THF (10 mL) with stirring under N_2 and cooled down to 0 °C in an ice–salt bath. To the reaction mixture was slowly added DIAD (0.54 mL, 2.75 mmol) via a syringe over a period of 15 min. The reaction was slowly warmed to room temperature and the stirring was continued 24 h. The solvent was removed and the residue was recrystallized from ethanol to afford **2** as a white solid (0.5424 g, 47 % yield). R_f = 0.60 (hexanes/EtOAc 75:25); m.p. 124–126 °C; $[\alpha]_D^{25}$ = +50.2 (c = 0.014 M, $CHCl_3$); ^{1}H NMR (400 MHz, $CDCl_3$): δ = 1.33 and 1.51 (2 s, 9H; CH_3 Boc rotamers), 2.05 (m, 1H; 1 × CH_2(3′)), 2.85 (m, 1H; 1 × CH_2(3′)), 3.59 and 3.73 (m, 1H; 1 × CH_2(5′) rotamers), 4.02 (m, 1H; 1 × CH(5′) rotamers), 4.52 and 4.61 (m, 1H; CH(4′) rotamers) 5.19 (m, 1H; CH(2′)), 6.99 (s, 1H; CHPh$_2$), 7.29 (s, 1H; C(6)H U^I), 7.37 (m, 10H; Dpm ArH), 7.51 (dd, J = 7.0, 7.4 Hz, 2H; CH(3,5) Bz), 7.68 (t, J = 7.1 Hz, 1H; CH(4) Bz), 7.88 ppm (m, 2H; CH(2,6) Bz); ^{13}C NMR (100 MHz, $CDCl_3$): δ = 28.1 and 28.3 (CH_3 Boc rotamers), 34.2 and 35.9 (CH_2(3′) rotamers), 49.6 and 49.9 (CH(5′) rotamers), 53.3 and 53.7 (CH(4′) rotamers), 57.4 and 57.5 (CH(2′) rotamers), 68.4 (C(5) U^I), 78.3 and 78.5 (CH Dpm rotamers), 81.6 (CCH_3 Boc), 127.1–128.8 (CH Ar Dpm), 129.2 and 130.5 (CH(2) and CH(3) Bz), 130.9 (C(1) Bz), 135.3 (C(4)H Bz), 139.2 (C Ar Dpm), 144.9 (CH(6) U^I), 149.6 (C(2) U^I), 153.4 (CO Boc), 158.5 (C(4) U^I), 167.4 (CO Bz), 171.2 ppm (CO proline); IR (ATR): $\tilde{\nu}_{max}$ = 1737.9, 1700.2, 1655.2, 1614.0, 1433.6, 1395.9, 1382.4, 1234.3, 1196.6, 1148.1, 983.8 cm^{-1}; HRMS (ESI+): m/z calcd for $C_{34}H_{32}O_7N_3I$+Na$^+$: 744.1183 [M+Na]$^+$; found: 744.1105.

*N-tert-Butoxycarbonyl-(4′R)-[5-(pyren-1-yl)uracil-1-yl]-(2′R)-proline diphenylmethyl ester (**4**)*

A round-bottomed flask was charged with *N-tert*-butoxycarbonyl-(4′*R*)-[3-benzoyl-5-iodouracil-1-yl]-(2′*R*)-proline diphenylmethyl ester (**2**; 0.3430 g, 0.475 mmol), pyren-1-boronic acid (0.1862 g, 0.755 mmol), and tetrakis(triphenylphosphine)palladium [Pd(PPh$_3$)$_4$] (0.0200 g, 0.0165 mmol). After flushing the reaction vessel with nitrogen to remove air, degassed CH_3CN (3 mL) and triethylamine (0.3 mL, 0.500 mmol) were added. The reaction mixture was heated to 80 °C with stirring under nitrogen. When the starting material was completely consumed (40 h, monitored by TLC), the solvent was removed under reduced pressure and the residue was separated by column chromatography on silica gel eluting with CH_2Cl_2/acetone (30:1). Without further characterization, the protected intermediate *N-tert*-butoxycarbonyl-(4′*R*)-[3-benzoyl-5-(pyren-1-yl)uracil-1-yl]-(2′*R*)-proline diphenylmethyl ester (**3**), was treated with ethanolamine (0.2 mL) in DMF (1 mL) for 20 min. After the reaction was finished, as indicated by TLC, the reaction mixture was diluted with CH_2Cl_2 (20 mL). The organic layer was washed with 10 % HCl (2 × 15 mL), dried with Na_2SO_4, and the solvent was removed. The residue was purified by column chromatography on silica gel eluting with hexanes/ethyl acetate (50:50) to obtain **4** as an off-white solid (0.2010 g, 60 % yield from **2**). R_f = 0.73 (hexanes/EtOAc 50:50); $[\alpha]_D^{25}$ = +46.6 (c = 0.014 M, $CHCl_3$); ^{1}H NMR (400 MHz, $CDCl_3$): δ = 1.33 and 1.51 (2 s, 9H; CH_3 Boc), 2.05 (m, 1H; 1 × CH_2(3′)), 2.85 (m, 1H; 1 × CH_2(3′)), 3.59 and 3.73 (m, 1H; 1 × CH_2(5′) rotamers), 4.02 (m, 1H; 1 × CH_2(5′)), 4.52 and 4.61 (m, 1H; CH(4′) rotamers), 5.19 (m, 1H; CH(2′)), 6.87 (s, 1H; CHPh$_2$), 7.25–7.51 (m, 10H; Ar Dpm), 7.42 and 7.45 (2 s, 1H; C(6)H U^{Py} rotamers), 7.86–8.24 (m, 9H; CH pyrene), 9.09 ppm (s, 1H; NH U^{Py}); ^{13}C NMR (100 MHz, $CDCl_3$): δ = 28.0 and 28.3 (CH_3 Boc rotamers), 34.2 and 35.5 (CH_2(3′) rotamers), 49.0 and 49.4 (CH(5′) rotamers), 52.8 and 53.6 (CH(4′) rotamers), 57.3 and 57.5 (CH(2′) rotamers), 77.9 and 78.2 (CH Dpm rotamers), 81.3 (CCH_3 Boc), 115.7 (C(5) U^{Py}), 124.6–126.1 (CH pyrene), 126.8–128.6 (CH Ar Dpm, CH and C pyrene), 129.1 (C pyrene), 130.8 (C pyrene), 131.2 (C pyrene), 131.7 (C pyrene), 139.2 (CH(6) U^{Py} and C Dpm), 150.7 (C(2) U^{Py}), 153.3 (CO Boc), 161.8 (C(4) U^{Py}), 170.9 ppm (CO proline); IR (ATR): $\tilde{\nu}_{max}$ = 1670.6, 1452.4, 1390.5, 1358.2, 1280.1, 1177.7, 1150.8, 964.9 cm^{-1}; HRMS (ESI+): m/z calcd for $C_{43}H_{37}O_6N_3$+Na$^+$: 714.2580 [M+Na]$^+$; found: 714.2519.

*N-Fluoren-9-ylmethoxycarbonyl-(4′R)-[5-(pyren-1-yl)uracil-1-yl]-(2′R)-proline (**1**)*

N-tert-Butoxycarbonyl-(4′*R*)-[5-(pyren-1-yl)uracil-1-yl]-(2′*R*)-proline diphenylmethyl ester (**4**) (0.1200 g, 0.170 mmol) was treated with *para*-toluenesulfonic acid monohydrate (0.0950 g, 0.5 mmol) in MeCN (2 mL) at 30 °C for 3 h. After the Boc deprotection was complete (as determined by TLC), diisopropylethylamine (DIEA) (150 μL, 0.85 mmol) was added to the reaction mixture followed by 9-fluorenylmethoxycarbonyl chloride (0.0660 g, 0.255 mmol). After the reaction was completed as indicated by TLC (ca. 1 h), the solvent was removed and the residue was purified by column chromatography on silica gel eluting with hexanes/ethyl acetate (50:50) to give the intermediate *N*-fluoren-9-ylmethoxycarbonyl-(4′*R*)-[5-(pyren-1-yl)uracil-1-yl]-(2′*R*)-proline diphenyl methyl ester. Without further characterization, this intermediate was treated with trifluoroacetic acid/CH_2Cl_2 (1:1) containing 10 % triisopropylsilane (1 mL) and left at 30 °C for 30 min. After that, the volatiles were removed by a gentle stream of nitrogen. The residue was triturated and washed with diethyl ether to give a white solid (0.0600 g, 55 % yield from **4**). R_f = 0.55 (hexanes/EtOAc 75:25+0.5 % HOAc); $[\alpha]_D^{25}$ = −4.7 (c = 0.015 M, DMF); ^{1}H NMR (400 MHz, CD_3OD): δ = 2.34 and 2.39 (2 m, 1H; 1 × CH_2(3′) rotamers), 2.78 and 2.85 (2 m, 1H; 1 × CH_2(3′) rotamers), 3.71 and 3.77 (m, 1H; 1 × CH_2(5′) rotamers), 3.87 and 4.04 (m, 1H; 1 × CH_2(5′) rotamers), 4.17 (m, 1H; CH Fmoc), 4.34 (m, 2H; CH_2 Fmoc), 4.31 and 4.43 (2 m, 1H; CH(2′) rotamers), 5.11 and 5.20 (2 m, 1H; CH(4′) rotamers), 6.80–7.80 (m, 8H; CH Fmoc), 7.92 (s, 1H; CH(6) U^{Py}), 7.95–8.23 ppm (m, 9H; CH pyrene); ^{13}C NMR (100 MHz, CD_3OD): δ = 34.2 and 34.9 (CH_2(3′) rotamers), 46.9 (CH Fmoc), 48.8 and 49.3 (CH(5′) rotamers), 53.2 and

 © 2011 Wiley-VCH Verlag GmbH & Co. KGaA, Weinheim

54.2 (*C*H(4′) rotamers), 58.6 and 58.9 (*C*H(2′) rotamers), 67.4 and 68.0 (*C*H_2 Fmoc rotamers), 114.6 (*C*H(5) U^{Py}), 119.4 (*C*H Ar Fmoc), 124.3–125.1 (*C*H and C pyrene), 125.7 (*C*H Ar Fmoc), 126.8–128.6 (*C*H Ar Fmoc, *C*H and *C* pyrene), 130.0 (*C* pyrene), 130.9 (*C* pyrene), 131.3 (*C* pyrene), 131.4 (*C* pyrene), 141.1 (*C* Ar Fmoc), 141.9 (*C*H(6) U^{Py}), 143.6–144.1 (*C* Ar Fmoc), 151.5 (*C*(2) U^{Py}), 154.9 and 155.2 (*C*O Fmoc), 163.7 (*C*(4) U^{Py}), 175.2 and 175.9 ppm (*C*O proline rotamers); IR (ATR): $\tilde{\nu}_{max}$ = 1681.4, 1447.1, 1414.7, 1280.1, 1175.1, 1115.8 cm^{-1}; HRMS (ESI^+): *m*/*z* calcd for $C_{40}H_{29}N_3O_6$+Na^+: 670.1954 [*M*+Na]$^+$; found: 670.1923.

Acknowledgements

This work was supported by the Alexander von Humboldt Foundation (to T.V.), the Development and Promotion of Science and Technology Talents Project (to C.B.), the Thailand Research Fund (RTA5280002), the Thai government stimulus package 2 (TKK2555, SP2) under the Project for Establishment of Comprehensive Center for Innovative Food, Health Products and Agriculture, the National Research University Grant from the Commission of Higher Education, and the Ratchadaphiseksomphot Endowment (AM1006A).

[1] R. W. Sinkeldam, N. J. Greco, Y. Tor, *Chem. Rev.* **2010**, *110*, 2579–2619.
[2] A. Okamoto, K. Tainaka, I. Saito, *J. Am. Chem. Soc.* **2003**, *125*, 4972–4973.
[3] A. Okamoto, K. Tanaka, T. Fukuta, I. Saito, *J. Am. Chem. Soc.* **2003**, *125*, 9296–9297.
[4] K. Matsumoto, Y. Shinohara, S. S. Bag, Y. Takeuchi, T. Morii, Y. Saito, I. Saito, *Bioorg. Med. Chem. Lett.* **2009**, *19*, 6392–6395.
[5] J. S. Mann, Y. Shibata, T. Meehan, *Bioconjugate Chem.* **1992**, *3*, 554–558.
[6] J. Telser, K. A. Cruickshank, L. E. Morrison, T. L. Netzel, *J. Am. Chem. Soc.* **1989**, *111*, 6966–6976.
[7] Y. Saito, Y. Miyauchi, A. Okamoto, I. Saito, *Chem. Commun.* **2004**, 1704–1705.
[8] A. Okamoto, K. Kanatani, I. Saito, *J. Am. Chem. Soc.* **2004**, *126*, 4820–4827.
[9] E. Mayer, L. Valis, C. Wagner, M. Rist, N. Amann, H.-A. Wagenknecht, *ChemBiochem.* **2004**, *5*, 865–868.
[10] C. Wagner, M. Rist, E. Mayer-Enthart, H.-A. Wagenknecht, *Org. Biomol. Chem.* **2005**, *3*, 2062–2063.
[11] G. T. Hwang, Y. J. Seo, S. J. Kim, B. H. Kim, *Tetrahedron Lett.* **2004**, *45*, 3543–3546.
[12] S. S. Bag, Y. Saito, K. Hanawa, S. Kodate, I. Suzuka, I. Saito, *Bioorg. Med. Chem. Lett.* **2006**, *16*, 6338–6341.
[13] Q. Xiao, R. T. Ranasinghe, A. M. P. Tang, T. Brown, *Tetrahedron* **2007**, *63*, 3483–3490.
[14] Y. Saito, K. Motegi, S. S. Bag, I. Saito, *Bioorg. Med. Chem.* **2008**, *16*, 107–113.
[15] G. T. Hwang, Y. J. Seo, B. H. Kim, *J. Am. Chem. Soc.* **2004**, *126*, 6528–6529.
[16] J. H. Ryu, Y. J. Seo, G. T. Hwang, J. Y. Lee, B. H. Kim, *Tetrahedron* **2007**, *63*, 3538–3547.
[17] T. Netzel, *Tetrahedron* **2007**, *63*, 3491–3514.
[18] T. L. Netzel, M. Zhao, K. Nafisi, J. Headrick, M. S. Sigman, B. E. Eaton, *J. Am. Chem. Soc.* **1995**, *117*, 9119–9128.
[19] E. Mayer, L. Valis, R. Huber, N. Amann, H.-A. Wagenknecht, *Synthesis* **2003**, 2335–2340.
[20] E. Mayer-Enthart, H.-A. Wagenknecht, *Angew. Chem.* **2006**, *118*, 3451–3453; *Angew. Chem. Int. Ed.* **2006**, *45*, 3372–3375.
[21] C. Wanninger-Weiss, H.-A. Wagenknecht, *Eur. J. Org. Chem.* **2008**, 64–71.
[22] N. Venkatesan, Y. J. Seo, B. H. Kim, *Chem. Soc. Rev.* **2008**, *37*, 648–663.
[23] a) T. Vilaivan, C. Srisuwannaket, *Org. Lett.* **2006**, *8*, 1897–1900; b) C. Vilaivan, C. Srisuwannaket, C. Ananthanawat, C. Suparpprom, J. Kawakami, Y. Yamaguchi, Y. Tanaka, T. Vilaivan, *Artificial DNA: PNA & XNA* **2011**, *2*, 50–59; XNA **2011**, 2, 50–59.
[24] C. Ananthanawat, T. Vilaivan, V. P. Hoven, X. D. Su, *Biosens. Bioelectron.* **2010**, *25*, 1064–1069.
[25] T. Pesnot, G. K. Wagner, *Org. Biomol. Chem.* **2008**, *6*, 2884–2891.
[26] N. Amann, H.-A. Wagenknecht, *Synlett* **2002**, 687–691.
[27] G. Lowe, T. Vilaivan, *J. Chem. Soc. Perkin Trans. 1* **1997**, 547–554.
[28] N. J. Greco, Y. Tor, *J. Am. Chem. Soc.* **2005**, *127*, 10784–10785.
[29] A. Omumi, D. G. Beach, M. Baker, W. Gabryelski, R. A. Manderville, *J. Am. Chem. Soc.* **2011**, *133*, 42–50.
[30] Pyrene has been shown to behave as a universal nucleobase in aegPNA: T. Tedeschi, A. Tornelli, S. Sforza, R. Corradini, R. Marchelli, *Artificial DNA: PNA & XNA* **2010**, *1*, 83–89; XNA **2010**, 1, 83–89.
[31] C. A. M. Seidel, A. Schulz, M. H. M. Sauer, *J. Phys. Chem.* **1996**, *100*, 5541–5553.
[32] O. Seitz, *Angew. Chem.* **2000**, *112*, 3389–3392; *Angew. Chem. Int. Ed.* **2000**, *39*, 3249–3252.
[33] Z. R. Grabowski, K. Rotkiewicz, W. Rettig, *Chem. Rev.* **2003**, *103*, 3899–4031.
[34] A. Trifonov, I. Buchvarov, H.-A. Wagenknecht, T. Fiebig, *Chem. Phys. Lett.* **2005**, *409*, 277–280.

Received: May 27, 2011
Published online: September 26, 2011

 © 2011 Wiley-VCH Verlag GmbH & Co. KGaA, Weinheim

Bioorganic & Medicinal Chemistry Letters 21 (2011) 6465–6469

Contents lists available at SciVerse ScienceDirect

Bioorganic & Medicinal Chemistry Letters

journal homepage: www.elsevier.com/locate/bmcl

3-Aminopyrrolidine-4-carboxylic acid as versatile handle for internal labeling of pyrrolidinyl PNA

Nisanath Reenabthue [a], Chalothorn Boonlua [b], Chotima Vilaivan [b], Tirayut Vilaivan [b], Chaturong Suparpprom [a,*]

[a] Department of Chemistry and Center of Excellence for Innovation in Chemistry, Faculty of Science, Naresuan University, Ta-Po District, Muang, Phitsanulok 65000, Thailand
[b] Organic Synthesis Research Unit, Department of Chemistry, Faculty of Science, Chulalongkorn University, Phayathai Road, Patumwan, Bangkok 10330, Thailand

ARTICLE INFO

Article history:
Received 3 June 2011
Revised 15 August 2011
Accepted 17 August 2011
Available online 23 August 2011

Keywords:
Peptide nucleic acid (PNA)
β-Amino acid
Foldamer
Molecular beacon
Fluorescence

ABSTRACT

Conformationally restricted pyrrolidinyl PNAs with an α/β-dipeptide backbone consisting of a nucleobase-modified proline and a cyclic five-membered amino acid spacer such as (1*S*,2*S*)-2-aminocyclopentanecarboxylic acid (ACPC) (acpcPNA) can form very stable hybrids with DNA with high Watson–Crick base pairing specificity. This work aims to explore the effect of incorporating 3-aminopyrrolidine-4-carboxylic acid (APC), which is isosteric to the ACPC spacer, into the acpcPNA. It is expected that the modification should not negatively affect the DNA binding properties, and that the additional nitrogen atom in the APC should provide a handle for internal modification. Orthogonally-protected (N^3-Fmoc/N^1-Boc and N^3-Fmoc/N^1-Tfa) APC monomers have been successfully synthesized and incorporated into the acpcPNA by Fmoc-solid-phase peptide synthesis. T_m, UV and CD spectroscopy confirmed that the (3*R*,4*S*)-APC could substitute the (1*S*,2*S*)-ACPC spacer in the acpcPNA with only slightly decreasing the stability of the hybrids formed between the modified acpc/apcPNA and DNA. In contrast, the (3*S*,4*R*) enantiomer of APC caused substantial destabilization of the hybrids. Furthermore, a successful on-solid-support internal labeling of the acpc/apcPNA via amide bond formation between pyrene-1-carboxylic acid or 4-(pyrene-1-yl) butyric acid and the pyrrolidine nitrogen atom of the APC spacer has been demonstrated. Fluorescence properties of the pyrene-labeled acpc/apcPNAs are sensitive to their hybridization states and can readily distinguish between complementary and single-mismatched DNA targets.
© 2011 Elsevier Ltd. All rights reserved.

Peptide nucleic acid or PNA[1,2]—an analogue of DNA with achiral, electrostatically neutral, peptide-like backbone—is an important tool in nucleic acid-related applications ranging from diagnostic, therapeutic, materials science and nanotechnology. Despite the completely different core structure of Nielsen's PNA from native nucleic acids, PNA can form a very stable hybrid with DNA/RNA in a highly sequence specific manner according to the Watson–Crick base pairing rules.[3] An additional advantage of the unnatural backbone of PNA is its high chemical/physiological stability.[4] The ability to functionalize PNA, for example, by biotin, a fluorophore or other reporter groups, is very important for many of its applications. In principle, the peptide backbone of PNA allows facile modification by standard amide bond formation. However, in practice this is generally true only for terminal modifications, whereby the amino group is already present (N-terminus) or can be incorporated without disrupting the overall structure of the PNA (e.g., as a lysine residue at the C-terminus).[5] Backbone modification at non-terminal positions requires incorporation of specialized monomers during the PNA synthesis on the solid support.[6–8] These modified PNA monomers often cause disturbance to the PNA structures and their DNA binding properties.[9] Recently, Appella et al. has developed Nielsen's type aegPNA monomers with a lysine side-chain attaching at the gamma-position with the aim to use as a handle for site-specific labeling through amide bond formation.[10] It was demonstrated that such modification had little effect on the stability of the resulting PNA·DNA hybrids and that a range of labels can be successfully incorporated at any desired positions.[11] Peptoid-like side chains have also been attached to the nitrogen atom of the aminoethyl group in aegPNA without reducing the hybridization affinity.[12] All of the above-mentioned works focus on labeling of the original aegPNA system with the aminoethylglycine backbone. Recently, we have introduced a conformationally constrained analogue of PNA consisting of proline/2-aminocyclopentane carboxylic acid α/β-dipeptide subunit called acpcPNA.[13–15] In addition to the ability to bind to its complementary DNA target with higher affinity and sequence specificity than DNA and aegPNA,[16] this acpcPNA exhibited a number of unusual properties not observed in aegPNA including the high preference for binding to DNA over RNA and the absence of self-pairing between two complementary strands.[14,15] Although terminal labeling of acpcPNA had been routinely performed,[16,17] there is no general

* Corresponding author. Tel.: +66 055 963 462; fax: +66 055 963 401.
E-mail address: chaturongs@nu.ac.th (C. Suparpprom).

0960-894X/$ - see front matter © 2011 Elsevier Ltd. All rights reserved.
doi:10.1016/j.bmcl.2011.08.079

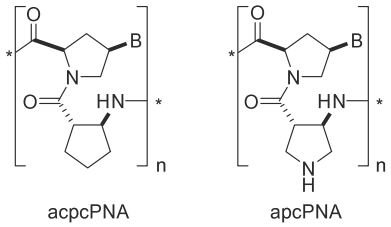

Scheme 1. Structure of acpcPNA and apcPNA.

solution for internal labeling available. We envisioned that the ability to site-specifically attach a label within the acpcPNA backbone would expand its utility further.

In this Letter, we report a new modification of our acpcPNA backbone by partial or total replacement of the 2-aminocyclopentanecarboxylic acid (ACPC) spacer with an isosteric 3-aminopyrrolidine-4-carboxylic acid (APC) spacer (Scheme 1).[18] We also evaluate the DNA binding properties of these novel apcPNA as well as mixed acpc/apcPNA chimeric oligomers, and compared to the corresponding unmodified acpcPNA. In addition, we have developed an orthogonally protected APC monomer and demonstrated its suitability as a handle for incorporation of fluorescence labels at the internal positions of acpcPNA via amide bond formation.

The Fmoc-protected, pentafluorophenyl (Pfp)-activated pyrrolidinyl PNA monomers **1a**–**1d** and the ACPC spacer (**2**) were synthesized following the literature procedure.[14] Since the *trans*-(3*R*,4*S*) APC should be isostructural with *trans*-(1*S*,2*S*)-ACPC spacer in acpcPNA, we decided to focus on this particular stereoisomer, but the *trans*-(3*S*,4*R*) stereoisomer of APC was also included for comparison purpose.

These monomers were required in Fmoc-protected, Pfp-activated forms (Scheme 2) in order to be compatible with our standard protocol for the solid phase peptide synthesis (SPPS) of acpcPNA.[14] In addition, the pyrrolidine nitrogen atom of the APC requires a semi-permanent protection that is compatible to the Fmoc-SPPS. The Boc group was chosen (monomers **3a**, **3b**) for initial evaluation of the DNA-binding behaviour of the modified acpcPNA. However, since the Boc group cannot be selectively removed without concomitant cleavage of the acpcPNA from the solid support equipped with Rink amide linker generally used in Fmoc-SPPS, an alternative protecting group is required to enable post-synthetic modifications of the acpcPNA on the solid support. The trifluoroacetyl (Tfa) group was chosen for this purpose because

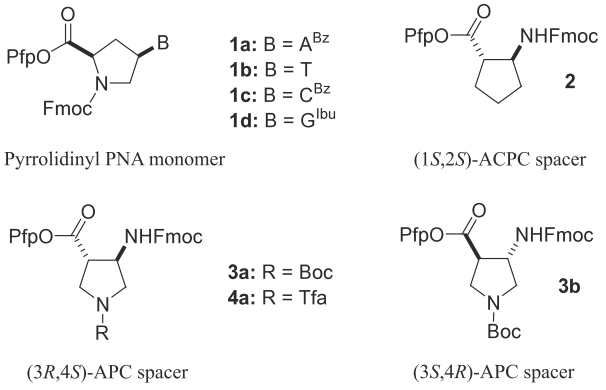

Scheme 2. Structure of acpcPNA monomers and spacers employed in this study (*Abbreviations:* Boc, *tert*-butoxycarbonyl; ACPC, 2-aminocyclopentanecarboxylic acid; APC, 3-aminopyrrolidine-4-carboxylic acid; Bz, benzoyl; Fmoc, fluorene-9-ylmethoxycarbonyl; Ibu, isobutyryl; Pfp, pentafluorophenyl; Tfa, trifluoroacetyl).

it is stable under non-aqueous basic conditions required for Fmoc deprotection, yet can be readily removed by treatment with an aqueous base where the Rink amide linker is completely stable. Syntheses of both enantiomers of the known Fmoc/Boc-protected *trans*-APC spacer were carried out following a protocol described by Gellman et al. (Scheme 3).[19] Diastereoselective reduction of the chiral enamines derived from ethyl 3-oxopyrrolidine-4-carboxylic acid (**5**)[20] and (*S*)-(−)-α-methylbenzylamine or (*R*)-(+)-α-methylbenzylamine as chiral auxiliaries gave the (3*R*,4*S*) and (3*S*,4*R*) amines **6a** and **6b**, respectively.

These intermediates were purified from the undesired diastereomers by recrystallization of the HCl salts (>98% of the desired diastereomer according to ^{1}H NMR and HPLC analysis). Cleavage of the chiral auxiliary, followed by protecting groups exchange and activation by pentafluorophenyl trifluoroacetate (PfpOTfa) provided the *trans*-(3*R*,4*S*)- and (3*S*,4*R*)-Pfp-activated spacers **3a** and **3b**. On the other hand, when the Boc group was removed by treatment with trifluoroacetic acid (TFA) prior to the activation with an excess of PfpOTfa, the Pfp-activated N^1-Tfa-protected (3*R*,4*S*)-APC spacer **4a** was obtained.

The acpcPNAs which were fully or partially modified with either enantiomer of the APC spacer were synthesized according to our previously published protocol.[14] The APC spacers **3a** and **3b** coupled at least as efficiently as the standard ACPC spacer on the solid support (>98% coupling yield for each step). The Boc group was removed during the cleavage from the resin with TFA. If the acpc/apcPNA was to be further functionalized on the solid support, the Tfa-protected APC spacer **4a** was employed instead of **3a**. After end-capping by acetylation or benzoylation, the nucleobase side chain protecting groups was removed by treatment with 1:1 aqueous ammonia/dioxane at 60 °C overnight. This condition also simultaneously removed the *N*-Tfa protecting group on the Tfa-protected APC unit. A label such as pyrene-1-carboxylic acid or 4-(pyrene-1-yl)butyric acid was then coupled onto the solid-supported acpc/apcPNA via HATU activation. After cleavage from the solid support by treatment with TFA, the acpc/apcPNA oligomers were purified by RP-HPLC and characterized by MALDI-TOF mass spectrometry (Table 1).

The stability of the hybrids formed between the synthesized acpc/apcPNA with their complementary DNA was determined by thermal denaturation experiments. The T_m data are summarized in Table 1 (melting curves shown in Fig. S9). To evaluate the compatibility of the APC to the ACPC backbone, the T_m values of the fully modified homothymine apcPNA nonamers **PNA1** (3*R*,4*S*) and **PNA2** (3*S*,4*R*) with dA_9 were compared with the corresponding unmodified acpcPNA. In accordance with our prediction, the **PNA1** with the (3*R*,4*S*)-APC spacer showed a clear melting behaviour, albeit with a considerably lower T_m compared to the unmodified acpcPNA ($\Delta T_m = -17.0$ °C). The **PNA2** showed no melting behaviour down to 20 °C, suggesting that the hybrid must have been very unstable. Interestingly, the T_m curve of **PNA1** was considerably broader than the unmodified acpcPNA, which may suggest the formation of multiple species, which was confirmed in the first derivative plot (Fig. S9b). The results from UV titration[21] (Fig. 1) also confirmed that the **PNA1** could form a hybrid with dA_9. They also further revealed that the **PNA1** could form both PNA·DNA and $(PNA)_2$·DNA hybrids as shown by the presence of two inflection points at ca. 50 and 35 mol % of DNA in the titration curve. CD spectra of the mixtures of **PNA1** and dA_9 at 1:1 and 2:1 ratios (Fig. 2) also confirmed the hybrid formation. The negative band originally at 250 nm in the dA_9 was slightly blue-shifted to 247 nm, with an increased intensity upon hybrid formation. In addition, a new negative band appeared at 267 nm. While other parts of the spectra remained unchanged, the intensity of this 267 nm band further increased when the ratio of the PNA:DNA was increased from 1:1 to 2:1 at a fixed concentration of the

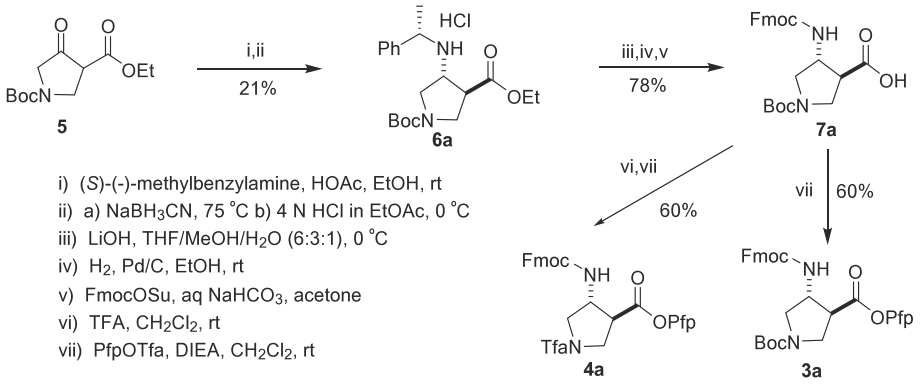

Scheme 3. Synthesis of the (3*R*,4*S*)-APC spacer (steps i–iv are adapted from Ref. 18). The enantiomeric (3*S*,4*R*)-APC derivatives **6b**, **7b** and **3b** were prepared in 17%, 66% and 66% yield, respectively starting from **5** and (*R*)-(+)-methylbenzylamine.

Table 1
Sequence, mass spectrometric and thermal melting data of the acpc/acpPNA

Code	Sequence (N→C)[a]	*m/z* (calcd)	*m/z* (found)	T_m[b] (°C)	ΔT_m[c] (°C)
PNA1	Bz-TTTTTTTT-LysNH$_2$	3250.5	3250.1	55.5[d,e]	−17.0
PNA2	Bz-TTTTTTTT-LysNH$_2$	3250.5	3251.2	<20[d]	—
PNA3	Bz-TTTTTTTTT-LysNH$_2$	3242.5	3242.6	71.1[d]	−1.4
PNA4	Bz-TTTTTTTTT-LysNH$_2$	3242.5	3243.7	28.3[d]	−44.2
PNA5	Bz-GTAGATCACT-LysNH$_2$	3621.9	3622.2	50.8[d]	−1.4
PNA6	Ac-TTTT(Py)TTTTT-LysNH$_2$	3409.6	3411.0	62.2[f]	−10.3
PNA7	Ac-GTAGA(Py)TCACT-LysNH$_2$	3788.9	3789.4	44.3[f]	−7.9
PNA8	Bz-GTAGA(PyBu)TCACT-LysNH$_2$	3893.0	3893.7	45.7[f]	−6.5

[a] T = ssACPC-T; T = (3*R*,4*S*)-APC-T; T = (3*S*,4*R*)-APC-T; (Py) = pyrene-1-carbonyl modification; (PyBu) = 4-(pyrene-1-yl)butyryl modification.
[b] With complementary DNA (dA$_9$ for **PNA1–PNA4** and **PNA6**; dAGTGATCTAC for **PNA5, PNA7** and **PNA8**).
[c] Values refer to the T_m decrease relative to that of unmodified acpcPNA under identical conditions (T_m of hybrids with complementary DNA Ac-TTTTTTTTT-LysNH$_2$: 72.5 °C; Ac-GTAGATCACT-LysNH$_2$: 52.2 °C).
[d] Conditions: 10 mM sodium phosphate buffer pH 7.0, 100 mM NaCl, [PNA] = 1.0 μM and [DNA] = 1.0 μM.
[e] Very broad and non-two-state melting curve.
[f] Conditions: 10 mM sodium phosphate buffer pH 7.0, [PNA] = 2.5 μM and [DNA] = 3.0 μM.

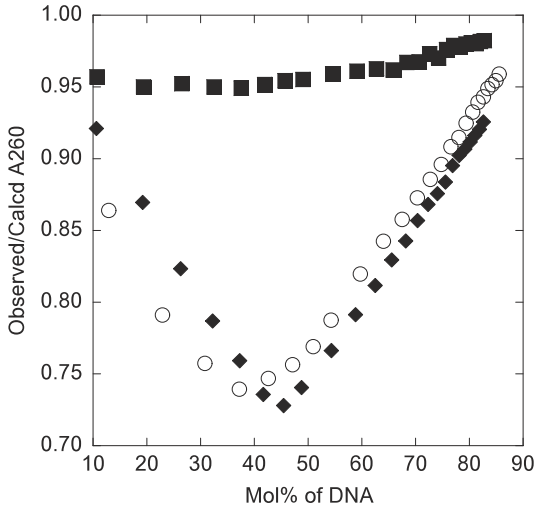

Figure 1. UV titration plots of **PNA1** (○), **PNA2** (■), **PNA3** (♦) and their complementary DNA (dA$_9$). The plots show the ratio of observed A_{260}/calculated A_{260} and mole fraction of DNA, and were measured in 10 mM sodium phosphate buffer pH 7.0, 100 mM NaCl at 25 °C, initial PNA concentration = 2 μM.

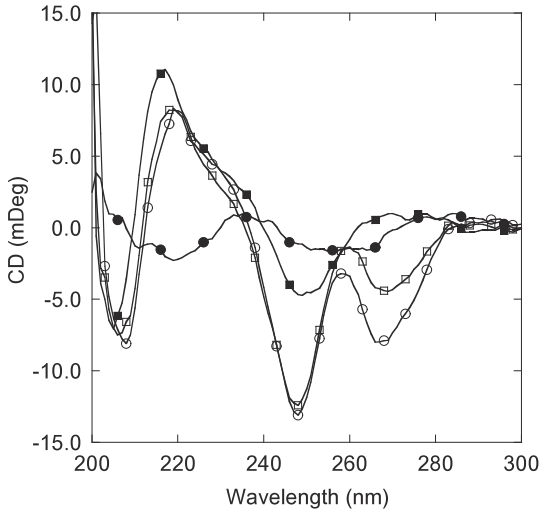

Figure 2. CD spectra of (a) dA$_9$ (–■–), **PNA1** (–●–), dA$_9$ + 1 equiv **PNA1** (–□–), and dA$_9$ + 2 equiv **PNA1** (–○–). The spectra were measured in 10 mM sodium phosphate buffer, pH 7.0, 100 mM NaCl at 25 °C, [PNA] = 2.5 or 5.0 μM and [DNA] = 2.5 μM.

DNA. This suggests the formation of different hybrids at different PNA:DNA ratios. No significant change in the CD spectra was observed in mixtures of **PNA2** and dA$_9$ at both 1:1 and 2:1 ratios relative to the sum of the CD spectrum of each component (Fig. S12). In addition, the UV titration curve of **PNA2** was essentially flat

without any hypochromicity (Fig. 1), indicating that it cannot form a stable hybrid at the temperature which the titration was carried out (25 °C). It can therefore be concluded that only the (3*R*,4*S*)-APC, but not the (3*S*,4*R*)-APC, could replace the (1*S*,2*S*)-ACPC spacer in acpcPNA as would be anticipated from their absolute configurations.

The UV titration curve of the **PNA3**, singly modified with a (3*R*,4*S*)-APC spacer at the middle of the strand, suggested that it could form only a duplex with dA_9 similar to the unmodified acpcPNA (Fig. 1). Most importantly, the T_m of the hybrid with complementary DNA of **PNA3** was only slightly decreased compared to the corresponding unmodified acpcPNA hybrid ($\Delta T_m = -1.4$ °C). On the other hand, the hybrid of **PNA4** carrying a single (3*S*,4*R*)-APC modification was much more destabilized ($\Delta T_m = -44.2$ °C). These results confirmed the conclusion from the aforementioned studies on the fully-modified **PNA1** and **PNA2** that only the (3*R*,4*S*)-APC could substitute the (1*S*,2*S*)-ACPC without much destabilizing effect. This conclusion is also true for mixed sequence acpc/apcPNA such as **PNA5**. In this case the T_m was again only slightly decreased ($\Delta T_m = -1.4$ °C) upon substitution of one ACPC by one (3*R*,4*S*)-APC unit. The specificity of DNA recognition by **PNA1** was demonstrated by the absence of a sigmoidal melting curve when the DNA was changed from dA_9 (complementary) to dA_4TA_4 (single mismatched). Likewise, the thermal stability of the hybrids formed between the singly APC-modified **PNA3** or **PNA5** and their single-mismatched DNA targets was also markedly decreased (−28.0 °C and −21.3 °C, respectively) compared to the fully complementary hybrids (Fig. S10). These results indicated that the high specificity of the DNA recognition is still retained in the apcPNA and acpc/apcPNA.

One distinctive feature of the homothymine **PNA1**, fully-modified with (3*R*,4*S*)-APC spacer, compared to the unmodified acpcPNA with the same sequence is that it forms a triplex with DNA in addition to the duplex. This could be explained by the favourable electrostatic attraction between the positively-charged backbone of the fully-modified PNA and the negatively-charged phosphate backbone of the DNA. The sharpening of the T_m curve at pH 8 (Fig. S11) supports this hypothesis because at higher pH, the pyrrolidine nitrogen (pK_a ~8.75)[22] would become less protonated, hence the electrostatic attraction should decrease. The behaviour of the APC spacer at high pH would therefore be more closely resemble that of the non-ionizable ACPC spacer. Since the singly-modified homothymine **PNA3** formed only duplex with complementary DNA, the triplex formation should not be a problem because for labeling purpose the PNA would need to be modified with only one or up to a few APC residues. Furthermore, upon modification by the amide bond formation, the APC residue should no longer be protonated at neutral pH.

In order to investigate the viability of using (3*R*,4*S*)-APC as a handle for internal modification of acpcPNA with a fluorophore, three pyrene-labeled acpc/apcPNA (**PNA6**, **PNA7** and **PNA8**) were synthesized as models. Pyrene-1-carboxylic acid and 4-(pyrene-1-yl)-butyric acid were chosen as the labels with the expectation that they should exhibit different fluorescence in the single stranded and duplex states. In the single stranded form, the pyrene should strongly interact with the nucleobases of the PNA resulting in fluorescence quenching.[23] Upon hybridization with the complementary DNA strand by Watson–Crick base pairing, the pyrene should interact differently with the nucleobases, leading to a fluorescence change.[10,24,25] A similar concept has previously been demonstrated in DNA system whereby the pyrene was attached to the nucleobase.[26,27] According to T_m analyses, labeling the acpc/apcPNA with pyrene cause further destabilization of the PNA·DNA duplexes, presumably due to steric effects (ΔT_m compared to the corresponding unmodified acpcPNA·DNA hybrids are −10.3, −7.9 °C and −6.5 °C for **PNA6**, **PNA7** and **PNA8**, respectively). The pyrene-1-carboxylic acid-modified homothymine **PNA6** in the single-stranded form exhibited two weak fluorescence emission bands at 382 and 400 nm. When it was hybridized with excess of dA_9, the fluorescence intensity at 382 nm increased ~2.6-fold over that of the single-stranded **PNA6** (Fig. S13). The change in the fluorescence could be visualized by naked eyes under UV irradiation (Fig. S14). Hybridization with a non-complementary DNA target (dA_4TA_4) gave barely noticeable change in the fluorescence compared to the single stranded **PNA6**. Consistently, the fluorescence increase was also observed in the mixed base sequence **PNA7**, although in this case the difference was considerably smaller (~1.3-fold enhancement upon hybridization) (Fig. 3a). Hybridization of **PNA7** with a single-mismatched DNA target yielded no significant fluorescence change, indicating the high specificity of the system.

A more pronounced fluorescence change was observed in **PNA8** with the same sequence as **PNA7** but with the pyrenebutyryl instead of the pyrenecarbonyl labels. Extending the pyrene from the acpc/apcPNA backbone by a three-carbon linker resulted in a 4.8 to 5-fold fluorescence enhancement of the 379 nm emission upon hybridization with the complementary DNA relative to the single stranded **PNA8** and its hybrid with single mismatched

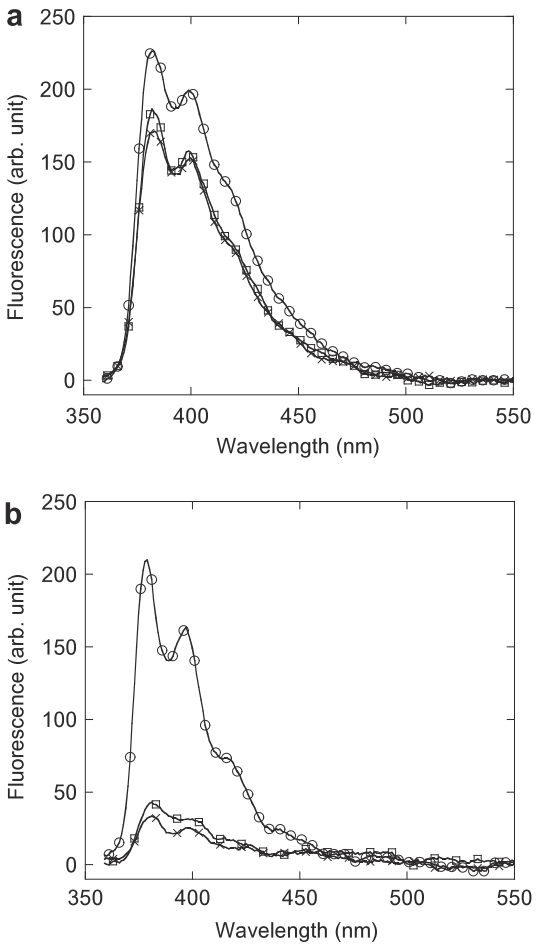

Figure 3. Fluorescence spectra of pyrene-labeled acpc/apcPNA (a) **PNA7** (–□–), **PNA7** + complementary DNA (–○–), **PNA7** + single mismatch DNA (–×–) and (b) **PNA8** (–□–), **PNA8** + complementary DNA (–○–), **PNA8** + single mismatch DNA (–×–); complementary DNA = (dAGTGATCTAC) and single mismatched DNA = (dAGTGACCTAC). The spectra were measured in 10 mM sodium phosphate buffer, pH 7.0 at 25 °C, [PNA] = 2.5 μM and [DNA] = 3.0 μM, excitation wavelength = 345 nm.

DNA (Fig. 3b). The better discrimination should be attributed to the more effective quenching of the pyrenebutyryl label in the single stranded **PNA8** than the pyrenecarbonyl label in **PNA7** as shown by the smaller fluorescence of **PNA8** compared to **PNA7**. After hybridization with the complementary DNA, both pyrene-labeled PNAs yielded similar fluorescence signals. Quenching of pyrene by nucleobases is known to occur via electron transfer from G, to T or to C.[28,29] The more effective quenching of the pyrenebutyryl label than the pyrenecarbonyl label can be attributed to at least two factors. First, the pyrenebutyryl group has a flexible linker, allowing more effective contact with neighboring nucleobases in the single stranded PNA. Second, the pyrenebutyryl label has an alkyl group, while the pyrenecarbonyl label has a carbonyl group, directly connect to the π-system of the pyrene. The redox properties of the pyrene chromophores in both labels are therefore different, resulting in different quenching behaviors.[23]

The generation of a positive (turn-on) fluorescence signal in this particular system is an advantage over many other related pyrene-labeled DNA probes whereby the fluorescence is often quenched upon hybridization with DNA as a result of intercalation of the pyrene chromophore between the base stack in the DNA duplex.[30] Only when the pyrene was linked to the nucleobase via relatively rigid linkers that a fluorescence enhancement was observed since no intercalation was possible without disrupting the Waston-Crick base pairing.[27,31,32] The fluorescence enhancement observed, together with the absence of duplex stabilization of the pyrene-labeled acpc/apcPNA relative to the unlabeled acpc/apcPNA, suggested the absence of intercalation of the pyrene labels between the base stack in acpc/apcPNA·DNA hybrids.[33] In effect, the pyrenecarbonyl- or pyrenebutyryl-labeled acpc/apcPNAs behave as quencher-free PNA beacons.[34] These singly-labeled probes are more easily synthesized than the corresponding dual-labeled PNA probes and should be less likely to have problems of aqueous solubility.[5,35] Although the fluorescence enhancement of these prototypic systems is relatively modest because of the high background fluorescence of the pyrene chromophores in the single stranded PNA, the excellent specificity warrants potential use of the system. As the extent of the quenching of pyrene by nucleobases is likely to be sequence-dependent,[23,24] work is now in progress to optimize the positions and structures of the label that will allow maximum fluorescence change to improve the efficiency of the DNA sequence determination.

Acknowledgments

We acknowledge the Thailand Research Fund (TRF) and Commission on Higher Education (MRG5180025 to C.S. and RTA5280002 to T.V.) and the Center of Excellence for Innovation in Chemistry (PERCH-CIC), Commission on Higher Education, Ministry of Education (to N.R.) for financial support.

Supplementary data

Supplementary data associated with this article can be found, in the online version, at doi:10.1016/j.bmcl.2011.08.079.

References and notes

1. Nielsen, P. E. *Acc. Chem. Res.* **1999**, *32*, 624.
2. Uhlmann, E.; Peyman, A.; Breipohl, G.; Will, D. W. *Angew. Chem., Int. Ed.* **1998**, *37*, 2796.
3. Egholm, M.; Buchardt, O.; Christensen, L.; Behrens, C.; Freier, S. M.; Driver, D. A.; Berg, R. H.; Kim, S. K.; Nordén, B.; Nielsen, P. E. *Nature* **1993**, *365*, 566.
4. Demidov, V. V.; Potaman, V. N.; Frank-Kamenetskii, M. D.; Egholm, M.; Buchardt, O.; Sönnichsen, S. H.; Nielsen, P. E. *Biochem. Pharmacol.* **1994**, *48*, 1310.
5. Kuhn, H.; Demidov, V. V.; Coull, J. M.; Fiandaca, M. J.; Gildea, B. D.; Frank-Kamenetskii, M. D. *J. Am. Chem. Soc.* **2002**, *124*, 1097.
6. Gasser, G.; Hüsken, N.; Köster, S. D.; Metzler-Nolte, N. *Chem. Commun.* **2008**, 3675.
7. Sosniak, A. M.; Gasser, G.; Metzler-Nolte, N. *Org. Biomol. Chem.* **2009**, *7*, 4992.
8. de la Torre, B. G.; Eritja, R. *Bioorg. Med. Chem. Lett.* **2003**, *16*, 391.
9. Kersebohm, T.; Kirin, S. I.; Metzler-Nolte, N. *Bioorg. Med. Chem. Lett.* **2006**, *16*, 2964.
10. Englund, E. A.; Appella, D. H. *Org. Lett.* **2005**, *7*, 3465.
11. Appella, D. H.; Englund, E. A. *Angew. Chem., Int. Ed.* **2007**, *46*, 1414.
12. Lu, X.-W.; Zeng, Y.; Liu, C. F. *Org. Lett.* **2009**, *11*, 2329.
13. Suparpprom, C.; Srisuwannaket, C.; Sangvanich, P.; Vilaivan, T. *Tetrahedron Lett.* **2005**, *46*, 2833.
14. Vilaivan, T.; Srisuwannaket, C. *Org. Lett.* **2006**, *8*, 1897.
15. Vilaivan, C.; Srisuwannaket, C.; Ananthanawat, C.; Suparpprom, C.; Kawakami, J.; Yamaguchi, Y.; Tanaka, Y.; Vilaivan, T. *Artificial DNA: PNA & XNA* **2011**, *2*, 50.
16. Ananthanawat, C.; Vilaivan, T.; Hoven, V. P.; Su, X. D. *Biosens. Bioelectron.* **2010**, *25*, 1064.
17. Korkaew, P.; Vilaivan, T. *Nucleic Acids Symp. Ser.* **2008**, *52*, 251.
18. Wang, X.; Espinosa, J. F.; Gellman, S. H. *J. Am. Chem. Soc.* **2000**, *122*, 4821.
19. Lee, H. S.; LePlae, P. R.; Porter, E. A.; Gellman, S. H. *J. Org. Chem.* **2001**, *66*, 3597.
20. Blake, J.; Willson, C. D.; Rapoport, H. *J. Am. Chem. Soc.* **1964**, *86*, 5293.
21. Vilaivan, T.; Lowe, G. *J. Am. Chem. Soc.* **2002**, *124*, 9326.
22. This is the calculated pK_a figure of the pyrrolidine nitrogen atom of *N*-Boc-(3*S*,4*R*)-3-aminopyrrolidine-4-carboxylic acid ethyl ester [955138-41-7] as provided by SciFinder database, accessed 07 April 2011.
23. Seidel, C. A. M.; Schulz, A.; Sauer, M. H. M. *J. Phys. Chem.* **1996**, *100*, 5541.
24. Nazarenko, I.; Piers, R.; Lowe, B.; Obaidy, M.; Rashtchian, A. *Nucleic Acids Res.* **2002**, *30*, 2089.
25. French, D. J.; Archard, C. L.; Brown, T.; McDowell, D. G. *Mol. Cell. Probes* **2001**, *15*, 363.
26. Saito, Y.; Motegi, K.; Bag, S. S.; Saito, I. *Bioorg. Med. Chem. Lett.* **2008**, *16*, 107.
27. Okamoto, A.; Kanatani, K.; Saito, I. *J. Am. Chem. Soc.* **2004**, *126*, 4820.
28. Manoharan, M.; Tivel, K. L.; Zhao, M.; Nafisi, K.; Netzel, T. L. *J. Phys. Chem.* **1995**, *99*, 17461.
29. Wilson, J. N.; Cho, Y.; Tan, S.; Cuppoletti, A.; Kool, E. T. *Chem. Biochem.* **2008**, *9*, 279.
30. Nakamura, M.; Fukunaga, Y.; Sasa, K.; Ohtoshi, Y.; Kanaori, K.; Hayashi, H.; Nakano, H.; Yamana, K. *Nucleic Acids Res.* **2005**, *33*, 5887.
31. Mayer, E.; Valis, L.; Wagner, C.; Rist, M.; Amann, N.; Wagenknecht, H.-A. *Chem. Biochem.* **2004**, *5*, 865.
32. Hwang, G. T.; Seo, Y. J.; Kim, S. J.; Kim, B. H. *Tetrahedron Lett.* **2004**, *45*, 3543.
33. Telser, J.; Cruickshank, K. A.; Morrison, L. E.; Netzel, T. L. *J. Am. Chem. Soc.* **1989**, *111*, 6966.
34. For a review on quencher-free DNA beacons see: Venkatesan, N.; Seo, Y. J.; Kim, B. H. *Chem. Soc. Rev.* **2008**, *37*, 648.
35. Seitz, O. *Angew. Chem., Int. Ed.* **2000**, *39*, 3249.

J Nanopart Res (2011) 13:6847–6857
DOI 10.1007/s11051-011-0592-8

RESEARCH PAPER

Surface-initiated atom transfer radical polymerization of poly(4-vinylpyridine) from magnetite nanoparticle

Boonjira Rutnakornpituk · Uthai Wichai · Tirayut Vilaivan · Metha Rutnakornpituk

Received: 20 May 2011 / Accepted: 23 September 2011 / Published online: 7 October 2011
© Springer Science+Business Media B.V. 2011

Abstract Surface modification of magnetite nanoparticles (MNP) with a covalently bonded poly(4-vinylpyridine) (P4VP) by surface-initiated atom transfer radical polymerization (ATRP) is reported in this article. MNP was first prepared via thermal decomposition of $Fe(acac)_3$ and grafted with an ATRP initiator on its surface. ATRP of 4-vinylpyridine was then initiated from the MNP surface in the presence of CuBr/PMDETA (1,1,4,7,7-pentamethyldiethylenetriamine) catalytic complex in dioxane. FTIR in combination with photocorrelation spectroscopy (PCS), thermogravimetric analysis (TGA), and vibrating sample magnetometry (VSM) techniques indicated the growth of P4VP on the particle surface with increasing ATRP reaction time. Transmission electron microscopy (TEM) disclosed that the average particle size was 8 nm in diameter with some nanoaggregation observed. The PCS results revealed that decreasing the solution pH enhanced the particle dispersibility because of the positive charge repulsion of the protonated P4VP on the particle surface. TGA was also performed to elucidate the composition of P4VP shell and magnetite core in the hybrid material.

Keywords Magnetite · Nanoparticle · Poly(4-vinylpyridine) · ATRP · pH sensitive · Surface science

Introduction

Surface modification of magnetite nanoparticle (MNP) by chemically bonded polymer has recently attracted a great attention owing to its potential biomedical applications, such as magnetic separation, controlled drug release (Zhang and Misra 2007), magnetic resonance imaging (Pei et al. 2007; Casula et al. 2010; Woo et al. 2004), and hyperthermia treatment of tumor cells (Laurent et al. 2008). For these applications, it is necessary that the particles must possess combined properties of physical and chemical stabilities, high magnetic saturation, biocompatibility, and interactive functions on its surface (Gupta and Gupta 2005). Hence, coating the particle surface with a polymeric thin film is essential, not only to prevent particle agglomeration, but also to provide a suitable surface for further functionalization by the attachment of various bioactive molecules, such as protein (Pan et al. 2005; Liu et al. 2004), amino acid (Hayashi et al. 2010; Marinescu et al. 2006), DNA (Lellouche et al.

Electronic supplementary material The online version of this article (doi:10.1007/s11051-011-0592-8) contains supplementary material, which is available to authorized users.

B. Rutnakornpituk · U. Wichai · M. Rutnakornpituk (✉)
Department of Chemistry and Center of Excellence for Innovation in Chemistry, Faculty of Science, Naresuan University, Phitsanulok 65000, Thailand
e-mail: methar@nu.ac.th

T. Vilaivan
Organic Synthesis Research Unit, Department of Chemistry, Faculty of Science, Chulalongkorn University, Phayathai Road, Patumwan, Bangkok 10330, Thailand

2005; Cheng et al. 2005; Mornet et al. 2000), peptide nucleic acid (PNA) (Milano et al. 2010), and folic acid (Zhang et al. 2002; Sonvico et al. 2005).

Surface modification of materials or particles with polymers via radical polymerization can be applied for a wide range of monomers and have widespread applications (Xu et al. 2009). However, the conventional radical polymerization gives rise for the lack of control over the polymer structure and molecular weight (Coessens et al. 2001; Hawker et al. 2001; Matyjaszewski and Xia 2001). Therefore, surface modification of MNP via controlled/living radical polymerizations (CRPs), including nitroxide-mediated radical polymerization (NMRP) (Chen et al. 2011), reversible addition fragmentation chain transfer (RAFT) polymerization (Tian et al. 2011), and metal-catalyzed living radical polymerizations (Zhou et al. 2011; Rutnakornpituk et al. 2011; Golas et al. 2010), have recently been attracting great interest because well-defined composition, architecture, and functionality of the polymeric stabilizer can be designed. Of the CRP techniques, atom transfer radical polymerization (ATRP) has been reported as one of the most potential "grafting from" method for surface modification of MNP (Zhou et al. 2008; Sun et al. 2007) with a wide range of usable monomers (Sun et al. 2007; Liu et al. 2005; Hermann High et al. 2007). Unlike the conventional radical polymerization, surface-initiated ATRP from MNP produced polymers with a narrow polydispersity index (PDI) and proceeded in a controlled manner (Xu et al. 2009; Matyjaszewski and Xia 2001). Moreover, when compared to other CRP reactions, the advantage of ATRP is that the reaction can be performed at a relatively low temperature, while other CRPs such as RAFT and NMRP involve a high reaction temperature to form radicals from azo or peroxide initiators (Rutnakornpituk et al. 2011).

The objective of this study is to use a "grafting from" strategy to modify MNP surface with poly(4-vinylpyridine) (P4VP) via ATRP. The major advantage of the "grafting from" strategy, an effective surface modification approach pioneered by Sogah (Hertler et al. 1990), is the capability of yielding a relatively high-density polymeric layer on particle surface as compared to the "grafting onto" strategy, in which steric hindrance interferes with further growth of polymers on the particle surface (Yang et al. 1998).

P4VP contains ionizable pyridyl groups in their backbone, making it a polyelectrolyte in an aqueous solution (Pinkrah et al. 2003; Gohy et al. 2002; Gil and Hudson 2004). It is thus anticipated that surface modification of MNP with P4VP via ATRP would produce a well-defined polyionizable P4VP stabilizer with narrow molecular weight distribution on the MNP surface. In addition to serving as steric and electrostatic stabilizers, the polyelectrolyte P4VP brushes should also exhibit interesting pH-responsive behaviors associated with their large electrostatic potentials (pK_a of 4-vinylpyridine is 5.62) (Perrin 1965; Mori et al. 2003). The "grafting from" polymerization of P4VP (Chen et al. 2011) and poly(3-vinylpyridine)(P3VP) (Kobayashi et al. 2006) brushes from magnetite surface via NMRP has previously been reported. However, the pH-responsive properties of such complexes were not investigated in detail. Utilization of NMRP for surface modification of magnetite particles with poly(3- or 4-vinylpyridine) (Kobayashi et al. 2006; Matsuno et al. 2004) and their copolymerization with other polymers, such as polystyrene (Matsuno et al. 2004), acrylamidoethylamine, and polyethyleneglycol (Thiessen et al. 2010) have been previously presented. In addition, surface modifications of Pd (Liu et al. 2011), Si (Tamami and Farjadian 2011), and Au (Chang and Lo 2011) nanoparticles with P4VP or poly(2-vinylpyridine)(P2VP) have also been investigated. However, the dependence of the solution pH on properties of these complexes was not reported.

In the current study, P4VP-coated MNPs were thus prepared via a surface-initiated ATRP using the "grafting from" strategy. FTIR was used to monitor the reaction progress in each step. TGA was used to investigate the percentage of each composition in the polymer–MNP complex. TEM technique was employed to monitor the particle size and its distribution. PCS was conducted to study the dependence of the solution pH on hydrodynamic diameter and electrophoretic mobility of the particles. VSM was also performed to reveal their magnetic properties.

Experimental

Materials

4-vinylpyridine, 95% (Acros) was fractionally distilled before use. Triethylamine (TEA), 97% (Carlo Erba), dioxane (Lab Scan), and toluene (Lab Scan)

were stirred over CaH_2 for 24 h and distilled prior to use. The following reagents were used as received: iron (III) acetylacetonate ($Fe(acac)_3$), (>99%, Acros); benzyl alcohol (98%, Unilab); 3-aminopropyl triethoxysilane (APS) (99%, Acros); 2-bromoisobutyryl bromide (BIBB) (98%, Acros); copper (I) bromide (98%, Acros); *N,N,N′,N″,N‴*-pentamethyldiethylenetriamine (PMDETA), (99%, Acros); ethyl-α-bromoisobutyrate (EBIB)(Aldrich); and oleic acid (Fluka).

Synthesis

Synthesis of oleic acid-coated MNP

In a typical synthesis, $Fe(acac)_3$ (5.0 g, 14.05 mmol) was dissolved in benzyl alcohol (90 mL) in a three-neck round-bottomed flask. It was stirred at 200 °C for 48 h under nitrogen blanket. The particles were isolated from the dispersion using an external magnet and washed repeatedly with ethanol and CH_2Cl_2 to remove the benzyl alcohol. The particles were then dried at room temperature *in vacuo*. To prepare oleic acid-coated MNP, the dried MNP (0.6 g) was suspended in an oleic acid solution in dried toluene (4 mL oleic acid in 30 mL toluene) and sonicated for 3 h.

Synthesis of 2-bromo-2-methyl-N-(3-(triethoxysilyl) propanamide (BTPAm)

The solution of 2-bromoisobutyryl bromide (BIBB) (0.1 mL, 0.8 mmol) in toluene (10 mL) was added dropwise to a solution of 3-aminopropyl triethoxysilane (APS) (0.18 mL, 0.8 mmol) in 10 mL of toluene containing triethylamine (TEA) (0.12 mL, 0.8 mmol) at 0 °C. The mixture was magnetically stirred for 2 h at 0 °C under nitrogen atmosphere, warmed to room temperature, and stirred for another 24 h at room temperature. The mixture was filtered to remove salts, evaporated to remove the unreacted TEA, and dried under reduced pressure. The resulting product, BTPAm, was obtained as yellowish oil (78% yield). ^{1}H NMR (400 MHz, $CDCl_3$) δ_H : 0.60 (m, 2H, Si–CH_2), 1.20 (t, 9H, O–CH_2–CH_3), 1.65 (m, 2H, Si–CH_2–CH_2), 1.95 (s, 6H, $(CH_3)_2$C–Br), 3.25 (m, 2H, CH_2–NH), 3.80 (m, 6H, CH_3–CH_2-O); FT–IR (KBr disk) ν_{max} : 3345 cm^{-1} (NH stretching), 2975–2889 cm^{-1} (C–H stretching), 1738 cm^{-1} (C=O of acid bromide stretching), 1658 cm^{-1} (C=O of amide stretching), 1532 cm^{-1} (NH bending), 1442 cm^{-1} (C–N stretching), 1286 cm^{-1} (C–Br stretching), 1112–1026 (Si–O stretching).

Immobilization of BTPAm, an ATRP initiating site, onto MNP surface

To immobilize BTPAm onto the oleic acid-coated MNP surface, the MNP–toluene dispersion (0.1 g of MNP in 5 mL toluene) (30 mL), BTPAm (0.90 mL) and 2 M TEA in toluene (6 mL) were added into a round-bottomed flask. The mixture was stirred for 24 h at room temperature under nitrogen atmosphere. The particles were subsequently precipitated with methanol, followed by a magnetic separation to obtain BTPAm-coated MNP. Then, the MNP was re-dispersed in toluene and re-precipitated in methanol. This procedure was repeated three times to completely remove unreacted BTPAm. The particles were finally dried *in vacuo*.

Surface-initiated ATRP of 4-vinylpyridine (4VP) from BTPAm-coated MNP

The BTPAm-coated MNP (0.1 g) was sonicated with 4-vinylpyridine (3 mL, 28 mmol) in a Schlenk tube for 1 h before an addition of a solution of CuBr (0.3 g, 2.1 mmol) and PMDETA (0.42 mL, 2.1 mmol) in dioxane (1 mL). The mixture was degassed by three freeze–pump–thaw cycles and heated at 80 °C for 24 h to commence ATRP reaction. For FTIR analyses, the dispersions were removed periodically via a syringe, and the P4VP-coated MNP was magnetically separated and washed thoroughly with methanol and dried *in vacuo*.

Characterization

FTIR was performed on a Perkin-Elmer Model 1600 Series FTIR Spectrophotometer. The solid samples were mixed with KBr to form pellets. ^{1}H NMR was performed on a 400-MHz Bruker NMR spectrometer using $CDCl_3$ as a solvent. TEM was performed on a Philips Tecnai 12 operated at 120 kV equipped with Gatan model 782 CCD camera. The particles were re-suspended in toluene with sonication before deposition on a TEM grid. Hydrodynamic diameter and electrophoretic mobility of the particles were measured at 25 °C via PCS using NanoZS4700 nanoseries Malvern instrument. The sample dispersions were

sonicated for 10 min before each measurement. The electrophoretic mobility was measured in various pH solutions with ionic strength of 0.1 M. Magnetic properties of the particles were measured at room temperature using a Standard 7403 Series, Lakeshore vibrating sample magnetometer. TGA was performed on SDTA 851 Mettler-Toledo at the temperature ranging between 25 and 600 °C at a heating rate of 20 °C/min under oxygen atmosphere.

Results and discussion

The objective of the current study is to modify MNP surface with P4VP using a "grafting from" strategy via ATRP reaction. The controlled/living radical polymerization allows coating of the polymer on MNP surface in a controlled fashion. It is conceived that P4VP grafted on the particle surfaces can provide both steric and electrostatic stabilizations, resulting in good dispersibility of the particles in a suitable media. Because the pyridine ring is protonated at pH below its pK_a (pK_a of 4-vinylpyridine is 5.62) (Perrin 1965), pH of the aqueous dispersion should play an important role on dispersibility of the P4VP-coated MNP. The effects of pH of the aqueous dispersions on their hydrodynamic diameter and electrophoretic mobility of the P4VP-coated MNP were also investigated.

Magnetite nanosolid supports used in this study were synthesized via a thermal decomposition of $Fe(acac)_3$ to eventually obtain MNP with a narrow size distribution. BTPAm, a linker between the particle surface and the polymer, was synthesized via an amide bond formation between APS and BIBB. It was then covalently immobilized on the surface of oleic acid-precoated MNP through a ligand exchange reaction followed by silanization (Fig. 1). The purpose of pre-coating MNP surface with oleic acid was to enhance the particle dispersibility in toluene before reacting with BTPAm (Rutnakornpituk et al. 2011).

Figure 2 shows FTIR spectra of P4VP-coated MNP withdrawn from the dispersions at 1, 6, 12 and 24 h of the ATRP reaction. A progressive growth of the pyridine ring signals ($\sim$1660 cm^{-1}) relative to those

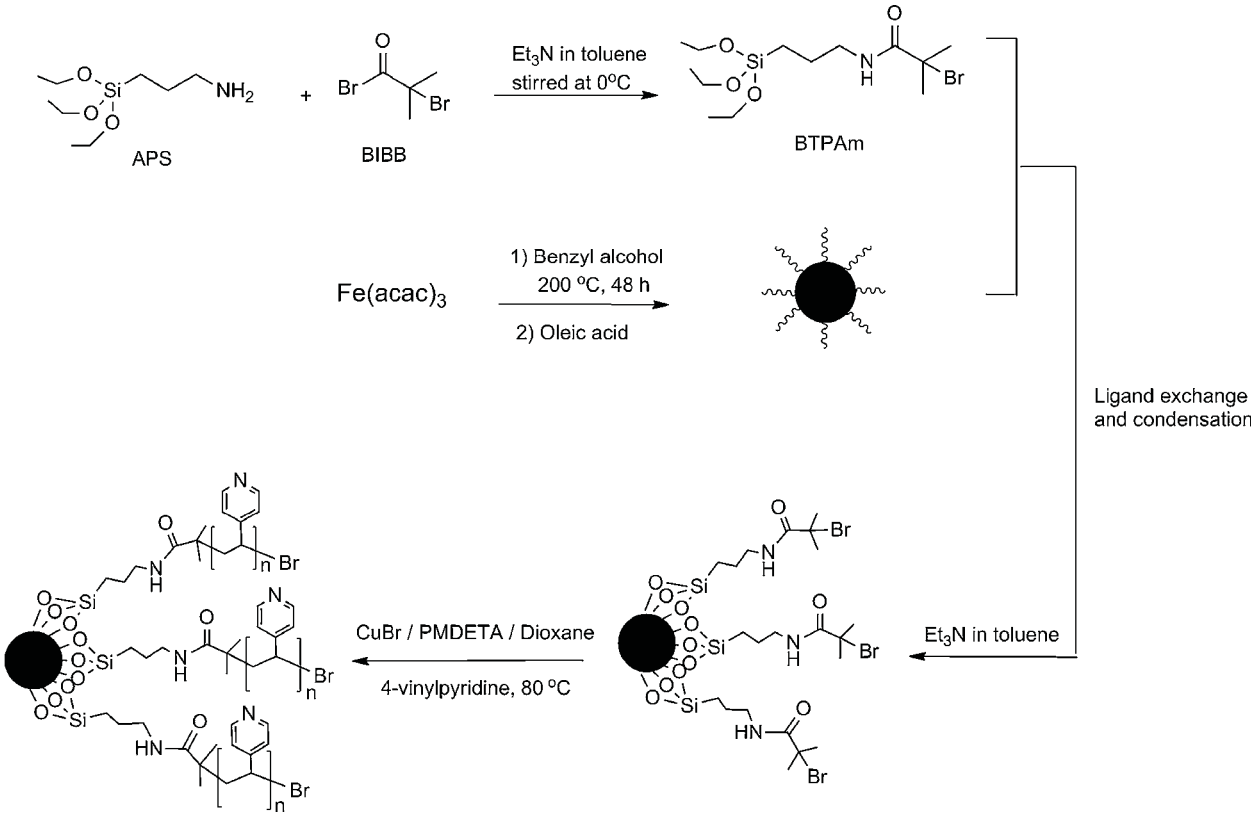

Fig. 1 Synthesis of poly(4-vinylpyridine)-coated magnetite nanoparticle

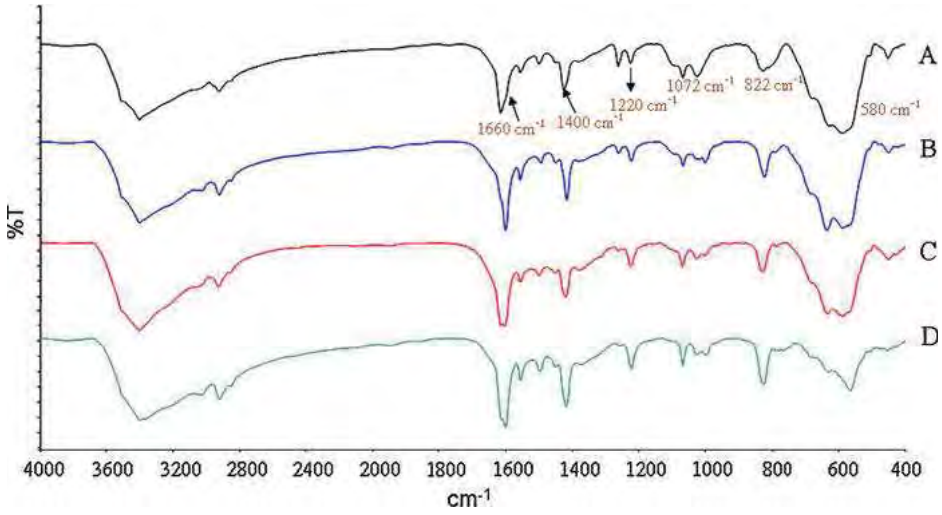

Fig. 2 FTIR spectra of P4VP-coated MNP after (*a*) 1 h, (*b*) 6 h, (*c*) 12 h, (*d*) 24 h of ATRP reactions at 80 °C

of Fe–O bond signals of the MNP core ($\sim$580 cm^{-1}) indicated the growing of P4VP on the MNP surfaces over the ATRP reaction time. In addition, the consistent decrease of the aliphatic C–N bond stretching from BTPAm (1260 cm^{-1}) and the increase of the aromatic amine of the pyridyl rings (1220 cm^{-1}) also supported the above conclusion. In addition, the characteristic signals of pyridyl rings, such as out-of-plane deformation vibrations of 4-monoalkyl pyridine (822 cm^{-1}) and hydrogen bending of 4-monosubstituted pyridine (1072 cm^{-1}), were also apparent, indicating the existence of P4VP in the complexes (Cook and Church 1957).

To investigate the molecular weight and the molecular weight distribution of P4VP, a small amount of ethyl bromoisobutylate (EBiB) was added in the dispersion as a "sacrificial initiator" to form free P4VP along with P4VP grafted on MNP. At a given ATRP reaction, the free P4VP, removed from the MNP complex periodically using an external magnet, was analyzed via GPC. The molecular weights of P4VP after 6 and 24 h of ATRP were 2,000 ($n = 19$) and 5,300 g/mol ($n = 50$), respectively, and the there molecular weight distributions ranged between 1.21 and 1.27. These narrow molecular weight distributions indicated the living mechanism of controlled radical polymerization. According to TEM and TGA results discussed in the later sections, the grafting density of P4VP chains on the particle can be calculated using the method reported by Rutnakornpituk (Rutnakornpituk et al. 2011), and it was found that there was about 0.66 P4VP chain/nm^2 (133 chains/particle). Examples of the calculation are illustrated in the supporting information. The density of pyridyl units on the particle surface, estimated using a similar calculation method, was 33 pyridyl units/nm^2 (6,700 pyridyl units/particle).

Because P4VP is known as a pH-sensitive polymer, dispersibility of the P4VP-coated MNP in water was investigated as a function of the solution pH. From the results in Fig. 3, the P4VP-coated particles after 24 h of ATRP were well dispersible in aqueous solutions without aggregation at pH lower than two. As the pH of the solution increased, dispersibility of the particles in the aqueous solution became poorer, and some particle aggregation was observed. It is hypothesized that, at highly acidic pH, pyridyl rings in P4VP on the particle surface were well protonated. The increase of surface polarity due to the presence of positive charges of the protonated pyridyl rings allowed the particles to well disperse in aqueous solutions because of the enhancement in electrostatic repulsion of positively

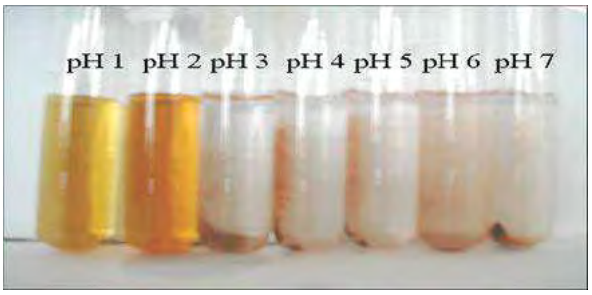

Fig. 3 Dispersibility of P4VP-coated MNP in water at various pHs

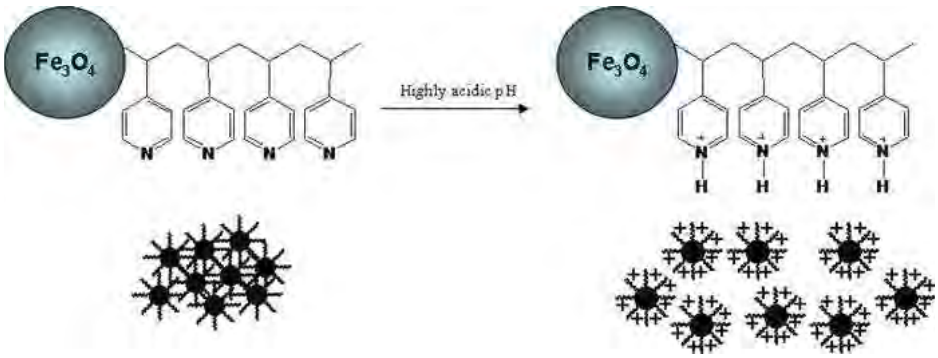

Fig. 4 The proposed stabilization mechanism of P4VP-coated MNP via electrostatic repulsion due to positively charged surface particle

charged surface particle (Fig. 4). The particles after 6 h of ATRP surface modification showed similar dispersibility of the particles in aqueous dispersions at the same pH range, implying that their dispersibility was not dependent on the chain length of P4VP on the particle surface.

How is that the pH values of the stable dispersions (pH $\leq$ 2) correlate with pK_a of the pyridyl ring? Because the reported pK_a of pyridine is 5.62 (Mori et al. 2003), we expected it to be fully protonated at pH around 3–4. The fully protonated dispersion at pH 2 seems to be two orders of magnitude lower than what we expected. However, the polymeric nature of the pyridine may decrease the pK_a by one or more unit because of the potential electrostatic repulsion of the many adjacent protonated pyridyl rings. One might suspect that the MNP complex may dissolve in aqueous solution at pH $\leq$ 2 and eventually form Fe^{2+}/Fe^{3+} ions and the free polymers. Therefore, the dispersions were centrifuged (14,000 rpm) to aggregate the particles, which were then collected by a permanent magnet. It was found that the MNP complexes still well responded to an external magnet, indicating that the MNP complex did not dissolve at low pH solution. This was in good agreement with PCS and TEM results discussed later that the polymer–MNP complexes still retained in the dispersions at pH $\leq$ 2. However, for uses in biomedical applications, the particles should exhibit excellent dispersions between pH 4 and 8. Formation of pyridinium ion on the particle surface via the reaction between alkyl halide and pyridyl rings of P4VP-coated MNP is another promising approach to obtain stable MNP dispersions at higher pH, and this warrants further studies.

Because pyridyl ring of P4VP is highly sensitive to protonation especially in acidic pH, it is thus interesting to understand how pH of aqueous solutions influences the hydrodynamic diameter and surface charge of the P4VP-coated MNP. The particles used in this study were surface modified with P4VP via ATRP reaction for 24 h. The pHs of the aqueous dispersions containing the P4VP-MNP complexes (0.2 mg/ml) were varied from 0.5 to 2.5, and their hydrodynamic diameters were determined via PCS technique. As pH of the dispersions decreased (more acidic pH), their hydrodynamic diameters rapidly decreased at pH ranging between 2.5 and 1.5, and reached the plateau state with pH decreasing between 1.5 and 0.5 (Fig. 5a). It was hypothesized that as pH of the

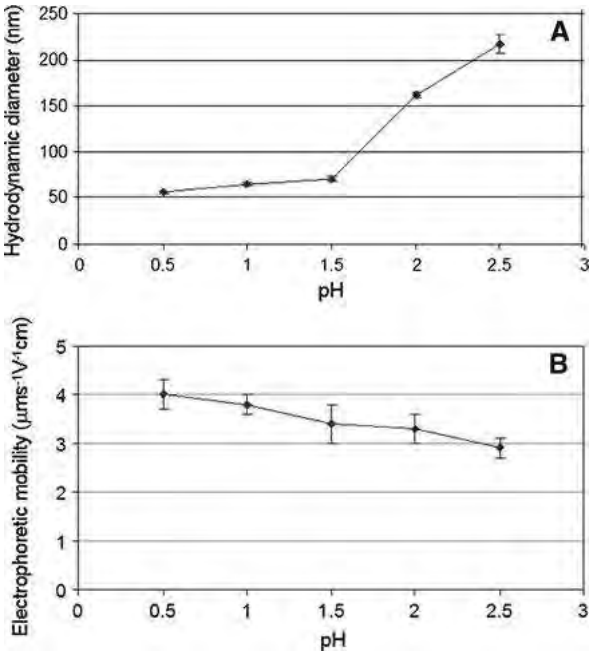

Fig. 5 **a** Hydrodynamic diameter and **b** electrophoretic mobility of P4VP-coated MNPs suspended in aqueous dispersions at various pHs. The particles were surface modified with P4VP via ATRP reaction for 24 h

dispersions decreased, the pyridyl rings on the surface of P4VP-coated MNP became more protonated. The formation of positive charges on their surfaces led to electrostatic repulsion toward neighboring particles, eventually preventing aggregation. These results supported the improved dispersibility of the particles at highly acidic pH.

The results from electrophoretic mobility measurements also supported this hypothesis. The samples were redispersed in the dispersions with pH ranging between 0.5 and 2.5 at ionic strength of 0.1 M for the electrophoretic mobility measurements. The obtained values were positive at all pH in the dispersions, implying that the surface of the P4VP-coated MNP have a net positive charge (Fig. 5b). The modified MNP showed an increase in electrophoretic mobility values with decreasing solution pH (more acidic pH). This was again attributed to the enhancement of protonation of pyridyl rings on the surface of the complex at highly acidic pH. It was also observed that the hydrodynamic diameter of P4VP-coated MNP steadily increased at the pH range of 0.5–1.5 and drastically changed at the pH range of 1.5–2.5, while its electrophoretic mobility showed a gradual change at the same pH range.

The dependence of ATRP reaction time on hydrodynamic diameter and electrophoretic mobility of P4VP-coated MNP was also investigated. According to the results in Fig. 6, when the ATRP reaction time was increased, the hydrodynamic diameters of the complex at pH 1.5 consistently decreased, while their surface charges became more positive. This result implied that increasing ATRP reaction time promoted the progressive growth of P4VP on the particle surface, leading to the increase in both steric and electrostatic repulsions of the protonated P4VP grafted onto the particle surface.

One might wonder if either steric or electrostatic repulsions of the grafted P4VP contributed a major effect on the particle stabilization. In order to demonstrate how well the P4VP stabilizing brushes can really perform, KNO_3 solution as background electrolyte was thus added in the dispersion to screen electrostatic repulsions. Others have reported on the effect of background electrolyte on the surface-enhanced Raman spectra (SERS) of pyridinium, and it was found that an obvious decrease of the intensity of pyridinium was observed as the concentration of KNO_3 background electrolyte was increased up to

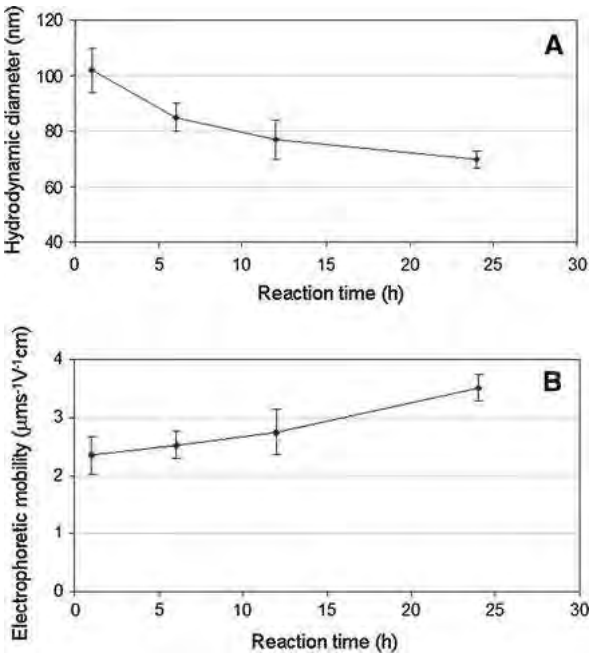

Fig. 6 **a** Hydrodynamic diameter and **b** electrophoretic mobility of P4VP-coated MNP at different ATRP reaction times. The P4VP-coated MNPs withdrawn at different time intervals were dispersed in pH 1.5 aqueous solutions

1.5 mol/L (Sun et al. 1985). According to this reported procedure, pH of the dispersion was monitored and carefully adjusted with HNO_3 to obtain pH = 2. Therefore, in the present study, an excess of 1.5 mol/L KNO_3 solution was added in P4VP-coated MNP dispersion to lessen the electrostatic repulsion of P4VP. It was found that the particles aggregated even though they were surface modified with P4VP via ATRP for 24 h. This result signified that electrostatic repulsion of the negatively charged surface played a major role on the particle stabilization. The chain length of the P4VP brush (the molecular weight of 5,300 g/mol) might be too short,and/or the grafting density of P4VP (0.66 chain/nm^2) might be too low to stabilize the particles sterically. Increase of the molecular weight of P4VP grafted on MNP surface might enhance the steric stabilization mechanism. This can be achieved by optimization of the ATRP conditions such as reaction temperature, time, solvent and the catalytic complex (type and ratio of ligand:catalyst).

The particles size and size distribution of the P4VP-coated MNP were investigated via TEM. The particles obtained from the 24 h ATRP reaction were re-suspended in acidic aqueous dispersion at pH 1.5

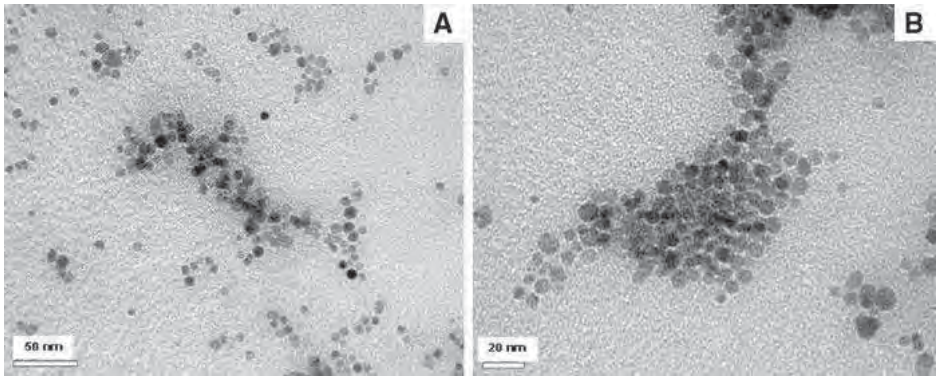

Fig. 7 TEM images of P4VP-coated MNP after 24 h of ATRP reaction, showing their good dispersibility and some nano-scale aggregation in pH 1.5-aqueous dispersions

before deposition on a TEM grid. From the TEM images (Fig. 7), the particle size was in the range of 6–11 nm with the average diameter of 8 nm. Although they were well dispersible in the media, some nano-scale aggregation of multiple particles was apparent. These particle clusters still existed in the TEM images even though the dispersions with more degree of dilution just enough to observe the presence of the particles were used for the TEM sample preparation. This indicated that these clusters were not drying artifact from the TEM sample preparation. The observation of these nanoclusters in TEM experiments was in good agreement with the PCS results that the hydrodynamic diameter of the particles (after 24 h of ATRP reaction) was in the range of 65–75 nm in aqueous solution at pH 1.5. This implies that the dispersions did not possess only the dispersed single particles, but also some stabilized clusters thoroughly dispersed in the system. It is striking to note that although these nano-clusters presented in the dispersions, these complexes were well dispersible in acidic aqueous dispersion without macroscopic aggregation visibly observed.

TGA experiments of P4VP-coated MNP at various ATRP reaction times were also performed to investigate the relative amounts of the organic components that can be grafted to the MNP surface. It should be noted that the P4VP-grafted MNP was repetitively extracted from other species in the reaction mixture with the use of ultracentrifugation and an external magnet. It was assumed that, at 600 °C under oxygen atmosphere, the weight residual was the weight of iron oxide core and the weight loss was thus attributed to the weight of the organic components including BTPAm and P4VP that was coated onto the particles surface. Hence, percent weight residual of bare MNP and MNP coated with BTPAm were investigated to obtain the percentage of BTPAm in the complex. According to TGA results, percentage of BTPAm in the complexes was about 2 wt%. Using a similar strategy, percentages of P4VP in each complex can be determined. It was found that percentages of P4VP in the P4VP-coated MNP at 1, 6, 12 and 24 h of ATRP reaction times increased from 13, 24, 35 and 53, respectively (Fig. 8). This was a supportive result to FTIR and PCS experiments that the chain length of P4VP was increased with increasing the ATRP reaction time.

The *M–H* curves of bare MNP and P4VP-coated MNP were shown in Fig. 9. They showed superparamagnetic behavior at room temperature as indicated by the absence of remanence and coercivity when the external applied magnetic field was removed. From the results in Fig. 9, the decrease of saturation

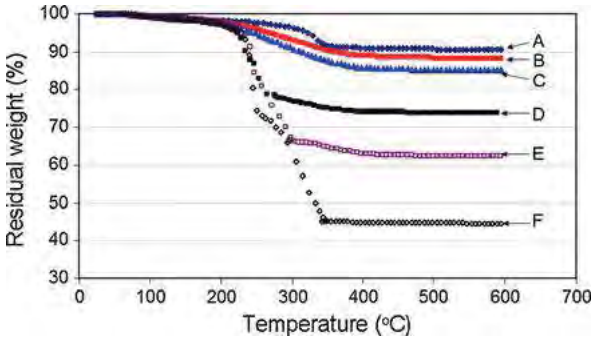

Fig. 8 TGA thermograms of (*a*) bare MNP. (*b*) BTPAm-coated MNP. P4VP-coated MNP at (*c*) 1 h, (*d*) 6 h, (*e*) 12 h, (*f*) 24 h of ATRP reactions

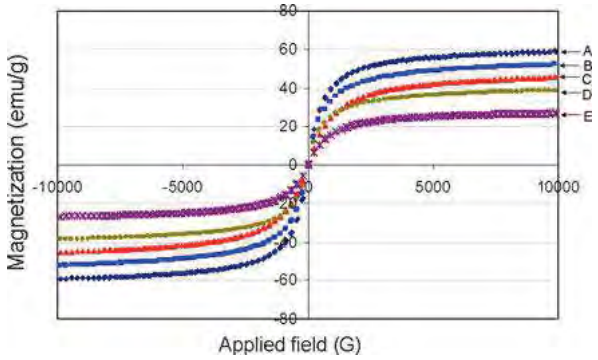

Fig. 9 *M–H* curves of (*a*) bare MNP, P4VP-coated MNP at (*b*) 1 h, (*c*) 6 h, (*d*) 12 h, (*e*) 24 h of ATRP reactions

Table 1 Percentage of magnetite in the complexes and their magnetic properties

Sample	emu/g sample[a]	% Fe_3O_4[b]	emu/g Fe_3O_4
Bare MNP	58	100	63
P4VP-coated MNP at			
1 h of ATRP	52	85	61
6 h of ATRP	45	73	62
12 h of ATRP	38	62	61
24 h of ATRP	27	44	61

[a] Estimated from the saturation magnetization (M_s) at 10,000 G from VSM technique

[b] Estimated from % char residual at 600 °C from TGA technique

magnetization (M_s) from 58 emu/g of bare MNP to 27–52 emu/g of P4VP-coated MNP was attributed to the presence of the organic coating, including BTPAm and P4VP, on their surface. The M_s values also dropped with increasing ATRP reaction time because of the growth of P4VP, resulting in the decrease of the percentage of magnetite core in the complexes. Interestingly, when taking percentage of magnetite in the complex (estimated from TGA technique) into account, the M_s values (in an emu/g magnetite unit) were almost constant, implying that magnetic properties of the magnetite core were not sacrificed after the surface modification (Table 1).

Conclusions

This study presented a "grafting from" strategy for surface modification of magnetite nanoparticles with a pH sensitive polymer, poly(4-vinylpyridine) (P4VP), via ATRP reaction. The living ATRP allowed a very good control on the growth of P4VP on the particle surface by tuning the ATRP reaction time. Many techniques, including FTIR, PCS, TGA, and VSM, were employed to confirm the growth of P4VP with increasing ATRP reaction time. The P4VP-coated MNP was well dispersible in acidic aqueous solutions with some nanoclusters observed. Decreasing the pH of the aqueous dispersions was proposed to promote protonation of the P4VP on their surface and enhance the magnetite nanoparticles' stabilization because of positively charged repulsion mechanism. These nanocomplexes with magnetically guidable properties might be used as an anion capture in aqueous solutions.

Acknowledgments The authors thank the Thailand Research Fund (TRF), the Commission on Higher Education (CHE) (RTA5280002), and The National Research Council of Thailand (NRCT) for providing financial supports. MR acknowledges T. Inphotha for the assistance in the syntheses, Dr.R.Traiphol and O. Ketchart for the discussions in electrophoretic mobility results, and Dr. Y. Udnan and Dr. P. Masawat for the discussions in the study on the addition of background electrolyte.

References

Casula MF, Floris P, Innocenti C, Lascialfari A, Marinone M, Corti M, Sperling RA, Parak WJ, Sangregorio C (2010) Magnetic resonance imaging contrast agents based on iron oxide superparamagnetic ferrofluids. Chem Mater 22: 1739–1748

Chang CC, Lo CT (2011) Effect of particles on the structure of solvent-annealed block copolymer/nanoparticle composite thin film. J Phys Chem B 115:2485–2493

Chen Z, Yang Q, Peng K, Guo Y (2011) Surface-initiated nitroxide-mediated radical polymerization of 4-vinylpyridine on magnetite nanoparticles. J Appl Polym Sci 119:3582–3590

Cheng G, Zhao J, Tu Y, He P, Fang Y (2005) A sensitive DNA electrochemical biosensor based on magnetite with a glassy carbon electrode modified by muti-walled carbon nanotubes in polypyrrole. Anal Chem Acta 533:11–16

Coessens V, Pintauer T, Matyjaszewski K (2001) Functional polymers by atom transfer radical polymerization. Prog Polym Sci 26:337–377

Cook GL, Church FM (1957) Correlations of the infrared spectra of some pyridines. J Phys Chem 61:458–462

Gil ES, Hudson SM (2004) Stimuli-responsive polymers and their bioconjugates. Prog Polym Sci 29:1173–1222

Gohy J, Lohmeijer BGG, Varshney SK, Decamps B, Leroy E, Boileau S, Schubert US (2002) Stimuli-responsive aqueous micelles from an ABC metallo-supramolecular triblock copolymer. Macromolecules 35:9748–9755

Golas PL, Louie S, Lowry GV, Matyjaszewski K, Tilton RD (2010) Comparative study of polymeric stabilizers for magnetite nanoparticles using ATRP. Langmuir 26:16890–16900

Gupta AK, Gupta M (2005) Synthesis and surface engineering of iron oxide nanoparticles for biomedical applications. Biomaterials 26:3995–4021

Hawker CJ, Bosman AW, Harth E (2001) New polymer synthesis by nitroxide mediated living radical polymerizations. Chem Rev 101:3661–3688

Hayashi K, Ono K, Suzuki H, Sawada M, Moriya M, Sakamoto W, Yogo T (2010) One-pot biofunctionalization of magnetic nanoparticles via thiol-ene click reaction for magnetic hyperthermia and magnetic resonance. Chem Mater 22: 3768–3772

Hermann High LR, Holder SJ, Penfold HV (2007) Synthesis of star polymers of styrene and alkyl (meth)acrylates from a porphyrin initiator core via ATRP. Macromolecules 40: 7157–7165

Hertler WR, Boettcher FP, Sogah DY (1990) Group transfer polymerization on a polymeric support. Macromolecules 23:1264–1268

Kobayashi M, Matsuno R, Otsuka H, Takahara A (2006) Precise surface structure control of inorganic solid and metal oxide nanoparticles through surface-initiated radical polymerization. Sci Technol Adv Mater 7:617–628

Laurent S, Forge D, Port M, Roch A, Robic C, Elst LV, Muller RN (2008) Magnetic iron oxide nanoparticles: synthesis, stabilization, vectorization, physicochemical characterizations, and biological applications. Chem Rev 108: 2064–2110

Lellouche J, Senthil G, Joseph A, Buzhansky L, Bruce I, Bauminger ER, Schlesinger J (2005) Magnetically responsive carboxylated magnetite-polydipyrrole/polydicarbazole nanocomposites of core-shell morphology. Preparation, characterization, and use in DNA hybridization. J Am Chem Soc 127:11998–12006

Liu X, Xing J, Guan Y, Shan G, Liu H (2004) Synthesis of amino-silane modified superparamagnetic silica supports and their use for protein immobilization. Colloids Surf A: Physicochem Eng 238:127–131

Liu G, Yan X, Lu Z, Curda SA, Lal J (2005) One-pot synthesis of block copolymer coated cobalt nanocrystals. Chem Mater 17:4985–4991

Liu JY, Cheng L, Song YH, Liu BF, Dong SJ (2011) Simple preparation method of multilayer polymer films containing Pd nanoparticles. Langmuir 17:6747–6750

Marinescu G, Patron L, Culita DC, Neagoe C, Lepadatu CI, Balint I, Bessais L, Cizmas CB (2006) Synthesis of magnetite nanoparticles in the presence of amino acids. J Nanopart Res 8:1045–1051

Matsuno R, Yamamoto K, Otsuka H, Takahara A (2004) Polystyrene- and poly(3-vinylpyridine)-grafted magnetite nanoparticles prepared through surface-initiated nitroxide-mediated radical polymerization. Macromolecules 37:2203–2209

Matyjaszewski K, Xia J (2001) Atom transfer radical polymerization. Chem Rev 101:2921–2990

Milano G, Musumeci D, Gaglione M, Messere A (2010) An alternative strategy to synthesize PNA and DNA magnetic conjugates forming nanoparticle assembly based on PNA/DNA duplexes. Mol Biosys 6:553–561

Mori H, Müller AHE, Klee JE (2003) Intelligent colloidal hybrids via reversible pH-induced complexation of polyelectrolyte and silica nanoparticles. J Am Chem Soc 125:3712–3713

Mornet S, Vekris A, Bonnet J, Duguet E, Grasset F, Choy JH, Portier J (2000) DNA–magnetite nanocomposite materials. Mater Lett 42:183–188

Pan BF, Gao F, Gu HC (2005) Dendrimer modified magnetite nanoparticles for protein immobilization. J Colloid Interface Sci 284:1–6

Pei W, Kumadaa H, Natusmea T, Saitoa H, Ishio S (2007) Study on magnetite nanoparticles synthesized by chemical method. J Magn Magn Mater 310:2375–2377

Perrin DD (1965) Dissociation constants of organic bases in aqueous solution. IUPAC Chem Data Ser, Buttersworth

Pinkrah VT, Snowden MJ, Mitchell JC, Seidel J, Chowdhry BZ, Fern GR (2003) Physicochemical properties of poly(*N*-isopropylacrylamide-co-4-vinylpyridine) cationic polyelectrolyte colloidal microgels. Langmuir 19:585–590

Rutnakornpituk M, Puangsin N, Theamdee P, Rutnakornpituk B, Wichai U (2011) Poly(acrylic acid)-grafted magnetic nanoparticle for conjugation with folic acid. Polymer 52:987–995

Sonvico F, Mornet S, Vasseur S, Dubernet C, Jaillard D, Degrouard J, Hoebeke J, Duguet E, Colombo P, Couvreur P (2005) Folate-conjugated iron oxide nanoparticles for solid tumor targeting as potential specific magnetic hyperthermia mediators: synthesis, physicochemical characterization, and in vitro experiments. Bioconjugate Chem 16: 1181–1188

Sun SC, Bernard I, Birke RL, Lombardi JR (1985) The effect of pH, Chloride ion and background electrolyte concentration on the SERS of acidified pyridine solutions. J Electroanal Chem 196:359–374

Sun Y, Ding X, Zheng Z, Cheng X, Hu X, Peng Y (2007) Surface initiated ATRP in the synthesis of iron oxide/polystyrene core/shell nanoparticles. Eur Polym J 43:762–772

Tamami B, Farjadian F (2011) Synthesis and applications of polyvinylpyridine-grafted silica containing palladium nanoparticles as a new heterogeneous catalyst for heck and suzuki coupling reactions. J Iran Chem Soc 8:S77–S88

Thiessen W, Dubavik A, Lesnyak V, Gaponik N, Eychmüller A, Wolff T (2010) Amphiphilic and magnetic behavior of Fe_3O_4 nanocrystals. Phys Chem Chem Phys 12:2063–2066

Tian J, Zheng F, Zhao HY (2011) Nanoparticles with Fe_3O_4-nanoparticle cores and gold-nanoparticle coronae prepared by self-assembly approach. J Phys Chem C 115:3304–3312

Woo K, Hong J, Choi S, Lee HW, Ahn JP, Kim CS, Lee SW (2004) Easy synthesis and magnetic properties of iron oxide nanoparticles. Chem Mater 16:2814–2818

Xu FJ, Neoh KG, Kang ET (2009) Bioactive surfaces and biomaterials via atom transfer radical Polymerization. Prog Polym Sci 34:719–761

Yang X, Shi J, Johnson S, Swanson B (1998) Growth of ultrathin covalently attached polymer films:# uniform thin films for chemical microsensors. Langmuir 14:1505–1507

Zhang J, Misra RDK (2007) Magnetic drug-targeting carrier encapsulated with thermosensitive smart polymer:

Core–shell nanoparticle carrier and drug release response. Acta Biomater 3:838–850

Zhang Y, Kohler N, Zhang M (2002) Surface modification of superparamagnetic magnetite nanoparticles and their intracellular uptake. Biomaterials 23:1553–1561

Zhou Y, Wang S, Ding B, Yang Z (2008) Modification of magnetite nanoparticles via surface-initiated atom transfer radical polymerization (ATRP). Chem Eng J 138:578–585

Zhou LL, Yuan JY, Yuan WZ, Sui XF, Wu SZ, Li ZL, Shen DZ (2011) Synthesis, characterization, and controllable drug release of pH-sensitive hybrid magnetic nanoparticles. J Magn Magn Mater 321:2799–2804

Talanta 88 (2012) 593–598

Contents lists available at SciVerse ScienceDirect

Talanta

journal homepage: www.elsevier.com/locate/talanta

FRET detection of DNA sequence via electrostatic interaction of polycationic phenyleneethynylene dendrimer with DNA/PNA hybrid

Paitoon Rashatasakhon[a], Kunnigar Vongnam[b], Warathip Siripornnoppakhun[a], Tirayut Vilaivan[a], Mongkol Sukwattanasinitt[a,*]

[a] Center for Petroleum, Petrochemicals and Advanced Materials, Department of Chemistry, Faculty of Science, Chulalongkorn University, Phayathai Road, Pathumwan, Bangkok 10330, Thailand
[b] Program of Petrochemistry and Polymer Science, Faculty of Science, Chulalongkorn University, Phayathai Road, Pathumwan, Bangkok 10330, Thailand

ARTICLE INFO

Article history:
Received 23 October 2011
Received in revised form
13 November 2011
Accepted 14 November 2011
Available online 19 November 2011

Keywords:
DNA
Dendrimer
Fluorescence sensor
FRET
Peptide nucleic acid

ABSTRACT

Interaction between a polycationic compound and DNA is a useful phenomenon for development of a new DNA sensing system. In this work, dendritic polycationic phenyleneethynylene fluorophores are investigated as a Förster resonance energy transfer (FRET) donor for the detection of DNA hybridization in conjunction with a fluorescein-labeled pyrrolidinyl peptide nucleic acid (Fl-acpcPNA) probe. The first generation dendrimer is an efficient energy donor for the fluorescein acceptor but also shows non-specific FRET signal with Fl-acpcPNA. The addition of *N*-methyl 2-pyrrolidone can virtually completely remove the non-specific interaction between Fl-acpcPNA and the dendrimer. Under the optimal condition, the complementary DNA gives a distinctively high FRET ratio (1.42) comparing with those of the non-complementary (0.26) and singly mismatched (0.51) DNAs. The FRET ratio responses linearly with the DNA concentration with the detection limit lower than 1 nM. The FRET ratio is even higher for the complementary target DNAs with extra hanging nucleotide sequences, which is a more frequently encountered scenario in real applications.

© 2011 Elsevier B.V. All rights reserved.

1. Introduction

Detection of DNA sequences is indispensable in medical diagnostics and biochemical analyses. During the past decades, we have witnessed several major developments of various techniques for the detection of DNA sequences based on DNA hybridization process including fluorimetry [1–3], colorimetry [4,5], electrochemistry [6–8], and surface plasmon resonance [9,10]. Homogeneous fluorescence analysis in solution is considered as one of the most convenient and sensitive methods. Direct use of fluorescent dyes which are capable of intercalating or binding into the grooves of double-stranded DNA (dsDNA) with concomitant fluorescence enhancement, such as ethidium bromide, SYBR Green® and PicoGreen®, as reporters for DNA hybridization is probably the most simple and common practice. Enhanced fluorescent signals by mismatched hybridized or even unhybridized single-stranded DNAs (ssDNA) are also often encountered due to their significant binding to these dyes [11,12]. To increase specificity of the analytical method, Förster resonance energy transfer (FRET) between energy donor and acceptor fluorophores has been successfully exploited [13,14]. One of the most intriguing developments involves the use of a polycationic π-conjugated polymer as a FRET donor and a flurophore-labeled ssDNA as a FRET acceptor [15,16]. Fluorescein-labeled peptide nucleic acid (Fl-PNA), a neutral peptide analog of DNA, has also been applied in a FRET-based detection of specific DNA sequences via PNA/DNA Watson–Crick hybridization [17–19]. The successful use of PNA probe has been attributed to two main reasons. First, PNA/DNA hybrid electrostatically interacts with the polycationic FRET donor more strongly, and second, the neutral unhybridized PNA and the PNA/DNA duplex is more readily and specifically formed than the analogous DNA/DNA duplex [20–23]. As a result, the use of PNA in place of DNA significantly increased the specificity such that even a single mismatched base in the DNA target can be readily distinguished with a considerably lower FRET signal [19].

Comparing with small molecule, conjugate polymers containing multiple fluorogenic moieties offer advantages in signal amplification and large molecular optical cross section [24–26]. The use of polycationic conjugated polymers as FRET donors for the detection of PNA/DNA hybridization however have been limited to a class of linear poly(phenylene-co-fluorene). The linear conjugated polymers usually possess broad distribution of molecular weights which may be not readily reproducible from lab to lab or even batch to batch. Unpredictable secondary structures of linear polymeric chains in aqueous media also add subtle issues in the interpretation of its intermolecular interaction. We are interested in exploring

* Corresponding author. Tel.: +66 2 2187620; fax: +66 2 2187598.
E-mail address: smongkol@chula.ac.th (M. Sukwattanasinitt).

0039-9140/$ – see front matter © 2011 Elsevier B.V. All rights reserved.
doi:10.1016/j.talanta.2011.11.041

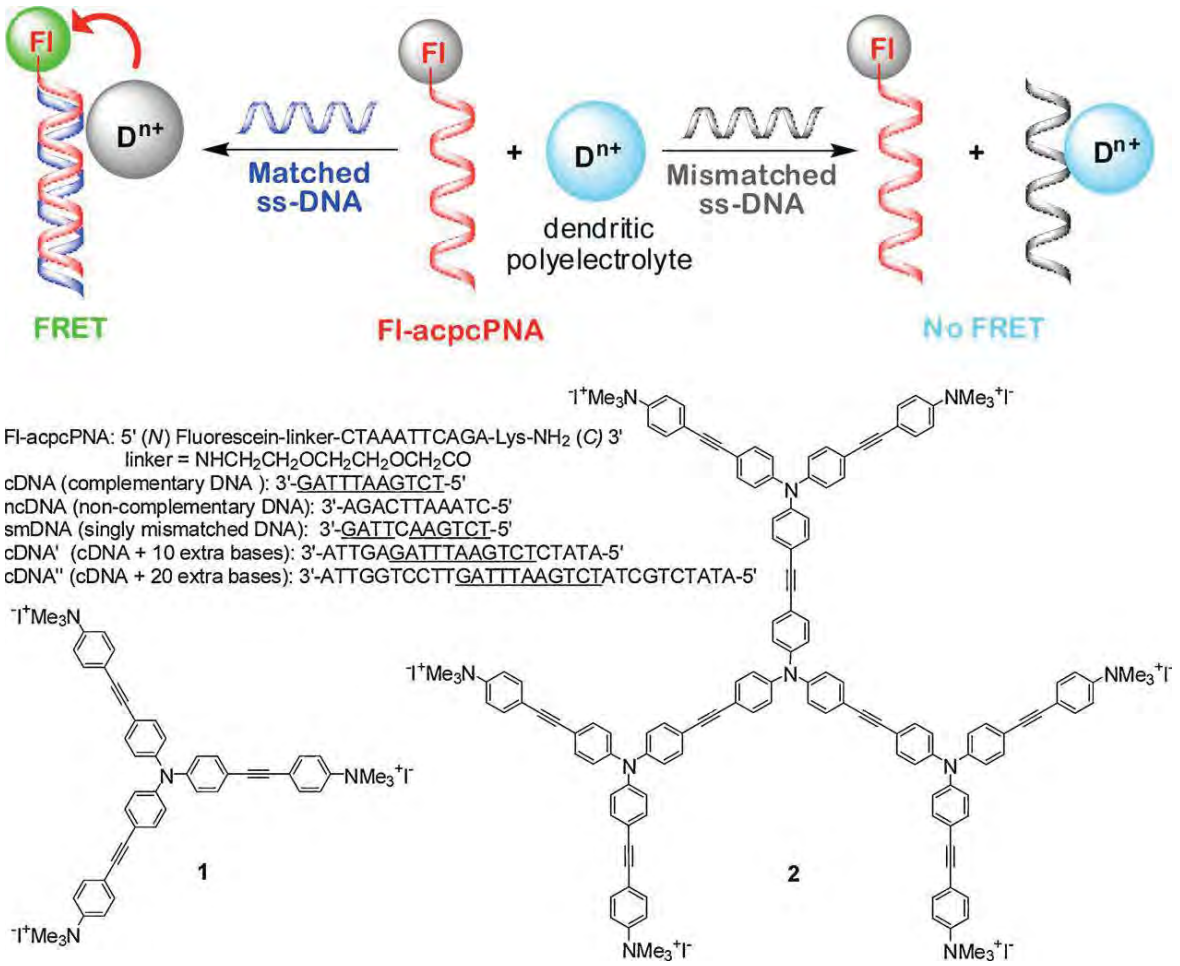

Fig. 1. Proposed detection of DNA/PNA hybridization via FRET from polycationic dendritic fluorophores $\mathbf{D^{n+}}$ (**1** and **2**) including their chemical structures and sequences of Fl-acpcPNA and DNAs used.

a class of polycationic fluorophores with definite molecular sizes and charges to be used as fluorescent transducers. Dendrimers are good candidates as their sizes and shapes can be controlled via convergent synthetic approach [27–30]. Recently, applications of dendritic phenylene-ethynylene polyelectrolytes as fluorescent signal transducer in sensing systems have been reported [31–36]. In this present work, we investigated the use of polycationic phenylene–ethynylene dendrimers **1** and **2** (Fig. 1) as a FRET donor in the detection of DNA sequence via the PNA/DNA hybridization principle. The specific PNA used in this work is a conformational constrained fluorescein-labeled pyrrolidinyl PNA (Fl-acpcPNA) derived from proline/2-aminocyclopentanecarboxylic acid backbone which exhibited superior specificity in DNA hybridization than the classical PNA [37,38].

2. Experimental

2.1. Chemicals and materials

Dendritic cationic fluorophores, **1** and **2**, were prepared as described in our previously reported procedures [34]. The acpcPNA probe was labeled at the *N*-terminus by 5(6)-carboxyfluorescein *N*-hydroxysuccinimidyl ester via an aminoethoxyethoxyacetyl spacer (–$NHCH_2CH_2OCH_2CH_2OCH_2CO$–) and was purified by HPLC after removal from the solid support [37,38]. HPLC-purified DNA oligo-nucleotides were purchased from Biodesign-Co., Ltd. (Thailand). Reagent grade formamide and *N*-methyl-2-pyrrolidinone were purchased from Merck and used without further purification.

2.2. Instruments

The UV–vis absorption spectra were recorded on a Varian Cary 50 UV–vis spectrophotometer. Fluorescence measurements were carried out with solution samples in a 3 mL quartz cuvette at room temperature using a Varian Cary Eclipse spectrofluorometer at 90° detection angle. The FRET ratios were calculated as the fluorescent intensity of the acceptor (fluorescein) over the intensity of the donor (**2**).

2.3. PNA/DNA sample preparation

Solutions of Fl-acpcPNA (0.6 μM) and DNA (0.6 μM) in 10 mM phosphate saline buffer pH 6.9 were mixed and allowed for hybridization at room temperature for overnight to provide a 0.3 μM Fl-acpcPNA/DNA duplex stock solution. For the fluorescence measurement, this stock solution was mixed with the fluorophore solution and the total volume was adjusted by 10 mM phosphate saline buffer pH 6.9, to give the final concentration of 1.0 μM for the fluorophore 0.1 μM for the DNA and PNA.

3. FRET experiments

To 1 mL of Fl-acpcPNA or Fl-acpcPNA/DNA stock solution (0.3 μM) was added 30 μL of **1** or **2** solution (100 μM), and the designated amount of 1-methyl-pyrrolidinone (NMP) or formamide at room temperature (25 °C). The final volume of the mixture was adjusted to 3 mL by 10 mM phosphate saline buffer pH 6.9 to afford the final concentration of 1 μM for the fluorophores and 0.1 μM for PNA and DNA. After the solution was thoroughly mixed for 1 min, the emission spectrum (410–700 nm) was recorded at room temperature with an excitation wavelength of 400 nm. The FRET signal and ratio were observed as the intensity of the fluorescein band peaked at 530 nm from the spectrum with the donor peak at 440 nm normalized.

4. Results and discussion

The basis of this work, as illustrated in Fig. 1, relies on the assumption that there is no significant interaction between the cationic dendritic fluorophores $\mathbf{D^{n+}}$ (**1** or **2**) and the electrostatically neutral Fl-acpcPNA. The addition of ssDNA with a complementary base sequence (cDNA) should give rise to a formation of a negatively charged DNA/PNA duplex, which in turn preferentially bind with the cationic dendrimer as a result of Coulombic interaction. A close proximity between $\mathbf{D^{n+}}$ and the fluorescein moiety on the acpcPNA should result in a FRET signal observed as enhanced fluorescein emission and reduced $\mathbf{D^{n+}}$ emission. On the other hands, if the DNA sequence has a non-complementary base sequence (ncDNA), there should be only the DNA/$\mathbf{D^{n+}}$ complexation, which gives no FRET signal.

The emission spectra of **1** and **2** along with the absorption and emission spectra of Fl-acpcPNA are shown in Fig. 2. Although the emission band of **1** has an ideal full overlapping integral with the absorption spectrum of Fl-acpcPNA, its broad emission band also cover a large portion of Fl-acpcPNA emission band. This precludes an efficient function of **1** as a FRET donor because the FRET signal detected from fluorescein emission would be greatly interfered by the donor emission. On the other hand, the emission band of the first generation dendrimer **2** advantageously appears at a significantly shorter wavelength probably due to its slower geometrical relaxation as a result of the bulkier dendritic arms. With a shorter emission wavelength, the overlapping area between the emission band of **2** and Fl-acpcPNA is considerably reduced and thus dendrimer **2** is a better choice as a FRET donor for Fl-acpcPNA. In addition, the higher number of positive charge (6+) on **2** should also provide a stronger electrostatic interaction with the PNA/DNA duplex that in turn enhance the efficiency of the FRET process.

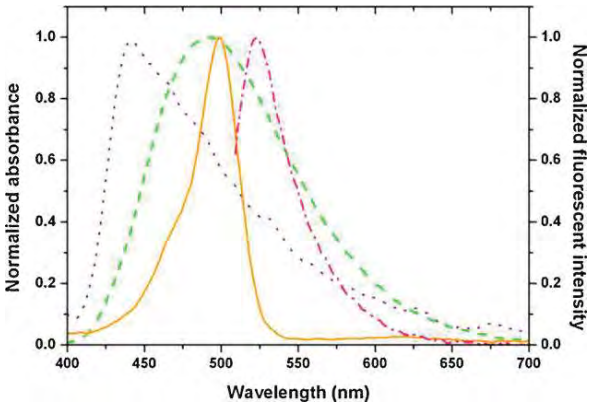

Fig. 2. Absorption spectrum of Fl-acpcPNA (–) and emission spectra of **1** (- - -), **2** (—) and Fl-acpcPNA (-·-).

Our initial FRET measurements showed that the use of **1** as the energy donor failed to give any distinguishable FRET signal even in the presence of the complementary DNA (Fig. 3a). On the other hand, the experiment with dendrimer **2** showed promising results. The strong emission signal of fluorescein was observed at 530 nm, especially for the system with cDNA (Fig. 3b). For the system with ncDNA, a much weaker FRET signal was observed. Interestingly, we observed a relatively strong FRET signal from the solution of only **2** and Fl-acpcPNA in the absence of any DNA. This result is somewhat deviate from our postulation proposed in Fig. 1 and it indicates a significant interaction between the donor and Fl-acpcPNA itself. This undesirable non-specific FRET signal may result from a relatively strong hydrophobic interaction between the dendritic core of **2** and the PNA backbone. Drastic reduction of the FRET signal in the presence of ncDNA implies that the Coulombic interaction of ncDNA with **2** is likely to be much stronger than the hydrophobic interaction between **2** and Fl-acpcPNA.

Recently, formamide has been successfully used as an additive to reduce non-specific hydrophobic interaction between DNA and PNA [39] while *N*-methylpyrrolidinone (NMP) has been used to reduce such interaction between DNA and cationic polyelectrolyte fluorophore [40]. These additives are known for their ability to

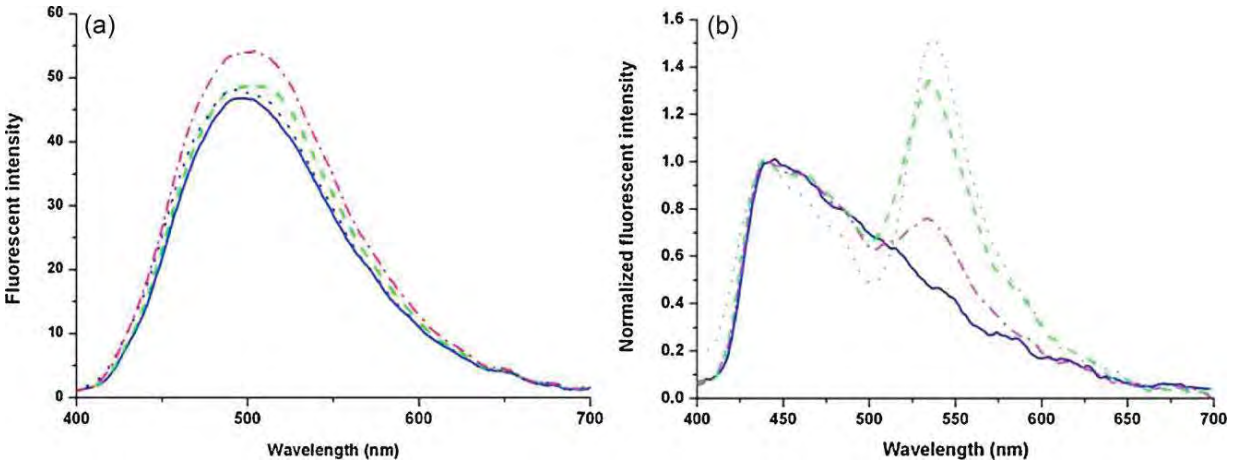

Fig. 3. (a) Emission spectra of **1** (–), **1**:Fl-acpcPNA (- - -), **1**:Fl-acpcPNA:cDNA (···) and **1**:Fl-acpcPNA:ncDNA (-·-) in phosphate saline buffer pH 6.9; [**1**] = 1.0 μM; [Fl-acpcPNA] = [DNA] = 0.1 μM. (b) Emission spectra of **2** (–), **2**:Fl-acpcPNA (- - -), **2**:Fl-acpcPNA:cDNA (···) and **2**:Fl-acpcPNA:ncDNA (-·-) in phosphate saline buffer pH 6.9; [**2**] = 1.0 μM; [Fl-acpcPNA] = [DNA] = 0.1 μM.

Table 1
Effects of additives on FRET ratios.

Additive	**2** + Fl-acpcPNA	**2** + Fl-acpcPNA + cDNA	**2** + Fl-acpcPNA + ncDNA
None	1.23 ± 0.14	1.40 ± 0.13	0.72 ± 0.11
Formamide (20%, v/v)	1.34 ± 0.16	1.66 ± 0.15	1.03 ± 0.09
NMP (20%, v/v)	0.58 ± 0.05	0.90 ± 0.07	0.47 ± 0.01
NMP (10%, v/v)	0.39 ± 0.15	1.42 ± 0.13	0.26 ± 0.18

solvate the PNA and DNA chain primarily via hydrogen bonding, which consequently reduce the hydrophobic interaction. In our tests, Table 1 shows that formamide cannot reduce the FRET ratio observed in the system containing only **2** and Fl-acpcPNA while NMP drastically decreases the FRET ratio of this system. At 10% (v/v) of NMP, the non-specific FRET ratio decreases without deteriorating the FRET signal generated from the desired Fl-acpcPNA/cDNA hybridization. Importantly, the FRET ratio of the PNA/ncDNA pair is also significantly reduced by NMP. Accordingly, the cDNA gives remarkably higher FRET signal than those of the ncDNA and the non-specific background in the presence of 10% (v/v) NMP (Fig. 4).

The effect of donor/acceptor ratio in the FRET process was studied at constant concentration of Fl-acpcPNA at 0.1 μM in the presence of 10% (v/v) NMP. The concentration of **2** was varied as 0.5, 1.0, and 1.5 μM. We compared the FRET ratios obtained from each condition in the presence of cDNA, ncDNA, and single mismatched DNA (smDNA), as well as in the absence of DNA. The plot in Fig. 5 indicates that the 1:10 M ratio of Fl-acpcPNA/**2** provide the best detection of cDNA while the non-specific signal, observed in the absence of DNA, is suppressed at a much lower level. This optimum ratio is probably governed by the countered balance between two concentration effects *i.e.* the increases of donor/acceptor complexation and the fluorescence background of **2**. It is also important to note that the cDNA (fully complementary DNA) can be clearly distinguished from the smDNA (singly mismatched DNA) at this optimal ratio.

We next investigated the effect of target DNA chain length on FRET efficiency by using 21-mer (cDNA′) and 31-mer DNA (cDNA″). Both cDNA′ and cDNA″ contain the complementary base sequence in the middle with extra base units extended from its both ends. The results are encouraging that the FRET ratio with cDNA′ and cDNA″ are successively higher than that in the case with cDNA (Fig. 6) and that the target DNAs with extra hanging nucleotide sequences is more likely the case encountered in real applications involving PCR-amplified or genomic DNA targets. The enhanced FRET signals by longer DNA chains highlight the importance of electrostatic interaction between the segment of DNA/PNA duplex and the cationic dendrimer in the FRET process.

The FRET ratio of the sensing system increased with the cDNA and a plot between corrected FRET ratio ($F_{(530)}$–$F_{0(530)}$) against concentration of cDNA yielded a linear line as shown in Fig. 7. The linear response suggests that the sensing system should be applicable for quantification of a designated DNA sequence. Fig. 7 also showed that the detection limit of this system is below 1 nM.

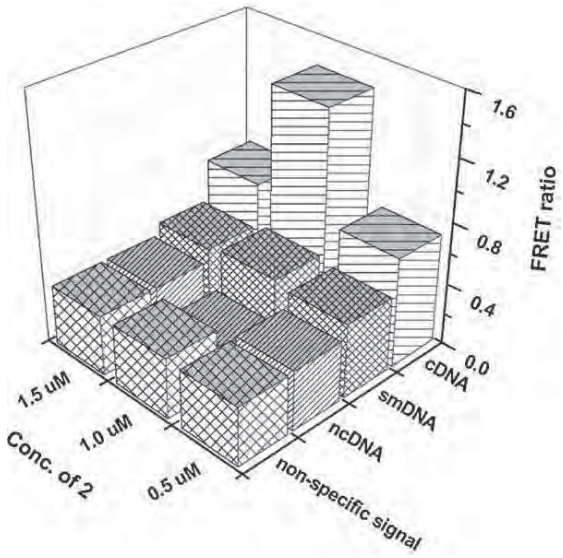

Fig. 5. FRET ratios obtained upon the addition of DNA (0.1 μM) to solutions containing varied concentrations of **2** and fixed Fl-acpcPNA concentration (0.1 μM).

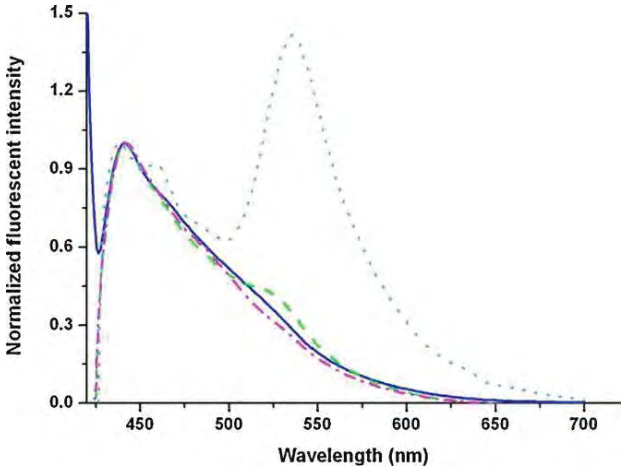

Fig. 4. Emission spectra of **2** (–), **2**:Fl-acpcPNA (- - -), **2**:Fl-acpcPNA:cDNA (···) and **2**:Fl-acpcPNA:ncDNA (-·-) in panel (a) phosphate saline buffer pH 6.9 with 10% (v/v) NMP [**2**] = 1.0 μM; [Fl-acpcPNA] = [DNA] = 0.1 μM.

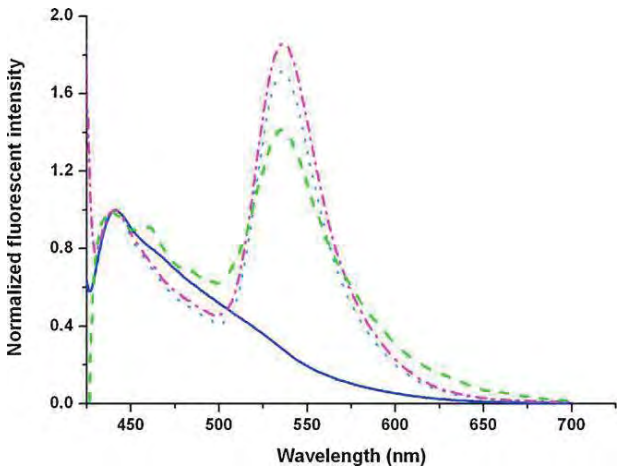

Fig. 6. Emission spectra of **2** (–), **2**:Fl-acpcPNA:cDNA (- - -), **2**:Fl-acpcPNA:cDNA′ (···) and **2**:Fl-acpcPNA:cDNA″ (-·-) in phosphate saline buffer pH 6.9 in the presence of 10% (v/v) NMP. [**2**] = 1.0 μM; [Fl-acpcPNA] = 0.1 μM; [DNA] = 0.1 μM.

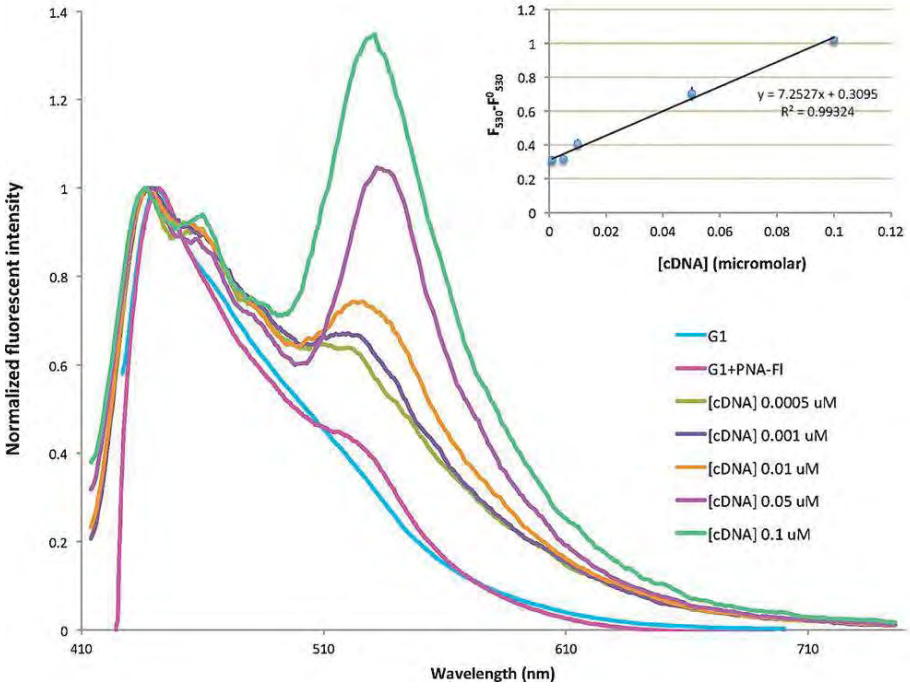

Fig. 7. Emission spectra and Linear plot between corrected FRET ratio ($F_{(530)}$–$F_{0(530)}$) and concentration of cDNA in phosphate saline buffer pH 6.9 with 10% (v/v) NMP [2] = 1.0 μM; [Fl-acpcPNA] = 0.1 μM.

5. Conclusion

In conclusion, we have demonstrated a detection of DNA hybridization by Förster resonance energy transfer (FRET) employing a cationic phenyleneethynylene dendritic fluorophore as a FRET donor and a fluorescein-labeled pyrrolidinyl peptide nucleic acid (Fl-acpcPNA) as the energy acceptor. The first generation fluorescent dendrimer with six positively charged ammonium peripheries provide adequate electrostatic interaction and spectral overlap resulted in readily distinguishable signals for the cases with complementary and non-complementary DNA. The background signal, which may be caused by the hydrophobic interaction between the inner part of the fluorophore and the peptide backbone of the acpcPNA could be eliminated by the addition of *N*-methyl-2-pyrrolidinone (NMP). Under optimum sensing condition, the sensing system readily detected fully complementary sequence DNA at submicromolar concentration level and distinguished it from the DNA with a single mismatch base. The cationic phenyleneethynylene dendrimer showed even higher FRET signal for detecting the target DNAs with extra hanging nucleotide sequences that should be useful for detecting PCR-amplified or genomic DNA targets in real applications.

Acknowledgement

This work is part of the Project for Establishment of Comprehensive Center for Innovative Food, Health Products and Agriculture supported by the Thai government stimulus package 2 (TKK2555, SP2) and receives financial support from the Thailand Research Fund (RTA5280002), the National Nanotechnology Center, NSTDA (NN-B-22-FN9-10-52-06), the 90th Anniversary of Chulalongkorn University Fund, the National Research University of CHE and the Ratchadaphiseksomphot Endowment Fund (AM1006A). KV thanks the Faculty of Science, Chulalongkorn University (A1B1-5) for her research fellowship. We also would like to thank Ms. Chalothorn Boonlua for Fl-acpcPNA samples.

References

[1] J. Zhu, Y. Lu, C. Deng, G. Huang, S. Chen, S. Xu, Y. Lv, K. Mitchelson, J. Cheng, Anal. Chem. 82 (2010) 5304–5312.
[2] I. Saaem, K-S. Ma, A.N. Marchi, T.H. LaBean, J. Tian, ACS Appl. Mater. Interfaces 2 (2010) 491–497.
[3] K. Boeneman, J.R. Deschamps, S. Buckhout-White, D.E. Prasuhn, J.B. Blanco-Canosa, P.E. Dawson, M.H. Stewart, K. Susumu, E.R. Goldman, M. Ancona, I.L. Medintz, ACS Nano 4 (2010) 7253–7266.
[4] A. Baeissa, N. Dave, B.D. Smith, J. Liu, ACS Appl. Mater. Interfaces 2 (2010) 3594–3600.
[5] R. Kanjanawarut, X. Su, Anal. Chem. 81 (2009) 6122–6129.
[6] E.G. Hvastkovs, D.A. Buttry, Analyst 135 (2010) 1817–1829.
[7] J.-Y. Park, S.-M. Park, Sensors 9 (2009) 9513–9532.
[8] X. Zhang, K. Jiao, S. Liu, Y. Hu, Anal. Chem. 81 (2009) 6006–6012.
[9] S. Ekgasit, G. Stengel, W. Knoll, Anal. Chem. 76 (2004) 4747–4755.
[10] B.P. Nelson, T.E. Grimsrud, M.R. Liles, R.M. Goodman, R.M. Corn, Anal. Chem. 73 (2001) 1–7.
[11] J.B. LePecq, C. Paoletti, J. Mol. Biol. 27 (1967) 87–106.
[12] J.T. Petty, J.A. Bordelon, M.E. Robertson, J. Phys. Chem. B 104 (2000) 7221–7227.
[13] R. Flehr, A. Kienzler, W. Bannwarth, M.U. Kumke, Bioconjugate Chem. 21 (2010) 2347–2354.
[14] Y.-N. Teo, E.T. Kool, Bioconjugate Chem. 20 (2009) 2371–2380.
[15] G. Liang, A.S. Susha, A.A. Lutich, F.D. Stefani, J. Feldmann, A.L. Rogach, ACS Nano 3 (2009) 4127–4131.
[16] R.R. Nayak, O.K. Nag, M. Kang, Y. Jin, H. Suh, K. Lee, H.Y. Woo, Macromol. Rapid Commun. 30 (2009) 633–638.
[17] B.S. Gaylord, A.J. Heeger, G.C. Bazan, Proc. Natl. Acad. Sci. U.S.A. 99 (2002) 10954–10957.
[18] B.S. Gaylord, A.J. Heeger, G.C. Bazan, J. Am. Chem. Soc. 125 (2003) 896–900.
[19] B.S. Gaylord, M.R. Massie, S.C. Feinstein, G.C. Bazan, Proc. Natl. Acad. Sci. U.S.A. 102 (2005) 34–39.
[20] E. Uhlman, A. Peyman, G. Breipohl, D.W. Will, Angew. Chem. Int. Ed. 37 (1998) 2796–2823.
[21] P.E. Nielsen, Acc. Chem. Res. 32 (1999) 624–630.
[22] B. Falkiewicz, Acta Biochim. Pol. 46 (1999) 509–529.
[23] K.N. Ganesh, P.E. Nielsen, Curr. Org. Chem. 4 (2000) 931–943.
[24] D.T. McQuade, A.E. Pullen, T.M. Swager, Chem. Rev. 100 (2000) 2537–2574.
[25] S.W. Thomas, G.D. Joly, T.M. Swager, Chem. Rev. 107 (2007) 1339–1386.
[26] C. Chi, A. Mikhailovsky, G.C. Bazan, J. Am. Chem. Soc. 129 (2007) 11134–11145.
[27] C.J. Hawker, J.M.J. Fréchet, J. Am. Chem. Soc. 112 (1990) 7638–7647.
[28] F. Zeng, S.C. Zimmerman, Chem. Rev. 97 (1997) 1681–1712.
[29] S.M. Grayson, J.M.J. Fréchet, Chem. Rev. 101 (2001) 3819–3867.
[30] P. Furuta, J.M.J. Fréchet, J. Am. Chem. Soc. 125 (2003) 13173–13181.

[31] B. Sandanaraj, R. Demont, S. Aathimanikandan, E.N. Savariar, S. Thayumanavan, J. Am. Chem. Soc. 128 (2006) 10686–10687.
[32] S. Jiwpanich, B.S. Sandanaraj, S. Thayumanavan, Chem. Commun. 80 (2009) 6–808.
[33] N. Niamnont, W. Siripornnoppakhun, P. Rashatasakhon, M. Sukwattanasinitt, Org. Lett. 11 (2009) 2768–2771.
[34] N. Niamnont, R. Mungkarndee, I. Techakriengkrai, P. Rashatasakhon, M. Sukwattanasinitt, Biosens. Bioelectron. 26 (2010) 863–867.
[35] B.W. Davis, N. Niamnont, C.D. Hare, M. Sukwattanasinitt, Q. Cheng, ACS Appl. Mater. Interfaces 2 (2010) 1798–1803.
[36] B.W. Davis, N. Niamnont, R. Dillon, B. Christopher, M. Sukwattanasinitt, Q. Cheng, Langmuir 27 (2011) 6401–6408.
[37] T. Vilaivan, C. Srisuwannaket, Org. Lett. 8 (2006) 1897–1900.
[38] C. Ananthanawat, T. Vilaivan, V.P. Hoven, X. Su, Biosens. Bioelectron. 25 (2010) 1064–1069.
[39] B. Boontha, J. Nakkuntod, N. Hirankarn, P. Chaumpluk, T. Vilaivan, Anal. Chem. 80 (2008) 8178–8186.
[40] F. Xia, X. Zou, R. Yang, Y. Xiao, D. Kang, A. Valle-Belisle, X. Gong, A.J. Heeger, K.W. Plaxco, J. Am. Chem. Soc. 132 (2010) 1252–1254.

Biosensors and Bioelectronics 33 (2012) 17–22

Contents lists available at SciVerse ScienceDirect

Biosensors and Bioelectronics

journal homepage: www.elsevier.com/locate/bios

Phenylene–ethynylene trication as an efficient fluorescent signal transducer in an aptasensor for potassium ion

Wannapa Yuanboonlim, Warathip Siripornnoppakhun, Nakorn Niamnont, Paitoon Rashatasakhon, Tirayut Vilaivan, Mongkol Sukwattanasinitt*

Center for Petroleum, Petrochemicals and Advanced Materials, Department of Chemistry, Faculty of Science, Chulalongkorn University, Bangkok 10330, Thailand

ARTICLE INFO

Article history:
Received 21 October 2011
Received in revised form
25 November 2011
Accepted 29 November 2011
Available online 30 December 2011

Keywords:
Aptamer
Biosensor
Fluorescence
Nucleic acid
Potassium detection
G-quadruplex

ABSTRACT

A tricationic phenylene–ethynylene (**N^{3+}**) fluorophore is investigated as a fluorescent transducer in homogeneous aptasensing system for potassium ion (K^+) assay in aqueous media. The enhancement of the fluorescent signal of **N^{3+}** by three K^+ aptamers consisting of 12, 15, and 21 nucleotides are observed and used for the determination of **N^{3+}**-aptamer binding affinities. The binding affinities increase with the length of the aptameric oligonucleotides and are proven to be important to the sensitivity and selectivity of the aptasensors. The enhanced fluorescent signal of each **N^{3+}**-aptamer solution is selectively quenched by K^+ due to the ability of K^+ in stabilizing the G-quadruplex structure of the aptamer. Among three aptamers, the 15-base aptamer provides optimal sensitivity and selectivity over other ions such as Li^+, Na^+, NH_4^+, Mg^{2+}, Ca^{2+} and Sr^{2+}. The sensing system shows the detection limit of 1 μM of K^+ in clean buffered solution and 30 μM of K^+ in the solution containing 4800-fold excess of Na^+, with wide linear dynamic ranges of micro- to millimolar concentration. This label-free fluorescence aptasensor is conveniently and effectively applicable for analysis of K^+ in urine samples.

© 2011 Elsevier B.V. All rights reserved.

1. Introduction

Potassium ion (K^+) are involved in many biological functions, such as maintenance of extracellular osmolarity, regulation of other ions in organisms, production of electrical signals in nerve systems related to Na^+–K^+ pump process (Yu et al., 2001; Walz, 2000), regulation of blood pressure and pH, enzyme activation of Na^+/K^+-ATPase, and the formation of collagen or elastin (Kofuji and Newman, 2004; Suter, 1998; Pedersen et al., 2006). An abnormal potassium ion concentration in biological fluids can lead to several diseases such as kidney, Addison's and adrenal gland diseases (Modesto et al., 2006; Michaud and Strickberger, 2001). The normal concentration range of potassium ion in human blood plasma is 3.5–5 mM (Huang and Chang, 2008). The daily reference intakes (DRI) of 4000 mg potassium has been proposed (Karger, 2004) and a lower risk of stroke was found to be associated with a little higher intakes (D'Elia et al., 2011). Development of a sensing system for rapid and reliable quantification of potassium ion is thus of importance for medical diagnosis and nutritional analysis.

In common medical practice, potassium ion concentration is determined by a medical instrument operated based on ion selective electrode technique (Szmacinski and Lakowicz, 1999). An optical method is a particularly interesting alternative to the electrochemical method as its detection is fast, sensitive and requires relatively inexpensive instrument. Among all optical methods, fluorometry is one of the most attractive methods due to its operational simplicity and high sensitivity. Simple fluorescent K^+-sensing systems are often encountered with poor selectivity against Na^+ ion, preventing them from practical usages (Yamauchi et al., 1999).

Recently, aptamer-based sensing systems, so-called aptasensors, have gained much attention due to their high sensitivity and selectivity. A typical aptamer is a single-stranded DNA or RNA chain, isolated from a large pool of random-sequence oligonucleotides, that is capable of binding a designated chemical or biological entity with high affinity and specificity (Zhang et al., 2008; Arthanari et al., 1998; Ho and Leclerc, 2004). Potassium aptamers are one of the best known classes of aptamers applied in sensing systems. They are G-rich oligonucleotides which can form the four-stranded helical conformation in solution with stacked arrays of G-quartets connected by Hoogsteen-type base pairing called G-quadruplex (Phan et al., 2006; Marathias and Bolton, 2000; Rujan et al., 2005; Radi and O'Sullivan, 2006). The stability of this conformation is greatly enhanced by K^+, hence highly selective detection of K^+ based on the formation of the G-quadruplex structure and fluorescent labeled probes have been reported (Ueyama et al., 2002; He et al., 2005; Chao et al., 2010). If the 5′- and 3′-ends of the aptameric oligonucleotide are labeled with a donor and an acceptor fluorophore, respectively, the formation of G-quadruplex structures

* Corresponding author. Tel.: +66 2 2187620; fax: +66 2 2187598.
E-mail address: smongkol@chula.ac.th (M. Sukwattanasinitt).

0956-5663/$ – see front matter © 2011 Elsevier B.V. All rights reserved.
doi:10.1016/j.bios.2011.11.049

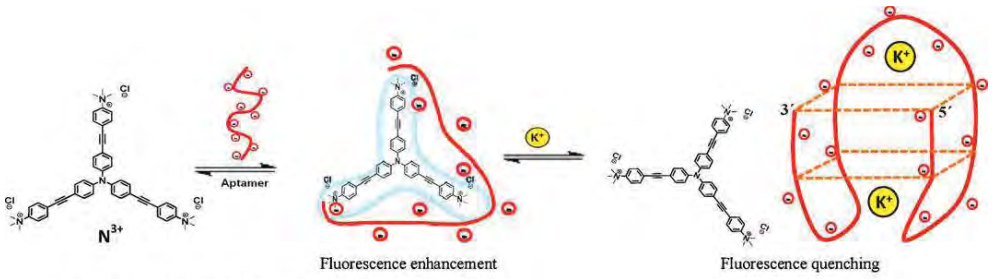

Apt12: d(5′- GGG GTT TTG GGG -3′)

Apt15: d(5′- GGT TGG TGT GGT TGG-3′)

Apt21: d(5′- GGG TTA GGG TTA GGG TTA GGG-3′)

nApt15: d(5′- CAT TCA TGT CAT TCA-3′)

Scheme 1. The proposed supramolecular interaction for K^+ detection using potassium aptamer (Apt) and tricationic fluorophore ($\mathbf{N^{3+}}$).

can bring the two fluorophores close to each other, thus resulting in fluorescence resonance energy transfer (FRET) (Nagatoishi et al., 2006; Juskowiak, 2006; Nagatoishi et al., 2007). This type of probe, frequently called molecular beacon, shows high selectivity and sensitivity for K^+ detection. However, it requires double labeling of the oligonucleotides which increase the cost of detection. Label-free aptasensors for potassium ion utilizing fluorescent dyes such as Oligreen (Huang and Chang, 2008), crystal violet (Kong et al., 2009), tetrakis-(diisopropylguanidino) zinc phthalocyanine (Qin et al., 2010), and Rhodamine B (Yu and Jiang, 2011) have also recently reported as a more economical alternative. The sensitivity and selectivity of these label-free sensing systems are likely to be interdependent on the supramolecular interactions among the signal transducing dye, the aptamer probe and the K^+ analyte. It is thus of interest to investigate effects of the interaction between the aptamer and the dye molecule on the sensitivity and selectivity of the sensing system. In this study, we used three known potassium aptamers (Apt12, Apt15 and Apt21 in Scheme 1) as the probe and one of our recently reported tricationic fluorophores (Niamnont et al., 2009) ($\mathbf{N^{3+}}$) as the signal transducer. $\mathbf{N^{3+}}$ is selected based on its multi-cationic nature to ensure appreciable water solubility and strong electrostatic interaction with the polyanionic oligonucleotide aptamers. The principle of the detection system, as illustrated in Scheme 1, relies on the assumption that there is a strong Coulombic interaction between the aptamer and $\mathbf{N^{3+}}$ that resulted in a strongly enhanced fluorescent signal. The addition of K^+ is expected to induce the aptamer to form a G-quadruplex which has a weaker interaction with $\mathbf{N^{3+}}$ leading to the reduction of the fluorescent intensity in relation to the K^+ concentration.

2. Experimental

2.1. Chemicals and materials

The fluorophore $\mathbf{N^{3+}}$ with an iodide counter ion was prepared according to our previously reported procedures (Niamnont et al., 2009) and it was eluted through an anionic exchange resin column (Amberlite IRA-410 Cl^- form) by DI water to exchange iodide with chloride counter ion. Metal salts i.e. LiCl, NaCl, KCl, $MgCl_2$, $CaCl_2$, $SrCl_2$ and Tris–HCl buffers used in the fluorescence measurement were analytical grade purchased from chemical vendors such as Sigma–Aldrich (USA), Fluka (Switzerland) or Merck (Germany). Oligonucleotides were ordered from BioDesign. Co. Ltd. (Bangkok, Thailand). All chemicals were used as received without further purification. Water was purified using a Millipore filtration system.

2.2. General methods

UV–vis absorption spectra were recorded on a Varian Cary 50 UV-Vis spectrophotometer. Fluorescence measurements were carried out with solution samples in a 2 mL quartz cuvette at room temperature using a Varian Cary Eclipse spectrofluorometer at 90° detection angle. The quantum efficiency was measured relative to quinine sulfate standard in 0.1 M H_2SO_4 ($\Phi_F = 0.54$).

2.3. Fluorescence sensing study

The stock solutions of $\mathbf{N^{3+}}$, aptamers and metal salts were prepared in Tris–HCl buffer pH 7.4 (10 mM). For spectrum measurements, the stock solutions of relevant compounds were mixed thoroughly and the total volumes were adjusted to 1.5 mL with the same buffer solution. The samples were allowed to equilibrate for at least 5 min at room temperature prior to the measurements. Each sample was prepared in triplicate solutions and each solution was measured for three times to provide the reported average values along with their standard deviation.

2.4. Fluorescence detection of K^+

The fluorescence spectrum of the mixture of $\mathbf{N^{3+}}$ (0.2 μM), the aptamer (0.02 μM) and one of the metal chlorides tested (LiCl, NaCl, KCl, NH_4Cl, $MgCl_2$, $CaCl_2$, and $SrCl_2$; 10 mM) in Tris–HCl buffer pH 7.4 (10 mM) was acquired in the range of 400–700 nm with the excitation wavelength of 372 nm. The quenching efficiency, $1 - (F/F_0)$, was plotted against the types of aptamers and metal ions, where F and F_0 are the fluorescence intensity in the presence and absence of the metal ion, respectively. For potassium concentration dependence study, the mixtures of $\mathbf{N^{3+}}$ (0.2 μM), Apt15 (0.02 μM) and potassium ion at various concentrations (0.004, 0.02, 0.2, 1, 2, 3, 4, 5, 10, 50, 100, 140 and 196 mM) were used. For interference test, the mixtures of $\mathbf{N^{3+}}$ (0.2 μM), Apt15 (0.02 μM), potassium ion (0.2 mM) and other metal chloride such as LiCl, NaCl, NH_4Cl, $MgCl_2$ $CaCl_2$, and $SrCl_2$ at ten times of potassium ion concentration (2 mM) were measured.

2.5. Application for K^+ assays in real samples

A calibration curve was prepared from the Tris–HCl buffered solutions of potassium ion (0.04–20 mM) in the presence of other simulated extracellular ions including NaCl (145 mM), $CaCl_2$ (2.5 mM), and $MgCl_2$ (1.5 mM) in the presence of $\mathbf{N^{3+}}$ fluorophore (1 μM) and Apt15 (0.1 μM). Urine samples were collected from four

healthy volunteers, centrifuged at 3500 Rev/min for 5 min, kept at 4 °C overnight and filtered through 0.45 μm Teflon membranes. For recovery test, KCl (10 mM) was also added into the urine samples prior to the analyses. The urine samples were then diluted 100-fold with Tris–HCl buffer (10 mM, pH 7.4) containing Apt15 (0.1 μM) and **N^{3+}** fluorophore (1 μM) and analyzed by fluorometer. For method validation, the same urine samples were analyzed by Inductively Coupled Plasma-Optical Emission Spectroscopy (ICP-OES Spectrometer, iCAP 6000 SERIES ICP Consumables Kit).

3. Results and discussion

3.1. Synthesis and photophysical properties of the tricationic fluorophore

The tricationic fluorophore **N^{3+}** in the form of iodide salt was synthesized according to the previously reported procedures (Scheme S1) (Niamnont et al., 2009). This iodide salt however gradually lost its water solubility upon storage in its solid state. The ^{1}H NMR spectra of the samples stored for a week revealed significant degree of demethylation from the ammonium groups (Fig. S1). The mixture of demethylated salts became poorly soluble in water and it is not suitable for further study. Ion exchange of the strongly nucleophilic iodide ion with a less nucleophilic chloride ion was thus performed by eluting the aqueous solution of the iodide salt through an Amberlite IRA-410 (Cl^- form) anionic ion exchange resin column. The fluorophore containing chloride counter ion, **N^{3+}** $3Cl^-$, was found to be more stable that it retains good water solubility upon storage. This chloride salt is thus utilized for further study as an analytical fluorescent transducing agent.

The solution of **N^{3+}** in Tris–HCl buffer solution pH 7.4 displayed absorption maximum at 372 nm (Fig. S2) with molar absorptivity of 3.42×10^4. When being excited at 372 nm, the fluorophore showed emission maximum at 486 nm and quantum efficiency of 13.6%. The addition of Apt15, a K^+ aptamer consisting of 15 nucleotide bases, enhanced the fluorescent intensity over five folds and blue shifted it to 454 nm (Fig. S3a). With one equivalent of Apt15, the system gave the quantum yield as high as 33.4%. These changes in the fluorescent signal reflect the expected interaction between the aptamer and **N^{3+}**. The interaction reduces the geometrical relaxation and self-associative quenching process resulting in the wavelength shift and intensity enhancement, respectively (Swager, 1998; Azagarsamy et al., 2010). The K^+ detection experiment gave results in good agreement with the principle proposed in Scheme 1. The fluorescence spectra shown in Fig. S3a demonstrate that the enhanced fluorescent signal of **N^{3+}**/Apt15 system decreases by over 50% upon the addition of 1 mM K^+. The positively charged K^+ is expected to bind with the aptamer reducing its binding with **N^{3+}** and reinstalling the self-associative quenching effect. To confirm that this behavior was a result of the specific binding between K^+ and the aptamer, a non-aptameric oligonucleotide (nApt15) having a random sequence which cannot form a G-quadruplex structure was also tested. In this case, the addition of K^+ did not cause any changes in the fluorescence intensity of the **N^{3+}**/nApt15 mixture (Fig. S3b).

3.2. Fluorescence responses of the fluorophore to ODNs

To gain insight into interactions between the fluorophore and aptamer, we investigated the mixtures of **N^{3+}** and four oligonucleotides (ODN) i.e. Apt12, Apt15 Apt21 and nApt15 (Scheme 1). The first three ODNs are K^+ aptamers while the last one is a non-aptameric ODN. At the same molar concentration, the ODNs with different lengths gave different enhancement and shift of the fluorescent signal of **N^{3+}** suggesting different binding affinity with the fluorophore (Fig. S4). With the assumption of 1:1 complexation

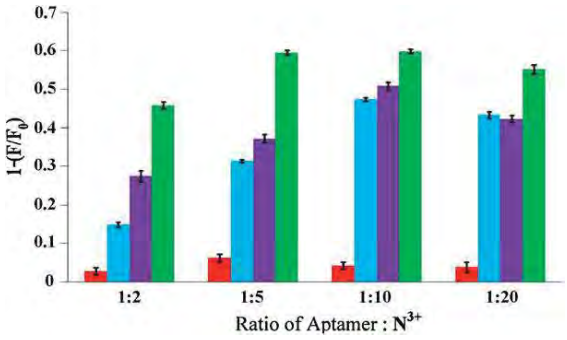

Fig. 1. Quenching efficiencies of K^+ in aptameric sensing systems using different ODNs: Apt12 ( ), Apt15 ( ), Apt21 ( ) and nApt15 ( ) at various ODN/fluorophore mole ratios.

between **N^{3+}** and the aptamer, the intercept/slope of a linear plot fit to the Benesi–Hildelbrand equation (Mukhopadhyay et al., 2005; Chakraborty and Guchhait, 2008; Upadhyay et al., 2007) gave the affinity constant (K_a) for each **N^{3+}**/ODN complex. The K_a values for Apt12, Apt15, Apt21 and nApt15 were determined as 3.2×10^7, 9.1×10^7, 3.0×10^8 and 9.4×10^7 M^{-1}, respectively (Fig. S5). The binding constants increase with the length of the ODNs in accordance to the increasing electrostatic interaction. The observation of similar values of the binding constants for the aptamer (Apt15) and non-aptamer (nApt15) also confirmed that the electrostatic force is the main binding contribution. Job's plot analysis of the fluorescence responses (Zachary, 1986) revealed that the Apt12 formed 2:1 complex with **N^{3+}**, while all the other ODNs formed 1:1 complexes (Fig. S6). The K_a obtained from the plot for Apt12 is thus likely to be the product of two binding steps ($K_{a1} \times K_{a2}$) and each Apt12 chain should have even much lower binding affinity than that obtained from the Benesi–Hildelbrand plot. We attribute the difference in binding ratios to the molecular length of ODN. From AM1 geometrical optimization, the distance between two ammonium groups of **N^{3+}** was determined to be 21.7 Å. Based on the length of a single nucleotide unit of 3.3 Å, the extended chain lengths of Apt12, Apt15 and Apt 21 are estimated to be 39.6, 49.5 and 69.3 Å, respectively. These values suggested that there is a good possibility of two Apt12 chains to interact with all three cationic sites of **N^{3+}** to form a 2:1 complex while only one chain of the longer aptamers (Apt15 and Apt21) is required to interact with all three cationic sites of **N^{3+}** (Fig. S7).

3.3. Condition for detection of K^+

According to the sensing mechanism presented in Scheme 1, the fluorescence quenching involves the competitive binding between K^+ and **N^{3+}** to the aptamer and greater sensitivity of K^+ may be obtained at the aptamer/fluorophore ratio lower than its stoichiometric ratio. We therefore investigated the effect of aptamer/fluorophore ratio on the sensitivity by varying the concentration of the aptamer from 0.1 to 0.01 μM at a fixed fluorophore concentration of 0.2 μM. The optimum aptamer/fluorophore ratio is determined as the ratio giving the highest quenching efficiency ($1 - F/F_0$) upon the addition of K^+ at a physiological concentration (10 mM). Fig. 1 shows the highest quenching efficiency at the aptamer/fluorophore ratio of 1:10 for all aptameric ODN lengths. While reducing the aptamer/fluorophore ratio decreases the initial fluorescence signal (F_0), this adverse effect can be offset by lower amount of K^+ required for effective competitive complexation. It is important to note that the reported binding constant of K^+ with Apt15 is 2×10^6 M^{-1} (Wilcox et al., 2008), which is about 50 times lower than the K_a values of **N^{3+}** with Apt15. Fig. 1 also shows that Apt12 has the highest quenching sensitivity at all

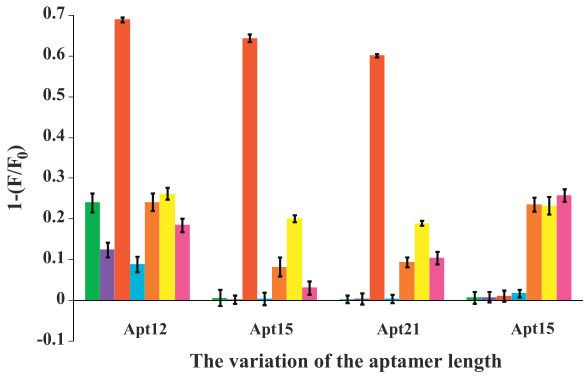

Fig. 2. Quenching efficiencies of physiological cations: Li^+ ( ), Na^+ ( ), K^+ ( ), NH_4^+ ( ), Mg^{2+} ( ), Ca^{2+} ( ) and Sr^{2+} ( ) in the sensing systems constructing from various ODNs.

ratios as expected for its lower binding affinity to the fluorophore, for each individual chain. It is also important to point out that the lower aptamer/fluorophore ratio is translated into the lower amount of expensive aptameric ODN required for the detection. In this particular aptasensing system, the optimum condition for K^+ sensing required only 20 nM of the aptamer and 200 nM of the fluorophore which is one of the lowest values have been reported (Huang and Chang, 2008; Kong et al., 2009; Qin et al., 2010). The plot also shows that K^+ gives very low quenching efficiency for the non-aptameric ODN, nApt15, confirming that the detection is based on the specific aptamer–K^+ interaction. Since the sensitivity of a sensor is generally traded off with selectivity, our next investigation is to compare the selectivity toward K^+ against other cations.

We investigated the selectivity of each aptamer/$\mathbf{N^{3+}}$ pair at the optimum 1:10 mole ratio by comparing the quenching efficiency of K^+ with other cations such as Li^+, Na^+, NH_4^+, Mg^{2+}, Ca^{2+} and Sr^{2+}. Fig. 2 clearly reveals that the aptameric sensing systems have high sensing selectivity toward K^+ while the non-aptameric system gave no K^+ selectivity. Among three aptamers, Apt12 provided the lowest selectivity against other monovalent cations such as Li^+, Na^+ and NH_4^+ that should again be attributed to its low binding affinity to the fluorophore. For the divalent cationic species such as Mg^{2+}, Ca^{2+} and Sr^{2+}, we observed lower selectivity against these ions. Comparing with the monovalent cations, the divalent cations possess greater electrostatic attraction with the ODN chains that led to greater quenching effect to the sensing system. Interestingly, the selectivity against divalent cations is rarely reported for K^+ aptasensors, it is thus important to point out that this tricationic fluorophore $\mathbf{N^{3+}}$ provided greater selectivity than the monocationic dye for K^+ aptasensing system (Kong et al., 2009). We thus attributed the factors for high selectivity not only to the specific binding between K^+ and the aptameric G-quadruplex structure but also to the binding affinity between the fluorophore and aptamer. Among the three aptamers, Apt15 presents the best choice for K^+ sensor as it give high selectivity with only slightly lower sensitivity comparing to Apt12.

3.4. Quantitative analysis of K^+

For quantitative analysis of K^+, the fluorescent signal of Apt15/$\mathbf{N^{3+}}$ (1:10) solution in the presence of KCl was measured. The fluorescent signal decreased with the increasing K^+ concentration (Fig. 3a). At low K^+ concentrations ($\leq$50 mM or $\leq 2.5 \times 10^5$ equiv.), the fluorescent signal was quenched without any peak shift. When the concentration of K^+ increased to 100 mM ($\geq 5 \times 10^5$ equiv.), the fluorescent signal was shifted to the original position of the free fluorophore. These results agree well with the stepwise formation of 1:1 and 2:1 complexes between K^+ and Apt15 (Yoshikawa, 2001; Declan and Wallace, 1998; Baigl and Yoshikawa, 2005). The 1:1 complex of K^+/Apt15 probably remains largely bound to $\mathbf{N^{3+}}$ while the 2:1 complex is likely to be dissociated from the fluorophore. This stepwise formation of 1:1 and 2:1 complexes is also evidenced from two linear dynamic ranges observed in the plot between quenching efficiency and log[K^+] before reaching the saturation (Fig. 3b). At low K^+ concentration, most complex formed is likely to be the 1:1 complex whereas the 2:1 complex becomes predominant at higher K^+ concentration. The 2:1 complex has lower negative charge and thus its binding with $\mathbf{N^{3+}}$ is weaker resulting in greater quenching sensitivity and the greater slope of the second dynamic range. With K^+ concentration higher than 100 mM (5×10^5 equiv.), the quenching effect is clearly saturated and the fluorescent signal returned to the original position of $\mathbf{N^{3+}}$. The plot in Fig. 3b demonstrates useful concentration range for quantitative analysis of K^+. The first linear dynamic range gave the limit of detection (LOD determined at the signal = 3 × noise) of K^+ as low as 9×10^{-7} M which is among the best for the label free systems reported to date (Huang and Chang, 2008; Kong et al., 2009; Qin et al., 2010).

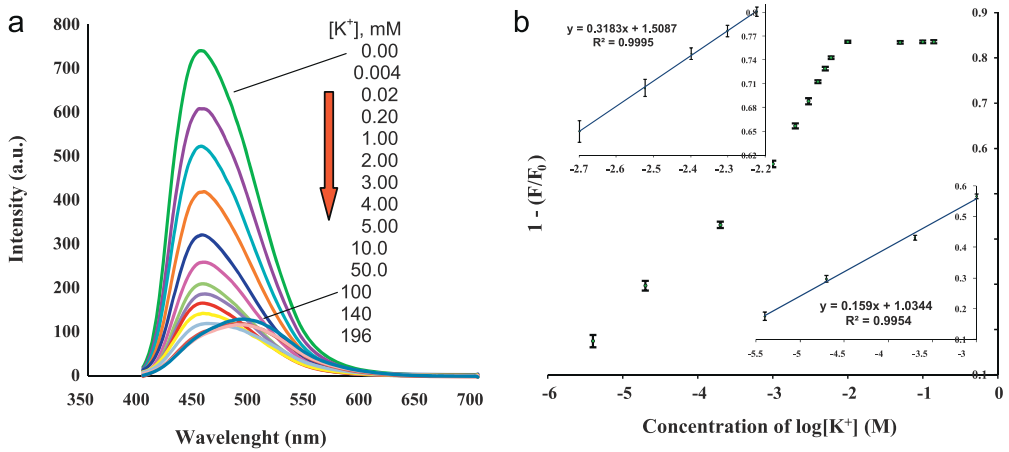

Fig. 3. (a) Fluorescence spectra (λ_{ex} = 372 nm) of the Apt15/$\mathbf{N^{3+}}$ (20/200 nM) in Tris–HCl buffer pH 7.4 (10 mM) in the presence of K^+ at various concentrations. (b) Plot of the quenching efficiency (λ_{em} = 456 nm) as a function of log[K^+]. The insets show two dynamic ranges of K^+ concentration (4 μM to 1 mM and 2–6 mM).

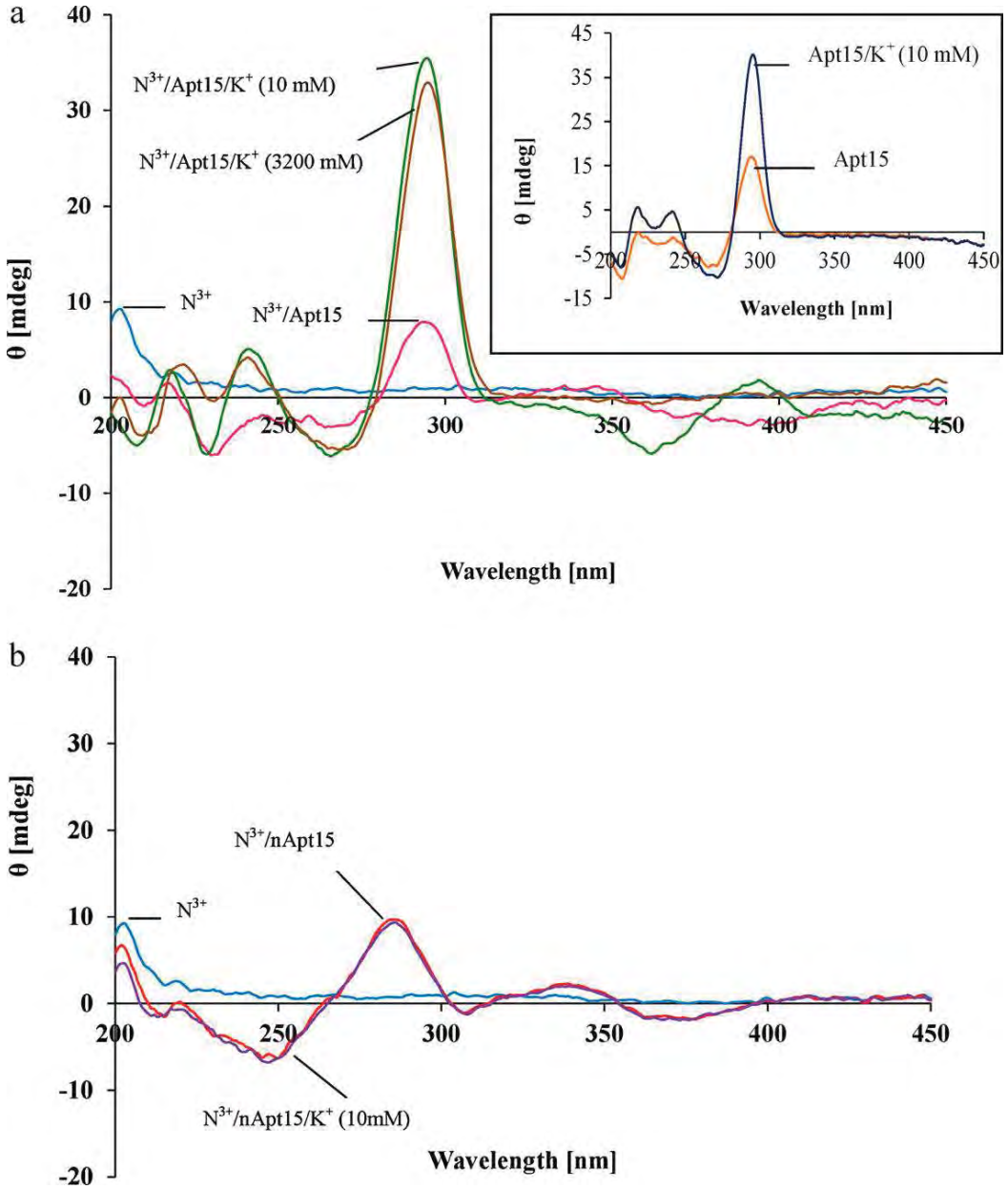

Fig. 4. Circular dichroism (CD) spectra of (a) aptameric system ([$\mathbf{N^{3+}}$] = 10 μM, [Apt15] = 10 μM, [K^+] = 10 and 3200 mM) and (b) non-aptameric system $\mathbf{N^{3+}}$ solution ([$\mathbf{N^{3+}}$] = 10 μM, [Apt15] = 10 μM, [K^+] = 10 mM) in Tris–HCl buffer pH 7.4 (10 mM). Inset is the system without $\mathbf{N^{3+}}$.

3.5. Supramolecular interaction study by circular dichroism (CD)

Circular dichroism (CD) spectroscopy was used to ascertain the changes in the interactions among $\mathbf{N^{3+}}$, Apt15 and K^+ at different K^+ concentration levels. The negative CD signal near the absorption of $\mathbf{N^{3+}}$ around 385 nm signifies the interaction between Apt15 and $\mathbf{N^{3+}}$ (Fig. 4a). In the presence of 10 mM K^+ (1.0×10^3 equiv.), the positive CD signal at 290 nm, corresponding to the signal of antiparallel G-quadruplex conformation of the aptamer (Kypr et al., 2009), is markedly increased. However, the signal near the absorption of $\mathbf{N^{3+}}$ did not return to the original nil value indicating some interaction between the aptamer and $\mathbf{N^{3+}}$ remained. The sign switching structure of the signal in this region also implies that the aptamer unevenly interacts with three branches of $\mathbf{N^{3+}}$. Further addition of K^+ to 3.20 M (3.2×10^5 equiv.) returns this CD signal back to zero confirming the full dissociation of the potassium–G-quadruplex complex from $\mathbf{N^{3+}}$. With similar interpretation, Fig. 4b confirms that the non-aptameric ODN, nApt15, interact with $\mathbf{N^{3+}}$ but not with K^+ as there is no CD signal change upon the addition of K^+.

3.6. K^+ assay in urine samples

In the final stage of this work, the application of Apt15-$\mathbf{N^{3+}}$ aptasensing system for determination of K^+ concentration in real human urine samples was evaluated. Using synthetic urine solutions containing 145 mM NaCl, 2.5 mM $CaCl_2$, 1.5 mM $MgCl_2$ and various concentrations of K^+ (0–20 mM) (Nagatoishi et al., 2005), a linear calibration line was obtained in the range of 0.04–2.0 mM (Fig. S8). Although the linearity range of the K^+ assay shifted to somewhat higher concentration range because of the impact of the

Table 1
Analytical results for K^+ content in urine samples from four healthy volunteers measured using the $\mathbf{N^{3+}}$–Apt15 fluorescence sensor[a] and ICP-OES.

Sample	$\mathbf{N^{3+}}$-Apt sensor Mean ± SD/mM ($n = 5$)	ICP-MS Mean ± SD/mM ($n = 5$)	*F*-Test between two methods[b]	Add K^+ (mM)	Found K^+ (mM)	Recovery (%)
Urine 1	4.20 ± 0.006	4.15 ± 0.033	S	10	9.875	98.8
Urine 2	11.17 ± 0.004	11.22 ± 0.152	3.15	10	9.952	99.5
Urine 3	14.58 ± 0.003	14.59 ± 0.063	2.30	10	9.753	97.5
Urine 4	23.21 ± 0.012	23.75 ± 0.091	3.67	10	9.741	97.4

[a] $[\mathbf{N^{3+}}]/[\text{Apt15}] = 1/0.1\ \mu M$.
[b] The *F*-test value is 6.39 at a 95% confidence level.

sample matrixes, as little as 30 μM K^+ could be detected, even in the presence of 145 mM Na^+ (4800-fold of K^+ concentration). On the basis of an *F*-test at a 95% confidence level, the K^+ concentrations in four volunteers' urine samples determined by Apt15–$\mathbf{N^{3+}}$ sensor agree very well with the values obtained from inductively coupled plasma-optical emission spectrometry (ICP-OES) (Table 1). The recovery level of 97.4–99.5% of K^+, intentionally spiked at 10 mM concentration into the urine sample solutions, also confirmed the effectiveness of this method for determination of K^+ content in urine. It is important to point out here that this fluorescence aptasensing assay provides the advantages of simple sample preparation, rapid detection and low cost instrumentation that are amenable to high throughput analysis.

4. Conclusion

The tricationic phenylene–ethynylene ($\mathbf{N^{3+}}$) is capable of transducing fluorescent signal in aptasensing system. The fluorescent signal of $\mathbf{N^{3+}}$ is enhanced upon electrostatic binding with the potassium aptamer. The addition of potassium ion selectively diminished this enhancement by inducing the formation G-quadruplex conformation of the aptamer chain which in turn weakens its electrostatic interaction with $\mathbf{N^{3+}}$. Sensitivity and selectivity of the sensing system was optimized by the variation of the aptamer length in order to tune the electrostatic interactions between the fluorophore and aptamer. The 15-base aptamer gave higher selectivity than the 12-base aptamer and higher sensitivity than the 21-base aptamer. The $\mathbf{N^{3+}}$–Apt15 aptasensor exhibits wide linear dynamic ranges from micro- to millimolar concentration of K^+ with the detection limit just below 1.0 μM. The sensing system is conveniently applicable for rapid K^+ assays in real urine samples.

Acknowledgements

The authors would like to acknowledge the financial support from the Research, Development and Engineering (RD&E) Fund through National Nanotechnology Center (NANOTEC), National Science and Technology Development Agency (Project NN-B-22-FN9-10-52-06). We would also like to thank The Thailand Research Fund (TRF: code RTA5280002) for research grants. This work is part of the Project for Establishment of Comprehensive Center for Innovative Food, Health Products and Agriculture supported by the Thai government stimulus package 2 (TKK2555, SP2) and National Research University of CHE and the Ratchadaphiseksomphot Endowment Fund (AM1006A). We would like to thank Assist. Prof. Dr. Narong Praphairaksit and his student for the experiments on the inductively coupled plasma-optical emission spectrometry (ICP-OES).

Appendix A. Supplementary data

Supplementary data associated with this article can be found, in the online version, at doi:10.1016/j.bios.2011.11.049.

References

Arthanari, H., Basu, S., Kawano, T.L., Bolton, P.H., 1998. Nucleic Acids Res. 26, 3724–3728.
Azagarsamy, M.A., Yesilyurt, V., Thayumanavan, S., 2010. J. Am. Chem. Soc. 132, 4550–4551.
Baigl, D., Yoshikawa, K., 2005. Biophys. J. 88, 3486–3493.
Chakraborty, A., Guchhait, N., 2008. J. Incl. Phenom. Macrocycl. Chem. 62, 91–97.
Chao, S., Hongxi, G., Cuiping, M., 2010. Anal. Biochem. 400, 99–102.
Declan, A.D., Wallace, B.A., 1998. Biophys. J. 75, 635–640.
D'Elia, L., Barba, G., Cappuccio, F., Strazzullo, P., 2011. J. Am. Coll. Cardiol. 57, 1210–1219.
He, F., Tang, Y., Wang, S., Li, Y., Zhu, D., 2005. J. Am. Chem. Soc. 127, 12343–12346.
Ho, H.A., Leclerc, M., 2004. J. Am. Chem. Soc. 126, 1384–1387.
Huang, C.C., Chang, H.T., 2008. Chem. Commun. 146, 1–1463.
Juskowiak, B., 2006. Anal. Chim. Acta 568, 171–180.
Karger, S., 2004. Ann. Nutr. Metab. 48, 1–16.
Kofuji, P., Newman, E.A., 2004. Neuroscience 129, 1045–1056.
Kong, D.M., Guo, J.H., Yang, W., Ma, Y.E., Shen, H.K., 2009. Biosens. Bioelectron. 25, 88–93.
Kypr, J., Kejnovska, L., Renciuk, D., Vorlickova, M., 2009. Nucleic Acids Res. 37, 1713–1725.
Marathias, V.M., Bolton, P.H., 2000. Nucleic Acids Res. 28, 1969–1977.
Michaud, G.F., Strickberger, S.A., 2001. J. Am. Coll. Cardiol. 38, 1224–1225.
Modesto, K.M., Møller, J.E., Freeman, W.K., Shub, C., Bailey, K.R., Pellikka, P.A., 2006. Am. J. Cardiol. 97, 1247–1249.
Mukhopadhyay, M., Banerjee, D., Koll, A., Mandal, A., Filarowski, A., Fitzmaurice, D., Das, R., Mukherjee, S., 2005. J. Photochem. Photobiol. A: Chem. 175, 94–99.
Nagatoishi, S., Nojima, T., Juskowiak, B., Takenaka, S., 2005. Angew. Chem. Int. Ed. Engl. 44, 5067–5070.
Nagatoishi, S., Nojima, T., Galezowska, E., Juskowiak, B., Takenaka, S., 2006. Chem. BioChem. 7, 1730–1737.
Nagatoishi, S., Nojima, T., Galezowska, E., Gluszynska, A., Juskowiak, B., Takenaka, S., 2007. Anal. Chim. Acta 581, 125–131.
Niamnont, N., Siripornnoppakhun, W., Rashatasakhon, P., Sukwattanasinitt, M., 2009. Org. Lett. 11, 2768–2771.
Pedersen, S.F., O'Donnell, M.E., Anderson, S.E., Cala, P.M., 2006. Am. J. Physiol. – Reg. I 291, R1–R25.
Phan, A.T., Kuryavyi, V.D., Patel, J., 2006. Curr. Opin. Struct. Biol. 16, 288–298.
Qin, H., Ren, J., Wang, J., Luedtke, N.W., Wang, E., 2010. Anal. Chem. 82, 8356–8360.
Radi, A.E., O'Sullivan, C.K., 2006. Chem. Commun. 343, 2–3434.
Rujan, L.N., Meleney, J.C., Bolton, P.H., 2005. Nucleic Acids Res. 33, 2022–2031.
Suter, P.M., 1998. Nutr. Rev. 56, 151–153.
Swager, T.M., 1998. Acc. Chem. Res. 31, 201–207.
Szmacinski, H., Lakowicz, J.R., 1999. Sens. Actuators B: Chem. 60, 8–18.
Ueyama, H., Takagi, M., Takenaka, S., 2002. J. Am. Chem. Soc. 124, 14286–14287.
Upadhyay, S.P., Pissurlenkar, R.R.S., Coutinho, E.C., Karnik, A.V., 2007. J. Org. Chem. 72, 5709–5714.
Walz, W., 2000. Neurochem. Int. 36, 291–300.
Wilcox, J.M., Rempel, D.L., Gross, M.L., 2008. Anal. Chem. 80, 2365–2371.
Yamauchi, A., Hayashita, T., Nishizawa, S., Watanabe, M., Teramae, N., 1999. J. Am. Chem. Soc. 121, 2319–2320.
Yoshikawa, K., 2001. Adv. Drug Deliv. Rev. 52, 235–244.
Yu., X., Jiang, Z., 2011. Anal. Lett. 44, 898–907.
Yu, S.P., Canzoniero, M.T., Choi, D.W., 2001. Curr. Opin. Cell Biol. 13, 405–411.
Zachary, D., 1986. J. Chem. Educ. 63, 162–170.
Zhang, J., Wang, L., Pan, D., Song, S., Boey, F.Y.C., Zhang, H., Fan, C., 2008. Small 4, 1196–1200.

TISSUE ANTIGENS
IMMUNE RESPONSE GENETICS

Tissue Antigens ISSN 0001-2815

BRIEF COMMUNICATION

A nested sequence-specific primer-polymerase chain reaction for the detection of *HLA-B*15:02*

S. Virakul[1], P. Kupatawintu[2], J. Nakkuntod[1], O. Kangwanshiratada[3], T. Vilaivan[4] & N. Hirankarn[3]

1 Medical Microbiology, Interdisciplinary Program, Graduate School, Chulalongkorn University, Bangkok, Thailand
2 National Blood Center, Thai Red Cross Society, Bangkok, Thailand
3 Department of Microbiology, Faculty of Medicine, Chulalongkorn University, Bangkok, Thailand
4 Department of Chemistry, Faculty of Science, Chulalongkorn University, Bangkok, Thailand

Key words
carbamazepine hypersensitivity; *HLA-B*15:02*; nested sequence-specific primer-polymerase chain reaction

Correspondence
N. Hirankarn, MD, PhD
Lupus Research Unit
Department of Microbiology
Faculty of Medicine
Chulalongkorn University
Rama 4 Road
Bangkok 10330
Thailand
Tel: +66 2 256 4132 ext. 624
Fax: +66 2 252 5952
e-mail: fmednpt@md.chula.ac.th

Received 21 July 2011; revised 29 November 2011; accepted 4 January 2012

doi: 10.1111/j.1399-0039.2012.01836.x

Abstract

In this study, we reported a new technique in detecting *HLA-B*15:02* by using a nested sequence-specific primer-polymerase chain reaction (SSP-PCR) that can be used on genomic DNA and whole blood for carbamazepine hypersensitivity prediction. We tested a total of 200 blind samples with known human leukocyte antigen (HLA)-B allelic types (44 positive for *HLA-B*15:02* and 156 negative for *HLA-B*15:02*) with this new nested SSP-PCR technique and compared its efficacy to that of commercial sequence-specific oligonucleotide probe-polymerase chain reaction (SSOP-PCR). Using starting materials from DNA and whole blood, we were able to detect *HLA-B*15:02* in 44 of our samples correctly. The test is very sensitive and is highly reproducible.

Certain human leukocyte antigen (HLA) alleles can be used as a marker for detecting Steven Johnson syndrome and toxic epidermal necrolysis. Although life-threatening drug hypersensitivities are rare, however, when it does occur, it can cause death in around 30% of its sufferers. In 2004, Chung et al. was the first to report using *HLA-B*15:02* as a genetic marker for predicting the patient's hypersensitivity to carbamazepine (1). Along the same lines, it has been reported that ethnicity plays an important role in patients becoming hypersensitive to certain drugs (2). *HLA-B*15:02* is strongly associated with carbamazepine hypersensitivity in Asians (3, 4) and not in Caucasians (5). As a result of this, the US Food and Drug Administration now recommends physicians to screen all Asian patients for the presence of *HLA-B*15:02* before initiating carbamazepine regimens (6).

Currently, HLA typing is frequently used in the field of transplantations, which require the detection of many alleles at the same time. However, for other medical fields, this is unnecessary, time consuming and costly. As a result of this, a simpler, cheaper and faster method to detect a specific allele is urgently needed. It has been shown that to detect *HLA-B*15*, the most polymorphic group, a multiple set of different primers are needed (7, 8). For example, a sequence-specific primer-polymerase chain reaction (SSP-PCR) technique would require at least six sets of primers in order to distinguish *HLA-B*15:02* from *B*15:13* and *B*15:21* (7).

Although SSP-PCR is the most cost effective method used to detect *HLA-B*15*, however, its DNA extraction procedure is highly dependent on DNA extraction kits which are quite expensive. Other techniques used to extract DNA such as the standard salting out method is very cheap but very time consuming and can take approximately 6 h to complete. A number of attempts have been used to type HLA and amplify the target DNA directly from whole blood to reduce the total assay time as much as possible (9). Mutant Taq DNA polymerase and high pH buffer were used to overcome the inhibitor in the whole blood samples such as anti-coagulating agent, hemoglobin, immunoglobulin G and lactoferrin (10, 11). Here, we report an alternative method

© 2012 John Wiley & Sons A/S

using a nested SSP-PCR in detecting *HLA-B*15:02* from purified genomic DNA and whole blood samples.

To find sequence-specific primers, all HLA-B sequences were obtained from the IMGT/HLA database (12). Nested PCR was used to increase the specificity of each round of amplification and to eliminate heterozygous combination from a number of separate reactions. Briefly, in the first PCR, some subtypes of *HLA-B*13, B*15, B*35, B*40, B*44* and *B*57* were amplified followed by a second PCR, which specifically amplified only *HLA-B*15:02*. All primer locations are shown in Figure 1 and all primer sequences are listed in Table 1. To predict which alleles will be amplified from the different combinations of primers used in the nested SSP-PCR, 10 bases from 3′ end of each primer sequence was entered into the PROBE and PRIMER Search Tool, IMGT/HLA database version 3.6 October 2011 (12). All possibilities of allele amplification from the prediction are shown in Table 2.

To test the specificity of primers, purified genomic DNAs were extracted from 13 samples with known HLA alleles identified by a commercial SSP-PCR Kit (Micro SSP™ HLA DNA Typing Trays, One Lambda, Inc., Canoga Park, CA) (Figure 2A). The results from the first PCR amplified the following alleles as expected: *HLA-B*13:01, 15:02, 15:13, 15:21* and *15:25*. Other alleles commonly found (more than

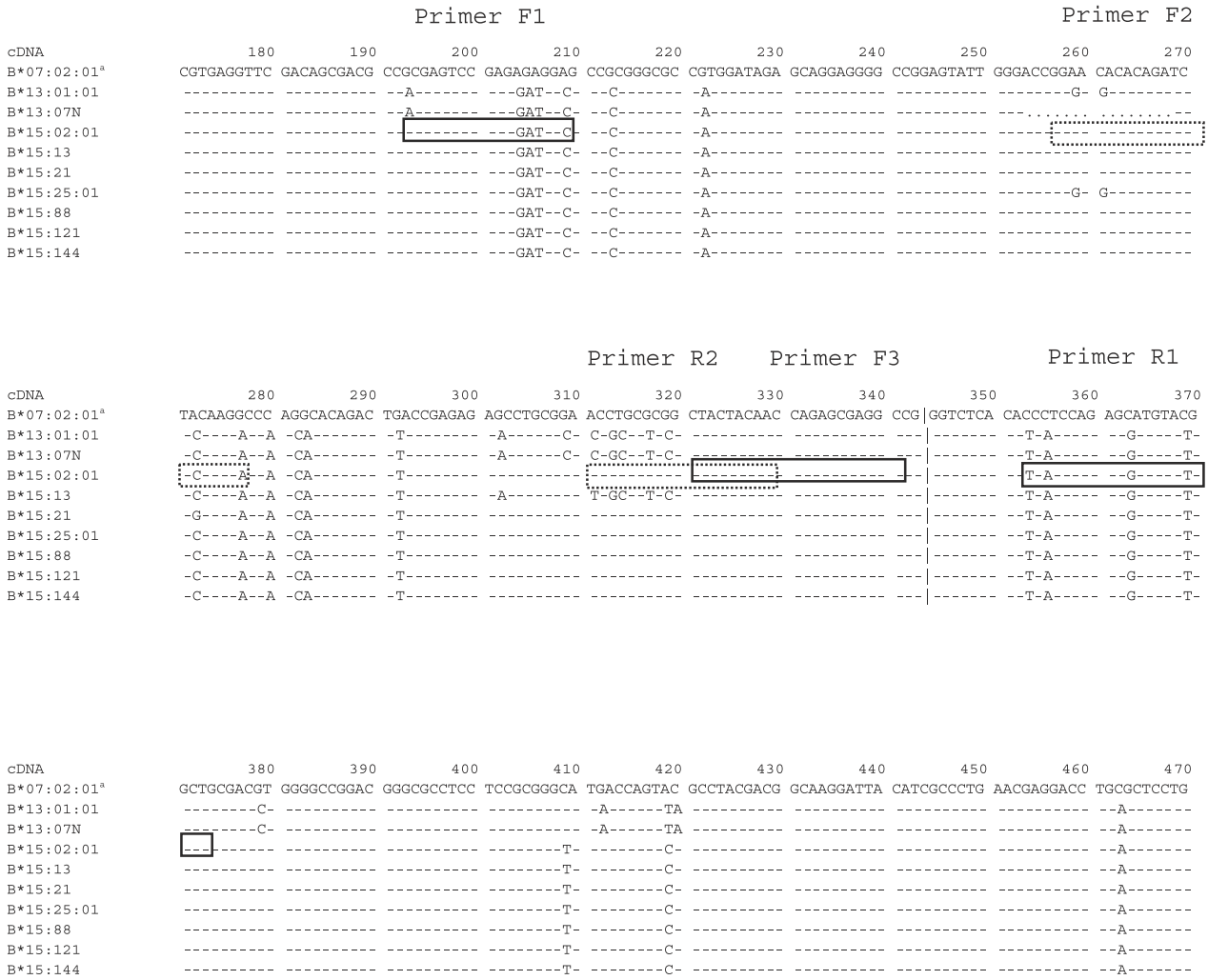

Figure 1 Primers were designed from regions within *HLA-B*15:02* exons 2 and 3. All these sequences were taken from IMGT/HLA database (12). For the first PCR, the sequences for *HLA-B*15:02* primers F1 are located in exon 2 and for R1, it is located in exon 3. For the second PCR, both F2 and R2 are all located in exon 2. The F3, a nested control primer is located in exon 2. All sequences for the primers are shown in Table 1. HLA, human leukocyte antigen.

[a] *HLA-B*07:02:01* was used as the consensus sequence. A dash (–) indicated that the sequences were similar to each other, whereas the dot (.) represented sequence insertions or deletions.

© 2012 John Wiley & Sons A/S

Table 1 Primers for *HLA-B*15:02* nested SSP-PCR[a]

SSP-PCR primers for *HLA-B*15:02*
F1:5′-GCGAGTCCGAGGATGGC-3′
R1:5′-AGCCATACATCCTCTGGATGA-3′
F2:5′-GGAGTATTGGGACCGGAAC-3′
R2:5′-TTGTAGTAGCCGCGCAGGT-3′
Primers for internal control (IFN-γ)
IF: 5′-CCTCACATGATATGACTTTGACAT-3′
IR: 5′-AACATCAGAAGCATTGACCTTG-3′
Primers for nested control (HLA)
F3:5′-CTACTACAACCAGAGCGAGGC-3′
R1:5′-AGCCATACATCCTCTGGATGA-3′

HLA, human leukocyte antigen; SSP-PCR, sequence-specific primer-polymerase chain reaction.
[a]In the first PCR, *HLA-B*15:02* primers (F1 and R1) were added to the reaction with an internal control primer (IF and IR). In the second PCR, F2 and R2 is used, in addition with F3 and R1 as nested control primer.

1%) in the Thai population (*HLA-B*07:05, 15:01, 27:04, 35:01, 40:01, 46:01, 57:01* and *58:01*) were not amplified. Using primers F2 and R2 in the second PCR, only *HLA-B*15:02* was amplified. PCR product sizes were detected by gel electrophoresis, which was performed on a 2% agarose at 100 V for 35 min with GeneRuler™ 50 bp (Fermentas, Glen Burnie, MD).

As shown in Table 2, some frequently found alleles were expected to be amplified in the first PCR such as *HLA-B*13:01, B*15:13, B*15:21* and *B*15:25* (430 bp). In the second PCR reactions, all other common alleles except *B*15:02* were expected to be eliminated. A sample would be identified as *HLA-B*15:02* if there was a positive band from F2&R2 (74 bp). To interpret the result, PCR products from first and second PCR were analyzed by gel electrophoresis. To avoid a false negative result, all samples must be positive from the internal control primer (150 bp) in the first PCR. In the second PCR, only positive samples from F1 and R1 will be amplified from the nested control primer (303 and/or 367 bp). The nested control primer (F3 and R1) will give a 303 bp band in the second PCR reaction. For *HLA-B*13:01*, products from F1 and R1 are fainter than other predicted

Table 2 Prediction of all possible amplified alleles and its frequencies (14) from different pairs of primers based on 10 mer from 3′ end of each primer[a]

Group	Alleles	Primers F1 and R1	Primers F2 and R2	Frequency in Thai population[b]	References	Frequency in Chinese population[c]	References
*B*13*	*B*13:01*	√		2.1–4.1	(15, 16)	3.6	(17)
	*B*13:06*	√		n/a		0.0	(18)
	*B*13:07N*	√		n/a		0.0	(18)
	*B*13:12*	√		n/a		0.0	(18)
	*B*13:13*	√		n/a		0.0	(18)
	*B*13:17*	√		n/a		n/a[d]	(19)
	*B*13:20*	√		n/a		n/a[d]	(19)
	*B*13:21*	√		n/a		n/a[d]	(19)
	*B*13:22*	√		n/a		n/a[d]	(19)
	*B*13:23*	√		n/a		n/a[d]	(19)
	*B*13:25*	√		n/a		n/a[d]	(19)
	*B*13:26*	√		n/a		n/a[d]	(19)
	*B*13:28*	√		n/a		n/a[d]	(19)
	*B*13:29*	√		n/a		n/a[d]	(19)
	*B*13:36*	√		n/a		n/a[d]	(19)
	*B*13:39*[e]	√	√	n/a		n/a[f]	
	*B*13:43*	√		n/a		n/a[f]	
	*B*13:50*	√		n/a		n/a[f]	
	*B*13:51*	√		n/a		n/a[f]	
	*B*13:52*	√		n/a		n/a[f]	
B*15	*B*15:02*	√	√	8.2–8.5	(15, 16, 20)	12.87	(21)
	*B*15:13*	√		0.1–1.8	(15, 20)	0.37	(21)
	*B*15:20*[e]	√	√	n/a		0.74	(21)
	*B*15:21*	√		0.7–1.0	(16, 20)	0.74	(21)
	*B*15:25*[g]	√	√	2.0–2.5	(15, 16)	1.84	(21)
	*B*15:36*	√		n/a		0.0	(18)
	*B*15:44*	√		n/a		0.0	(18)
	*B*15:77*[e]	√	√	n/a		0.0	(18)
	*B*15:85*[e]	√	√	n/a		0.0	(18)
	*B*15:88*[h]	√	√	n/a		0.0	(18)
	*B*15:89*	√		n/a		0.0	(18)
	*B*15:121*[h]	√	√	n/a		n/a[d]	(19)
	*B*15:139*	√		n/a		n/a[d]	(19)

© 2012 John Wiley & Sons A/S

Table 2 *Continued*

Group	Alleles	Primers F1 and R1	Primers F2 and R2	Frequency in Thai population[b]	References	Frequency in Chinese population[c]	References
	*B*15:144*[h]	√	√	n/a		n/a[d]	(19)
	*B*15:154*[g]	√	√	n/a		n/a[d]	(19)
	*B*15:194*[h]	√	√	n/a		n/a[f]	
	*B*15:204*[e]	√	√	n/a		n/a[f]	
	*B*15:213*[h]	√	√	n/a		n/a[f]	
	*B*15:214*[h]	√	√	n/a		n/a[f]	
	*B*15:223*[h]	√	√	n/a		n/a[f]	
*B*35*	*B*35:46*	√		n/a		0.0	(18)
*B*40*	*B*40:137*[e]	√	√	n/a		n/a[f]	
*B*44*	*B*44:08*	√		n/a		0.10	(17)
	*B*44:57*	√		n/a		n/a[d]	(19)
	*B*44:60*	√		n/a		n/a[d]	(19)
*B*57*	*B*57:05*	√		n/a		0.0	(18)

HLA, human leukocyte antigen; SSP-PCR, sequence-specific primer-polymerase chain reaction.

[a]To predict which alleles will be amplified from the different combinations of primers used in the nested SSP-PCR, 10 bases from 3′ end of each primer were entered into the IMGT/HLA PROBE and PRIMER Search Tool, database version 3.6 October 2011. Frequencies of all alleles were from the Allele Frequency Net Database (14).

[b]Frequency of these alleles in the Thai population both from Bangkok and from the Northeast region which has the highest population in Thailand.

[c]Frequency of these alleles in the Chinese population. Majority of the Asian population is composed of Chinese ethnicity. Because most of the data is available for the Chinese North Han population, this data is used here to determine the frequency of these alleles in the Chinese population.

[d]This data is only from Morocco Settat Chaouya population. The frequency of these alleles is 0.0%.

[e]The behavior of these primers with *HLA-B*15:25* can imply that rare alleles such as *HLA-B*13:39, 15:20, 15:77, 15:85, 15:154, 15:204* and *40:137* will not be amplified by this system.

[f]There are no frequency information about these alleles.

[g]*HLA-B*15:25* failed to be amplified by F2 and R2, which was first predicted by 10-base analysis. This is because the condition is stringent enough for nested control primer (F3 and R1) to overcome a reaction from the second PCR primer (F2 and R2). This is because nested control primer can bind 100% to *HLA-B*15:25*, whereas *HLA-B*15:25* has two mismatches near 5′ end of F2.

[h]*HLA-B*15:88, 15:121, 15:144, 15:194, 15:213, 15:214* and *15:223* are expected to be positive for both reactions. It should be noted that these alleles are extremely rare worldwide. This assay can be used to identify *HLA-B*15:02* with very low false positive results.

alleles, as there is one mismatch on F1. There are also fewer 303 bp products in the second PCR. The additional 367 bp fainted band can also be seen in *B*15:21* and *B*15:25* in the second PCR as a product from F2 and R1. It should be noted that *HLA-B*15:02* and *15:13* can be amplified by F2 and R1 much better than F3 and R1. This can be explained by a perfect match of F2 primer to these two alleles and a melting temperature of each primer. F2 (60.6°C) has the same melting temperature as R1, while F3 has 64.5°C. Interestingly, *HLA-B*15:25* failed to be amplified by F2 and R2, which was firstly predicted by 10 bases analysis. This is because the condition is stringent enough for nested control primer (F3 and R1) to overcome a reaction from the second PCR primer (F2 and R2). The nested control primer can bind 100% to *HLA-B*15:25*, whereas *HLA-B*15:25* has two mismatches near 5′ end of F2. The behavior of these primers implies that rare alleles such as *HLA-B*13:39, 15:20, 15:77, 15:85, 15:154, 15:204* and *40:137* will not be amplified by this system, which will have only *HLA-B*15:88, 15:121, 15:144, 15:194, 15:213, 15:214* and *15:223* as default amplifications.

We validated our nested PCR with 104 purified genomic DNA collected from blood or bone marrow donors from the Thai Red Cross Society, Bangkok, Thailand, which was approved by the Ethics Committee for Human Research Protection from the Faculty of Medicine, Chulalongkorn University, and consent forms were obtained from all subjects. These samples have been HLA typed by the commercial sequence-specific oligonucleotide probe-polymerase chain reaction (SSOP-PCR) (LABType® SSO B Locus, One Lambda, Inc., Canoga Park, CA). These 104 samples were then sent to us, blind. We detected 20/20 *HLA-B*1502*. Other HLA-B alleles ($n = 84$) were not detected by our system (Table 3). According to our primer design, rare alleles such as *HLA-B*15:88, 15:121, 15:144, 15:194, 15:213, 15:214* and *15:223* were also expected to be amplified from this nested SSP-PCR technique by using 10 bases from 3′ end of each primer to predict. However, these alleles are very rare worldwide, and we could not detect them, which suggests the specificity of this assay to be >99.9%, with 100% sensitivity.

Nested SSP-PCR was also performed directly from whole blood using KAPA Blood PCR Kit (Kapa Biosystems, Woburn, MA). For the first PCR reaction, a total final volume of 10 µl consisted of the following components: final concentration of 1× KAPA Blood PCR Mix B, 1.0 µM primer, 0.25 µM internal control primer and 1.0 µl of whole blood as

© 2012 John Wiley & Sons A/S

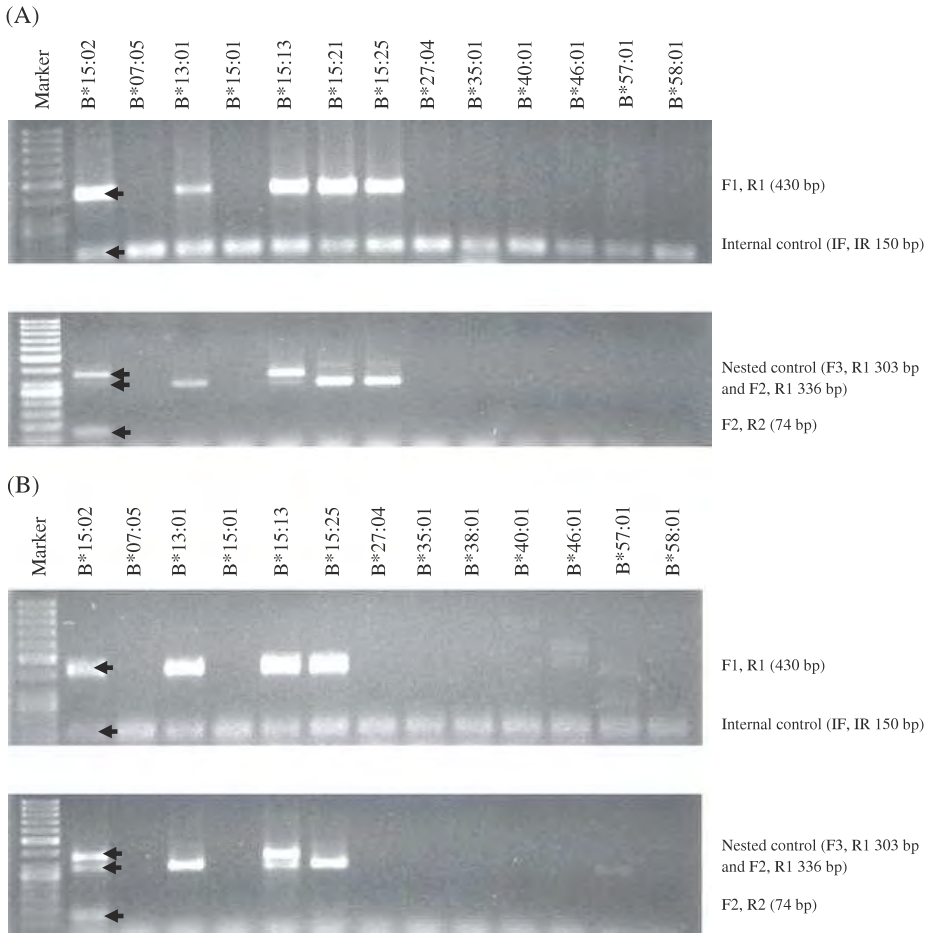

Figure 2 Migration patterns of *HLA-B*15:02* compared to other alleles. These products were detected by nested sequence-specific primer-polymerase chain reaction from both DNA (A) and whole blood samples (B). The composition of PCR from DNA the first PCR with a final volume of 10 μl contained the following components: final concentrations of 1× *Taq* buffer, 2.5 mM MgCl2, (Fermentas, Glen Burnie, MD) and total genomic DNA of 50 ng per reaction. For the second PCR, a total final volume of 10 μl reaction had the same components as the first PCR with 0.6 mM of nested control primer and had an additional 2.5 μl of 100 times diluted PCR product from the first step, region amplified by primers F1 and R1, as template. PCR cycles for both DNA and whole blood are the same. The first PCR was performed with an initial denaturation at 95°C for 5 min followed by a touchdown program of: (1) 5 cycles at 95°C for 30 s, 70°C for 30 s and 72°C for 30 s, (2) 5 cycles at 95°C for 30 s, 68°C for 30 s and 72°C for 30 s, (3) 5 cycles at 95°C for 30 s, 67.1°C for 30 s and 72°C for 30 s, (4) 10 cycles at 95°C for 30 s, 65°C for 30 s and 72°C for 30 s, and (5) 20 cycles at 95°C for 30 s, 55°C for 30 s and 72°C for 30 s. The final extension step was performed at 72°C for 5 min and later was held at 4°C. For the second PCR, denaturation was performed in one cycle at 95°C for 5 min and followed by 10 cycles at 95°C for 30 s, 70°C for 30 s and 72°C for 30 s. The final extension step was performed at 72°C for 5 min and held at 4°C. Two positive bands from the first (430 bp from F1 and R1) and second PCR (74 bp F2 and R2) will be reported as *HLA-B*15:02*. Alleles that are positive in the first step, but not *HLA-B*15:02*, will only be positive from nested control band (303 bp from F3 and R1) in the second step. Negative results will only have the internal control band (150 bp) from the first PCR. HLA, human leukocyte antigen. Arrow head (◄) indicates the expected product.

template. As for the second PCR, the same components from the first PCR were used with 0.6 mM of nested control primers and with an additional 2.5 μl of 100 times diluted PCR product from the first PCR, product amplified from using primers F1 and R1, as template. We tested our in-house nested SSP-PCR on another 96 independent blood samples from blood or bone marrow donors from the Thai Red Cross Society. These samples have been HLA typed by the commercial SSOP-PCR (LABType® SSO B Locus, One Lambda, Inc.). We were able to detect *HLA-B*15:02* in all 24 samples and another 72 samples of other *HLA-B* alleles with 100% sensitivity and >99.9% specificity (Table 3). A representative gel electrophoresis is shown in Figure 2B.

HLA-B15 group is one of the most diverse families of HLA-B alleles. Identifying a broad *HLA-B*15* group might be a good choice to avoid the use of carbamazepine. However,

© 2012 John Wiley & Sons A/S

Table 3 Numbers of samples defined by each method

Alleles[a]	Purified genomic DNA[b]	Whole blood[c]
*B*07:02*	0/2	—
*B*07:05*	0/8	0/2
*B*08:01*	0/1	—
*B*13:01*	0/8	0/15
*B*13:02*	0/4	—
*B*15:01*	0/3	0/6
*B*15:02*	20/20	24/24
*B*15:11*	0/2	—
*B*15:13*	0/1	0/1
*B*15:21*	0/1	—
*B*15:25*	0/2	0/7
*B*15:32*	0/1	0/1
*B*18:01*	0/7	0/9
*B*18:02*	0/1	0/1
*B*27:04*	0/3	0/6
*B*27:06*	0/3	—
*B*35:01*	0/4	0/2
*B*35:03*	0/2	—
*B*35:05*	0/7	—
*B*38:02*	0/5	0/4
*B*39:01*	0/1	0/3
*B*40:01*	0/8	0/12
*B*40:02*	—	0/1
*B*40:06*	0/7	—
*B*44:03*	0/7	—
*B*46:01*	0/23	0/20
*B*48:01*	0/1	0/3
*B*49:01*	0/1	—
*B*51:01*	0/4	0/5
*B*51:02*	0/1	0/2
*B*52:01*	0/5	0/3
*B*54:01*	0/1	—
*B*55:01*	0/1	—
*B*56:01*	0/1	—
*B*57:01*	0/4	0/3
*B*58:01*	0/11	0/9

HLA, human leukocyte antigen.

[a]It should also be noted that extremely rare alleles such as *HLA-B*13:39, 15:20, 15:77, 15:85, 15:88, 15:121, 15:144, 15:154, 15:194, 15:204, 15:213, 15:214, 15:223* and *40:137* were not detected in this study.

[b]The first number is the number of samples detected by the new nested PCR method using purified genomic DNA as template, and the second number shows alleles defined by SSOP commercial technique.

[c]The first number is the number of samples detected by the new nested PCR method using whole blood as template, and the second number shows alleles defined by SSOP commercial technique.

there have been false positive results for *HLA-B*15:01, 15:11, 15:12, 15:13, 15:18, 15:21, 15:25* and *15:32*, which are found in more than 1% of the Thai population. As a result, patients with false positive results of these alleles have to pay for expensive drugs that they may be allergic to. Moreover, the use of alternative drugs could result in other consequences. For example, the exposure of valproate *in utero* was associated with increased risk of impaired cognitive function at 3 years of age (13). Therefore, the development of methods to specifically and accurately detect *HLA-B*15:02* is important. Previous SSP-PCR methods have reported the use of at least six sets of primers in six separate reactions with 30 cycles from touchdown phase to detect *HLA-B*15:02* (7, 8). We report an alternative method to specifically detect *HLA-B*1502* without the use of multiple sets of primers. In this study, our in-house SSP-PCR required two reactions. With the help of nested PCR, the second reaction can specifically identify *HLA-B*15:02*. We have also validated that the use of as little as 1 μl whole blood in this alternative method gave clear and consistent results comparable to genomic DNA sampling. Although SSP-PCR is the most cost effective method, its DNA extraction step can become expensive depending on which DNA extraction kit is used. In addition, if a cheaper alternative technique such as a standard salting out method is used to extract DNA, this can result in a longer turnaround time. However, the nested SSP-PCR method carries a contamination risk, and it should be tightly controlled. Further development into a single closed tube is recommended.

In conclusion, *HLA-B*15:02* can be identified by our in-house nested SSP-PCR method with 100% sensitivity and >99.9% specificity, from both purified DNA and whole blood. This technique also requires a smaller amount of the starting material compared to other methods. Patient benefits include the prevention of adverse events from taking carbamazepine, lower costs and shorter turnaround time.

Acknowledgments

This work was supported by the 90th Anniversary of Chulalongkorn University Fund (Ratchadaphiseksomphot Endowment Fund) and the Thailand Research Fund (Senior Research Scholar Grant – RTA5280002).

Conflict of interest

The authors have declared no conflicting interests.

References

1. Chung WH, Hung SI, Hong HS et al. Medical genetics: a marker for Stevens-Johnson syndrome. *Nature* 2004: **428**: 486.
2. Chung WH, Hung SI, Chen YT. Human leukocyte antigens and drug hypersensitivity. *Curr Opin Allergy Clin Immunol* 2007: **7**: 317–23.
3. Man CB, Kwan P, Baum L et al. Association between HLA-B*1502 allele and antiepileptic drug-induced cutaneous reactions in Han Chinese. *Epilepsia* 2007: **48**: 1015–8.
4. Locharernkul C, Loplumlert J, Limotai C et al. Carbamazepine and phenytoin induced Stevens-Johnson syndrome is associated

© 2012 John Wiley & Sons A/S

with HLA-B*1502 allele in Thai population. *Epilepsia* 2008: **49**: 2087–91.
5. Alfirevic A, Jorgensen AL, Williamson PR, Chadwick DW, Park BK, Pirmohamed M. HLA-B locus in Caucasian patients with carbamazepine hypersensitivity. *Pharmacogenomics* 2006: **7**: 813–8.
6. Ferrell PB Jr, McLeod HL. Carbamazepine HLA-B*1502 and risk of Stevens-Johnson syndrome and toxic epidermal necrolysis: US FDA recommendations. *Pharmacogenomics* 2008: **9**: 1543–6.
7. Yu N, Ohashi M, Alosco S et al. Typing of HLA-B*15 alleles using sequence-specific primers. *Tissue Antigens* 1998: **52**: 260–9.
8. Bunce M, O'Neill CM, Barnardo MC et al. Phototyping: comprehensive DNA typing for HLA-A, B, C, DRB1, DRB3, DRB4, DRB5 & DQB1 by PCR with 144 primer mixes utilizing sequence-specific primers (PCR-SSP). *Tissue Antigens* 1995: **46**: 355–67.
9. Sayer DC, Cassell HS, Christiansen FT. HLA-B*27 typing by sequence specific amplification without DNA extraction. *Mol Pathol* 1999: **52**: 300–1.
10. Bu Y, Huang H, Zhou G. Direct polymerase chain reaction (PCR) from human whole blood and filter-paper-dried blood by using a PCR buffer with a higher pH. *Anal Biochem* 2008: **375**: 370–2.
11. Kermekchiev MB, Kirilova LI, Vail EE, Barnes WM. Mutants of Taq DNA polymerase resistant to PCR inhibitors allow DNA amplification from whole blood and crude soil samples. *Nucleic Acids Res* 2009: **37**: e40.
12. Robinson J, Mistry K, McWilliam H, Lopez R, Parham P, Marsh SG. The IMGT/HLA database. *Nucleic Acids Res* 2011: **39**: D1171–6.
13. Meador KJ, Baker GA, Browning N et al. Cognitive function at 3 years of age after fetal exposure to antiepileptic drugs. *N Engl J Med* 2009: **360**: 1597–605.
14. Gonzalez-Galarza FF, Christmas S, Middleton D, Jones AR. Allele frequency net: a database and online repository for immune gene frequencies in worldwide populations. *Nucleic Acids Res* 2011: **39**: D913–9.
15. Chandanayingyong D. HLA class II (DRB1, DQA1 and DQB1) allele and haplotype frequencies among HIV infected discordant couples in thais. *7th Asia-Oceania Histocompatibility Workshop and Conference. Karuizawa, Japan, 2003*.
16. Pimtanothai N, Charoenwongse P, Mutirangura A, Hurley CK. Distribution of HLA-B alleles in nasopharyngeal carcinoma patients and normal controls in Thailand. *Tissue Antigens* 2002: **59**: 223–5.
17. Yang G, Deng YJ, Hu SN et al. HLA-A, -B, and -DRB1 polymorphism defined by sequence-based typing of the Han population in Northern China. *Tissue Antigens* 2006: **67**: 146–52.
18. Hu ZH, Liu ZH, Xiong YJ et al. A novel HLA-DRB1*15 allelic sequence isolated from the Han population of Guangdong, China. *Int J Immunogenet* 2005: **32**: 221–2.
19. Canossi A, Piancatelli D, Aureli A et al. Correlation between genetic HLA class I and II polymorphisms and anthropological aspects in the Chaouya population from Morocco (Arabic speaking). *Tissue Antigens.* 2010: **76**: 177–93.
20. Romphruk AV, Romphruk A, Kongmaroeng C, Klumkrathok K, Paupairoj C, Leelayuwat C. HLA class I and II alleles and haplotypes in ethnic Northeast Thais. *Tissue Antigens* 2010: **75**: 701–11.
21. Yang G, Deng YJ, Qin H et al. HLA-B*15 subtypes distribution in Han population in Beijing, China, as compared with those of other populations. *Int J Immunogenet* 2010: **37**: 205–12.

© 2012 John Wiley & Sons A/S

ORGANIC LETTERS

2012
Vol. 14, No. 6
1440–1443

Pyrrolidinyl Peptide Nucleic Acid Homologues: Effect of Ring Size on Hybridization Properties

Woraluk Mansawat,[†] Chotima Vilaivan,[†] Árpád Balázs,[‡] David J. Aitken,[‡] and Tirayut Vilaivan*,[†]

Organic Synthesis Research Unit, Department of Chemistry, Faculty of Science, Chulalongkorn University, Phayathai Road, Patumwan, Bangkok 10330, Thailand, and Laboratoire de Synthèse Organique & Méthodologie, ICMMO – CNRS UMR 8182, Université Paris-Sud, 15 rue Georges Clemenceau, 91405 Orsay cedex, France

vtirayut@chula.ac.th

Received January 23, 2012

ABSTRACT

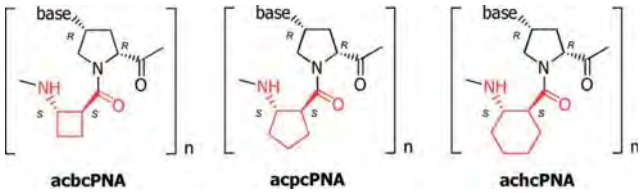

The effect of ring size of four- to six-membered cyclic β-amino acid on the hybridization properties of pyrrolidinyl peptide nucleic acid with an alternating α/β peptide backbone is reported. The cyclobutane derivatives (acbcPNA) show the highest T_m and excellent specificity with cDNA and RNA.

Nucleic acids form higher order structures in a predictable fashion as a result of the highly specific Watson–Crick type base pairing. This property is essential for the function of nucleic acids in the storage and transfer of genetic information in all living organisms. It is also the basis of various applications, ranging from biomedical sciences through biotechnologies to material sciences.[1] In recent years, there has been considerable interest in the design of alternative nucleic acid recognition systems that may offer advantages over DNA or RNA in terms of chemical stability, binding affinities, and/or specificities toward different types of nucleic acids. Peptide nucleic acid (PNA) is a class of nucleic acid analogues in which a peptide-like backbone replaces the deoxyribose-phosphate backbone of DNA. In addition to being able to recognize its cDNA/RNA with high affinity and sequence specificity, the electrostatically neutral nonphosphate backbone of PNA gives rise to a number of unique properties not observed in other classes of DNA analogues, such as complete resistance to nucleases and the relative insensitivity of PNA·DNA hybrids to ionic strength.[2] Conformational restriction of the *N*-aminoethylglycyl backbone of the original PNA (now known as aegPNA), for example, by incorporation of a cyclic moiety or one or more substituents along the PNA backbone, can provide PNA with an improved binding affinity as well as specificity.[3−5]

[†] Chulalongkorn University.
[‡] Université Paris-Sud.

(1) Reviews: (a) Silverman, S. K. *Angew. Chem., Int. Ed.* **2010**, *49*, 7180–7201. (b) Aldaye, F. A.; Palmer, A. L.; Sleiman, H. F. *Science* **2008**, *321*, 1795–1799. (c) Seeman, N. C. *Mol. Biotechnol.* **2007**, *37*, 246–257. (d) Leumann, C. J. *Bioorg. Med. Chem.* **2002**, *10*, 841–854.

(2) (a) Nielsen, P. E. *Chem. Biodiversity* **2010**, *7*, 796–804. (b) Lundin, K. E.; Good, L.; Strömberg, R.; Gräslund, A.; Smith, C. I. E. *Adv. Genet.* **2006**, *56*, 1–51. (c) Egholm, M.; Buchardt, O.; Christensen, L.; Behrens, C.; Freier, S. M.; Driver, D. A.; Berg, R. H.; Kim, S. K.; Norden, B.; Nielsen, P. E. *Nature* **1993**, *365*, 566–568.

(3) Reviews: (a) Corradini, R.; Sforza, S.; Tedeschi, T.; Totsingan, F.; Manicardi, A.; Marchelli, R. *Curr. Top. Med. Chem.* **2011**, *11*, 1535–1554. (b) Efimov, V. A.; Aralov, A. V.; Chakhmakhcheva, O. G. *Russ. J. Bioorg. Chem.* **2010**, *36*, 663–683. (c) Kumar, V. A.; Ganesh, K. N. *Acc. Chem. Res.* **2005**, *38*, 404–412.

(4) Selected examples of PNA incorporating cyclic structures in the backbone: (a) Pokorski, J. K.; Witschi, M. A.; Purnell, B. L.; Appella, D. H. *J. Am. Chem. Soc.* **2004**, *126*, 15067–15073. (b) Govindaraju, T.; Kumar, V. A.; Ganesh, K. N. *J. Am. Chem. Soc.* **2005**, *127*, 4144–4145.

(5) Selected examples of PNA with backbone substituents: (a) Dragulescu-Andrasi, A.; Rapireddy, S.; Frezza, B. M.; Gayathri, C.; Gil, R. G.; Ly, D. H. *J. Am. Chem. Soc.* **2006**, *128*, 10258–10267. (b) Englund, E. A.; Appella, D. H. *Angew. Chem., Int. Ed.* **2007**, *46*, 1414–1418. (c) Manicardi, A.; Calabretta, A.; Bencivenni, M.; Tedeschi, T.; Sforza, S.; Corradini, R.; Marchelli, R. *Chirality* **2010**, *22*, E161–E172.

10.1021/ol300190u © 2012 American Chemical Society
Published on Web 02/29/2012

Inspired by the discovery that oligomers of cyclic β-amino acids can adopt well-defined helical conformations,[6,7] we previously developed a series of pyrrolidinyl PNA with an α/β peptide backbone consisting of an alternating sequence of nucleobase-modified proline and cyclic β-amino acid "spacer" such as 1-aminopyrrolidinecarboxylic acid (dapcPNA)[8] or 2-aminocyclopentanecarboxylic acid (acpcPNA).[9] These pyrrolidinyl PNAs bind to DNA with higher affinity and sequence specificity compared to aegPNA.[10] They also exhibited some unusual features, including the preference for binding to DNA over RNA as well as the inability to form self-hybrids. The failure of pyrrolidinyl PNA carrying acyclic spacers to recognize DNA/RNA targets[11] suggested that the cyclic five-membered ring spacer locks the conformation of the PNA into a form that is close to optimal for DNA binding. The work carried out so far has been limited to a five-membered ring spacer, and in order to gain further insight into the structural properties of these pyrrolidinyl PNA, an investigation of the effect of the ring size of the spacer part was warranted. Modification of the ring size should change both the rigidity and the torsional angle (θ) of the NH−C2−C1−CO which is an integral part of the PNA backbone[7] and could in turn significantly affect the hybridization properties of the resulting PNA.

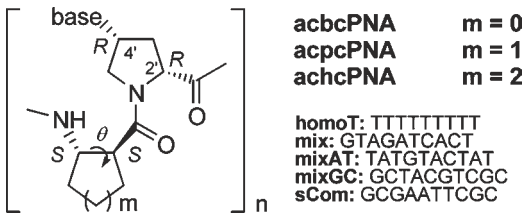

Figure 1. Structures and sequences of PNA.

We now report on the behavior of two new PNA manifolds, which incorporate 2-aminocyclobutanecarboxylic acid (ACBC) or 2-aminocyclohexanecarboxylic acid (ACHC) spacers, referred to here as acbcPNA and achcPNA respectively, and compare them with acpcPNA which contains a 2-aminocyclopentanecarboxylic (ACPC) spacer (Figure 1). Since the (1*S*,2*S*) configuration was previously found to be optimal for the ACPC spacer,[9] the same (1*S*,2*S*) configuration was a logical starting point for the new ring systems. Thus, the Fmoc-derivative of (1*S*,2*S*)-ACBC[12] was prepared, along with the known Fmoc-(1*S*,2*S*)-ACHC,[13] and each of these derivatives was combined with the (4′*R*)-nucleobase-modified (2′*R*)-proline employing the Fmoc solid-phase peptide synthesis previously developed[14] to give eight new pyrrolidinyl PNA sequences as shown in Table S1, Supporting Information. All of these pyrrolidinyl PNA possess the same (2′*R*,4′*R*) configuration at the proline part except for ***epi*-acbcPNA-sCom**. This latter PNA, with a (2′*R*,4′*S*) configuration, was synthesized in order to investigate the self-pairing abilities not observed in the (2′*R*,4′*R*) epimer of acpcPNA.[15] The PNA was purified by HPLC (>90% purity), and the identities confirmed by matrix-assisted laser desorption ionization time-of-flight (MALDI-TOF) mass spectrometry. It is noteworthy that the intrinsically labile ACBC[16] is compatible with the basic conditions required during Fmoc group removal and nucleobase side chain deprotection procedures.

Table 1. Thermal Stabilities of DNA and RNA Hybrids of Homologous Pyrrolidinyl PNA[a]

entry	PNA	apDNA	pDNA	apRNA	pRNA
1	**acbcPNA-homoT**	73.8	–	n.d.	n.d.
		(72.5)	–	–	–
2	**acbcPNA-mixAT**	63.2	<20	50.8	25.8
		(54.2)	(<20)	(32.6)	(<20)
3	**acbcPNA-mix**	66.1	<20	58.2	31.7
		(53.3)	(<20)	(42.3)	(<20)
4	**acbcPNA-mixGC**	69.8	34.1	62.9	48.6
		(54.5)	(<20)	(48.0)	(32.9)
5	**achcPNA-homoT**	<20	–	n.d.	n.d.
		(72.5)	–	–	–
6	**achcPNA-mix**	<20	<20	<20	<20
		(53.3)	(<20)	(42.3)	(<20)

[a] T_m values of the corresponding acpcPNA hybrids under identical conditions[9] are shown in parentheses, and ap and p are antiparallel and parallel, respectively. Conditions: 10 mM sodium phosphate buffer pH 7.0, 100 mM NaCl, and [PNA] = [DNA] = 1 μM. T_m values are accurate to within ±0.5 °C.

The hybridization properties of **acbcPNA-homoT** and **achcPNA-homoT** with cDNA (dA_9) were investigated by thermal denaturation experiments (monitored by UV−vis at 260 nm) (Table 1, entries 1 and 5). A well-defined thermal denaturation curve was observed only with **acbcPNA-homoT**. The melting temperature (T_m) of

(6) (a) Appella, D. H.; Christianson, L. A.; Klein, D. A.; Powell, D. R.; Huang, X.; Barchi, J. J., Jr.; Gellman, S. H. *Nature* **1997**, *387*, 381–382. (b) Cheng, R. P.; Gellman, S. H.; DeGrado, W. F. *Chem. Rev.* **2001**, *101*, 3219–3232.

(7) (a) Vasudev, P. G.; Chatterjee, S.; Shamala, N.; Balaram, P. *Chem. Rev.* **2011**, *111*, 657–687. (b) Fülöp, F.; Martinek, T. A.; Tóth, G. K. *Chem. Soc. Rev.* **2006**, *35*, 323–334.

(8) Vilaivan, T.; Lowe, G. *J. Am. Chem. Soc.* **2002**, *124*, 9326–9327.

(9) (a) Vilaivan, T.; Srisuwannaket, C. *Org. Lett.* **2006**, *8*, 1897–1900. (b) Vilaivan, C.; Srisuwannaket, C.; Ananthanawat, C.; Suparpprom, C.; Kawakami, J.; Yamaguchi, Y.; Tanaka, Y.; Vilaivan, T. *Artif. DNA: PNA XNA* **2011**, *2*, 50–59.

(10) Ananthanawat, C.; Vilaivan, T.; Hoven, V. P.; Su, X. *Biosens. Bioelectron.* **2010**, *25*, 1064–1069.

(11) (a) Vilaivan, T.; Suparpprom, C.; Harnyuttanakorn, P.; Lowe, G. *Tetrahedron Lett.* **2001**, *42*, 5533–5536. (b) Vilaivan, T.; Suparpprom, C.; Duanglaor, P.; Harnyuttanakorn, P.; Lowe, G. *Tetrahedron Lett.* **2003**, *44*, 1663–1666. (c) Ngamwiriyawong, P.; Vilaivan, T. *Nucleosides, Nucleotides Nucleic Acids* **2011**, *30*, 97–112.

(12) (a) Fernandes, C.; Pereira, E.; Faure, S.; Aitken, D. J. *J. Org. Chem.* **2009**, *74*, 3217–3220. (b) Declerck, V.; Aitken, D. J. *Amino Acids* **2011**, *41*, 587–595.

(13) (a) Schinnerl, M.; Murray, J. K.; Langenhan, J. M.; Gellman, S. H. *Eur. J. Org. Chem.* **2003**, 721–726. (b) Xu, D.; Prasad, K.; Repič, O.; Blacklock, T. J. *Tetrahedron: Asymmetry* **1997**, *8*, 1445–1451.

(14) Lowe, G.; Vilaivan, T. *J. Chem. Soc., Perkin Trans. 1* **1997**, 555–560.

(15) Taechalertpaisarn, J.; Sriwarom, P.; Boonlua, C.; Yotapan, N.; Vilaivan, C.; Vilaivan, T. *Tetrahedron Lett.* **2010**, *51*, 5822–5826.

(16) Aitken, D. J.; Gauzy, C.; Pereira, E. *Tetrahedron Lett.* **2004**, *45*, 2359–2361.

73.8 °C is comparable to that of acpcPNA with the same sequence (72.5 °C). Circular dichroism (CD) experiments also clearly confirmed that the **acbcPNA-homoT**, but not **achcPNA-homoT**, could form a stable hybrid with dA_9 (Figure S9, Supporting Information). The melting curve of the hybrid between **acbcPNA-homoT** and dA_9, as monitored by CD spectroscopy, was in good agreement with that obtained from UV−vis experiments (Figure 2).

Although homopyrimidine PNAs generally form $(PNA)_2$·DNA triplexes by Watson−Crick/Hoogsteen base pairing,[17] UV and CD titrations of **acbcPNA-homoT** and dA_9 (Figure S10, Supporting Information) clearly showed that only the 1:1 duplex was formed. The lack of triplex formation is analogous to acpcPNA, which may be ascribed to the steric repulsion of the bulky acpcPNA/acbcPNA backbone that destabilizes such triplexes.[9]

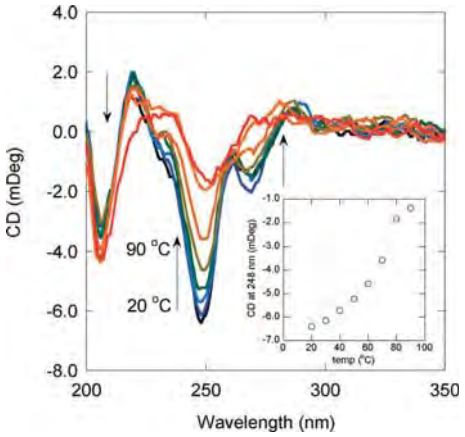

Figure 2. CD spectra of hybrid of **acbcPNA-homoT** and dA_9 at different temperatures (a) and change of CD signal at 248 nm as a function of temperature (b). Conditions: 10 mM sodium phosphate buffer pH 7.0, 100 mM NaCl, and [PNA] = [DNA] = 1 μM.

The binding studies of a mixed sequence PNA with DNA and RNA in both antiparallel and parallel orientations were performed on three different acbcPNA sequences with various G+C contents (**acbcPNA-mixAT**, **acbcPNA-mix**, **acbcPNA-mixGC**) and one achcPNA sequence (**achcPNA-mix**) (Table 1 and Figure S11, Supporting Information). The results were compared with the corresponding T_m values from acpcPNA with identical sequences.[9] Several important observations were made. First, the acbcPNA binds to DNA and RNA preferentially in an antiparallel direction, although it can also form quite stable parallel acbcPNA·RNA hybrids. Second, both acbcPNA·DNA and acbcPNA·RNA hybrids show higher thermal stabilities than the corresponding acpcPNA hybrids. The extent of T_m increase depends on G+C content, ranging from 9 °C (20% G+C) to 15 °C (70% G+C) in acbcPNA·DNA hybrids and from 15 °C (70% G+C) to 18 °C (20% G+C) in acbcPNA·RNA hybrids. Third, the general preference for binding to DNA over RNA in the original acpcPNA was still observed in acbcPNA. Finally, the achcPNA with a mix sequence (**achcPNA-mix**) did not show any binding to cDNA or RNA in both antiparallel and parallel orientations.

The results from T_m experiments were also further confirmed by CD spectroscopy. The binding of **acbcPNA-mix** to antiparallel DNA, antiparallel RNA and parallel RNA resulted in a significant change in CD spectra compared to the sum of each component (Figure S12, Supporting Information). On the other hand, no such change was observed upon binding of **acbcPNA-mix** to parallel DNA as well as in all DNA and RNA hybrids with **achcPNA-mix** (Figure S13, Supporting Information).

Table 2. Thermal Stabilities of Mismatched DNA Hybrids of **acbcPNA-mix**

entry	DNA (5′→3′)	T_m (°C)[a]	ΔT_m (°C)[b]
1	dAGTGATCTAC	66.1 (53.3)	–
2	dAGTAATCTAC	40.4 (26.4)	−25.7 (−26.9)
3	dAGTTATCTAC	40.6 (27.8)	−25.5 (−25.5)
4	dAGTCATCTAC	42.8 (31.0)	−23.3 (−22.3)
5	dAGTGGTCTAC	36.4 (23.9)	−29.4 (−29.5)
6	dAGTGTTCTAC	46.6 (29.4)	−19.5 (−23.9)
7	dAGTGCTCTAC	39.8 (23.8)	−26.3 (−29.5)
8	dAGTGAGCTAC	46.0 (26.5)	−20.1 (−26.8)
9	dAGTGAACTAC	47.0 (28.4)	−19.1 (−24.9)
10	dAGTGACCTAC	45.1 (28.8)	−21.0 (−24.5)
11	dAGTGATGTAC	41.2 (26.4)	−24.9 (−26.9)
12	dAGTGATATAC	38.3 (24.2)	−27.8 (−29.1)
13	dAGTGATTTAC	44.6 (28.5)	−21.5 (−24.8)

[a] T_m values of the corresponding acpcPNA hybrids under identical conditions[9] are shown in parentheses. Conditions: 10 mM sodium phosphate buffer pH 7.0, 100 mM NaCl, and [PNA] = [DNA] = 1 μM. [b] T_m (complementary) − T_m (mismatched). T_m values are accurate to within ±0.5 °C.

Specificity is perhaps one of the most important aspects of any nucleic acid recognition systems. The T_m of hybrids between the PNA **acbcPNA-mix** and various DNA targets carrying a mismatched base at the positions 4−7 (Table 2) showed that the specificity (determined from the difference of T_m values between mismatched and cDNA hybrids) was comparable to acpcPNA. A T_m decrease of >20 °C was observed in all but two cases (pT·dT and pA·dA mismatch, which showed ΔT_m of −19.5 and −19.1 °C, respectively). This level of mismatch discrimination is better than the corresponding DNA and the original aegPNA (typical ΔT_m −10 to −14 °C).[2]

Another unique property of acpcPNA is the inability to form self-pairing hybrids between two complementary acpcPNA sequences.[9] This could lead to a number of useful applications in targeting DNA duplexes by a double duplex invasion mechanism that has been traditionally achieved with pseudocomplementary aegPNA bearing modified bases (2,4-diaminopurine/2-thiouracil).[18]

(17) Kim, S. K.; Nielsen, P. E.; Egholm, M.; Buchardt, O.; Berg, R. H.; Nordén, B. *J. Am. Chem. Soc.* **1993**, *115*, 6477–6481.

(18) Lohse, J.; Dahl, O.; Nielsen, P. E. *Proc. Natl. Acad. Sci. U.S.A.* **1999**, *96*, 11804–11808.

According to UV and CD melting studies, the PNA **acpcPNA-sCom** with a 10-mer self-complementary sequence showed no cooperative melting. On the other hand, **acbcPNA-sCom** showed a broad UV melting curve with apparent T_m of ca. 45 °C. At 20 °C, the same PNA showed a positive CD signal at 260 nm and a strong negative CD signal at 280 nm, which is distinctly different from the CD spectra of nonself-complementary acbcPNA (compare Figures S12 and S16, Supporting Information). These signals disappeared upon heating and reappeared upon cooling. The results suggest that **acbcPNA-sCom** can form a self-complementary hybrid. We also synthesized the (2′*R*,4′*S*) epimer of both acbcPNA and acpcPNA to compare the self-pairing behavior with the "normal" acpcPNA and acbcPNA. As shown in Table 3 and Figures S15 and S16, Supporting Information, the ***epi*-acbcPNA-sCom** self-pairing hybrid was considerably more stable than the corresponding ***epi*-acpcPNA-sCom** self-pairing hybrid. All self-complementary pyrrolidinyl PNAs can form stable hybrids with DNA with T_m values in the range of 67 °C (acpcPNA) to 73−78 °C (acbcPNA). In all cases, the PNA·DNA hybrids are more stable than the PNA·PNA hybrids at the same total strands concentration. The difference between T_m of PNA·DNA and PNA·PNA hybrids is smallest in *epi*-acbcPNA (ΔT_m = 14 °C) and greatest in acpcPNA (ΔT_m > 46 °C).

Table 3. Thermal Stabilities of Self-Complementary and DNA Hybrids of acbcPNA and acpcPNA[a]

entry	PNA	config	T_m self	T_m apDNA
1	**acbcPNA-sCom**	2′*R*,4′*R*	45.7	77.7
2	**acpcPNA-sCom**	2′*R*,4′*R*	<20	66.8
3	***epi*-acbcPNA-sCom**	2′*R*,4′*S*	59.3	73.3
4	***epi*-acpcPNA-sCom**	2′*R*,4′*S*	32.7	66.8

[a] Conditions: 10 mM sodium phosphate buffer pH 7.0, 100 mM NaCl, and [PNA] = 2 μM (self-hybridization) or [PNA] = [DNA] = 1 μM (PNA·DNA hybridization). T_m values are accurate to within ±0.5 °C.

Since the absence of NH in proline residues does not allow the formation of regular 11- and 14/15-helices usually observed in α/β peptides,[19] the preorganization into helical conformations of these α/β pyrrolidinyl PNA should be governed by the limited conformational space available to the cyclic β-amino acid spacer rather than hydrogen bonding. Based on our previous molecular dynamics simulations,[20] the origin of stabilization of acbcPNA·DNA relative to acpcPNA·DNA hybrids might be explained by a more favorable preorganization of acbcPNA as follows: Models of dapcPNA and acpcPNA showed the values of torsional angle NH−C2−C1−CO (θ) (Figure S17, Supporting Information) of the D-APC and (*S*,*S*)-ACPC spacers of 99.2 ± 6.4° and 99.2 ± 3.1° (averaged from 10 D-APC and 13 ACPC residues, respectively). A relatively large difference between these values compared to the corresponding θ figure from an X-ray structure of (*R*,*R*)-ACPC oligomer (−85.9 ± 12.2°; averaged from 6 residues)[21] suggests that there must be a substantial conformational reorganization of the ACPC moiety to allow optimal binding to DNA. While the five-membered ring of ACPC is flexible enough to allow this, there is an entropic penalty associated with the conformational reorganization process. On the other hand, the torsional angle θ obtained from an X-ray structure of (*R*,*R*)-ACBC oligomer (−95.5 ± 3.7°; averaged from 8 residues)[22] is closer to the optimal θ values shown above. Hence, the acbcPNA is better preorganized for binding to DNA when compared to acpcPNA. The torsional angle θ of ACHC obtained from an X-ray structure of (*S*,*S*)-ACHC hexamer was in the range of only 51.5−61.4°.[23] The large deviation from the optimal θ, together with the rigidity of the cyclohexane ring system which does not allow efficient conformational reorganization, should explain the inability of achcPNA to pair with DNA. The origin of the greater stabilization of acbcPNA·RNA compared to acpcPNA·RNA hybrids cannot be explained without further structural information, but the ability to bind strongly to RNA in addition to DNA clearly suggests potential of applications of acbcPNA involving RNA targets.

In conclusion, we have successfully synthesized homologues of acpcPNA with four-membered ring (acbcPNA) and six-membered ring (achcPNA) spacers. The replacement of ACPC with ACBC resulted in a new pyrrolidinyl PNA with general binding properties similar to acpcPNA but with an increase of T_m with cDNA and RNA hybrids by 0.9−1.8 °C per modification without compromising the specificity. In contrast, the replacement of ACPC with ACHC resulted in total loss of binding to both DNA and RNA. The results are explained by a more favorable conformational preorganization of the ACBC residue compared to ACPC and ACHC.

Acknowledgment. Financial supports to this work come from the Thailand Research Fund (RTA5280002) (to T.V.) and the Ratchadaphiseksomphot Endowment Fund from Chulalongkorn University (postdoctoral fellowship to W.M.).

Supporting Information Available. Synthesis of Fmoc-(1*S*,2*S*)-ACBC-OH and NMR spectra, analytical HPLC and MALDI-TOF mass spectral data of PNA, and additional UV and CD spectra. This material is available free of charge via the Internet at http://pubs.acs.org.

The authors declare no competing financial interest.

(19) Choi, S. H.; Guzei, I. A.; Spencer, L. C.; Gellman, S. H. *J. Am. Chem. Soc.* **2008**, *130*, 6544–6550.
(20) Siriwong, K.; Chuichay, P.; Saen-oon, S.; Suparpprom, C.; Vilaivan, T.; Hannongbua, S. *Biochem. Biophys. Res. Commun.* **2008**, *372*, 765–771.
(21) Appella, D. H.; Christianson, L. A.; Klein, D. A.; Richards, M. R.; Powell, D. R.; Gellman, S. H. *J. Am. Chem. Soc.* **1999**, *121*, 7574–7581.
(22) Fernandes, C.; Faure, S.; Pereira, E.; Théry, V.; Declerck, V.; Guillot, R.; Aitken, D. J. *Org. Lett.* **2010**, *12*, 3606–3609.
(23) Appella, D. H.; Christianson, L. A.; Karle, I. L.; Powell, D. R.; Gellman, S. H. *J. Am. Chem. Soc.* **1999**, *121*, 6206–6212.

Provided for non-commercial research and education use.
Not for reproduction, distribution or commercial use.

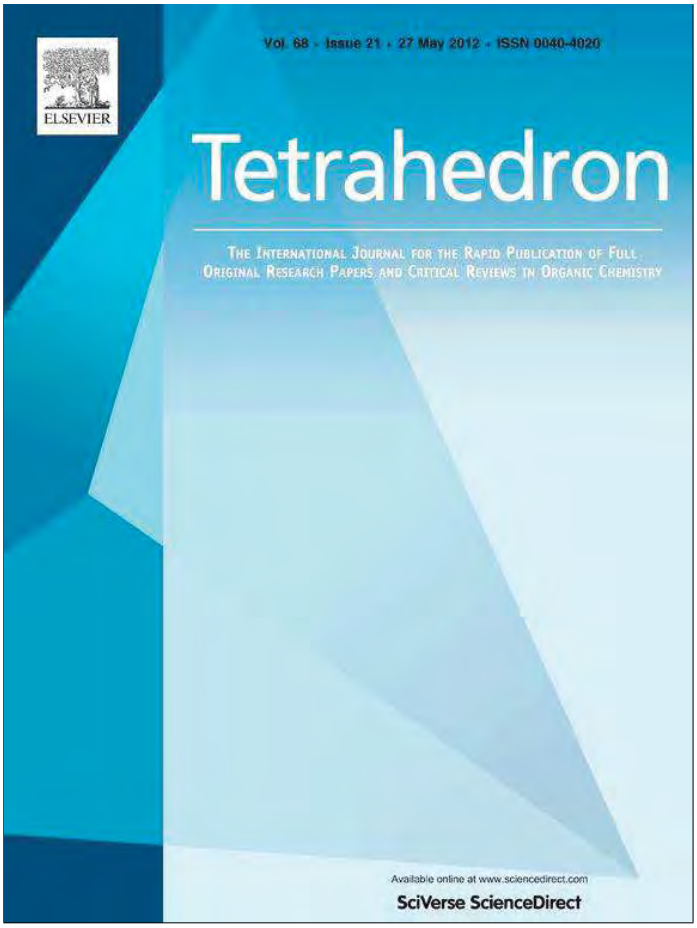

This article appeared in a journal published by Elsevier. The attached copy is furnished to the author for internal non-commercial research and education use, including for instruction at the authors institution and sharing with colleagues.

Other uses, including reproduction and distribution, or selling or licensing copies, or posting to personal, institutional or third party websites are prohibited.

In most cases authors are permitted to post their version of the article (e.g. in Word or Tex form) to their personal website or institutional repository. Authors requiring further information regarding Elsevier's archiving and manuscript policies are encouraged to visit:

http://www.elsevier.com/copyright

Author's personal copy

Tetrahedron 68 (2012) 3988–3995

Contents lists available at SciVerse ScienceDirect

Tetrahedron

journal homepage: www.elsevier.com/locate/tet

Clicked polycyclic aromatic hydrocarbon as a hybridization-responsive fluorescent artificial nucleobase in pyrrolidinyl peptide nucleic acids

Woraluk Mansawat [a], Chalothorn Boonlua [a], Khatcharin Siriwong [b], Tirayut Vilaivan [a,*]

[a] Organic Synthesis Research Unit, Department of Chemistry, Faculty of Science, Chulalongkorn University, Phayathai Road, Patumwan, Bangkok 10330, Thailand
[b] Department of Chemistry and Center for Innovation in Chemistry, Faculty of Science, Khon Kaen University, Khon Kaen 40002, Thailand

ARTICLE INFO

Article history:
Received 1 December 2011
Received in revised form 2 March 2012
Accepted 19 March 2012
Available online 28 March 2012

Keywords:
Click chemistry
Fluorescence
Polycyclic aromatic hydrocarbon
Peptide nucleic acid

ABSTRACT

Pyrene as well as other aromatic hydrocarbons could be successfully incorporated into pyrrolidinyl peptide nucleic acid bearing a D-prolyl-2-aminocyclopentane carboxylic acid backbone (acpcPNA) as a base surrogate via a triazole linker employing Cu-catalyzed alkyne–azide cycloaddition (click chemistry). The labeling can be performed via a pre-clicked pyrene monomer or by post-synthetic modification of azide-containing acpcPNA on solid support. Thermal denaturation experiments suggested that the pyrene–triazole unit can behave as a universal base in the acpcPNA system. The mode of base-pairing has been proposed based on molecular dynamics simulations. Importantly, the fluorescence spectra of the pyrene-labeled single stranded acpcPNA and its hybrid with DNA are quite different. The ratio of emissions at 380 and 460 nm changed significantly (up to a factor of 7) upon hybrid formation with complementary DNA.

© 2012 Elsevier Ltd. All rights reserved.

1. Introduction

Polycyclic aromatic hydrocarbons, such as pyrene can behave as a universal base[1] in DNA that can 'pair' against all four natural nucleobases (i.e., adenine, cytosine, guanine, and thymine) without specific preference due to the lack of hydrogen bonding.[2,3] When incorporated into peptide nucleic acid (PNA), an electrostatically neutral analogue of DNA with a peptide-like backbone, pyrene could also behave as a fluorescent universal base.[4,5] As the fluorescence properties of pyrene are very sensitive to its microenvironment, pyrene-modified DNA and PNA are potentially useful as fluorescence probes for DNA or RNA hybridization.[6] Our interest has long been focused on a conformationally restricted pyrrolidinyl PNA bearing an alternating D-proline/2-amino-cyclopentanecarboxylic acid backbone (acpcPNA).[7,8] We have demonstrated some unusual properties of this acpcPNA system[9] and have reported interesting DNA-hybridization-responsive fluorescence properties of pyrene-containing acpcPNA.[10,11]

In recent years, the copper(I)-catalyzed Huisgen azide–alkyne cycloaddition (CuAAC) reaction to give 1,4-disubstituted-1,2,3-triazole derivatives (known as 'click chemistry') has become one of the most useful tools in biomolecular research.[12–15] While it has been extensively used for conjugation of DNA with various molecules, such as dyes and other reporter groups as well as for making DNA with modified backbones[16,17] and nucleobases,[18–22] the application of click chemistry in PNA research is relatively underexplored.[23] The majority of click reactions involving PNA is usually performed via terminally azide or alkyne-labeled PNA,[24,25] although examples of internal labeling are known.[26] In this work, we have developed methods based on click chemistry to incorporate polycyclic aromatic hydrocarbons, such as pyrene as a substitute for canonical nucleobases in acpcPNA (Scheme 1). In addition, we also investigated the ability of the clicked pyrene to behave as a fluorescent universal nucleobase and have modeled the system by molecular dynamics (MD) simulations.

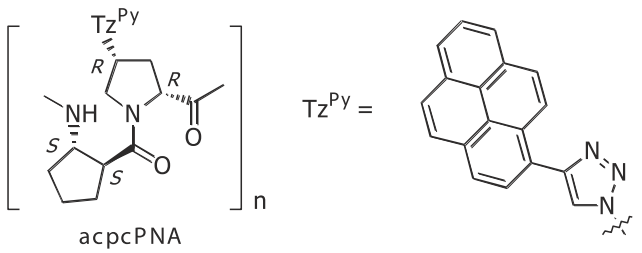

Scheme 1. Structure of acpcPNA with clicked pyrene (Tz^{Py}) as an artificial nucleobase.

* Corresponding author. Tel.: +66 2 2187627x101; fax: +66 2 2187598; e-mail address: vtirayut@chula.ac.th (T. Vilaivan).

0040-4020/$ – see front matter © 2012 Elsevier Ltd. All rights reserved.
doi:10.1016/j.tet.2012.03.062

Author's personal copy

2. Results and discussions

2.1. Synthesis of Tz^{Py} and azide building blocks

In the first method, we decided to start with the pre-clicked pyrene (Tz^{Py}) monomer to be incorporated into acpcPNA by solid phase peptide synthesis. The Fmoc-protected acpcPNA monomer (**4**) was synthesized as outlined in Scheme 2. The synthesis started from the known intermediate **1**, which was obtained in four steps from *trans*-4-hydroxy-L-proline.[27] Nucleophilic substitution with sodium azide afforded the intermediate **2** in 95% yield. The Tz^{Py} chromophore was formed by clicking 1-ethynylpyrene to the azide **2** in the presence of CuI as a catalyst in 57% yield. Subsequent cleavage of the protecting groups followed by Fmoc protection and *C*-protecting group removal gave the desired clicked pyrene acpcPNA monomer (**4**) in 68% yield over three steps from **3**. In the second method, we wished to explore the possibility of performing the click reaction after the acpcPNA synthesis but prior to the cleavage from the solid support ('post-synthetic click reaction'), hence the Fmoc-protected azide-substituted amino acid (**5**)[28] was also synthesized from **2**.

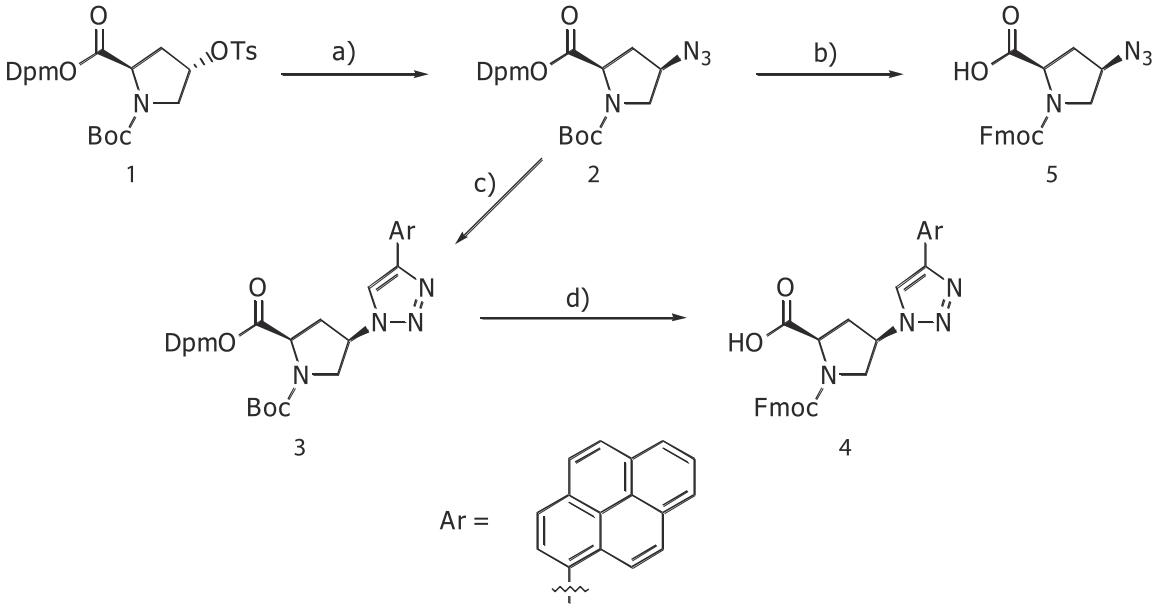

Scheme 2. Reagents and conditions: (a) NaN_3 1.1 equiv, anhydrous K_2CO_3 1.2 equiv, dry DMF, 2–3 h, 70 °C under N_2, 95%; (b) i. TFA in anisole, 2 h, rt, ii. FmocOSu 0.9 equiv, $NaHCO_3$ 2.5 equiv, CH_3CN/H_2O=1:1, overnight, rt, quantitative; (c) 1-ethynylpyrene, CuI (15 mol %), DIEA 2 equiv, CH_3CN, 12 h, 80 °C, 57%; (d) i. *p*-TsOH 3.2 equiv in CH_3CN, 3 h, rt, ii. FmocCl 1.3 equiv, DIEA 3.8 equiv, rt, 85%, iii. TFA/CH_2Cl_2=1:1 in anisole, 15 min, rt, 68%.

2.2. Solid-phase synthesis of pyrene-containing acpcPNA via a pre-formed clicked pyrene monomer

Starting from standard acpcPNA building blocks, together with the clicked pyrene monomer (**4**), the **PNA1** with a sequence of Bz-GCATTATz^{Py}AGATAC-LysNH$_2$ was successfully synthesized on a Tentagel resin equipped with a Rink amide linker employing a standard Fmoc-solid phase strategy previously developed in our laboratory.[29] The monomer **4** was incorporated using 2-(1*H*-7-azabenzotriazol-1-yl)-1,1,3,3-tetramethyluronium hexafluorophosphate (HATU) as an activator during the coupling step. The successful synthesis of the **PNA1** was confirmed by MALDI-TOF mass spectrometry (*m*/*z* calcd 4779.2; found 4782.3). The coupling efficiency per step was generally >95% as determined by spectrophotometry during the solid-phase synthesis. The low isolated yield (3.5%) was comparable to unlabeled PNA and was attributed to the loss during the HPLC purification step. The **PNA2** and **PNA3**, carrying a cytosine base (C) and an azide group (N_3) in place of the Tz^{Py}, respectively, were also synthesized by the same protocol to be used as controls (**PNA2**: *m*/*z* calcd 4621.0; found 4621.9; **PNA3**: *m*/*z* calcd 4552.9; found 4554.4).

2.3. Thermal stabilities of pyrene-containing acpcPNA–DNA hybrids

The hybridization properties of **PNA1** bearing the triazole-linked pyrene (X=Tz^{Py}) at the middle position with oligodeoxynucleotides were investigated by thermal denaturation experiments (Table 1). The complementary DNA targets containing one of the four natural nucleobases opposite to the pyrene in **PNA1** were chosen to test the ability of pyrene to behave as a universal base. The absorbance at 260 nm versus temperature plots showed sigmoidal curves in all cases, which indicated co-operative dissociation of the base pairs similar to the unmodified acpcPNA. The T_m values revealed that each of the four nucleobases in the DNA strand can pair equally well to the pyrene in the PNA strand. The T_m values range from 68.1 °C (vs dT in **DNA4**) to 69.8 °C (vs dG in **DNA1**), with a ΔT_m of 1.8 °C (Table 1, entries 1–4). On the other hand, the un-

Table 1
T_m data of **PNA1**, **PNA2**, and **PNA3** (*N*-GCATTA**X**AGATAC-*C*) and their hybrids with **DNA1-4** (5′-GTATCT**Y**TAATGC-3′)

Entry	PNA	X	DNA	Y	T_m (°C)[a]	$\Delta G_{binding}$ (kcal/mol)[b]
1	**PNA1**	Tz^{Py}	**DNA1**	G	69.8	−90.8
2		Tz^{Py}	**DNA2**	A	69.0	−88.9
3		Tz^{Py}	**DNA3**	C	68.9	−87.7
4		Tz^{Py}	**DNA4**	T	68.1	−85.2
5	**PNA2**	C	**DNA1**	G	85.0	−94.0
6		C	**DNA2**	A	72.0	−86.1
7		C	**DNA3**	C	69.0	−75.0
8		C	**DNA4**	T	65.7	−79.3
9	**PNA3**	N_3	**DNA4**	T	61.2	—

[a] Conditions: 2.5 μM PNA, 3.0 μM DNA, 10 mM sodium phosphate buffer pH 7.0.
[b] Derived from 10 ns MD trajectories using MM–GBSA method and larger negative value indicates the higher thermodynamic stability.

Author's personal copy

modified **PNA2** with a cytosine instead of the triazole-linked pyrene showed a strong preference for pairing with dG in the opposite DNA strand (**DNA1**) as shown by a high T_m of 85.0 °C (Table 1, entry 5). The three other mismatched hybrids between **PNA2** and **DNA2**–**DNA4** showed a significant decrease in the T_m values by 13.0–19.3 °C, with the pC·dC pair being the most destabilized (Table 1, entries 6–8). The T_m of the mismatched hybrids of **PNA2** are in the same range as those of **PNA1** hybrids, although the T_m range is much smaller for the latter, indicating that the Tz^{Py} acpcPNA could form stable duplexes with little discrimination between the four natural DNA bases. To confirm the active role of the Tz^{Py} in pairing with the opposite base in the DNA strand, the T_m of the **PNA3**·**DNA4** duplex was also determined. The T_m value of only 61.2 °C for this 'abasic' PNA·DNA duplex compared to the T_m of 68.1 °C (ΔT_m=6.9 °C) of the **PNA1**·**DNA4** duplex suggested that the π–π stacking provided by the triazole-linked pyrene is contributing to the duplex stabilities (Table 1, entries 4 and 9). In the case of **PNA2**·**DNA4** duplex, although the two opposite mismatched bases cannot form the Watson–Crick hydrogen bonding, there is still considerable stabilization of the duplex compared to that of the **PNA3**·**DNA4** duplex, which could also be explained by the presence of similar π–π stacking interactions.

2.4. Molecular dynamics simulations of pyrene-containing acpcPNA–DNA hybrids

To get further insight in the possible mode of pairing of the pyrenetriazole base in acpcPNA, molecular dynamics (MD) simulations were performed on various hybrids of **PNA1** and compared with **PNA2**. The $\Delta G_{binding}$ values calculated from the MD trajectories using MM–GBSA approach[30–32] are in good agreement with the thermal stabilities obtained experimentally (Table 1). The $\Delta G_{binding}$ range for the hybrids of **PNA1** with DNA is −85.2 to −90.8 kcal/mol while the corresponding figures of **PNA2** were −75.0 to −86.1 kcal/mol (mismatched hybrids) and −94.0 kcal/mol (complementary hybrid). The model of **PNA1**·**DNA1** hybrid suggests that the pyrene is not directly interacting with the opposite nucleobase in the complementary DNA strand, but rather pointing out to the major groove (Fig. 1a) probably due to the bulkiness of the pyrene ring that does not allow effective pairing with the nucleobase despite the possibilities of obtaining further stabilization due to π–π stacking. The MD structures also show additional hydrogen bonding between the triazole part and the opposite nucleobase and a stacking interaction of the pyrene part with the adjacent base A in the same PNA strand. The triazole can form up to two hydrogen bonds with base G, and form one bond with other bases (Fig. S12). The hydrogen bond distance between the acceptor (nitrogen atom of triazole) and donor (nitrogen atom of the opposite G, A, C, and T bases) averaged over 10,000 structures of each MD trajectory were 3.32±0.29, 3.23±0.25, 3.30±0.30, and 4.58±0.69 Å, respectively. Note that the criterion of hydrogen bond distance is within 3.5 Å. For **PNA1**·**DNA4** hybrid, although some simulated structures of 10 ns MD trajectory (for example, the snapshot shown in Fig. S12) exhibit the hydrogen bond interaction between triazole and thymine, the average distance of 4.58 Å implies that the hydrogen bond strength is lower compared with those of others, which could explain the lower stability of **PNA1**·**DNA4** system. Similarly, the two hydrogen bonds of Tz^{Py}-G in the duplex **PNA1**·**DNA1** may account for its higher stability than **PNA1**·**DNA2** and **PNA1**·**DNA3** duplexes, even though the average hydrogen bond distances of these two duplexes are slightly shorter. Generally, however, according to $\Delta G_{binding}$ values listed in Table 1, one can say that the stabilities of pyrene–triazole binding to nucleobases are not significantly different. The overall conformation of the Tz^{Py}-containing **PNA1**·**DNA1** hybrid is similar to the normal duplex **PNA2**·**DNA1** (Fig. 1b). The MD simulation thus clearly explains the role of the Tz^{Py} as a universal base in acpcPNA.

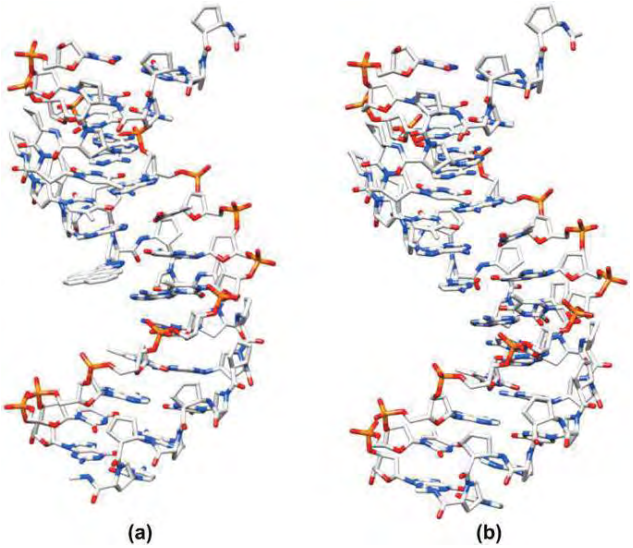

Fig. 1. Energy minimized structures of (a) **PNA1**·**DNA1** (pTz^{Py}-dG) and (b) **PNA2**·**DNA1** (pC-dG) duplexes.

2.5. Optical properties of Tz^{Py}-containing acpcPNA·DNA hybrids

It is expected that the environments of the pyrene chromophore in the single-stranded PNA should be quite different from that of its hybrid with DNA. One related study on Nielsen's type aegPNA[4] with pyrene as an artificial nucleobase showed that the fluorescence emission of the pyrene is quenched (up to fivefolds) upon hybridization to its complementary DNA and RNA targets, which was explained by stacking of the pyrene unit within the PNA·DNA or PNA·RNA duplexes. Having demonstrated that the Tz^{Py} could behave as a universal base in acpcPNA, it would be interesting to study how the optical properties of the Tz^{Py} acpcPNA change in response to the hybridization event.

Absorption spectra of the single-stranded **PNA1** showed a broad, unstructured pyrene peak with λ_{max} of ca. 350 nm due to the electronic coupling between the pyrene and the conjugated triazole (Fig. 2a). Upon excitation at 350 nm, the **PNA1** displayed an emission spectrum showing both the pyrene monomer or locally excited state (LE) bands at λ_{max}=390, 410, and 435 nm, as well as another band that appeared as a weaker, broad shoulder around 460 nm (Fig. 2b). The latter emission band could be attributed to exciplex[33] or intramolecular charge transfer (ICT) species[34,35] that are typically observed in non-polar solvents. We propose that the hydrophobic Tz^{Py} base in the single stranded acpcPNA is not free but associates with other nucleobases to avoid direct contact with water. This process is facilitated in single-stranded PNA due to the possibilities of folding of the PNA backbone into a compact structure.[36] Such folding is obviously unlikely in the much more rigid PNA–DNA duplex.

Interestingly, when the **PNA1** was hybridized with either of the complementary **DNA1**–**DNA4**, the absorption as well as the fluorescence spectra of the hybrid changed dramatically compared to the single-stranded PNA. The absorption spectra of the hybrids showed a splitting of the pyrene absorption band into two peaks of equal intensities at 354 and 368 nm. The bathochromic shift of the pyrene absorption indicated the presence of stacking interactions between the pyrene and the nucleobase, which is consistent with the MD simulation results. In addition, the CD spectrum of the

Author's personal copy

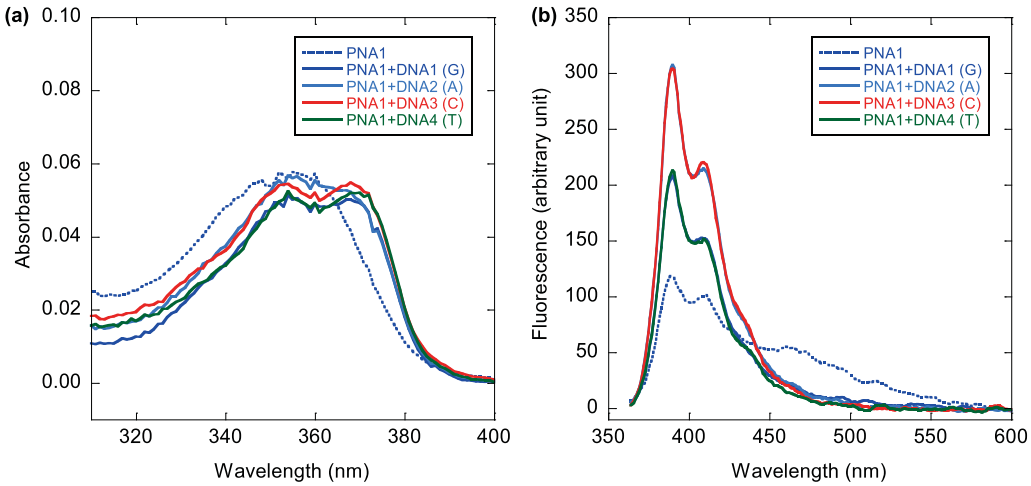

Fig. 2. Absorption (a) and fluorescence spectra (b) of **PNA1** and its hybrids with **DNA1**–**DNA4** (conditions: 2.5 μM PNA, 3.0 μM DNA in 10 mM sodium phosphate buffer pH=7.0, λ_{excit}=350 nm).

PNA1·**DNA2** hybrid showed a weak, but definite, signal in the pyrene absorption region (Fig. 3), confirming the presence of interaction between the pyrene and the nucleobase. In the fluorescence spectra, the exciplex emission disappeared upon hybridization, with a concomitant increase of the monomer emission at 390 nm (1.8–2.6-folds). The increase of the monomer emission could be ascribed to the change of the environment of the pyrene to a more hydrophilic one upon hybridization as shown by the location of the pyrene moiety in the major groove, with only one face stacking to the adjacent A base in the N-terminal direction (Fig. 1a). Although the change of emission spectra at a single wavelength is relatively small, the ratio of the monomer (390 nm) to exciplex (460 nm) emissions changed quite significantly from 2.1 in single-stranded **PNA1** to between 9.4 and 15.0 in its DNA hybrids, which translated to the response change from 4.4 to 7.0-fold (Table 2). Compared to conventional PNA with pyrene as a universal base,[4]

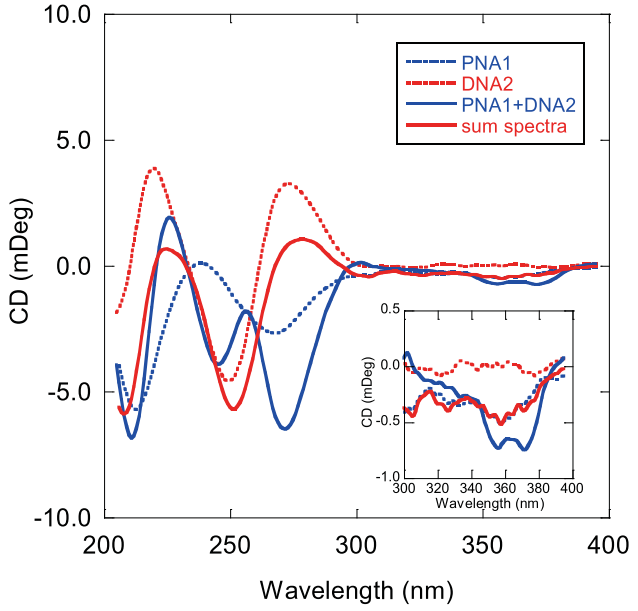

Fig. 3. CD spectra of **PNA1** and its hybrid with **DNA2** (conditions: 2.5 μM PNA, 3.0 μM DNA in 10 mM sodium phosphate buffer pH 7.0).

Table 2
Fluorescence data of **PNA1** (*N*-GCATTA**Tz**^{Py}AGATAC-*C*) and their hybrids with **DNA1**–**DNA4** (5′-GTATCT**Y**TAATGC-3′)

Entry	Y in DNA	I_{390}/I_{460}	$I_{390}/I_{390(ss)}$	$I_{460}/I_{460(ss)}$	$(I_{390}/I_{460})/(I_{390}/I_{460})_{ss}$
1	ssPNA	2.1	1.0	1.0	1.0
2	G	9.4	1.8	0.40	4.4
3	A	13.0	2.6	0.43	6.1
4	C	15.0	2.6	0.37	7.0
5	T	14.5	1.8	0.27	6.8

the present system of Tz^{Py}-modified acpcPNA behaves quite differently, and in a more advantageous way because the change in the fluorescence response can be monitored in a ratiometric fashion rather than at a single wavelength. The large difference between the monomer and exciplex emission (390 vs 460 nm) also means that not only the intensity, but also the color of the fluorescence change upon hybridization with DNA. Indeed, the fluorescence color change from green-blue to blue could even be observed by naked eyes under black light illumination (Fig. S11). Hence, the Tz^{Py} unit can behave as fluorescence universal artificial base in acpcPNA that exhibits fluorescence change upon pairing with all four natural nucleobases.

2.6. Synthesis of pyrene- and other aromatic-hydrocarbon-containing acpcPNA by post-synthetic click reactions on solid support

Although the synthesis and incorporation of the pyrenyltriazole monomer into acpcPNA were straightforward, it would be highly desirable to develop a general strategy to perform a click reaction at a later stage of the PNA synthesis. This post-synthetic click reaction would allow attachment of a diverse set of chromophores on the same azide-containing acpcPNA intermediate, such as **PNA3** without having to synthesize all the monomers and oligomers separately. To explore this new strategy, the resin-supported and fully-protected azide **PNA3**[37] was treated with 1-ethynylpyrene in the presence of Cu(I)–TBTA[38] complex in DMSO/^{t}BuOH/H_2O (3:1:1) (Scheme 3).[39] This solvent mixture was compatible with the solid support used in the PNA synthesis (Tentagel®), allowing efficient swelling to permit quantitative click reaction. The completeness of the reaction was monitored by HPLC (Fig. S9) and MALDI-TOF mass spectrometry (Fig. 4). In both

Author's personal copy

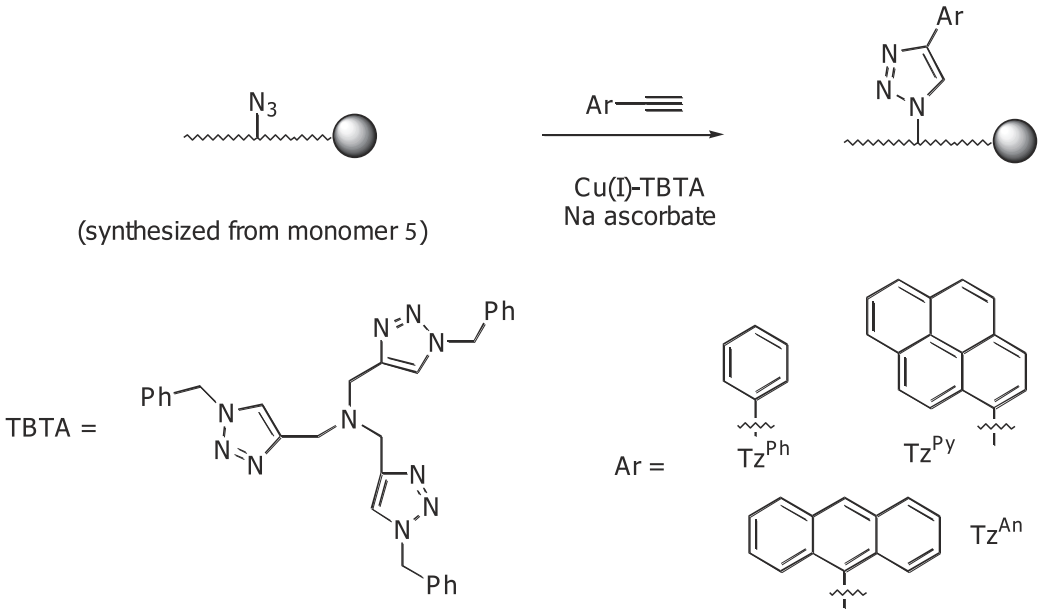

Scheme 3. Synthesis of aromatic-hydrocarbon-clicked acpcPNA via post-synthetic click reactions.

analyses, the signals due to the **PNA3** (t_R=53.0 min, m/z 4555.4) were completely absent with concomitant appearance of the new signal of the **PNA1** (t_R=62.1 min, m/z 4780.8) after a single click reaction performed overnight. The mass increase of 225.4 amu after the click reaction indicated a successful incorporation of the ethynylpyrene unit (MW 226.3). The **PNA1** prepared by this post-synthetic strategy is identical in all respects to the **PNA1** synthesized through the pre-formed monomer **4**. In addition, pyrene as well as other aromatic hydrocarbons including benzene and anthracene were successfully attached to another azide-containing PNA **PNA4** (GCATTT**N$_3$**TGATAC) via their ethynyl derivatives using the same strategy to afford **PNA5**, **PNA6**, and **PNA7**, which were labeled by pyrene-1-yl, phenyl and anthracene-9-yl triazoles, respectively (Table 3, Figs. S6–S8). While the single stranded Tz^{Ph} **PNA6** as well as its DNA hybrid is practically non-fluorescent, the Tz^{An} **PNA7** showed a weak emission at 420 nm in single stranded form, which increased only slightly upon hybridization with DNA. On the other hand, the characteristic switch between monomer/exciplex was observed in the Tz^{Py} **PNA5** and its DNA hybrid (Fig. S13), indicating the general fluorescence properties of the Tz^{Py} base irrespective of the identity of flanking bases (A/A in **PNA1** and T/T in **PNA5**).

3. Conclusion

In conclusion we had demonstrated that pyrene could be successfully incorporated into acpcPNA as a base surrogate via a triazole linker using 'click' chemistry via a pre-formed pyrene-labeled

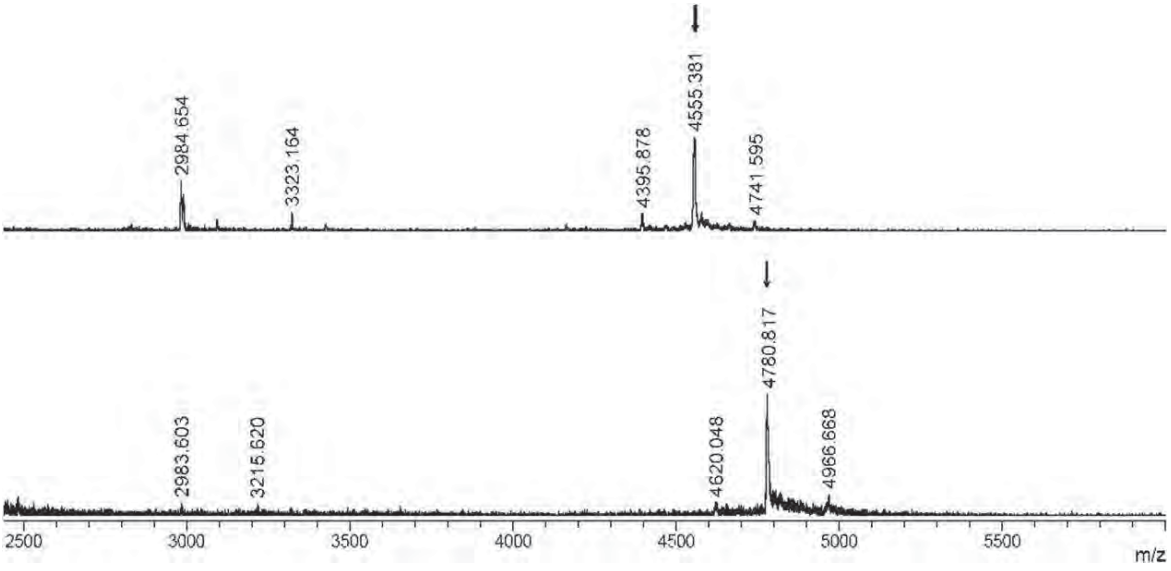

Fig. 4. MALDI-TOF mass spectra of crude **PNA3** (Bz-GCATTAN$_3$AGATAC-LysNH$_2$) before (top) and after (bottom) the on-solid-support click reaction with 1-ethynylpyrene (MW 226.3). The peaks of interest are indicated by an arrow.

Author's personal copy

Table 3
Characterization data of the clicked acpcPNA synthesized via post-synthetic click reaction

Entry	PNA	Sequence ($N\rightarrow C$)[a] GCATTY**X**YGATAC	m/z (calcd)[b]	m/z (found)[c]	Isolated yield[d] (%)
1	**PNA1**	X=Tz^{Py}; Y=A	4779.2	4779.4	4.4 (3.5)
2	**PNA5**	X=Tz^{Py}; Y=T	4761.2	4762.8	5.1
3	**PNA6**	X=Tz^{Ph}; Y=T	4637.0	4638.2	2.1
4	**PNA7**	X=Tz^{An}; Y=T	4737.1	4738.2	2.8

[a] All sequences were N-terminal benzoylated, C-terminal L-lysinamide capped.
[b] Average mass calculated for [M+H^+].
[c] MALDI-TOF, CCA matrix, linear mode.
[d] The yield in parentheses was obtained from the pre-formed monomer strategy.

monomer or by post-synthetic modification of azide-containing acpcPNA with 1-ethynylpyrene. The latter protocol allows attaching of pyrene, as well as other aromatic hydrocarbons including anthracene and benzene, to the same common azide-modified acpcPNA intermediate without the need for synthesizing each monomer separately. In addition, the click reaction protocol was conveniently carried out on the solid support, which allowed facile purification of the modified PNA from the excess reagents. Thermal denaturation experiments suggested that the pyrene–triazole unit can behave as a universal base in the acpcPNA system with little discrimination among the four canonical nucleobases. Molecular dynamics simulations suggested that the triazole can form weak hydrogen bonds with all nucleobases and that the pyrene was pointing away to the major groove rather than intercalating into the duplex. Furthermore, the fluorescence of the Tz^{Py} chromophore is sensitive to the hybridization state of the acpcPNA as shown by a significant increase of the pyrene monomer emission at 390 nm with concomitant decrease in the exciplex emission at 460 nm upon pairing with a complementary DNA carrying either A, T, C or G opposite to the pyrene.

4. Experimental section

4.1. General

Chemicals and solvents were purchased from standard suppliers and were used without further purification. RP-HPLC experiments were performed on a Water Delta 600™ HPLC system. ^{1}H and ^{13}C NMR spectra were recorded on a Bruker Avance 400 NMR spectrometer operating at 400 MHz for ^{1}H and 100 MHz for ^{13}C. MALDI-TOF mass spectra were obtained on a Microflex MALDI-TOF mass spectrometry (Bruker Daltonics) using α-cyano-4-hydroxycinnamic acid (CCA) as the matrix. High resolution mass spectra were obtained on a Bruker Daltonics micrOTOF in positive ESI mode. IR spectra were recorded on Nicolet iS10 FT-IR spectrometer.

Oligonucleotides were obtained from Biodesign (Pathumthani, Thailand) and were used as received. The concentration of oligonucleotides and acpcPNAs was determined from the absorbance at 260 nm using the reported molar extinction coefficients at 260 nm (ε_{260}) for DNA monomers.[40] The molar extinction coefficient of Tz^{Py} was obtained from the free monomer in methanol (2.84×10^4 L mol^{-1} cm^{-1}) was used for calculation of Tz^{Py}-containing acpcPNA. UV, fluorescence, and CD measurements were carried out in sodium phosphate buffer solution (10 mM, pH 7.0) using 10 mm quartz glass cuvettes. Absorption spectra and the melting temperatures (2.5 μM PNA, 3.0 μM DNA, 20–90 °C, 1.0 °C/min) were recorded on a Varian Cary 100 UV–vis spectrophotometer. CD spectra were measured on a Jasco-J815 spectropolarimeter and fluorescence spectra were measured on a Varian Eclipse spectrofluorimeter.

4.2. Synthesis

*4.2.1. N-9-Fluorenylmethoxycarbonyl-(2′R,4′R)-[4-(pyren-1-yl)triazol-1-yl]-proline (**4**).* A 50 mL round bottom flask was charged with compound **1** (0.55 g, 1 mmol), sodium azide (71.5 mg, 1.1 mmol), and anhydrous K_2CO_3 (0.17 g, 1.2 mmol) in 3 mL dry DMF. The slurry was heated at 70 °C with stirring under N_2 for 3 h. When the starting material was completely consumed (monitored by TLC), DMF was removed under reduced pressure. The reaction mixture was partitioned in dichloromethane/water and the dichloromethane layer was washed with water (three times). The organic layer was dried over Na_2SO_4 and concentrated in vacuo to get the azide intermediate **2** as a white solid (0.40 g, 95% yield); δ_H (400 MHz; $CDCl_3$) 1.26 and 1.47 (9H, 2×s, C*H*$_3$ Boc rotamers), 2.16 and 2.20 [1H, 2×m, 1×C*H*$_2$(3′) rotamers], 2.37–2.52 [1H, 2×m, 1×C*H*$_2$(3′) rotamers], 3.43 and 3.52 [1H, 2×m, 1×C*H*$_2$(5′) rotamers], 3.67 and 3.76 [1H, 2×m, C*H*$_2$(2′) rotamers], 4.15 [1H, m, C*H*(4′)], 4.43 and 4.57 [1H, 2×m, 1×C*H*(5′) rotamers], 6.90 and 6.95 (1H, 2×s, C*H*Ph$_2$ Dpm rotamers), 7.26–7.34 (10H, m, Ar C*H* Dpm). A mixture of **2** (0.40 g, 0.95 mmol), 1-ethynylpyrene (186 mg, 0.82 mmol), DIEA (0.35 mL, 2 mmol), and CuI (28.6 mg, 0.15 mmol, 15 mol %) were dissolved in CH_3CN (5 mL). The reaction mixture was heated at 80 °C under N_2 for 12 h (monitored by TLC). The solvent was removed and the residue was purified by column chromatography with EtOAc/hexanes (40:60) as eluent to obtain the Boc-protected intermediate **3** as a brown solid (0.31 g, 57% yield); δ_H (400 MHz; $CDCl_3$) 1.31 and 1.51 (9H, 2×s, C*H*$_3$ Boc rotamers), 2.53–2.72 [1H, m, 1×C*H*$_2$(3′) rotamers], 3.05–3.17 [1H, m, 1×C*H*$_2$(3′) rotamers], 3.99–4.15 [1H, m, 1×C*H*$_2$(5′) rotamers], 4.28–4.37 [1H, m, C*H*$_2$(2′) rotamers], 4.61–4.76 [1H, 2×m, 1×C*H*(5′) rotamers], 5.41–5.50 [1H, m, C*H*(4′)], 6.89 (1H, s, C*H*Ph$_2$ Dpm), 7.07–7.30 (10H, m, Ar C*H* Dpm), 8.01–8.21 (9H, m, Ar C*H* Pyrene), 8.54 and 8.56 (1H, 2×s, C*H* Triazole rotamers). Compound **3** (0.27 g, 0.42 mmol) was then treated with *p*-TsOH (254 mg, 1.3 mmol, 3.2 equiv) in CH_3CN (5 mL) at room temperature. After 3 h, the Boc protecting group was completely removed (as monitored by TLC). DIEA (0.28 mL, 1.6 mmol, 3.8 equiv) was then added to the yellow slurry formed to give a brown solution followed by FmocCl (141 mg, 0.54 mmol). The reaction was stirred at room temperature until a brownish precipitate was observed (3 h). The solvent was removed and the residue was purified by column chromatography with EtOAC/hexanes (40:60) as eluent to receive a Fmoc-protected intermediate as a light yellow solid (0.27 g, 85% yield); δ_H (400 MHz; $CDCl_3$) 2.55–2.78 [1H, m, 1×C*H*$_2$(3′) rotamers], 2.97–3.17 [1H, m, 1×C*H*$_2$(3′) rotamers], 3.90–4.77 [6H, m, C*H*$_2$(5′), CH(2′), Fmoc aliphatic C*H* and C*H*$_2$ rotamers], 5.24–5.44 [1H, m, C*H*(4′)], 6.85 and 6.91 (1H, 2×s, C*H*Ph$_2$ Dpm rotamers), 6.96–8.23 (27H, m, aromatic C*H*), 8.64 and 8.67 (1H, 2×s, C*H* Triazole rotamers). This intermediate (0.10 g, 0.13 mmol) was treated with 1:4:4 anisole/TFA/CH_2Cl_2 (2 mL) for 15 min at room temperature. After removal of the volatiles under a stream of N_2 gas, the residue was washed with Et_2O to give the product **4** as a yellow solid (54.5 mg, 68% yield). The overall yield from **1** was 31%; R_f 0.22 (EtOAc/MeOH 9:1); ν_{max} (film) 3130, 3045, 2960, 2898, 1708, 1610, 1595, 1479, 1452, 1422, 1357, 1248, 1200, 1183, 1172, 1120, 1054 cm^{-1}; $[\alpha]_D^{24}$ −5.00 (*c* 0.50, MeOH); δ_H (400 MHz; DMSO-d_6) 2.74–2.92 [1H, m, 1×C*H*$_2$(3′) rotamers], 3.05–3.21 [1H, m, 1×C*H*$_2$(3′) rotamers], 4.09–4.16 [1H, m, 1×C*H*$_2$(5′)], 4.20–4.25 [1H, m, 1×C*H*$_2$(5′)], 4.20–4.38 (3H, m, C*H* and C*H*$_2$ Fmoc), 4.44–4.48 and 4.61–4.65 [1H, 2×m, C*H*(2′) rotamers], 5.40–5.52 [1H, m, C*H*(4′)], 7.32–7.38 (2H, m, Fmoc Ar C*H*), 7.40–7.46 (2H, m, Fmoc Ar C*H*), 7.68–7.75 (2H, m, Fmoc Ar C*H*), 7.91 (2H, d, *J* 7.6, Fmoc Ar C*H*), 8.12 (1H, t, *J* 7.6, pyrene C*H*), 8.25–8.40 (7H, m, pyrene C*H*), 8.90 (1H, d, *J* 9.7, pyrene C*H*), 8.94 (1H, s, triazole C*H*); δ_C (100 MHz; DMSO-d_6) δ=34.5 and 35.5 [CH_2 (3′) rotamers], 46.6 and 46.7 (*C*H Fmoc rotamers), 50.8 and 51.4 [CH_2(5′) rotamers], 57.0 and 57.3 [*C*H(4′)

Author's personal copy

rotamers], 57.7 and 57.8 [CH(2′) rotamers], 67.0 and 67.3 [Fmoc CH_2 rotamers], 120.1 (Fmoc Ar *C*H), 123.8 (*C*), 123.9 (*C*), 124.3 (*C*), 125.0 (*C*H), 125.1 (*C*H), 125.1 (*C*H), 125.3 (Fmoc Ar *C*H), 126.5 (*C*H), 127.1 (*C*H), 127.2 (Fmoc Ar *C*H), 127.3 (*C*H), 127.7 (Fmoc Ar *C*H), 127.5 (*C*),128.0 (*C*H), 130.4 (*C*), 130.6(*C*), 130.9 (*C*), 140.7 (Fmoc Ar *C*), 143.6 (Fmoc Ar *C*), 146.3 (*C*), 153.8 (*C*O Fmoc), 172.3 and 172.8 (*C*OOH rotamers); HRMS (ESI^+) *m*/*z*: found 605.2218. $C_{38}H_{29}O_4N_4$ ($M{\cdot}H^+$) requires 605.2189.

4.2.2. Synthesis of PNA. All acpcPNA oligomers were synthesized manually from the corresponding Fmoc-protected acpcPNA monomers and β-amino acids spacers by Fmoc-solid phase peptide synthesis on a Tentagel resin equipped with an acid-labile Rink amide linker as described previously (0.5–1.5 μmol scale).[7,29] The acpcPNAs were end-capped by benzoylation. If required, the post-synthetic modification is carried out at this stage. After completion of the synthesis, the nucleobase side-chain was deprotected by treatment with 1:1 aq NH_3/dioxane at 60 °C overnight. After cleavage from the resin using 95% TFA (3×30 min), the PNA was precipitated using diethyl ether and purified by reverse-phase HPLC (C18 column 4.6×150 mm, 0.1% TFA in water/methanol gradient from 90:10 to 10:90 over 85 min with 5 min equilibration time). The purity was determined by MALDI-TOF mass spectrometry and by reverse-phase HPLC using the following conditions: C18 column 4.6×50 mm, particle size 3 μ; mobile phase *A*=0.1% TFA in water; *B*=0.1% TFA in MeCN; gradient=10–90% B over 25 min with 5 min equilibration time at a flow rate of 0.5 mL/min.

4.2.3. Post-synthetic click reaction on-solid support. The reaction vessel for solid-phase synthesis was filled with resin-supported azide PNA (0.5 μmol). 1-Ethynylpyrene (150 μL, 50 mM), tris[(1-benzyl-1*H*-1,2,3-triazol-4-yl)methyl]amine (300 μL, 100 mM), tetrakis(acetonitrile)copper(I)-hexafluorophosphate (150 μL, 100 mM) (each in DMSO/^{t}BuOH 3:1), and sodium-L-ascorbate (150 μL, 400 mM in H_2O) were added to the resin and the mixture was kept overnight at room temperature, with occasional agitation.[39] The completeness of the reaction was monitored by MALDI-TOF analysis of the sampled resin following TFA cleavage. After the starting azide PNA was completely consumed, the resin was washed with DMSO, H_2O, and MeOH (three times each) and dried under a stream of N_2 gas. Cleavage and purification was carried out as described above.

4.2.4. Molecular dynamics simulation. To get further information concerning the stability of duplexes in the molecular level, molecular dynamics (MD) simulations of **PNA1·DNA** and **PNA2·DNA** duplexes, in total eight systems, in aqueous conditions have been performed using AMBER 9 package.[41] Since the three-dimensional structure of acpcPNA is not available, its starting structure was built up based on that of the DNA·DNA duplex by one-to-one mapping of the PNA backbone atoms onto DNA backbone atoms. The coordinates of the missing atoms were added using geometric calculation. To improve the structure of this modified backbone, partial optimization was then performed using molecular mechanics calculations. The structure of pyrenyltriazole (Tz^{Py}) base was optimized with B3LYP/6-31G* calculation using Gaussian 09 program[42] before inserting into the PNA backbone. The force field parameters of PNA and pyrenyltriazole were prepared within the standard procedure (for more details, see Ref. 32).

Each duplex was embedded into a rectangular box of water extended by 10 Å in each direction from the duplex and then neutralized by adding 12 Na^+ counterions. We employed the force fields of FF03[43] complemented with the prepared parameters. The simulations were performed at the temperature of 300 K and pressure of 1 atm with the standard conditions described elsewhere.[32] The unconstrained MD trajectories were generated for 10 ns and the snapshots were stored every 1 ps.

Binding free energy calculation: The binding free energy, $\Delta G_{binding}$, for a duplex can be calculated as

$$\Delta G_{binding} = G^{duplex} - G^{strand1} - G^{strand2}. \quad (1)$$

Each free energy G^x was computed for the snapshots from the 10 ns MD trajectories, according to the following equation:

$$G^x = H^x_{gas} + H^x_{trans/rot} + G^x_{solvation} - TS^x \quad (2)$$

where H_{gas} is the gas-phase energy calculated using the molecular mechanics (MM) method, and $H_{trans/rot}$ corresponds to the energy due to six translational and rotational degrees of freedom, which is $6\times1/2RT$ and equals 1.79 kcal/mol at 300 K. $G_{solvation}$ is the solvation free energy estimated using a continuum approach based on the generalized Born/surface area (GB/SA) model developed by Onufriev et al.[30] The entropic term, *TS*, can be estimated by normal mode (NMODE) analysis[44] at 300 K. More details of the calculation and applied parameters have been described elsewhere.[31,32]

Acknowledgements

Financial supports to this work come from the Thailand Research Fund (RTA5280002) (to T.V.), the Ratchadaphiseksomphot Endowment Fund from Chulalongkorn University (postdoctoral fellowship to W.M.), the Development and Promotion of Science and Technology Talents Project (DPST) (to C.B.), the Higher Education Research Promotion and National Research University Project of Thailand, Office of the Higher Education Commission, through the Advanced Functional Material Cluster of Khon Kaen University (to K.S.) and Advanced Organic Materials Cluster of Chulalongkorn University (AM1006A, to T.V.), and the Thai government stimulus package 2 (TKK2555, SP2) under the Project for Establishment of Comprehensive Center for Innovative Food, Health Products and Agriculture. The Center for Innovation in Chemistry (PERCH-CIC), and National Electronics and ComputerTechnology Center, National Science and Technology Development Agency (URL: http://www.lsr.nectec.or.th) are acknowledged for providing computing resources. We also thank Prof. Polkit Sangvanich for obtaining HRMS spectra.

Supplementary data

Supplementary data associated with this article can be found in the online version, at doi:10.1016/j.tet.2012.03.062. These data include MOL files and InChiKeys of the most important compounds described in this article.

References and notes

1. Loakes, D. *Nucleic Acids Res.* **2001**, *29*, 2437–2447.
2. (a) Matray, T. J.; Kool, E. T. *J. Am. Chem. Soc.* **1998**, *120*, 6191–6192; (b) Schweitzer, B. A.; Kool, E. T. *J. Am. Chem. Soc.* **1995**, *117*, 1863–1872.
3. Balakin, K. V.; Korshun, V. A.; Mikhalev, I. I.; Maleev, G. V.; Malakhov, A. D.; Prokhorenko, I. A.; Berlin, Y. A. *J. Biosens. Bioelectron.* **1998**, *13*, 771–778.
4. Tedeschi, T.; Tonelli, A.; Sforza, S.; Corradini, R.; Marchelli, R. *Artif. DNA PNA XNA* **2010**, *1*, 83–89.
5. MacKinnon, K. F.; Qualley, D. F.; Woski, S. A. *Tetrahedron Lett.* **2007**, *48*, 8074–8077.
6. éstergaard, M. E.; Hrdlicka, P. J. *Chem. Soc. Rev.* **2011**, *40*, 5771–5788.
7. Vilaivan, T.; Srisuwannaket, C. *Org. Lett.* **2006**, *8*, 1897–1900.
8. Vilaivan, C.; Srisuwannaket, C.; Ananthanawat, C.; Suparpprom, C.; Kawakami, J.; Yamaguchi, Y.; Tanaka, Y.; Vilaivan, T. *Artif. DNA PNA XNA* **2011**, *2*, 50–59.
9. Taechalertpaisarn, J.; Sriwarom, P.; Boonlua, C.; Yotapan, N.; Vilaivan, C.; Vilaivan, T. *Tetrahedron Lett.* **2010**, *51*, 5822–5826.
10. Reenabthue, N.; Boonlua, C.; Vilaivan, C.; Vilaivan, T.; Suparpprom, C. *Bioorg. Med. Chem. Lett.* **2011**, *21*, 6465–6469.
11. Boonlua, C.; Vilaivan, C.; Wagenknecht, H.-A.; Vilaivan, T. *Chem.—Asian. J.* **2011**, *6*, 3251–3259.
12. Meldal, M.; Tornøe, C. W. *Chem. Rev.* **2008**, *108*, 2952–3015.
13. Best, M. D. *Biochemistry* **2009**, *48*, 6571–6584.
14. El-Sagheer, A. H.; Brown, T. *Chem. Soc. Rev.* **2010**, *39*, 1388–1405.

Author's personal copy

15. Gramlich, P. M. E.; Wirges, C. T.; Manetto, A.; Carell, T. *Angew. Chem., Int. Ed.* **2008**, *47*, 8350–8358.
16. Isobe, H.; Fujino, T.; Yamazaki, N.; Guillot-Nieckowski, M.; Nakamura, E. *Org. Lett.* **2008**, *10*, 3729–3732.
17. Nuzzi, A.; Massi, A.; Dondoni, A. *QSAR Comb. Sci.* **2007**, *26*, 1191–1199.
18. Nakahara, M.; Kuboyama, T.; Izawa, A.; Hari, Y.; Imanishi, T.; Obika, S. *Bioorg. Med. Chem. Lett.* **2009**, *19*, 3316–3319.
19. Spadafora, M.; Postupalenko, V. Y.; Shvadchak, V. V.; Klymchenko, A. S.; Mély, Y.; Burger, A.; Benhida, R. *Tetrahedron* **2009**, *65*, 7809–7816.
20. Chittepu, P.; Sirivolu, V. R.; Seela, F. *Bioorg. Med. Chem.* **2008**, *16*, 8427–8439.
21. Berndl, S.; Herzig, N.; Kele, P.; Lachmann, D.; Li, X.; Wolfbeis, O. S.; Wagenknecht, H.-A. *Bioconjugate Chem.* **2009**, *20*, 558–564.
22. éstergaard, M. E.; Guenther, D. C.; Kumar, P.; Baral, B.; Deobald, L.; Paszczynski, A. J.; Sharma, P. K.; Hrdlicka, P. J. *Chem. Commun.* **2010**, 4929–4931.
23. Howarth, N. M.; Ricci, J. *Tetrahedron* **2011**, *67*, 9588–9594 and references cited therein.
24. Gogoi, K.; Mane, M. V.; Kunte, S. S.; Kumar, V. A. *Nucleic Acids Res.* **2007**, *35*, e139.
25. Lim, S. Y.; Chung, W.-Y.; Lee, H. K.; Park, M. S.; Park, H. G. *Biochem. Biophys. Res. Commun.* **2008**, *376*, 633–636.
26. Gasser, G.; Hüsken, N.; Köster, S. D.; Metzler-Nolte, N. *Chem. Commun.* **2008**, 3675–3677.
27. Lowe, G.; Vilaivan, T. *J. Chem. Soc., Perkin Trans. 1* **1997**, 547–554.
28. Bonger, K. M.; Kapoerchan, V. V.; Grotenbreg, G. M.; van Koppen, C. J.; Timmers, C. M.; van der Marel, G. A.; Overkleeft, H. S. *Org. Biomol. Chem.* **2010**, *8*, 1881–1884.
29. Lowe, G.; Vilaivan, T. *J. Chem. Soc., Perkin Trans. 1* **1997**, 555–560.
30. Onufriev, A.; Bashford, D.; Case, D. A. *J. Phys. Chem. B* **2000**, *104*, 3712–3720.
31. Gohlke, H.; Case, D. A. *J. Comput. Chem.* **2004**, *25*, 238–250.
32. Siriwong, K.; Chuichay, P.; Saen-oon, S.; Suparpprom, C.; Vilaivan, T.; Hannongbua, S. *Biochem. Biophys. Res. Commun.* **2008**, *372*, 765–771.
33. van Daele, I.; Bomholt, N.; Filichev, V. V.; van Calenbergh, S.; Pedersen, E. B. *ChemBioChem* **2008**, *9*, 791–801.
34. Bag, S. S.; Kundu, R. *J. Org. Chem.* **2011**, *76*, 3348–3356.
35. Grabowski, Z. R.; Rotkiewicz, K.; Rettig, W. *Chem. Rev.* **2003**, *103*, 3899–4031.
36. Seitz, O. *Angew. Chem., Int. Ed.* **2000**, *39*, 3249–3252.
37. Although the nucleobase side chain protection is probably not required during the click reaction, in view of potential instability of organic azides under high temperature conditions necessary for side-chain deprotection it is preferred to leave the protecting groups at this stage.
38. Chan, T. R.; Hilgraf, R.; Sharpless, K. B.; Fokin, V. V. *Org. Lett.* **2004**, *6*, 2853–2855.
39. Beyer, C.; Wagenknecht, H.-A. *Chem. Commun.* **2010**, 2230–2231.
40. Egholm, M.; Nielsen, P. E.; Buchardt, O.; Berg, R. H. *J. Am. Chem. Soc.* **1992**, *114*, 9677–9678.
41. Case, D. A.; Darden, T. A.; Cheatham, T. E., III; Simmerling, C. L.; Wang, J.; Duke, R. E.; Luo, R.; Merz, K. M.; Pearlman, D. A.; Crowley, M.; Walker, R. C.; Zhang, W.; Wang, B.; Hayik, S.; Roitberg, A.; Seabra, G.; Wong, K. F.; Paesani, F.; Wu, X.; Brozell, S.; Tsui, V.; Gohlke, H.; Yang, L.; Tan, C.; Mongan, J.; Hornak, V.; Cui, G.; Beroza, P.; Mathews, D. H.; Schafmeister, C.; Ross, W. S.; Kollman, P. A. *AMBER 9*; University of California: San Francisco, 2006.
42. Gaussian 09, Revision B.01; Gaussian,: Wallingford, Connecticut, 2009.
43. Duan, Y.; Wu, C.; Chowdhury, S.; Lee, M. C.; Xiong, G.; Zhang, W.; Yang, R.; Cieplak, P.; Luo, R.; Lee, T.; Caldwell, J.; Wang, J.; Kollman, P. *J. Comput. Chem.* **2003**, *24*, 1999–2012.
44. Kottalam, J.; Case, D. A. *Biopolymers* **1990**, *29*, 1409–1421.

Biosensors and Bioelectronics 38 (2012) 430–435

Contents lists available at SciVerse ScienceDirect

Biosensors and Bioelectronics

journal homepage: www.elsevier.com/locate/bios

Short communication

Label-free capacitive DNA sensor using immobilized pyrrolidinyl PNA probe: Effect of the length and terminating head group of the blocking thiols

Orawan Thipmanee [a,b,c], Saluma Samanman [a,b,c], Supannee Sankoh [a,b,c], Apon Numnuam [a,b,c], Warakorn Limbut [a,b,d], Proespichaya Kanatharana [a,b,c], Tirayut Vilaivan [e], Panote Thavarungkul [a,b,f,*]

[a] Trace Analysis and Biosensor Research Center, Prince of Songkla University, Hat Yai, Songkhla 90112, Thailand
[b] Center of Excellence for Innovation in Chemistry, Faculty of Science, Prince of Songkla University, Hat Yai, Songkhla 90112, Thailand
[c] Department of Chemistry, Faculty of Science, Prince of Songkla University, Hat Yai, Songkhla 90112, Thailand
[d] Department of Applied Science, Faculty of Science, Prince of Songkla University, Hat Yai, Songkhla 90112, Thailand
[e] Organic Synthesis Research Unit, Department of Chemistry, Faculty of Science, Chulalongkorn University, Bangkok 10330, Thailand
[f] Department of Physics, Faculty of Science, Prince of Songkla University, Hat Yai, Songkhla 90112, Thailand

ARTICLE INFO

Article history:
Received 8 June 2012
Accepted 13 June 2012
Available online 19 June 2012

Keywords:
Blocking thiol
acpcPNA
Self-assembled monolayer
Capacitance measurement
DNA sensor
Trace analysis

ABSTRACT

This paper reports, for the first time, the influence of the length and the terminating head group of blocking thiols on the sensitivity and specificity of a label-free capacitive DNA detection system using immobilized pyrrolidinyl peptide nucleic acid (acpcPNA) probes. A C-terminal lysine-modified acpcPNA was immobilized through four different alkanethiol self-assembled monolayers (SAMs), i.e., 3-mercaptopropionic acid (MPA), thioctic acid (TA), thiourea (TU) and mercaptosuccinic acid (MSA). The hybridization between the acpcPNA probes and the target DNA was directly measured using the capacitive system. Five blocking thiols of various lengths (C=3, 6, 8, 9 and 11), with the –OH terminating head group, i.e., 3-mercapto-1-propanol (3-MPL), 6-mercapto-1-hexanol (6-MHL), 8-mercapto-1-octanol (8-MOL), 9-mercapto-1-nonanol (9-MNL), 11-mercapto-1-undecanol (11-MUL) and another blocking thiol (C=11) with a $-CH_3$ terminating head group, and 1-dodecanethiol (1-DDT) were investigated. The blocking thiol with the same length as the total spacer of the immobilized acpcPNA gave the highest sensitivity and specificity with the –OH terminating head group providing a slightly better signal than the $-CH_3$ group. Under the optimized conditions, the immobilized acpcPNA probes provided a wide linear range for DNA detection (1.0×10^{-11}–1.0×10^{-8} M) with a very low detection limit in the picomolar range. The modified acpcPNA electrode could be reused through at least 58 cycles. The high sensitivity and very low detection limits are potentially useful for the analysis of ultra-trace levels of DNA in samples. Preliminary studies were also performed to see the effect of probe concentration and target length.

© 2012 Elsevier B.V. All rights reserved.

1. Introduction

The development of sensors for specific DNA sequences has attracted a lot of attention due to their potential applications. A number of parameters can affect the sensitivity and specificity of the sensor, one of which is the way the probes were immobilized onto the transducer surface (Lucarelli et al., 2004, 2008; Tichoniuk et al., 2008). DNA probes can be immobilized onto a gold electrode sensor via a mixed binary monolayer of thiolated DNA and diluents (Wong et al., 2005). Alternatively the probes can be immobilized via a self-assembled monolayer (SAM) followed by the blocking of any free sensing surfaces using a thiol compound. The latter procedure has generally provided better DNA hybridization than the first technique (Herne and Tarlov, 1997). This is because the blocking thiol can help to project the immobilized probes away from the electrode surface. This prevents non-specific DNA–surface interactions and also helps the probes to be well packed onto the gold surface (Mannelli et al., 2005; Peeters et al., 2008). Both the length and the terminating head group of the blocking thiols have been reported to affect the hybridization and the discrimination efficiency of DNA sensors (Dharuman and Hahn, 2007, 2008; Degefa and Kwak, 2008; Dharuman et al., 2010).

Recently peptide nucleic acid (PNA) has gained considerable attention as a sensing probe. PNA is a DNA mimic in which the natural deoxyribose-phosphate backbone is replaced by a neutral pseudopeptide chain consisting of repeating *N*-(2-aminoethyl)-glycine units (aegPNA) linked by amide bonds (Nielsen, 2001). Pyrrolidinyl PNA with a conformationally rigid D-prolyl-2-aminocyclopentanecarboxylic acid (ACPC) backbone (acpcPNA) is a relatively new PNA system developed by our group (Suparpprom et al., 2005; Vilaivan and Srisuwannaket, 2006). Compared to DNA

* Corresponding author at: Department of Physics, Faculty of Science, Prince of Songkla University, Hat Yai, Songkhla 90112, Thailand. Tel.: +66 7428 8753; fax: +66 74 55 8849.
E-mail address: panote.t@psu.ac.th (P. Thavarungkul).

0956-5663/$ - see front matter © 2012 Elsevier B.V. All rights reserved.
http://dx.doi.org/10.1016/j.bios.2012.06.021

and aegPNA, it provided a stronger binding affinity and better sequence specificity towards DNA.

The aim of this work was to develop a new platform for a DNA biosensor based on a combination of a highly sensitive, simple to operate and relatively inexpensive electrochemical capacitive transducer (Loyprasert et al., 2008; Numnuam et al., 2009; Wannapob et al., 2010; Samanman et al., 2011) and a acpcPNA probe. A simple protocol for immobilization between the acpcPNA probe and SAMs of four alkanethiols with various chain lengths is explored. This work also aimed to investigate the influence of the blocking thiols with various chain lengths and terminating head groups (–OH and $–CH_3$). Finally, the performances of the developed capacitive DNA sensor were studied. A preliminary study was also performed using different PNA probes and DNA targets with different sequence and lengths.

2. Experimental

2.1. Materials

The 9-mer lysine-modified acpcPNA (Ac-TTT TTT TTT-LysNH_2), PNA-T9 probe and the 12-mer mixed base lysine-modified acpcPNA (Bz-TGT CAA CTG ACT-LysNH_2), PNA-M12 probe, were synthesized by Mrs. Chotima Vilaivan at Chulalongkorn University, Thailand according to the published protocol (Vilaivan and Srisuwannaket, 2006).

Oligonucleotide target DNAs were purchased from the Bioservice Unit, National Science and Technology Development Agency and BioDesign Co., Ltd., Thailand. The sequences are mentioned below.

For the PNA-T9 probe
Complementary DNA
D6comp:5′-AAAAAA-3′
D9comp:5′-AAAAAAAAA-3′
D12comp:5′-AAAAAAAAAAAA-3′
D15comp:5′-AAAAAAAAAAAAAAA-3′
D27comp:5′- AAAAAAAAAAAAAAAAAAAAAAAAAAA-3′
D27compM18a:5′-*TTTTTTTTT*AAAAAAAAA*TTTTTTTTT*-3′
D27compM18b:5′-*TGCTCAGCT*AAAAAAAAA*TGCTCAGCT*-3′
Single mismatched DNA
D9M1G:5′-AAAA*G*AAAA-3′
D9M1C:5′-AAAA*C*AAAA-3′
D9M1T:5′-AAAA*T*AAAA-3′
Double mismatched DNA
D9M2G:5′-AAA*G*A*G*AAA-3′
D9M2C:5′-AAA*C*A*C*AAA-3′
D9M2T:5′-AAA*T*A*T*AAA-3′
Non-complementary DNA
D9non-compa:5′-*TTTTTTTTT*-3′
D9non-compb:5′-*TATTATTAT*-3′
For the PNA-M12 probe
Complementary DNA
D9comp:5′-CAGTTGACA-3′
D12comp:5′-AGTCAGTTGACA-3′
D15compM3:5′-*GCT*AGTCAGTTGACA-3′
D30compM18:5′-*GACTGCACC*AGTCAGTTGACA*TGTTGCGAC*-3′
Single mismatched DNA
D12M1T:5′-AGTCA*T*TTGACA-3′
D12M1C:5′-AGTCA*C*TTGACA-3′
D12M1A:5′-AGTCA*A*TTGACA-3′
Double mismatched DNA
D12M2T:5′-AGT*TA*TTGACA-3′
D12M2CG:5′-AGT*GA*CTTGACA-3′
D12M2A:5′-AGT*AAA*TTGACA-3′
Non-complementary DNA
D12non-comp:5′-*TCAGTCAACTGT*-3′

Five blocking thiols of various lengths ($C=3$, 6, 8, 9 and 11), with the –OH terminating head group, i.e., 3-mercapto-1-propanol (3-MPL), 6-mercapto-1-hexanol (6-MHL), 8-mercapto-1-octanol (8-MOL) and 9-mercapto-1-nonanol (9-MNL) were obtained from Aldrich (Milwaukee, USA) and 11-mercapto-1-undecanol (11-MUL) was from Aldrich (Steinheim, Germany). Another blocking thiol ($C=11$) with a different terminating head group ($–CH_3$), 1-dodecanethiol (1-DDT) from Aldrich (Milwaukee, USA) was also studied. Four alkanethiols, mercaptosuccinic acid (MSA, Fluka, Buchs, Switzerland), 3-mercaptopropionic acid (MPA, Aldrich, Steinheim, Germany), thioctic acid (TA, Aldrich, Milwaukee, USA) and thiourea (TU, Sigma, Saint Louis, USA) were used to prepare the SAM surface.

2.2. Immobilization of the acpcPNA

The PNA-T9 probe was used in the initial optimization as the model. The cleaned gold electrodes (diameter 3 mm, 99.99%) were immersed in 250 mM alkanethiol solutions of MSA (Shervedani and Hatefi-Mehrjardi, 2007), MPA and TA for 12 h and in TU for 24 h at room temperature (Limbut et al., 2006). The SAMs formed from MSA, MPA and TA were activated for amide bond formation with lysine acpcPNA using 0.05 M EDC/0.03 M NHS in phosphate buffer (pH 5.00) for 5 h. Glutaraldehyde was used to activate the amino group of TU for coupling to the acpcPNA probe. Then 20 μL of a 5.0 μM (Wittung-Stafshede et al., 2000; Hejazi et al., 2010) of the acpcPNA was placed on the SAMs for 24 h at 4 °C. The electrode with the SAM of TU was further treated with 1.0 mM ethanolamine pH 8.00 for 7 minutes to deactivate all the remaining aldehyde groups not coupled to the immobilized acpcPNA. Finally, all immobilized acpcPNA electrodes were immersed in 1.0 mM of the six blocking thiol solutions for 1 h.

A 12-mer mixed base sequence (PNA-M12) was also immobilized, under the optimal immobilization conditions and also with the best blocking thiol to represent a more realistic scenario in analyses of real DNA samples.

2.3. Capacitance measurement

The modified electrode was used as the working electrode in a flow injection system under the following operating conditions: 10 mM phosphate buffer pH 7.00 as the running buffer, sample volume 300 μL and flow rate 50 μL min^{-1}. The capacitance was determined from the obtained current response when a potential step of 50 mV was applied to the working electrode as previously described (Limbut et al., 2006) (Supplementary data Fig. 1S). When DNA was injected into the flow system, it hybridized to the immobilized acpcPNA on the working electrode and the capacitance decreased. The capacitance change (ΔC) due to the PNA–DNA hybridization could then be determined. The regeneration solution, 300 μL of 50 mM NaOH (Ananthanawat et al., 2009b), was then applied to break the binding between the probe and the target DNA, ready for a new analytical cycle (Supplementary data Fig. 1S inset).

2.4. Sensitivity determination

To determine the influence of the chain length and the terminating head group of the blocking thiols, a calibration curve was first obtained by injecting 1.0×10^{-11}–1.0×10^{-8} M ($n=3$) of complementary target DNA with a subsequent regeneration step.

The sensitivity, i.e. the slope of the plot between the capacitance changes ($-$nF cm^{-2}) versus the logarithm of concentration of the complementary target DNA (log M) (Supplementary data Fig. 1S inset), was used to indicate the efficiency of the hybridization of the target DNA and the immobilized acpcPNA probe. A higher sensitivity reflects a more efficient system.

2.5. Specificity determination

The % signal suppression (%SS) of the mismatched DNA response was calculated according to Eq.(1). A large %SS indicated a better specificity:

$$\%\mathrm{SS} = \frac{\Delta c_{\text{complementary DNA}} - \Delta c_{\text{mismatched DNA}}}{\Delta c_{\text{complementry DNA}}} \times 100 \quad (1)$$

3. Results and discussion

3.1. Effect of the length of the blocking thiols

The effect of the chain length of the blocking thiols was evaluated in terms of the sensitivity of the capacitance change caused by the hybridization of the complementary DNA target to the immobilized PNA-T9 probe.

The PNA-T9 probe was immobilized using the SAM of four different alkanethiols, i.e., TA(6C), TU(1C+1N), MSA(2C or 3C) and MPA(3C) via an amide bond with the ε-NH_2 side chain of the C-terminal lysine residue. The spacer from these alkanethiols when combined with the lysine spacer of the immobilized acpcPNA (5C+1N) became 11C+1N, 11C+2N, 7C+1N or 8C+1N and 8C+1N, respectively (Fig. 1(a–d)). The effect of the six blocking thiols with different chain lengths, i.e., 3-MPL(3C), 6-MHL(6C), 8-MOL(8C), 9-MNL(9C), 11-MUL(11C) with their -OH terminating head group and 1-DDT(11C) with its –CH_3 terminating head group, were compared.

Fig. 2(a) shows the sensitivities of the MPA-acpcPNA electrode to the blocking thiols, the one with the same length as that of the total spacer, 9-MNL (9 atoms, 8C+1N), provided the highest sensitivity (20.4 ± 0.7 -nF cm^{-2} (log M)$^{-1}$). The blocking thiol with a shorter length, i.e., 3-MPL, 6-MHL and 8-MOL gave a lower sensitivity. This is also true for the blocking thiol with a longer length, i.e., 11-MUL and 1-DDT also gave lower sensitivities.

For the SAM of TA and TU with a total spacer length of 11C+1N and 11C+2N, respectively, the highest sensitivities of

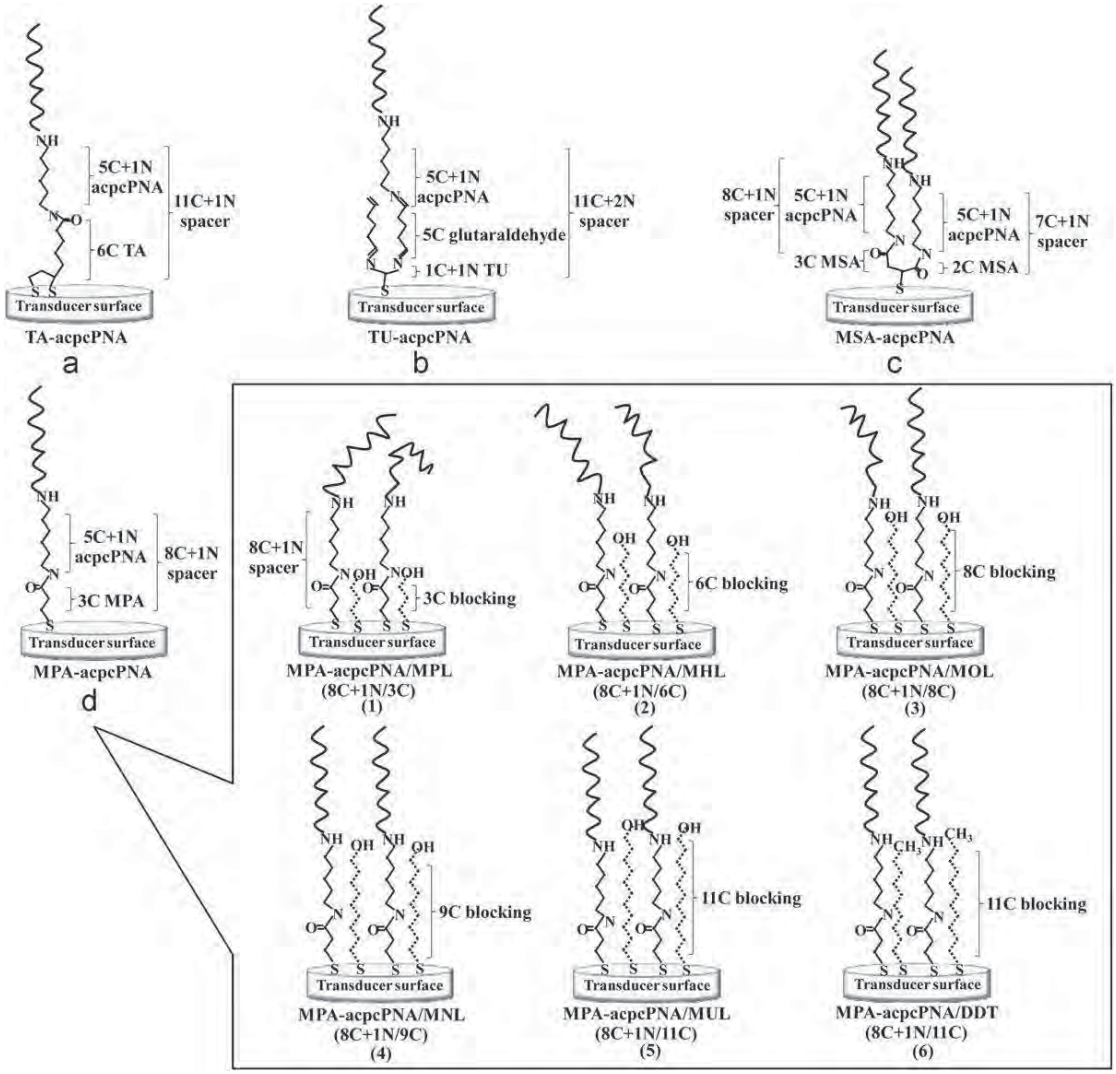

Fig. 1. The total spacer of the acpcPNA modified on four types of self-assembled monolayers (a) TA, (b) TU, (c) MSA and (d) MPA. Inset (d) schematic diagram of the six interfaces of the MPA immobilized acpcPNA electrode (total of 8C+1 N spacer) with different chain lengths of the blocking thiols, (d1) 3-MPL (3C), (d2) 6-MHL (6C), (d3) 8-MOL (8C), (d4) 9-MNL (9C), (d5) 11-MUL (11C) with the –OH terminating head group and (d6) 1-DDT (11C) with the –CH_3 terminating head group.

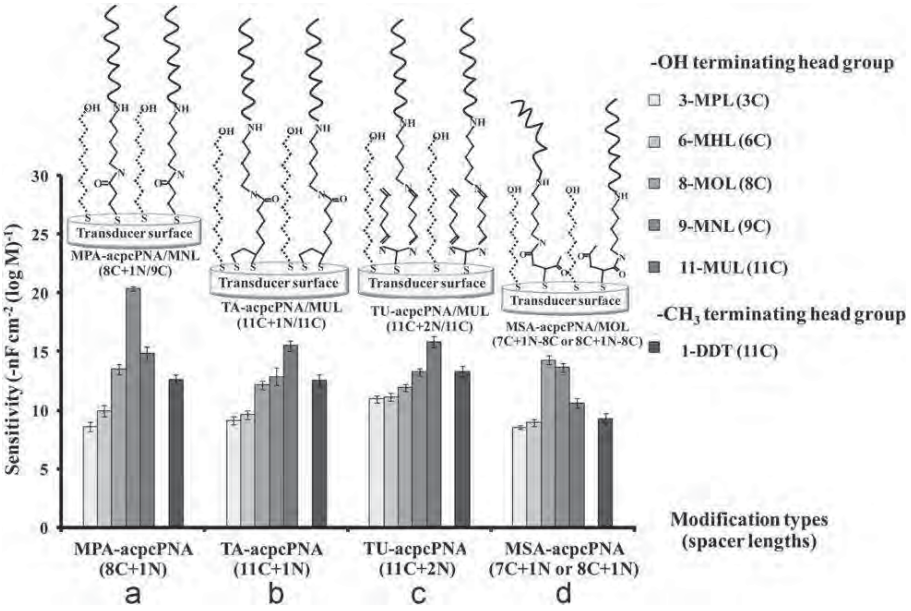

Fig. 2. Effect of the length and terminating head group of the blocking thiol on the sensitivity for the detection of the complementary target DNA.

15.5 ± 0.5 $-$nF cm^{-2} (log M)$^{-1}$ for TA and 15.8 ± 0.4 $-$nF cm^{-2} (log M)$^{-1}$ for TU were obtained using the longest blocking thiol (11-MUL; 11C) (Fig. 2(b) and (c)). Other blocking thiols with shorter chain length gave lower sensitivities. (Note: Longer blocking thiols ($>$11C) were not commercially available.)

In the case of MSA with a branched structure the total spacer of the immobilized acpcPNA is either 7C+1N or 8C+1N (Fig. 1(c)). The blocking thiols with the same length as the acpcPNA spacer (8-MOL or 9-MNL) showed the highest sensitivities of 14.3 ± 0.5 and 13.6 ± 0.3 -nF cm^{-2} (log M)$^{-1}$, respectively (Fig. 2(d)). The two sensitivities were not much different since the immobilized acpcPNA probes could be attached on either the 7C+1N or 8C+1N spacer branches. Lower sensitivities were obtained from the use of blocking thiols with a shorter or longer length.

From the results it is clear that the blocking thiol with the same length as the total spacer of the immobilized acpcPNA showed the highest sensitivity. This is possibly because this length can help arrange the acpcPNA probes to be more readily available for hybridization. These results corresponded well with other reports, using various techniques to study the orientation of the probe, which showed that the use of blocking thiols or diluents helped to orient the probe to extend further into the solvent phase (Lee et al., 2006, 2007), making it more favorable for hybridization resulting in a maximum hybridization efficiency (Boozer et al., 2006; Gong et al., 2006; Su et al., 2005). For the blocking thiol with a shorter length than the total spacer, the end of the blocking thiol was further away from the acpcPNA probe. This could be explained by the probe not now being in an optimum position for access of the DNA target resulting in a lower sensitivity. For the blocking thiol with a longer chain length the lower sensitivity could be due to the overlapping of the blocking thiol with the base of the acpcPNA probes resulting in lower hybridization efficiency. The results are in line with the study made by Wong and coworkers on DNA–DNA hybridization (Wong et al., 2005).

3.2. Effect of the terminating head group

To test the effects of the terminating head groups, two blocking thiols with the same length were investigated, 11-MUL with an –OH terminating head group and 1-DDT with a –CH_3 terminating head group. The –OH terminating head group (with the lone pair electron) consistently provided slightly better sensitivity than the –CH_3 terminating head group (without a lone pair electron) (Fig. 2(a–d)). This is possibly because of the more hydrophilic characteristic of the –OH terminating head group than the –CH_3 terminating head group (Dharuman and Hahn, 2007). This higher hydrophilicity will help the target DNA in an aqueous solution to move closer to the electrode surface (Gillmor et al., 2000), i.e., closer to the immobilized probe resulting in a more efficient hybridization. However, the effect is much less than the effect of the chain length of the blocking thiols.

3.3. Effect of PNA probe concentration

The amount of accessible immobilized probe is a major factor that would influence hybridization efficiency (Keighley et al., 2008; Liu et al., 2005). A preliminary study of the effect of concentration of the probe to be immobilized (3.0–7.0 μM) via the four SAMs, which should correlate with the amount of immobilized probe, was investigated. The sensitivity increased with concentration and leveled off at 5.0 μM (Supplementary data Fig. 2S). For all concentrations the blocking thiol with the same length as the total spacer of the immobilized PNA-T9 showed the highest sensitivity. The results indicated that a good sensor sensitively depends on both the probe concentration and the length of the blocking thiol.

3.4. Linear range and detection limit

The immobilized PNA-T9 probes (5.0 μM) using the blocking thiols that provided the highest sensitivities (Fig. 2) were tested i.e., MPA blocked with MNL, TA blocked with MUL, TU blocked with MUL and MSA blocked with MOL. The capacitance change was studied from 1.0×10^{-14} to 1.0×10^{-7} M of the target DNA. A linear relationship between the capacitance change and the logarithm of the target DNA was found between 1.0×10^{-11} and 1.0×10^{-8} M for all four systems and the detection limits (Buck and Lindner, 1994) of the four systems were between 6 and 10 pM (Supplementary data Table 1S). The proposed capacitive DNA sensor provided a much better detection limit than other methods such as QCM that gave a detection limit of 5 μM and SPR that had a detection limit of 0.2 μM studied by Ananthanawat

et al. (2009a,b) using a similar T9 acpcPNA probe. Therefore, this capacitive DNA sensor offers a promising alternative and more sensitive probe for the detection of ultra-trace levels of DNA.

3.5. Reusability

The reusability of the immobilized acpcPNA electrode was evaluated by repeatedly injecting the same concentration of complementary DNA (1.0×10^{-10} M) with a subsequent regeneration step. The electrodes modified with four SAMs with blocking solutions that provided the best sensitivities were tested. The reusability was evaluated in terms of the percentage of residual activity:

$$\text{Residualactivity}\ (\%) = \frac{\Delta C_2}{\Delta C_1} \times 100 \quad (2)$$

where ΔC_1 and ΔC_2 were the capacitance change when the immobilized acpcPNA probe hybridized to the DNA target for the first time and after each regeneration, respectively (Supplementary data Fig. 1S inset). The electrodes could be reused for between 58 and 73 times with an average residual activity of $\geq 98\%$ (Supplementary data Table 1S). After the decrease of the response the electrode was tested (Supplementary data Fig. 3S(e)) and the cyclic voltammogram suggested that it is most likely caused by the loss of the SAM together with its attached acpcPNA from the gold electrode.

3.6. Reproducibility

The reproducibility of the responses of the PNA-T9 electrodes from two different preparations of MPA, TU and TA was tested by comparing the sensitivities. The sensitivities of the two electrodes were 20.4 ± 0.7 and 20.6 ± 0.5 $-\text{nF cm}^{-2}$ $(\log \text{M})^{-1}$ for MPA; 15.8 ± 0.4 and 16.3 ± 0.5 $-\text{nF cm}^{-2}$ $(\log \text{M})^{-1}$ for TU; 13.3 ± 0.5 and 13.5 ± 0.4 $-\text{nF cm}^{-2}$ $(\log \text{M})^{-1}$ for TA. The sensitivities did not differ between each preparation, i.e., good reproducibility was obtained for different preparations.

3.7. Specificity

To investigate the specificity the PNA-T9 immobilized on MPA was employed because it provided the best sensitivity (Fig. 2(a)). Three blocking thiols with shorter length, the same length and longer length relative to the total spacer of the SAM modified PNA-T9 were also compared. The hybridization with the complementary target DNA, single and double base mismatched DNAs at 1.0×10^{-8} M were monitored. Fig. 3(a), (b), and (c) shows the results. The complementary DNA (D9comp) provided a much higher capacitance change compared to the single and double mismatched DNA target. The %SS obtained from the blocking thiol (9C) with the same length as the spacer (8C+1N) was the highest (76–79%) followed by the one with the next shorter length (8C) (70–74%) and the next longer length (11C) (68–69%). As expected, the %SS for the double mismatched target was higher than that for the single mismatched. Two different non-complementary DNAs were also tested (Fig. 3(b)) and gave the highest %SS of 99%.

PNA-M12 probe immobilized under optimal conditions obtained for the PNA-T9 probe, i.e. 5 μM on MPA followed by blocking with MNL (the thiol with the same length as the spacer), was also investigated. In agreement with the results obtained

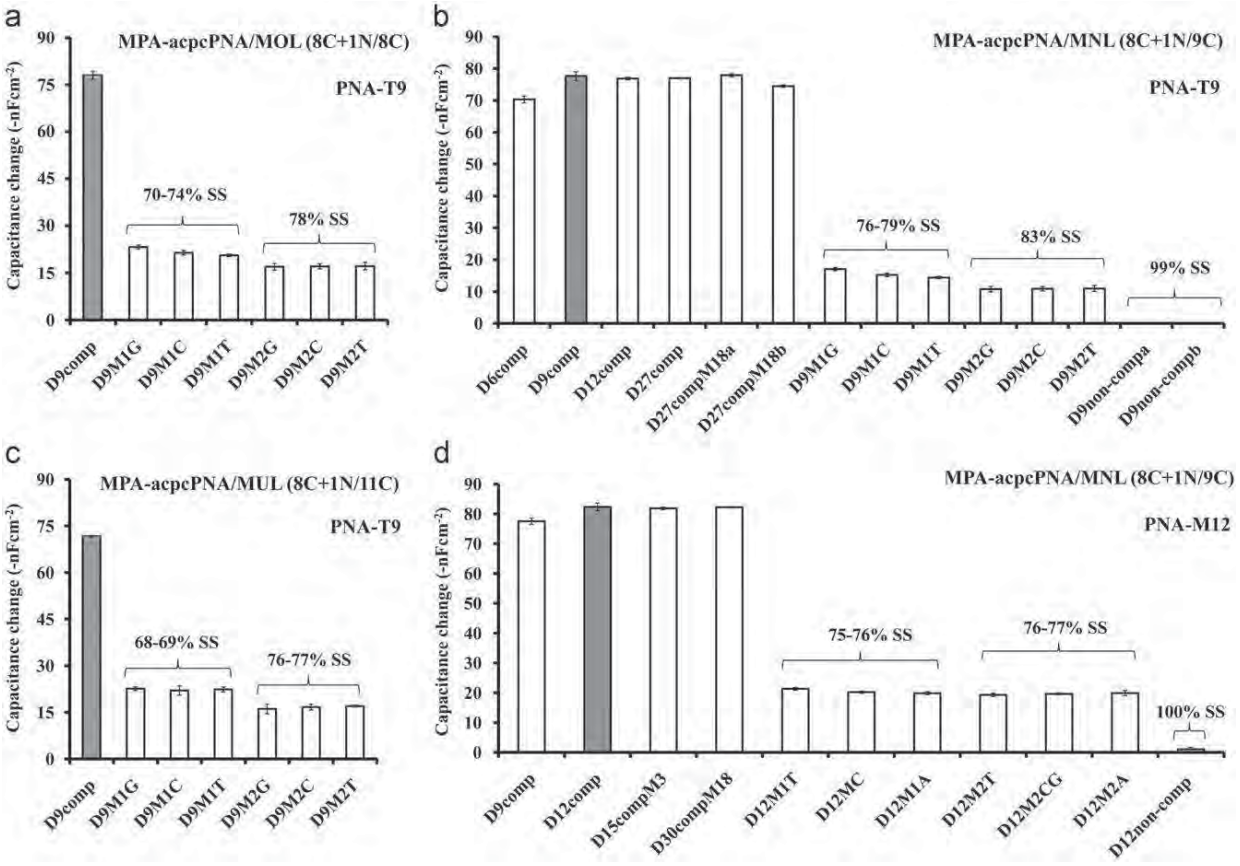

Fig. 3. The measured capacitance change ($n=3$) of the complementary, single, double mismatched and non-complementary target DNAs using immobilized acpcPNA probes (PNA-T9 and PNA-M12) on a MPA modified electrode (8C+1 N spacer) with different chain lengths of the blocking thiol, (a) 8-MOL (8C), (b) and (d) 9-MNL (9C), (c) 11-MUL (11C), tested at 1.0×10^{-8} M DNAs showing the %SS. Solid columns indicate the complementary target DNAs with the same length as the PNA probe.

with the 9-mer probe, good specificity was also obtained from this 12-mer mixed base probe, i.e., very high %SS for the single and double mismatched and a complete signal suppression for the non-complementary DNA (Fig. 3(d)).

3.8. Effect of target length

In the case of the complementary DNAs with different lengths, a shorter target length (D6comp for PNA-T9 and D9comp for PNA-M12) provided a lower capacitance signal than the fully complementary DNAs (D9comp for PNA-T9 and D12comp for PNA-M12) (Fig. 3(b) cf. 3(d)). This is because when the target DNA binds to the PNA probe, water and electrolyte molecules will be displaced by the DNA sample thereby giving a change in capacitance (Berggren et al., 1999). A longer duplex length caused a larger change since the water and electrolyte molecules were pushed further away from the electrode. It was of interest to observe that longer target DNAs gave a similar capacitance change to DNA with the same length as the probe. This implies that the overhanging unhybridized part of the DNA target, which is more flexible than the duplex, does not directly affect the performance of the biosensor, supporting the mechanism of capacitance change by water and electrolyte molecule displacement explained.

4. Conclusions

In this research, the effect of the length and terminating head group of the blocking thiol were studied using a highly sensitive capacitive system. The one with an equal length to the –OH terminating head group of the blocking thiol provided the highest sensitivity. The blocking thiol with an equal length also provided the highest %SS, so this also indicated the high binding specificity. These sensors based on acpcPNA probes provided very good performances such as they produced a linear concentration response over a wide linear range (1.0×10^{-11}–1.0×10^{-8} M), a very low detection limit (picomolar) and good reusability of at least 58 cycles. The high sensitivity and very low detection limits are potentially useful for the analysis of DNA at ultra-trace levels in samples. The hybridization response was also found to be correlated to the concentration of the probe to be immobilized and the length of the target DNAs. In this work, a probe concentration of 5.0 μM is sufficient to give maximum coverage of the sensor leading to the best response. As for the target length, there are correlations between the response and the length of the target that can form a duplex with the probe whereby a longer target length provided a larger response. No further increase in response was observed with targets carrying extra region that does not form hybrid with the probe. Further studies on this aspect would be useful.

Acknowledgements

The authors are grateful to Grants from the Thailand Research Fund (TRF, RTA528002); the Royal Golden Jubilee Ph.D-program (RGJ) supported by The Thailand Research Fund (3.C.PS/50/B.1 and 3.C.PS/51/B.1); the Office of the Higher Education Commission (CHE-SSR-Ph.D-THA); the Center of Excellence for Innovation in Chemistry (PERCH-CIC), the Office of the Higher Education Commission; the Higher Education Research Promotion and National Research University Project of Thailand, Office of the Higher Education Commission; the Trace Analysis and Biosensor Research Center (TAB-RC), and Graduate School, Prince of Songkla University, Hat Yai, Thailand are all gratefully acknowledged. The authors thank Dr. Brian Hodgson, Prince of Songkla University, Hat Yai, Songkhla, Thailand for assistance with English.

Appendix A. Supporting information

Supplementary data associated with this article can be found in the online version at http://dx.doi.org/10.1016/j.bios.2012.06.021.

References

Ananthanawat, C., Vilaivan, T., Hoven, V.P., 2009a. Sensors and Actuators B: Chemical 137, 215–221.
Ananthanawat, C., Vilaivan, T., Mekboonsonglarp, W., Hoven, V.P., 2009b. Biosensors and Bioelectronics 24, 3544–3549.
Berggren, C., Stalhandske, P., Brundell, J., Johansson, G., 1999. Electroanalysis 11, 156–160.
Boozer, C., Chen, S., Jiang, S., 2006. Langmuir 22, 4694–4698.
Buck, R.P., Lindner, E., 1994. Pure and Applied Chemistry 66, 2527–2536.
Degefa, T.H., Kwak, J., 2008. Journal of Electroanalytical Chemistry 612, 37–41.
Dharuman, V., Hahn, J.H., 2007. Sensors and Actuators B: Chemical 127, 536–544.
Dharuman, V., Hahn, J.H., 2008. Biosensors and Bioelectronics 23, 1250–1258.
Dharuman, V., Chang, B.Y., Park, S.M., HahnN, J.H., 2010. Biosensors and Bioelectronics 25, 2129–2134.
Gillmor, S.D., Thiel, T.C., Strother, T.C., Smith, L.M., Lagally, M.G., 2000. Langmuir 16, 7223–7228.
Gong, P., Lee, C.Y., Gamble, L.J., Castner, D.G., Grainger, D.W., 2006. Analytical Chemistry 78, 3326–3334.
Hejazi, M.S., Pournaghi-Azar, M.H., Ahour, F., 2010. Analytical Biochemistry 399, 118–124.
Herne, T.M., Tarlov, M.J., 1997. Journal of the American Chemical Society 119, 8916–8920.
Keighley, T.D., Estrela, P., Li, P., Migliorato, P., 2008. Biosensors and Bioelectronics 24, 906–911.
Lee, C.Y., Gong, P., Harbers, G.M., Grainger, W.D., Castner, D.G., Gamble, L.J., 2006. Analytical Chemistry 78, 3326–3334.
Lee, C.Y., Nguyen, T.P.-C., Grainger, D.W., Gamble, L.J., Castner, D.G., 2007. Analytical Chemistry 79, 4390–4400.
Liu, J., Tian, S., Nielsen, P.E., Knoll, W., 2005. Chemical Communications, 2969–2971.
Limbut, W., Kanatharana, P., Mattiasson, B., Asawatreratanakul, P., Thavarungkul, P., 2006. Biosensors and Bioelectronics 22, 233–240.
Loyprasert, S., Thavarungkul, P., Asawatreratanakul, P., Wongkittisuksa, B., Limsakul, C., Kanatharana, P., 2008. Biosensors and Bioelectronics 24, 78–86.
Lucarelli, F., Marrazza, G., Turner, A.P.F., Mascini, M., 2004. Biosensors and Bioelectronics 19, 515–530.
Lucarelli, F., Tombelli, S., Minunni, M., Marrazza, G., Mascini, M., 2008. Analytica Chimica Acta 609, 139–159.
Mannelli, I., Minunni, M., Tombelli, S., Wang, R., Spiriti, M.M., Mascini, M., 2005. Bioelectrochemistry 66, 129–138.
Nielsen, P.E., 2001. Current Opinion in Biotechnology 12, 16–20.
Numnuam, A., Kanatharana, P., Mattiasson, B., Asawatreratanakul, P., Wongkittisuksa, B., Limsakul, C., Thavarungkul, P., 2009. Biosensors and Bioelectronics 24, 2559–2565.
Peeters, S., Stakenborg, T., Reekmans, G., Laureyn, W., Lagae, L., Van Aerschot, A., Van Ranst, M., 2008. Biosensors and Bioelectronics 24, 72–77.
Samanman, S., Kanatharana, P., Chotigeat, W., Decahmag, P., Thavarungkul, P., 2011. Journal of Virological Methods 173, 75–84.
Shervedani, R.K., Hatefi-Mehrjardi, A., 2007. Sensors and Actuators B: Chemical 126, 415–423.
Su, X., Wu, Y.J., Robelek, R., Knoll, W., 2005. Langmuir 21, 348–353.
Suparpprom, C., Srisuwannaket, C., Sangvanich, P., Vilaivan, T., 2005. Tetrahedron Letters 46, 2833–2837.
Tichoniuk, M., Ligaj, M., Filipak, M., 2008. Sensors and Actuators 8, 2118–2135.
Vilaivan, T., Srisuwannaket, C., 2006. Organic Letters 8, 1897–1900.
Wannapob, R., Kanatharana, P., Limbut, W., Numnuam, A., Asawatreratanakul, P., Thammakhet, C., Thavarungkul, P., 2010. Biosensors and Bioelectronics 26, 357–364.
Wittung-Stafshede, P., Rodahl, M., Kasemo, B., Nielsen, P., Norden, B., 2000. Colloids and Surface A 174, 269–273.
Wong, E.L.S., Chow, E., Gooding, J.J., 2005. Langmuir 21, 6957–6965.

ChemistryOPEN

Open Access

DOI: 10.1002/open.201200016

Conformational Control of Dual Emission by Pyrrolidinyl PNA–DNA Hybrids

Sabrina Sezi,[a] Reji Varghese,[a] Tirayut Vilaivan,*[b] and Hans-Achim Wagenknecht*[a]

The current interest in using nucleic acids as supramolecular scaffolds for the precise arrangement of chromophores is extremely high.[1] This is triggered by the potential to control chromophore interactions through the geometry of the double helical structure and is also driven by the search for new multifluorescent probes for bioanalytics and for new multiluminescent organic materials.[2–6] However, the construction of nucleic acid-based multichromophores requires the understanding of photophysical interactions in chromophore pairs as the simplest unit along the helix. Wilhemsson et al. used rigid nucleic acid base analogues to study the influence of the relative orientation on energy transfer.[6] Recently, we published on white light-emitting DNA by combining ethynyl pyrene and ethynyl nile red as blue-green and red emitters.[4] Herein, we extend this concept to pyrrolidinyl PNA–DNA hybrids to study the influence of a conformationally restricted nucleic acid geometry.

Peptide nucleic acid (PNA) is a class of DNA analogues that consists of nucleobases attached to a peptide-like backbone. The original PNA with a flexible *N*-(2-aminoethyl)glycine backbone introduced by Nielsen et al. was shown to bind strongly to DNA and preferentially to RNA with high affinity and sequence specificity.[7,8] We,[9–11] as well as others,[12–14] have shown that incorporating conformational rigidity into the PNA backbone could further improve the binding affinity, especially to DNA, as a result of decreased entropy loss upon hybridization. PNA systems derived from nucleobase-modified proline in (2′*R*,4′*R*) configurations in combination with cyclic β-amino acids including (*R*)-aminopyrrolidine-2-carboxylic acid (dapcPNA),[9] (2*S*)-aminocyclopentane-(1*S*)-carboxylic acid (acpcPNA)[10] and (2*S*)-aminocyclobutane-(1*S*)-carboxylic acid (acbcPNA)[11] formed very stable hybrids with complementary DNA. Much less stable hybrids were formed with RNA, and no self-pairing hybrids could be obtained in acpcPNA.[10] These properties have not been observed in other PNA systems. Recently, the artificial nucleobase 5-(1-pyrenyl)uracil was incorporated into acpcPNA to probe the sequence selectivity by fluorescence of hybrids with DNA.[15]

We applied, herein, dual-emitting oligonucleotides bearing ethynyl pyrene adjacent to ethynyl nile red to probe the differences in interactions in DNA duplexes compared to conformationally constrained acpcPNA–DNA hybrids. Using our published synthetic protocols,[4,10] we prepared doubly labeled oligonucleotides **DNA1** to **DNA4** and the corresponding acpcPNA counterstrands, **PNA1** to **PNA4**. These strands can form fully complementary DNA–PNA hybrids in the binding region (e.g., **DNA1**–**PNA1**) in which the two fluorophores are embedded in four different sequential contexts (X-----Y, Scheme 1). **DNA5** to **DNA8** represent oligonucleotide counterstrands to **DNA1** to **DNA4**, respectively, in order to compare the optical properties of the PNA–DNA hybrids with the corresponding doubly modified DNA duplexes (e.g., **DNA1**–**DNA5**). Additionally, PNA–DNA hybrids or DNA duplexes with two mismatches can be formed (e.g., **DNA1**–**PNA2** or **DNA1**–**DNA6**). **DNA9** to **DNA12** represent reference oligonucleotides to measure the thermal stability of the unmodified acpcPNA–DNA hybrids (e.g,. **DNA9**–**PNA1**).

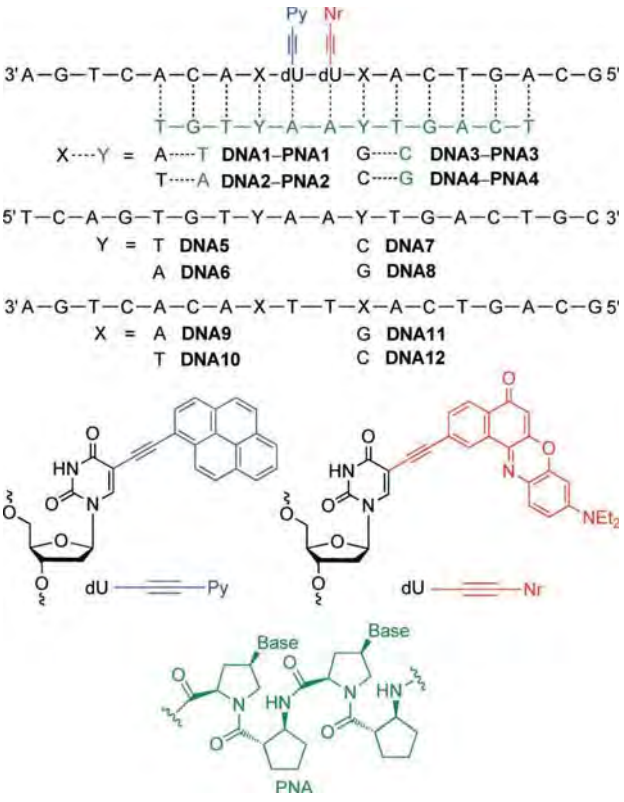

Scheme 1. Sequences of modified oligonucleotides **DNA1** to **DNA4**, acpcPNA counterstrands **PNA1** to **PNA4**, oligonucleotide counterstrands **DNA5** to **DNA8** and reference oligonucleotides **DNA9** to **DNA12**.

[a] *S. Sezi, Dr. R. Varghese, Prof. H.-A. Wagenknecht*
Institute for Organic Chemistry, Karlsruhe Institute of Technology
Fritz-Haber-Weg 6, 76131 Karlsruhe (Germany)
E-mail: Wagenknecht@kit.edu

[b] *Prof. T. Vilaivan*
Department of Chemistry, Faculty of Science, Chulalongkorn University
Phyathai Road, Pathumwan, Bangkok 10330 (Thailand)
E-mail: vtirayut@chula.ac.th

Supporting information for this article is available on the WWW under http://dx.doi.org/10.1002/open.201200016.

© 2012 The Authors. Published by Wiley-VCH Verlag GmbH & Co. KGaA. This is an open access article under the terms of the Creative Commons Attribution Non-Commercial License, which permits use, distribution and reproduction in any medium, provided the original work is properly cited and is not used for commercial purposes.

The optical properties of the acpcPNA–DNA hybrids in comparison with the corresponding DNA duplexes were characterized by UV/Vis absorption spectra, including melting temperatures (T_m), and steady-state fluorescence spectroscopy (Table 1). The unmodified hybrids **DNA9**–**PNA1** to **DNA12**–**PNA4** exhibit T_m values ranging from 71.8 °C to >90 °C. Considering the fact that the PNA counterstrands **PNA1** to **PNA4** represent only a partial, 12 bases long complement, these T_m values are extremely high and show the extraordinary stabilizing effect of acpcPNA.[10] On the other hand, it is highly interesting that the thermal stabilities of the acpcPNA–DNA hybrids contradict the known sequential effects in normal DNA. The only difference is that **DNA9**–**PNA1** and **DNA10**–**PNA2** contain two A-T base pairs where **DNA11**–**PNA3** and **DNA12**–**PNA4** bear two G-C base pairs. In normal DNA, an exchange of A-T by G-C base pairs increases the T_m values. With acpcPNA, the opposite effect is obtained, and the thermal stability is enhanced with A-T base pairs. The T_m values of **PNA1** and **PNA3** with their exactly complementary, unmodified DNA targets were 85.4 and 71.0 °C, respectively. These values are comparable to those obtained from the long target sequences used in this work, indicating that the binding should occur at the expected region. All four doubly labeled hybrids, **DNA1**–**PNA1** to **DNA4**–**PNA4**, show reduced T_m values of 58.2–82.3 °C, due to the presence of the two fluorophores. On the other hand, the T_m values of these acpcPNA–DNA hybrids are generally higher compared with the corresponding doubly labeled DNA duplexes (i.e., **DNA1**–**DNA5** to **DNA4**–**DNA8,** except **DNA3**–**DNA7** in comparison with **DNA3**–**PNA3**). Mismatch-containing DNA duplexes (e.g., **DNA1**–**DNA6**) show strongly reduced thermal stabilities (−9.3 °C to −27.9 °C), while mismatch-containing acpcPNA–DNA hybrids are not formed at all (e.g. **DNA1**–**PNA2**), as expected based on our previous results and as supported by the low absorption differences in the melting temperature experiments.[10]

Table 1. Melting temperatures (T_m) and optical properties of acpcPNA–DNA hybrids in comparison with DNA duplexes.

Sequence[a]		T_m[b] [°C]	$\Delta A_{402}/\Delta A_{379}$[c]	λ [nm][d]	I_{665}/I_{440}[e]
DNA1	–	–	0.97	621	8.9
DNA1–DNA5	m	58.5	0.99	622	2.7
DNA1–DNA6	mm	48.7	1.02	624	9.0
DNA1–PNA1	m	82.3	0.92	618	3.6
DNA1–PNA2	mm	–[f]	0.96	622	9.1
DNA9–PNA1	m	86.0	–	–	–
DNA2	–	–	0.94	618	>10
DNA2–DNA6	m	57.2	0.97	620	4.3
DNA2–DNA5	mm	47.9	0.99	618	11.5
DNA2–PNA2	m	76.5	0.90	631	1.2
DNA2–PNA1	mm	–[f]	0.96	619	6.3
DNA10–PNA2	m	>90	–	–	–
DNA3		–	1.03	621	8.5
DNA3–DNA7	m	63.5	1.01	621	5.2
DNA3–DNA8	mm	51.2	1.06	622	>10
DNA3-PNA3	m	58.2	0.95	623	2.2
DNA3–PNA4	mm	–[f]	1.03	621	7.4
DNA11–PNA3	m	71.8	–	–	–
DNA4	–	–	0.91	622	>10
DNA4–DNA8	m	64.3	0.98	623	1.7
DNA4–DNA7	mm	36.4	0.91	621	>10
DNA4–PNA4	m	77.4	0.90	637	1.0
DNA4–PNA3	mm	–[f]	0.91	622	8.9
DNA12–PNA4	m	>90	–	–	–

[a] m = match, mm = mismatch. [b] *Conditions:* duplex (2.5 μM), buffer (10 mM Na-P_i, 250 mM NaCl, pH 7), 20–90 °C, 0.7 °C min^{-1}. [c] Absorption ratios at 402 nm versus 379 nm. [d] Absorption maximum of the nile red chromophore. [e] Fluorescence intensity ratios at 665 nm versus 440 nm. [f] $\Delta\Delta A < 0.05$.

The UV/Vis absorption of both the doubly modified acpcPNA–DNA hybrids and the DNA duplexes show the presence of both chromophores at ~370–400 nm (ethynyl pyrene) and ~620 nm (ethynyl nile red). If excited at 380 nm, which is highly selective for ethynyl pyrene, the various single strands, hybrids and duplexes show dual emission at ~440 nm (ethynyl pyrene) and ~665 nm (ethynyl nile red) as the result of an energy transfer between both chromophores. In the most interesting case from the supramolecular point of view, the contributions of the blue-green and the red emission are equal, and thereby an emission of white light is generated.[4] A careful examination reveals two major differences in the UV/Vis absorption of the various samples (Figure 1 and the Supporting Information): Both the ratio of the two absorption bands of ethynyl pyrene at ~402 nm and ~379 nm as well as the maximum of nile red absorption varies significantly (Table 1). According to our previous results, the UV/Vis band at approximately 402 nm represents the absorption of an excitonically coupled complex of the ethynyl pyrene chromophore with one of the adjacent DNA bases.[16] In the randomly folded single stranded DNA, these interactions are generally less pronounced. However, a higher extent of prestacking between the ethynyl pyrene and purines (A or G) exist in **DNA1** and **DNA3**, respectively, as the corresponding absorption ratios ($\Delta A_{402}/\Delta A_{379}$) are higher compared with those of **DNA2** and **DNA4**. In principle, ground state interactions interfere with energy transfer, because the latter process requires the excitation of an uncoupled chromophore as energy donor (ethynyl pyrene) and subsequent transfer of excitation energy to an uncoupled and unexcited chromophore as acceptor (ethynyl nile red). Hence, it is not surprising that those single stranded oligonucleotides (**DNA2** and **DNA4**), in which the ethynyl pyrene is less coupled in the ground state (according to the ratios $\Delta A_{402}/\Delta A_{379}$), exhibit better energy-transfer efficiencies (indicated by higher nile red emission, and displayed by higher fluorescence intensity ratios $I_{665}/I_{440} > 10$).

If the single strands **DNA1** to **DNA4** are annealed with the corresponding fully complementary counterstrands **DNA5** to **DNA8**, the absorption side band at ~402 nm gets intensified, and the ratios $\Delta A_{402}/\Delta A_{379}$ increase accordingly. This is not a new result and has been reported previously.[14] However, intensified ground state interactions of the ethynyl pyrene chromophore with adjacent DNA bases in double stranded DNA inhibits energy transfer to ethynyl nile red. As a result, the fluorescence intensity at ~665 nm gets decreased significantly *without* a corresponding increase of the ethynyl pyrene emis-

 © 2012 The Authors. Published by Wiley-VCH Verlag GmbH & Co. KGaA, Weinheim

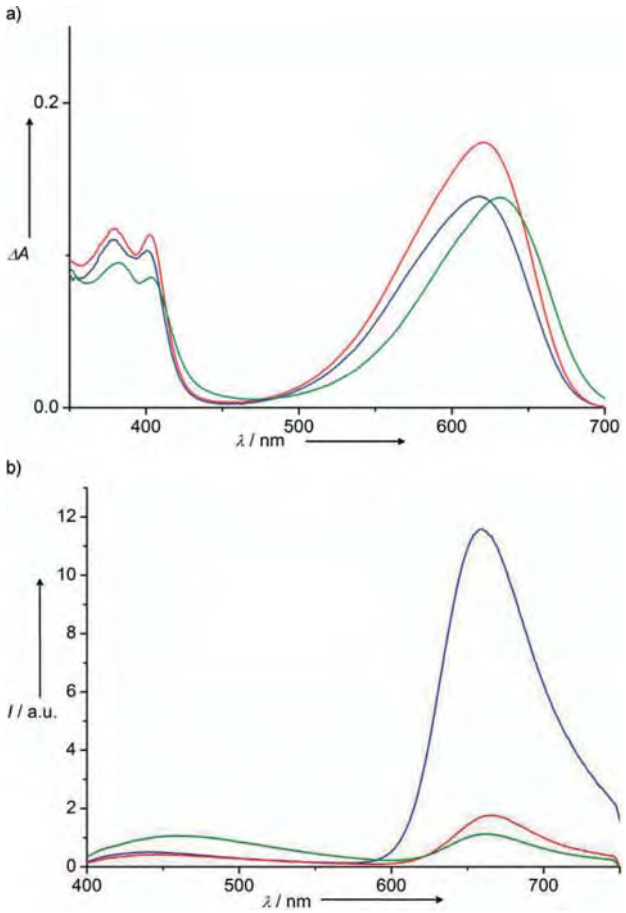

Figure 1. a) UV/Vis absorption and b) fluorescence representatively shown for single stranded **DNA2** (——), double stranded **DNA2**–**DNA6** (——) and **DNA2**–**PNA2** (——; 2.5 μM each) in buffer (10 mM Na-P_i, 250 mM NaCl, pH 7) at 20 °C and λ_{exc} 380 nm.

sion at ~440 nm. The ratio of the fluorescence intensities I_{665}/I_{440} are reduced to values between 1.7 (**DNA4**–**DNA8**) and 5.2 (**DNA3**–**DNA7**). It is important to note here that the excitonic interactions do not require the fully matched DNA architecture around them, as they are formed also in the mismatched DNA duplexes (**DNA1**–**DNA6** to **DNA4**–**DNA7**). However, in the latter duplexes they do not interfere with energy transfer. Obviously, transition dipole moments of the nonstacked subensemble can—due to higher conformational flexibility—adapt an orientation that is more suitable for efficient energy transfer. Thus, fluorescence intensity ratios I_{665}/I_{440} in the mismatched duplexes are similar to those of the corresponding single strands **DNA1** to **DNA4**.

If the single strands **DNA1** to **DNA4** are annealed with corresponding fully complementary acpcPNA strands **PNA1** to **PNA4**, the optical properties change quite significantly compared with the DNA duplexes. Except for **DNA1**–**PNA1**, the I_{665}/I_{440} ratios are generally lower than that of the corresponding DNA duplexes, ranging between 1.0 (**DNA4**–**PNA4**) to 3.6 (**DNA1**–**PNA1**). The fluorescence intensity ratio bears no relationship to the duplex stability as can be seen by the lower I_{665}/I_{440} ratio, despite the lower thermal stability of **DNA3**–**PNA3** compared with **DNA3**–**DNA7**. In addition, the absorption side bands of ethynyl pyrene at ~402 nm get reduced and the absorption ratios $\Delta A_{402}/\Delta A_{379}$ get decreased accordingly. This observation indicates that the stacking interactions between the ethynyl pyrene chromophore and adjacent DNA bases are interrupted by the conformational constrain, which is introduced in acpcPNA–DNA hybrids. According to our discussion for the matched DNA duplexes above, this should yield stronger nile red fluorescence intensity at ~665 nm compared with DNA double strands. However, the opposite effect is observed: the red emission is also reduced in the acpcPNA–DNA hybrids. This result can be explained by two different effects that are probably combined to various extents in the different acpcPNA–DNA hybrids. Firstly, except for **DNA1**–**PNA1**, the ethynyl pyrene fluorescence in acpcPNA–DNA hybrids increases slightly relative to DNA duplexes. The observed difference of the energy-transfer efficiencies is likely due to the change in the relative orientation of the chromophore dipole moments[3] upon duplex formation with PNA (helically twisted conformation), which partially prohibits an efficient energy transfer. With the published doubly modified DNA–DNA duplexes[4] we observed that even if the difference in the energy transfer is small (according to the rather small increase of ethynyl pyrene fluorescence intensity), the significant drop of the red emission intensity in the duplex is due to the large molar extinction coefficient and the high fluorescence quantum yield of ethynyl nile red. Secondly, a careful examination of the ethynyl nile red absorption reveals changes of its maximum wavelength (most pronounced in **DNA2**–**PNA2**). This again supports ground state interactions between nile red and ethynyl pyrene, and thereby again interferes with ethynyl nile red emission induced by energy transfer.

The inspection of photophysical interactions in chromophore pairs is crucial for using the geometries of nucleic acid hybrids with artificial backbones for the development of multichromophore systems. From our results it becomes clear that the strong binding to DNA (high T_m values) and the pronounced sequence selectivity including mismatch discrimination of acpcPNA provides added value to the basic concept of self-assembled nucleic acid-based nanostructures and multichromophore arrangements. Among the samples presented herein, especially hybrids **DNA2**–**PNA2** and **DNA4**–**PNA4** show nearly equal contributions of the blue-green and red emission and, thus, represent white-light emitters with better thermal stability than the previously published white light-emitting DNA (WED).[4] These results demonstrate that the control of photophysical interactions between chromophores can be much better realized with the sterically constrained pyrrolidinyl PNA. Especially acpcPNA has a significant potential and should play an increasing role for the development of both fluorescent probes and nucleic acid-based nanomaterials.

 © 2012 The Authors. Published by Wiley-VCH Verlag GmbH & Co. KGaA, Weinheim

Acknowledgements

This work was supported by the Alexander von Humboldt Foundation (R.V. and T.V.), the Deutsche Forschungsgemeinschaft (DFG) (GRK 640) and the Thailand Research Fund (RTA5280002).

Keywords: biosensors · fluorescence · nanomaterials · nucleic acids · peptides

[1] a) R. Varghese, H.-A. Wagenknecht, *Chem. Commun.* **2009**, 2615 – 2624; b) V. L. Malinovskii, D. Wenger, R. Haner, *Chem. Soc. Rev.* **2010**, *39*, 410 – 422; c) A. Ruiz-Carretero, P. G. A. Janssen, A. Kaeser, A. P. H. J. Schenning, *Chem. Commun.* **2011**, *47*, 4340 – 4347; d) T. J. Bandy, A. Brewer, J. R. Burns, G. Marth, T. Nguyen, E. Stulz, *Chem. Soc. Rev.* **2011**, *40*, 138 – 148.

[2] a) M. E. Østergaard, P. J. Hrdlicka, *Chem. Soc. Rev.* **2011**, *40*, 5771 – 5788; b) S. P. Sau, P. J. Hrdlicka, *J. Org. Chem.* **2012**, *77*, 5 – 16.

[3] a) Q.-H. Xu, B. S. Gaylord, S. Wang, G. C. Bazan, D. Moses, A. J. Heeger, *Proc. Natl. Acad. Sci. USA* **2004**, *101*, 11634 – 11639; b) M. Endo, T. Shiroyama, M. Fujitsuka, T. Majima, *J. Org. Chem.* **2005**, *70*, 7468 – 7472; c) T. Nguyen, A. Brewer, E. Stulz, *Angew. Chem.* **2009**, *121*, 2008 – 2011; *Angew. Chem. Int. Ed.* **2009**, *48*, 1974 – 1977; d) D. Navarathne, Y. Ner, J. G. Grote, G. A. Sotzing, *Chem. Commun.* **2011**, *47*, 12125 – 12127; e) W. Su, M. Schuster, C. R. Bagshaw, U. Rant, G. A. Burley, *Angew. Chem.* **2011**, *123*, 2764 – 2767; *Angew. Chem. Int. Ed.* **2011**, *50*, 2712 – 2715.

[4] a) R. Varghese, H.-A. Wagenknecht, *Chem. Eur. J.* **2009**, *15*, 9307 – 9310; b) R. Varghese, H.-A. Wagenknecht, *Org. Biomol. Chem.* **2010**, *8*, 526 – 528.

[5] R. E. Dale, J. Eichinger, *Biopolymers* **1974**, *13*, 1573 – 1605.

[6] K. Börjesson, S. Preus, A. H. El-Sagheer, T. Brown, B. Albinsson, L. M. Wilhemsson, *J. Am. Chem. Soc.* **2009**, *131*, 4288 – 4293.

[7] a) P. E. Nielsen, M. Egholm, R. H. Berg, O. Buchardt, *Science* **1991**, *254*, 1497 – 1500; b) M. Egholm, O. Buchardt, L. Christensen, C. Behrens, S. M. Freier, D. A. Driver, R. H. Berg, S. K. Kim, B. Norden, P. E. Nielsen, *Nature* **1993**, *365*, 566 – 568.

[8] B. Hyrup, P. E. Nielsen, *Bioorg. Med. Chem.* **1996**, *4*, 5 – 23.

[9] T. Vilaivan, G. Lowe, *J. Am. Chem. Soc.* **2002**, *124*, 9326 – 9327.

[10] a) T. Vilaivan, C. Srisuwannaket, *Org. Lett.* **2006**, *8*, 1897 – 1900; b) C. Vilaivan, C. Srisuwannaket, C. Ananthanawat, C. Suparpprom, J. Kawakami, Y. Yamaguchi, Y. Tanaka, T. Vilaivan, *Artificial DNA, PNA & XNA* **2011**, *2*, 50 – 59.

[11] W. Mansawat, C. Vilaivan, Á. Balázs, D. J. Aitken, T. Vilaivan, *Org. Lett.* **2012**, *14*, 1440 – 1443.

[12] V. A. Kumar, K. N. Ganesh, *Acc. Chem. Res.* **2005**, *38*, 404 – 412.

[13] J. K. Pokorski, M. A. Witschi, B. L. Purnell, D. H. Appella, *J. Am. Chem. Soc.* **2004**, *126*, 15067 – 15073.

[14] R. J. Worthington, A. P. O'Rourke, J. Morral, T. H. S. Tan, J. Micklefield, *Org. Biomol. Chem.* **2007**, *5*, 249 – 259.

[15] C. Boonlua, C. Vilaivan, H.-A. Wagenknecht, T. Vilaivan, *Chem. Asian J.* **2011**, *6*, 3251 – 3259.

[16] a) E. Mayer, L. Valis, C. Wagner, M. Rist, N. Amann, H.-A. Wagenknecht, *ChemBioChem* **2004**, *5*, 865 – 868; b) C. Wagner, M. Rist, E. Mayer-Enthart, H.-A. Wagenknecht, *Org. Biomol. Chem.* **2005**, *3*, 2062 – 2063; c) A. Trifonov, M. Raytchev, I. Buchvarov, M. Rist, J. Barbaric, H.-A. Wagenknecht, T. Fiebig, *J. Phys. Chem. B* **2005**, *109*, 19490 – 19495.

Received: May 4, 2012
Published online on July 11, 2012

 © 2012 The Authors. Published by Wiley-VCH Verlag GmbH & Co. KGaA, Weinheim

THE JOURNAL OF PHYSICAL CHEMISTRY B

Article

pubs.acs.org/JPCB

Inclusion Complexes between Amphiphilic Phenyleneethynylene Fluorophores and Cyclodextrins in Aqueous Media

Warathip Siripornnoppakhun,[†] Nakorn Niamnont,[‡] Akachai Krumsri,[†] Gamolwan Tumcharern,[§] Tirayut Vilaivan,[†] Paitoon Rashatasakhon,[†] S. Thayumanavan,[∥] and Mongkol Sukwattanasinitt*[,†]

[†]Department of Chemistry, Faculty of Science, Chulalongkorn University, Bangkok 10330, Thailand

[‡]Department of Chemistry, Faculty of Science, King Mongkut's University of Technology Thonburi, Bangkok 10140, Thailand

[§]Thailand National Nanotechnology Center, National Science and Technology Development Agency, Patumthanee 12120, Thailand

[∥]Department of Chemistry, University of Massachusetts at Amherst, Amherst, Massachusetts 01003, United States

Supporting Information

ABSTRACT: Binding events of cyclodextrins (CyD's) in aqueous media are important for designing and explaining the host−guest chemistry applied in sensing and controlled release systems. A water-soluble tricationic compound ($\mathbf{3N^+}$) with three branches of phenyleneethynylene fluorescent moieties and its related amphiphilic compounds ($\mathbf{3C^-}$, $\mathbf{N^0N^+}$, $\mathbf{N^+}$, and $\mathbf{2N^+}$) are employed as molecular probes in the systematic characterization of the supramolecular interactions with CyD's (α, β, and γ). The strong fluorescence enhancement, combined with induced circular dichroism (CD) signals and ^{1}H NMR data, is evidence of 1:1 static inclusion complexes of $\mathbf{3N^+}$/γ-CyD and $\mathbf{2N^+}$/γ-CyD. $\mathbf{3N^+}$ presents a structural design which can form inclusion complexation with γ-CyD with one of the highest binding constants of 3.0×10^4. The relatively moderate fluorescence enhancement, shift of ^{1}H NMR signals, and weak induced CD signals indicate fast exchange complexation of β-CyD with the amphiphilic guest molecules. The interaction with α-CyD is perceived only for $\mathbf{N^0N^+}$, the only nonbranched fluorescent guest model, via its strong fluorescence enhancement. However, the lack of ^{1}H NMR signal splitting and the lack of induced CD signals suggest the noninclusion mode of binding between $\mathbf{N^0N^+}$ and α-CyD.

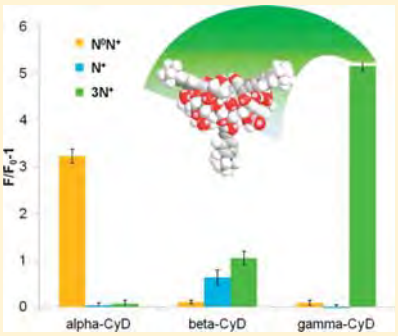

INTRODUCTION

Cyclodextrins (CyD's), a well-known class of host compounds used in sensing and controlled release applications,[1] are cyclic oligosaccharides that selectively form inclusion complexes with guest molecules. Their unique configurations have a hydrophilic outer surface and a hydrophobic inner surface with the inner cavity diameters reported at 5.0, 6.2, and 8.0 Å for α-CyD, β-CyD, and γ-CyD, respectively.[2] In the aqueous phase, CyD's are amphiphilic and may interact with other chemical species that interfere with their collisional probability and hydration dynamics, leading to changes in their physical and chemical properties.[3] These changes may be observed by various techniques to study the interactions between CyD's and guest molecules; examples include ^{1}H NMR,[4] mass spectrometry,[5] electrophoresis,[6] UV−vis absorption spectroscopy,[7] fluorescence spectroscopy,[8] circular dichroism (CD) spectroscopy,[9] X-ray crystallography,[10] and computational calculations.[11] Understanding the binding events of CyD's in aqueous media is crucial for employing their host−guest chemistry in sensing and controlled release systems. The inclusion complexes of CyD's have so far been held responsible for most spectroscopic changes observed in solution. In the solid phase, X-ray crystallography can generally provide unarguable proof of an inclusion complex. It is however trickier to have definitive evidence of an inclusion complex in solution, due to its dynamic nature. We have thus taken the task of gathering evidence for inclusion complexes of CyD's in aqueous solution as our current research problem. We also aim to find structural attributes of the guest compounds that can enhance the stability of the inclusion complex in an aqueous system. Other parts, besides the hydrophobic cavity of the CyD structure (i.e., secondary hydroxyl groups on the wider rim, primary hydroxyl groups on the narrow rim, and the polar oxygen lone pair on the outer annulus)[12] may also take part in the binding events.

To study the inclusion complexes of CyD's in an aqueous system, amphiphilic molecular probes which allow comprehensive characterization by various spectroscopic methods are desirable. We have recently developed a water-soluble tricationic compound ($\mathbf{3N^+}$) with phenyleneethynylene fluorescent moieties which shows strong fluorescence responses upon protein and DNA binding.[13] Interaction of this amphiphilic fluorophore with the nanoconfined environment of CyD's is thus easily probed by fluorescence measurement. Extensive spectroscopic investigation of this compound and its

Received: June 12, 2012
Revised: September 6, 2012
Published: September 8, 2012

ACS Publications © 2012 American Chemical Society

dx.doi.org/10.1021/jp3057652 | J. Phys. Chem. B 2012, 116, 12268−12274

family ($3C^-$, N^0N^+, N^+, and $2N^+$) provides useful information toward our objectives of obtaining evidence for CyD inclusion complexes in solution and molecular designs of suitable guest compounds.

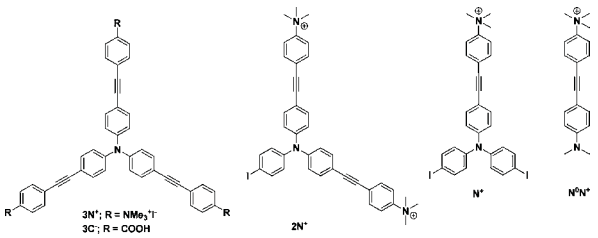

EXPERIMENTAL SECTION

Absorption, Emission, and CD Spectroscopies. All spectroscopic measurements were performed on the solution samples in sodium phosphate buffer (pH 7, 10 mM) containing NaCl (100 mM) in a quartz cuvette (10 mm light path). The instruments used in data acquisition were a Varian Cary 50 UV−vis spectrophotometer, Varian Cary Eclipse spectrofluorometer, and JASCO CD spectrometer. The solutions of the fluorophore and CyD were thoroughly mixed and allowed to stand for 5 min before each measurement.

MS Spectroscopies. A mixture of each fluorophore/CyD pair was prepared in Milli-Q water at room temperature. The final concentrations of the fluorophores and CyD's are 10 and 40 μM (fluorophore:CyD = 1:4). The MS data were acquired using the positive ion mode on a Micromass Quattro micro TM API electrospray ionization mass spectrometer (Waters, Milford, MA).

Synthesis. Synthesis procedures and characterization data of new amphiphilic fluorophores are described in the Supporting Information.

RESULTS AND DISCUSSION

We started our investigation by observing the changes of the fluorescence signal of $3N^+$ (5 μM) upon the addition of α-, β-, and γ-CyD's (20 μM). As shown in Figure 1a, γ-CyD dramatically enhanced the emission signal of $3N^+$, while β-CyD increased the signal only slightly and α-CyD did not create any changes of the spectrum at all. These results suggested that $3N^+$ interacted strongly with γ-CyD and only weakly with β-CyD but may not interact with α-CyD. It is also interesting to note that the signal enhancement goes hand-in-hand with the blue shift, which implies the interaction with γ-CyD is involved in either a reduction of the π-conjugation length of the fluorophore or a reduction in its geometrical relaxation and intramolecular charge transfer (ICT).[3a,d,11,14]

To identify the cause of this blue shift, the absorption spectra of $3N^+$ in the absence and presence of CyD's were recorded. The absorption spectra revealed that only γ-CyD caused a significant blue shift of the maximum absorption wavelength (λ_{max}) of the fluorophore from 370 to 364 nm (Figure 1b). This 6 nm (0.055 eV) shift is much smaller than the 40 nm (0.225 eV) shift present in the emission spectra, which indicates only a minor contribution of the change of the π-conjugation length to the blue shift of the emission maximum. The restriction of geometrical relaxation and the ICT process are thus the main contributors that indeed support the formation of an inclusion complex between $3N^+$ and γ-CyD in the aqueous medium.

In our next investigation, ^{1}H NMR spectra of $3N^+$ and its mixture with each CyD, at a 1:4 mole ratio, were compared. The $3N^+/\alpha$-CyD mixture gave sharper and slightly downfield shifted ^{1}H NMR signals of $3N^+$, indicating some interactions between $3N^+$ and α-CyD. This interaction was not observed in the form of fluorescence enhancement as noted earlier, which is likely due to a much lower concentration (~1/400) used in the fluorescence experiment. Therefore, the interaction between $3N^+$ and α-CyD is probably rather weak. For the mixture with β-CyD, all four aromatic signals of $3N^+$ became even sharper and more downfield shifted (Figure 2), which signified stronger interaction. In the case of $3N^+/\gamma$-CyD, the four aromatic signals of $3N^+$ split into seven peaks which could be assigned to two sets of chemically inequivalent phenyleneethynylene branches. One set consisted of the signals at 7.94, 7.71, 7.03, and 6.87 ppm (a, b, c, and d), and the other set contained the peaks at 7.83, 7.77, and 7.30 ppm (a′, b′, c′, and d′). The peak pattern in the first set looked quite similar to those of the original $3N^+$, while the second set appeared with a quite different pattern. These two sets of peaks indicate unsymmetrical interaction of the three phenyleneethynylene branches of $3N^+$ with γ-CyD. The 2:1 integration ratio between the first and second sets also signifies that two phenyleneethynylene branches of $3N^+$ interact only weakly with γ-CyD while the other branch interacts quite strongly, probably via inclusion complexation. As the mixture contained excess γ-CyD (4 equiv), the ^{1}H NMR spectrum also showed the original signals of γ-CyD (for ^{1}H

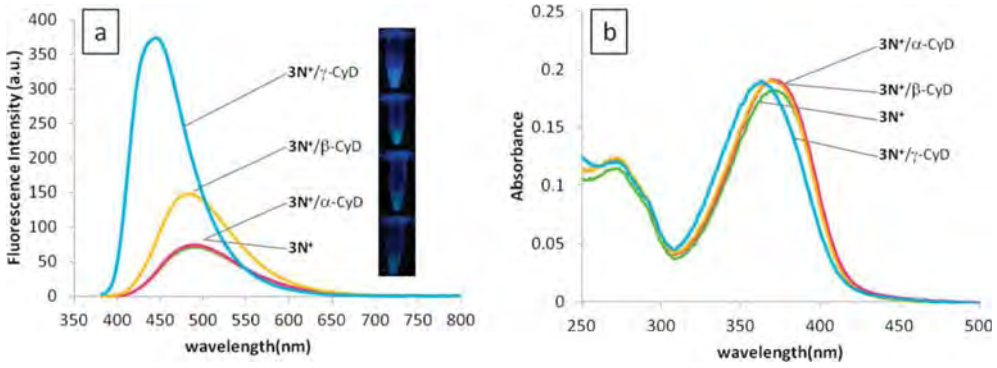

Figure 1. (a) Emission spectra and (b) absorption spectra of $3N^+$ (5 μM) in the presence of α-, β-, and γ-cyclodextrins (20 μM), excited at 370 nm. Inset: photographs of mixtures of $3N^+$ with CyD's under black light irradiation.

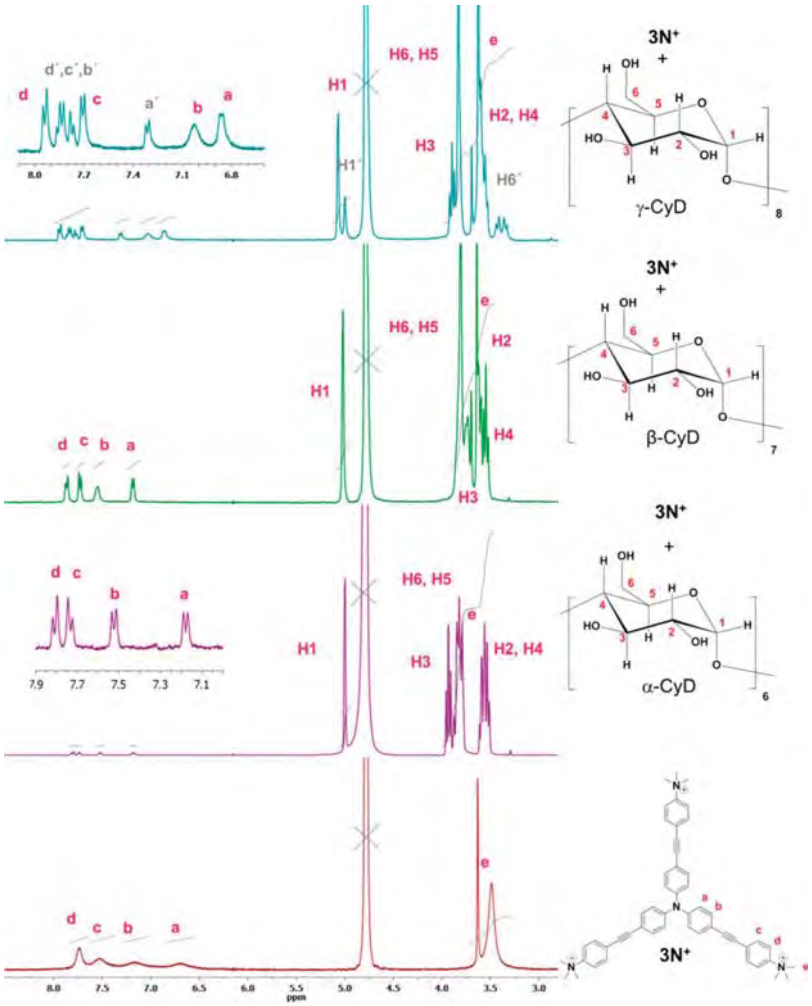

Figure 2. ^{1}H NMR spectra of **3N**$^+$ in D_2O (bottom) and in the presence of α-cyclodextrin, β-cyclodextrin, or γ-cyclodextrin (top).

NMR of pure CyD's, see Figure S1a, Supporting Information) noted specifically for the anomeric protons (H1) at 5.07 ppm. Near this signal, another peak was also observed at a slightly more upfield chemical shift (5.00 ppm), which could be reasonably assigned to the corresponding proton (H1′) of γ-CyD complexing with **3N**$^+$. The integration ratio between H1′ and a′ (or b′, c′, or d′) was found to be 4:1. This value agrees well with the 1:1 complex of **3N**$^+$/γ-CyD in which γ-CyD contains eight H1′ atoms and **3N**$^+$ contains two a′ protons.

The 1:1 complex was also confirmed by Job's plot of the fluorescence intensity, which peaked at a 0.5 mole ratio of **3N**$^+$ (Figure S2, Supporting Information). In summary, the NMR data described here clearly support that the fluorescence enhancement of **3N**$^+$ is involved in the formation of a stable inclusion complex with γ-CyD but a fast-exchange complex with β-CyD.[2d,4p]

In the CD spectroscopy study, **3N**$^+$, as an achiral compound, did not give any CD peaks in the range of 200−500 nm (Figure 3). In the presence of α- and β-CyD's, the CD spectra of the mixtures remained structureless. However, γ-CyD gave a strong induced CD signal of **3N**$^+$ with at least four CD peaks. The CD peaks in the range of 300−400 nm correspond to the $\pi-\pi^*$ absorption of the phenyleneethynylene conjugated system (Figure 1b). The Cotton effect of the CD signal in this range is strong evidence for the tight interaction between the fluorophore and chiral γ-CyD cavity.

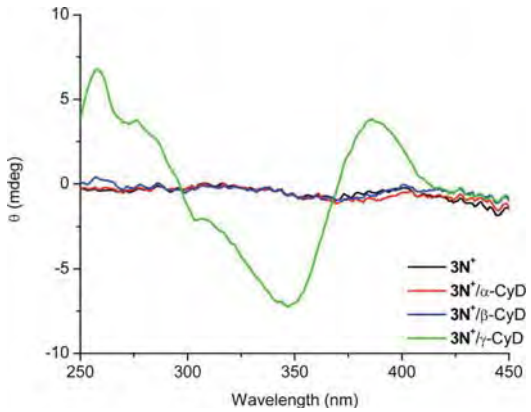

Figure 3. CD spectra of **3N**$^+$ (10 μM) in the presence of α-, β-, and γ-cyclodextrins (10 μM) in sodium phosphate buffer (pH 7, 10 mM) and NaCl (100 mM) at 20 °C.

dx.doi.org/10.1021/jp3057652 | J. Phys. Chem. B 2012, 116, 12268−12274

The binding constant (K_b) between $3N^+$ and CyD was determined by using Benesi–Hilderbrand's double reciprocal plot for a 1:1 complex according to the following equation:

$$\frac{1}{I - I_0} = \frac{1}{I - I_0} + \frac{1}{(I_1 - I_0)K_b}\frac{1}{[\mathrm{CyD}]}$$

where I_0, I, and I_1 are the fluorescence intensities of the free $3N^+$, $3N^+$/CyD mixture, and $3N^+$/CyD complex, respectively.[15] The plot of $1/(I - I_0)$ against the reciprocal molar concentration of CyD provides the y-intercept as $1/(I_1 - I_0)$ and the gradient as $1/(I_1 - I_0)K_b$. Thus, K_b was obtained from the y-intercept/gradient ratio, which were 1.53×10^4 and 3.00×10^4 for β- and γ-CyD, respectively (Figure S3, Supporting Information). It is important to point out here that the binding constant of $3N^+$ is one of the highest for 1:1 complexation with γ-CyD.[16] To our surprise, the binding constant for $3N^+/\beta$-CyD was also relatively high despite it showing only moderate fluorescence enhancement and no clear CD signal change. This relatively high K_b with little effect on fluorescence and CD signals may result from several weak interaction sites with the fast-exchange process as observed by ^{1}H NMR. In fact, we even believe that the $3N^+/\beta$-CyD complex may not be an inclusion mode of interaction. The NOESY NMR spectra also did not show any correlations between aromatic protons of $3N^+$ and β-CyD protons (Figure S1b, Supporting Information), but several correlations were clearly observed in the case of γ-CyD (Figure S1c).

From the size of the ammonium headgroup of $3N^+$ (4.4 Å) and the minimum internal diameter of CyD's (α, 4.4 Å; β, 5.8 Å; γ, 7.4 Å),[2d] the headgroup should be able to insert into β- and γ-CyD's (Figure 4). However, all the spectroscopic results

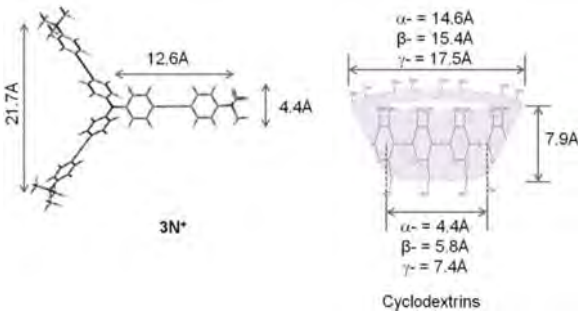

Figure 4. Structural parameters of $3N^+$ and CyD's.

described above gave only evidence for the inclusion complex of $3N^+/\gamma$-CyD. There thus remain intriguing questions of whether other structural traits besides the hydrophobicity and size of the cavity can contribute to the inclusion process.

Three more fluorophores ($3C^-$, N^+, and $2N^+$) were synthesized and studied for the fluorescence responses to CyD's in aqueous solution. Tricarboxylate anion $3C^-$ did not show a significant signal change upon the addition of each CyD (Figure S4, Supporting Information), suggesting no interaction between this fluorophore and CyD's. The results are not totally surprising as the hydroxyl rims of CyD's possess a negative potential.[1] In the case of electrostatically positive fluorophores (N^+ and $2N^+$), each CyD induced different fluorescence changes (Figure 5). The responses of $2N^+$ were similar to those of $3N^+$, the signals of which were strongly enhanced by γ-CyD, moderately enhanced by β-CyD, and not enhanced by α-CyD. The results can again be rationalized as the formation of an inclusion complex of $2N^+$ with only γ-CyD. Surprisingly, N^+, which also contains a positively charged ammonium group, did not show any fluorescence responses to γ-CyD. It however still gave a small fluorescence enhancement with the addition of β-CyD. Also, only $2N^+$ showed an induced CD signal in the presence of γ-CyD (Figure S5, Supporting Information). All the results described above strongly suggested that the inclusion complex was formed only in the case of the $2N^+/\gamma$-CyD pair. The observations also clearly revealed the role of the positive potential on the guest molecule in stabilizing the complex probably via favorable attraction with the negative potential on the CyD rim.

^{1}H NMR spectra of $2N^+$ and CyD mixtures in D_2O were acquired, and we found that only γ-CyD induced significant signal shifts (Figure 6; for α- and β-CyD's, see Figure S6, Supporting Information). There was again a new peak at 5.00 ppm (H1′) corresponding to the anomeric H1 protons of the complexing γ-CyD. These results are quite similar to those observed for $3N^+$, indicating the inclusion complex between $2N^+$ and γ-CyD. However, there was only one set of ^{1}H NMR signals for protons a–f in the case of $2N^+$, while there were two sets (a–d and a′–d′) observed in the case of $3N^+$. The single set of ^{1}H NMR indicates that two phenyleneethynylene branches are in the same environment, which is only possible with the inclusion of γ-CyD at the iodophenyl branch. In addition, there were significant downfield shifts of aromatic protons on the iodobenzene ring (e and f) and upfield shifts along with some broadening of inner aromatic protons on the phenylacetylene branches (a and b). The spectral shifts indicated that the inclusion restrained the C–N bond rotation, causing opposite effects on the electron density of the iodophenyl ring and that of the inner benzene rings of the phenylacetylene branches. The signal broadening also supported the restriction of C–N bond rotation. This part of the ^{1}H NMR observation suggested that the whole iodophenyl ring of $2N^+$ must be deeply inserted into the γ-CyD cavity to affect C–N bond rotation and the dipole–dipole interaction between the two electropositive branches and the electronegative γ-CyD rim should be one of the main driving forces. The insertion of the iodophenyl group of $2N^+$, instead of one of its two ammonium branches, into the γ-CyD cavity was initially quite surprising. It however later served as an interesting finding in this work that the two electropositive branches preferred the interaction from the outside with the electronegative γ-CyD wider rim rather than penetrating through the γ-CyD cavity to interact with its narrower rim. The MM2 geometrical optimization also revealed that the γ-CyD cavity was capable of engulfing the entire triphenylamine core, placing its hydrophilic wider rim in close proximity with the strongly polarized trimethylanilinium rings (Figure S7, Supporting Information). At this point, we strongly believed that two electropositive groups on the fluorophores provide strong dipole–dipole interaction with the CyD wider rim in collaboration with the hydrophobic interaction, inside the cavity, for the formation of inclusion complexes with γ-CyD.

To reassure that two ammonium groups are necessary for inclusion complexation with γ-CyD, a linear monocationic pheneyleneethynylene fluorophore (N^0N^+) was tested as a guest molecule. As expected, there was no fluorescence change of this compound in the presence of γ-CyD (or β-CyD), confirming the absence of inclusion complex formation. To our surprise, the fluorescence signal was however considerably

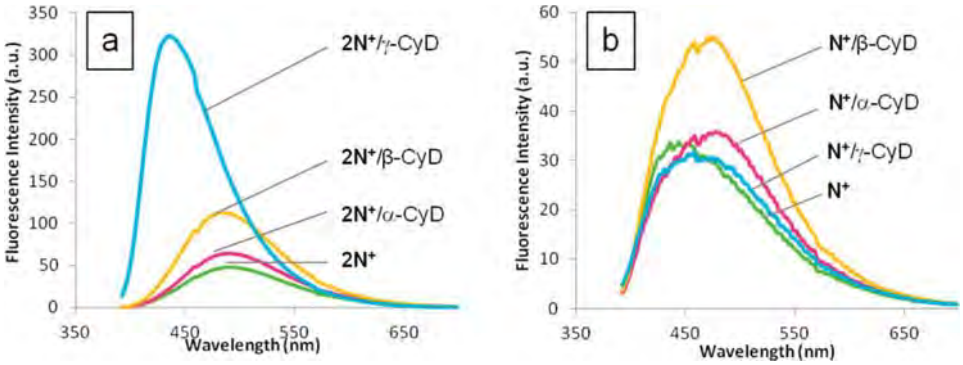

Figure 5. Fluorescence spectra of $\mathbf{2N}^+$ (5 μM) and $\mathbf{N}^+$ (5 μM) in the presence of α-, β-, and γ-CyD's (20 μM) in sodium phosphate buffer (pH 7, 10 mM) and NaCl (100 mM), excited at 368 nm.

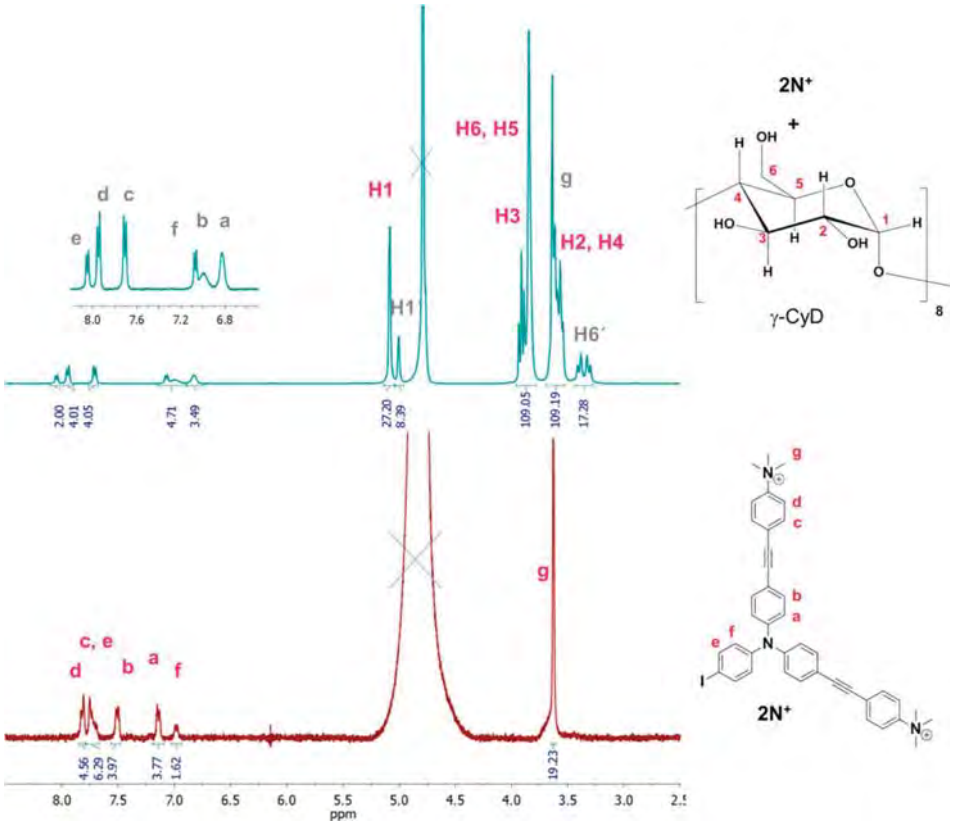

Figure 6. ^{1}H NMR spectra of $\mathbf{2N}^+$ in D_2O only (bottom) and in the presence of γ-cyclodextrin (top).

enhanced in the presence of α-CyD (Figure 7). The results suggested that only α-CyD strongly interacted with $\mathbf{N^0N^+}$, possibly via the inclusion complex. The ^{1}H NMR spectrum of the $\mathbf{N^0N^+}$/α-CyD mixture showed some shifts of the signals of aromatic protons and only one peak of α-CyD anomeric protons around 5.02 ppm (Figure S8, Supporting Information). This ^{1}H NMR observation did not support the formation of a stable inclusion complex but was more consistent with the fast-exchange complexation. The CD spectra of $\mathbf{N^0N^+}$ and its mixture with α-CyD were essentially identical (Figure S10, Supporting Information), which also did not support the formation of an inclusion complex. We therefore believe that the strong fluorescence enhancement and ^{1}H NMR signal shift are caused by fast-exchange complexation rather than inclusion complexation.

The ESI-MS spectra of a 1:4 mixture of each fluorophore/CyD pair in water showed ion peaks at m/z corresponding to both the fluorophore and its 1:1 CyD complex (Figures S11–S14, Supporting Information) that confirmed the formation of a 1:1 complex. The intensity ratios between the complex and fluorophore peaks in the cases of N^{3+}/γ-CyD and N^{2+}/γ-CyD pairs were considerably higher than those observed for other fluorophore/CyD pairs (Table 1), which also indicated the stronger host/guest binding within these two complexes.

dx.doi.org/10.1021/jp3057652 | J. Phys. Chem. B 2012, 116, 12268–12274

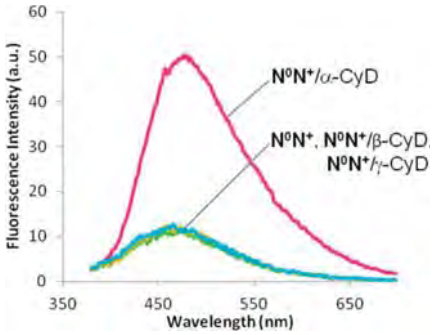

Figure 7. Fluorescence spectra of N^0N^+ (5 μM) in the presence of α-, β-, and γ-CyD's (20 μM) in sodium phosphate buffer (pH 7, 10 mM) and NaCl (100 mM), excited at 328 nm.

Table 1. Abundance of Ions Corresponding to m/z of the Fluorophore (I_{Flu}^{n+}) and Its 1:1 CyD Complex (I_{Cpx}^{n+}) Obtained from ESI-MS Spectra of an Aqueous Solution of Fluorophore/CyD (1:4) Mixtures

fluorophore	cyclodextrin	I_{Flu}^{n+}	I_{Cpx}^{n+}	$I_{Flu}^{n+}/I_{Cpx}^{n+} \times 10^3$
$3N^+$	α-CyD	1.15×10^7	3.18×10^4	2.8
	β-CyD	9.04×10^6	1.58×10^4	1.8
	γ-CyD	2.00×10^5	8.97×10^4	450
$2N^+$	α-CyD	5.21×10^6	2.68×10^4	5.1
	β-CyD	6.10×10^6	7.91×10^3	1.3
	γ-CyD	2.35×10^5	8.73×10^3	37
N^0N^+	α-CyD	3.26×10^5	442	1.4
	β-CyD	1.57×10^6	ND[a]	0
	γ-CyD	3.08×10^6	354	0.1

[a]ND = not detected.

The fluorescence responses of all fluorophores to CyD's are summarized as a histogram plot in Figure 8a. The fluorescence signals of $3N^+$ and $2N^+$ were enhanced strongly ($F/F_0 > 4$) by γ-CyD and moderately enhanced by β-CyD ($F/F_0 \approx 2$), while the signals of N^+ and N^0N^+ were enhanced exclusively by β-CyD and α-CyD, respectively. These differentiable fluorescence responses should be useful for simple identification of CyD's. As demonstrated in Figure 8b, the fluorescence responses of three selected fluorophores (N^0N^+, N^+, and $3N^+$) showed easily distinguishable patterns for α-, β-, and γ-CyD's.

CONCLUSIONS

The series of cationic phenyleneethynylene fluorophores are useful as molecular probes for spectroscopic studies of the interaction modes with CyD's. We found that the stable inclusion complexes were formed only between γ-CyD and the tri- and dicationic fluorophores. The finding suggests that cooperative bindings via hydrophobic and dipole−dipole forces are important for inclusion complexation. No clear evidence of an inclusion complex between β-CyD and the cationic fluorophores was observed. The fluorescence signal of 4-((4-(dimethylamino)phenyl)ethynyl)-*N*,*N*,*N*-trimethylanilinium (N^0N^+) was strongly enhanced by α-CyD, with no other evidence supporting the formation of an inclusion complex. The spectroscopic data in this work are useful references for host−guest chemistry study of CyD's. The structure of the tri- and dicationic fluorophores should also be helpful in designing guest molecules for sensor applications and CyD-based controlled release systems.

ASSOCIATED CONTENT

Supporting Information

Spectroscopic data and synthesis procedures of the compounds. This material is available free of charge via the Internet at http://pubs.acs.org.

AUTHOR INFORMATION

Corresponding Author

*E-mail: smongkol@chula.ac.th.

Notes

The authors declare no competing financial interest.

ACKNOWLEDGMENTS

We thank the National Nanotechnology Center (NANOTEC) (NSTDA code NN-B-22-FN9-10-52-06), The Thailand Research Fund (TRF codes RTA5280002 and PHD/0050/2549), the National Research University of CHE and the Ratchadaphiseksomphot Endowment Fund (Grant AM1006A), and the 90th Anniversary of Chulalongkorn University Fund for financial support and student scholarships. This work is also part of the Project for Establishment of Comprehensive Center for Innovative Food, Health Products and Agriculture supported by Thai government stimulus package 2 (Grant TKK2555, SP2).

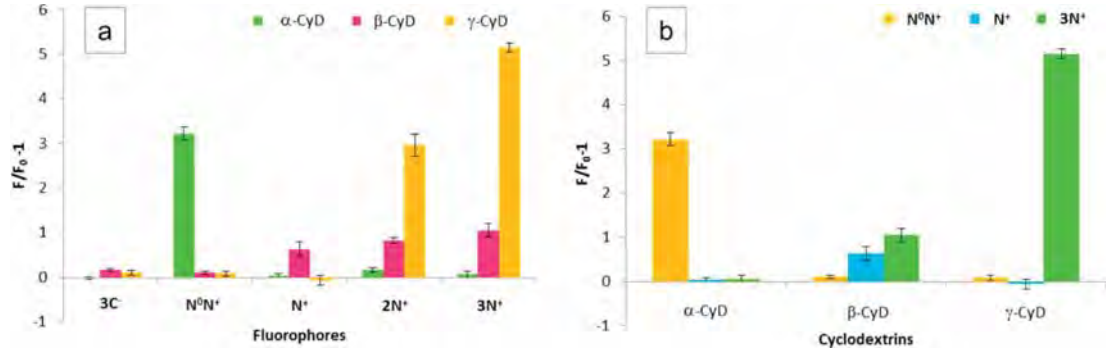

Figure 8. (a) Bar chart representing fluorescence responses of the fluorophores to CyD's (10 μM) in sodium phosphate buffer (pH 7, 10 mM) and NaCl (100 mM) using excitation wavelengths of 378, 328, 368, 368, and 370 nm, respectively, and (b) bar chart representing different fluorescence response patterns, based on three selected fluorophores, created by α-, β-, and γ-CyD's.

REFERENCES

(1) (a) Maeztu, R.; Tardajos, G.; Gonzalez-Gaitano, G. *J. Phys. Chem. B* **2010**, *114*, 2798−2806. (b) Uekama, K.; Hirayama, F.; Irie, T. *Chem. Rev.* **1998**, *98*, 2045−2076. (c) Dsouza, R. N.; Pischel, U.; Nau, W. M. *Chem. Rev.* **2011**, *111*, 7941−7980. (d) Horvath, G.; Premkumar, T.; Boztas, A.; Lee, E.; Jon, S.; Geckeler, K. E. *Mol. Pharmaceutics* **2008**, *5*, 358−361. (e) Xu, D.; Wang, X.; Ding, L. *Carbohydr. Polym.* **2011**, *83*, 1257−1262. (f) Hedges, A. R. *Chem. Rev.* **1998**, *98*, 2035−2044. (g) Chaturvedi, K.; Ganguly, K.; Kulkarni, A. R.; Kulkarni, V. H.; Nadagouda, M. N.; Rudzinski, W. E.; Aminabhavi, T. M. *Expert Opin. Drug Delivery* **2011**, *8*, 1455−1468. (h) Moya-Ortega, M. D.; Alvarez-Lorenzo, C.; Sigurdsson, H. H.; Concheiro, T. L. *Carbohydr. Polym.* **2012**, *87*, 2344−2351.

(2) (a) Dodziuk, H. *Cyclodextrins and Their Complexes: Chemistry, Analytical Methods, Applications*; Wiley-VCH Verlag: Wienheim, Germany, 2006. (b) Szejtli, J. *Chem. Rev.* **1998**, *98*, 1743−1753. (c) Connors, K. A. *Chem. Rev.* **1997**, *97*, 1325−1357. (d) Wenz, G.; Han, B.-H.; Müller, A. *Chem. Rev.* **2006**, *106*, 782−817.

(3) (a) Douhal, A. *Chem. Rev.* **2004**, *104*, 1955−1976. (b) Sahu, K.; Kumar Mondal, S.; Ghosh, S.; Bhattacharyya, K. *Bull. Chem. Soc. Jpn.* **2007**, *80*, 1033−1043. (c) Das, P.; Chakrabarty, A.; Haldar, B.; Mallick, A.; Chattopadhyay, N. *J. Phys. Chem. B* **2007**, *111*, 7401−7408. (d) Rao, V. G.; Ghatak, C.; Pramanik, R.; Sarkar, S.; Sarkar, N. *J. Phys. Chem. B* **2011**, *115*, 10500−10508. (e) Champaiboon, T.; Tumcharern, G.; Potisatityuenyong, A.; Wacharasindhu, S.; Sukwattanasinitt, M. *Sens. Actuators, B* **2009**, *139*, 532−537.

(4) (a) Schneider, H.-J.; Hacket, F.; Rüdiger, V.; Ikeda, H. *Chem. Rev.* **1998**, *98*, 1755−1785. (b) Chen, M.; Diao, G.; Zhang, E. *Chemosphere* **2006**, *63*, 522−529. (c) Sompornpisut, P.; Deechalao, N.; Vongsvivut, J. *Sci. Asia* **2002**, *28*, 263−270. (d) Kato, K.; Sasakawa, H.; Kamiya, Y.; Utsumi, M.; Nakano, M.; Takahashi, N.; Yamaguchi, Y. *Biochim. Biophys. Acta.* **2008**, *1780*, 619−625. (e) Onnainty, R.; Longhi, M. R.; Granero, G. E. *Carbohydr. Res.* **2011**, *346*, 1037−1046. (f) Garg, A.; Gupta, B.; Prakash, R.; Singh, S. *Chem. Pharm. Bull.* **2010**, *58*, 1313−1319. (g) Danel, C.; Azaroual, N.; Foulon, C.; Goossens, J.-F.; Vermeersch, G.; Bonte, J.-P.; Vaccher, C. *Tetrahedron: Asymmetry* **2006**, *17*, 975−983. (h) Bendeby, B.; Kenne, L.; Sandström, C. *J. Inclusion Phenom. Macrocyclic Chem.* **2004**, *50*, 173−181. (i) Acuna-Rougier, C.; Mera-Adasme, R.; Jullian, C.; Olea-Azar, C. *J. Inclusion Phenom. Macrocyclic Chem.* **2010**, *68*, 339−346. (j) Sadlej-sosnowska, N.; Kozerski, L.; Bednarek, E.; Sitkowski, J. *J. Inclusion Phenom. Macrocyclic Chem.* **2000**, *37*, 383−394. (k) Zheng, W.; Tarr, M. A. *Spectrochim. Acta, A* **2006**, *65*, 1098−1103. (l) Ma, H. L.; Wu, J. J.; Liang, W. J.; Chao, J. B. *J. Inclusion Phenom. Macrocyclic Chem.* **2007**, *58*, 221−226. (m) Terekhova, I.; Kozbial, M.; Kumeev, R.; Gierycz, P. *Chem. Phys. Lett.* **2011**, *514*, 341−346. (o) Jover, A.; Budal, R. M.; Meijide, F.; Hugo Soto, V.; Vazquez Tato, J. *J. Phys. Chem. B* **2004**, *108*, 18850−18859. (p) Herrmann, W.; Keller, B.; Wenz, G. *Macromolecules* **1997**, *30*, 4966−4972.

(5) (a) Cong, X.; Czerwieniec, G.; McJimpsey, E.; Ahn, S.; Troy, F. A.; Lebrilla, C. B. *J. Am. Soc. Mass Spectrom.* **2006**, *17*, 442−454. (b) Kwon, S.; Lee, W.; Shin, H.-J.; Yoon, S.; Kim, Y.; Kim, Y.-J.; Lee, K.; Lee, S. *J. Mol. Struct.* **2009**, *938*, 192−197.

(6) Verlaysen, K.; Sabah, S.; Scriba, G.; Chen, A.; Sandra, P. *J. Chromatogr., A* **1998**, *824*, 91−97.

(7) Hbaieb, S.; Kalfat, R.; Chevalier, Y.; Amdouni, N.; Parrot-Lopez, H. *Mater. Sci. Eng., C* **2008**, *28*, 697−704.

(8) (a) Wang, L.; Bian, G.; Wang, L.; Dong, L.; Chen, H.; Xia, T. *Spectrochim. Acta, A* **2005**, *61*, 1201−1205. (b) Al-Hassan, K. A.; Saleh, N.; Abu-Abdoun, I. I.; Yousef, Y. A. *J. Inclusion Phenom. Macrocyclic Chem.* **2008**, *61*, 361−365. (c) Zhang, H.-X.; Huang, X.; Zhang, M. *J. Fluoresc.* **2008**, *18*, 753−760. (d) Chakraborty, A.; Guchhait, N. *J. Inclusion Phenom. Macrocyclic Chem.* **2008**, *62*, 91−97. (e) Vijayan Enoch, M.; Rajamohan, R.; Swanimathan, M. *Spectrochim. Acta, A* **2010**, *77*, 473−477.

(9) Mori, T.; Ho, Ko, Y.; Kim, K.; Inoue, Y. *J. Org. Chem.* **2006**, *71*, 3232−3247. (b) Allenmark, S. *Chirality* **2003**, *15*, 409−422.

(10) (a) Anibarro, M.; Gabler, K.; Uson, I.; Sheldrick, G. M.; Saenger, W. *Carbohydr. Res.* **2001**, *333*, 251−256. (b) Enju, W.; Guangying, C.; Changri, H. *Chin. J. Chem.* **2011**, *29*, 617−622. (c) Ding, J.; Steiner, T.; Zebel, V.; Hingerty, B. E.; Mason, S. A.; Saenger, W. *J. Am. Chem. Soc.* **1991**, *113*, 8081−8089. (d) Steiner, T.; Mason, S. A.; Saenger, W. *J. Am. Chem. Soc.* **1991**, *113*, 5676−5687.

(11) Lipkowicz, K. B. *Chem. Rev.* **1998**, *98*, 1829−1873.

(12) Martin Del Valle, E. M. *Process Biochem.* **2004**, *39*, 1033−1046. Chernykh, E. V.; Brichkin, S. B. *High Energy Chem.* **2010**, *44*, 83−100.

(13) (a) Niamnont, N.; Siripornnoppakhun, W.; Rashatasakhon, P.; Sukwattanasinitt, M. *Org. Lett.* **2009**, *11*, 2768−2771. (b) Niamnont, N.; Mungkarndee, R.; Techakriengkrai, I.; Rashatasakhon, P.; Sukwattanasinitt, M. *Biosens. Bioelectron.* **2010**, *26*, 863−867. (c) Davis, B. W.; Niamnont, N.; Dillon, R.; Bardeen, C. J.; Sukwattanasinitt, M.; Cheng, Q. *Langmuir* **2011**, *27*, 6401−6408. (c) Yuanboonlim, W.; Siripornnoppakhun, W.; Niamnont, N.; Rashatasakhon, P.; Vilaivan, T.; Sukwattanasinitt, M. *Biosens. Bioelectron.* **2012**, *33*, 17−22. (d) Rashatasakhon, P.; Vongnam, K.; Siripornnoppakhun, W.; Vilaivan, T.; Sukwattanasinitt, M. *Talanta* **2012**, *88*, 593−598.

(14) Sen, T.; Kanta Haldar, K.; Patra, A. *J. Phys. Chem. C* **2012**, *114*, 11409−11413.

(15) (a) Kuntz, I. D.; Gasparro, F. P.; Johnston, M. D.; Taylor, R. P. *J. Am. Chem. Soc.* **1986**, *90*, 4778−4781. (b) Almansa López, E.; Bosque-Sendra, J. M.; Cuadros Rodríguez, L.; García Campanña, A. M.; Aaron, J. J. *Anal. Bioanal. Chem.* **2003**, *375*, 414−423.

(16) (a) Kumar Mandal, A.; Kumar Das, D.; Kumar Das, A.; Sen Mojumdar, S.; Bhattachayya, K. *J. Phys. Chem. B* **2011**, *115*, 10456−10461. (b) Das, P.; Mallick, A.; Sarkar, D.; Chattopadhyay, N. *J. Phys. Chem.* **2008**, *112*, 9600−9603. (c) Tanhuanpaa, K.; Hon Cheng, K.; Anttonen, K.; Virtanen, J. A.; Somerharju, P. *Biophys. J.* **2001**, *81*, 1501−1510. (d) Pumera, M.; Matalova, R.; Jalinek, I.; Jindrich, J.; Juza, J. *Molecules* **2001**, *6*, 221−229. (e) Funasaki, N.; Ishikawa, S.; Neya, S. *Langmuir* **2002**, *18*, 1786−1790. (f) Dodziuk, H.; Demchuk, O. M.; Bielejewska, A.; Komiski, W.; Dolgonos, G. *Supramol. Chem.* **2004**, *16*, 287−292. (g) Smith, V. J.; Rougier, N. M.; de Rossi, R. H.; Caira, M. R.; Bujan, E. I.; Fernandez, M. A.; Bourne, S. A. *Carbohydr. Res.* **2009**, *344*, 2388−2393. (h) Green, T. K.; Denoroy, L.; Parrot, S. *J. Org. Chem.* **2010**, *75*, 4048−4055. (i) He, Y.; Fu, P.; Shen, X.; Gao, H. *Micron* **2008**, *39*, 495−516. (j) Wu, A.; Shen, X.; He, Y. *J. Colloid Interface Sci.* **2006**, *302*, 87−94. (k) Farcas, A.; Ghosh, I.; Jarroux, N.; Harabagiu, V.; Guegan, P.; Nau, W. M. *Chem. Phys. Lett.* **2008**, *465*, 96−101. (l) Wu, A.; Shen, X.; He, Y. *J. Colloid Interface Sci.* **2006**, *297*, 525−533. (m) Srinivasan, K.; Kayalvizhi, K.; Sivakumar, K.; Stalin, T. *Spectochim. Acta, A* **2011**, *79*, 169−178. (m) Krois, D.; Brinker, U. H. *J. Am. Chem. Soc.* **1998**, *120*, 11627−11632.

(17) Umezawa, H.; Okada, S.; Oikawa, H.; Matsuda, H.; Nakanishi, H. *J. Phys. Org. Chem.* **2005**, *18*, 468−472.

Analyst

RSC Publishing

PAPER

View Article Online
View Journal | View Issue

Cite this: *Analyst*, 2013, **138**, 269

Positively charged polymer brush-functionalized filter paper for DNA sequence determination following Dot blot hybridization employing a pyrrolidinyl peptide nucleic acid probe†

Praethong S. Laopa,[ab] Tirayut Vilaivan[c] and Voravee P. Hoven*[c]

As inspired by the Dot blot analysis, a well known technique in molecular biology and genetics for detecting biomolecules, a new paper-based platform for colorimetric detection of specific DNA sequences employing peptide nucleic acid (PNA) as a probe has been developed. In this particular study, a pyrrolidinyl PNA bearing a conformationally rigid D-prolyl-2-aminocyclopentanecarboxylic acid backbone (acpcPNA) was used as a probe. The filter paper was modified to be positively charged with grafted polymer brushes of quaternized poly(dimethylamino)ethyl methacrylate (QPDMAEMA) prepared by surface-initiated polymerization of 2-(dimethylamino)ethyl methacrylate from the filter paper *via* ARGET ATRP followed by quaternization with methyl iodide. Following the Dot blot format, a DNA target was first immobilized *via* electrostatic interactions between the positive charges of the QPDMAEMA brushes and negative charges of the phosphate backbone of DNA. Upon hybridization with the biotinylated pyrrolidinyl peptide nucleic acid (b-PNA) probe, the immobilized DNA can be detected by naked eye observation of the yellow product generated by the enzymatic reaction employing HRP-labeled streptavidin. It has been demonstrated that this newly developed assay was capable of discriminating between complementary and single base mismatch targets at a detection limit of at least 10 fmol. In addition, the QPDMAEMA-grafted filter paper exhibited a superior performance to the commercial membranes, namely Nylon 66 and nitrocellulose.

Received 15th August 2012
Accepted 16th October 2012

DOI: 10.1039/c2an36133g

www.rsc.org/analyst

Published on 19 October 2012 on http://pubs.rsc.org | doi:10.1039/C2AN36133G
Downloaded on 28 November 2012

Introduction

DNA sequence determination plays an important role in many biotechnology-related applications ranging from medical,[1,2] forensic,[3,4] agriculture and food sciences.[5] Several methodologies have been continuously developed in order to attain practical and reliable techniques that should be simple, rapid, inexpensive, highly specific and sensitive. In addition, the ability to be implemented in a high-throughput fashion is a highly desirable feature from the economical perspective. Conventional detection mostly relies on the specific hybridization between the designed nucleic acid probe and the complementary sequence which is a part of the DNA analyte. The recognition event can then be transformed into a physically measurable variable which can be determined either by the techniques requiring labels/tags or by label-free techniques based on electrochemical,[6–11] optical,[12–14] and piezoelectric methods.[5,15]

Since 1991, the Nielsen group has introduced a unique DNA analogue called peptide nucleic acid (PNA).[16,17] In PNA, the negatively charged sugar-phosphate backbone of DNA is totally replaced by an uncharged peptide-like backbone (Scheme 1b). The reduced electrostatic repulsion between PNA and DNA

[a]*Program in Petrochemistry, Faculty of Science, Chulalongkorn University, Phayathai Road, Patumwan, Bangkok 10330, Thailand*

[b]*Center for Petroleum, Petrochemicals, and Advanced Materials, Chulalongkorn University, Phayathai Road, Patumwan, Bangkok 10330, Thailand*

[c]*Organic Synthesis Research Unit, Department of Chemistry, Faculty of Science, Chulalongkorn University, Phayathai Road, Patumwan, Bangkok 10330, Thailand. E-mail: vipavee.p@chula.ac.th; Fax: +66-2218-7598; Tel: +66-2218-7627 ext. 102*

† Electronic supplementary information (ESI) available: PNA and DNA sequences, GPC traces, water contact angles, SEM images, FTIR spectra, XPS spectra and atomic composition of the surface-modified filter papers, and additional test results. See DOI: 10.1039/c2an36133g

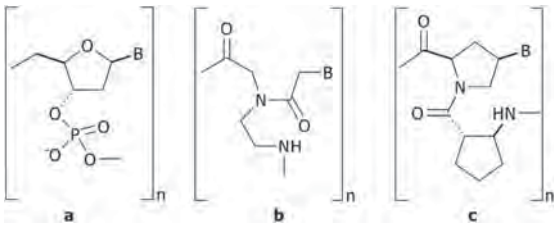

Scheme 1 Structures of (a) DNA, (b) Nielsen's aegPNA, and (c) Vilaivan's acpcPNA.

This journal is © The Royal Society of Chemistry 2013

Published on 19 October 2012 on http://pubs.rsc.org | doi:10.1039/C2AN36133G
Downloaded on 28 November 2012

backbones resulted in superior hybridization characteristics, *e.g.*, higher thermal stability, stronger affinity with less dependence on the salt concentration, greater sequence specificity, and higher capability of strand invasion to double-stranded DNA. The high specificity of PNA makes it an excellent probe for DNA sequence determination. Despite these advantages, there are many attempts to improve the original PNA further during the past 20 years. Among several variants of PNA developed to date, the conformationally rigid pyrrolidinyl PNA derived from D-prolyl-2-aminocyclopentane carboxylic acid (acpc) backbones (acpcPNA),[18,19] introduced by Vilaivan and co-workers (Scheme 1c), shows great promise because it can form a PNA·DNA duplex with even higher affinity and specificity than the original Nielsen's aegPNA. The potential of acpcPNA as a probe to detect the DNA base sequence has been recently demonstrated by employing various techniques including quartz crystal microbalance (QCM),[20] surface plasmon resonance (SPR)[21–23] and MALDI-TOF mass spectrometry.[24] However, these techniques require advanced instruments that are suitable for only well-equipped laboratories and hence cannot be used on-site in remote or rural areas having limited clinical experts and medical facilities.

Dot blot hybridization is a technique widely used in molecular biology and genetics for detecting biomolecules. The sample containing the biological target (mostly proteins or DNA) to be detected is spotted directly on a membrane (such as nitrocellulose, Nylon 66 and poly(vinylidene fluoride) (PVDF)) without prior separation. The presence or absence of a specific target can be detected by binding with a probe that can report the binding event by radioactivity,[25] fluorescence,[26] chemiluminescence,[27–29] or enzyme-based colorimetric assays.[26,30–35] Dot blot hybridization can analyze multiple samples inexpensively with high accuracy and in a high-throughput fashion.

In order to develop an assay based on the concept of Dot blot hybridization, three major components must be considered including the membrane, the probe and the detection method. Commercial membranes designed for DNA blotting including nitrocellulose,[26,33] PVDF,[36] and Nylon 66[37] are generally hydrophobic, which may cause undesirable non-specific adsorption that complicates the analysis. This unwanted characteristic becomes a serious problem particularly with hydrophobic probes such as PNA. To suppress such non-specific interactions, a strong buffer solution containing metal ion ($MgCl_2$),[32] organic solvent (acetonitrile, formamide),[24,32,33,37] anionic detergent (sodium dodecyl sulfate)[24,32,33,37] or combinations thereof must be employed, which may negatively affect the PNA·DNA hybridization. Previously, we have succeeded in using Q-sepharose as an anion-exchanger for capturing the acpcPNA·DNA hybrid in combination with mass spectrometry as a platform for multiplex SNP detection in DNA samples.[24] Based on a similar principle, this research aims to develop a hydrophilic and positively charged membrane for DNA sequence analysis in Dot blot format using acpcPNA probes. It is anticipated that the positive charges on the membrane not only provide a platform for selective capturing of PNA·DNA hybrids, but should also help preventing non-specific adsorption of other non-DNA components in the samples as well as the PNA probe itself.

Due to its availability and inexpensiveness, filter paper-based platforms for analytical applications have received considerable attention in recent years.[38,39] In this research, a hydrophilic and positively charged membrane is developed from filter paper functionalized with quaternized poly(2-(dimethylamino)ethyl methacrylate) (QPDMAEMA) brushes.[40–42] Although the formation of the surface-grafted polymer brushes of QPDMAEMA on a cellulosic membrane has been previously described,[40] to the best of our knowledge, their specific application in DNA sequence determination has never been reported. In principle, the QPDMAEMA-grafted filter paper should readily capture the negatively charged DNA, but not the neutral acpcPNA, by electrostatic interaction. Only when the sequences of the DNA and the biotinylated acpcPNA probe (b-PNA) are complementary, the probe will be immobilized through hybridization with the surface-bound DNA. The non-complementary as well as the excess PNA probes may be removed by simple washing. The presence of the b-PNA·DNA hybrid on the membrane can then be visualized by an enzyme-based colorimetric assay employing horseradish peroxidase streptavidin (SA–HRP) conjugate and a chromogenic substrate such as *o*-phenylenediamine (OPD)[26,30–35] (Fig. 1).

Experimental section

Materials

Whatman no. 1 filter paper was used as the membrane. 2-(Dimethylamino)ethyl methacrylate (DMAEMA) (Aldrich, 98%) was passed through a column filled with basic alumina to remove the inhibitor. The ligand, tris[2-(dimethylamino)ethyl] amine (Me_6TREN), was synthesized according to the published procedure[43] from tris(2-aminoethyl)amine (98%, Aldrich). Ethyl 2-bromoisobutyrate (EBiB) (Fluka, >97%), 2-bromoisobutyryl bromide (Aldrich, 98%), copper(II) bromide (Fluka, 99%), tin(II) 2-ethylhexanoate ($Sn(EH)_2$) (Aldrich, 95%), L-ascorbic acid (Sigma-Aldrich, >99%), 4-*N*,*N*-dimethylaminopyridine (DMAP)

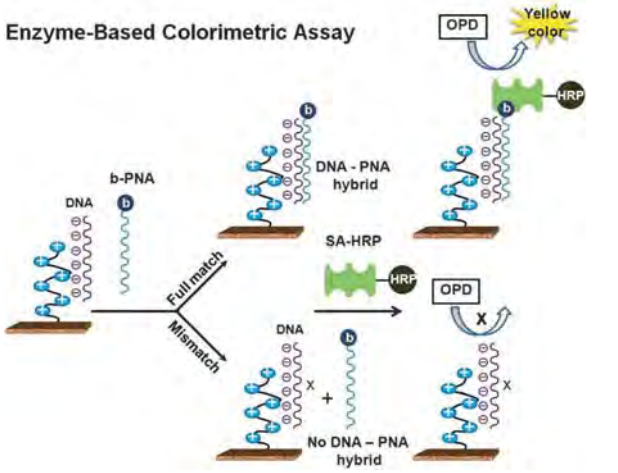

Fig. 1 Schematic representation of enzymatic amplified colorimetric detection of DNA following Dot blot hybridization using filter paper functionalized with positively charged polymer brushes and the peptide nucleic acid probe.

This journal is © The Royal Society of Chemistry 2013

Published on 19 October 2012 on http://pubs.rsc.org | doi:10.1039/C2AN36133G
Downloaded on 28 November 2012

(Fluka, 95%), methyl iodide (Aldrich, >99%), streptavidin–horseradish peroxidase conjugate (SA–HRP) (Sigma-Aldrich, ≥80% protein content, 80–150 units per mg protein), bovine serum albumin (BSA) (Sigma-Aldrich, >96%), *o*-phenylenediamine (OPD) (Aldrich, 98%), 3,3′,5,5′-tetramethylbenzidine (TMB) (Sigma-Aldrich, ≥99%), urea–hydrogen peroxide (urea–H_2O_2) substrate kit (Merck, for analysis 35%), blotting-Nylon 66 membranes, type B, positive (Fluka, 0.45 μm pore size), Hybond ECL nitrocellulose membrane or Amersham Hybond™ ECL™ (GE Healthcare Life Sciences, 0.45 μm pore size) were used as received. All solvents used were of reagent grade. Oligonucleotides were purchased from Bioservice Unit, National Science and Technology Development Agency (Thailand). Ultrapure distilled water was obtained after purification using a Millipore Milli-Q system (USA) that involves reverse osmosis, ion exchange, and filtration steps.

Instrumentation

^{1}H and ^{13}C NMR spectra were recorded in a solution of $CDCl_3$ or DMSO-d_6 on a Varian Mercury-400 nuclear magnetic resonance spectrometer operating at 400 MHz. Chemical shifts were reported in parts per million (ppm) relative to tetramethylsilane (TMS). Infrared spectra of materials scraped from the surface-modified filter paper and prepared as KBr pellets were collected on a Nicolet Impact 6700 FT-IR spectrometer with 32 scans at a resolution of 4 cm^{-1} in a frequency range of 400–4000 cm^{-1}. The molecular weight and polydispersity index of the free poly(2-(dimethylamino)ethyl methacrylate (PDMAEMA) formed in solution were measured using a Waters GPC system (USA), performed at 35 °C using THF (1.0 mL min^{-1}) as the mobile phase and a Waters E600 column connected to the RI detector. Narrow polystyrene standards were used for generating a calibration curve. The water contact angles were measured in air at ambient temperature using a contact angle goniometer, model 200-F1, equipped with a Gilmont syringe and a 24-gauge flat-tipped needle (Ramé-Hart, USA). The data for each sample were taken from five different areas of the substrate and analyzed by DROPimage standard 2.0, after which they were expressed as the arithmetic mean value ± standard deviation (SD). The surface morphology of the filter paper before and after stepwise modification was observed by SEM on a JEOL (JSM-6480LV, Japan) instrument. Surface composition of the surface-modified filter paper was characterized by X-ray photoelectron spectroscopy (XPS) on a Physical Electronics Quantum 2000, using monochromatic Al k-alpha X-rays, and standard dual ion-electron neutralization.

The mass spectra of acpcPNA were recorded on a Microflex MALDI-TOF mass spectrometer (Bruker Daltonics, Germany). The sample (1 μL) was mixed with 10 μL of the matrix solution consisting of α-cyano-4-hydroxycinnamic acid (CCA) in 0.1% TFA in acetonitrile–water (1 : 1) solution. This mixture (1 μL) was deposited onto the target, allowed to dry, and analyzed in positive ion linear time-of-fight mode with an accelerating voltage of +20 kV. All spectra were recorded by averaging between 20 and 30 individual laser shots.

The scanned images of the tested results on filter papers were recorded on a XEROX Workcentre 3119 scanner in 24 bit RGB mode. The brightness/contrast/resolution was set to 128/128/300. The images were saved as TIFF-files. The intensity of each spot was determined using Scion Image software by first converting to gray scale at 300 dpi. Intensity measurements were carried out using the Line tool to select an area for analysis to obtain profile images.

Preparation of QPDMAEMA-grafted filter paper

The initiator immobilized filter paper was prepared according to the published procedure by Lee and co-workers.[40] The filter paper (3.5 × 8 cm^2) was first cleaned by sonicating in dichloromethane (CH_2Cl_2) for 2 min prior to immersion in a solution of triethylamine (2.4 mL, 17 mmol) and a catalytic amount of DMAP (39 mg, 0.3 mmol) in 25 mL of CH_2Cl_2 under stirring for 10 min. Then, 2-bromoisobutyryl bromide (0.6 mL, 1.9 mmol) was slowly added to this solution. After the reaction proceeded for 16 h at ambient temperature (27–33 °C) with gentle agitation, the filter paper was thoroughly rinsed with CH_2Cl_2 followed by methanol and then air-dried.

The initiator immobilized filter paper was placed in a 32 mL scintillation vial containing DMAEMA (16.8 mL, 100 mmol), $CuBr_2$ (1.2 mg, 0.005 mmol), Me_6TREN (57.0 mg (0.25 mmol), and EBiB (74 μL, 0.5 mmol) dissolved in 4.5 mL acetone. After stirring for 10 min, a solution of $Sn(EH)_2$ (490 mg, 1.2 mmol) in 3 mL acetone was then added into the mixture. The vial was then sealed with a rubber septum. The volume of free space above the solution was 7.7 mL. The reaction was left stirring for a specified reaction time (24 h) at ambient temperature (27–33 °C). The filter paper was removed from the vial, successively washed with THF and MeOH to remove the residual monomer and catalysts, and was finally air-dried to yield PDMAEMA-grafted filter paper.

The PDMAEMA-grafted filter paper was placed in 25 mL DMF containing an excess amount of methyl iodide (100 μL). After stirring for 20 h, the filter paper was removed from the solution and washed three times with MeOH followed by THF under sonication and then air-dried. The filter paper was immersed in 100 mL of 0.1 M NaCl solution for 24 h, soaked in 500 mL of deionized water for 48 h and was finally air-dried to obtain QPDMAEMA-grafted filter paper.

Preparation of the biotinylated acpcPNA probe

Three acpcPNA probes, two 13 mer sequences (SLE1 and SLE2) corresponding to two different SNPs at the position −1082 of human *IL-10* promoter gene and one 12 mer random sequence (TG), were used in the study (Table 1). We chose PNA probes with length between 12 and 13 bases which should give a good balance between sensitivity and specificity. The practicality of such 13-base long probes for detection of real human DNA samples has previously been demonstrated.[24] The biotinylated acpcPNA probes (b-PNA) were synthesized according to literature procedures.[18–24] The biotin was attached at the N-termini of acpcPNA while still on the solid support *via* two successive aminoethoxyethoxyacetyl (egl) linkers employing biotin

Published on 19 October 2012 on http://pubs.rsc.org | doi:10.1039/C2AN36133G
Downloaded on 28 November 2012

Table 1 Mass characteristic and T_m of biotinylated acpcPNA probes

Name	PNA sequence	*m/z* (calculated)	*m/z* (observed)	T_m (°C)
b-PNA (SLE1)	*N*-Biotin-(egl)$_2$-TTCCCCCTCCCAA-LysNH$_2$-*C*	4880.36	4879.92	59.3
b-PNA (SLE2)	*N*-Biotin-(egl)$_2$-TTCCCCTTCCCAA-LysNH$_2$-*C*	4895.37	4898.64	65.4
b-PNA (TG)	*N*-Biotin-(egl)$_2$-TGATGCTATGAC-LysNH$_2$-*C*	4722.12	4724.46	not measured

pentafluorophenyl ester in the presence of HOAt/DIPEA. After nucleobase side-chain deprotection and cleavage from the solid support, the crude b-PNA was purified by reversed-phase HPLC with UV detection at 260 nm. A Varian Polaris C18 analytical HPLC column (3 μm particle size 4.6 × 50 mm) was used and eluted with a gradient of 0.1% TFA in MeOH and 0.1% TFA in water. After purification, the solution of PNA was lyophilized and the identity of the acpcPNA oligomers was confirmed by MALDI-TOF mass spectrometry and by thermal denaturation experiments (after hybridization with complementary DNA sequences) (Table 1).

General protocol for DNA sequence determination

The QPDMAEMA-grafted filter paper was cut into 1.0 × 7.0 cm^2 pieces and the spot positions were marked with a pencil. The designated DNA and b-PNA sequences from the list in Table S1 (ESI†) were spotted on the filter paper following a sequence indicated in Table S2 (ESI†). Two microliters of the DNA sample (1 μM in the solution of 0.4 M NaOH containing 10 mM EDTA) was spotted on the filter paper using a micropipette. The filter paper was air-dried and 2 μL of the b-PNA probe (1 μM solution in 0.1 M sodium phosphate buffer (PBS) pH 7.4) was subsequently introduced. The filter paper was rinsed immediately three times with phosphate buffer solution and Milli-Q water followed by incubation in a blocking solution (1% BSA, w/v) at ambient temperature for 30 min. Two microliters of SA–HRP (20 μg mL^{-1}) was then spotted onto the filter paper at the position where the DNA sample was immobilized. The filter paper was then rinsed three times with PBS, Milli-Q water, and citrate buffer (CTB, 0.1 M, pH 5). Two concentrations of the PBS solutions (0.1 M or 50 mM) with or without added 0.1 M NaCl used in the step of washing and blocking were tested in order to find the optimal condition that yields the most efficient detection. Without drying, the filter paper was immersed in a solution consisting of 250 μL of 1.6 mg mL^{-1} OPD substrate (freshly prepared prior to use) and 250 μL of 1.6 mg mL^{-1} urea–H_2O_2 for 1 min and was finally washed with deionized water.

Results and discussion

Preparation and characterization of QPDMAEMA-grafted filter paper

The QPDMAEMA-grafted filter paper was prepared by surface-initiated polymerization (SIP) of 2-(dimethylamino)ethyl methacrylate (DMAEMA) on the filter paper followed by quaternization with methyl iodide (Scheme 2). The initiator immobilized filter paper was prepared by acylation of the hydroxyl groups on the filter paper with 2-bromoisobutyryl bromide in the presence of triethylamine/DMAP. The surface of the filter paper became hydrophobic with a water contact angle of 125.5 ± 1.0° (image of the water droplet is shown in Fig. S1a, ESI†), as opposed to the completely wettable virgin filter paper (water contact angle ~ 0°) suggesting that the immobilization of the 2-bromoisobutyrate moieties on the filter paper was successful. This water contact is much greater than that observed on a gold-coated glass slide grafted onto a monolayer of 2-bromoisobutyrate groups (72°).[44] It is suspected that the additional hydrophobicity may come from the intrinsic roughness of the filter paper causing the water drop to be pinned while performing contact angle measurement. It should be emphasized that this unexpected high contact angle was only observed when at least 16 h of reaction time was used. In the presence of a catalytic amount of DMAP, it is believed that acylation should be more effective and thus yielded a greater graft density of 2-bromoisobutyrate groups on the filter paper than that of the work reported previously by Carlmark and Malmstrom[45] of which the acylation was conducted in the absence of a catalyst. Intuitively, the wetting behavior of the filter paper that may be less covered by 2-bromoisobutyrate groups should be largely governed by the extremely hydrophilic nature of the origin filter paper. This may be the reason why the contact angle of their 2-bromoisobutyrate-modified filter paper was not measurable.

The 2-bromoisobutyrate-functionalized filter paper was then subjected to SIP of the DMAEMA monomer *via* a recently developed living radical polymerization process, activators regenerated by electron transfer for atom transfer radical

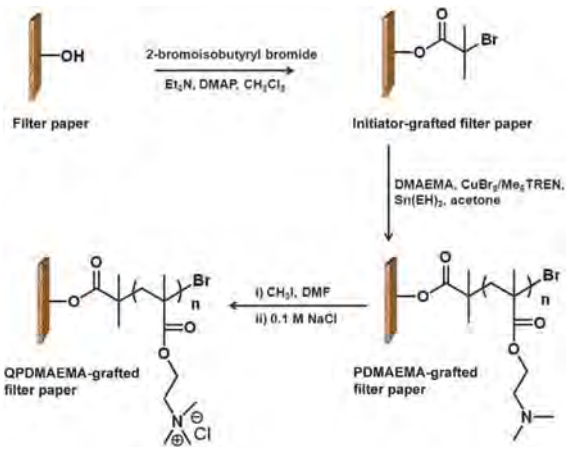

Scheme 2 A synthetic pathway for the preparation of QPDMAEMA-grafted filter paper.

This journal is © The Royal Society of Chemistry 2013

Published on 19 October 2012 on http://pubs.rsc.org | doi:10.1039/C2AN36133G
Downloaded on 28 November 2012

polymerization (ARGET ATRP).[46–48] This mode of polymerization has been chosen as a method for fabricating the positively charged membrane in this particular case due to the fact that the polymerization is living so the molecular weight or graft density of the attached polymer chains can be well controlled. More importantly, the reaction can be performed in a limited amount of air using a ppm level of a catalyst in the presence of a reducing agent without a need for rigorous deoxygenation. This simple handling strategy really opens up an opportunity to produce this paper-based membrane at a larger scale for future DNA sensor applications.

In this research, the ARGET ATRP of DMAEMA was conducted using the $CuBr_2$–Me_6TREN complex and $Sn(EH)_2$ as a catalytic system and reducing agent, respectively. To monitor the molecular weight of the PDMAEMA formed in solution, the sacrificial initiator, EBiB, was added. For the target degree of polymerization (DP) at 200 ($[DMAEMA]_0/[EBiB]_0 = 200:1$), it was found that the $[Sn(EH)_2]_0/[CuBr_2]_0$ of 400 was the optimal ratio that gave the polymer with well-controlled characteristic (M_n (exp) = 28 495 being close to a M_n (theo) of 28 260 and PDI = 1.28) (Table S3, ESI† entry 3). Increasing the ratio to 667 did not provide a positive impact on the polymerization process (Table S3, ESI† entry 4). On the other hand, the PDI tended to be high at a ratio of 200. It should be emphasized that acetone is a better solvent for polymerization of DMAEMA using this catalytic system than anisole (Table S3, ESI† entry 1), the solvent used for the synthesis of PDMAEMA *via* ARGET ATRP using the $CuCl_2$–tris[(2-pyridyl)methyl]amine (TPMA) complex as the catalyst, previously reported by others.[46] This is quite desirable given that acetone is a non-toxic organic solvent having a low boiling point so it can be easily removed from the filter paper after the SIP process by air drying without the need for heat treatment.

The ability to control the molecular weight of PDMAEMA is demonstrated in Table 2. Apparently, the molecular weight of PDMAEMA correspondingly increases as a function of $[DMAEMA]_0/[EBiB]_0$ from 100 : 1 to 200 : 1 and 400 : 1 or a target DP of 100, 200, and 400, respectively. The PDI values approaching 1.0 suggest that the polymerization can be well controlled and gave PDMAEMA with narrow molecular weight distribution. GPC traces of the synthesized PDMAEMA having different target DP are displayed in Fig. S2, ESI.†

Quaternization of PDMAEMA-grafted filter paper was accomplished by methylation of the amino groups of PDMAEMA on filter paper with methyl iodide at ambient temperature as shown in Scheme 2. The iodide counter ion must be exchanged for chloride by treatment with 0.1 M NaCl. This step is mandatory because it was found that iodide ion can be oxidized into iodine which makes the paper turn slightly yellowish upon storage. After it was air-dried, the QPDMAEMA-grafted filter paper having chloride as the counter ion was obtained. The filter paper became extremely hydrophilic after being grafted with PDMAEMA. Although a contact angle of ~50° can be roughly estimated from the drop image promptly captured at the initial contact using the Adobe Photoshop CS2, the water drop was rapidly absorbed into the PDMAEMA-grafted filter paper and disappeared within a second after the contact. This is much more hydrophilic than that has been observed for PDMAEMA-grafted on relatively flat surfaces (~50°).[49,50] This wetting behavior remained unaltered after quaternization. Images of water droplets during water contact angle measurements of both samples are shown in Fig. S1b and c (ESI†).

As examined by SEM (Fig. S3, ESI†), there was no visible changes of surface morphology of the filter paper particularly after being grafted with PDMAEMA having a target DP of 200 (both before and after quaternization) implying that the layer of the coated polymer is relatively thin. This observation coincides with the fact that the physical strength and resistance to bending of the filter paper were not affected by polymer grafting. On the other hand, the filter paper became tougher and plastic-like upon grafting with PDMAEMA having a higher target DP of 400 (SEM micrograph not shown) suggesting that a thicker polymer layer was deposited on the filter paper.

The functional group identity of each surface-modified filter paper was determined by FT-IR as shown in Fig. S4 (ESI†). The FTIR spectra of the initiator immobilized filter paper (Fig. S4b, ESI†) show a band at ~1728 cm^{-1} (C=O stretching of 2-bromoisobutyrate ester) which is not present in the virgin filter paper (Fig. S4a, ESI†). After being grafted with PDMAEMA, the absorption peak for the carbonyl group appears at the same position with greater intensity (Fig. S4c, ESI†), which is a characteristic of the C=O stretching of PDMAEMA.[40,41] No significant change in the IR bands was observed after quaternization (Fig. S2d, ESI†).

The elemental compositions of all surface-modified filter papers were evaluated by XPS and the corresponding spectra are shown in Fig. S5–S9 (ESI†). From the XPS atomic composition data illustrated in Table S4 (ESI†), the detection of 0.8% bromine on the initiator immobilized filter paper suggests that there are bromoester groups available for initiating polymerization from the surface of filter paper. A trace amount of bromine (~0.2%) detected on the PDMAEMA- and QPDMAEMA-grafted filter papers indicated that there were still living polymer chain ends in the form of dormant bromoester species. The presence of an atomic signal of nitrogen on the PDMAEMA- and QPDMAEMA-grafted filter papers clearly confirms the successful polymer attachment *via* the SIP process. The C/N ratio of 8.1 (Table S4, ESI†) corresponds quite well with the theoretical value of PDMAEMA (8.0). An increase in C/N ratio to 11.9 together with the emergence of the N_{1s} peak at 402.0 eV on the QPDMAEMA-grafted filter paper (Fig. 2) strongly indicates that

Table 2 Characteristic of PDMAEMA synthesized by ARGET ATRP having varied target DP

Entry	Target DP[a]	% Conv[b]	M_n (theo)[c]	M_n (exp)[d]	PDI[d]
1	100	85	13 345	21 010	1.24
2	200	90	28 260	28 495	1.28
3	400	69	43 332	42 650	1.18

[a] $EBiB/CuBr_2/Me_6TREN = 1:0.006:0.25$. The polymerization was conducted in a scintillation vial with volume of free space = 7.7 mL. [b] Determined by ^1H NMR in $CDCl_3$. [c] M_n (theo) = ($[DMAEMA]_0/[EBiB]_0$) × conversion. [d] Determined by GPC in THF, based on polystyrene standards.

Published on 19 October 2012 on http://pubs.rsc.org | doi:10.1039/C2AN36133G
Downloaded on 28 November 2012

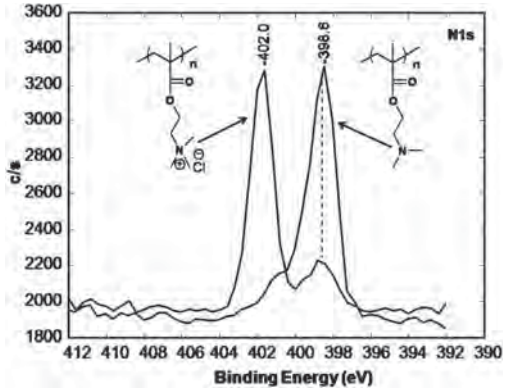

Fig. 2 N_{1s} XPS spectra of PDMAEMA- (right) and QPDMAEMA- (left) grafted filter papers.

additional carbon atoms have been introduced upon quaternization and that most nitrogen atoms existed in the less electronegative form of quaternary ammonium groups.[42] The extent of surface quaternization estimated from the relative ratio between the area of the N_{1s} from the quaternary ammonium entities and that of the regular, non-quaternized one appearing at 398.6 eV was about 80% (Fig. 2). This figure is relatively high suggesting that the QPDMAEMA-grafted filter paper should be positively charged irrespective of pH and readily available to electrostatically adsorb DNA. To test such adsorption ability, a synthetic 13 mer DNA corresponding to a partial sequence of human *IL-10* promoter gene (DNA SLE2) was used as a model. A 1 μL of 10 μM DNA in 0.4 M NaOH containing 10 mM EDTA was spotted on the QPDMAEMA-grafted filter paper. XPS analysis of the paper after extensive washing to remove the unbound DNA (Table S4, ESI†) revealed a characteristic signal of the phosphate group, with a phosphorus content of 1.2%, implying that the DNA molecules were successfully adsorbed on the QPDMAEMA-grafted filter paper.

DNA detection following Dot blot hybridization

It should be emphasized that most of the tests were performed on the QPDMAEMA-grafted filter paper prepared using a target DP of 200. The results are displayed in two formats: scanned images (column A) and profile images as analyzed by Scion Image (column B). The profile image should provide the semi-quantitative intensity of the colorimetric readout and therefore reflecting the testing efficiency and facilitating the background and signal differentiation. A preliminary optimization was first carried out with 1 pmol of b-DNA SLE2 as a positive control by varying the enzyme, substrate, concentration and reaction time. The results shown in Fig. S10 (ESI†) suggest that SA–HRP was superior to avidin–HRP, and the optimal amount was 20 ng per spot since this condition provided a high signal and a minimal background due to non-specific adsorptions (Fig. S10d, ESI†). According to Fig. S11 (ESI†), the optimum concentration of the substrate mixture is 250 μL of 1.6 mg mL^{-1} OPD and 250 μL of 1.6 mg mL^{-1} urea–H_2O_2 and the optimum activation time is 1 min because this condition gave a high signal to background ratio (Fig. S11c, ESI†). Increasing the concentration of substrate mixtures and/or reaction time gave a stronger signal, but so as the non-specific adsorption (background). When TMB[34,35] was used as a substrate in place of OPD, a stronger color was obtained, but also with higher background (Fig. S11a, ESI†). In addition, the blue color disappeared after storage at room temperature suggesting that the complex formed was not stable and that TMB was not the appropriate substrate. The use of a blocking solution (especially 1% BSA) has been found to be essential in preventing the non-specific interaction between the SA–HRP and QPDMAEMA-grafted filter paper as demonstrated in Fig. S12a (ESI†). As seen in Fig. S12b, ESI† signals from both expected specific hybridization and unwanted non-specific adsorption were largely suppressed after blocking with 1% skim milk, a common blocking reagent for various bioassays, suggesting that it is not a suitable blocking reagent.

To test the ability of QPDMAEMA-grafted filter paper as a membrane for DNA sequence determination by Dot blot hybridization, two closely related synthetic 13 mer oligodeoxynucleotides (DNA SLE1 and DNA SLE2) differing by just one base were spotted onto the membrane and the sequences were detected by the b-PNA SLE2 probe. Details of DNA and PNA sequences and the description of samples/probes applied in each spot (1–6) are displayed in Tables S1 and S2 (ESI†), respectively. A biotinylated DNA (b-DNA SLE2) was included as a positive control to show the maximum signal that can be generated by the enzymatic reaction. The effects of washing and blocking solutions were examined using the optimal conditions mentioned above (see results in Fig. S10d, S11c, and S12a, ESI†). Only the positions with b-DNA SLE2 [(+)1)] and DNA SLE2/b-PNA SLE2 [(+)4] (Table S1, ESI†) show yellow spots visible to the naked eyes (Fig. 3). Lowering the PBS concentration down from 0.1 M to 50 mM in the absence of 0.1 M NaCl (Fig. 3d) gave inferior detection efficiency, with slight yellowish tints observed

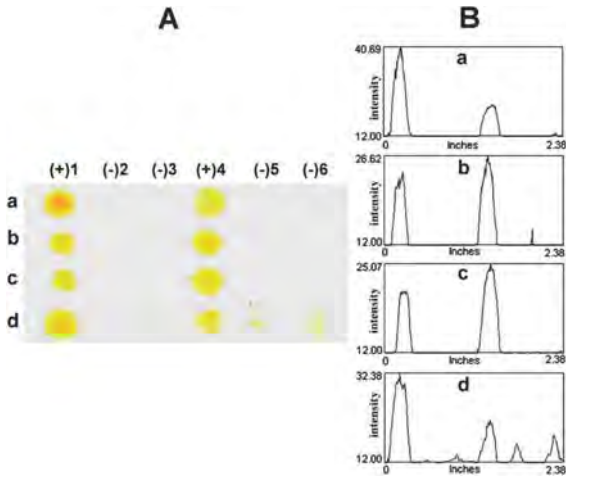

Fig. 3 Representative images (column A: scanned image and column B: profile image) of the test results demonstrating the effect of PBS concentration and salt addition in washing and blocking solutions: (a) 0.1 M PBS w/ 0.1 M NaCl, (b) 0.1 M PBS w/o 0.1 M NaCl, (c) 50 mM PBS w/ 0.1 M NaCl, and (d) 50 mM PBS w/o 0.1 M NaCl.

This journal is © The Royal Society of Chemistry 2013

Published on 19 October 2012 on http://pubs.rsc.org | doi:10.1039/C2AN36133G
Downloaded on 28 November 2012

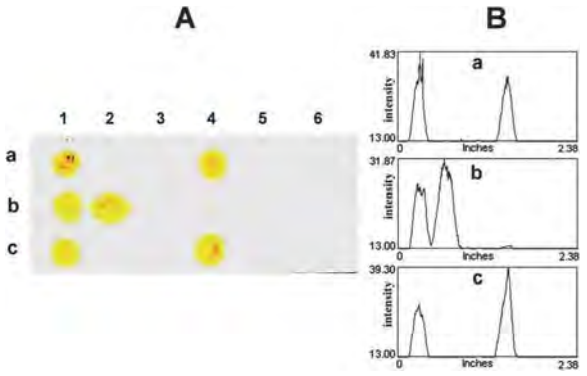

Fig. 4 Representative images (column A: scanned image and column B: profile image) of the test results demonstrating the specificity and efficiency of (a) b-PNA SLE2, (b) b-PNA SLE1 to distinguish complementary and single mismatched DNA (SLE2 and SLE1) targets or (c) complementary DNA (AC) and non-complementary DNA (AG) using b-PNA (TG). The positive results are shown by the yellow spots at position 4 for the tests in entries a and b, and 2 for entry b.

on the two negative controls [(−)5) and (−)6)]. Such non-specific adsorption disappeared and a good detection result was obtained (comparable to the result shown in Fig. 3b) upon addition of 0.1 M NaCl (Fig. 3c). For this reason, 0.1 M PBS without salt addition (Fig. 3b) was chosen as washing and blocking buffers for all subsequent experiments.

Three acpcPNA probes, b-PNA SLE2 and b-PNA SLE1, which differ by only one base, and an unrelated b-PNA (TG) were chosen for specificity determination. Details of DNA and PNA sequences and the description of samples/probes applied in each spot (1–6) are illustrated in Tables S1 and S5 (ESI†), respectively. The data presented in Fig. 4a and b reveal that the Dot blot hybridization using the QPDMAEMA-grafted filter paper and acpcPNA probes offers an excellent specificity to distinguish single base mismatches in the DNA target

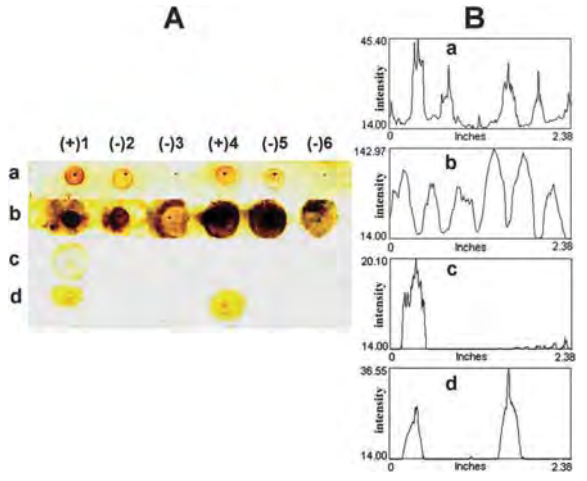

Fig. 5 Representative images (column A: scanned image and column B: profile image) of the test results demonstrating the performance of the QPDMAEMA-grafted filter paper in comparison with commercial membranes: (a) nitrocellulose, (b) Nylon 66, (c) PDMAEMA-, and (d) QPDMAEMA-grafted filter paper.

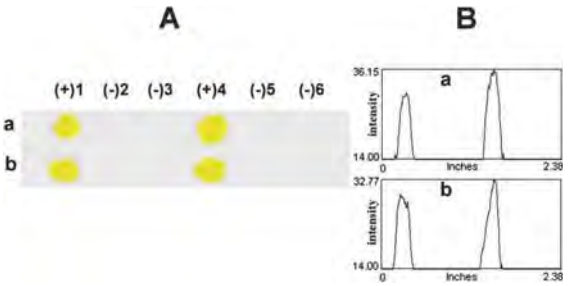

Fig. 6 Representative images (column A: scanned image and column B: profile image) of the test results demonstrating sequence determination of the DNA SLE2 sample using the b-PNA SLE2 probe on the QPDMAEMA-grafted filter paper: (a) freshly prepared and (b) stored at room temperature (27–33 °C) for 1 month.

consisting a partial sequence of human *IL-10* promoter gene (SLE1 and SLE2) by showing only the signal of b-PNA that was hybridized with the complementary DNA target. In addition to these two sequences, the same technique employing b-PNA (TG) as a probe can also successfully distinguish between the complementary and non-complementary DNA targets since the yellow spot was only observed at the position of the complementary DNA target (AC) (Fig. 4c). This illustrates the general applicability of the membrane for detection of various DNA sequences.

For the results shown in Fig. 5–7, details of DNA and PNA sequences and the description of samples/probes applied in each spot (1–6) are displayed in Tables S1 and S2 (ESI†), respectively. To compare the performance of the modified filter paper described in this work with commercial membranes, the detection of DNA SLE2 with b-PNA SLE2 was selected for the

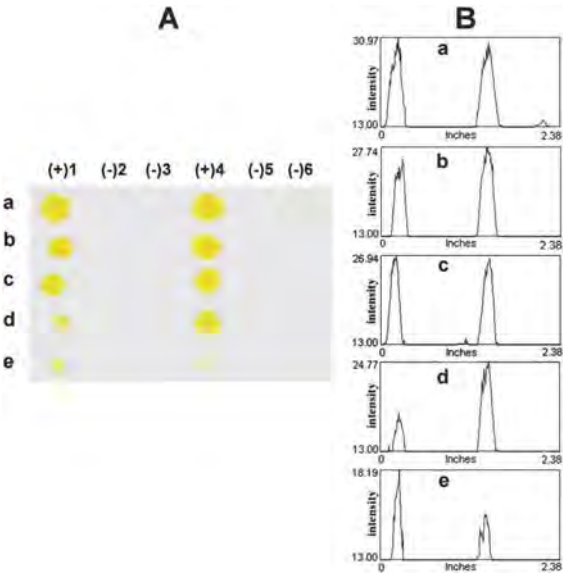

Fig. 7 Representative images (column A: scanned image and column B: profile image) of the test results demonstrating the detection limit of complementary DNA SLE2 and single mismatched DNA SLE1 using 2 μL of 1 μM b-PNA SLE2 as the probe: (a) 2 pmol (2 μL of 1 μM), (b) 1 pmol (1 μL of 1 μM), (c) 100 fmol (1 μL of 100 nM), (d) 50 fmol (0.5 μL of 100 nM), and (e) 10 fmol (1 μL of 10 nM).

Published on 19 October 2012 on http://pubs.rsc.org | doi:10.1039/C2AN36133G
Downloaded on 28 November 2012

investigation. The results presented in Fig. 5 showed that only the QPDMAEMA-grafted filter paper (Fig. 5d) provided a clear-cut discrimination between the complementary [(+)4] and single mismatched DNA [(−)2]. On the other hand, the unquaternized PDMAEMA-grafted filter paper (Fig. 5c) gave low signals even with the positive control [(+)1], indicating that the quaternary ammonium groups of QPDMAEMA are essential for the efficient capture of DNA. The commercial nitrocellulose (Fig. 5a) and Nylon 66 (Fig. 5b) membranes showed substantial non-specific interactions as shown by the presence of dark spots in places where negative results should be observed. In the case of nitrocellulose (Fig. 5a), the appearance of signals whenever the b-PNA was applied, even in the absence of the correct DNA target [(−)2 and (−)5], suggested that there were non-specific interactions between the surface of the membrane and the b-PNA probe. With Nylon 66 (Fig. 5b), the colored spots were observed in all six positions implying that there were non-specific interactions between the membrane surface and SA–HRP as well.

To test the stability of the QPDMAEMA-functionalized filter paper upon storage, the Dot blot experiments were carried out using a membrane that has been stored at room temperature (27–33 °C) for 1 month in comparison with the freshly prepared membranes. The results shown in Fig. 6 demonstrate that both membranes provided comparable results in distinguishing complementary and mismatched DNA targets suggesting that the modified filter paper is stable and the detection efficiency is not affected upon storage for at least one month. This outcome is quite desirable from the practical perspective.

The lowest amount of DNA that can still allow a clear discrimination between fully complementary (DNA SLE2) and single-mismatched DNA (DNA SLE1) was evaluated by spotting different quantities of the DNA targets (2 pmol to 10 fmol) followed by the detection using 2 pmol of the b-PNA SLE2 probe. The results in Fig. 7 show that unambiguous discrimination, which can be quoted as the detection limit of this colorimetric method, is at least down to 10 fmol (equivalent to 1 μL of 10 nM DNA). Although this detection limit is somewhat higher than some other reports,[32,34,35] our main objective to develop a positively charged filter paper-based membrane for simple naked eye detection of DNA using a PNA probe and rapid analysis of multiple DNA samples with a short reaction time (less than 1 hour from DNA spotting to color readout) has been fulfilled. We have previously demonstrated that this level of sensitivity is more than sufficient to detect DNA samples from standard PCR products[24] and, if necessary, it should be possible to improve the detection limit further using polybiotin tags[35,51,52] or polymeric enzymes.[35]

The limitation of this present technique is similar to all blotting techniques that use non-specific interaction to immobilize DNA. If the DNA target to be detected is contaminated by other DNA sequences, there will be a competition between different DNA targets in binding to the membrane and the desired sequence may not be detectable. In such a scenario, a sandwich assay in which two acpcPNA probes that bind to different regions of the DNA target – one probe is immobilized on the surface for capturing the DNA target and the other is labeled with enzyme for detection – should solve the problem.[35]

Conclusions

QPDMAEMA was successfully grafted onto the filter paper by surface-initiated polymerization of DMAEMA *via* ARGET ATRP followed by quaternization with methyl iodide. The molecular weight and polydispersity index of the polymer can be controlled by adjusting the ratio of the $Sn(EH)_2$/initiator and reaction time. The QPDMAEMA-grafted filter paper showed better performance than Nylon 66 and nitrocellulose to be used as a membrane for DNA sequence detection following a Dot blot format employing a biotinylated acpcPNA probe and an enzyme-mediated colorimetric assay. The low non-specific interaction of the modified filter paper, together with the high specificity of the PNA probe, allows single mismatch discrimination down to 10 fmol of DNA targets under non-stringent conditions.

Acknowledgements

The financial support for this project was provided by Research Team Consolidation Grant, the Thailand Research Fund (RTA 5280002), the National Research University Project of Commission of Higher Education (CHE) and the Ratchadapiseksomphot Endowment Fund (Project Code AM1006A), and the Thai Government Stimulus Package 2 (TKK2555), under the Project for Establishment of Comprehensive Center for Innovative Food, Health Products and Agriculture. The authors are indebted to Dr Jack Hirsch of Polymer Science and Engineering Department, University of Massachusetts, Amherst, for assistance with XPS analysis. PSL acknowledges Kasetsart University, Chalermphrakiat Sakon Nakhon Province Campus and the Development and Promotion of Science and Technology Talents Project (DPST) for a PhD scholarship.

References

1 C.-P. Chak, J. M. Y. Lai, K. W. Y. Sham, C. H. K. Cheng and K. C.-F. Leung, *RSC Adv.*, 2011, **1**, 1342.
2 J. Baur, C. Gondran, M. Holzinger, E. Defrancq, H. Perrot and S. Cosnier, *Anal. Chem.*, 2009, **82**, 1066.
3 A. Akane, S. Seki, H. Shiono, H. Nakamura, M. Hasegawa, M. Kagawa, K. Matsubara, Y. Nakahori, S. Nagafuchi and Y. Nakagome, *Forensic Sci. Int.*, 1992, **52**, 143.
4 H. Pfitzinger, B. Ludes and P. Mangin, *Int. J. Leg. Med.*, 1993, **105**, 213.
5 M. Passamano and M. Pighini, *Sens. Actuators, B*, 2006, **118**, 177.
6 B. Kannan, D. E. Williams, M. A. Booth and J. Travas-Sejdic, *Anal. Chem.*, 2011, **83**, 3415.
7 H. Yin, Y. Zhou, C. Chen, L. Zhu and S. Ai, *Analyst*, 2012, **137**, 1389–1395.
8 K.-H. Lee, J. O. Lee, S. Choi, J.-B. Yoon and G.-H. Cho, *Biosens. Bioelectron.*, 2012, **31**, 343.

 This journal is © The Royal Society of Chemistry 2013

Published on 19 October 2012 on http://pubs.rsc.org | doi:10.1039/C2AN36133G
Downloaded on 28 November 2012

9 S. Hason, H. Pivonkova, V. Vetterl and M. Fojta, *Anal. Chem.*, 2008, **80**, 2391.
10 X. Tang, H. Liu, B. Zou, D. Tian and H. Huang, *Analyst*, 2012, **137**, 309.
11 Z. Gao, *Analyst*, 2012, **137**, 1674.
12 D. Berdat, A. Marin, F. Herrera and M. A. M. Gijs, *Sens. Actuators, B*, 2006, **118**, 53.
13 M. Kaatz, H. Schulze, I. Ciani, F. Lisdat, A. R. Mount and T. T. Bachmann, *Analyst*, 2012, **137**, 59.
14 M. Liu, X. Lou, J. Du, M. Guan, J. Wang, X. Ding and J. Zhao, *Analyst*, 2012, **137**, 70.
15 X. Mao, L. Yang, X.-L. Su and Y. Li, *Biosens. Bioelectron.*, 2006, **21**, 1178.
16 M. Egholm, O. Buchardt, L. Christensen, C. Behrens, S. M. Freier, D. A. Driver, R. H. Berg, S. K. Kim, B. Norden and P. E. Nielsen, *Nature*, 1993, **365**, 566.
17 P. E. Nielsen, M. Egholm, R. H. Berg and O. Buchardt, *Science*, 1991, **254**, 1497.
18 C. Suparpprom, C. Srisuwannaket, P. Sangvanich and T. Vilaivan, *Tetrahedron Lett.*, 2005, **46**, 2833.
19 T. Vilaivan and C. Srisuwannaket, *Org. Lett.*, 2006, **8**, 1897.
20 C. Ananthanawat, T. Vilaivan and V. P. Hoven, *Sens. Actuators, B*, 2009, **137**, 215.
21 C. Ananthanawat, V. P. Hoven, T. Vilaivan and X. Su, *Biosens. Bioelectron.*, 2011, **26**, 1918.
22 C. Ananthanawat, T. Vilaivan, V. P. Hoven and X. D. Su, *Biosens. Bioelectron.*, 2010, **25**, 1064.
23 C. Ananthanawat, T. Vilaivan, W. Mekboonsonglarp and V. P. Hoven, *Biosens. Bioelectron.*, 2009, **24**, 3544.
24 B. Boontha, J. Nakkuntod, N. Hirankarn, P. Chaumpluk and T. Vilaivan, *Anal. Chem.*, 2008, **80**, 8178.
25 M. A. Cook, A. M. Osborn, J. Bettandorff and P. A. Sobecky, *Microbiology*, 2001, **147**, 2089.
26 M. S. Urdea, B. D. Warner, J. A. Running, M. Stempien, J. Clyne and T. Horn, *Nucleic Acids Res.*, 1988, **16**, 4937.
27 E. Heinicke, U. Kumar and D. G. Munoz, *J. Immunol. Methods*, 1992, **152**, 227.
28 M. Musiani, M. Zerbini, D. Gibellini, G. Gentilomi, S. Venturoli, G. Gallinella, E. Ferri and S. Girotti, *J. Clin. Microbiol.*, 1991, **29**, 2047.
29 M. Schäferling and S. Nagl, *Anal. Bioanal. Chem.*, 2006, **385**, 500.
30 N. Graf, S. Kassube and R. Krämer, *Bioorg. Med. Chem. Lett.*, 2008, **18**, 4786.
31 N. Graf and R. Krämer, *Chem. Commun.*, 2006, 4375.
32 J. J. Leary, D. J. Brigati and D. C. Ward, *Proc. Natl. Acad. Sci. U. S. A.*, 1983, **80**, 4045.
33 M. Renz and C. Kurz, *Nucleic Acids Res.*, 1984, **12**, 3435.
34 X. Su, H. F. Teh, X. H. Lieu and Z. Q. Gao, *Anal. Chem.*, 2007, **79**, 7192.
35 N. Zhang and D. H. Appella, *J. Am. Chem. Soc.*, 2007, **129**, 8424.
36 C. Kemper, K. Berggren, Z. Diwu and W. F. Patton, *Electrophoresis*, 2001, **22**, 881.
37 K. C. Reed and D. A. Mann, *Nucleic Acids Res.*, 1985, **13**, 7207.
38 C.-M. Cheng, A. W. Martinez, J. Gong, C. R. Mace, S. T. Phillips, E. Carrilho, K. A. Mirica and G. M. Whitesides, *Angew. Chem., Int. Ed.*, 2010, **49**, 4771.
39 A. W. Martinez, S. T. Phillips, G. M. Whitesides and E. Carrilho, *Anal. Chem.*, 2010, **82**, 3.
40 S. B. Lee, R. R. Koepsel, S. W. Morley, K. Matyjaszewski, Y. J. Sun and A. J. Russell, *Biomacromolecules*, 2004, **5**, 877.
41 D. Roy, J. S. Knapp, J. T. Guthrie and S. Perrier, *Biomacromolecules*, 2008, **9**, 91.
42 F. Zhou, Z. Zheng, B. Yu, W. Liu and W. T. S. Huck, *J. Am. Chem. Soc.*, 2006, **128**, 16253.
43 M. Ciampolini and N. Nardi, *Inorg. Chem.*, 1966, **5**, 41.
44 P. Akkahat and V. P. Hoven, *Colloids Surf., B*, 2011, **86**, 198.
45 A. Carlmark and E. Malmstrom, *J. Am. Chem. Soc.*, 2002, **124**, 900.
46 H. Dong and K. Matyjaszewski, *Macromolecules*, 2008, **41**, 6868.
47 K. Matyjaszewski, H. C. Dong, W. Jakubowski, J. Pietrasik and A. Kusumo, *Langmuir*, 2007, **23**, 4528.
48 K. Matyjaszewski, W. Jakubowski, K. Min, W. Tang, J. Y. Huang, W. A. Braunecker and N. V. Tsarevsky, *Proc. Natl. Acad. Sci. U. S. A.*, 2006, **103**, 15309.
49 S. Gupta, M. Agrawal, M. Conrad, N. A. Hutter, P. Olk, F. Simon, L. M. Eng, M. Stamm and R. Jordan, *Adv. Funct. Mater.*, 2010, **20**, 1756.
50 J.-K. Chen and B.-J. Bai, *J. Phys. Chem. C*, 2011, **115**, 21341.
51 A. Emileh, E. Vasheghani-Farahani and M. Imani, *Eur. Polym. J.*, 2007, **43**, 1986.
52 A. H. Al-Hakim and R. Hull, *Biochem. J.*, 1988, **251**, 935.

Talanta 105 (2013) 1–7

Contents lists available at SciVerse ScienceDirect

Talanta

journal homepage: www.elsevier.com/locate/talanta

New calix[4]arene derivatives as ionophores in polymeric membrane electrodes for Ag(I): Comparative selectivity studies and detection of DNA hybridization

Wanwisa Janrungroatsakul [a], Tirayut Vilaivan [a], Chotima Vilaivan [a], Sarayut Watchasit [a], Chomchai Suksai [b], Wittaya Ngeontae [c], Wanlapa Aeungmaitrepirom [a], Thawatchai Tuntulani [a,*]

[a] Department of Chemistry, Faculty of Science, Chulalongkorn University, Bangkok 10330, Thailand
[b] Department of Chemistry and Center of Excellence for Innovation in Chemistry, Faculty of Science, Burapha University, Chonburi 20131, Thailand
[c] Materials Chemistry Research Unit, Department of Chemistry and Center of Excellence for Innovation in Chemistry, Faculty of Science, Khon Kaen University, Khon Kaen 40002, Thailand

ARTICLE INFO

Article history:
Received 1 November 2012
Received in revised form
19 November 2012
Accepted 21 November 2012
Available online 27 November 2012

Keywords:
Silver ion selective electrode
Peptide nucleic acid
Silver nanoparticles
DNA hybridization

ABSTRACT

Four calix[4]arene derivatives containing various donor atoms and different topology (**L1**−**L4**) have been synthesized and used as neutral ionophores to fabricate silver ion selective electrodes (Ag-ISEs) which were characterized in terms of their potentiometric selectivities and complex formation constants. The ionophore **L2** having two nitrogen and two sulfur donors showed stronger interactions with Ag^+ and the highest selectivity coefficient towards Ag^+. The best membrane electrode was prepared from **L2** and used to fabricate silver ion selective microelectrodes (Ag-ISμEs) which could detect silver ions in 1000 μL samples with detection limit around 1 μM using sodium ion microelectrodes as a pseudo reference electrode. Such potentiometric measurement was then applied to detect DNA hybridization on a gold substrate, employing immobilized lipoic acid-modified pyrrolidinyl PNA (Lip-acpcPNA) as a probe. The hybridization between the neutral Lip-acpcPNA probe and DNA target led to a negatively charged surface that could bind positively charged silver nanoparticles ($AgNPs^+$) via electrostatic interactions. The hybridization signal was observed by dissolution of the electrostatically adsorbed $AgNPs^+$ with hydrogen peroxide. Excellent discrimination of complementary from single mismatched and non-complementary DNA targets was achieved under non-stringent conditions. The detection limit of DNA was 0.2 μM in 1000 μL samples.

© 2012 Elsevier B.V. All rights reserved.

1. Introduction

Potentiometry based on ion selective electrodes (ISEs) has been widely used for determining the activity of metal ions for several decades [1]. Since ISEs offer several advantages, especially low cost, simplicity and obvious compatibility with miniaturization, they are an excellent tool in analytical applications such as clinical measurements, industrial process control and environmental monitoring. Recently, there has been an increasing interest in using miniaturized ISEs for monitoring protein immunoassays [2] or DNA hybridization [3–5] using Ag, CdS-nanocrystal labels, enzyme tags or liposomes.

Peptide nucleic acid (PNA) is a DNA analog containing nucleobase-modified *N*-(2-aminoethyl)glycine subunits linked together by amide bonds. PNA can form duplexes with complementary DNA with high thermal stability owing to the absence of electrostatic repulsion between PNA and DNA strands. PNA also discriminates single-base mismatched DNA with high specificity [6]. Employing the unique uncharged properties of PNA backbone, two research groups [7,8] reported the use of PNA as a probe to detect non-labeled oligonucleotides specifically through electrostatic interactions between positively charged metallic nanoparticles and negatively charged backbone of DNA hybridized with the neutral PNA probe.

We aim to fabricate a polymer membrane silver ion selective microelectrode (Ag-ISμE) that can detect DNA hybridization with the neutral PNA probe using positively charged silver nanoparticles ($AgNPs^+$) as a potentiometric marker. A variety of ionophores containing π-electrons [9–11] or heteroatoms [12–17] as coordinate sites have been successfully used to construct Ag-ISEs for monitoring and determining silver ions. Nevertheless, Szigeti and co-workers showed that selectivity coefficients of membranes containing π-coordinating calix[4]arene ionophores were worse than those containing calix[4]arene incorporating sulfur donors, resulting in less discrimination of Ag^+ from other cations [18].

* Corresponding author. Tel.: +66 2 2187643; fax: +66 2 2187598.
E-mail address: tthawatc@chula.ac.th (T. Tuntulani).

0039-9140/$ - see front matter © 2012 Elsevier B.V. All rights reserved.
http://dx.doi.org/10.1016/j.talanta.2012.11.046

Therefore, we designed and synthesized four calix[4]arene derivatives **L1**–**L4** containing various donor atoms and different topology, which were used as neutral ionophores to fabricate Ag-ISEs. The characteristics such as selectivity, lower detection limit and formation constant of the four ionophores synthesized towards Ag^+ in polymeric membranes were compared in order to choose the best ionophore from which to fabricate a microelectrode to be used in combination with PNA for monitoring DNA hybridization.

The principle of our potentiometric sensors for detection of DNA hybridization is illustrated in Fig. 1. Pyrrolidinyl PNA with a D-propyl-2-aminocyclopentanecarboxylic acid backbone (acpcPNA) [19–21] which shows excellent specificity for DNA recognition is used as a probe in this work. The acpcPNA is modified at the *N*-terminus with lipoic acid and the so-obtained Lip-acpcPNA is covalently immobilized on the surface of a gold substrate. The target DNA is hybridized with the electrostatically neutral Lip-acpcPNA resulting in a negatively charged surface due to the phosphate backbone of the target DNA. Addition of $AgNPs^+$ [22,23] results in adsorption of the $AgNPs^+$ on the gold substrate through electrostatic interactions. The adsorbed $AgNPs^+$ on the gold surface is then oxidized by H_2O_2 to release silver ions, which can be detected with our fabricated Ag-ISμE.

2. Experimental

2.1. Materials

p-tert-Butylcalix[4]arene-tetraacetic acid tetraethyl ester (Na(X)), potassium tetrakis[4–chlorophenyl]borate (KT*p*ClPB), bis(2-ethylhexyl)sebacate (DOS), *o*-nitrophenyl octyl ether (*o*-NPOE), high molecular weight poly(vinyl chloride) (PVC), and tetrahydrofuran (THF) were purchased in selectophore® or puriss quality from Fluka. Nitrate salts of cations were of analytical grade obtained from Merck, Fluka, Sigma–Aldrich, Reidel and Carlo Erba. 30% (v/v) Hydrogen peroxide (H_2O_2) was purchased from Fisher Scientific. All solutions were prepared with deionized water with the specific resistivity of 18.2 MΩ cm (Milli-Q water purification system; Bedford, MA, USA).

Chemicals for synthesis of $AgNPs^+$, i.e., silver nitrate ($AgNO_3$), cetyltrimethylammonium bromide (CTAB) and sodium borohydride ($NaBH_4$) were purchased from Merck.

All oligonucleotides were purchased from Biogenomed Co., Ltd. The sequences of complementary, single base mismatched and non-complementary DNA targets were 5′-GTCATAGCATCA-3′, 5′-GTCATCGCATCA-3′ and 5′-AAGGCCTATGTC-3′, respectively.

2.2. Preparation of membrane electrodes

The membrane contained 1 wt% ionophore, KT*p*ClPB (75 mol% relative to ionophore), 33 wt% PVC and 66 wt% *o*-NPOE. All components (220 mg in total) were dissolved in 2.5 mL of THF or MeOH/$CHCl_3$/THF (1:2:10 v/v) and poured into a glass ring (30 mm i.d.) fixed on a glass plate. Then, the solvent was allowed to evaporate at room temperature overnight. A transparent membrane of about 200 μm in thickness was obtained. The membrane was punched into circular films (7.5 mm i.d.) and glued with a PVC/THF slurry on the top of a PVC tube and connected to a micropipette tip as an electrode body. An internal filling solution containing 10 mM $AgNO_3$ was put into this PVC tube which connected to a micropipette tip and a AgCl-coated silver wire was placed into it. The prepared membrane electrode was conditioned in 10 mM $AgNO_3$ solution for overnight prior to use.

2.3. Selectivity measurements

The potentiometric selectivity coefficients were determined by the separate solution method (SSM) [24]. The membranes were conditioned overnight in the solution of interfering metal ions (nitrate salt). The response of the electrode was first measured against the interfering metal ions (10^{-7}–10^{-2} M) by using 10 mM of the same interfering cations (chloride salt) as an inner filling solution. The electrode was then used to measure the response of silver nitrate solutions. Selectivity coefficients of each metal were performed in triplicate (using a new membrane for each replicate). The interfering ions in this study were Na^+, K^+, Ca^{2+}, Mg^{2+}, Ni^{2+}, Cu^{2+}, Zn^{2+}, Cd^{2+}, Pb^{2+} and Hg^{2+}. To determine the selectivity coefficients of Hg^{2+} and Pb^{2+}, the pH of solution was

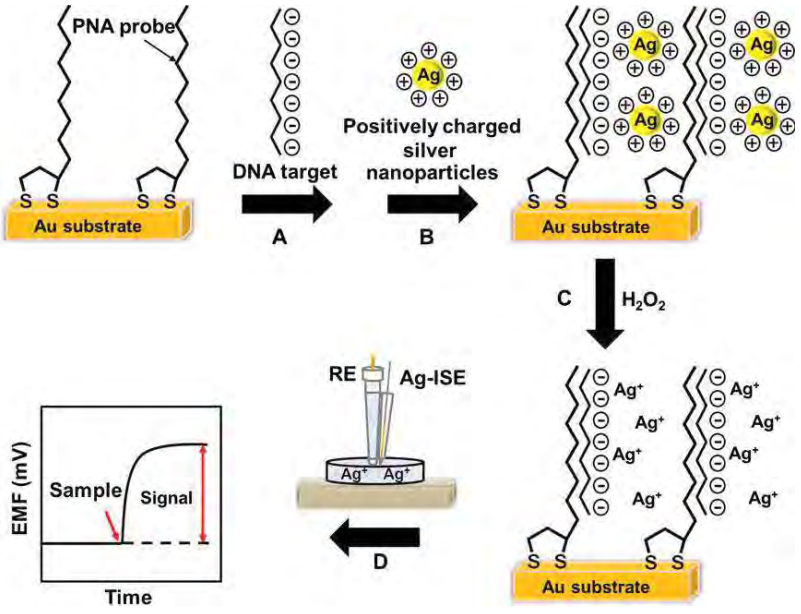

Fig. 1. Representation of $AgNPs^+$-based label-free potentiometric DNA detection.

adjusted to 2 and 4, respectively with HNO_3. The selectivity coefficients were calculated from the mean value of triplicate experiments with the standard deviation.

2.4. Preparation of sandwich membranes

In order to determine ion–ionophore complex formation constants in the solvent polymeric membrane, it requires membrane potential measurements on two-layer sandwich membranes [25–27], where only one side contains the ionophore. The membrane compositions and the formation constant are shown in Table 1.

The conventional standard size membranes, with and without ionophore, were conditioned in 5 mM $AgNO_3$ overnight. The sandwich membrane was prepared by attaching two individual membranes together and visibly checked for air bubbles before placing in the electrode body. The membrane with the ionophore was contacted with sample solution (5 mM $AgNO_3$) that is the same solution as the conditioning and inner filling solutions. All potentiometric measurements were carried out at ambient temperature in unstirred salt solution versus a Ag/AgCl reference electrode with 1 M LiOAc as a salt bridge electrolyte. The range of time required from attaching the membrane until the membrane potential measurement was less than 1 min. The potential value was continuously recorded for several hours.

Membrane potential values, E_M, were determined by subtracting the cell potential for membrane without ionophore from that of the sandwich membrane. The formation constants were calculated using Eq. (1).

$$\log\beta_{IL_n} = \left(\frac{E_M z_I F}{2.303RT}\right) - n\log\left(L_T - \frac{nR_T}{z_I}\right) \quad (1)$$

L_T is the total concentration of the ionophore. R_T is the concentration of lipophilic ion exchanger. R, T, F, n and z_I are the gas constant, the absolute temperature, the Faraday constant, the complex stoichiometry and the charge of the tested ion, respectively.

2.5. Preparation of Lip-acpcPNA

The 12-mer acpcPNA probe with a sequence of TGATGCTATGAC-Lys (Mtt) was synthesized from the respective *N*-Fmoc-protected monomers on a solid support (Tentagel, Rink amide linker) according to a previously published protocol [19–21]. After *N*-Fmoc and nucleobase side-chain deprotections, it was further modified at the *N*-terminus with an aminoethoxyethoxyacetyl (O) linker followed by DL-lipoic acid (HATU/DIEA activation). The Lip-acpcPNA was then cleaved from the solid support using trifluoroacetic acid (TFA) and purified by reverse phase HPLC. The sequence was confirmed by MALDI-TOF mass spectrometry (Lip-O-TGATGCTATGAC-$LysNH_2$, Calcd.: m/z=4540.0, Found: m/z=4539.7) and by hybridization with its complementary DNA (d 5′-GTCATAGCATCA-3′) (T_m=76.7 °C at 1.0 μM PNA, 1.0 μM DNA in 10 mM sodium phosphate buffer pH 7.0 containing 100 mM NaCl).

2.6. Preparation of fabricated Ag-ISμE and EMF measurements for DNA biosensor

The membrane for the Ag-ISμE was prepared as reported previously [28]. The cocktail membrane containing **L2** (0.74 wt%, 10.31 mmol kg^{-1}), KT*p*ClPB (0.25 wt%, 5.03 mmol kg^{-1}), PVC (32.99 wt%) and *o*-NOPE (66.02 wt%) was prepared in an appropriate volume of THF after stirring 1 h. The Ag-ISμE was fabricated from the tip of 1000 μL micropipette (0.5 mm i.d.) dipped into membrane cocktail for 3 s. It was left to stand in vertical position to allow the solvent to evaporate. The membrane thickness is around 0.5 mm. The resulting microelectrodes were conditioned in 10 mM $AgNO_3$ solution for overnight prior to use. An internal filling solution containing 10 mM $AgNO_3$ was put into a micropipette tip and a AgCl-coated silver wire was placed into the solution.

Sodium ion selective microelectrode (Na-ISμE) prepared from Na(X) (0.99 wt%, 10.00 mmol kg^{-1}), KT*p*ClPB (0.25 wt%, 5.03 mmol kg^{-1}), PVC (32.85 wt%) and DOS (65.91 wt%) was used as a reference electrode. The components were dissolved in THF. The inner filling solution was 10 mM NaCl, and the conditioning solution was 10 mM $NaNO_3$.

Potentiometric measurements were performed in 1000 μL samples with a Na-ISμE as pseudo reference electrode in unstirred solutions with a 16-channel electrode monitor (Lawson Labs Inc., Malvern, PA 19355, USA) at room temperature. The activity coefficients of silver ions in sample solutions were calculated according to the Debye–Hückel approximation [29].

2.7. Preparation of $AgNPs^+$

The preparation of CTAB-coated silver nanoparticles was carried out using the previous published procedure with modifications [22,23]. The solution of CTAB (2 mL, 1 mM) in ethanol was added in aqueous solution of $AgNO_3$ (25 mL, 5 mM) and stirred for 10 min. Then, 1% v/v freshly prepared aqueous $NaBH_4$ was added under vigorous stirring. The mixture immediately turned yellow-green and left stirring for 1 h.

Fig. 2 shows the UV–vis spectrum of the synthesized CTAB-coated AgNPs with a strong surface plasmon band at 397 nm.

Table 1
Membrane compositions, response properties based on ionophores **L1**–**L4** and experimental membranes potentials and corresponding ionophore complex formation constants determined with segmented sandwich membranes for ionophores **L1**–**L4** in PVC membrane assuming 1:1 stoichiometry of their complexes with Ag^+.

Ionophore	Membrane composition (wt%)				Slope (mV/decade)	Linear range (M)	Detection limit (M)	Membrane potential E_M (mV)	Formation constant log β_{ILn}
	Ionophore, L_T (mmol kg^{-1})	KT*p*ClPB, R_T (mmol kg^{-1})	PVC	Plasticizer					
L1	0.59 (10.27)	0.37 (7.47)	32.91	*o*-NPOE, 66.13	43.1 ± 0.6	10^{-5} to 10^{-2}	3.9×10^{-6}	126 ± 6	4.66 ± 0.10
L2	0.73 (10.10)	0.37 (7.49)	32.93	*o*-NPOE, 65.97	58.8 ± 0.6	10^{-6} to 10^{-2}	4.8×10^{-7}	162 ± 3	5.25 ± 0.05
L3	0.88 (9.96)	0.37 (7.40)	33.00	*o*-NPOE, 65.75	56.3 ± 0.8	10^{-6} to 10^{-2}	1.0×10^{-6}	162 ± 5	5.31 ± 0.08
L4	1.15 (10.24)	0.37 (7.40)	32.78	*o*-NPOE, 65.70	51.0 ± 0.9	10^{-6} to 10^{-2}	5.0×10^{-6}	134 ± 9	4.80 ± 0.16
o-NPOE	–	0.37 (7.46)	33.11	*o*-NPOE, 66.52	44.3 ± 1.5	10^{-5} to 10^{-2}	4.9×10^{-6}	–	–

Transmission electron microscopy (TEM) has been used to characterize shape and size of the $AgNPs^{+}$. A TEM image in Fig. 3 clearly indicates that $AgNPs^{+}$ are spherical and have an average particle size of 20 nm. The particles have been found to be colloidally stable for at least two months.

2.8. Preparation of immobilized Lip-acpcPNA on gold substrate and DNA hybridization

The gold substrates obtained from Sigma–Aldrich were cut to $10 \times 5\ mm^2$ pieces with uniform thickness (0.25 mm) by a shearing machine. They were cleaned with piranha solution (3:1 H_2SO_4: 30% (v/v) H_2O_2), thoroughly rinsed with Milli-Q water, absolute ethanol and dried under pure nitrogen gas. The Lip-acpcPNA solution (10 μM in 10 mM $NaNO_3$, 100 μL) was dropped on the gold substrate and the substrate was incubated at 4 °C for 40 h, followed by washing with Milli-Q water.

The immobilized Lip-acpcPNA on the gold substrate was treated with a target DNA solution in 10 mM $NaNO_3$ (0, 2, 5, 10, 15, 20, 40 and 80 μM, 100 μL) at room temperature for 3 h. The washing procedure was performed in three times to remove any unbound DNA. Then, a solution of $AgNPs^{+}$ (250 ppm, 50 μL) was deposited onto the gold substrate. After 2 h at room temperature, the gold substrate was washed three times with Milli-Q water.

Hydrogen peroxide was used for dissolution of the $AgNPs^{+}$ to silver ions. A 0.2 M solution of H_2O_2 (100 μL) was added on the gold substrate and left for 45 min. The solution on the gold substrate was then transferred to an eppendorf tube and the volume adjusted to 1000 μL with 10 mM $NaNO_3$. The solution was stirred to decompose the remaining H_2O_2. The detection of silver ions in the sample was performed in the 1000 μL eppendorf tube by using a Na-ISμE as a reference electrode.

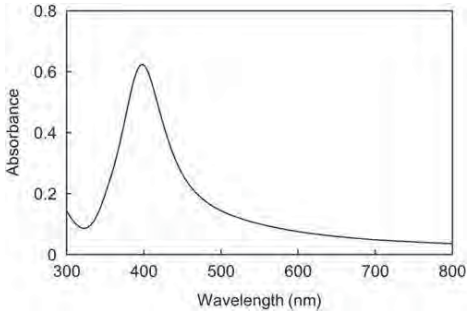

Fig. 2. The plasmon absorption band of diluted $AgNPs^{+}$ (λ_{max}=397 nm).

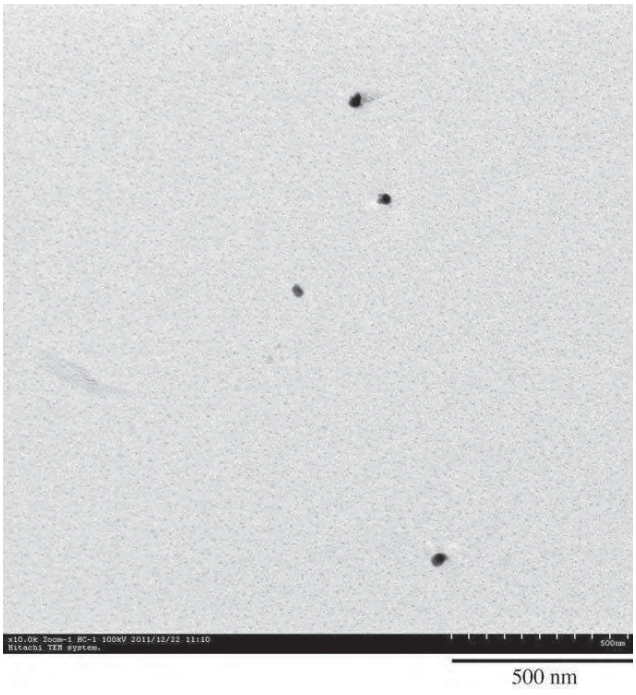

Fig. 3. TEM image of the synthesized $AgNPs^{+}$.

3. Results and discussion

3.1. Design and synthesis of ionophores

Calix[4]arene derivatives were designed and synthesized by attaching different functional groups to obtain different topology with various donor atoms for binding Ag^{+}. Each compound was modified at one or two opposite phenolic groups of calix[4]arene by benzothiazole and dipicolylamine derivatives yielding calix[4]-arene derivatives, **L1**–**L4** (Fig. 4). **L1** and **L2** [28] contained soft nitrogen and sulfur as donor atoms and **L3** and **L4** [30] contained soft nitrogen and hard oxygen donor atoms. In preliminary studies, all synthesized ionophores incorporated in polymeric membranes response to Ag^{+}. Ionophore **L4** showed high selectivity towards Ag^{+} as investigated by fluorescence, absorption, and ^{1}H NMR spectroscopy [30]. Generally, Hg^{2+} was a major interference for Ag-ISEs because soft metal ions, Ag^{+}, Hg^{2+} and Pb^{2+} preferred to coordinate to soft donor atoms such as sulfur and nitrogen according to Pearson [31].

3.2. Complex formation constants of L1 – L4 with Ag^{+}

The complex formation constants between Ag^{+} and ionophores **L1**–**L4** were determined with segmented sandwich membranes, assuming a 1:1 ion–ionophore stoichiometry, and the results are shown in Table 1. The results showed that **L2** and **L3** possessed higher complex formation constants than **L1** and **L4**.

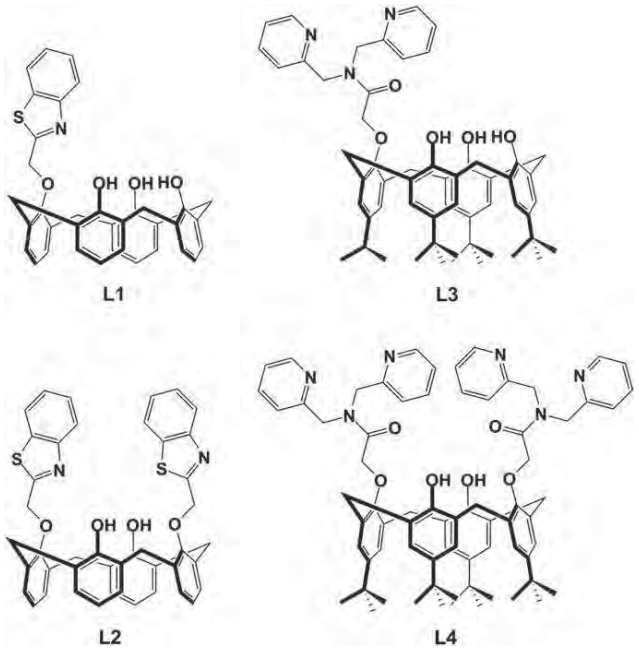

Fig. 4. Structures of four synthesized ionophores **L1**–**L4**.

Ionophores **L2** and **L3** formed strong and stable complexes with Ag^+ in the same order with logarithmic complex formation constants of 5.25 ± 0.05 and 5.31 ± 0.08 for **L2** and **L3**, respectively. The higher formation constant could result in a better selectivity towards the analyte ions due to the superior ability of the ionophore to discriminate between primary ions and interfering ions.

3.3. Effect of functional groups and the number of substituents on the selectivity

The ion selectivity of electrodes based on calix[4]arene singly modified with benzothiazole (**L1**) and dipicolylamine (**L3**) were investigated (Fig. 5). These ionophores possessed soft nitrogen donors capable of forming complexes with Ag^+. The ionophore **L3** containing three nitrogen and one oxygen donors from dipicolylamine and carbonyl, respectively exhibited more interference from Hg^{2+}. The introduction of heteroatoms of one sulfur and one nitrogen donors from benzothiazole **L1** resulted in better selectivity towards Ag^+ than **L3** as well as decreased interference from Hg^{2+}.

Two substituents on the opposite phenolic groups of calix[4]arene with two benzothiazole **L2** and two dipicolylamine **L4** were synthesized in order to investigate the effect of increasing number of donor groups on ion selectivity compared to the singly-substituted calix[4]arene ionophores **L1** and **L3**. The ionophores having two substituted phenolic groups consistently gave higher selectivity coefficients to Ag^+/Hg^{2+}: **L2** > **L1** and **L4** > **L3**. This suggested that more donor atoms of the disubstituted calix[4]arene could coordinate with Ag^+ more effectively. Furthermore, the increased lipophilicity of two substituted phenolic groups can prevent leaching of the ionophore from the membranes. Therefore, **L2** gave the best ion selectivity towards Ag^+ compared to other ionophores and exhibited a good discrimination with $> 10^4$ times higher than all tested cations except Hg^{2+}. The best selectivity towards Ag^+ of **L2** corresponded to its high complex formation value. This characteristic may be attributed to the two symmetrical benzothiazole groups on the calix[4]arene bearing two nitrogen and two sulfur donors which could rearrange in a suitable geometry for complexing Ag^+ better than other interfering ions. The results from complex formation and selectivity studies suggested that **L2** was the most appropriate ionophore to fabricate Ag-ISμEs.

3.4. Fabrication of Ag-ISμE

Our fabricated Ag-ISE has been successfully employed in speciation analysis of the AgNPs solution [28] and in glucose biosensor by using AgNPs as cation maker [32]. In addition, the fabricated Ag-ISE can be used in a wide range of solution pH from pH 2 to 8 with no significant change in the EMF value [28]. In this work, a Ag-ISμE is developed for monitoring of DNA hybridization. The calibration curve of Ag^+-microelectrode was performed in 1000 μL and used 10 mM $NaNO_3$ (pH 6.0) as background by using a Na^+-microelectrode as pseudo reference electrode as shown in Fig. 6. Na^+-microelectrode was chosen as a reference electrode and Na^+ was selected as the background electrolyte since this Ag^+-microelectrode showed a distinctive discrimination of the logarithmic selectivity coefficient as compared to Na^+ with $\log K^{pot}_{Ag,Na} = -6.70$ [28]. The Ag-ISμE showed a low detection limit of 9.12×10^{-7} M (~ 1 μM) in 1000 μL solution with near the theoretical Nernstian slope of 58.7 mV per decade (inset, Fig. 6).

3.5. Detection of DNA hybridization

Molecules carrying a thiol or a disulfide group can be immobilized by chemisorption onto a gold surface to form self-assembled monolayer (SAM). Covalent immobilization of lipoic

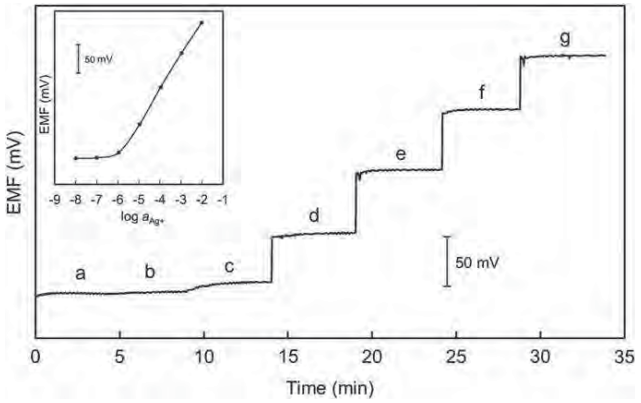

Fig. 6. Time trace line response of the Ag-ISμE to increasing level of Ag^+: (a) 10^{-8}; (b) 10^{-7}; (c) 10^{-6}; (d) 10^{-5}; (e) 10^{-4}; (f) 10^{-3}; (g) 10^{-2} M in 1000 μL of solution with 10 mM $NaNO_3$ as background with Na-ISμE as the pseudo reference electrode. Inset displays the corresponding calibration plot.

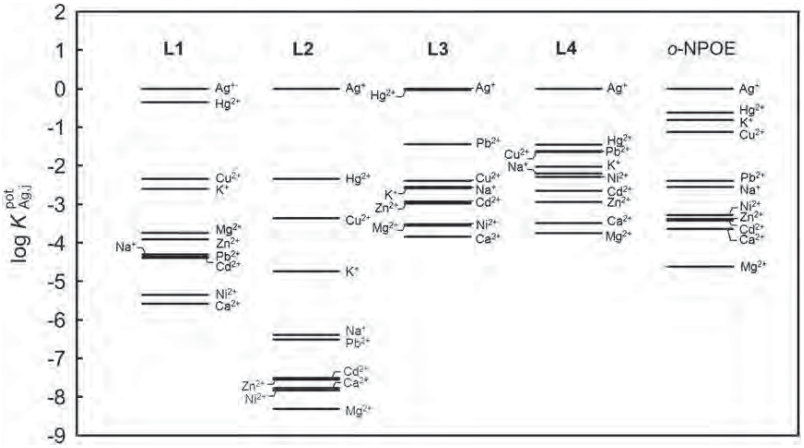

Fig. 5. Comparison of selectivity coefficients (log $K^{pot}_{Ag,j}$) of electrodes based on **L1**–**L4** and the blank membrane (without ionophores). The membrane compositions are 10 mmol kg^{-1} ionophore and 7.5 mmol kg^{-1} KT*p*ClPB in PVC plasticized with *o*-NPOE.

acid derivatives on gold surface provided a more stable SAM than that of the simple thiol via two S–Au bonds [33]. The disulfide group of Lip-acpcPNA was attached on the gold substrate by immersing in PNA solutions of various concentrations (1, 5 and 10 μM) to investigate the suitable concentration of the PNA probe that allows efficient detection of DNA and discrimination of complementary and mismatched DNA. The potentials of solutions containing Ag^+ obtained from a bare gold substrate, the substrate after Lip-acpcPNA immobilization, and after hybridization with the target DNA on gold substrate were compared after treatment with $AgNPs^+$ followed by H_2O_2 oxidation (Fig. 7). The hybridization signals with complementary DNA were obtained when the gold surface was treated with 10 μM of Lip-acpcPNA. Initially, non-specific adsorption between $AgNPs^+$ and the bare gold substrate was observed as shown by the non-zero ΔEMF values. The signals were lowered after immobilization with Lip-acpcPNA (at 10 μM), indicating that the probe can self-assemble onto gold substrate and that $AgNPs^+$ could not effectively bind to the electrostatically neutral PNA. After hybridization with DNA, the signal was increased compared to without DNA, suggesting that the electrostatic interactions between the negatively charged of DNA backbone and $AgNPs^+$ had taken place. At lower concentrations of Lip-acpcPNA, i.e. 1 and 5 μM, no difference in EMF values were observed before and after hybridization with target DNA. This suggests that there was not enough immobilized PNA to hybridize effectively with the target DNA. Therefore, 10 μM of Lip-acpcPNA was selected for further experiments.

To determine the specificity of the DNA detection, the Lip-acpcPNA immobilized on gold substrate was hybridized with fully complementary, single base mismatched and non-complementary DNA under the same hybridization condition (10 mM $NaNO_3$, pH 6.0). The results illustrated in Fig. 8 showed that the hybridization with fully complementary DNA produced the highest signal, 144 ± 3 mV. Hybridization with single base mismatched and non-complementary DNA gave very low signals which were indistinguishable from the control signal, indicating that there were no hybridization between single base mismatched and non-complementary DNA to Lip-acpcPNA immobilized on the gold substrate. The time trace lines in Fig. 8 clearly showed that this Lip-acpcPNA probe could discriminate fully complementary DNA from non-complementary DNA and single base mismatched DNA under non-stringent conditions.

The Lip-acpcPNA immobilized on gold substrate (at 10 μM concentration) was next hybridized with complementary DNA at different concentrations (2, 5, 10, 15, 20, 40 and 80 μM). Fig. 9 showed that EMF values of hybridization depended on the increasing in concentration of the target DNA. Higher concentrations of the target DNA resulted in more negative charges from phosphate backbone of DNA and gave larger detectable signals of Ag^+. The lower detection limit was 0.2 μM of the target DNA in 1000 μL sample with a linear range from 0.2 to 2.0 μM target DNA correlating with concentration of Ag^+ in micromolars (μM) was obtained as shown in Fig. 9.

The results indicate that the proposed system can detect DNA hybridization by following signals of Ag^+ which obtained from dissolution of positively charged CTAB-coated AgNPs interacting with negatively charged DNA. In addition, this detection system is inexpensive and requires fewer steps for detecting the hybridization between Lip-acpcPNA probe and the DNA target as compared to other systems using electrostatic interactions between positively charged nanoparticles and negatively charged backbone of DNA hybridized with the neutral PNA probe [7,8].

4. Conclusion

The potentiometric studies of electrodes from compounds **L1**–**L4** showed that they could be used as ionophores in Ag-ISEs. The ionophore **L2** containing two nitrogen and two sulfur donor atoms showed optimum selectivity towards Ag^+ compared to other ionophores. The complex formation constant of **L2** was relatively high corresponding to its best selectivity towards Ag^+. Furthermore, we have demonstrated that the simple potentiometric method based on Ag-ISμE using **L2** as an ionophore in combination with pyrrolidinyl peptide nucleic acid probe could be used to detect DNA hybridization from the signal of silver ions, which derived from the electrostatic interactions between the

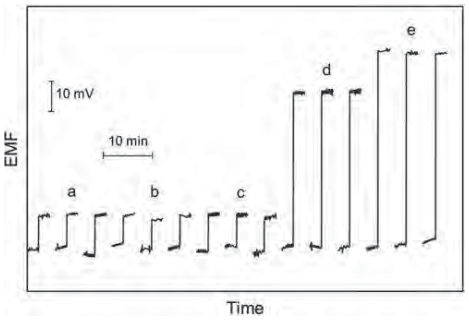

Fig. 8. Potentiometric hybridization response: (a) control solution (10 mM $NaNO_3$, zero target), (b) 40 μM non-complementary DNA, (c) 40 μM single base mismatched DNA, (d) 20 μM target DNA, and (e) 40 μM target DNA (as complementary targets) after DNA hybridization. Potentiometric measurements were performed in 1000 μL samples with Na-ISμE as the pseudo reference electrode and 10 mM $NaNO_3$ as a background solution.

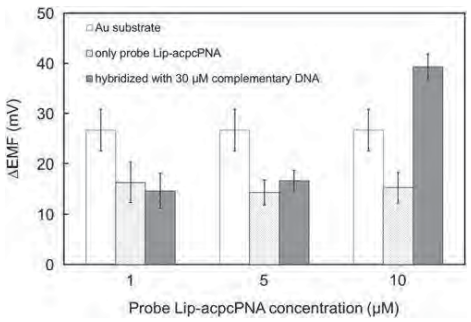

Fig. 7. Effect of concentration of probe Lip-acpcPNA on the response (ΔEMF values obtained from the subtraction from the background solution).

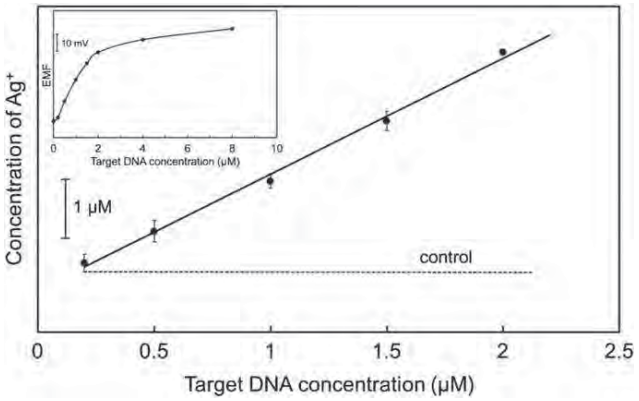

Fig. 9. Calibration plot for the potentiometric monitoring of $AgNPs^+$-based label-free DNA hybridization in 1000 μL eppendorf tube (error bars: SD, $N=3$). The dashed line corresponds to control signal (no target DNA).

$AgNPs^{+}$ and the negatively charged target DNA hybridized to the neutral Lip-acpcPNA probe immobilized on the gold substrate.

Acknowledgments

WJ would like to thank the Commission on Higher Education, Thailand for supporting by grant fund under the program Strategic Scholarships for Frontier Research Network for the Join Ph.D. Program Thai Doctoral degree for this research. Additionally, the authors gratefully acknowledge financial support from the Thailand Research Fund (RTA5380003 to TT and RTA5280002 to TV).

Appendix A. Supporting information

Supplementary data associated with this article can be found in the online version at http://dx.doi.org/10.1016/j.talanta.2012.11.046.

References

[1] J. Wang, Analytical Electrochemistry, 3rd ed., Wiley, New York, 2006.
[2] K.Y. Chumbimuni-Torres, Z. Dai, N. Rubinova, Y. Xiang, E. Pretsch, J. Wang, E. Bakker, J. Am. Chem. Soc. 128 (2006) 13676–13677.
[3] A. Numnuam, K.Y. Chumbimuni-Torres, Y. Xiang, R. Bash, P. Thavarungkul, P. Kanatharana, E. Pretsch, J. Wang, E. Bakker, J. Am. Chem. Soc. 130 (2008) 410–411.
[4] J. Wu, K.Y. Chumbimuni-Torres, M. Galik, C. Thammakhet, D.A. Haake, J. Wang, Anal. Chem. 81 (2009) 10007–10012.
[5] K.Y. Chumbimuni-Torres, J. Wu, C. Clawson, M. Galik, A. Walter, G. -U. Flechsig, E. Bakker, L. Zhang, J. Wang, Analyst 135 (2010) 1618–1623.
[6] J. Wang, E. Palecek, P.E. Nielson, G. Rivas, X. Cai, H. Shiraishi, N. Dontha, D. Luo, P.A.M. Farias, J. Am. Chem. Soc. 118 (1996) 7667–7670.
[7] L. Fabris, M. Dante, G. Braun, S.J. Lee, N.O. Reich, M. Moskovits, T.-Q. Nguyen, G.C. Bazan, J. Am. Chem. Soc. 129 (2007) 6086–6087.
[8] S.K. Kim, H. Cho, J. Jeong, J.N. Kwon, Y. Jung, B.H. Chung, Chem. Commun. 46 (2010) 3315–3317.
[9] K. Kimura, S. Yajima, K. Tatsumi, M. Yokoyama, M. Oue, Anal. Chem. 72 (2000) 5290–5294.
[10] S. Yajima, N. Yoshioka, M. Tanaka, K. Kimura, Electroanalysis 15 (2003) 1319–1326.
[11] J. Bobacka, T. Lahtinen, H. Koskinen, K. Rissanen, A. Lewenstam, A. Ivaska, Electroanalysis 14 (2002) 1353–1357.
[12] D. Siswanta, K. Nagatsuka, H. Yamada, K. Kumakura, H. Hisamoto, Y. Shichi, K. Toshima, K. Suzuki, Anal. Chem 68 (1996) 4166–4172.
[13] Z. Yan, Y. Lu, X. Li, Sens. Actuators B 122 (2007) 174–181.
[14] A. Demirel, A. Doğan, G. Akkuş, M. Yilmaz, E. Kiliç, Electroanalysis 18 (2006) 1019–1027.
[15] X. Zeng, L. Weng, L. Chen, X. Leng, Z. Zhang, X. He, Tetrahedron Lett. 41 (2000) 4917–4921.
[16] L. Chen, H. Ju, X. Zeng, X. He, Z. Zhang, Anal. Chim. Acta 437 (2001) 191–197.
[17] X. Zeng, L. Weng, L. Chen, F. Xu, Q. Li, X. Leng, X. He, Z.-Z. Zhang, Tetrahedron 58 (2002) 2647–2658.
[18] Z. Szigeti, A. Malon, T. Vigassy, V. Csokai, A. Grün, K. Wygladacz, N. Ye, C. Xu, V.J. Chebny, I. Bitter, R. Rathore, E. Bakker, E. Pretsch, Anal. Chim. Acta 572 (2006) 1–10.
[19] T. Vilaivan, C. Srisuwannaket, Org. Lett. 8 (2006) 1897–1900.
[20] C. Vilaivan, C. Srisuwannaket, C. Ananthanawat, C. Suparpprom, J. Kawakami, Y. Yamaguchi, Y. Tanaka, T. Vilaivan, Artif. DNA: PNA & XNA 2 (2011) 50–59.
[21] C. Ananthanawat, T. Vilaivan, V.P. Hoven, X. Su, Biosens. Bioelectron. 25 (2010) 1064–1069.
[22] V. Patil, R.B. Malvankar, M. Sastry, Langmuir 15 (1999) 8197–8206.
[23] G. Wei, L. Wang, H. Zhou, Z. Liu, Y. Song, Z. Li, Appl. Surf. Sci. 252 (2005) 1189–1196.
[24] E. Bakker, P. Bühlmann, E. Pretsch, Chem. Rev. 97 (1997) 3083–3132.
[25] Y. Mi, E. Bakker, Anal. Chem. 71 (1999) 5279–5287.
[26] E. Bakker, M. Willer, M. Lerchi, K. Seiler, E. Pretsch, Anal. Chem. 66 (1994) 516–521.
[27] Y. Qin, Y. Mi, E. Bakker, Anal. Chim. Acta 421 (2000) 207–220.
[28] W. Ngeontae, W. Janrungroatsakul, N. Morakot, W. Aeungmaitrepirom, T. Tuntulani, Sens. Actuators B 134 (2008) 377–385.
[29] P.C. Meier, Anal. Chim. Acta 136 (1982) 363–368.
[30] R. Joseph, B. Ramanujam, A. Acharya, C.P. Rao, J. Org. Chem. 74 (2009) 8181–8190.
[31] R.G. Pearson, J. Am. Chem. Soc. 85 (1963) 3533–3539.
[32] W. Ngeontae, W. Janrungroatsakul, P. Maneewattanapinyo, S. Ekgasit, W. Aeungmaitrepirom, T. Tuntulani, Sens. Actuators B 137 (2009) 320–326.
[33] T.M. Willey, A.L. Vance, C. Bostedt, T. van Buuren, R.W. Meulenberg, L.J. Terminello, C.S. Fadley, Langmuir 20 (2004) 4939–4944.

Provided for non-commercial research and education use.
Not for reproduction, distribution or commercial use.

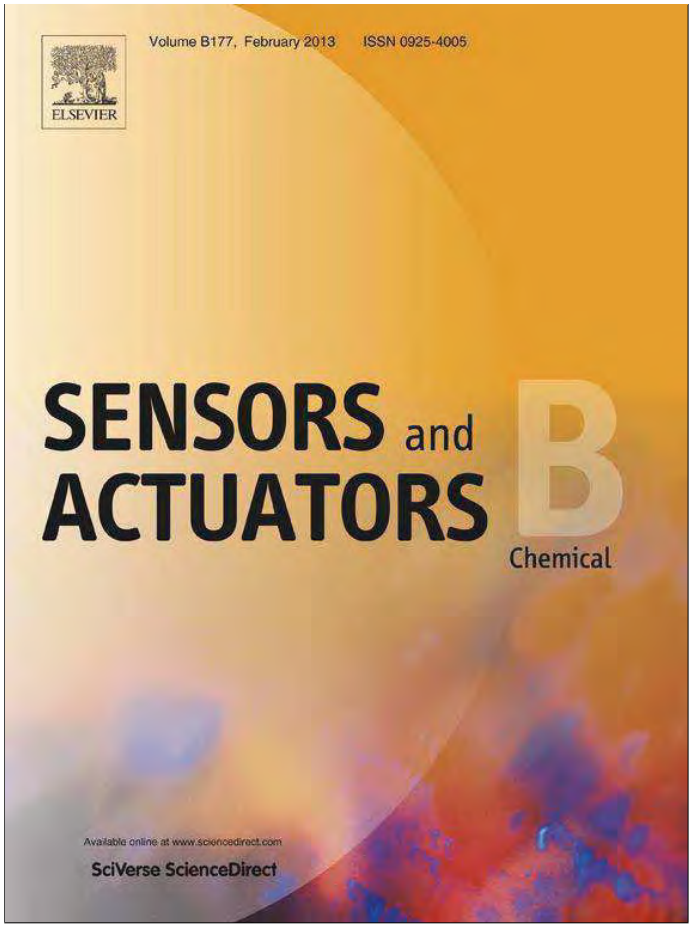

This article appeared in a journal published by Elsevier. The attached copy is furnished to the author for internal non-commercial research and education use, including for instruction at the authors institution and sharing with colleagues.

Other uses, including reproduction and distribution, or selling or licensing copies, or posting to personal, institutional or third party websites are prohibited.

In most cases authors are permitted to post their version of the article (e.g. in Word or Tex form) to their personal website or institutional repository. Authors requiring further information regarding Elsevier's archiving and manuscript policies are encouraged to visit:

http://www.elsevier.com/copyright

Author's personal copy

Sensors and Actuators B 177 (2013) 543–554

Contents lists available at SciVerse ScienceDirect

Sensors and Actuators B: Chemical

journal homepage: www.elsevier.com/locate/snb

A comparative study of a label-free DNA capacitive sensor using a pyrrolidinyl peptide nucleic acid probe immobilized through polyphenylenediamine and polytyramine non-conducting polymers

Supannee Sankoh[a,b,c], Saluma Samanman[a,b,c], Orawan Thipmanee[a,b,c], Apon Numnuam[a,b,c], Warakorn Limbut[a,b,d], Proespichaya Kanatharana[a,b,c], Tirayut Vilaivan[e], Panote Thavarungkul[a,b,f,*]

[a] Trace Analysis and Biosensor Research Center, Prince of Songkla University, Hat Yai, Songkhla 90112, Thailand
[b] Center of Excellence for Innovation in Chemistry, Faculty of Science, Prince of Songkla University, Hat Yai, Songkhla 90112, Thailand
[c] Department of Chemistry, Faculty of Science, Prince of Songkla University, Hat Yai, Songkhla 90112, Thailand
[d] Department of Applied Science, Faculty of Science, Prince of Songkla University, Hat Yai, Songkhla 90112, Thailand
[e] Organic Synthesis Research Unit, Department of Chemistry, Faculty of Science, Chulalongkorn University, Bangkok 10330, Thailand
[f] Department of Physics, Faculty of Science, Prince of Songkla University, Hat Yai, Songkhla 90112, Thailand

ARTICLE INFO

Article history:
Received 12 September 2012
Received in revised form
19 November 2012
Accepted 21 November 2012
Available online 30 November 2012

Keywords:
Non-conducting polymer
Polyphenylenediamine
Polytyramine
acpcPNA
Capacitive system
Sensor

ABSTRACT

This work has, for the first time, reported a comparative study on the performances of a label-free capacitive DNA sensor based on an immobilized pyrrolidinyl peptide nucleic acid with a D-prolyl-2-aminocyclopentanecarboxylic acid backbone (acpcPNA) attached to three easy to prepare non-conducting polymers. Two phenylenediamine (PD) isomers (*ortho*- and *para*-) and one tyramine monomer were electropolymerized to form polymer films. The hybridization between the acpcPNA probes, immobilized on the polymer layer, and the target DNA was detected directly by measuring the capacitance change. Using the optimal electropolymerized conditions, the highest sensitivity of 20.9 ± 0.6-nF cm^{-2} (log M)$^{-1}$ was obtained from poly-*para*-PD (P*p*PD) with a lowest detection limit of 0.2 pM. A wide linear range, 1.0×10^{-12} to 1.0×10^{-8} M, was obtained for both the P*p*PD and polytyramine (Pty). A narrower linear range of 1.0×10^{-11} to 1.0×10^{-8} M was obtained from the poly-*ortho*-PD (P*o*PD). The surface morphology was observed using scanning electron microscopy and atomic force microscopy. The polymer with the better surface morphology, i.e., smoother, denser and more homogeneous was the one with more immobilized probes and a better overall performance. All modified polymers gave a high % signal suppression (%SS) for both the single and double mismatched target DNAs, and indicated its high specificity. The electrodes can be reused for at least 68 analytical cycles. The effects of the target length and probe concentrations were also investigated. Under the operating conditions of this work the system would be very useful for the cost-effective analysis of ultra-trace levels of DNA in samples.
© 2012 Elsevier B.V. All rights reserved.

1. Introduction

Label-free DNA sensors are now being widely investigated due to their low cost, simplicity of operation and fast response times. In recent years, there has been an increase in the use of synthetic peptide nucleic acid (PNA) probes instead of DNA probes because of their higher stability [1]. They also provide a higher specificity with faster hybridization kinetics [2,3]. Many transducers have been successfully employed for label-free DNA detection such as mass sensitive [4,5], optical [6,7] and electrochemical transducers [8,9]. One of the systems that has attracted recent interest due to its high sensitivity, simplicity of operation and is relatively inexpensive is the potential step capacitive technique [10–13].

The principle of the potential step capacitive system is based on measuring changes in dielectric properties when a target binds with the sensing element on the electrode surface. One of the important factors to facilitate detection of the change is the insulating property of the immobilized surface. This is to prevent possible interference from electroactive species in the electrolyte solution and reduces the Faradaic current [14,15]. The insulating layer is generally based on the use of a self-assembled monolayer (SAM) of thiol compounds [9,10,12,14–16] for the immobilization of the sensing elements. However, the self-assembly process requires a relatively long preparation time (12–24 h) and a very smooth surface of the gold electrode is a necessity [16,17]. To overcome these problems electropolymerization of a non-conducting

* Corresponding author at: Department of Physics, Faculty of Science, Prince of Songkla University, Hat Yai, Songkhla 90112, Thailand. Tel.: +66 74 288753; fax: +66 74 558849.
E-mail address: panote.t@psu.ac.th (P. Thavarungkul).

0925-4005/$ – see front matter © 2012 Elsevier B.V. All rights reserved.
http://dx.doi.org/10.1016/j.snb.2012.11.077

Author's personal copy

polymer on the working electrode is an attractive alternative. It can be produced much more quickly (8 min) and the roughness of the gold electrode is not such a critical factor for the formation of the polymer [18]. Furthermore, these insulator layers [19,20] can be prepared as an ultra-thin film (10–100 nm) [21–24] and provides a large number of surface amine group reactive sites for the immobilization of sensing molecules [19]. Poly-*ortho*-phenylenediamine (P*o*PD) [17,25], poly-*para*-phenylenediamine (P*p*PD) [24], and polytyramine (Pty) [16,26] are non-conducting polymers that have been successfully employed as immobilization films for various recognition elements. However, there has not been any report on a DNA sensor based on an immobilized PNA probe prepared on such polymers.

The objective of this work was to compare the performances of a label-free capacitive DNA sensor using an acpcPNA probe immobilized on each of three electropolymerized non-conducting polymers of P*o*PD, P*p*PD and Pty. This is the first time such a comparative study has been attempted. The optimal electropolymerized conditions, i.e., the monomer concentration and number of scans, were first investigated together for each polymer. This is also the first time the performances were compared under optimal conditions for each polymer. The sensing element was acpcPNA, a conformationally constrained peptide nucleic acid derived from a D-prolyl-2-aminocyclopentanecarboxylic acid (ACPC) backbone. This is a relatively new PNA system developed by our group [27,28]. This PNA provides a stronger binding affinity and better sequence specificity toward DNA compared to DNA itself [29,30] and aminoethylglycyl PNA (aegPNA) [4,28,31]. The surface morphology of the polymer films was observed using scanning electron microscopy and images obtained from an atomic force microscope. These together with the amount of the immobilized acpcPNA probes were correlated to the performances.

2. Experimental

2.1. Materials

The 9-mer lysine-modified acpcPNA (Ac-TTTTTTTTT-LysNH_2) denoted as 'acpcPNA-T9 probe' and the 12-mer mixed base lysine-modified acpcPNA (Bz-TGTCAACTGACT-LysNH_2) denoted as 'acpcPNA-M12 probe', were synthesized by Mrs. Chotima Vilaivan at Chulalongkorn University, Thailand according to the published protocol [27,28]. The acpcPNA probes were purified by reverse phase HPLC (to >90% purity) and their identities were verified by MALDI-TOF mass spectrometry (acpcPNA-T9: *m*/*z* calcd. 3179.4 found 3179.4; acpcPNA-M12: *m*/*z* calcd. 4270.6 found 4271.6).

Oligonucleotides (DNAs), complementary, single mismatched, double mismatched and non-complementary target DNAs were from Bioservice Unit, National Science and Technology Development Agency and BioDesign Co., Ltd., Thailand. The DNA sequences are shown as follows (non-complementary regions are indicated by italicized letters):

For the acpcPNA-T9 probe
Complementary DNA
D6comp: 5′-AAAAAA-3′
D9comp: 5′-AAAAAAAAA-3′
D12comp: 5′-AAAAAAAAAAAA-3′
D27comp: 5′-AAAAAAAAAAAAAAAAAAAAAAAAAAA-3′
D27compM18a: 5′-*TTTTTTTTT*AAAAAAAAA*TTTTTTTTT*-3′
D27compM18b: 5′-*TGCTCAGCT*AAAAAAAAA*TGCTCAGCT*-3′
Single mismatched DNA
D9M1G: 5′-AAAA*G*AAAA-3′
D9M1C: 5′-AAAA*C*AAAA-3′
D9M1T: 5′-AAAA*T*AAAA-3′
Double mismatched DNA
D9M2G: 5′-AAA*G*A*G*AAA-3′
D9M2C: 5′-AAA*C*A*C*AAA-3′
D9M2T: 5′-AAA*T*A*T*AAA-3′
Non-complementary DNA
D9non-compa: 5′-*TTTTTTTTT*-3′
D9non-compb: 5′-*TATTATTAT*-3′

For the acpcPNA-M12 probe
Complementary DNA
D9comp: 5′-CAGTTGACA-3′
D12comp: 5′-AGTCAGTTGACA-3′
D15compM3: 5′-*GCT*AGTCAGTTGACA-3′
D30compM18: 5′-*GACTGCACC*AGTCAGTTGACA*TGTTGCGAC*-3′
Single mismatched DNA
D12M1T: 5′-AGTCA*T*TTGACA-3′
D12M1C: 5′-AGTCA*C*TTGACA-3′
D12M1A: 5′-AGTCA*A*TTGACA-3′
Double mismatched DNA
D12M2T: 5′-AGT*TA*T*T*TGACA-3′
D12M2CG: 5′-AGTCA*G*TTGACA-3′
D12M2A: 5′-AGTA*AA*TTGACA-3′
Non-complementary DNA
D12non-comp: 5′-*TCAGTCAACTGT*-3′

The three non-conducting monomers, *ortho*-phenylenediamine (*o*-PD), *para*-phenylenediamine (*p*-PD) and tyramine were obtained from BDH (Poole, England), laboratory UNILAB reagent (Sydney–Melbourne, Australia) and Aldrich (Steinheim, Germany), respectively. Glutaraldehyde and 11-mercapto-1-undecanol (11-MUL) were obtained from Sigma-Aldrich® (Steinheim, Germany). All buffers were prepared with deionized water treated with a reverse osmosis-deionizing system (Pentair, Inc., USA). Before use, buffers were filtered through a nylon membrane filter (Vertical®, Albet, Spain, pore size 0.2 μm) with subsequent degassing. Other chemicals were of analytical grade and were used as received.

2.2. Gold electrode preparation

Gold rod electrodes (99.99% purity) with a diameter of 3.0 mm were polished by hand using alumina slurries with particle diameters of 5, 1 and 0.3 μm, respectively and subsequently cleaned by rinsing with distilled water. The electrodes were then placed in a plasma cleaner (Model PDC-32G, Harrick, New York, USA) for 15 min to remove any organic materials adsorbed onto the surface electrode.

2.3. acpcPNA probe immobilization

The acpcPNA-T9 probe possessing a T9 sequence was chosen for the initial optimization of the model because it is the simplest probe that can form a sufficiently stable hybrid with a complementary DNA target at room temperature ($T_m \sim 73\,^{\circ}C$) and this probe forms only a duplex (not a triplex) with its complementary DNA (dA_9) [28]. Because of its short length and simple composition, this PNA can be synthesized with high efficiency. Furthermore the homo-T sequence contains no exocyclic amino groups that could complicate the immobilization and it also has no electroactive G base that may complicate the interpretation of the results [27,28].

Monomers of *o*-PD and *p*-PD were prepared in 10 mM sodium acetate buffer pH 5.18 [17] and the tyramine monomer was prepared in a solution containing 2.0 mM phosphate buffer pH 7.00 and ethanol (volume ratio of 3:1) [16]. For the immobilization of acpcPNA-T9, the monomer concentration and the number of scans for electropolymerization were optimized at the same time. From the literature 5 mM of *o*-PD [21,32,33], 5 mM of *p*-PD [21,32], and 50 mM of tyramine [16,26] have been used. Therefore, monomer concentrations close to these values were used. For *o*-PD and *p*-PD, 1, 5, 10 and 20 mM of monomer was electropolymerized by cyclic voltammetry at 5, 10, 15 and 20 scans using the potential range from 0.0 to 0.8 V vs. Ag/AgCl with a scan rate of 50 mV s^{-1}. Electropolymerization of tyramine was performed using the same conditions but at concentrations of 5, 15, 35, 50 and 60 mM. The

Author's personal copy

polymer-coated electrodes were cleaned by rinsing with distilled water and treated with 5% (v/v) glutaraldehyde in 10 mM sodium phosphate buffer pH 7.00 at room temperature for 20 min to activate the aldehyde group. Next, 20 μL of a 5.0 μM aqueous solution of acpcPNA-T9 was placed on the polymer coated electrode and the coupling reaction was allowed to proceed overnight at 4 °C [9]. The electrodes were then treated with 1.0 mM ethanolamine pH 8.00 for 7 min to deactivate all the remaining aldehyde groups not coupled to the immobilized acpcPNA-T9 probe. Finally the modified electrodes were immersed in 1.0 mM of 11-MUL blocking solution for 1 h at room temperature to block any remaining pinholes on the electrode surface.

The acpcPNA-M12 probe was also immobilized under the optimal electropolymerized conditions obtained from the above experiments. This is to demonstrate the applicability in a more realistic situation, i.e., to show that the presence of G bases and exocyclic amino groups do not negatively affect the fabrication and performance of the sensor. Different sequences and lengths of DNA targets were also tested to demonstrate the applicability in a more realistic scenario for analyses of real DNA samples where the length of the DNA target is unlikely to be the same as that of the probe.

The electrochemical behavior of each immobilization step was studied by cyclic voltammetry. Electrochemical measurements were carried out using a potentiostat (Methrohm Autolab B.V., The Netherlands) coupled to an electrochemical cell containing the modified working electrode, an Ag/AgCl reference electrode as reference and a platinum wire as an auxiliary electrode.

2.4. Amount of the immobilized acpcPNA probe on the modified electrode surface

The absorbance of the acpcPNA-T9 probe in water was measured at 260 nm using a spectrophotometer (AvaSpec-2048-USB2-UA, Avantes Technical Support, The Netherlands) combined with a SpectroPipetter (Spectropipetter-SPT-2, World Precision Instruments, USA). The A_{260} was used to calculate the concentration from the equation $A = \varepsilon bc$, where A is the absorbance, ε is the molar extinction coefficient (79.2 mL μmol^{-1} cm^{-1}) of acpcPNA-T9 at 260 nm [34], b is the path length of the SpectroPipetter (1.0 mm) and c is the concentration (μmol mL^{-1}). The amount of the acpcPNA probe was then calculated from the concentration of the probe and the volume (20 μL) used for the immobilization. The amount of the immobilized acpcPNA-T9 probe on the modified electrode prepared under the optimal electropolymerized conditions was determined as the difference between the amount of the probe in the solution prepared before the immobilization and the solution collected from the electrode surface after the immobilization.

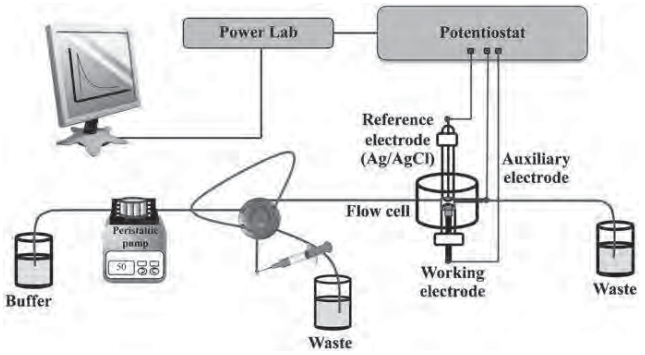

Fig. 1. Schematic diagram showing the flow injection capacitive DNA sensor system.

2.5. Surface morphology characterization

The surface morphology of the polymer coated electrodes was observed by scanning electron microscopy (SEM) and atomic force microscopy (AFM). Polymer surfaces were imaged with a JSM 5800 SEM from JEOL, Japan, operated at an accelerating voltage of 20 kV. AFM imaging was performed in a tapping mode with a Nanosurf easyScan 2 from NANOSURF AG, Switzerland.

2.6. Capacitance measurement

The experimental set-up of the flow injection capacitive DNA sensor system is shown in Fig. 1. The modified gold electrode (working electrode), a stainless steel tube (auxiliary electrode) and a custom made Ag/AgCl (reference electrode) were placed in a custom-made measuring flow cell (10 μL) and they were connected to a potentiostat (Model EA161, EDAQ, New South Wales, Australia).

The capacitance was determined from the obtained current response when a potential step of 50 mV (pulse width 6.4 ms) was applied to the working electrode. The system can be represented by a simple RC circuit model and the current-time response can be expressed by Eq. (1) [14]

$$i(t) = \frac{u}{R_s} \exp\left(\frac{-t}{R_s C_{total}}\right) \quad (1)$$

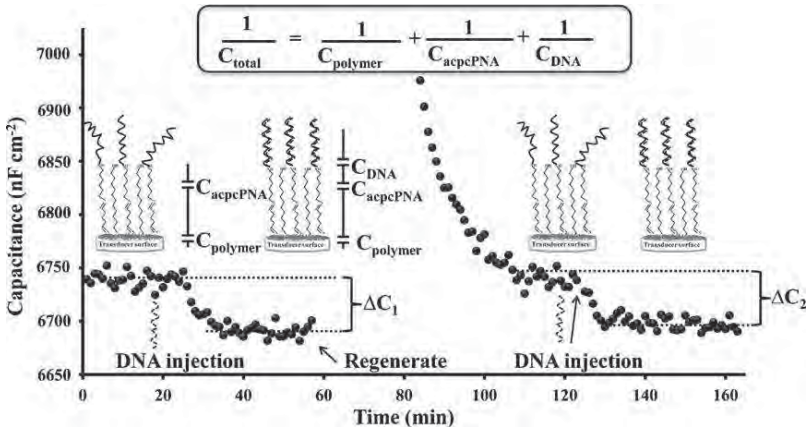

Fig. 2. Capacitance response of the immobilized acpcPNA-T9 modified electrode. The baseline signal of the carrier buffer was first recorded. After the injection of DNA, the hybridization between the DNA and the immobilized acpcPNA-T9 probe caused the capacitance to decrease (ΔC). The regeneration solution was then injected to remove the DNA from the immobilized acpcPNA-T9. When the signal baseline was recovered a new analysis cycle was applied.

Author's personal copy

where $i(t)$ is the current in the circuit as a function of time, u is the applied pulse potential, R_s is the dynamic resistance of the recognition layer, t is the time elapsed after the potential step is applied, and C_{total} is the total capacitance measured at the working electrode/solution interface. Eq. (2) is obtained by taking the logarithm of Eq. (1)

$$\ln i(t) = \ln \frac{u}{R_s} - \frac{t}{R_s C_{total}} \quad (2)$$

From the linear least-square fitting of $\ln i(t)$ versus t, the R_s and C_{total} were calculated from the intercept and slope of the linear regression equation, respectively. During the continuous flow of the running buffer, a baseline capacitance was obtained. When the target DNA was injected into the flow system it hybridized to the immobilized acpcPNA on the working electrode and the C_{total} decreased (Fig. 2) as described by Eq. (3)

$$\frac{1}{C_{total}} = \frac{1}{C_{polymer}} + \frac{1}{C_{acpcPNA}} + \frac{1}{C_{DNA}} \quad (3)$$

where C_{total} is the total double layer capacitance measured at the working electrode/solution interface, $C_{polymer}$ is the capacitance of the polymer modified layer, $C_{acpcPNA}$ is the capacitance of the acpcPNA layer, and C_{DNA} is the capacitance of the DNA layer. C_{total} was measured every minute and the results were later plotted as a function of time. The capacitance change (ΔC) could be determined (Fig. 2) as

$$\Delta C = C_{before\ \ hybridizing\ \ with\ \ DNA} - C_{after\ \ hybridizing\ \ with\ \ DNA} \quad (4)$$

The regeneration solution, 300 μL of 50 mM NaOH [6], was then applied to break the binding between the acpcPNA probe and the target DNA after hybridization. The capacitance then returned to its original baseline, ready for a new analytical cycle (Fig. 2).

2.7. Specificity determination

The specificity of the proposed DNA sensor was studied by comparing the signal of the complementary DNA and the single base and double base mismatched DNA, the % signal suppression (%SS) was calculated according to Eq. (5). A higher %SS reflexes a better specificity.

$$\%SS = \frac{\Delta C_{complementry\ \ DNA} - \Delta C_{mismatched\ \ DNA}}{\Delta C_{complementry\ \ DNA}} \times 100 \quad (5)$$

3. Results and discussion

3.1. Characterization of the immobilization steps

Fig. 3 shows the cyclic voltammograms of the three monomers at the concentration that provided the highest capacitance response (see Section 3.2), i.e. 5 mM for *o*-PD (Fig. 3(a)) and *p*-PD (Fig. 3(b)), and 50 mM for tyramine (Fig. 3(c)). After the first scan the peak current continuously decreased with each further scan indicating that more and more of the non-conducting polymer was formed and covered the electrode surface.

The degree of insulation of the modified gold electrode after each immobilization step was examined by cyclic voltammetry (Eco Chemie μ-autolab B.V., Utrecht, Netherlands) with 10 mM $K_3[FeCN_6]$ in 0.1 M KCl between −0.3 and 0.7 V at a scan rate of 0.1 V/s vs. a Ag/AgCl electrode. An example of a cyclic voltammogram recorded from a PoPD modified electrode with the immobilized acpcPNA-T9 probe is shown in Fig. 4. The cleaned gold surface showed a voltammogram with large oxidation and reduction peaks (Fig. 4(a) inset). Both peaks decreased substantially when the polymer was coated onto the gold surface (Fig. 4(b)). The insulating property of the electrode surface was further

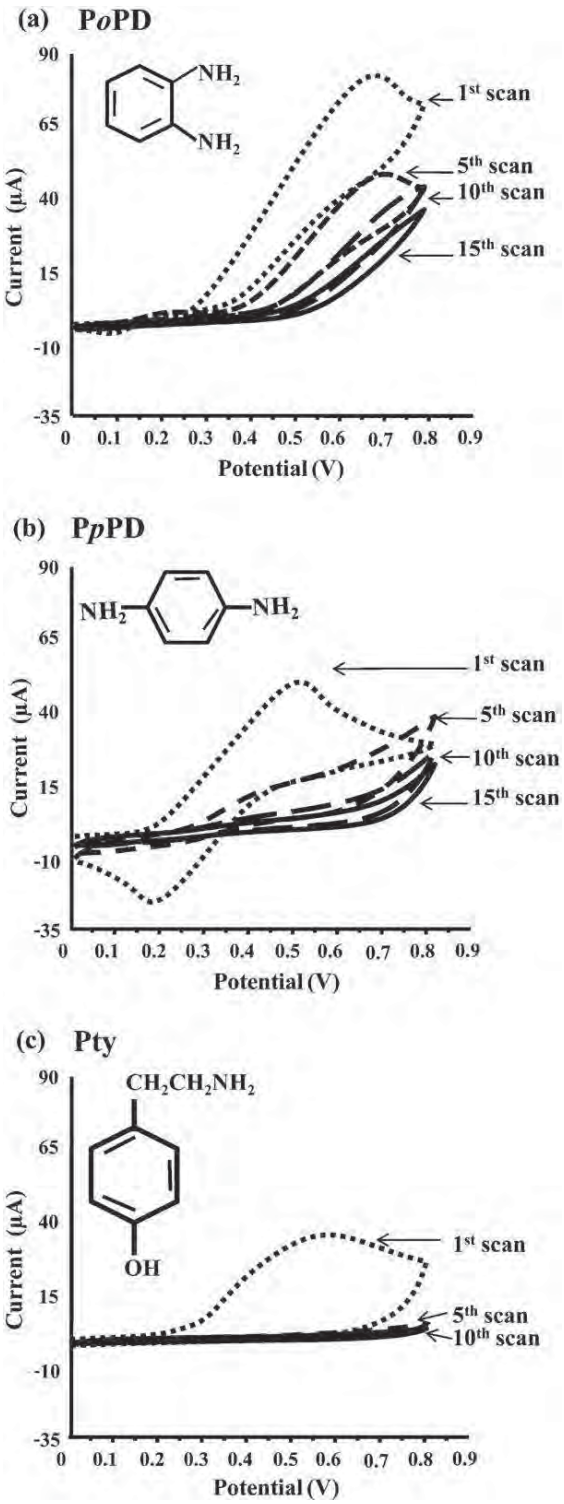

Fig. 3. Cyclic voltammograms of the electropolymerization of the three polymers (a) PoPD, (b) PpPD and (c) Pty in their monomer solution.

increased when the acpcPNA-T9 was immobilized (Fig. 4(c)). This indicated that the acpcPNA-T9 had been successfully immobilized onto the modified gold electrode. The modified surface was then reacted with ethanolamine pH 8.50; this step was to occupy all the remaining aldehyde groups that had not been coupled to the immobilized acpcPNA-T9. After the treatment with 11-MUL

Author's personal copy

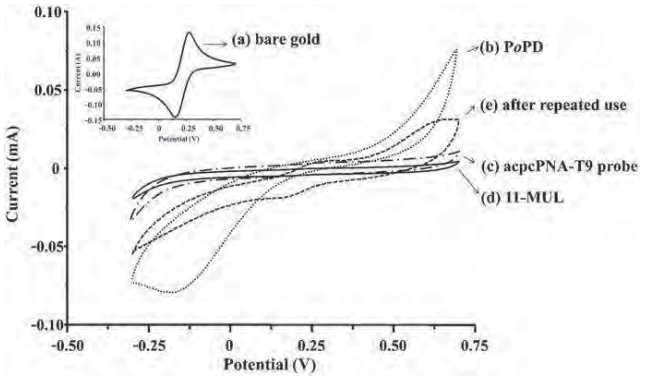

Fig. 4. An example of a cyclic voltammograms obtained from a PoPD immobilized acpcPNA-T9 probe (a) bare gold, (b) PoPD, (c) acpcPNA-T9 probe, (d) 11-MUL before use and (e) after repeated use.

the electrode surface was completely insulated as shown by the disappearance of the redox peaks (Fig. 4(d)). This insulation property is a necessary condition for the non-Faradaic detection of the employed capacitive system [35].

3.2. Effect of monomer concentration and number of scans

The monomer concentration and the number of scans for the electropolymerization that may affect the immobilization, and hence the system performance, were optimized together. The optimal conditions were chosen from the conditions that provided the highest capacitance change using the same concentration of the DNA target at 1.0×10^{-10} M. The measurements were carried out using the following operating conditions: regeneration solution 300 μL of 50 mM NaOH [6], 10 mM phosphate buffer pH 7.00 as the running buffer, sample volume 300 μL and flow rate 50 μL min^{-1}. Fig. 5 shows the capacitance change vs. the concentration of the monomers. At every monomer concentration both PoPD (Fig. 5(a)) and PpPD (Fig. 5(b)) showed an increase of the capacitance change with the number of electropolymerization scan up to 15 scans and then decreased. The optimal concentration was 5 mM and the number of scans was 15 for both PoPD and PpPD. For the Pty modified electrode (Fig. 5(c)) for an increase between 5 and 35 mM, the capacitance change increased with the number of electropolymerization scans whereby the capacitance change decreased with the number of scans at 60 mM. For 50 mM, the capacitance change increased with the number of scans up to 10 scans before the signal decreased. Hence the optimal concentration of Pty was 50 mM and the number of scans was 10. This could be explained from the surface morphology of the polymer coated film and the amount of immobilized acpcPNA which will be discussed in the following sections.

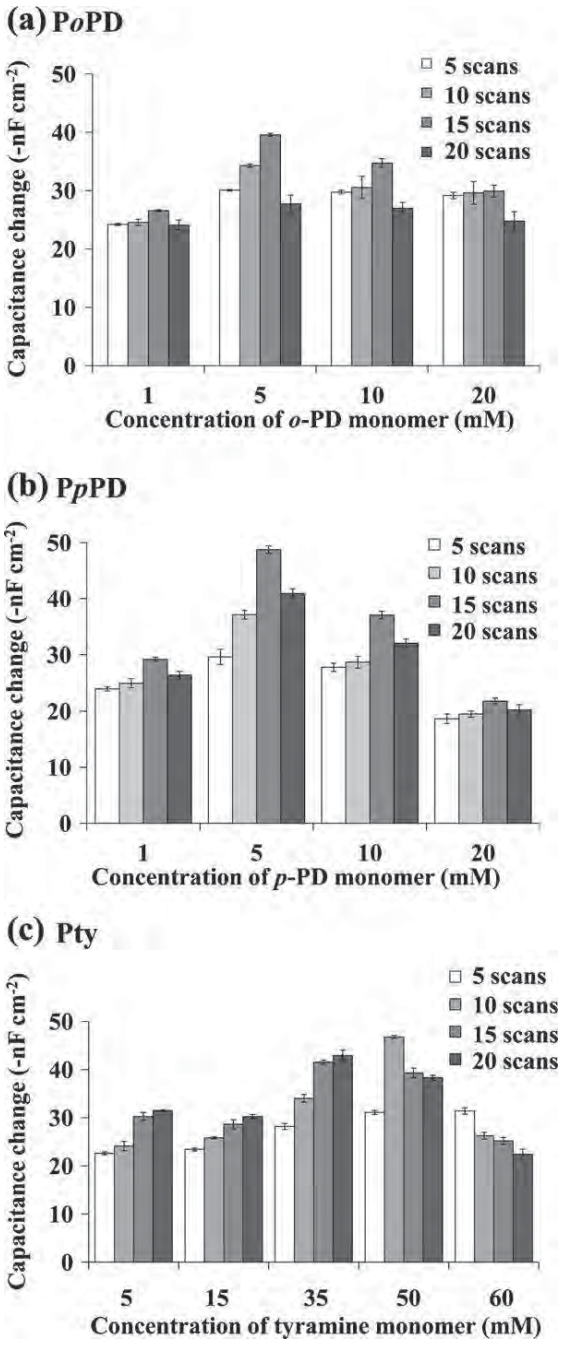

Fig. 5. Effect of monomer concentrations (1, 5, 10 and 20 mM for *o*-PD and *p*-PD, and 5, 15, 35, 50 and 60 mM for tyramine) and number of scans (5, 10, 15 and 20 scans) on the electropolymerization of the three non-conducting polymers, (a) PoPD, (b) PpPD and (c) Pty.

3.3. Surface morphology

3.3.1. Scanning electron microscopy

Fig. 6 shows the SEM images of the three polymer coated surfaces. They are distinctly different from the bare gold electrode surface (Fig. 6a inset). At the optimal concentration and number of scans, 5 mM and 15 scans for PoPD and PpPD, 50 mM and 10 scans for Pty, the surfaces were relatively smooth and the polymer film fully covered the gold electrode surface (Fig. 6(c), (g) and (j)). Some free spaces (dark areas) were observed for the surfaces with a lower number of scans (Fig. 6(a), (b), (e), (f) and (i)). The higher number of scans showed a closely packed lumpy morphology caused by the overlay of the polymer layer (Fig. 6(d), (h), (k) and (l)).

3.3.2. Atomic force microscope

Additional information on the film morphology was obtained from the AFM, employed in a tapping mode. An example of the AFM images of the bare gold electrode, the PpPD modified electrode with the lowest number of scans (5 scans), the optimal number of scans (15 scans) and the highest number of scans (20 scans) are presented in Fig. 7. Topographic AFM images of the bare gold electrode showed a relatively rough surface (Fig. 7a1 and a2). The average peak height from several line scans ($n = 10$ lines, 256 points per line) is shown in Fig. 7(a3). The AFM-tip deflections were larger

Author's personal copy

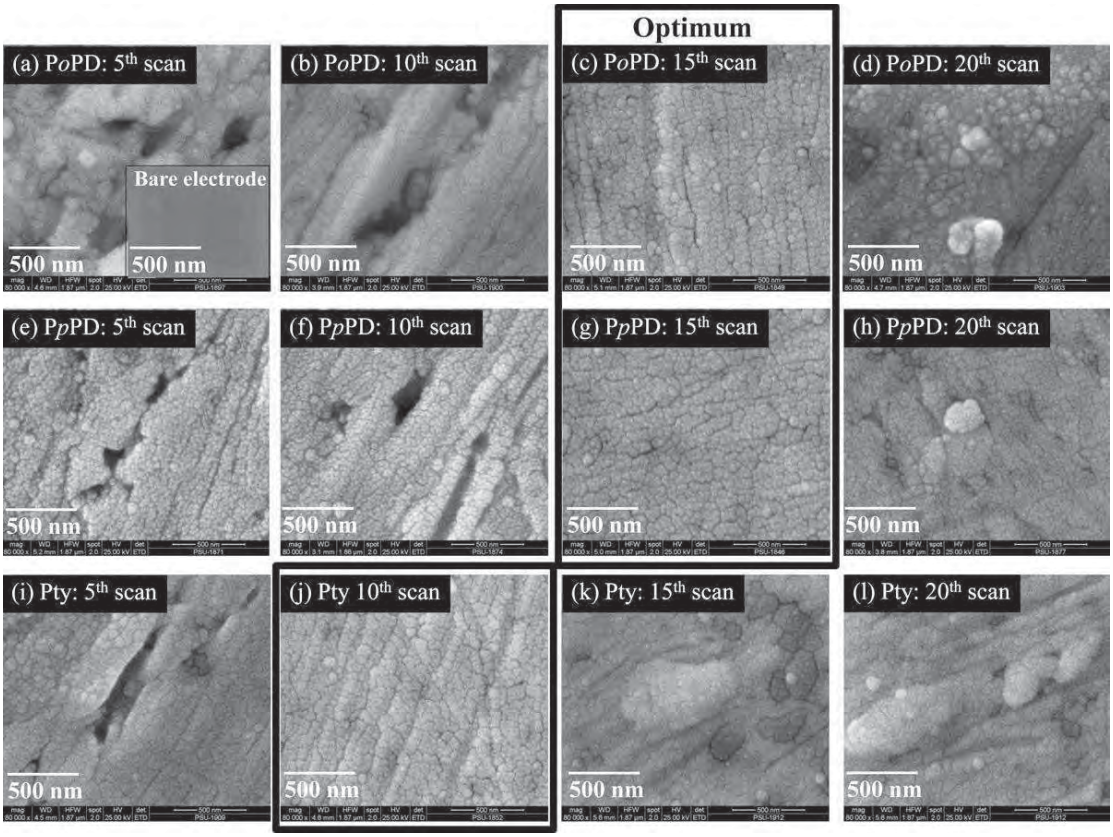

Fig. 6. SEM images of bare gold electrode surfaces electropolymerized with 5 mM of *o*-PD at different numbers of scans (a)–(d), with 5 mM *p*-PD at different numbers of scans (e)–(h), and with 50 mM tyramine monomer concentration at different numbers of scans (i)–(l) from 5 to 20 scans. The images at the optimal number of scan are indicated by the solid frame. Inset (a) is the SEM image of a bare gold electrode.

than 5 nm with a root mean square roughness (RMS) of 10 ± 1 nm. For the P*p*PD surface with 5 scans, there were some dark spots of an uncoated surface (Fig. 7(b1)) with a lot of jagged peaks (Fig. 7(b2)) observed. This is possibly due to the different height of the coated and uncoated areas. The RMS value was 7.6 ± 0.1 nm, lower than the bare gold surface to indicate that the polymer coated surface was smoother. A lower RMS value of 4.4 ± 0.3 nm, was obtained from the 15 scans, that indicated a more uniform, smoother surface (Fig. 7(c1) and (c2)) with more deposited polymer than for the 5 scans. For 20 scans, the RMS value was 7.9 ± 0.2 nm that is higher than for the 15 scans. This is possibly because of its inhomogenous surface (Fig. 7(d1) and (d2)). A larger peak height difference was clearly evident in the profile (Fig. 7(d3)). The results from the AFM images corresponded well with those obtained from the SEM images.

Fig. 8 shows the AFM images of the surfaces coated with the three polymers at their optimal concentration and number of scans. For the P*o*PD modified electrode, the RMS value was 6.8 ± 0.8 nm and the AFM images presented a relatively rough surface (Fig. 8(a1) and (a2)). This is clearly evident in the profile (Fig. 8(a3)). The topography of the P*p*PD modified electrode (Fig. 8(b1) and (b2)) provided a smoother, denser and more homogeneous surface than the P*o*PD modified electrode. It also provided a better profile (Fig. 8(b3)) and a lower RMS of 4.4 ± 0.3 nm. For the Pty modified electrode, the RMS value of 5.9 ± 0.5 nm was higher than the P*p*PD modified electrode, to indicate that it had a rougher surface (Fig. 8(c1) and (c2)). Compared to the P*p*PD modified electrode, the profile was also more rugged (Fig. 8(c3)).

From the surface morphologies obtained from both the SEM and AFM images it is reasonable to say that there exists an optimal concentration and number of scans of the polymer that provides a smooth coated electrode surface. For a particular concentration when the number of scans was too few the surfaces were not fully coated. However, too many scans made the coated layer too thick and lumpy. This is part of the reasons behind the different responses shown in Fig. 5. At a lower number of scans (5 and 10 scans for P*o*PD and P*p*PD, 5 scans for Pty) a lower signal was obtained because less polymer was coated onto the electrode surface hence a lower amount of the acpcPNA-T9 probe could be immobilized (see Section 3.4). At a higher number of scans (20 scans for P*o*PD and P*p*PD or 15 and 20 scans for Pty) the layer of the polymer was too thick and this reduced the total capacitance of the modified layer after the final blocking steps (C_{mod}) ($C \propto 1/\text{thickness}$) and resulted in a lower signal. This can be explained as follows.

Let C_{mod} be the total capacitance of all the modified layers and C_{DNA} the capacitance of the bound target DNA, the total capacitance C_{total} according to Eq. (3) is

$$\frac{1}{C_{total}} = \frac{1}{C_{\text{mod}}} + \frac{1}{C_{DNA}} \tag{6}$$

If the C_{mod} is low it will dominate the total capacitance and the capacitance change caused by the target DNA was less detectable. Therefore, it is important to have a surface with the highest possible capacitance [14]. For all the modified surfaces at the optimal number of scans the C_{mod} values after the final blocking steps were found to be the highest. That is, the C_{mod} for the P*o*PD modified electrode at 15 scans was $(7.03 \pm 0.02) \times 10^3$ compared to $(4.230 \pm 0.004) \times 10^3$ nF cm^{-2} at 20 scans and $(12.38 \pm 0.01) \times 10^3$ compared to $(11.88 \pm 0.02) \times 10^3$ nF cm^{-2} for P*p*PD. For the Pty modified electrode the C_{mod} was $(9.52 \pm 0.02) \times 10^3$,

Author's personal copy

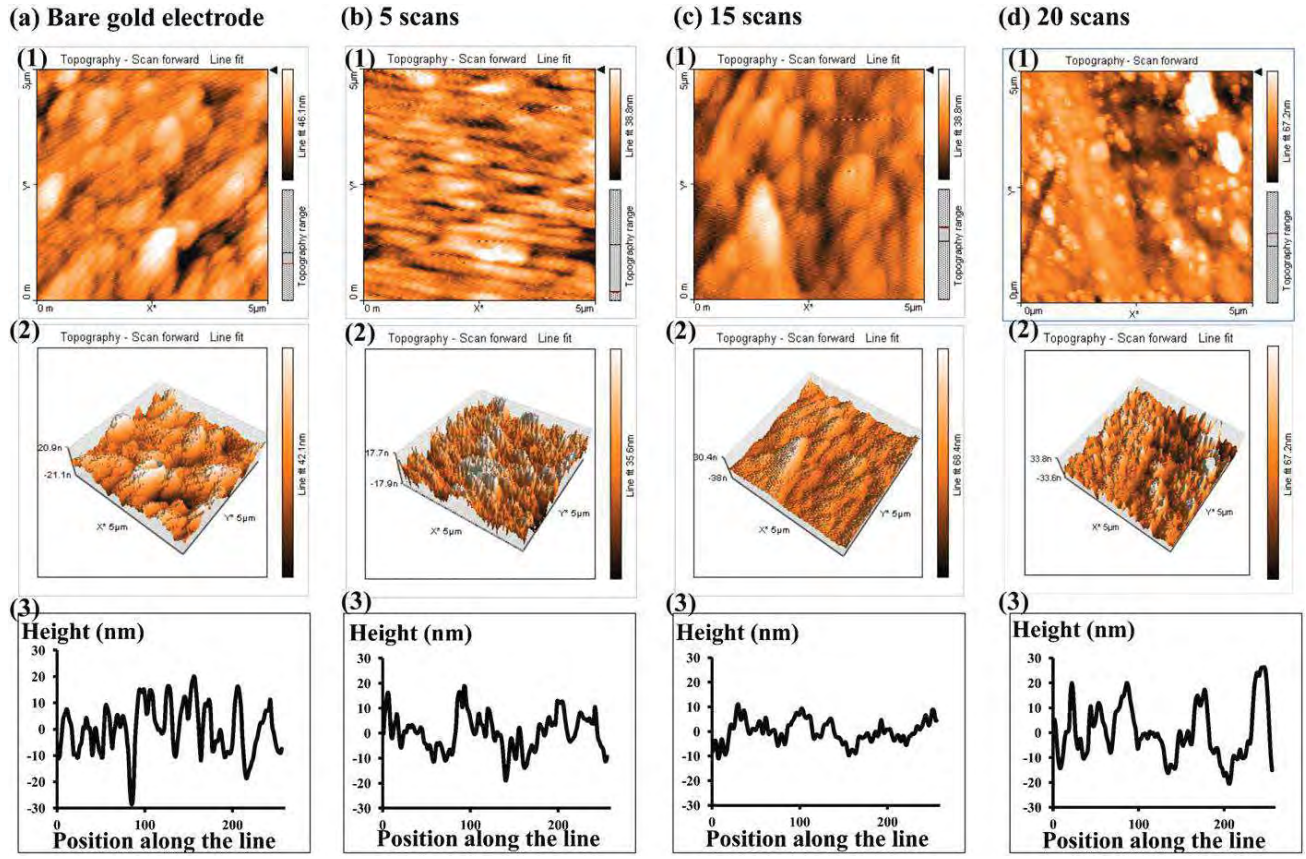

Fig. 7. AFM images of a bare gold electrode from 5 μm × 5 μm (a), with a 5 mM P*p*PD modified electrode surfaces and different numbers of scans (b) 5 scans, (c) 15 scans and (d) 20 scans. (1) and (2) are the 2D and 3D topographic images, (3) the AFM image profile showing tip deflections along the line (n = 10 lines, 256 points per line).

$(5.38 \pm 0.01) \times 10^3$ and $(5.08 \pm 0.01) \times 10^3$ nF cm^{-2} for 10, 15 and 20 scans, respectively. From the results it is clear that the optimal number of scans for each polymer produced the highest C_{mod} value, hence the highest capacitance change (ΔC) was obtained. Another reason for a lower signal at a higher number of scans was probably because the surface was lumpy due to the overlying layers of polymer. This may reduce the active sites, resulting in a lower amount of the acpcPNA-T9 probes being immobilized (see Section 3.4).

Comparing the three polymers under the optimal electropolymerization conditions, the P*p*PD modified electrode provided a slightly higher capacitance change than the Pty modified electrode, but it was much higher than the P*o*PD modified electrode. This is because it provided the best surface morphology – smooth, dense and homogenous – that resulted in the higher C_{mod} value. The surface with the best morphology also provided the highest amount of immobilized acpcPNA probe and this generally leads to a large signal (see Section 3.4).

3.4. Effect of the probe concentration and the amount of the immobilized acpcPNA probe

The amount of the immobilized acpcPNA-T9 probe on the electrodes coated with the three non-conducting polymers was tested by 3 replications per electrode. The electrode electropolymerized under the optimal conditions (5 mM *o*PD and *p*PD with 15 scans, and 50 mM tyramine with 10 scans) provided the highest amount of the immobilized acpcPNA-T9 probe (Table 1). This agreed well with the capacitance change as presented in Section 3.2.

To further test whether the best sensitivity was due to the different modified polymers, the probe concentration or both, three concentrations of the acpcPNA-T9 probe (3.0, 5.0 and 7.0 μM), were prepared and tested for immobilization. Fig. 9 shows the obtained sensitivity, i.e., the slope of the calibration plot of the capacitance change against the logarithm of the DNA target concentration of between 1.0×10^{-11} and 1.0×10^{-8} M. A low probe concentration (3.0 μM) showed a low sensitivity because of the lower amount of

Table 1
Effect of the number of scans used for electropolymerization with an optimal concentration of each monomer on the amount of the immobilized acpcPNA-T9 probe (5.0 μM) on the modified electrode surface (n = 3 per electrode).

The number of scans (scans)	Amount of the immobilized 5.0 μM acpcPNA-T9 probe on the modified electrode surface under the optimal monomer concentration of each polymer		
	*Po*PD (5 mM) (×10^2 pmol cm^{-2})	*Pp*PD (5 mM) (×10^2 pmol cm^{-2})	Pty (50 mM) (×10^2 pmol cm^{-2})
5	2.8 ± 0.2	3.7 ± 0.2	3.9 ± 0.1
10	4.6 ± 0.2	4.9 ± 0.2	7.77 ± 0.04
15	5.4 ± 0.1	7.9 ± 0.2	5.8 ± 0.2
20	2.8 ± 0.2	5.3 ± 0.2	5.0 ± 0.2

Author's personal copy

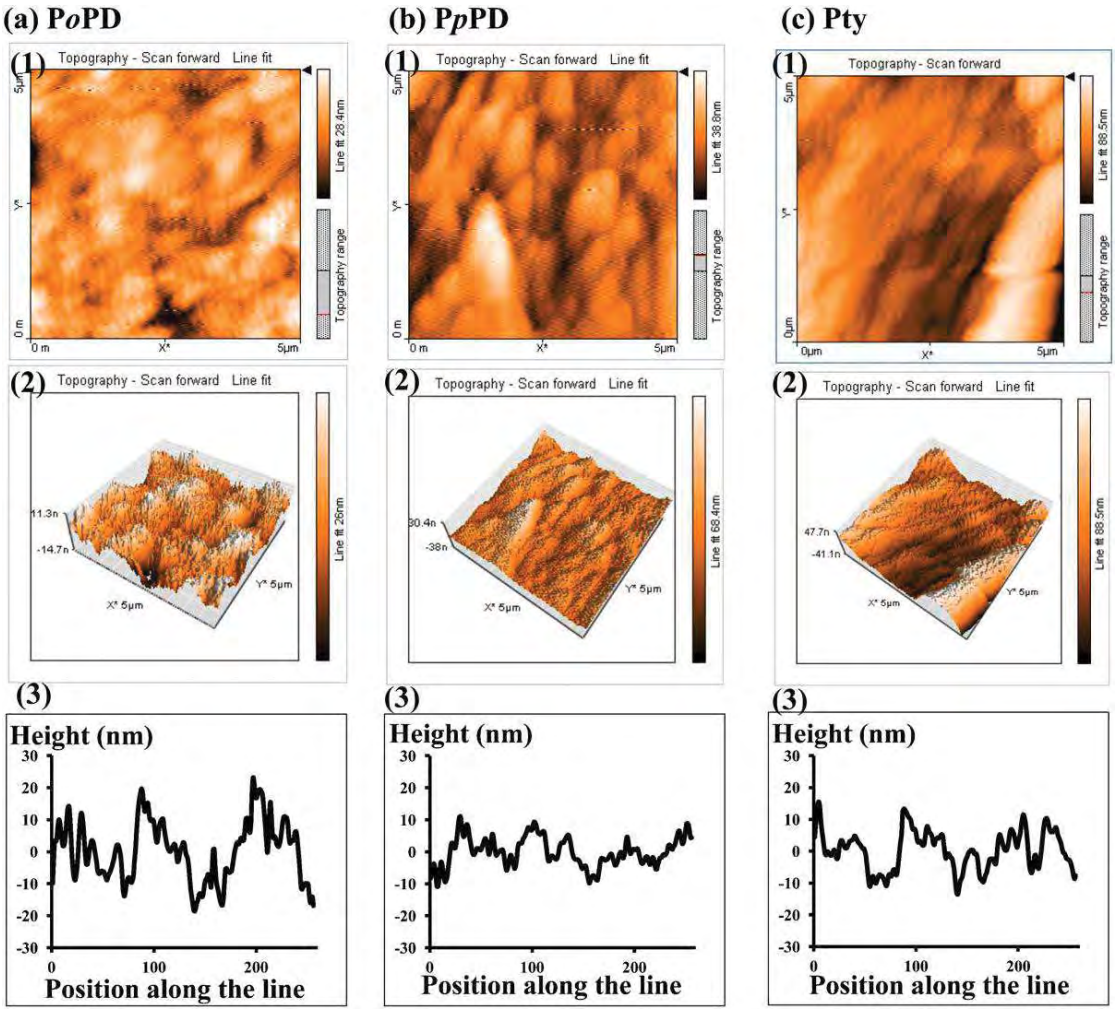

Fig. 8. AFM images of each polymer under optimal conditions obtained from 5 μm × 5 μm (a) (PoPD), (b) PpPD and (c) a Pty modified electrode surface. (1) and (2) are the 2D and 3D topographic images, (3) the AFM image profile showing large tip deflections along the line (n = 10 lines, 256 points per line).

the immobilized acpcPNA-T9 probe. For the probe concentrations of 5.0 and 7.0 μM the sensitivities were about the same. This is probably because the surfaces had the same amount of the immobilized acpcPNA-T9 probe.

The amount of the immobilized acpcPNA-T9 probe using three different concentrations of acpcPNA-T9 (3.0, 5.0 and 7.0 μM) are shown in Table 2. The amount of the immobilized acpcPNA probes reflects the results of Fig. 9. That is, the maximal immobilized probe was achieved at 5.0 μM. It is clear that the different capacitance signals also depended on the probe concentration. But at the same probe concentration the response depended on the modified polymer surface.

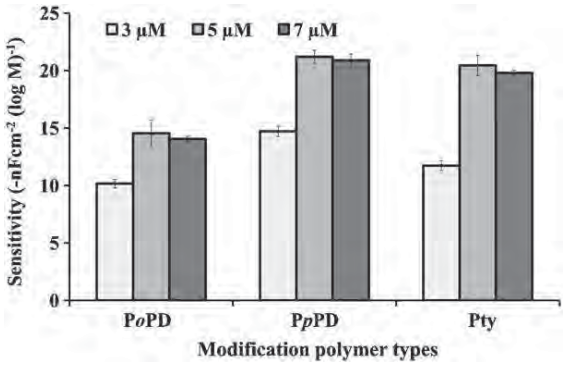

Fig. 9. Effect of the probe concentration (3.0, 5.0 and 7.0 μM) of acpcPNA-T9 probe on the sensitivity under the optimal concentration and the number of electropolymerization scans for each polymer, PoPD, PpPD and Pty.

3.5. Linear range and detection limit

The capacitive responses of various concentrations of the target DNA was studied from 1.0×10^{-14} to 1.0×10^{-7} M under the conditions; a sample volume of 300 μL, carrier buffer 10 mM phosphate, pH 7.00, and a flow rate of 50 μL min^{-1} with a regeneration step using 300 μL of 50 mM NaOH [6]. The relationship between the capacitance change and the logarithm of the target DNA concentration using the three polymers is shown in Fig. 10. Since the calibration curve has an s-shape, the limit of detection (LOD) was determined by following IUPAC recommendation 1994 where it is taken as the concentration of an analyte at the point of intersection of the extrapolated linear range and the final lowest concentration level segment of the calibration plot [36]. As expected, the best performances were from PpPD. It provided the highest sensitivity (20.9 ± 0.6-nF cm^{-2} $(log\,M)^{-1}$), lowest LOD (0.2 pM) and had a very wide linear range between 1.0×10^{-12} and 1.0×10^{-8} M. The

Author's personal copy

Table 2
Effect of the probe concentration (3.0, 5.0 and 7.0 μM) of the acpcPNA-T9 probe using the optimal conditions for electropolymerization on the amount of the immobilized acpcPNA-T9 probe on the modified electrode ($n = 3$ per electrode).

Modification polymer types	Amount of the immobilized acpcPNA-T9 probe of each polymer on the different concentrations of the acpcPNA-T9 probe		
	3.0 μM ($\times 10^2$ pmol cm^{-2})	5.0 μM ($\times 10^2$ pmol cm^{-2})	7.0 μM ($\times 10^2$ pmol cm^{-2})
PoPD (5 mM, 15 scans)	4.6 ± 0.1	5.7 ± 0.2	5.6 ± 0.1
PpPD (5 mM, 15 scans)	5.6 ± 0.1	7.9 ± 0.2	7.8 ± 0.2
Pty (50 mM, 10 scans)	5.0 ± 0.1	7.8 ± 0.1	7.7 ± 0.1

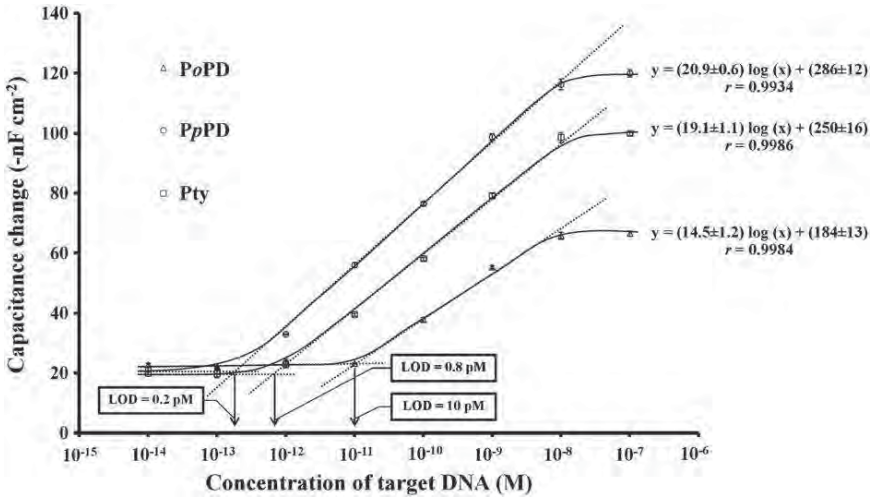

Fig. 10. The relationship between capacitance change and the logarithm of the DNA concentration with the immobilized acpcPNA probe under optimal electropolymerized conditions for each polymer (△) PoPD, (○) PpPD and (□) Pty showing the linear equation and the limit of detection (LOD).

Pty modified electrode performances were slightly inferior to the PpPD that provided the same linear range but with a lower sensitivity (19.1 ± 1.1-nF cm^{-2} (log M)$^{-1}$) and LOD (0.8 pM). The one with the PoPD coated polymer had the worst performance with the lowest sensitivity (14.5 ± 1.2-nF cm^{-2} (log M)$^{-1}$), the most narrow linear range (1.0×10^{-11} to 1.0×10^{-8} M) and the largest value of LOD (10 pM).

The maximum concentration of the linear range of all polymers was 1.0×10^{-8} M, the question is whether the amount of the probe is the limiting factor. The amount of the DNA target was then calculated for this concentration, to be 3.0 pmol using the sample volume of 300 μL. Considering the results from Table 2 where the amount of the immobilized acpcPNA-T9 probe was $(7.9 \pm 0.2) \times 10^2$ and $(7.8 \pm 0.1) \times 10^2$ pmol cm^{-2} for the PpPD and Pty modified electrode, respectively thus the acpcPNA probe was more than enough to bind with the analyte. However, the highest amount of the target DNA, at the highest concentration, was only 3.0 pmol which is 20 times lower than the amount of the immobilized probe. This is because the detection was operated in a flow system where the binding of the target DNA and the immobilized acpcPNA probe also depended on the flow rate and sample volume. A longer residence time for the sample in the flow cell would allow more target DNA to be transported to the sensor surface. Therefore, decreasing the flow rate or increasing the sample volume could help improve the analytical performances.

Under the operating conditions used in this work the system is sufficient for the analysis of ultra-trace levels of DNA in samples. The proposed capacitive DNA sensor based on an electrode covered with a non-conducting polymer film provided a much better detection limit than other methods such as QCM (detection limit of 5 μM) and SPR (detection limit of 0.2 μM) studied by Ananthanawat et al. [4,6], using similar acpcPNA-T9 probes. Comparing the performance of the best polymer modified surface, PpPD to the best of a SAM modified electrode – 3-mercaptopropionic acid (MPA) – in our previous work using the same acpcPNA-T9 probe [9], the PpPD modified electrode provided a wider linear range – 1.0×10^{-12} to 1.0×10^{-8} M compared to 1.0×10^{-11} to 1.0×10^{-8} M of the MPA modified electrode. The PpPD also gave a lower detection limit, 0.2 pM compared to 6 pM for the MPA. This is possibly because the polymer has a three-dimensional structure, enabling more active groups to interact with the acpcPNA probes and resulting in more acpcPNA probes being immobilized, $(7.9 \pm 0.2) \times 10^2$ pmol cm^{-2} compared to $(5.0 \pm 0.2) \times 10^2$ pmol cm^{-2} on the MPA modified electrode (unpublished data). Hence, this allows for more target DNA to be hybridized.

3.6. Reusability

The reusability of the immobilized acpcPNA electrode was investigated by repeating the injections of the complementary DNA at the same concentration 1.0×10^{-10} M following a regeneration step after each measurement. The reusability was evaluated in terms of the percentage of residual activity determined from the capacitance change when the immobilized acpcPNA probe hybridized to the target DNA for the first time (ΔC_1) and after each regeneration (ΔC_2) (Fig. 2) using Eq. (7).

$$\text{Residual activity } (\%) = \frac{\Delta C_2}{\Delta C_1} \times 100 \quad (7)$$

The electrodes modified with the three polymers, PoPD, PpPD and Pty could be reused 68, 74 and 77 times, respectively with an average residual activity of ≥98%. After that the residual activity decreased rapidly. The electrode was then tested by cyclic voltammetry. An example of the voltammogram of the PoPD modified electrode surface after repeated use is shown in Fig. 4(e). As can be seen the redox peaks after use are higher than the redox peaks

Author's personal copy

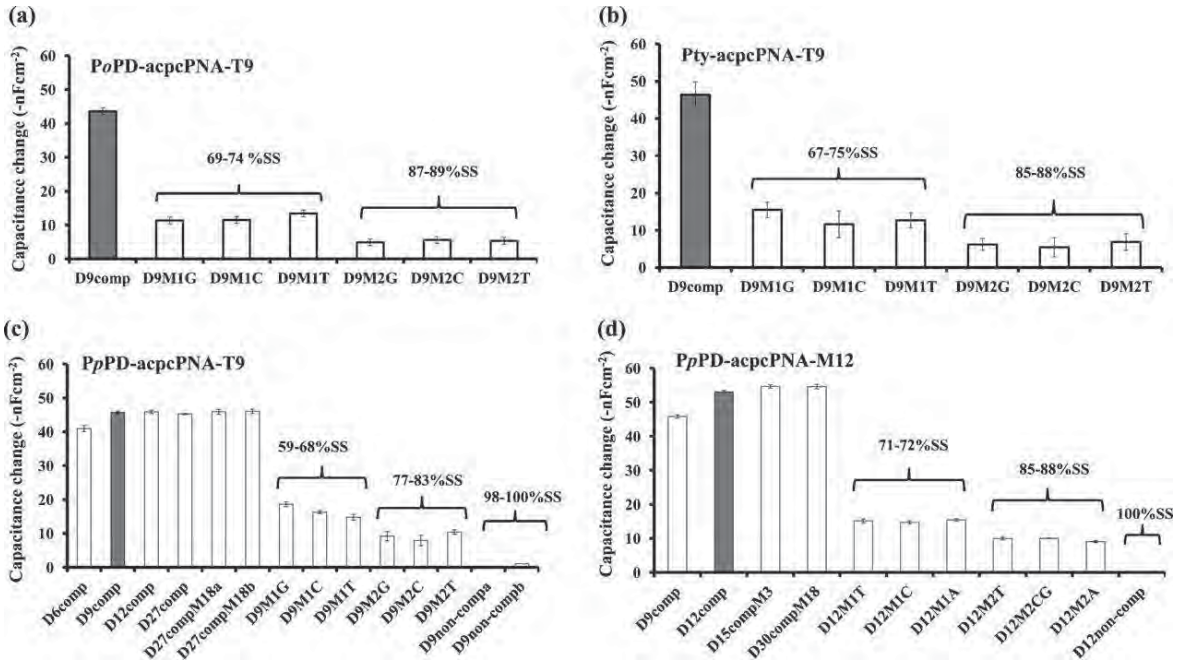

Fig. 11. The measured capacitance change ($n = 3$) of the complementary and mismatched DNAs using immobilized acpcPNA probes on the three types of non-conducting polymer modified electrode (a) PoPD, (b) Pty and (c) P*p*PD with the immobilized acpcPNA-T9 probes, and (d) P*p*PD with the immobilized acpcPNA-M12 probes, tested at 1.0×10^{-10} M DNAs showing the % signal suppression (%SS).

when the surface was modified with the acpcPNA (Fig. 4(c)). That is, the decrease of responses is most likely caused by the loss of the attached acpcPNA-T9 from the polymer layer on the gold electrode.

3.7. Reproducibility

The reproducibility of the responses of the acpcPNA-T9 electrodes from two different preparations of the three polymers were tested by comparing their sensitivities. The sensitivities of the two electrodes were 14.5 ± 1.2 and 14.6 ± 1.3-nF cm^{-2} (log M)$^{-1}$ for PoPD, 20.9 ± 0.6 and 21.1 ± 1.1-nF cm^{-2} (log M)$^{-1}$ for P*p*PD, and 19.1 ± 1.1 and 19.0 ± 1.2-nF cm^{-2} (log M)$^{-1}$ for Pty. The sensitivities did not differ between each preparation. This means that good reproducibility was obtained from the different preparations.

3.8. Specificity

To investigate the specificity, the hybridization of the immobilized acpcPNA-T9 probes with the complementary target DNA, single, double mismatched DNAs and non-complementary target DNAs (see Section 2.1) at 1.0×10^{-10} M were monitored (Fig. 11(a)–(c)). A much higher capacitance change was obtained from the complementary DNA (D9comp) compared to the single and double mismatched DNA target. As expected, the %SS for the double mismatched target was higher than for the single mismatched. Two different non-complementary DNAs were also tested (Fig. 11(c)) and gave the highest %SS.

An acpcPNA-M12 immobilized under optimal conditions for electropolymerization obtained for the acpcPNA-T9 probe on P*p*PD was also investigated (Fig. 11(d)). In agreement with the results obtained with the acpcPNA-T9 probe, it had good specificity, and a very high %SS for the single and double mismatched DNA and a complete signal suppression for the non-complementary DNA.

3.9. Effect of target length

Different target lengths of the complementary DNAs were tested, a shorter target length (D6comp for acpcPNA-T9 and D9comp for acpcPNA-M12) gave a lower capacitance response than the fully complementary DNAs (D9comp for acpcPNA-T9 and D12comp for acpcPNA-M12) (Fig. 11(c) cf. 11(d)). This is most likely because a longer duplex can push water and electrolyte molecules further away from the electrode surface. This behavior gives rise to a greater capacitance change [14]. Comparing the capacitance response between a longer target DNA and the DNA with the same range as the probe a similar capacitance response was obtained. It is possible that the overhanging unhybridized part of the DNA target is more flexible than the duplex, thus, does not directly affect the measured capacitance change as explained above. The results are in line with the study made by Thipmanee et al. on a SAM modified electrode [9]. Further investigations on this aspect would be useful.

4. Conclusions

In this research, a comparative study of three electropolymerized non-conducting polymers was used to immobilize a target acpcPNA probe for detecting DNA. The performance of the label-free DNA sensor was studied using the highly sensitive capacitive system. The modified electrode under optimal concentrations and numbers of electropolymerization scans provided the highest capacitance signal and this was related to the best surface morphology and the highest amount of the immobilized acpcPNA probe. The response was also related to the concentration of the immobilized probe. The electrode modified with P*p*PD provided a slightly higher sensitivity than the Pty modified electrode with the same linear range, and it had a much better sensitivity than obtained with a PoPD modified electrode. The detection limit of the three polymers was in the picomolar range. All modified polymers gave a high %SS

Author's personal copy

for both the single and double mismatched target DNAs, and indicated a high specificity. The electrodes can be reused for at least 68 cycles. The system could easily determine the target DNA analyte at ultra trace levels. The capacitance response also depended on the length of the formed duplex where a longer target length gave a larger signal. It was a surprise to show that the overhanging unhybridized part of the target DNA did not seem to affect the response. This effect should be further studied with a longer target length.

Acknowledgements

The authors are grateful to grants from the Thailand Research Fund (TRF, RTA5280002); the Royal Golden Jubilee Ph.D-program (RGJ) supported by The Thailand Research Fund (3.C.PS/50/B.1 and 3.C.PS/51/B.1); the Office of the Higher Education Commission (CHE-SSR-Ph.D-THA); the Center of Excellence for Innovation in Chemistry (PERCH-CIC), the Office of the Higher Education Commission; the Higher Education Research Promotion and National Research University Project of Thailand, Office of the Higher Education Commission; the Trace Analysis and Biosensor Research Center (TAB-RC), and Graduate School, Prince of Songkla University, Hat Yai, Thailand. The authors also thank Dr. Brian Hodgson, Prince of Songkla University, Hat Yai, Songkhla, Thailand for assistance with the English.

References

[1] J.P. Vernille, L.C. Kovell, J.W. Schneider, Peptide nucleic acid (PNA) amphiphiles: synthesis, self-assembly, and duplex stability, Bioconjugate Chemistry 15 (2004) 1314–1321.
[2] P.E. Nielsen, Peptide nucleic acid: a versatile tool in genetic diagnostics and molecular biology, Current Opinion in Biotechnology 12 (2001) 16–20.
[3] P.E. Nielsen, M. Egholm, An introduction to peptide nucleic acid, Current Issues in Molecular Biology 1 (1999) 89–104.
[4] C. Ananthanawat, T. Vilaivan, V.P. Hoven, Synthesis and immobilization of thiolated pyrrolidinyl peptide nucleic acids on gold-coated piezoelectric quartz crystals for the detection of DNA hybridization, Sensors and Actuators B 137 (2009) 215–221.
[5] M. Duman, R. Saber, E. Pişkin, DNA point mutation detection based on DNA ligase reaction and nano-Au amplification: a piezoelectric approach, Biosensors and Bioelectronics 18 (2003) 1355–1363.
[6] C. Ananthanawat, T. Vilaivan, W. Mekboonsonglarp, V.P. Hoven, Thiolated pyrrolidinyl peptide nucleic acids for the detection of DNA hybridization using surface plasmon resonance, Biosensors and Bioelectronics 24 (2009) 3544–3549.
[7] A.I.K. Lao, X. Su, K.M.M. Aung, SPR study of DNA hybridization with DNA and PNA probes under stringent conditions, Biosensors and Bioelectronics 24 (2009) 1717–1722.
[8] T.H. Degefa, J. Kwak, Electrochemical impedance sensing of DNA at PNA self assembled monolayer, Journal of Electroanalytical Chemistry 612 (2008) 37–41.
[9] O. Thipmanee, S. Samanman, S. Sankoh, A. Numnuam, W. Limbut, P. Kanatharana, T. Vilaivan, P. Thavarungkul, Label-free capacitive DNA sensor using immobilized pyrrolidinyl PNA probe: effect of the length and terminating head group of the blocking thiols, Biosensors and Bioelectronics 38 (2012) 430–435.
[10] W. Limbut, P. Kanatharana, B. Mattiasson, P. Asawatreratanakul, P. Thavarungkul, A comparative study of capacitive immunosensors based on self-assembled monolayers formed from thiourea, thioctic acid, and 3-mercaptopropionic acid, Biosensors and Bioelectronics 22 (2006) 233–240.
[11] S. Loyprasert, P. Thavarungkul, P. Asawatreratanakul, B. Wongkittisuksa, C. Limsakul, P. Kanatharana, Label-free capacitive immunosensor for microcystin-LR using self-assembled thiourea monolayer incorporated with Ag nanoparticles on gold electrode, Biosensors and Bioelectronics 24 (2008) 78–86.
[12] S. Samanman, P. Kanatharana, W. Chotigeat, P. Deachamag, P. Thavarungkul, Highly sensitive capacitive biosensor for detecting white spot syndrome virus in shrimp pond water, Journal of Virological Methods 173 (2011) 75–84.
[13] R. Wannapob, P. Kanatharana, W. Limbut, A. Numnuam, P. Asawatreratanakul, C. Thammakhet, P. Thavarungkul, Affinity sensor using 3-aminophenylboronic acid for bacteria detection, Biosensors and Bioelectronics 26 (2010) 357–364.
[14] C. Berggren, B. Bjarnason, G. Johansson, Capacitive biosensors, Electroanalysis 13 (2001) 173–180.
[15] C. Berggren, G. Johansson, Capacitance measurements of antibody–antigen interactions in a flow system, Analytical Chemistry 69 (1997) 3651–3657.
[16] S. Loyprasert, M. Hedström, P. Thavarungkul, P. Kanatharana, B. Mattiasson, Sub-attomolar detection of cholera toxin using a label-free capacitive immunosensor, Biosensors and Bioelectronics 25 (2010) 1977–1983.
[17] K. Teeparuksapun, P. Kanatharana, W. Limbut, C. Thammakhet, P. Asawatreratanakul, B. Mattiasson, B. Wongkittisuksa, C. Limsakul, P. Thavarungkul, Disposable electrodes for capacitive immunosensor, Electroanalysis 21 (2009) 1066–1074.
[18] M. Ujvári, G. Láng, G. Inzelt, The problem of the low-frequency dispersion in the case of polymer film electrodes – an experimental impedance study on Au|poly(o-phenylenediamine) electrodes, Electrochemistry Communications 2 (2000) 497–502.
[19] L.D. Tran, B. Piro, M.C. Pham, T. Ledoan, C. Angiari, L.H. Dao, F. Teston, A polytyramine film for covalent immobilization of oligonucleotides and hybridization, Synthetic Metals 139 (2003) 251–262.
[20] D. Zane, A. Raffaele, A. Curulli, G.B. Appetecchi, S. Passerini, Electrosynthesis of poly(o-phenylenediamine) in a room temperature ionic liquid, Electrochemistry Communications 9 (2007) 2037–2040.
[21] Y.-Q. Dai, D.-M. Zhou, K.-K. Shiu, Permeability and permselectivity of polyphenylenediamine films synthesized at a palladium disk electrode, Electrochimica Acta 52 (2006) 297–303.
[22] M. Yuqing, C. Jianrong, W. Xiaohua, Using electropolymerized non-conducting polymers to develop enzyme amperometric biosensors, Trends in Biotechnology 22 (2004) 227–231.
[23] Z. Zhang, H. Liu, J. Deng, A glucose biosensor based on immobilization of glucose oxidase in electropolymerized o-aminophenol film on platinized glassy carbon electrode, Analytical Chemistry 68 (1996) 1632–1638.
[24] D.-M. Zhou, Y.-Q. Dai, K.-K. Shiu, Poly(phenylenediamine) film for the construction of glucose biosensors based on platinized glassy carbon electrode, Journal of Applied Electrochemistry 40 (2010) 1997–2003.
[25] Z. Cheng, E. Wang, X. Yang, Capacitive detection of glucose using molecularly imprinted polymers, Biosensors and Bioelectronics 16 (2001) 179–185.
[26] S. Samanman, P. Kanatharana, P. Asawatreratanakul, P. Thavarungkul, Characterization and application of self-assembled layer by layer gold nanoparticles for highly sensitive label-free capacitive immunosensing, Electrochimica Acta 80 (2012) 202–212.
[27] C. Suparpprom, C. Srisuwannaket, P. Sangvanich, T. Vilaivan, Synthesis and oligodeoxynucleotide binding properties of pyrrolidinyl peptide nucleic acids bearing prolyl-2-aminocyclopentanecarboxylic acid (ACPC) backbones, Tetrahedron Letters 46 (2005) 2833–2837.
[28] T. Vilaivan, C. Srisuwannaket, Hybridization of pyrrolidinyl peptide nucleic acids and DNA: selectivity, base-pairing specificity, and direction of binding, Organic Letters 8 (2006) 1897–1900.
[29] H. Arlinghaus, M. Ostrop, O. Friedrichs, J. Feldner, Genome diagnostics with TOF-SIMS, Applied Surface Science 203 (2003) 689–692.
[30] H. Arlinghaus, M. Schröder, J. Feldner, O. Brandt, J. Hoheisel, D. Lipinsky, Development of PNA microarrays for gene diagnostics with TOF-SIMS, Applied Surface Science 231 (2004) 392–396.
[31] C. Ananthanawat, T. Vilaivan, V.P. Hoven, X. Su, Comparison of DNA, aminoethylglycyl PNA and pyrrolidinyl PNA as probes for detection of DNA hybridization using surface plasmon resonance technique, Biosensors and Bioelectronics 25 (2010) 1064–1069.
[32] S.J. Killoran, R.D. O'Neill, Characterization of permselective coatings electrosynthesized on Pt–Ir from the three phenylenediamine isomers for biosensor applications, Electrochimica Acta 53 (2008) 7303–7312.
[33] S. Myler, S. Eaton, S.P.J. Higson, Poly(o-phenylenediamine) ultra-thin polymer-film composite membranes for enzyme electrodes, Analytica Chimica Acta 357 (1997) 55–61.
[34] E. van Pelt-Verkuil, A. Van Belkum, J.P. Hays, Principles and Technical Aspects of PCR Amplification, Springer Verlag, New York, 2008.
[35] B. Wongkittisuksa, C. Limsakul, P. Kanatharana, W. Limbut, P. Asawatreratanakul, S. Dawan, S. Loyprasert, P. Thavarungkul, Development and application of a real-time capacitive sensor, Biosensors and Bioelectronics 26 (2011) 2466–2472.
[36] R.P. Buck, E. Lindner, Recommendations for nomenclature of ion-selective electrodes, Pure and Applied Chemistry 66 (1994) 2527–2536.

Biographies

Supannee Sankoh is a Ph.D. candidate in Chemistry at Prince of Songkla University, Thailand. Her research covers chemical sensors and biosensors.

Saluma Samanman is a Ph.D. candidate in Chemistry at Prince of Songkla University, Thailand. Her research covers chemical sensors and biosensors.

Orawan Thipmanee is a Ph.D. candidate in Chemistry at Prince of Songkla University, Thailand. Her research covers affinity biosensors.

Apon Numnuam has a Ph.D. in Chemistry obtained in 2008 at Prince of Songkla University, Thailand. He is a faculty member of the Department of Chemistry, Prince of Songkla University, Thailand. He is also a member of the Trace Analysis and Biosensor Research Center, Prince of Songkla University. His research interests include electrochemistry, biosensors and chemical sensors.

Warakorn Limbut has a Ph.D. in Chemistry obtained in 2007 at Prince of Songkla University. He is a faculty member of the Department of Applied Science, Prince of Songkla University, Thailand. He is also a member of the Trace Analysis and Biosensor Research Center, Prince of Songkla University. His research interests include biosensors, chemical sensors and electroanalytical chemistry.

Author's personal copy

Proespichaya Kanatharana has a Ph.D. in Analytical Chemistry obtained in 1982 at Villanova University, USA. She is an Associate Professor at the Department of Chemistry, Prince of Songkla University, Thailand. She is also the Director of the Trace Analysis and Biosensor Research Center, Prince of Songkla University. Her research interests include trace analysis, chemical sensors, biosensors, synthesis and development of nanomaterials and techniques, analytical methods development, application and techniques for flux measurement (greenhouse gases) from ecosystem.

Tirayut Vilaivan has a D. Phil. in Organic Chemistry obtained in 1996 at Oxford University, England. He is an Associate Professor at the Department of Chemistry, Chulalongkorn University, Thailand. His research interests include the synthesis of new peptide nucleic acid systems and their applications in diagnostics and synthetic methodology developments.

Panote Thavarungkul has a D. Phil. in Biophysics obtained in 1985 at University of Waikato, New Zealand. She is an Associate Professor at the Department of Physics, Prince of Songkla University, Thailand. She is also a member of the Trace Analysis and Biosensor Research Center, Prince of Songkla University. Her research interests include biosensors and chemical sensors for medical, environmental and industrial applications.

คำขอรับสิทธิบัตร/อนุสิทธิบัตร

☑ การประดิษฐ์
☐ การออกแบบผลิตภัณฑ์
☐ อนุสิทธิบัตร

ข้าพเจ้าผู้ลงลายมือชื่อในคำขอรับสิทธิบัตร/อนุสิทธิบัตรนี้ขอรับสิทธิบัตร/อนุสิทธิบัตร ตามพระราชบัญญัติสิทธิบัตร พ.ศ.2522 แก้ไขเพิ่มเติมโดยพระราชบัญญัติสิทธิบัตร (ฉบับที่2) พ.ศ.2535 และพระราชบัญญัติสิทธิบัตร (ฉบับที่3) พ.ศ.2542

สำหรับเจ้าหน้าที่	
วันรับคำขอ 14 ส.ค. 2555	เลขที่คำขอ
วันยื่นคำขอ 14 ส.ค. 2555	1201004109
สัญลักษณ์จำแนกการประดิษฐ์ระหว่างประเทศ	
ใช้กับแบบผลิตภัณฑ์ ประเภทผลิตภัณฑ์	
วันประกาศโฆษณา	เลขที่ประกาศโฆษณา
วันออกสิทธิบัตร/อนุสิทธิบัตร	เลขที่สิทธิบัตร/อนุสิทธิบัตร
ลายมือชื่อเจ้าหน้าที่	

1 ชื่อที่แสดงถึงการประดิษฐ์/การออกแบบผลิตภัณฑ์

อานาล็อกดีเอ็นเอสังเคราะห์และโอลิโกนิวคลีโอไทด์สังเคราะห์เพื่อการตรวจสารพันธุกรรมของไวรัสโรคเหี่ยวสับปะรดซนิดพีเอ็มดับเบิลยูเอวี (PMWaV)1 และ 2 และวิธีตรวจสอบสารพันธุกรรม

2 คำขอรับสิทธิบัตรการออกแบบผลิตภัณฑ์นี้เป็นคำขอสำหรับแบบผลิตภัณฑ์อย่างเดียวกันและเป็นคำขอลำดับที่

ในจำนวน 1 คำขอ ที่ยื่นในคราวเดียวกัน

3 ผู้ขอรับสิทธิบัตร/อนุสิทธิบัตร และที่อยู่ (เลขที่ ถนน ประเทศ)	
นายปิยะศักดิ์ ชอุ่มพฤกษ์ ที่อยู่เลขที่ 511/715 จรัลสนิทวงศ์ 37 แขวงบางขุนศรี เขต บางกอกน้อย กรุงเทพฯ 10700ประเทศไทย และ นายธีรยุทธ วิไลวัลย์ ที่อยู่เลขที่ 186 ตรอก/ซอย นาคนิวาส 21 แขวง ลาดพร้าว เขต ลาดพร้าว จังหวัดกรุงเทพมหานคร ประเทศไทย	3.1 สัญชาติ ไทย 3.2 โทรศัพท์ 02-218-5494 02-412 9571 3.3 โทรสาร 02-218-5494 3.4 อีเมล์ piyasakcha@gmail.com

4 สิทธิในการขอรับสิทธิบัตร/อนุสิทธิบัตร

☑ ผู้ประดิษฐ์/ผู้ออกแบบ ☐ ผู้รับโอน ☐ ผู้ขอรับสิทธิโดยเหตุอื่น

5 ตัวแทน (ถ้ามี)/ที่อยู่ (เลขที่ ถนน จังหวัด รหัสไปรษณีย์)	
	5.1 ตัวแทนเลขที่
	5.2 โทรศัพท์
	5.3 โทรสาร
	5.4 อีเมล์

6 ผู้ประดิษฐ์/ผู้ออกแบบผลิตภัณฑ์ และที่อยู่ (เลขที่ ถนน ประเทศ)

นายปิยะศักดิ์ ชอุ่มพฤกษ์ ที่อยู่เลขที่ 511/715 จรัลสนิทวงศ์ 37 แขวงบางขุนศรี เขต บางกอกน้อย กรุงเทพฯ 10700ประเทศไทย และ
นายธีรยุทธ วิไลวัลย์ ที่อยู่เลขที่ 186 ตรอก/ซอย นาคนิวาส 21 แขวง ลาดพร้าว เขต ลาดพร้าว จังหวัดกรุงเทพมหานคร ประเทศไทย

7 คำขอรับสิทธิบัตร/อนุสิทธิบัตรนี้แยกจากหรือเกี่ยวข้องกับคำขอเดิม

ผู้ขอรับสิทธิบัตร/อนุสิทธิบัตร ขอให้ถือว่าได้ยื่นคำขอรับสิทธิบัตร/อนุสิทธิบัตรนี้ ในวันเดียวกับคำขอรับสิทธิบัตร เลขที่ วันยื่น เพราะคำขอรับสิทธิบัตร/อนุสิทธิบัตรนี้แยกจากหรือเกี่ยวข้องกับคำขอเดิมเพราะ

☐ คำขอเดิมมีการประดิษฐ์หลายอย่าง ☐ ถูกคัดค้านเนื่องจากผู้ขอไม่มีสิทธิ ☐ ขอเปลี่ยนแปลงประเภทของสิทธิ

หมายเหตุ ในกรณีที่ไม่อาจระบุรายละเอียดได้ครบถ้วน ให้จัดทำเป็นเอกสารแนบท้ายแบบพิมพ์นี้โดยระบุหมายเลขกำกับข้อและหัวข้อที่แสดงรายละเอียดเพิ่มเติมดังกล่าวด้วย

(ต้นฉบับสำหรับผู้ขอรับใบอนุญาตฯ ใช้ติดไว้ ณ สถานที่ขายยาในที่เปิดเผยและเห็นได้ง่าย)

กรมสนับสนุนบริการสุขภาพ
สถานที่ขายยาแผนปัจจุบันประเภทที่ ข
ใบอนุญาตขายยาแผนปัจจุบันประเภทที่ ข

เลขที่ 076 หมดอายุ 20 ธันวาคม 2565

ใบแจ้งรายการชำระเงินเลขที่ 2013081400100005 วันที่ชำระเงิน 14 สิงหาคม 2556

ได้รับอนุญาตให้ขายยาแผนปัจจุบันประเภทที่ ข ตามรายการดังต่อไปนี้

รายการ	จำนวนเงิน
ค่าธรรมเนียมใบอนุญาตขายยาแผนปัจจุบันประเภทที่ ข	5000.00
ค่าธรรมเนียมการตรวจสถานที่ขายยา	500.00

ผู้ได้รับใบอนุญาต ( )

ผู้อนุญาต

ตำแหน่ง

คำขอรับสิทธิบัตร/อนุสิทธิบัตร

☑ การประดิษฐ์
☐ การออกแบบผลิตภัณฑ์
☐ อนุสิทธิบัตร

ข้าพเจ้าผู้ลงลายมือชื่อในคำขอรับสิทธิบัตร/อนุสิทธิบัตรนี้ ขอรับสิทธิบัตร/อนุสิทธิบัตร ตามพระราชบัญญัติสิทธิบัตร พ.ศ.2522 แก้ไขเพิ่มเติมโดยพระราชบัญญัติสิทธิบัตร (ฉบับที่2) พ.ศ.2535 และพระราชบัญญัติสิทธิบัตร (ฉบับที่3) พ.ศ.2542

สำหรับเจ้าหน้าที่	
วันรับคำขอ	เลขที่คำขอ
วันยื่นคำขอ	
สัญลักษณ์จำแนกการประดิษฐ์ระหว่างประเทศ	
ใช้กับแบบผลิตภัณฑ์ ประเภทผลิตภัณฑ์	
วันประกาศโฆษณา	เลขที่ประกาศโฆษณา
วันออกสิทธิบัตร/อนุสิทธิบัตร	เลขที่สิทธิบัตร/อนุสิทธิบัตร
ลายมือชื่อเจ้าหน้าที่	

1.ชื่อที่แสดงถึงการประดิษฐ์/การออกแบบผลิตภัณฑ์

อานาล็อกดีเอ็นเอสังเคราะห์และโอลิโกนิวคลีโอไทด์สังเคราะห์เพื่อการตรวจสารพันธุกรรมของไวรัสโรคเหี่ยวสับปะรดชนิดพีเอ็มดับเบิลยูเอวี (PMWaV)1 และ 2 และวิธีตรวจสอบสารพันธุกรรม

2.คำขอรับสิทธิบัตรการประดิษฐ์นี้เป็นคำขอสำหรับแบบประดิษฐ์อย่างเดียวกันและเป็นคำขอลำดับที่

ในจำนวน 1 คำขอ ที่ยื่นในคราวเดียวกัน

3.ผู้ขอรับสิทธิบัตร/อนุสิทธิบัตร และที่อยู่ (เลขที่ ถนน ประเทศ)

นายปิยะศักดิ์ ชอุ่มพฤกษ์ ที่อยู่เลขที่ 511/715 จรัลสนิทวงศ์ 37 แขวงบางขุนศรี เขต บางกอกน้อย กรุงเทพฯ 10700ประเทศไทย และ
นายธีรยุทธ วิไลวัลย์ ที่อยู่เลขที่ 186 ตรอก/ซอย นาคนิวาส 21 แขวง ลาดพร้าว เขต ลาดพร้าว จังหวัดกรุงเทพมหานคร ประเทศไทย

3.1 สัญชาติ ไทย
3.2 โทรศัพท์ 02-218-5494 02-412 9571
3.3 โทรสาร 02-218-5494
3.4 อีเมล์ piyasakcha@gmail.com

4.สิทธิในการขอรับสิทธิบัตร/อนุสิทธิบัตร

☑ ผู้ประดิษฐ์/ผู้ออกแบบ ☐ ผู้รับโอน ☐ ผู้ขอรับสิทธิโดยเหตุอื่น

5.ตัวแทน (ถ้ามี)/ที่อยู่ (เลขที่ ถนน จังหวัด รหัสไปรษณีย์)

5.1 ตัวแทนเลขที่
5.2 โทรศัพท์
5.3 โทรสาร
5.4 อีเมล์

6.ผู้ประดิษฐ์/ผู้ออกแบบผลิตภัณฑ์ และที่อยู่ (เลขที่ ถนน ประเทศ)

นายปิยะศักดิ์ ชอุ่มพฤกษ์ ที่อยู่เลขที่ 511/715 จรัลสนิทวงศ์ 37 แขวงบางขุนศรี เขต บางกอกน้อย กรุงเทพฯ 10700ประเทศไทย และ
นายธีรยุทธ วิไลวัลย์ ที่อยู่เลขที่ 186 ตรอก/ซอย นาคนิวาส 21 แขวง ลาดพร้าว เขต ลาดพร้าว จังหวัดกรุงเทพมหานคร ประเทศไทย

7.คำขอรับสิทธิบัตร/อนุสิทธิบัตรนี้แยกจากหรือเกี่ยวข้องกับคำขอเดิม

ผู้ขอรับสิทธิบัตร/อนุสิทธิบัตร ขอให้ถือว่าได้ยื่นคำขอรับสิทธิบัตร/อนุสิทธิบัตรนี้ ในวันเดียวกับคำขอรับสิทธิบัตร เลขที่ วันยื่น เพราะคำขอรับสิทธิบัตร/อนุสิทธิบัตรนี้แยกจากหรือเกี่ยวข้องกับคำขอเดิมเพราะ

☐ คำขอเดิมมีการประดิษฐ์หลายอย่าง ☐ ถูกคัดค้านเนื่องจากผู้ขอไม่มีสิทธิ ☐ ขอเปลี่ยนแปลงประเภทของสิทธิ

หมายเหตุ ในกรณีที่ไม่อาจระบุรายละเอียดได้ครบถ้วน ให้จัดทำเป็นเอกสารแนบท้ายแบบพิมพ์นี้โดยระบุหมายเลขกำกับข้อและหัวข้อที่แสดงรายละเอียดเพิ่มเติมดังกล่าวด้วย

8.การยื่นคำขอนอกราชอาณาจักร

วันยื่นคำขอ	เลขที่คำขอ	ประเทศ	สัญลักษณ์จำแนกการประดิษฐ์ระหว่างประเทศ	สถานะคำขอ
8.1				
8.2				
8.3				

8.4 ☐ ผู้ขอรับสิทธิบัตร/อนุสิทธิบัตรให้ถือว่าได้ยื่นคำขอนี้ในวันที่ได้ยื่นคำขอรับสิทธิบัตร/อนุสิทธิบัตรในต่างประเทศเป็นครั้งแรก โดย

☐ ได้ยื่นเอกสารหลักฐานพร้อมคำขอนี้ ☐ ขอยื่นเอกสารหลักฐานหลังจากวันยื่นคำขอนี้

9.การแสดงการประดิษฐ์หรือการออกแบบผลิตภัณฑ์ ผู้ขอรับสิทธิบัตร/อนุสิทธิบัตรได้แสดงการประดิษฐ์ที่หน่วยงานของรัฐเป็นผู้จัด

วันแสดง วันเปิดงานแสดง ผู้จัด

10.การประดิษฐ์เกี่ยวกับจุลชีพ

10.1 เลขทะเบียนฝากเก็บ	10.2 วันที่ฝากเก็บ	10.3 สถาบันฝากเก็บ/ประเทศ

11.ผู้ขอรับสิทธิบัตร/อนุสิทธิบัตร ขอยื่นเอกสารภาษาต่างประเทศก่อนในวันที่ยื่นคำขอนี้ และจะจัดยื่นคำขอรับสิทธิบัตร/อนุสิทธิบัตรนี้ที่จัดทำเป็นภาษาไทยภายใน 90 วัน นับจากวันยื่นคำขอนี้ โดยขอยื่นเป็นภาษา

☐ อังกฤษ ☐ ฝรั่งเศส ☐ เยอรมัน ☐ ญี่ปุ่น ☐ อื่น ๆ

12.ผู้ขอรับสิทธิบัตร/อนุสิทธิบัตร ขอให้อธิบดีประกาศโฆษณาคำขอรับสิทธิบัตร หรือรับจดทะเบียน และประกาศโฆษณาอนุสิทธิบัตรนี้หลังจากวันที่ เดือน พ.ศ.

☑ ผู้ขอรับสิทธิบัตร/อนุสิทธิบัตรขอให้ใช้รูปเขียนหมายเลข 1 ในการประกาศโฆษณา

13.คำขอรับสิทธิบัตร/อนุสิทธิบัตรนี้ประกอบด้วย

ก.แบบพิมพ์คำขอ 2 หน้า

ข.รายละเอียดการประดิษฐ์ หรือคำพรรณนาแบบผลิตภัณฑ์ 8 หน้า

ค.ข้อถือสิทธิ 1 หน้า

ง.รูปเขียน 1 รูป 1 หน้า

จ.ภาพแสดงแบบผลิตภัณฑ์

☐ รูปเขียน รูป - หน้า

☐ ภาพถ่าย รูป - หน้า

ฉ.บทสรุปการประดิษฐ์ 1 หน้า

14.เอกสารประกอบด้วย

☑ เอกสารแสดงสิทธิในการขอรับสิทธิบัตร/อนุสิทธิบัตร

☑ หนังสือรับรองการแสดงการประดิษฐ์/การออกแบบผลิตภัณฑ์

☐ หนังสือมอบอำนาจ

☐ เอกสารรายละเอียดเกี่ยวกับจุลชีพ

☐ เอกสารการขอนับวันยื่นคำขอในต่างประเทศเป็นวันยื่นคำขอในประเทศไทย

☐ เอกสารขอเปลี่ยนแปลงประเภทของสิทธิ

☐ เอกสารอื่น ๆ

15.ข้าพเจ้าขอรับรองว่า

☑ การประดิษฐ์นี้ไม่เคยยื่นขอรับสิทธิบัตร/อนุสิทธิบัตรมาก่อน

☐ การประดิษฐ์นี้ได้พัฒนาปรับปรุงมาจาก.....

16.ลายมือชื่อ (☑ ผู้ขอรับสิทธิบัตร/อนุสิทธิบัตร; ☐ ตัวแทน)

หมายเหตุ บุคคลใดยื่นขอรับสิทธิบัตรการประดิษฐ์หรือการออกแบบผลิตภัณฑ์ หรืออนุสิทธิบัตร โดยการแสดงข้อความอันเป็นเท็จแก่พนักงานเจ้าหน้าที่เพื่อให้ได้ไปซึ่งสิทธิบัตรหรืออนุสิทธิบัตร ต้องระวางโทษจำคุกไม่เกินหกเดือน หรือปรับไม่เกินห้าพันบาท หรือทั้งจำทั้งปรับ

รายละเอียดของการประดิษฐ์

ชื่อที่แสดงถึงการประดิษฐ์

อานาล็อกดีเอ็นเอสังเคราะห์และโอลิโกนิวคลีโอไทด์สังเคราะห์เพื่อการตรวจสารพันธุกรรมของไวรัสโรคเหี่ยวสับปะรดชนิด พีเอ็มดับเบิลยูเอวี (PMWaV)1 และ 2 และวิธีตรวจสอบสารพันธุกรรม

ลักษณะและความมุ่งหมายของการประดิษฐ์

การประดิษฐ์นี้เกี่ยวข้องกับ อานาล็อกดีเอ็นเอและชุดของโอลิโกนิวคลีโอไทด์ที่ออกแบบและสังเคราะห์ขึ้นด้วยกระบวนการทางเคมีให้มีความจำเพาะเจาะจงต่อบริเวณของยีนโปรตีนเปลือกหุ้มของไวรัสโรคเหี่ยวสับปะรดชนิดพีเอ็มดับเบิลยูเอวี 1 และ 2 และวิธีการนำเอาชุดของโอลิโกนิวคลีโอไทด์และอานาล็อกดีเอ็นเอ ที่ออกแบบ และสังเคราะห์ขึ้นนี้ไปใช้งานร่วมกับ

1. เทคนิคการเพิ่มปริมาณสารพันธุกรรม ด้วยเอนไซม์ดีเอ็นเอพอลิเมอร์เลส ได้แก่ แทคดีเอ็นเอพอลิเมอร์เลส พีเอฟยูดีเอ็นเอพอลิเมอร์เลส ทีทีเอชดีเอ็นเอพอลิเมอร์เลส เคโอดีพอลิเมอร์เลส ดีปเวนท์ดีเอ็นเอพอลิเมอร์เลส พีดับบลิวยูพอลิเมอร์เลส บีเอสทีพอลิเมอร์เลส ทีแอลไอพอลิเมอร์เลส ลำพังหรือร่วมกับเอนไซม์รีเวอร์สทรานสคริปเทส
2. การใช้งานบนพื้นฐานการไฮบริไดเซชันของกรดนิวคลีอิก ด้วยโพรบที่เป็นอานาล็อกดีเอ็นเอหรือเป็ปไทด์นิวคลีอิก ในรูปสารละลายหรือบนสื่อจำพวกเมมเบรนหรือกระดาษ
3. การใช้งานโดยการติดฉลากที่บริเวณ 5' และ 3' ของอานาล็อกดีเอ็นเอและโอลิโกนิวคลีโอไทด์สังเคราะห์ ที่ออกแบบและสังเคราะห์ขึ้นร่วมโมเลกุลที่เป็นฟูออโรฟอร์ ได้แก่ อะเล็กซ่า 488 (ALEXA-488) แฟม (FAM) โจ (JOE) แทมรา (TAMRA) ไซทรี (CY3) ไซไฟว์ (CY5) บีเฮชคิว (BHQ) เฮก (HEX) หรือร็อก (ROX)
4. การใช้งานร่วมกับดีเอ็นเอไบนด์เดอร์ และแคลซีน (calcine) เพื่อก่อให้เกิดการเปลี่ยนแปลงทางไฟฟ้า หรือทาง แสง
5. การใช้งานร่วมกับคอลลอยด์ของอนุภาคนาโนของโลหะ เพื่อตรวจการเปลี่ยนแปลงทางกายภาพ (physic)

ทั้งนี้เพื่อบ่งบอกภาวะการตรวจสอบสารพันธุกรรมบริเวณยีนโปรตีนเปลือกหุ้มของไวรัสโรคเหี่ยวสับปะรด พีเอ็มดับเบิลยูเอวี 1 และ 2

ในอีกลักษณะหนึ่งการประดิษฐ์นี้เกี่ยวข้องกับการตรวจสารพันธุกรรมของเชื้อไวรัสโรคเหี่ยวสับปะรด พีเอ็มดับเบิลยูเอวี ทั้งชนิดที่ 1 และ 2 ในทางวิทยาศาสตร์อย่างเฉพาะเจาะจง

สาขาวิทยาการที่เกี่ยวข้องกับการประดิษฐ์

ตัวองค์ความรู้นี้ จัดอยู่ในสาขาที่เกี่ยวข้องกับการออกแบบ สังเคราะห์และใช้โอลิโกนิวคลีโอไทด์หรืออานาล็อกติเอ็นเอที่มีลำดับนิวคลิโอไทด์เฉพาะและสังเคราะห์ขึ้นด้วยกระบวนการทางเคมี เพื่อการใช้งานในการตรวจสอบสารพันธุกรรมด้วยกระบวนการทางเคมีโดยเอนไซม์ สำหรับการประยุกต์ทางเคมี ชีวโมเลกุล แพทยศาสตร์และพันธุศาสตร์

ภูมิหลังของศิลปะหรือวิทยาการที่เกี่ยวข้อง

ปัจจุบันความต้องการในการตรวจวิเคราะห์สารพันธุกรรมของไวรัสที่ก่อโรคในพืชมีความสำคัญต่อระบบการผลิตทางการเกษตรทั้งนี้เนื่องจากเพื่อให้ได้ข้อมูลในการวางแผนป้องกันควบคุม และจัดการโรคอย่างมีประสิทธิภาพ สำหรับประเทศไทย การผลิตสับปะรดเป็นอุตสาหกรรมที่สำคัญ คิดเป็นรายได้หมุนเวียนประเทศในปี พ.ศ. 2547 สูงถึง 17951.08 ล้านบาท และมีมูลค่าส่งออกสูงถึง 51 ล้านบาท อย่างไรก็ดีด้วยการผลิตที่ประสบปัญหาด้านคุณภาพและการให้ผลผลิตที่ไม่สม่ำเสมอ เนื่องจากปัญหาการระบาดของโรคเหี่ยวที่เกิดจากไวรัส ส่งผลกระทบต่อเสถียรภาพในการส่งวัตถุดิบเข้าสู่ภาคอุตสาหกรรมอย่างรุนแรง

โรคเหี่ยวสับปะรดเกิดจากไวรัสพีเอ็มดับเบิลยูเอวี (Pineapple mealybug with associated virus; PMWaV) ทั้งชนิด 1 และ 2 เมื่อติดเชื้อต้นสับปะรดจะแสดงอาการ เริ่มจากการหยุดการเจริญเติบโตของราก รากเน่า จากนั้นจึงสังเกตพบอาการที่ใบ โดยใบล่างจะเปลี่ยนสีจากเขียวเป็นเหลืองอมชมพู ในกรณีรุนแรงใบจะแห้งและม้วนตัวเข้าและแสดงอาการเหี่ยวชัดเจน อย่างไรก็ดีหากสับปะรดมีการเจริญเติบโตที่ดีในช่วงหน้าฝนจะพบว่าบางครั้งอาการของโรคจะไม่ชัดเจน การติดเชื้อดังกล่าวส่งผลต่อการหยุดการเจริญเติบโต และทำให้เก็บเกี่ยวผลผลิตไม่ได้

ประเทศไทย นิยมปลูกสับปะรดพันธุ์ปัตตาเวีย ซึ่งอ่อนแอต่อไวรัสทั้ง 2 ชนิด และเนื่องจากการขยายพันธุ์สับปะรดเพื่อปลูกในพื้นที่ใหม่ๆ นิยมใช้หน่อ ตะเกียง และจุกเป็นท่อนพันธุ์ หากท่อนพันธุ์เหล่านั้นติดเชื้อ จะส่งผลต่อการแพร่ระบาดของโรคอย่างรวดเร็ว ดังนั้นการตรวจวิเคราะห์รหัสพันธุกรรมและวินิจฉัยไวรัสสาเหตุของโรคอย่างมีประสิทธิภาพ ด้วยวิธีการที่รวดเร็วและแม่นยำ จึงส่งผลต่อการควบคุม และลดความเสี่ยงจากโรคได้

การตรวจสารพันธุกรรมของไวรัสจากตัวอย่างสับปะรด จะพบสารพันธุกรรมเริ่มต้นในปริมาณที่น้อยมาก การใช้ชุดของโอลิโกนิวคลีโอไทด์ที่สังเคราะห์ขึ้น จะมีความจำเพาะต่อปริมาณของยีนโปรตีนเปลือกหุ้มของไวรัส การศึกษาสายพันธุ์ไวรัสพบว่าไวรัสโรคเหี่ยวในสับปะรดมีพันธุ์ต่างกัน 3 พันธุ์ ได้แก่ ชนิดที่ 1 2 และ 3 (PMWaV-1, PMWaV-2, PMWaV-3) การศึกษาเบื้องต้น พบว่าในประเทศพบการระบาดเฉพาะชนิดที่ 1 และ 2 เท่านั้น โดยทั้ง 2 ชนิด มีสารพันธุกรรมเป็นอาร์เอ็นเอสาย ขนาด 13071 และ 13250-13400 นิวคลีโอไทด์ โดยยีนโปรตีนเปลือกหุ้มของไวรัสชนิดที่ 1 และ 2 โดยเฉพาะบริเวณยีนโปรตีนเปลือกหุ้มมีความคล้ายคลึงกันต่ำกว่า 42% การตรวจสอบสารพันธุกรรมของไวรัสทั้ง 2 จึงต้องแยกดำเนินการอย่างอิสระ แม้ที่ผ่านมาจะมีผู้พัฒนา

เทคนิคการตรวจสารพันธุกรรมแต่การตรวจไม่ได้อยู่บนพื้นฐานของยีนโปรตีนเปลือกหุ้ม (Sethan and Hen, 2002) นอกจากนี้การตรวจยังอยู่บนพื้นฐานของไวรัสสายพันธุ์ที่พบในฮาวาย ซึ่งแตกต่างไปจากสายพันธุ์ไทย

สำหรับการตรวจทางพันธุกรรม ความแม่นยำ ความจำเพาะ และความไวของปฏิกิริยาในการตรวจวิเคราะห์ ขึ้นอยู่กับความเหมาะสมกับโอลิโกนิวคลีโอไทด์ที่ใช้เป็นไพร์เมอร์และอานาล็อกดีเอ็นเอที่ใช้เป็นโพรบที่สังเคราะห์ขึ้น เนื่องจากจะเกี่ยวข้องกับการจับตัวที่สมบูรณ์ ตามหลักคู่สม (complementary) ช่วยให้ระยะระหว่างโมเลกุล ใกล้กัน และอยู่ในระดับที่มีความเหมาะสมจนเกิดปฏิกิริยาทางเคมีในภาวะจำลอง (In vitro) ดังนั้นหัวใจสำคัญในการตรวจวิเคราะห์จึงขึ้นอยู่กับการคัดเลือกและออกแบบโอลิโกนิวคลีโอไทด์สังเคราะห์และอานาล็อกดีเอ็นเอโพรบที่เหมาะสมนี้

การประดิษฐ์ในครั้งนี้ ได้จากการโคลนยีนและศึกษาเปรียบเทียบลำดับนิวคลีโอไทด์ในบริเวณยีนโปรตีนเปลือกหุ้มของสายพันธุ์ไวรัสที่ติดเชื้อในสับปะรดในประเทศ ในระหว่างปี พ.ศ. 2552-2554 และเปรียบเทียบกับไวรัสในกลุ่มเดียวกันหรือกลุ่มใกล้เคียงกัน เพื่อหาบริเวณเฉพาะพิเศษที่เป็นบริเวณอ้างอิง และนำองค์ความรู้มาออกแบบเป็นชุดโอลิโกนิวคลีโอไทด์ที่มีลำดับเฉพาะ และอานาล็อกดีเอ็นเอคู่สมกับยีนเป้าหมาย และสังเคราะห์ชุดนิวคลีโอไทด์และอานาล็อกดีเอ็นเอเหล่านั้นด้วยกระบวนการทางเคมี โดยเมื่อนำชุดนิวคลีโอไทด์และอานาล็อกดีเอ็นเอที่มีลำดับนิวคลิโอไทด์จำเพาะมาใช้งานร่วมกับเทคนิคทางชีววิทยาโมเลกุลจะช่วยให้สามารถตรวจสอบและแยกวิเคราะห์ความแตกต่างของสารพันธุกรรมของไวรัสโรคเหี่ยวสับปะรดทั้งชนิดที่ 1 และ 2 ออกจากกัน หรือออกจากไวรัสชนิดอื่นในกลุ่มเดียวกันได้อย่างมีประสิทธิภาพ

ลักษณะและความมุ่งหมายของการประดิษฐ์

การประดิษฐ์นี้มุ่งถึงชุดของโอลิโกนิวคลีโอไทด์และอานาล็อกดีเอ็นเอที่มีลำดับนิวคลิโอไทด์จำเพาะต่อยีนโปรตีนเปลือกหุ้มของไวรัสโรคเหี่ยวสับปะรดทั้งชนิดที่ 1 และ 2 ที่ได้ออกแบบและสังเคราะห์ขึ้นด้วยกระบวนการทางเคมี เพื่อการนำไปใช้ร่วมกับเทคนิคชีววิทยาโมเลกุล ทำให้การตรวจสอบสารพันธุกรรมของไวรัสโรคเหี่ยวสับปะรดทั้งชนิดที่ 1 และ 2 ออกจากกัน และแยกออกจากสารพันธุกรรมของไวรัสชนิดอื่นในกลุ่มเดียวกันหรือต่างกลุ่ม ให้ทำได้อย่างเฉพาะเจาะจงและมีประสิทธิภาพ

การเปิดเผยการประดิษฐ์โดยสมบูรณ์

การประดิษฐ์นี้เกี่ยวข้องกับ การออกแบบชุดของโอลิโกนิวคลีโอไทด์และอานาล็อกดีเอ็นเอสังเคราะห์ที่ดำเนินการออกแบบตามหลักคู่สม และสังเคราะห์ขึ้นด้วยกระบวนการทางเคมี ให้มีความจำเพาะกับบริเวณของยีนโปรตีนเปลือกหุ้มของไวรัสโรคเหี่ยวสับปะรดทั้งชนิดที่ 1 และ 2 และการนำชุดโอลิโกนิวคลีโอไทด์และอานาล็อกดีเอ็นเอไปใช้งานร่วมกับ

1. เทคนิคการเพิ่มปริมาณสารพันธุกรรม ด้วยเอนไซม์ดีเอ็นเอพอลิเมอร์เลส ได้แก่ แทคดีเอ็นเอพอลิเมอร์เลส พีเอฟยูดีเอ็นเอพอลิเมอร์เลส ทีทีเฮชดีเอ็นเอพอลิเมอร์เลส เคโอดีพอลิเมอร์เลส ดีป เวนท์ดีเอ็นเอพอลิเมอร์เลส พีดับบลิวยูพอลิเมอร์เลส

บีเอสทีพอลิเมอร์เลส ทีแอลไอพอลิเมอร์เลส สำพังหรือร่วมกับเอนไซมรีเวอร์สทรานสคริปเทส

2. การใช้งานบนพื้นฐานขการไฮบริไดเซชันของกรดนิวคลิอิก ด้วยโพรบที่เป็นอานาล็อกดีเอ็นเอหรือเป็ปไทด์นิวคลีอิก ในรูปสารละลายหรือบนสื่อจำพวกเมมเบรนหรือกระดาษ

3. การใช้งานโดยการติดฉลากที่บริเวณ 5' และ 3' ของอานาล็อกดีเอ็นเอและโอลิโกนิวคลีโอไทด์สังเคราะห์ ที่ออกแบบและสังเคราะห์ขึ้นร่วมโมเลกุลที่เป็นฟูออโรฟอร์ ได้แก่ อะเล็กซ่า 488 (ALEXA-488) แฟม (FAM) โจ (JOE) แทมรา (TAMRA) ไซทรี (CY3) ไซไฟว์ (CY5) บีเฮชคิว (BHQ) เฮก (HEX) หรือร็อก (ROX)

4. การใช้งานร่วมกับดีเอ็นเอไบนด์เดอร์ และแคลซีน (calcine) เพื่อก่อให้เกิดการเปลี่ยนแปลงทางไฟฟ้า หรือทาง แสง

5. การใช้งานร่วมกับคอลลอยด์ของอนุภาคนาโนของโลหะ เพื่อตรวจการเปลี่ยนแปลงทางกายภาพ (physic)

เพื่อการตรวจสอบสารพันธุกรรมบริเวณยีนโปรตีนเปลือกหุ้มของไวรัสโรคเหี่ยวสับปะรดทั้งชนิดที่ 1 และ 2 ออกจากกัน และออกจากสารพันธุกรรมของไวรัสชนิดอื่นอย่างเฉพาะเจาะจง

ชุดโอลิโกนิวคลีโอไทด์ที่ออกแบบและสังเคราะห์ขึ้นด้วยวิธีทางเคมี มีการเรียงตัวของลำดับนิวคลิโอไทด์เป็นดังแสดงตามรูปที่ 1

ไวรัสโรคเหี่ยวสับปะรด เป็นไวรัสที่มีความสำคัญต่อการเกิดโรคเหี่ยวในสับปะรดอย่างรุนแรง การติดเชื้อมีผลต่อการเจริญเติบโตและการให้ผลผลิตของสับปะรด โดยเฉพาะกับสายพันธุ์ปัตตาเวียที่อ่อนแอต่อเชื้อทั้ง 2 ชนิด

การศึกษาโครงสร้างทางพันธุกรรม โดยการเก็บตัวอย่างไวรัสจากต้นสับปะรดที่เป็นโรค มาสกัดสารพันธุกรรมด้วยวิธีสกัดด้วยสารละลายฟีนอล จากนั้นนำสารพันธุกรรมที่ได้มาเพิ่มปริมาณดีเอ็นเอบริเวณยีนโปรตีนเปลือกหุ้มโดยชุดไพรเมอร์หมายเลข 1 และ 2 ที่จำเพาะต่อบริเวณ โอเพ่นรีดดิง (open reading) และบริเวณรหัสหยุด (stop codon) ของยีนโปรตีนเปลือกหุ้มของไวรัสทั้ง 2 ชนิด และตรวจสอบลำดับนิวคลิโอไทด์เปรียบเทียบระหว่างไวรัสหวัดที่พบระบาดอยู่ กับลำดับนิวคลิโอไทด์ของไวรัสที่พบระบาดอยู่ในต่างประเทศ พบว่าสารพันธุกรรมของไวรัสนี้มีความแตกต่างระหว่างกัน 75-80% และต่างจากไวรัสชนิดอื่น เช่น จีแอลอาร์เอวี สี่และห้า GLRaV-4, GLRaV-5, (grapevine leafroll associated virus) แอลซีเอชวี สอง LChV-2(Little Cherry Virus-2) มากกว่า 80 % ความแตกต่างของลำดับพันธุกรรมเหล่านี้ ช่วยให้การจำแนกสายพันธุ์บนพื้นฐานของลำดับนิวคลีโอไทด์สามารถทำได้

จากการวิเคราะห์ลำดับนิวคลีโอไทดีปรากฏในธนาคารข้อมูลยีน (GenBank) หมายเลข AF414119, NC_010178, EU769114, JN995531, JN995532, EU 769144, FJ 209048 EU769116 DQ225114 และกับลำดับนิวคลิโอไทด์ที่ได้จากสายพันธุ์ในประเทศ

ผลวิเคราะห์โดยการเปรียบเทียบลำดับนิวคลิโอไทด์รวมหรืออไลน์เมนท์ (alignment) ด้วยโปรแกรมคลัสตัล ดับเบิ้ลยู (Clustal W) เพื่อหาบริเวณที่เหมือนและต่างกันของไวรัสเน้นการวิเคราะห์บนชิ้นส่วนของยีน โปรตีนเปลือกหุ้ม

ซึ่งเป็นยีนสร้างโปรตีนที่ผิวอนุภาคซึ่งส่งผลต่อคุณสมบัติทั้งในแง่การก่อโรค ความรุนแรง ความสามารถในการแพร่กระจายด้วยพาหะ และสมบัติในการจำแนกชนิด และชับไทป์ของไวรัสด้วยวิธีการทางอณูชีววิทยา

ผลการค้นหา คัดเลือกบริเวณนิวคลิโอไทด์ที่ให้ความจำเพาะสูงสุด และเหมาะสมที่จะนำมาออกแบบเป็นไพร์เมอร์ โดยการเปรียบเทียบค่า ทีเอ็ม (Tm) ด้วยโปรแกรมคอมพิวเตอร์ เพื่อเลือกสรรอีกครั้ง จะสามารถคำนวณค่าอุณหภูมิที่เหมาะสม ความยาวและขนาดของโอลิโกนิวคลิโอไทด์ที่ลงตัวในการนำไปสังเคราะห์ และสามารถนำไปใช้ตรวจสอบได้ หรือใช้เพื่อเลือกลำดับนิวคลีโอไทด์เพื่อที่ได้โอลิโกนิวคลีโอไทด์ต้นแบบ ที่เมื่อสังเคราะห์ขึ้นจะนำไปใช้ในการตรวจวินิจฉัยเชื้อไวรัสโรคเหี่ยวได้โดยตรง

ในการตรวจสอบ สามารถใช้โครงสร้าง

โอลิโกนิวคลิโอไทด์ หมายเลข1คู่กับ สายคู่สมของโอลิโกนิวคลิโอไทด์หมายเลข 3 – 6

โอลิโกนิวคลิโอไทด์หมายเลข 2 คู่กับ สายคู่สมของโอลิโกนิวคลิโอไทด์ หมายเลข 4 – 6

โอลิโกนิวคลิโอไทด์หมายเลข 3 คู่กับสายคู่สมของโอลิโกนิวคลิโอไทด์ หมายเลข 5 – 6

หรือ

สายคู่สมของโอลิโกนิวคลิโอไทด์หมายเลข 4 คู่กับ โอลิโกนิวคลิโอไทด์ หมายเลข 1-2

สายคู่สมของโอลิโกนิวคลิโอไทด์หมายเลข 5 คู่กับ โอลิโกนิวคลิโอไทด์ หมายเลข 1-3

สายคู่สมของโอลิโกนิวคลิโอไทด์หมายเลข 6 คู่กับ โอลิโกนิวคลิโอไทด์ หมายเลข 1-4

โอลิโกนิวคลิโอไทด์หมายเลข 7 คู่กับ สายคู่สมของโอลิโกนิวคลิโอไทด์ หมายเลข 9-12

โอลิโกนิวคลิโอไทด์หมายเลข 8 คู่กับ สายคู่สมของโอลิโกนิวคลิโอไทด์ หมายเลข 10-12

โอลิโกนิวคลิโอไทด์หมายเลข 9 คู่กับ สายคู่สมของโอลิโกนิวคลิโอไทด์ หมายเลข 11-12

หรือ

สายคู่สมของโอลิโกนิวคลิโอไทด์หมายเลข 10 คู่กับ โอลิโกนิวคลิโอไทด์ หมายเลข 7-8

สายคู่สมของโอลิโกนิวคลิโอไทด์หมายเลข 11 คู่กับ โอลิโกนิวคลิโอไทด์ หมายเลข 7-10

สายคู่สมของโอลิโกนิวคลิโอไทด์หมายเลข 12 คู่กับ โอลิโกนิวคลิโอไทด์ หมายเลข 7-11

การจับคู่ดังกล่าวใช้สำหรับการเพิ่มปริมาณดีเอ็นเอของไวรัสโรคเหี่ยวในลับปะรด การนำโอลิโกนิวคลิโอไทด์มาใช้เป็นคู่ไพร์เมอร์ ใช้ได้กับปฏิกิริยาการจำลองตัวของดีเอ็นเอแบบลูกโซ่พอลิเมอร์เลส ในการเพิ่มปริมาณ DNA หรือ cDNA โดยเอนไซม์ในกลุ่มโพลวันไทป์ (Pol I Type) หรือ อัลฟาไทป์ (α Type) ในสารละลายที่ประกอบไปด้วย 10mM Tris.HCl (pH. 8.3) 1.5mM MgCl2 50mM KCl 1mM DTT 0.5% Tween 0.5% Nonidet P-40 2.5mM dNTP each โดยใช้ปริมาณโอลิโกนิวคลิโอไทด์ 5 พิโคโมลต่อปฏิกิริยาและปริมาณสารพันธุกรรม 50-100 นาโนกรัม บ่มปฏิกิริยาให้ดีเอ็นเอเสียสภาพที่อุณหภูมิ 93 องศาเซลเซียส 1 นาที annealing อุณหภูมิ 55 องศาเซลเซียส 1 นาที และทำปฏิกิริยาสังเคราะห์ดีเอ็นเอ หรือ extention ที่อุณหภูมิ 72 องศาเซลเซียส 2 นาที จำนวน 40 รอบผลการดำเนินการจะเฉพาะเจาะจงกับยีนโปรตีนเปลือกหุ้ม เฉพาะกับ

ตัวอย่างที่เกี่ยวข้องกับเชื้อไวรัสโรคเหี่ยวในสับปะรดชนิดที่ 1 และ2 นี้เท่านั้นจึงจะให้ผลิตภัณฑ์ดีเอ็นเอที่เพิ่มปริมาณจนสามารถตรวจสอบโดยหลักทางฟิสิกส์ได้

สำหรับโครงสร้างโอลิโกนิวคลิโอไทด์หมายเลข 13-14 และ 15-16 เป็นโครงสร้างสังเคราะห์ โครงสร้างเหล่านี้เกิดจากการจงใจออกแบบโอลิโกนิวคลิโอไทด์ขึ้นมาใหม่ให้โอลิโกนิวคลิโอไทด์ทั้งหมดเกิดจาก 1 หรือ 2 บริเวณของโอลิโกนิวคลิโอไทด์ มาร่วมเชื่อมกันให้อยู่ในรูปโนโอลิโกนิวคลิโอไทด์เดียวกัน โดยจะออกแบบให้เมื่อใช้งานโอลิโกนิวคลิโอไทด์จะจับตัวกับบริเวณ 6 บริเวณ ภายในยีนโปรตีนเปลือกหุ้มพร้อมกัน และเกิดได้เฉพาะกับสายพันธุ์ไวรัสโรคเหี่ยว แต่จะไม่เกิดหรือไม่จับกับลำดับนิวคลิโอไทด์ของไวรัสสายพันธุ์ย่อยชนิดอื่น การใช้โครงสร้างโอลิโกนิวคลิโอไทด์หมายเลข 1 3 7 10 13 14 15 และ16 หรือคู่สม ร่วมกัน หรือการใช้โอลิโกนิวคลิโอไทด์หมายเลข 1 3 13 14 หรือคู่สม ร่วมกัน หรือ 7 10 15 16 หรือคู่สม ร่วมกัน แยกเป็นปฏิกิริยาอิสระ โดยใช้สารเคมี กับปฏิกิริยาการเพิ่มปริมาณดีเอ็นเอด้วยอุณหภูมิระนาบเดียว (isothermal DNA amplification) ด้วยเอนไซม์บีเอสทีโพลิเมอร์เลส ในสารละลายที่ประกอบไปด้วย 40 mM Tris pH 8.8 20 mM KCl 40mM $MgSO_4$ 20 mM $(NH_4)_2SO_4$ 0.2% Tween 20 1.6 M Betaine 2.8 mM dNTP และ 16 U. *Bst* DNA polymerase โดยปฏิกิริยาประกอบด้วยชุดโอลิโกนิวคลิโอไทด์ ร่วมกับโอลิโกนิวคลิโอไทด์ 13-16 โดยปมปฏิกิริยาในอุณหภูมิ 63^{0}C 40 นาที จะช่วยเพิ่มสัญญาณดีเอ็นเอจำเพาะของยีนโปรตีนเปลือกหุ้มของไวรัสที่มีอยู่แม้เพียงน้อยนิดระดับ 100 copies ให้สามารถเพิ่มปริมาณมากขึ้นจนอยู่ในระดับตรวจวัดทางฟิสิกส์ได้

การวัดสัญญาณทำได้หลายรูปแบบ ตัวอย่างที่นิยมได้แก่

1) การทำปฏิกิริยาทางเคมีที่ตำแหน่ง 5' หรือ 3' ของโอลิโกนิวคลิโอไทด์ที่ระบุ กับโมเลกุลพิเศษ เกี่ยวข้องกับการเปลี่ยนแปลงสัญญาณทางฟิสิกส์ เช่นการใช้การเรืองตามหลักการฟูออเรสเซ็น รีโซแนนท์ เอ็นเนจีทรานสเฟอร์ (fluorescence resonance energy transfer (FRET)) การเรืองตามหลักปกติเมื่อใช้ฟูออโรฟอร์ เป็นตัวจับ ทั้งสองมีการวัดสัญญาณโดยการวัดแสงที่ความยาวคลื่นจำเพาะ การวัดการเรืองแสง หรือการใช้กัมมันตรังสีที่เป็นนิวคลิโอไทด์ ซึ่งมีการวัดสัญญาณโดยการวัดปริมาณรังสีด้วยเครื่องซินทิลเลชันเคาท์เตอร์ (scintillation counter) จากนั้นนำโอลิโกนิวคลิโอไทด์ที่ระบุไว้ข้างต้น ไปทำปฏิกิริยาเพิ่มปริมาณดีเอ็นเอด้วยระบบ ปฏิกิริยาการจำลองตัวของดีเอ็นเอแบบลูกโซ่พอลิเมอร์เลส หรือ การเพิ่มปริมาณดีเอ็นเอด้วยอุณหภูมิระนาบเดียว ปริมาณดีเอ็นเอของตัวอย่างเป้าหมายเท่านั้นที่สามารถเพิ่มปริมาณได้เป็นจำนวนมากระดับปริมาณดังกล่าวยิ่งมากก็จะเชื่อมโยงไปสู่ระดับปริมาณสัญญาณที่ตรวจวัดได้ทางฟิสิกส์มากตาม

2) การกระตุ้นให้เกิดการจับตัวของโมเลกุลดีเอ็นเอที่เพิ่มปริมาณอย่างจำเพาะด้วยโมเลกุลที่จับตัวกับดีเอ็นเอในรูปดีเอ็นเอไบนด์เดอร์

ดีเอ็นเอไบนด์เดอร์เป็นโมเลกุลที่เมื่อจับกับดีเอ็นเอหรือผลลัพท์ของดีเอ็นเอที่เพิ่มในปฏิกิริยา จะส่งผลในรูปการเปลี่ยนแปลงทางกายภาพ เช่น กระตุ้นให้เกิดการเรืองแสง หรือการเปลี่ยนแปลงของค่าทางไฟฟ้า ขณะที่โมเลกุลแคลซีน ซึ่งเป็นโมเลกุลที่เมื่อจับกับ บายโพรดักท์ (by products) ได้แก่ไพโรฟอสเฟตที่พบในกระบวนการเพิ่มปริมาณดีเอ็นเอ

จะก่อให้เกิดการเปลี่ยนแปลงทางกายภาพ เช่น กระตุ้นให้เกิดการเรืองแสง โมเลกุลดีเอ็นเอไบนด์เดอร์ตัวอย่างนี้นำมาปรับให้ได้ 3 กลุ่ม ได้แก่

1. ดีเอ็นเอไบนด์เดอร์ ในกลุ่มอินเตอร์คาเลเตอร์ (intercalator) อาศัยหลักการแทรกตัวในระหว่างสายของดีเอ็นเอ ได้แก่ เมธิลีนบลู โปรปิเดียมไอโอไดด์ อะมิโนอะคริดีน อีลิปทริซิน

2. ดีเอ็นเอไบนด์เดอร์ในกลุ่มไมเนอร์กรูฟ (minor groove binder) ซึ่งจะจับตัวกับโครงสร้างไมเนอร์กรูฟ ในโครงสร้างเกลียวคู่ (double helix) ในโมเลกุลดีเอ็นเอ ได้แก่ โฮกซ์ 33258 (Hoechst 33258) นิวเคลียร์เยลโลว์ เดฟวัน (DEF 1) เบอร์เรนิล ไซเบอร์กรีน แดบปี้ (DAPI) พิโคกรีน และอีวากรีน

3. โมเลกุล DNA binder ที่อาศัยการติดฉลากที่ปลาย 5 หรือ 3 โดยอาจอยู่ในรูป ดีเอ็นเอหรืออาร์เอ็นเอหรือโอลิโกนิวคลีโอไทด์หรือดีเอ็นเออานาล็อก โดยฉลากที่ติดที่ปลาย 5 หรือ 3 ในรูป อะเล็กซ่า 488 (ALEXA-488) แฟม (FAM) โจ (JOE) แทมรา (TAMRA) ไซทรี (CY3) ไซไฟว์ (CY5) บีเฮชคิว (BHQ) เฮก (HEX) ร็อก (ROX) แดบซิล (DABCYL) เตท (TET) บอดิพิล เอฟแอล (BODIPY FL) ดีดีคิว (DDQ)

4. หรือโมเลกุลเรืองแสงสังเคราะห์ ความเข้มข้นใช้งานของโมเลกุลเมื่อติดฉลากลงบนดีเอ็นเอหรืออาร์เอ็นเอหรือโอลิโกนิวคลีโอไทด์ อยู่ในช่วง 10-100 pmole/ปฏิกิริยา

สำหรับการใช้สารเคมีแคลซีนเพื่อทำปฏิกิริยาโดยตรงสามารถใช้โมเลกุลแคลซีนความเข้มข้น 50μM ร่วมกับ 1mM $MnCl_2$ ร่วมไปกับปฏิกิริยาตั้งแต่ต้น โดยในขณะเริ่มต้นของปฏิกิริยา โมเลกุล calcein จะจับตัวอยู่กับ Mn^{2+} และยังไม่เรืองแสง แต่เมื่อปฏิกิริยาการเพิ่มปริมาณดีเอ็นเอสัมฤทธิ์ผล จะพบว่ามีการใช้ dNTP มากจนเกิดเป็น ไพโรฟอสเฟต (PPi) ที่เป็นบายโพรดักท์ มากตาม PPi มีความสามารถที่จะไปแย่งจับ Mn^{2+} ทำให้โมเลกุลแคลซีนเป็นอิสระ เมื่อรับพลังงานจากรังสี UV ตั้งแต่ความยาวคลื่น 240-370 nm จะกระตุ้นให้เกิดการคายพลังงาน โดยการเรืองแสงที่ช่วงความยาวคลื่น 515 nm การวัดผลสัมฤทธิ์ของปฏิกิริยาจากทั้ง ดีเอ็นเอไบนด์เดอร์ และจากโมเลกุล calcein ทำได้โดยดูการเรืองแสง เมื่อส่องดูด้วย black light หรือ UV light

5. การใช้โอลิโกนิวคลีโอไทด์ที่ระบุเป็นโมเลกุลตรวจจับ บนหลักการ ไฮบริไดเซชัน หรือใช้โอลิโกนิวคลีโอ ไทด์ที่ระบุเป็นกลไกในการจับตัวร่วมกับ กรดนิวคลีอิกอื่น ได้แก่ดีเอ็นเออานาล็อก หมายเลข 1 และ 2 อย่างใดอย่างหนึ่งแยกกัน ร่วมกับ โอลิโกนิวคลีโอไทด์หมายเลข 17 และ โอลิโกนิวคลีโอไทด์ หมายเลข 18 รวมถึงการใช้ดีเอ็นเออานาล็อก ที่เป็นเป็ปไทด์นิวคลีอิกแอซิด หรือ เบต้าไพโรริดินิลเป็ปไทด์นิวคลีอิกแอซิด การตรวจจับด้วยหลักการนี้อาศัยการจับตัวของโอลิโกนิวคลีโอไทด์ที่ระบุร่วมกับลำดับนิวคลีโอไทด์อื่น รวมถึง เป็ปไทด์นิวคลีอิกแอซิดที่เป็นดีเอ็นเออานาล็อก หมายเลข 1 และ 2 ร่วมกับลำดับนิวคลีโอไทด์เป้าหมายของยีนของไวรัสโรคเหี่ยวทั้งสองชนิด ส่งผลให้เกิดการเปลี่ยนแปลงทางสัญญาณที่ตรวจสอบได้ทางฟิสิกส์ การเปลี่ยนแปลงทางสัญญาณอาจ

กระตุ้นผ่านโอลิโกนิวคลิโอไทด์ที่ระบุ หรือลำดับนิวคลิโอไทด์อื่นหรือเป็ปไทด์นิวคลิอิกแอซิด หรือร่วมกันก็ได้ การใช้โอลิโกนิวคลิโอไทด์ที่ระบุนี้ ร่วมกับคอลลอยด์ของอนุภาคนาโนของโลหะ ในลักษณะที่กระตุ้นให้เกิดการจับตัวของอนุภาคนาโนของโลหะ บนโมเลกุลของโอลิโกนิวคลิโอไทด์ที่ระบุ หรือใช้โมเลกุลของโอลิโกนิวคลิโอไทด์ที่ระบุเป็นสื่อให้เกิดการจับตัวของอนุภาคนาโนของโลหะ บนโมเลกุลของลำดับนิวคลิโอไทด์เป้าหมายของไวรัสโรคเหี่ยวส่งผลให้เกิดการเปลี่ยนแปลงทางสัญญาณที่ตรวจสอบได้ทางฟิสิกส์ในรูป การเรืองแสง การเปลี่ยนคุณสมบัติทางแสง การเปลี่ยนสีทางแสง ที่เกิดจากปรากฏการณ์พลาสมอน (plasmon) การใช้โอลิโกนิวคลิโอไทด์ที่ระบุสามารถใช้ร่วมกับระบบการเพิ่มปริมาณดีเอ็นเอ และหรือระบบการแสดงสัญญาณผ่านปฏิกิริยาเคมีที่ตำแหน่ง 5' หรือ 3'ของโอลิโกนิวคลิโอไทด์ที่ระบุ หรือระบบ ไฮบริไดเซชัน หรือทั้งหมด

โดยดำเนินการสามารถทำได้ในรูปสารละลาย สารละลายที่เป็นของเหลวสามารถไหลซึมผ่านไปบนสื่อได้แก่ ซิลิโคนสังเคราะห์ในรูปแบบชิปหรือ ซิลิกอนในรูปแบบชิปที่มีโครงสร้างเหมาะสม หรือบนเมมเบรน หรือบนกระดาษ การใช้โอลิโกนิวคลิโอไทด์และดีเอ็นเอ อานาล็อกที่ระบุร่วมกับชิป หรือบนเมมเบรน หรือบนกระดาษนี้ช่วยให้การการนำเสนอผลการเปลี่ยนแปลงของสัญญาณดีเอ็นเอหรืออาร์เอ็นเอที่ตรวจสอบได้ทางฟิสิกส์ ทำได้อย่างเป็นระบบและมีประสิทธิภาพ โดยเมื่อมีการใช้งานร่วมดังกล่าว จะก่อให้เกิดการเปลี่ยนแปลงของสัญญาณที่เกิดโดยตรงหรือโดยอ้อมผ่านโอลิโกนิวคลิโอไทด์และหรือดีเอ็นเออานาล็อกที่ระบุ ทำให้สัญญาณดีเอ็นเอหรืออาร์เอ็นเอที่เกิดขึ้น ตรวจสอบได้ทางฟิสิกส์ เช่นผ่านการเรืองแสง การเปลี่ยนคุณสมบัติทางแสง การเปลี่ยนสี การเปลี่ยนแปลงทางกัมมันตรังสี ระดับปริมาณดีเอ็นเอที่มีลำดับนิวคลิโอไทด์ที่จำเพาะผ่านการเพิ่มของปริมาณดีเอ็นเอ การเปลี่ยนแปลงทางไฟฟ้า การเปลี่ยนแปลงทางสนามแม่เหล็ก

สัญญาณการเปลี่ยนแปลงดังกล่าวนำไปสู่รูปแบบการใช้งานโอลิโกนิวคลิโอไทด์และหรือ ดีเอ็นเออานาล็อกที่ระบุที่ระบุเพื่อตรวจสารพันธุกรรมของเชื้อไวรัสโรคเหี่ยวในสับปะรด เพื่อการตรวจวินิจฉัยทางห้องปฏิบัติการหรือกับตัวอย่างที่ได้จากในแปลงปลูก หรือเพื่อการตรวจคัดกรองเชื้อไวรัสอย่างเฉพาะเจาะจงได้

<u>วิธีการประดิษฐ์ที่ดีที่สุด</u>

เหมือนกับที่ได้กล่าวไว้แล้วในหัวข้อการเปิดเผยการประดิษฐ์โดยสมบูรณ์

โอลิโกนิวคลิโอไทด์ หมายเลข 1 5'-ACTCTGGGCCTAAGACAGT-3'

โอลิโกนิวคลิโอไทด์ หมายเลข 2 5'-GGAAGACCAAGTCAAGGAA-3'

โอลิโกนิวคลิโอไทด์ หมายเลข 3 5'-GGAGGTAGGACTACTGTGTCG-3'

โอลิโกนิวคลิโอไทด์ หมายเลข 4 5'-ATGCACACAAGGTGATAGG-3'

โอลิโกนิวคลิโอไทด์ หมายเลข 5 5'-GCATGATTAACGTTCCGATCC-3'

โอลิโกนิวคลิโอไทด์ หมายเลข 6 5'-ACGTTTGAAGATTTGATAGCAGCCG-3'

โอลิโกนิวคลิโอไทด์ หมายเลข 7 5'-ACTATATAGAAACAGAGACGC-3'

โอลิโกนิวคลิโอไทด์ หมายเลข 8 5'-AATATACATCAAGGACGTGAGT-3'

โอลิโกนิวคลิโอไทด์ หมายเลข 9 5'-GCGATGAATTCGGGGTACGAA-3'

โอลิโกนิวคลิโอไทด์ หมายเลข 10 5'-AGAACTATGGCTCATCACG-3'

โอลิโกนิวคลิโอไทด์ หมายเลข 11 5'-ATGGTAAAATAACACCTAACGAG-3'

โอลิโกนิวคลิโอไทด์ หมายเลข 12 5'-ACCCGTTTAGGCAATATATGCG-3'

โอลิโกนิวคลิโอไทด์ หมายเลข 13 5'-CGACACAGTAGTCCTACCTCCGGAAGACCAAGTCAAGGAA-3'

โอลิโกนิวคลิโอไทด์ หมายเลข 14 5'-ACGTTTGAAGATTTGATAGCAGCCGATCGGAACGTTAATCATGC-3'

โอลิโกนิวคลิโอไทด์ หมายเลข 15 5'-TCGTACCCCGAATTCATCGCAATATACATCAAGGACGTGAGT-3'

โอลิโกนิวคลิโอไทด์ หมายเลข 16 5'-ACCCGTTTAGGCAATATATGCGCTCGTTAGGTGTTATTTTACCAT-3'

โอลิโกนิวคลิโอไทด์ หมายเลข 17 5'-AATCAATGGG-3'

โอลิโกนิวคลิโอไทด์ หมายเลข 18 5'-TTAGTGTGGG-3'

อานาล็อกดีเอ็นเอ หมายเลข 1 5'- TATAATTGATT -3'

อานาล็อกดีเอ็นเอ หมายเลข 2 5'- TATAACACTAA -3'

ข้อถือสิทธิ

1. ชุดของโอลิโกนิวคลีโอไทด์ และดีเอ็นเออานาล็อก ที่ออกแบบและสังเคราะห์ขึ้นในรูปโอลิโกนิวคลิโอไทด์ อานาล็อกดีเอ็นเอรูปแบบเป็ปไทด์นิวคลีอิกแอซิด ที่ประกอบด้วยลำดับนิวคลิโอไทด์หรือส่วนหนึ่งส่วนใดรวมทั้งสายคู่สมของลำดับนิวคลิโอไทด์ที่แสดงตามรูปที่ 1 ชุดของโอลิโกนิวคลีโอไทด์ที่ระบุมีความจำเพาะเจาะจงต่อการเพิ่มสัญญาณของยีนโปรตีนเปลือกหุ้มของไวรัสโรคเหี่ยว ทำให้การตรวจสารพันธุกรรมของไวรัสนี้โดยเฉพาะเกิดขึ้นได้อย่างมีประสิทธิภาพโดยไม่มีผลต่อการเพิ่มสัญญาณไวรัสสายพันธุ์อื่นที่ไม่ใช่ไวรัสโรคเหี่ยว พีเอ็มดับบริวเอวี ชนิดที่ 1 และ 2 ทั้งนี้เพื่อตรวจสารพันธุกรรมของเชื้อ และการตรวจคัดกรองสารพันธุกรรมของเชื้อไวรัสในห้องปฏิบัติการหรือในสภาวะจำลอง(in vitro)

2. การใช้งานชุดของโอลิโกนิวคลีโอไทด์ ตามข้อถือสิทธิ 1 ในการเพิ่มปริมาณสัญญาณกรดนิวคลีอิก ด้วยเอมไซม์โพลิเมอร์เลส ได้แก่ แทคโพลิเมอร์เลส พีเอฟยูโพลิเมอร์เลส ทีทีเฮชโพลิเมอร์เลส เคโอดีโพลิเมอร์เลส ดีปเวนท์โพลิเมอร์เลส พีดับบลิวยูโพลิเมอร์เลส บีเอสทีโพลิเมอร์เลส ทีแอลไอโพลิเมอร์เลส ลำพังหรือร่วมกับเอนไซมรีเวอร์สทรานสคริปเทส หรือด้วยปฏิกิริยาลูบอุณหภูมิเดียวด้วยเอมไซม์โพลิเมอร์เลส ได้แก่บีเอสทีโพลิเมอร์เลส

3.การใช้งานชุดโอลิโกนิวคลีโอไทด์ ตามข้อถือสิทธิ 1 เพื่อการใช้งาน บนชิป บนระบบปฏิบัติการวิเคราะห์ทางเคมีในหลอดทดลองหรือบนเมมเบรนหรือกระดาษ

4.การใช้งานชุดโอลิโกนิวคลีโอไทด์ ตามข้อถือสิทธิ 1 เพื่อการตรวจสอบลำดับนิวคลิโอไทด์ด้วยเทคนิคไฮบริไดเซชั่น (hybridization) ในรูปของโพรบที่เป็นกรดนิวคลีอิกสังเคราะห์ เป็นอานาล็อกดีเอ็นเอหรือเป็นเป็ปไทด์นิวคลีอิกแอซิดที่สังเคราะห์ขึ้นจากส่วนหนึ่งส่วนใดของแบบของชุดโอลิโกนิวคลีโอไทด์ที่ได้ออกแบบขึ้นตามข้อถือสิทธิ 1

5.การใช้งานชุดโอลิโกนิวคลีโอไทด์ และดีเอ็นเออานาล็อก ตามข้อถือสิทธิ 1 โดยการติดฉลากที่บริเวณ 5' และ 3' ของชุดโอลิโกนิวคลีโอไทด์นั้น ด้วยโมเลกุลอะเล็กซ่า 488 (ALEXA-488) แฟม (FAM) โจ (JOE) แทมรา (TAMRA) ไซทรี (CY3) ไซไฟว์ (CY5) บีเฮชคิว (BHQ) เฮก (HEX) ร็อก (ROX) แดบซิล (DABCYL) เตท (TET) บอดิพิล เอฟแอล (BODIPY FL) ดีดีคิว (DDQ) เพื่อให้เรืองแสง

6. การใช้งานชุดโอลิโกนิวคลีโอไทด์ ตามข้อถือสิทธิ 1 ร่วมกับโมเลกุลดีเอ็นเอไบนด์เดอร์ โฮกซ์ 33258 (Hoechst 33258) นิวเคลียร์เยลโลว์ เดฟวัน (DEF 1) เบอร์เรนิล ไซเบอร์กรีน แดบปี้ (DAPI) พิโคกรีน และอีวากรีน และแคลซีน ที่ก่อให้เกิดการเปลี่ยนแปลงทางกระแสไฟฟ้า และหรือ การเปลี่ยนแปลงทางแสง

7. การใช้งานชุดโอลิโกนิวคลีโอไทด์ ตามข้อถือสิทธิ 1 ร่วมกับคอลลอยด์ของอนุภาคนาโนของโลหะ เงิน ทองคำ พลาตินัม เพื่อการตรวจการเปลี่ยนแปลงทางพลาสมอน

บทสรุปการประดิษฐ์

การประดิษฐ์นี้เกี่ยวกับชุดของโอลิโกนิวคลิโอไทด์ที่มีลำดับนิวคลิโอไทด์เฉพาะที่เกิดจากการออกแบบและสังเคราะห์ขึ้นด้วยกระบวนการทางเคมี และรูปแบบการใช้งานชุดของโอลิโกนิวคลิโอไทด์เฉพาะ ร่วมกับระบบการสกัดสารพันธุกรรม (นิวคลีอิกแอซิด) ของไวรัสจากตัวอย่างผ่านระบบการเพิ่มปริมาณสารพันธุกรรมของไวรัสด้วยยีนโปรตีนเปลือกหุ้มที่เฉพาะเจาะจงกับไวรัสโรคเหี่ยวของสับปะรด ด้วยเอนไซม์พอลิเมอร์เลสใดๆ ในระบบจำลอง(in vitro) หรือร่วมกับระบบการตรวจวิเคราะห์บนชิปหรือระบบการตรวจในหลอดทดลองหรือบนเมมเบรนหรือบนกระดาษ หรือร่วมกับระบบการแสดงผลในรูปของการเรืองแสงด้วยโมเลกุลดีเอ็นเอไบนด์เดอร์ หรือร่วมกับ ระบบ hybridization ด้วยกรดนิวคลิอิคอื่นหรือเปปไทด์นิวคลิอิคแอซิด(PNA) หรือร่วมกับนาโนคอลลอยด์ของโลหะ ทำให้เกิดการเปลี่ยนแปลงทางกายภาพในรูปสัญญาณดีเอ็นเอ ทำให้การตรวจวิเคราะห์สารพันธุกรรมของไวรัส ทำได้ง่าย รวดเร็วและแม่นยำ โดยระบบที่ประดิษฐ์ขึ้นช่วยให้การตรวจไวรัสโรคเหี่ยวของสับปะรดทำได้อย่างมีประสิทธิภาพ ส่งผลดีต่อการเตรียมการในการป้องกันการแพร่ระบาดและการขยายตัวของโรค

ภาคผนวก 2

บทคัดย่องานประชุม

(เนื่องจากเอกสารมีความหนามาก จึงไม่ได้เย็บรวมในเล่มรายงานฉบับสมบูรณ์
ผู้สนใจโปรดดูรายละเอียดในแผ่น CD)

L-22

Pyrrolidinyl Peptide Nucleic Acids as Probes for DNA Biosensor Applications

Cheeraporn Ananthanawat, Boonjira Boontha, Pratchayaporn Korkaew, Voravee Hoven and Tirayut Vilaivan*
Organic Synthesis Research Unit, Department of Chemistry, Faculty of Science, Chulalongkorn University, Phayathai Road, Patumwan, Bangkok 10210 Thailand.
E-mail: *vtirayut@chula.ac.th*

We have recently reported the synthesis and nucleic acid binding properties of a new conformationally constraint pyrrolidinyl peptide nucleic acid (PNA) carrying an alternate α,β dipeptide backbone derived from D-proline and (1*S*,2*S*)-2-aminocyclopentane carboxylic acid (ACPC). Apart from binding strongly, yet sequence specifically, to DNA, the new PNA exhibited many unusual properties including the preferential binding to DNA over RNA, the inability to self-hybridize and the relative independency of PNA·DNA hybrid stability to G·C content. These properties suggest a potential of using the PNA as probes for DNA sequence analysis.

In an example, we have developed a new ion-exchange capture technique for DNA sequence analysis. The uncharged PNA cannot be absorbed onto a solid anion exchanger unless it is first hybridized with complementary DNA to form a negatively charged PNA·DNA hybrid. By observing the presence of absorbed PNA by MALDI-TOF MS or fluorescence microscopy, the sequence of the DNA target can be deduced from the sequence of the PNA probe. The high specificity of the PNA probe allows unambiguous discrimination between complementary and single mismatched DNA targets in standard buffers at ambient temperature. The technique has been successfully applied in single nucleotide polymorphism (SNP) genotyping of human DNA. Importantly, the analysis can be done in multiplex fashion whereby three different SNP sites in the same DNA sample are simultaneously analyzed.

In addition, the PNA probes were also immobilized onto gold surfaces with a view of using them as DNA biosensors. It has been demonstrated by QCM and SPR that the immobilized PNA probes still retain the ability to discriminate between complementary and non-complementary DNA targets. Thus we have demonstrated that the new PNA can be used as highly specific probes for DNA sequence analysis.

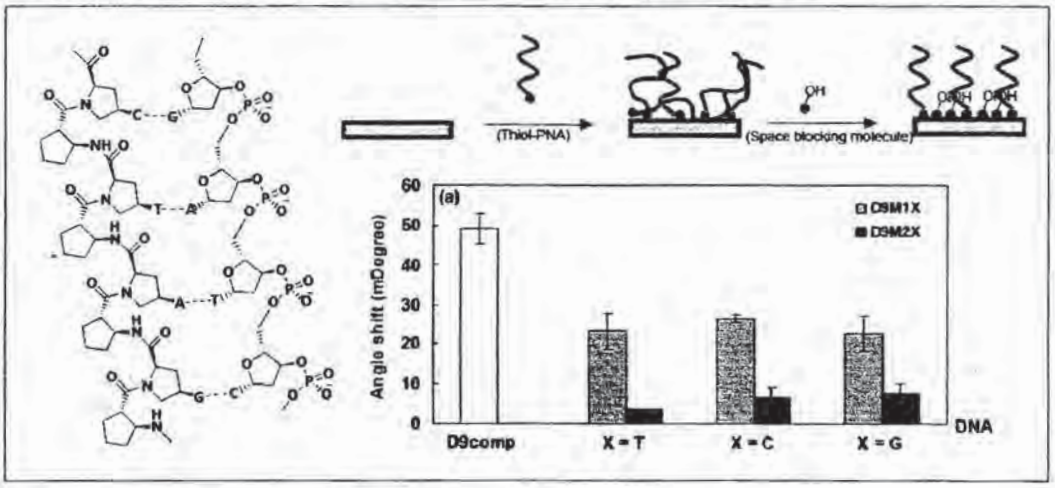

1. Ananthanawat, C. et al. *Biosens. Bioelectron.* **2009**, *24*, 3544–3549.
2. Ananthanawat, C. et al. *Sens. Acutators B: Chem.* **2009**, *137*, 215–221.
3. Boontha B.et al. *Anal. Chem.* **2008**, *80*, 8178–8186.

Tirayut Vilaivan (ธีรยุทธ วิไลวัลย์), b 1971 in Bangkok, Thailand. Chulalongkorn University (BSc 1992), Oxford Univ. (DPhil 1996, Prof. G. Lowe), Associate Professor, Department of Chemistry, Faculty of Science, Chulalongkorn University (2004-present). Research field: asymmetric catalysis, peptide nucleic acids, medicinal chemistry.

L-22

Pyrrolidinyl Peptide Nucleic Acids as Probes for DNA Biosensor Applications

Cheeraporn Ananthanawat, Boonjira Boontha, Pratchayaporn Korkaew, Voravee Hoven and Tirayut Vilaivan*
Organic Synthesis Research Unit, Department of Chemistry, Faculty of Science, Chulalongkorn University, Phayathai Road, Patumwan, Bangkok 10210 Thailand.
E-mail: *vtirayut@chula.ac.th*

We have recently reported the synthesis and nucleic acid binding properties of a new conformationally constraint pyrrolidinyl peptide nucleic acid (PNA) carrying an alternate α,β dipeptide backbone derived from D-proline and (1*S*,2*S*)-2-aminocyclopentane carboxylic acid (ACPC). Apart from binding strongly, yet sequence specifically, to DNA, the new PNA exhibited many unusual properties including the preferential binding to DNA over RNA, the inability to self-hybridize and the relative independency of PNA·DNA hybrid stability to G·C content. These properties suggest a potential of using the PNA as probes for DNA sequence analysis.

In an example, we have developed a new ion-exchange capture technique for DNA sequence analysis. The uncharged PNA cannot be absorbed onto a solid anion exchanger unless it is first hybridized with complementary DNA to form a negatively charged PNA·DNA hybrid. By observing the presence of absorbed PNA by MALDI-TOF MS or fluorescence microscopy, the sequence of the DNA target can be deduced from the sequence of the PNA probe. The high specificity of the PNA probe allows unambiguous discrimination between complementary and single mismatched DNA targets in standard buffers at ambient temperature. The technique has been successfully applied in single nucleotide polymorphism (SNP) genotyping of human DNA. Importantly, the analysis can be done in multiplex fashion whereby three different SNP sites in the same DNA sample are simultaneously analyzed.

In addition, the PNA probes were also immobilized onto gold surfaces with a view of using them as DNA biosensors. It has been demonstrated by QCM and SPR that the immobilized PNA probes still retain the ability to discriminate between complementary and non-complementary DNA targets. Thus we have demonstrated that the new PNA can be used as highly specific probes for DNA sequence analysis.

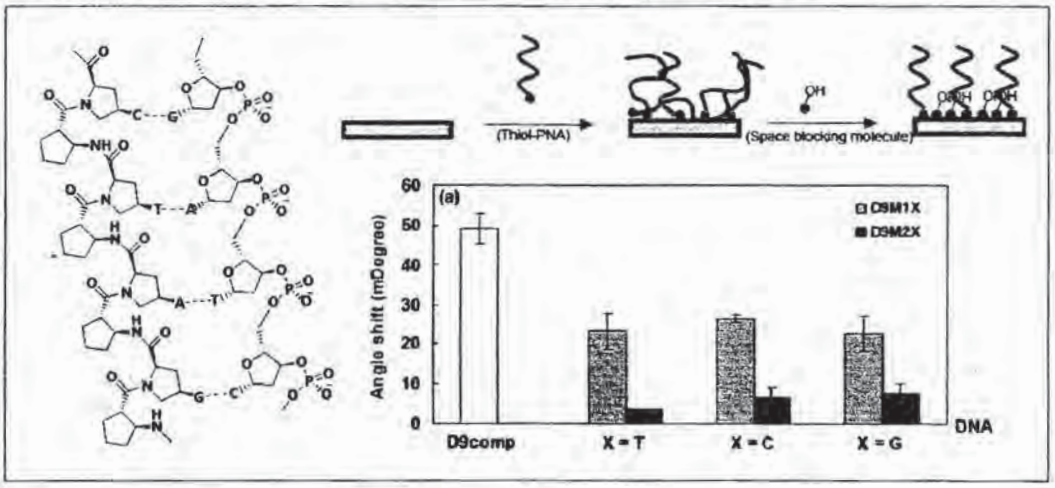

1. Ananthanawat, C. et al. *Biosens. Bioelectron.* **2009**, *24*, 3544–3549.
2. Ananthanawat, C. et al. *Sens. Acutators B: Chem.* **2009**, *137*, 215–221.
3. Boontha B.et al. *Anal. Chem.* **2008**, *80*, 8178–8186.

Tirayut Vilaivan (ธีรยุทธ วิไลวัลย์), b 1971 in Bangkok, Thailand. Chulalongkorn University (BSc 1992), Oxford Univ. (DPhil 1996, Prof. G. Lowe), Associate Professor, Department of Chemistry, Faculty of Science, Chulalongkorn University (2004-present). Research field: asymmetric catalysis, peptide nucleic acids, medicinal chemistry.

3.1(2)

β-Pyrrolidinyl Peptide Nucleic Acids: Synthesis and Applications as Probes for DNA Sequence Analysis

Vilaivan, T.

Organic Synthesis Research Unit, Department of Chemistry, Faculty of Science, Chulalongkorn University, Bangkok 10330, Thailand
E-mail: vuravus@chula.ac.th

Keywords: PNA, DNA, Diagnostic, β-Amino acid, Foldamer

Abstract

A new class of conformationally constraint pyrrolidinyl peptide nucleic acid (PNA) derived from an alternate proline and 2-aminocyclopentane carboxylic acid (ACPC) backbone has been synthesized and evaluated for nucleic acid biding and self-pairing properties. The new PNA exhibited many unusual properties not found in other PNA systems including high single base mismatch specificity even under low-stringency conditions, the preferential binding to DNA over RNA, the inability to self-hybridize and the relative independency of PNA·DNA hybrid stability to base composition. These properties suggest that the new PNA is potentially useful in diagnostic applications, especially in DNA sequence analysis. Applications of the new PNA as probes for highly specific DNA sequence determination with a single base mismatch resolution will also be demonstrated.

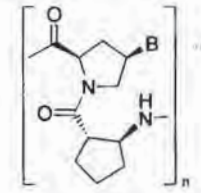

B = nucleobases (A, T, C, G)

n = 9 to 15

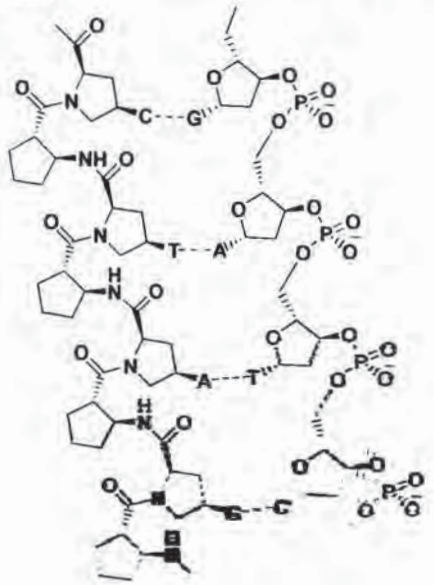

Pyrrolidinyl Peptide Nucleic Acids with Unusual Pairing Properties as Potential Antigene Agents

Tirayut Vilaivan
Department of Chemistry, Faculty of Science, Chulalongkorn University,
Phayathai Road, Patumwan, Bangkok 10330, Thailand
vtirayut@chula.ac.th

Selective and efficient targeting DNA is a potentially powerful strategy for control of gene expression. Despite its potential advantages over RNA targeting by antisense oligonucleotides, the strategy is relatively underexplored. One major obstacle is the relative inaccessibility of DNA compared to RNA. The other is the lack of suitable antigene agents that can bind strongly and specifically to double-stranded DNA with unlimited sequence restriction. The usefulness of peptide nucleic acid (PNA) – a neutral-backbone analogue of DNA – as antisense and antigene agents has been demonstrated in a number of model systems. However, unlike RNA targeting, targeting double stranded DNA by PNA suffers sequence limitation due to the inherent unfavourable binding properties of the classical aminoethylglycyl (aeg) PNA.

We have recently developed a new conformationally rigid PNA system based on a D-prolyl-2-aminocyclopentanecarboxylic acid (acpc) backbone. The new acpcPNA displays strong affinity and high sequence specificity in binding to DNA similar to aegPNA. On the other hand, while two strands of complementary aegPNA interact strongly by Watson-Crick base pairing, the new acpcPNA fails to show such self-pairing property. Self-pairing in aegPNA was undesirable in DNA-targeting by the so-called double duplex invasion strategy, and it was necessary to modulate the self-pairing of PNA by appropriate modification of nucleobase and/or the backbone. Our preliminary experiments indicated that the non self-pairing acpcPNA is a potentially useful agent for double duplex invasion of dsDNA.

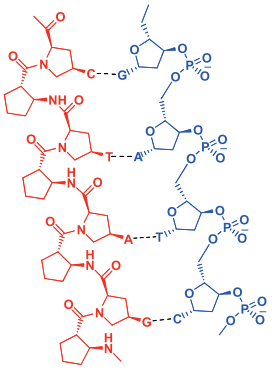

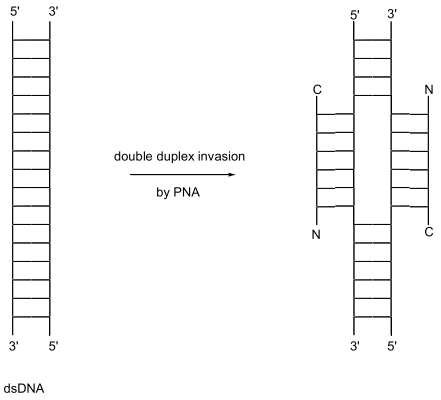

1. Vilaivan, T.; Srisuwannaket, C. *Org. Lett.* **2006**, *8*, 1897–1900.
2. Suparpprom, C.; Srisuwannaket, C.; Sangvanich, P.; Vilaivan, T. *Tetrahedron Lett.* **2005**, *46*, 2833–2837.
3. Vilaivan, T.; Lowe, G. *J. Am. Chem. Soc.* **2002**, *124*, 9326–9327.

Tirayut Vilaivan, Chulalongkorn Univ. (B.Sc. 1992), Oxford Univ. (D.Phil. 1996, Prof. G. Lowe), Visiting associate professor Osaka at City Univ. (Prof. Y. Ohfune, 2003), Humboldt research fellow (Prof. O. Reiser, 2009), TRF Senior Research Scholar (2009-present). Lecturer (1996–1999), Assistant Professor (1999–2004), Associate Professor (2004–present), all at Chulalongkorn University. Research field: Catalytic Asymmetric Synthesis, Unnatural Amino Acids and Peptides, Medicinal Chemistry.

3.1(4)

Synthesis and pairing properties of pyrrolidinyl peptide nucleic acid: beyond PNA·DNA duplexes

Tirayut Vilaivan*

Organic Synthesis Research Unit, Department of Chemistry, Faculty of Science, Chulalongkorn University, Phayathai Road, Patumwan, Bangkok, Thailand 10300

**E-mail: vtirayut@chula.ac.th, Tel: +66-2-218-7627*

The high affinity and specificity of pairing between peptide nucleic acids (PNA) and single stranded DNA or RNA have been extensively exploited in DNA/RNA-related diagnostic and therapeutic applications. PNA can, in addition, form a variety of unique high-order structures, either on its own or with nucleic acids. These structures include triplexes, DNA invasion complexes, and self-pairing hybrids. We have previously reported the synthesis of a new pyrrolidinyl PNA carrying a D-prolyl-2-aminocyclopentanecarboxylic acid (acpc) backbone that can bind to DNA with high sequence specificity. Applications of such pyrrolidinyl PNA in DNA sequence determination had been well demonstrated. In this presentation, synthesis and ability of conformationally constrained pyrrolidinyl peptide nucleic acids to form various high-order structures other than the already well-studied PNA·DNA duplex will be discussed. The ability to form high order structures in a predictable and controllable fashion makes these PNAs potentially useful molecules in applications that require programmable self-assembly building blocks.

REFERENCES

Lowe, G.; Vilaivan, T. *J. Am. Chem. Soc.* **2002**, 124, 9326-9327.
Vilaivan, T.; Srisuwannaket, C. *Org. Lett.* **2006**, 8, 1897-1900.

3.1(5)

Synthesis and DNA binding properties of *(2R,4S)* pyrrolidinyl peptide nucleic acid

Jaru Taechalertpaisarn, Pitchanun Sriwarom, Chotima Vilaivan and Tirayut Vilaivan*

Organic Synthesis Research Unit, Department of Chemistry, Faculty of Science, Chulalongkorn University, Phayathai Road, Patumwan, Bangkok, Thailand 10300

**E-mail: vtirayut@chula.ac.th, Tel: +66-2-218-7627*

Peptide Nucleic Acid (PNA) is a structural mimic of DNA. PNA binds to DNA with high affinity and sequence specificity following the Watson-Crick base pairing rules. This property is useful for detecting DNA sequences or gene therapies. Recently, a new conformationally-restricted PNA based on a (2*R*,4*R*)-prolyl-(1*S*,2*S*)-2-aminocyclopentanecarboxylic acid backbone has been extensively studied. The PNA showed excellent binding properties with DNA. On the other hand, other diastereomeric pyrrolidinyl PNAs have not been systematically investigated. It was reasoned that changing the configuration at the C-4 position of the pyrrolidine ring should not much affect the global conformation of the PNA backbone, and the resulting PNA should retain the DNA binding properties. In this research, Fmoc-protected pyrrolidinyl PNA monomers with (2*R*,4*S*) configuration have been synthesized. The four PNA monomers carried the four natural nucleobases, Adenine (A), Thymine (T), Cytosine (C) and Guanine (G). These PNA monomers were used for synthesizing the corresponding oligomers, using (1*S*,2*S*)-2-aminocyclopentanecarboxylic acid (*SS*-ACPC) as a spacer by Fmoc solid phase peptide synthesis. Preliminary binding studies with complementary DNA by melting temperature (T_m) suggested that the new PNA can bind to DNA, albeit with lower affinity compared to the (2*R*,4*R*) diastereomer.

REFERENCES

1. Lowe, G.; Vilaivan, T *J. Chem. Soc., Perkin Trans. 1*, **1997**, 539-546.
2. Lowe, G.; Vilaivan, T. *J. Am. Chem. Soc.* **2002**, 124, 9326-9327.
3. Vilaivan, T.; Srisuwannaket, C. *Org. Lett.* **2006**, 8, 1897-1900.

3.1(6)

Rapid detection of oseltamivir resistant mutation at amino acid residue 274 of novel 2009 human influenza A virus (H1N1) based on blue silver nanoparticle

Nussara Donraman,[1] Sanong Ekgasit,[2] Tirayut Vilaivan,[3] Yong Poovorawan[4] and Piyasak Chaumpluk[1,5*]

[1]*Laboratory of Plant Transgenic Technology and Biosensor, Department of Botany, Faculty of Science, Chulalonkorn University, Phyathai, Pathumwan, Bangkok, Thailand 10330*

[2]*Sensor Research Unit, Department of Chemistry, Faculty of Science, Chulalongkorn University, Bangkok, Thailand 10330*

[3]*Department of Chemistry, Faculty of Science, Chulalongkorn University, Thailand 10330*

[4]*Center of Excellence in Clinical Virology, Faculty of Medicine, Chulalongkorn University, Bangkok, Thailand 10330*

[5]*Food Research and Testing Laboratory, Faculty of Science, Chulalongkorn University, Phyathai, Pathumwan, Bangkok, Thailand 10330*

**E-mail: piyasakcha@yahoo.com, Tel: +66-2-218-5494*

The rapid widespread of the novel 2009 H1N1 human influenza A virus, transmissible from human to human, has raised concerns with respect to the control and the prevention of ongoing transmission. Although the most effective antiviral agent, oseltamivir (OTV), is recommended by The World Health Organization (WHO), recently it has been informed by health authorities in Denmark, Japan and the Special Administrative Region of Hong Kong, China of the appearance of novel 2009 H1N1 viruses which are resistant to the antiviral drug oseltamivir based on laboratory testing. Those oseltamivir resistant mutations in N1, were detected at position H274Y. Therefore, rapid detection of mutation at this position allowing a prompt action taken for next pandemic of potential higher resistance oseltamivir resistant H1N1 strains' preparedness is required. We have developed a genotypic identification method involving a reverse transcription polymerase chain reaction followed by rapid liquid phase hybridization using silver nanoparticles and beta-pyrrolidinyl peptide nucleic acid designed at residue H274Y which are associated strongly with oseltamivir resistance. Hybridization of probe to target DNAs allowed DNA signals to be detected visually within 20 min. Hybridization of the probe to wild type virus induced aggregation of blue silver particles whereas no such an induction was observed to those mutants. Demonstration of the test for the presence of mutants via silver nanoparticles revealed the consistency of the test compared with standard Southern hybridization. This method provides a rapid genotypic identification of the oseltamivir resistant viruses by confirmation test for the presence of mutation domain via rapid Southern hybridization's principle.

11th PACIFIC POLYMER
CONFERENCE 2009
INCORPORATING
31st AUSTRALASIAN POLYMER SYMPOSIUM
PROGRAM
Organic and Polymer Solar Cells
(satellite meeting sponsored by DIISR ISL International Consortium on Organic Solar Cells)
Inaugural Australian Microplasma Workshop
(satellite meeting sponsored by DIISR)
2nd International Symposium on Ultimate Stability
of Nanostructured Polymers and Composites
PPC11
6 – 10 DECEMBER
CAIRNS CONVENTION CENTRE,
CAIRNS, AUSTRALIA
www.ppc11.org

P298	Morphology and Properties of TPS/EVA Biomass Alloy by Melt Blending *Sheng-Ju Liao*, Jeremy Chen, Cheng Feng Liao
P299	Investigation of flow marks in PP composites *Soonho Lim*, Hyun-Deung Shin, Min-Hyung Kim, Jae-Gon Lim, Chun-Soo Lee
P300	Compositions and manufacturing of high viscosity recycle PET *Kou-Chuan Lin*
P301	Cell Repelling and Attracting Implant Surfaces respectively tailored via Plasma Polymers of Hexamethyldisiloxane and Allylamine *Alexander Lotz*, Matthias Gabriel, Jennifer Kroth, Sebastian Kuhn, Ingo Köper, Renate Förch
P302	Dielectric Relaxation of Polyvinyl Alcohol doped with nano-CdS *Salah Mahrous*, Taha Hanafy, Gomaa Khabery
P303	Vacuum Chamber with Heating Up to 300ºC Dispositive: Application on Grafting Process by Electron Beam Irradiation Pedro Cardozo, *José Manzoli*, Áurea Geraldo, Elizabeth Somessari, Carlos Silveira, Hélio Paes, Wagner Fernandes, Carlos Souza
P304	Mechanical Behavior Analysis of LDPE Foams Irradiated by Electron Beam Paulo Pirolla, Djalma Dias, *José Manzoli*, Leonardo Silva
P305	Thermal and mechanical properties of constrained polypropylene fibres *Anton Marcincin*, Marcela Hricova, Konstantin Marcincin, Alena Hoferikova, Anna Ujhelyiova
P306	Synthesis of Ion Conductive Epoxy-Based Networked Polymers *Kozo Matsumoto*, Takeshi Endo
P307	Determination of DNA Sequences using Peptide Nucleic Acid in combination with Chitosan Particles by MALDI-TOF Mass Spectrometry *Jittima Meebungpraw*, Tirayut Vilaivan, Suda Kiatkamjornwong, Voravee Hoven
P308	Radical Copolymerization of (±) Menthyl Methacrylate and Methyl Methacrylate for Polymer Optical Fibres *Eun Hee Min*, KoK Hou Wong, Mark Straton, Alexander Argyros, François Ladouceur
P309	Characterization of Methacrylate Copolymers by Means of Multivariate Analysis of 13C NMR Spectra *Hikaru Momose*, Tomoya Maeda, Tatsuya Naono, Kosuke Hattori, Tomohiro Hirano, Koichi Ute
P310	Radiation-induced crosslinking and post-processing of poly(L-lactic acid) composite *Naotsugu Nagasawa*, Noboru Kasai, Fumio Yoshii, Masao Tamada
P311	Formation of Poly(vinyl alcohol) Hydrogel under the different Freeze/thaw Cycle *Tatsuro Nakano*, Takahiko Nakaoki
P312	Neurite penetration into PCL scaffold implanted in the brain David Finkelstein, Mal Horne, John Forsythe, *David Nisbet*
P313	Molecular Structure at Cross-linking Point and Bound structure in Solvent of Isotactic Polystyrene Gel *Takuya Nishimura*, Takahiko Nakaoki
P314	Synthesis of New Epoxy Resin with Stilbene Structure into the Main Chain *Naoki Nishimura*, Masaharu Sugimoto, Hideo Honma, Hiroaki Kouzai
P315	Synthesis of polyrotaxane composedy-cyclodextrin and hydroxyl-terminated polybutadiene *Mutsuaki Numata*, Kouzai Hiroaki
P316	Novel Fabrication of Poly(Vinyl Alcohol) Hydrogel Beads by Quenching Technique *Se Heang Oh*, Cheon Soo Lim, Hye Jin Jeon, Hyun Hoon Song, Jin Ho Lee
P317	Plasmid DNA-Loaded Hydrophilized PLGA Porous Scaffold for the Chondrogenesis of Mesenchymal Stem Cells *Se Heang Oh*, Sung Hwan Jang, Kyoung Seon Yeon, Hye Joung Kim, Gun Il Im, Jin Ho Lee
P318	Electrical bistability of crossbar-structured organic memory devices based on polymer nanocomposite *Jong Hoe Oh*, Jae-eun Park, Tae-hoon Lim, Sung Chul Hong, Seungmoon Pyo, Do-Hoon Hwang
P319	Alternating Copolymerization of Bicyclic Bis(γ-butyrolactone) with Epoxides Initiated by Phosphines *Sousuke Ohsawa*, Kazuhide Morino, Atsushi Sudo, Takeshi Endo
P320	Changes of the chemical structure of isotactic-polypropylene induced by ion-beam irradiation Toshitaka Oka, *Akihiro Oshima*, Ryota Motohashi, Naoto Seto, Yuji Watanabe, Ryoji Kobayashi, Hisaaki Kudo, Takeshi Murakami, Masakazu Washio, Yoshimasa Hama
P321	Controlled Surface Grafting of Poly(tBA-co-AA) Using Atom Transfer Radical Polymerisation and the 'Grafting From' Approach *Huey Wen Ooi*, Lisbeth Grondahl, Firas Rasoul, Andrew Whittaker
P322	Surface Modification of Polymeric Materials Using Ultra Low Energy Electron Beam Irradiation *Akihiro Oshima*, Fumiya Shiraki, Masakazu Washio
P323	Ring-Opening Polymerization of ε-Caprolactone Using Rare-Earth Perfluoroalkanesulfonates and Perfluoroalkanimides *Miyuki Oshimura*, Akinori Takasu
P324	Synthesis of imine-functionalized poly(L-lysine) and recombination reaction of the side chains *Yui Ozaki*, Akio Takahashi, Toshiyuki Oyama

Determination of DNA Sequences using Peptide Nucleic Acid in combination with Chitosan Particles by MALDI-TOF Mass Spectrometry

Jittima Meebungpraw[1,2], *Tirayut Vilaivan*[3], *Suda Kiatkamjornwong*[4], *Voravee P. Hoven*[3*]

[1]Program in Petrochemistry and Polymer Science, Faculty of Science
[2]Center for Petroleum, Petrochemicals, and Advanced Materials
[3]Organic Synthesis Research Unit, Department of Chemistry, Faculty of Science
[4]Department of Imaging and Printing Technology, Faculty of Science
Chulalongkorn University, Phayathai Road, Pathumwan, Bangkok 10330, Thailand
*E-mail: treasure_jt@hotmail.com, vipavee.p@chula.ac.th**

Determination of DNA sequences are significantly important for many biotechnology-related applications ranging from medical, forensic, agriculture and food science. The concept of using a new conformationally rigid pyrrolidinyl peptide nucleic acid (PNA), strong anion-exchange captures such as commercially available Q-Sepharose in combination with MALDI-TOF mass spectrometry has been proven as a simple and effective way for single nucleotide polymorphism genotyping.[1] This research has introduced chitosan particles having different moieties as alternative anion-exchange captures that may be applicable for the same purpose. The strategy is schematically outlined in Figure 1.

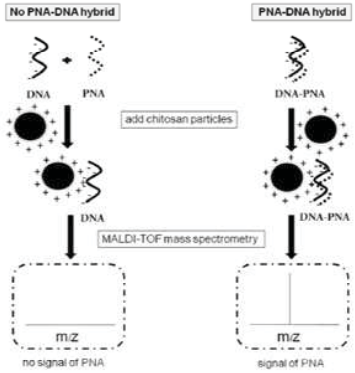

***Figure* 1:** Schematic diagram showing the concept of using chitosan particles as anion-exchange capture of PNA-DNA hybrid in combination with MALDI-TOF mass spectrometry in DNA sequence analysis

In principle, the positively charged chitosan particles can only bind ionically with the negatively charged DNA. The neutral PNA cannot be adsorbed by the particles unless it is hybridized with the negatively charged complementary DNA to form a negatively charged DNA-PNA hybrid. The facts that the complementary PNA-DNA hybrid can be selectively captured by the positively charged chitosan particles which can be easily separated from non-complementary and unhybridized PNA should allow direct detection of the PNA-DNA hybridization by MALDI-TOF mass spectrometry after washing. To test the ability of all chitosan particles as anion-exchange captures of complementary PNA-DNA hybrid, PNA1 probe, T9 was first hybridized with the DNA target (listed in Table 1), followed by an addition of the designated chitosan particles. MALDI-TOF analysis of all particles (except DMBz) after being washed by deionized water, shown in Figure 2, revealed mainly the signal of PNA1, only when the complementary DNA1 (D9) was employed. There were no signals detected in the cases of both single-mismatched (A8C) and full-mismatched (F2) DNA targets suggesting the specificity of the detection. The success of analysis was further

demonstrated by the fact that there was no appearance of PNA1 signal in the absence of the hybridized DNA implying that there were no non-specific interactions between the positively-charged particles and the neutral and uncharged PNA1. And that the PNA1 can only be linked to the particles through the hybridization with the complementary DNA that was later attracted ionically to the particles. However, the mismatch discrimination cannot be realized in the case of the DMBz particles. The signals of PNA1 probe were seen on the particles regardless of the mismatching of the DNA target. This non-specific interactions are believed to stem from the presence of hydrophobic benzyl moieties introduced to the DMBz particles. Among all particles tested, HTACC particles seem to give the best performance considering that they did not exhibit non-specific interactions with PNA2 probe, so that the detection of PNA1 was possible even in the presence of PNA2. It should be noted that the signal of PNA1 and PNA2, typically appear at m/z 3180 and 3260, respectively. That was not the case for CS, QAC, and DMBz particles. The hydrophilic hydroxyl groups which is a part of quaternary ammonium groups render the HTACC particles superior anion-exchange captures.

Table 1 PNA and DNA sequences used in this study

Code	Sequence	Note
PNA1 (T9)	Ac-TTTTTTTTT-LysNH_2	-
DNA (A9)	d(5'-AAAAAAAAA-3')	complementary to PNA1
DNA (A8C)	d(5'-AAAACAAAA-3')	single-mismatch to PNA1
DNA (F2)	d(5'-AGTGATCTAC-3′)	full-mismatch to PNA1
PNA2 (A9)	Ac-AAAAAAAAA-LysNH_2	-

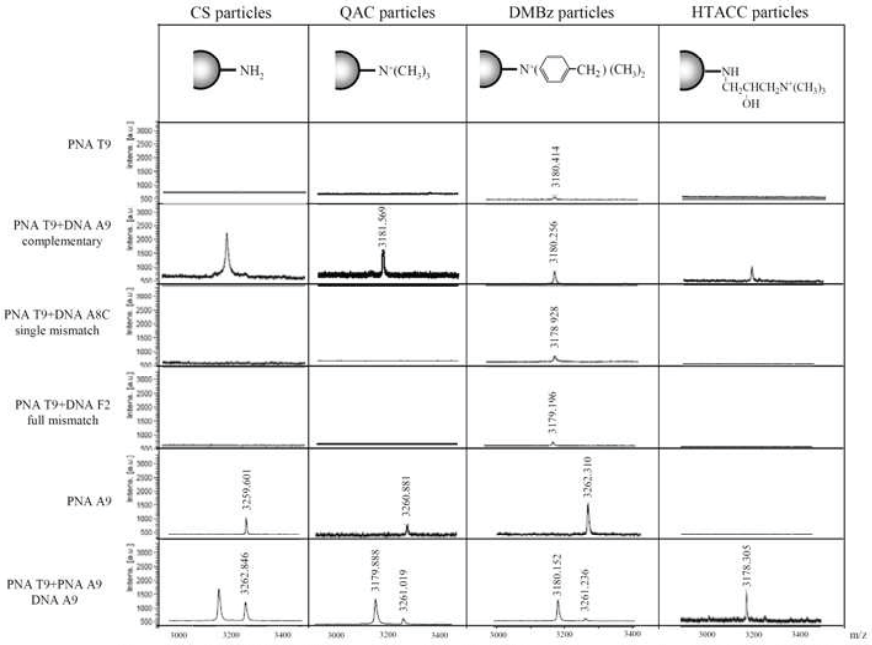

Figure 2: MALDI-TOF mass spectra of particles after capturing the PNA-DNA hybrid

References

[1] Boontha, B.; Nakkuntod, J.; Hirankarn, N.; Chumpluk, P.; Vilaivan, T. *Anal. Chem.* **2008,** *80*, 8178-8186.

[2] Hoven, V. P.; Tangpasuthadol, V.; Angkitpaiboon, Y.; Vallapa, N.; Kiatkamjornwong, S. *Carbohydr. Polym.* **2007,** 68(1), 44-53.

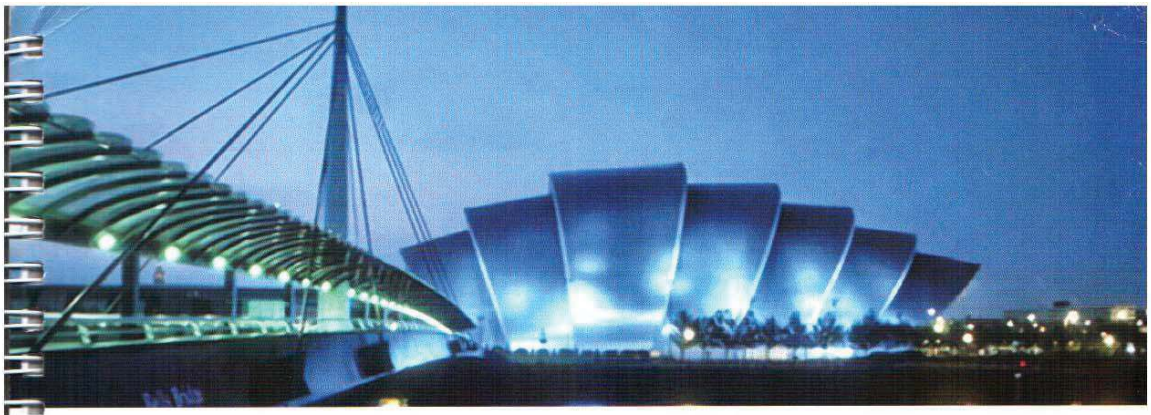

BIOSENSORS2010

20TH ANNIVERSARY WORLD CONGRESS ON BIOSENSORS

26-28 May 2010 • Glasgow, UK

Organised and Sponsored by

ELSEVIER

Cranfield UNIVERSITY

Main Sponsor

ERCON

www.biosensors-congress.elsevier.com

Thursday, 27 May 2010

	Room A – Clyde Auditorium	*Room B – Forth*	*Room C - Boisdale*	*Room D - Alsh*
09:00	**Plenary Session 4** Chair: Prof Frieder Scheller, University of Potsdam, Germany			
09:00	04.1 Stimuli-responsive materials - their role in the realisation of next generation autonomous sensing devices **Prof Dermot Diamond**, *Dublin City University, Ireland*			
09:40	04.2 Active arrays **Prof Frank Bier**, *IBMT, Germany*			
10:20	***Refreshments & Poster Session 2 Viewing***			
11:00	**Parallel Session 5A** **Nanobiosensors, nanomaterials & nanoanalytical systems** Chair: Prof Harold Craighead, Cornell University, United States	**Parallel Session 5B** **DNA chips & nucleic acid sensors** Chair: Dr Ulrich Rant, Technical University Munich, Germany	**Parallel Session 5C** **Proteomics, single-cell analysis and electronic noses** Chair: Prof Patricia Connolly, University of Strathclyde, United Kingdom	**Parallel Session 5D** **Enzyme-based biosensors** Chair: Prof Loïc Blum, University of Lyon, France
11:00	05A.1 Single nanosensors based on molecularly imprinted polymer nanocomposites as synthetic receptors, and on plasmonic enhancement K Haupt*[1], Y De Wilde[2], M Bompart[1]; [1]Compiègne University of Technology, France, [2]ESPCI ParisTech, France	05B.1 Magnetic luminescent nanoparticle-nucleic acid sensors for environmental applications KR Hristova*, A Son, D Dosev, IM Kennedy; University of California, Davis, United States	05C.1 Ligand fishing in human plasma using SPR biosensors and mass spectrometry P Ducoroy*[2], A Rouleau[1], G Lucchi[2], L Sylvius[2], C Elie-Caille[1], W Boireau[1], et al; [1]Université de Franche-Comté, France, [2]Centre Hospitalier Universitaire Dijon, France	05D.1 Random micro-confinement of bacteria into picolitre emulsion droplets for rapid detection and enumeration by enzymatic activity determination PR Marcoux*[1,2], M Dupoy[1,2], R Mathey[1,3], A Novelli Rousseau[1,3], PL Joly[1,2], F Rivera[1,2], et al; [1]bioMérieux - CEA Joint Team, France, [2]Commissariat à l'Energie Atomique (CEA), LETI, MINATEC, France, [3]bioMérieux Grenoble, France
11:20	05A.2 An interference localized surface plasmon resonance sensor specialized for the detection of biomolecular interactions HM Ha, H Yoshikawa, E Tamiya*; Osaka University, Japan	05B.2 Studying PNA interactions with duplex DNA using surface plasmon resonance technique C Ananthanawat*[1], V Hoven[1], T Vilaivan[1], X Su[2]; [1]Chulalongkorn University, Thailand, [2]Institute of Materials Research and Engineering, Singapore	05C.2 Label-free sub-picomolar protein detection with extended-gate field-effect transistors P Estrela*[1], D Paul[2], LKJ Stadler[3], L Wang[4], P Ko Ferrigno[3], P Migliorato[2], et al; [1]University of Bath, United Kingdom, [2]University of Cambridge, United Kingdom, [3]Leeds Institute of Molecular Medicine, United Kingdom, [4]Rutherford Appleton Laboratory, United Kingdom	05D.2 A new amperometric bienzymatic biosensor based on biocomposites for determination of gluconic acid in wines X Ceto, F Cespedes, M del Valle*; Autonomous University of Barcelona, Spain

[05B.2]

Studying PNA interactions with duplex DNA using surface plasmon resonance technique

C Ananthanawat*[1], V Hoven[1], T Vilaivan[1], X Su[2]

[1]*Chulalongkorn University, Thailand,* [2]*Institute of Materials Research and Engineering, Singapore*

Peptide nucleic acids (PNAs) are DNA mimics, in which the negatively charged sugar-phosphate backbone of DNA is replaced by a neutral polyamide backbone. Due to their electrically neutral backbone, PNAs have superior hybridization properties (high affinity and specificity) relative to their DNA counterparts. In addition, PNA can bind to duplex DNA to form higher-order complexes that render them important reagents in antisense/antigene therapy and in drug discovery.

In this contribution, the application of surface plasmon resonance (SPR) technique for studying the binding of PNA to duplex DNA is reported for the first time. We have developed SPR protocols to verify the sequence rules and binding conditions (pH and ionic strength) of conventional homopyrimidine and homopurine PNA in forming PNA/DNA_2 complexes with different structural identifications (triplex formation and duplex invasion) (Figure 1). With the real-time SPR measurement, we have quantified the PNA hybridization efficiency, determined PNA binding directions (antiparallel vs parallel), distinguished sequence dependent structural identifications of the PNA/DNA_2 complexes, and evaluated the binding kinetics identified by the binding mode.

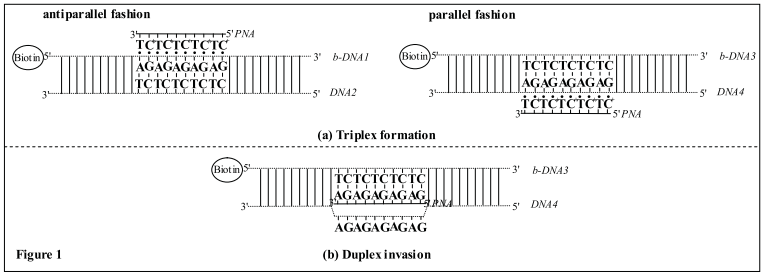

Figure 1

We have correlated the SPR results to those obtained using other conventional methods to demonstrate the utility of the SPR technique for studying higher-order nucleic acids complexes on solid-liquid interface. Based on the protocols developed for the conventional PNA bearing *N*-(2-aminoethyl) glycine linkages, we have extended the study to another synthetic PNA bearing a conformationally rigid D-prolyl-2-aminocyclopentane-carboxylic acid (acpc) backbone. This is the first report on the acpcPNA's dsDNA binding properties.

Keywords: peptide nucleic acid, surface plasmon resonance, triplex formation, duplex invasion

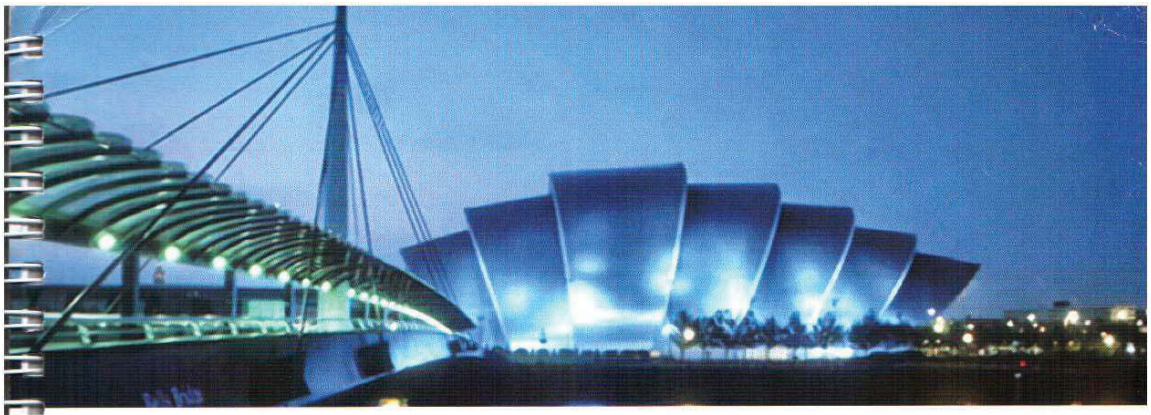

BIOSENSORS2010

20TH ANNIVERSARY WORLD CONGRESS ON BIOSENSORS

26-28 May 2010 • Glasgow, UK

Organised and Sponsored by

ELSEVIER

Cranfield UNIVERSITY

Main Sponsor

ERCON

www.biosensors-congress.elsevier.com

[P3.2.009] **High sensitivity glucose biosensors based on patterned single-walled carbon nanotube electrodes using transfer printing and photolithograpy**
CW Park*[1], SG Kim[2], MJ Kim[2], CJ Lee[2], NK Min[2], [1]*Kangwon University, Korea, Republic of*, [2]*Korea University, Korea, Republic of*

[P3.2.010] **Amperometric biosensor based on cellobiose dehydrogenase from the ascomycete corynascus thermophilus (ctCDH) for detection of glucose**
MN Zafar[1], F Tasca[1], G Nöll[2], W Harreither[3], R Ludwig[3], L Gorton*[1], [1]*Lund University, Sweden*, [2]*Siegen University, Germany*, [3]*BOKU-University of Natural Recources and Applied Life Sciences Vienna, Austria*

[P3.2.011] **Immobilization of biomolecules by a new affinity system based on biotin and poly(pyrrole-nitrilotriacetic acid-Cu^{2+}) film.**
J Baur[1], M Holzinger[1], S Cosnier*[1], [1]*Université Joseph Fourier-CNRS, France*

[P3.2.012] **Imaging protein kinases involved in cell proliferation and cancer progression through intracellular delivery of fluorescent peptide biosensors**
L Kurzawa[1], M Pellerano[1], MC Morris*[1], [1]*University of Montpellier, CRBM-CNRS UMR5237, France*

[P3.2.013] **Cytochrome c loaded mesoporous indium tin oxide (ITO) superoxide biosensor**
S Frasca*[1], BM Smarsly[2], JJ Feng[3], P Hildebrandt[3], A Thomas[3,4], U Wollenberger[1], [1]*University of Potsdam, Germany*, [2]*Justus Liebig University, Germany*, [3]*Technical University of Berlin, Germany*, [4]*Max Planck Institute of Colloids and Interfaces, Germany*

[P3.2.014] **Pesticide biosensors using acetylcholinesterase immobilized on carbon nanotubes**
Y Gao*[1], I Kyratzis[1], R Taylor[1], C Huynh[1], M Hickey[1], [1]*CSIRO Materials Science and Engineering, Australia*

[P3.2.015] **Fabrication of multiwalled carbon nanotubes/polyaniline modified Au electrode for ascorbic acid determination**
N Chauhan*[1], J Narang[1], CS Pundir[1], [1]*M D University Rohtak, India*

[P3.2.016] **Construction of a laccase biosensor for phenolic compound detection**
E Tastan[1], K Kazmanli[1], FN Kok*[1], [1]*Istanbul Technical University, Turkey*

[P3.2.017] **Enzymatic amplified calorimetric detection of DNA following "Dot Blot" format employing filter paper functionalized with quaternized polymer brushes and peptide nucleic acid probe**
P Srikaenjun*[1], T Vilaivan[1], VP Hoven[1], [1]*Chulalongkorn University, Thailand*

[P3.2.018] **An amperometric lactate biosensor based on a screen-printed carbon electrode containing Meldola`s Blue-Reinecke salt, coated with lactate dehydrogenase and NAD^+, for flow injection analysis of lactate in serum**
M Piano*[1], S Serban[2], R Pittson[2], GA Drago[1], JP Hart[3], [1]*Gwent Group (Applied Enzyme Technology Ltd), United Kingdom*, [2]*Gwent Group (Gwent Electronic Materials Ltd), United Kingdom*, [3]*University of the West of England, United Kingdom*

[P3.2.019] **Investigation into pulsed laser technology for the fabrication of microelectrodes and micro-biosensors**
LJ Jones*[1], S Serban[1], RW Pittson[1], JP Hart[2], [1]*Gwent Group (Gwent Electronic Materials Ltd), United Kingdom*, [2]*University of the West of England, United Kingdom*

[P3.2.020] **Development of a biosensor based on screen-printed carbon electrodes for the determination of inorganic phosphate for applications in biomedical and environmental samples**
L Gilbert*[1], JP Hart[1], ATA Jenkins[2], S Browning[3], [1]*University of the West of England, United Kingdom*, [2]*University of Bath, United Kingdom*, [3]*The Environment Agency, United Kingdom*

[P3.2.021] **Sensitivity and long-term stability of an amperometric enzyme based gas sensor for formaldehyde**
M Hämmerle*[1], T Falkner[1], K Hilgert[1], S Achmann[1], R Moos[1], [1]*University of Bayreuth, Germany*

[P3.2.022] **Nitrite biosensors based on catalase coated surfaces containing insulated silicon structures**
A Zazoua[1], H Bétatache[1], J Bausells[1], A Errachid*[1], N Jaffrezic-Renault[1], [1]*Jijel University, Algeria*, [2]*Centro Nacional de Microelectronica Barcelona, Spain*, [3]*Université Lyon 1, France*

[P3.2.023] **Improved poly-pyrrole based biosensors using EIS as electrochemical technique of detection**
D Zane[1], C Bianchini*[1], A Curulli[1], GB Appetecchi[2], S Passerini[3], [1]*CNR Institute for Nanostructured Materials, Italy*, [2]*ENEA, Italy*, [3]*University of Muenster, Germany*

[P3.2.024] **Electroanalysis of chemical modifications on acetylcholinesterase**
V Dounin*[1], K Kerman[1], [1]*University of Toronto, Canada*

[P3.2.025] **Direct detection of enzyme-catalyzed product by FET sensor with ferrocene modified electrode**
Y Ishige*[1], S Takeda[1], M Kamahori[1], [1]*Hitachi Ltd, Japan*

[P3.2.017]

Enzymatic amplified calorimetric detection of DNA following “Dot Blot” format employing filter paper functionalized with quaternized polymer brushes and peptide nucleic acid probe

P Srikaenjun*, T Vilaivan, VP Hoven
Chulalongkorn University, Thailand

As inspired by the “Dot blot” technique, a well known method in molecular biology and genetics for detecting biomolecules, a new PNA-based colorimetric detection of DNA sequence has been developed. Positively charged membrane to be used for DNA blotting was prepared by surface-initiated polymerization of 2-(dimethylamino)ethyl methacrylate on filter paper followed by quaternization with methyl iodide. Using a recently developed living radical polymerization process, activators regenerated by electron transfer for atom transfer radical polymerization (ARGET ATRP), the molecular weight and the positive charge density along the chain of the resulting polymer brushes of quaternized poly(dimethylamino)ethyl methacrylate (PQDMAEMA) can be tailored. The fact that the polymerization can be performed under a limited amount of air using a ppm level of metal catalyst in the presence of reducing agent without a need for rigorous deoxygenation truly adds simplicity to the method.

Following the “Dot blot” format, a DNA target was first captured via ionic interactions between the positive charges of the PQDMAEMA brushes and the phosphate backbone of DNA. Upon hybridization with biotinylated peptide nucleic acid probe (b-PNA), the immobilized DNA can be detected by naked eye observation of the yellow product generated by the enzymatic amplification employing HRP-labelled streptavidin. In this particular study, a synthetic PNA bearing a conformationally rigid D-prolyl-2-aminocyclopentanecarboxylic acid backbone (acpcPNA) was used as a probe to detect a region of human *IL-10* promoter gene. It has been demonstrated that this newly developed assay was capable of discriminating a single base mismatch. Due to its simplicity, rapidity and inexpensiveness, it is believed that this format of detection can be implemented into a high-throughput fashion, a highly desirable feature of biosensor.

Keywords: calorimetric detection, peptide nucleic acid probe, polymer brushes, Dot Blot

PACCON

SWU 2011

January 5-7, 2011

Miracle Grand Hotel
Bangkok, Thailand

PACCON

PURE AND APPLIED CHEMISTRY INTERNATIONAL CONFERENCE 2011

ABSTRACTS

Sustainable Development: from Basic to Applied Chemistry

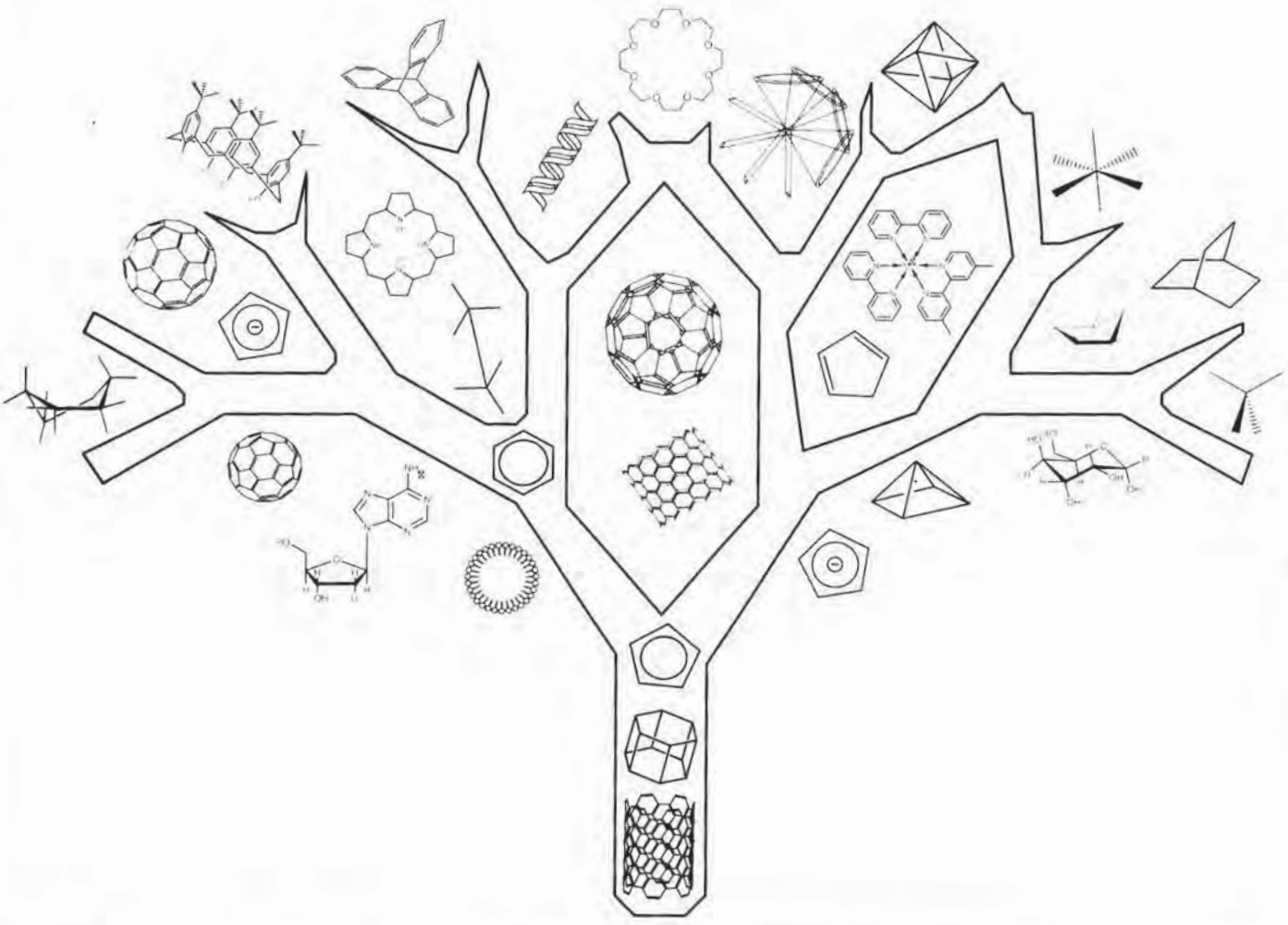

Organized by

Supported by

OM_O0017: Synthesis and nucleic acid binding properties of novel pyrrolidinyl peptide nucleic acid carrying 3-aminopyrrolidine-4-carboxylic acid spacer

Nisanath Reenabthue[1], Tirayut Vilaivan[2], Chaturong Suparpprom[1]
[1]*Department of Chemistry, and Center of Excellence for Innovation in Chemistry, Faculty of Science, Naresuan University, Phitsanulok 65000, THAILAND.*
[2]*Department of Chemistry, Faculty of Science, Chulalongkorn University, Bangkok 10330, THAILAND.*

Peptide nucleic acid (PNA) is a DNA mimic in which the deoxyribose phosphate backbone was substituted with a peptide chain. In this research, novel pyrrolidinyl PNA carrying 3-aminopyrrolidine-4-carboxylic acid (*aza-acpc*) spacers were synthesized. These spacers were designed based on our previously reported PNA system bearing (1*S*,2*S*)-2-aminocyclopentanecarboxylic acid (*acpc*) spacer, with additional nitrogen atom in the cyclopentane ring of the β-amino acid. It is expected that the new spacer will improve the solubility of the PNA and provide a handle for internal modification. The *trans*-(3*R*,4*S*)- and (3*S*,4*R*)- isomers of N^3-Fmoc/N^1-Boc-protected *aza-acpc* were synthesized following a known route. Diatereoselective reductive amination of the keto-ester intermediate, obtained via a Diekmann cyclization of Boc-glycine ethyl ester, with (*S*)- and (*R*)-α-methylbenzylamine followed by protecting group exchange gave the (3*R*,4*S*)- and (3*S*,4*R*) isomers of the protected spacers in 6.5% and 4.9% overall yield, respectively. These spacers have been successfully incorporated into model PNA sequences by Fmoc solid phase peptide synthesis. Successful incorporation of the new spacers was confirmed by MALDI-TOF MS. DNA binding studies by T_m measurement of two PNA sequences, each of which was modified with a single *aza-acpc* unit in the middle of the strand, suggested that the *trans*-(3*R*,4*S*)-*aza-acpc* spacer was compatible with the original PNA backbone carrying (1*S*,2*S*)-2-aminocyclopentanecarboxylic acid (*acpc*) spacer as shown by their essentially unchanged T_m. The possibilities of incorporation of fluorophores such as pyrene in the middle of the PNA strand via the N^1 position of the aza-acpc spacer is under investigation.

OM_O0018: Isolation of alkaloids from crude extract of longan leaves, *Dimocarpus longan Lour.*

Nattawut Jaiboon, Jamjuree Jino, Apiwat Baramee and Sairoong Saowsupa*
Department of Chemistry, Faculty of Science, Chiang Mai University, Chiang Mai, Thailand 50200
**E-mail: ssairoong@chiangmai.ac.th, Tel: +66-5-394-3341 ext.307*

Thai longan leaves, *Dimocarpus longan Lour.* cultivars Dor, and Heaw, were dried and powdered. The powdered plants were subjected to extract with three different solvents, *n*-hexane, CH_2Cl_2 and MeOH. The antibacterial activities showed that the methanol extracts of these cultivars exhibited significantly against *E. coli*, *P. aeruginosa* and *S. aureus* with diameters of inhibition zone of 10, 18, 14 mm and 10, 16.5, 12 mm, respectively. According to the interesting biological activities, the methanol extracts were subjected to extract by dichloromethane and then 4% acetic acid (pH 2-2.5). Crude alkaloids were isolated and detected with Dragendoff's reagent. By the use of chromatographic technique, the isolated alkaloids were studied by Infrared spectroscopy (IR), Nuclear Magnetic Resonance (NMR), and Mass spectrometry (MS).

OM_O0020: Pentacyclic triterpenoids and steroids from the rhizomes of *Agapetes Hosseana* diels

P. Kornwongwan and S. Luangkamin*
Department of Chemistry and Centre for Innovation in Chemistry (PERCH-CIC), Faculty of Science, Chiang Mai University, Chiang Mai 50200, Thailand
**E-mail: suwaporn@chiangmai.ac.th*

Agapetes hosseana Diels, locally named Saphaolom, belongs to the family ERICACEAE. Its rhizomes have been use in traditional medicine for nourishment after having a fever. Three pentacyclic triterpenoids (1-3) and two steroids (4-5) were isolated from the dichloromethane extract of the dried rhizomes of *Agapetes hosseana* Diels. Their structures were determined to be taraxerone (1), taraxerol (2), 3-acetyl oleanolic acid (3), β-sitosterol (4) and stigmast-4-en-3-one (5), by

PACCON

SWU 2011

January 5-7, 2011

Miracle Grand Hotel
Bangkok, Thailand

PACCON

PURE AND APPLIED CHEMISTRY INTERNATIONAL CONFERENCE 2011

ABSTRACTS

Sustainable Development: from Basic to Applied Chemistry

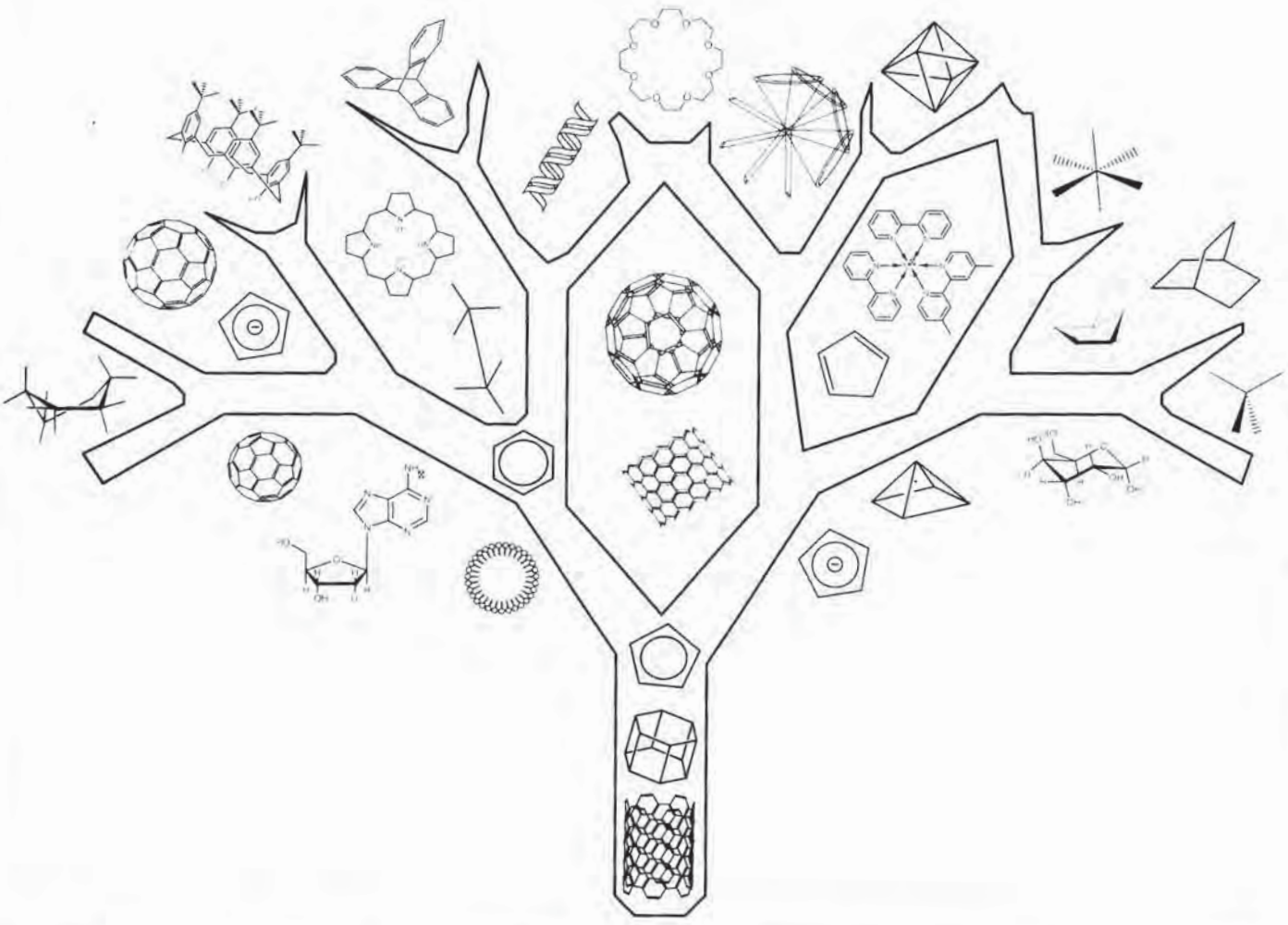

Organized by

Supported by

OM_O0040: Anionic water soluble terphenylene diethynylene fluorophores

Kunnigar Vongnam[1] Tirayut Vilaivan[2] Mongkol Sukwattanasinitt[2] and Paitoon Rashatasakhon[2]*
[1] *Program of Petrochemistry and Polymer Science, Faculty of Science, Chulalongkorn University*
[2] *Department of Chemistry, Faculty of Science, Chulalongkorn University*
**E-mail:paitoon.r@chula.ac.th, Tel: +66-2-2187620*

Dendritic water soluble fluorophores containing terphenylene diethynylene units and carboxylic group as anionic peripheries are designed and synthesized. The synthesis relies on a regioselective tri-iodination of triphenylamine and a Sonogashira cross-coupling with trimethylsilylacetylene. Removal of the protecting group provides a dendritic core in 78% yield. Starting from hydroquinone, a series of alkylation, iodination, and Sonogashira coupling with methyl 4-ethynylbenzoate give rise to the dendritic arms in moderate to good yields. The Sonogashira coupling between the core and an excess amount of dendritic arm gave rise to a zeroth generation dendrimer. All of the compounds synthesized were characterized by ^{1}H, ^{13}C NMR, and mass spectrometry. The photophysical properties of these novel fluorophores and a preliminary screening for metal ion sensing will also be presented.

OM_O0042: Gas chromatography-mass spectrometry and comprehensive two-dimensional gas chromatography analysis of organic components in bio-oil from tea waste

Rueansap Charoenphon[1*], Sugunya Wongpornchai[1] and Suparin Chaiklangmuang[2]
[1]*Department of Chemistry, Faculty of Science, Chiang Mai University, Chiang Mai, Thailand 50200*
[2]*Department of Industrial Chemistry, Faculty of Science, Chiang Mai University, Chiang Mai, Thailand 50200*
**E-mail: Rueansap.cha@gmail.com*

Bio-oil is a renewable liquid fuel that is produced from biomass by pyrolysis process. The chemical composition of each bio-oil type relies on many factors, such as biomass type and pyrolysis conditions. In this study, pyrolysis of tea waste using temperature of 600 °C, heating rate of 10 °C/min and hold time of 3 hr yielded two layers of bio-oil samples, which were then subjected to analysis of their chemical compositions by GC-MS and GC×GC technique. Results revealed the detection of 78 and 42 components in the top and bottom layer, respectively. Among these, there were 65 and 36 identified components, respectively. The major components of bio-oil samples from the top layer and the bottom layer were phenolics. However, hydrocarbons that were found only in the top layer of the tea waste bio-oil accounted for 23 % of the total content. When GC×GC was applied to analysis of the tea waste bio-oil samples, additional components were detected which resulted in the total of at least 296 and 136 components found in the top and bottom layer, respectively. In comparison with GC-MS, GC×GC showed greater ability to differentiate the quality of bio-oils in terms of their chemical compositions.

OM_O0043: Microbial transformation of α-mangostin

Panarat Arunrattiyakorn [1*], Sunit Suksumrarn [1], Nuttika Suwannasai [2] and Hiroshi Kanzaki [3]
[1]*Department of Chemistry, Faculty of Science, Srinakharinwirot University, Bangkok 10110, Thailand*
[2]*Department of Biology, Faculty of Science, Srinakharinwirot University, Bangkok 10110, Thailand*
[3]*The Graduate School of Natural Science and Technology, Okayama University, Okayama 700-8530, Japan*
**E-mail: panarata@swu.ac.th*

Recently, mangosteen products have become widely commercially available and are highly popular because of their perceived role in enhancing human health. The major secondary metabolite of mangosteen fruits is α-mangostin (**1**), a tetraoxygenated diprenylated xanthone which exhibit various biological activities including antibacterial, antifungal, anti-inflammatory, antimycobacterial, antioxidant, antiplasmodial, and cytotoxic activities. It also exhibited potential as a possible cancer chemopreventive compound. Thus α-mangostin has attracted much attention recently. In the present study, the microbial transformation of **1** by endophytic fungi was investigated. Our aims are to obtain various structurally modified derivatives of **1** that might increase the bioactivity by microbial metabolic activation and to attain a better understanding of microbial model metabolism of **1**. Incubation of **1** with *Colletotrichum gloeosporioides* (EYL131) gave four new xanthone derivatives

PACCON

SWU 2011

January 5-7, 2011

Miracle Grand Hotel
Bangkok, Thailand

PACCON

PURE AND APPLIED CHEMISTRY INTERNATIONAL CONFERENCE 2011

ABSTRACTS

Sustainable Development: from Basic to Applied Chemistry

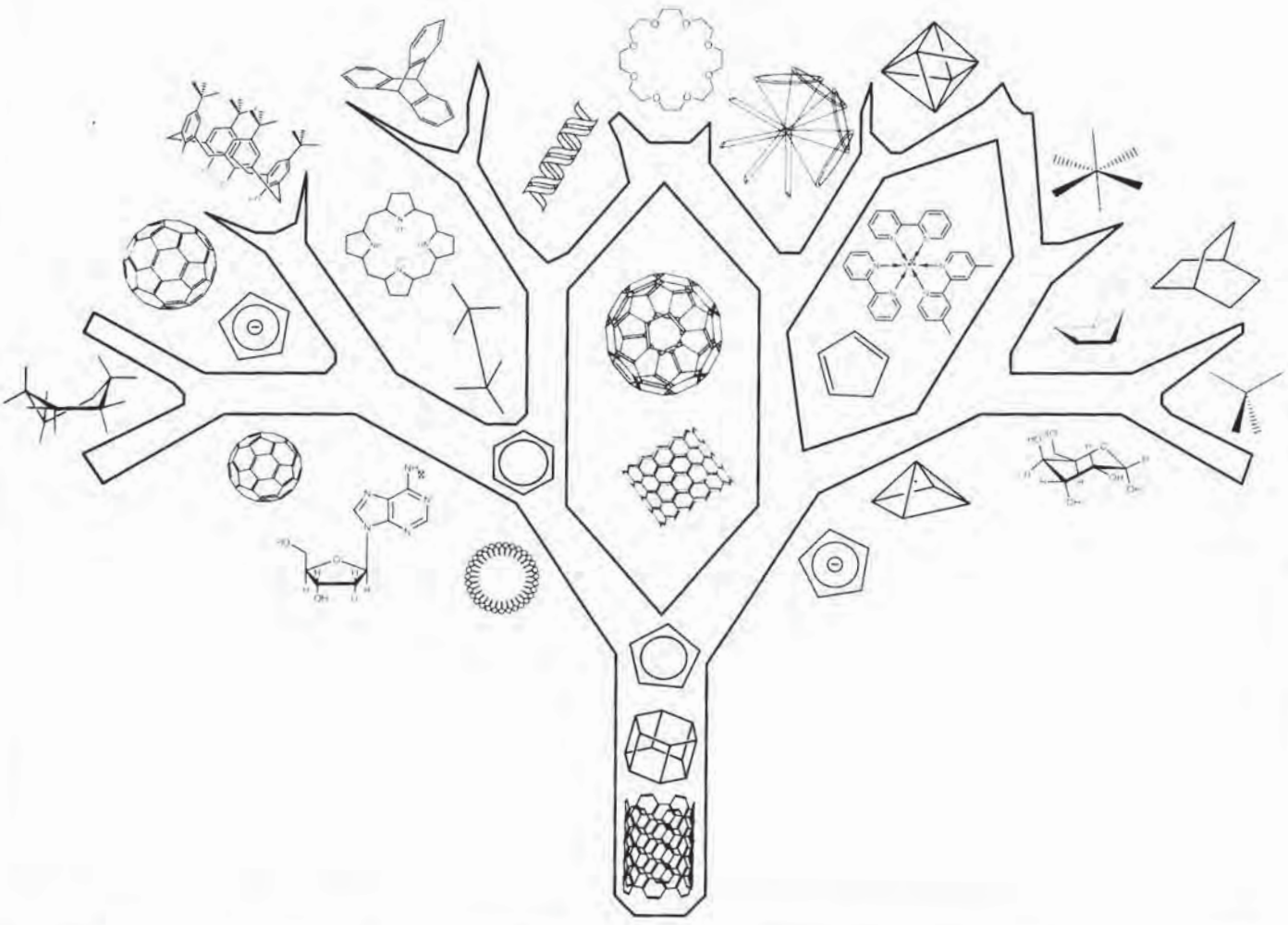

Organized by

Supported by

weight reduction. To avoid using toxic metal containing catalysts, we envisioned introduced phthalic anhydride as a covalent linker into the system under the same heating condition. Thermal degradation significantly decreased. Furthermore, melting temperature and processing temperature were also reduced, while decomposition temperature was elevated. Other mechanical properties were also characterized in order to adjust the optimum condition to chemically modify PHB to fit various application requirement such as coating materials, adhesives, plastic film and biocomposites. Moreover, this method can also be used to increase molecular weight block copolymers as linear, grafted or cross-linked depending on type of alcohols used instead of PEGs.

MN_M0072: Synthesis of poly(4-vinylpyridine) *via* atom transfer radical polymerization (ATRP) from surface of magnetite nanoparticle

Metha Rutnakornpituk[1*], Teerawat Inpotha[1], Boonjira Rutnakornpituk[1], Uthai Wichai[1], Tirayut Vilaivan[2]
[1] *Department of Chemistry and Center of Excellence for Innovation in Chemistry, Faculty of Science, Naresuan University, Phitsanulok, 65000 Thailand*
[2] *Department of Chemistry, Faculty of Science, Chulalongkorn University, 10330 Thailand*
**E-mail:methar@nu.ac.th*

Surface modification of magnetite nanoparticle (MNP) with a covalently bonded poly(4-vinylpyridine) (P4VP) shell *via* surface initiated atom transfer radical polymerization (ATRP) is presented herein. MNPs were prepared by thermal decomposition of $Fe(acac)_3$ in benzyl alcohol. An ATRP initiating site, BTPAm (2-bromo-2-methyl-N-(3-(triethoxysilyl)propyl)propanamide), was then covalently bound onto the surface of the particles through a combination of a ligand exchange reaction and condensation of triethoxysilane. An ATRP of 4-vinylpyridine mediated by copper bromide catalyst and PMDETA (1,1,4,7,7-pentamethyldiethylenetriamine) ligand was carried out in dioxane for 24 h. The presence of P4VP coated on the particles was verified by fourier transform infrared spectroscopy (FT-IR). Transmission electron microscopy (TEM) disclosed that the average particle size was about 8 nm in diameter. These hybrid nanoparticles were well dispersible in acidic solutions especially at the range of pH 1-3. Effect of the solution pH on their surface charge and hydrodynamic diameter was investigated *via* photocorrelation spectrophotometry (PCS). As decreasing the solution pH from 2.5 to 0.5, its hydrodynamic diameter gradually decreased from 220 to 52 nm, while its zeta potential continuously increased from 38 to 55 mV. This was attributed to the presence of positively charged repulsion of protonated surface of the P4VP-coated MNP. Their magnetic properties were determined via vibrating sample magnetometry (VSM). Percent of P4VP and MNP in the complexes were revealed using thermogravimetric analysis (TGA). It was observed that, as increasing the ATRP reaction time, percent of P4VP in the complexes increased due to the high content of polymeric P4VP coated on the MNP core.

MN_M0077: Titanium dioxide coated zinc oxide compound for dye-sensitized solar cells

Rungroj Tuayjareon [1*] Tarinee Nootong [1,2] Tanattha Rattana [1] Prayoon Suapadkron [1,2], Panita Chinvetkitvanich [1,2] Tula Jutarosaga [1,2*] Pichet Limsuwan [1,2]
[1] *Department of Physics, Faculty of Science, King Mongkut's University of Technology Thonburi, 126 Pracha-uthit Rd, Bangmod, Tungkru, Bangkok, Thailand 10140*
[2] *Thin Film Technology Research Laboratory, ThEP Center, CHE, 328 Si Ayutthaya Road, Ratchathewi, Bangkok, 10400*
**E-mail:s1400503@kmutt.ac.th, tula.jut@kmutt.ac.th*

Metal oxide nanowires were successfully fabricated via vapor-solid-liquid (VLS) mechanism at 630°C on indium tin oxide/borosilicate glass for a dye-sensitized solar cell (DSSC) application. The crystallinity and the morphology of synthesized nanostructure were verified using X-ray diffraction (XRD) technique and scanning electron microscopy (SEM), respectively. XRD confirmed that the synthesized material consist of face-center cubic Zn_2SnO_4, hexagonal ZnO and tetragonal SnO_2. SEM showed wire-like nanostructures having the height and the diameter of 61 μm and 61±22 nm. respectively. Before applying as electrode for DSSCs, the nanowires were then coated with TiO_2 thin film via D.C. magnetron sputtering process. The electrical characteristics of the fabricated cell under

Polymer Preprints, Japan

Vol.59, No.2

59th SPSJ Symposium on Macromolecules
Sapporo, Japan
September 15-17, 2010

高分子学会 THE SOCIETY OF POLYMER SCIENCE, JAPAN

1Pd074 Preparation and functions of temperature-responsive dendrimers encapsulating gold nanopartides
Keishi Takeda,Eiji Yuba,Atsushi Harada,Kenji Kono 4801

1Pc075 Preparation and Investigation of Solution Behavior of Thermosensitive Polypeptide with Sulfobetaine Group
Akihiro Banno,Hideki Sugimoto,Katsuhiro Inomata,Eiji Nakanishi 4802

1Pd076 Preparation and aggregation behavior of thermo-responsive block copolymer containing polypeptide
Takahito Osawa,Mina Endo,Hideki Sugimoto,Katsuhiro Inomata,Eiji Nakanishi 4803

1Pc077 Design of temperature-responsive vesicles using poly(amidoamine) dendron-based lipids
Yuki Hiranaka,Eiji Yuba,Atsushi Harada,Kenji Kono 4804

1Pd078 Neural differentiation of NT2 cells usmg microwell chip
Yukiko Yoshiura,Shirou Yoshida,Kohji Nakazawa 4805

1Pc079 Preparation and function of dual-signal-responsive liposomes based on hyperbranched poly(glycidol)s with temperature- and pH-sensitive properties
Tomohiro Kaiden,Eiji Yuba,Atsushi Harada,Yuichi Sakanishi,Kenji Kono 4806

1Pd080 Synthesis and Evaluation of Alginate Hydrogel Using Self-assembly beta-Strand Peptides
Naotaka Nishimura,Yoshiaki Hirano 4807

1Pc081 The interacdon and tumor delivery of porfimer sodium, a photosensitive agent, by poly(L-lysine)-graft-polyethyleneglycol
Arihiro Kano,Izumi Nakamura,Kenji Moriyama,Naohiko Shimada,Atsushi Maruyama 4808

1Pd082 Effect of polymer backbone structure on antigen dehvery function of pH-sensitive polymer-modified liposomes
Eiii Yuba,Atsushi Harada,Yuichi Sakanishi,Shinobu Watarai,Kenji Kono 4809

1Pc083 Interaction of novel phenylboronic acid containing polymers with glycoproteins
Yuki Inami,Taka-aki Asoh,Akihiko Kikuchi 4810

1Pc085 Development of Polyamine-Lipid Conjugates for Gene Transfer and Resolution of Transfection Mechanism
Kiyoshi Kato,Takehisa Dewa,Misa Uchida,Yusuke Kozuma,Kouji Iida,Tomohiro Asai,Naoto Oku,Mamoru Nango 4811

1Pd086 Using poly(acrylic acid) brushes as SPR-Precursor layer for DNA sensor
Piyaporn Akkahat,Wanwimon Mekboonsonglarp,Suda Kiatkamjornwong,Tirayut Vilaivan,Voravee Hoven 4812

1Pc087 Functional Cycloamylose far Nucleic acid Delivery System
Savaka Toita,Kazunari Akiyoshi 4813

1Pd088 Role of Ionic States of Cationic lipids in the Stability of Assemblies and their Transfection Efficiency
Satya Ranjan Sarker,Shinji Takeoka 4814

1Pc089 Stimuli-responsiveness of polyion complex nanoparticles coinposed of hydrophobically-modified poly(amino acid).
Kazuki Watanabe,Takami Akagi,Mitsuru Akashi 4815

1Pd090 Design of acid-labile nanogels
Savaka Hirano,Nobuyuki Morimoto,Shigeru Shimizu,David H. Thompson,Kazunari Akiyoshi 4816

1Pc091 Design and Biodistribution Analysis of Novel PEGylated Iron Oxide Nanoparticles for Tumor Diagnosis and Treatment
Kodai Ujiie,Naoki Kanayama,Masao Kamimura,Shogo Sumitani,Mikio Kishimoto,Hideto Yanagihara,Yusuke Ohara,Keiichi Yamada,Shinji Hashimoto,Tatsuya Oda,Nobuhiro Ohkochi,Eiji Kita,Yukio Nagasaki 4817

1Pd086

Using Poly(Acrylic Arid) Brushes as SPR-Precursor Layer for DNA Sensor

Akkahat, P.[1,2], Mekboonsonglarp, W.[3], Kiatkamjornwong, S.[4], Vilaivan, T.[5] and Hoven, V. P.[5]
([1]Program in Petrochemistry, Faculty of Science, [2]Center for Petroleum, Petrochemicals, and Advanced Materials, [3]Scientific and Techuological Research Equipment Center, [4]Department of Imaging and Printing Technology, Faculty of Science, [5]Organic Synthesis Research Unit, Department of Chemistry, Faculty of Science, Chulalongkorn University, Bangkok, 10330, Thailand)

Introduction Development of DNA biosensor largely relies on the probe immobilization on the sensing surface in order lo maximize the sensitivity and specificity.[1,2] This research introduces "surface-initiated atom transfer radical polymerization" (SI-ATRP) as alternative way to produce a precursor layer of poly(acrylic acid) (PAA) brushes on SPR sensor chip (3D chip). It is anticipated that the 3 0 platform based on the nuface–tetheredPAA brushes should yield high binding capacity to sensing probe aud subsequently give high DNA tiytmdization response.

Experiments PAA brushes were prepared on SPR chip via SI-ATRP of sodium acrylate in aqueous solution at room temperature. The chip was seated in the SPR cell. PNA probes were immobilized on PAA brushes by two procedures. After the probe immobilization, the 50 μM of target DNA was then applied.

Results and Discussion The direct covalent attachment of streptavidin on PAA brushes via amine coupling showed the highest PNA probe binding. Subsequently, the PNA probes were employed for the detection of DNA hybridization. As shown in Fig. 1. the hybridization with complementary DNA (A9) provided the highest SPR angle shift and the angle shift decreased with increasing number of mismatched bases in the target DNA. This result suggests that this sensing platform showed highly specific detection.

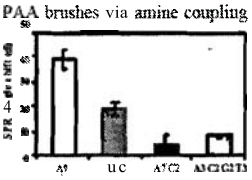

Figure 1 SPR angle shifts of hybridization reaction between PNA probe immobilized 3D directed with complementary and mismatched DNAs

[1] Mannelli, I. et al. Bioelectrochemistry 2005, 66, 129.
[2] Wang, Q. et al. Sens. Actuators B: Chem. 2007, 123, 227.

Using Poly(Acrylic Acid) Brushes as SPR-Precursor Layer for DNA Sensor

Akkahat, P.[1,2], Mekboonsonglarp, W.[3], Kiatkamjornwong, S.[4], Vilaivan, T.[5], and Hoven, V. P.[5] ([1]Program in Petrochemistry, Faculty of Science, [2]Center for Petroleum, Petrochemicals, and Advanced Materials, [3]Scientific and Technological Research Equipment Center, [4]Department of Imaging and Printing Technology, Faculty of Science, [5]Organic Synthesis Research Unit, Department of Chemistry, Faculty of Science. Chulalongkorn University, Bangkok, 10330, Thailand) [1]Tel: +81-8-04232-2623, E-mail: akkahat_p@yahoo.com

Key Word: Poly(Acrylic Acid) Brushes, DNA, SPR, Biosensor.

Abstract: Carboxyl groups along poly(acrylic acid) (PAA) brushes attached to the surface of gold-coated glass substrate served as precursor moieties for immobilization of peptide nucleic acids (PNA), synthetic DNA analogues to act as sensing platform for DNA analysis using surface plasmon resonance (SPR) technique. Surface-modified PAA brushes were obtained by surface initiated atom transfer radical polymerization (SI-ATRP) of sodium acrylate monomer in aqueous solution at room temperature. Two immobilization procedures were employed; (1) specific recognition of streptavidin on biotin immobilized PAA brushes and (2) direct covalent attachment of streptavidin on PAA brushes via amine coupling. The streptavidin molecules have available sites for further binding with biotinylated PNA (biotin-PNA probe) via streptavidin-biotin bridge chemistry. The 9-mer single-stranded PNA (5'-biotin-egl-TTT TTT TTT-LysNH$_2$-3') was chosen for probe immobilization. According to SPR analysis, it was found that the direct covalent coupling of streptavidin on PAA layer provided greater number of binding sites for biotin-PNA than the streptavidin layer adsorbed on the biotin immobilized PAA brushes. Subsequently, the biotinylated PNA probes were employed for the detection of DNA hybridization. The sensing platform showed highly specific detection towards the complementary DNA in 10 mM PBS at 25°C. This investigation has demonstrated the potential of the PAA brushes as SPR-precursor layer for PNA-based DNA sensing applications.

JAIST
JAPAN
ADVANCED INSTITUTE OF
SCIENCE AND TECHNOLOGY
1990

JAIST 20th ANNIVERSARY

7th International Symposium on Advanced Materials in Asia-Pacific

JAIST International Symposium on Nano Technology 2010

Sep.30 – Oct.1, 2010

Ishikawa High-Tech Exchange Center, Ishikawa, Japan

Book of Abstracts

Japan Advanced Institute of Science and Technology (JAIST)

17:00-17:20 A107 Prof. Nantanit Wanichacheva, Silpakorn Univ.
Rhodamine-based fluorescent and colorimetric chemosensors for the selective and rapid detection of mercury (II) ions

17:20-17:40 A108 Prof. Radzali Othman, USM
Dry mechanosynthesis of carbonate-substitued hydroxypatite

18:00-20:00 Room C
Banquet

Oct. 1 (Friday)

8:30-8:50 Registration (Entrance)

Room A
Chair Prof. S. Maenosono (JAIST)

9:00-9:20 B211 Prof. T. Matsushima, JAIST
Enhancement of hole injection at organic/organic heterojunction interface due to control of molecular orientation

9:20-9:40 B212 Dr. Mohammad Ferdows, Japan Atomic Energy Agency
Reverse Monte Carlo simulation approach on the structure of C59N

9:40-10:00 B213 Dr. Lee Siew Ling, UTM
Nanocrystalline bismuth phosphate material synthesized via hot injection method

10:00-10:20 B214 Prof. Mariatti Jaafar, USM
Flexural properties of hybrid nano silver and micron silver in epoxy composites for conductive adhesive application

10:20-10:40 Coffee Break

Chair Prof. Nantanit Wanichacheva, Silparkorn Univ.

10:40-11:00 B215 Prof. Voravee P. Hoven, Chulalongkorn Univ.
The power of polymer brushes in biosensing applications

11:00-11:20 B216 Dr. Anawat Ajavakom, Chulalongkorn Univ.
The novel synthetic method for 1,4-dihydropyridine and its application for fluorescent chemosensor

G1-6 Thichamporn Eaidkong, Chulalongkorn Univ.
Colorimetric paper based array from polydiacetylenes: new sensor platform for volatile organic compounds

G1-7 Sasikarn Ampornpun, Chulalongkorn Univ.
Effect of methylene chain length on the thermochromic behaviors of PDAs containing diamido groups

G1-8 Nadda Booranabunyat, Chulalongkorn Univ.
Quaternized chitosan particles prepared by self assembly of amphiphilic chitosan

G1-9 Arithat Leuchai, Chulalongkorn Univ.
Synthesis of triazine containing porphyrin as photoactive compounds for solar cells

G1-10 Kanlaya Phaphon, Chulalongkorn Univ.
Acid catalyzed tautomerization of 1,3-dihydroxyacetone to lactic acid

G1-11 Sukanya Jiamworanunkul, Chulalongkorn Univ.
Fluorescent marker derived from cardanol

G1-12 Paweena Ekkaphan, Chulalongkorn Univ.
Rigid polyurethane foams from seed oils

G1-13 Sathaporn Poonsawat, Chulalongkorn Univ.
Physical properties of maleated polylactide/functionalized multiwall carbon nanotube composites

G2-1 Lalita Nammueng, Chulalongkorn Univ.
Theoretical study of olefination of carbonyl compounds catalyzed by copper oxide-pillared montmorillonite

G2-2 Parisa Dumrongsakda, Chulalongkorn Univ.
Theoretical investigation of conversion of ethanol to ethylene over transition metal ions ZSM-5 catalysts

G2-3 Suphat Korkiatithaweechai
Controlled release of diclofenac from pH-sensitive matrix polymer of chitosan and oxidized konjac glucomannan

G2-4 Kulwadee Pinwattana, Chulalongkorn Univ.
Application of CdSe quantum dots for biological labeling

G2-5 Wijitar Dungchai, Chulalongkorn Univ.
Wax for new fabrication method to use in microfluidic system

The power of polymer brushes in biosensing applications

Vipavee P. Hoven[1*], *Piyaporn Akkahat*[2,3], *Paethong Srikaenjan*[2,3], *Tirayut Vilaivan*[1], *Suda Kiatkamjornwong*[4]

[1]Organic Synthesis Research Unit, Department of Chemistry, Faculty of Science, Chulalongkorn University, Bangkok 10330, Thailand
[2]Program in Petrochemistry, Faculty of Science, Chulalongkorn University, Bangkok 10330, Thailand
[3]Center for Petroleum, Petrochemicals, and Advanced Materials, Chulalongkorn University, Bangkok 10330, Thailand
[4]Department of Imaging and Printing Technology, Faculty of Science, Chulalongkorn University, Bangkok 10330, Thailand
*Tel: (02) 218-7627 ext 102, Fax. (02) 218-7598, E-mail: vipavee.p@chula.ac.th

Abstract

Development of biosensor largely relies on the immobilization of bioactive species to sensor or measurement platforms. The density of immobilized bioactive species significantly affects sensitivity, detection limit of biosensor. This research introduces "grafting from" or "surface-initiated polymerization" as an alternative approach to produce functional precursor matrices for immobilizing biomolecules. Using "living" atom transfer radical polymerization (ATRP), the functional group density along the chains of polymer brushes can be tailored as a function of polymerization condition. Biosensing applications of two specific polymer brushes will be presented. The first system relies on poly(acrylic acid) (PAA) brushes. Using surface plasmon resonance (SPR) technique, the potential of the PAA brushes for the biosensing applications based on specific molecular recognition between biotin and streptavidin can be demonstrated. The analyte detectability as a function of immobilized probe density, swellability of the PAA brushes will be discussed. The second system is based on positively charged polymer brushes of quarternized poly(2-(dimethylamino)ethyl methacrylate) (QPDMAEMA). As inspired by the "Dot blot" technique – a well known method in molecular biology and genetic for detecting biomolecules, the cellulose membrane-grafted QPDMAEMA, that was prepared by ATRP process, was used for capturing the DNA target via ionic interactions between the positive charges along the chain of PQDMAEMA and the phosphate backbone of DNA. Upon hybridization with its complementary neutral peptide nucleic acid probe which was tagged with biotin (b-PNA), the immobilized DNA can be detected by naked eye observation of the yellow staining generated by the enzymatic amplification employing HRP-labeled streptavidin. Preliminary results are available on the detection of target DNA causing a well-recognized autoimmune disease, SLE.

Keywords: polymer brushes, biosensor, ATRP, DNA, biotin, streptavidin.

G 1-8

Quaternized chitosan particles prepared by self assembly of amphiphilic chitosan

Nadda Booranabunyat[1,2], *Voravee P. Hoven*[3*]

[1] Program in Petrochemistry and Polymer Science, Faculty of Science, Chulalongkorn University, Bangkok 10330, Thailand

[2] Center for Petroleum, Petrochemicals, and Advanced Materials, Chulalongkorn University, Bangkok 10330, Thailand

[3] Organic Synthesis Research Unit, Department of Chemistry, Faculty of Science, Chulalongkorn University, Bangkok 10330, Thailand

* Tel: (02) 218-7627 ext 102, Fax. (02) 218-7598, E-mail: vipavee.p@chula.ac.th

Abstract

Phthaloyl (Ph), hexanoyl (Hex) and dodecyl (Dod) -groups as hydrophobic entities and poly(ethylene glycol) (PEG) and *N*-[(2-hydroxyl-3-trimethylammonium)]propyl (HTAP) as hydrophilic entities were immobilized on chitosan backbone via chemical reactions of amino and hydroxyl groups, respectively. Degree of substitution (%DS) of each functional group was determined by ^{1}H NMR. Formation of particles was then induced by self assembly of the resulting amphiphilic chitosan derivatives upon dialysis in water. Unlike the chitosan particles having HTAP moieties, a subsequent heterogeneous methylation was necessary to introduce positively charged quaternary ammonium groups to the chitosan particles having PEG moieties. In this research, effects of molecular weight of chitosan, type of hydrophobic and hydrophilic groups as well as relative %DS of hydrophobic/hydrophilic groups on the particle size/morphology were determined.

Keywords: chitosan particles, self-assembly, quaternary ammonium groups.

PACCON

SWU 2011

January 5-7, 2011

Miracle Grand Hotel
Bangkok, Thailand

PACCON
PURE AND APPLIED CHEMISTRY INTERNATIONAL CONFERENCE 2011

ABSTRACTS

Sustainable Development: from Basic to Applied Chemistry

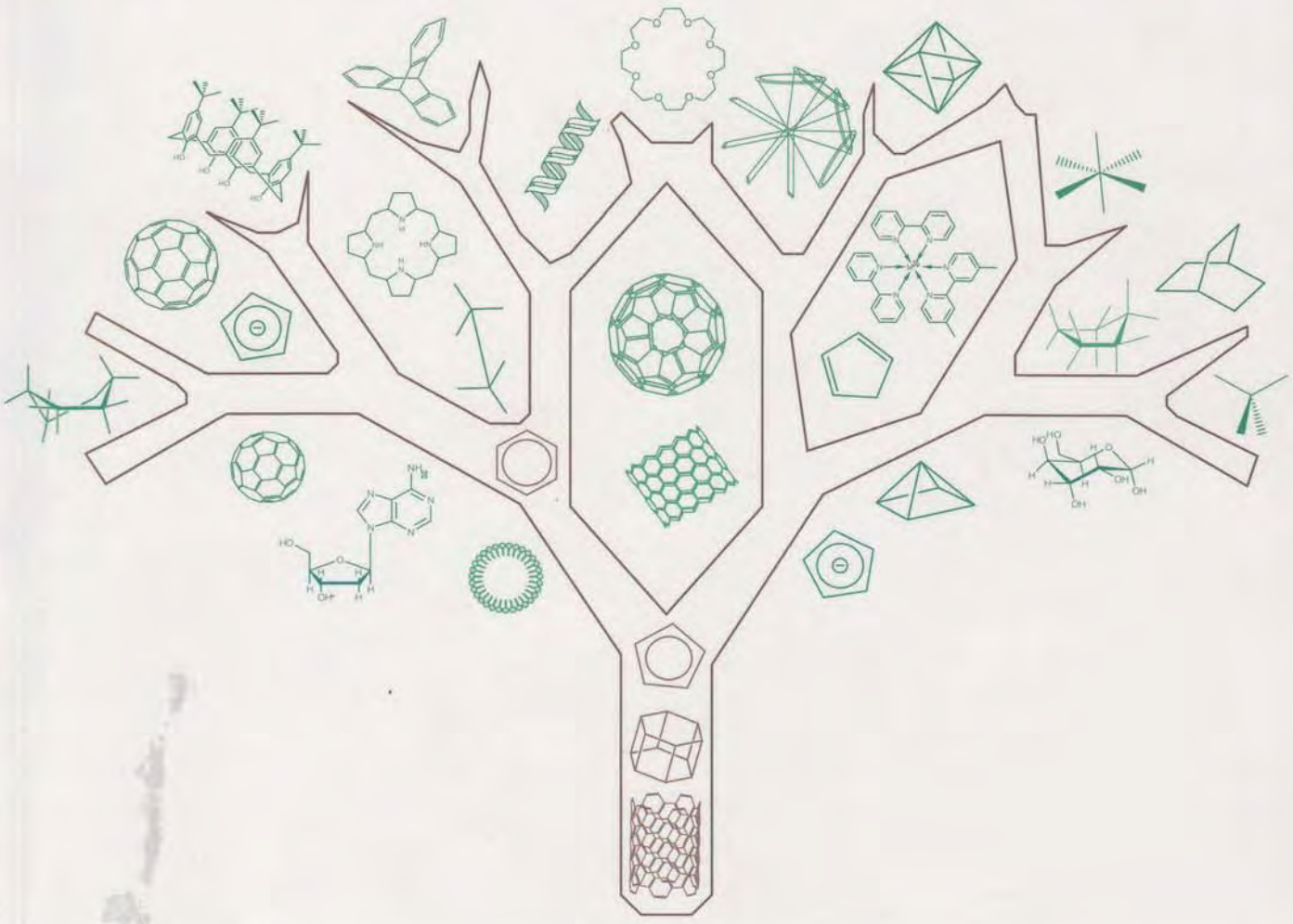

Organized by

Supported by

International Year of CHEMISTRY 2011

NSTDA

SHARP

BRUKER

NANOTEC

THAILAND convention & exhibition bureau

FRIDAY: January 7th, 2011

Time	*Miracle Grand ballroom*						
09.00-09.40	**Plenary lecture IV** Chairperson: Prof. Dr. Apichart Suksamrarn Prof. Dr.Timothy C. Gallagher Title: "Cytisine – From Synthesis to Smoking Cessation"						
09.40-10.20	**Plenary lecture V** Chairperson: Prof. Dr. Apichart Suksamrarn Prof.Dr.Thawatchai Tuntulani Title "Synthetic Molecular Sensors and Devices Based on Calix[4]arene Derivatives"						
10.20-10.35	Coffee break						
	Miracle Grand A room	**Miracle Grand B room**	**Gemini room**	**Virgo room**	**Leo room**	**Libra room**	**Mar room**
	Material Science and Nanotechnology 1	**Analytical Chemistry**	**Organic Chemistry and Medicinal Chemistry**	**Petroleum Chemistry and Catalysis**	**Inorganic Chemistry**	**Cosmetics**	**Polymer Chemistry**
10.35-11.05	Invited Lecture MN-INV-4: Gamolwan Tumcharern	Invited Lecture AC-INV-9: Warakorn Limbut	Invited Lecture OM-INV-7: Jay S. Siegel	Invited Lecture PC-INV-2: Tawan Sooknoi	Invited Lecture IC-INV-1: John H. K. Yip	Invited Lecture CM-INV-1: Supason Wanichwecharungruang	Invited Lecture PM-INV-4: Voravee Hoven
11.05-12.05	MN-OR-26 MN-OR-27 MN-OR-28 MN-OR-29	Invited Lecture AC-INV-10: Wijitar Dungchai AC-OR-15 AC-OR-16	Invited Lecture OM-INV-8: Boon-ek Yingyongnarongkul OM-OR-9 OM-OR-10	PC-OR-10 PC-OR-11 PC-OR-12	IC-OR-1 IC-OR-2 IC-OR-3 IC-OR-4	Invited Lecture CM-INV-2: Rapepun Wititsuwannakul CM-OR-1 CM-OR-2	PM-OR-15 PM-OR-16 PM-OR-17 PM-OR-18
12.05-13.00	Lunch at the Jupiter room (3rd Floor)						
13.00-16.00	Best Poster Award and Closing Ceremony at *Miracle Grand ballroom*						

EXCURSION:

PM-INV-4

Featuring Biosensing Applications of Chitosan

Pornpen Sae-ung[1] Jittima Meebungpraw[1]
Gamolwan Tumcharern[2] Tirayut Vilavan[3]
Suda Kiatkamjornwong[4] and Voravee P. Hoven[3]*

[1] *Program in Petrochemistry and Polymer Science, Faculty of Science, Chulalongkorn University, Bangkok, 10330, Thailand*
[2] *National Nanotechnology Center, National Science and Technology Development Agency, Thailand Science Park, Pathumthani 12120, Thailand*
[3] *Organic Synthesis Research Unit, Department of Chemistry, Faculty of Science, Chulalongkorn University, Bangkok 10330, Thailand*
[4] *Department of Imaging and Printing Technology, Faculty of Science, Chulalongkorn University, Bangkok 10330, Thailand*
**E-mail: vipavee.p@chula.ac.th*

Due to its favorable physico-chemical characteristics, chitosan (CS) has been widely used for a number of biomedical-related applications such as drug carrier, antibacterial agent. Here in this presentation, an unconventional, yet powerful application of chitosan in biosensing area is featured. It has been recently demonstrated that a large number of amino groups in the CS structure can act as both reducing and stabilizing agent for the synthesis of gold nanoparticles (AuNPs). This readily available amino functionality was capable of binding with bovine serum albumin (BSA), an antibody model. The synthesized AuNPs having BSA-modified chitosan as the stabilizing agent (BSA-CS) were stable up to more than one month but aggregated in the presence of anti-BSA due to the antigen-antibody specific interactions which can be visualized by naked eye. These results demonstrated the potential of AuNPs stabilized by biomolecule-attached chitosan as chromogenic biosensor based on the aggregation of AuNPs. Another work is related to the development of a label-free technique based on the use of a conformationally rigid pyrrolidinyl PNA having D-prolyl-2-aminocyclopentane-carboxylic acid backbones (*acpc*PNA) and quaternized chitosan particles which act as anion exchanger. Since PNA is a neutral molecule, it cannot be adsorbed by quaternized chitosan particles unless it is hybridized with the negatively charged complementary DNA to form a negatively charged DNA-PNA hybrid. The facts that the complementary PNA-DNA hybrid can be selectively captured by the positively charged quaternized chitosan particles and the particles can be easily separated from non-complementary and unhybridized PNA allow direct detection of the PNA-DNA hybridization by MALDI-TOF mass spectrometry after simple washing without the use of enzyme treatment or heating. DNA sequence determination was carried out on synthetic DNA sequences which are T9, A9 and a 14-mer, mixed base DNA of which sequence mimics mutant K-*ras* DNA, a mutated region that is associated with cancer.

ISSN 0953-8178

international immunology

AUGUST 2010VOLUME 22 SUPPLEMENT
NUMBER 1
www.intimm.oxfordjournals.org

14th International Congress of Immunology

Kobe, Japan

Day 5 (5/5)

Friday, August 27, 2010

14th ICI KANSAI 2010

OXFORD OPEN

OXFORD JOURNALS
OXFORD UNIVERSITY PRESS

international immunology AUGUST 2010VOLUME 22 SUPPLEMENT NUMBER 1
OXFORD

(OVA) as the foreign antigen, blocking murine CD32B enhanced primary but not secondary immune responses. Interestingly, IgG production was preferentially boosted with anti-CD32B mAb treatment in an adjuvant (e.g., LPS) and CD4 dependant manner, indicating that these mAbs may also act indirectly on CD4+ T cells. In experiments with human B-cell lymphoma cells and human CD32B transgenic mice, administration of anti-human CD32B mAb (AT10) was shown to have a modest effect on B cell/tumour depletion. However, when combined with rituximab, improved depletion was observed to a far greater extent than with either mAb alone. These data support the hypotheses that CD32B is a promising target for augmenting immune responses and potentiating immunotherapy of B-cell lymphoproliferative disorders.

WS/PP-095-04 Differences in functioning of neutrophil IgA receptor (FcalphaRI) and IgG receptors (FcgammaRs)

J. Bakema, L. van der Steen, C. Tuk, R. Beelen, M. van Egmond.
VUMC, amsterdam, Netherlands

Immunoglobulin A (IgA) is the principal antibody class in mucosal areas and plays a key role in mucosal defense. The Fc receptor for IgA (FcalphaRI) is expressed by myeloid cells, including neutrophils, and can trigger both pro- and anti-inflammatory responses in vitro. Despite considerable progress in understanding the role FcαRI on monocytes, functions of neutrophil FcαRI are ill-understood. We now demonstrate that cross-linking of FcαRI with monomeric serum IgA leads to active neutrophil migration through the release of leukotriene B4, which is a potent neutrophil chemoattractant. Dimeric IgA (dIgA), but neither secretory IgA, was equally capable of inducing neutrophil recruitment. Neutrophils do express the Fc receptors for IgG and signaling via IgG Fc-receptors is dependent on ITAM phosphorylation, similar to FcalphaRI signaling. However, induction of neutrophil migration was not observed when IgG was used. We are now investigating what determines the functional difference between FcalphaRI and FcgammaRs on neutrophils. In detail, we are now determining whether the observed lack of IgG mediated neutrophil migration can be explained by differences in Fc receptors, ITAM signaling or threshold of ITAM signaling.

In summary, since neutrophils are the first cells that arrive at inflammatory sites once pathogens have crossed the epithelial barrier and neutrophils are now also recognized as potent effector cells in antibody mediated cellular cytotoxicity, we propose that FcαRI is a highly important (overlooked) Fc receptor on neutrophils.

WS/PP-095-05 Human papillomavirus virus-like particles and NK cell interactions: role of CD16

V. Renoux[1], I. Langers[1], B. Clénanceau[2], M. Thiry[3], N. Antoine[4], E. Dortu[1], A. Reschner[1], J. Boniver[1], P. Delvenne[5], **N. Jacobs**[1].
[1]*GIGA-I3, University of Liège, Liège, Belgium,* [2]*Inserm U892 University of Nantes, Nantes, France,* [3]*GIGA-neurosciences, University of Liège, Liège, Belgium,* [4]*Department of Morphology and Pathology, Faculty of Veterinary medicine, University of Liège, Liège, Belgium,* [5]*GIGA-Cancer, University of Liège, Liège, Belgium*

Persistent infection with oncogenic human papillomavirus (HPV) genotypes is a necessary cause of uterine cervical cancer. Recombinant HPV L1 protein self-assembles into virus-like particles (VLP) that are morphologically and immunologically similar to native virions. These HPV-VLP were recently licensed as a prophylactic vaccine against cervical cancer. Dendritic cell activation by internalisation of HPV-VLP has been demonstrated, but despite the fact that CD16 have been described as a co-receptor for HPV-VLP, their interactions with other CD16+ cells, such as Natural Killer (NK) cells, have not been assessed.

To study HPV-VLP internalisation in NK cells, we used fluorescent HPV-VLP with flow cytometry and confocal microscopy. A weak entry of HPV-VLP in the NK cell line, NK92 (CD16-) was observed, whereas NK cells isolated from blood (CD16+) internalised HPV-VLP rapidly. We confirmed these results by electronic microscopy. Interestingly, CD16 transduction in NK92 cell line restored partially the HPV-VLP internalisation. Drugs inhibiting clathrin or caveolar virus entry pathways did not significantly affect the HPV-VLP uptake and electronic microscopy pictures suggested a macropinocytosis mechanism for HPV-VLP entry.

To test if NK activity could be influenced by HPV-VLP, we studied the lytic granule exocytosis by a CD107 assay and observed an increased cell degranulation in the presence of HPV-VLP. The expression of CD16 seemed necessary to induce the degranulation since only NK92 CD16+, and not NK92 CD16-, showed CD107 positivity.

Our results suggest that CD16 on NK cells plays a role in HPV-VLP internalisation and lytic granule exocytosis induced by HPV-VLP.

Supported by the Belgian FNRS.

WS/PP-095-06 Identification and characterization of the elusive IgM Fc receptor (FcμR)

H. Kubagawa[1], S. Oka[1], Y. Kubagawa[1], I. Torii[1], E. Takayama[1], D. Kang[1], G. L. Gartland[2], L. Bertoli[3], H. Mori[4], H. Takatsu[4], T. Kitamura[5], H. Ohno[4], J. Y. Wang[4]. [1]*Department of Pathology, University of Alabama at Birmingham, Birmingham, AL, United States,* [2]*Department of Medicine, University of Alabama at Birmingham, Birmingham, AL, United States,* [3]*Brookwood Medical Center, Birmingham, AL, United States,* [4]*RIKEN Research Center for Allergy and Immunology, Yokohama, Japan,* [5]*5Institute of Medical Science, University of Tokyo, Tokyo, Japan*

While Fc receptors (FcRs) for switched Ig isotypes have been extensively characterized, an FcR for IgM (FcμR) has defied genetic identification despite cellular evidence for its existence first published more than 30 years ago. By retroviral expression and functional cloning, we have identified a cDNA encoding a *bona fide* FcμR in human B-lineage cDNA libraries. FcμR is defined as a transmembrane sialoglycoprotein of ~60 kD, which contains an extracellular Ig-like domain homologous to two other IgM-binding receptors (the polymeric Ig receptor and Fcα/μR) but has an exclusive Fcμ-binding specificity and a high affinity (~10 nM for pentameric IgM). The cytoplasmic tail of FcμR contains conserved tyrosine and serine residues, but none of the tyrosine residues are located in the known immunoreceptor tyrosine-based activation, inhibitory or switch motifs. Upon receptor ligation with preformed IgM immune complexes, both tyrosine and serine residues in FcμR-transductants are phosphorylated. Unlike other FcRs, the major cell types expressing FcμR are adaptive immune cells, including B and T lymphocytes. After antigen-receptor ligation or phorbol myristate acetate stimulation, FcμR expression is up-regulated on B cells but down-modulated on T cells, suggesting differential regulation of its expression during B and T cell activation. Although this receptor was initially designated as Fas apoptosis inhibitory molecule 3 (FAIM3) or TOSO, our results clearly indicate that FcμR *per se* has no inhibitory activity in Fas-mediated apoptosis and that such inhibition is only achieved when anti-Fas antibody of an IgM but not IgG isotype is used for inducing apoptosis.

WS/PP-095-07 Enhanced levels of both membrane-bound and soluble forms of IgM Fc receptor (FcμR) in patients with chronic lymphocytic leukemia (CLL)

Y. Kubagawa[1], T. Motohashi[1], F. J. Li[1], L. S. Wilson[1], L. F. Bertoli[2], J. C. Barton[2], S. Barnes[1], R. S. Davis[1], H. Kubagawa[1]. [1]*University of Alabama at Birmingham, Birmingham, AL, United States,* [2]*Brookwood Medical Center, Birmingham, AL, United States*

We have recently isolated the full length FcμR cDNA encoding a 390-aa type I membrane protein (17-aa signal peptide, 236-aa extracellular region, 19-aa transmembrane segment, and 118-aa cytoplasmic tail). By using receptor-specific mAbs and IgM ligands, FcμR is defined as a transmembrane sialoglycoprotein of ~60 kD expressed on B and T lymphocytes in humans. We also identified an alternatively spliced form of FcμR cDNA derived by direct splicing of exon 4 (membrane-proximal extracellular domain) to exon 6 (cytoplasmic domain 1), excluding exon 5 (transmembrane domain). This splicing event results in a reading frame shift in exon 6, generating a novel 70-aa hydrophilic carboxyl-terminal tail, suggesting that this splice variant encodes a soluble form of FcμR (solFcμR). In this study, we examined the surface density of FcμR on B cells in blood samples from normal individuals and patients with CLL by immunofluorescence analysis and the serum levels of solFcμR by sandwich ELISA. Many CLL B cells expressed a significantly higher density of FcμR on their cell surface than normal B cells, and we are currently determining whether the level of FcμR correlates with that of CLL prognostic markers (FCRL2, ZAP70, CD38) or with the *IGHV* mutation status. Many CLL patients were also found to have high serum titers of solFcμR when compared to normal individuals. The solFcμR was resolved as an ~40 kD protein by Western blot analysis and shown by mass spectrometric analysis to be generated from the alternatively spliced FcμR transcript, rather than by cleavage of the membrane-bound form.

WS-096 Genetic factors and epidemiology of allergic diseases

Chairpersons: Mayumi Tamari, Kenji Izuhara

WS/PP-096-01 Evaluation of correlation of haptoglobin phenotypes in allergic rhinitis

H. A. Khazaei. *Zahedan medical sciences university, Zahedan, Islamic Republic of Iran*

Introduction: Haptoglobin is a plasma α2- glycoprotein that has huge biological roles mainly play in stability of Th1 and Th2 immune responses with three phenotypes as Hp1-1, Hp 2-1, and Hp 2-2. Their high frequency of each of them is associated with some diseases such as allergic diseases. The aim of this study was to determine possible association of haptoglobin phenotypes and correlation of serum IgG, IgM and IgE levels with each phenotype of patients suffering from allergic rhinitis disease.

Material and methods: This analytic and descriptive study was carried out on 240 allergic rhinitis patients and healthy control aged from 1 to 65 years old at hospitals of Zahedan city. 5 ml blood sample was taken and serum was examined for determination of Hp phenotyping by gel electrophoresis and peroxidase staining method. The amount of serum IgG, IgA and IgE level was measured by ELISA and SRID methods and data from analyzing of each immunoglobulins levels related to specific phenotype was reporting as the mean +SD.

The results and conclusion: The results of this study were indicated firstly the distribution of HP phenotypes in the study population and slightly changes in hapyoglobin phenotypes and secondly elevated of total IgE levels in patients compared to control group, was associated with Hp2-2 frequency phenotypes and this may play crucial role in the establishment of the Th2 immune reactions in patients and when this happens, it will issue new insights in terms of better diagnostic issues.

WS/PP-096-02 Immunomodulators in breast milk and development of eczema in infancy

Y. Morita[1], N. Shimojo[1], H. Ohnishi[2], M. Kawamoto[2], E. Matui[2], N. Kondo[2], Y. Kohno[1]. [1]*Department of pediatrics, Graduate School of Medicine, Chiba University, Chiba, Japan,* [2]*Department of pediatrics, Graduate School of Medicine, Gifu University, Gifu, Japan*

Objective: Our objective was to assess the relationship between development of eczema and the content of the cytokines in breast milk.

Material & methods: Nine hundred pairs of mothers and newborns were recruited to this prospective study on development of eczema. Breast milk samples were collected at 3-5days and 1 month after delivery. We asked skin condition of the babies by questionnaires at 1, 4 and 6 month. Eczema was defined as a pruritic, eczematous dermatosis, the symptoms of which lasting at least 2months. We selected 154 samples randomly (71 eczema and 83 healthy infants at age of 6month). Then we measured breast milk samples for TGF-β1, TGF-β2 and soluble CD14 (sCD14) by commercial ELISA systems and investigated relation between levels of cytokines and sCD14 in the breast milk and development of eczema at the age of 6 month.

Results: The median concentrations of sCD14 is lower in infants who suffer from eczema than healthy infants (11.8 and 14.6 ug/ml, respectively; $p < 0.01$). The median change of TGF-β1 colostrum to mature milk is lower in infants who suffer from eczema than healthy infants (-16.5 and 0.61 pg/ml, respectively; $p < 0.01$).

Conclusion: There are relations between sCD14 in colostrums, the change of breast milk TGF-β1 in a month after delivery and the development of eczema.

WS/PP-096-03 Loss of SOCS1 in B cells results in hyper IgE syndrome (HIES) and predisposes to allergy in mice

T. Kobayashi[1], Y. Matsunaga[2], M. Kawasumi[1], S. Fukuyama[2], H. Inoue[2], A. Yoshimura[3]. [1]*Center for Integrated Medical Research, Keio University School of Medicine, Tokyo, Japan,* [2]*Research Institute for Diseases of the Chest, Kyushu University, Fukuoka, Japan,* [3]*Department of Microbiology and Immunology, Keio University School of Medicine, Tokyo, Japan*

Suppressor of cytokine signaling-1 (SOCS1) is a negative regulator of cytokine responses. We have previously shown that SOCS1 deficiency in T cells and dendritic cells results in hypersensitivity to interferon-gamma (IFN-gamma) leading to stronger cellular immune responses (Th1-type responses) both in vitro and in vivo. Indeed, SOCS1 deficient mice die within three weeks after birth due to IFN-gamma-dependent severe multiorgan inflammation.

To explore the physiologic roles of SOCS1 in B cells, we generated B cell-specific SOCS1 knockout (SOCS1ΔB) mice. SOCS1ΔB mice grew normally and did not develop inflammatory disease, however, total serum IgG1 and IgE levels were significantly elevated. Antigen-specific IgE production was also augmented in SOCS1ΔB mice immunized with DNP-KLH/Alum. B cells lacking SOCS1 were highly sensitive to both IFN-gamma and IL-4 in vitro resulting in prolonged phosphorylation of STAT1 and STAT6, respectively. However, the increased levels of IgE were canceled by crossing SOCS1ΔB with STAT6-deficient but not with STAT1-deficent mice suggesting that the hyperproduction of IgE in SOCS1-deficient B cells was due to excessive activation of STAT6 pathway. To examine whether SOCS1ΔB mice were more susceptible to allergic responses, active cutaneous anaphylaxis (ACA) and OVA-induced allergic airway responses were assessed. Reflecting increased levels of IgE, ACA to DNP-hapten were enhanced in the ears of the mutant mice compared with those of WT mice. The number of eosinophils in bronchoalveolar lavage fluid was also increased in SOCS1ΔB mice after OVA challenge. These data suggest that SOCS1 levels in B cells regulate the susceptibility of mice to IgE-dependent allergic responses.

WS/PP-096-04 A simple nested sequence specific primer-polymerase chain reaction for HLA-B*1502

S. Virakul[1], P. Kupatawintu[2], R. Reantragoon[3], J. Nakkuntod[1], O. Kangwanshiratada[3], N. Hirankarn[3]. [1]*Chulalongkorn University, Bangkok, Thailand,* [2]*National Blood Center, Thai Red Cross Society, Bangkok, Thailand,* [3]*Department of Microbiology, Faculty of Medicine, Chulalongkorn University, Bangkok, Thailand*

Certain HLA alleles can be used as a pharmacogenetic marker with high specificity for Steven Johnson Syndrome (SJS) and toxic epidermal necrolysis (TEN), the life-threatening drug hypersensitivity conditions. Recently, HLA-B*1502 shows strong association with carbamazepine hypersensitivity in Asian ethnicity. Thus, the screening test for HLA-B*1502 before initiation of carbamazepine therapy is recommended. Here, we reported a simple nested sequence specific primer polymerase chain reaction (SSP-PCR) for HLA-B*1502. The nested reaction helps discriminate false positive reaction from heterozygous combination. We performed this test in the 105 blind DNA samples from the Thai Red Cross Society with known HLA-B allelic types by commercial SSP-PCR and SBT determined alleles. We can detect 25 HLA-B*1502 samples correctly and did not amplify any other HLA-B alleles ($n = 80$). Although we cannot differentiate B*1502 from some rare HLA-B alleles namely HLA-B*1577, 1585, 1588, 9521 and 9544, these alleles are very rare in the world population (<0.1%). We can consistently detect a positive result in a sample contains as little as 1 ng DNA template. The test is very sensitive and has high rate of reproducibility.

WS/PP-096-05 Childhood allergic diseases in Zimbabwe

E. N. Sibanda. *University of Zimbabwe, Harare, Zimbabwe*

The purpose of the review was to profile childhood allergic diseases amongst attendants of an Asthma, Allergy and Immune Dysfunction Clinic in Harare, Zimbabwe.

A sample of 400 patients who were not older than 15 years at presentation were included in the analysis. The history was guided by a standard questionnaire which included demographic details and a family history of atopy. The interventions were skin prick testing, serological documentation of total and allergen specific IgE. A diagnosis of an allergic condition was based on a combination of the clinical and laboratory findings.

A whole range of allergic conditions was represented in the group. The leading allergic condition was rhinitis. Others were dermatitis, asthma, conjunctivitis, urticaria and food allergy. The most commonly recurring allergen sources were house dust mites (D. pter. and D. farinae) and grass pollen. Animal dander was less frequent. Food allergen source sensitization was more common in the younger age groups. Wheat, peanut and soya were the commonest food allergen sources. However, when the patients were stratified by age, dermatitis was the commonest presentation in children under the age of two years and this was frequently associated with food allergen source sensitization.

Allergic conditions are common world-wide and are increasing in frequency in Africa. The profile of the conditions and associated allergen sources are the same in this population as in well resourced countries.

WS-097 Environmental factors in allergies

Chairpersons: Hirohisa Saito, Mubeccel Akdis

WS/PP-097-01 Involvement of innate immune cell response to allergens in the pathogenesis of allergic airway inflammation

S. Kamijo, T. Takai, T. Tokura, T. Kuhara, M. Hara, H. Ogawa, K. Okumura. *Atopy (Allergy) Research Center, Juntendo University School of Medicine, Bunkyo-ku, Tokyo, Japan*

Background: Pollens and house dust are considered as sources of immunomodulatory substances responsible for the pathogenesis of allergic diseases. Allergenic pollens contain enzymes and lipids. House dust mite major group 1 allergens and papain, an occupational allergen, are known to possess protease activity. Protease activity of papain stimulates mouse basophils to release IL-4 and is responsible to Th2 induction. We examined the response of dendritic cells and basophils to, and induction of allergic airway inflammation by, pollen grains, mite protease allergens and papain in mice.

Methods: We analyzed activity of proteases and NADPH oxidase and release of eicosanoid-like substances in allergenic pollen grains. Murine bone marrow-derived dendritic cells, basophils or mast cells were stimulated with pollen grains or mite allergens. Cytokine release, cell surface marker expression and mRNA expression were analyzed by ELISA, flowcytometry, and real-time PCR. Japanese cedar pollen grains, mite protease allergens, or papain was intranasally administered to mice.

Results: Release of proteases, and eicosanoid-like substances from pollen grains into PBS was observed. NADPH oxidase activity was detected in the pollen grains. Pollen grains induced maturation and cytokine production of dendritic cells without eliciting IL-12 production. Pollen grains and mite protease allergens induced IL-4 production of basophils similarly to papain. Intranasal administration of Japanese cedar pollen grains, mite protease allergens, and papain resulted in allergic airway inflammation.

WS/PP-097-02 Lipopolysaccharide enhances histamine responsiveness in human coronary artery endothelial cells by stimulating the expression of histamine H1 receptors

V. V. Raveendran[1], X. Tan[1], B. Levant[2], D. J. Stechschulte[1], K. N. Dileepan[1]. [1]*Department of Medicine, University of Kansas Medical Center, Kansas City, KS, United States,* [2]*Department of Pharmacology and Toxicology, University of Kansas Medical Center, Kansas City, KS, United States*

Histamine (HIS) is a major product of mast cells and basophils. HIS is well-recognized for its vasodialtory and immunomodulatory functions in allergic

PO-S13-03

Polycyclic Aromatic Hydrocarbons as Fluorescent Universal Bases in Pyrrolidinyl Peptide Nucleic Acids

Woraluk Mansawat, Chalothorn Boonlua, Chotima Vilaivan, Tirayut Vilaivan

Chemistry, Chulalongkorn University, Thailand

Polycyclic aromatic hydrocarbons are known to intercalate between base pairs of DNA duplexes. In this work, the ability of pyrene to behave as a fluorescent nucleobase surrogate in pyrrolidinyl peptide nucleic acid (acpcPNA) is evaluated. To achieve the goal, one of the nucleobase in a 12-mer acpcPNA was substituted with a pyrene-triazole unit. This could be accomplished through a Cu-catalyzed clock reaction either via a preformed monomer or a post-synthetic modification of azide-containing acpcPNA. Thermal denaturation experiments suggested that the pyrene-triazole unit can behave as a universal base in the acpcPNA system. Furthermore, the fluorescence of the pyrene chromophore is sensitive to the hybridization state of the acpcPNA as shown by a significant increase of the pyrene emission at 380 nm (up to a factor of 3) upon adding a complementary DNA carrying either A, T, C or G opposite to the pyrene.

OR-G6-11

Water-Soluble Polycationic Dendritic Fluorophores for CMC Determination and DNA Detection

Warathip Siripornnoppakhun, Nakorn Naimnont, Paitoon Rachtasakhon, Tirayut Vilaivan, Mongko Sukwattanasinitt

Organic Synthesis Research Unit, Department of Chemistry, Faculty of Science, Chulalongkorn University, Thailand

Water-soluble polycationic dendritic fluorophores containing phenyleneethynylene branches and quarternary ammonium peripheral groups were synthesized. Fluorescent enhancement of the fluorophores upon the addition of anionic, cationic or non-ionic surfactants and deoxyribonucleic acids (DNAs) are investigated. The critical micelle concentration (CMC) was determined by plotting of the fluorescent intensity against the surfactant concentration in which the signal enhancement is associated with the micellization process. Zeroth generation fluorophore also showed emission enhancement in the presence of DNAs while its signal reduction is observed in the presence of a synthetic polyanionic polymer, poly(vinyl) sulfate (PVSK). At the same negative charge (or nucleotide base) concentration, the fluorogenic response is greater for the longer DNAs suggesting that the longer DNAs interact more strongly than the shorter chains to the zeroth generation fluorophore. The DNAs however do not change the emission signal of the first generation fluorophore. The binding between the DNAs and the first generation fluorophore is recognized from the FRET signal to SBG II, a commercialized DNA binding dye. The interaction between the DNAs and these dendritic polycationic fluorophores can be applied for DNA and its specific sequence detection.

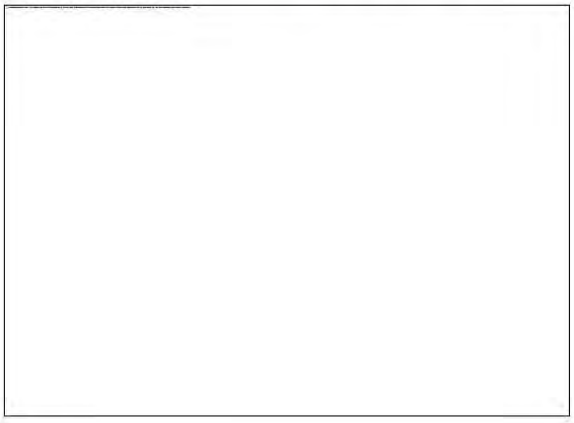

OR-G1-14

Detection of Dna Following "Dot Blot" Format Employing Filter Paper Functionalized with Quaternized Polymer Brushes and Peptide Nucleic Acid Probe

Praethong S. Laopa, Tirayut Vilaivan, Voravee P. Hoven

Department of Chemistry, Faculty of Science, Chulalongkorn University, Bangkok, Thailand

As inspired by the Dot blot technique, a well known method in molecular biology and genetics for detecting biomolecules, a new PNA-based colorimetric detection of DNA sequence has been developed. The filter paper was modified to be positively charged with grafted polymer brushes of quaternized poly(dimethylamino)ethyl methacrylate (QPDMAEMA) to be used for DNA detection. It was prepared by surface-initiated polymerization of 2-(dimethylamino)ethyl methacrylate from filter paper via ARGET ATRP followed by quaternization with methyl iodide. Following the Dot Blot format, a DNA target was first captured via ionic interactions between the positive charges of the QPDMAEMA brushes and negative charges of the phosphate backbone of DNA. Upon hybridization with biotinylated peptide nucleic acid probe (b-PNA), the immobilized DNA can be detected by naked eye observation of the yellow product generated by the enzymatic amplification employing HRP-labeled streptavidin. In this particular study, a synthetic PNA bearing a conformationally rigid D-prolyl-2-aminocyclopentanecarboxylic acid backbone (acpcPNA) was used as a probe to detect a region of human IL-10 promoter gene. It has been demonstrated that this newly developed assay was capable of discriminating a single base mismatch and the detection limit of this method was as low as 1 picomole. In addition, the QPDMAEMA grafted filter paper exhibited a superior performance to the commercial membranes, nylon 66 and nitrocellulose.

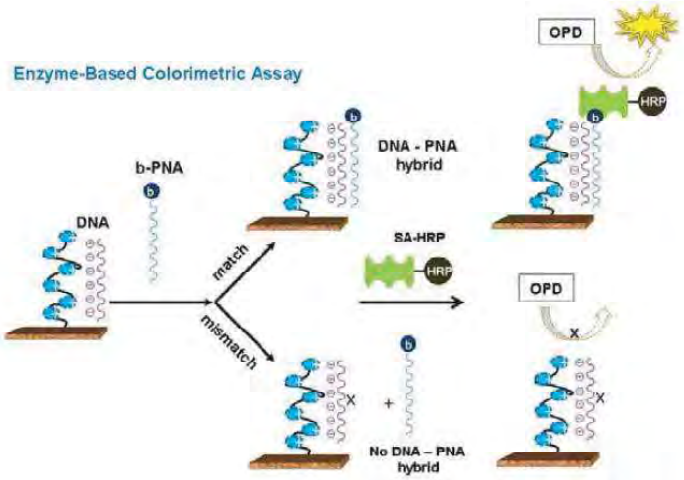

OR-G1-15

Quaternized Chitosan Particles Prepared by Self Assembly of Amphiphilic Chitosan

Nadda Booranabunyat, Tirayut Vilaivan, Voravee P. Hoven

Quaternized chitosan particles were prepared from amphiphilic chitosan containing phthaloyl groups (Ph), hexyl groups (He) or dodecyl groups (Do) as hydrophobic entities and poly(ethylene glycol) (PEG) or N-[(2-hydroxyl-3-trimethylammonium)]propyl (HTAP) as hydrophilic entities immobilized via chemical reactions of amino and hydroxyl groups, respectively. Degree of substitution (%DS) of each functional group was determined by 1H NMR. Formation of particles was then induced by self assembly of the resulting amphiphilic chitosan derivatives upon dialysis in water. Unlike the chitosan particles having HTAP moieties, a subsequent heterogeneous methylation was necessary to introduce positively charged quaternary ammonium groups to the chitosan particles having PEG moieties. In this research, the effects of type and mole ratio of hydrophilic groups and hydrophobic groups as well as relative %DS of hydrophobic/hydrophilic groups on the particle size/morphology were studied. According to SEM analysis, the mean particle size was not significantly affected by %DS variation. The particles have spherical morphology and a size range of 100-200 nm. And only the particles obtained from the amphiphilic chitosan grafted with HTAP exhibited positive charges as determined by PCS.

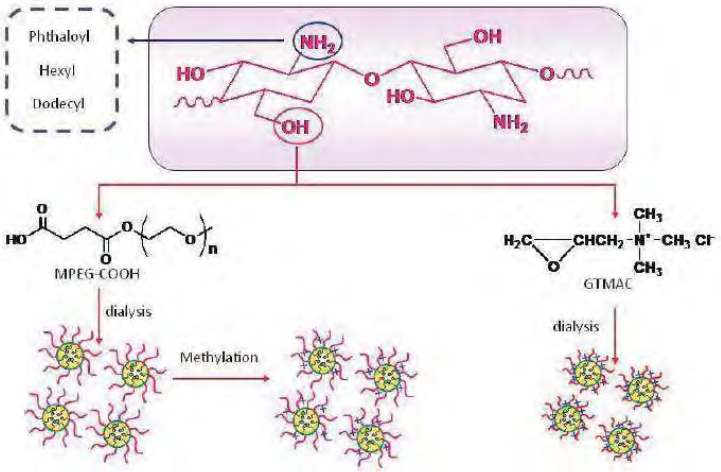

PO-G2-40

Effect of Blocking Reagents on The Capacitive Detection of PNA-DNA Hybridization

Orawan Thipmanee[1], Saluma Samanman[1], Supannee Sankoh[1], Apon Numnuam[2], Warakorn Limbut[3] , Proespichaya Kanatharana[2] , Tirayut Vilaivan[4] , Panote Thavarungkul[5]

[1]Trace Analysis and Biosensor Research Center, Prince of Songkla University, Thailand
[2]Department of Chemistry, Faculty of Science, Prince of Songkla University, Thailand
[3]Department of Applied Science, Faculty of Science, Prince of Songkla University, Thailand
[4]Department of Chemistry, Faculty of Science, Chulalongkorn University, Thailand
[5]Department of Ph, Faculty of Scienceysics, Prince of Songkla University, Thailand

A capacitive DNA sensor was investigated based on the immobilization of a peptide nucleic acid (PNA) probe on the gold electrode surface. The hybridization of PNA with its DNA target was quantified by the capacitance change at the electrode-electrolyte interface using the potentiostatic step method. The most critical step for the fabrication of this highly sensitive capacitive sensor is the insulation of the immobilized layer to prevent interference from redox couples in the electrolyte solution and high faradaic background currents. In addition the orientation of the PNA probe is also a crucial factor for DNA hybridization. Therefore, two blocking reagents of different lengths, 3-mercaptopropanol (3-MPL) and 6-mercaptohexanol (6-MHL), were studied to investigate their ability to provide an insulation layer that prevented non-specific PNA-Au interaction and also helped the PNA molecules to remain upright on the surface. That helped to increase the hybridization reaction. The lysine peptide nucleic acid (Lys-PNA) probes were immobilized on the gold electrode surface by using a self-assembled monolayer (SAM) of 11-mercaptoundecanoic acid (11-MUA) and blocked with the blocking reagent. The sensitivity (slope of the calibration curve) of the capacitive DNA sensor when using 3-MPL was 10.6 ± 0.3 nF cm^{-2} M^{-1} and 14.5 ± 0.2 nF cm^{-2} M^{-1} for 6-MHL. The results indicated that the longer alkane chain of 6-MHL used for blocking provided better signal and a greater sensitivity than the shorter chain of the 3-MPL.

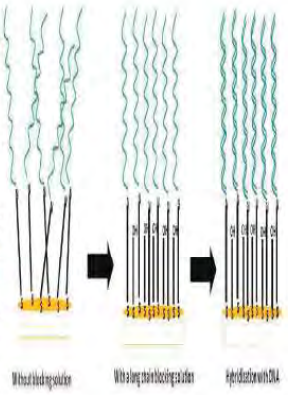

SYN-P-001

SYNTHESIS AND OPTICAL PROPERTIES OF INTERNALLY THIAZOLE ORANGE-LABELED PYRROLIDINYL PEPTIDE NUCLEIC ACID

Boonsong Ditmangklo[1], Chaturong Suparpprom[1], Tirayut Vilaivan[2,*]

[1] *Department of Chemistry and Center of Excellence for Innovation in Chemistry, Faculty of Science, Naresuan University, Phitsanulok, 65000, Thailand*
[2] *Department of Chemistry, Faculty of Science, Chulalongkorn University, Bangkok 10330, Thailand*
**Corresponding Author : vtirayut@chula.ac.th*

ABSTRACT

Thiazole orange (TO) is a cyanine dye that exhibits low quantum yield and weak fluorescence in solution. Upon binding to DNA, large fluorescence enhancements are generally observed due to restriction of the molecule in a planar conformation. In this work, an alkyne-modified thiazole orange derivative (aTO) was synthesized and incorporated internally into a pyrrolidinyl PNA consisting of an alternating sequence of nucleobase-modified D-proline/(1*S*,2*S*)-2-aminocyclopentanecarboxylic acid (acpcPNA) by our previously developed sequential reductive alkylation-click chemistry. The reductive alkylation of the acpcPNA backbone, site-specifically modified with a (3*R*,4*S*)-3-amino pyrrolidine-4-carboxylic acid (APC) spacer, was carried out on solid support by first reacting the APC-modified acpcPNA with 4-azidobutanal in the presence of $NaBH_3CN$/HOAc. The azide-modified acpcPNA was then reacted with aTO in the presence of a Cu(I) catalyst (click chemistry). The reactions were monitored by MALDI-TOF mass spectrometry, which revealed quantitative labeling in two different PNA sequences. The fluorescence of the TO-labeled acpcPNA was enhanced by a factor of 20 or more upon pairing with complementary DNA target.

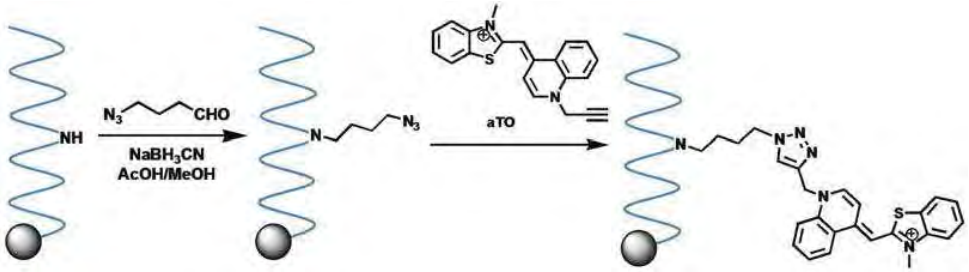

Keywords Thiazole orange dye; PNA probe; Reductive alkylation; Click chemistry; Molecular beacon

HST-P-036

A POLYCATIONIC PHENYLENE-ETHYNYLENE AS A FLUORESCENT TRANSDUCER IN AN APTASENSOR FOR POTASSIUM ION

Wannapa Yuanboonlim, Warathip Siripornnoppakhun, Paitoon Rashatasakhon, Tirayut Vilaivan, Mongkol Sukwattanasinitt*

Organic Synthesis Research Unit, Department of Chemistry, Faculty of Science, Chulalongkorn University, Bangkok, Thailand 10330
**Corresponding Author : smongkol@chula.ac.th.*

ABSTRACT

Polycationic phenylene-ethynylene fluorophore and oligonucleotide aptamers (Apt21: s(5′-GGG TTA GGG TTA GGG TTA GGG-3′) of potassium are investigated for homogeneous assay in aqueous solution for detection of potassium ion (K^+). The experiment measured affinity constants for fluorophore-aptamer complex. The analysis is based on the reduced fluorescence signals upon addition of K^+ into a fluorophore solution containing an aptamer. The aptamer forms complex with the fluorophore that enhances and blue shift its fluorescence signals probably by the reduction of geometrical relaxation process. Upon the addition of K^+, the aptamer switches to form a potassium-aptamer complex leading to the reduction of the fluorescence signal probably by the reduction of deaggregation process and the fluorescence change with the variation of K^+ concentration. The system shows selectivity toward K^+ over other ions such as Li^+, Na^+, NH_4^+, Mg^{2+}, Ca^{2+} and Sr^{2+} due to the ability of K^+ in stabilizing the G-quadruplex structure of the aptamer and shows good sensitivity due to the structure has multiple charge which is designed for strong coulombic interaction with the aptamers. The assay is rapid, simple, specific, label-free, reproducible and low costs. This test has great potential applications for analysis of K^+ in biological samples such as serum and urine.

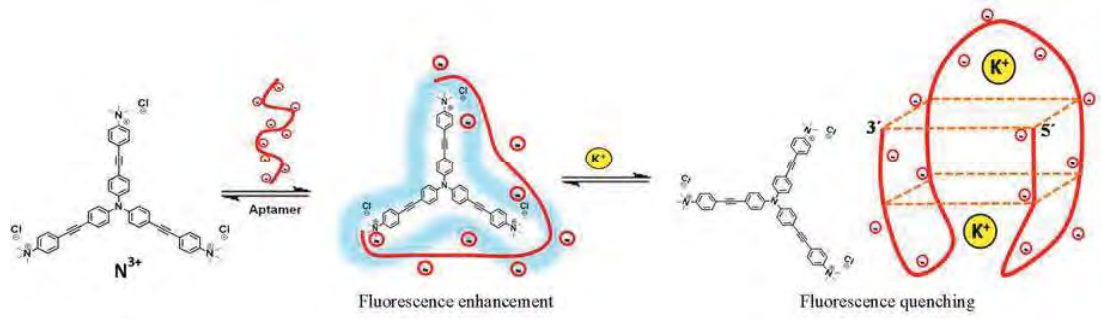

Keywords Aptamer; Fluorescence; Potassium detection; G-quadruplex

MNT-O-042

BLACKBERRY-LIKE PARTICLES ASSEMBLED FROM FLUORESCENT-LABELED QUATERNIZED AMPHIPHILIC CHITOSAN

Kanya Taboonpong[1,2], Tirayut Vilaivan[3], Voravee P. Hoven[3,*]

[1] *Program in Petrochemistry and Polymer Science, Faculty of Science, Chulalongkorn University, Phayathai Road, Pathumwan, Bangkok 10330, Thailand*
[2] *Center for Petroleum, Petrochemicals and Advanced Materials, Chulalongkorn University, Phayathai Road, Pathumwan, Bangkok 10330, Thailand*
[3] *Organic Synthesis Research Unit, Faculty of Science, Chulalongkorn University, Phayathai Road, Pathumwan, Bangkok 10330, Thailand*
**Corresponding Author : vipavee.p@chula.ac.th*

ABSTRACT

Upon self-assembly of amphiphilic chitosan having *N*-[(2-hydroxyl-3-trimethylammonium)]propyl (HTAP) as hydrophilic entities and ethynylpyrene (fluorescent dye) as hydrophobic entities, fluorescent-labeled quaternized chitosan (Pyr-CS-HTAP) particles can be formed. The functionality of the quaternized chitosan particles was verified by FT-IR and NMR spectroscopy. According to SEM analysis, the particles had a size range of 1-2 μm with blackberry-like morphology. And the particles exhibited positive charges with a zeta-potential of +40 mV as determined by PCS. The particles had bright green fluorescence and were stable in a broad pH and temperature range. These particles are developed to be used for monitoring antibacterial mechanism by fluorescence technique.

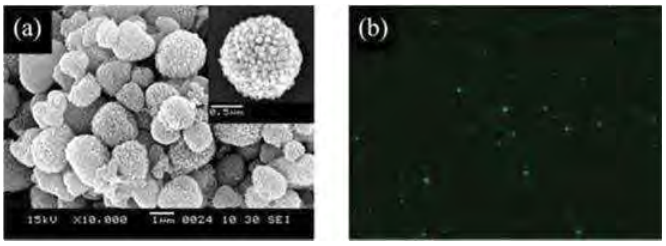

Figure 1 SEM (a) and fluorescence (b) micrographs of Pyr-CS-HTAP particles.

Keywords Self-assembly; Amphiphilic; Chitosan Particles; Fluorescent-labeled; Blackberry-like

MNT-P-291

DEVELOPMENT OF SIGNAL AMPLIFICATION METHOD ASSISTED BY POLYMERIZATION FOR DNA DETECTION

Praethong Laopa[1,2], Tirayut Vilaivan[3], Voravee P. Hoven[*]

[1] *Program in Petrochemistry, Faculty of Science, Chulalongkorn University, Phayathai Road, Patumwan, Bangkok 10330*

[2] *Center for Petroleum, Petrochemicals, and Advanced Materials, Chulalongkorn University, Phayathai Road, Patumwan, Bangkok 10330*

[3] *Organic Synthesis Research Unit, Department of Chemistry, Faculty of Science, Chulalongkorn University, Phayathai Road, Patumwan, Bangkok 10330*

**Corresponding Author : vipavee.p@chula.ac.th*

ABSTRACT

Signal amplification by polymerization has been recently emerged as a simple, rapid, sensitive, and inexpensive way to detect DNA binding. In principle, hundreds to millions of times of signals can be amplified through the chain propagation of the designated monomer from the initiator immobilized on biosensor surface under appropriate condition. The resulting polymer would thus change the optical property of the sensing spot, which later becomes visually distinguishable from the background. Here in this research, two monomers were used for investigation: poly(ethylene glycol)methacrylate (PEGMA) and rhodamine B-functionalized 2-hydroxyethylmethacrylate (RhB-HEMA). These two monomers yielded colored copolymer that can be visualized by naked eye without the equipment requirement and are water-soluble, the characteristic mandatorily required to assure that the copolymer unbound to the biosensor surface can be removed by aqueous washing. According to our preliminary investigation, the desired copolymer appearing in red can grow from the initiator grafted on paper with minimal background from non-specific adsorption of unbound copolymer. The employment of a purge-free controlled polymerization based on activators regenerated by electron transfer for atom transfer radical polymerization (ARGET ATRP) truly add simplicity to the detection process. It is our on-going investigation to determine the ability of a peptide nucleic acid probe bearing a conformationally rigid D-prolyl-2-aminocyclopentanecarboxylic acid backbone (acpcPNA) end-capped with ARGET ATRP initiator in amplifying the signal upon hybridization with target DNA that was immobilized on paper-based biosensor.

Keywords Polymerization; Signal amplification; DNA; PNA; ARGET ATRP

MNT-O-038

SURFACE FUNCTIONALIZATION OF MAGNETITE NANOPARTICLE WITH POLYCATION AND ITS BIOCONJUGATION

Thapanapong Theppaleak[1], Boonjira Rutnakornpituk[1], Uthai Wichai[1], Tirayut Vilaivan[2], Metha Rutnakornpituk[1,*]

[1] *Department of Chemistry and Center of Excellence for Innovation in Chemistry, Faculty of Science, Naresuan University, Phitsanulok 65000, Thailand*

[2] *Organic Synthesis Research Unit, Department of Chemistry, Faculty of Science, Chulalongkorn University, Phayathai Road, Patumwan, Bangkok 10330, Thailand*

**Corresponding Author : methar@nu.ac.th*

ABSTRACT

The magnetite nanoparticles (MNP) were surface modified with the copolymer of poly(ethylene glycol) methyl ether methacrylate (PEGMA) and 2-diethylamino ethyl methacrylate (DEAEMA) via atom transfer radical polymerization (ATRP) for use as a cationic nanosolid to immobilize PNA probe for detection of DNA sequence. Molar ratio of the PEGMA:DEAEMA copolymer was systematically varied (100:0, 75:25, 50:50, 25:75 and 0:100, respectively) for fine adjustment of the positive charges on the particle surface after theirs quaternization. Kinetic studies of the (co)polymerizations were investigated using ^{1}H-NMR technique to reveal the relative reactivity of the polymers in the grafting reaction. Zeta potential of the (co)polymer-coated MNP was analyzed by photo correlation spectroscopy (PCS). Transmission electron microscopy (TEM) and PCS indicated that the water dispersibility of the particles was improved upon quaternization of the DEAEMA entities grafted on the particle surface. The preliminary results showed that these copolymer-grafted MNP can be used as a solid support to differentiate synthetic DNA sequence. These novel cationic magnetic nanocaptures might be applicable to use for detection of DNA sequences.

Keywords Magnetite nanoparticle; DEAEMA; PNA; DNA

HST-P-056

THE CHAIN LENGTH EFFECT OF BLOCKING REAGENT ON THE CAPACITIVE DETECTION OF PNA-DNA HYBRIDIZATION

Supannee Sankoh[1,2,3], Orawan Thipmanee[1,2,3], Saluma Samanman[1,2,3], Warakorn Limbut[1,2,4], Apon Numnuam[1,2,3], Proespichaya Kanatharana[1,2,3], Tirayut Vilaivan[5], Panote Thavarungkul[1,2,6,*]

[1] *Trace Analysis and Biosensors Research Centre, Faculty of Science, Prince of Songkla University, Hat Yai, SongKhla 90112, Thailand*
[2] *Center of Excellence for Innovation in Chemistry, Faculty of Science, Prince of Songkla University, Hat Yai, SongKhla 90112, Thailand*
[3] *Department of Chemistry, Faculty of Science, Prince of Songkla University, Hat Yai, SongKhla 90112, Thailand*
[4] Department *of* Applied Science, *Faculty of Science, Prince of Songkla University, Hat Yai, SongKhla 90112, Thailand*
[5] *Organic Synthesis Research Unit, Department of Chemistry, Faculty of Science, Chulalongkorn University, Phayathai Road, Patumwan, Bangkok 10330, Thailand*
[6] *Department of Physic, Faculty of Science, Prince of Songkla University, Hat Yai, SongKhla 90112, Thailand*
**Corresponding Author : panote.t@psu.ac.th*

ABSTRACT

A capacitive DNA sensor was investigated based on the immobilization of a peptide nucleic acid (PNA) probe on the gold electrode surface. This DNA sensor measures the capacitance change as a result of the hybridization between an immobilized PNA and DNA target. The orientation of the PNA probe is also an important factor for DNA hybridization. The immobilization of PNA probe is obtained *via* a self assembled monolayer (SAM) of 11-mercaptoundecanoic acid (MUA). Three blocking reagents of different lengths, 3-mercapto-1-propanol (MPL), 6-mercapto-1-hexanol (MHL) and 11-mercapto-1undecanol (MUL) were investigated for their ability to provide an insulation layer that was suited for the capacitive system and prevented non-specific PNA-Au interaction. This also helped the PNA molecules to remain upright on the surface, and, hence, increased of the hybridization reaction. The PNA probes were immobilized on the gold electrode surface by using a SAM of MUA and blocked with the blocking reagent. The sensitivity [omit (slope of the calibration curve)] of the capacitive DNA sensor when using MPL, MHL and MUL were 10.6±0.3 $nFcm^{-2}M^{-1}$, 14.5±0.2 $nFcm^{-2}M^{-1}$ and 17.4±0.6 $nFcm^{-2}M^{-1}$, respectively. The results indicated that the longer alkane chain of MUL used for blocking provided better signal and greater sensitivity than the shorter chain of the MPL and MHL. Each modified electrode can be reused up to 73 times.

Keywords DNA sensor; 11-Mercaptoundecanoic acid; PNA probe; Capacitive biosensor; Blocking reagent

BORDEAUX 2012 SYMPOSIUM ON FOLDAMERS

a COST Action CM0803 – Marie Curie IAPP FOLDAPPI joint event

January 30 - February 2 2012

European Institute of Chemistry and Biology
Bordeaux-Pessac, FRANCE

BOOK OF ABSTRACTS

Plenary lectures 1-6

Keynote lectures 1-11

Oral Communications 1-14

Posters 1-33

Cyclobutane β-amino acid–proline PNA: a ring size effect?

David J. Aitken,[a] Árpád Balás,[a] Woraluk Mansawat,[b] Chotima Vilaivan,[b] Tirayut Vilaivan[b]

[a]*Laboratoire de Synthèse Organique & Méthodologie, ICMMO, Université Paris-Sud, 91400 Orsay, France.* [b]*Organic Synthesis Research Unit, Department of Chemistry, Chulalongkorn University, Bangkok 10330, Thailand*

david.aitken@u-psud.fr, vtirayut@.chula.ac.th

Peptide nucleic acid (PNA) is a class of bio-inspired synthetic material which displays a sequence of nucleic bases on a peptide backbone, this latter feature replacing the deoxyribose-phosphate backbone of DNA. In previous work, the Thai group has examined a new type of PNA: mixed α/β peptides comprised of alternating nucleobase-substituted-D-proline and a five-membered cyclic β-amino acid, *trans*-(1*S*,2*S*)-2-amino-1-cyclopentanecarboxylic acid (Figure 1, left). These PNA materials bound selectively to complementary DNA, according to the Watson-Crick base pairing rules.[1,2]

In the present work, the Orsay group has profited from their recently established practical access to enantiomerically pure *trans*-(1*S*,2*S*)-2-amino-1-cyclobutanecarboxylic acid (ACBC),[3,4] to facilitate the preparation of analogous PNA materials featuring a four-membered cyclic β-amino acid (Figure 1, right). This communication will present the syntheses of these new materials, and their hybridization properties. In particular, the consequences of the ring-size modification on binding stability will be considered.

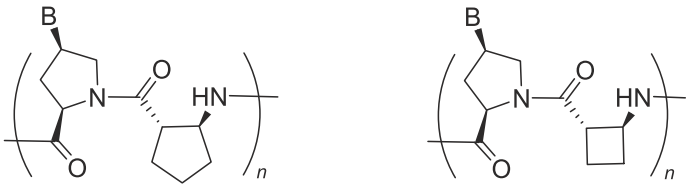

Figure 1. Mixed α/β PNA containing cyclic β-amino acids: previously studied (left), and new materials discussed in this communication (right).

References

[1] T. Vilaivan, C. Srisuwannaket, *Org. Lett*. **2006**, *9*, 1897.
[2] C. Suparpprom, C. Srisuwannaket, P. Sangvanich, T. Vilaivan, *Tetrahedron Lett*. **2005**, *46*, 2833.
[3] C. Fernandes, E. Pereira, S. Faure, D. J. Aitken, *J. Org. Chem.* **2009**, *74*, 3217.
[4] V. Declerck, D. J. Aitken, *Amino Acids* **2011**, *41*, 587.

TISSUE ANTIGENS
IMMUNE RESPONSE GENETICS

ABSTRACTS

Joint 16th International HLA and Immunogenetics Workshop, 26th European Federation for Immunogenetics Conference and 23rd British Society of Histocompatibility and Immunogenetics Conference

Liverpool, United Kingdom

May 31st–June 3rd, 2012

© 2012 John Wiley & Sons A/S

ORGANISING COMMITTEE

Co-chairs:
Derek Middleton (Liverpool)
Steven GE Marsh (London)

Members:
Brendan Clarke (Leeds)
Ann-Margaret Little (Glasgow)
Susan Martin (Manchester)
David Wilson (Aberdeen)

EFI SCIENTIFIC COMMITTEE AND REVIEWERS

R. Bontrop (The Netherlands)	Chairman
A. Amoroso (Italy)	
R. Blasczyk (Germany)	
M. Colonna (USA)	
F. Koning (The Netherlands)	
D. Middleton (UK)	Loc (*ex-offocio*)
L. Sollid (Norway)	
J. Trowsdale (UK)	
R. Vaughan (UK)	(*ex-offocio* BSHI)

EFI EXECUTIVE COMMITTEE

I.N. Doxiadis (The Netherlands)	President
G. Fischer (Austria)	President-Elect
A-M. Little (UK)	Secretary
M. Bengtsson (Sweden)	Deputy Secretary
V. Dubois (France)	Treasurer
G. Guidicelli (France)	Deputy Treasurer

K. Fleischhauer (Italy)
J. Mytilineos (Germany)
M. Petrek (Czech Republic)
M. Toungouz Nevessignsky (Belgium)
B. Vidan-Jeras (Slovenia)
C. Vilches (Spain)

BSHI EXECUTIVE COMMITTEE

J. Cornish	President
S. Fuggle	Chairman
A. Poles	Secretary
D. Turner	Secretary Elect
V. Carter	Treasurer
A. Anaud	Meetings Secretary
N. Diaz Burlinson	Membership Secretary
S. Martin	BEB Chairperson
K. Poulton	BPAG Chairperson

D. Singleton
A. Karasu
D. McKensie

© 2012 John Wiley & Sons A/S

Foreword of the Chairmen of the 16th International HLA and Immunogenetics Workshop and Local Organising Committee

On behalf of the organising committee, we are delighted to welcome you to Liverpool for the Joint Conference of the 16th International HLA and Immunogenetics Workshop, 26th Federation for European Immunogenetics Conference and 23rd British Society of Histocompatibility and Immunogenetics Conference.

This is the first time that the three organisations have come together in a single event and we are excited that so many people have registered to extend our knowledge and understanding of immunogenetics and histocompatibility.

Liverpool, the 2008 European Capital of Culture, is a perfect venue for the event and we hope that you will all take time to explore the city and take advantage of the activities arranged for you.

Needless to say coordinating and organising a meeting of this sort involves a great many people, all of whom we most sincerely thank. In particular we would like to express our deep appreciation to the members of the EFI and BSHI Executive Committees, EFI Scientific Committee and EFI Education Committee for their help and support in organising the Scientific Program, the Teaching Sessions and in the evaluation of the abstracts. More than 500 abstracts have been submitted from all over the world, which is probably some kind of record, but more than anything reflects the excellent work being carried out across the world in this field. We would also like to thank all of our sponsors without whom meetings of this kind would simply not be possible.

We are delighted to host you on Liverpool's famous waterfront, a UNESCO world heritage site, and hope that you will be stimulated by both the meeting and your surroundings.

Derek Middleton and Steven Marsh
Chairmen 16th IHIWC

Foreword of the President of EFI

With great pleasure, I welcome the participants of the combined European Federation for Immunogenetics and British Society for Histocompatibility and Immunogenetics Conference in Liverpool. It is a historical masterpiece of vision having not only two societies cooperating for the annual meeting but also harbouring the International HLA and Immunogenetics Workshop Conference. It is work at its best. It mimics the tri-molecular structure of MHC, peptide and receptor. In this case the T-cell receptor. Other members of the community could see different things such as the three important immune cells; the three classes of MHC or even other associations.

The program is excellent and the organising committee have done their utmost to offer to the community all the attributes for an excellent and wonderful meeting. However, a meeting lives with its participants, their input to discussions in the lectures and abstract sessions, it lives with the awardees and their vision and it lives with all the educational activities, and last but not least, with the input and efforts of the sponsors of the societies and the meeting. All of the aforementioned have done their best beforehand. A grateful thank-you to all: participant; sponsor and local organiser and not forgetting, to the committees of EFI and BSHI with all their members. I wish you a fruitful unforgettable Conference, for both the scientific and personal experience.

Ilias Doxiadis
President of EFI

Foreword of the Chairman of BSHI

As Chair of the British Society for Histocompatibility and Immunogenetics (BSHI) and on behalf of the BSHI, I am delighted to welcome you to Liverpool to the joint 16th International HLA and Immunogenetics Workshop Conference, 26th European Federation for Immunogenetics (EFI) and 23rd BSHI Conference. We are grateful to the organisers and the committee for compiling a stimulating and diverse scientific programme and are pleased to welcome eminent speakers for the BSHI lectures, the Hilliard Festenstein lecture, the Terasaki lecture and the BSHI Presidential Address. Thanks, too, to the corporate partners and sponsors of this Conference whose support is vital. This Conference promises to be a great opportunity for exchange of ideas and to develop collaborations with colleagues internationally. I hope that you will find the Conference stimulating and that you are able to take time to visit the fascinating city of Liverpool.

Susan Fuggle,
Chair BSHI

© 2012 John Wiley & Sons A/S

P333

IL-12B GENE POLYMORPHISMS INFLUENCE PSORIATIC ARTHRITIS CLINICAL SUBTYPES IN ROMANIAN POPULATION

Olivia M. Popa[1], Eva Kriegova[1], Luis Popa[2], Petra Schneiderova[1], Monica I. Dutescu[3], Mihai Bojinca[4], Violeta Bojinca[4], Constantin Bara[4], Martin Petrek[1]

[1]Faculty of Medicine and Dentistry, Palacky University, Olomouc, Czech Republic, [2]Grigore Antipa National Museum of Natural History, Bucharest, Romania, [3]National Institute of Hematology and Blood Transfusion, Bucharest, Romania, [4]Faculty of Medicine, University Carol Davila, Bucharest, Romania
Correspondence: oliviapopa@yahoo.com

Psoriatic arthritis (PsA) is a chronic disorder characterized by skin psoriasis and the inflammation of the peripheral joints (oligo or polyarticular) and/or spine (axial). PsA has a genetic predisposition and recent findings indicate that the genes participating in interleukin (IL)-12/23 signaling play an important role in the disease pathogenesis. IL-12B gene encodes the common subunit p40 of both IL-12 and IL-23. The aim of this study was to investigate a possible influence of IL-12B gene single nucleotide polymorphisms (SNPs) on the clinical symptoms of PsA in Romanian patients. PsA patients (n = 94, 42.5% polyarticular disease, 33% axial involvement, 24.5% isolated oligoarticular) and 161 controls of Romanian ethnicity were genotyped for 6 SNPs in the IL-12B gene. Genotyping was performed with the Sequenom MassARRAY platform (Sequenom, San Diego, CA). Association tests for each polymorphism, linkage disequilibrium (LD) and haplotype frequency estimations were performed with the software PLINK v 1.07 and p values $\leq$0.05 were considered significant. The rs6887695 variant was associated with polyarthritis subtype (MAF 16.2% in patients versus 32.6% in controls, p = 0.003, pcorr = 0.01, OR 0.401, 95% CI 0.211–0.759). Two other SNPs showed associations with the same subtype (rs3212227, MAF 16.2% in patients vs 27.1% in controls, p = 0.04 and rs1363670, MAF 22.5% in patients vs 12.9% in controls, p = 0.03). These associations did not remain significant after correction. The combined haplotype CATACC of all studied SNPs (rs3212227/rs2853694/rs3212220/rs1433048/rs1363670/rs6887695) was associated with polyarthritis subtype (7.6% in patients vs 21.8% in controls, p = 0.004). No association of the investigated SNPs was found with other disease characteristics. In conclusion, in the Romanian population, IL-12B gene influences the clinical phenotype of PsA, mainly of the polyarticular subtype. Grant support: IGA PU_LF_2012_007.

P334

HLA AND TUMOR NECROSIS FACTOR POLYMORPHISMS IN PATIENTS WITH PROSTATE CANCER

Katarina Stingl, Tvrtko Hudolin, Renata Zunec, Zeljko Kastelan, Eleonora Goluza, Zorana Grubic

University Hospital Centre Zagreb, Zagreb, Croatia
Correspondence: kstingl@kbc-zagreb.hr

Tumor necrosis factor-alpha (TNF-alpha) is a proinflammatory cytokine that has been implicated in pathogenesis of many forms of cancer, including prostate cancer. The polymorphisms located within the gene for TNF-alpha have shown an influence on the production of this cytokine. The aim of the study was to evaluate the potential association of TNFa, TNFb and TNFd as well as HLA-A, -B and -DRB1 with prostate cancer. Eighty-nine patients, diagnosed and treated for prostate cancer at the University Hospital Centre Zagreb in the period 2009–2011, were included in the study. The HLA typing was performed using sequence specific oligo probes and Luminex methodology. TNF microsatellites were analyzed using sequence specific primers and PCR followed by electrophoresis on a polyacrylamide gel in an automated sequencer (ALFexpress). The control subjects were healthy individuals (n = 150) typed for HLA-A, -B, -DRB1, TNFa, TNFb and TNFd polymorphisms. The analysis of the patients' HLA typing results revealed *HLA-A*02* (33.7%), *-B*51* (14.6%) and *DRB1*11* (16.9%) as the most frequent specificities. This, as well as the distribution of other HLA specificities at tested loci did not show any significant difference in comparison to the controls. The most frequent alleles at TNF loci were TNFa2 (28.1%), TNFb (36.5%) and TNFd (47.8%). The distribution of TNF alleles revealed a significant difference only for TNFa2 and TNFd5 alleles that were present significantly more among patients in comparison to controls (TNFa2: 28.1% vs. 16.7%, p = 0.0043; TNFd5: 32.0% vs. 21.3%, p = 0.0128). When the patients were divided according to the Gleason score, those two TNF alleles showed a significant increase only among patients with a higher Gleason score (GS equal or higher of 7; TNFa2: 28.4% vs. 16.7%, p = 0.0214; TNFd5: 36.4% vs. 21.3%, p = 0.0062). The obtained results indicate an association of TNFa and TNFd polymorphisms with prostate cancer, especially in cases of higher tumor grade.

P335

LOOP-MEDIATED ISOTHERMAL AMPLIFICATION AS A SCREENING TEST FOR HLA-B*57:01 AND 58:01 IN DRUG HYPERSENSITIVITY PREDICTION

Sita Virakul[1], Pawinee Kupatawintu[2], Piyasak Chaumpluk[3], Tirayut Vilaivan[3], Nattiya Hirankarn[1]

[1]Faculty of Medicine, Chulalongkorn University, Bangkok, Thailand, [2]Thai Red Cross Society, Bangkok, Thailand, [3]Faculty of Science, Chulalongkorn University, Bangkok, Thailand
Correspondence: Nattiyap@gmail.com

© 2012 John Wiley & Sons A/S

Association studies between *HLA-B*57:01* and abacavir hypersensitivity, and *HLA-B*58:01* and allopurinol hypersensitivity in many Asian populations including the Thai population have been reported in recent years. A mortality rate of those who suffer with Stevens Johnson Syndrome and toxic epidermal necrolysis (SJS-TEN), severe drug hypersensitivity, is about 30%. Screening for these alleles before initiating the drug drastically prevents the severe adverse reaction. Most HLA typing techniques depend on conventional techniques e.g. sequence specific primer – polymerase chain reaction or sequence specific oligonucleotide probe – polymerase chain reaction that require well equipped laboratory and specialized scientists. Thus it is important to develop an alternative method to allow HLA typing in a limited resources area. In this report, we used LAMP (Loop-mediated isothermal amplification), an isothermal amplification technique, to amplify *HLA-B*57:01* and *B*58:01*. This technique requires 4 primers which specifically target 6 regions allowing both *HLA-B*57:01* and *B*58:01* to be detected. From 99 blind purified DNA samples, in 40 minutes we could successfully achieve 100% sensitivity and 98.99% specificity (4 positive for *HLA-B*57:01*, 12 positive for *B*58:01* and 82 negative for *HLA-B*57:01* and *B*58:01*) with one false positive sample, compared to commercial SSOP-PCR technique. This technique is faster than PCR and also allows instant detection by using SYBR green. In addition, an expensive thermocycler machine is not required. However, there is a potential problem of false positive results. Therefore, this technique still needs further development to make it more specific. Ongoing research includes the use of an oligonucleotide probe labelled with fluorescence to increase detection specificity and further differentiate *HLA-B*57:01* from *B*58:01*.

P336

BLACK PATIENTS OF AFRICAN DESCENT AND HLA-DRB1*1503 FREQUENCY OVERREPRESENTED IN EPIDERMOLYSIS BULLOSA ACQUISITA

Pascale Loiseau[1], Marc Busson[2], Françoise Aucouturier[3], Coralie Zumelzu[4], Christelle Le Roux-Villet[4], Michel Heller[4], Valérie Pendaries[5], Nicole Lièvre[4], Francis Pascal[4], Marie-Dominique Brette[3], Serge Doan[6], Frédéric Caux[4], Liliane Laroche[4], Antoine Petit[3], Dominique Charron[1], Catherine Prost-Squarcioni[4]

[1]Hôpital Saint-Louis, AP-HP and Inserm, Paris, France, [2]Inserm, Paris, France, [3]Hôpital Saint-Louis, AP-HP, Paris, France, [4]Hôpital Avicenne, AP-HP, Bobigny, France, [5]Inserm, Toulouse, France, [6]Hôpital Bichat, AP-HP, Paris, France
Correspondence: pascale.loiseau@univ-paris-diderot.fr

Epidermolysis bullosa acquisita (EBA) is a rare autoimmune bullous disease (AIBD). A higher EBA incidence and HLA predisposing genetic factor have been suspected in some populations. A retrospective study from the French Referral Center for Autoimmune and Toxic Acquired Bullous Dermatoses showed that 54% EBA in contrast to 3% AIBD patients were black people ($p = 10^{-6}$) and that 54% black patients suffering from AIBD had EBA. Between 1983 and 2009, 19 black EBA patients were seen. Among the 19 black EBA patients, 9 were natives of sub-Saharan Africa, 1 from Reunion Island, 7 from West Indies and 2 were of mixed ancestry. The frequency of *HLA-DRB1*1503* was 50% for African patients, significantly higher than for the control population ($p < 10^{-3}$) and 21% for the West Indians (ns). A high EBA frequency has already been reported in American blacks significantly associated with HLA-DR2. In conclusion, this retrospective study assessed the overrepresentation of black patients with EBA, its link with HLA-*DRB1*1503* allele, and suggests that EBA should be evoked systematically for every AIBD seen in this population.

P337

IMPACT OF HLA AND CYTOKINE POLYMORPHISMS ON INHIBITOR DEVELOPMENT IN CHILDREN WITH SEVERE HAEMOPHILIA A.

Ioanna Varela[1], Helen Pergantou[2], Kleopatra Spanou[1], Marina Economou[3], Zoey Kapsimali[2], Helen Platokouki[2], Olga Moraloglou[1], Nikki A. Constantinidou[1]

[1]Immunology-Histocompatibility, Aghia Sophia Children's Hospital, Athens, Greece, [2]Haemophilia Centre/Haemostasis Unit, Aghia Sophia Children's Hospital, Athens, Greece, [3]Haemophilia Centre, 1st Paediatric Department of Aristotle University, Ippokration Hospital, Thessaloniki, Greece
Correspondence: anosia@paidon-agiasofia.gr

The development of inhibitors (Inh) against factor VIII in Hemophilia A (HA) patients is the most serious complication and seems to be multifactorial. The type of FVIII gene mutation, HLA genes and cytokine polymorphisms are included among genetic predisposing factors for Inh formation. To investigate any possible correlation of FVIII gene intron-22 inversion, HLA alleles and cytokine polymorphisms with the risk for Inh development in 52 Greek children with severe HA, exclusively treated with recombinant products, we performed Long Range PCR for detection of intron-22 inversion. PCR-SSP and PCR-SSO were applied for HLA Class I and II genotyping and also for polymorphisms of TNF-a, TGF-b1, IL-10, IL-6, IFN-gamma. Statistical analysis was performed by χ^2 test and Fischer's exact test. Twenty-eight children had developed inhibitors (Group I), while 24 had not (Group II). Analysis of HLA frequencies between the two groups showed statistically significant differences in the following genotypes i) positive associations with Inh development: *DRB1*01* ($p = 0.014$, OR = 10.9), *DRB1*01:01* ($p = 0.011$), *DQB1*05:01* ($p = 0.005$, OR = 12.8), and ii) negatively associated with Inh development: *DRB1*11* ($p = 0.011$, OR = 0.2), *DRB1*11:01* ($p = 0.031$, OR = 0.15), *DQB1*03* ($p = 0.004$, OR = 0.15), *DQB1*03:01* ($p = 0.014$, OR = 0.22). The differences between the two groups regarding the polymorphisms of cytokines were not statistically significant. However, the homozygocity of the haplotypes ACC and ATA for IL-10 -1082G>A, -819C>T and -592C>A polymorphisms showed a trend for Inh development. This study shows that *HLA-DRB1*01*, *DRB1*01:01*

© 2012 John Wiley & Sons A/S

IUPAC
International Union of Pure and Applied Chemistry

World Polymer Congress
June 24–29, 2012

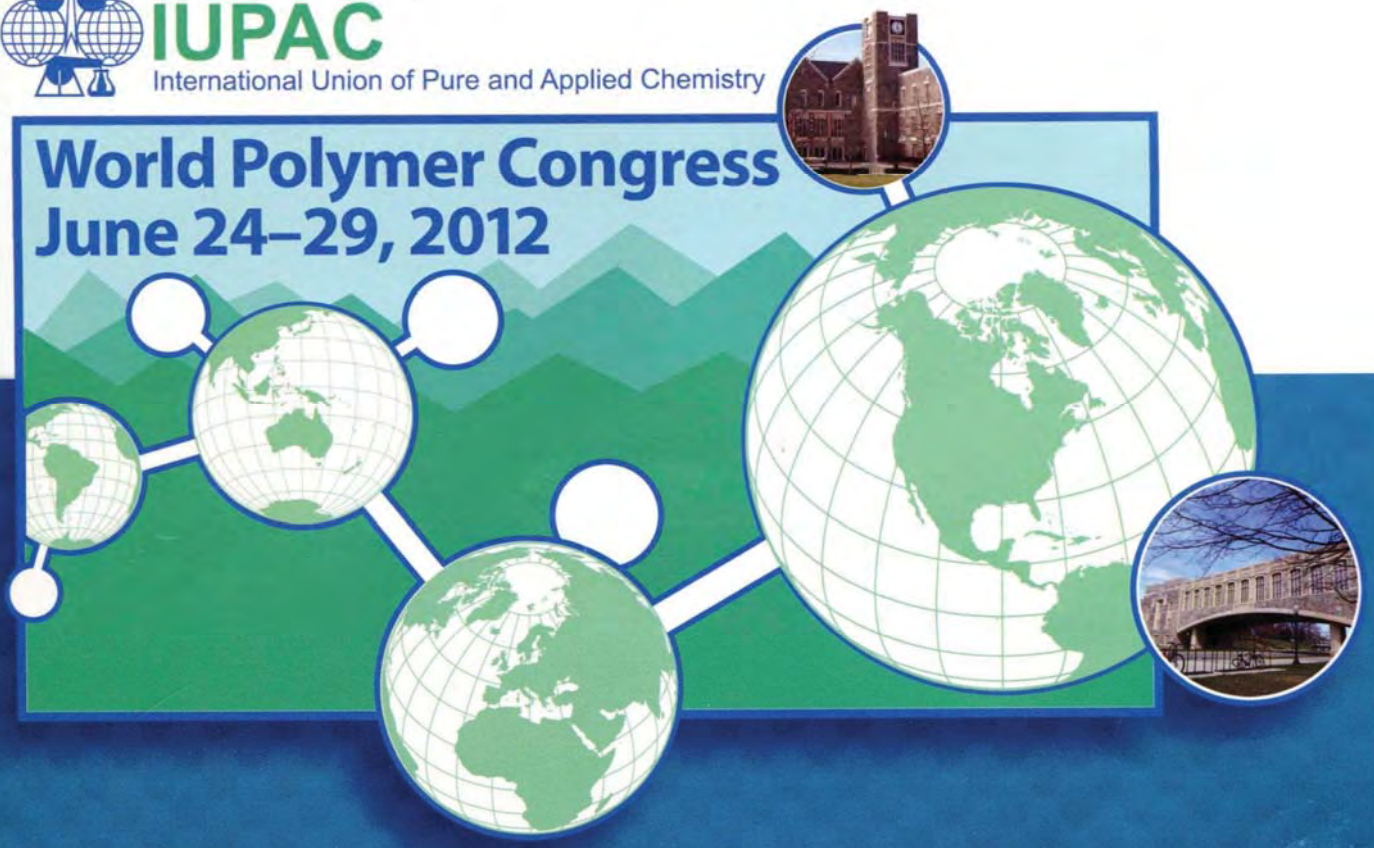

MACRO2012

Enabling Technologies for a Safe, Sustainable, Healthy World

VirginiaTech
Invent the Future®

Blacksburg, Virginia • USA

PROGRAM

BLACKBERRY-LIKE PARTICLES ASSEMBLED FROM FLUORESCENT-LABELED QUATERNIZED AMPHIPHILIC CHITOSAN: PREPARATION AND THEIR POTENTIAL FOR BIOIMAGING

*Kanya Taboonpong[1,2], Tirayut Vilaivan[3], Voravee P. Hoven[3]**

[1]Program in Petrochemistry and Polymer Science, Faculty of Science, Chulalongkorn University, Pathumwan, Bangkok 10330, Thailand
[2]Center for Petroleum, Petrochemicals and Advanced Materials, Chulalongkorn University, Pathumwan, Bangkok 10330, Thailand
[3]Organic Synthesis Research Unit, Faculty of Science, Chulalongkorn University, Pathumwan, Bangkok 10330, Thailand

Introduction

Self-assembly is well recognized as a versatile technique for inducing particle formation from amphiphilic polymer having both hydrophobic and hydrophilic entities. In particular, the method has been successfully employed to generate particles with controllable size range and great potential as drug carriers from amphiphilic chitosan, a natural, non-toxic, and biodegradable biopolymer.[1-2] Fluorescent labeling has been known as an effective tool to monitor substance uptake by biological systems. In the case of particle, the fluorescent dye can be either chemically tagged to or physically encapsulated in the particles. Taking advantage of pyrene being a hydrophobic fluorescent dye, fluorescent labeled quaternized chitosan particles can be conveniently prepared by self-assembly of amphiphilic chitosan having pyrene as a hydrophobic entity and *N*-[(2-hydroxyl-3-trimethylammonium)]propyl (HTAP) as a hydrophilic entity. It is anticipated that the quaternary ammonium groups from HTAP should enhance electrostatic attraction between the particles and negatively charged phospholipid cell membranes and subsequently promote cellular uptake so that the particles may be applicable for bioimaging applications.

Experimental

Stepwise procedure for the preparation of fluorescent-labeled amphiphilic chitosan is schematically outlined in Figure 1. *N*-phthaloylchitosan (PhCS) was first synthesized in order to protect amino groups of chitosan. The *C-6*-azido-*N*-phthaloylchitosan (N_3-PhCS) was then obtained after bromination of *C6* hydroxyl group of chitosan followed by azidation.[3] Click reaction between the N_3-PhCS and 1-ethynylpyrene was conducted using Cu(I) as catalyst and *N,N*-diisopropylethylamine as base to yield pyrene-functionalized PhCS (Pyr-PhCS). Deprotection of phthaloyl groups was carried out via hydrolysis using hydrazine solution. The positively charged HTAP groups were then introduced by a reaction between Pyr-PhCS and glycidyltrimethylammonium chloride (GTMAC) in DMF. Finally, fluorescent-labeled quaternized chitosan particles were obtained by self-assembly of the resulting amphiphilic chitosan (Pyr-CS-HTAP) after dialysis against deionized water for 4 days and lyophilization.

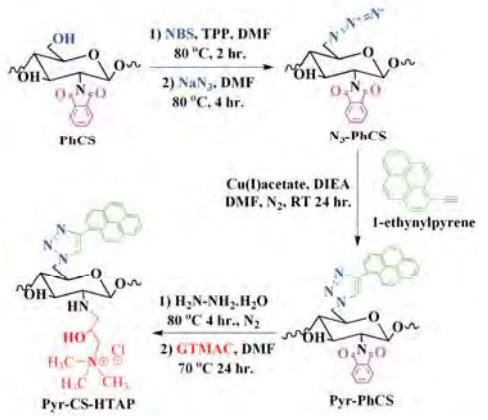

Figure 1. Schematic representation of stepwise procedure used for the preparation of fluorescent-labeled amphiphilic chitosan.

Results and Discussion

FT-IR technique was used to monitor the stepwise functionalization of chitosan. As shown in Figure 2, a characteristic stretching of azide group in N_3-PhCS emerges at 2100 cm^{-1} and disappears after the click reaction with ethynylpyrene (See Pyr-CS-HTAP spectrum). The presence of C-H stretching peak of -$N(CH_3)_3$ at 1480 cm^{-1} and the absence of C=O stretching at 1700 cm^{-1} (found in PhCS) in the Pyr-CS-HTAP spectrum verified the success of HTAP incorporation and the complete removal of phthaloyl entities, respectively.

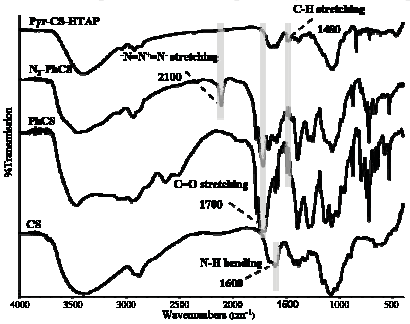

Figure 2. FT-IR spectra of chitosan (CS), PhCS, N_3-PhCS and Pyr-CS-HTAP.

According to SEM analysis (Figure 3a), the self-assembly of the amphiphilic Pyr-CS-HTAP interestingly yielded particles with blackberry-like morphology and a size range of 1-2 µm. As expected, the particles exhibited positive charges with a zeta-potential of +40 mV as determined by photon correlation spectroscopy. The bright green fluorescence of the particles appeared in Figure 3b indicated the existence of pyrene in the structure of Pyr-CS-HTAP particles.

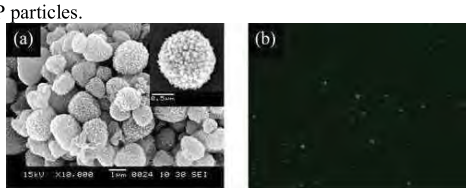

Figure 3. SEM (a) and fluorescence (b) micrographs of Pyr-CS-HTAP particles.

The self-assembled Pyr-CS-HTAP particles are relatively stable considering that there was no detectable morphological change under extreme variation of temperature (0-100°C) and pH (1-12). The de-aggregation only occurred upon the treatment with non-polar hexane. Nonetheless, the blackberry-like particles can be recovered after hexane removal and water replacement indicating that the self-assembly process is reversible. Interactions of the Pyr-CS-HTAP particles with representative biological systems such as bacteria (*S.aureus* and *E.coli)* and cells (macrophage, cancer cells) are being investigated to demonstrate their potential for bioimaging applications.

Conclusions

Fluorescent-labeled quaternized chitosan particles can be successfully prepared by self-assembly of amphiphilic chitosan. These positively charged particles have an interesting blackberry-like morphology and are relatively stable. With these desirable characteristics, the particles should potentially be used for bioimaging applications.

Acknowledgement. The financial support for this project was provided by The Thailand Research Fund (RTA 5280002).

References

(1) Opanasopit, P.; Ngawhirunpat, T.; Rojanarata, T.; Choochottiros, C.; Chirachanchai, S. *Colloids Surf. B Biointerfaces* **2007**, *60*, 117.
(2) Choochottiros, C.; Yoksan, R.; Chirachanchai, S. *Polymer* **2009**, *50*, 1877.
(3) Gao, Y.; Zhang, Z.; Chen, L.; Gu, W.; Li, Y. *Biomacromolecules* **2009**, *10*, 2175.

Postharvest Non-destructive Determination of Fruits: a Model on Fruit Maturity Assay via Biosensor Based on Colorimetric Change of Gold Nanoparticles

P. Chaumpluk*
Laboratory of Plant Transgenic Technology and Biosensor, Department of Botany
Faculty of Science,
Chulalongkorn University
Phyathai, Bangkok 10330
Thailand

P. Chaiprasart
Postharvest Innovation Center,
Faculty of Agriculture, Natural Resource and Environment,
Naresuan University,
Phitsanulok, 65000
Thailand

T. Vilaivan
Department of Chemistry, Faculty of Science,
Chulalongkorn University, Bangkok 10330
Thailand

Keywords: pineapple, *Ananus comosus*, *AcSUT*1

Abstract

New approach for non-destructive fruit maturity determination using pineapple as a model had been established. The assay was based on expression patterns of the putative sucrose transporter (*AcSUT*1) in crown leaves during the course of physiological maturity that could be employed as an index marker for fruit maturity. Determination of *AcSUT*1 cDNA was initially designed using isothermal cDNA amplification and the DNA signal detection via biosensor based on colorimetric platform with gold colloid nanoparticles, 20 nm in diameter. In the immature fruit, the *AcSUT*1 gene was expressed allowing target DNA amplification to occur. DNA signals detection in later step was based on plasmon phenomena of gold nanoparticles. Presence of target DNA affected gold colloid nanoparticles in term of non aggregation with no colour change (still ruby red). However, in the mature fruit, the expression of the *AcSUT*1 gene was terminated resulting in no target cDNA product amplification. When this was tested with gold colloid nanoparticles, it induced aggregation of particles which in turn resulted in a plasmonic change of colloid solution from ruby red to dark purple, visible by naked eye. All processes from RNA extraction to cDNA signal detection could be completed within 80 min without the need for a thermocycler as normally employed during RT-PCR. The developed assay demonstrated the integration of the novel DNA biosensor approach for a non-destructive determination of fruit quality.

*** piyasakcha@gmail.com**

INTRODUCTION

Maturity of fruit at harvest is an important factor determining fruit quality. Especially, in several fruits, immature fruit may leads to inferior flavor quality and undesirable physiological changes, which in turn shortening their shelf-life(Kader, 1999). In general, fruits reach their best quality when they were left maturity ripen on plant. Nevertheless, most practical harvesting can not wait until reaching that stage. Measuring

the maturity through some characters or markers was then required. When considering maturity measurement, maturity of fruits for customer was basically determined by their appearance quality including freshness firmness and color, however, for farmer maturity indices were further employed as important factors for determination of time for fruit harvesting. So far several indices including total solid, soluble solid concentration, titratable acidity concentration and ratio between soluble solid to titratable acidity, and flesh firmness were used for determining maturity and quality of fruit (Pattee, 1985). Nevertheless, those appearance factors and chemical indices alone could not perfectly predict real maturity of fruits. Moreover, measurement through most of those indices was performed with risk of destructive manner.

Maturation is a stage of development leading to the attainment of physiological maturity. In most fruits, even fruits were detached from plant the processes of development were still going on. We had interested in investigation of pineapple fruit development as a model because it was the most agronomical important to Thailand with annual gross export value more than 690 million US$.

Pineapple is classified as a non-climacteric fruit whose processes of ripening can not markedly be continued once removed from the plant. It produces small quantities amount of ethylene and has almost no response to it (Kader, 1999). Thus any abundance of transcripts relating to fruit quality along the period of development may not be influenced by ethylene as found in the other of climacteric one.

So far several genes of pineapple had been investigated for their expression profiles. Taira *et al*., (2005) had studied a group of chitinase genes and found the different among their stage of expression and physiological roles. Type A chitinase expressed at all stages while type B and C was terminate at early stage of fruit development. These early termination were not related directly to fruit maturation. Moyle *et al*., (2005) had surveyed a range of expressed sequences during fruit development from green unripe to yellow ripe fruit and found that some genes, for example, fruit bromelain gene and their inhibitors, were abundant at unripe fruit stage, while MADS box and others associated with protein synthesis (ribosomal L10 and some translation factors) were expressed at yellow ripe fruit. Although the expressions were covering stages of fruit maturation, these un unique expression profiles were not able to employ as marker for maturity detection.

During fruit maturation, sugar storage and assimilate partitioning in fruit play an important role in fruit carbohydrate metabolism. The genes involving to these storage and assimilate partitioning phenomena were then attacked interests since sugar accumulation was one of the importance phenomena influencing fruit maturity and quality. Zhang *et al*., (2010) had reported the important of sucrose phosphate synthase (SPS) as a key enzyme over invertase and sucrose synthase, and had cloned gene SPS of pineapple (*Ac-SPS1*). Expression studies of this *Ac-SPS1* gene revealed low expression at early stage of fruit growth, increasing from 20 days after anthesis and gradually decreasing again on 40 days after anthesis. The results although implied *Ac-SPS1* and an activator of this gene might be important regulatory events of sugar during pineapple fruit maturation, its uninterrupted transcription pattern could not be employed for fruit maturation detection.

Antony *et al*., (2008) had investigated the sugar storage in pineapple (*Ananus comosus*) and had identified a putative hexose transporter gene (*AcMST1*: *A comosus* monosaccharide transporter), a putative inositol transporter gene (*AcINT1*), a putative sucrose transporter (*AcSUT1*) and tonoplast hexose transporter like (*AcMST2*). In pineapple, *AcMST1* was more highly expressed in fruits compared to leaves, whilst transcripts of *AcINT1, AcSUT1, and AcMST2* were more abundant in leaves (Antony *et*

al., 2008). The expression patterns of *AcMST1* and *AcSUT1* implied the incidence of the synthesis and accumulation periods of monosaccharide in fruit, and also the transportation of monosaccharide from leaf during maturation, which might be employed in fruit maturation detection.

In this paper, we had further studied the abundance of transcripts of both *AcMST1* and *AcSUT1* comparing with that of 18S rRNA in fruits and in crown leaf of during the course of fruit development. Results revealed pattern of gene expression of *AcSUT1* in crown leaf was finally terminated when fruit was in mature stage. Based on this, we had demonstrated the feasibility of using the *AcSUT1* expression phenomenon as an indicator for fruit maturity determination. It was based on biosensor technique, combining a rapid cDNA amplification of *AcSUT1* transcripts using reverse transcription loop mediated isothermal platform and a novel rapid nucleic acid hybridization using colorimetric change of gold nanoparticles for a simple non destructive determination of fruit maturity.

MATERIALS AND METHODS

Pineapple fruits used in the experiment were Smooth Cayenne type *Ananus comosus* (L.) Merr., cv. Sriraja from local orchards in Cholburi province, Thailand. Fruits were picked up covering all 5 stages of fruit developments; stage1 anthesis (2 months after flowering treatment), stage2 late anthesis stage (2.5 months after stage 1), stage3 small fruit stage (3.5 months after flowering treatment), stage 4 medium fruit stage (4-4.5 months after treatment), and stage 5 mature fruit (5 months after flowering treatment)(Fig. 1.). Transportation of fruits to laboratory was finished within two hours post detachment.

The transcripts abundance of each genes were investigated using RT-PCR (Antony *et al*., 2008). Amplification of primers set for the *AcMST1, AcSUT1* gene and for the 18S rRNA gene, were based on criteria of specific DNA amplification to both genes without leaving non-specific products. In detail, first, total RNA was extracted from 500 mg of fruit and the second crown leaf (scale) from basal closed to fruit of each treatment with TRIZOL solution according to the manufacturer's protocol (Invitrogen, USA). Two-step RT-PCR of each samples was performed using reverse M-MuLV transcriptase (New England Biolabs Inc., USA), and *Taq* DNA polymerase (Promega, USA) with incubation condition for reverse transcription at 42°C 60 min and 90°C for 10 min inactivation of enzyme, and for PCR using denaturation at 93°C 40 sec, annealing at 53°C 1 min, and extension at 72°C 1min with 40 cycles of amplification as described (Sambrook *et al*., 1989). RT-PCR products were visualized after electrophoresis.

For detection of cDNA of *AcSUT1* gene using reverse transcription loop mediated isothermal amplification (RT-LAMP), set of primers was designed to recognize 6 distinct areas of *AcSUT1* gene of pineapple (accession number EF460878) as described (Chaumpluk and Chaiprasart, 2010) (Figure 3.) and reaction preparations were carried out as described (Notomi *et al*., 2000). The mixture was incubated at 63°C for 30 min. No post heat incubation at 80°C was applied. The detection limit of the reaction was determined using equivalent copy numbers of cloned *AcSUT1* at 10-fold dilutions as described (Anonymous, 2003, Kuribara *et al.*, 2002). The sensitivity of the assay was also confirmed and compared with that of RT-PCR by the gel electrophoresis (Antony *et al*., 2008).

Confirmation of the *AcSUT1* cDNA was by novel colorimetric nucleic acid hybridization in gold colloid solution. This was based on plasmonic change of gold nanoparticles upon hybridized with probe (Kanjanawarut and Su, 2009). Gold nanoparticles 20 nm in size in water solution were prepared and selected under increasing alkaline condition using soluble starch as reducing agent (Pienpinijtham *et al.*, 2010). Analog nucleic acid probe (5'Flu-O-aatcagtaatta-LysNH_2) was synthesized according to the previously reported Fmoc solid-phase peptide synthesis protocol (Suparpprom *et al*., 2005, Vilaivan and Srisuwannaket, 2006). The crude oligo probe was cleaved from the solid support by treatment with trifluoroacetic acid (TFA) and purified using reversed-phase HPLC with UV detection at 260 nm. A Varian Polaris C18 (3 μm particle size 4.6x50 mm) analytical HPLC column was used and eluted with a gradient of 0.1% TFA in acetonitrile and 0.1% TFA in deionized water. Binding of probe to surface of gold nano particles was performed by adding probe to a final concentration of 100 pM to 20μL gold solution (1000 ppm) at room temperature. Nucleic acid hybridization was performed after adding 1 μL of RT-LAMP products and 1mM PBS. Changing of gold color was observed with naked eye and measured through UV-Visible Spectroscopy (Ocean Optics ® USB2000, USA) with λ=380-800nm.

RESULTS AND DISCUSSION

Sugar accumulation was found in fruit during maturation. Close correlation of the abundance of *AcMST1* in fruits was demonstrated (Antony *et al*., 2008). However in fruit, there were limited expressions of *AcSUT1* gene especially during fruit maturation due to the processes of sugar transportation was nearly ceased during that period. Although abundance of both gene were studied in fruit(Antony *et al*., 2008), there were no investigation of both gene following the course of fruit development as well as the fate of the gene in crown leaf at each stages. Thus, in order to find the relationships between transcripts abundance of both gene during the course of fruit development in both fruit and crown leaf, cDNA corresponding to both genes covering all 5 stages ranking from stage1 anthesis (2 months after flowering treatment), stage2 late anthesis stage (2.5 months after stage1), stage3 small fruit stage (3.5 months after flowering treatment), stage 4 medium fruit stage (4-4.5months after flowering treatment), and stage 5 mature fruit (5 months after flowering treatment)(Fig. 1) were carried out. The mature fruit at stage 5 was selected based on 80% of yellow ripen which represent stage of physiological maturity. The investigation of *AcMST1 and AcSUT1* gene expression of in crown leaf during fruit development were shown in Fig. 2.

Results revealed that, in fruit, the expression of *AcMST1* increased from stage 2 and steadily expressed with a level more than that of 18S, house keeping rRNA. Also the expression of *AcSUT1* started to express at similar stage with that of *AcMST1*. The expression of *AcSUT1* though continued to the last, its level of expression decreased after stage 3. Interestingly, level of expression of both genes, in crown leaf, were much lower than that found in fruit. Also level of expression of both genes continued to decrease after stage 4 and the expression of *AcSUT1* was totally discontinued at stage 5.

AcSUT1 protein is a sucrose transporter localized to pre-vacuoles. Since in Arabidopsis a similar protein called SUT2, localized at plasma membrane of sieve element, was found to highly express in sink tissues, similar to *AcSUT1*, a role of

AcSUT1 as efflux carriers, implicated in phloem unloading had been proposed (Antony *et al*., 2008).

The halting of *AcSUT1* expression in crown leaf at stage of fruit maturity was attracted interest because this phenomenon could be employed for maturity prediction. Based on this, a method for a simple non destructive determination of fruit maturity using the *AcSUT1* expression phenomenon in crown leaf as an indicator was developed. It was based on specific cDNA amplification via reverse transcription loop mediated isothermal amplification platform in combination with nucleic acid hybridization based on colorimetric assay of gold nanoparticles (Kanjanawarut and Su, 2009).

Reverse transcription loop-mediated isothermal amplification (RT-LAMP) provides an alternative simple yet rapid testing option (Notomi *et al*., 2000, Mori *et al*., 2001). The mechanisms of RT-LAMP and its accesses had been described elsewhere (Notomi *et al*., 2000, Parida *et al*., 2008). RT-LAMP has several advantages comparing with RT-PCR and real-time RT-PCR especially in reaction simplicity, its rapidness, its highly specific to target RNA due to the simultaneously primed of multi primers on RNA, and its higher amplification efficiency, all attributes that clearly distinguish RT-LAMP from the existing detection methods (Parida *et al*., 2008).

Likewise, the novel nucleic acid hybridization, based on colorimetric assay of gold nanoparticles, was employed for further identify cDNA signals. In the colorimetric detection, the β-pyrrolidinyl peptide nucleic acid (PNA) was used as probe. β-pyrrolidinyl PNA is a derivative of oligonucleotide analogues, in which the sugar phosphate backbone had been replaced by a pseudopeptide chain of *N*-aminoethylglycine monomers, the recognition of target DNA via PNA/DNA hybridization could be performed at exceptionally high affinity and specificity (Suparpprom et al., 2005, Vilaivan and Srisuwannaket, 2006). The merits of using PNA here were not only property of PNA that allowed complementary DNAs to be hybridized according to the Watson–Crick hydrogen-bonding rules, it also offered advantages over classical DNA hybridization since its neutral-charged backbone increases the binding strength (Vilaivan and Srisuwannaket, 2006). This provided a rapid sequence-specific detection in solution without the need of membrane in short period of time. Moreover, this PNA probe typically showed superior selectivity against mismatches compared to DNA probes and would not hybridize with RNA molecules in the system, the latter was not found in that of Nielsen (Nielsen and Haaima 1997). Thus these properties improve discrimination of target DNA to a perfect level.

PNA also acts as a coagulant to alter the intrinsic stability of gold nanoparticles when mixing together allowing nucleic acid hybridization to be simply and rapidly carried out. In principle, the binding of PNA probe on surface of gold nanoparticles is by both the nitrogen-/oxygen-containing and the hydrophobic neutral structure of peptide backbone leading to a higher affinity to gold than that of DNA. During hybridization, PNA oligomers can induce immediate particle aggregation, if they are not bind with their target DNA, however, when target DNAs are available, successful PNA-DNA hybridizations result in forming of hybridization complexes, although having a stable double helix structure similar to dsDNA, that can effectively protect gold nanoparticles from salt induced aggregation (Kanjanawarut and Su, 2009). The result of gold nanoparticles aggregation provides a colorimetric change of colloid particles from ruby red to purple that can be seen with naked eye.

In the first step of experiment, a primer set for *AcSUT1* cDNA amplification, comprising two outer (F3 and B3) and two inner primers (FIP and BIP), was chosen and

depicted in Fig. 3. It was specific to 6 area of *AcSUT1* (Accession No. 460878) between position 1574 to 1741(see Fig. 3 for detail).

Amplification using the designed primer set at 63 °C delivered ladder DNA products of multiplied size of ~170 nucleotides (Fig. 4) within 30 min. Only sample having *AcSUT1* RNA had been amplified. The primer set was priori tested by computer program Blastn for specific amplification of only target RNA but not others (Altschul *et al.*, 1990) and tested for non-reacting with RNA of plant viruses (TMV, CMV, PRSV) (data not shown). When compared with RT-PCR of Antony *et al.*, (2008), RT-LAMP provided similar results (Fig. 4., lower).

Sensitivity in *AcSUT1* detection using known copy number of clone cDNA of *AcSUT1* as templates was also performed. Results, in Fig. 5, revealed the LAMP unique DNA pattern observed even when the template molecules were diluted to a level of 10 copies per reaction. Results of cDNA amplifications were also well corresponding with that of previously reported RT-PCR (Antony *et al.*, 2008). All these results supported the reliability of amplification system for *AcSUT1* signals amplification.

Further step confirmation of the nucleotide sequence of target products was by novel nucleic acid hybridization based on colorimetric assay of gold nanoparticles. Successful detection of *AcSUT1*'s cDNA each time when fruit were still immature came with ladder like DNA products that hybridized well with PNA at surface of gold nanoparticles. This resulted in effective protection of gold nanoparticles from salt induced aggregation, thus, remaining of ruby red color for gold solution. Whereas in mature fruit, where the expression of *AcSUT1* in crown leaf had terminated, no DNA amplification were observed. The PNA oligomers, not binding with their target DNA, were remained on the gold surface and could induce immediate particle aggregation changing the color of gold solution from ruby red to purple one. Ruby red color of gold solution after hybridization could be detected in samples having *AcSUT1* expression within 2 min(Fig. 4 and Fig 5, bottom). They provided further evidences of nucleic acid specific detection following *AcSUT1* amplification system. These specificity and sensitivity indicated a satisfactory performance of the combined RT-LAMP and rapid nucleic acid hybridization method for maturity detection. The result of clear color of ruby red signals came from the yield of DNA products, delivered more by reverse transcription isothermal DNA amplification than that of PCR, especially at near limit of detection. The RT-LAMP/nucleic acid hybridization also provided several merits of RT-LAMP in cDNA amplification and signals detection in terms of the incubation at constant temperature which eliminates the need for a thermocycler device, making possible to perform DNA amplification outside laboratory (Mori *et al.*, 2001, Nagamine *et al.*, 2001) and detection rapidly at room temperature. Furthermore, time for amplification reaction is reduced to 30 min which enables the whole processes of the detection to be completed within 1 hour. Additionally, this detection can be observed visually with naked eye

Further demonstrations of fruit maturity determination using the above method, an application for field testing had been carried out to using 25 samples randomly selected from fields (15 mature and 10 immature fruits, based on color and soluble solid criteria). Results revealed the complete detection of all blind 15 samples of mature fruits among 25 samples tested but one false negative result was found from both tests. The mature fruit results predicted by RT-LAMP were agreed with the results previously judged by the physiological criteria. Based on the data tested (n=25), sensitivity of the test was

calculated from number of positive results divided by sum of number of positive plus number of false negative, which equally to 15/16 or 93.75%. Similarly, the specificity of the test was calculated from number of negative results divided by sum of number of negative plus number of false positive, which equally to 10/10 or 100% (Fig.6.) . It should be noted that the detection of gene expression here was a qualitative test, suitable to detect on and off gene expression, for quantitative assay further modification of the method was needed.

Detection of target *AcSUT1* gene expression in crown leaf was a sample model for non destructive determination of fruit maturity. In the rest of fruits, either climacteric or non climacteric one, the incidences of the synthesis and accumulation periods of monosaccharide in fruit, and also the transportation of monosaccharide from leaf during maturation, were still key factors in fruit development, fruit quality and fruit maturity, awaited elucidation. These exploring could be employed in fruit maturation detection.

Based on the above results, we had developed the method for simple fruit maturity detection and demonstrated the use of this method for fruit maturity determination. By detecting of *AcSUT1* gene expression in crown leaf, one can predict state of fruit maturity without damage the fruit. This was the first time that isothermal nucleic amplification platform together with nucleic acid hybridization on the surface of gold nanoparticles were applied for fruit maturity detection. The detection via RT-LAMP and nanoparticles here costs approximately US$8 per test, at least 8 times cheaper than the cost of a standard laboratory test. Also reaction can be adjusted to an easy-to-operate reagent kit which better provides an opportunity to monitor the expression of *AcSUT1* gene wherever needed.

CONCLUSION

A technique for the pineapple fruit maturity detection based on RT-LAMP of *AcSUT1* and nucleic acid hybridization on the surface of gold nanoparticles was developed. Direct amplification of *AcSUT1* by reverse transcription isothermal DNA amplification using a set of primers allowed target gene to be ready for nucleic acid hybridization in 30 min. Target gene products in ladder DNA starting from size of 170 nt. could be observed. Determination of technique's sensitivity revealed the limit of detection at 10 copies of *AcSUT1* gene. Further detection of *AcSUT1* signals was based on colorimetric nucleic acid hybridization platform with gold colloid nanoparticles, 20 nm in diameter. In the immature fruit, the *AcSUT*1 gene was expressed allowing target DNA amplification to occur. Presence of target DNA affected gold colloid nanoparticles in term of non aggregation with no color change (still ruby red). However, in the mature fruit, the expression of the *AcSUT*1 gene was terminated resulting in no target cDNA product amplification. When this was tested with gold colloid nanoparticles, it induced aggregation of particles which in turn resulted in a plasmonic change of colloid solution from ruby red to dark purple, visible by naked eye. The technique has several merits on its rapidity and simplicity in performing the test, on the characteristic of colorimetric change of gold nanoparticles which required no sophisticated devices, and on its ability to perform the test wherever needed.

ACKNOWLEDGEMENTS
We would like to thank the Integration Project: Innovations for the Improvement of Food Safety and Food Quality for New World Economy, Chulalongkorn University, Bangkok, Thailand, for the support in sub-project "DNA molecule for novel development in quality and safety analysis of raw materials and processed foods". Thanks were also to Thailand Research Fund, for the support of the project "Synthesis, properties and applications of conformationally constrained beta-pyrrolidinyl peptide nucleic acids".

Literature cited

Altschul S.F., Gish W., Miller W., Myers E.W., and Lipman D.J. 1990. Basic local alignment search tool. Journal of Molecular Biology 215: 403–410.

Anonymous. 2003. Creating standard curves with genomic DNA or plasmid DNA templates for use in quantitative PCR, Applied Biosystems Protocol 1-9. (available at www.appliedbiosystems.com/support/tutorials/pdf/ quant_pcr.pdf)

Antony E., Taybi, T., Courbot, M., Mugford, S.T., Smith, J.A.C., and Borland, A.M. 2008. Cloning, localization and expression analysis of vacuolar sugar transporters in the CAM plant *Ananus comosus* (pineapple). J. Experimental Botany 59:1895-1908.

Chaumpluk, P., Chaiprasart, P. 2010. Fluorescene biosensor for a simple and rapid detection of Escherichia coli in fresh-cut fruits. Acta Horticulturae 880:547-554.

Kader, A.A. 1999. Fruit maturity, ripening and quality relationships. Acta Hort 485:203-208.

Kanjanawarut, R and Su, X. 2009. Colorimetric detection of DNA using unmodified metallic nanoparticles and peptide nucleic acid probes. Analytical Chemistry 81: 6122–6129.

Kuribara, H., Shindo,Y., Matsuoka, T., Takuro, K., Futo, S., Aoki, N., Hirao, T., Akiyama, H., Goda, Y., Toyoda, M. and Hino, A. 2002. A novel reference molecules for quantification of genetically modified maize and soybean. J. AOAC Int. 85: 1077-1089.

Mori, Y., Nagamine, K., Tomita N., and Notomi T. 2001. Detection of loop-mediated isothermal amplification reaction by turbidity derived from magnesium pyrophosphate formation, Biochem. Biophys. Res. Commun. 289 :150–154.

Moyle, R., Fairbairn, D.J., Ripi, J., Crowe, M. and Botella, J.R. 2005. Developing pineapple fruit has a small transcriptome dominated by metallothionein. J. Experimental Botany 56:101-112.

Nagamine, K., Watanabe, K., Ohtsuka, K., Hase T., and Notomi, T. 2001. Loop-mediated isothermal amplification reaction using a nondenatured template, Clin. Chem. 47 : 1742–1743.

Nielsen P.E., and Haaima G.1997. Peptide nucleic acid (PNA). A DNA mimic with a pseudopeptide backbone. Chem. Soc. Rev. 26:73-78.

Notomi, T., Okayama, H., Masubuchi, H., Yonekawa, T., Watanabe, K., Amino N., and T. Hase. 2000. Loop-mediated isothermal amplification of DNA. Nucleic Acids Res. 28 : e63.

Parida, M., Sannarangaiah, S., Dash, P.K., Rao, P. V. L., Morita, K. 2008. Loop mediated isothermal amplification (LAMP): a new generation of innovative gene amplification technique; perspectives in clinical diagnosis of infectious diseases. Rev. Med. Virol. 18: 407–421.

Pattee, H.E.(ed,).1985. Evaluation of quality of Fruits and vegetables. AVI Publishing Co. Inc. Westport, CT.p. 410.

Pienpinijtham, P., Thammacharoen, C., and Ekgasit S. 2010. Enhacement of reducing efficiency of soluble starch for green synthesis of gold nanoparticles. Pure and Applied Chemistry International Conference 21-23 January 2010 Sunee Grand Hotel Ubon Ratchathani, Thailand. p. 366.

Sambrook, J., Fritsch, E.F., and Maniatis., T. 1989. Molecular cloning: a laboratory manual.Cold Spring Harbor Laboratory Press. New York.

Suparpprom, C., Srisuwannaket, C., Sangvanich, P., Vilaivan, T. 2005. Synthesis and oligodeoxynucleotide binding properties of pyrrolidinyl peptide nucleic acids bearing prolyl-2-aminocyclopentanecarboxylic acid (ACPC) backbones. Tetrahedron Lett. 46: 2833-2837.

Taira, T., Toma, N., Ichi, M., Takeuchi, M., and Ishihara, M. 2005. Tissue distribution, synthesis stage and ethylene induction of pineapple (*Ananus comosus*) chitinase. Biosci. Biotechnol. Biochem. 69:852-854.

Vilaivan, T., Srisuwannaket, C. 2006. Hybridization of pyrrolidinyl peptide nucleic acids and DNA: Selectivity, base-pairing specificity, and direction of binding. Org. Lett. 8:1897-1900.

Zhang, X., Du, L., Xie, M.A., Wang, W., Mo, Y., and Sun, G. 2010. Cloning and expression of pineapple sucrose phosphate synthase gene during fruit development. African J. of Biotechnology 9:8296-8303.

Figures

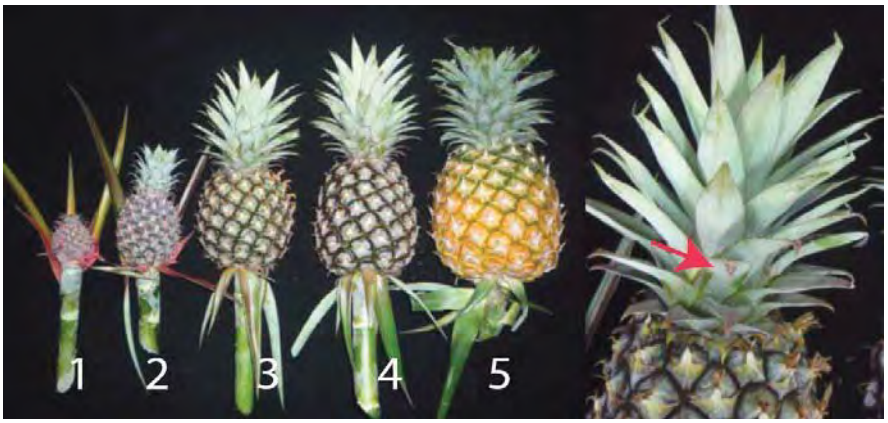

Figure 1. Stage of fruits development of Sriraja, a Cayenne type pineapple. A) From left to right, Stage1 anthesis (2 months after flowering treatment), Stage2 late anthesis stage (2.5 months after stage1), Stage3 small fruit stage (3.5 months after flowering treatment), Stage 4 medium fruit stage (4-4.5months after flowering treatment), and Stage 5 mature fruit (5 months after flowering treatment). B) Position of crown leaf used for maturity detection (arrow).

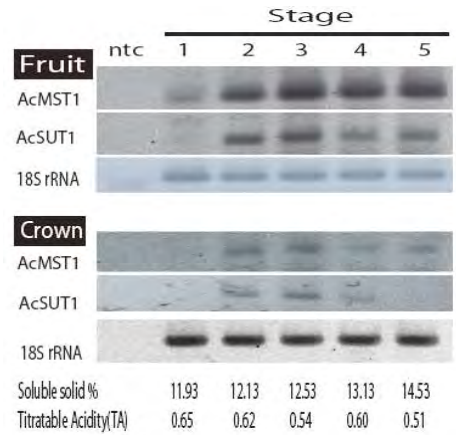

Figure 2. Abundance of transcripts of AcMST1 and AcSUT1 in fruits and in crown leave during the course of fruit development (Stage 1 anthesis to stage 5 mature fruit) compared with the 18S rRNA house keeping gene. Soluble solid and titratable acidity (TA) of each stage were also shown. The ntc represents non template control.

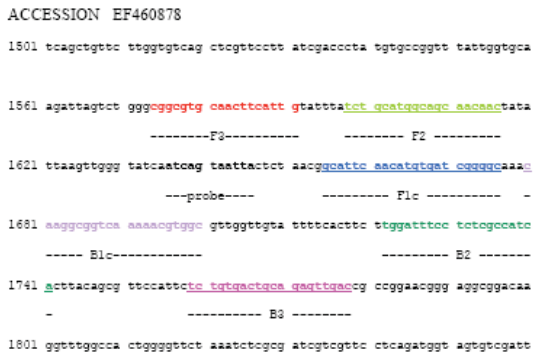

Primer	Sequence	Location
F3	CGGCGTGCAACTTCATTG	1574-1591
B3	GTCAACTCTGCAGTCACAGA	1759-1778
FIP	GCCCCGATCACATGTTGAATGC TTTTTCTGCATGGCAGCAACAAC	1597-1616 and 1655-1676
BIP	CAAGGCGGTCAAAAACGTGGC TTTTTGATGGCGAGAGGAAATCCA	1680-1700 and 1722-1741

Figure 3. Schematic illustration of related sequence of *AcSUT1* where 6 locations of primers were assigned on the sequence including F3, F2, F1, B1, B2 and B3 respectively. The detail of primers was demonstrated on the right.

Figure 4. Amplification of target *AcSUT1* using RT- LAMP, their corresponding RT-PCR detection (lower) and the confirmation by nucleic acid hybridization using gold nanoparticles. Lane M, 100 nucleotide ladder, Lane NTC, non template control, Lane –ve, negative amplification of *AcSUT1*, and +ve, positive amplification of *AcSUT1*.

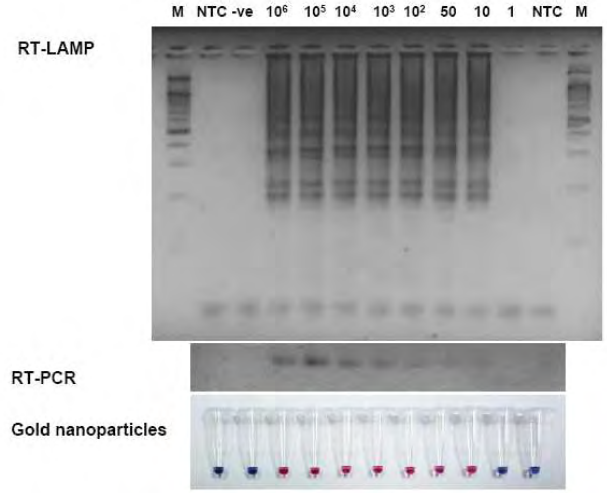

Figure. 5. Sensitivity of primers for amplification of target cDNA of known copies using cloned *AcSUT1* gene via LAMP (upper) and its nucleic acid hybridization using gold nanoparticles (lower). The confirmation by PCR based on Antony, (2008) was shown in the middle. Lane M, 100 nt ladder marker. Lane –ve , negative amplification of DNA using *AcMST1* gene as a template, Lanes with numbers represent the number of DNA copies involved in detection.

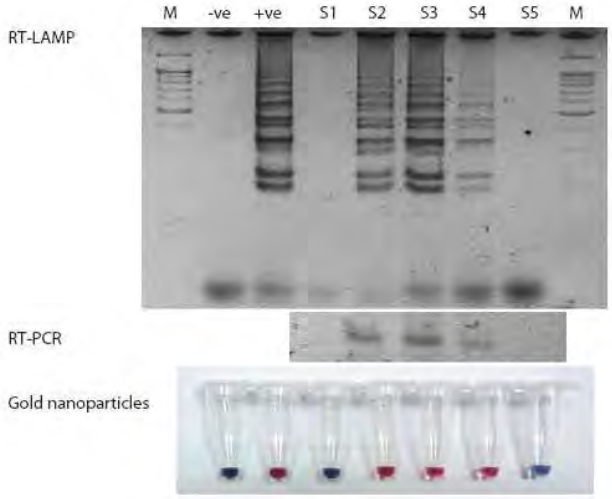

	Sample*	RT-PCR	RT-LAMP+ Goldnano
Mature (true positive)	15	15	15
False positive	-	0	0
Immature(true negative)	10	9	9
False negative	-	1	1

n = 25

$$\text{Sensitivity} = \frac{\text{true positive}}{\text{true positive+false negative}} = \frac{15}{15+1} = 93.75\%$$

$$\text{Specificity} = \frac{\text{true negative}}{\text{true negative+false positive}} = \frac{10}{10+0} = 100\%$$

Figure 6. A) Representative detection of *AcSUT1* in pineapple fruits collected from fields. Results based on RT-LAMP (upper) and RT-PCR as previously reported (Antony, *et al*., 2008) (middle) and nucleic acid hybridization using gold nanoparticles (lower) were illustrated. Lane M, 100 nt ladder marker, Lane –ve , negative amplification of *AcMST1*, Lane +ve , positive *AcSUT1* DNA, Lanes S with numbers represent the commercial samples from source 1 to 5. B) Overall fruit maturity detection using 15 mature fruits and 10 immature fruits revealed a precise testing results of mature fruits with one of false negative in both methods. The sensitivity and specificity were demonstrated.

SYN-O-004

CYCLODEXTRINS DISCRIMINATION BY TRICATIONIC PHENYLENE-ETHYLYNYLENE FLUOROPHORE

Warathip Siripornnoppakhun, Paitoon Rashatasakhon, Mongkol Sukwattanasinitt*

Department of Chemistry, Faculty of Science, Chulalongkorn University Bangkok 10330 Thailand
**Corresponding Author : smongkol@chula.ac.th*

ABSTRACT

The cyclodextrins (CyDs) containing six (α), seven (β) and eight (γ) glucosyl-membered cyclic structure are widely used in controlled release system, separation and molecular recognition due to their complexation ability and low cytotoxicity. Size selective inclusion complexation with CyDs and detection of this phenomenon are thus important for development toward these applications. In this contribution, the complexation of trimethylphenyl quaternary ammonium groups with γ–CyD is readily observed by fluorescence enhancement and ^{1}H NMR signals shifts of tricationic phenylene-ethynylene fluorophore. Benesi-Hilderbrand plot and the NMR data revealed a 1:1 complexation between the fluorophore and γ-CyD. The data also indicate no inclusion interaction between the fluorophore and other CyDs (α and β). This tricationic fluorophore should be useful for identify γ–CyD from the other sizes CyDs and probing its inclusion interaction.

Keywords Fluorescence; Sensor; Inclusion complex

Chulalongkorn University
จุฬาลงกรณ์มหาวิทยาลัย
Pillar of the Kingdom

Abstract Book

The 8th Mathematics and Physical Science Graduate Congress 2012

Connect Science
Connect ASEAN

8 - 10 December 2012

Faculty of Science
Chulalongkorn University, Thailand

Participating Universities :

UNIVERSITY OF MALAYA
The Leader in Research & Innovation

NUS
National University of Singapore

Cytocompatibility and Cellular Uptake of Blackberry-like Particles Assembled from Fluorescent-labeled Quaternized Chitosan

Kanya Taboonpong[1,2], Naunpun Sangphech[3], Tanapat Palaga[3], Tirayut Vilaivan[4] and Voravee P. Hoven[4*]

[1]*Program in Petrochemistry and Polymer Science, Faculty of Science, Chulalongkorn University, Bangkok 10330, Thailand*
[2]*Center for Petroleum, Petrochemicals and Advanced Materials, Chulalongkorn University, Bangkok 10330, Thailand*
[3]*Department of Microbiology, Faculty of Science, Chulalongkorn University, Bangkok 10330, Thailand*
[4]*Organic Synthesis Research Unit, Faculty of Science, Chulalongkorn University, Bangkok 10330, Thailand*
**Corresponding auther. E-Mail: vipavee.p@chula.ac.th*

Abstract

Upon self-assembly of amphiphilic chitosan having *N*-[(2-hydroxyl-3-trimethylammonium)] propyl (HTAP) as hydrophilic entities and ethynylpyrene (fluorescent dye) as hydrophobic entities, fluorescent-labeled quaternized chitosan (Pyr-CS-HTAP) particles can be formed. The functionality of the quaternized chitosan particles were verified by FT-IR and NMR spectroscopy. According to SEM analysis, the particles had a size range of 1-2 μm with blackberry-like morphology. And the particles exhibited positive charges with a zeta-potential of +40 mV as determined by PCS. The particles had bright green fluorescence and were stable in a broad pH and temperature range. The cytotoxicity test revealed that the particles were biocompatible with Macrophage cells (RAW 264.7 cells). Moreover, cellular uptake of the particles by the cells can be determined by confocal laser scanning microscopy (CLSM) and flow cytometry techniques. The results showed that approximately 42% of cellular uptake was observed after 1 h incubation. It has also been found that the aggregation of the particles has a strong impact on the extent of cellular uptake. These fluorescent-labeled quaternized chitosan particles possess a number of desirable features that may be used for bioimaging application.

Keywords: blackberry-like particles; fluorescent-labeled particles; self-assembly; chitosan particles; cytocompatible particles

Chulalongkorn University
จุฬาลงกรณ์มหาวิทยาลัย
Pillar of the Kingdom

Abstract Book

The 8th Mathematics and Physical Science Graduate Congress 2012

Connect Science
Connect ASEAN

8 - 10 December 2012

Faculty of Science
Chulalongkorn University, Thailand

Participating Universities :

UNIVERSITY OF MALAYA
The Leader in Research & Innovation

NUS
National University of Singapore

Functional Polymer-stabilized Gold Nanoparticles: Preparation and Peptide Nucleic Acid Immobilization

Pornpen Sae-ung[1], Gamolwan Tumcharern[2], Tirayut Vilaivan[3], and Voravee P. Hoven[3*]

[1]*Program in Macromolecular Science, Faculty of Science, Chulalongkorn University, Bangkok 10330, Thailand*
[2]*National Nanotechnology Center, National Science and Technology Development Agency, Thailand Science Park, Pathumthani 12120, Thailand*
[3]*Organic Synthesis Research Unit, Department of Chemistry, Faculty of Science, Chulalongkorn University, Bangkok 10330, Thailand*
**Corresponding author. E-mail: vipavee.p@chula.ac.th*

Abstract

Poly(methacrylic acid)-*ran*-(2-methacryloyloxyethyl phosphorylcholine) (PMAMPC) which can provide binding site and protein-repellent property was prepared via Reversible Addition-Fragmentation Chain Transfer (RAFT) polymerization and grafted onto citrate-stabilized gold nanoparticles (citrate-AuNPs) to obtain functionalizable AuNPs having anti-fouling characteristic. Optical property, size, and morphology of PMAMPC-stabilized AuNPs (PMAMPC-AuNPs) were evaluated by UV-vis spectroscopy, dynamic light scattering (DLS) technique and transmission electron microscopy (TEM). The presence of PMAMPC around the AuNPs was also confirmed by Fourier transform infrared spectroscopy (FTIR). PMAMPC-AuNPs were highly stable because of both electrostatic and steric stabilizations of the polymeric shell. Then, fluorescein-labeled peptide nucleic acid (PNA-flu) was immobilized to carboxyl groups of PMAMPC on PMAMPC-AuNPs via EDC/NHS coupling chemistry. Effects of PMAMPC molecular weight, surfactant (Tween-80) concentration on PNA-flu immobilization was determined. The amount of immobilized PNA-flu as determined by fluorescence spectroscopy after KCN digestion was found to be 2.72×10^{13} probe/cm^2. This value is two times higher than that (1.28×10^{13} probe/cm^2) obtained via a direct PNA immobilization by self-assembly monolayer (SAM) formation of PNA-terminated thiol compound. This discovery strongly suggests that the 3-D structure of the polymeric shell can provide greater probe binding capacity than the 2-D SAM system. It is anticipated that this newly developed polymer-stabilized AuNPs can potentially be developed into effective PNA-based DNA biosensor.

Keywords: Gold nanoparticles; Zwitterionic polymer; Peptide nucleic acid; Protein repellent surface

NANYANG TECHNOLOGICAL UNIVERSITY

NUS National University of Singapore

THE 7TH INTERNATIONAL CONFERENCE ON CUTTING-EDGE ORGANIC CHEMISTRY IN ASIA

THE 3RD NEW PHASE INTERNATIONAL CONFERENCE ON CUTTING-EDGE ORGANIC CHEMISTRY IN ASIA

(ICCEOCA-7 / NICCEOCA-3)

11 - 14 Dec 2012, Singapore
Nanyang Technological University

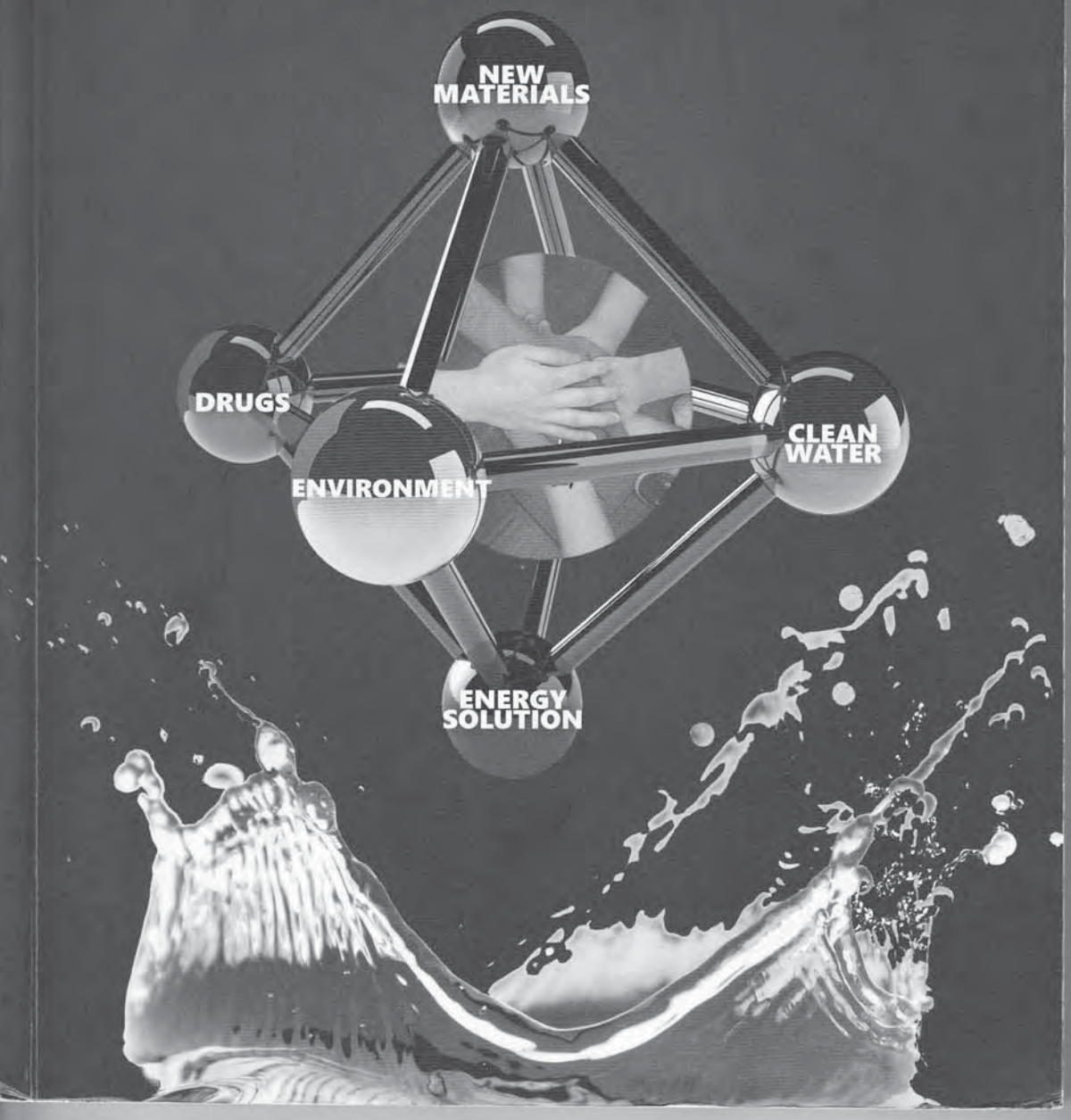

17:30 OP12 p.37
Interfacial Self-Assembly and Theranostic Applications of Organic-Inorganic Hybrid Nanomaterials
Ken C.-F. Leung, *Hong Kong Baptist University / The Chinese University of Hong Kong*

18:00 OP13 p.38
Biomimetic Total Synthesis of Complex Sesquiterpenoid
Xiaoguang Lei, *National Institute of Biological Sciences*

THU - 13 DEC 2012

Oral Presentation | Classroom 1

08:30 - 10:00 | Session Chair: Sunggak Kim

08:30 OP14 p.39
Formation of Ligand-Assisted Complex of Two RNA Hairpin Loops
Kazuhiko Nakatani, *Osaka University,The Institute of Scientific and Industrial Research*

09:00 OP15 p.40
Protein Total Synthesis
Xuechen Li, *The University of Hong Kong*

09:30 OP16 p.41
Bioactive Compounds from Endophytic and Marine-Derived Fungi
Prasat Kittakoop, *Laboratory of Natural Products, Chulabhorn Research Institute/Chulabhorn Graduate Institute*

11:00 - 12:30 | Session Chair: Somsak Ruchirawat

11:00 OP17 p.42
Highly Efficient Methodologies via Nitrogenation
Ning Jiao, *Peking University, School of Pharmaceutical Sciences*

11:30 OP18 p.43
Efficient synthesis of biologically active chromenone derivatives via Pd-catalyzed direct cross-coupling
Sungwoo Hong, *KAIST*

12:00 OP19 p.44
D-D-π-A Type Organic Dyes for Dye-Sensitized Solar Cells: Structure-Property Relationships
Vinich Promarak, *Department of Chemistry, Faculty of Science, Ubon Ratchathani University*

13:30 - 15:30 | Session Chair: Yixin Lu

13:30 OP20 p.45
Organocatalyst in Total Synthesis
Yujiro Hayashi, *Tohoku University*

14:00 OP21 p.46
Asymmetric Diels-Alder Reactions via HOMO-activation
Ying-Chun Chen, *Department of Medicinal Chemistry, West China School of Pharmacy, Sichuan University*

14:30 OP22 p.47
N-Heterocyclic Carbene Catalysis: Towards Developing New Activation Modes
Robin Chi, *NTU-SPMS-CBC*

15:00 OP23 p.48
Transition Metal-Catalyzed Fluorination
Guosheng Liu, *Shanghai Institute of Organic Chemistry, Chinese Academy of Sciences*

16:30 - 18:00 | Session Chair: Atsushi Nishida

16:30 OP24 p.49
Functionalized Nanoparticle for Cell Targeting and Protein Enrichment
Chun-Cheng Lin, *National Tsing Hua University*

17:00 OP25 p.50
Internally-Labeled Pyrrolidinyl Peptide Nucleic Acid as Hybridization-Responsive Fluorescence Probes for DNA Sequence Detection
Tirayut Vilaivan, *Department of Chemistry, Faculty of Science, Chulalongkorn University*

17:30 OP26 p.51
Catalytic Asymmetric Construction of Stereochemically Diversified Pyrrolidines
Takayoshi Arai, *Chiba University*

18:00 OP27 p.52
Structural Revisions/Assignments of Marine Natural Products by Total Synthesis
Tao Ye, *Dept. of Applied Biology and Chemical Technology, The Hong Kong Polytechnic University*

FRI - 14 DEC 2012

Oral Presentation | Classroom 1

08:30 - 10:00 | Session Chair: Minoru Isobe

08:30 OP28 p.53
Modulation of oxacarbenium ions: a Simple Approach for Stereoselective Glycosidic bond formations
Kwok Kong Mong, *National Chao Tung University*

09:00 OP29 p.54
Ni-Catalyzed Multi-component Coupling Reaction of Organozinc Reagents, Unsaturated Hydrocarbons, and Carbonyl Compounds
Masanari Kimura, *Nagasaki University*

09:30 OP30 p.55
Aromatic C-H Bond Functionalization: Transition Metal-Free SET C-H Arylation, Pd-Catalyzed Cross-Dehydrogenative-Coupling (CDC) and Ketone-Directed Hydroxylation Reaction
Fuk Yee Kwong, *The Hong Kong Polytechnic University*

10:30 - 12:00 | Session Chair: Pauline Chiu

10:30 OP31 p.56
Weak Hydrogen Bonding as Stereocontrolling Element in Asymmetric Palladium Catalysis
Steve Zhou, *NTU-SPMS-CBC*

11:00 OP32 p.57
Synthesis of Azabicycles via Lewis- and Brφnsted-Acid-Promoted Cyclization of N-Containing Cyclic Enynols
Ming-Chang Yeh, *National Taiwan Normal University*

11:30 OP33 p.58
Site Selective Borylation of Unactivated Internal C(sp3)–H Bonds Catalyzed by Rh or Ir Complexes with Silica-Supported Monophoshine Ligands
Masaya Sawamura, *Hokkaido University*

WED - 12 DEC 2012

Poster Session A | NTU -

10:30 - 11:30, 15:30 - 16:30

PA01
Design, Synthesis, and Electr Phthalocyanine Analogues
Atsuya Muranaka, *Advanced Elem*

PA02
Collective Syntheses of Tetro
Toshio Nishikawa, *Nagoya Univ*

PA03
The Use of Functionalized Ra Resolution
Kwunmin Chen, *National Taiwan N*

PA04
Structure-based Optimizatio G-quadruplex DNA Stabilize
Edmond Dik Lung Ma, *Hong Kong*

PA05
Selective Synthesis of Hetero
Boshun Wan, *Dalian Institute of Ch*

PA06
Palladium-Catalyzed Arylati Malonate Esters with Aryl H
Hideki Yorimitsu, *Kyoto Universit*

PA07
Pd(II)-Catalyzed C-H Activat Hydrogen Phosphates
Sunggak Kim, *NTU-SPMS-CBC*

PA08
Hydrogen Bonded Aryl Ami
Zhan-Ting Li, *Department of Chemis*

PA09
π-Extended, Expanded Arom Protonation-Coupled Redox
Chang Hee Lee, *Kangwon National U*

PA10
ortho-Methyl Substituted W the DNA strand displacemer
Shigeki Sasaki, *Kyushu University*

PA11
Small Molecule Regulator o
Zhang Yan, *Department of Chemistry*

PA12
Enantioselective Conjugate Catalyzed by Ni(acac)2 and
Biing-Jiun Uang, *National Tsing Hua*

PA13
Deacylation of Unactivated Transamidation
Takashi Ohshima, *Kyushu Universi*

PA14
Muraymycins: A Guide to a
Satoshi Ichikawa, *Hokkaido Universi*

OP25

Internally-Labeled Pyrrolidinyl Peptide Nucleic Acid as Hybridization-Responsive Fluorescence Probes for DNA Sequence Detection

Tirayut Vilaivan,* Boonsong Ditmangklo, Chalothorn Boonlua
Organic Synthesis Research Unit, Department of Chemsitry, Faculty of Science, Chulalongkorn University, Phayathai Road, Patumwan, Bangkok 10330, Thailand
E-mail: vtirayut@chula.ac.th

Classical molecular beacons require two different labels, usually a fluorophore and a quencher attached to different end of the same DNA strand. The sequence of DNA beacons are designed so that the fluorophore and hte quencher are in close proximity in the normal state, resulting in suppression of the fluorescence. Upon hybridization with the correct DNA target, the fluorophore and quencher are separated and this is accompanied by fluorescence increase. There are attempts to simplify the design of molecular beacons by using just one fluorophore that can change its fluorescence in response to the different microenvironment in the single- and double-stranded DNA. Little work in this area had been applied to peptide nucleic acid (PNA) – a DNA analogue with the deoxyribose phosphate backbone is replaced by a peptide-like backbone. PNA recognizes DNA/RNA with higher affinity and specificity than DNA, and offered a number of other advantages such as complete resistant to proteases and nucleases.

In this work, we summarize progress in the design of hybridization responsive fluorescence probe for DNA sequence determination based on our recently-developed pyrrolidinyl peptide nucleic acid consisting of D-prolyl-(1*S*,2*S*)-2-aminocyclopentanecarboxylic acid backbone (acpcPNA). As an example, we had developed reliable reductive alkylation and Click chemistry-based protocols for site-specific labeling of acpcPNA backbone by pyrene or thiazole orange. The pyrene-labeled acpcPNA showed a fluorescence increase (4–14 folds) in the presence of the correct DNA target. The thiazole orange-labeled acpcPNA showed even higher fluorescence increase (up to 100 folds) upon binding to DNA. The specificity can be further improved with the help of S1 nuclease digestion, which allows perfect discrimination between complementary and single mismatched DNA at ambient conditions under a wide sequence context.

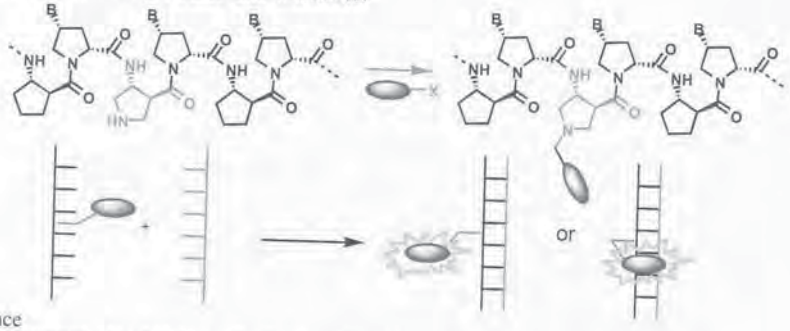

Reference
1. (a) Mansawat, W.; Vilaivan, C.; Balázs, Á.; Aitken, D.; Vilaivan, T. *Org. Lett.* **2012**, *14*, 1440–1443.; (b) Vilaivan, T.; Srisuwannaket, C. *Org. Lett.* **2006**, *8*, 1897–1900.
2. (a) Boonlua, C.; Vilaivan, C.; Wagenknecht, H.-A.; Vilaivan, T. *Chem. Asian J.* **2011**, *6*, 3251–3259.;(b) Reenabthue, N.; Boonlua, C.; Vilaivan, C.; Vilaivan, T.; Suparpprom C. *Bioorg. Med. Chem. Lett.* **2011**, *21*, 6465–6569.

Tirayut Vilaivan (ธีรยุทธ วิไลวัลย์). Chulalongkorn University (B.Sc., 1992), Oxford University (D.Phil., 1996). Associate Professor, Department of Chemistry, Faculty of Science, Chulalongkorn University (since 2004). Research field: peptide nucleic acids, asymmetric catalysis, medicinal chemistry.

OP26

Catalytic Asymme

Department of Ch
1-3

Precise control of stereoche
is a highly desired goal
asymmetric synthesis
functionalized molecules.
exploring efficient asymm
we prepared a library
imidazoline-aminophenol
catalysts, and developed
throughput screening metho
reaction mixtures carried
solid-phase catalysts were di
by circular dichroism (CD).
"Solid-phase catalysis/CD-
the catalysts for [3+2] cy
imino esters and nitro
explored to give the tetrasub
pyrrolidines. The chiral

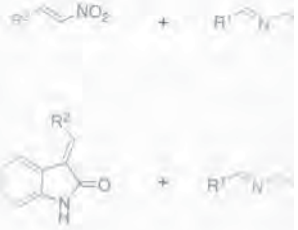

Reference
1. Arai, T.; Watanabe, M.;
Chem. Int. Ed. **2006**, *45*,
2. Arai, T.; Yokoyama, N.;
3. Arai, T.; Yokoyama, N.;
7895.
4. Awata, A.; Arai, T. *Chem.*

Takayoshi
Univ. of
Postdoc. H
Prof. Chib
asymmetric
throughput
organic-ino

PURE AND APPLIED CHEMISTRY INTERNATIONAL CONFERENCE 2013

January 23-25, 2013

Bangsaen Beach

THAILAND

PEPTIDE NUCLEIC ACID PROBE FOR ELECTROCHEMICAL DETECTION OF HUMAN PAPILLOMA VIRUS DNA TYPE 16

Sakda Jampasa[1], Wanida Wonsawat[2], Tirayut Vilaivan[3], Orawon Chailapakul[1, 4, 5,*]

[1] *Program in Petrochemicals and Polymer Science, Faculty of Science, Chulalongkorn University, Thailand*

[2] *Department of Chemistry, Faculty of science and Technology, Suan Sunandha Rajabhat University, 1 U-Thong Nok Road, Dusit, Bangkok, Thailand*

[3] *Organic Synthesis Research Unit, Faculty of Science, Chulalongkorn University, Thailand*

[4] *Electrochemistry and Optical Spectroscopy Research Unit, Department of Chemistry, Faculty of Science, Chulalongkorn University, Thailand*

[5] *National Center of Excellence for Petroleum, Petrochemicals, and Advanced Materials, Chulalongkorn University, Thailand*

**Corresponding Author: corawon@chula.ac.th*

ABSTRACT

A novel electrochemical biosensor for the detection of high-risk human papilloma virus (HPV) DNA type 16 based on pyrrolidinyl peptide nucleic acid (acpcPNA) as a sensor probe was proposed. A 14-mer PNA probe was designed to specifically target the DNA sequence of HPV type 16. The probe was modified at the N-terminus via N-acylation with anthraquinone (AQ) as a redox-active label. The success of the synthesis of the AQ labeled PNA (PNA-AQ) was confirmed by MALDI-TOF mass spectrometry and by thermal denaturation study with a complementary synthetic DNA target with a sequence corresponding to the HPV DNA (T_m= 69.9 ^oC). An inexpensive screen print carbon electrode (SPCE) was used in this study. Ink compositions containing graphite powder, carbon ink and binder solution were mixed together with the ratio of 0.2 g: 1 g: 1 mL, respectively. The PNA-AQ probe (20 μM) was covalently immobilized onto the electrode surface using 1-ethyl-3-(3-dimethylaminopropyl) carbodiimide) (EDC) as a coupling agent after the electrochemical pretreatment of electrode. Hybridization between the PNA-AQ probes and the synthetic DNA target was studied by measuring the peak current of AQ using a square-wave voltammetric (SWV) method. The results showed that the redox signal response decreased by three folds after addition of the DNA. This is explained by the rigidity of PNA-DNA duplexes, which affected the accessibility and electron transfer between the AQ label and the electrode surface. It is hoped that this method will be applicable in screening for the HPV-DNA type 16 in the primary stage of cervical cancer in the developing country.

Keywords Human Papilloma Virus (HPV); Peptide Nucleic Acid (PNA); Anthraquinone (AQ); screen print carbon electrode (SPCE); Redox-active label

ANC O 001 SIZE CHARACTERIZATION OF SILVER NANOPARTICLES (AgNPs) PREPARED UNDER VARIOUS CONDITIONS AND UPON INCUBATION IN *IN VITRO* GASTROINTESTINAL DIGESTION

Jakrawan Yostawonkul, Juwadee Shiowatana, Atitaya Siripinyanond
Faculty of Science, Mahidol University, Thailand

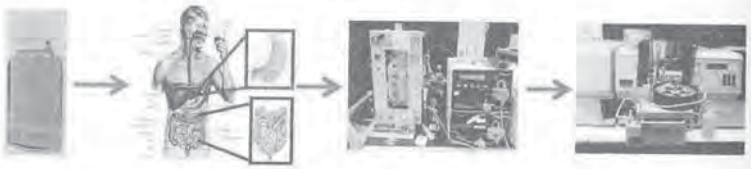

Keywords Silver nanoparticles; Tannic acid; Flow field-flow fractionation

ANC O 002 METHOD DEVELOPMENT FOR ESTIMATION OF *IN VITRO* BIOACCESSIBILITY OF PHYTOESTROGENS IN SOYBEAN MILK USING HIGH PERFORMANCE LIQUID CHROMATOGRAPHY AFTER DIALYSIS METHOD

N. Butboon, J. Shiowatana, T. Tiensing, A. Siripinyanond
Faculty of Science, Mahidol University, Thailand

Keywords Phytoestrogens; Daidzein; Genistein; Solid-phase extraction; Bioaccessibility

ANC O 003 DUAL OPTICAL DETECTION OF A HIGHLY SENSITIVE MERCURY SENSOR THROUGH FRET PROCESS

O. Hanmeng, T. Puangsamlee, C. Wainiphithapong, K. Suksat, K. Grudpan, N.Wanichacheva
Faculty of Science, Silpakorn University, Thailand

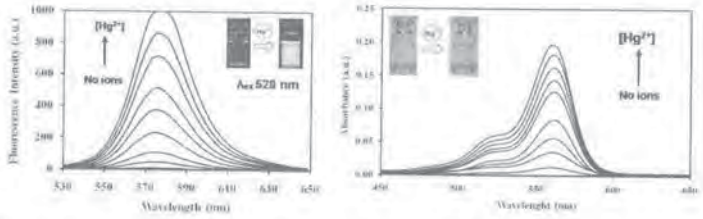

Keywords Mercury sensor; Fluorescence sensor; Hg2+-selectivity

ANC O 004 SIMULTANEOUS DETERMINATION OF ISOPROTURON AND CARBENDAZIM IN WATER SAMPLES BY SQUARE WAVE ANODIC STRIPPING VOLTAMMETRY

Peeyanun Noyrod, Suchada Chuanuwatanakul, Orawon Chailapakul, Wanida Wonsawat
Faculty of Science, Chulalongkorn University, Thailand

An electrochemical method for simultaneous determination of two pesticides, namely isoproturon and carbendazim, in water samples are presented. The determinations are established by square wave anodic stripping voltammetry (SWASV) using graphene-based electrochemical sensor fabricated in our laboratory. Linear calibration graphs were established in the range of 0.02 - 10.0 mg L^{-1} for isoproturon and 0.50 - 10.0 mg L^{-1} for carbendazim. The limits of detection were 0.02 mg L^{-1} for isoproturon and 0.11 mg L^{-1} for carbendazim. The relative standard deviations were 9.17 and 10.0 % for isoproturon and carbendazim, respectively. The satisfactory recoveries of 106.9% for isoproturon and 85.46% for carbendazim in rice-field water and 92.06% for isoproturon and 84.41% for carbendazim in Chao Phraya river water, were obtained.

Keywords Pesticides; Isoproturon; Carbendazim; Modified-electrodes; Graphene

ANC O 005 MULTILAYER ELECTROCHEMICAL PAPER-BASED ANALYTICAL DEVICE WITH SODIUM DODECYL SULPHATE FOR THE SELECTIVE DETERMINATION OF DOPAMINE IN HUMAN SERUM

Poomrat Rattanarat, Wijitar Dungchai, Weena Siangproh, Orawon Chailapakul, Charles S. Henry
Faculty of Science, Chulalongkorn University, Thailand

A modern platform of paper-based analytical device for selective detection of dopamine over uric acid and ascorbic acid in serum is introduced. Multilayer paper-based analytical device was constructed for preconcentration and selectively electrochemical detection of catecholamines in complex matrix. DA determination in the presence of AA and UA was performed using square-wave voltammetry between −0.2 and 0.8 V vs. Ag/AgCl, and linear range and detection limit (S/N = 3)were found to be 1–100 μM and 0.37 μM, respectively. Nonetheless, novel preconcentration mechanism based on electrostatic interactions between dopamine and sodium dodecyl sulfate will be discussed.

Keywords Paper-based analytical device; Dopamine; Ascorbic acid; Uric acid

ANC O 006 PEPTIDE NUCLEIC ACID PROBE FOR ELECTROCHEMICAL DETECTION OF HUMAN PAPILLOMA VIRUS DNA TYPE 16

Sakda Jampasa, Wanida Wonsawat, Tirayut Vilaivan, Orawon Chailapakul
Faculty of Science, Chulalongkorn University,Thailand

A novel electrochemical biosensor for the detection of high-risk human papilloma virus (HPV) DNA type 16 based on pyrrolidinyl peptide nucleic acid (acpcPNA) as a sensor probe was proposed. Anthraquinone (AQ) was used as a redox-active label. The success of the synthesis of the AQ labeledPNA (PNA-AQ) was confirmed by MALDI-TOF mass spectrometry and by thermal denaturation study. An inexpensive screen print carbon electrode (SPCE) was used in this study. The PNA-AQ probe was covalently immobilized onto the electrode surface. The result showed that, the redox signal response decreased by three folds after the hybridization between the PNA-AQ probes and the synthetic DNA target.

Keywords Human Papilloma Virus (HPV); Peptide Nucleic Acid (PNA)

ORAL PRESENTATION PROGRAM

Thursday, 24 Jan 2013

Presidential Symposium : Thai-Korean Nanotechnology (SYM-II)			
24 Jan 2013		15.30 - 17.20 Pacific 2	Room:
17.00-17.30	SYM-I-008	Kajornsak Fuangnawakij	Nanostructured Spinel Oxides and Their Applications in Heterogeneous Catalysis
Analytical Chemistry (ANC-I)			
24 Jan 2013		10.40 - 12.10 Pacific 1	Room:
Chairperson : Assoc.Prof.Dr.Orawan Chailapakul Co-Chair : Dr.Apinya Navakun			
10.40-11.10	ANC-I-001	Takashi Kaneta	Selective Detection of Glycoproteins by Two-Color Laser-Induced Fluorescence in Capillary Electrophoresis
11.10-11.30	ANC-O-001	Jakrawan Yostawonkul	Size Characterization of Silver Nanoparticles(AgNPs) Prepared Under Various Conditions and Upon Incubation in In Vitro Gastrointestinal
11.30-11.50	ANC-O-002	Nathanika Butboon	Method Development for Estimation of In Vitro Bioaccessibility of Phytoestrogens in Soybean Milk Using High Performance Liquid Chromatography (HPLC) after Dialysis Method
11.50-12.10	ANC-O-003	Thamon Puangsamlee	Dual Optical Detection of a Highly Sensitive Mercury Sensor Through Fret Process
Analytical Chemistry (ANC-II)			
24 Jan 2013		13.10 - 15.10	Room: Pacific1
Chairperson : Dr.Yupaporn Sameenoi ; Co-chair : Dr.Nudnuda Rodthongkhum			
13.10-13.40	ANC-I-002	Charles Sherman Henry	Personal Exposure Assessment Using a Paper-Based Analytical Devices

ORAL PRESENTATION PROGRAM

Thursday, 24 Jan 2013

Analytical Chemistry (ANC-II)			
24 Jan 2013		13.10 - 15.10	Room: Pacific1
Chairperson : Dr.Yupaporn Sameenoi ; Co-chair : Dr.Nudnuda Rodthongkhum			
13.40-14.00	ANC-O-004	Peeyanun Noyrod	Simultaneous Determination of Isoproturon and Carbendazim in Water Samples by Square Wave Anodic Stripping Voltammetry
14.00-14.20	ANC-O-005	Poomrat Rattanarat	Multilayer Electrochemical Paper-Based Analytical Device with Sodium Dodecyl Sulphate for the Selective Determination of Dopamine in Human Serum
14.20-14.40	ANC-O-006	Sakda Jampasa	Peptide Nucleic Acid Probe For Electrochemical Detection of Human Papilloma Virus DNA Type 16
14.40-15.00	ANC-O-007	Thanakorn Pluangklang	Improvements of Membraneless Vaporization Device and Its Application with Sequential Injection Analysis
Analytical Chemistry (ANC-III)			
24 Jan 2013		15.30 - 17.20	Room: Pacific 1
Chairperson : Prof.Dr. Charles Sherman Henry ; Co-Chair : Dr.Yupaporn Sameenoi			
15.30-16.00	ANC-I-003	Nadnudda Rodthongkum	Selective Enrichment and Sensitive Detection of Cancer Biomarkers Using Amphiphilic Nanoassemblies along with MALDI-MS
16.00-16.20	ANC-O-008	Nupattaranee Thammasoontaree	Ultra Fast Liquid Chromatography Coupled With Graphene Modified Electrode for Simultaneous Determination of Sulfonamides
16.20-16.40	ANC-O-009	Nipapan Ruecha	Nanodroplets Graphene-Polymer as a Novel Electrodes for Cholesterol Detection
16.40-17.00	ANC-O-010	Jirapom Kitikul	Development of Glutamate Biosensor Based on Immobilized Glutamate Oxidase on the Chitosan Cross Linked with Carbon Nanotube Modified Gold Nanowire
17.00-17.20	ANC-O-011	Dakhil.N.Taha	Simple and Highly Sensitive FIA Method for Determination of Vanadium (V) Ion by Using Merging Z zone Technique

การสังเคราะห์พิร์โรลิดินิลเพปไทด์นิวคลีอิกแอซิด (พีเอ็นเอ) ที่มียูนิเวอร์ซัลเบส

SYNTHESIS OF PYRROLIDINYL PEPTIDE NUCLEIC ACID (PNA) CARRYING UNIVERSAL BASE

วิมลมาศ ศรีนาราง, ชโลธร บุญเหลือ, ณัฐวุฒิ โยธาพันธ์, โชติมา วิไลวัลย์, ธีรยุทธ วิไลวัลย์*

Wimonmas Srinarang, Chalothorn Boonlua, Nuttawut Yothapan, Chotima Vilaivan, Tirayut Vilaivan*

Organic Synthesis Research Unit, Department of Chemistry, Faculty of Science, Chulalongkorn University, Bangkok 10330 e-mail: vtirayut@chula.ac.th

บทคัดย่อ: การจดจำระหว่างดีเอ็นเอสองสายอาศัยการเข้าคู่กันอย่างจำเพาะเจาะจงของเบสไทมีน- อะดีนีน และไซโตซีน- กัวนีน แต่ความจำเพาะเจาะจงดังกล่าวเป็นสิ่งที่ไม่พึงประสงค์ในบางวัตถุประสงค์ ตัวอย่างเช่น การตรวจสอบลำดับเบสของดีเอ็นเอที่มีลำดับเบสคล้ายคลึงกัน แต่ไม่เหมือนกันเสียทีเดียว หากส ามารถเตรียมยูนิเวอร์ซัลโพรบที่สามารถจับยึดกับดีเอ็นเอที่มีความแตกต่างกันเพียงเล็กน้อยเหล่านี้ได้ดีพอๆ กันก็จะช่วยลดจำนวนโพรบที่ต้องสังเคราะห์ลงไปได้มาก โดยยูนิเวอร์ซัลโพรบจะต้องมียูนิเวอร์ซัลเบสซึ่งแสดงสมบัติการจับยึดกับเบสธรรมชาติทั้งสี่ชนิดได้ใกล้เคียงกัน ในงานวิจัยที่ผ่านมามีผู้สังเคราะห์และศึกษาการจับยึดของดีเอ็นเอที่มียูนิเวอร์ซัลเบสอยู่บ้าง แต่มีการศึกษาพีเอ็นเอที่มียูนิเวอร์ซัลเบสมีน้อยมาก ดังนั้นในงานวิจัยนี้จึงมีแนวคิดที่จะสังเคราะห์พีเอ็นเอชนิดพิร์โรลิดินิลที่มีอิโนซีนเป็นยูนิเวอร์ซัลเบสและศึกษาสม บัติการจับยึดของ พีเอ็นเอดังกล่าวกับดีเอ็นเอที่มีเบสธรรมชาติโดยเริ่มจากการสังเคราะห์อิโนซีนยูนิเวอร์ซัลเบสโมโนเมอร์ ที่มีหมู่ปกป้องเป็น Fmoc โดยพบว่าสามารถสังเคราะห์มอนอเมอร์ดังกล่าวได้ และสามารถสังเคราะห์พิร์โรลิดินิลพีเอ็นเอที่มีมอนอเมอร์ดังกล่าวได้จริง และจะได้ศึกษาความสามารถในการเป็นยูนิเวอร์ซัลโพรบของพีเอ็นเอที่สังเคราะห์ได้ต่อไป

Abstract: Recognition between two strands of DNA relies on highly specific base pairing between thymine-adenine and cytosine-guanine. Such a high specificity is undesirable in certain purposes, for example, in determination of DNA sequences that are closely related, but not identical. A universal probe that can bind to these similar DNA targets with equal affinities will reduce the number of probes to be synthesized. The universal probe must contain one or more universal base which can bind to all four natural nucleobases with equal strength. A considerable progress in this area has been made with DNA probe, but not PNA. The purpose of this work is to synthesize and determine the DNA binding properties of a new pyrrolidinyl PNA carrying inosine as a universal base. The Fmoc-protected inosine universal base monomer has been successfully synthesized and incorporated into the pyrrolidinyl PNA. The ability of the synthesized PNA to behave as universal probe is being investigated.

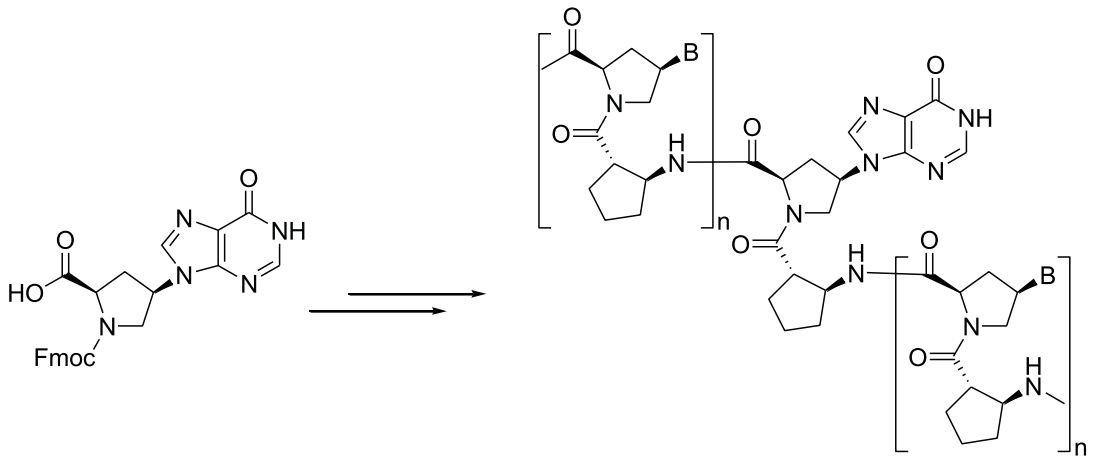
HO
O
N
NH
N
N
N
Fmoc
O
B
N
O
H
N
n
O
N
N
NH
N
O
N
H
N
O
B
N
O
H
N
n

การสังเคราะห์เพปไทด์นิวคลีอิกแอซิดชนิดใหม่ที่มีสะพานเชื่อมเป็นบีตา-2-อะมิโนไซโคลโพรเพนคาร์บอกซิลิกแอซิด

SYNTHESIS OF NOVEL PEPTIDE NUCLEIC ACIDS BEARING *β*-2-AMINOCYCLOPROPANE CARBOXYLIC ACID SPACER

บุญจิรา บุญทา,[1] โอลิเวอร์ ไรเซอร์,[2] ธีรยุทธ วิไลวัลย์[1]*

Boonjira Boontha,[1] Oliver Reiser,[2] Tirayut Vilaivan[1]*

[1]Organic Synthesis Research Unit, Department of Chemistry, Faculty of Science, Chulalongkorn University, Bangkok 10330. e-mail: vtirayut@chula.ac.th

[2]Institute for Organic Chemistry, University of Regensburg, 93053, Regensburg, Germany

บทคัดย่อ: การสังเคราะห์และสมบัติการจับยึดดีเอ็นเอของเพปไทด์นิวคลีอิกแอซิด (พีเอ็นเอ) ที่มีคอนฟอร์เมชันจำกัดเป็นหัวข้อที่มีผู้ให้ความสนใจมากในช่วงหลายปีที่ผ่านมา กลุ่มวิจัยของเราได้เคยรายงานพิโรลิดินิลพีเอ็นเอชนิดใหม่ที่ประกอบไปด้วยโปรลีนและกรดเบตาอะมิโนที่เป็นวงห้าเหลี่ยมที่ชื่อ (1*S*,2*S*)-2-อะมิโนไซโคลเพนเทนคาร์บอกซิลิกแอซิดในโครงสร้างหลัก (*acpc*PNA) พีเอ็นเอชนิดนี้แสดงสมบัติการจับยึดกับดีเอ็นเอที่มีลำดับเบสคู่สมได้อย่างแข็งแรงและจำเพาะเจาะจง แต่แสดงความแข็งแรงและจำเพาะเจาะจงต่ออาร์เอ็นเอน้อยกว่า แม้ว่าพีเอ็นเอที่มีกรดบี ตาอะมิโนแบบวงห้าเหลี่ยมเป็นตัวเชื่อมจะให้ผลการทดลองที่ดี แต่วงห้าเหลี่ยมยังคงมีความยืดหยุ่นในโครงสร้างค่อนข้างสูง ซึ่งอาจมีผลกระทบในทางลบต่อการจับยึดกับดีเอ็นเอ ดังนั้นในงานวิจัยนี้จึงมุ่งเน้นถึงการสังเคราะห์พีเอ็นเอชนิดใหม่ (*β-acc*PNA) ที่มีตัวเชื่อมเป็นกรดบีตาอะมิโนที่เป็นวงสามเหลี่ยมซึ่งเป็นโครงสร้างที่มีความยืดหยุ่นน้อยกว่าเดิม การสังเคราะห์เริ่มจากการเตรียมมอนอเมอร์ของ *β-acc*PNA ที่มีไทมีนเป็นเบสและมีหมู่ปกป้องเป็น Fmoc ในรูปแบบที่เป็นอิแนนชิโอเมอร์เดี่ยวโดยเริ่มต้นจากเอ็น-บอค-พิร์โรล จากนั้นจึงนำมอนอเมอร์ดังกล่าวไปใช้ในการสังเคราะห์พีเอ็นเอที่เป็นไทมีนโอลิโกเมอร์โดยใช้วิธีการสังเคราะห์บนวัฏภาคของแข็ง และจะได้ศึกษาสมบัติการจับยึดกับดีเอ็นเอเทียบกับพีเอ็นเอที่มีตัวเชื่อมเป็นวงแหวนห้าเหลี่ยมต่อไป

Abstract: Synthesis and DNA binding properties of conformationally restricted peptide nucleic acid (PNA) have been the subject of intense research in the past few years. Our group previously reported a pyrrolidinyl peptide nucleic acids consisting of proline and a five-membered cyclic β-amino acid namely (1*S*,2*S*)-2-aminocyclopentanecarboxylic acid in the backbone (*acpc*PNA). This PNA system showed a strong binding affinity and high sequence specificity with DNA, but less so with RNA targets. Although, the 5-membered cyclic β-amino acid spacer has been successfully employed as spacer in PNA, the 5-membered ring system appeared to be flexible which could compromise the

DNA binding properties. In this work, a new PNA system bearing potentially more rigid 3-membered cyclic β-amino acid (β-*acc*PNA) was synthesized. The *N*-Fmoc protected *β-acc*PNA monomers containing thymine base have been successfully synthesized in enantiomerically pure form starting from pyrrole. These monomers were used to synthesize homothymine PNA by solid phase peptide synthesis. DNA binding properties of the PNA with DNA will be explored and compared with the 5-membered ring analogue.

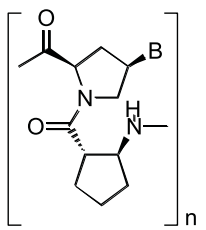

*acpc*PNA

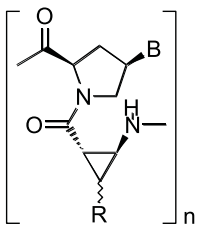

*βacc*PNA

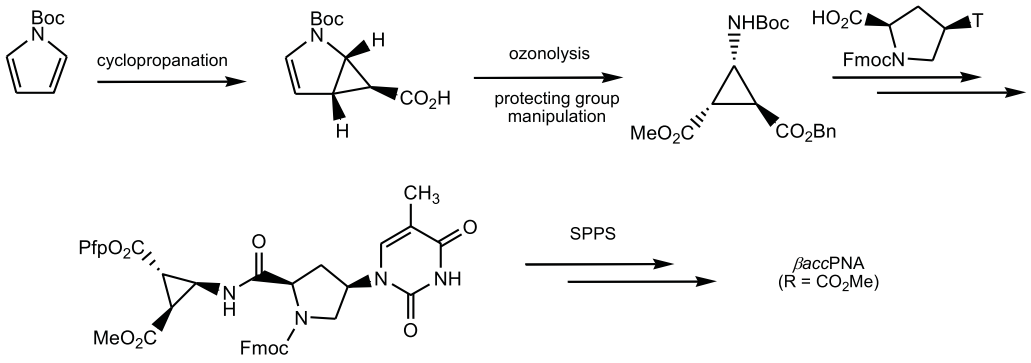

Abstracts

THE 36th CONGRESS on SCIENCE and TECHNOLOGY of THAILAND (STT 36)

การประชุมวิชาการวิทยาศาสตร์และเทคโนโลยีแห่งประเทศไทย ครั้งที่ 36 (วทท 36)

Towards a Better Society through Science and Technology

วิทยาศาสตร์และเทคโนโลยีเพื่อสังคมที่ดีขึ้น

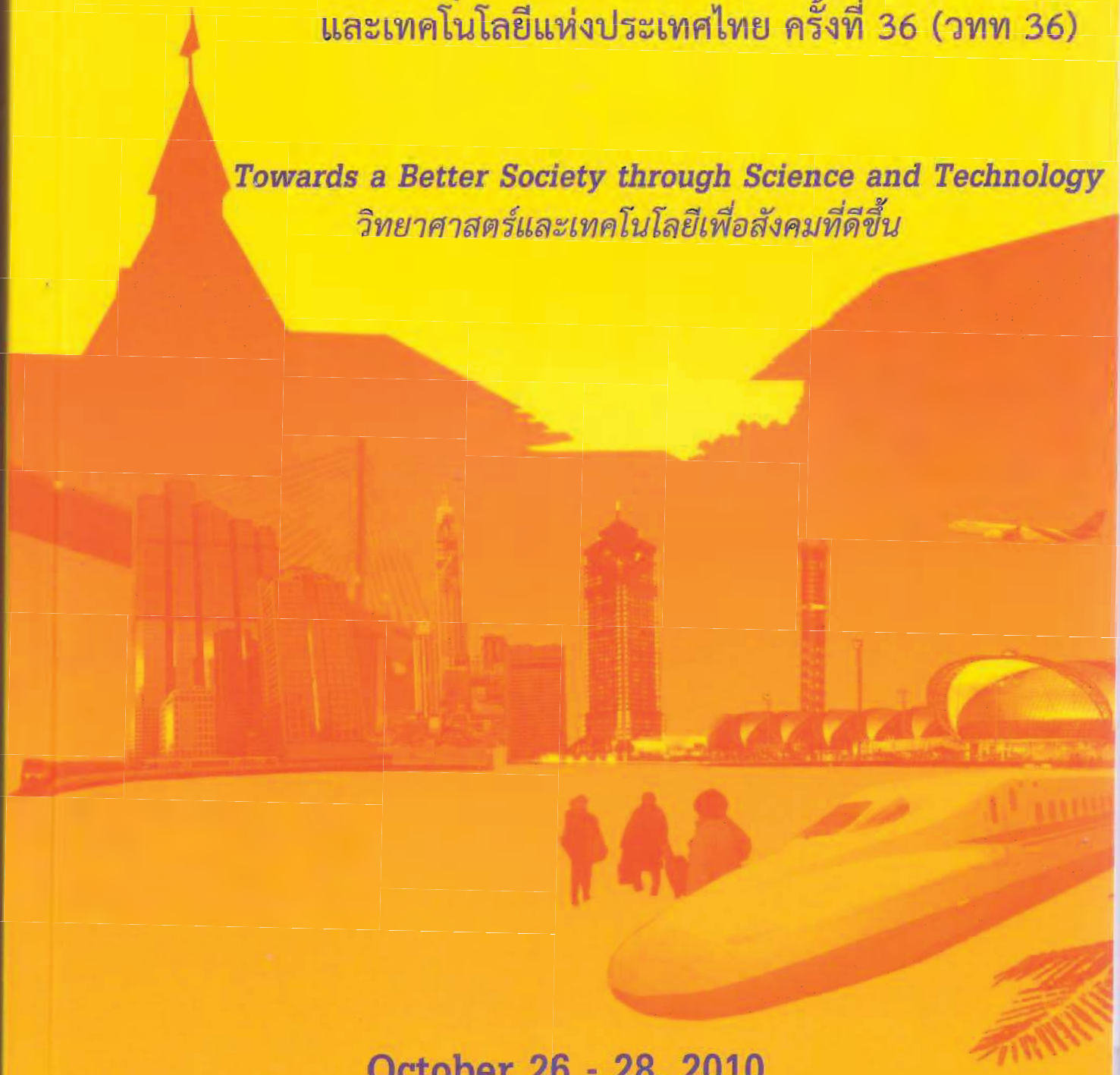

October 26 - 28, 2010

Venue: Bangkok International Trade & Exhibition Centre (BITEC). Bangkok, Thailand.

26 - 28 ตุลาคม 2553 ณ ศูนย์นิทรรศการและการประชุมไบเทค กรุงเทพฯ

www.stt36.scisoc.or.th

Organic Synthesis Research Unit, Department of Chemistry, Faculty of Science, Chulalongkorn Univ
Phayathai Road, Patumwan, Bangkok 10330, Thailand
*e-mail: vtirayut@chula.ac.th

Abstract: Traditional fluorescent labeled probes for nucleic acid hybridization carrying a fluoroph
either end of the molecule are not responsive to the hybridization state since the position of the fluor
is remote from the base pair. In this work a pyrene-labeled uridine pyrrolidinyl peptide nucleic acid
monomer was synthesized and incorporated into a PNA molecule. The modified PNA retains the ab
specifically recognize its DNA target as determined by melting temperature (T_m) experiments. Further
the fluorescence of the modified PNA was enhanced significantly when the PNA was hybridized
complementary target. As a result, the pyrene-modified is potentially useful as a hybridization resp
fluorescence probe for DNA sequence determination.

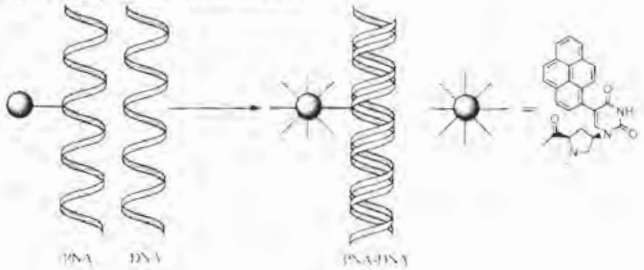

C3_C0054: Carbazole alkaloids from *Murraya koenigii* stems

Cholpisut Tantapakul*, Surat Laphookieo
Natural Products Laboratory Research, School of Science, Mae Fah Luang University, Tasud, Muang, Chiang Rai 57100, Thailand
*e-mail: solica_b@hotmail.com

Abstract: Chemical investigations of *Murraya koenigii* stems led to the isolation and identification of se
carbazole alkaloids, murrayazoline (**1**), mahanimbine (**2**), *O*-methylmahanine (**3**), girinimbine (**4**), mukol
(**5**), murrayazolidine (**6**) and murrayanine (**7**). Their structures were elucidated by spectroscopic meth
Moreover, structure of **1** was also comfirmed by X-ray diffraction data.

C3_C0055: Flavanones and dihydrochalcones from *Etlingera littoralis* rhizomes

Chotika Jeerapong[1,*], Thongchai Kruahong[1], Surat Laphookhieo[2]
[1] Department of Chemistry and Center of Excellence for Innovation in Chemistry, Faculty of Science and Technology, Suratthani Rajabhat University, Mueang, Surat Thani 84100, Thailand
[2] Natural products Research Laboratory, School of Science of Mae Fah Luang University, Muang, Chiang Rai 57100, Thailand
*e-mail: phooying@gmail.com

Abstract: The studies of chemical constituents from rhizomes of *Etlingera littoralis* led to the isolation
two flavanones, pinocembrin (1) and pinostrobin (2) and four dihydrochalcones, 2', 6'-dihydroxy-4
methoxydihydrochalcone (3), 2',4',6'-trihydroxydihydrochalcone (4) , 2',6'-dihydroxy-4',4-dimethoxydihy
drochalcone (5) and 2',6',4-trihydroxy-4'-methoxydihydrochalcone (6), respectively. All structures wer
characterized by extensive 1D and 2D NMR spectroscopic methods except compound 3 was characterize
by using ^{1}H NMR and X-ray diffraction data.

C3_C0056: Coumarins from *Feronia limonia* roots

Ittipon Siridechakorn*, Tawanun Sripisut, Surat Laphookhieo
Natural Products Research Laboratory, School of Science of Mae Fah Luang University, Muang, Chiang Rai 57100, Thailand
*e-mail: siridechakorn@yahoo.com

Abstract: Phytochemical investigation of the roots of *Feronia limonia* led to the isolation of four coumarins: isopimpinellin (**1**), osthol (**2**), auraptene (**3**) and 6-methoxy-7-geranyloxycoumarin (**4**). Their structures were elucidated by extensive 1D and 2D NMR spectroscopic methods.

C3_C0058: Chemical interactions between β-carotene and chitosan by coagulation and flocculation: A study on light scattering intensity and infrared spectrum

6th NCCC
The Sixth National Chitin Chitosan Conference

Proceedings

The Sixth National Chitin–Chitosan Conference

In conjunction with

The Sixth Thailand Materials Science and Technology Conference

Thailand Textile Symposium 2010

August 26-27, 2010
Miracle Grand Convention Hotel,
Bangkok, Thailand

Organized by

MTEC
a member of NSTDA

O-08 **Water-based Nano-sized Chitosan for Food Additive: A Case Study of Pacific White Shrimp Preservation** 54
P. Chantarasataporn, R. Yoksan, R. Pichayangkura, W. Visessanguan and S. Chirachanchai

O-09 **Chitosan Nanospheres for Allergen Delivery System: Molecular Design, Synthesis, and Allergen Incorporation** 58
Jatesuda Jirawutthiwongchai, Katanchalee Mai-ngam and Suwabun Chirachanchai

O-10 **Chitin – Chitosan Production form Golden Apple Snail for Agricultural Benefit** 61
Nitchamon Thamaragsa, Path Kojinok and Danuwat Peng - ont

O-11 **Glucose-encapsulated Efficiencies in Chitosan Nanoparticles** 66
Yuwaporn Sornsiri and Pariya Na Nakorn

O-12 **Utilization of Quaternized Chitosans for Improving Water Solubility and Control Releases of Poorly Water Soluble Drugs** 71
Sasikarn Sripetthong, Chitchamai Ovatlarnporn and Warayuth Sajomsang

O-13 **Preparation of Chitosan Anti-inflammatory Agent, 5-Aminosalicylic Acid Conjugates for Colonic Drug Delivery** 78
Sirinporn Nalinbenjapun, Chitchamai Ovatlarnporn and Warayuth Sajomsang

O-14 **Chitosan and Trimethyl Chitosan Particles as Oral Vaccine Delivery Systems: Comparison the Potential to Initiate Immune Responses** 85
Supavadee Boontha, Hans E. Junginger, Neti Waranuch, Assadang Polnok and Tasana Pitaksuteepong

O-15 **Preparation of Chitosan Films and Beads by Cross-link Reaction with Epoxidized Natural Rubber as Drug Delivery Systems** 90
S. Paichamnan , C. Ovatlarnporn and P. Klinpitak

O-16 **Gamma-Ray Radiation on Succinylated Chitosan and Their Characterization** 96
Chutima Vanichvattanadecha, Ratana Rujiravanit, Hiroshi Tamura and Seiichi Tokura

POSTER PRESENTATIONS

P-01 **Preparation and Antibacterial Property of Wound Dressing from Quaternary Ammonium Chitin** 100
Ekkachai Sukpaiboon, Onruthai Pinyakong and Wanpen Tachaboonyakiat

P-02 **Quaternized *N*-(3-pyridylmethyl) Chitosan/DNA Nanocomplexes as Gene Carriers: Effect of Molecular Weight** 104
Pattarapond Gonil, Maleenart Petchsangsai, Nuttaporn Pimpha, Uracha Ruktanonchai, Warayuth Sajomsang and Praneet Opanasopit

P-03 **Quaternized Chitosan Particles Prepared by Self Assembly of Amphiphilic Chitosan** 109
Nadda Booranabunyat and Voravee P. Hoven

P-04 **Adsorption of Reactive Dye Water on Nanochitin Particle** 113
Sukumal Boonurapeepinyo, Nichada Jearanaikkon and Niramol Sakkayawong

P-05 **Preparation of Chitosan Nanoparticles by Electrospray Method** 118
Dolaya Polchai, Krisana Siralertmukul and Cholthacha Harnirattisai

P-06 **Poly(Phenylene Vinylene)/Zeolite Y Composites Respond Toward Ammonium Nitrate Vapor** 121
Jirarat Kamonsawas, Anuvat Sirivat, Pimpa Hormnirun and Walaiporn Prissanaroon

อนุภาคควอเทอร์ไนซ์ไคโทซานเตรียมโดยการประกอบตัวเองของแอมฟิฟิลิกไคโทซาน

Quaternized Chitosan Particles Prepared by Self Assembly of Amphiphilic Chitosan

Nadda Booranabunyat[1,2], Voravee P. Hoven[3*]

[1]Program in Petrochemistry and Polymer Science, Faculty of Science, Chulalongkorn University
[2]Center for Petroleum, Petrochemicals, and Advanced Materials, Chulalongkorn University
[3]Organic Synthesis Research Unit, Department of Chemistry, Faculty of Science, Chulalongkorn University, Bangkok 10330, Thailand
Tel: 0-2218-7627 ext 102, Fax: 0-2218-7598, E-Mail: vipavee.p@chula.ac.th

บทคัดย่อ

การตรึงหมู่ทาโลอิลซึ่งเป็นหมู่ที่ไม่ชอบน้ำและตรึงหมู่พอลิ(เอทิลีน ไกลคอล) หรือ เอ็น-[(2-ไฮดรอกซิล-3-ไตรเมทิลแอมโมเนียม)]โพรพิลซึ่งเป็นหมู่ที่ชอบน้ำทำได้โดยการทำปฏิกิริยาทางเคมีของหมู่อะมิโนและหมู่ไฮดรอกซิลบนโครงสร้างไคโทซาน ตามลำดับ สามารถวิเคราะห์เปอร์เซ็นต์การแทนที่ของแต่ละหมู่ที่ตรึงได้โดยโปรตอนเอ็นเอ็มอาร์ สามารถเหนี่ยวนำให้เกิดอนุภาคโดยการประกอบตัวเองของอนุพันธ์แอมฟิฟิลิกไคโทซานที่ได้ผ่านไดอะไลซิสในน้ำ การเพิ่มความเป็นประจุบวกของหมู่ควอเทอร์นารีแอมโมเนียมบนผิวของอนุภาคไคโทซานชนิดที่ตรึงด้วยหมู่พอลิ(เอทิลีน ไกลคอล) จำเป็นต้องอาศัยการทำปฏิกิริยาเมทิลเลชันแบบต่างวัฏภาค ซึ่งแตกต่างจากอนุภาคที่มีหมู่เอ็น-[(2-ไฮดรอกซิล-3-ไตรเมทิลแอมโมเนียม)]โพรพิล ในงานวิจัยนี้สนใจที่ศึกษาผลของน้ำหนักโมเลกุลไคโทซาน ชนิดของหมู่ที่ชอบน้ำ ตลอดจนเปอร์เซ็นต์การแทนที่ของหมู่ที่ชอบน้ำและไม่ชอบน้ำต่อขนาด/สัณฐานวิทยา

Abstract

Phthaloyl groups (Ph) as hydrophobic entities and poly(ethylene glycol) (PEG) or *N*-[(2-hydroxyl-3-trimethylammonium)]propyl (HTAP) as hydrophilic entities were immobilized on chitosan backbone via chemical reactions of amino and hydroxyl groups, respectively. Degree of substitution (%DS) of each functional group was determined by ^{1}H NMR. Formation of particles was then induced by self assembly of the resulting amphiphilic chitosan derivatives upon dialysis in water. Unlike the chitosan particles having HTAP moieties, a subsequent heterogeneous methylation was necessary to introduce positively charged quaternary ammonium groups to the chitosan particles having PEG moieties. In this research, effects of molecular weight of chitosan, type of hydrophilic groups as well as relative %DS of hydrophobic/hydrophilic groups on the particle size/morphology will be determined.

Introduction

Chitosan is a partially deacetylated form of chitin, the second most abundant polysaccharide next to cellulose, which was found in the exoskeleton of insect, shell of crustaceans and fungal cell walls. Chitosan has a number of unique characteristics such as biocompatibity, biodegradability, low toxicity and antibacterial [1]. Chitosan shows its antibacterial activity only in acidic medium above its pKa (pH 6.5). Introducing quaternary ammonium groups to chitosan via quaternization of amino groups has been recognized as a potential way to enhance the antibacterial activity of chitosan in a broader pH range. In addition, it has been recently demonstrated that chitosan as well as quaternized chitosan in the form of nanoparticles exerted higher antibacterial activity than chitosan solution because the greater surface area of the particles provides intimate contact with the surface of bacterial cells. In this research, we have proposed to generate chitosan particles having positive charges of quaternary ammonium groups by self assembly of amphiphilic chitosan. It is believed that this approach should be an efficient way to fabricate the sub-micron particles whose size can be tuned by varying hydrophobic and hydrophilic proportions and types and eligible for a large scale production.

Materials and Methods

Materials:

Chitosan flakes (degree of deacetylation 85%, molecular weight 45,000 Da and degree of deacetylation 95%, molecular weight 100,000 Da) were obtained from Seafresh Chitosan (Lab) Co., Ltd. (Thailand). Phthalic anhydride, poly(ethylene glycol)methyl ether (mPEG) (Mn = 5000), succinic anhydride (SA), *N*-hydroxysuccinamide (NHS) and 1-ethyl-3-(3'-dimethylaminopropyl)carbodiimide (EDC) were purchased from Aldrich. Methyl iodide (MeI), sodium hydroxide (NaOH), sodium iodide (NaI), and glycidyltrimethylammonium chloride (GTMAC) were purchased from Fluka (Switzerland). Methanol (MeOH) was purchased from Merck (Germany). Dimethyl formamide (DMF) was purchased from Carlo. All reagents and materials are analytical grade and used without further purification.

Methods:

Synthesis of phthaloylchitosan (PhCS) was done by a reaction of 3.0 g chitosan with phthalic anhydride (3 mole equiv.) in 20 mL DMF at 110 °C under N_2 atmosphere for 6 h then the temperature was reduced to 60°C and left overnight under N_2 atmosphere. Light yellow powder was obtained as a product after precipitation in cool water and dried *in vacuo*.

Synthesis of poly(ethylene glycol) methyl ether terminated with carboxyl groups (mPEG-COOH) [2]: was done by reacting mPEG (3g) with SA (1 mole equiv. to mPEG) in DMF 10 mL using pyridine as a catalyst at 60°C overnight. White powder was obtained after precipitation in diethyl ether and dried *in vacuo*.

Preparation of amphiphilic chitosan particles

- *Phthaloylchitosan-graft-mPEG (PhCS-g-mPEG) particles* [3]: PhCS(0.2g) was reacted with mPEG-COOH (1, 3, 5 mole equiv.) in 4 mL DMF. NHS (1 mole equiv.) was added and stirred until the solution became clear. Then EDC (1 mole equiv.) was added and stirred for 24 h. Light yellow powder was obtained after dialysis against deionized water for 4 days and lyophilization.
- *Quaternized PhCS-graft-mPEG (QPhCS-g-mPEG) particles:* An anhydrous methanol solution (10 mL) was added into a flask containing 0.05 g PhCS-g-mPEG particles. NaOH (0.13 g, 3.3 mmol) and NaI (0.28 g, 1.9 mmol) were added to the flask. Subsequently, MeI (0.4 mL, 6.4 mmol) was added every 4 h to the mixture. The reaction mixture was stirred at 50°C for 8 h. The QPhCS-*g*-mPEG particles were isolated by centrifugation at 10,000 rpm for 30 min. Supernatant was discarded and the particles were extensively rinsed with methanol and dried *in vacuo*.
- *Phthaloylchitosa-grafted-HTAP (PhCS-g-HTAP) particles:* PhCS (0.2g) was dissolved in 4 mL DMF at ambient temperature. Then GTMAC (1, 3, 5 mole equiv.) was added into the solution. The reaction was stirred at 70°C for 24 h. Light yellow powder was obtained after dialysis against deionized water for 4 days and lyophilization.

Results and Discussion

^{1}H NMR technique was used to confirm the success of amphiphilic chitosan particle formation. Signals at 3.1 ppm appearing in Fig.1C and 1D can be assigned to $-N^+(CH_3)_3$ groups of QPhCS-*g*-mPEG and PhCS-*g*-HTAP, respectively. The signal at 2.1 ppm was assigned to the methoxy group of mPEG (Fig.1B) while the signal at 7.2-8.0 ppm assigned to aromatic groups of phthaloyl entities shown in all spectra.

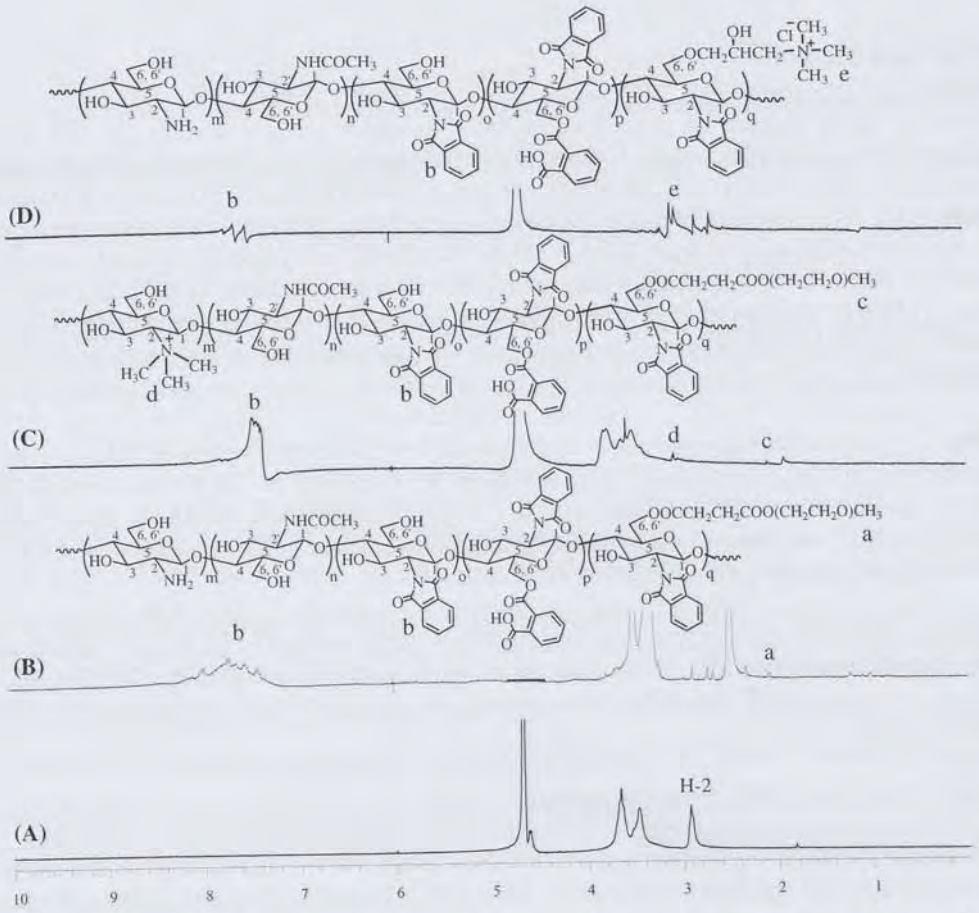

Fig.1: ^{1}H NMR spectra of (A) chitosan, (B) PhCS-*g*-mPEG, (C) QPhCS-*g*-mPEG, and (d) PhCS-*g*-HTAP.

Degree of substitution (%DS) of phthaloyl groups were determined from the relative ratio between the integral of H signal from phthaloyl groups and the signal of H-2 from glucosamine units. As shown in Table 1, %DS of phthaloyl groups in PhCS was 72 and 52% for the chitosan having molecular weight of 45,000 Da and 100,000 Da, respectively. %DS of mPEG was determined from the relative ratio between the integral of H signal from -OCH_3 in mPEG and the signal of H-2 from glucosamine units. Degree of quaternization (%DQ) of QPhCS-*g*-mPEG and PhCS-*g*-HTAP were evaluated from the relative ratio between the integral of H signal from $(CH_3)_3$ and the signal of H-2 from glucosamine units. As demonstrated in Table 1 and 2, the relative ratio between hydrophobic entities (%DS of Ph) and the hydrophilic entities (%DS of mPEG or HTAP) can be varied as a function of mole ratio of PhCS:mPEG and PhCS:HTAP in the case of PhCS-*g*-mPEG, and PhCS-*g*-HTAP, respectively. %DQ was ranged from 6 to 17%.

Table 1. %DS and %DQ of QPhCS-*g*-mPEG

Sample	Mole of PhCS:mPEG	%DS of PhCS	%DS of mPEG	%DQ
$PhCS_{45,000}$-*g*-mPEG	5:1	72	2.67	8.60
	5:3		27.3	9.33
	5:5		16.0	16.1
$PhCS_{100,000}$-*g*-mPEG	5:1	52	5.67	4.00
	5:3		17.3	10.7
	5:5		11.6	10.5

Table 2. %DS of PhCS-*g*-HTAP

Sample	Mole of PhCS:HTAP	%DS of PhCS	%DS of HTAP
$PhCS_{45,000}$-*g*-HTAP	5:1	72	6.56
	5:3		15.1
$PhCS_{100,000}$-*g*-HTAP	5:1	52	5.89
	5:3		16.8

Morphological appearances of PhCS-*g*-mPEG particles determined by SEM are shown in Fig.2. The particles are spherical in shape and have an average size in a range of 100-150 nm. The morphologies of other particles and zeta potential of all particles are yet to be determined to verify whether the sub-micron particles having positive charges can be formed.

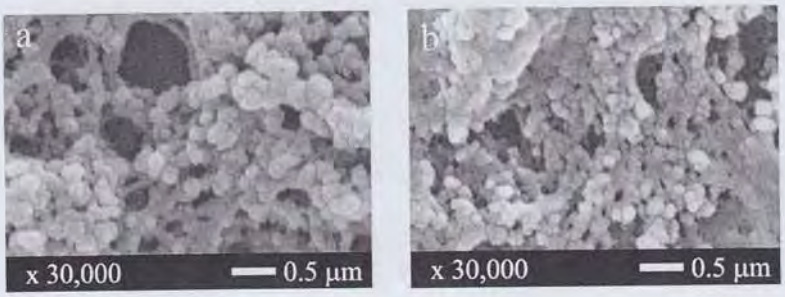

Fig.2: SEM micrographs of (a) $PhCS_{100,000}$-*g*-mPEG (5:1); (b) $PhCS_{45,000}$-*g*-mPEG (5:1)

Conclusion

Amphiphilic chitosan can be successfully synthesized. Self-assembly of the resulting derivatives upon dialysis gave stable colloidal solution in water at room temperature. According to ^{1}H NMR analysis, the relative %DS of hydrophobic/hydrophilic groups can be varied as a function of reagent mole ratio. SEM analysis of representative particles suggested that the sub-micron particles with well-defined spherical morphology can be formed. The investigation on the effects of molecular weight of chitosan, type of hydrophilic groups as well as relative %DS of hydrophobic/hydrophilic groups on the particle size/morphology and zeta potential is on-going and will be presented at the meeting.

Acknowledgements

The financial support for this project was provided by Research Team Consolidation Grant, The Thailand Research Fund and Commission of Higher Education (RTA 5280002) and Center for Petroleum, Petrochemicals, and Advanced Materials.

References

1. Sang-Hoon, L, Samuel, HM. (2003) Review of chitosan and its derivatives as antimicrobial agents and their uses as textile chemicals. *Journal of Macromolecular Science*, 43, 223-269.
2. Anumansirikul, N, Wittayasuporn, M, Klinubol P, Tachaprutinun, A, Wanichwecharungruang, SP. (2008) UV-screening chitosan nanocontainers:increasing the photostability of encapsulated materials and controlled release. *Nanotechnology*, 205101.
3. Choochottiros, C, Yoksan, R, Chirachanchai, S. (2009) Amphiphilic chitosan nanospheres: Factors to control nanosphere formation and its consequent pH responsive performance. *Polymer*, 50, 1877-1886.

The 11th Graduate Research Conference 2010

รวมบทคัดย่อ

การประชุมวิชาการเสนอผลงานวิจัยระดับบัณฑิตศึกษา ครั้งที่ 11

บัณฑิตวิทยาลัย มหาวิทยาลัยขอนแก่น
GRADUATE SCHOOL KHON KAEN UNIVERSITY

Detection of *HLA-B*5801* by In-House PCR-SSP

วิธีการตรวจหาเอชแอลเอบี 5801 ด้วยวิธีพีซีอาร์เอสเอสพี

Sita Virakul (ศิตา วีรกุล)[*] Jeerawat Nakkuntod (จีรวัฒน์ นาคขุนทด)[*] Pawinee Kupatawintu[**] (ภาวิณี คุปตวินทุ)
Oratai Kangwanshiratada (อรทัย กังวาลชิรธาดา)[***] Suppaporn Paiboonkasarp (ศุภพร ไพบูลย์กษาปน์)[***]
Dr.Nattiya Hirankarn, (ดร. พญ.ณัฏฐิยา หิรัญกาญจน์)[****]

ABSTRACT

Pharmacogenetics in HLA allele is very useful for risk assessment in life-threatening drug hypersensitivity. In 2004, *HLA-B*1502* first showed strong association with carbamazepine hypersensitivity in Asian ethnicity. Another association, *HLA-B*5801* involves with allopurinol hypersensitivity with 26% mortality rate. Since allele frequency of *HLA-B*5801* is quite common in some Asian ethnicity, it is important to develop a rapid and cost effective test for Asian, including our Thai population. To get HLA typing result, commercially available PCR-SSP is too expensive. As a result, in-house PCR-SSP would be the most interesting candidates comparing to other molecular techniques. The results showed that only one set of primer can differentiate *HLA-B*5801* from other alleles specifically in 200 DNA samples with 100% sensitivity and >99.9% specificity. The benefit of these tests would help patients to avoid any life-threatening adverse consequences from allopurinol.

บทคัดย่อ

ในปัจจุบันสามารถทำนายการเกิดการแพ้ยาอย่างรุนแรงได้โดยการหาอัลลีลของเอชแอลเอยีน โดยเอชแอลเอแรกที่มีการรายงานคือ เอชแอลเอบี 1502 ซึ่งแสดงความสัมพันธ์ในการเกิดการแพ้ยารุนแรงกับยากันชักชื่อคาร์บามาซีพีน อีกยีนหนึ่งคือเอชแอลเอบี 5801 กับยาโรคเกาต์ชื่ออัลโลพูรินอล ยีนเหล่านี้มีความสำคัญมากเนื่องจากเป็นยีนที่พบมากในกลุ่มประชากรเอเชีย ร่วมกับอัตราการตายอยู่ประมาณ 26 เปอร์เซ็นต์ ดังนั้นจึงมีความสำคัญในการหาวิธีหายีนที่ได้ผลถูกต้องราคาเหมาะสม และรวดเร็ว วิธีหนึ่งก็คือ พีซีอาร์เอสเอสพี ในปัจจุบันมีชุดตรวจสำเร็จแต่ราคายังคงแพงเกินไป จึงควรมีการพัฒนาพีซีอาร์เอสเอสพีอย่างง่าย และราคาถูกเพื่อใช้เอง จากผลการทดสอบพบว่าสามารถทำนายเอชแอลเอบี 5801 ในตัวอย่างดีเอนเอจำนวน 200 รายได้ความไว 100 เปอร์เซ็นต์ และแม่นยำ >99.9% ประโยชน์ของผลการทดลองครั้งนี้ทำให้สามรถช่วยคนไข้ไม่ให้เกิดอาการแพ้ที่รุนแรงถึงชีวิตได้ตั้งแต่ก่อนการให้ยา

Key Words: *HLA-B*5801*, PCR-SSP
คำสำคัญ: เอชแอลเอบี 5801 พีซีอาร์เอสเอสพี

[*] *Student, Medical Microbiology, Interdisciplinary Program, Graduate School, Chulalongkorn University*
[**] *National Blood Center, Thai Red Cross Society*
[***] *Immunology Department, Department of Microbiology, Faculty of Medicine, Chulalongkorn University*
[****] *Associate Professor, Lupus Research Unit, Department of Microbiology, Faculty of Medicine, Chulalongkorn University*

1. Introduction

Drug response in each patient is different. Up to date, there are many evidence on genetic factors which play an important role in these responses, such as cytochrome P450, thiopurine methyltransferase and human leukocyte antigen (HLA) (Ingelman-Sundberg, 2008). Study in inherited predisposing factors which determine drug response is widely known as pharmacogenetics (Wolf et al., 2000). These diverse reactions include not only level of effectiveness in treatment, but also life-threatening severe symptom. For severe drug-induced reaction aspect, although the incident rate is quite low, identification of these genetic markers helps reduce cause of death dramatically. The strongest and the most specific marker for risk assessment so far is HLA gene (Ingelman-Sundberg, 2008).

The poorest prognosis among severe drug-induced skin reactions are Stevens-Johnson syndrome (SJS) and toxic epidermal necrolysis (TEN) (Mockenhaupt, 2009). They are a life-threatening syndrome with high mortality rate. The appearances on mouth, lips, conjunctiva and genital area vary from erythema to blistering second degree burn-like.

In 2004, Chung, *et al.*, first reported HLA gene as a genetic marker for SJS by carbamazepine (Chung et al., 2004). Year after, many other studies in pharmacogenetics of HLA alleles and drug hypersensitivity have also been reported. In addition to HLA-drug specific induced SJS, reports on ethnicity shows important role as well (Chung et al., 2007). Among Asian ethnicity, *HLA-B*5801* involved with severe side effect from antihyperuricemic agents, allopurinol. Its mortality rate is around 26% (Hung et al., 2005). Since allele frequency of this HLA antigens are quite common in some Asian ethnicities, as listed in table 1 (http://www.allelefrequencies.net/default.asp), it is important to develop a rapid test for Asian including our population.

Ethnicity	*HLA-B*5801* (%)
China North Han	2.9
China South Han	8.9
Taiwan	9.8
Japan	0.5
Korea	6.5
Singapore	5.8
Thailand	7.7
Vietnam	6.5

Table1. *HLA–B*5801* frequencies in Asian ethnicity.

For HLA typing, standard serological tests give inconclusive results which were caused by cross reactivity of monoclonal antibodies. As a result, HLA subtypes cannot be identified accurately. Years after, molecular techniques become commercially available and are applied to many routine laboratories. It's still

expensive and also gives lots of unnecessary information, as all alleles are interpreted (Martin et al., 2005). Testing HLA gene from genomic DNA, most laboratories may apply either of four different techniques. First, polymerase chain reaction-sequence specific oligonucleotide probe (PCR-SSOP). This technique use sets of probes to detect HLA types of multiple samples at the same time. This is suitable for high throughput HLA typing, preferable used in donor center. Second, reverse SSOP is quite expensive due to the development of high efficiency probes that were designed to bind target allele at the same temperature. The third technique is PCR-SSOP-luminex® system which applies flow cytometry to detect different alleles with up to 100 DNA probe attached colorimetric beads (Itoh et al., 2005). Its limitations are cost and requirement of special instrument. Finally, sequence-specific primer polymerase chain reaction (PCR-SSP) technique works by amplification HLA gene with many sets of primers to specifically differentiate closely related alleles. This technique is available in many forms of commercial sets of primers, which cost is still quite expensive. In order to get the most specific, rapid and cost effective test for *HLA-B*5801*, it's challenging to develop an in-house PCR-SSP to predict drug allergy for each patients before prescription.

2. Objective

To develop an in-house PCR-SSP for *HLA-B*5801* and validate with PCR-SSP commercial kit and direct sequencing.

3. Materials and methods

Sample

In a setup step, known *HLA-B*5801*, *B*1517* and *B*5701*, which have the closest sequences to *HLA-B*5801* and are present in Thai population, along with other alleles (*HLA-B*0705, 1301, 1501, 1511/12/13, 1525, 1801, 3501, 3801, 3901, 4001/02, 4402, 4601, 4801, 5101/02, 5201* and *5701*) that have high frequency in Thai population (http://www.allelefrequencies.net/default.asp), were used. In a validation step, two hundred genomic DNA samples of blood or bone marrow donors at the Thai Red Cross were analyzed by gold standard methods using PCR-SSP commercial kit (Micro SSP™ HLA DNA Typing Trays, One Lambda, Inc.) and direct sequencing. These genomic DNA samples were sent to us blindly to test for *HLA-B*5801*, with 9.5% of *HLA-B*5801*.

Sequence-specific Primer design

*HLA*B* is the most polymorphic gene in human genome. Around 1,249 variants are reported in 2009 from the IMGT/HLA database (http://www.ebi.ac.uk/imgt/hla). In order to design specific primer, HLA-B sequence alignment was

taken from the database with *HLA-B*070201* as consensus sequence (Figure 1). It's noted that polymorphism among *HLA-B*58* group is scattered around the whole sequence, so rare *HLA-B*5705* and other rare subtypes of *HLA-B*58* cannot be differentiated. Reaction mix at 20 µl contains final concentration of 1x Taq buffer, 1.5 mM $MgCl_2$, 0.2 mM dNTP, 1.25 µM primer (F1: 5'-ACGGAACATGAAGGCCTCC-3' and R1: 5'-CAGCCATACATCCTCTGGATGA-3'), 0.25 µM internal control primer (IF: 5'-CCTCACATGATATGACTTTGACAT-3' and IR: 5'-AACATCAGAAGCATTGACCTTG-3') and 0.25 U Platinum® Taq DNA polymerase (Invitrogen). Touchdown PCR cycles are used to increase specificity, set up by gradient of temperature and cycles that results in both positive band for *HLA-B*5801* and housekeeping gene. They are composed of 95°C 2 min for 1 cycle; 95°C 30s, 70°C 30s and 72°C 30s for 5 cycles; 95°C 30s, 68°C 30s and 72°C 30s for 5 cycles; 95°C 30s, 67.1°C 30s and 72°C 30s for 5 cycles; 95°C 30s, 65°C 30s and 72°C 30s for 10 cycles; 95°C 30s, 55°C 30s and 72°C 30s for 20 cycles; 72°C 5 min for 1 cycle and holding at 4°C. Total genomic DNA is 100 ng. Electrophoresis uses 2% agarose gel to determine PCR product size by running with 100bp DNA Ladder at 100 V for 40 min.

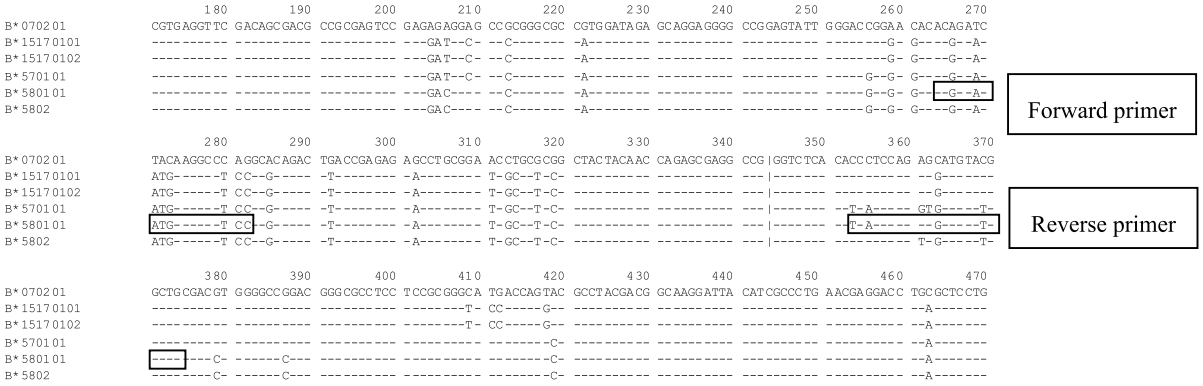

Figure 1 Related *HLA-B* alleles sequence alignment with primer regions. *HLA-B*5801* can be differentiated specifically within those closely related alleles, *HLA-B*1517*, *5701* and *5802*.

Assay Analysis

To compare the efficiency between the new developed method with traditional one, sensitivity and specificity of the assay is determined (Altman and Bland, 1994).

Sensitivity = $\frac{\text{number of true positive}}{\text{number of true positive + number of false negative}}$

Specificity = $\frac{\text{number of true negative}}{}$

number of true negative + number of false positive

4. Results and discussion

Previous report on *HLA-B*5801* detection composed of two sets of primer (Bunce et al., 1995). From the reference, first primer set amplifies *HLA-B*5801, 5104, 5301 and 1513*, while another set amplifies *HLA-B*5801-3*. A successful typing for *HLA-B*5801* will give two positive bands from both sets of primer in separated reactions. The limitation of this method can occur with the combination of non *HLA-B*5801* heterozygote, for example, patient with *HLA-B*1513* and *HLA-B*5802* will result as two positive bands and misinterpret as *HLA-B*5801*. Here, we used only one set of primer to reduce assay number to one reaction and to also exclude false positive from heterozygote. Of 200 samples, we can detect 19 *B*5801* samples correctly. Moreover, this current test could reduce the HLA typing cost from 3,000 baht/test by commercial PCR-SSP to 1,000 baht/test.

In addition, within these 200 samples, all HLA-B alleles presented more than 1% in Thai population including *HLA-B*0705, 1301, 1501, 1511/12/13, 1525, 1801, 3501, 3801, 3901, 4001/02, 4402, 4601, 4801, 5101/02, 5201 and 5701* gave negative result with our primer. A representative gel picture is shown in Fig 2.

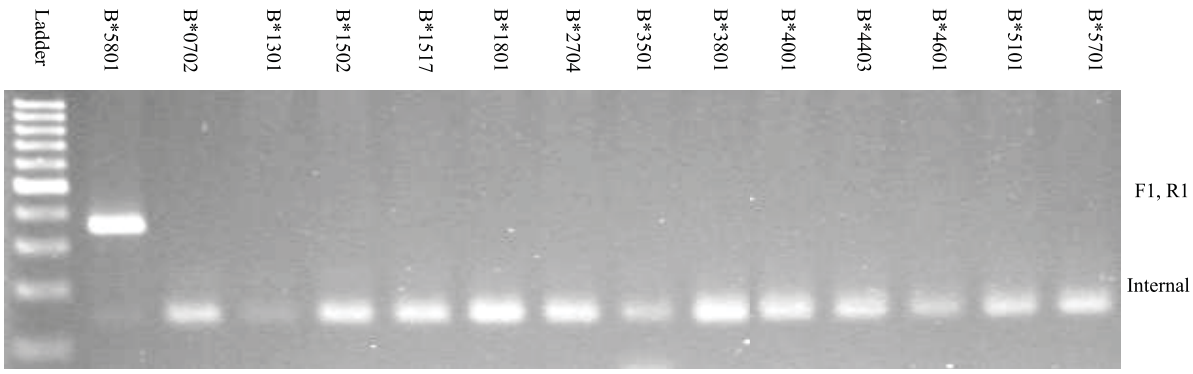

Figure 2 Migration patterns from both *HLA-B*5801* (F1, R1) and housekeeping primer.

As mentioned earlier, polymorphisms among other related alleles, both in intron and exon, are scattered around the sequences, so *HLA-B*5705* and other subtype of *HLA-B*58* cannot be differentiated. Predicted amplified alleles are *HLA-B*5705, 5801, 5804-5, 5809, 5810N, 5811-13, 5815, 5817N, 5819* and *5821-24*. However, from the allele frequencies database (http://www.allelefrequencies.net/default.asp) of world populations, those cross reactive alleles are very

rare, close to 0%. From 200 blind samples, this assay gives 100% sensitivity and >99.9% specificity, as extremely rare alleles mentioned above can still be amplified. According to our samples, we didn't found those extremely rare alleles, positive predictive value and negative predictive value are 100%. Therefore, this SSP assay with one set of primer pairs can be used with high specificity in our Thai population.

5. Conclusion

This PCR-SSP system can be used to define *HLA-B*5801*. The benefit of these tests would help patients to avoid any life-threatening adverse consequences from allopurinol with less cost.

6. Acknowledgement

This work is supported by the Lupus Research Unit and the Thailand Research Fund (Senior Research Scholar Grant – RTA5280002).

7. References

Altman D. G. and Bland J. M. 1994. Diagnostic tests. 1: Sensitivity and specificity. *BMJ* **308**, 1552.

Bunce M., O'Neill C. M., Barnardo M. C., Krausa P., Browning M. J., Morris P. J. and Welsh K. I. 1995. Phototyping: comprehensive DNA typing for HLA-A, B, C, DRB1, DRB3, DRB4, DRB5 & DQB1 by PCR with 144 primer mixes utilizing sequence-specific primers (PCR-SSP). *Tissue Antigens* **46**, 355-67.

Chung W. H., Hung S. I. and Chen Y. T. 2007. Human leukocyte antigens and drug hypersensitivity. *Curr Opin Allergy Clin Immunol* **7**, 317-23.

Chung W. H., Hung S. I., Hong H. S., Hsih M. S., Yang L. C., Ho H. C., Wu J. Y. and Chen Y. T. 2004. Medical genetics: a marker for Stevens-Johnson syndrome. *Nature* **428**, 486.

Hung S. I., Chung W. H., Liou L. B., Chu C. C., Lin M., Huang H. P., Lin Y. L., Lan J. L., Yang L. C., Hong H. S., Chen M. J., Lai P. C., Wu M. S., Chu C. Y., Wang K. H., Chen C. H., Fann C. S., Wu J. Y. and Chen Y. T. 2005. HLA-B*5801 allele as a genetic marker for severe cutaneous adverse reactions caused by allopurinol. *Proc Natl Acad Sci U S A* **102**, 4134-9.

Ingelman-Sundberg M. 2008. Pharmacogenomic biomarkers for prediction of severe adverse drug reactions. *N Engl J Med* **358**, 637-9.

Itoh Y., Mizuki N., Shimada T., Azuma F., Itakura M., Kashiwase K., Kikkawa E., Kulski J. K., Satake M. and Inoko H. 2005. High-throughput DNA typing of HLA-A, -B, -C, and -DRB1 loci by a PCR-SSOP-Luminex method in the Japanese population. *Immunogenetics* **57**, 717-29.

Martin A. M., Nolan D. and Mallal S. 2005. HLA-B*5701 typing by sequence-specific amplification: validation and comparison with sequence-based typing. *Tissue Antigens* **65**, 571-4.

Mockenhaupt M. 2009. Severe drug-induced skin reactions: clinical pattern, diagnostics and

rare, close to 0%. From 200 blind samples, this assay gives 100% sensitivity and >99.9% specificity, as extremely rare alleles mentioned above can still be amplified. According to our samples, we didn't found those extremely rare alleles, positive predictive value and negative predictive value are 100%. Therefore, this SSP assay with one set of primer pairs can be used with high specificity in our Thai population.

5. Conclusion

This PCR-SSP system can be used to define *HLA-B*5801*. The benefit of these tests would help patients to avoid any life-threatening adverse consequences from allopurinol with less cost.

6. Acknowledgement

This work is supported by the Lupus Research Unit and the Thailand Research Fund (Senior Research Scholar Grant – RTA5280002).

7. References

Altman D. G. and Bland J. M. 1994. Diagnostic tests. 1: Sensitivity and specificity. *BMJ* **308**, 1552.

Bunce M., O'Neill C. M., Barnardo M. C., Krausa P., Browning M. J., Morris P. J. and Welsh K. I. 1995. Phototyping: comprehensive DNA typing for HLA-A, B, C, DRB1, DRB3, DRB4, DRB5 & DQB1 by PCR with 144 primer mixes utilizing sequence-specific primers (PCR-SSP). *Tissue Antigens* **46**, 355-67.

Chung W. H., Hung S. I. and Chen Y. T. 2007. Human leukocyte antigens and drug hypersensitivity. *Curr Opin Allergy Clin Immunol* **7**, 317-23.

Chung W. H., Hung S. I., Hong H. S., Hsih M. S., Yang L. C., Ho H. C., Wu J. Y. and Chen Y. T. 2004. Medical genetics: a marker for Stevens-Johnson syndrome. *Nature* **428**, 486.

Hung S. I., Chung W. H., Liou L. B., Chu C. C., Lin M., Huang H. P., Lin Y. L., Lan J. L., Yang L. C., Hong H. S., Chen M. J., Lai P. C., Wu M. S., Chu C. Y., Wang K. H., Chen C. H., Fann C. S., Wu J. Y. and Chen Y. T. 2005. HLA-B*5801 allele as a genetic marker for severe cutaneous adverse reactions caused by allopurinol. *Proc Natl Acad Sci U S A* **102**, 4134-9.

Ingelman-Sundberg M. 2008. Pharmacogenomic biomarkers for prediction of severe adverse drug reactions. *N Engl J Med* **358**, 637-9.

Itoh Y., Mizuki N., Shimada T., Azuma F., Itakura M., Kashiwase K., Kikkawa E., Kulski J. K., Satake M. and Inoko H. 2005. High-throughput DNA typing of HLA-A, -B, -C, and -DRB1 loci by a PCR-SSOP-Luminex method in the Japanese population. *Immunogenetics* **57**, 717-29.

Martin A. M., Nolan D. and Mallal S. 2005. HLA-B*5701 typing by sequence-specific amplification: validation and comparison with sequence-based typing. *Tissue Antigens* **65**, 571-4.

Mockenhaupt M. 2009. Severe drug-induced skin reactions: clinical pattern, diagnostics and

therapy. *J Dtsch Dermatol Ges* **7**, 142-60; quiz 161-2.

Wolf C. R., Smith G. and Smith R. L. 2000. Science, medicine, and the future: Pharmacogenetics. *BMJ* **320**, 987-90.

PERCH-CIC

CONGRESS VII

Theme: Chemistry, Environment and Society

การประชุมวิชาการ

ศูนย์ความเป็นเลิศด้านนวัตกรรมทางเคมี ครั้งที่ 7

Jomtien Palm Beach Hotel & Resort Pattaya, Chonburi

PERCH-CIC

PERDO

Center of Excellence for Innovation in Chemistry

Poster Presentations

Session S1 - Analytical Technology

Coordinators: Prapin Wilairat / Proespichaya Kanatharana / Jaroon Jakmunee / Somchai Lapanantnoppakhun / Wanlop Harasai / Apinya Nacapricha / Rattikan Chantiratikul / Kanchana Ueasiri / Pichaya Mungkornsasmakul / Chongdar Thammakhet / Wanakorn Limbut / Apon Numnuam

S1-P1	Fabrication of a Home-made Spectrophotometric Detector for Flow Injection System	อภิเดช ทองอ่อน	Apidech Thongson
S1-P2	A Compact Flow Injection Colorimetric Detection for Determination of Ethanol in Distilled Liquor	วิมุเศียญ คงศีร	Wimpen Khongpet
S1-P3	Determination of Salinity in Seawater with a Reagent-free Flow Injection System	ปิยวรรณ พันธ์	Piyawan Phanit
S1-P4	A Simple Flow Injection Analysis Spectrophotometric Method for Determination of Trace Nitrite in Water Samples	ปวีณสา ประเสริฐบุญโชคชัย	Paweelada Prasertboonyai
S1-P5	Determination of Ammonia by Reverse Flow Injection Analysis	นพวรรณ ทันธิน	Nopphawan Thunthin
S1-P6	Comparison of the Efficiency of Gas Collection Units for Determination of Nitrogen Dioxide by Flow Injection Analysis	นพดล แย้มมณี	Noppadon Mameyen
S1-P7	Application of CdS Quantum Dots as Luminescent Probes for Arsenic Determination by Gas-Diffusion Flow Injection Analysis	ณัฏฐิกานต์ บุพวงศ์	Natthaya Buswong
S1-P8	Development of a Flow Injection-capillary Electrophoresis System	ธราธิดา มูลดี	Thararat Moonta
S1-P9	Sequential Injection Spectrophotometric Determination of Aluminium(III) Using Quercetin	พรนิธี หนอพึ่ง	Pornthree Norfun
S1-P10	Spectrophotometric Sequential Injection Analysis for Determination of Phenol in Water	ธนากร เปลื้องทอง	Thanakorn Pluangklang
S1-P11	Determination of Orthophosphate by Cross Injection Analysis	สสิธันท์ จายา	Sasitan Jaya
S1-P12	Possibility Study of Continuous Flow Sequential Extraction and Determination of Phosphorus in Soil	ศิริมา กองวิจา	Sirinart Prewha
S1-P13	Monolith-based Immobilized Enzyme Micro-reactor for Determination of Organophosphorus Pesticides	ภาวี รัตนกิจ	Panwee Rattanakit
S1-P14	Monolithic Materials for a Microfluidic System	วิสาขะ ชูเดชกุล	Visakha Chuedchukorn
S1-P15	Rapid Fabrication of PMMA Chips Using mini-CNC Machine Modified with Laser Diode	นนทิพย ธีรกุลวิทย์	Nuntiba Teerarungs
S1-P16	Low Cost Lithography and Sputtering Process for Electrochemical-based Microfluidic Device Fabrication	จันทร์เพ็ญ พรุวรรณ์	Chanpen Karuwan
S1-P17	Surface Plasmon Resonance Immunosensor Based on Immobilized Antibody on Electropolymerized Poly(o-phenylenediamine)	สุรนาท ยอดบุตร	Suparnat Yodbut
S1-P18	Surface Plasmon Resonance Immunosensor for Melioidosis Detection	สุภาพร ดาวัลย์	Supaporn Dawan
S1-P19	Detection of Total Bacteria Using Surface Plasmon Resonance Affinity Biosensor	จงจิต จันดา	Jongjit Janr
S1-P20	Capacitive DNA Sensor Using Immobilized PNA	สุพรรณี สีแสวะ	Supannee Sankoh
S1-P21	Capacitive Immunosensor Using para-Phenylenediamine Modified Electrode for HSA Detection	อรวรรณ ทิพย์เนตร์	Orawan Thipnetee
S1-P22	Multilayer Modified Electrode for Label-free Impedimetric Immunosensing of Small Molecule	เกษร ฉลัยนต์	Kochaporn Chalianat
S1-P23	Preparation of Magnetic Iron Oxide Particles by Co-precipitation	ชาริสิณี สีวิชาม	Charisinee Sirichan
S1-P24	Utilization of Metal Oxide Semiconductor as Sensor for Determination of Ethanol	อำนาจ เรืองศักดิ์พิพัฒ	Amnat Ruangchaiwat
S1-P25	Simple and Direct Determination of Ethanol in Gasohol by Raman Spectrometry	พูนศรี แซ่เล้ง	Phoonthavee Saenge
S1-P26	Sensitivity Enhancement of Glucose Fluorescence Sensor Based on Alizarin-Boronic Acid Complex in Aqueous Micelle	เกษรินทร์ งามดี	Kesarin Ngamdee
S1-P27	Development of Oxygen Biosensor Based on Entrapping of Laccase on the Nanocomposite Film of Carbon Nanotubes-Chitosan	ยุวเรศ เสนารี	Yuwakorn Senari

S1-P20

Capacitive DNA Sensor Using Immobilized PNA

Supannee Sankoh,[a,b,c] Orawan Thipmanee,[a,b,c] Saluma Samanman,[a,b,c] Warakorn Limbut,[a,b,d] Apon Numnuam,[a,b,c] Proespichaya Kanatharana,[a,b,c] Tirayut Vilaivan[e] and Panote Thavarungkul[a,b,f]

[a]*Trace Analysis and Biosensors Research Centre, Faculty of Science, Prince of Songkla University, Hat Yai, SongKhla 90112, Thailand.*
[b]*Center of Excellence for Innovation in Chemistry, Faculty of Science, Prince of Songkla University, Hat Yai, SongKhla 90112, Thailand.*
[c]*Department of Chemistry, Faculty of Science, Prince of Songkla University, Hat Yai, SongKhla 90112, Thailand.*
[d]*Department of Applied Science, Faculty of Science, Prince of Songkla University, Hat Yai, SongKhla 90112, Thailand.*
[e]*Organic Synthesis Research Unit, Department of Chemistry, Faculty of Science, Chulalongkorn University, Phayathai Road, Patumwan, Bangkok 10330, Thailand.*
[f]*Department of Physic, Faculty of Science, Prince of Songkla University, Hat Yai, SongKhla 90112, Thailand.*

Introduction and Objective

Peptide nucleic acid (PNA) is a DNA mimic that has the ability to form extremely stable complexes with the complementary DNA oligomers. This work reports the development of a flow-injection capacitive DNA sensor with immobilized lipoic acid modified PNA (Lip-PNA) probe for the direct detection of DNA using a capacitive system.

Methods

Lip-PNA was directly immobilized on cleaned gold electrode by chemical adsorption. The modification of the modified electrode was investigated by cyclic voltammetry. The modified electrode was used as the working electrode (WE) in a flow injection system to detect the hybridization between DNA target and Lip-PNA probe by measuring the change in capacitance.

Results

The electrochemical characterization of the electrode surface studied using cyclic voltammetry confirmed that Lip-PNA probe was immobilized on the cleaned gold electrode. The affinity hybridization between DNA target and PNA probe causes the decrease of the measured capacitance. Under the optimum conditions, the linear dynamic range was 1.0×10^{-11} to 1.0×10^{-8} M with a detection limit of 1.0×10^{-11} M.

Conclusion

The capacitive DNA sensor with Lip-PNA probe is suitable for the direct detection of affinity hybridization.

Keywords: affinity biosensor, DNA sensor, PNA, capacitive biosensor

Selected References:

1. Ananthanawat, C.; Vilaivan, T.; Hoven, V.P.; Su, X. *Biosens. Bioelectron.*, **2010**, *25*, 1064-1069.
2. Limbut, W.; Thavarungkul, P.; Kanatharana, P.; Wongkittisuksa, B.; Asawatreratanakul, P.; Limsakul, C. *Electrochim. Acta*, **2010**, *55*, 3268-3274.

Supannee Sankoh (สุพรรณี สังเกาะ) **Ph.D. Student**
b 1985 in Satun, Thailand
Prince of Songkla University, Thailand, Chemistry, B.Sc. 2008
Research field: sensors

PERCH-CIC

CONGRESS VII

Theme: Chemistry, Environment and Society

การประชุมวิชาการ

ศูนย์ความเป็นเลิศด้านนวัตกรรมทางเคมี ครั้งที่ 7

4-7 May 2011

Jomtien Palm Beach Hotel & Resort Pattaya, Chonburi

PERCH-CIC
PERDO

Center of Excellence for Innovation in Chemistry

www.perch-cic.org

S2A-O12

Synthesis and Nucleic Acid Binding Properties of Novel Pyrrolidinyl Peptide Nucleic Acid Carrying 3-Aminopyrrolidine-4-carboxylic Acid Spacer

Nisanath Reenabthue,[a] Tirayut Vilaivan[b] and Chaturong Suparpprom[a]

[a]Department of Chemistry and Center of Excellence for Innovation in Chemistry, Faculty of Science, Naresuan University, Phitsanulok 65000, Thailand.
[b]Department of Chemistry, Faculty of Science, Chulalongkorn University, Bangkok 10330, Thailand.

Introduction and Objective

Peptide nucleic acid (PNA) is a DNA mimic which deoxyribose phosphate is replaced by peptide backbone. From our previous study, a new conformationally rigid PNA base on a pyrrolidinyl backbone bearing a (1*S*,2*S*)-2-amino-1-cyclopentanecarboxylic acid (*acpc*) spacer showed excellent binding with DNA. In this research, novel pyrrolidinyl PNA bearing a 3-aminopyrrolidine-4-carboxylic acid (*aza-acpc*) spacer was synthesized and investigated its DNA binding properties for improve the solubility of this PNA and provide a handle for internal modification.

Methods

The *trans*-(3*R*,4*S*)- and (3*S*,4*R*)-isomers of *aza-acpc* were synthesized following the known route. The synthetic protocol starting by diastereoselective reductive amination of the keto-ester intermediate, obtained via a Diekmann cyclization of Boc-glycine ethyl ester, with (*S*)- and (*R*)-α-methylbenzylamine followed by protecting group exchange gave the (3*R*,4*S*)- and (3*S*,4*R*)-isomers of the protected spacers. These spacers have been successfully incorporated into model PNA sequences by Fmoc solid phase peptide synthesis. Successful incorporation of the new spacers was confirmed by MALDI-TOF MS and purified by HPLC.

Results

The *trans*-(3*R*,4*S*)- and (3*S*,4*R*)-isomers of *aza-acpc* were synthesized in 6.5% and 4.9% overall yield, respectively. The results of T_m data showed that (3*R*,4*S*)-*aza-acpc* PNA and singly modified in the middle of the strand which possess the same absolute configuration as (1*S*,2*S*)-*acpc* could bind with complementary DNA in high T_m (55.5 and 71.1 °C) with T_m only slightly lower than unmodified *acpc*PNA. The UV-titration data showed interesting manner of singly modified PNA with (3*R*,4*S*)-*aza-acpc* spacer formed complexes with 1:1 stoichiometry and fully modified formed PNA 2:DNA 1 ratio while (3*S*,4*R*)-*aza-acpc* PNA not show any equivalent point. CD spectroscopy also clearly demonstrates the formation of stable hybrids between the singly modified (3*R*,4*S*)-*aza-acpc* PNA with dA_9. These results confirm the ability of (3*R*,4*S*)-*aza-acpc* to mimic the (1*S*,2*S*)-*acpc* in PNA.

Conclusion

New pyrrolidinyl PNA carrying *trans*-(3*R*,4*S*)-*aza-acpc* spacer have been successfully synthesized. UV titration, Tm and CD experiments clearly revealed that this PNA can bind with DNA without compromising the ability of original (1*S*,2*S*)-*acpc* PNA.

Keywords: *aza-acpc*PNA, *acpc*PNA, DNA, β-amino acid

Selected References:

1. Suparpprom, C.; Srisuwannaket, C.; Sangvanich, P.; Vilaivan, T. *Tetrahedron Lett.*, **2005**, *46*, 2833-2837.
2. Lee, H. S.; LePlae, P. R.; Porter, E. A.; Gellman, S. H. *J. Org. Chem.*, **2001**, *66*, 3597-3599.

Nisanath Reenabthue (นิสานาถ รีน้ำยื่อ) **M.Sc. Student**
Naresuan University, Thailand, Chemistry, B.Sc. 1994
Research field: synthesis of peptide nucleic acid (PNA)

A NEW STRATEGY FOR ON-SOLID-SUPPORT LABELING OF PYRROLIDINYL PEPTIDE NUCLEIC ACID BY REDUCTIVE ALKYLATION AND CLICK CHEMISTRY

Boonsong Ditmangklo,[1] Chaturong Suparpprom,[1] Tirayut Vilaivan[2,*]

[1]Department of Chemistry and Center of Excellence for Innovation in Chemistry, Faculty of Science, Naresuan University, Ta-Po District, Muang, Phitsanulok 65000, Thailand
[2]Organic Synthesis Research Unit, Department of Chemistry, Faculty of Science, Chulalongkorn University, Phayathai Road, Patumwan, Bangkok 10330, Thailand
*e-mail: vtirayut@chula.ac.th

Abstract: A new strategy for site-specific modification of pyrrolidinyl peptide nucleic acid consisting of an alternating sequence of nucleobase-modified D-proline/(1*S*,2*S*)-2-aminocyclopentanecarboxylic acid (acpcPNA) has been developed. The reductive *N*-alkylation of the acpcPNA, previously modified with a (3*R*,4*S*)-3-amino pyrrolidine-4-carboxylic acid (azaACPC) spacer, was carried out on solid support by first reacting the azaACPC-modified acpcPNA(**1**) with 4-azidobutanal in the presence of $NaBH_3CN$ under mildly acidic conditions. The azide-modified acpcPNA (**2**) was further labeled with 1-ethynylpyrene, a representative alkyne-functionalized fluorophore, using Cu(I)-catalyzed Huisgen azide-alkyne cycloaddition (click chemistry). The two-step reaction sequence proceeded in quantitative yield without side reactions as verified by MALDI-TOF mass spectrometry after cleavage of the acpcPNA from the solid support. This strategy offers a convenient and effective way for the development of internally-labeled fluorescent acpcPNA probes.

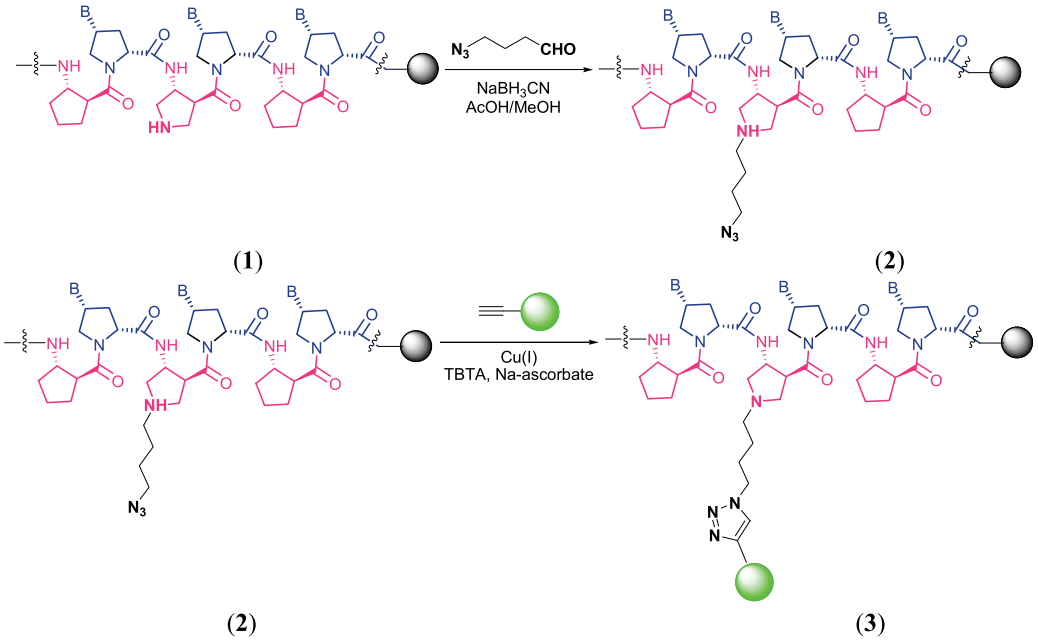

(**1**) (**2**)

(**2**) (**3**)

Acknowledgements: This work was supported by Center of Excellence for Innovation in Chemistry (PERCH-CIC) and the Thailand Research Fund (RTA5280002).
Keywords: fluorescence, PNA probe, reductive alkylation, click chemistry, molecular beacon

DUAL-PYRENE-LABELED PYRROLIDINYL PEPTIDE NUCLEIC ACID PROBES

Nattapon Maneelun, Chalothorn Boonlua, Tirayut Vilaivan*

Organic Synthesis Research Unit, Department of Chemistry, Faculty of Science, Chulalongkorn University, Phayathai Road, Patumwan, Bangkok 10330, Thailand
*e-mail: vtirayut@chula.ac.th

Abstract: In this study, dual-pyrene-labeled pyrrolidinyl peptide nucleic acid (acpcPNA) probes have been rationally designed by site-specifically attaching two pyrene chromophores onto the backbone of the same acpcPNA strand. The fluoresecence spectra of the single stranded acpcPNA showed mainly the excimer emission at 470 nm, indicating that the two pyrene chromophores were in close proximity. Upon hybridization with the complementary DNA target, the two chromophores were separated, resulting in the enhancement of the pyrene monomer emission at 380 nm. The ratios of monomer to excimer emissions of the modified acpcPNA were between 0.27 to 0.43 in the single stranded form, and between 0.48 to 1.19 after hybridization, depending on the distance between the two pyrene chromophores. These dual-labled acpcPNA should be useful as probes for detecting sequences of DNA. The advantage of this design over conventional molecular beacons is that not only intensity, but also the emission wavelength, change significantly upon hybridization with the DNA target.

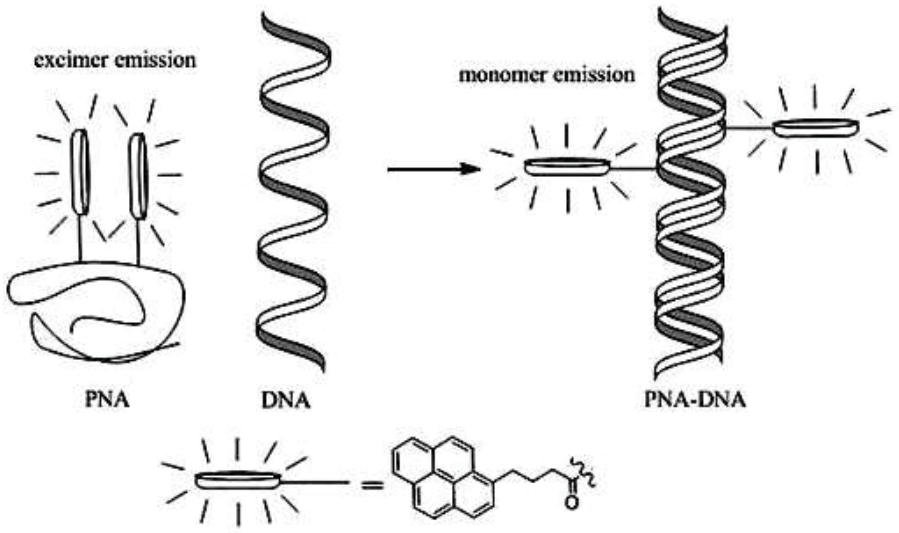

Acknowledgements: This work was supported by the Thailand Research Fund (RTA5280002) and the Development and Promotion of Science and Technology Talents Project (DPST).

Keywords: pyrene, fluorescence, PNA probe, excimer, molecular beacon

PYRROLIDINYL PEPTIDE NUCLEIC ACID TERMINALLY-LABELED WITH THIAZOLE ORANGE AS A FLUORESCENT DNA PROBE

Chaiwat Maneethamwong,[1] Boonsong Ditmangklo,[2] Chaturong Suparpprom,[2] Tirayut Vilaivan[1,*]
[1]Organic Synthesis Research Unit, Department of Chemistry, Faculty of Science, Chulalongkorn University, Phayathai Road, Patumwan, Bangkok 10330, Thailand
[2]Department of Chemistry, Faculty of Science, Naresuan University, Ta-Po District, Muang, Phitsanulok 65000, Thailand
*e-mail: vtirayut@chula.ac.th

Abstract: The unsymmetrical cyanine dye thiazole orange (TO) was attached at the *N*-terminus of pyrrolidinyl PNA with D-proline/(1*S*,2*S*)-2-aminocyclopentanecarboxylic acid backbone (acpcPNA) with the aim to be used as a fluorescent probe for DNA sequence determination. The *N*-terminus of the acpcPNA was first functionalized with azidobutyl group by reductive alkylation with 4-azidobutanal. The TO label, previously functionalized with an alkyne group at the *N*-atom of the quinoline ring, was next attached to the azidobutyl acpcPNA *via* Click chemistry on soild-support. Fluorescence properties of the terminally TO-labeled mix-base 10mer acpcPNA in the absence and presence of complementary DNA targets were next studied. The single stranded TO-labeled acpcPNA showed very weak fluorescence, which did not increase significantly upon hybridization to the complementary DNA target having exactly the same length. On the other hand, hybridization of the TO-labeled acpcPNA with a 21-base DNA consisting of a 10-base region complementary to the labeled acpcPNA resulted in a 12-fold fluorescence increase. Addition of another short DNA sequence complementary to the overhanging single stranded region resulted in a dramatic increase of fluorescence (up to 89-fold) while addition of non-complementary DNA did not give the same fluorescence increase. The results are explained by the interaction between the TO label and the DNA duplex. The large fluorescence increase suggests that the terminally-labeled acpcPNA may be used for developing a probe for specific DNA sequence determination.

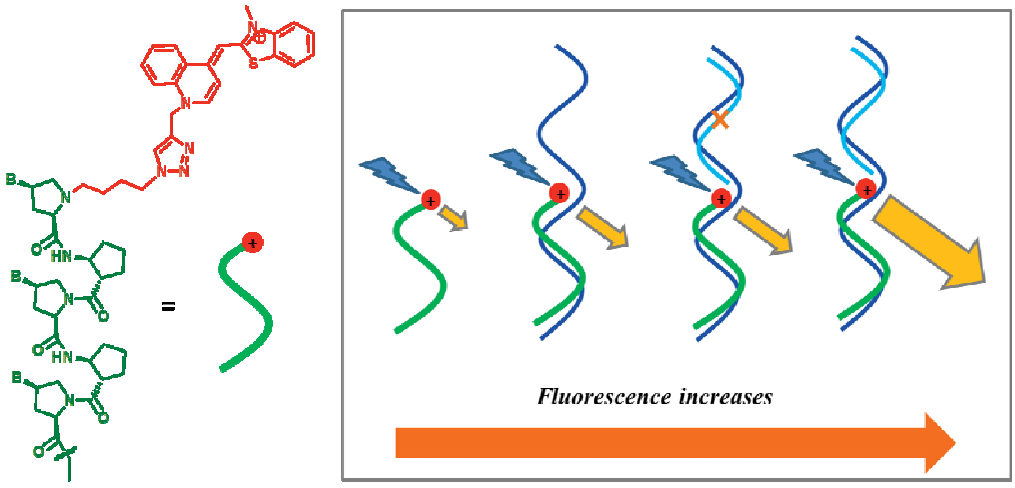

Acknowledgements: This work was supported by the Thailand Research Fund (RTA5280002).

Keywords: PNA, Thiazole Orange, fluorescence, click chemistry, molecular beacon

ORTHOGONALLY-PROTECTED 3-AMINOPYRROLIDINE-4-CARBOXYLIC ACIDS FOR SYNTHESES OF DOUBLY-LABELED PYRROLIDINYL PEPTIDE NUCLEIC ACIDS

Nattawut Yotapan, Tirayut Vilaivan*
Organic Synthesis Research Unit, Department of Chemistry, Faculty of Science,
Chulalongkorn University, Phayathai Road, Patumwan, Bangkok 10330, Thailand
*e-mail: vtirayut@chula.ac.th

Abstract: Pyrrolidinyl peptide nucleic acids (acpcPNA) labeled at the backbone with a suitable Fluorescence Resonance Energy Transfer (FRET) pair are potentially useful as fluorescence probes that can change their fluorescence intensity and/or emission wavelength upon hybridization to correct DNA targets. While single labeling of acpcPNA at the backbone has previously been achieved through replacement of the usual 2-aminocyclopentanecarboxylic acid (ACPC) monomer in acpcPNA with *N*-Tfa-protected 3-aminopyrrolidine-4-carboxylic acid (APC) monomer, synthesis of doubly-labeled PNA requires an additional APC protecting group that must be compatible with the Fmoc chemistry (removable by non-aqueous base) used for the synthesis of the acpcPNA and with the Tfa group (removable by aqueous base) used for protection of the first APC residue. In this work, we had synthesized *N*-(*o*-nosyl)- (removable by thiolate) and *N*-Teoc-protected (removable by fluoride) APC derivatives and evaluated their potential to be used in combination with the *N*-Tfa-protected APC monomer for the synthesis of doubly-modified acpcPNA. While the *N*-Tfa group could be selectively removed in the presence of either *N*-Teoc or *N*-(*o*-nosyl) groups, only removal of the latter could be selectively achieved in the presence of *N*-Tfa group. The combination of *N*-(*o*-nosyl)- and *N*-Tfa-protected APC monomers provided excellent level of orthogonality in the synthesis of model doubly-modified acpcPNAs as demonstrated by MALDI-TOF mass spectrometry.

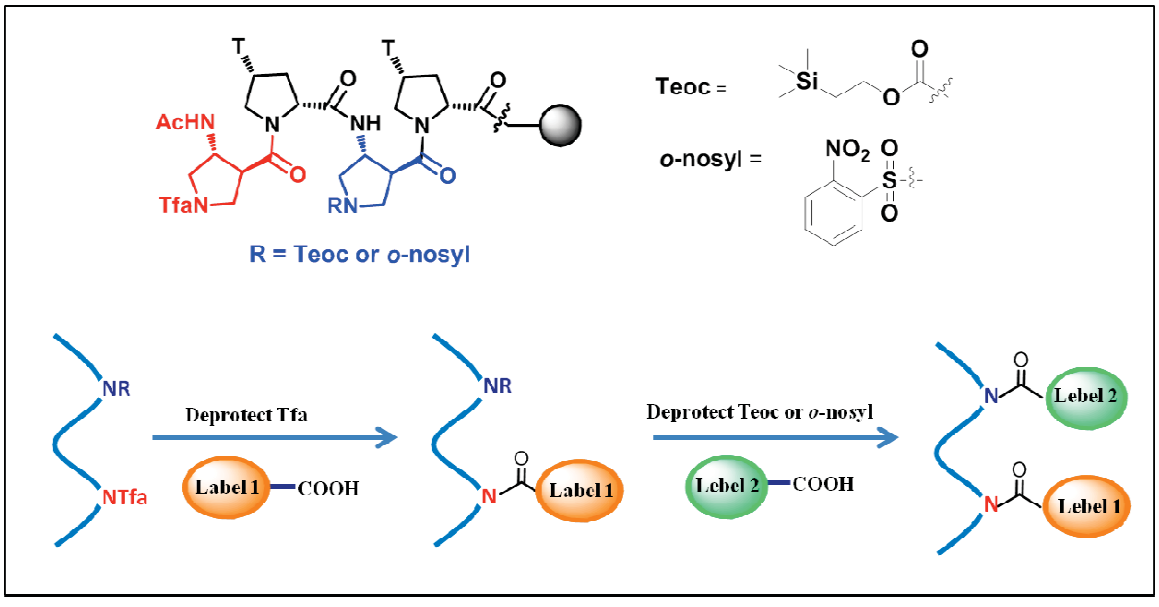

Acknowledgements: This work was supported by the Thailand Research Fund (RTA5280002).

Keywords: PNA, fluorescence, FRET, orthogonal protection, molecular beacon

HIGHLY SPECIFIC DNA SEQUENCE DETERMINATION BY PYRENE-LABELED PYRROLIDINYL PEPTIDE NUCLEIC ACID PROBES IN COMBINATION WITH ENZYMATIC DIGESTION

Chalothorn Boonlua,[1] Boonsong Ditmangklo,[2] Chaturong Suparpprom,[2] Chotima Vilaivan,[1] Tirayut Vilaivan[1,*]

[1]Organic Synthesis Research Unit, Department of Chemistry, Faculty of Science, Chulalongkorn University, Bangkok 10330, Thailand

[2]Department of Chemistry, Faculty of Science, Naresuan University, Phitsanulok, 65000, Thailand

*e-mail: vtirayut@chula.ac.th

Abstract: Oligonucleotide probes labeled with environment-sensitive fluorophores are powerful tools for studies of molecular diagnostics, and biotechnology. In this work, we have synthesized a hybridization-responsive pyrrolidinyl peptide nucleic acid (acpcPNA) probe. The acpcPNA probe was covalently modified at the backbone with a pyrene chromophore through a flexible linker *via* acylation or reductive alkylation of 3-aminopyrrolidine-4-carboxylic acid (APC)-modified acpcPNA. The fluorescence of the pyrene-labeled acpcPNA is quenched by the nucleobases (especially T and C) in the single-stranded state. Hybridization of the pyrene-labeled acpcPNA to its complementary DNA target resulted in a large increase in fluorescence signal (up to 14-fold). Hybridization to mismatched DNA gave variable results (unchanged, decreased or increased fluorescence relative to the single-stranded PNA), depending on the position and type of the mismatch pairs. Fluorescence analysis showed that the complementary PNA·DNA hybrid was much more resistant to digestion by nuclease S1, an enzyme that specifically hydrolyzes single-stranded DNA, than mismatched hybrids. Accordingly, perfect discrimination between complementary and mismatched DNA targets had been achieved after 10-min digestion of the hybrids by the enzyme, whereby the fluorescence of the mismatched hybrids returned to baseline (i.e. similar to single-stranded PNA) and that of the complementary hybrid remained unchanged.

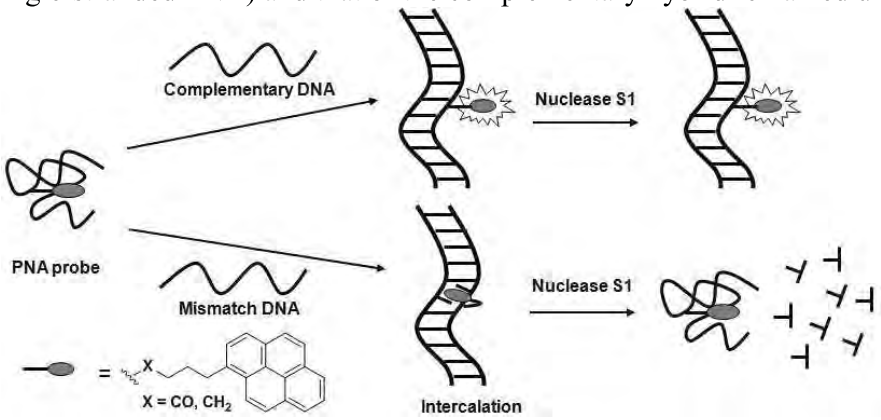

References:

1. Reenabthue N, Boonlua C, Vilaivan C, Vilaivan T, Suparpprom C. Bioorg Med Chem Lett 2011;21:6465-6569.
2. Komiyama M, Ye S, Liang X, Yamamoto Y, Tomita T, Zhou J-M, Aburatani H. J Am Chem Soc 2003;125:3758-3762.

Acknowledgements: The Thailand Research Fund (RTA5280002) and the Development and Promotion of Science and Technology Talents Project (DPST).

Keywords: peptide nucleic acid, nuclease S1, fluorescence, molecular beacon

ภาคผนวก 3

เอกสารรวมคัดย่องานประชุมประจำปีกลุ่มวิจัย

(เนื่องจากเอกสารมีความหนามาก จึงไม่ได้เย็บรวมในเล่มรายงานฉบับสมบูรณ์
ผู้สนใจโปรดดูรายละเอียดในแผ่น CD)

สัญญาเลขที่ RTA5280002

รายงานการประชุมประจำปีครั้งที่ 1
ทุนส่งเสริมกลุ่มวิจัย ปี 2552

วันศุกร์ที่ 21 มกราคม 2554 เวลา 08:30 – 15:00
ห้องประชุม ศ.ดร.แถบ นีละนิธิ (ห้อง 1119) ชั้น 11 อาคารมหามกุฏ
ภาควิชาเคมี คณะวิทยาศาสตร์ จุฬาลงกรณ์มหาวิทยาลัย

โครงการ การสังเคราะห์ สมบัติ และการประยุกต์ใช้เบต้าพิโรลิดินิลเพปไทด์นิวคลีอิกแอซิดที่มีคอนฟอร์เมชันถูกจำกัด

Synthesis, Properties and Applications of Conformationally Constrained β-Pyrrolidinyl Peptide Nucleic Acids

หัวหน้าโครงการ รศ.ดร.ธีรยุทธ วิไลวัลย์
ภาควิชาเคมี คณะวิทยาศาสตร์ จุฬาลงกรณ์มหาวิทยาลัย

สนับสนุนโดยสำนักงานกองทุนสนับสนุนการวิจัย
(งานวิจัยนี้ยังไม่เสร็จสมบูรณ์ โปรดอย่านำไปใช้อ้างอิง)

คำนำ

โครงการ “การสังเคราะห์ สมบัติ และการประยุกต์ใช้เบต้าพิโรลิดินิลเพปไทด์นิวคลีอิกแอซิดที่มีคอนฟอร์เมชันถูกจำกัด” นี้ได้รับการสนับสนุนจากสำนักงานกองทุนสนับสนุนการวิจัย (สกว.) ภายใต้ทุนส่งเสริมกลุ่มวิจัย (เมธีวิจัยอาวุโส) ตามเงื่อนไขในสัญญารับทุนจาก สกว . หัวหน้าโครงการจะต้องจัดการประชุมวิชาการประจำทุกปี ประกอบกับขณะนี้งานได้ดำเนินการมาเป็นระยะเวลา 18 เดือนแล้ว จึงเห็นควรที่จะจัดงานประชุมนี้ขึ้น เพื่อให้ผู้ร่วมโครงการได้มีโอกาสนำ เสนอความก้าวหน้าของโครงการวิจัย ร่วมกัน และแลกเปลี่ยนความรู้ระหว่างกลุ่มวิจัย- สาขา และรับฟังข้อเสนอแนะจากผู้ทรงคุณวุฒิ อันจะทำให้เกิดการพัฒนางานวิจัยไปในทิศทางที่ดีขึ้น

คณะผู้วิจัยขอขอบพระคุณสำนักงานกองทุนสนับสนุนการวิจัยและสถาบันต้นสังกัดของหัวหน้าโครงการ และผู้ร่วมโครงการทุกท่าน รวมทั้งแหล่งทุนอื่นที่ได้ให้การสนับสนุนงานวิจัยแม้จะ ไม่ใช่ทางตรง ตลอดจนผู้ช่วยวิจัย และนักศึกษา ที่ทำให้โครงการดำเนินไปได้ด้วยดี มีผลงานที่มีคุณภาพสูงตามที่ตั้งเป้าหมายไว้

อนึ่ง งานวิจัยนี้ยังไม่เสร็จสมบูรณ์ ข้อมูลทั้งหมดนี้เป็นเพียงผลการศึกษาเบื้องต้นที่ยังไม่ได้ผ่านการประเมินอย่างเป็นทางการจากผู้เชี่ยวชา ญ โปรดอย่านำไปเผยแพร่หรืออ้างอิงจนกว่าผลงานจะได้ตีพิมพ์ในวารสารวิชาการแล้ว

รศ.ดร.ธีรยุทธ วิไลวัลย์
หัวหน้าโครงการ

กำหนดการประชุมทุนส่งเสริมกลุ่มวิจัย (เมธีวิจัยอาวุโส) ครั้งที่ 1

โครงการ “การสังเคราะห์ สมบัติ และการประยุกต์ใช้เบต้าพิโรลิดินิลเพปไทด์นิวคลีอิกแอซิด ที่มีคอนฟอร์เมชันถูกจำกัด” (รหัสโครงการ: RTA5280002)

วันศุกร์ที่ 21 มกราคม 2554 เวลา 08:30 – 15:00

ห้องประชุม ศ.ดร.แถบ นีละนิธิ (ห้อง 1119) ชั้น 11 อาคารมหามกุฏ

ภาควิชาเคมี คณะวิทยาศาสตร์ จุฬาลงกรณ์มหาวิทยาลัย

08:30-08:50	ลงทะเบียน
08:50-09:00	กล่าวเปิดงานโดยคณบดีคณะวิทยาศาสตร์
09:00-09:30	สรุปภาพรวมของโครงการโดยหัวหน้าโครงการ (รศ.ดร.ธีรยุทธ วิไลวัลย์)
09:30-10:00	3-Aminopyrrolidine-4-carboxylic acid: A versatile handle for internal labeling of pyrrolidinyl PNA (ดร.จตุรงค์ สุภาพพร้อม ภาควิชาเคมี คณะวิทยาศาสตร์ มหาวิทยาลัยนเรศวร)
10:00-10:30	Dendritic fluorophores and polydiacetylenes for DNA sensors (รศ.ดร.มงคล สุขวัฒนาสินิทธิ์ ภาควิชาเคมี คณะวิทยาศาสตร์ จุฬาลงกรณ์มหาวิทยาลัย)
10:30-11:00	Detection of DNA following “Dot Blot” format employing filter paper functionalized with quaternized polymer brushes and peptide nucleic acid probe (รศ.ดร.วรวีร์ โฮเว่น ภาควิชาเคมี คณะวิทยาศาสตร์ จุฬาลงกรณ์มหาวิทยาลัย) (อาหารว่างในห้องประชุม)
11:00-11:30	Surface-functionalized magnetic nanoparticles for immobilization of PNA and DNA (รศ.ดร.เมธา รัตนากรพิทักษ์ ภาควิชาเคมี คณะวิทยาศาสตร์ มหาวิทยาลัยนเรศวร)
11:30-12:00	Capacitive biosensor based on immobilized PNA probe through *ortho*-phenylenediamine (o-PD) (รศ.ดร.ปณต ถาวรังกูร ภาควิชาฟิสิกส์ คณะวิทยาศาสตร์ มหาวิทยาลัยสงขลานครินทร์)
12:00-13:00	รับประทานอาหารกลางวันและชมโปสเตอร์
13:00-13:30	Point of care detection of oseltamivir resistant mutation in novel 2009 human influenza A virus (H1N1) based on β-pyrrolidinyl peptide nucleic acid hybridization (ผศ.ดร.ปิยะศักดิ์ ชอุ่มพฤกษ์ ภาควิชาพฤกษศาสตร์ คณะวิทยาศาสตร์ จุฬาลงกรณ์มหาวิทยาลัย)
13:30-14:00	Using PNA probe as a rapid detection of LAMP and PCR product for drug hypersensitivity prediction (รศ.ดร.พญ.ณัฏฐิยา หิรัญกาญจน์ ภาควิชาจุลชีววิทยา คณะแพทยศาสตร์ จุฬาลงกรณ์มหาวิทยาลัย)
14:00-15:00	ประชุมโต๊ะกลม (เฉพาะหัวหน้าโครงการย่อยและผู้ทรงคุณวุฒิ) และอาหารว่าง
15:00-16:00	ชมโปสเตอร์

	โครงการย่อย	ผู้ร่วมโครงการ	ตำแหน่ง
1	Conformationally restriced PNA : synthesis and binding properties	1. รศ.ดร.ธีรยุทธ วิไลวัลย์ 2. ดร.จตุรงค์ สุภาพพร้อม 3. ดร.ซ่อลัดดา ศรีสุวรรณเกศ 4. ดร.วรลักษณ์ มั่นสวัสดิ์ 5. นางโชติมา วิไลวัลย์ 6. น.ส. ชโลธร บุญเหลือ 7. น.ส. นิธินาถ รีนับถือ 8. น.ส. บุญส่ง ดิษมังคล้อ 9. นายณัฐพล มณีลุน	หัวหน้าโครงการ นักวิจัย นักวิจัย ผู้ช่วยนักวิจัย ผู้ช่วยนักวิจัย นักศึกษาปริญญาเอก นักศึกษาปริญญาโท นักศึกษาปริญญาโท นักศึกษาปริญญาโท
2	Dendritic fluorophores for detection of DNA/PNA hybridization	1. รศ.ดร.มงคล สุขวัฒนาสินิทธิ์ 2. ผศ.ดร.ไพฑูรย์ รัชตะสาคร 3. น.ส. วราทิพย์ ศิริพรนพคุณ 4. น.ส. กรรณิการ์ วงศ์นาม 5. นายนคร เนียมนนท์ 6. น.ส. วรรณนภา ย้วนบุญหลิม 7. น.ส. ณัฐพร กิมพิทักษ์	หัวหน้าโครงการ นักวิจัย นักศึกษาปริญญาเอก นักศึกษาปริญญาโท นักศึกษาปริญญาเอก นักศึกษาปริญญาโท นักศึกษาปริญญาโท
3	Development of positively charged polymeric support for high throughput DNA sequence analysis using PNA probes	1. รศ.ดร.วรวีร์ โฮเว่น 2. น.ส. นัดดา บูรณบัญญัติ 3. น.ส. จิตติมา มีบึงพร้าว 4. น.ส. แพทอง ศรีแก่นจันทร์	หัวหน้าโครงการ นักศึกษาปริญญาโท นักศึกษาปริญญาโท นักศึกษาปริญญาเอก
4	Surface functionalized magnetic nanoparticles for immobilization of PNA and DNA	1. รศ.ดร.เมธา รัตนากรพิทักษ์ 2. ดร.บุญจิรา รัตนากรพิทักษ์ 3. ดร.อุทัย วิชัย 4. นายฐาปณพงศ์ เทพฤกษ์ 5. น.ส. ยิ่งรัก พรายอินทร์ 6. นายกฤษดา ดันกันยา	หัวหน้าโครงการ นักวิจัย นักวิจัย นักศึกษาปริญญาเอก นักศึกษาปริญญาโท นักศึกษาปริญญาโท
5	Development of label-free electrochemical DNA biosensor based on immobilized PNA probes	1. รศ.ดร.ปณต ถาวรังกูร 2. รศ.ดร.เพริศพิชญ์ คณาธารณา 3. ดร.วรากร ลิ่มบุตร 4. ดร.อาภรณ์ นุ่มน่วม 5. น.ส. อรวรรณ ทิพย์มณี 6. น.ส. สาลูมา สมานหมาน 7. น.ส. สุพรรณี สันเกาะ	หัวหน้าโครงการ นักวิจัย นักวิจัย นักวิจัย นักศึกษาปริญญาโท นักศึกษาปริญญาโท นักศึกษาปริญญาโท
6.1	Applications of PNA based diagnostics in medical, food and agricultural science	1. ผศ.ดร.ปิยะศักดิ์ ชอุ่มพฤกษ์ 2. น.ส. อลิษา โล่วาณิชย์พัฒน์	หัวหน้าโครงการ ผู้ช่วยนักวิจัย
6.2	Applications of PNA based diagnostics in medical, food and agricultural sciences	1. รศ.พญ.ดร.ณัฏฐิยา หิรัญกาญจน์ 2. นพ.ดร.อมรพันธุ์ เสรีมาศพันธุ์ 3. นายจีรวัฒน์ นาคขุนทด 4. น.ส. ศิตา วีรกุล	หัวหน้าโครงการ นักวิจัย นักศึกษาปริญญาเอก ผู้ช่วยนักวิจัย

3-Aminopyrrolidine-4-carboxylic acid: A versatile handle for internal labeling of pyrrolidinyl PNA

Nisanath Reenabthue[a], Chotima Vilaivan[b], Tirayut Vilaivan[b], Chaturong Suparpprom[a,*]

[a]Department of Chemistry and Center of Excellence for Innovation in Chemistry, Faculty of Science, Naresuan University, Pahonyothin Road, Ta-Po District, Muang, Phitsanulok, 65000
[b]Organic Synthesis Research Unit, Department of Chemistry, Faculty of Science, Chulalongkorn University, Phayathai Road, Patumwan, Bangkok, 10330

*E-mail: chaturongs@nu.ac.th

Abstract: In this research, the cyclic beta-amino acid 3-aminopyrrolidine-4-carboxylic acid (aza-acpc) was synthesized and used as a spacer in the pyrrolidinyl PNA. The (3*R*,4*S*)- and (3*S*,4*R*)-aza-acpc spacers which are structural analogues of (1*S*,2*S*)- and (1*R*,2*R*)-acpc spacers, respectively, were prepared according to the literature and were introduced into a few model PNA sequences by standard Fmoc-solid-phase peptide synthesis. The DNA-binding studies results revealed that incorporation of the (3*R*,4*S*)-aza-acpc spacer into the PNA only slightly decreased the stability of the hybrids (71.1°C compared with 76.7°C) as confirmed by T_m, UV-titration and CD spectroscopy. Furthermore, the nitrogen atom of the aza-acpc spacer was successfully labeled by pyrene-1-carboxylic acid to give an internally-labeled fluorescence PNA probe. Fluorexcence experiments showed that this new PNA probe can discriminate between single-stranded PNA and PNA·DNA hybrid based on the fluorescence enhancement (1-3 fold, depending on sequences).

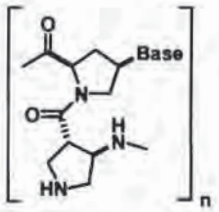

aza-acpcPNA

Publication status

[ ] Published
Citation information:
[x] To be published
Proposed submission date: Feb 2011

Dendritic fluorophores and polydiacetylenes for DNA sensors

Mongkol Sukwattanasinitt,[1,*] Paitoon Rashatasakhon,[1] Tirayut Vilaivan,[1] Nakorn Niamnont,[1] Warathip Siripornnoppakhun,[1] Kunnigar Vongnam[2]

[1] Organic Synthesis Research Unit, Department of Chemistry, Faculty of Science, Chulalongkorn University
[2] Program of Petrochemistry and Polymer Science, Faculty of Science, Chulalongkorn University

*E-mail: smongkol@chula.ac.th

Abstract: Two classes of pi-conjugated systems *i.e.* 1) dendritic phenylacetylene fluorophors and 2) polydiacetylene vesicles are currently investigated in our laboratory for the applications in detection and analysis of biological agents such as proteins and DNA. A series of water soluble dendritic fluorophores, composed of phenylacetylene repeating units and ionic charged peripheral groups, are synthesized. The charge variation on the dendritic structures is proven to be valuable for constituting a sensing array for protein discrimination. The polycationic fluorophores exhibit distinct fluorescence enhancement by DNA, which is potentially useful for DNA detection and sequencing applications. Biotin funtionalized polydiacetylene vesicles are synthesized and investigated for selective colorimetric response to Neutravidin and Streptavidin for future applications in DNA sequencing.

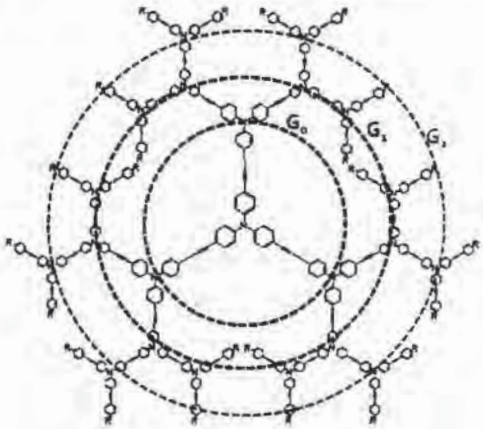

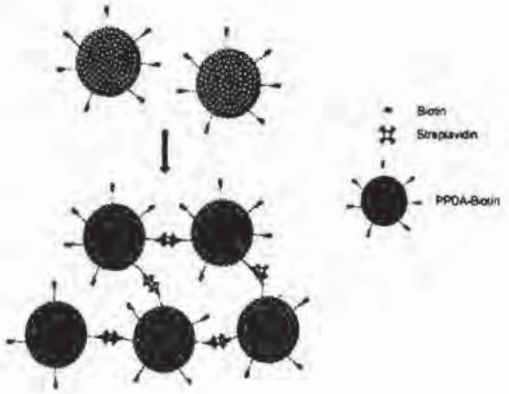

Publication status

[ ] Published

Citation information:

[x] To be published

Proposed submission date: March 2011

Detection of DNA following "Dot Blot" format employing filter paper functionalized with quaternized polymer brushes and peptide nucleic acid probe

Paethong Srikaenjan[1,2], Tirayut Vilaivan[3], Voravee P. Hoven[3,*]

[1]Program in Petrochemistry, Faculty of Science, Chulalongkorn University, Phayathai Road, Patumwan, Bangkok 10330
[2]Center for Petroleum, Petrochemicals, and Advanced Materials, Chulalongkorn University, Phayathai Road, Patumwan, Bangkok 10330
[3]Organic Synthesis Research Unit, Department of Chemistry, Faculty of Science, Chulalongkorn University, Phayathai Road, Patumwan, Bangkok 10330

*E-mail: vipavee.p@chula.ac.th

Abstract: As inspired by the "Dot blot" technique, a well known method in molecular biology and genetics for detecting biomolecules, a new PNA-based colorimetric detection of DNA sequence has been developed. The filter paper was modified to be positively charged with grafted polymer brushes of quaternized poly(dimethylamino)ethyl methacrylate (QPDMAEMA) to be used for DNA detection. It was prepared by surface-initiated polymerization of 2-(dimethylamino)ethyl methacrylate from filter paper via ARGET ATRP followed by quaternization with methyl iodide. Following the "Dot Blot" format, a DNA target was first captured via ionic interactions between the positive charges of the QPDMAEMA brushes and negative charges of the phosphate backbone of DNA. Upon hybridization with biotinylated peptide nucleic acid probe (b-PNA), the immobilized DNA can be detected by naked eye observation of the yellow product generated by the enzymatic amplification employing HRP-labeled streptavidin. In this particular study, a synthetic PNA bearing a conformationally rigid D-prolyl-2-aminocyclopentanecarboxylic acid backbone (acpcPNA) was used as a probe to detect a region of human *IL-10* promoter gene. It has been demonstrated that this newly developed assay was capable of discriminating a single base mismatched from fully complementary DNA targets at 1 pmol level.. In addition, the QPDMAEMA grafted filter paper exhibited a superior performance to commercial membranes including nylon-66 and nitrocellulose.

Publication status

[ ] Published
Citation information:
[x] To be published
Proposed submission date: March 2011

Surface-functionalized magnetic nanoparticles for immobilization of PNA and DNA

Thapanapong Theppaleak[1], Boonjira Rutnakornpituk[1], Uthai Wichai[1], Metha Rutnakornpituk[1,*], Tirayut Vilaivan[2]
[1]Department of Chemistry, Faculty of Science, Naresuan University, Muang, Phitsanulok 65000
[2]Organic Synthesis Research Unit, Department of Chemistry, Faculty of Science, Chulalongkorn University, Phayathai Road, Patumwan, Bangkok 10330

*E-mail: methar@nu.ac.th

Abstract: We here report the synthesis of surface-functionalized magnetite nanoparticle with the copolymer of poly(ethylene glycol) methyl ether methacrylate (PEGMA) and diethylamino ethyl methacrylate (DEAEMA) *via* atom transfer radical polymerization (ATRP). The polymer grafted on the particles was subsequently quarternized to obtain the particles with positively charged surface for adsorption with PNA-DNA hybrid by ionic interaction. Molar ratio of the (co)polymer was systematically varied (100:0, 75:25, 50:50, 25:75 and 0:100, respectively) to tune the degree of positive charge on their surface and also obtain well dispersible particles in aqueous media. Kinetic studies of the copolymerization indicated that PEGMA showed a slightly higher reactivity than that of DEAEMA. Polydispersity of the copolymers, determined *via* gel permeation chromatography (GPC), was in the range of 1.3-1.7, indicating the living/controlled radical mechanism of ATRP. Photon correlation spectroscopy (PCS) disclosed that zeta potential of the particles ranged between +22 to +32 mV and consistently increased as increasing DEAEMA contents in the copolymer. Transmission electron microscopy (TEM) revealed that the particles with about 6 nm in diameter have an improved dispersibility in water after quarternization. From the preliminary results, MALDI-TOF mass spectrometry indicated that negatively charged PNA-DNA hybrid can ionically adsorb onto the positively charged surface of the particle.

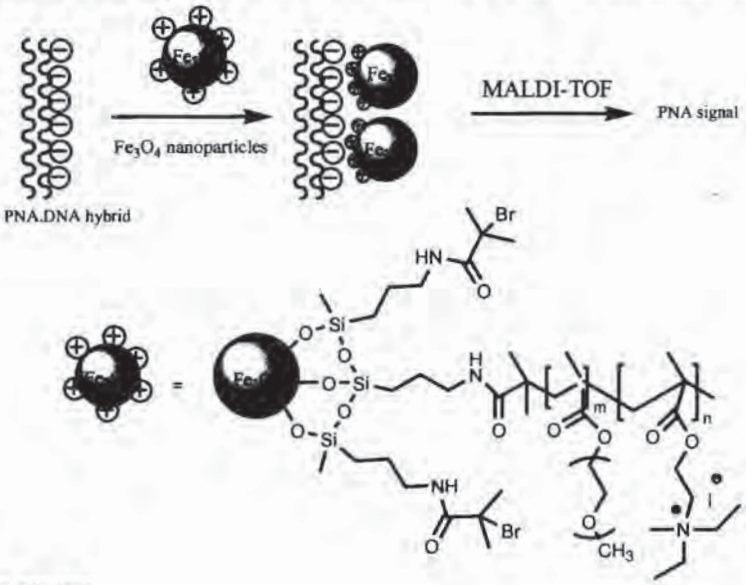

Publication status

[ ] Published

Citation information:

[x] To be published

Proposed submission date: April 2011.

Capacitive biosensor based on immobilized PNA probe through *ortho*-phenylenediamine (*o*-PD)

Orawan Thipmanee[1,2], Saluma Samanman[1,2], Supannee Sankoh[1,2], Warakorn Limbut[1,3], Apon Numnuam[1,2], Proespichaya Kanatharana[1,2], Tirayut Vilaivan[4], Panote Thavarungkul[1,5,*]

[1]Trace Analysis and Biosensor Research Center, Prince of Songkla University, Hat Yai, Songkhla 90112, Thailand
[2]Department of Chemistry, Faculty of Science, Prince of Songkla University, Hat Yai, Songkhla 90112, Thailand
[3]Department of Applied Science, Faculty of Science, Prince of Songkla University, Hat Yai, Songkhla 90112, Thailand
[4]Organic Synthesis Research Unit, Department of Chemistry, Faculty of Science, Chulalongkorn University, Phayathai Road, Pathumwan, Bangkok 10330, Thailand
[5]Department of Physics, Faculty of Science, Prince of Songkla University, Hat Yai, Songkhla 90112, Thailand

*E-mail: panote.t@psu.ac.th

Abstract: The immobilization of PNA probe on the gold electrode surface was obtained via a layer of electropolymerized *ortho*-phenylenediamine (*o*-PD) film. 11-mercaptoundecanol was used as the spacer molecule for the PNA probes making it easier to hybridize with the target DNA. The binding between DNA target and immobilized PNA probe was directly detected by measuring the change of capacitance in a flow system. The proposed capacitive detection provided a wide linear dynamic range between 1.0×10^{-11} M and 1.0×10^{-7} M with the detection limit of 1.0×10^{-11} M. It also exhibited high discrimination against a single-base and double-base mismatch DNA. The immobilized PNA probe on *o*-PD modified electrode was stable and good reproducibility of the residual activity ($96.1 \pm 3.1\%$) could be obtained up to 56 times with a relative standard deviation of 3.2 %.

Publication status

[ ] Published
Citation information:
[x] To be published
Proposed submission date: July 2011
Note: The content of this work will be combined with the work based on self-assembled monolayer for the publication.

Point of care detection of oseltamivir resistant mutation in novel 2009 human influenza A virus (H1N1) based on β-pyrrolidinyl peptide nucleic acid hybridization

Piyasak Chaumpluk,[1,*] Tirayut Vilaivan,[2] Sanong Ekgasit,[2] Wasun Chantratita,[3] Yong Poovorawan[4]

[1] Laboratory of Plant Transgenic Technology and Biosensor, Department of Botany, Faculty of Science, Chulalongkorn University, Bangkok 10330, Thailand
[2] Department of Chemistry, Faculty of Science, Chulalongkorn University, Bangkok 10330, Thailand
[3] Unit of Virology and Molecular Microbiology, Department of Pathology, Faculty of Medicine, Ramathibodi Hospital, Mahidol University, Bangkok, 10400, Thailand
[4] Center of Excellence in Clinical Virology, Faculty of Medicine, Chulalongkorn University, Bangkok, 10330 Thailand

*E-mail: piyasakcha@yahoo.com

Abstract: The rapid widespread of the novel 2009 H1N1 human influenza A virus, transmissible from human to human has raised concerns with respect to the control and the prevention of ongoing transmission. Although the most effective antiviral agent, oseltamivir (OTV), is recommended by The World Health Organization (WHO), recently it has been informed by health authorities in Denmark, Japan and the Special Administrative Region of Hong Kong, China of the appearance of novel 2009 H1N1 viruses which are resistant to the antiviral drug OTV based on laboratory testing. Those oseltamivir resistant mutations in neuraminidase gene (N1), were detected at position H274Y. Therefore, rapid detection of mutation at this position allowing a prompt action taken for next pandemic of potential higher resistance oseltamivir resistant H1N1 strains' preparedness is required. We have developed two genotypic identification methods, both involving a reverse transcription isothermal DNA amplification specific to N1 followed either by rapid liquid phase competitive hybridization using 6-carboxyfluorescein labeled □-pyrrolidinyl peptide nucleic acid and its corresponding oligonucleotide quencher designed across residue H274Y which are associated strongly with oseltamivir resistance or 6-carboxyfluorescein labeled beta-pyrrolidinyl peptide nucleic acid with blue silver nanoparticles. In the first method, hybridization of probe to target DNAs allowed DNA signals to be detected visually within 1 min. Hybridization of the probe to wild type virus induced fluorescence signals upon UV illumination, whereas no such an induction was observed to those mutants. In the second, hybridization of probe to target DNAs allowed DNA signals to be detected visually within 20 min. Hybridization of the probe to wild type virus did not induced aggregation of blue silver nanoparticles whereas an induction was observed to those mutants resulting in translucent color of blue silver nanoparticles. Demonstration of the test for the presence of mutants via both methods revealed the consistency of the test compared with standard sequencing method. These methods provides a rapid genotypic identification of the oseltamivir resistant viruses by confirmation test for the presence of mutation domain via rapid Southern hybridization's principle.

Publication status

[ ] Published
Citation information:
[x] To be published
Proposed submission date: Mar 2011

* Part of the content was presented at PACCON 2010
Donraman *et al.*, 2010. Rapid detection of Oseltamivir Resistant Mutation at Amino Acid Residue 274 of Novel 2009 Human Influenza A Virus (H1N1) based on blue silver nanoparticles. Pure and Applied Chemistry International Conference 2010. 21-23 Jan 2010. Sunee Grand Hotel, Ubon Rachathani. 228.

Using PNA probe as a rapid detection of LAMP and PCR product for drug hypersensitivity prediction

Sita Virakul[1], Tirayut Vilaivan[2], Piyasak Chaumpluk[2], Nattiya Hirankarn[3,*]

[1] Interdisciplinary program, Medical Microbiology, Chulalongkorn University, Bangkok, Thailand
[2] Faculty of Science, Chulalongkorn University, Bangkok, Thailand
[3] Faculty of Medicine, Chulalongkorn University, Bangkok, Thailand

*E-mail: nattiyap@gmail.com

Abstract: The nested SSP-PCR (sequence-specific primer-polymerase chain reaction) of HLA-B*15:02 and HLA-B*58:01 were developed as the conventional methods for anti-seizure (carbamazepine) and anti-hyperuricemic (allopurinol) drug hypersensitivity prediction, respectively. This new simpler and more cost effective assay could achieve 100% sensitivity and specificity comparing to the commercial SSP-PCR. Alternatively, LAMP (Loop-mediated isothermal amplification), an isothermal amplification technique, was successfully amplified HLA-B*58:01 with 95.24% sensitivity and 83.78% specificity. This assay significantly reduced the assay time from 3 hours of SSP-PCR to 40 minutes of LAMP reaction. In order to increase the specificity of this assay, pyrrolidinyl peptide nucleic acid (PNA), a DNA analog, was used due to the high specific and high affinity binding to DNA. In this study, PNA-DNA strand displacement probe was used as a LAMP product detection tool. Purified and heating LAMP product to facilitate PNA probe binding failed to give fluorescent signal. This might be explained by the PNA probes' sequence and length. Moreover, a simple SSP-PCR reaction for HLA-B*15:02 was developed to couple with the PNA probe for sequence-specific detection in a dot blot platform in order to reduce number of assay reaction and the risk of PCR product contamination from nested PCR.

Publication status

[ ] Published
Citation information:
[x] To be published
Proposed submission date: Mar 2011

5-(Pyren-1-yl)uracil as a base-discriminating fluorophore in pyrrolidinyl peptide nucleic acids

Chalothorn Boonlua, Chotima Vilaivan, Tirayut Vilaivan*

Organic Synthesis Research Unit, Department of Chemistry, Faculty of Science, Chulalongkorn University, Phayathai Road, Patumwan, Bangkok 10330

*E-mail: vtirayut@chula.ac.th

Abstract: A pyrene-labeled uridine (pyU) pyrrolidinyl peptide nucleic acid (PNA) monomer was synthesized and incorporated into the PNA. The pyU base in PNA could specifically recognize the base A in its complementary DNA strand as determined by thermal denaturation (T_m) experiments. The fluorescence of the pyU-containing single-stranded PNA was very weak in aqueous buffer. In the presence of a complementary DNA target, the fluorescence was enhanced significantly (4–40 fold, depending on sequences). Experiments with mismatched DNA targets revealed that the fluorescence enhancement was specific to the pairing between pyU and A. As a result, the pyrene-modified pyrrolidinyl PNA is potentially useful as a hybridization responsive fluorescence probe for DNA sequence determination.

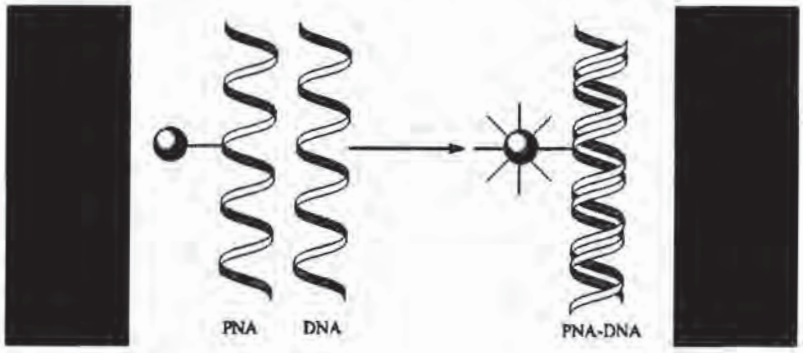

Publication status

[ ] Published
Citation information:
[x] To be published
Proposed submission date: Feb 2011

Polycyclic aromatic hydrocarbons as fluorescent universal bases in pyrrolidinyl peptide nucleic acids

Woraluk Mansawat, Chalothorn Boonlua, Chotima Vilaivan, Tirayut Vilaivan*

Organic Synthesis Research Unit, Department of Chemistry, Faculty of Science, Chulalongkorn University, Phayathai Road, Patumwan, Bangkok 10330

*E-mail: vtirayut@chula.ac.th

Abstract: A pyrene-labeled pyrrolidinyl peptide nucleic acid (PNA) monomer was synthesized by Cu-catalyzed click chemistry. The monomer was incorporated into the PNA with the aim to investigate the ability of the pyrene to behave as a nucleobase surrogate. Thermal denaturation studies between a mixed sequence PNA probe containing the triazole-linked pyrene at the middle position and a complementary DNA strand containing one of the four natural nucleobases (*i.e.*, adenine, cytosine, guanine, and thymine) facing the pyrene label indicated that the pyrene can behave as a universal base, with little discrimination between the four natural DNA bases. Importantly, the fluorescence of the pyrene-labeled single stranded PNA and it hybrid with DNA are quite different. The former showed a weak pyrene emission at 380 nm as well as a broad shoulder around 460 nm, suggesting the formation of an exciplex. The exciplex emission disappeared upon hybridization, with a concomitant increase of the pyrene monomer emission at 380 nm (up to a factor of 3).

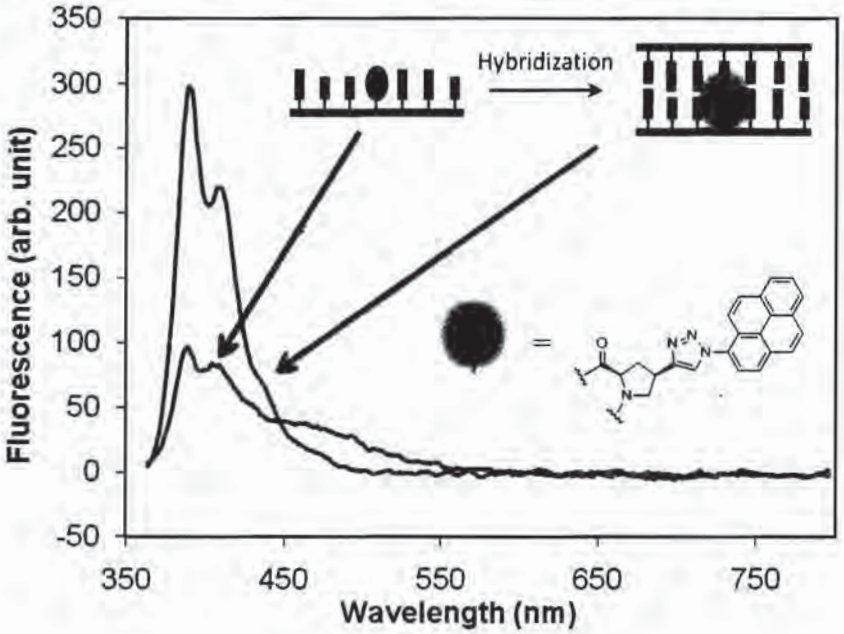

Publication status

[ ] Published
Citation information:
[x] To be published
Proposed submission date: Oct 2011

Polycationic fluorophores containing phenyleneethynylene building block for detection of oligonucleotides

Warathip Siripornnoppakhun, Paitoon Rachtasakhon, Tirayut Vilaivan, Mongkol Sukwattanasinitt*
Organic Synthesis Research Unit, Department of Chemistry, Faculty of Science, Chulalongkorn University, Phayathai Road, Patumwan, Bangkok 10330

*E-mail: smongkol@chula.ac.th

Abstract: Zeroth and first generation dendritic polycationic fluorophores containing phenyleneethynylene branches and quarternary ammonium peripheral groups are synthesized. Zeroth generation fluorophore showed emission enhancement in the presence of oligonucleotides (ODNs) while its signal reduction is observed in the presence of a synthetic polyanionic polymer, poly(vinyl) sulfate (PVSK). At the same negative charge (or nucleotide base) concentration, the fluorogenic response is greater for the longer ODNs suggesting that the longer ODNs interact more strongly than the shorter chains to the zeroth generation fluorophore. The ODNs however do not change the emission signal of the first generation fluorophore. The binding between the ODNs and the first generation fluorophore is recognized from the FRET signal to a known DNA binding dye, SyBrGreen II. The interaction between the ODNs and these dendritic polycationic fluorophores can be applied for detection of ODN.

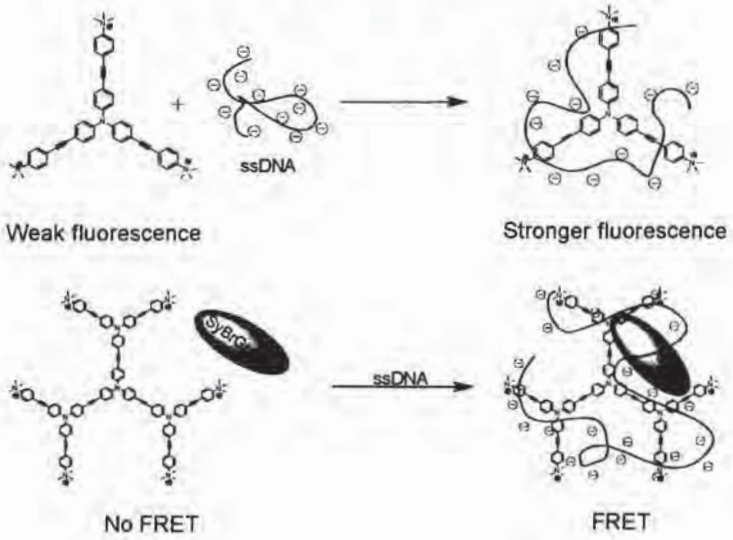

Publication status

[ ] Published
Citation information:
[x] To be published
Proposed submission date: Feb 2011

A cationic dendritic polycationic fluorophore as a FRET donor for the detection of DNA-PNA hybridization

Kunnigar Vongnam[1], Tirayut Vilaivan[2], Paitoon Rashatasakhon[2] and Mongkol Sukwattanasinitt[2,*]

[1] Program of Petrochemistry and Polymer Science, Faculty of Science, Chulalongkorn University
[2] Organic Synthesis Research Unit, Department of Chemistry, Faculty of Science, Chulalongkorn University

*E-mail: smongkol@chula.ac.th

Abstract: The use of a conjugated dendritic polycationic fluorophore as a donors in the Förster resonance energy transfer (FRET) process to a fluorescein-labeled peptide nucleic acid is investigated in a context of DNA sensor development. The non-specific FRET signal which may have caused by the hydrophobic interaction between PNA backbone and dendrimer inner structure can be weakened by the addition of formamide or *N*-methyl-2-pyrrolidinone. The FRET ratio greater than one is obtained for the case of complementary target DNA. The sequence specificity is also evaluated by using a single-mismatched DNA and DNAs with extra 10-20 base pairs.

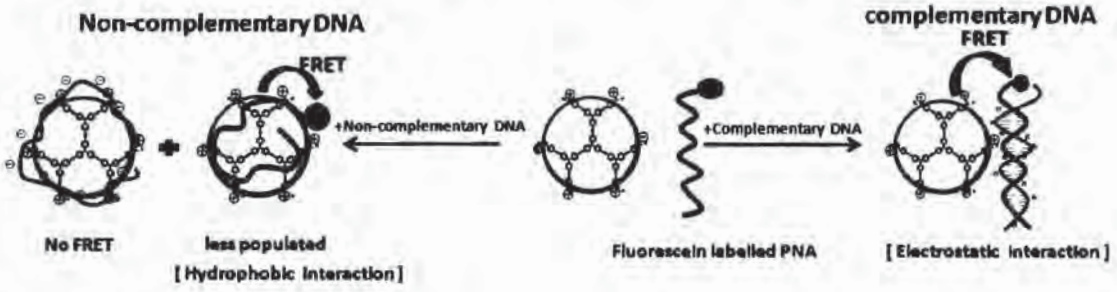

Publication status

[ ] Published
Citation information:
[x] To be published
Proposed submission date: Feb 2011

Determination of K-*ras* DNA using peptide nucleic acid probe in combination with chitosan particles by MALDI-TOF mass spectrometry

Jittima Meebungpraw[1,2], Tirayut Vilaivan[3], Suda Kiatkamjornwong[4], Voravee P. Hoven[3,*]

[1]Program in Petrochemistry and Polymer Science, Faculty of Science, Chulalongkorn University, Phayathai Road, Patumwan, Bangkok 10330
[2]Center for Petroleum, Petrochemicals, and Advanced Materials, Chulalongkorn University, Phayathai Road, Patumwan, Bangkok 10330
[3]Organic Synthesis Research Unit, Department of Chemistry, Faculty of Science Chulalongkorn University, Phayathai Road, Patumwan, Bangkok 10330
[4]Department of Imaging and Printing Technology, Faculty of Science Chulalongkorn University, Phayathai Road, Pathumwan, Bangkok 10330

*E-mail: vipavee.p@chula.ac.th

Abstract: The ability to accurately determine the base sequence of DNA has a range of important biotechnology-related applications including medical, forensic, agriculture and food sciences. The concept of using a new conformationally constrained pyrrolidinyl peptide nucleic acid (*acpc*PNA) in combination with Q-sepharose as an anion exchanger and MALDI-TOF mass spectrometry has been recently proven as a simple and effective way for DNA sequence analysis. This research has introduced chitosan and quatemized chitosan particles as a new anion-exchanger that may be applicable for the same purpose. The particles were prepared by ionic crosslinking of chitosan followed by quatemization via reductive alkylation/methylation. The success of particle formation was verified by TEM, FT-IR and ^{1}H NMR analyses. The applicability of the particles in DNA sequence determination was demonstrated using two 14mer PNA probes having the sequences corresponding to wild-type and mutant K-*ras* genes.

Publication status

[ ] Published
Citation information:
[x] To be published
Proposed submission date: February 2011

Quaternized chitosan particles prepared by self assembly of amphiphilic chitosan

Nadda Booranabunyat[1,2], Tirayut Vilaivan[3], Voravee P. Hoven[3,*]

[1]Program in Petrochemistry and Polymer Science, Faculty of Science, Chulalongkorn University, Phayathai Road, Patumwan, Bangkok 10330
[2]Center for Petroleum, Petrochemicals, and Advanced Materials, Chulalongkorn University, Phayathai Road, Patumwan, Bangkok 10330
[3]Organic Synthesis Research Unit, Department of Chemistry, Faculty of Science Chulalongkorn University, Phayathai Road, Patumwan, Bangkok 10330

*E-mail: vipavee.p@chula.ac.th

Abstract: Quaternized chitosan particles were prepared from amphiphilic chitosan containing phthaloyl groups (Ph), hexanoyl groups (He) or dodecyl groups (Do) as hydrophobic entities and poly(ethylene glycol) (PEG) or *N*-[(2-hydroxyl-3-trimethylammonium)]propyl (HTAP) as hydrophilic entities. The two types of modifiers were grafted onto the chitosan via chemical reactions of amino and hydroxyl groups, respectively. Degree of substitution (%DS) of each functional group was determined by ^{1}H NMR. Formation of particles was then induced by self assembly of the resulting amphiphilic chitosan derivatives upon dialysis in water. Unlike the chitosan particles having HTAP moieties, a subsequent heterogeneous methylation was necessary to introduce positively charged quaternary ammonium groups to the chitosan particles having PEG moieties. The effects of type and mole ratio of hydrophilic groups and hydrophobic groups as well as relative %DS of hydrophobic/hydrophilic groups on the particle size/morphology were studied. According to SEM analysis, the mean particle size was not significantly affected by %DS variation. The particles have spherical morphology and a size range of 100–200 nm. Only the particles obtained from the amphiphilic chitosan grafted with HTAP exhibited positive charges as determined by Photon Correlation Spectroscopy (PCS).

Publication status

[ ] Published
Citation information:
[x] To be published
Proposed submission date: October 2011

Synthesis of poly(4-vinylpyridine) *via* atom transfer radical polymerization (ATRP) from surface of magnetite nanoparticle

Metha Rutnakornpituk[1,*], Teerawat Inpotha[1], Boonjira Rutnakornpituk[1], Uthai Wichai[1], Tirayut Vilaivan[2]
[1]Department of Chemistry, Faculty of Science, Naresuan University, Muang, Phitsanulok 65000
[2]Organic Synthesis Research Unit, Department of Chemistry, Faculty of Science, Chulalongkorn University, Phayathai Road, Patumwan, Bangkok 10330

*E-mail: methar@nu.ac.th

Abstract: Surface modification of magnetite nanoparticle (MNP) with a covalently bonded poly(4-vinylpyridine) (P4VP) shell *via* surface initiated atom transfer radical polymerization (ATRP) is presented herein. The MNPs were prepared by thermal decomposition of $Fe(acac)_3$ in benzyl alcohol. An ATRP initiating site, BTPAm (2-bromo-2-methyl-N-(3-(triethoxysilyl)propyl)propanamide), was then covalently attached onto the surface of the particles through a combination of a ligand exchange reaction and condensation of triethoxysilane. An ATRP of 4-vinylpyridine mediated by copper bromide catalyst and PMDETA (1,1,4,7,7-pentamethyldiethylenetriamine) ligand was carried out in dioxane for 24 h. The presence of P4VP coating on the particles was verified by Fourier transform infrared spectroscopy (FT-IR). Transmission electron microscopy (TEM) disclosed that the average particle size was about 8 nm in diameter. These hybrid nanoparticles were well dispersible in acidic solutions especially at the range of pH 1-3. Effect of the solution pH on their surface charge and hydrodynamic diameter was investigated *via* photocorrelation spectrophotometry (PCS). As decreasing the solution pH from 2.5 to 0.5, its hydrodynamic diameter gradually decreased from 220 to 52 nm, while its zeta potential continuously increased from 38 to 55 mV. This was attributed to the presence of positively charged repulsion of protonated surface of the P4VP-coated MNP. Their magnetic properties were determined via vibrating sample magnetometry (VSM). Percentage of P4VP and MNP in the complexes were revealed using thermogravimetric analysis (TGA). It was observed that, as increasing the ATRP reaction time, percentage of P4VP in the complexes increased due to the high content of polymeric P4VP coated on the MNP core.

Publication status
[ ] Published
Citation information:
[x] To be published
Proposed submission date: December 2011

Picomolar detection of DNA-PNA binding based on capacitance measurement

Apon Numnuam[1,2], Proespichaya Kanatharana[1,2], Warakorn Limbut[1,3], Orawan Thipmanee[1,2], Saluma Samanman[1,2], Supannee Sankoh[1,2], Tirayut Vilaivan[4], Panote Thavarungkul[1,5,*]

[1]Trace Analysis and Biosensor Research Center, Prince of Songkla University, Hat Yai, Songkhla 90112, Thailand
[2]Department of Chemistry, Faculty of Science, Prince of Songkla University, Hat Yai, Songkhla 90112, Thailand3
[3]Department of Applied Science, Faculty of Science, Prince of Songkla University, Hat Yai, Songkhla 90112, Thailand
[4]Organic Synthesis Research Unit, Department of Chemistry, Faculty of Science, Chulalongkorn University, Phayathai Road, Pathumwan, Bangkok 10330, Thailand
[5]Department of Physics, Faculty of Science, Prince of Songkla University, Hat Yai, Songkhla 90112, Thailand

*E-mail: panote.t@psu.ac.th

Abstract: The lysine modified PNA probes (Lys-PNA) were immobilized on a gold electrode on a self-assembled monolayer (SAM) of 11-mercaptoundecanoic acid (11-MUA). The SAM of 11-MUA was activated with EDC/NHS for the immobilization of Lys-PNA followed by immersing the electrode in 1-dodecanethiol to block the remaining pinholes on the gold electrode surface. Hybridization between the target DNA and the immobilized PNA was determined by capacitance measurement. The capacitive system could detect the target DNA with a very wide linear range, between 1.0×10^{-11} and 1.0×10^{-5} M, and provided a very low detection limit of 4.0×10^{-12} M. The system was highly selective to the complementary DNA target, providing very good discrimination against single- and double-base mismatch DNA. The modified Lys-PNA probe provided good reproducibility of residual activity (97.4 ± 1.7 %) and could be reused up to 47 times for one electrode preparation with a relative standard deviation (RSD) of 1.7% that helps to reduce the analysis costs.

Publication status

[ ] Published
Citation information:
[x] To be published
Proposed submission date: July 2011
Note: The content of this work will be combined with the work based on polymer for the publication.

Multi-detection of shrimp viral diseases using fluorescence peptide nucleic acid probes

Piyasak Chaumpluk,[1]* Tirayut Vilaivan[2]

[1] Laboratory of Plant Transgenic Technology and Biosensor, Department of Botany, Faculty of Science, Chulalongkorn University, Bangkok 10330, Thailand
[2] Department of Chemistry, Faculty of Science, Chulalongkorn University, Bangkok 10330, Thailand

*E-mail: piyasakcha@yahoo.com

Abstract: Emerging disease epizootics frequently cause substantial losses among populations of shrimp, resulting in large economic losses in commercial aquaculture and threats to valuable stocks of wild shrimps. The extent of disease spread and impacts are often exacerbated by a problem of a delay in developing tools for the confirmatory diagnosis of disease or identification of the causative agent that allows infected animals to go undetected. So far, at least four major viruses affecting penaeid shrimp production in Thailand, including yellow-head virus (YHV), white spot syndrome virus (WSSV), Taura syndrome virus (TSV), and infectious hypodermal and hematopoietic necrosis virus (IHHNV) were reported. Although several PCR methods were developed for detection of shrimp viruses, these methods had a limitation on retention time for the test, depending on devices, their expenses, their specificities only on single viral infection per test, and therefore not fit for field application. A simple and rapid point of care method to detect the present of four major viruses was developed through the pathogenic viral genes. Detection method was based isothermal nucleic acid amplification both reverse transcription loop mediated isothermal amplification and normal loop mediated isothermal amplification using each of four set of primers specific to 6 area of viral virulent genes. Detection of the amplified nucleic acid products was based on competitive hybridization of DNA products with beta-pyrrolidinyl peptide nucleic acid probes specific to each of four major viruses with their appropriated oligonucleotide quenchers. The method was able to detect 20 copies of viral nucleic acid at limit of detection with high specificity and detect the presence of virus(es) in specimen within 60 min including nucleic acid preparation without relying on laboratory facilities. Confirmation of the test was measured through fluorescence signals upon PNA hybridization and UV illumination. This provides an alternative for screening and point of care control of the viruses in long run.

Publication status

[ ] Published
Citation information:
[x] To be published
Proposed submission date: Apr 2011

A simple and rapid colorimetric detection of pineapple mealy bug wilt-associated viruses (PMWaVs) based on gold nanoparticles

Piyasak Chaumpluk,[1]* Najwa Yanya,[1] Tirayut Vilaivan[2]

[1] Laboratory of Plant Transgenic Technology and Biosensor, Department of Botany, Faculty of Science, Chulalongkorn University, Bangkok 10330, Thailand
[2] Department of Chemistry, Faculty of Science, Chulalongkorn University, Bangkok 10330, Thailand

*E-mail: piyasakcha@yahoo.com

Abstract: Pineapple mealybug wilt disease is a devastating disease found in most areas where pineapples are grown commercially. Strong correlations between disease symptoms and Pineapple mealybug wilt-associated virus (PMWaV1 and 2) have been addressed. Since pineapple is vegetatively propagated, therefore a rapid screening of virus in propagules from one generation to the next is needed. We had developed a rapid colorimetric PMWaV detection method with high degree of accuracy based on gold nanoparticle's plasmon property. Detection processes were based on the specific cDNA amplification of common element in viral gene of both PMWaV-1 and -2. at 65°C using isothermal temperature platform. DNA signals were then measured visually through a colorimetric change of gold particle (20 nm) after probe hybridized to the target gene products. The method could detected both viruses and had a limit of detection at 10 copies of cloned viral DNA. No cross-reactivity was observed from samples contaminated with other viruses. Detection could be completed within 40 min of operation without the need of thermo cycler. This method constitutes a basis for a rapid yet simple and accurate detection of pathogenic virus suitable for field application.

Publication status

[ ] Published
Citation information:
[x] To be published
Proposed submission date: Apr 2011

สัญญาเลขที่ RTA5280002

รายงานการประชุมประจำปีครั้งที่ 2
ทุนส่งเสริมกลุ่มวิจัย ปี 2552

วันศุกร์ที่ 9 ธันวาคม 2554 เวลา 08:30 – 16:00
ห้อง SC4-209 ภาควิชาเคมี คณะวิทยาศาสตร์ มหาวิทยาลัยนเรศวร

โครงการ การสังเคราะห์ สมบัติ และการประยุกต์ใช้เบต้าพิโรลิดินิลเพปไทด์นิวคลีอิกแอซิดที่มีคอนฟอร์เมชันถูกจำกัด

Synthesis, Properties and Applications of Conformationally Constrained β-Pyrrolidinyl Peptide Nucleic Acids

หัวหน้าโครงการ รศ.ดร.ธีรยุทธ วิไลวัลย์
ภาควิชาเคมี คณะวิทยาศาสตร์ จุฬาลงกรณ์มหาวิทยาลัย

สนับสนุนโดยสำนักงานกองทุนสนับสนุนการวิจัย
(งานวิจัยนี้ยังไม่เสร็จสมบูรณ์ โปรดอย่านำไปใช้อ้างอิง)

คำนำ

โครงการ “การสังเคราะห์ สมบัติ และการประยุกต์ใช้เบต้าพิโรลิดินิลเพปไทด์นิวคลีอิกแอซิดที่มีคอนฟอร์เมชันถูกจำกัด” นี้ได้รับการสนับสนุนจากสำนักงานกองทุนสนับสนุนการวิจัย (สกว.) ภายใต้ทุนส่งเสริมกลุ่มวิจัย (เมธีวิจัยอาวุโส) ตามเงื่อนไขในสัญญารับทุนจาก สกว. หัวหน้าโครงการจะต้องจัดการประชุมวิชาการประจำทุกปี ประกอบกับขณะนี้งานได้ดำเนินการมาเป็นระยะเวลา 28 เดือนแล้ว จึงเห็นควรที่จะจัดงานประชุมนี้ขึ้นเพื่อให้ผู้ร่วมโครงการได้มีโอกาสนำเสนอความก้าวหน้าของโครงการวิจัยร่วมกัน และแลกเปลี่ยนความรู้ระหว่างกลุ่มวิจัย-สาขา และรับฟังข้อเสนอแนะจาก อันจะทำให้เกิดการพัฒนางานวิจัยไปในทิศทางที่ดีขึ้น

คณะผู้วิจัยขอขอบพระคุณสำนักงานกองทุนสนับสนุนการวิจัยและสถาบันต้นสังกัดของหัวหน้าโครงการ และผู้ร่วมโครงการทุกท่าน รวมทั้งแหล่งทุนอื่นที่ได้ให้การสนับสนุนงานวิจัยแม้จะไม่ใช่ทางตรง ตลอดจนผู้ช่วยวิจัย และนักศึกษา ที่ทำให้โครงการดำเนินไปได้ด้วยดี มีผลงานที่มีคุณภาพสูงตามที่ตั้งเป้าหมายไว้ นอกจากนี้ยังต้องขอขอบคุณมหาวิทยาลัยนเรศวร ที่ให้ความอนุเคราะห์สภานที่จัดการประชุมและอำนวนความสะดวกอื่นๆ

อนึ่ง งานวิจัยนี้ยังไม่เสร็จสมบูรณ์ ข้อมูลทั้งหมดนี้เป็นเพียงผลการศึกษาเบื้องต้นที่ยังไม่ได้ผ่านการประเมินอย่างเป็นทางการจากผู้เชี่ยวชาญ โปรดอย่านำไปเผยแพร่หรืออ้างอิงจนกว่าผลงานจะได้ตีพิมพ์ในวารสารวิชาการแล้ว

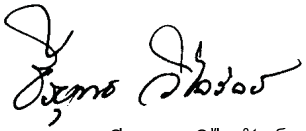

รศ.ดร.ธีรยุทธ วิไลวัลย์
หัวหน้าโครงการ

กำหนดการประชุมทุนส่งเสริมกลุ่มวิจัย (เมธีวิจัยอาวุโส) ครั้งที่ 2

โครงการ “การสังเคราะห์ สมบัติ และการประยุกต์ใช้เบต้าพิโรลิดินิลเพปไทด์นิวคลีอิกแอซิด ที่มีคอนฟอร์เมชันถูกจำกัด” (รหัสโครงการ: RTA5280002)

วันศุกร์ที่ 9 ธันวาคม 2554 เวลา 08:30 – 16:00

ภาควิชาเคมี คณะวิทยาศาสตร์ มหาวิทยาลัยนเรศวร

08:30-08:50	ลงทะเบียน
08:50-09:00	กล่าวรายงานโดย รองศาสตราจารย์ ดร.ชยันต์ บุณยรักษ์ คณบดี คณะวิทยาศาสตร์ และเปิดงานโดย ศาสตราจารย์ ดร.สุจินต์ จินายน อธิการบดีมหาวิทยาลัยนเรศวร
09:00-09:30	สรุปภาพรวมของโครงการโดยหัวหน้าโครงการ รศ.ดร.ธีรยุทธ วิไลวัลย์ (นักวิจัยดีเด่นแห่งชาติ สาขาวิทยาศาสตร์เคมีและเภสัช ปี 2554)
09:30-10:00	Internally-labeled pyrrolidinyl peptide nucleic acids as a quencher-free molecular beacon (รศ.ดร.ธีรยุทธ วิไลวัลย์ ภาควิชาเคมี คณะวิทยาศาสตร์ จุฬาลงกรณ์มหาวิทยาลัย)
10:00-10:30	FRET Detection of DNA sequence via electrostatic interaction of polycationic phenyleneethynylene dendrimer with DNA/PNA hybrid (ผศ.ดร.ไพฑูรย์ รัชตะสาคร ภาควิชาเคมี คณะวิทยาศาสตร์ จุฬาลงกรณ์มหาวิทยาลัย)
10:30-11:00	Development of signal amplification method assisted by polymerization for DNA detection (น.ส.แพทอง เหลาภา ภาควิชาเคมี คณะวิทยาศาสตร์ จุฬาลงกรณ์มหาวิทยาลัย)
11:00-11:30	อาหารว่าง
11:30-12:00	Surface-functionalized magnetite nanoparticles for immobilization of PNA and DNA (ดร.บุญจิรา รัตนากรพิทักษ์ ภาควิชาเคมี คณะวิทยาศาสตร์ มหาวิทยาลัยนเรศวร)
12:00-13:00	รับประทานอาหารกลางวันและชมโปสเตอร์
13:00-13:30	Effect of the length and terminating head group of blocking thiols on the label-free capacitive detection of DNA using immobilized pyrrolidinyl acpcPNA probe (น.ส. อรวรรณ ทิพย์มณี ภาควิชาเคมี คณะวิทยาศาสตร์ มหาวิทยาลัยสงขลานครินทร์)
13:30-14:00	Monitoring interactions of acpcPNA with DNA duplexes by gel electrophoresis (น.ส. ศิตา วีรกุล ภาควิชาจุลชีววิทยา คณะแพทยศาสตร์ จุฬาลงกรณ์มหาวิทยาลัย)
14:00-15:00	ประชุมโต๊ะกลม (เฉพาะหัวหน้าโครงการย่อยและผู้ทรงคุณวุฒิ) และอาหารว่าง
15:00-16:00	ชมโปสเตอร์

บทความนำเสนอแบบ oral **หน้า**

O001: *Internally-labeled pyrrolidinyl peptide nucleic acids as a quencher-free molecular beacon* 1
Chalothorn Boonlua, Chotima Vilaivan, Nisanath Reenabthue, Boonsong Ditmangklo, Chaturong Suparpprom, Tirayut Vilaivan (sub-project 1)

O002: *FRET Detection of DNA sequence via electrostatic interaction of polycationic phenyleneethynylene dendrimer with DNA/PNA hybrid* 2
Kunnigar Vongnam, Warathip Siripornnoppakhun, Tirayut Vilaivan, Paitoon Rashatasakhon, Mongkol Sukwattanasinitt (sub-project 2)

O003: *Development of signal amplification method assisted by polymerization for DNA detection* 3
Praethong Laopa, Tirayut Vilaivan, Voravee P. Hoven (sub-project 3)

O004: *Surface-functionalized magnetite nanoparticles for immobilization of PNA and DNA* 4
Thapanapong Theppaleak, Boonjira Rutnakornpituk, Uthai Wichai, Tirayut Vilaivan, Metha Rutnakornpituk (sub-project 4)

O005: *Effect of the length and terminating head group of blocking thiols on the label-free capacitive detection of DNA using immobilized pyrrolidinyl acpcPNA probe* 5
Orawan Thipmanee, Saluma Samanman, Supannee Sankoh, Apon Numnuam, Warakorn Limbut, Proespichaya Kanatharana, Tirayut Vilaivan, Panote Thavarungkul (sub-project 5)

O006: *Monitoring interactions of acpcPNA with DNA duplexes by gel electrophoresis* 6
Sita Virakul, Paethong S. Laopa, Tirayut Vilaivan, Nattiya Hirankarn (sub-project 6b)

บทความนำเสนอแบบโปสเตอร์ **หน้า**

P001: *Pyrrolidinyl peptide nucleic acid homologues* 7

Woraluk Mansawat, Chotima Vilaivan, David Aitken, Tirayut Vilaivan (sub-project 1)

P002: *Dual-pyrene-labeled pyrrolidinyl peptide nucleic acid probes* 8

Nattapon Maneelun, Chalothorn Boonlua, Tirayut Vilaivan (sub-project 1)

P003: *Cyclodextrins discrimination by tricationic phenylene-ethylnylene fluorophore* 9

Warathip Siripornnoppakhun, Paitoon Rashatasakhon, Tirayut Vilaivan, Mongkol Sukwattanasinitt (sub-project 2)

P004: *Fluorescent-labeled quaternized chitosan particles prepared by self-assembly of amphiphilic chitosan* 10

Kanya Taboonpong, Tirayut Vilaivan, Voravee P. Hoven (sub-project 2)

P005: *Surface-initiated atom transfer radical polymerization of poly(4-vinylpyridine) from magnetite nanoparticle* 11

Boonjira Rutnakornpituk, Uthai Wichai, Tirayut Vilaivan, Metha Rutnakornpituk (sub-project 4)

P006: *Label-free capacitive DNA sensor based on tyramine modified pyrrolidinyl PNA probe* 12

Supannee Sankoh, Saluma Samanman, Orawan Thipmanee, Apon Numnuam, Warakorn Limbut, Proespichaya Kanatharana, Tirayut Vilaivan, Panote Thavarungkul (sub-project 5)

P007: *Multiple detection of shrimp's white spot syndrome virus and infectious hypodermal and hematopoietic necrosis virus using multiplex loop mediated isothermal DNA amplification and colorimetric signals detection via gold nanoparticles* 13

Piyasak Chaumpluk, Tirayut Vilaivan (sub-project 6a)

P008: *Establishment of hemoglobin E lateral flow strip test by peptide nucleic acid: A preliminary study* 14

Theeradet Khomwan, Nattiya Hirankan, Tirayut Vilaivan, Amornpun Sereemaspun (sub-project 6c)

Internally-labeled pyrrolidinyl peptide nucleic acids as a quencher-free molecular beacon

Chalothorn Boonlua,[1] Chotima Vilaivan,[1] Nisanath Reenabthue,[2] Boonsong Ditmangklo,[2] Chaturong Suparpprom,[2] Tirayut Vilaivan[1,*]

[1]Organic Synthesis Research Unit, Department of Chemistry, Faculty of Science, Chulalongkorn University, Phayathai Road, Patumwan, Bangkok 10330
[2]Department of Chemistry and Center of Excellence for Innovation in Chemistry, Faculty of Science, Naresuan University, Ta-Po District, Muang, Phitsanulok, 65000

*E-mail: vtirayut@chula.ac.th

Abstract: DNA or PNA probes labeled with one or more environment-sensitive chromophores are potentially useful as diagnostic tools. In this study, we had developed a reliable method for site-specific internal labeling of pyrrolidinyl peptide nucleic acid (acpcPNA) *via* acylation or reductive alkylation of 3-aminopyrrolidine-4-carboxylic acid (apc)-modified acpcPNA. When pyrene was used as the label through a flexible linker, the fluorescence of the pyrene-labeled single stranded acpcPNA was very low due to the effective quenching of pyrene by pyrimidine bases. The fluorescence increases up to 14-fold upon hybridization of the acpcPNA to the complementary DNA. No fluorescence increase was observed in the presence of single base mismatch DNA targets, provided that the mismatch base located in close proximity to the site of label attachment. As a result, the pyrene-labeled acpcPNA can behave as an effective quencher-free molecular beacon. The scope and limitation of this new PNA beacon, as well as the mechanism of fluorescence change, are being explored.

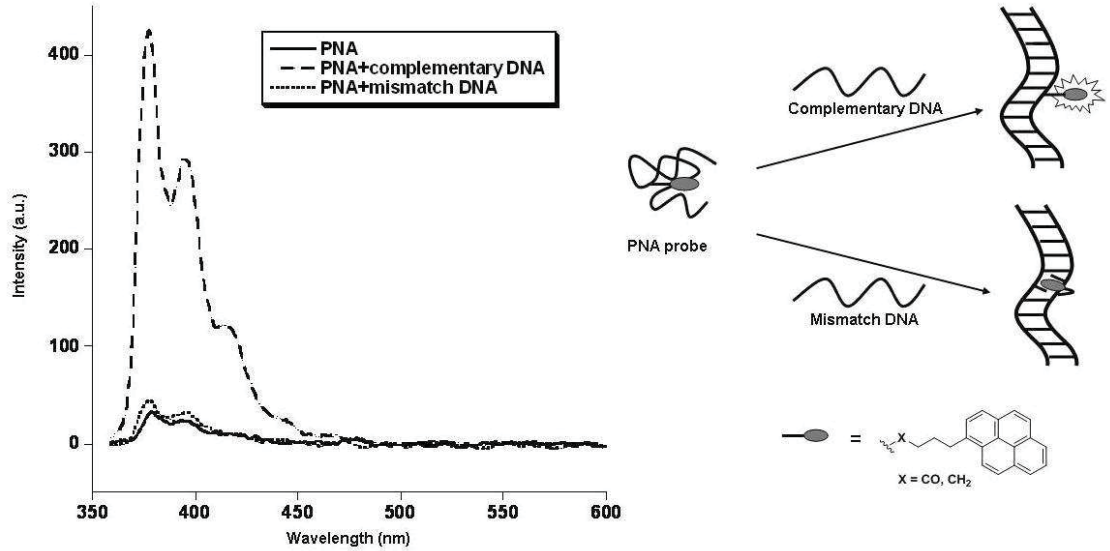

Publication status

[ ] Published
Citation information:
[x] To be published
Proposed submission date: Dec 2011

FRET Detection of DNA sequence via electrostatic interaction of polycationic phenyleneethynylene dendrimer with DNA/PNA hybrid

Kunnigar Vongnam[1], Warathip Siripornnoppakhun[2], Tirayut Vilaivan[2], Paitoon Rashatasakhon[2] and Mongkol Sukwattanasinitt[2]

[1] Program of Petrochemistry and Polymer Science, Faculty of Science, Chulalongkorn University
[2] Organic Synthesis Research Unit, Department of Chemistry, Faculty of Science, Chulalongkorn University

*E-mail: smongkol@chula.ac.th

Abstract: Interaction between a polycationic compound and DNA is a useful phenomenon for development of a new DNA sensing system. In this work, dendritic polycationic phenyleneethynylene fluorophores are investigated as a Förster resonance energy transfer (FRET) donor for the detection of DNA hybridization in conjunction with a fluorescein-labeled pyrrolidinyl peptide nucleic acid (Fl-acpcPNA) probe. The first generation dendrimer is an efficient energy donor for the fluorescein acceptor but also shows non-specific FRET signal with Fl-acpcPNA. The addition of *N*-methyl 2-pyrrolidone can virtually completely remove the non-specific interaction between Fl-acpcPNA and the dendrimer. Under the optimal condition, the complementary DNA gives a distinctively high FRET ratio (1.42) comparing with those of the non-complementary (0.26) and singly mismatched (0.51) DNAs. The FRET ratio responses linearly with the DNA concentration with the detection limit lower than 1 nM. The FRET ratio is even higher for the complementary target DNAs with extra hanging nucleotide sequences, which is a more frequently encountered scenario in real applications.

Publication status

[ ] Published
Citation information:
[x] To be published
Proposed submission date: under revision (Talanta)

Development of signal amplification method assisted by polymerization for DNA detection

Praethong Laopa[1,2], Tirayut Vilaivan[3], Voravee P. Hoven[3,*]

[1]Program in Petrochemistry, Faculty of Science, Chulalongkorn University, Phayathai Road, Patumwan, Bangkok 10330
[2]Center for Petroleum, Petrochemicals, and Advanced Materials, Chulalongkorn University, Phayathai Road, Patumwan, Bangkok 10330
[3]Organic Synthesis Research Unit, Department of Chemistry, Faculty of Science, Chulalongkorn University, Phayathai Road, Patumwan, Bangkok 10330

*E-mail: vipavee.p@chula.ac.th

Abstract: Signal amplification by polymerization has been recently emerged as a simple, rapid, sensitive, and inexpensive way to detect DNA binding. In principle, hundreds to millions of times of signals can be amplified through the chain propagation of the designated monomer from the initiator immobilized on biosensor surface under appropriate condition. The resulting polymer would thus change the optical property of the sensing spot, which later becomes visually distinguishable from the background. Here in this research, two monomers were used for investigation: poly(ethylene glycol)methacrylate (PEGMA) and rhodamine B-functionalized 2-hydroxyethylmethacrylate (RhB-HEMA). These two monomers yielded colored copolymer that can be visualized by naked eye without the equipment requirement and are water-soluble, the characteristic mandatorily required to assure that the copolymer unbound to the biosensor surface can be removed by aqueous washing. According to our preliminary investigation, the desired copolymer appearing in red can grow from the initiator grafted on paper with minimal background from non-specific adsorption of unbound copolymer. The employment of a purge-free controlled polymerization based on activators regenerated by electron transfer for atom transfer radical polymerization (ARGET ATRP) truly add simplicity to the detection process. It is our on-going investigation to determine the ability of a peptide nucleic acid probe bearing a conformationally rigid D-prolyl-2-aminocyclopentanecarboxylic acid backbone (acpcPNA) end-capped with ARGET ATRP initiator in amplifying the signal upon hybridization with target DNA that was immobilized on paper-based biosensor.

Publication status

[ ] Published
Citation information:
[x] To be published
Proposed submission date: October 2012

Surface-functionalized magnetite nanoparticles for immobilization of PNA and DNA

Thapanapong Theppaleak[1], Boonjira Rutnakornpituk[1], Uthai Wichai[1], Tirayut Vilaivan[2] and Metha Rutnakornpituk[1]*

[1]Department of Chemistry and Center of Excellence for Innovation in Chemistry, Faculty of Science, Naresuan University, Phitsanulok, 65000
[2]Organic Synthesis Research Unit, Department of Chemistry, Faculty of Science, Chulalongkorn University, Phayathai Road, Patumwan, Bangkok 10330

*E-mail: methar@nu.ac.th

Abstract: We here report the surface modification of magnetite nanoparticle (MNP) with the copolymer of poly(ethylene glycol) methyl ether methacrylate (PEGMA) and diethylamino ethyl methacrylate (DEAEMA) *via* atom transfer radical polymerization (ATRP) for use as a cationic nanosolid capture for detection of DNA sequence using PNA probe. Molar ratio of the PEGMA:DEAEMA copolymer was systematically varied to obtain 100:0, 75:25, 50:50, 25:75 and 0:100, respectively, to tune the positive charges on the particle surface after quaternization. Kinetic studies of the (co)polymerizations were also investigated *via* ^{1}H NMR to disclose the relative reactivity of the polymers in the grafting reaction. Zeta potential of the (co)polymer-coated MNP was analyzed by photo correlation spectroscopy (PCS). Transmission electron microscopy (TEM) and PCS indicated an improvement in the particle dispersibility in water upon quaternization of the DEAEMA entities grafted on the particle surface. From the preliminary results, these copolymer-grafted MNP can be used as a solid support to differentiate between full match and single-base mismatch DNA sequences using PNA probe. These novel cationic nanocaptures might be applicable for use as a magnetic guidable tool for detection of DNA sequences.

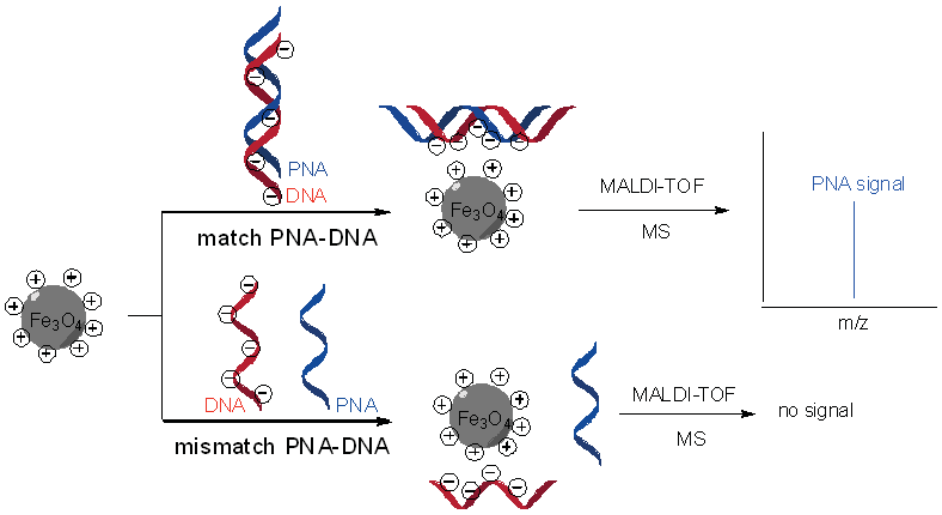

Publication status

[ ] Published
Citation information:
[x] To be published
Proposed submission date: January 2012

Effect of the length and terminating head group of blocking thiols on the label-free capacitive detection of DNA using immobilized pyrrolidinyl acpcPNA probe

Orawan Thipmanee[1,2,3], Saluma Samanman[1,2,3], Supannee Sankoh[1,2,3], Apon Numnuam[1,2,3], Warakorn Limbut[1,2,4], Proespichaya Kanatharana[1,2,3], Tirayut Vilaivan[5] and Panote Thavarungkul[1, 2,6,*]

[1] Trace Analysis and Biosensor Research Center, Prince of Songkla University, Hat Yai, Songkhla 90112
[2] Center of Excellence for Innovation in Chemistry, Faculty of Science, Prince of Songkla University, Hat Yai, Songkhla 90112
[3] Department of Chemistry, Faculty of Science, Prince of Songkla University, Hat Yai, Songkhla 90112
[4] Department of Applied Science, Faculty of Science, Prince of Songkla University, Hat Yai, Songkhla 90112
[5] Organic Synthesis Research Unit, Department of Chemistry, Faculty of Science, Chulalongkorn University, Bangkok 10330
[6] Department of Physics, Faculty of Science, Prince of Songkla University, Hat Yai, Songkhla 90112

*E-mail: panote.t@psu.ac.th

Abstract: The influence of the length and the terminating head group of blocking thiols on the sensitivity and specificity of a label-free capacitive DNA detection system using immobilized pyrrolidinyl peptide nucleic acid (acpcPNA) probes was studied. A C-terminal lysine-modified acpcPNA was immobilized through four different alkanethiol self-assembled monolayers (SAMs), i.e., 3-mercaptopropionic acid (MPA), thioctic acid (TA), thiourea (TU) and mercaptosuccinic acid (MSA). The hybridization between the acpcPNA probes and the target DNA was directly measured using the capacitive system. Five blocking thiols of various length (C=3, 6, 8, 9 and 11), with the -OH terminating head group, i.e., 3-mercapto-1-propanol (3-MPL), 6-mercapto-1-hexanol (6-MHL), 8-mercapto-1-octanol (8-MOL), 9-mercapto-1-nonanol (9-MNL), 11-mercapto-1-undecanol (11-MUL) and another blocking thiol (C=11) with a -CH3 terminating head group, 1-dodecanethiol (1-DDT) were investigated. The blocking thiol with the same length as the total spacer of the immobilized acpcPNA gave the highest sensitivity and specificity with the -OH terminating head group providing a slightly better signal than the -CH3 group. Under the optimized conditions, the immobilized acpcPNA probes provided a wide linear range for DNA detection (1.0×10-11 to 1.0×10-8 M) with a very low detection limit in the picomolar range. The modified acpcPNA electrode could be reused through at least 58 cycles. The high sensitivity and very low detection limits are potentially useful for the analysis of ultra-trace levels of DNA in samples.

Publication status

[ ] Published
Citation information:
[X] To be published
Submitted 27 October 2011

Monitoring interactions of acpcPNA with DNA duplexes by gel electrophoresis

Sita Virakul,[1] Paethong S. Laopa,[2] Tirayut Vilaivan,[2] Nattiya Hirankarn[1,*]

[1] Faculty of Medicine, Chulalongkorn University, Bangkok
[2] Faculty of Science, Chulalongkorn University, Bangkok,

*E-mail: nattiyap@gmail.com

Abstract: The knowledge of using certain HLA allele for drug hypersensitivity prediction is one of the major breakthroughs to drastically prevent patients from suffering with a lethal Stevens - Johnson syndrome in recent years. Currently, HLA gene detection systems are developed mostly on traditional molecular techniques for transplantation which is too informative to find one allele for drug hypersensitivity prediction. Fluorescein-labeled pyrrolidinyl peptide nucleic acid (FAM-labeled acpcPNA) is introduced to further increase the specificity of conventional PCR and LAMP-based detection. However, the results obtained so far had not been successful despite the ability of the PNA probe to bind to single stranded synthetic deoxyoligonucleotide was confirmed by thermal denaturation experiments. The aim of this study is to understand the nature of interaction of acpcPNA with double-stranded DNA derived from PCR amplification using gel electrophoresis. A FAM-labeled acpcPNA was designed to detect interferon gamma gene (IFN-g). The successful hybrid formation with single stranded synthetic deoxyoligonucleotide target was confirmed by agarose gel electrophoresis under non-denaturing conditions as shown by a new fluorescent band that migrates into the gel as opposed to the baseline band of the unhybridized FAM-labeled acpcPNA. No new band was observed with non-specific target, suggesting that the interaction is specific. The amount of 10 pmol PNA was found to be the minimum quantity that allows convenient direct visualization. When the FAM-labeled acpcPNA was hybridized with heat-denatured PCR products containing the target sequence, only partial binding was observed as evidenced by the presence of both excess PCR product and PNA, as well as a new band corresponding to the PNA-PCR product complex. The temperature and hybridization time were varied, and it was observed that the longer the hybridization time lead to less efficient binding of PNA. This might be due to the fact that PNA is much smaller than the complementary PCR product strand, hence the short PNA-DNA duplex initially formed is not stable enough compared to the longer DNA-DNA duplex. As a result, the DNA-DNA duplex reformed after prolonged hybridization time, leading to expelling of the PNA strand. Addition of the second pseudocomplementary PNA strand appears to improve the stability of the PNA-PCR product complex, although the invasion was still incomplete. The results suggest a rather complex interaction between acpcPNA and real DNA samples, which requires careful optimization to enable applications of this PNA in real sample analysis.

Publication status

[ ] Published
Citation information:
[X] To be published
Proposed submission date:

Pyrrolidinyl peptide nucleic acid homologues

Woraluk Mansawat,[1] Chotima Vilaivan,[1] David Aitken,[2] Tirayut Vilaivan[1,*]

[1] Organic Synthesis Research Unit, Department of Chemistry, Faculty of Science, Chulalongkorn University, Phayathai Road, Patumwan, Bangkok 10330, Thailand
[2] Laboratoire de Synthèse Organique et Méthodologie, ICMMO - Bât 420 - 3ème étage, Université Paris-Sud XI, 15, rue Georges Clemenceau, 91405 Orsay cedex, France

*E-mail: vtirayut@chula.ac.th

Abstract: The original pyrrolidinyl PNA bearing the alternate sequence of nucleobase-modified proline/2-aminocyclopentanecarboxylic acid (acpcPNA) has been a subject of intensive investigation by our group during the past decade. While the effect stereochemistry of the proline and the ACPC spacer on the DNA/RNA binding properties of the pyrrolidinyl PNA is well understood, no information is available about the effect of changing the ring size. This work aims to investigate the effect of changing the ring size of the spacer part, which would result in a change in both the rigidity (increased rigidity is expected in six- and four-membered relative to five-membered rings) and the conformation of the PNA backbone (due to the change in the torsional angle (θ) of the NH-C2-C1-CO which is an integral part of the backbone). The replacement of (1*S*,2*S*)-2-aminocyclopentanecarboxylic acid (ACPC) with (1*S*,2*S*)-2-aminocyclobutanecarboxylic acid (ACBC) resulted in a new pyrrolidinyl PNA (acbcPNA) with general binding properties similar to acpcPNA, but with an increase of T_m with both complementary DNA and RNA hybrids by 0.7–1.5 °C per modification without compromising the specificity. In contrast, the replacement of ACPC with (1*S*,2*S*)-2-aminocyclohexanecarboxylic acid (ACHC) resulted in total loss of binding to both DNA and RNA. The results are explained by a more favourable conformational pre-organization of the ACBC residue.

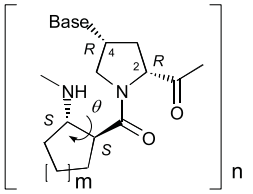

acbcPNA **m = 0**
acpcPNA **m = 1**
achcPNA **m = 2**

Publication status

[ ] Published
Citation information:
[x] To be published
Proposed submission date: Dec 2011

Dual-pyrene-labeled pyrrolidinyl peptide nucleic acid probes

Nattapon Maneelun, Chalothorn Boonlua, Tirayut Vilaivan*

Organic Synthesis Research Unit, Department of Chemistry, Faculty of Science, Chulalongkorn University, Phayathai Road, Patumwan, Bangkok 10330

*E-mail: vtirayut@chula.ac.th

Abstract: Dual-pyrene-labeled pyrrolidinyl peptide nucleic acid (acpcPNA) probes have been rationally designed by site-specifically attaching two pyrene chromophores onto the same strand of acpcPNA. Single-stranded acpcPNA with two pyrenebutyryl labels showed a strong fluorescence emission at 470 nm (pyrene excimer) and a weaker emission at 380 nm (pyrene monomer), indicating that the two pyrene chromophores were in close proximity. Hybrid formation with the complementary DNA target resulted in an enhancement of the monomer emission with concomitant decrease of the excimer emission due to the disruption of the excimer. Separation between the two pyrenebutyryl labels by 3 nucleotide units resulted in a larger change in the ratios of monomer to excimer emissions (0.43 in ss, 1.19 in ds) than 2 (0.27 in ss, 0.62 in ds) and 1 nucleotide (0.43 in ss, 0.48 in ds) units. Replacement of the pyrene label from pyrenebutyryl ($PyCH_2CH_2CH_2CO$-) to pyrenebutyl ($PyCH_2CH_2CH_2CH_2$-) resulted in a more dramatic change in excimer/monomer emissions ratio at 3 nucleotides separation (0.65 in ss, 2.53 in ds). The ratios of monomer to excimer emission changed very little if the DNA target carried a single mismatched base, indicating a high specificity. These dual-pyrene-labled acpcPNA should be useful as probes for detecting sequences of DNA. The advantage of this design over conventional molecular beacons is that not only intensity, but also the emission wavelength, change significantly upon hybridization with the DNA target.

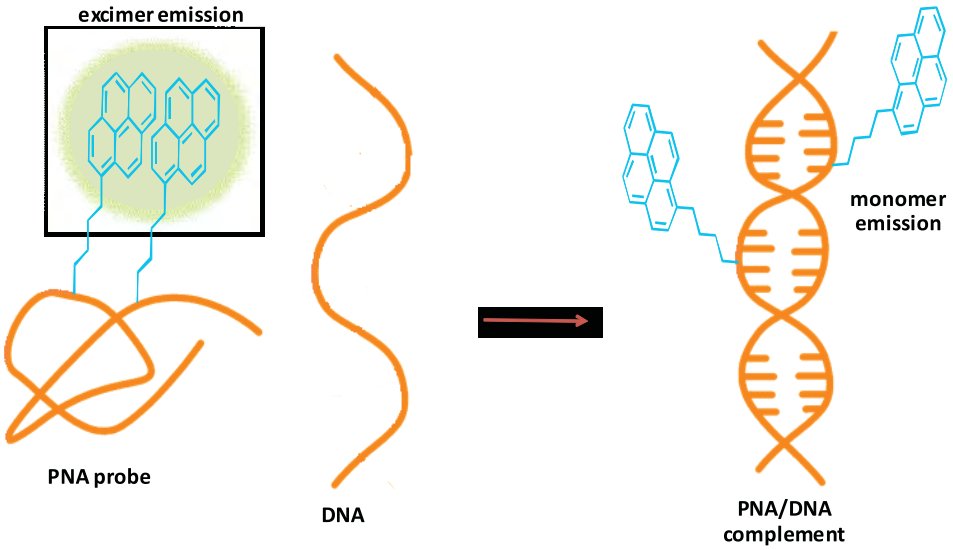

Publication status

[ ] Published
Citation information:
[x] To be published
Proposed submission date: July 2012

Cyclodextrins discrimination by tricationic phenylene-ethylnylene fluorophore

Warathip Siripornnoppakhun, Paitoon Rashatasakhon, Tirayut Vilaivan, Mongkol Sukwattanasinitt*

Organic Synthesis Research Unit, Department of Chemistry, Faculty of Science, Chulalongkorn University, Phayathai Road, Patumwan, Bangkok 10330

*E-mail: smongkol@chula.ac.th

Abstract: The cyclodextrins (CyDs) containing six (α), seven (β) and eight (γ) glucosyl-membered cyclic structure are widely use in controlled release system, separation and molecular recognition due to their complexation ability and low cytotoxicity. Size selective inclusion complexation with CyDs and detection of this phenomenon are thus important for development toward these applications. In this contribution, the complexation of trimethylphenyl quaternary ammonium groups with γ–CyD is readily observed by fluorescence enhancement and ^{1}H NMR signals shifts of tricationic phenylene-ethynylene fluorophore. Benesi-Hilderbrand plot and the NMR data revealed a 1:1 complexation between the fluorophore and γ-CyD. The data also indicate no inclusion interaction between the fluorophore and other CyDs (α and β). This tricationic fluorophore should be useful for identify γ–CyD from the other sizes CyDs and probing its inclusion interaction.

Publication status

[ ] Published
Citation information:
[x] To be published
Proposed submission date: Jan 2012

Fluorescent-labeled quaternized chitosan particles prepared by self-assembly of amphiphilic chitosan

Kanya Taboonpong[1,2], Tirayut Vilaivan[3] and Voravee P. Hoven[3,*]

[1]Program in Petrochemistry and Polymer Science, Faculty of Science, Chulalongkorn University, Bangkok 10330
[2]Center for Petroleum, Petrochemicals and Advanced Materials, Chulalongkorn University, Bangkok 10330
[3]Organic Synthesis Research Unit, Faculty of Science, Chulalongkorn University, Bangkok 10330

[*]E-mail: vipavee.p@chula.ac.th

Abstract: Upon self-assembly of amphiphilic chitosan having *N*-[(2-hydroxyl-3-trimethylammonium)]propyl (HTAP) as hydrophilic entities and ethynylpyrene (fluorescent dye) as hydrophobic entities, fluorescent-labeled quaternized chitosan (Pyr-CS-HTAP) particles can be formed. The functionality of the quaternized chitosan particles were verified by FT-IR and NMR spectroscopy. According to SEM analysis, the particles had a size range of 1-2 μm with blackberry-like morphology. And the particles exhibited positive charges with a zeta-potential of +40 mV as determined by PCS. The particles had bright green fluorescence and were stable in a broad pH and temperature range.

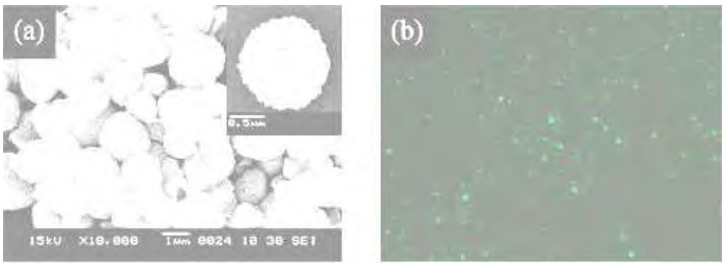

Figure 1. SEM (a) and fluorescence (b) micrographs of Pyr-CS-HTAP particles

Publication status

[ ] Published
Citation information:
[x] To be published
Proposed submission date: June 2012

Surface-initiated atom transfer radical polymerization of poly(4-vinylpyridine) from magnetite nanoparticle

Boonjira Rutnakornpituk[1], Uthai Wichai[1], Tirayut Vilaivan[2] and Metha Rutnakornpituk[1,*]

[1]Department of Chemistry and Center of Excellence for Innovation in Chemistry, Faculty of Science, Naresuan University, Phitsanulok, 65000
[2]Organic Synthesis Research Unit, Department of Chemistry, Faculty of Science, Chulalongkorn University, Phayathai Road, Patumwan, Bangkok 10330
*E-mail: methar@nu.ac.th

Abstract: Surface modification of magnetite nanoparticles (MNP) with a covalently bonded poly(4-vinylpyridine) (P4VP) by surface initiated atom transfer radical polymerization (ATRP) is reported herein. MNP was first prepared *via* thermal decomposition of $Fe(acac)_3$ and grafted with an ATRP initiator on its surface. ATRP of 4-vinylpyridine was then initiated from the MNP surface in the presence of CuBr/PMDETA (1,1,4,7,7-pentamethyldiethylenetriamine) catalytic complex in dioxane. FTIR in combination with photocorrelation spectroscopy (PCS), thermogravimetric analysis (TGA) and vibrating sample magnetometry (VSM) techniques indicated the growth of P4VP on the particle surface with increasing the ATRP reaction time. Transmission electron microscopy (TEM) disclosed that the average particle size was 8 nm in diameter with some nanoaggregation observed. From PCS results, decreasing the solution pH enhanced the particle dispersibility due to the positive charge repulsion of the protonated P4VP on the particle surface. TGA was also performed to elucidate the composition of P4VP shell and magnetite core in the hybrid material.

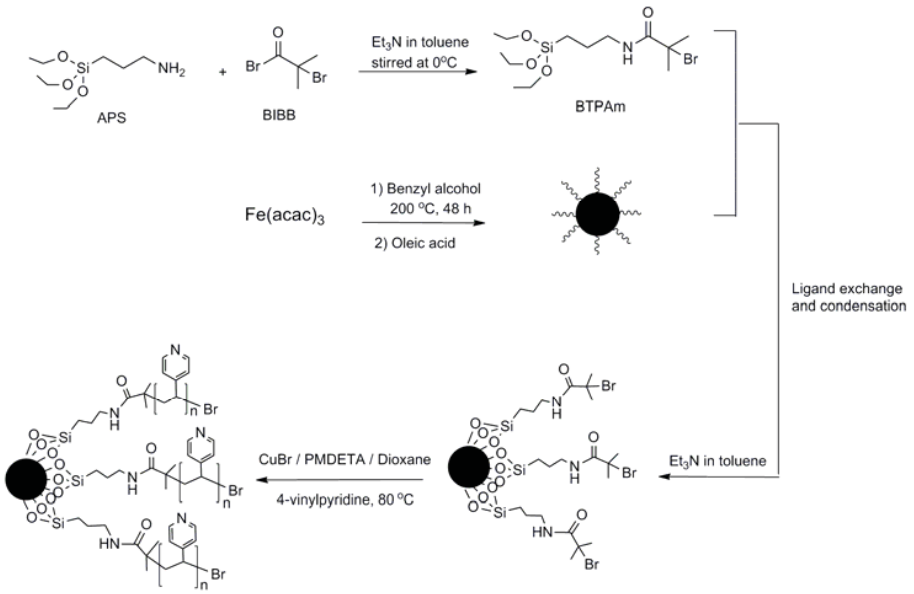

Publication status

[x] Published

Citation information: B. Rutnakornpituk, U. Wichai, T. Vilaivan and M. Rutnakornpituk, Surface-initiated atom transfer radical polymerization of poly(4-vinylpyridine) from magnetite nanoparticle, *Journal of Nanoparticle Research*, In Press (2011). (Impact factor (2010) = 3.25) DOI 10.1007/s11051-011-0592-8

[ ] To be published: Proposed submission date:

Label-free capacitive DNA sensor based on tyramine modified pyrrolidinyl PNA probe

Supannee Sankoh[1,2,3], Saluma Samanman[1,2,3], Orawan Thipmanee[1,2,3], Apon Numnuam[1,2,3], Warakorn Limbut[1,2,4], Proespichaya Kanatharana[1,2,3], Tirayut Vilaivan[5] and Panote Thavarungkul[1,2,6*]

[1] Trace Analysis and Biosensor Research Center, Prince of Songkla University, Hat Yai, Songkhla 90112
[2] Center of Excellence for Innovation in Chemistry, Faculty of Science, Prince of Songkla University, Hat Yai, Songkhla 90112
[3] Department of Chemistry, Faculty of Science, Prince of Songkla University, Hat Yai, Songkhla 90112
[4] Department of Applied Science, Faculty of Science, Prince of Songkla University, Hat Yai, Songkhla 90112
[5] Organic Synthesis Research Unit, Department of Chemistry, Faculty of Science, Chulalongkorn University, Bangkok 10330
[6] Department of Physics, Faculty of Science, Prince of Songkla University, Hat Yai, Songkhla 90112

*E-mail: panote.t@psu.ac.th

Abstract: Pyrrolidinyl peptide nucleic acid (acpcPNA) is a new PNA that offers many advantages for target hybridization. In this work, the acpcPNA probes were immobilized on a gold electrode through a layer of polytyramine film, modified on a gold electrode surface by electropolymerization process. The functional groups of the polymer were activated with glutaraldehyde for acpcPNA probes immobilization. The final step was to immerse the electrode in a 11-mercapto-1-undecanol (11-MUL) solution to block any pinholes on the gold electrode surface. The hybridization between the target DNA and the immobilized acpcPNA probe was detected by capacitance measurement. The capacitive system could detect the target DNA with a wide linear range (1.0 x 10-12 and 1.0 x 10-8 M) and a very low detection limit (0.8 pM). The system provided very good discrimination against single and double base mismatched DNAs. The modified acpcPNA probe provided good reproducibility of residual activity (97.9 ± 1.5 %) and one preparation of the modified electrode could be reused up to 77 times with a relative standard deviation (RSD) of 1.5% and this helps to reduce the analysis costs.

Publication status

[ ] Published
Citation information: Submitted
[X] To be published
Proposed submission date: March 2012

Multiple detection of shrimp's white spot syndrome virus and infectious hypodermal and hematopoietic necrosis virus using multiplex loop mediated isothermal DNA amplification and colorimetric signals detection via gold nanoparticles

Piyasak Chaumpluk,[1,*] Tirayut Vilaivan[2]

[1] Laboratory of Plant Transgenic Technology and Biosensor, Department of Botany, Faculty of Science, Chulalongkorn University, Bangkok 10330, Thailand
[2] Department of Chemistry, Faculty of Science, Chulalongkorn University, Bangkok 10330, Thailand

*E-mail: piyasakcha@yahoo.com

Abstract: White spot syndrome virus (WSSV) and Infectious hypodermal and hematopoietic necrosis virus (IHHNV) are two DNA viral pathogens of major economic importance in shrimp aquaculture through out the world. A highly specific and sensitive diagnostic system for detection of WSSV and IHHNV was designed based on the multiplex LAMP method and the colorimetric signals detection using gold nanoparticles. Multiple sets of primers specific to 12 area of target transmembrane signal peptide and NS-1 gene of both viruses were used in 60 min reaction at 63°C. DNA signals were then measured visually through a colorimetric change of gold particles (20nm) after each of PNA probes specific to each genes hybridized to the target gene products. The method could detect either of these viruses or both and had same limit of detection to each viruses at 50 copies of cloned viral DNA. No cross reactivity was observed from samples contaminated with other viruses. This provides an alternative for simple screening and point of care control of the viruses in long run.

Publication status

[ ] Published

Citation information:

[x] To be published

Proposed to integrate data to the previous Singleplex LAMP data and plan to complete a manuscript in the first quarter of year 2012.

Establishment of hemoglobin E lateral flow strip test by peptide nucleic acid: A preliminary study

Theeradet Khomwan[1], Nattiya Hirankan[2], Tirayut Vilaivan[3], Amornpun Sereemaspun[1,*]

[1] Nanobiomedicine Laboratory, Department of Anatomy, Faculty of Medicine, Chulalongkorn University, Rama 4 Road, Pratumwan District, Bangkok 10330
[2] Department of Microbiology, Faculty of Medicine, Chulalongkorn University, Rama 4 Road, Pratumwan District, Bangkok 10330
[3] Department of Chemistry, Faculty of Science, Chulalongkorn University, Rama 4 Road, Pratumwan District, Bangkok 10330

*E-mail: amornpun.s@chula.ac.th

Abstract: Hemoglobin E disease is the most common β-structural hemoglobin variant that is constituted for 13 % of Thai population. Interestingly, around 50-60 % of β-Thalassemia/Hb E was found in the northeast of Thailand. To date, the screening test for β-Thalassemia/Hb E is the detection of hemoglobin precipitation, but this assay is time-comsuming and requires skilled person to interpret results. In addition, the temperature may affect the test that has very fragile erythrocyte and may lead to the false-positive results. The objective of this study is to develop a screening test that uses nanotechnology and PNA probe by sandwich hybridization. The results from this technique are shown in red band on test strips that are easily visible by naked eyes, less time-consuming, easy to carry and high-specificity. Preliminary results with synthetic DNA that have been made as a placebo to the genomic DNA of the patients show that PNA probes have high-specificity and is capable to get results within 30 minutes. These findings suggest a new promising method for clinical applications in the near future.

Publication status

[ ] Published
Citation information:
[x] To be published
Proposed submission date: N/A

ภาคผนวก 1: รายนามผู้เข้าร่วมประชุม

	โครงการย่อย	ผู้ร่วมประชุม	ตำแหน่ง
1	Conformationally restriced PNA : synthesis and binding properties	1. รศ.ดร.ธีรยุทธ วิไลวัลย์ 2. ดร.จตุรงค์ สุภาพพร้อม 3. ดร. วรลักษณ์ มั่นสวัสดิ์ 4. น.ส. ชโลธร บุญเหลือ 5. น.ส. บุญส่ง ดิษมังคล้อ 6. นายณัฐพล มณีลุน 7. นางโชติมา วิไลวัลย์	หัวหน้าโครงการ นักวิจัย ผู้ช่วยนักวิจัย นักศึกษาปริญญาเอก นักศึกษาปริญญาโท นักศึกษาปริญญาโท เจ้าหน้าที่โครงการ
2	Dendritic fluorophores for detection of DNA/PNA hybridization	1. น.ส. วราทิพย์ ศิริพรนพคุณ 2. น.ส. กรรณิการ์ วงษ์นาม	นักศึกษาปริญญาเอก นักศึกษาปริญญาโท
3	Development of positively charged polymeric support for high throughput DNA sequence analysis using PNA probes	1. รศ.ดร.วรวีร์ โฮเว่น 2. น.ส. แพรทอง เหลาภา 3. น.ส. กัญญา ตะบูนพงศ์	หัวหน้าโครงการ นักศึกษาปริญญาเอก นักศึกษาปริญญาโท
4	Surface functionalized magnetic nanoparticles for immobilization of PNA and DNA	1. รศ.ดร.เมธา รัตนากรพิทักษ์ 2. ดร.บุญจิรา รัตนากรพิทักษ์ 3. ดร.อุทัย วิชัย 4. นายฐาปณพงศ์ เทพฤกษ์ 5. น.ส. ยิ่งรัก พรายอินทร์ 6. นายกฤษดา ตันกันยา 6. นส ศิรประภา มีรอด 7. นส นันทรักษ์ รอดเกตุ 8. นส. ภาวิณี เทียมดี 9. นายบัณฑิต ทองอ่อน 10. นายรฐนนท์ จันแก้ว 11. นายกฤษฎา ตันกันยา	หัวหน้าโครงการ นักวิจัย นักวิจัย นักศึกษาปริญญาเอก นักศึกษาปริญญาเอก นักศึกษาปริญญาโท นักศึกษาปริญญาโท นักศึกษาปริญญาโท นักศึกษาปริญญาโท นักศึกษาปริญญาโท นักศึกษาปริญญาโท นักศึกษาปริญญาโท
5	Development of label-free electrochemical DNA biosensor based on immobilized PNA probes	1. รศ.ดร.ปณต ถาวรังกูร 2. รศ.ดร.เพริศพิชญ์ คณาธารณา 3. ดร.อาภรณ์ นุ่มน่วม 4. น.ส. อรวรรณ ทิพย์มณี 5. น.ส. สาลูมา สมานหมาน 6. น.ส. สุพรรณี สันเกาะ	หัวหน้าโครงการ นักวิจัย นักวิจัย นักศึกษาปริญญาโท นักศึกษาปริญญาโท นักศึกษาปริญญาโท
6.1	Applications of PNA based diagnostics in medical, food and agricultural science	1. น.ส. อัจจิมา เมืองชื่น	ผู้ช่วยนักวิจัย
6.2	Applications of PNA based diagnostics in medical, food and agricultural sciences	1. น.ส. ศิตา วีรกุล	ผู้ช่วยนักวิจัย
6.3	Applications of PNA based diagnostics in medical, food and agricultural sciences	1. นายธีระเดช ขมหวาน	ผู้ช่วยนักวิจัย

ภาคผนวก 2: Output จากโครงการได้รับการตีพิมพ์ในวารสารวิชาการระดับนานาชาติ

1. Taechalertpaisarn, J.; Sriwarom, P.; Boonlua, C.; Yotapan, N.; Vilaivan, C.; Vilaivan, T. "DNA-, RNA- and self-pairing properties of pyrrolidinyl peptide nucleic acids with (2'R,4'S)-prolyl-(1*S*,2*S*)-aminocyclopentanecarboxylic acid backbone" *Tetrahedron Lett.* **2010**, *51*, 5822–5826. (IF2010 = 2.618) (เป็น output จากโครงการย่อย 1)

2. Ananthanawat, C.; Hoven, V. P.; Vilaivan, T.; Su, X. D. “Surface Plasmon Resonance Study of PNA Interactions with Double Stranded DNA” *Biosens. Bioelectron.* **2011**, *26*, 1918–1923. (IF2010 = 5.361) (เป็น output จากโครงการย่อย 1)

3. Ngamwiriyawong, P.; Vilaivan, T. "Synthesis and nucleic acids binding properties of diasteromeric aminoethylprolyl peptide nucleic acids (aepPNA)" *Nucleosides Nucleotides and Nucleic Acids* **2011**, 30, 97–112. (IF2010 = 1.132) (เป็น output จากโครงการย่อย 1)

4. Vilaivan, C.; Srisuwannaket, C.; Ananthanawat, C.; Suparpprom, C.; Kawakami, J.; Yamaguchi, Y.; Tanaka, Y.; Vilaivan, T. "Pyrrolidinyl peptide nucleic acid with α/β-peptide backbone: A conformationally constrained PNA with unusual hybridization properties" *Artificial DNA: PNA and XNA* **2011**, 2, 50–59. (IF2010 = ยังไม่มี เนื่องจากเป็นวารสารใหม่) (เป็น output จากโครงการย่อย 1)

5. Boonlua, C.; Vilaivan, C.; Wagenknecht, H.-A.; Vilaivan, T. "5-Pyren-1-yl uracil as a base discriminating fluorophore in pyrrolidinyl peptide nucleic acids" *Chem. Asian J.* **2011**, in press (DOI: 10.1002/asia.201100490). (IF2010 = 4.188) (เป็น output จากโครงการย่อย 1)

6. Reenabthue, N.; Boonlua, C.; Vilaivan, C.; Vilaivan, T.; Suparpprom, C. "3-Aminopyrrolidine-4-carboxylic acid as versatile handle for internal labeling of pyrrolidinyl PNA" *Bioorganic Med. Chem. Lett.* **2011**, *21*, 6465–6469. (IF2010 = 2.661) (เป็น output จากโครงการย่อย 1 ร่วมกับผลงานจากทุนวิจัยหลังปริญญาเอกของ ดร.จตุรงค์ สุภาพพร้อม)

7. Rutnakornpituk, B.; Wichai, U.; Vilaivan, T.; Rutnakornpituk, M. "Surface-initiated atom transfer radical polymerization of poly(4-vinylpyridine) from magnetite nanoparticle" *J. Nanoparticle Research*, in press (DOI: 10.1007/s11051-011-0592-8). (IF2010 = 3.253) (เป็น output จากโครงการย่อย 4)

8. Rashatasakhon, P.; Vongnam, K.; Siripornnoppakhun, W.; Vilaivan, T.; Sukwattanasinitt, M. "FRET Detection of DNA sequence via electrostatic interaction of polycationic phenylene-ethynylene dendrimer with DNA/PNA hybrid" *Talanta*, in press (DOI: 10.1016/j.talanta.2011.11.041). (IF2010 = 3.772) (เป็น output จากโครงการย่อย 2)

สัญญาเลขที่ RTA5280002

รายงานการประชุมประจำปีครั้งที่ 3
ทุนส่งเสริมกลุ่มวิจัย ปี 2552

วันศุกร์ที่ 11 มกราคม 2556 เวลา 08:30 – 16:00
ณ ห้องสัมมนา คณะวิทยาศาสตร์ มหาวิทยาลัยสงขลานครินทร์

โครงการ การสังเคราะห์ สมบัติ และการประยุกต์ใช้เบต้าพิโรลิดินิลเพปไทด์นิวคลีอิกแอซิดที่มีคอนฟอร์เมชันถูกจำกัด

Synthesis, Properties and Applications of Conformationally Constrained β-Pyrrolidinyl Peptide Nucleic Acids

หัวหน้าโครงการ รศ.ดร.ธีรยุทธ วิไลวัลย์
ภาควิชาเคมี คณะวิทยาศาสตร์ จุฬาลงกรณ์มหาวิทยาลัย

สนับสนุนโดยสำนักงานกองทุนสนับสนุนการวิจัย
(งานวิจัยนี้ยังไม่เสร็จสมบูรณ์ โปรดอย่านำไปใช้อ้างอิง)

คำนำ

โครงการ “การสังเคราะห์ สมบัติ และการประยุกต์ใช้เบต้าพิโรลิดินิลเพปไทด์นิวคลีอิกแอซิดที่มีคอนฟอร์เมชันถูกจำกัด” นี้ได้รับการสนับสนุนจากสำนักงานกองทุนสนับสนุนการวิจัย (สกว.) ภายใต้ทุนส่งเสริมกลุ่มวิจัย (เมธีวิจัยอาวุโส) ตามเงื่อนไขในสัญญารับทุนจาก สกว. หัวหน้าโครงการจะต้องจัดการประชุมวิชาการประจำทุกปี ประกอบกับขณะนี้งานได้ดำเนินการมาจนถึงสิ้นสุดโครงการแล้ว จึงเห็นควรที่จะจัดงานประชุมนี้ขึ้นเพื่อให้ผู้ร่วมโครงการได้มีโอกาสนำเสนอความก้าวหน้าของโครงการวิจัยร่วมกัน และแลกเปลี่ยนความรู้ระหว่างกลุ่มวิจัย-สาขา และรับฟังข้อเสนอแนะจากผู้ทรงคุณวุฒิ อันจะทำให้เกิดการพัฒนางานวิจัยไปในทิศทางที่ดีขึ้น

คณะผู้วิจัยขอขอบพระคุณสำนักงานกองทุนสนับสนุนการวิจัยและสถาบันต้นสังกัดของหัวหน้าโครงการ และผู้ร่วมโครงการทุกท่าน รวมทั้งแหล่งทุนอื่นที่ได้ให้การสนับสนุนงานวิจัยแม้จะไม่ใช่ทางตรง ตลอดจนผู้ช่วยวิจัย และนักศึกษา ที่ทำให้โครงการดำเนินไปได้ด้วยดี มีผลงานที่มีคุณภาพสูงตามที่ตั้งเป้าหมายไว้ นอกจากนี้ยังต้องขอขอบคุณคณะทำงานจากมหาวิทยาลัยสงขลานครินทร์ และคณะวิทยาศาสตร์ มหาวิทยาลัยสงขลานครินทร์ ที่ให้ความอนุเคราะห์สถานที่จัดการประชุมและอำนวยความสะดวกอื่นๆ

อนึ่ง งานวิจัยนี้ยังไม่เสร็จสมบูรณ์ ข้อมูลทั้งหมดนี้เป็นเพียงผลการศึกษาเบื้องต้นที่ยังไม่ได้ผ่านการประเมินอย่างเป็นทางการจากผู้เชี่ยวชาญ โปรดอย่านำไปเผยแพร่หรืออ้างอิงจนกว่าผลงานจะได้ตีพิมพ์ในวารสารวิชาการแล้ว

รศ.ดร.ธีรยุทธ วิไลวัลย์
หัวหน้าโครงการ

กำหนดการประชุมทุนส่งเสริมกลุ่มวิจัย (เมธีวิจัยอาวุโส) ครั้งที่ 3

โครงการ “การสังเคราะห์ สมบัติ และการประยุกต์ใช้เบต้าพิโรลิดินิลเพปไทด์นิวคลีอิกแอซิด ที่มีคอนฟอร์เมชันถูกจำกัด” (รหัสโครงการ: RTA5280002)

วันศุกร์ที่ 11 มกราคม 2556 เวลา 08:30 – 16:00

ณ ห้องสัมมนา คณะวิทยาศาสตร์ มหาวิทยาลัยสงขลานครินทร์

08:30-09:00	ลงทะเบียน
09:00-09:15	กล่าวเปิดงานโดยคณบดี คณะวิทยาศาสตร์ มหาวิทยาลัยสงขลานครินทร์
09:15-09:45	สรุปภาพรวมของโครงการโดยหัวหน้าโครงการ (รศ.ดร.ธีรยุทธ วิไลวัลย์)
09:45-10:15	**O001:** A sequential reductive alkylation-Click chemistry for site-specific labeling of PNA (อ.ดร.จตุรงค์ สุภาพพร้อม ภาควิชาเคมี คณะวิทยาศาสตร์ มหาวิทยาลัยนเรศวร)
10:15-11:00	อาหารว่างและ poster session
11:00-11:30	**O002:** Establishment of hemoglobin E lateral flow strip test by peptide nucleic acid: A preliminary study with human genomic DNA (อ.ดร.นพ.อมรพันธุ์ เสรีมาศพันธุ์ ภาควิชากายวิภาคศาสตร์ คณะแพทยศาสตร์ จุฬาลงกรณ์มหาวิทยาลัย)
11:30-12:00	**O003:** Paper-based lab-on-chip for optical detection of novel 2009 human influenza A virus (H1N1) based on β-pyrrolidinyl peptide nucleic acid hybridization in colloidal of blue silver nanoplates (ผศ.ดร.ปิยะศักดิ์ ชอุ่มพฤกษ์ ภาควิชาพฤกษศาสตร์ คณะวิทยาศาสตร์ จุฬาลงกรณ์มหาวิทยาลัย)
12:00-13:00	รับประทานอาหารกลางวัน
13:00-13:30	**O004:** Surface-functionalized magnetite nanoparticles for immobilization of PNA and DNA (ผศ.ดร.บุญจิรา รัตนากรพิทักษ์ ภาควิชาเคมี คณะวิทยาศาสตร์ มหาวิทยาลัยนเรศวร)
13:30-14:00	**O005:** Positively charged polymeric support for DNA sequence analysis using PNA probes: Success, failure, and opportunity (รศ.ดร. วรวีร์ โฮเว่น ภาควิชาเคมี คณะวิทยาศาสตร์ จุฬาลงกรณ์มหาวิทยาลัย)
14:00-14:30	**O006:** Effect of DNA target length on a label-free capacitive DNA sensor based on poly-para-phenylenediamine modified pyrrolidinyl PNA probe (น.ส.อรวรรณ ทิพย์มณี ภาควิชาเคมี คณะวิทยาศาสตร์ มหาวิทยาลัยสงขลานครินทร์)
14:30-15:30	อาหารว่างและ poster session
15:30-16:30	ประชุมโต๊ะกลม (เฉพาะหัวหน้าโครงการย่อยและผู้ทรงคุณวุฒิ) และอาหารว่าง

บทความนำเสนอแบบ oral **หน้า**

O001: A sequential reductive alkylation-Click chemistry for site-specific labeling of PNA 1
Boonsong Ditmangklo, Chaturong Suparpprom, Tirayut Vilaivan

O002: Establishment of hemoglobin E lateral flow strip test by peptide nucleic acid: A preliminary study with human genomic DNA 2
Amornpun Sereemaspun, Teeradet Khomvarn

O003: Paper-based lab-on-chip for optical detection of novel 2009 human influenza A virus (H1N1) based on β-pyrrolidinyl peptide nucleic acid hybridization in colloidal of blue silver nanoplates 3
Piyasak Chaumpluk, Tirayut Vilaivan, Sanong Ekgasit, Yong Poovorawan

O004: Surface-functionalized magnetite nanoparticles for immobilization of PNA and DNA 4
Thapanapong Theppaleak, Boonjira Rutnakornpituk, Uthai Wichai, Tirayut Vilaivan, Metha Rutnakornpituk

O005: Positively charged polymeric support for DNA sequence analysis using PNA probes: Success, failure, and opportunity 5
Jittima Meebungpraw, Nadda Booranabunyat, Kanya Taboonpong, Praethong S. Laopa, Tirayut Vilaivan, Voravee P.Hoven

O006: Effect of DNA target length on a label-free capacitive DNA sensor based on poly-para-phenylenediamine modified pyrrolidinyl PNA probe 6
Orawan Thipmanee, Saluma Samanman, Supannee Sankoh, Apon Numnuam, Warakorn Limbut, Proespichaya Kanatharana, Tirayut Vilaivan, Panote Thavarungkul

บทความนำเสนอแบบโปสเตอร์ **หน้า**

P001: *Electrochemically active peptide nucleic acid probes* 7

Jutatip Kongpeth, Sakda Jumpasa, Orawon Chailapakul, Tirayut Vilaivan (sub-project 1)

P002: *Synthesis and optical properties of pyrrolidinyl peptide nucleic acid carrying 1-pyrenylethynyladenine (A^{PyE}) base* 8

Duangrat Nim-anussornkul, Tirayut Vilaivan (sub-project 1)

P003: *Poly(ethylene glycol)-modified pyrrolidinyl peptide nucleic acid* 9

Thanesuan Nuanyai, Tirayut Vilaivan (sub-project 1)

P004: *Synthesis and optical properties of nile Nile blueBlue- and nNile rRed-labeled pyrrolidinyl peptide nucleic acids* 10

Chayan Charoenpakdee, Pawinee Wathanathavorn, Nattawut Yotapan, Tirayut Vilaivan (sub-project 1)

P005: *Cytocompatibility and cellular uptake of blackberry-like particles assembled from fluorescent-labeled quaternized chitosan* 11

Kanya Taboonpong, Naunpun Sangphech, Tanapat Palaga, Tirayut Vilaivan, Voravee P. Hoven (sub-project 3)

P006: *Functional polymer-stabilized gold nanoparticles: Preparation and peptide nucleic acid immobilization* 12

Pornpen Sae-ung, Gamolwan Tumcharern, Tirayut Vilaivan, Voravee P. Hoven (sub-project 3)

P007: *Surface-initiated atom transfer radical polymerization of poly(4-vinylpyridine) from magnetite nanoparticle* 13

Boonjira Rutnakornpituk, Uthai Wichai, Tirayut Vilaivan and Metha Rutnakornpituk (sub-project 4)

P008: *A comparative study of a label-free capacitive DNA sensor based on non-conducting polymers modified pyrrolidinyl PNA probe* 14

Supannee Sankoh, Saluma Samanman, Orawan Thipmanee, Apon Numnuam, Warakorn Limbut, Proespichaya Kanatharana, Tirayut Vilaivan, Panote Thavarungkul (sub-project 5)

P009: *Postharvest non-destructive determination of fruits: A model on fruit maturity assay via biosensor based on colorimetric change of gold nanoparticles* 15

Piyasak Chaumpluk, Peerasak Chaiprasart, Tirayut Vilaivan (sub-project 6)

O001: A sequential reductive alkylation-Click chemistry for site-specific labeling of PNA

Boonsong Ditmangklo,[1] Chaturong Suparpprom,[1] Tirayut Vilaivan[2,*]

[1]Department of Chemistry and Center of Excellence for Innovation in Chemistry, Faculty of Science, Naresuan University, Phitsanulok 65000, Thailand
[2]Organic Synthesis Research Unit, Department of Chemistry, Faculty of Science, Chulalongkorn University, Phayathai Road, Patumwan, Bangkok 10330, Thailand
*E-mail: vtirayut@chula.ac.th

Abstract: A general strategy for site-specific labeling of pyrrolidinyl PNA with D-prolyl/2-aminocyclopentanecarboxylic acid backbone (acpcPNA) was developed. The acpcPNA was first modified by replacement of the (1*S*,2*S*)-2-aminocyclopentanecarboxylic acid (acpc) linker with *N*-trifluoroacetyl (Tfa)-protected (3*R*,4*S*)-3-aminopyrrolidine-4-carboxylic acid (apc) linker. After selective deprotection of the *N*-Tfa group, various labels including those containing reactive functional groups like protected amino, alkynes and azides could be post-synthetically introduced *via* reductive alkylation. Subsequent secondary modification by Click reaction with azide- or alkyne-containing labels allowed efficient incorporation of various dyes including pyrene and thiazole orange to the acpcPNA backbone. The internally-labeled acpcPNA are useful as probes that can yield fluorescence change upon binding to specific DNA targets.

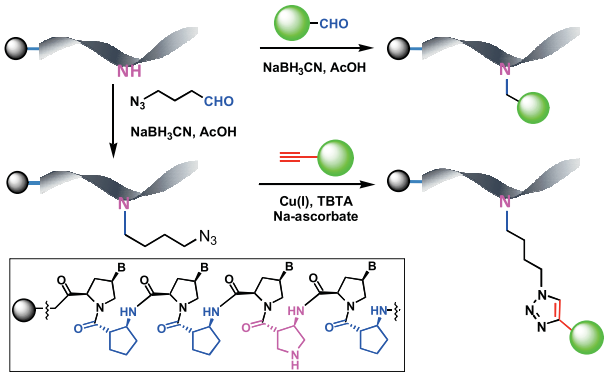

Publication status
[ ] Published
[×] To be published
Proposed submission date: Nov 2012 (under review)

O002: Establishment of hemoglobin E lateral flow strip test by peptide nucleic acid: A preliminary study with human genomic DNA

Amornpun Sereemaspun* and Teeradet Khomvarn

Nanobiomedicine Laboratory, Department of Anatomy, Faculty of Medicine,
Chulkalongkorn University, Rama 4 Road, Patumwan District, Bangkok 10330
*E-mail: amornpun.s@chula.ac.th

Abstract: Hemoglobin E disease is the most common β-structural hemoglobin variant that is constituted for 13 % of Thai population. Interestingly, around 50-60 % of β-Thalassemia/Hb E was found in the northeast of Thailand. To date, the screening test for β-Thalassemia/Hb E is the detection of hemoglobin precipitation, but this assay is time-consuming and requires skilled person to interpret results. In addition, the temperature may affect the test that has very fragile erythrocyte and may lead to the false-positive results. The objective of this study is to develop a nucleic acid lateral flow strip test that uses peptide nucleic acid (PNA) probesfor sandwich hybridization. Preliminary results with synthetic DNA that have been made as a placebo to the genomic DNA of the patients show that PNA probes have high-specificity and is capable to get results within 30 minutes. For further clinical applications in the near future, interesting data of PNA-based nucleic lateral flow strip test with human genomic DNA would be presented. In vitro alternative assay for enhancing the sensitivity and specificity of this test strip would be discussed.

Publication status
[ ] Published
[×] To be published
Proposed submission date: N/A

O003: Paper-based lab-on-chip for optical detection of novel 2009 human influenza A virus (H1N1) based on β-pyrrolidinyl peptide nucleic acid hybridization in colloidal of blue silver nanoplates

Piyasak Chaumpluk,[1*] Tirayut Vilaivan,[2] Sanong Ekgasit,[2] Yong Poovorawan[3]

[1]Laboratory of Plant Transgenic Technology and Biosensor, Department of Botany, Faculty of Science, Chulalongkorn University, Bangkok 10330, Thailand
[2]Department of Chemistry, Faculty of Science, Chulalongkorn University, Bangkok 10330, Thailand
[3]Center of Excellence in Clinical Virology, Faculty of Medicine, Chulalongkorn University, Bangkok, 10330 Thailand
*E-mail: piyasakcha@yahoo.com

Abstract: A novel, low cost, and highly sensitive paper-based lab-on-chip optical sensor for the detection of a target DNA via nucleic acid hybridization probe using blue colloidal silver nanoplates (AgNPls) as the colorimetric indicator was developed. The single unit chip was fabricated on Whatman filter paper using plastic lamination. It has 2.5x3 cm^2 dimension and divided into 2 parts, one for nucleic acid amplification and the other for signal detection. Novel numan influenza virus H1N1 assay was by viral specific HA gene amplification in an amplification part via isothermal reverse transcription loop mediated DNA amplification platform using primer set specific to 6 areas of the gene. Further DNA signals detection, at signal detection part, was based on AgNPls exhibiting blue-colored surface plasmon resonance and turning colorless upon aggregation. This related with target nucleic hybridization but not non target one with β-pyrrolidinyl peptide nucleic acid forming no color changes. Assay had a limit of detection at 10 copies of target HA gene with high specificity against other types of infectious viruses. It spent only one hour to complete all detection processes and could be visually observed with naked eye.

Publication status
[ ] Published
[×] To be published
Proposed submission date: Dec 2012

O004: Surface-functionalized magnetite nanoparticles for immobilization of PNA and DNA

Thapanapong Theppaleak[1], Boonjira Rutnakornpituk[1], Uthai Wichai[1], Tirayut Vilaivan[2] and Metha Rutnakornpituk[1,*]

[1]Department of Chemistry and Center of Excellence for Innovation in Chemistry, Faculty of Science, Naresuan University, Phitsanulok, 65000
[2]Organic Synthesis Research Unit, Department of Chemistry, Faculty of Science, Chulalongkorn University, Phayathai Road, Patumwan, Bangkok 10330
*E-mail: methar@nu.ac.th

Abstract: We here report the surface modification of magnetite nanoparticle (MNP) with the copolymer of poly(ethylene glycol) methyl ether methacrylate (PEGMA) and diethylamino ethyl methacrylate (DEAEMA) *via* atom transfer radical polymerization (ATRP) for use as a cationic nanosolid capture for detection of DNA sequence using PNA probe. Molar ratio of the PEGMA:DEAEMA copolymer was systematically varied to obtain 100:0, 75:25, 50:50, 25:75 and 0:100, respectively, to tune the positive charges on the particle surface after quaternization. Photo correlation spectroscopy (PCS) indicated an increase in degrees of positive charge of the particles after quaternization. Transmission electron microscopy (TEM) and PCS indicated an improvement in the particle dispersibility in water upon quaternization of the DEAEMA entities grafted on the particle surface.

Application of the (co)polymer-grafted MNP as a cationic support for detection of DNA sequences with the use of acpc-PNA as a probe was investigated using ion exchange capture strategy. The particles coated with 50:50 and 100:0 molar ratio of PEGMA:DEAEMA copolymers were used in this study to represent those with different degrees of surface charges (27 and 33 mV, respectively). Fluorescence spectroscopy revealed that the binding capability of the particles to DNA tagged with fluorescein at 5'-position (FAM-dA_9) was 88 and 171 nmole nucleotide/g MNP, respectively. PNA signals of PNA-DNA hybrids adsorbed on the cationic MNP were examined by the matrix-assisted laser desorption ionization-time-of-flight (MALDI-TOF) mass spectrometry. It was found that minimum detectable quantity of PNA-DNA hybrids adsorbed on the particle was 70 pmole in both samples. Two DNA sequences including the sequence stimulating to C-methylation cancer cells and Kirsten Rat Sarcoma (*K-ras*) gene were used in this study. The samples can differentiate between full match and single-base mismatch targeting DNA sequences using both single and double PNA probes. This polymer-grafted MNP might be applicable for use as a magnetically guidable tool for detection of real DNA samples in the future.

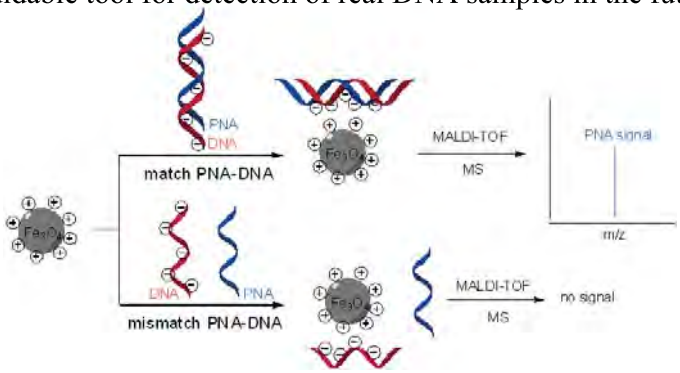

Publication status

[ ] Published - Citation information:
[×] To be published
Proposed submission date: Submitted to Journal of Biomedical Nanotechnology

O005: Positively charged polymeric support for DNA sequence analysis using PNA probes: Success, failure, and opportunity

Jittima Meebungpraw[1], Nadda Booranabunyat[1], Kanya Taboonpong[1], Praethong S. Laopa[2], Tirayut Vilaivan[3], Voravee P.Hoven[3,*]

[1] Program in Petrochemistry and Polymer Science, Faculty of Science, Chulalongkorn University, Phayathai Road, Patumwan, Bangkok 10330, Thailand
[2] Program in Petrochemistry, Faculty of Science, Chulalongkorn University, Phayathai Road, Patumwan, Bangkok 10330, Thailand
[3] Organic Synthesis Research Unit, Department of Chemistry, Faculty of Science, Chulalongkorn University, Phayathai Road, Pathumwan, Bangkok 10330, Thailand
*E-mail: vipavee.p@chula.ac.th

Abstract: Taking advantage of the charge difference between peptide nucleic acid (PNA), a DNA analog, having an uncharged peptide-like backbone and DNA having negatively charged sugar-phosphate backbone, this research aimed to develop positively charged polymeric platforms that are capable of capturing PNA which acts as a probe only when it is hybridized with its complementary DNA. DNA sequence in the duplex captured by the positively charged polymeric platforms was then identified by non-labeling techniques. The first platform is based on quaternized chitosan particles obtained by ionic crosslinking of chitosan followed by heterogeneous methylation. Using the conformationally rigid pyrrolidinyl PNA derived from D-prolyl-2-aminocyclopentane-carboxylic acid (acpc) backbones (acpcPNA) as a probe, a synthetic 14-mer, mixed base DNA of which sequence mimics mutant K-*ras* DNA, a mutated region associated with cancer, can be detected at 10 pmol level by MALDI-TOF mass spectrometry employing the quaternized chitosan particles as anion exchange captures. Quaternized chitosan particles can also be prepared by an alternative method based on self-assembly of amphiphilic chitosan. The self-assembled particles, however, failed to serve as effective anion exchange captures for DNA analysis. Nonetheless, it has been later discovered that one of the synthesized amphiphilic chitosan having pyrene as hydrophobic entity yielded fluorescent-labeled particles with unique blackberry-like morphology which are quite stable in broad pH and temperature ranges and exhibit a number of desirable characteristics that may be applicable for bioimaging. The second platform, on the other hand, was developed from filter paper functionalized with quaternized poly(2-(dimethylamino)ethyl methacrylate (QPDMAEMA) brushes. It showed superior performance to commercially available membranes, Nylon 66 and nitrocellulose, for DNA sequence detection following a Dot blot format employing biotinylated acpcPNA probe and the enzyme-mediated colorimetric assay. The low non-specific interaction of the modified filter paper, together with the high specificity of the PNA probe allows single mismatch discrimination down to 10 fmol of DNA targets. It is our ongoing effort to determine the possibility of improving detection limit by using electrochemical detection based on the same capturing strategy.

Publication status
[ ] Published
[ ] To be published
Proposed submission date: N/A

O006: Effect of DNA target length on a label-free capacitive DNA sensor based on poly-*para*-phenylenediamine modified pyrrolidinyl PNA probe

Orawan Thipmanee[1,2,3], Saluma Samanman[1,2,3], Supannee Sankoh[1,2,3], Apon Numnuam[1,2,3], Warakorn Limbut[1,2,4], Proespichaya Kanatharana[1,2,3], Tirayut Vilaivan[5] and Panote Thavarungkul[1,2,6,*]

[1] Trace Analysis and Biosensor Research Center, Prince of Songkla University, Hat Yai, Songkhla 90112
[2] Center of Excellence for Innovation in Chemistry, Faculty of Science, Prince of Songkla University, Hat Yai, Songkhla 90112
[3] Department of Chemistry, Faculty of Science, Prince of Songkla University, Hat Yai, Songkhla 90112
[4] Department of Applied Science, Faculty of Science, Prince of Songkla University, Hat Yai, Songkhla 90112
[5] Organic Synthesis Research Unit, Department of Chemistry, Faculty of Science, Chulalongkorn University, Bangkok 10330
[6] Department of Physics, Faculty of Science, Prince of Songkla University, Hat Yai, Songkhla 90112
[*]E-mail address: panote.t@psu.ac.th

Abstract: The influence of the DNA target length on the sensitivity of a label-free capacitive DNA sensor using a pyrrolidinyl peptide nucleic acid (acpcPNA) probe with 11 mixed bases was studied. A C-terminal lysine-modified acpcPNA probe was immobilized through a thin film of a non-conducting polymer, poly-*para*-phenylenediamine (P*p*PD). The hybridization between the acpcPNA probes and the target DNAs was directly measured using the capacitive system. Four DNA targets with different length (11, 41, 61 and 65 bases) were investigated. The DNA target with the longest overhang on the electrode surface gave the highest sensitivity. Under the optimized conditions, the immobilized acpcPNA probes provided a wide linear range for DNA detection (1.0×10^{-12} to 1.0×10^{-8} M) with a very low detection limit in the picomolar range. The modified acpcPNA electrode could be reused through at least 85 cycles. The high sensitivity and very low detection limits are potentially useful for the analysis of ultra-trace levels of DNA in the samples.

Publication status
[ ] Published
[×] To be published
Proposed submission date: N/A

P001: Electrochemically active peptide nucleic acid probes

Jutatip Kongpeth,[1] Sakda Jumpasa,[2] Orawon Chailapakul,[2] Tirayut Vilaivan[1,*]

[1] Organic Synthesis Research Unit, Department of Chemistry, Faculty of Science, Chulalongkorn University, Phayathai Road, Patumwan, Bangkok 10330, Thailand
[2] Electrochemical Analysis Research Unit, Department of Petrochemical and polymer science, Faculty of Science, Chulalongkorn University, Phayathai Road, Patumwan, Bangkok 10330, Thailand
*E-mail: vtirayut@chula.ac.th

Abstract: Electrochemical detection offers a rapid, sensitive and inexpensive mean for DNA sensing applications. This work aims to develop electrochemically active pyrrolidinyl peptide nucleic acid (acpcPNA) probes for electrochemical detection of DNA sequence. To enable electrochemical detection, the acpcPNA was first labeled with a redox active label such as methylene blue (MB) or anthraquinone (2-AQ) at the *N*-termini via acylation with the carboxyl-containing label. The 2-AQ- and MB-labeled acpcPNA with a T_9 sequence when hybridized with complementary DNA (dA9) shows an increased in melting temperature (T_m) by 4.3–5.6 °C compared to unlabeled acpcPNA. The results can be explained by π-π interaction between the redox active unit and the terminal base pairs. Hybridization with single mismatched DNA decreases the T_m by 26–28 °C, suggesting the high specificity of the DNA hybridization. The labeled acpcPNAs were next studied by square-wave voltammetric (SWV) method, which yield the signals at –0.70 (2-AQ) and –0.24 (MB) V respectively. The signals decreased dramatically (to less than 10% of the original values) after adding complementary DNA, thus validating the concept of using redox active PNA as a probe for electrochemical detection of DNA sequence.

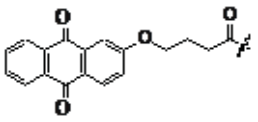

Anthraquinone

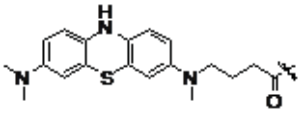

Methylene blue

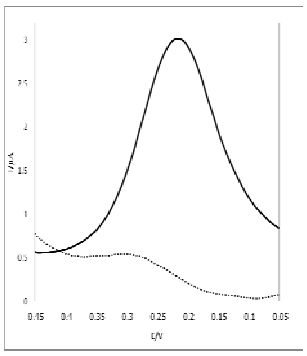

CVs of MB labeled acpcPNA before (black curve) and after (gray curve) hybridized with complementary DNA in phosphate buffer pH 7.4

Publication status

[ ] Published
[×] To be published
Proposed submission date: More studies are required before publication.

P002: Synthesis and optical properties of pyrrolidinyl peptide nucleic acid carrying 1-pyrenylethynyladenine (A^{PyE}) base

Duangrat Nim-anussornkul, Tirayut Vilaivan*

Organic Synthesis Research Unit, Department of Chemistry, Faculty of Science, Chulalongkorn University, Phayathai Road, Patumwan, Bangkok 10330, Thailand
*E-mail: vtirayut@chula.ac.th

Abstract: Pyrene-modified DNA and its analogues are useful hybridization-responsive fluorescence probes for DNA or RNA sequence determinations. DNA probes carrying pyrenylethynyl-labeled adenine (A^{PyE}) possess interesting optical properties, although their base-pairing do not strictly follow Watson-Crick base pairing rules. In this work, the A^{PyE} base was incorporated into pyrrolidinyl peptide nucleic acid bearing proline/2-aminocyclopentanecarboxylic acid backbone (acpcPNA). The A^{PyE} acpcPNA monomer was synthesized *via* Sonogashira coupling reaction between the corresponding 8-bromoadenine acpcPNA monomer and 1-ethynylpyrene. A model acpcPNA carrying the A^{PyE} base, $T^4A^{PyE}T^4$, showed the specific recognition between the base A^{PyE} in acpcPNA and the base T in DNA according to UV melting analyses. Most importantly, the fluorescence of A^{PyE} was increased by 1.6 folds upon pairing with complementary DNA. On the other hand, the fluorescence signal was decreased by 0.7–0.9 fold in the presence of single-base mismatched DNA. These results showed that the acpcPNA containing A^{PyE} is potentially useful as a fluorescent DNA probe.

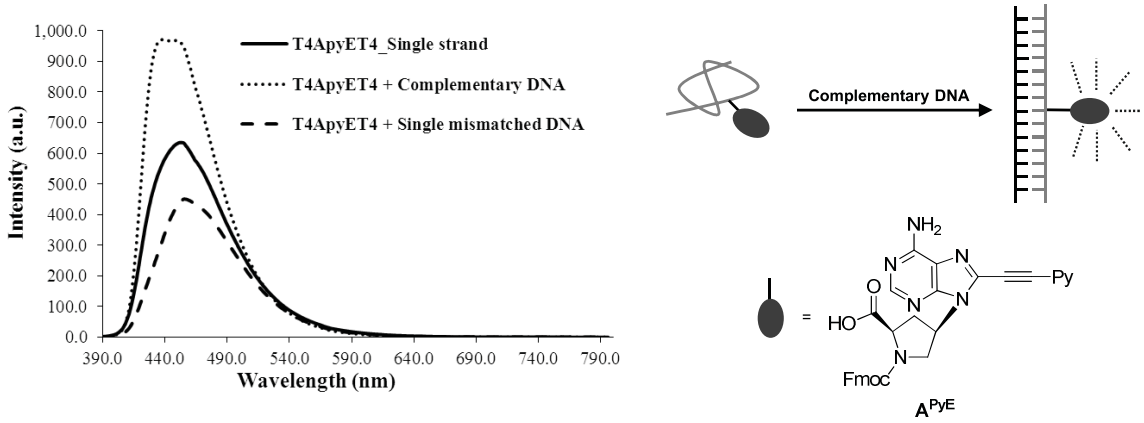

Publication status

[ ] Published

[×] To be published

Proposed submission date: More studies are required before publication.

P003: Poly(ethylene glycol)-modified pyrrolidinyl peptide nucleic acid

Thanesuan Nuanyai, Tirayut Vilaivan*

Organic Synthesis Research Unit, Department of Chemistry, Faculty of Science,
Chulalongkorn University, Phayathai Road, Patumwan, Bangkok 10330, Thailand
*E-mail: vtirayut@chula.ac.th

Abstract: One of the problems associated with pyrrolidinyl peptide nucleic acid (acpcPNA) system previously developed by our group was hydrophobicity. Thus, acpcPNA has limited aqueous solubility and showed significant non-specific interactions with non-polar molecule such as pyrene and other non-polar dyes. To overcome the problem, the acpcPNA backbone was modified by poly(ethylene glycol) derivatives with different numbers of repeating unit (1–3) and end groups (OH, NH_2). *N*-Fmoc-amino poly(ethylene glycol) and *O*-trityl-poly(ethylene glycol) were prepared from di-, tri- and tetra-ethylene glycol by selective modification of one end of the molecules. IBX oxidation of the mono-alcohols afforded aldehyde derivatives of poly(ethylene glycol). Reductive alkylation of apc-modified acpcPNA with these aldehydes gave poly(ethylene glycol)- modified acpcPNA. The modified acpcPNA with hydroxy substitution gave slightly lowered T_m with complementary DNA when compared with unmodified acpcPNA. On the other hand, an increase in Tm was observed with modified acpcPNA carrying amino-substitution. This can be explained by the electrostatic interaction between the amino-modifier and the negatively-charged DNA backbone.

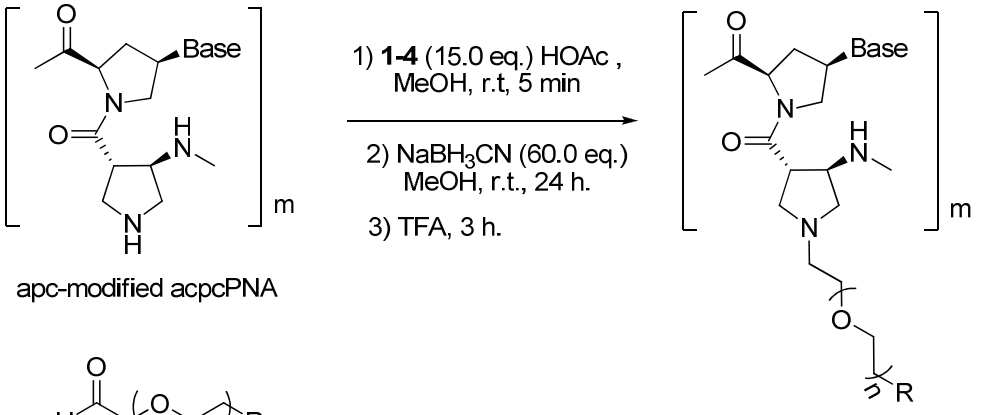

apc-modified acpcPNA

1: n = 1, R = OTr
2: n = 2, R = OTr
3: n = 3, R = OTr
4: n = 2, R = NHFmoc

p1: n = 1, R = OH
p2: n = 2, R = OH
p3: n = 3, R = OH
p4: n = 2, R = NH_2

Publication status

[ ] Published

[×] To be published

Proposed submission date: More studies are required before publication.

P004: Synthesis and optical properties of Nile blue- and Nile red-labeled pyrrolidinyl peptide nucleic acids

Chayan Charoenpakdee, Pawinee Wathanathavorn, Nattawut Yotapan, Tirayut Vilaivan

Organic Synthesis Research Unit, Department of Chemistry, Faculty of Science, Chulalongkorn University, Phayathai Road, Patumwan, Bangkok 10330, Thailand
*E-mail: vtirayut@chula.ac.th

Abstract: Nile Blue and Nile Red are members of phenoxazine dyes. Their emission wavelengths and intensities are known to be sensitive to environments such as solvent polarity. In this study, we propose to modify pyrrolidinyl peptide nucleic acid with prolyl/2-aminocyclopentanecarboxylic acid backbone (acpcPNA) with Nile Blue and Nile Red, with the aim to develop fluorescence acpcPNA probes whose fluorescence properties are responsive to the presence or absence of the correct DNA target. To achieve this goal, we synthesized two new propargylated Nile Blue and Nile Red derivatives, and demonstrated their successful attachment *via* Cu(I)-catalyzed alkyne-azide cycloaddition (CuAAC) (also known as Click chemistry) onto the backbone of acpcPNA previously modified with azidobutyl functional group. Successful introduction of the dyes onto the acpcPNA backbone was confirmed by MALDI-TOF MS. The ability of the labeled acpcPNAs to recognize their DNA targets as well as their optical properties (UV, fluorescence) will be next studied.

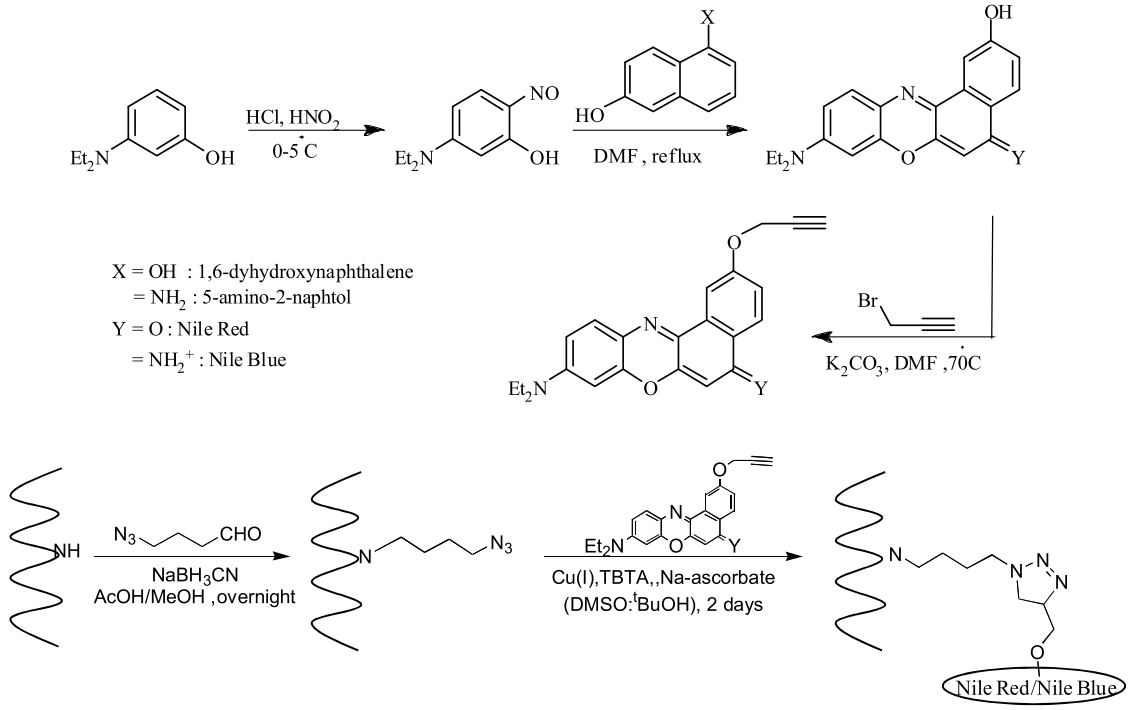

Publication status

[ ] Published

[×] To be published

Proposed submission date: More studies are required before publication

P005: Cytocompatibility and cellular uptake of blackberry-like particles assembled from fluorescent-labeled quaternized chitosan

Kanya Taboonpong[1,2], Naunpun Sangphech[3], Tanapat Palaga[3], Tirayut Vilaivan[4], Voravee P. Hoven[4,*]

[1]Program in Petrochemistry and Polymer Science, Faculty of Science, Chulalongkorn University, Phayathai Road, Patumwan, Bangkok 10330, Thailand
[2]Center for Petroleum, Petrochemicals and Advanced Materials, Chulalongkorn University, Phayathai Road, Patumwan, Bangkok 10330, Thailand
[3]Department of Microbiology, Faculty of Science, Chulalongkorn University, Phayathai Road, Patumwan, Bangkok 10330, Thailand
[4]Organic Synthesis Research Unit, Faculty of Science, Chulalongkorn University, Phayathai Road, Patumwan, Bangkok 10330, Thailand
*E-mail: vipavee.p@chula.ac.th

Abstract: Upon self-assembly of amphiphilic chitosan having N-[(2-hydroxyl-3-trimethylammonium)]propyl (HTAP) as hydrophilic entities and ethynylpyrene (fluorescent dye) as hydrophobic entities, fluorescent-labeled quaternized chitosan (Pyr-CS-HTAP) particles can be formed. The functionality of the quaternized chitosan particles were verified by FT-IR and NMR spectroscopy. According to SEM analysis, the particles had a size range of 1-2 μm with blackberry-like morphology. And the particles exhibited positive charges with a zeta-potential of +40 mV as determined by PCS. The particles had bright green fluorescence and were stable in a broad pH and temperature range. The cytotoxicity test revealed that the particles were biocompatible with Macrophage cells (RAW 264.7 cells). Moreover, cellular uptake of the particles by the cells can be determined by confocal laser scanning microscopy (CLSM) and flow cytometry techniques. The results showed that approximately 42% of cellular uptake was observed after 1 h incubation. It has also been found that the aggregation of the particles has a strong impact on the extent of cellular uptake. These fluorescent-labeled quaternized chitosan particles possess a number of desirable features that may be used for bioimaging application.

Publication status
[ ] Published
[×] To be published
Proposed submission date: March 2013

P006: Functional polymer-stabilized gold nanoparticles: Preparation and peptide nucleic acid immobilization

Pornpen Sae-ung[1], Gamolwan Tumcharern[2], Tirayut Vilaivan[3], Voravee P. Hoven[3*]

[1]Program in Macromolecular Science, Faculty of Science, Chulalongkorn University, Phayathai Road, Patumwan, Bangkok 10330, Thailand
[2]National Nanotechnology Center, National Science and Technology Development Agency, Thailand Science Park, Paholyothin Road, Klong Luang, Pathumthani 12120, Thailand
[3]Organic Synthesis Research Unit, Department of Chemistry, Faculty of Science, Chulalongkorn University, Phayathai Road, Patumwan, Bangkok 10330, Thailand
*E-mail: vipavee.p@chula.ac.th

Abstract: Poly(methacrylic acid)-*ran*-(2-methacryloyloxyethyl phosphorylcholine) (PMAMPC) which can provide binding site and protein-repellent property was prepared via Reversible Addition-Fragmentation Chain Transfer (RAFT) polymerization and grafted onto citrate-stabilized gold nanoparticles (citrate-AuNPs) to obtain functionalizable AuNPs having anti-fouling characteristic. Optical property, size, and morphology of PMAMPC-stabilized AuNPs (PMAMPC-AuNPs) were evaluated by UV-vis spectroscopy, dynamic light scattering (DLS) technique and transmission electron microscopy (TEM). The presence of PMAMPC around the AuNPs was confirmed by Fourier transform infrared spectroscopy (FTIR). PMAMPC-AuNPs were highly stable because of both electrostatic and steric stabilizations of the polymeric shell. Then, fluorescein-labeled peptide nucleic acid (PNA-flu) was immobilized to carboxyl groups of PMAMPC on PMAMPC-AuNPs via EDC/NHS coupling chemistry. Effects of PMAMPC molecular weight, surfactant (Tween-80) concentration on PNA-flu immobilization was determined. The amount of immobilized PNA-flu as evaluated by fluorescence spectroscopy after KCN digestion was found to be 2.72×10^{13} probe/cm^2. This value is two times higher than that (1.28×10^{13} probe/cm^2) obtained via a direct PNA immobilization by self-assembly monolayer (SAM) formation of PNA-terminated thiol compound. This discovery strongly suggests that the 3-D structure of the polymeric shell can provide greater probe binding capacity than the 2-D SAM system. It is anticipated that this new polymer-stabilized AuNPs can potentially be developed into effective PNA-based DNA biosensor.

Publication status

[ ] Published
[×] To be published
Proposed submission date: September 2013

P007: Surface-initiated atom transfer radical polymerization of poly(4-vinylpyridine) from magnetite nanoparticle

Boonjira Rutnakornpituk[1], Uthai Wichai[1], Tirayut Vilaivan[2] and Metha Rutnakornpituk[1]*

[1]Department of Chemistry and Center of Excellence for Innovation in Chemistry, Faculty of Science, Naresuan University, Phitsanulok, 65000
[2]Organic Synthesis Research Unit, Department of Chemistry, Faculty of Science, Chulalongkorn University, Phayathai Road, Patumwan, Bangkok 10330
*E-mail: methar@nu.ac.th

Abstract: Surface modification of magnetite nanoparticles (MNP) with a covalently bonded poly(4-vinylpyridine) (P4VP) by surface initiated atom transfer radical polymerization (ATRP) is reported herein. MNP was first prepared *via* thermal decomposition of $Fe(acac)_3$ and grafted with an ATRP initiator on its surface. ATRP of 4-vinylpyridine was then initiated from the MNP surface in the presence of CuBr/PMDETA (1,1,4,7,7-pentamethyldiethylenetriamine) catalytic complex in dioxane. FTIR in combination with photocorrelation spectroscopy (PCS), thermogravimetric analysis (TGA) and vibrating sample magnetometry (VSM) techniques indicated the growth of P4VP on the particle surface with increasing the ATRP reaction time. Transmission electron microscopy (TEM) disclosed that the average particle size was 8 nm in diameter with some nanoaggregation observed. From PCS results, decreasing the solution pH enhanced the particle dispersibility due to the positive charge repulsion of the protonated P4VP on the particle surface. TGA was also performed to elucidate the composition of P4VP shell and magnetite core in the hybrid material.

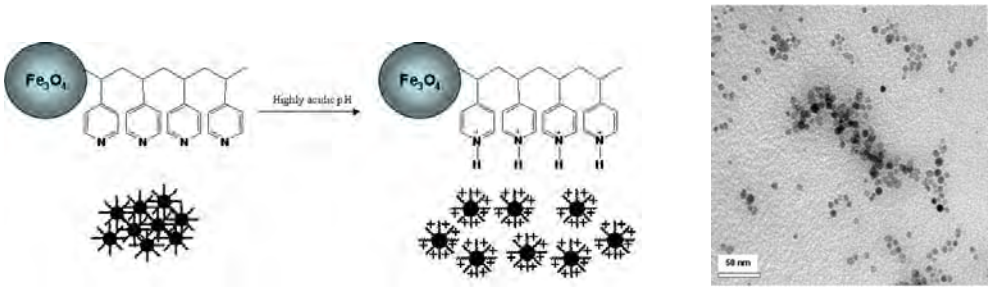

A proposed mechanism for nanoparticle stabilization and a TEM image of the particles

Publication status

[×] Published

Citation information: B. Rutnakornpituk, U. Wichai, T. Vilaivan and M. Rutnakornpituk, Surface-initiated atom transfer radical polymerization of poly(4-vinylpyridine) from magnetite nanoparticle, *Journal of Nanoparticle Research* **2011**, *13*, 6847-6857. (Impact factor (2010) = 3.25). DOI 10.1007/s11051-011-0592-8

[ ] To be published

P008: A comparative study of a label-free capacitive DNA sensor based on non-conducting polymers modified pyrrolidinyl PNA probe

Supannee Sankoh[1,2,3], Saluma Samanman[1,2,3], Orawan Thipmanee[1,2,3], Apon Numnuam[1,2,3], Warakorn Limbut[1,2,4], Proespichaya Kanatharana[1,2,3], Tirayut Vilaivan[5] and Panote Thavarungkul[1,2,6,]*

[1] Trace Analysis and Biosensor Research Center, Prince of Songkla University, Hat Yai, Songkhla 90112
[2] Center of Excellence for Innovation in Chemistry, Faculty of Science, Prince of Songkla University, Hat Yai, Songkhla 90112
[3] Department of Chemistry, Faculty of Science, Prince of Songkla University, Hat Yai, Songkhla 90112
[4] Department of Applied Science, Faculty of Science, Prince of Songkla University, Hat Yai, Songkhla 90112
[5] Organic Synthesis Research Unit, Department of Chemistry, Faculty of Science, Chulalongkorn University, Bangkok 10330
[6] Department of Physics, Faculty of Science, Prince of Songkla University, Hat Yai, Songkhla 90112
*E-mail: panote.t@psu.ac.th

Abstract: This work reported a comparative study on the performances of a label-free capacitive DNA sensor using pyrrolidinyl peptide nucleic acid with D-prolyl-2-aminocyclopentanecarboxylic acid backbone (acpcPNA) immobilized on three non-conducting polymers. Two phenylenediamine (PD) isomers (ortho- and para-) and one tyramine monomer were electropolymerized to form polymer films. The hybridization between the target DNA and the immobilized acpcPNA probe was detected by capacitance measurement. Under the optimal electropolymerized conditions, the highest sensitivity of 20.9±0.6 –nF cm^{-2} M^{-1} was obtained from poly-*para*-PD (P*p*PD) with the lowest detection limit of 0.2 pM. A wide linear range, 1.0×10^{-12}–1.0×10^{-8} M, was obtained for both the P*p*PD and polytyramine (Pty). A narrower linear range of 1.0×10^{-11}–1.0×10^{-8} M was obtained from poly-*ortho*-PD (P*o*PD). The surface morphology of polymer film was observed using scanning electron microscopy and atomic force microscopy. The polymer with the better surface morphology, i.e., smoother, denser and more homogeneous was the one with more immobilized probes and a better overall performance. All modified polymers gave a high % signal suppression (%SS) for both the single and double mismatched target DNAs, indicating its high specificity. The electrodes can be reused for at least 68 analytical cycles and this helps to reduce the analysis costs.

Publication status

[×] Published

Citation information: Sankoh, S.; Samanman, S.; Thipmanee, O.; Numnuam, A.; Limbut, W.; Kanatharana, P.; Vilaivan, T.; Thavarungkul, P. A "A comparative study of a label-free DNA capacitive sensor using a pyrrolidinyl peptide nucleic acid probe immobilized through polyphenylenediamine and polytyramine non-conducting polymers" *Sens. Actuators B: Chem.* **2013**, *177*, 543–554.

[ ] To be published:

P009: Postharvest non-destructive determination of fruits: A model on fruit maturity assay via biosensor based on colorimetric change of gold nanoparticles

Piyasak Chaumpluk,[1*] Peerasak Chaiprasart,[2*] Tirayut Vilaivan[3]

[1] Laboratory of Plant Transgenic Technology and Biosensor, Department of Botany, Faculty of Science, Chulalongkorn University, Bangkok 10330, Thailand
[2] Postharvest Innovation Center, Faculty of Agriculture, Natural Resource and Environment, Naresuan University, Phitsanulok, 65000, Thailand
[3]Department of Chemistry, Faculty of Science, Chulalongkorn University, Bangkok 10330, Thailand
*E-mail: piyasakcha@yahoo.com

Abstract: New approach for non-destructive fruit maturity determination using pineapple as a model had been established. The assay was based on expression patterns of the putative sucrose transporter (*AcSUT*1) in crown leaves during the course of physiological maturity that could be employed as an index marker for fruit maturity. Determination of *AcSUT*1 cDNA was initially designed using isothermal cDNA amplification and the DNA signal detection via biosensor based on colorimetric platform with gold colloid nanoparticles, 20 nm in diameter. In the immature fruit, the *AcSUT*1 gene was expressed allowing target DNA amplification to occur. DNA signals detection in later step was based on plasmon phenomena of gold nanoparticles. Presence of target DNA affected gold colloid nanoparticles in term of non aggregation with no colour change (still ruby red). However, in the mature fruit, the expression of the *AcSUT*1 gene was terminated resulting in no target cDNA product amplification. When this was tested with gold colloid nanoparticles, it induced aggregation of particles which in turn resulted in a plasmonic change of colloid solution from ruby red to dark purple, visible by naked eye. All processes from RNA extraction to cDNA signal detection could be completed within 80 min without the need for a thermocycler as normally employed during RT-PCR. The developed assay demonstrated the integration of the novel DNA biosensor approach for a non-destructive determination of fruit quality.

Publication status

[×] Published

Citation information: *Acta Horticulturae* 945:205–211.*

[ ] To be published

* indexed in AgBiotech News and Information; AGRICOLA; CAB Abstracts; Chemical Abstracts; Food Science and Technology Abstracts; Forestry Abstracts; SCOPUS.

ภาคผนวก 1: ผลงานตีพิมพ์ของโครงการ (ข้อมูลถึง 8 มกราคม 2556)

1. Taechalertpaisarn, J.; Sriwarom, P.; Boonlua, C.; Yotapan, N.; Vilaivan, C.; Vilaivan, T. "DNA-, RNA- and self-pairing properties of pyrrolidinyl peptide nucleic acids with (2'*R*,4'*S*)-prolyl-(1*S*,2*S*)-aminocyclopentanecarboxylic acid backbone" *Tetrahedron Lett.* **2010**, *51*, 5822–5826.

2. Ananthanawat, C.; Hoven, V. P.; Vilaivan, T.; Su, X. D. “Surface Plasmon Resonance Study of PNA Interactions with Double Stranded DNA” *Biosens. Bioelectron.* **2011**, *26*, 1918–1923.

3. Ngamwiriyawong, P.; Vilaivan, T. "Synthesis and nucleic acids binding properties of diasteromeric aminoethylprolyl peptide nucleic acids (aepPNA)" *Nucleosides Nucleotides and Nucleic Acids* **2011**, 30, 97–112.

4. Vilaivan, C.; Srisuwannaket, C.; Ananthanawat, C.; Suparpprom, C.; Kawakami, J.; Yamaguchi, Y.; Tanaka, Y.; Vilaivan, T. "Pyrrolidinyl peptide nucleic acid with α/β-peptide backbone: A conformationally constrained PNA with unusual hybridization properties" *Artificial DNA: PNA and XNA* **2011**, 2, 50–59.

5. Boonlua, C.; Vilaivan, C.; Wagenknecht, H.-A.; Vilaivan, T. "5-Pyren-1-yl uracil as a base discriminating fluorophore in pyrrolidinyl peptide nucleic acids" *Chem. Asian J.* **2011**, 6, 3251–3259.

6. Reenabthue, N.; Boonlua, C.; Vilaivan, C.; Vilaivan, T.; Suparpprom, C. "3-Aminopyrrolidine-4-carboxylic acid as versatile handle for internal labeling of pyrrolidinyl PNA" *Bioorganic Med. Chem. Lett.* **2011**, *21*, 6465–6469.

7. Rutnakornpituk, B.; Wichai, U.; Vilaivan, T.; Rutnakornpituk, M. "Surface-initiated atom transfer radical polymerization of poly(4-vinylpyridine) from magnetite nanoparticle" *J. Nanopart. Res.* **2011**, *13*, 6847–6857.

8. Rashatasakhon, P.; Vongnam, K.; Siripornnoppakhun, W.; Vilaivan, T.; Sukwattanasinitt, M. "FRET Detection of DNA sequence via electrostatic interaction of polycationic phenylene-ethynylene dendrimer with DNA/PNA hybrid" *Talanta*, **2012**, *88*, 593–598.

9. Yuanboonlim, W.; Siripornnoppakhun, W.; Rashatasakhon, P.; Vilaivan, T.; Sukwattanasinitt, M. "Phenylene-ethynylene trication as an efficient fluorescent signal transducer in an aptasensor for potassium ion" *Biosens. Bioelectron.* **2012**, *12*, 17–22.

10. Virakul, S.; Kupatawintu, P.; Nakkuntod, J.; Kangwanshiratada, O.; Vilaivan, T.; Hirankarn, N. "A Nested Sequence Specific Primer-Polymerase Chain Reaction for the detection of HLA-B*15:02" *Tissue Antigens* **2012**, *79*, 295–301.

11. Mansawat, W.; Vilaivan, C.; Balázs, A.; Aitken, D.; Vilaivan, T. "Pyrrolidinyl peptide nucleic acid homologues: Effect of ring size on hybridization properties" *Org. Lett.* **2012**, *14*, 1440–1443.

12. Mansawat, W.; Boonlua, C.; Siriwong, K.; Vilaivan, T. "Clicked polycyclic aromatic hydrocarbon as a hybridization-responsive fluorescent artificial nucleobase in pyrrolidinyl peptide nucleic acids" *Tetrahedron.* **2012**, *68*, 3988–3995.

13. Thipmanee, O.; Samanman, S.; Sankoh, S.; Numnuam, A.; Limbut, W.; Kanatharana, P.; Vilaivan, T.; Thavarungkul, P. "Label-free capacitive DNA sensor using immobilized PNA probe: Effect of the length and terminated head group of blocking thiols" *Biosens. Bioelectron.* **2012**, *38*, 430–435.

14. Sezi, S.; Varghese, R.; Vilaivan, T.; Wagenknecht, H.-A. "Conformational control of dual emission by pyrrolidinyl PNA–DNA hybrids" *ChemistryOpen* **2012**, *1*, 173–176.

15. Siripornnoppakhun, W.; Niamnont, N.; Krumsri, A.; Tumcharern, G.; Vilaivan, T.; Rashatasakhon, P.; Thayumanavan, S.; Sukwattanasinitt, M. "Inclusion complexes between amphiphilic phenyleneethynylene fluorophores and cyclodextrins in aqueous media" *J. Phys. Chem. B* **2012**, *116*, 12268–12274.

16. Laopa, P.S.; Vilaivan, T.; Hoven, V. P. "Positively charged polymer brushes-functionalized filter paper for DNA sequence determination following Dot Blot hybridization employing pyrrolidinyl peptide nucleic acid probe" *Analyst* **2013**, *138*, 269–277.

17. Janrungroatsakul, W.; Vilaivan, T.; Vilaivan, C.; Watchasit, S.; Suksai, C.; Ngeontae, W.; Aeungmaitrepirom, W.; Tuntulani, T. "New calix[4]arene derivatives as ionophores in polymeric membrane electrodes for Ag(I): Comparative selectivity studies and detection of DNA hybridization" *Talanta* **2013**, *105*, 1–7.

18. Sankoh, S.; Samanman, S.; Thipmanee, O.; Numnuam, A.; Limbut, W.; Kanatharana, P.; Vilaivan, T.; Thavarungkul, P. “Ultra trace label-free DNA sensor using immobilized pyrrolidinyl PNA on non-conducting polymer based on capacitive system” *Sens. Actuator B.* **2013**, *177*, 543–554.

ภาคผนวก 2: รายนามของนักวิจัยผู้ร่วมโครงการ

1. รศ.ดร.ธีรยุทธ วิไลวัลย์ (Assoc. Prof. Dr. Tirayut Vilaivan) — หัวหน้าโครงการ
   สังกัด ภาควิชาเคมี คณะวิทยาศาสตร์ จุฬาลงกรณ์มหาวิทยาลัย
   โทรศัพท์ 022187627 ext 101 E-mail vtirayut@chula.ac.th
2. อ.ดร.จตุรงค์ สุภาพพร้อม (Dr. Chaturong Suparpprom) — ผู้ร่วมวิจัย
   สังกัด ภาควิชาเคมี คณะวิทยาศาสตร์ มหาวิทยาลัยนเรศวร — โครงการย่อยที่ 1
   โทรศัพท์ 055963462 E-mail chaturongs@nu.ac.th
3. อ.ดร.ช่อลัดดา ศรีสุวรรณเกศ (Dr. Choladda Srisuwannaket) — ผู้ร่วมวิจัย
   สังกัด ภาควิชาเคมี คณะวิทยาศาสตร์ มหาวิทยาลัยพระจอมเกล้าธนบุรี — โครงการย่อยที่ 1
   โทรศัพท์ 024709556 E-mail choladda.sri@kmutt.ac.th
4. รศ.ดร.มงคล สุขวัฒนาสินิทธิ์ (Assoc. Prof. Dr. Mongkol Sukwattanasinitt) — ผู้ร่วมวิจัย
   สังกัด ภาควิชาเคมี คณะวิทยาศาสตร์ จุฬาลงกรณ์มหาวิทยาลัย — โครงการย่อยที่ 2
   โทรศัพท์ 022187620 E-mail smongkol@chula.ac.th
5. รศ.ดร.วรวีร์ โฮเว่น (Assoc. Prof. Dr. Voravee Hoven) — ผู้ร่วมวิจัย
   สังกัด ภาควิชาเคมี คณะวิทยาศาสตร์ จุฬาลงกรณ์มหาวิทยาลัย — โครงการย่อยที่ 3
   โทรศัพท์ 022187627 ext 102 E-mail vipavee.p@chula.ac.th
6. รศ.ดร.เมธา รัตนากรพิทักษ์ (Assoc. Prof. Dr. Metha Rutnakornpituk) — ผู้ร่วมวิจัย
   สังกัด ภาควิชาเคมี คณะวิทยาศาสตร์ มหาวิทยาลัยนเรศวร — โครงการย่อยที่ 4
   โทรศัพท์ 055963464 E-mail methar@nu.ac.th
7. อ.ดร.บุญจิรา บุญทา (Dr. Boonjira Boontha) — ผู้ร่วมวิจัย
   สังกัด ภาควิชาเคมี คณะวิทยาศาสตร์ มหาวิทยาลัยนเรศวร — โครงการย่อยที่ 4
   โทรศัพท์ 055963466 E-mail b_boonjira@hotmail.com
8. อ.ดร.อุทัย วิชัย (Dr. Uthai Wichai) — ผู้ร่วมวิจัย
   สังกัด ภาควิชาเคมี คณะวิทยาศาสตร์ มหาวิทยาลัยนเรศวร — โครงการย่อยที่ 4
   โทรศัพท์ 055963466 E-mail uthaiw@nu.ac.th
9. รศ.ดร.ปณต ถาวรังกูร (Assoc. Prof. Dr. Panote Thavarungkul) — ผู้ร่วมวิจัย
   สังกัด ภาควิชาฟิสิกส์ คณะวิทยาศาสตร์ มหาวิทยาลัยสงขลานครินทร์ — โครงการย่อยที่ 5
   โทรศัพท์ 074288753 E-mail panote.t@psu.ac.th
10. รศ.ดร.เพริศพิชญ์ คณาธารณา (Assoc. Prof. Dr. Proespichaya Kanatharana) — ผู้ร่วมวิจัย
    สังกัด ภาควิชาเคมี คณะวิทยาศาสตร์ มหาวิทยาลัยสงขลานครินทร์ — โครงการย่อยที่ 5
    โทรศัพท์ 074288420 E-mail proespichaya.k@psu.ac.th
11. อ.ดร.วรากร ลิ่มบุตร (Dr. Warakorn Limbut) — ผู้ร่วมวิจัย
    สังกัด ภาควิชาวิทยาศาสตร์ประยุกต์ คณะวิทยาศาสตร์ มหาวิทยาลัยสงขลานครินทร์ — โครงการย่อยที่ 5
    โทรศัพท์ 074288563 E-mail warakorn.l@psu.ac.th
12. อ.ดร.อาภรณ์ นุมน่วม (Dr. Apon Numnuam) — ผู้ร่วมวิจัย
    สังกัด ภาควิชาเคมี คณะวิทยาศาสตร์ มหาวิทยาลัยสงขลานครินทร์ — โครงการย่อยที่ 5
    โทรศัพท์ 074288457 E-mail apon.n@psu.ac.th
13. ผศ.ดร.ปิยะศักดิ์ ชะอุ่มพฤกษ์ (Assist. Prof. Dr. Piyasak Chaumpluk) — ผู้ร่วมวิจัย
    สังกัด ภาควิชาพฤกษศาสตร์ คณะวิทยาศาสตร์ จุฬาลงกรณ์มหาวิทยาลัย — โครงการย่อยที่ 6
    โทรศัพท์ 022185494 E-mail piyasakcha@gmail.com
14. รศ.พญ.ดร.ณัฏฐิยา หิรัญกาญจน์ (Assoc. Prof. Dr. Nattiya Hirankarn) — ผู้ร่วมวิจัย
    สังกัด ภาควิชาจุลชีววิทยา คณะแพทยศาสตร์ จุฬาลงกรณ์มหาวิทยาลัย — โครงการย่อยที่ 6
    โทรศัพท์ 022564132 E-mail fmednpt@md.chula.ac.th
15. อ.นพ.ดร.อมรพันธ์ เสรีมาศพันธ์ (Dr. Amornpun Sereemaspun) — ผู้ร่วมวิจัย
    สังกัด ภาควิชากายวิภาคศาสตร์ คณะแพทยศาสตร์ จุฬาลงกรณ์มหาวิทยาลัย — โครงการย่อยที่ 6
    โทรศัพท์ 022564281 E-mail amornpun.s@chula.ac.th
16. ผศ.ดร.ไพฑูรย์ รัชตะสาคร (Assist. Prof. Dr. Paitoon Rashtaskon) — ผู้ร่วมวิจัย
    สังกัด ภาควิชาเคมี คณะวิทยาศาสตร์ จุฬาลงกรณ์มหาวิทยาลัย — โครงการย่อยที่ 2
    โทรศัพท์ 022187620 E-mail paitoon.r@chula.ac.th

ภาคผนวก 4

รายละเอียดทางวิชาการของโครงการย่อย 1–6

(เนื่องจากเอกสารมีความหนามาก จึงไม่ได้เย็บรวมในเล่มรายงานฉบับสมบูรณ์
ผู้สนใจโปรดดูรายละเอียดในแผ่น CD)

Project 1: Conformationally restricted PNA: Synthesis and binding properties

หัวหน้าโครงการ ธีรยุทธ วิไลวัลย์

รายงานในช่วง 1 สิงหาคม 2552-31 กรกฎาคม 2556

โครงการนี้มีวัตถุประสงค์หลักประการหนึ่งคือเพื่อศึกษาสมบัติการจับยึดของพีเอ็นเอระบบ (2*R*,4*R*)-prolyl-(1*S*,2*S*)-ACPC-PNA (acpcPNA) (รูปที่ 1) ซึ่งเป็นพีเอ็นเอที่ได้จากการบุกเบิกของคณะผู้วิจัยเองโดยได้รับการสนับสนุนทุนวิจัยจากสำนักงานกองทุนสนับสนุนการวิจัยมาอย่างต่อเนื่อง พีเอ็นเอระบบดังกล่าวมีความสามารถในการจับยึดกับดีเอ็นเอที่ดีเทียบเท่ากับพีเอ็นเอของ Nielsen ซึ่งเป็นพีเอ็นเอที่มีการใช้งานอย่างกว้างขวางในงานวิจัยและการประยุกต์ใช้ด้านต่างๆ โดยเฉพาะอย่างยิ่งในการเป็นส่วนประกอบของระบบหรืออุปกรณ์สำหรับการตรวจสอบลำดับเบสของสารพันธุกรรม โดยสมบัติของ acpcPNA ที่ทราบอยู่แล้วอย่างละเอียดจะเป็นความแข็งแรง ความจำเพาะเจาะจง และทิศทางของการจับยึดกับดีเอ็นเอเป็นส่วนใหญ่ และมีผลการทดลองเบื้องต้นที่แสดงให้เห็นว่าพีเอ็นเอระบบนี้นอกจากจะจับกับดีเอ็นเอได้ดีแล้วยังแสดงสมบัติบางประการที่ไม่มีในพีเอ็นเอระบบอื่น เช่น การเลือกจับกับดีเอ็นเอได้ดีกว่าอาร์เอ็นเอ และการที่มันไม่สามารถจับคู่กันเอง [Vilaivan and Srisuwannaket, 2006] แต่งานวิจัยที่ผ่านมายังทดลองในขอบเขตที่จำกัดเพียงไม่กี่ลำดับเบสเท่านั้น ในงานวิจัยนี้จึงได้เพิ่มจำนวนพีเอ็นเอที่นำมาทดสอบให้มากขึ้น และศึกษาเปรียบเทียบความสามารถของพีเอ็นเอ P1 ที่มีลำดับเบสที่แตกต่างกันในแง่ของการจับยึดกับดีเอ็นเอ อาร์เอ็นเอ และกับตัวของมันเอง และศึกษาปัจจัยทางโครงสร้างที่ส่งผลต่อสมบัติการจับยึดที่เป็นลักษณะเฉพาะของพีเอ็นเอดังกล่าว

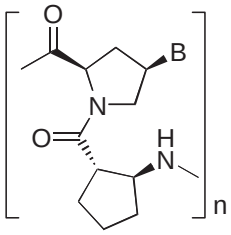

acpcPNA

รูปที่ 1 โครงสร้างของพีเอ็นเอที่เป็นระบบที่ใช้ศึกษาหลักในงานวิจัยนี้

วัตถุประสงค์อีกประการหนึ่งของโครงการวิจัยนี้คือการศึกษาระบบพีเอ็นเอที่มีคอนฟอร์เมชันที่ถูกจำกัดระบบอื่นๆ ที่นอกเหนือจาก acpcPNA ที่ได้ศึกษาไปค่อนข้างมากแล้ว โดยงานวิจัยจะแบ่งออกเป็น การสังเคราะห์และศึกษาสมบัติจับยึดของ acpcPNA ที่มี modified base หรือ unnatural base และการการสังเคราะห์และศึกษาสมบัติจับยึดของพีเอ็นเอที่มี modified backbone ที่มาจากกรดเบต้าอะมิโนชนิดอื่น เช่น 3-, 4- หรือ 6-membered ring cyclic beta-amino acids โดยคาดหวังว่าจะพบพีเอ็นเอระบบอื่นเพิ่มเติมที่อาจแสดงการจับยึดกับดีเอ็นเอหรืออาร์เอ็นเอที่แตกต่างจาก acpcPNA ซึ่งอาจนำไปสู่การประยุกต์ใช้ประโยชน์ในวัตถุประสงค์ที่แตกต่างกัน

1. การสังเคราะห์และศึกษาสมบัติจับยึดของ acpcPNA

งานวิจัยในส่วนนี้เป็นการสังเคราะห์และศึกษาสมบัติการจับยึดของ acpcPNA ซึ่งเป็นระบบพีเอ็นเอดั้งเดิมที่คณะผู้วิจัยได้ศึกษามาเป็นระยะเวลาหนึ่งตั้งแต่ก่อนรับทุนวิจัยนี้แล้ว โดยงานส่วนที่ทำเพิ่มเติมคือการสังเคราะห์ acpcPNA ที่มีลำดับเบสที่หลากหลายมากขึ้น โดยให้มีความยาวเท่ากันคือ 10 เบส แต่มีสัดส่วนของเบส AT และ CG แตกต่างกัน (**10mer1**, **10mer2**, **10mer3**) เพื่อศึกษาสมบัติการจับยึดกับดีเอ็นเอ เปรียบเทียบกับอาร์เอ็นเอ เพื่อยืนยันผลการทดลองเบื้องต้นที่พบว่าพีเอ็นเอชนิดนี้มีความเลือกจำเพาะในการจับกับดีเอ็นเอมากกว่าอาร์เอ็นเอว่าจะยังคงเป็นจริงในลำดับเบสอื่นๆ อีกหรือไม่ นอกจากนี้ยังได้ออกแบบสายพีเอ็นเอให้มีลำดับ

เบสเป็นคู่สมกันทั้งในแบบแอนติพาราเรล (**10mer1** vs **10mer4**, **10mer2** vs **10mer6**, **10mer3** vs **10mer8**) และพาราเรล (**10mer1** vs **10mer5**, **10mer2** vs **10mer7**, **10mer3** vs **10mer9**) เพื่อศึกษาความเป็นไปได้ในการจับกันเองระหว่างพีเอ็นเอกับพีเอ็นเออีกด้วย ลำดับเบสและ *m/z* ของ acpcPNA ที่สังเคราะห์ได้เป็นดังแสดงในตารางที่ 1

ตารางที่ 1 Sequences and characterization data of PNA used in this study.

SequenceID	PNA sequence	*m/z* (calcd for $M{\cdot}H^+$)	*m/z* (found)
10mer1	GTAGATCACT	3556.7	3555.9
10mer2	GCTACGTCGC	3533.7	3533.9
10mer3	TATGTACTAT	3546.7	3546.9
10mer4	AGTGATCTAC	3556.7	3556.0
10mer5	CATCTAGTGA	3556.7	3556.5
10mer6	GCGACGTAGC	3582.7	3582.6
10mer7	CGATGCAGCG	3582.7	3582.6
10mer8	ATAGTACATA	3564.7	3564.6
10mer9	ATACATGATA	3564.7	3564.5

ตารางที่ 2 Orientation of binding between mixed base PNA and DNA

entry	PNA	T_m (antiparallel DNA) (^oC)		T_m (parallel DNA) (^oC)	
		0 mM NaCl	100 mM NaCl	0 mM NaCl	100 mM NaCl
1	**10mer1**	57.0	53.3	< 20	< 20
2	**10mer2**	60.4	54.5	< 20	< 20
3	**10mer3**	59.6	54.2	< 20	< 20
4	**10mer4**	57.2	52.8	< 20	< 20
5	**10mer5**	60.6	56.1	< 20	< 20
6	**10mer6**	65.2	60.8	< 20	< 20
7	**10mer7**	65.1	59.1	< 20	< 20
8	**10mer8**	65.5	61.0	< 20	< 20
9	**10mer9**	65.3	59.8	< 20	< 20

Conditions: 1 μM PNA, 1 μM DNA, 10 mM sodium phosphate buffer pH 7.0, 0 or 100 mM NaCl, heating rate 1.0 ^oC/min. T_m values are accurate within $\pm$0.5 ^oC.

ในเบื้องต้นได้ศึกษาสมบัติการจับยึดระหว่างพีเอ็นเอทุกลำดับเบสที่สังเคราะห์ขึ้นกับดีเอ็นเอที่มีลำดับเบสคู่สมกัน ทั้งในทิศทางแอนติพาราเรล และพาราเรล โดยใช้เทคนิค UV melting โดยตัวแปรที่จะนำมาเปรียบเทียบกันคือค่า T_m (melting temperature) ซึ่งวัดที่ความเข้มข้นเดียวกันคือ 1 μM เนื่องจากความแข็งแรงของการจับยึดของพีเอ็นเอและดีเอ็นเอขึ้นกับความเข้มข้นของเกลือบ้าง แม้จะไม่มากเท่ากับการจับยึดกันระหว่าง

ดีเอ็นเอกับดีเอ็นเอก็ตาม ในการทดลองจึงทำที่ความเข้มข้นของเกลือต่างกัน 2 ความเข้มข้นคือ 0 และ 100 mM NaCl ผลการทดลองที่ได้เป็นดังแสดงในตารางที่ 2

ตารางที่ 3 T_m of PNA·RNA hybrids

entry	PNA	%G·C content	T_m (antiparallel RNA) ($^{\circ}$C)	T_m (parallel RNA) ($^{\circ}$C)
1	**10mer1**	40	42.3	< 20
2	**10mer2**	70	48.0	32.9
3	**10mer3**	20	32.6	< 20
4	**10mer4**	40	40.8	N.D
5	**10mer5**	40	40.9	N.D
6	**10mer6**	70	49.3 (150)	30.2
7	**10mer7**	70	51.2 (150)	28.5
8	**10mer8**	20	39.7	N.D
9	**10mer9**	20	37.7	N.D

Conditions: 1 μM PNA, 1 μM DNA, 10 mM sodium phosphate buffer pH 7.0, 100 mM NaCl, heating rate 1.0 $^{\circ}$C/min. T_m values are accurate within $\pm$0.5 $^{\circ}$C.

จากตารางที่ 2 จะเห็นได้ว่าพีเอ็นเอทุกลำดับเบสที่สังเคราะห์ขึ้นสามารถจับยึดกับดีเอ็นเอที่มีลำดับเบสคู่สมกันได้เฉพาะในทิศทางแอนติพาราเรลเท่านั้น โดยมีค่า T_m อยู่ในช่วง 57.0–65.3 $^{\circ}$C ที่ 0 mM NaCl และ 52.8–61.0 $^{\circ}$C ที่ 100 mM NaCl ส่วนในทิศทางการจับแบบพาราเรลไม่พบว่าเกิดการจับยึดกันระหว่างพีเอ็นเอกับดีเอ็นเอ (ไม่เกิดการ melt ซึ่งแสดงว่า T_m <20 $^{\circ}$C ในทุกกรณี) ซึ่งเป็นการยืนยันว่าระบบ acpcPNA มีการเลือกจำเพาะต่อทิศทางการจับกับดีเอ็นเอในแบบแอนติพาราเรลที่สูงมากในทุกๆ ลำดับเบสที่นำมาทดสอบ

ในการทดลองต่อมาได้ศึกษาความสามารถในการจับยึดกับอาร์เอ็นเอ ทั้งในรูปแบบแอนติพาราเรล และพาราเรล (ตารางที่ 3) พบว่า การจับยึดระหว่างพีเอ็นเอกับอาร์เอ็นเอในรูปแบบแอนติพาราเรลมีค่า T_m อยู่ในช่วง 32.6–49.3 $^{\circ}$C ซึ่งต่ำกว่าการจับกันระหว่างพีเอ็นเอกับดีเอ็นเอแบบแอนติพาราเรลที่ภาวะเดียวกันในทุกกรณี (ช่วง T_m 52.8–61.0 $^{\circ}$C) นอกจากนี้ยังพบว่าพีเอ็นเอที่มี %GC content ค่อนข้างสูงสามารถจับกับอาร์เอ็นเอในทิศทางแบบพาราเรลได้ แม้จะได้โมเลกุลลูกผสมที่มีความเสถียรน้อยกว่าแบบแอนติพาราเรลก็ตาม (ดู entry 2,6 และ 7)

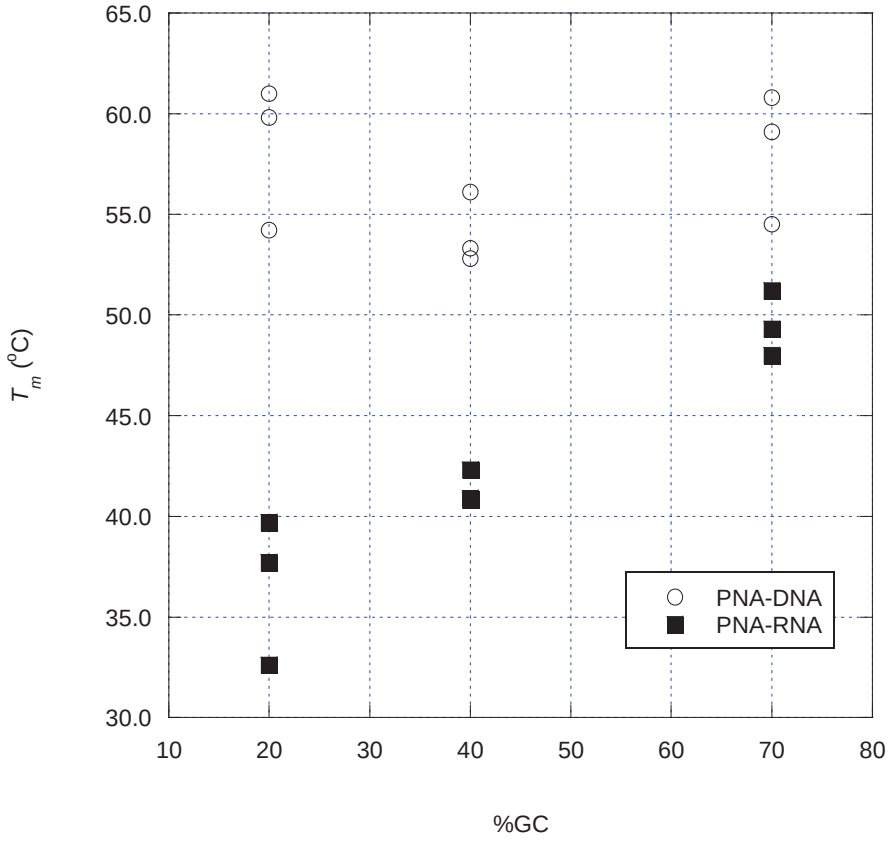

รูปที่ 2 A plot showing relationship between G·C content and stability of PNA·DNA and PNA·RNA hybrids. Conditions: 1 μM PNA, 1 μM DNA, 10 mM sodium phosphate buffer pH 7.0, 100 mM NaCl, heating rate 1.0 °C/min. T_m values are accurate within ±0.5 °C.

เมื่อเปรียบเทียบค่า T_m ของโมเลกุลลูกผสมแบบแอนติพาราเรลระหว่างพีเอ็นเอกับดีเอ็นเอ และพีเอ็นเอกับอาร์เอ็นเอ ที่สัดส่วนของ GC เบสแตกต่างกันจะพบแนวโน้มที่น่าสนใจดังแสดงในรูปที่ 2 กล่าวคือ ในกรณีของพีเอ็นเอกับดีเอ็นเอ ค่า T_m จะค่อนข้างคงที่ โดยไม่ขึ้นกับสัดส่วนของ GC เบส ในขณะที่ค่า T_m ของพีเอ็นเอกับอาร์เอ็นเอจะมีค่าขึ้นกับสัดส่วนของ GC เบส ในลักษณะเดียวกับที่พบในดีเอ็นเอและอาร์เอ็นเอธรรมชาติ นั่นคือถ้ายิ่งสัดส่วนของคู่เบส GC มีมากก็จะมีค่า T_m ที่สูงขึ้น (รูปที่ 1) ดังนั้น ความแตกต่างของ Tm ระหว่างโมเลกุลลูกผสมพีเอ็นเอ-ดีเอ็นเอ กับพีเอ็นเอ-อาร์เอ็นเอ จะขึ้นกับลำดับเบส โดยที่ความแตกต่างจะมากเมื่อพีเอ็นเอมีสัดส่วนของเบส AT มาก และความแตกต่างนี้จะน้อยลงเมื่อพีเอ็นเอมีสัดส่วนของเบส GC มากขึ้น อย่างไรก็ตาม ในทุกกรณีความเสถียรของ โมเลกุลลูกผสมพีเอ็นเอ-ดีเอ็นเอจะมากกว่าพีเอ็นเอ-อาร์เอ็นเอเสมอ

ผลการทดลองทั้งหมดยืนยันสมบัติที่เป็นเอกลักษณ์เฉพาะตัวของ acpcPNA 2 ประการที่ไม่เคยมีการรายงานในพีเอ็นเอ หรือแอนาล็อกของดีเอ็นเอชนิดอื่นๆ มาก่อนคือ 1. ความสามารถในการเลือกจับกับดีเอ็นเอได้ดีกว่าอาร์เอ็นเอ และ 2. ความเสถียรของโมเลกุลลูกผสมระหว่างพีเอ็นเอกับดีเอ็นเอที่ไม่ขึ้นกับสัดส่วนของเบสที่เป็นองค์ประกอบ สมบัติประการแรกเป็นการบ่งชี้ข้อจำกัดของ acpcPNA ว่าน่าจะเหมาะกับงานที่เกี่ยวข้องกับเป้าหมายของการจับยึดที่เป็นดีเอ็นเอมากกว่าอาร์เอ็นเอ เช่นงานทางด้าน DNA-based diagnostics และ antigene therapeutics ส่วนสมบัติประการที่สองน่าจะเป็นประโยชน์ในการนำไปใช้เป็นโพรบสำหรับตรวจวินิจฉัยแบบ high throughput เช่นในการทำไมโครแอเรย์ เนื่องจากสามารถออกแบบพีเอ็นเอโพรบหลายๆ ชนิดเพื่อให้

จับกับดีเอ็นเอเป้าหมายได้หลายๆ ตำแหน่งพร้อมกัน โดยที่โมเลกุลลูกผสมที่เกิดขึ้นมีความเสถียรใกล้เคียงกันและไม่ขึ้นกับลำดับเบสของดีเอ็นเอที่เป็นเป้าหมาย โดยทางกลุ่มวิจัยได้เคยนำสมบัตินี้ของ acpcPNA ไปใช้ในการตรวจลำดับเบสของดีเอ็นเอในรูปแบบ multiplex เป็นผลสำเร็จมาแล้ว [Boontha et al., 2008]

ตารางที่ 4. Evidences for the lack of self-hybridization between two complementary PNA sequences

entry	PNA pairs	%G·C content	T_m (°C)	Note
1	**10mer1·10mer4**	40	<20	antiparallel
2	**10mer1·10mer5**	40	24.2	parallel
3	**10mer2·10mer6**	70	<20	antiparallel
4	**10mer2·10mer7**	70	35.1	parallel
5	**10mer3·10mer8**	20	<20	antiparallel
6	**10mer3·10mer9**	20	<20	parallel

Conditions: 1 μM PNA, 1 μM DNA, 10 mM sodium phosphate buffer pH 7.0, 100 mM NaCl, heating rate 1.0 °C/min. T_m values are accurate within ±0.5 °C.

นอกจากการศึกษาการจับยึดกันระหว่าง acpcPNA กับดีเอ็นเอและอาร์เอ็นเอแล้ว ยังได้มีการศึกษาความสามารถในการจับยึดกันเองระหว่าง acpcPNA สองสายที่มีลำดับเบสคู่สมกัน ทั้งในแบบแอนติพาราเรลและพาราเรล โดยผลการทดลองเป็นดังแสดงในตารางที่ 4 ซึ่งแสดงให้เห็นว่า acpcPNA ไม่สามารถเกิดโมเลกุลลูกผสมกับตัวมันเองในทิศทางแอนติพาราเรล (entries 1, 3, 5) แต่ในกรณีที่มีสัดส่วนของ GC เบสสูง (entries 2,4) อาจเกิดโมเลกุลลูกผสมกับตัวเองในทิศทางพาราเรลได้ อย่างไรก็ตาม โมเลกุลลูกผสมที่เกิดขึ้นถือว่ามีความเสถียรต่ำมากเมื่อเทียบกับการเกิดโมเลกุลลูกผสมระหว่างพีเอ็นเอ-ดีเอ็นเอ หรือแม้แต่ดีเอ็นเอ-ดีเอ็นเอ การที่ acpcPNA ไม่เกิดโมเลกุลลูกผสมกับตัวเองในทิศทางแอนติพาราเรลนับเป็นสมบัติเฉพาะที่เป็นเอกลักษณ์ของพีเอ็นเอชนิดนี้อีกประการหนึ่งที่อาจนำไปประยุกต์ใช้ประโยชน์ได้ในการออกแบบพีเอ็นเอสองสายเพื่อให้จับกับดีเอ็นเอเป้าหมายที่เป็นโมเลกุลแบบเกลียวคู่โดยการเกิด double duplex invasion ซึ่งน่าจะช่วยเพิ่มประสิทธิภาพของการจับยึดระหว่างพีเอ็นเอกับดีเอ็นเอแบบเกลียวคู่ ซึ่งในงานวิจัยที่ผ่านมาที่ทำโดยกลุ่มวิจัยอื่นยังพบว่ามีข้อจำกัดอยู่มากทั้งในแง่ของประสิทธิภาพและความจำเพาะเจาะจงต่อลำดับเบสของดีเอ็นเอที่เป็นเป้าหมาย [Lohse et al., 1999] ซึ่งการประยุกต์ใช้งาน acpcPNA ในลักษณะนี้จะได้มีการศึกษาต่อไปในอนาคต งานวิจัยที่เกี่ยวข้องกับ acpcPNA ในส่วนนี้ได้รับการตีพิมพ์แล้วในวารสาร Artificial DNA: PNA&XNA [Vilaivan et al., 2011]

ในขณะนี้ยังไม่สามารถอธิบายปัจจัยทางโครงสร้างที่มีอิทธิพลต่อสมบัติการจับยึดที่เป็นลักษณะเฉพาะของ acpcPNA เนื่องจากยังไม่มีข้อมูลโครงสร้าง 3 มิติระหว่างพีเอ็นเอกับดีเอ็นเอ, อาร์เอ็นเอ และกับพีเอ็นเอด้วยกันเอง โดยกำลังอยู่ระหว่างดำเนินการศึกษาโครงสร้างดังกล่าวทั้งทางทฤษฎีโดยใช้การคำนวณแบบ Molecular Dynamics (ร่วมกับกลุ่มวิจัยของ ศ.ดร.สุพจน์ หารหนองบัว และ ผศ.ดร.คัชรินทร์ ศิริวงศ์) และการใช้เทคนิคทาง X-ray crystallography (ร่วมกับกลุ่มวิจัยของ รศ.ดร.พลังพล คงเสรี)

2. การสังเคราะห์และศึกษาสมบัติจับยึดของ acpcPNA ที่มี modified base

เพื่อเป็นการขยายขอบเขตการใช้งานของพีเอ็นเอชนิด acpcPNA ให้กว้างขวางขึ้นได้มีแนวคิดการแทนที่เบสธรรมชาติ (A, T, C, G) ในหน่วยของพีเอ็นเอโมโนเมอร์ด้วยเบสอื่นๆ ที่ไม่ใช่เบสธรรมชาติ โดยเบสที่ไม่ใช่เบสธรรมชาติกลุ่มที่สนใจมีอยู่ 2 กลุ่ม กลุ่มแรกคือเบสที่สามารถจับยึดกับเบสธรรมชาติทั้งสี่ชนิด (A, T, C, G) ได้อย่างไม่จำเพาะเจาะจง ซึ่งเรียกว่ายูนิเวอร์แซลเบส พีเอ็นเอโพรบที่มียูนิเวอร์แซลเบสจะมีประโยชน์ในการจับยึดกับดีเอ็นเอเป้าหมายมีความผันแปรของลำดับเบสในบางตำแหน่ง (ที่ไม่ใช่ตำแหน่งที่สนใจจะศึกษา) สูง โดยสมบัติของยูนิเวอร์แซลเบสที่พึงประสงค์จะต้องสามารถจับยึดกับเบสธรรมชาติทั้งสี่ชนิดได้ดีใกล้เคียงกันโดยไม่ขึ้นกับชนิดของเบสที่มาเข้าคู่กัน และเบสที่อยู่ข้างเคียง

เบสที่ไม่ใช่เบสธรรมชาติกลุ่มที่สองที่สนใจศึกษาคือกลุ่มอนุพันธ์ของยูเรซิล (U) ที่มีการแทนที่บนตำแหน่งที่ 5 ของหมู่เบสด้วยหมู่ฟังก์ชันที่สามารถแสดงสัญญาณเช่นฉลากเรืองแสง ข้อดีของโมเลกุลเหล่านี้คือสามารถใส่ฉลากเรืองแสงเข้าไปในตำแหน่งอื่นที่นอกเหนือจากส่วนปลายของโมเลกุล ซึ่งน่าจะมีประโยชน์ในการเป็นโพรบสำหรับการตรวจลำดับเบสของดีเอ็นเอโดยแนวคิดใหม่ๆ เช่น quencher-free molecular beacon [Englund and Appella, 2005] เป็นต้น

2.1 Hypoxanthine as a modified base

ยูนิเวอร์แซลเบสตัวแรกที่ได้ศึกษาคือไฮโปแซนทีน (hypoxanthine, H) (รูปที่ 3) ซึ่งมีการศึกษากันมากในระบบของดีเอ็นเอ [Sun and Lee, 2010; Case-Green and Southern, 1994] และพีเอ็นเอต้นแบบของ Nielsen โดยในระบบพีเอ็นเอของ Nielsen พบว่าเบสชนิดนี้แสดงสมบัติของยูนิเวอร์แซลเบสที่ไม่ดีนัก กล่าวคือเมื่อมี A เป็นเบสข้างเคียง H จะแสดงสมบัติการจับยึดที่ดีเป็นพิเศษกับเบส C (คล้ายเบส G) แต่เมื่อมี T เป็นเบสข้างเคียง H กลับแสดงสมบัติการจับยึดที่จำเพาะเจาะจงกับเบส A (คล้ายเบส T) โดยในกรณีหลังนี้เชื่อว่าเกิดจาก Hoogsteen base pairing ส่วนในกรณีแรกจะคล้ายกับ Watson-Crick base pairing อย่างไรก็ตาม ความแตกต่างของ T_m ในกรณีที่เกิดการจับยึดได้ดีที่สุด กับกรณีที่แย่ที่สุดมีค่าไม่มากนัก (อยู่ในช่วง 6.5–14 °C) [Timár et al. 1999]

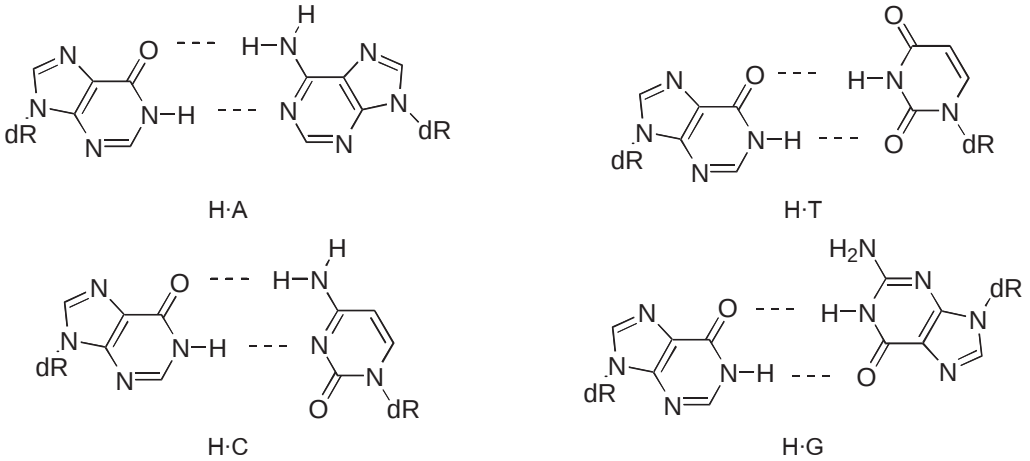

รูปที่ 3 แสดงการเกิดคู่เบสระหว่าง H กับ natural nucleobases

ในงานวิจัยนี้ได้ทดลองประเมินความสามารถในการเป็นยูนิเวอร์แซลเบสของ H ใน acpcPNA ซึ่งอาจให้ผลต่างจากพีเอ็นเอระบบของ Nielsen โดยเริ่มจากการสังเคราะห์ H โมโนเมอร์ที่ถูกปกป้องด้วยหมู่ Fmoc ความพยายามสังเคราะห์ไฮโปแซนทีนโมโนเมอร์จากการแทนที่หมู่โทซิเลตใน *trans*-4-tosyloxy-D-proline ที่มีหมู่ปกป้องอะมิโนเป็น Boc และหมู่ปกป้องคาร์บอกซิลเป็น diphenylmethyl ester ด้วยเบสไฮโปแซนทีนโดยตรงไม่

ประสบความสำเร็จ แต่สามารถสังเคราะห์โมโนเมอร์ดังกล่าวจากสารตั้งต้นตัวเดียวกันได้โดยผ่าน 6-chloropurine monomer ตามด้วยการทำไฮโดรลิซิสเพื่อเปลี่ยนหมู่คลอโรให้เป็นหมู่ไฮดรอกซิล [Baker and Tanna, 1965] ดังแสดงในรูปที่ 4

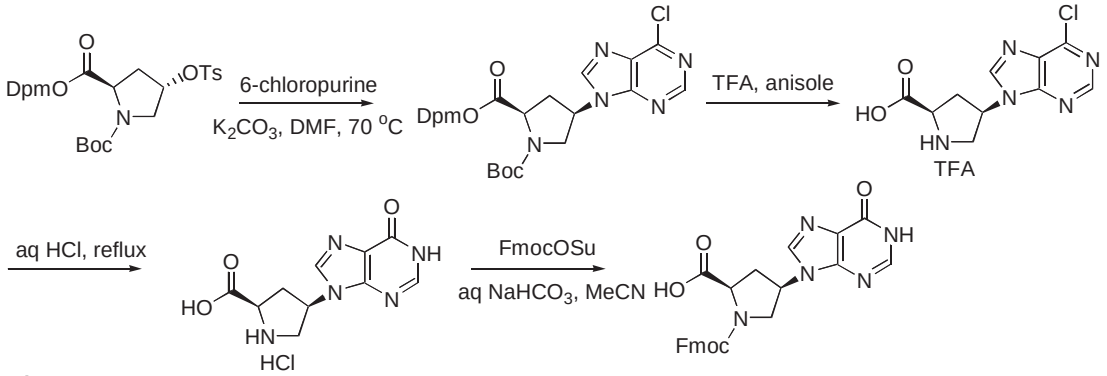

รูปที่ 4 แผนภาพแสดงการสังเคราะห์โมโนเมอร์ของไฮโปแซนทีนเบส (H)

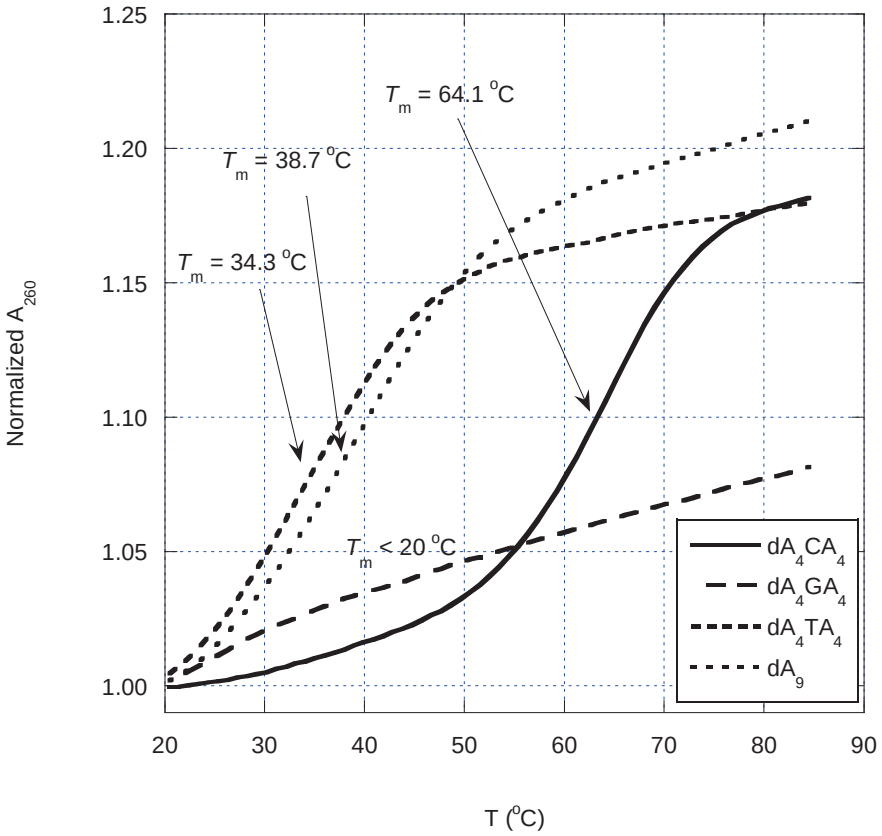

รูปที่ 5 แสดง melting curve ของไฮบริดระหว่างพีเอ็นเอ T_4HT_4 และดีเอ็นเอ dA_4YA_4 เมื่อ H คือไฮโปแซนทีน และ Y คือ A, T, C หรือ G

ในเบื้องต้นได้ทดลองประเมินความสามารถของไฮโปแซนทีนในการเป็นยูนิเวอร์แซลเบสสำหรับ acpcPNA โดยการสังเคราะห์พีเอ็นเอที่มีลำดับเบสเป็น T_4HT_4 โดยใช้วิธีการสังเคราะห์พีเอ็นเอโดยวิธี Fmoc-SPPS โดยอาศัย Fmoc/Pfp monomer ตามที่ได้เคยรายงานไปแล้ว [Vilaivan and Srisuwannaket, 2006] เว้น

แต่ในขั้นที่ใส่เบส H จะใช้โมโนเมอร์ในรูปที่เป็นกรดคาร์บอกซิลิก ที่ผ่านการกระตุ้นด้วย HATU/DIEA แทนการใช้ Fmoc/Pfp โมโนเมอร์ พีเอ็นเอที่ได้สามารถทำให้บริสุทธิ์โดย HPLC ตามวิธีการมาตรฐาน (*m/z* calcd: 3189.43 found: 3190.87) ผลการหาค่า T_m ของโมเลกุลลูกผสมระหว่างพีเอ็นเอดังกล่าวกับดีเอ็นเอที่มีลำดับเบสเป็น A_4YA_4 เมื่อ Y = A, T, C และ G เป็นดังสรุปในรูปที่ 5

ข้อมูลในรูปที่ 5 แสดงว่าเบสไฮโปแซนทีนไม่มีสมบัติเป็นยูนิเวอร์แซลเบสใน acpcPNA แต่กลับแสดงสมบัติคล้ายกับเบส G แม้จะมีเบสข้างเคียงเป็น T ก็ตาม กล่าวคือสามารถเกิดโมเลกุลลูกผสมที่ค่อนข้างเสถียรกับดีเอ็นเอในกรณีที่เบสที่อยู่ตรงข้ามเป็น C (T_m = 64.1 °C) ซึ่งใกล้เคียงกับในกรณีของโมเลกุลลูกผสมที่เกิดจากพีเอ็นเอ T_4GT_4 และดีเอ็นเอ dA_4CA_4 (T_m = 64.2 °C) แต่เมื่อเบสที่อยู่ตรงข้ามเป็น A, T หรือ G จะมีค่า T_m ลดต่ำลงมาค่อนข้างมาก โดยเฉพาะอย่างยิ่งเมื่อเบสตรงข้ามเป็น G ซึ่งมีความเกะกะสูง โดยค่า T_m ที่ลดต่ำลงมาอยู่ในเกณฑ์ใกล้เคียงกับในกรณีที่เป็น single base mismatch ตามปกติคือ ΔT_m ~ 25–30 °C ซึ่งสมบัตินี้แตกต่างจากพีเอ็นเอต้นแบบของ Nielsen อย่างชัดเจน

แม้ผลการทดลองจะไม่เป็นตามที่คาดไว้ แต่การที่เบส H สามารถแสดงสมบัติเสมือนกับเป็นเบส G ก็เปิดโอกาสให้สามารถใช้แทนเบส H แทนเบส G ใน acpcPNA ได้ ซึ่งข้อดีของเบส H คือโมโนเมอร์สามารถสังเคราะห์ได้ง่ายกว่าโมโนเมอร์ของเบส G มาก เนื่องจาก regioselectivity ของการแทนที่ค่อนข้างสูง และไม่จำเป็นต้องมีหมู่ปกป้อง อีกทั้งในการสังเคราะห์พีเอ็นเอยังสามารถแทรกโมโนเมอร์ที่มีเบส H เข้าไปได้อย่างมีประสิทธิภาพมากกว่าโมโนเมอร์ของเบส G อย่างไรก็ตาม เพื่อเป็นการยืนยันว่าเบส I สามารถแทนที่เบส G ได้ในกรณีที่ลำดับเบสเปลี่ยนไป โดยเฉพาะอย่างยิ่งเมื่อมีเบสข้างเคียงเป็นตัวอื่นที่ไม่ใช่ T จึงได้สังเคราะห์ acpcPNA อีก 4 ชนิดที่มีเบส H แทรกอยู่ระหว่างคู่เบสต่างๆ กัน โดยลำดับเบสที่สังเคราะห์จะเป็นลำดับเดียวกับที่ใช้ในการศึกษาที่มีมาก่อนหน้านี้ในระบบพีเอ็นเอของ Nielsen นอกจากนี้ยังได้สังเคราะห์ acpcPNA อีก 2 ชนิดที่มีเบส G แทนที่ตำแหน่งของเบส H เพื่อเปรียบเทียบการจับยึดกับดีเอ็นเอที่เป็นคู่สมและไม่เป็นคู่สมกันด้วย โดยได้ยืนยันโครงสร้างของพีเอ็นเอทั้งหมดที่สังเคราะห์ได้ด้วยเทคนิค MALDI-TOF mass spectrometry ดังแสดงในตารางที่ 5

ตารางที่ 5 ข้อมูลลำดับเบสและ *m/z* ของพีเอ็นเอที่สังเคราะห์ได้

sequence	*m/z* (calcd)	*m/z* (found)
Ac-CCTTTITCATC-LysNH_2	3803.11	3801.05
Ac-CCTTAIACATC-LysNH_2	3821.14	3820.08
Ac-CCTTCICCATC-LysNH_2	3773.09	3772.52
Ac-CCTTGIGCATC-LysNH_2	3853.14	3853.91
Ac-CCTTTGTCATC-LysNH_2	3818.13	3816.70
Ac-CCTTAGACATC-LysNH_2	3836.16	3836.96

ผลการตรวจวัดค่า T_m กับดีเอ็นเอที่มีลำดับเบสเป็นคู่สม และไม่เป็นคู่สมกันโดยเปลี่ยนแปลงเฉพาะตำแหน่งของเบสที่จับคู่กับเบส H หรือ G ที่ตรงกลางสายเป็นดังแสดงในรูปที่ 6

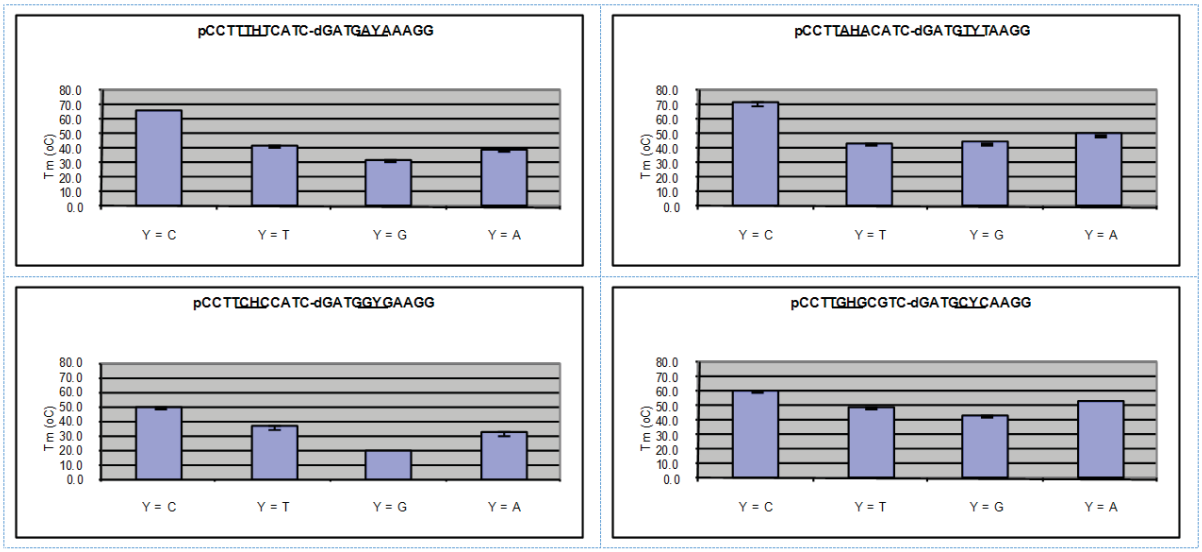

รูปที่ 6 เปรียบเทียบค่า T_m ของ PNA·DNA duplex ที่มีเบส I เป็นองค์ประกอบ; T_m measured at 1.0 μM duplex concentration, 10 mM sodium phosphate buffer pH 7.0, 100 mM NaCl, heaing rate 1 ºC/min

ผลการทดลองในรูปที่ 6 แสดงให้เห็นว่าเบส H ที่อยู่บนพีเอ็นเอสามารถจับคู่กับเบส C บนดีเอ็นเอได้ดีกว่าเบสตัวอื่น (G, C และ A) ไม่ว่าจะมีเบสข้างเคียงเบส H เป็นอะไรก็ตาม โดยเมื่อเบสข้างเคียงเป็น A หรือ T จะมีความแตกต่างของ T_m ระหว่างคู่เบส H·C กับคู่เบสอื่นมากกว่าเมื่อเบสข้างเคียงเป็น C หรือ G และเมื่อเปรียบเทียบกับพีเอ็นเอที่มีลำดับเบสเหมือนกัน เว้นแต่เปลี่ยนจาก H เป็น G จะเห็นว่าเบส H ในพีเอ็นเอมีความจำเพาะเจาะจงต่อ C เช่นเดียวกับเบส G ทุกประการ (รูปที่ 7) และเมื่อเปรียบเทียบกับระบบพีเอ็นเอของ Nielsen ที่มีลำดับเบสเดียวกันพบว่า T_m ของ acpcPNA ที่มีเบส H อยู่ตรงกลางสายจะมีค่าสูงกว่า และแสดงความจำเพาะเจาะจงต่อเบส C ที่ชัดเจนกว่ามาก (ค่า ΔT_m ในทุกกรณี > 20 ºC เมื่อเทียบกับระบบพีเอ็นเอของ Nielsen ที่มี ΔT_m สูงสุดเพียง 10.8 ºC) (ตารางที่ 6)

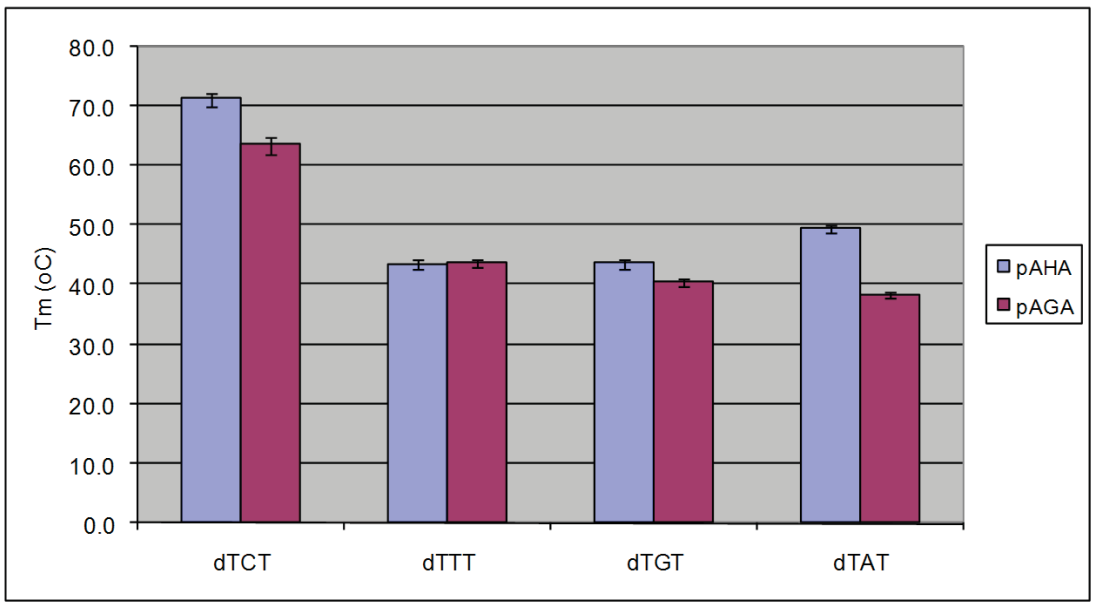

pCCTTAXACATC + dGATGTYTAAGG (X = H,G; Y = C,T,G,A)

(a)

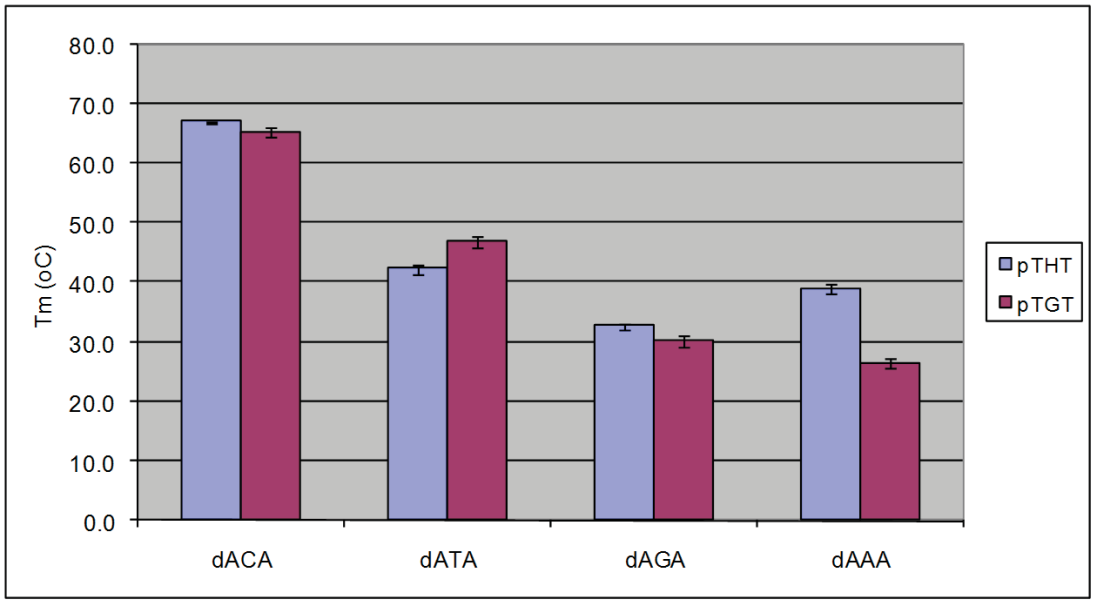

pCCTTTXTCATC + dGATGAYAAAGG (X = H,G, Y = C,T,G,A)

(b)

รูปที่ 7 เปรียบเทียบค่า T_m ของ PNA·DNA duplex ที่มีเบส H เป็นองค์ประกอบ กับที่มีเบส G เป็นองค์ประกอบ เมื่อมีเบสข้างเคียง H เป็น A (a) และเมื่อมีเบสข้างเคียง H เป็น T (b); T_m measured at 1.0 μM duplex concentration, 10 mM Sodium phosphate buffer pH 7.0, 100 mM NaCl, heating rate ºC /min

ตารางที่ 6 เปรียบเทียบค่า T_m ของ PNA·DNA duplex ที่มีเบส H เป็นองค์ประกอบในพีเอ็นเอสองชนิดคือ acpcPNA ของกลุ่มผู้วิจัย และ aegPNA ของ Nielsen

PNA (N⟶C)	DNA	T_m (acpcPNA)[a] (ΔT_m, ºC)[c]	T_m (aegPNA)[b] (ΔT_m, ºC)[c]
CCTTAHACATC	..TCT..	71.2 (0)	45.3 (0)
	..TTT..	43.5 (27.7)	34.5 (10.8)
	..TGT..	43.6 (27.6)	38.0 (7.3)
	..TAT..	49.4 (21.8)	36.9 (8.4)
CCTTTHTCATC	..ACA..	67.1 (0)	45.7 (0)
	..ATA..	42.4 (24.7)	38.2 (7.5)
	..AGA..	32.7 (34.4)	41.0 (4.7)
	..AAA..	38.9 (28.2)	52.2 (–6.5)

[a] T_m measured at 1.0 μM duplex concentration, 10 mM Sodium phosphate buffer pH 7.0, 100 mM NaCl

[b] T_m data from [Timár et al. 1999] measured under the same contitions

[c] $\Delta T_m = T_m$ (H·C) – T_m (H·X), when X is the base under consideration

เป็นที่น่าประหลาดใจว่าแม้คู่เบส G·C จะมีถึง 3 พันธะไฮโดรเจน ในขณะที่คู่เบส H·C สร้างได้เพียง 2 พันธะไฮโดรเจนแต่ความแข็งแรงของคู่เบส H·C ใน acpcPNA กลับค่อนข้างใกล้เคียง หรือสูงกว่าคู่เบส G·C อยู่เล็กน้อยเมื่อพิจารณาจากค่า T_m เปรียบเทียบกันในแต่ละกรณี ซึ่งเป็นพฤติกรรมที่แตกต่างจากทั้งดีเอ็นเอและพีเอ็นเอของ Nielsen เป็นที่น่าสังเกตว่าคู่เบส G·C ใน acpcPNA มีความเสถียรน้อยกว่าคู่เบส A·T เช่นกัน ดังนั้นอาจเป็นไปได้ว่าในระบบ acpcPNA คู่เบส G·C ไม่ได้อยู่ในคอนฟอร์เมชันที่เหมาะสมที่จะเกิดพันธะไฮโดรเจนได้ครบทั้งสามพันธะ จึงทำให้ความเสถียรของคู่เบส G·C ต่ำกว่าที่ควรจะเป็น การค้นพบว่าคู่เบส H·C แสดงความเสถียรใกล้เคียงกับคู่เบส G·C นั้นสอดคล้องกับสมมติฐานข้างต้น อย่างไรก็ตาม การอธิบายปรากฏการณ์ดังกล่าวในระดับโมเลกุลจำเป็นต้องมีการทดลองเพิ่มเติมที่จะให้ข้อมูลเกี่ยวกับโครงสร้างสามมิติของสารประกอบเชิงซ้อนระหว่างพีเอ็นเอและดีเอ็นเอ เช่น NMR หรือ X-ray crystallography หรือการใช้แบบจำลองโมเลกุลประกอบการคำนวณทางทฤษฎี แต่อย่างน้อยที่สุด การค้นพบนี้ได้เสนอแนะว่าสามารถแทนที่เบส G ใน acpcPNA ด้วยเบส H ได้โดยไม่มีผลกระทบต่อ specificity ในการจดจำเบส C และยังช่วยเพิ่มความเสถียรของ PNA·DNA duplex แทนที่จะลดความเสถียรดังที่พบในกรณีของ DNA·DNA duplex ซึ่งถือว่ามีความสำคัญอย่างยิ่งต่อการนำ acpcPNA ไปประยุกต์ใช้ประโยชน์ในด้านต่างๆ ด้วยเหตุผลที่กล่าวไปแล้วข้างต้นว่าโมโนเมอร์ของเบส H สามารถสังเคราะห์ได้ง่ายกว่าโมโนเมอร์ของ G และสามารถแทรกเข้าไปในสายของพีเอ็นเอได้ง่ายกว่ามากโดยวิธีสังเคราะห์บนวัฏภาคของแข็ง นอกจากนี้ ด้วยการที่ G เป็นเบสที่มี oxidation potential ต่ำกว่าเบสตัวอื่นๆ มันจึงสามารถรับอิเล็กตรอนได้ดี [Kawai et al., 2002] ทำให้มันมักจะรบกวนการ assay ที่ใช้พีเอ็นเอเป็นโพรบในบางเทคนิค โดยเฉพาะอย่างยิ่ง fluorescence เนื่องจาก G สามารถทำให้เกิดการ quench ของฟลูออโรฟอร์เป็นจำนวนมากผ่านกลไก photoexcited oxidative charge transfer [Mayer et al., 2004] นอกจากนี้ การแทนที่ G ด้วย I ยังได้ใช้ในการทำ electrochemical detection ของ DNA hybridization โดยอาศัยการดูจาก oxidation signal ของ guanine ซึ่งมีข้อจำกัดคือโพรบที่ใช้จะต้องไม่มี G เป็นองค์ประกอบเนื่องจากจะให้สัญญาณรบกวนการตรวจวัด [Wang et al, 1995] แต่สามารถหลีกเลี่ยงได้ด้วยการแทนที่ G ในโพรบด้วย H [Wang et al, 1998] โดยยังคงสามารถรักษา specificity ไว้ได้เหมือนเดิม

ตารางที่ 7 เปรียบเทียบค่า T_m ของ PNA·DNA duplex ที่มีเบส H และ G เป็นองค์ประกอบ (ลำดับเบสของพีเอ็นเอคือ *N*-AATTTXCATCA-*C* และลำดับเบสของดีเอ็นเอคือ 5'-TGATGYAAATT-3'

Y in DNA	T_m (X=G)[a] (ΔT_m, ºC)[b]	T_m (X=I)[a] (ΔT_m, ºC)[b]
C	71.7 (0)	74.9 (0)
T	55.6 (16.1)	53.0 (21.9)
G	46.8 (24.9)	49.1 (25.8)
A	41.1 (30.6)	49.9 (25.0)

[a] T_m measured at 1.0 μM duplex concentration, 10 mM Sodium phosphate buffer pH 7.0, 100 mM NaCl

[b] $\Delta T_m = T_m$ (I·C) – T_m (I·X), when X is the base under consideration

สุดท้ายเพื่อเป็นการยืนยันเพิ่มเติมว่าการแทนที่เบส G ด้วย H ในระบบ acpcPNA จะสามารถใช้ได้ทั่วๆ ไป โดยไม่จำกัดอยู่เฉพาะแต่ในกรณีทดสอบข้างต้น จึงได้ทดลองสังเคราะห์ acpcPNA ความยาว 11 เบส ที่มีเบส

G และ H ที่ตำแหน่งเดียวกันอีกคู่หนึ่ง ซึ่งเป็น biologically relevance sequence ผลการตรวจวัดค่า T_m ดังแสดงในตารางที่ 7 สามารถยืนยันการค้นพบในข้างต้น กล่าวคือการแทนที่ G ด้วย H ทำให้ได้พีเอ็นเอที่สามารถเกิดไฮบริดที่เสถียรขึ้นกับดีเอ็นเอเป้าหมาย และยังคงมี specificity ต่อเบส C เหนือกว่าเบสอื่นๆ โดยเฉพาะอย่างยิ่งเมื่อเปรียบเทียบในกรณีที่ mismatch เบสเป็น T ซึ่งมักจะเกิด wobble pair กับเบส G ได้ค่อนข้างดี ทำให้ G·T mismatch มีค่า T_m ลดต่ำลงกว่า G·C perfect match น้อยกว่าคู่เบสอื่น แต่เมื่อแทนที่ด้วยเบส H พบว่า H·T mismatch มีความเสถียรลดลงกว่า G·T mismatch ประกอบกับความเสถียรที่เพิ่มขึ้นของ H·C perfect match ทำให้ค่า T_m ที่เปลี่ยนแปลงไปเห็นได้ชัดเจนมากขึ้น นั่นคือการแทนที่เบส G ด้วยเบส H จะทำให้สามารถบอกความแตกต่างของเบส T กับเบส C ได้ดียิ่งขึ้น งานส่วนนี้กำลังอยู่ระหว่างการเตรียมต้นฉบับบทความเพื่อตีพิมพ์

2.2 Hybridization of PNA with fluorescent-modified DNA

กลุ่มวิจัยของ Prof. Hans-Achim Wagenknecht (University of Regensburg, Germany) ได้พัฒนาดีเอ็นเอเรืองแสงสีขาว (White light emitting DNA, WED) ที่มีฟลูออโรฟอร์สองชนิดได้แก่ ethynylpyrene และ ethynyl Nile red ต่อกับหน่วยของยูริดีนที่อยู่ติดกันในลำดับเบสของดีเอ็นเอ (รูปที่ 8) และได้แสดงให้เห็นว่าการเกิด energy transfer ของฟลูออโรฟอร์ทั้งสองจะเปลี่ยนแปลงไปตามสถานะการไฮบริไดซ์ของดีเอ็นเอ [Varghese and Wagenknecht, 2009] กล่าวคือในสภาพที่เป็นสายเดี่ยว จะเกิด energy transfer จาก pyrene ไปยัง Nile red ทำให้เมื่อ excite ที่ λ_{max} ของ pyrene (~380 nm) จะเห็นเฉพาะการเรืองแสงของ Nile red (λ_{em} ~665 nm) สารละลายของ ssDNA จึงเรืองแสงเป็นสีแดง แต่เมื่อดีเอ็นเออยู่ในสภาพที่เป็น double helix ฟลูออโรฟอร์ทั้งสองจะถูกบังคับให้บิดออกจากกันเนื่องจากถูกบังคับด้วยโครงสร้างที่ค่อนข้าง rigid ของ DNA double helix การเกิด energy transfer จึงไม่ดีเท่าในสภาพสายเดี่ยว ดังนั้นการ excite ที่ λ_{max} ของ pyrene (~380 nm) จะทำให้เห็นการเรืองแสงทั้งของ pyrene (λ_{em} ~440 nm) และ Nile red (λ_{em} ~665 nm) จึงเห็นเป็นการเรืองแสงสีขาว

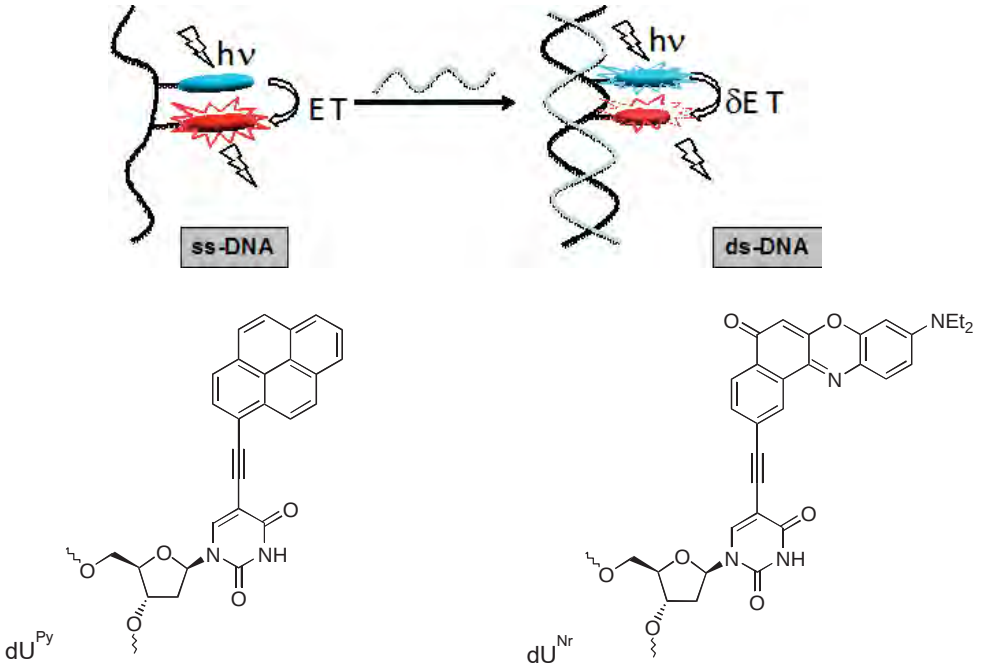

รูปที่ 8 หลักการทำงานของ White light emitting DNA (WED) และโครงสร้างของ ethynylpyrene modified dU และ ethynyl Nile red modified dU

งานวิจัยนี้มีวัตถุประสงค์เพื่อทดสอบความสามารถในการไฮบริไดซ์ระหว่าง WED DNA กับ acpcPNA ที่มีลำดับเบสคู่สมกัน และศึกษาสมบัติเชิงแสงของ PNA·DNA hybrid ที่เกิดขึ้น โดยลำดับเบสของดีเอ็นเอและพีเอ็นเอที่ใช้เป็นดังแสดงในรูปที่ 9 ซึ่งจะเป็นชุดเดียวกับที่ได้มีข้อมูลการศึกษาสมบัติเชิงแสงมาก่อนหน้านี้แล้ว โดยเป็นงานวิจัยที่ทำภายใต้ความร่วมมือกับ Prof. Wagenknecht

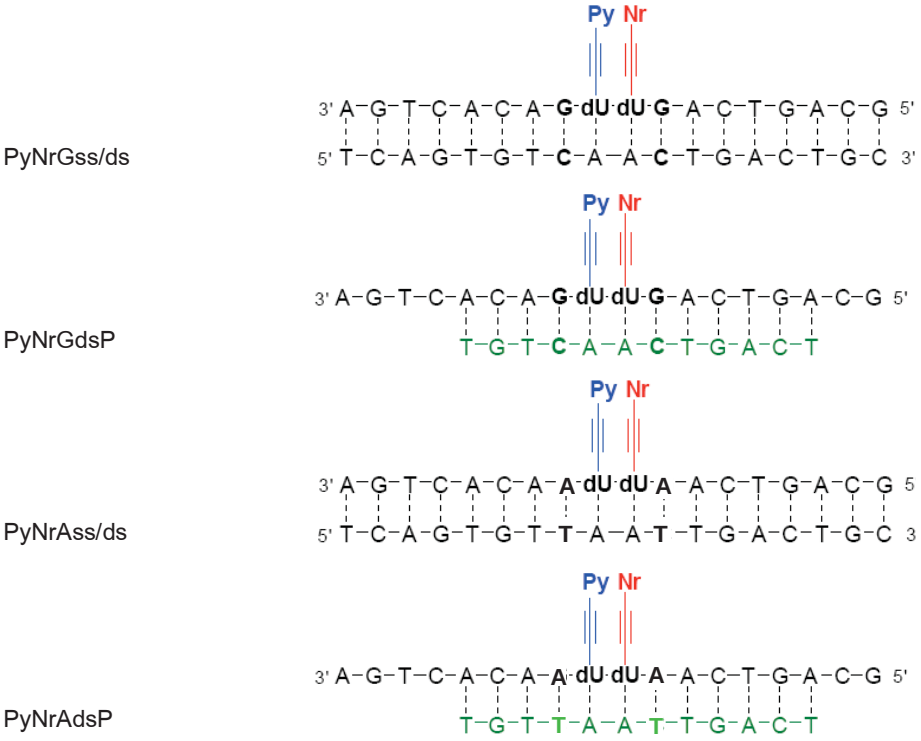

รูปที่ 9 ลำดับเบสของพีเอ็นเอและดีเอ็นเอที่ใช้ในงานวิจัยนี้

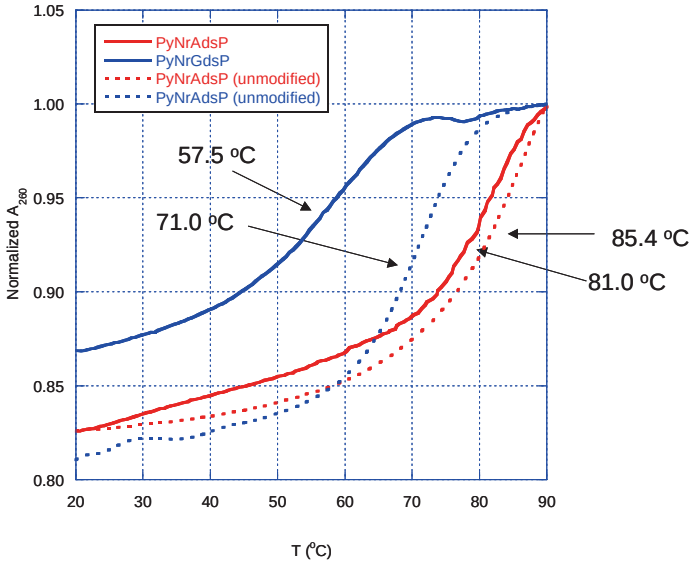

รูปที่ 10 T_m curves ของ PNA·DNA hybrid (modified vs unmodified); T_m measured at 2.5 μM duplex concentration, 10 mM sodium phosphate buffer pH 7.0, 250 mM NaCl, heaing rate 0.7 ºC /min

ในเบื้องต้นได้ทดสอบความสามารถในการเกิดไฮบริดระหว่างพีเอ็นเอกับดีเอ็นเอที่ผ่านการดัดแปลงด้วยฟลูออโรฟอร์โดยเทคนิค UV melting ซึ่งพบว่าพีเอ็นเอสามารถเกิดไฮบริดที่เสถียรกับดีเอ็นเอได้แม้ว่าจะใช้พีเอ็นเอที่มีความยาวเพียง 12 เบส เท่านั้น โดยพบว่า T_m ของ PNA·DNA hybrid ที่ผ่านการดัดแปลงด้วยฟลูออโรฟอร์จะต่ำกว่าของ PNA·DNA hybrid ที่ไม่ได้ผ่านการดัดแปลงอยู่พอสมควร (รูปที่ 7) เมื่อเปรียบเทียบกันระหว่างค่า T_m ของ PNA·DNA hybrid ด้วยกันเองจะเห็นว่าไฮบริดที่มีคู่เบส A·T อยู่ขนาบข้างฟลูออโรฟอร์ทั้งสองจะเสถียรกว่าไฮบริดที่มีคู่เบส G·C ในอยู่ตำแหน่งเดียวกัน จากนั้นจึงได้วัดการเกิดฟลูออเรสเซนส์ของดีเอ็นเอสายเดี่ยวและ PNA·DNA hybrid เปรียบเทียบกับ DNA·DNA hybrid ข้อมูลที่ได้แสดงอยู่ในรูปของ FRET ratio ซึ่งเป็นอัตราส่วนระหว่าง emission ที่ λ_{max} ของ Nile red (I_{665}) ต่อ pyrene (I_{440}) โดยตัวเลขมากจะแสดงถึงการเกิด energy transfer ที่มีประสิทธิภาพมากกว่าตัวเลขที่มีค่าน้อย (ตารางที่ 8 และรูปที่ 8)

ข้อมูลในตารางที่ 8 แสดงว่าในกรณีที่เป็น single strand DNA จะเกิด energy transfer ระหว่าง pyrene และ Nile red ได้ดี โดยพิจารณาได้จากอัตราส่วน I_{665}/I_{440} ที่มีค่าสูง (14.2–30.4) แต่เมื่อเกิดเป็น DNA·DNA hybrid ตัวเลขนี้จะลดลงอย่างมากเหลือเพียง 5.8–6.0 ส่วนในกรณีของ PNA·DNA hybrid ก็พบการลดลงของ I_{665}/I_{440} ในทำนองเดียวกัน แต่ความแตกต่างของอัตราส่วนนี้ มีช่วงที่กว้างกว่าในกรณีของดีเอ็นเอ (2.7–6.6) ซึ่งนำไปสู่สมมติฐานว่าน่าจะเกิดจากการที่คู่เบส G·C ทำให้เกิดการบิด (twist angle) มากกว่าคู่เบส A·T และสามารถนำไปสู่คำอธิบายว่าทำไมคู่เบส G·C ในพีเอ็นเอ **P1** จึงมีความเสถียรน้อยกว่าคู่เบส A·T อย่างไรก็ตามสมมติฐานนี้ยังรอการพิสูจน์จากการศึกษาโครงสร้างในสามมิติของ PNA·DNA hybrid ต่อไป ผลงานในส่วนนี้ร่วมกับงานวิจัยที่ได้ศึกษาโดยละเอียดร่วมกับ Ms. Sabrina Sezi นักศึกษาปริญญาเอกจาก Karlsruhe Institute of Technology ประเทศเยอรมันได้รับการตอบรับให้ตีพิมพ์แล้วในวารสาร ChemistryOpen [Sezi, 2012]

ตารางที่ 8 เปรียบเทียบค่า T_m และการเกิด energy transfer ในดีเอ็นเอสายเดี่ยวและไฮบริดของมัน

Sample	T_m[a]	I_{665}/I_{440}[a,b]
PyNrGss	-	14.2
PyNrGds	62.1	6.0
PyNrGds (PNA)	57.5	2.7
PyNrAss	-	30.4
PyNrAds	58.3	5.8
PyNrAds (PNA)	81.0	6.6

[a] All measurements were carried out at 2.5 μM modified DNA and 3.0 μM DNA/PNA in 10 mM sodium phosphate buffer pH 7.0, 250 mM NaCl

[b] λ_{ex} 380 nm, 20 ºC

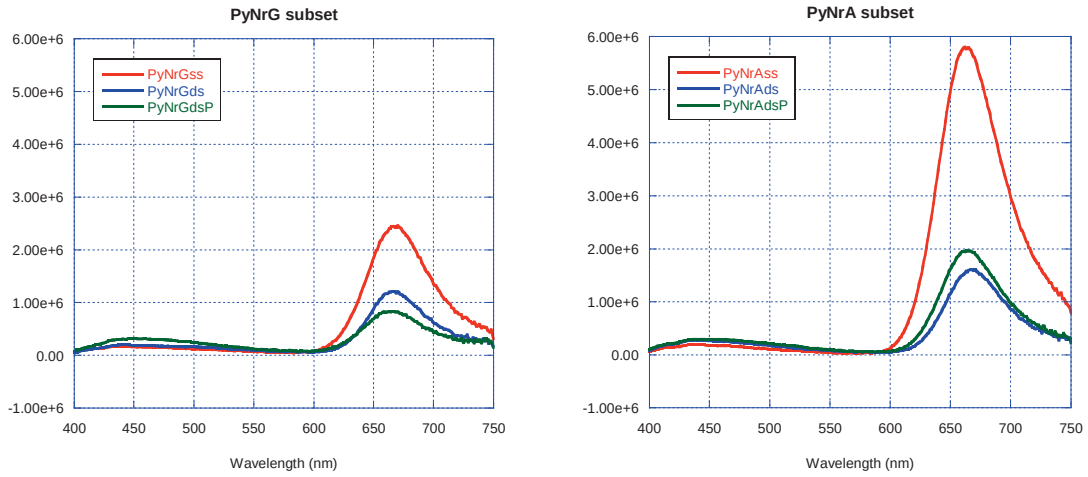

รูปที่ 10 Fluorescence spectra ของ pyrene/Nile red modified DNA (left: PyNrG, right PyNrA) และไฮบริดของมันกับ DNA และ PNA; measured at 2.5 μM duplex concentration, 10 mM sodium phosphate buffer pH 7.0, 250 mM NaCl, λ_{ex} 380 nm, 20 ºC

2.3 Synthesis and Hybridization of PNA containing fluorescent-modified uracil base

แม้ว่าการสังเคราะห์พีเอ็นเอที่ติดฉลากเรืองแสงจะได้ทำมานานแล้วในกลุ่มของผู้วิจัย แต่การติดฉลากที่เคยศึกษามาทั้งหมดจะกระทำผ่านการเกิดพันธะเอไมด์ที่ปลายด้านใดด้านหนึ่งของโมเลกุล ดังนั้นฟลูออโรฟอร์จึงอยู่ห่างไกลจากบริเวณที่เกิดพันธะไฮโดรเจนหรือการ stack ของคู่เบส ฟลูออโรฟอร์ที่ติดอยู่ในลักษณะดังกล่าวจึงมีประโยชน์เพียงแค่เป็น reporter ที่ไม่ sensitive กับการเกิดไฮบริไดเซชัน ซึ่งหากจะนำไปใช้ในการตรวจวัดการเกิดการไฮบริไดซ์กับดีเอ็นเอเป้าหมายจะต้องมีการแยกพีเอ็นเอที่เกิดการไฮบริไดซ์ออกจากที่ไม่เกิดการไฮบริไดซ์ก่อน เช่น โดยอาศัย ion exchange capture [Korkaew and Vilaivan, 2008] จึงจะสามารถตรวจวัดได้ หรือมิฉะนั้นจะต้องอาศัยเทคนิคพิเศษอื่น เช่น molecular beacon ที่จะทำให้การเรืองแสงของฟลูออโรฟอร์แตกต่างกันในสภาพก่อนและหลังการเกิดไฮบริด [Marras, 2008]

จากข้อจำกัดข้างต้น งานวิจัยในส่วนนี้จึงมีวัตถุประสงค์ที่จะสังเคราะห์ acpcPNA ที่มีเบสที่ติดฉลากด้วยฟลูออโรฟอร์ โดยมีสมมติฐานว่าการที่ฟลูออโรฟอร์อยู่ติดกับคู่เบสน่าจะทำให้ได้พีเอ็นเอเรืองแสงที่สามารถเปลี่ยนแปลงสมบัติการเรืองแสง (ความเข้ม, ความยาวคลื่น, fluorescence life time) ตามสภาวะของการเกิดไฮบริไดเซชัน ซึ่งอาจเป็นในรูปของฟลูออโรฟอร์ชนิดเดียว หรือมากกว่าหนึ่งชนิดภายใต้แนวคิดคล้ายคลึงกับ WED ที่ได้นำเสนอในหัวข้อ 2.2 โดยในเบื้องต้นได้เลือกเบสคือยูเรซิล และฟลูออโรฟอร์คือ pyrene ซึ่งมีวิธีการสังเคราะห์ซับซ้อนน้อยที่สุด และมีการศึกษากันมาค่อนข้างดีแล้วในระบบของดีเอ็นเอ [Mayer et al., 2004; Wanninger-Weiss, 2008] เป็นระบบสำหรับทดสอบ โมเลกุลของโมโนเมอร์ที่เป็นเป้าหมายเป็นดังแสดงในรูปที่ 11

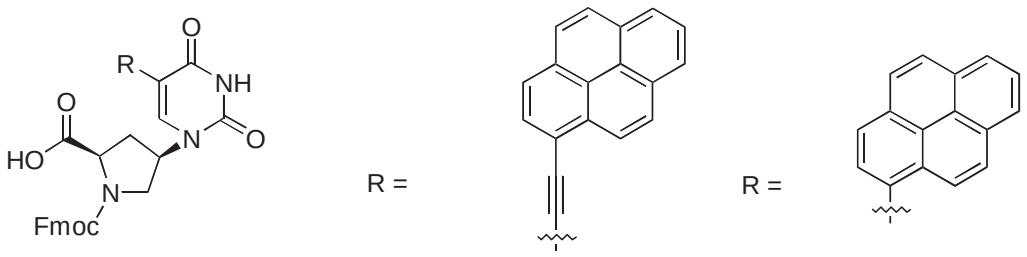

U^{CCPy} monomer **U^{Py} monomer**

รูปที่ 11 โครงสร้างของ pyrene-modified acpcPNA โมโนเมอร์

ในเบื้องต้นได้พยายามสังเคราะห์โมโนเมอร์ **U^{CCPy}** ทำตามวิธีการเดียวกับที่ใช้ในการสังเคราะห์ดีเอ็นเอโมโนเมอร์ [Mayer et al., 2004] โดยเริ่มต้นจาก protected iodouracil PNA monomer ทำปฏิกิริยา Sonogashira coupling กับ 2-ethynylpyrene ภายใต้ภาวะมาตรฐาน สามารถแยกผลิตภัณฑ์ที่ต้องการออกมาได้ในปริมาณผลผลิต 88% และสามารถเปลี่ยนหมู่ปกป้องอะมิโนจาก Boc เป็น Fmoc ได้โดยใช้วิธีการเดียวกับโมโนเมอร์อื่นๆ ที่เคยศึกษามาแล้ว แต่ปัญหาที่พบคือในขั้นตอนสุดท้ายที่จะต้องกำจัดหมู่ปกป้องคาร์บอกซิล (ไดฟีนิลเมทิลเอสเทอร์) ออกภายใต้ภาวะกรด พบว่าภายใต้ภาวะมาตรฐานที่ใช้กรดไตรฟลูออโรอะซิติกที่ความเข้มข้นต่างๆ ไม่ว่าจะมี carbocation scavenger (ในที่นี้ใช้ triethylsilane) อยู่ด้วยหรือไม่ก็ตามจะทำให้เกิดการปิดวงได้เป็น อนุพันธ์ของfuranopyrimidine ที่มีโครงสร้างดังแสดงในรูปที่ 12 โครงสร้างดังกล่าวได้จากการศึกษาโดยเทคนิค ^{1}H และ ^{13}C NMR โดยคาดว่าผลิตภัณฑ์ดังกล่าวเกิดจากการที่วงแหวน pyrene ช่วย stabilize vinyl cation ที่เกิดจากการโปรโตเนตหมู่แอลไคน์ระหว่างการทำ acidolysis ซึ่ง vinyl cation นี้จะทำปฏิกิริยาต่อกับ O^4 ของยูเรซิล จึงเกิดการปิดวงพร้อมกับการสูญเสียหมู่เบนโซอิลไป ปัจจุบันยังไม่สามารถแก้ปัญหานี้ได้ จึงยังไม่สามารถสังเคราะห์ ethynylpyrene โมโนเมอร์ **U^{CCPy}** ได้สำเร็จตามต้องการ แต่อย่างไรก็ตาม ผลิตภัณฑ์ข้างเคียงที่ได้คือ furopyrimidine นั้นก็มีความน่าสนใจเนื่องจากมันสามารถเรืองแสงได้ และมีรายงานว่า furanopyrimidine สามารถเกิดคู่เบสกับ G ได้แม้จะไม่ค่อยเสถียรนักก็ตาม [Lahoud et al. 2008; Woo et al 1996]

สำหรับการสังเคราะห์พีเอ็นเอโมโนเมอร์ **U^{Py}** ที่มีวงแหวนไพรีนต่อตรงกับตำแหน่ง 5 ของยูเรซิลสามารถทำได้โดยใช้ปฏิกิริยา Suzuki-Miyura cross coupling ระหว่าง iodouracil monomer กับ pyrene 1-boronic acid เดียวกับการสังเคราะห์ดีเอ็นเอโมโนเมอร์ [Amann and Wagenknecht, 2002] ดังแสดงในรูปที่ 13 จากนั้นจึงได้ทดลองสังเคราะห์ acpcPNA ที่มีลำดับเบสเป็น $T_4U^{Py}T_4$ (**PNA1**) โดยวิธีการมาตรฐานเช่นเดียวกับพีเอ็นเอโมโนเมอร์ปกติ พีเอ็นเอที่ได้แสดงค่า *m/z* (MALDI-TOF) ซึ่งสอดคล้องกับผลิตภัณฑ์ที่ต้องการ ($M{\cdot}H^+$ calcd. *m/z* 3365.6, found 3366.8) ผลการทดสอบการไฮบริไดซ์กับดีเอ็นเอที่มีลำดับเบสเป็น dA_4XA_4 เป็นดังแสดงในรูปที่ 14 เมื่อพิจารณาค่า T_m ในกรณีที่ X = A (complementary) แสดงให้เห็นว่าการ modify ตำแหน่งที่ 5 ของยูเรซิลด้วย pyrene จะทำให้ความแข็งแรงของคู่เบส $U^{Py}{\cdot}A$ น้อยกว่าคู่เบส T·A ปกติ (T_m $pT_9{\cdot}dA_9$ ~ 73 ºC ภายใต้ภาวะเดียวกัน) เนื่องมาจากอิทธิพลของ steric effect ของหมู่ pyrene จึงรบกวนกับการเกิด PNA·DNA duplex อย่างไรก็ตาม เป็นที่น่ายินดีว่าหน่วยเบส PyU ในพีเอ็นเอที่ผ่านการดัดแปลงด้วย U^{Py} โมโนเมอร์ยังแสดงสมบัติการเลือกจดจำเฉพาะกับเบส A เช่นเดียวกับเบส T หรือ U ตามปกติ อันจะเห็นได้จาก sigmoidal melting transition ที่มี T_m ~ 60 ºC เฉพาะในกรณีที่ X = A แต่เมื่อ X เป็นเบสอื่นจะไม่เห็นการเกิด melting แสดงว่าไม่เกิดการไฮบริดเมื่อเบสไม่เป็นคู่สมกัน งานที่จะทำต่อไปคือการศึกษาสมบัติการเรืองแสงของพีเอ็นเอที่ผ่านการดัดแปลงด้วยเบส U^{Py} ทั้งในสภาพที่เป็นสายเดี่ยว และเมื่อมีดีเอ็นเอที่มีลำดับเบสเป็นคู่สมและไม่เป็นคู่สมกัน

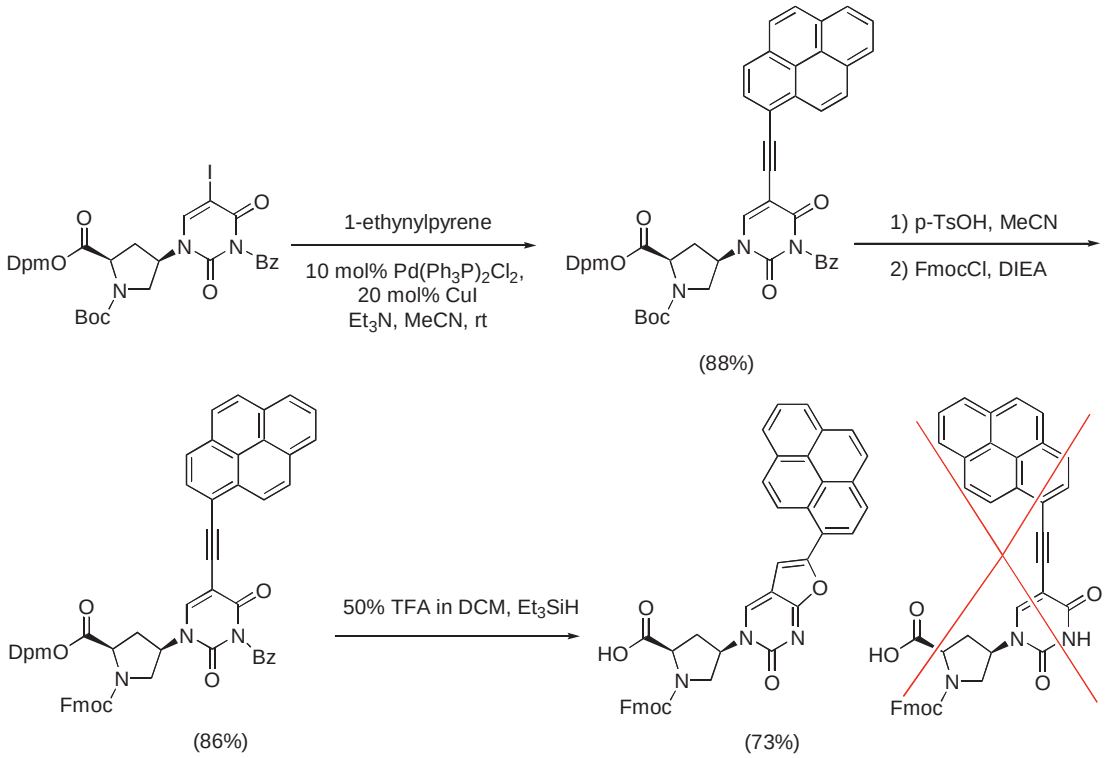

รูปที่ 12 แผนการสังเคราะห์พีเอ็นเอโมโนเมอร์ $\mathbf{U}^{\mathbf{CCPy}}$

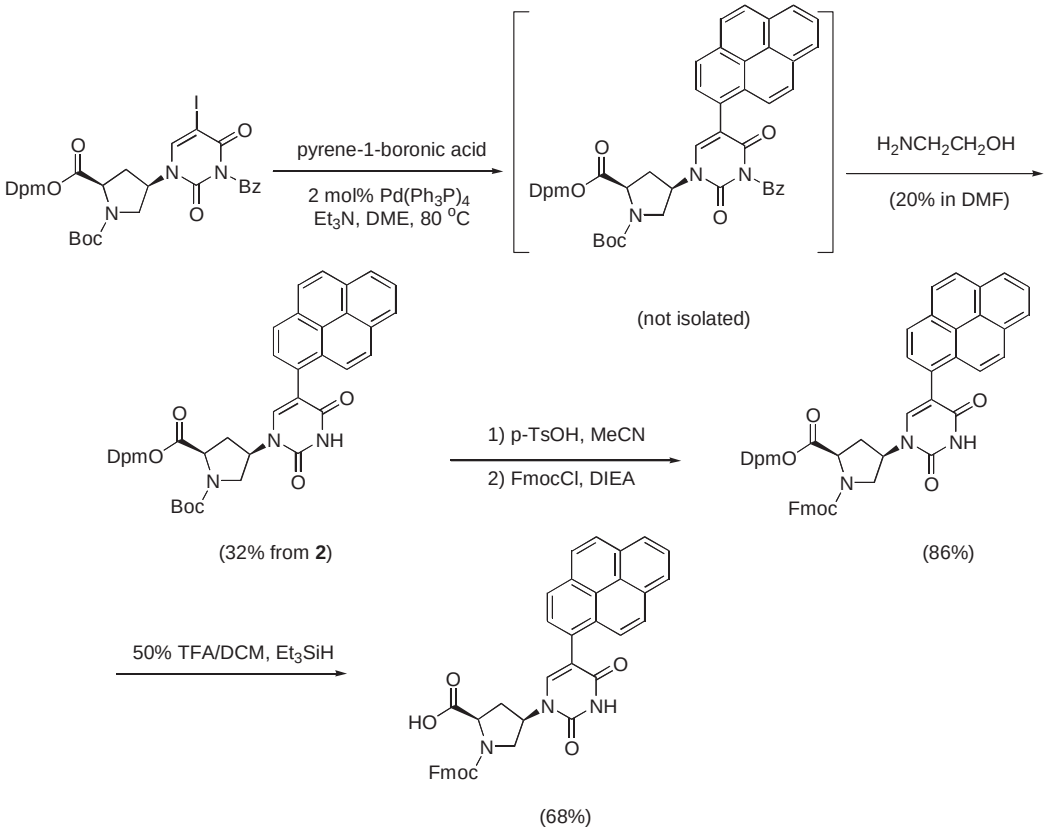

รูปที่ 13 การสังเคราะห์พีเอ็นเอโมโนเมอร์ $\mathbf{U}^{\mathbf{Py}}$

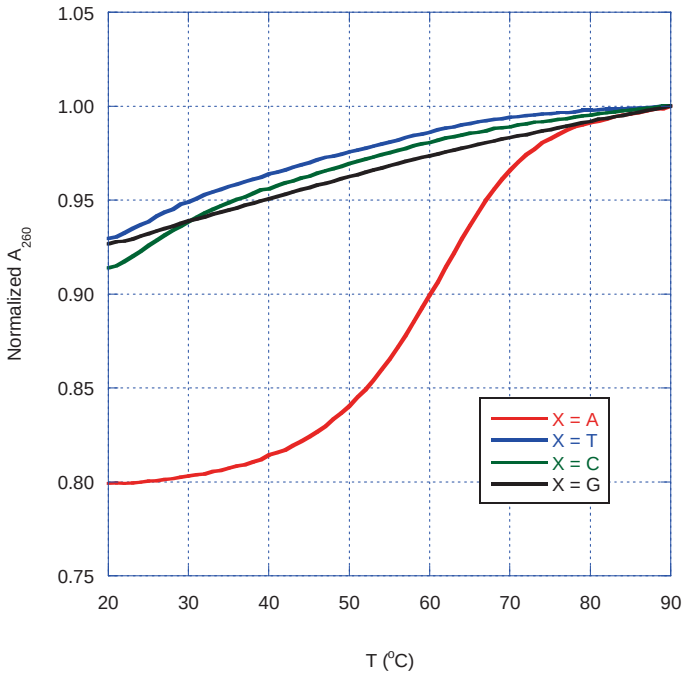

รูปที่ 14 T_m curves ของ PNA·DNA hybrid (pT_4PyUT_4 vs dA_4XA_4; X = A,T,C,G); T_m measured at 2.5 μM duplex concentration, 10 mM sodium phosphate buffer pH 7.0, 250 mM NaCl, heating rate 0.7 ºC/min.

งานที่ได้ทำต่อมาคือการศึกษาสมบัติการจับยึดกับดีเอ็นเอ และสมบัติการเรืองแสงของพีเอ็นเอที่ผ่านการดัดแปลงด้วยเบส U^{Py} ที่มีลำดับเบสที่หลากหลายมากขึ้นทั้งในสภาพที่เป็นสายเดี่ยว และเมื่อมีดีเอ็นเอที่มีลำดับเบสเป็นคู่สมและไม่เป็นคู่สมกัน U^{Py}-modified acpcPNA และดีเอ็นเอที่ใช้ในการศึกษาทั้งหมดมีลำดับเบสดังสรุปในรูปที่ 15 โครงสร้างของพีเอ็นเอทุกตัวที่สังเคราะห์ได้รับการพิสูจน์ทราบโดยเทคนิค MALDI-TOF mass spectrometry ผลการทดสอบการไฮบริไดซ์ระหว่าง **PNA1** ซึ่งมีลำดับเบสเป็น $T_4U^{Py}T_4$ กับดีเอ็นเอที่มีลำดับเบสเป็น dA_4XA_4 แสดงให้เห็นว่าเบส U^{Py} ใน acpcPNA สามารถจดจำเบส A ในดีเอ็นเอได้อย่างจำเพาะเจาะจง แต่ความแข็งแรงของคู่เบส U^{Py}·A จะน้อยกว่าคู่เบส T·A ปกติ (T_m pT_9·dA_9 ~ 73 ºC เทียบกับ T_m **PNA1**·dA_9 ~ 66 ºC ภายใต้ภาวะเดียวกัน ดูตารางที่ 1) คาดว่าเนื่องมาจากอิทธิพลของ steric effect ของหมู่ pyrene เมื่อพิจารณาที่ absorption spectrum ของ **PNA1** (รูปที่ 16A) จะพบสัญญาณของหน่วยไพรีนที่มีลักษณะ broad และมี λ_{max} อยู่บริเวณ 345 nm ซึ่งสอดคล้องกับ absorption spectra ของดีเอ็นเอที่มี U^{Py} เบสซึ่งเคยมีผู้ศึกษามาก่อนหน้านี้ [Wanninger-Weiss and Wagenknecht, 2008] เมื่อเกิดไฮบริดกับดีเอ็นเอ เฉพาะ **DNA1** ที่มีลำดับเบสเป็นคู่สมเท่านั้นที่มีการเปลี่ยนแปลงของ absorption spectrum ในส่วนของไพรีนอย่างชัดเจน กล่าวคือสเปกตรัมจะมีลักษณะ broad มากขึ้น shoulder ที่บริเวณ 340 nm หายไป และเกิด bathochromic shift ของ λ_{max} ไปที่บริเวณ 345 nm พร้อมกับเกิด hyperchromism ลักษณะของสเปกตรัมที่เปลี่ยนไปนี้บ่งชี้ว่ามีการเปลี่ยนแปลงของ electronic transition ใน U^{Py} โครโมฟอร์หลังการเกิดไฮบริด ที่อุณหภูมิสูงกว่าค่า T_m สเปกตรัมนี้จะกลับคืนมาเหมือนของ **PNA1** ที่เป็นสายเดี่ยว และเมื่อทำให้เย็นลงอีกครั้งก็จะได้สเปกตรัมของไฮบริดกลับคืนมา แสดงว่าการเปลี่ยนแปลงลักษณะของสเปกตรัมนี้สามารถผันกลับได้ เมื่อพิจารณา fluorescence spectrum ของ **PNA1** (รูปที่ 16B) พบว่าในสภาพที่เป็นสายเดี่ยวมีการเรืองแสงที่ต่ำมากเมื่อ excited ที่ 350 nm โดยมีค่า quantum yield (Φ_F) เพียง 0.006 แต่เมื่อเกิดไฮบริดกับ dA_9 การเรืองแสงจะเพิ่มขึ้นอย่างมาก โดยมี maximum emission

อยู่ที่ 465 nm ค่าการเรืองแสงที่เพิ่มขึ้นเมื่อ **PNA1** เปลี่ยนจากสภาพที่เป็นสายเดี่ยวเป็นไฮบริดสูงถึง 42 เท่า (วัดที่ 465 nm) และค่า quantum yield (Φ_F) จะเพิ่มสูงขึ้นถึง 0.130 (ตารางที่ 1) ส่วนในกรณีอื่นที่ดีเอ็นเอไม่เป็นคู่สม (มี single mismatched base ในตำแหน่งที่ตรงกับเบส U^{Py}) นอกจากจะไม่สามารถวัดค่า T_m ได้ (เนื่องจากไม่เกิดไฮบริด หรือเกิดไฮบริดที่มีความเสถียรต่ำมาก) แล้ว การเพิ่มขึ้นของการเรืองแสงก็เกิดขึ้นในระดับที่ต่ำกว่ากรณีที่เป็นดีเอ็นเอคู่สมมาก (3.0–8.7 เท่า) คิดเป็นอัตราส่วนของการเรืองแสงระหว่างกรณีที่เป็นดีเอ็นเอคู่สมเทียบกับเมื่อเป็น single mismatched อยู่ที่ระหว่าง 4.8–13 เท่า โดยการเปลี่ยนแปลงการเรืองแสงนี้สามารถสังเกตเห็นได้ด้วยตาเปล่าอย่างชัดเจนภายใต้แสง UV (black light) (รูปที่ 17)

(N) T–T–T–X–U^{Py}–X–T–T–T (C)	**PNA1**: X = T; **PNA2**: X = A; **PNA3**: X = G; **PNA4**: X = C
(3') A–A–A–Y– Z –Y–A–A–A (5')	**DNA1a**: Y = A; Z = A; **DNA1b**: Y = A; Z = T **DNA1c**: Y = A; Z = C; **DNA1d**: Y = A; Z = G **DNA2**: Y = T; Z = A; **DNA3**: Y = C; Z = A **DNA4**: Y = G**;** Z = A
(N) T–T–T–T–T–C–U^{Py}–C–T–T–T–T–T–T (C)	**PNA5**
(3') A–A–A–A–A–G– T –G–A–A–A–A–A–A (5')	**DNA5**
(N) A–G–T–T–A–U^{Py}–C–C–C–T–G–C (C)	**PNA6**
(3') T–C–A–A–T– X – Y –G–G–A–C–G (5')	**DNA6a**: X = A; Y = G (complementary) **DNA6b**: X = C; Y = G (C mismatch) **DNA6c**: X = G; Y = G (G mismatch) **DNA6d**: X = T; Y = G (T mismatch) **DNA6e**: X = A; Y = A (indirect mismatched) **DNA6f**: X = G; Z = A (double mismatched)
(N) C–T–A–A–X–U^{Py}–T–C–A–G–A (C)	**PNA7**: X = A; **PNA8**: X = T
(3') G–A–T–T–Y– A – A –G–T–C–T (5')	**DNA7**: Y = T; **DNA8**: Y = A
(N) U^{Py}–T–T–T–T–T–T–T–T–T (C)	**PNA9**
(3') A –A–A–A–A–A–A–A–A–A (5')	**DNA9**

รูปที่ 15 ลำดับเบสของพีเอ็นเอและดีเอ็นเอที่ใช้ในงานวิจัยนี้

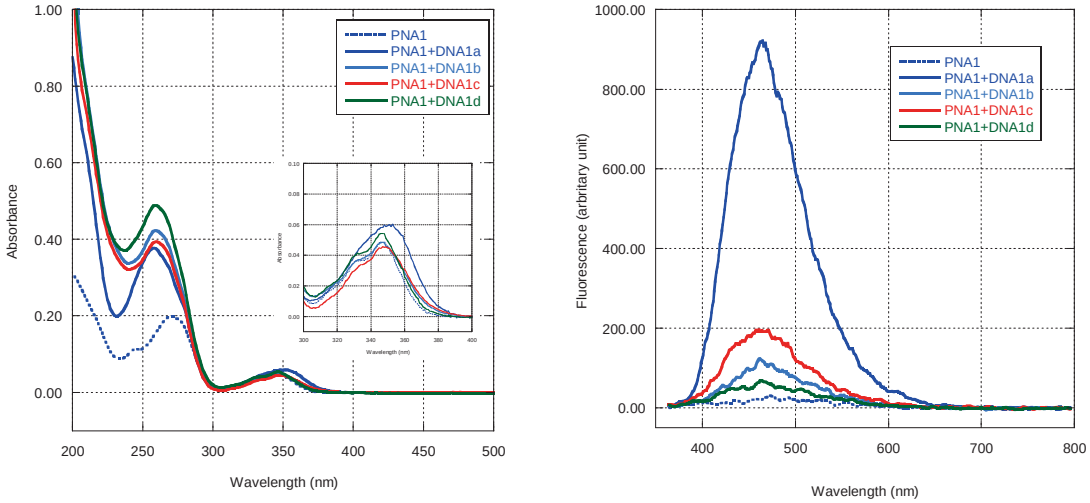

A B

รูปที่ 16 Absorption (A) และ fluorescence spectra (B) ของ **PNA1** และไฮบริดของมันกับ **DNA1a–1d** conditions: 2.5 μM PNA, 3.0 μM DNA, 10 mM sodium phosphate buffer pH 7.0, λ_{excit} = 350 nm.

ตารางที่ 9 สรุปค่า T_m และสมบัติเชิงแสงของ **PNA1** และไฮบริดของมันกับดีเอ็นเอ

Entry	System	T_m (°C)[a]	Φ_F[b]	$I_{465}(ds)/I_{465}(ss)$[c]	Note
1	**PNA1**	-	0.006	-	ss, $TU^{Py}T$
2	**PNA1+DNA1a**	65.8	0.131	41.9	ds, complementary
3	**PNA1+DNA1b**	< 20	0.022	5.3	ds, mismatched
4	**PNA1+DNA1c**	< 20	0.039	8.7	ds, mismatched
5	**PNA1+DNA1d**	< 20	0.013	3.0	ds, mismatched

[a] conditions: 2.5 μM PNA, 3.0 μM DNA, 10 mM Sodium phosphate buffer pH 7.0

[b] measured using quinine sulfate (Φ_F = 0.546) as standard, λ_{excit} = 350 nm

[c] non-two-state melting curve

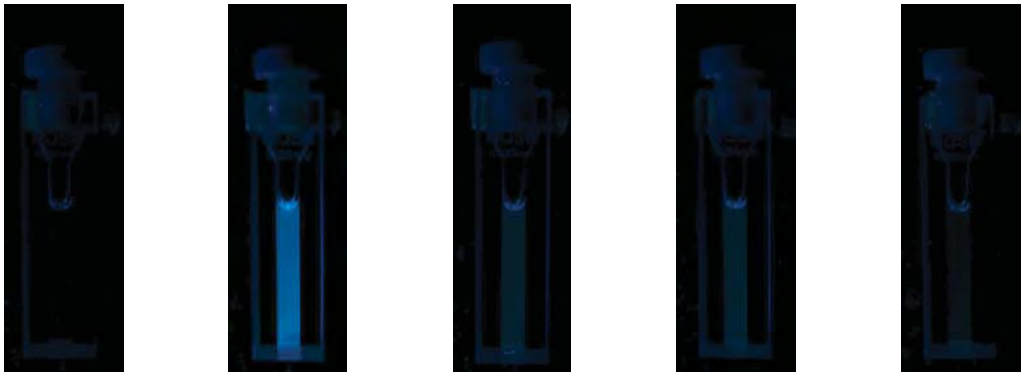

PNA1 **PNA1+DNA1a** **PNA1+DNA1b** **PNA1+DNA1c** **PNA1+DNA1d**

รูปที่ 17 ภาพถ่ายภายใต้ UV light เพื่อเปรียบเทียบการเรืองแสงของ **PNA1** และไฮบริดของมันกับ **DNA1a–1d** conditions: 2.5 μM PNA, 3.0 μM DNA, 10 mM Sodium phosphate buffer pH 7.0.

การศึกษาค่า T_m แสดงให้เห็นว่า **PNA4** ที่มีเบสข้างเคียงหมู่ U^{Py} เป็น C/C นั้นไม่เกิดไฮบริดกับดีเอ็นเอที่มีลำดับเบสคู่สม แสดงว่าการเรืองแสงที่ไม่เปลี่ยนแปลงอย่างชัดเจนนี้น่าจะเกิดจากการที่พีเอ็นเอไม่สามารถเกิดไฮบริด ไม่ใช่ไฮบริดที่เกิดขึ้นไม่เรืองแสง ซึ่งไม่เป็นที่น่าประหลาดใจเท่าใดนักเนื่องจากผลการศึกษาในระบบ acpcPNA ได้พบมาก่อนหน้านี้แล้วว่าเมื่อพีเอ็นเอชนิดนี้มีเบส TC หรือ C/T ในตำแหน่งที่ติดกันความเสถียรของไฮบริดที่เกิดขึ้นกับดีเอ็นเอคู่สมจะต่ำกว่าปกติ โดยในกรณีที่ของพีเอ็นเอ T_4CT_4 ที่ไม่ได้มีการดัดแปลงใดๆ จะมี T_m ของไฮบริดกับดีเอ็นเอคู่สม (A_4GA_4) อยู่ที่ 53.5 ºC เทียบกับพีเอ็นเอ T_9 ซึ่งมี T_m ของไฮบริดกับดีเอ็นเอคู่สมสูงถึง 76.8 C (1 μM PNA, 0 mM NaCl in 10 mM sodium phosphate buffer) [Srisuwannaket and Vilaivan, 2006] การเพิ่มหมู่ไพรีนเข้าไปยิ่งทำให้ความเสถียรของไฮบริดที่เกิดขึ้นลดลงไปอีก เพื่อแก้ปัญหานี้จึงต้องเพิ่ม T เข้าไปที่ปลายทั้งสองด้านของ **PNA4** ให้เป็น **PNA5** ที่มีความยาว 13 เบส พบว่าในกรณีของ **PNA5** นี้สามารถเกิดไฮบริดที่เสถียรกับดีเอ็นเอคู่สมได้ และไฮบริดที่เกิดขึ้นมีการการเรืองแสงที่เพิ่มขึ้นจากเมื่อเป็นสายเดี่ยวอย่างชัดเจน เมื่อเปรียบเทียบความสามารถในการเรืองแสงของไฮบริดจะอยู่ที่ T/T>>C/C~A/A>G/G ซึ่งค่อนข้างสอดคล้องกับ redox potential ของเบสข้างเคียง (T – most easily reduced, G – most easily oxidized) [Manoharan et al, 1995] แม้การเรืองแสงของ U^{Py} ฟลูออโรฟอร์ในพีเอ็นเอทั้งในสภาพสายเดี่ยวและไฮบริด รวมทั้งการเปลี่ยนแปลงการเรืองแสงจะขึ้นอยู่กับเบสข้างเคียง แต่ผลที่ได้ก็แสดงให้เห็นว่าในทุกกรณีจะมีการเปลี่ยนแปลงการเรืองแสงในทิศทางเดียวกันคือการเรืองแสงจะเพิ่มขึ้นเมื่อเกิดไฮบริด (fluorescence turn-on) ซึ่งเป็นลักษณะที่ไม่พบเสมอไปนักในดีเอ็นเอที่มีเบสเรืองแสงชนิดอื่นๆ

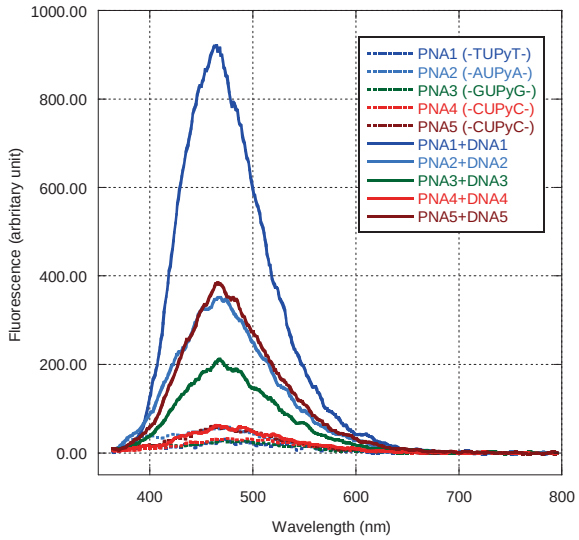

รูปที่ 18 Fluorescence spectra ของ **PNA2–5** และไฮบริดของมันกับ **DNA2–5** conditions: 2.5 μM PNA, 3.0 μM DNA, 10 mM Sodium phosphate buffer pH 7.0, λ_{excit} = 350 nm.

แม้ผลการศึกษากับ **PNA1** จะเป็นที่น่าพอใจ แต่ในการใช้งานจริงพีเอ็นเอหรือดีเอ็นเอที่เกี่ยวข้องจะมีลำดับเบสที่ซับซ้อนกว่านี้มาก การทดลองต่อไปจึงได้ศึกษากับพีเอ็นเอที่ลำดับเบสผสม **PNA6** ที่มีเบส U^{Py} อยู่ตรงกลางสาย (ระหว่างเบส A และ C) พบว่าเมื่อเกิดการไฮบริไดซ์กับ **DNA6a** ซึ่งมีลำดับเบสคู่สมกันจะมีการเรืองแสงเพิ่มขึ้นถึง 6.5 เท่า เมื่อเทียบกับ **PNA6** ในสภาพที่เป็นสายเดี่ยว ในขณะที่การไฮบริไดซ์กับ single mismatched DNA targets **DNA6b–6d** ที่มี mismatched base ตรงกับตำแหน่งของ U^{Py} พอดีจะไม่ทำให้การเรืองแสงเปลี่ยนแปลงไปมากนัก โดย G-mismatched จะทำให้เกิดการเรืองแสงเพิ่มขึ้นมากที่สุดเมื่อเทียบกับ

mismatched base อื่นๆ คือ 1.6 เท่าเมื่อเทียบกับ **PNA6** สายเดี่ยว แต่ก็ยังมีความแตกต่างจาก complementary target อย่างชัดเจน ดังนั้นจึงสามารถสรุปได้ว่าเบส U^{Py} ใน acpcPNA แสดงความเป็น base discriminating fluorophore (BDF) กล่าวคือสามารถแยกแยะความแตกต่างระหว่างเบส A ซึ่งเป็นเบสคู่สมของมัน กับเบสอื่นในดีเอ็นเอเป้าหมายได้ โดยไม่ขึ้นกับเบสข้างเคียง

ตารางที่ 10 T_m และสมบัติเชิงแสงของ **PNA2–5** และไฮบริดของมันกับดีเอ็นเอ

Entry	System	T_m (°C)[a]	Φ_F[b]	$I_{465}(ds)/I_{465}(ss)$[c]	Note
1	**PNA2**	-	0.011	-	ss, $AU^{Py}A$
2	**PNA2+DNA2**	60.2	0.051	6.2	ds, complementary
3	**PNA3**	-	0.006	-	ss, $GU^{Py}G$
4	**PNA3+DNA3**	54.1	0.032	8.3	ds, complementary
5	**PNA4**	-	0.006	-	ss, $CU^{Py}C$
6	**PNA4+DNA4**	< 20	0.010	2.0	ds, complementary
7	**PNA5**	-	0.009	-	ss, $CU^{Py}C$ (extended)
8	**PNA5+DNA5**	72.7	0.048	6.8	ds, complementary

[a] conditions: 2.5 μM PNA, 3.0 μM DNA, 10 mM Sodium phosphate buffer pH 7.0

[b] measured using quinine sulfate (Φ_F = 0.546) as standard, λ_{excit} = 350 nm

[c] non-two-state melting curve

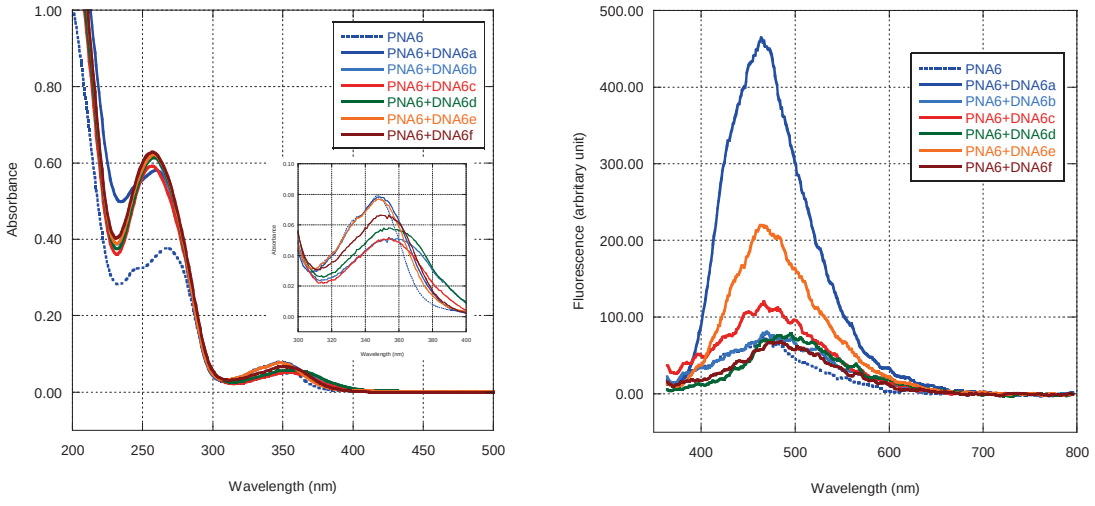

(A) (B)

รูปที่ 19 Absorption (A) และ fluorescence spectra (B) ของ **PNA6** และไฮบริดของกับ **DNA6a–6f** conditions: 2.5 μM PNA, 3.0 μM DNA, 10 mM sodium phosphate buffer pH 7.0, λ_{excit} = 350 nm.

ตารางที่ 11 T_m และสมบัติเชิงแสงของ **PNA6–8** และไฮบริดของมันกับดีเอ็นเอ

Entry	System	T_m (ºC)[a]	Φ_F[b]	$I_{465}(ds)/I_{465}(ss)$	Note
1	**PNA6**	-	0.009	-	ss, $AU^{Py}C$
2	**PNA6+DNA6a**	66.3	0.052	6.5	ds, complementary
3	**PNA6+DNA6b**	54.3	0.018	1.1	ds, C mismatch
4	**PNA6+DNA6c**	54.2	0.025	1.6	ds, G mismatch
5	**PNA6+DNA6d**	54.5	0.014	1.0	ds, T mismatch
6	**PNA6+DNA6e**	46.1	0.029	3.1	ds, indirect mismatched
7	**PNA6+DNA6f**	40.0	0.011	0.8	ds, double mismatched
8	**PNA7**	-	0.030	-	ss, $AU^{Py}T$
9	**PNA7+DNA7**	-[c]	0.066	2.7	ds, complementary
10	**PNA8**	-	0.027	-	ss, $TU^{Py}T$
11	**PNA8+DNA8**	-[c]	0.084	4.0	ds, complementary

[a] conditions: 2.5 μM PNA, 3.0 μM DNA, 10 mM Sodium phosphate buffer pH 7.0

[b] measured using quinine sulfate (Φ_F = 0.546) as standard, λ_{excit} = 350 nm

[c] non-two-state melting curve

เมื่อพิจารณา absorption spectra ของ **PNA6** และไฮบริดของมันกับ **DNA6a–6d** (รูปที่ 19 และตารางที่ 11) พบว่าสเปกตรัมในบริเวณการดูดกลืนของไพรีนของพีเอ็นเอ-ดีเอ็นเอไฮบริดจะแตกต่างจากของพีเอ็นเอสายเดี่ยว และสเปกตรัมของไฮบริดที่เป็นคู่สม (**DNA6a**) จะแตกต่างจากกรณีที่เป็น single mismatched hybrid อย่างชัดเจน โดยในกรณีของไฮบริดที่เป็นคู่สมสเปกตรัมจะมี λ_{max} ที่เคลื่อนไปทางความยาวคลื่นที่เพิ่มขึ้น (bathaochromic shift) เพียงเล็กน้อยและพีกมีลักษณะกว้างมากขึ้น ในขณะที่ไฮบริดที่ไม่เป็นคู่สมจะมีการเปลี่ยนแปลงที่ชัดเจนมาก คือจะมี bathochromic shift ที่ชัดเจนกว่า (λ_{max}~355 nm) และเกิด hypochromism ด้วย ลักษณะการเกิด bathochromic shift และ hypochromism นี้เสนอแนะว่าหน่วยของไพรีนอาจเกิดการซ้อนทับ (stacking) กับคู่เบสที่อยู่ข้างเคียงได้ ซึ่งมีลักษณะใกล้เคียงกับที่พบในดีเอ็นเอที่มีเบส U^{Py} แต่ในกรณีของดีเอ็นเอที่เคยมีผู้ศึกษามาแล้วนั้นพบว่า U^{Py} ไม่แสดงสมบัติการเป็น BDF กล่าวคือไม่ว่าเบสที่อยู่ตรงข้ามกับ U^{Py} จะเป็นอะไรก็จะมีการเปลี่ยนแปลงของ absorption และ fluorescence spectrum ในลักษณะเดียวกัน [Wanninger-Weiss and Wagenknecht, 2008] ซึ่งเสนอแนะว่าเบส U^{Py} ในดีเอ็นเอน่าจะอยู่ในลักษณะที่หันเอาด้านไพรีนเข้าไปซ้อนกับคู่เบสในทุกกรณี เนื่องจากพลังงานของระบบที่ลดลงจากการซ้อนทับกันนี้มีค่ามากกว่าพลังงานที่ลดลงจากการเกิดพันธะไฮโดรเจนและการซ้อนทับของส่วน U ในเบส U^{Py} กับคู่เบสอื่นที่อยู่ข้างเคียง (การเกิดพันธะไฮโดรเจนและการซ้อนทับกันของไพรีนกับคู่เบสไม่สามารถเกิดพร้อมกันได้เนื่องจากทั้งสองส่วนอยู่คนละด้านกันของโมเลกุล) แต่เบส U^{Py} ใน acpcPNA จะแสดงพฤติกรรมการซ้อนทับของไพรีนกับคู่เบสเฉพาะเมื่อเบสที่อยู่ตรงข้ามไม่ใช่ A ซึ่งบ่งชี้ว่าความแข็งแรงของคู่เบส U^{Py}-A ในระบบ acpcPNA มีมากกว่าดีเอ็นเอปกติ และทำให้มันสามารถแสดงสมบัติเป็น BDF ได้

เป็นที่น่าสังเกตว่าไฮบริดระหว่าง **PNA6** กับดีเอ็นเอเป้าหมายเป็น single mismatched target แต่เบสที่ mismatched นั้นไม่ได้อยู่ตรงกันกับ U^{Py} เช่น **DNA6e** นั้นจะมีการเรืองแสงเพิ่มขึ้นอย่างมากเมื่อเทียบกับ **PNA6** ที่เป็นสายเดี่ยว ทั้งๆ ที่ความเสถียรของ **PNA6·DNA6e** นั้นน้อยกว่า คู่ mismatched อื่นๆ ที่มีเบสที่ไม่เป็นคู่สม

ตรงกับตำแหน่งของ U^{Py} (พิจารณาจาก T_m) นอกจากนี้ electronic absorption spectrum ของไฮบริด **PNA6·DNA6e** จะมีลักษณะคล้ายคลึงกับของไฮบริด **PNA6·DNA6a** ซึ่งเป็นคู่สมกันมาก แสดงว่าการเปลี่ยนแปลงการเรืองแสงขึ้นกับการเกิดพันธะไฮโดรเจนระหว่าง U^{Py}-A และการซ้อนทับกันของคู่เบส U^{Py}-A กับเบสข้างเคียง โดยไม่เกี่ยวข้องกับความเสถียรของไฮบริดที่เกิดขึ้นโดยรวม และเมื่อดีเอ็นเอเป้าหมายเป็น double mismatched DNA การเปลี่ยนแปลงการเรืองแสงจะเป็นไปในทิศทางตรงกันข้าม กล่าวคือการเรืองแสงจะลดลงไปอีกเมื่อเทียบกับในสภาพที่เป็นสายเดี่ยว

ในอีกตัวอย่างหนึ่งที่แสดงให้เห็นความสามารถของ U^{Py} ในการเป็น BDF ในระบบของ acpcPNA ได้แก่ **PNA7** และ **PNA8** ซึ่งมีเบส U^{Py} อยู่ระหว่างเบส A/T และ T/T ตามลำดับ พบว่าในทั้งสองกรณีก็สังเกตเห็นการเปลี่ยนแปลงการเรืองแสงเช่นเดียวกัน (ตารางที่ 11 และรูปที่ 20) แม้ว่าการเพิ่มขึ้นจะไม่ชัดเจนเท่ากับในกรณีที่ผ่านมา เนื่องจากในกรณีนี้พีเอ็นเอในสภาพที่เป็นสายเดี่ยวทั้งสองตัวมีการเรืองแสงค่อนข้างสูง แสดงให้เห็นว่าการเรืองแสงของพีเอ็นเอในสภาพที่เป็นสายเดี่ยวก็มีความความสัมพันธ์กับลำดับเบสของมัน โดยอาจจะมีขอบเขตที่จะต้องพิจารณามากกว่าเฉพาะคู่เบสที่อยู่ติดกัน เนื่องจากเมื่อเทียบกันระหว่าง **PNA8** กับ **PNA1** ซึ่งมีคู่เบสที่อยู่ติดกับ U^{Py} เป็น T/T เหมือนกันแต่กลับมีการเรืองแสงในสภาพที่เป็นสายเดี่ยวแตกต่างกันมาก ขณะนี้กำลังอยู่ระหว่างการศึกษาอิทธิพลของลำดับเบสที่มีต่อการเรืองแสงทั้งของพีเอ็นเอสายเดี่ยวและเมื่อเป็นไฮบริดกับดีเอ็นเอ ซึ่งจะเป็นแนวทางในการพัฒนาพีเอ็นเอที่สามารถเปลี่ยนแปลงการเรืองแสงได้อย่างชัดเจนมากยิ่งขึ้น

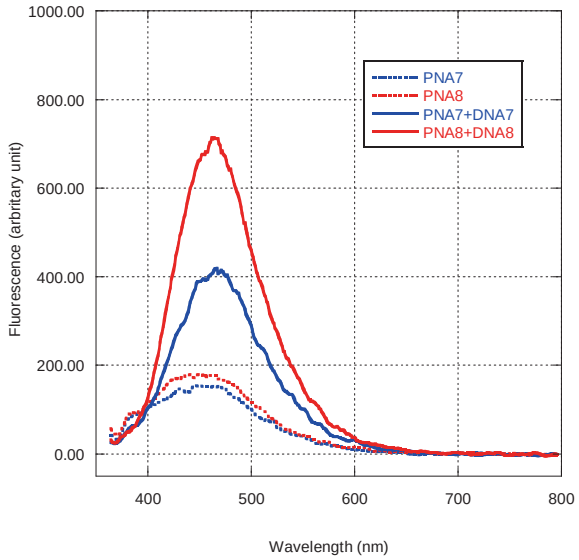

รูปที่ 20 Fluorescence spectra ของ **PNA7–8** และไฮบริดของมันกับ **DNA7–8** conditions: 2.5 μM PNA, 3.0 μM DNA, 10 mM Sodium phosphate buffer pH 7.0, λ_{excit} = 350 nm.

จากข้อมูลที่แสดงในข้างต้นทั้งหมดสามารถได้ข้อสรุปที่ชัดเจนว่าเบส U^{Py} สามารถทำหน้าที่เป็น BDF ในระบบ acpcPNA ได้ โดยที่ U^{Py} กับ A จะทำให้การเรืองแสงเพิ่มขึ้นตั้งแต่ 2.7 – 42 เท่า ขึ้นกับลำดับเบสของพีเอ็นเอ ในขณะที่การเข้าคู่ของ U^{Py} กับเบสอื่นจะมีผลให้มีการเปลี่ยนแปลงการเรืองแสงน้อยมาก จึงสามารถนำมาใช้เป็นโมเลคิวลาร์บีคอนที่ไม่ต้องอาศัยตัวดับการเรืองแสง (quencher) ซึ่งงานส่วนนี้ได้รับการตีพิมพ์แล้ว [Boonlua et al., 2011] งานที่ได้ทำต่อมาคือการศึกษาสมบัติเชิงแสงของ acpcPNA ที่มี U^{py} เบสเพิ่มเติมเพื่อที่จะหาความสัมพันธ์ระหว่างลำดับเบสกับการเรืองแสง ซึ่งจะนำไปสู่ความเข้าใจของกลไกของการเกิดการเปลี่ยนแปลง

การเรืองแสง และการพัฒนาพีเอ็นเอโพรบที่มีความแตกต่างของการเรืองแสงในสภาพที่เป็นสายเดี่ยวและเมื่อเกิดไฮบริดกับดีเอ็นเอได้ดียิ่งขึ้น

เมื่อพิจารณาข้อมูลการเรืองแสงของระบบพีเอ็นเอที่มี U^{py} เบสในสภาพที่เป็นสายเดี่ยวเทียบกับที่เป็นไฮบริดกับดีเอ็นเอคู่สมพบว่า ในกรณีที่มีการเปลี่ยนแปลงการเรืองแสงน้อยส่วนใหญ่จะเกิดจากการที่พีเอ็นเอในสภาพที่เป็นสายเดี่ยวมีการเรืองแสงค่อนข้างสูง ตัวอย่างเปรียบเทียบที่น่าสนใจคือ **PNA1** (TTTTU^{py}TTTT) และ **PNA8** (CTAATU^{py}TCAGA) ซึ่งมีการเรืองแสงของพีเอ็นเอในสภาพที่เป็นสายเดี่ยวแตกต่างกันอย่างมาก ($\Phi_{F\ (PNA8)}/\Phi_{F\ (PNA1)}$ = 14 เท่า) ทั้งๆ ที่ เบส U^{py} ในพีเอ็นเอทั้งสองจะมี T เป็นเบสข้างเคียงเหมือนกัน แสดงว่าปัจจัยที่เป็นตัวกำหนดการเรืองแสงของ U^{py} ในพีเอ็นเอสายเดี่ยวอาจจะมีขอบเขตที่จะต้องพิจารณามากกว่าเฉพาะคู่เบสที่อยู่ติดกัน ซึ่งอาจไม่ใช่เรื่องที่น่าประหลาดใจนักเมื่อพิจารณาว่าพีเอ็นเอในสภาพที่เป็นสายเดี่ยวในสภาวะแวดล้อมที่เป็นน้ำน่าจะสามารถพับตัวเป็นโครงสร้างที่กระชับเพื่อลดอันตรกิริยาระหว่างนิวคลีโอเบสกับน้ำ ทำให้เบส U^{py} สามารถสัมผัสกับเบสตัวอื่นที่ไม่ใช่ nearest neighbour ได้

สิ่งที่ต้องทำความเข้าใจคือเบสแต่ละชนิดมีผลต่อการเรืองแสงของเบส U^{py} อย่างไร การที่ **PNA1** ซึ่งเป็น homothymine sequence มีการเรืองแสงที่ต่ำมาก ($\Phi_{F\ (PNA1)}$ = 0.006) แสดงให้เห็นว่าเบส T น่าจะเป็น quencher ที่ดีสำหรับเบส U^{py} ในพีเอ็นเอสายเดี่ยว การทดลองที่ได้กระทำต่อมาคือการสังเคราะห์ acpcPNA ที่เป็น homo-sequence อื่นๆ ได้แก่ **PNA9** (AAAAU^{py}AAAA), **PNA10** (CCCCU^{py}CCCC) และ **PNA11** (GGGGU^{py}GGGG) อย่างไรก็ตาม พบว่าพีเอ็นเอทุกชนิดที่สังเคราะห์ได้ในสภาพสายเดี่ยวให้สัญญาณฟลูออเรสเซนต์ที่ไม่แตกต่างกันนัก โดยลำดับของความสว่าง (เทียบจากค่า Φ_F) จะเป็น G > A > C > T แสดงว่าการที่พีเอ็นเอบางตัวเช่น **PNA7** และ **PNA8** มีความสว่างมากเป็นพิเศษในสภาพที่เป็นสายเดี่ยวไม่ได้ขึ้นกับลำดับเบสเท่านั้น แต่อาจมีปัจจัยอื่นเช่นการเกิด secondary structure มาเกี่ยวข้องด้วย ซึ่งเป็นสิ่งที่ควรจะต้องศึกษาต่อไป

2.4 Synthesis and Hybridization of PNA containing fluorescence universal base

Eric T. Kool ได้รายงานมาก่อนหน้านี้ว่าการแทนที่นิวคลีโอเบสในดีเอ็นเอด้วยอะโรมาติกไฮโดรคาร์บอนที่ไม่สร้างพันธะไฮโดรเจน เช่น ไพรีน จะทำให้ได้ดีเอ็นเอที่สามารถเกิดไฮบริดที่ค่อนข้างเสถียรได้ [Schweitzer and Kool, 1995] แสดงว่าอะโรมาติกไฮโดรคาร์บอนเหล่านี้ สามารถประพฤติตัวเลียนแบบดีเอ็นเอเบส แต่เนื่องจากการที่มันไม่สามารถสร้างพันธะไฮโดรเจนได้ มันจึงไม่น่าจะสามารถบอกความแตกต่างระหว่างเบสของดีเอ็นเออีกสายหนึ่งที่อยู่ตรงกันข้ามได้ และควรจะประพฤติตัวเป็นยูนิเวอร์แซลเบส โดยได้มีรายงานมาก่อนหน้านี้ในระบบ aegPNA ของ Nielsen ว่าพอลิไซคลิกอะโรมาติกไฮโดรคาร์บอนเช่น ไพรีน แอนทราซีน อะซีแนฟทีน สามารถเป็นยูนิเวอร์แซลเบสได้ [MacKinnon et al., 2007] สิ่งที่น่าสนใจคือพอลิไซคลิกอะโรมาติกไฮโดรคาร์บอนส่วนใหญ่สามารถเรืองแสงได้ และเป็นที่ทราบกันดีว่าการเรืองแสงของสารเหล่านี้ขึ้นกับสภาพแวดล้อมของตัวฟลูออโรฟอร์อย่างมาก ฟลูออโรฟอร์ที่อยู่ในดีเอ็นเอในสภาพที่เป็นสายเดี่ยวกับเกลียวคู่ควรจะอยู่ในสิ่งแวดล้อมที่แตกต่างกันและน่าจะแสดงการเรืองแสงที่ต่างกันด้วย แต่กลับไม่ค่อยมีผู้รายงานความสามารถในการเรืองแสงของพอลิไซคลิกไฮโดรคาร์บอนเหล่านี้เท่าใดนัก ในงานวิจัยนี้จะศึกษาความสามารถในการเป็นยูนิเวอร์แซลเบสของพอลิไซคลิกอะโรมาติกไฮโดรคาร์บอนในระบบ acpcPNA และเปรียบเทียบการเรืองแสงของ acpcPNA ที่มีพอลิไซคลิกอะโรมาติกไฮโดรคาร์บอนอยู่ด้วยในสภาพที่เป็นสายเดี่ยวและเมื่อเกิดไฮบริดกับดีเอ็นเอ

ในการศึกษาระยะเริ่มต้นของงานวิจัยนี้จะเน้นไปที่การใช้ไพรีน ซึ่งมีผู้ศึกษามาพอสมควรในระบบของดีเอ็นเอเพื่อเป็นตัวแทนของพอลิไซคลิกอะโรมาติกไฮโดรคาร์บอน การสังเคราะห์ acpcPNA ที่มีไพรีนเป็นนิวคลีโอเบสจะจะต้องหาวิธีติดไพรีนเข้าไปตรงตำแหน่ง 4’ ของวงแหวนพิร์โรลิดีนแทนที่จะเป็นนิวคลีโอเบส โดยในที่นี้จะเลือกต่อผ่านวงแหวนไตรอะโซลใช้ปฏิกิริยา Cu-catalyzed 1,3-dipolar cycloaddition (Click chemistry) ระหว่าง

protected 4-azidoproline กับ 1-ethynylpyrene ได้ผลิตภัณฑ์เป็น **Tz^{Py}** monomer วิธีการสังเคราะห์เป็นดังสรุปในรูปที่ 21

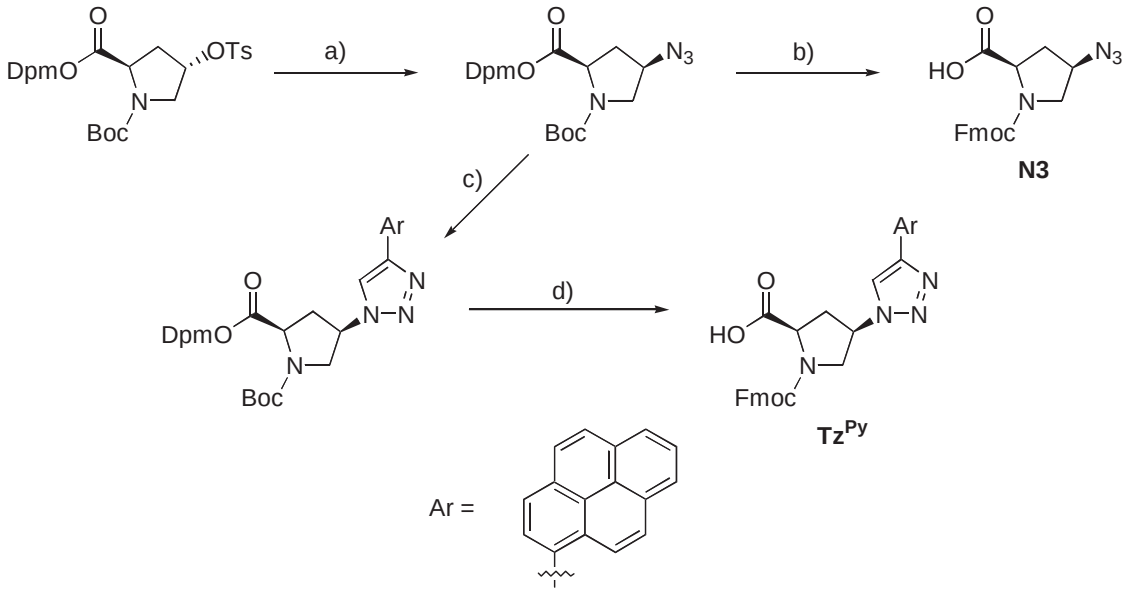

รูปที่ 21 วิธีการสังเคราะห์พีเอ็นเอโมโนเมอร์ **Tz^{Py}** และ **N3**; reagents and conditions: a) NaN_3 1.1 equiv, anhydrous K_2CO_3 1.2 equiv, dry DMF, 2-3 h, 70 °C under N_2, 95%; b) i. TFA in anisole, 2 h, rt, ii. FmocOSu 0.9 equiv, $NaHCO_3$ 2.5 equiv, CH_3CN:H_2O = 1:1, overnight, rt, quantitative yield; c) 1-Ethynylpyrene, CuI (15 mol%), DIEA 2 equiv, CH_3CN, 12 h, 80 °C, 57%; d) i. *p*-TsOH 3.2 equiv in CH_3CN, 3 h, rt, ii. FmocCl 1.3 equiv, DIEA 1.3 equiv, rt, 85%, iii. TFA:CH_2Cl_2 = 1:1 in anisole, 15 min, rt, 68%.

เมื่อได้ **Tz^{Py}** โมโนเมอร์แล้วจึงนำมาสังเคราะห์เป็น acpcPNA ที่มีลำดับเบสเป็น Bz-GCATTA(Tz^{Py})AGATAC–LysNH$_2$ นอกจากนี้ยังได้สังเคราะห์ acpcPNA ที่มีเบส C แทนที่เบส Tz^{Py} (Bz-GCATTACAGATAC–LysNH$_2$) เพื่อเป็นตัวเปรียบเทียบ โครงสร้างของพีเอ็นเอทั้งสองได้รับการยืนยันโดย MALDI-TOF mass spectrometry จากนั้นจึงได้ศึกษาความเสถียรของไฮบริดกับดีเอ็นเอที่มีลำดับเบสเป็นคู่สมกันแต่มีเบสที่อยู่ตำแหน่งที่ตรงกับ Tz^{Py}/C เป็น A, G, C และ T ตามลำดับ ค่า T_m ที่ได้เป็นดังแสดงในตารางที่ 12

ข้อมูลจากตารางที่ 12 แสดงให้เห็นอย่างชัดเจนว่า **Tz^{Py}** สามารถประพฤติตัวเป็นยูนิเวอร์แซลเบส กล่าวคือไม่มีการเลือกเข้าคู่กับเบสธรรมชาติตัวใดตัวหนึ่ง ดังจะเห็นได้จากค่า T_m ที่ใกล้เคียงกันมากไม่ว่าเบสตรงข้ามจะเป็นเบสอะไร (ΔT_m = 1.7 ºC) ในขณะที่พีเอ็นเอที่มีเบส C แทนที่ตำแหน่งของ **Tz^{Py}** จะแสดงการเลือกจับกับเบส G อย่างชัดเจน (ΔT_m = 19.3 ºC) เนื่องจากไพรีนมีสมบัติเรืองแสง จึงได้ศึกษาสมบัติเชิงแสงของไฮบริดระหว่าง **Tz^{Py}** พีเอ็นเอนี้กับดีเอ็นเอโดย absorption และ fluorescence spectroscopy ผลที่ได้เป็นดังแสดงในรูปที่ 22

ตารางที่ 12 ข้อมูล T_m ของ PNA (GCATTAXAGATAC) และไฮบริดของมันกับ DNA (GTATCTYTAA TGC)

Entry	X in PNA	Y in DNA	T_m (ºC)[a]	ΔT_m (ºC)[b]
1	**Tz^{Py}**	A	69.0	1.7
2	**Tz^{Py}**	G	69.8	
3	**Tz^{Py}**	C	68.9	
4	**Tz^{Py}**	T	68.1	
5	**C**	A	72.0	19.3
6	**C**	G	85.0	
7	**C**	C	69.0	
8	**C**	T	65.7	

[a] conditions: 2.5 μM PNA, 3.0 μM DNA, 10 mM sodium phosphate buffer pH 7.0

[b] $\Delta T_m = T_m(\text{max}) - T_m(\text{min})$

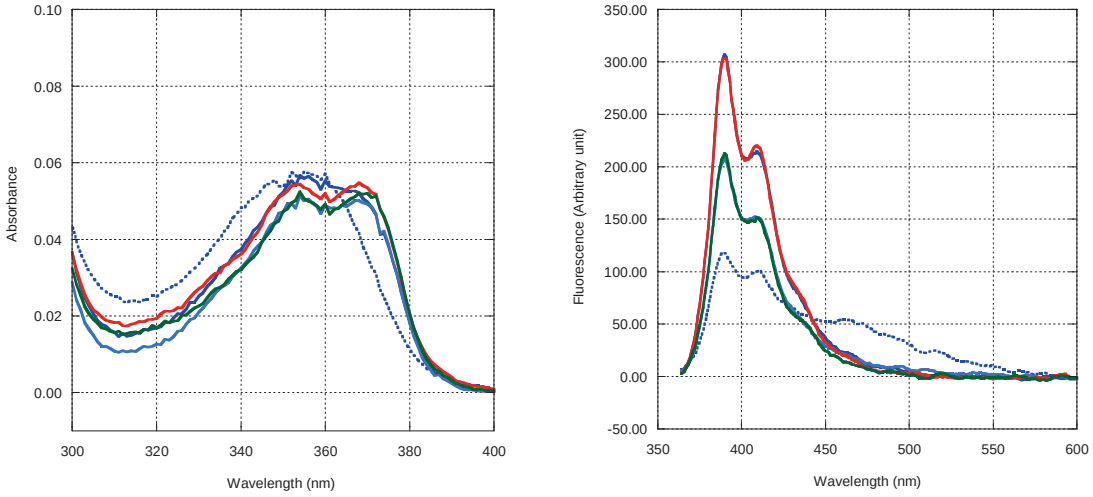

(A) (B)

รูปที่ 22 Absorption (A) และ fluorescence (B) ของ **Tz^{Py} PNA** (·····) และไฮบริดกับ DNA Y = A (–), G (–), C (–), T (–) conditions: 2.5 μM PNA, 3.0 μM DNA, 10 mM sodium phosphate buffer pH 7.0, λ_{excit} 350 nm.

PNA **+ DNA (A)** **+ DNA (G)** **+ DNA (C)** **+ DNA (T)**

รูปที่ 23 ภาพถ่ายภายใต้ UV light เพื่อเปรียบเทียบการเรืองแสงของ **Tz^{Py} PNA** และไฮบริดของมันกับดีเอ็นเอ conditions: 2.5 μM PNA, 3.0 μM DNA, 10 mM sodium phosphate buffer pH 7.0.

เมื่อพิจารณาที่ absorption spectra ของ **Tz^{Py} PNA** จะเห็นแถบการดูดกลืนของไพรีนที่บริเวณ 352 nm ซึ่งมีลักษณะ broad ไม่แสดง fine structure ที่เป็นเอกลักษณ์ของไพรีน แสดงว่ามี electronic coupling ระหว่างไพรีนโครโมฟอร์กับนิวคลีโอเบสหรือกับไตรอะโซลที่ใช้เป็นตัวเชื่อม เมื่อเกิดเป็นไฮบริดกับดีเอ็นเอ ไม่ว่าจะมีเบสที่ตรงกับไพรีนเป็นอะไรก็ตามก็จะมีการเปลี่ยนแปลงของการดูดกลืนของไพรีนในลักษณะเดียวกันกล่าวคือจะเกิดการแยกออกของแถบการดูดกลืนเป็น 2 แถบ พร้อมทั้งมี bathochromic shift ไปที่ 352 และ 372 nm แสดงให้เห็นถึงสิ่งแวดล้อมของไพรีนโครโมฟอร์ที่เปลี่ยนแปลงไป ส่วน fluorescence spectrum ของ **Tz^{Py} PNA** แสดงสัญญาณที่ค่อนข้างอ่อนในช่วง ~390-430 nm โดยมี λ_{max} อยู่ที่ 388, 400 และ 430 nm ซึ่งเป็นลักษณะเฉพาะของไพรีนโมโนเมอร์ นอกจากนี้ยังพบสัญญาณที่ค่อนข้าง broad ที่บริเวณ 460 nm ซึ่งน่าจะเกิดจาก exciplex ของไพรีนที่ยังไม่ทราบโครงสร้างแน่ชัด และยังอยู่ระหว่างการศึกษารายละเอียด ทำให้เห็นการเรืองแสงเป็นสีเขียว-ฟ้า (รูปที่ 23) แต่เมื่อเกิดการไฮบริไดซ์กับดีเอ็นเอ จะทำให้เกิดการเปลี่ยนแปลงของสเปกตรัมอย่างชัดเจน กล่าวคือ emission ในส่วนของไพรีนโมโนเมอร์จะเพิ่มขึ้นราว 2–3 เท่า และ emission ของ exciplex จะหายไป ทำให้การเรืองแสงเปลี่ยนเป็นสีออกน้ำเงินมากขึ้น ปรากฏการณ์นี้เกิดขึ้นกับดีเอ็นเอทุกตัว ซึ่งเป็นการยืนยันว่าไพรีนทำหน้าที่เป็นยูนิเวอร์แซลเบสโดยไม่เลือกจับกับเบสใดเบสหนึ่งดีเป็นพิเศษ

แม้ผลการทดลองเบื้องต้นจะเป็นที่น่าพอใจในแง่ที่ว่าไพรีนสามารถทำหน้าที่เป็นยูนิเวอร์แซลเบสในระบบ acpcPNA โดยค่า T_m ของไฮบริดของพีเอ็นเอที่มีไพรีนอยู่กับดีเอ็นเอคู่สมที่มีเบสตรงข้ามกับไพรีนเป็น A, T, C และ G มีความแตกต่างของค่า T_m น้อยมาก นอกจากนี้พีเอ็นเอที่มีไพรีนยูนิเวอร์แซลเบสยังแสดงความแตกต่างของการเรืองแสงในสภาพที่เป็นสายเดี่ยวและเมื่อเกิดไฮบริดกับดีเอ็นเอ แต่ก็ยังต้องมีการศึกษาต่ออีกมากในแง่ของกลไกของการเปลี่ยนแปลงการเรืองแสง และอิทธิพลของเบสข้างเคียงที่อาจมีต่อการเปลี่ยนแปลงการเรืองแสง อย่างไรก็ตาม การศึกษาโดยละเอียดจำเป็นจะต้องใช้พีเอ็นเอในปริมาณมาก ซึ่งต้องอาศัยการพัฒนาวิธีการสังเคราะห์ให้มีประสิทธิภาพมากขึ้นโดยแนวทางคือการการติดส่วนของไพรีน หรืออะโรมาติกไฮโดรคาร์บอนชนิดอื่น ลงไปโดยตรงบนพีเอ็นเอที่มีเอไซด์โมโนเมอร์ ผ่าน click reaction (post-synthetic modification) [Bonger et al., 2010]

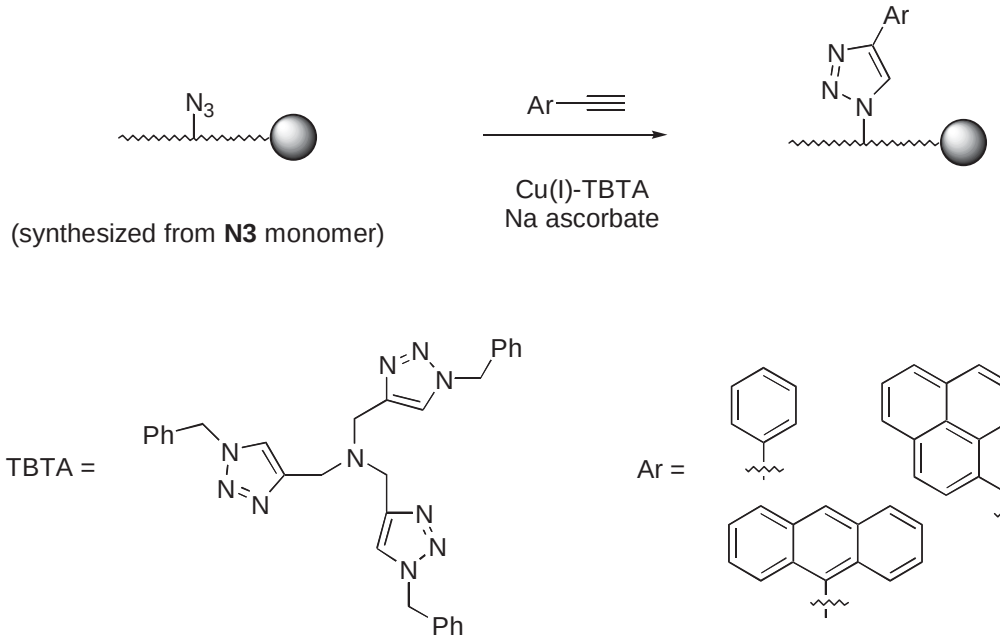

รูปที่ 24 วิธีการสังเคราะห์ acpcPNA ที่มี modified triazole base โดยผ่าน post-synthetic click reaction

งานวิจัยที่ได้ทำต่อมาจึงเน้นไปที่การพัฒนาวิธีการสังเคราะห์พีเอ็นเอที่มีเบส $\mathbf{Tz^{Py}}$ ที่มีประสิทธิภาพมากขึ้นโดยการติดส่วนของไพรีน หรือพอลิไซคลิกอะโรมาติกไฮโดรคาร์บอนชนิดอื่นลงไปโดยตรงบนพีเอ็นเอที่มีหมู่เอไซด์อยู่ด้วยผ่าน post-synthetic click reaction (รูปที่ 24) ซึ่งวิธีการดังกล่าวจะทำให้สามารถติดส่วนของเบสเรืองแสงที่หลากหลายเข้าไปที่พีเอ็นเอได้โดยไม่จำเป็นต้องสังเคราะห์โมโนเมอร์ขึ้นมาก่อน และสามารถทำได้โดยตรงบนวัฏภาคของแข็งซึ่งสะดวกมากในทางปฏิบัติ

เพื่อศึกษาความเป็นไปได้ของการสังเคราะห์พีเอ็นเอที่มีเบส Tz^{py} ตามหลักการดังกล่าวข้างต้นจึงได้ทดลองทำปฏิกิริยาคลิกของเอไซด์พีเอ็นเอที่มีลำดับเบสผสมและมีความยาว 13 เบส (Bz-GCATTTA(N_3)AGATAC-LysNH_2) กับ 1-ethynylpyrene บนวัฏภาคของแข็ง ผลการติดตามการเกิดปฏิกิริยาโดยเทคนิค MALDI-TOF mass spectroscopy **(รูปที่ 25)** เสนอแนะว่าปฏิกิริยา click เกิดอย่างสมบูรณ์ให้ผลิตภัณฑ์เป็น Bz-GCATTTA(Tz^{Py})AGATAC-LysNH_2 โดยไม่มีเอไซด์พีเอ็นเอเหลือ และไม่มีปฏิกิริยาข้างเคียงอื่น

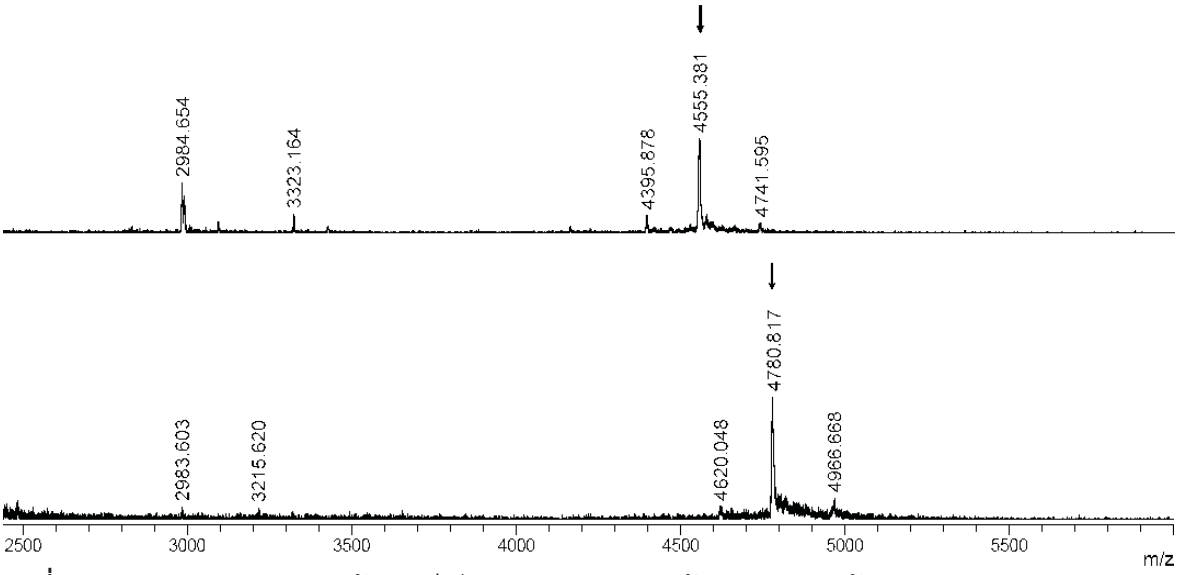

รูปที่ 25 MALDI-TOF แมสสเปกตรัมของพีเอ็นเอก่อน (บน) และหลังปฏิกิริยาคลิกกับ 1-ethynylpyrene (MW 226.3) (ล่าง) บนวัฏภาคของแข็ง พีกของสารที่สนใจแสดงโดยลูกศรชี้

ตารางที่ 13 ลำดับเบส มวลโมเลกุล และปริมาณผลผลิตของพีเอ็นเอที่สังเคราะห์โดยกระบวนการ post-synthetic click reaction

Entry	Sequence[a] GCATTY**X**YGATAC	*m/z* (calcd.)[b]	*m/z* (found)[c]	isolated yield (%)
1	X = Tz^{Py}; Y = A	4779.2	4779.4	4.38
2	X = Tz^{Py}; Y = T	4761.2	4762.8	5.13
3	X = Tz^{Ph}; Y = T	4637.0	4638.2	2.12
4	X = Tz^{An}; Y = T	4737.1	4738.2	2.79

[a]All sequences were N-terminal benzoylated, C-terminal L-lysinamide capped.

[b]Average mass calculated for $[M+H^+]$.

[c]MALDI-TOF, CCA matrix, linear mode.

จากนั้นจึงได้นำวิธีการนี้ไปสังเคราะห์พีเอ็นเอตัวอื่นๆ โดยพีเอ็นเอที่ได้สังเคราะห์ตามวิธีการ post-synthetic click reaction ดังกล่าวเป็นดังสรุปในตารางที่ 13

PNA ที่มีหมู่ Tz^{Ph} (GCATTTTz^{Ph}TGATAC) ไม่แสดงการเรืองแสงทั้งในสภาพที่เป็นสายเดี่ยวและเมื่อมีดีเอ็นเอคู่สมอยู่ด้วย PNA ที่มีหมู่ Tz^{An} (GCATTTTz^{An}TGATAC) (Tz^{An}) ในสภาพที่เป็นสายเดี่ยวแสดงการเรืองแสงที่ต่ำ โดยมี emission peak ที่มีลักษณะ broad และ unstructured โดยมี λ_{max} อยู่ที่ 425 nm ซึ่งน่าจะเป็นของ exciplex และพบว่าการเรืองแสงเพิ่มขึ้นเพียงเล็กน้อย (~ 2 เท่า) เมื่อมีดีเอ็นเอคู่สมอยู่ด้วย โดยไม่เห็นการเรืองแสงเพิ่มเติมที่ความยาวคลื่นอื่น ส่วน PNA ที่มีหมู่ Tz^{Py} (GCATTTTz^{Py}TGATAC) ในสภาพสายเดี่ยวมีการเรืองแสงที่ต่ำ และพบทั้ง emission ของ pyrene monomer (388 nm) และ exciplex (~ 460 nm) แต่เมื่อเกิดไฮบริดกับดีเอ็นเอคู่สมจะมีการเพิ่มขึ้นของ monomer emission ถึงเกือบ 11 เท่า และ exciplex emission จะลดลงเล็กน้อย ซึ่งสอดคล้องกับผลของ Tz^{Py} PNA ที่ได้ศึกษามาก่อนหน้านี้ แสดงว่าการเปลี่ยนแปลงของ monomer/exciplex emission ของเบส Tz^{Py} นี้สามารถเกิดได้ทั้งเมื่อเบสข้างเคียงเป็น A/A และ T/T **(รูปที่ 26)**

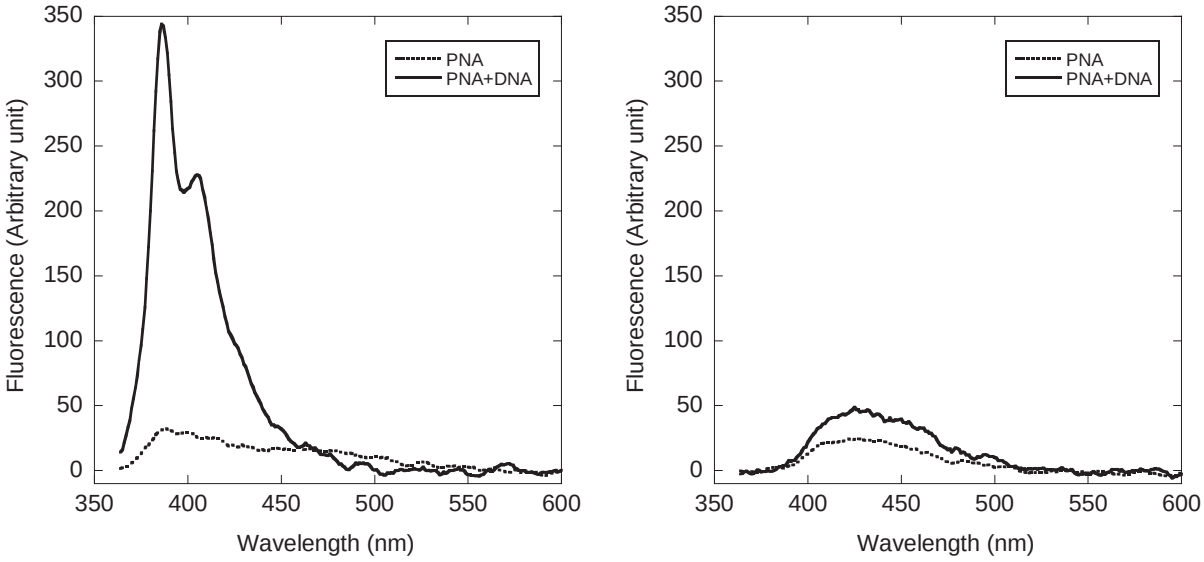

รูปที่ 26 ฟลูออเรสเซนต์สเปกตรัมของ **Tz^{Py} PNA** (GCATTTTz^{Py}TGATAC) (a) และ **Tz^{An} PNA** (GCATTTTz^{An}TGATAC) (b) ในสภาพที่เป็นสายเดี่ยว (–) และเมื่อมีดีเอ็นเอที่มีลำดับเบสคู่สม (···) (5'-GTATCAGAAATGC-3') อยู่ด้วย (conditions: 2.5 μM PNA, 3.0 μM DNA in 10 mM sodium phosphate buffer pH=7.0, λ_{excit} = 350 nm).

ผลการทดลองทั้งหมดได้แสดงถึงวิธีการสังเคราะห์และศักยภาพของการประยุกต์ใช้ clicked polycyclic aromatic hydrocarbon เพื่อเป็น fluorescence artificial nucleobase ในระบบ acpcPNA ที่แสดงการเปลี่ยนแปลงการเรืองแสงที่ตอบสนองต่อการเกิดไฮบริดกับดีเอ็นเอ ซึ่งค่อนข้างเสร็จสมบูรณ์แล้ว และได้รับการตีพิมพ์เรียบร้อยแล้ว [Mansawat et al., 2012a]

3. การสังเคราะห์และศึกษาสมบัติจับยึดของพีเอ็นเอที่มี modified backbone

3.1 PNA with alternative configuration of the pyrroldine ring

งานวิจัยที่ผ่านมาของกลุ่มได้เน้นการสังเคราะห์และศึกษาสมบัติการจับยึดของ acpcPNA ที่มีคอนฟิกกิวเรชันเป็น (2'*R*,4'*R*)-prolyl-(1*S*,2*S*)-ACPC เป็นหลัก ซึ่งการที่เลือกศึกษาไอโซเมอร์นี้ได้มาจากการสังเคราะห์และเปรียบเทียบสมบัติการจับยึดกับดีเอ็นเอของพีเอ็นเอไดอะสเตอริโอเมอร์ต่างๆ โดยเลือก optimize โครงสร้างส่วนวงแหวนพิโรลิดีนและส่วน spacer แยกกันทำให้สามารถลดจำนวนสเตอริโอไอโซเมอร์ที่ต้องสังเคราะห์และทดสอบสมบัติการจับยึดจากทั้งสิ้น 16 ไดอะสเตอริโอเมอร์เหลือเพียง 7 ไดอะสเตอริโอเมอร์ โดยโครงสร้างของสเตอริโอไอโซเมอร์อื่นที่นอกเหนือจากระบบ (2'*R*,4'*R*)-prolyl-(1*S*,2*S*)-ACPC ที่ได้ศึกษาโดยละเอียดไปแล้ว เป็นดังแสดงในรูปที่ 27

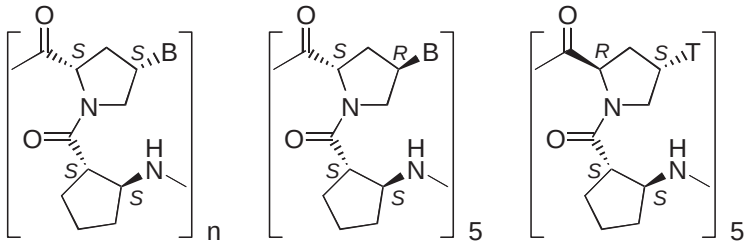

(2'*S*,4'*S*)/(1*S*,2*S*) **(2'*S*,4'*R*)/(1*S*,2*S*)** **(2'*R*,4'*S*)/(1*S*,2*S*)**

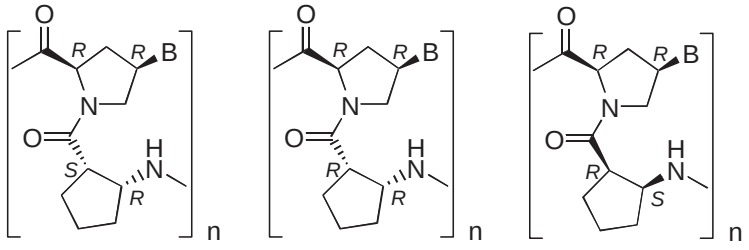

(2'*R*,4'*R*)/(1*S*,2*R*) **(2'*R*,4'*R*)/(1*R*,2*R*)** **(2'*R*,4'*R*)/(1*R*,2*S*)**

รูปที่ 27 ไดอะสเตอริโอเมอร์ของพีเอ็นเอที่ได้ทำการศึกษาเพิ่มเติมนอกเหนือจาก *RR*-Pro/*SS*-ACPC (acpcPNA)

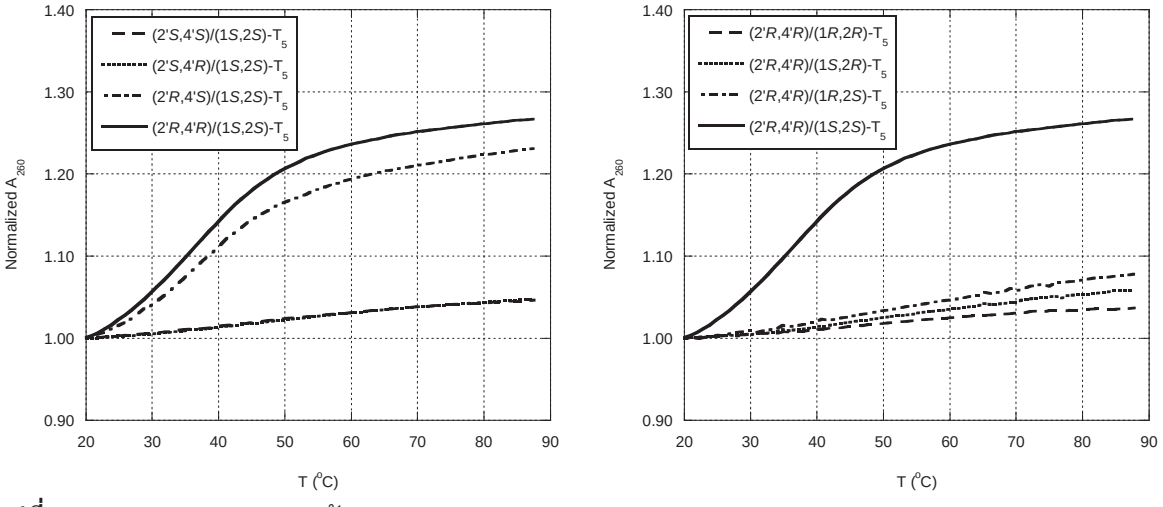

รูปที่ 28 T_m curve ของ PNA T_5 กับ poly(dA), T_m measured at 1 μM duplex concentration, 10 mM Sodium phosphate buffer pH 7.0, 100 mM NaCl, heaing rate 1 ºC/min.

ในงานวิจัยได้สังเคราะห์พีเอ็นเอที่เหลืออีก 6 ไดอะสเตอริโอเมอร์ที่มีลำดับเบสเป็น T_5 และนำไปศึกษาสมบัติการจับยึดกับดีเอ็นเอคู่สม ซึ่งในที่นี้ใช้ poly(dA) ซึ่งสามารถเกิดไฮบริดที่เสถียรกว่า dA_5 เนื่องจาก end-stacking effect เป็นตัวแทนของ DNA ผลการวัดค่า T_m พบว่านอกเหนือจาก (2'*R*,4'*R*)-prolyl-(1*S*,2*S*)-ACPC-PNA (acpcPNA) ที่เป็นระบบที่ได้ศึกษามาอย่างละเอียดแล้ว ก็ยังมีอีกไดอะสเตอริโอเมอร์หนึ่งคือ (2'*R*,4'*S*)-prolyl-(1*S*,2*S*)-ACPC PNA (*epi*-acpcPNA) ที่แสดงสมบัติการจับยึดกับดีเอ็นเอเช่นเดียวกัน (รูปที่ 29)

การที่ *epi*-acpcPNA สามารถจับยึดกับดีเอ็นเอได้ไม่ใช่เรื่องที่เกินความคาดหมายนักเมื่อพิจารณาว่าการเปลี่ยนคอนฟิกกิวเรชันของคาร์บอนที่ตำแหน่ง 4 ในวงแหวนพิโรลิดีนไม่ได้เปลี่ยน overall configuration ของ PNA backbone ไปจาก acpcPNA แต่ประการใด เนื่องจากคาร์บอนดังกล่าวไม่ได้เป็นส่วนของ backbone โดยตรง นอกจากนี้ยังได้มีผู้รายงานว่าดีเอ็นเอที่ประกอบด้วยแอลฟ่าอะโนเมอริกนิวคลีโอไซด์ (α-DNA) ซึ่งมีคอนฟิกกิวเรชันของอะโนเมอริกคาร์บอนตรงกันข้ามกับดีเอ็นเอปกติ (β-DNA) ยังสามารถจับยึดกับดีเอ็นเอได้อย่างแข็งแรง และที่น่าสนใจกว่านั้นคือ α-DNA จับกับ β-DNA เกิดเป็น duplex ที่มีทิศทางของดีเอ็นเอทั้งสองสายจัดเรียงตัวในลักษณะ parallel แทนที่จะเป็น antiparallel เหมือน duplex ที่เกิดจาก β-DNA ตามปกติ [Morvan et al., 1987] ดังนั้น งานวิจัยนี้จึงได้ทดลองสังเคราะห์ และศึกษาสมบัติการจับยึดกับดีเอ็นเอ อาร์เอ็นเอ และการเกิด self hybrid ของ *epi*-acpcPNA โดยคาดหวังว่าจะได้ระบบพีเอ็นเอใหม่ที่มีสมบัติการจับยึดที่แตกต่างไปจากระบบเดิม ซึ่งอาจนำไปสู่การประยุกต์ใช้งานในวัตถุประสงค์ที่แตกต่างกัน

จากผลการทดลองที่เป็นบวกเบื้องต้นนี้ทำให้กลุ่มวิจัยหันมาศึกษาสมบัติการจับยึดดีเอ็นเอและอาร์เอ็นเอของ *epi*-acpcPNA มากขึ้น โดยเริ่มต้นจากการสังเคราะห์พีเอ็นเอโมโนเมอร์ทั้งสี่ชนิด (A, T, C และ G) ที่มีคอนฟิกกิวเรชันของวงแหวนพิโรลิดีนเป็น (2'*R*,4'*S*) โดยเริ่มต้นจาก protected *cis*-4-hydroxy-D-proline (**8a**) ตามวิธีการดังที่สรุปในรูปที่ 29 พีเอ็นเอโมโนเมอร์ดังกล่าวสามารถนำไปสังเคราะห์เป็นพีเอ็นเอที่มีคอนฟิกกิวเรชันของวงแหวนพิโรลิดีนเป็น (2'*R*,4'*S*) ได้โดยวิธี Fmoc solid phase peptide synthesis มาตรฐานตามที่ได้เคยทำกับ acpcPNA [Vilaivan and Srisuwannaket, 2006] และได้สังเคราะห์พีเอ็นเอใหม่ขึ้นมา 3 ชนิดดังแสดงในตารางที่ 14 นอกจากนี้ยังได้สังเคราะห์ acpcPNA ที่มีลำดับเบสเดียวกันด้วยเพื่อใช้เป็นตัวเปรียบเทียบ

ตารางที่ 14 ข้อมูลลำดับเบสและ *m/z* ของ *epi*-acpcPNA ที่สังเคราะห์ได้

PNA	sequence (N⟶C)	length (bases)	*m/z* (calcd.)[a]	*m/z* (found)[b]
***RS*-T_9**	Lys-TTTTTTTTT-LysNH_2	9	3266.15	3265.58
***RS*-mix**	Bz-GTAGATCACT-LysNH_2	10	3620.91	3618.85
***RS*-sc**	Ac-CGCGAATTCGCG-LysNH_2	12	4233.18	4234.54

[a] Average mass

[b] MALDI-TOF, linear mode, CCA matrix

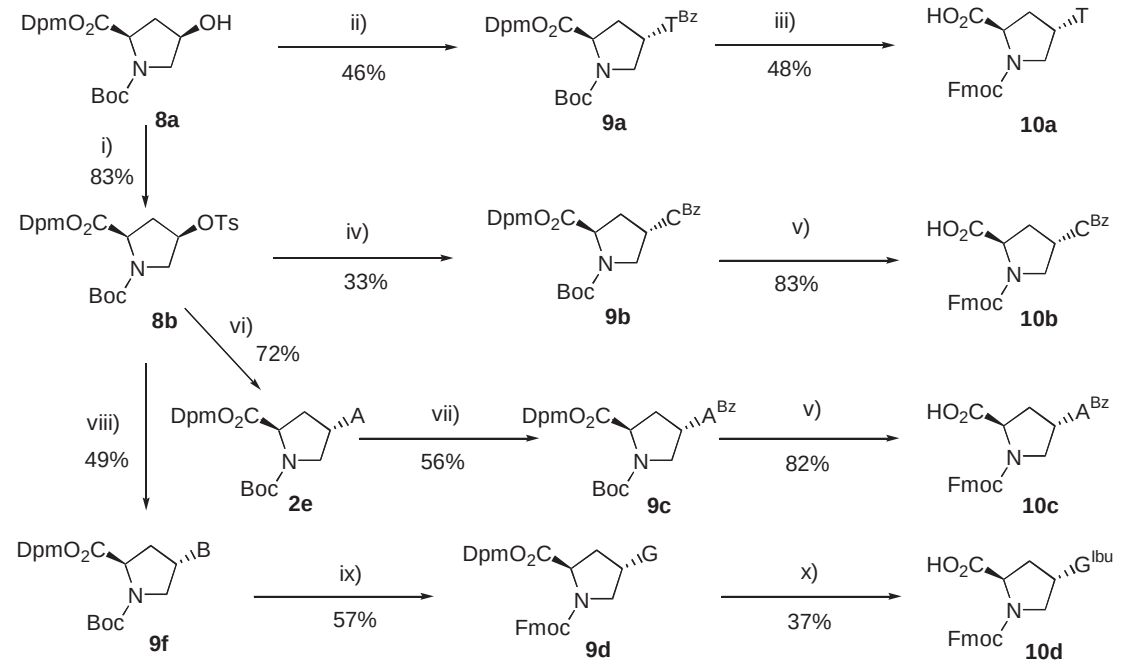

B = 2-chloro-6-aminopurin-9-yl

i) TsCl, Et_3N, cat. DMAP, CH_2Cl_2, rt, 4 h
ii) N^3-BzT, Ph_3P, DIAD, THF, 0 ^oC-rt, O/N
iii) a) TsOH, MeCN, rt, 3h b) FmocCl, DIEA, rt, 1 h
c) TFA, anisole, rt, O/N
iv) N^4-BzC, K_2CO_3, DMF, 80 ^oC, 8 h
v) a) TFA, anisole, rt, 3 h
b) FmocOSu, $NaHCO_3$, aq. MeCN, O/N
vi) adenine, K_2CO_3, DMF, 80 ^oC, 6 h
vii) a) BzCl, pyridine, 0 ^oC, 2h b) aq. NH_3, MeOH, rt
viii) 2-amino-6-chloropurine, K_2CO_3, DMF, 80 ^oC, 2 h
ix) a) TFA, rt, 2 h b) 2M HCl, reflux, 2 h
c) FmocOSu, $NaHCO_3$, aq. MeCN, rt, O/N
d) Ph_2CHN_2, EtOAc-MeOH, rt, 2 h
x) a) IbuCl, pyridine, 0 ^oC-rt, O/N b) TFA, 1 h

รูปที่ 29 แสดงการสังเคราะห์พีเอ็นเอโมโนเมอร์ทั้ง 4 ชนิดของ *RS*-Pro/*SS*-ACPC PNA (*epi*-acpcPNA)

ตารางที่ 15 T_m ของไฮบริดระหว่างพีเอ็นเอ **RS-mix** และ DNA/RNA

DNA/RNA sequence (5'→3')	T_m (ºC)[a] acpcPNA (2'*R*,4'*R*)	T_m (ºC)[a] *epi*-acpcPNA (2'*R*,4'*S*)	Note
dAGTGATCTAC	53.3	50.8	antiparallel, perfect matched
dAGTGCTCTAC	23.8	26.5	antiparallel, single mismatched
dAGTGTTCTAC	29.4	27.4	antiparallel, single mismatched
dAGTGGTCTAC	23.9	28.1	antiparallel, single mismatched
dCATCTAGTGA	<20	<20	parallel, perfect matched
rAGUGAUCUAC	42.3	40.7	antiparallel, perfect matched
rCAUCUAGUGA	<20	<20	parallel, perfect matched

[a] T_m measurements were carried out at 1 μM PNA and 1 μM DNA in 10 mM Sodium phosphate buffer pH 7.0, 100 mM NaCl

การศึกษาการจับยึด กับ DNA ของ acpcPNA (2'*R*,4'*R*) และ epi-acpcPNA (2'*R*,4'*S*) เปรียบเทียบกันด้วยการวัด T_m แสดงให้เห็นว่าพีเอ็นเอทั้งสองระบบแสดงการจับยึดกับดีเอ็นเอที่แข็งแรงใกล้เคียงกัน ตัวอย่างเช่น ไฮบริดระหว่าง epi-acpcPNA ***RS*-T$_9$** กับ dA$_9$ มีค่า T_m เท่ากับ 67.8 ºC ซึ่งต่ำกว่าของ acpcPNA ที่มีลำดับเบสเดียวกัน (72.9 ºC) เพียงเล็กน้อยเท่านั้น เมื่อศึกษาในระบบที่เป็นเบสผสม (***RS*-mix**) (ตารางที่ 15) ก็ให้ผลสอดคล้องกัน โดยจะสังเกตเห็นว่าพีเอ็นเอทั้งสองระบบแสดงความแข็งแรงและความจำเพาะเจาะจงของการจับยึดกับดีเอ็นเอที่สูง โดยระบบ *epi*-acpcPNA จะมีความแข็งแรงและความจำเพาะเจาะจงต่อดีเอ็นเอที่ต่ำกว่า ระบบ acpcPNA เล็กน้อย เป็นที่น่าสังเกตว่าพีเอ็นเอทั้งสองระบบจดจำเฉพาะดีเอ็นเอที่มีลำดับเบสคู่สมในทิศทาง antiparallel เท่านั้น ซึ่งต่างจาก α-anomeric DNA ที่จะจดจำเฉพาะดีเอ็นเอที่มีลำดับเบสคู่สมในทิศทาง parallel และเมื่อเปรียบเทียบในแง่ของความสามารถในการจดจำ RNA พบว่า *epi*-acpcPNA มีความจำเพาะในการจดจำ DNA ได้เหนือกว่า RNA เช่นเดียวกับ acpcPNA

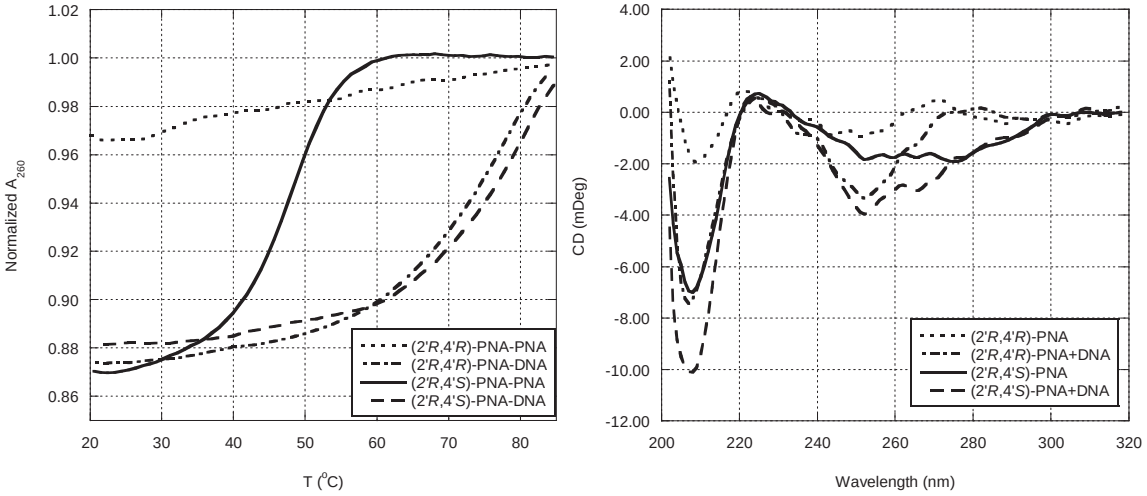

(A) (B)

รูปที่ 30 (A) T_m curves (B) CD spectra ของ ของ self complementary acpcPNA (2'*R*,4'*R*) และ *epi*-acpcPNA (2'*R*,4'*S*) ที่มีลำดับเบสตรงกับ ***RS*-sc** ในตารางที่ 15 เมื่อไม่มี และมี DNA เป้าหมายอยู่ด้วย; conditions: 1 μM duplex concentration, 10 mM sodium phosphate buffer pH 7.0, 100 mM NaCl.

ผลการทดลองทั้งหมดข้างต้นแสดงให้เห็นว่า *epi*-acpcPNA แสดงการจดจำดีเอ็นเอที่คล้ายคลึงกับ acpcPNA แต่เมื่อพิจารณาถึงสมบัติการเข้าคู่กันเองของพีเอ็นเอทั้งสองระบบพบว่ามีความแตกต่างกันอย่างชัดเจน กล่าวคือใน acpcPNA นั้นได้เป็นที่ยืนยันจากงานวิจัยก่อนหน้านี้แล้วว่า ไม่สามารถเกิด self hybrid ได้ระหว่างพีเอ็นเอสองสายที่มีลำดับเบสคู่สมกัน แต่ในระบบ *epi*-acpcPNA กลับพบว่าสามารถเกิด self hybrid ที่ค่อนข้างเสถียรได้ ถ้าพีเอ็นเอทั้งสองสายมีทิศทาง antiparallel ซึ่งกันและกัน โดยพีเอ็นเอ ***RS*-sc** ซึ่งเป็น self-complementary sequence ของ *epi*-acpcPNA จะแสดง sigmoidal transition เมื่อนำไปให้ความร้อนและติดตามการเปลี่ยนแปลงของ UV absorbance ที่ 260 nm (T_m ~47.8 ºC) ในขณะที่ acpcPNA ที่มีลำดับเบสเดียวกันไม่แสดงพฤติกรรมเช่นนั้น (รูปที่ 30A) จึงแสดงให้เห็นว่าเฉพาะ *epi*-acpcPNA เท่านั้นที่สามารถเกิดเป็น antiparallel PNA·PNA homoduplex แต่เมื่อเติมดีเอ็นเอที่เป็นคู่สมลงไป พบว่าในทั้งสองกรณีจะทำให้เกิด PNA·DNA heteroduplex ดังจะเห็นได้จาก sigmoidal curve ที่มี T_m ~ 77.0 (***RR*-sc**) และ 78.6 ºC (***RS*-sc**)

นอกจากนี้ยังสามารถยืนยันการเกิด PNA·PNA homoduplex เฉพาะกรณีระบบของ *epi*-acpcPNA ได้จาก CD spectroscopy (รูปที่ 30B)

แม้สมบัติการจดจำกับดีเอ็นเออย่างแข็งแรงและจำเพาะเจาะจงของ *epi*-acpcPNA อาจไม่ใช่เรื่องสำคัญมากนักเนื่องจากเป็นสมบัติที่ acpcPNA มีอยู่แล้ว แต่สิ่งที่น่าสนใจกว่าคือการที่ *epi*-acpcPNA สามารถเกิด self hybrid ได้ ซึ่งแตกต่างจาก acpcPNA อย่างชัดเจน และอาจนำไปสู่การประยุกต์ใช้ที่แตกต่างกันของพีเอ็นเอทั้งสองระบบ โดย acpcPNA น่าจะเหมาะสำหรับ applications ที่เกี่ยวกับ DNA ที่ไม่ต้องการการเกิด self hybrid เช่น การ target cellular DNA ด้วย double duplex invasion mechanism [Lohse et al., 1999] ในขณะที่ *epi*-acpcPNA น่าจะเหมาะสมกับการนำไปใช้ทางด้านนาโนเทคโนโลยี/เครื่องมือระดับโมเลกุลที่อาศัยการจดจำระหว่างพีเอ็นเอสองสาย [Gothlef et al., 2005] จากข้อมูลที่มีอยู่ในปัจจุบันยังไม่สามารถอธิบายปัจจัยในระดับโมเลกุลที่ส่งผลถึงความแตกต่างของสมบัติการเกิด self hybrid ของพีเอ็นเอทั้งสองระบบได้ แต่อย่างน้อยที่สุดคำอธิบายที่ว่า acpcPNA ไม่สามารถเกิด self hybrid ได้ด้วยปัจจัยทางสเตอริกเป็นหลักนั้นไม่น่าจะถูกต้อง ผลงานส่วนนี้ได้รับการตีพิมพ์แล้ว [Taechalertpaisarn et al., 2010]

3.2 PNA incorporating β-amino acids other than ACPC in the backbone

3.2.1 β-2-aminocyclopropanecarboxylic acid (β-ACC)

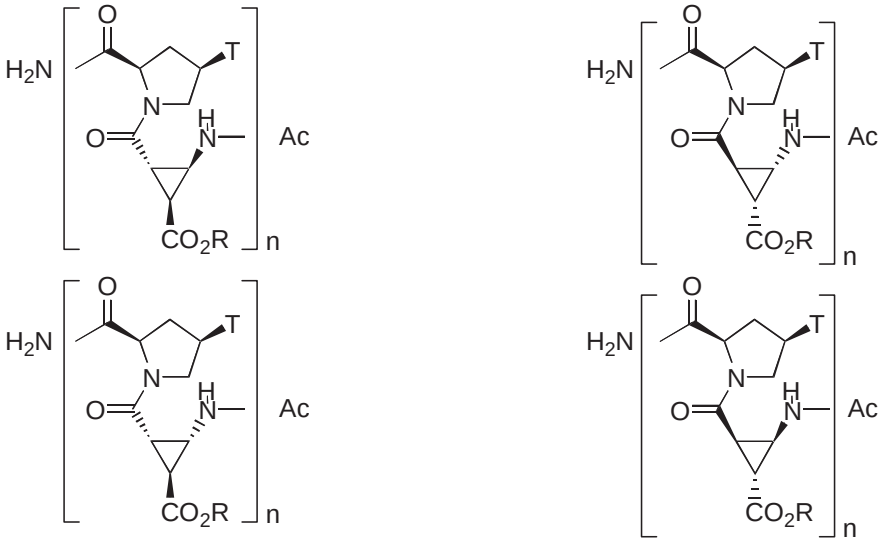

รูปที่ 31 โครงสร้างของ β-ACC PNA ที่จะสังเคราะห์ในงานวิจัยนี้

งานวิจัยในส่วนนี้เริ่มต้นที่การศึกษาพีเอ็นเอระบบใหม่ที่มี 2-aminocyclopropane-1-carboxylic acid (β-ACC) เป็นส่วนประกอบของโครงสร้างหลัก (backbone) (รูปที่ 31) แทนที่จะเป็น 2-aminocyclopentane-carboxylic acid (ACPC) โดยมีสมมติฐานว่า β-ACC จะมีคอนฟอร์เมชันที่ถูกจำกัดมากกว่า ACPC ซึ่งอาจนำไปสู่พีเอ็นเอระบบใหม่ที่สามารถจับยึดกับดีเอ็นเอ/อาร์เอ็นเอได้แข็งแรงกว่าระบบพีเอ็นเอดั้งเดิมที่มี ACPC เป็นส่วนประกอบของโครงสร้างหลัก โดยงานวิจัยในส่วนนี้ได้ร่วมมือกับ Professor Oliver Reiser จาก Institute of Organic Chemistry, University of Regensburg ประเทศเยอรมนี ซึ่งมีความเชี่ยวชาญในการสังเคราะห์และศึกษาเพปไทด์ที่มี β-ACC เป็นส่วนประกอบ เนื่องจาก β-ACC จะเกิดปฏิกิริยาแตกวงได้ง่ายในรูปที่เป็นหมู่อะมิ

โนอิสระ จึงไม่เหมาะที่จะคัพลิงโมโนเมอร์ของ β-ACC บนวัฏภาคของแข็งโดยตรง แผนการสังเคราะห์จึงต้อง "ปกป้อง" หมู่อะมิโนของ β-ACC ก่อนโดยการสร้างพันธะเพพไทด์ระหว่างหมู่คาร์บอกซิลของโพรลีนกับหมู่อะมิโนของ β-ACC เกิดเป็นไดเพพไทด์ Fmoc-Pro-β-ACC-OH แล้วจึงคัพลิงไดเพพไทด์นี้บนวัฏภาคของแข็งแทน ซึ่งจะสามารถหลีกเลี่ยงการเปิดเผยหมู่อะมิโนของ β-ACC โดยไม่จำเป็นได้ โดยอาศัยฐานความรู้ที่มีมาก่อนว่าสเตอริโอเคมีของส่วนโพรลีนที่แสดงการจับยึดกับดีเอ็นเอได้ดีที่สุดเมื่อมีตัวเชื่อมในโครงสร้างหลักเป็น ACPC น่าจะเป็น (2′*R*,4′*R*) งานวิจัยนี้จึงได้ยึดสเตอริโอไอโซเมอร์นี้ของโพรลีนเป็นหลัก และศึกษาสเตอริโอไอโซเมอร์ของ β-ACC ทั้ง 4 ไอโซเมอร์ โดยจะเริ่มจากไอโซเมอร์ที่มีคอนฟิกกิวเรชันเป็น (1*S*,2*S*) ซึ่งสอดคล้องกับ *SS*-ACPC เป็นไอโซเมอร์แรก แผนการสังเคราะห์เป็นดังแสดงในรูปที่ 32 โดยเริ่มจากสารตั้งต้น Boc-(-)-*trans*-(1*S*,2*S*)-β-ACC-OBn สารตั้งต้นที่เลือกใช้มีหมู่คาร์บอกซิลสองหมู่ ซึ่งมีหมู่ปกป้องที่ orthogonal ซึ่งกันและกัน (Me/Bn) หมู่หนึ่งอยู่ในตำแหน่ง *trans*- อีกหมู่หนึ่งอยู่ในตำแหน่ง *cis*- กับ หมู่ -NH_2 ซึ่งมีข้อดีเหนือกว่า unsubstituted β-ACC คือสามารถสังเคราะห์ไอโซเมอร์ของ β-ACC ทั้ง 4 ไอโซเมอร์โดยอาศัยสารตั้งต้นเพียงสองชนิด โดยการเลือกกำจัดหมู่ปกป้องที่จำเพาะเจาะจงเท่านั้น

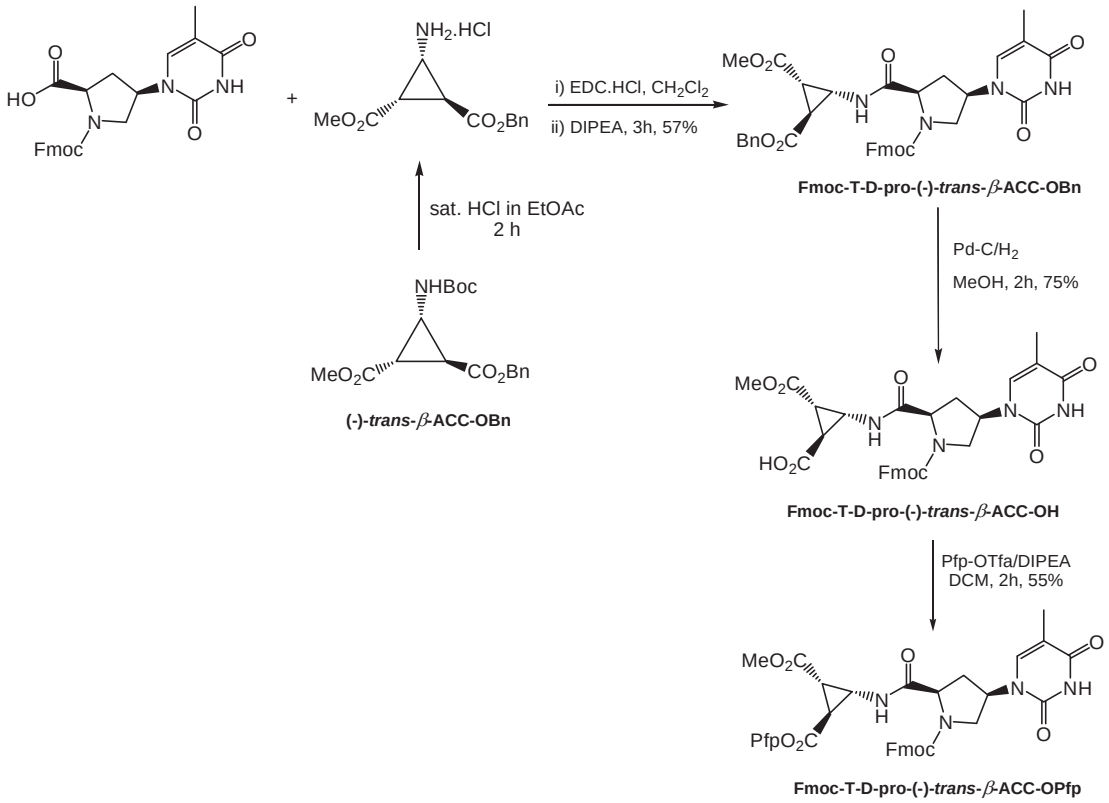

รูปที่ 32 แผนภาพแสดงการสังเคราะห์ β-ACC PNA โมโนเมอร์ Fmoc-(2′*R*,4′*R*)-Pro(T)-(1*S*,2*S*)-β-ACC-OPfp

การสังเคราะห์เริ่มต้นจากการกำจัดหมู่ Boc ซึ่งเป็นหมู่ปกป้องของหมู่อะมิโนใน β-ACC ออก โดยใช้ HCl ใน EtOAc ซึ่งหมู่อะมิโนนี้จะเสถียรในสภาพที่เป็นเกลือ HCl แต่จะทำให้เกิดการเปิดวงอย่างรวดเร็วในภาวะที่เป็นเบส เพื่อลดการเกิดปฏิกิริยาข้างเคียงดังกล่าวจึงต้องทำเกลือที่ได้ให้เป็นกลางแบบ in situ โดยใช้ DIPEA และทำปฏิกิริยาเพพไทด์คัพพลิง กับ (2*R*,4*R*)-Fmoc-T-OH ที่ผ่านการกระตุ้นด้วย EDC·HCl ซึ่งปฏิกิริยาดังกล่าว

ให้ปริมาณผลผลิต 57% ในขั้นต่อมาเป็นการกำจัดหมู่เบนซิล ซึ่งเป็นหมู่ปกป้องเอสเทอร์โดยวิธีไฮโดรจิโนไลซิส และตามด้วยการกระตุ้นหมู่คาร์บอกซิลโดยการเปลี่ยนเป็นเพนตะฟลูออโรฟีนิลเอสเทอร์ตามวิธีมาตรฐาน ซึ่งได้ปริมาณผลผลิต 75 และ 55% ตามลำดับ ซึ่งอยู่ในเกณฑ์ที่ยอมรับได้

โมโนเมอร์ดังกล่าวสามารถนำมาต่อกันเป็นพีเอ็นเอที่มีลำดับเบสเป็น T_{10} โดยเทคนิคการสังเคราะห์เพพไทด์บนวัฏภาคของแข็งมาตรฐาน โดยพีเอ็นเอที่ได้เมื่อทำให้บริสุทธิ์แสดงค่า *m/z* = 3813.60 ซึ่งสอดคล้องกับค่าที่ได้จากการคำนวณ (*m/z* calcd. for R = Me, 3810.63) (รูปที่ 33) แสดงว่าสามารถสังเคราะห์พีเอ็นเอที่มีลำดับเบสตามที่ต้องการได้จริง โดยไม่มีการแตกสลายของวงไซโคลโพรเพนระหว่างการสังเคราะห์บนวัฏภาคของแข็งและหมู่เมทิลเอสเทอร์ซึ่งเป็นหมู่ปกป้องคาร์บอกซิลที่เป็นโซ่ข้างก็เสถียรภายใต้ภาวะดังกล่าว

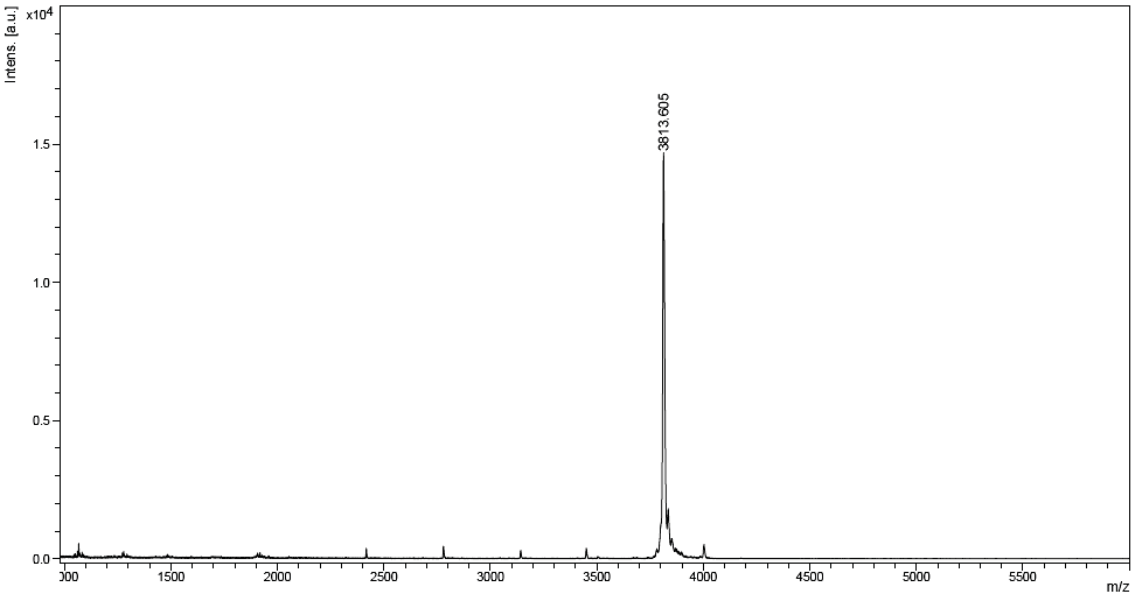

รูปที่ 33 MALDI-TOF analysis ของ T_{10} β-ACC PNA ที่ได้จากโมโนเมอร์ Fmoc-(2′*R*,4′*R*)-Pro(T)-(1*S*,2*S*)-β-ACC-OPfp

การสังเคราะห์โมโนเมอร์ของ β-ACC พีเอ็นเอไอโซเมอร์อื่นที่เหลืออีก 3 ชนิดได้แก่ Fmoc-(2'*R*,4'*R*)-Pro(T)-(1*S*,2*R*)-β-ACC-OPfp, Fmoc-(2'*R*,4'*R*)-Pro(T)-(1*R*,2*S*)-β-ACC-OPfp และ Fmoc-(2'*R*,4'*R*)-Pro(T)-(1*R*,2*R*)-β-ACC-OPfp สามารถทำได้ในทำนองเดียวกัน และได้นำโมโนเมอร์ดังกล่าวไปสังเคราะห์เป็นพีเอ็นเอที่มีลำดับเบสเป็น T_{10} ได้สำเร็จครบทุกตัว แต่เป็นที่น่าเสียดายว่าพีเอ็นเอที่สังเคราะห์ได้ไม่มีตัวใดแสดงสมบัติการจับยึดกับดีเอ็นเอเป้าหมาย (dA_{10}) เลย คาดว่าการที่ β-ACC PNA ไม่สามารถจับยึดกับดีเอ็นเอเป้าหมายน่าจะเป็นเพราะโครงสร้างของ β-ACC มีความ rigid เกินกว่าที่จะสามารถปรับตัวให้อยู่ในคอนฟอร์เมชันที่จะจับยึดกับ DNA ได้อย่างมีเสถียรภาพ งานที่จะดำเนินการต่อไปคือการเปลี่ยนขนาดวงแหวนเป็น 6 เหลี่ยม และ/หรือการสังเคราะห์วงแหวนขนาด 4 เหลี่ยม ซึ่งน่าจะมีความ rigid น้อยกว่า β-ACC และน่าจะส่งผลให้การจับยึดกับดีเอ็นเอเป้าหมายดีขึ้น

3.2.2 2-aminocyclobutanecarboxylic acid (ACBC) และ 2-aminocyclohexanecarboxylic acid (ACHC)

ในหัวข้อก่อนหน้านี้ (**3.2.1**) ได้กล่าวถึงการพัฒนาอนุพันธ์ของ acpcPNA ที่ได้แทนที่ส่วนตัวเชื่อม ACPC ด้วย 2-aminocylopropanecarboxylic acid (β-ACC) ซึ่งพบว่าพีเอ็นเอที่สังเคราะห์ได้ไม่แสดงสมบัติการจับยึดกับดีเอ็นเอ งานวิจัยที่ได้ทำต่อมาคือการแทนที่ส่วนของตัวเชื่อม ACPC ด้วย cyclic beta-amino acid ชนิดอื่น เช่น (1*S*,2*S*)-2-aminocyclobutanecarboxylic acid (ssACBC) ทำให้ได้เป็นพีเอ็นเอชนิดใหม่ขึ้น (acbcPNA) (รูปที่ 34) โดยโมโนเมอร์ของตัวเชื่อมที่ต้องการได้แก่ Fmoc-(1*S*,2*S*)-2-aminocyclobutanecarboxylic acid (Fmoc-ssACBC-OH) ซึ่งได้รับความอนุเคราะห์จาก Prof. David J. Aitken จาก Université Paris-Sud XI ประเทศฝรั่งเศส สารดังกล่าวสังเคราะห์ได้จากปฏิกิริยา photochemical [Fernandes et al., 2009] ที่กลุ่มวิจัยของ Prof. Aitken เป็นผู้พัฒนาขึ้น

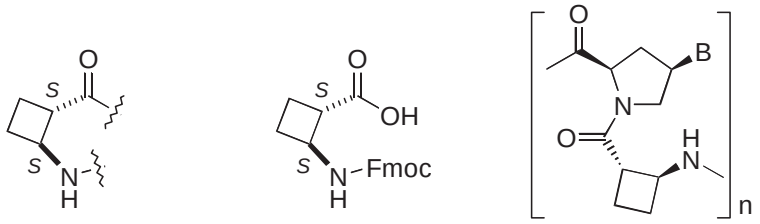

รูปที่ 34 โครงสร้างของตัวเชื่อม (1*S*,2*S*)-2-aminocyclobutanecarboxylic acid (ssACBC) โมโนเมอร์ และ acbcPNA

acbcPNA ที่สังเคราะห์ขึ้นใหม่มีลำดับเบสเป็น T_9 (**acbcPNA-T9**) และ GTAGATCACT (**acbcPNA-mix**) โดยที่ทุกตำแหน่งของ ACPC ถูกแทนที่ด้วย ACBC อย่างสมบูรณ์ acbcPNA ทั้งสองชนิดนี้ได้รับการพิสูจน์เอกลักษณ์โดยเทคนิค MALDI-TOF mass spectrometry เป็นที่น่าสังเกตว่า 2-aminocyclobutanecarboxylic acid ซึ่งหากมีหมู่อะมิโนอิสระจะไม่เสถียรในภาวะที่เป็นเบสเนื่องจากการแตกออกของวงไซโคลบิวเทน [Aitken et al., 2004] อย่างไรก็ตาม ไม่พบว่ามีปัญหาใดๆ เกิดขึ้นในการสังเคราะห์ acbcPNA ทั้งสองชนิด แสดงว่า 2-aminocyclobutanecarboxylic acid ที่ถูก acylate แล้วมีความเสถียรต่อภาวะที่ใช้ในการสังเคราะห์พีเอ็นเอ (ที่ใช้ 20% piperidine เป็น deprotection reagent ซ้ำหลายๆ รอบ) และการกำจัดหมู่ปกป้องของนิวคลีโอเบส (ใช้สารละลาย 1:1 แอมโมเนีย-ไดออกเซน ที่ 60 ºC เป็นเวลา 8–12 ชั่วโมง)

ไฮบริดของ **acbcPNA-T9** กับ DNA คู่สม (dA_9) แสดงค่า T_m ถึง 74 ºC ซึ่งสูงใกล้เคียงกับ acpcPNA ที่มีลำดับเบสเป็น T_9 เหมือนกัน (T_m = 73 ºC ภายใต้ภาวะเดียวกัน) และการจับยึดมีความจำเพาะเจาะจงสูงดังจะเห็นได้จากการที่ไฮบริดของมันกับ single mismatched DNA มี T_m ที่ลดต่ำลงประมาณ 18–25 ºC นอกจากนี้ยังได้ยืนยันการเกิดไฮบริดโดยใช้ CD spectroscopy ซึ่งแสดงการเปลี่ยนแปลงสัญญาณอย่างชัดเจนเมื่อเกิดไฮบริดระหว่างพีเอ็นเอกับดีเอ็นเอคู่สม โดยสัญญาณนี้จะลดต่ำลงเมื่อเพิ่มอุณหภูมิ แสดงถึงการแยกตัวของสายพีเอ็นเอกับดีเอ็นเอที่อุณหภูมิสูง

ผลการศึกษา T_m ของ **acbcPNA-mix** กับดีเอ็นเอและอาร์เอ็นเอชนิดต่างๆ เปรียบเทียบกับ acpcPNA ซึ่งมีลำดับเบสเดียวกันเป็นดังสรุปในตารางที่ 16 ผลการทดลองแสดงให้เห็นว่าไฮบริดระหว่าง acbcPNA กับดีเอ็นเอคู่สมในทิศทางแอนติพาราเรลมีความเสถียรสูงกว่าของ acpcPNA โดยมีความจำเพาะเจาะจงของการเกิดไฮบริดต่ำลงดังจะเห็นได้จากความเสถียรของ single mismatched hybrid ที่เพิ่มขึ้นด้วยเมื่อเทียบกับ acpcPNA เมื่อเปรียบเทียบความสามารถในการเกิดไฮบริดกับอาร์เอ็นเอ พบว่า acbcPNA เกิดไฮบริดที่แข็งแรงกว่า acpcPNA ทั้งในทิศทางแอนติพาราเรลและพาราเรล โดยไฮบริดของแอนติพาราเรลอาร์เอ็นเอจะมีความเสถียรมากกว่าพาราเรลอาร์เอ็นเอ

ตารางที่ 16 เปรียบเทียบค่า T_m ของไฮบริดต่างๆ ของ **acbcPNA-mix** และ acpcPNA ที่มีลำดับเบสเดียวกัน (ภาวะ: ความเข้มข้นของ PNA = 1.0 μM DNA = 1.0 μM, 10 mM sodium phosphate buffer, 100 mM NaCl)

Entry	Target	T_m (ºC) (acbcPNA)	T_m (ºC) (acpcPNA)[a]	Note
1	dAGTGATCTAC	66.1	53.3	Antiparallel, perfect matched
2	dAGTGCTCTAC	39.8	23.8	Antiparallel, single mismatched
3	dAGTGTTCTAC	46.6	29.4	Antiparallel, single mismatched
4	dAGTGGTCTAC	36.4	23.9	Antiparallel, single mismatched
5	dCATCTAGTGA	<20	<20	Parallel, perfect matched
6	rAGUGAUCUAC	58.2	42.3	Antiparallel, perfect matched
7	rCAUCUAGUGA	31.7	<20	Parallel, perfect matched

[a]Data from Taechalertpaisarn et al., 2010

นอกจากนี้ยังได้ศึกษาความสามารถในการเกิดไฮบริดของ acbcPNA ที่มีลำดับเบสอื่นกับดีเอ็นเอและอาร์เอ็นเอ ผลที่ได้เป็นดังแสดงใน**ตารางที่ 17** (ข้อมูลใน entry 1 ซ้ำกับข้อมูลในตารางที่ 16)

ตารางที่ 17 T_m ของ complementary hybrids ของ acbcPNA กับ DNA และ RNA ชนิดต่างๆ ตัวเลขในวงเล็บแสดงค่า T_m acpcPNA-DNA hybrids ภายใต้ภาวะเดียวกัน [Vilaivan, 2011] (Conditions: [PNA] = [DNA] = 1 μM, 10 mM sodium phosphate buffer pH 7.0, 100 mM NaCl).

Entry	PNA	Sequence	% G+C	T_m (ºC) (apDNA)	T_m (ºC) (pDNA)	T_m (ºC) (apDNA)	T_m (ºC) (pRNA)
1	**acbcPNA-mix**	GTAGATCACT	40	66.1	<20	58.2	31.7
				(53.3)	(<20)	(42.3)	(<20)
2	**acbcPNA-mixAT**	TATGTACTAT	20	63.2	<20	50.8	25.8
				(54.2)	(<20)	(32.6)	(<20)
3	**acbcPNA-mixGC**	GCTACGTCGC	70	69.8	34.1	62.9	48.6
				(54.5)	(<20)	(48.0)	(32.9)

ข้อมูลที่ได้แสดงให้เห็นว่าการแทนที่ตัวเชื่อม ACPC ในพีเอ็นเอด้วย ACBC จะทำให้ความเสถียรของไฮบริดกับดีเอ็นเอและอาร์เอ็นเอเพิ่มขึ้น โดยค่า T_m ที่เพิ่มขึ้นจะอยู่ในช่วง 9–15 °C สำหรับดีเอ็นเอ และ 15–18 °C สำหรับอาร์เอ็นเอ ในขณะที่ยังคงมีความจำเพาะเจาะจงของการยึดจับในทิศทางแอนติพาราเรลที่สูงอยู่ ยกเว้นใน RNA ที่มี G/C rich ซึ่งสามารถตรวจพบการจับยึดกับ acbcPNA ในทิศทางพาราเรลได้ด้วย ซึ่งสอดคล้องกับสมบัติของ acpcPNA การที่ acbcPNA สามารถจับยึดกับอาร์เอ็นเอได้แข็งแรงกว่า acpcPNA มากเสนอแนะว่า acbcPNA น่าจะเหมาะสมในการนำไปประยุกต์ใช้กับโมเลกุลเป้าหมายที่เป็นอาร์เอ็นเอด้วย

ตารางที่ 18 T_m ของ self complementary และ DNA ไฮบริดของ acbcPNA และ acpcPNA (Conditions: [PNA] = [DNA] = 1 μM or [PNA] = 2 μM for self complementary studies, 10 mM sodium phosphate buffer pH 7.0, 100 mM NaCl).

Entry	PNA	Config	T_m self	T_m apDNA
1	**acbcPNA-sCom**	2'*R*,4'*R*	45.7	77.7
2	**acpcPNA-sCom**	2'*R*,4'*R*	<20	66.8
3	***epi*-acbcPNA-sCom**	2'*R*,4'*S*	59.3	73.3
4	***epi*-acpcPNA-sCom**	2'*R*,4'*S*	32.7	66.8

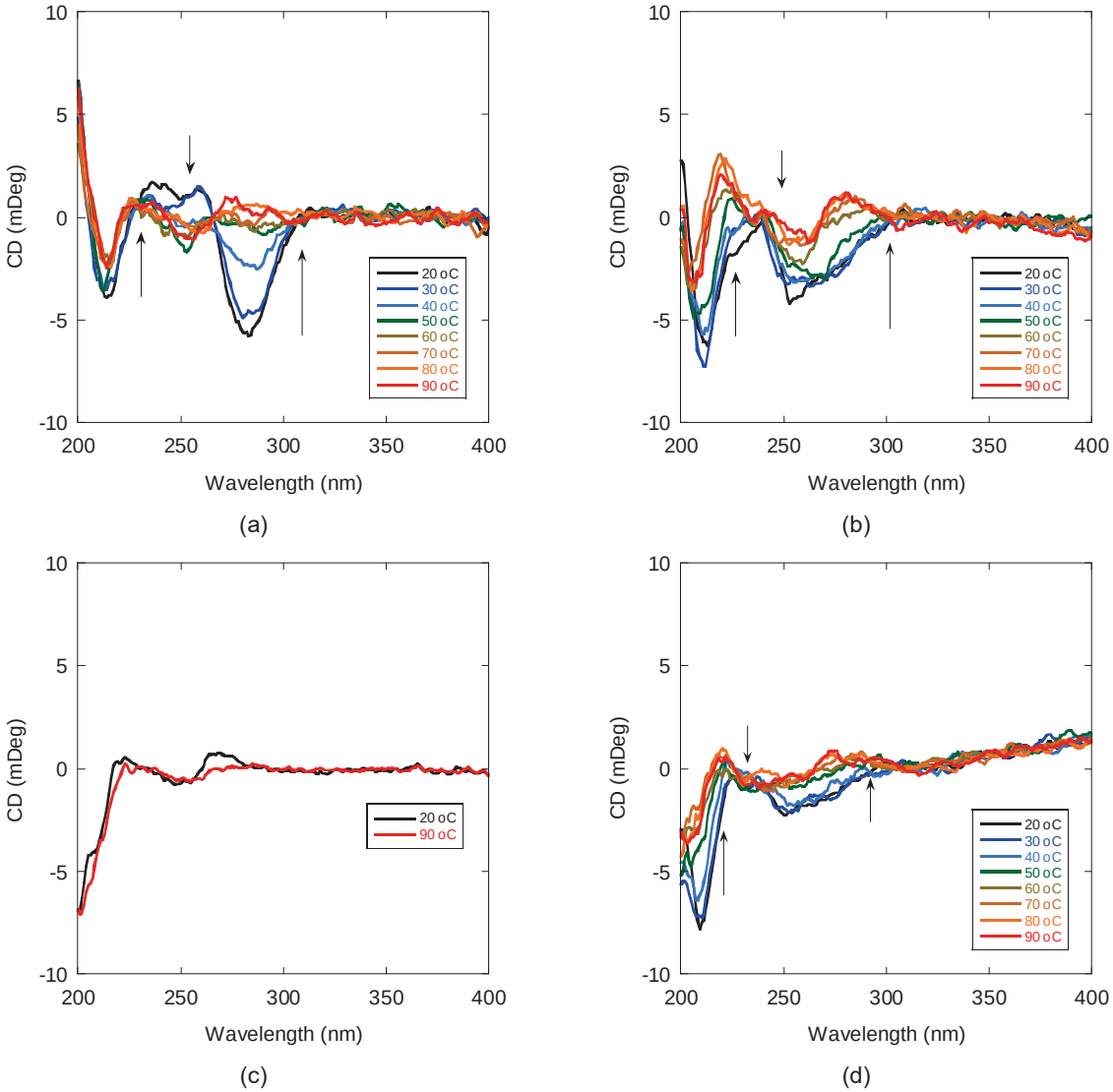

รูปที่ 35 CD spectra ของ self-complementary PNA **acbcPNA-sCom** (a) ***epi*-acbcPNA-sCom** (b) **acpcPNA-sCom** (c) and ***epi*-acpcPNA-sCom** (d) ที่อุณหภูมิต่างๆ (Conditions: 10 mM sodium phosphate buffer pH 7.0, 100 mM NaCl, [PNA] = 2 μM).

สุดท้ายนี้ยังได้ศึกษาความสามารถในการเกิด self-hybrid ของ acbcPNA ที่มีลำดับเบสเป็น self-complementary sequence (**acbcPNA-sCom**) โดยได้ศึกษาทั้งในกรณีที่เป็น (2'*R*,4'*R*) และ (2'*R*,4'*S*) (*epi*-acbcPNA) ไอโซเมอร์ เนื่องจากเป็นที่ทราบมาก่อนหน้านี้แล้วว่า (2'*R*,4'*S*) ไอโซเมอร์ของ acpcPNA สามารถเกิด self-complementary hybrid ที่เสถียรกว่า (2'*R*,4'*R*) ไอโซเมอร์ [Taechalertpaisarn et al., 2010] และยังได้เปรียบเทียบกับ acpcPNA ที่มีลำดับเบสเดียวกัน ผลที่ได้เป็นดังแสดงในตารางที่ 18 และรูปที่ 35

ข้อมูลในตารางที่ 18 แสดงให้เห็นว่า acbcPNA สามารถเกิด self complementary hybrid ที่เสถียรกว่า acpcPNA ซึ่งอาจเนื่องมาจาก steric effect ที่ลดลงของวงแหวนไซโคลบิวเทนเมื่อเทียบกับวงแหวนไซโคลเพนเทน โดยได้ยืนยันการเกิด self complementary hybrid ด้วย variable temperature CD spectroscopy ซึ่งแสดงการเปลี่ยนแปลงสัญญาณ CD ที่อุณหูมิต่ำกับสูงอย่างชัดเจน โดยในกรณีของ **acpcPNA-sCom** ซึ่งไม่สามารถเกิด self complementary hybrid จะไม่เห็นการเปลี่ยนแปลงสัญญาณ CD ดังกล่าว

ในขณะที่การแทนที่วงแหวนไซโคลเพนเทนใน acpcPNA ด้วยวงแหวนไซโคลบิวเทนใน acbcPNA ทำให้ได้พีเอ็นเอชนิดใหม่คือ acbcPNA ที่แสดงสมบัติการจับยึดกับดีเอ็นเอและอาร์เอ็นเอได้ดีขึ้น การแทนที่วงแหวนไซโคลเพนเทนด้วยวงแหวนไซโคลเฮกเซนจะได้ achcPNA ที่ไม่แสดงสมบัติการจับยึดกับดีเอ็นเอและอาร์เอ็นเอทั้งในกรณีที่มีลำดับเบสเป็น T_9 (**achcPNA-homoT**) และลำดับเบสผสม (**achcPNA-mix**) เมื่อพิจารณาแบบจำลองโมเลกุลของพีเอ็นเอ-ดีเอ็นเอที่ได้เคยศึกษามาก่อนหน้านี้ [Siriwong et al., 2008] สามารถอธิบายผลของขนาดของวงแหวนได้ว่าเกี่ยวข้องกับค่า torsional angle (θ) ซึ่งมีผลกระทบโดยตรงกับคอนฟอร์เมชันของสายพีเอ็นเอ กล่าวคือ แบบจำลองโมเลกุลแสดงว่าค่า θ ของ dapcPNA และ acpcPNA จะอยู่ที่ 99.2±6.4 $^\circ$ และ 99.2±3.1 $^\circ$ ตามลำดับ [Siriwong et al., 2008] ในขณะที่ค่า θ ที่ได้จากโครงสร้างผลึกของโอลิโกเมอร์ของ ACBC, ACPC และ ACHC คือ 85.9±12.2 [Fernandes et al., 2010], 95.5±3.7 [Appella et al., 1999b] และ 51.5–61.4 $^\circ$ [Appella et al., 1999a] ตามลำดับ จะเห็นได้ว่าค่า θ ของ ACBC ค่อนข้างใกล้เคียงกับค่าที่เหมาะสมมากที่สุด จึงกล่าวได้ว่า acbcPNA น่าจะมีการจัดตัวอยู่ในคอนฟอร์เมชันที่เหมาะสมที่จะเกิดไฮบริดกับดีเอ็นเอได้ดีกว่า acpcPNA ส่วนในกรณีของ achcPNA จะเห็นว่าค่า θ แตกต่างไปจากค่าที่เหมาะสมมาก ประกอบกับวงแหวนไซโคลเฮกเซนไม่สามารถบิดตัวได้อย่างอิสระเท่ากับวงแหวนไซโคลเพนเทนหรือไซโคลบิวเทน จึงทำให้ achcPNA สูญเสียความสามารถในการจับยึดกับดีเอ็นเอไป ข้อมูลเหล่านี้จะเป็นพื้นฐานของการออกแบบพีเอ็นเอที่แสดงสมบัติการจับยึดกับดีเอ็นเอและ/หรืออาร์เอ็นเอได้แข็งแรงและ/หรือมีความจำเพาะเจาะจงที่ดีขึ้น งานในส่วนนี้ได้รับการตีพิมพ์แล้ว [Mansawat et al., 2012b]

3.2.3 3-aminopyrrolidine-4-carboxylic acid (APC)

งานวิจัยส่วนนี้เป็นการขยายผลเพิ่มเติมจากทุนวิจัยหลังปริญญาเอกของ ดร.จตุรงค์ สุภาพพร้อม ที่เกี่ยวข้องกับการนำ 3-aminopyrrolidine-4-carboxylic acid (APC) ซึ่งเป็น aza-analogue ของ2-aminocyclopentanecarboxylic acid (ACPC) มาเป็นส่วนของตัวเชื่อมแทน ACPC ในระบบ acpcPNA โดยมีสมมติฐานว่าตัวเชื่อม APC น่าจะเพิ่มการละลายของ acpcPNA เนื่องจากมีไนโตรเจนอะตอมที่มีความชอบน้ำในสภาพที่ถูกโปรโตเนต และเป็นตำแหน่งให้ต่อฉลากต่างๆ เช่นไบโอตินหรือสารเรืองแสงได้ที่บริเวณกลางสายของ acpcPNA โดยไม่มีผลกระทบต่อความเสถียรมากนัก งานวิจัยในส่วนแรกจะเป็นการสังเคราะห์พีเอ็นเอที่มีส่วนของตัวเชื่อมถูกแทนที่ด้วย APC สองไอโซเมอร์ได้แก่ (3*R*,4*S*) และ (3*S*,4*R*) ซึ่งมีคอนฟิกกิวเรชันที่สอดคล้องกับ (1*S*,2*S*)- และ (1*R*,2*R*)- ACPC ตามลำดับ (รูปที่ 36 และ รูปที่ 37)

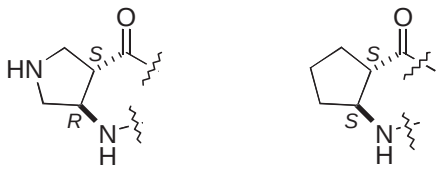

รูปที่ 36 เปรียบเทียบโครงสร้างของตัวเชื่อม (3*R*,4*S*)-APC และ ssACPC

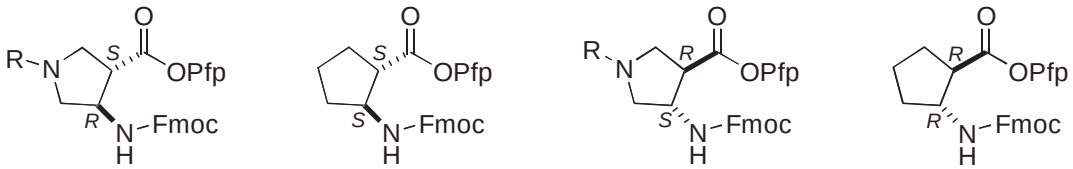

***RS*-APC1**: R = Boc (ssACPC) ***SR*-APC1**: R = Boc (rrACPC)

***RS*-APC2**: R = Tfa

รูปที่ 37 เปรียบเทียบโครงสร้างของ APC และ ACPC monomer

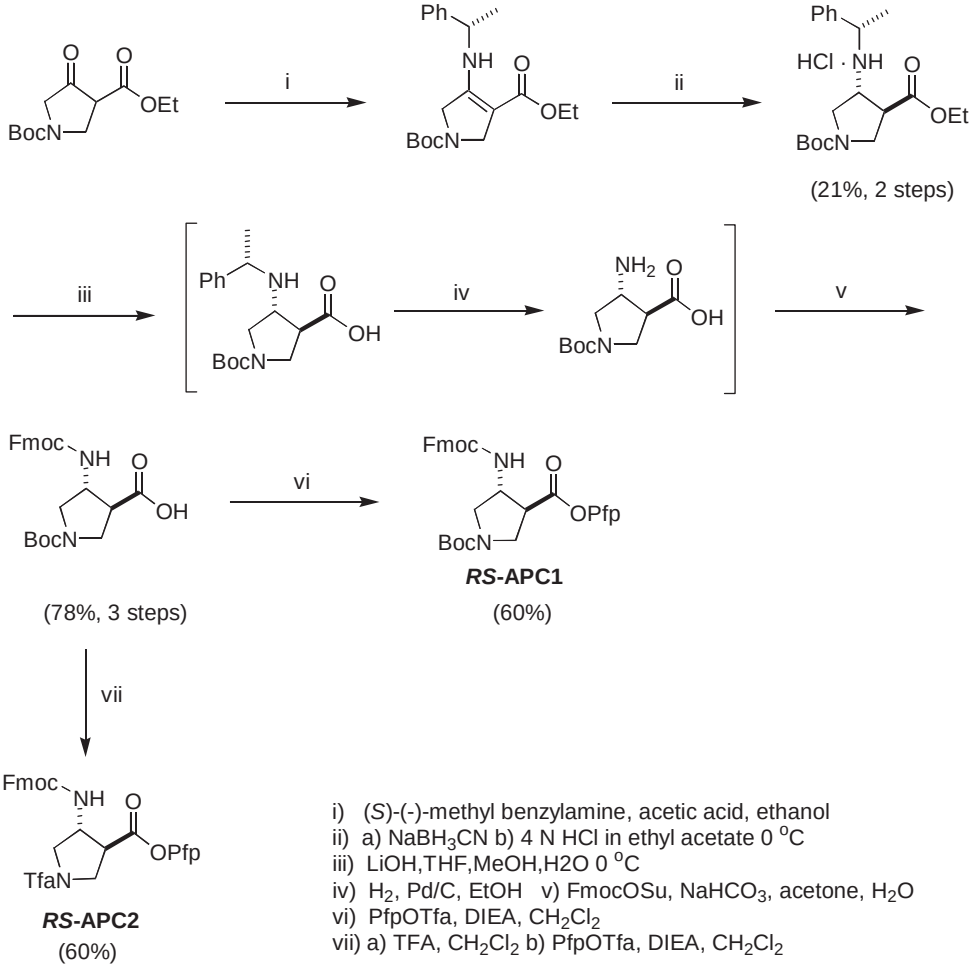

รูปที่ 38 การสังเคราะห์ APC โมโนเมอร์ ***RS*-APC1** และ ***RS*-APC2**

ในเบื้องต้นได้สังเคราะห์ orthogonally-protected APC โมโนเมอร์ ***RS*-APC1** และ ***SR*-APC1** ซึ่งใช้หมู่ Boc- และ ***RS*-APC2** ซึ่งใช้หมู่ Tfa (trifluoroacetyl) เป็นหมู่ปกป้องพิร์โรลิดีนไนโตรเจนอะตอม และมีหมู่ Fmoc เป็นหมู่ปกป้อง primary amino group โดยใช้วิธีการตามเอกสารอ้างอิง [Lee et al., 2001] ซึ่งอาศัยการทำปฏิกิริยา diastereoselective reduction ของอีนามีนที่ได้จาก (*S*)-methylbenzylamine เป็น chiral auxiliary และแยกผลิตภัณฑ์ไอโซเมอร์ที่ต้องการโดยใช้การตกผลึกของเกลือไฮโดรคลอไรด์ และเปลี่ยนให้เป็น NH_2-Fmoc-protected acid การแลกเปลี่ยนหมู่ปกป้องจาก Boc เป็น Tfa ทำได้โดยการกำจัดหมู่ Boc ออก ตามด้วยการ activate ด้วย pentafluorophenyl acetate (PfpOTfa) ซึ่งจะเป็นการเติมหมู่ปกป้อง Tfa ไปด้วยพร้อมกัน การสังเคราะห์ azaACPC โมโนเมอร์ ***RS*-APC1** และ ***SR*-APC1** เป็นดังสรุปในรูปที่ 38 ส่วนการสังเคราะห์โมโนเมอร์ ***SR*-APC1** ก็ทำได้โดยวิธีเดียวกัน แต่ใช้ (*R*)-methylbenzylamine เป็น chiral auxiliary แทน โดยได้ปริมาณผลผลิตใกล้เคียงกัน

ตารางที่ 19 ลำดับเบสของ APC-modified acpcPNA (apc/acpcPNA) ที่สังเคราะห์ขึ้นและข้อมูล MALDI-TOF MS และ T_m

Code	Sequence (N→C)[a]	*m/z* (calcd)	*m/z* (found)	T_m (°C)[b]
***RS*-t9**	Bz-$\underline{\text{TTTTTTTTT}}$-Lys$NH_2$	3250.5	3251.6	55.5 (76.7)[c,d]
***SR*-t9**	Bz-$\underline{\underline{\text{TTTTTTTTT}}}$-Lys$NH_2$	3250.5	3250.0	no Tm[c]
***RS*-T4tT4**	Bz-TTTT$\underline{\text{T}}$TTTT-LysNH_2	3242.5	3242.4	71.1[c]
***SR*-T4tT4**	Bz-TTTT$\underline{\underline{\text{T}}}$TTTT-Lys$NH_2$	3242.5	3243.8	28.3[c]
***RS*-mix**	Bz-GTAGA$\underline{\text{T}}$CAC T-LysNH_2	3621.9	3622.5	50.8 (57.6)[c,d]
***RS*-T4tT4(PyC)**	Ac-TTTT(PyC)$\underline{\text{T}}$TTTT-LysNH_2	3409.6	3411.4	62.2[e]
***RS*-mix(PyC)**	Ac-GTAGA(PyC)$\underline{\text{T}}$CACT-LysNH_2	3788.5	3789.3	45.2[e]
***RS*-T4tT4(PyB)**	Ac-TTTT(PyB)$\underline{\text{T}}$TTTT-LysNH_2	3451.6	3452.0	60.3[e]
***RS*-mix(PyB)**	Ac-GTAGA(PyB)$\underline{\text{T}}$CACT-LysNH_2	3893.0	3893.7	45.7[e]

[a] T = ssACPC-T; $\underline{\text{T}}$ = (3*R*,4*S*)-APC-T; $\underline{\underline{\text{T}}}$ = (3*S*,4*R*)-APC-T; (PyC) = pyrene-1-carbonyl modification; (PyB) = 3-(pyrene-1-yl)butyryl modification

[b] with complementary DNA (dA_9 for ***RS*-t9**, ***SR*-t9**, ***RS*-T4tT4**, ***SR*-T4tT4**, ***RS*-T4tT4(PyC)** and ***RS*-T4tT4(PyB)**; 5'- dAGTGATCTAC -3' for ***RS*-mix**, ***RS*-mix(PyC)** and ***RS*-mix(PyB)**

[c] Conditions: 10 mM sodium phosphate buffer pH 7.0, 100 mM NaCl, [PNA] = 1 μM and [DNA] = 1 μM

[d] Values in parentheses refer to the T_m of unmodified acpcPNA under identical conditions.

[e] Conditions: 10 mM sodium phosphate buffer pH 7.0, 0 mM NaCl, [PNA] = 2.5 μM and [DNA] = 3 μM

เมื่อได้โมโนเมอร์ของตัวเชื่อม APC มาแล้ว จึงนำไปทำเป็นพีเอ็นเอโอลิโกเมอร์ด้วยวิธีการสังเคราะห์เพปไทด์บนวัฏภาคของแข็งด้วยวิธีการตามเอกสารอ้างอิง โดยได้สังเคราะห์ apc/acpcPNA ทั้งหมด 5 ชนิดที่มีลำดับเบส ชนิด จำนวน และตำแหน่งของตัวเชื่อมแตกต่างกัน ดังแสดงในตารางที่ 19 โดยพีเอ็นเอ ***RS*-t9**, ***SR*-t9**, และ ***SR*-T4tT4** ซึ่งจะไม่ได้มีการดัดแปลงเพิ่มเติมสามารถสังเคราะห์ได้โดยอาศัย Boc-protected โมโนเมอร์ ***RS*-APC1** และ ***SR*-APC1** ส่วนพีเอ็นเอ ***RS*-T4tT4** และ ***RS*-mix** สามารถสังเคราะห์โดยใช้ Tfa-protected โมโนเมอร์ ***RS*-APC2** การใช้ Tfa โมโนเมอร์ทำให้สามารถกำจัดหมู่ปกป้องพิร์โรลิดีนไนโตรเจนออกได้โดยไม่ทำให้สายพีเอ็น

เอหลุดออกจากวัฏภาคของแข็ง จึงสามารถทำการต่อฉลากเรืองแสงเช่น pyrene-1-carboxylic acid หรือ 3-(pyrene-1-yl)butyric acid ซึ่งสามารถเปลี่ยนแปลงการเรืองแสงได้ตามสภาพแวดล้อม เข้าที่พีเอ็นเอบนวัฏภาคของแข็งได้โดยตรง ได้เป็นพีเอ็นเอ ***RS*-T4tT4(PC)**, ***RS*-T4tT4(PB)**, **RS-mix(PC)** และ ***RS*-mix(PB)** เพื่อพัฒนาเป็นพีเอ็นเอโพรบที่มีการเรืองแสงที่ตอบสนองต่อสถานะของการเกิดไฮบริดกับดีเอ็นเอเป้าหมายได้อย่างจำเพาะเจาะจง

จากการทดลองหาค่า T_m พบว่าการเปลี่ยนตัวเชื่อมจาก ssACPC เป็น (3*R*,4*S*)-azaACPC ทั้งสาย (***RS*-t9**) จะทำให้ค่า T_m ลดลงจาก 76.7 °C เป็น 55.5 °C หรือเฉลี่ยประมาณ 2.5 °C ต่อการแทนที่ ssACPC ด้วย (3*R*,4*S*)-APC หนึ่งครั้ง ส่วนการแทนที่ ssACPC หนึ่งตัวที่ตำแหน่งตรงกลางสายด้วย (3*R*,4*S*)-APC ดังในกรณีของ ***RS*-T4tT4** และ ***RS*-mix** ซึ่งเป็น homothymine และ mixed base acpcPNA ตามลำดับจะทำให้ค่า T_m นั้นลดลงไปเพียงเล็กน้อย (5.6–6.8 °C) ในขณะที่การแทนที่ ssACPC ด้วย (3*S*,4*R*)-APC ทั้งสาย (***SR*-t9**) จะทำให้พีเอ็นเอที่ได้สูญเสียความสามารถในการจับกับดีเอ็นเอโดยสิ้นเชิง (ยืนยันโดยเทคนิค CD และ UV titration) แม้แต่ ***SR*-T4tT4** ซึ่งมีการแทนที่ ssACPC เพียงหน่วยเดียวตรงกลางสายด้วย (3*S*,4*R*)-APC ก็แสดงค่า T_m ที่ลดลงอย่างมากถึง 48.4 °C เมื่อเทียบกับ acpcPNA ที่ไม่ได้มีการดัดแปลงใดๆ แสดงให้เห็นว่าโครงสร้างของตัวเชื่อม (3*S*,4*R*)-APC ไม่สามารถปรับตัวให้เข้ากับคอนฟอร์เมชันของ acpcPNA ได้ ซึ่งไม่เป็นที่เกินความคาดหมายนักเมื่อพิจารณาจากสเตอริโอเคมีของมันที่ตรงกันข้ามกับ ssACPC ส่วนในกรณีของ (3*R*,4*S*)-APC ที่มีโครงสร้างที่สอดคล้องกับ ssACPC จะทำให้ได้พีเอ็นเอที่มีความเสถียรมากกว่ามาก นอกจากนี้เมื่อพิจารณาในแง่ของ specificity การเปรียบเทียบการจดจำระหว่าง homothymine PNA ***RS*-t9** กับดีเอ็นเอคู่สม (dA_9) กับดีเอ็นเอที่เป็น single-base mismatch (dA_4TA_4) พบว่า T_m จะลดลงไป 28 °C (จาก 71.1 ไปเป็น 43.1 °C) แสดงว่า acpcPNA ที่ดัดแปลงด้วยตัวเชื่อม APC นี้ยังคงแสดงความจำเพาะเจาะจงในการจดจำกับดีเอ็นเอเป้าหมายที่สูงมากอยู่ งานที่ทำต่อจึงเน้นศึกษา acpcPNA ที่ดัดแปลงด้วย (3*R*,4*S*)-APC เป็นหลัก โดยได้เพิ่มหมู่ไพรีนเข้าไปที่ตำแหน่งของ (3*R*,4*S*)-APC ซึ่งผลการศึกษา T_m ของ ***RS*-T4tT4(PyC)**, ***RS*-T4tT4(PyB)**, ***RS*-mix(PyC)** และ ***RS*-mix(PyB)** แสดงให้เห็นว่าการต่อหมู่ไพรีนเข้าไปจะทำให้ความเสถียรของไฮบริดลดลงไปอีกประมาณ 5–10 °C เมื่อเทียบกับพีเอ็นเอที่ยังไม่ได้เติมหมู่ไพรีน ซึ่งความเสถียรที่ลดลงนี้น่าจะเกิดจากความเกะกะของหมู่ไพรีนรวมทั้งพันธะเอไมด์ที่เกิดขึ้นด้วย

สิ่งที่น่าสนใจคืออนุพันธ์ของไพรีนเหล่านี้สามารถเปลี่ยนแปลงการเรืองแสงได้ตามสถานะการเกิดไฮบริดของพีเอ็นเอ (รูปที่ 39) พีเอ็นเอ ***RS*-T4tT4(PyC)** ที่ดัดแปลงด้วย pyrene-1-carboxylic acid แสดงแถบการเรืองแสงที่เป็นลักษณะเฉพาะของไพรีนที่ 382 และ 400 nm เมื่อถูกกระตุ้นที่ 340 nm โดยการเรืองแสงมีค่าต่ำในสภาพที่เป็นสายเดี่ยว แต่เมื่อเติมดีเอ็นเอคู่สม (dA_9) เข้าไปจะทำให้การเรืองแสงเพิ่มขึ้น ~2.6 เท่า (ที่ 382 nm) โดยไม่มีการเปลี่ยนแปลงความยาวคลื่นของการเรืองแสง และเมื่อมี single mismatched DNA อยู่ด้วยจะไม่มีการเปลี่ยนแปลงการเรืองแสงเมื่อเทียบกับพีเอ็นเอสายเดี่ยว แต่เมื่อติดฉลากไพรีนเดียวกันนี้ใน ***RS*-mix(PyC)** ซึ่งมีลำดับเบสผสม พบว่าการเปลี่ยนแปลงการเรืองแสงเกิดขึ้นน้อยกว่ากรณีที่เป็น homothymine sequence มาก โดยค่าการเรืองแสงที่เพิ่มขึ้นเมื่อมีดีเอ็นเอคู่สมอยู่ด้วยคือ 1.3 เท่า และไม่มีการเปลี่ยนแปลงเมื่อมี single mismatched DNA

ฉลาก 3-(pyrene-1-yl)butyric acid (PB) แสดงการเปลี่ยนแปลงการเรืองแสงที่ชัดเจนกว่า pyrene-1-carboxylic acid กล่าวคือ ในกรณีที่ลำดับเบสเป็น homothymine ***RS*-T4tT4(PyB)** ในสภาพที่เป็นสายเดี่ยวมีการเรืองแสงที่ต่ำมาก และการเรืองแสงที่ ~380 nm เพิ่มขึ้นถึง 72 และ 10.5 เท่าเมื่อเกิดไฮบริดกับดีเอ็นเอคู่สม และ single mismatched DNA ตามลำดับ แต่สำหรับ ***RS*-mix(PyB)** ซึ่งมีลำดับเบสผสม จะมีค่าการเรืองแสงที่เพิ่มขึ้น

5.2 เท่าเมื่อเมื่อเกิดไฮบริดกับดีเอ็นเอคู่สม และไม่มีการเปลี่ยนแปลงการเรืองแสงเมื่อเกิดไฮบริดกับ single mismatched DNA โดยเมื่อเปรียบเทียบเฉพาะค่าการเรืองแสงของพีเอ็นเอสายเดี่ยวที่ติดฉลาก PB พบว่า ***RS*-mix(PyB)** ซึ่งมีลำดับเบสผสม มีค่าค่อนข้างสูงกว่า ***RS*-T4tT4(PyB)** ซึ่งเป็น homothymine อยู่ประมาณ 10 เท่า แสดงว่าปัจจัยหนึ่งที่ทำให้การเปลี่ยนแปลงการเรืองแสงน้อยลงใน ***RS*-mix(PyB)** เกิดจากการที่มี background fluorescence สูง ผลงานส่วนนี้ได้รับการตีพิมพ์ไปแล้ว [Reenabthue et al., 2011] งานที่จะทำต่อไปคือการศึกษาอิทธิพลของเบสแต่ละชนิดที่มีต่อการเรืองแสงของฉลาก 3-(pyrene-1-yl)butyric acid เพื่อพัฒนาพีเอ็นเอโพรบที่มี background fluorescence ต่ำลง

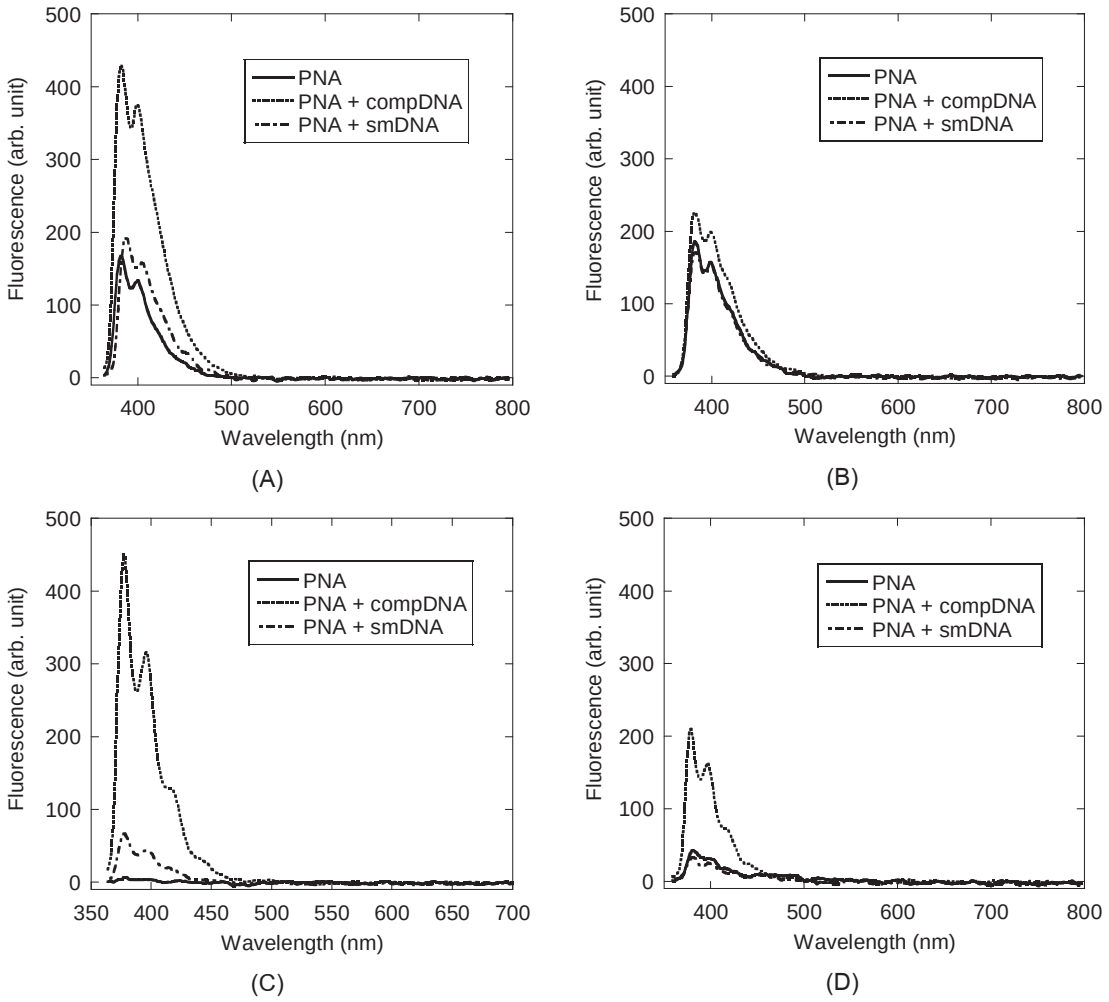

รูปที่ 39 Fluorescence spectra of pyrene-labeled acpc/apcPNA (A) ***RS*-T4tT4(PyC)** (A), ***RS*-mix(PyC)** (B), ***RS*-T4tT4(PyB)** (C), ***RS*-mix(PyB)** (D) and their hybrids with complementary DNA (dA_9 for ***RS*-T4tT4(PyC)** and ***RS*-T4tT4(PyB)**; dAGTGATCTAC for ***RS*-mix(PyC)** and ***RS*-mix(PyB)**) and single mismatched DNA (dA_4TA_4 for ***RS*-T4tT4(PyC)** and ***RS*-T4tT4(PyB)**; dAGTGACCTAC for ***RS*-mix(PyC)** and ***RS*-mix(PyB)**). The spectra were measured in 10 mM sodium phosphate buffer, pH 7.0 at 25 ºC, [PNA] = 2.5 μM and [DNA] = 3.0 μM, excitation wavelength = 345 nm (***RS*-T4tT4(PyC)** and ***RS*-mix(PyC)**) or 340 nm (***RS*-T4tT4(PyB)** and ***RS*-mix(PyB)**).

เพื่อเป็นการศึกษาผลของการติดฉลากไพรีนบิวทีริล (PyB) ที่ตำแหน่งต่างๆ ของพีเอ็นเอที่มีต่อการเรืองแสงของฉลาก PyB ในงานวิจัยได้เปรียบเทียบการเรืองแสงพีเอ็นเอที่มีลำดับเบสเดียวกันคือ GTAGATCACT แต่มีการดัดแปลงด้วย PyB ที่ตำแหน่งภายในของสายพีเอ็นเอ และที่ปลายด้าน N และด้าน C ทั้งในสภาพที่เป็นสายเดี่ยวและเมื่อเข้าคู่กับดีเอ็นเอที่เป็นคู่สมและไม่เป็นคู่สม โดยการติดฉลากที่ตำแหน่ง internal กระทำผ่านตัวเชื่อม (3*R*,4*S*)-APC ที่อยู่ทางด้าน N ของเบสที่แสดงตำแหน่งโดยการขีดเส้นใต้ ส่วนการติดฉลากที่ตำแหน่ง C-terminus และ N-terminus กระทำผ่านโซ่ข้างของ C-terminal lysine และ N-terminal ACPC ตามลำดับ ผลที่ได้เป็นดังแสดงในตารางที่ 20

ตารางที่ 20 ข้อมูลการเรืองแสงของพีเอ็นเอที่ติดฉลากด้วย PyB ในสภาวะที่มีและไม่มีดีเอ็นเอคู่สมอยู่ด้วย (conditions: 2.5 μM PNA, 3.0 μM DNA, 10 mM sodium phosphate buffer pH=7.0, λ_{excit} = 345 nm).

Entry	System	Φ_F(ss)	Φ_F(ds)	Φ_F(ds/ss)	F_{377}(ds/ss)	Note
1	GTAGATCACT 3'-CATCTAGTGA-5'	0.0424	0.1873	4.41	5.20	comp.
2	GTAGATCACT 3'-CATCCAGTGA-5'	0.0444	0.0446	1.00	0.87	internal mismatch
3	GTAGATCACT 3'-CATCTAGTGA-5'	0.0348	0.1675	4.81	4.65	comp.
4	GTAGATCACT 3'-CATCCAGTGA-5'	0.0348	0.0659	1.89	1.12	internal mismatch
5	PyB-GTAGATCACT 3'-CATCTAGTGA-5'	0.0492	0.0105	0.21	0.23	comp.
6	PyB-GTAGATCACT 3'-CATCCAGTGA-5'	0.0447	0.0116	0.26	0.34	internal mismatch
7	GTAGATCACT-PyB 3'-CATCTAGTGA-5'	N.D.	N.D.	N.D.	0.46	Comp.
8	GTAGATCACT-PyB 3'-CATCCAGTGA-5'	N.D.	N.D.	N.D.	0.50	internal mismatch

ข้อมูลจาก**ตารางที่ 20** แสดงให้เห็นว่าในทุกกรณี ฉลาก PyB จะมีการเรืองแสงเมื่อเริ่มต้นไม่แตกต่างกันมากนัก โดยมี Φ_F(ss) 0.04-0.05 ภายใต้ภาวะเดียวกัน แต่เฉพาะกรณีที่มีการติดฉลาก PyB เข้าที่ตำแหน่งกลางสายของพีเอ็นเอเท่านั้นที่การเกิดไฮบริดกับดีเอ็นเอที่มีลำดับเบสคู่สมทำให้เกิดการเพิ่มขึ้นของการเรืองแสงถึง 4.4 เท่า เมื่อพิจารณาจาก Φ_F(ds/ss) หรือ 5.2 เท่า เมื่อพิจารณาจาก F_{377}(ds/ss) ในขณะที่การเกิดไฮบริดกับดีเอ็นเอที่มีลำดับเบสผิดไป 1 ตำแหน่งจะทำให้การเรืองแสงเปลี่ยนแปลงไปโดยลดต่ำลงกว่าพีเอ็นเอสายเดี่ยวเล็กน้อย และการติด PyB ที่ตำแหน่งปลายสายของพีเอ็นเอไม่ว่าจะเป็นด้าน N หรือ ด้าน C จะทำให้การเรืองแสงลดลงอย่างมากเมื่อเกิดไฮบริดกับดีเอ็นเอทั้งที่เป็นคู่สมและไม่เป็นคู่สม

เพื่อยืนยันว่าการเรืองแสงที่เพิ่มขึ้นเมื่อมีการเข้าคู่ระหว่างพีเอ็นเอที่ติดฉลาก PyB ที่ตำแหน่งกลางสายกับดีเอ็นเอคู่สมเกิดขึ้นกับพีเอ็นเอทั่วๆ ไปโดยไม่เจาะจงกับลำดับเบสนี้เท่านั้น จึงได้ทดลองสังเคราะห์พีเอ็นเอที่มีลำดับเบสอื่น และติดฉลาก PyB ไว้ที่ตำแหน่งกลางสายเหมือนกัน โดยให้อยู่ระหว่างเบสที่แตกต่างกันได้แก่ A/T และ T/T **(ตารางที่ 21)** พบว่าในทั้งสองกรณีมีการเรืองแสงที่เพิ่มขึ้นจริงเมื่อมีการเข้าคู่กับดีเอ็นเอที่มีลำดับเบสคู่

สม และการเข้าคู่กับดีเอ็นเอที่มีเบสผิดไปหนึ่งตำแหน่งจะทำให้การเรืองแสงเปลี่ยนแปลงแตกต่างกันออกไป โดยความแตกต่างนี้ขึ้นกับตำแหน่งของเบสที่ผิดไป หากเบสที่ผิดไปอยู่ใกล้กับตำแหน่งที่ติดฉลากจะทำให้การเรืองแสงมีค่าต่ำ แต่ถ้าอยู่ห่างจากตำแหน่งที่ติดฉลากออกไป การเรืองแสงจะมีค่าสูงขึ้น (ตารางที่ 21 และรูปที่ 40)

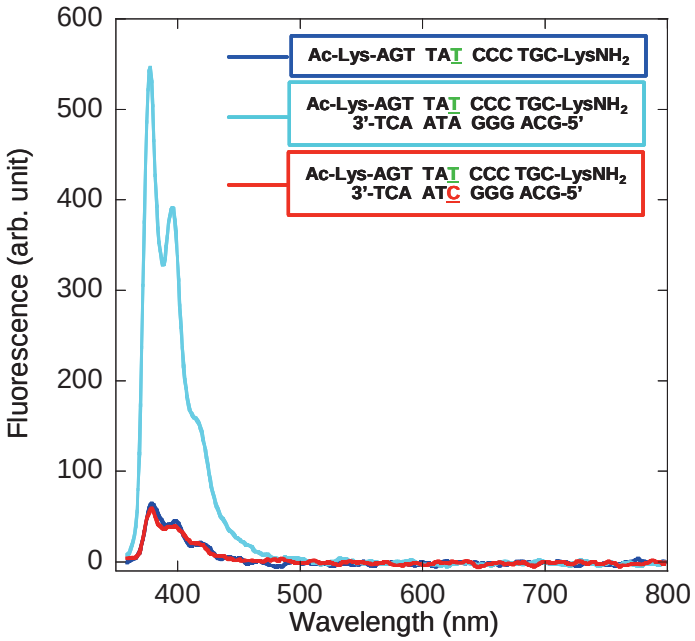

รูปที่ 40 ฟลูออเรสเซนต์สเปกตรัมของพีเอ็นเอที่ติดฉลากด้วย PyB (Ac-Lys-AGTTATCCCTGC-LysNH$_2$) ในสภาพที่เป็นสายเดี่ยวและเมื่อมี DNA ที่มีลำดับเบสคู่สม (5'-GCAGGGATAACT-3') และ DNA ที่เป็น single mismatched (5'-GCAGGGCTAACT-3') (conditions: 10 mM sodium phosphate buffer, pH 7.0 at 25 ºC, [PNA] = 2.5 μM and [DNA] = 3.0 μM, excitation wavelength = 345 nm)

ตารางที่ 21 การเรืองแสงของพีเอ็นเอที่ติดฉลากด้วย PyB ที่ตำแหน่ง internal (ตำแหน่งที่ติดฉลากแสดงโดยการขีดเส้นใต้) ในสภาวะที่มีและไม่มีดีเอ็นเอคู่สมอยู่ด้วย (conditions: 2.5 μM PNA, 3.0 μM DNA, 10 mM sodium phosphate buffer pH=7.0, λ_{excit} = 345 nm).

Entry	System	Φ_F	Φ_F(ds/ss)	F_{377}(ds/ss)	Note
1	AGTTATCCCTGC	0.0203	-	-	single stranded
2	AGTTATCCCTGC 3'-TCAATAGGGACG-5'	0.2839	14.0	6.14	comp.
3	AGTTATCCCTGC 3'-TCAATCGGGACG-5'	0.0347	1.08	0.92	internal mismatch (T·C)
4	AGTTATCCCTGC 3'-TCAATTGGGACG-5'	0.1695	8.34	5.99	internal mismatch (T·T)
5	AGTTATCCCTGC 3'-TCAATGGGGACG-5'	0.0132	0.65	0.70	internal mismatch (T·G)
6	CTAAATTCAGA	0.0518	-	-	single stranded
7	CTAAATTCAGA 3'-GATTTAAGTCT-5'	0.3259	6.36	6.82	comp.
8	CTAAATTCAGA 3'-GATTTACGTCT-5'	0.0412	0.80	0.64	internal mismatch (T·C)

ตารางที่ 21 (ต่อ)

Entry	System	Φ_F	Φ_F(ds/ss)	F_{377}(ds/ss)	Note
9	CTAAATTCAGA 3'-GATTTATGTCT-5'	0.1571	3.07	2.36	internal mismatch (T·T)
10	CTAAATTCAGA 3'-GATTTAGGTCT-5'	0.0524	1.02	0.67	internal mismatch (T·G)
11	CTAAATTCAGA 3'-GATTTGAGTCT-5'	0.0805	1.57	1.01	internal mismatch (T·G)
12	CTAAATTCAGA 3'-GATTTTAGTCT-5'	0.3757	7.33	4.10	internal mismatch (T·T)
13	CTAAATTCAGA 3'-GATTCAAGTCT-5'	0.2828	5.52	4.36	indirect mismatch (A·C)
14	CTAAATTCAGA 3'-GATTAAAGTCT-5'	0.3119	6.08	5.98	indirect mismatch (A·A)
15	CTAAATTCAGA 3'-GATTGAAGTCT-5'	0.2624	5.12	5.02	indirect mismatch (A·G)
16	CTAAATTCAGA 3'-GATTTAACTCT-5'	0.0849	1.66	1.69	indirect mismatch (C·C)
17	CTAAATTCAGA 3'-GATTTAATTCT-5'	0.1578	3.08	2.92	indirect mismatch (C·T)
18	CTAAATTCAGA 3'-GATTTAAATCT-5'	0.1660	3.24	2.72	indirect mismatch (C·A)
19	CTAAATTCAGA	0.1463	-	-	single stranded
20	CTAAATTCAGA 3'-GATTTAAGTCT-5'	0.3378	2.31	2.91	comp.
21	CTAAATTCAGA 3'-GATTTAAATCT-5'	0.0795	0.54	0.33	internal mismatch (C·A)
22	CTAAATTCAGA 3'-GATTTAACTCT-5'	0.0493	0.34	0.23	internal mismatch (C·C)
23	CTAAATTCAGA 3'-GATTTAATTCT-5'	0.0471	0.32	0.22	internal mismatch (C·T)
24	CTAAATTCAGA 3'-GATTAAAGTCT-5'	0.2770	1.89	1.55	indirect mismatch (A·A)
25	CTAAATTCAGA 3'-GATTCAAGTCT-5'	0.2692	1.84	1.50	indirect mismatch (A·C)
26	CTAAATTCAGA 3'-GATTTAAGTCT-5'	0.1952	1.33	1.04	indirect mismatch (A·T)

จากพฤติกรรมการเรืองแสงของพีเอ็นเอที่ติดฉลาก PyB ตรงกลางสายดังกล่าว ประกอบกับข้อมูลจาก UV spectroscopy ของพีเอ็นเอที่เกิดไฮบริดกับดีเอ็นเอคู่สมที่แสดงการเกิด hypsochromic shift ของ pyrene absorption band จาก 346 nm ในพีเอ็นเอสายเดี่ยวไปเป็น 343 nm ในพีเอ็นเอ-ดีเอ็นเอไฮบริด และ ของพีเอ็นเอที่เกิดไฮบริดกับดีเอ็นเอที่ไม่เป็นคู่สมที่แสดงการเกิด bathochromic shift ของ pyrene absorption band จาก 346 nm ในพีเอ็นเอสายเดี่ยวไปเป็น 348 nm ในพีเอ็นเอ-ดีเอ็นเอไฮบริด ซึ่งการเปลี่ยนแปลงของ λ_{max} ของ pyrene absorption band นี้มีความสัมพันธ์กับการเกิด stacking กล่าวคือการเกิด bathochromic shift แสดงถึงการเกิด stacking ของไพรีน ดังนั้นไพรีนในพีเอ็นเอ-ดีเอ็นเอไฮบริดที่ไม่เป็นคู่สมจะมีการ stack ของไพรีนมากที่สุด

เนื่องจากคู่เบสไม่แข็งแรงทำให้ไพรีนซึ่งไม่ชอบน้ำสามารถแทรกตัวเข้าไปแทนคู่เบสที่ไม่เป็นคู่สม ตามด้วยพีเอ็นเอสายเดี่ยว และพีเอ็นเอ-ดีเอ็นเอไฮบริดที่เป็นคู่สม ในกรณีนี้คู่เบสมีความแข็งแรง ไพรีนไม่สามารถแทรกตัวเข้าไปได้ จึงต้องอยู่ในสภาพที่ยื่นออกไปจาก PNA·DNA duplex ซึ่งสอดคล้องกับการเรืองแสงที่วัดได้ (การเกิด stacking จะทำให้การเรืองแสงจะลดลง) การเปลี่ยนแปลงการเรืองแสงของพีเอ็นเอที่ติดฉลากด้วยไพรีนจึงสามารถอธิบายได้ดังรูปที่ 41

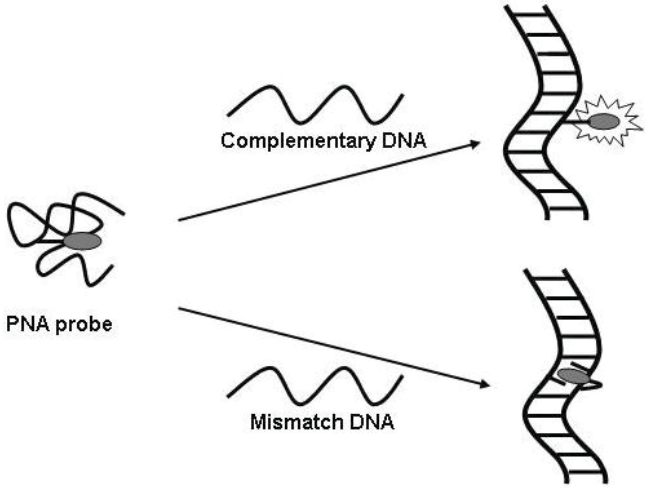

รูปที่ 41 แบบจำลองเพื่ออธิบายการเปลี่ยนแปลงการเรืองแสงของพีเอ็นเอที่ติดฉลากด้วย PyB ที่ตำแหน่ง internal

แม้การเปลี่ยนแปลงการเรืองแสงของ PyB PNA จะเป็นไปในลักษณะที่เพิ่มขึ้นเมื่อมีดีเอ็นเอคู่สมอยู่ด้วย การเปลี่ยนแปลงการเรืองแสงเมื่อมีดีเอ็นเอที่ไม่เป็นคู่สมจะทำนายผลได้ยากกว่า โดยอาจเพิ่มขึ้น เท่าเดิม หรือลดลง โดยขึ้นอยู่กับตำแหน่ง และชนิดของ mismatch base pair ที่เกี่ยวข้อง ข้อสรุปทั่วๆ ไปคือหาก mismatched base อยู่ในตำแหน่งใกล้เคียงกับตำแหน่งของ PyB เลเบล จะทำให้การเรืองแสงเท่าเดิมหรือลดลงเมื่อเทียบกับ single stranded PNA และเมื่อ mismatched base อยู่ห่างออกไป การเรืองแสงจะสูงขึ้นตามลำดับ ซึ่งสอดคล้องกับแบบจำลองที่เสนอในรูปที่ 41 อย่างไรก็ตาม มีข้อยกเว้นอยู่ในกรณีที่มี mismatch pair เป็น T·T อยู่ใกล้กับตำแหน่งของ PyB เลเบล พบว่าจะให้การเรืองแสงที่เพิ่มขึ้นสูงมากใกล้เคียงกับกรณีที่เป็น complementary ซึ่งยังไม่สามารถอธิบายได้จากผลการทดลองเท่าที่มีอยู่ในขณะนี้

เพื่อศึกษาต่อไปว่าอะไรคือปัจจัยที่ทำให้พีเอ็นเอที่ติดฉลากที่ปลายสายจึงมีการเรืองแสงที่ลดลงเมื่อเข้าคู่กับทั้งดีเอ็นเอคู่สมและไม่เป็นคู่สมจึงได้ทำการทดลองกับพีเอ็นเอที่มีลำดับเบสเป็น PyB-XGTTATCCCTGC (X = A, C, G, T) และ PyB-CTAAATTCAGA กับดีเอ็นเอที่มีลำดับเบสเป็นคู่สมและไม่เป็นคู่สมต่างๆ กัน ผลที่ได้เป็นดังแสดงในตารางที่ 22

ตารางที่ 22 การเรืองแสงของพีเอ็นเอที่ติดฉลากด้วย PyB ที่ตำแหน่ง terminal ในสภาวะที่มีและไม่มีดีเอ็นเอคู่สมอยู่ด้วย (conditions: 2.5 μM PNA, 3.0 μM DNA, 10 mM sodium phosphate buffer pH=7.0, λ_{excit} = 345 nm).

Entry	System	Φ_F	Φ_F(ds/ss)	F_{377}(ds/ss)	Note
1	PyB-AGTTATCCCTGC	0.0956	-	-	single stranded
2	PyB-AGTTATCCCTGC 3'-TCAATAGGGACG-5'	0.0221	0.23	0.32	comp. (A·T)
3	PyB-AGTTATCCCTGC 3'-GCAATAGGGACG-5'	0.1522	1.59	2.29	terminal mismatch (A·G)
4	PyB-AGTTATCCCTGC 3'-CCAATAGGGACG-5'	0.1297	1.36	2.50	terminal mismatch (A·C)
5	PyB-AGTTATCCCTGC 3'-ACAATAGGGACG-5'	0.1874	1.96	2.00	terminal mismatch (A·A)
6	PyB-AGTTATCCCTGC 3'-TCAATCGGGACG-5'	0.0225	0.24	0.20	internal mismatch (T·C)
7	PyB-AGTTATCCCTGC 3'-ATCAATAGGGACG-5'	0.0524	0.55	0.45	N-terminal extended (+A)
8	PyB-AGTTATCCCTGC 3'-TTCAATAGGGACG-5'	0.0104	0.11	0.13	N-terminal extended (+T)
9	PyB-AGTTATCCCTGC 3'-CTCAATAGGGACG-5'	0.0359	0.38	0.14	N-terminal extended (+C)
10	PyB-AGTTATCCCTGC 3'-GTCAATAGGGACG-5'	0.0148	0.15	0.36	N-terminal extended (+G)
11	PyB-AGTTATCCCTGC 3'-_CAATAGGGACG-5'	0.1647	1.72	2.11	N-terminal deleted (-T)
12	PyB-AGTTATCCCTGC 3'-__AATAGGGACG-5'	0.1634	1.71	2.15	N-terminal deleted (-TC)
13	PyB-CTAAATTCAGA	0.0262	-	-	single stranded
14	PyB-CTAAATTCAGA 3'-GATTTAAGTCT-5'	0.0104	0.40	0.46	comp. (C·G)
15	PyB-CTAAATTCAGA 3'-AATTTAAGTCT-5'	0.0453	1.73	2.49	terminal mismatch (C·A)
16	PyB-CTAAATTCAGA 3'-GATTTCAGTCT-5'	0.0030	1.73	0.22	internal mismatch (T·C)
17	PyB-CTAAATTCAGA 3'-TGGGATTTAAGTCT-5'	0.0167	0.64	0.62	N-terminal extended (+TGG)

จากผลการทดลองทั้งหมดสามารถสรุปได้ว่า acpcPNA ที่ติดฉลาก PyB สามารถ sense local environment ของพีเอ็นเอเบสได้ และสามารถใช้เป็น quencher free molecular beacon [Venkatesan, 2008] ได้

โดยหากติดฉลาก PB เข้าที่ตำแหน่งกลางสายของพีเอ็นเอ โดยจะทำให้เกิดการเรืองแสงเพิ่มขึ้นหากมีการเข้าคู่กับดีเอ็นเอที่มีเบสคู่สม เนื่องจากหมู่ไพรีนไม่สามารถเกิดการ intercalate เข้าไปในพีเอ็นเอ-ดีเอ็นเอไฮบริดที่เป็นคู่สม ซึ่งเป็นพฤติกรรมที่แตกต่างจากดีเอ็นเออย่างชัดเจน (เป็นที่ทราบกันดีว่าดีเอ็นเอที่ติดฉลากด้วยไพรีนตรงตำแหน่ง 2' ของวงแหวนดีออกซีไรโบสจะมีการเรืองแสงลดลงในสภาพที่เป็น duplex เนื่องจากการเกิด intercalation) [Yamana, 1999] ในขณะที่การติดฉลาก PyB ตรงปลายสายของพีเอ็นเอจะทำให้การเรืองแสงลดลงหากมีการเข้าคู่กับดีเอ็นเอที่มีเบสคู่สม เนื่องจากการ stack ของไพรีนกับคู่เบสที่อยู่ตรงปลายของพีเอ็นเอ-ดีเอ็นเอไฮบริด และการเรืองแสงจะเพิ่มขึ้นถ้าดีเอ็นเอไม่มีเบสตรงปลาย หรือมีเบสที่ไม่เป็นคู่สม เนื่องจากไม่เกิดการ stacking ของไพรีนกับคู่เบส

แม้พีเอ็นเอที่ติดฉลากด้วย PyB ที่ตำแหน่งกลางสายจะมีการเปลี่ยนแปลงการเรืองแสงในทิศทางที่เพิ่มขึ้น (turn on) เมื่อเกิดไฮบริดกับดีเอ็นเอคู่สม ปัญหาหนึ่งที่พบคือการที่พีเอ็นเอสายเดี่ยวมี background fluorescence สูง ซึ่งจากแบบจำลองที่แสดงในรูปที่ 41 การเรืองแสงของพีเอ็นเอสายเดี่ยวควรจะต่ำเนื่องจากการ quench ด้วยนิวคลีโอเบส แต่นิวคลีโอเบสต่างชนิดกันจะมีความสามารถในการ quench ไพรีนได้ไม่เท่ากัน โดยงานวิจัยก่อนหน้านี้ได้แสดงว่าความสามารถในการ quench pyrene ของนิวคลีโอเบสในดีเอ็นเอเรียงลำดับได้ดังนี้ T>C>G>A [Wilson, 2008] เพื่อเป็นการยืนยันว่าลำดับดังกล่าวยังคงเป็นจริงในระบบ acpcPNA จึงได้สังเคราะห์พีเอ็นเอที่มีลำดับเบสเป็น AA, TT, CC และ GG โดยติดหมู่ PB ที่ระหว่างเบสทั้งสอง และวัดการเรืองแสงในสภาพที่เป็นสายเดี่ยวเปรียบเทียบกัน พบว่าลำดับของความสว่าง (ที่ความเข้มข้นเดียวกัน) คือ AA >> GG > CC> TT ซึ่งสอดคล้องกัน (ตารางที่ 23) และเบส A ให้ความสว่างใกล้เคียงกับเมื่อไม่มีเบสใดๆ (P = abasic PNA) ดังนั้น การออกแบบระบบ quencher free molecular beacon ที่ให้มี background ต่ำควรจะต้องอาศัยลำดับเบสที่เป็น pyrimidine rich และหลีกเลี่ยงการติดฉลาก PyB ในตำแหน่งที่ใกล้กับเบส A อย่างไรก็ตาม ผลการทดลองที่ได้ทำเพิ่มเติม ซึ่งจะไม่ขอกล่าวรายละเอียดในที่นี้แสดงให้เห็นว่าการ quench ของฉลาก PyB ไม่ได้จำกัดอยู่เฉพาะโดยนิวคลีโอเบสตัวที่อยู่ติดกับฉลาก PyB เท่านั้น

ตารางที่ 23 การเรืองแสงของพีเอ็นเอสายเดี่ยวที่ติดฉลากด้วย PyB ที่ตำแหน่งตรงกลางระหว่างเบส 2 ตัว (conditions: 2.5 μM PNA, 3.0 μM DNA, 10 mM sodium phosphate buffer pH=7.0, λ_{excit} = 345 nm).

Entry	System	Φ_F
1	P(PB)P	0.4096
2	A(PB)A	0.3322
3	C(PB)C	0.0102
4	G(PB)G	0.1240
5	T(PB)T	0.0020
6	A(PB)T	0.0705
7	T(PB)A	0.0533

แม้ว่าการเปลี่ยนแปลงการเรืองแสงของฉลาก PyB จะให้ข้อมูลเกี่ยวกับ local environment ของมันได้ แต่ในบางกรณีก็สามารถแปลผลได้ยาก โดยเฉพาะอย่างยิ่งในกรณีที่มี mismatch base อยู่ห่างจากตำแหน่งที่ติดฉลาก PyB หรือเมื่อมี T·T mismatch เพื่อเป็นการแก้ปัญหานี้จึงได้มีแนวคิดที่จะใช้เอนไซม์ nuclease S1 ที่จำเพาะเจาะจงต่อการย่อย DNA สายเดี่ยวมาช่วยเพิ่มความจำเพาะเจาะจงของการตรวจสอบลำดับเบสของดีเอ็นเอโดย PyB-labeled acpcPNA probes หลักการคือเป็นที่ทราบกันมาก่อนหน้านี้แล้วว่า DNA ที่เป็นส่วนหนึ่งของ

complementary PNA·DNA hybrid จะเสถียรต่อการถูกย่อยโดย nuclease S1 กว่า DNA ที่อยู่ใน mismatched PNA·DNA hybrid มาก [Komiyama et al. 2003] ดังนั้นจึงได้ทดลองวัดการเรืองแสงของพีเอ็นเอที่ไฮบริไดซ์กับดีเอ็นเอที่เป็นคู่สมและไม่เป็นคู่สมชนิดต่างๆ จากนั้นจึงเติมเอนไซม์ลงไป และติดตามการเปลี่ยนแปลงการเรืองแสงเมื่อเวลาผ่านไป (รูปที่ 41) พบว่าผลที่ได้เป็นที่น่าพอใจ กล่าวคือเมื่อตอนเริ่มต้น พบว่า single mismatched hybrid ที่มีตำแหน่งของ mismatch ไม่ตรงกับฉลาก PB จะมีการเรืองแสงที่สูงกว่า background อยู่พอสมควร (ตัวเลข F/F_0 อยู่ระหว่าง 2–6 เท่า ซึ่งไม่ตรงกับข้อมูลในตารางที่ 21 เนื่องจากภาวะที่ใช้ในการศึกษาการเรืองแสงต่างกัน กล่าวคือการทดลองนี้ทำใน S1 buffer ซึ่งเป็น 30 mM sodium acetate pH 4.6) หลังให้ทำปฏิกิริยาไป 10 นาที พบว่าสัญญาณที่เกิดจาก mismatched hybrid ลดลงเหลือเท่ากับพีเอ็นเอสายเดี่ยว (F/F_0 = 1) ในทุกกรณี ในขณะที่สัญญาณของ complementary hybrid ลดลงไปเพียงเล็กน้อย (F/F_0 จาก 14 เท่า เหลือประมาณ 10 เท่า) แสดงว่าดีเอ็นเอที่เข้าคู่อย่างไม่สมบูรณ์ถูกย่อยได้เร็วกว่าดีเอ็นเอที่เข้าคู่กับพีเอ็นเออย่างสมบูรณ์ ดังนั้นจึงสามารถใช้ nuclease S1 ในการเพิ่มความจำเพาะเจาะจงของการตรวจสอบลำดับเบสของดีเอ็นเอด้วย PyB-labeled PNA ได้

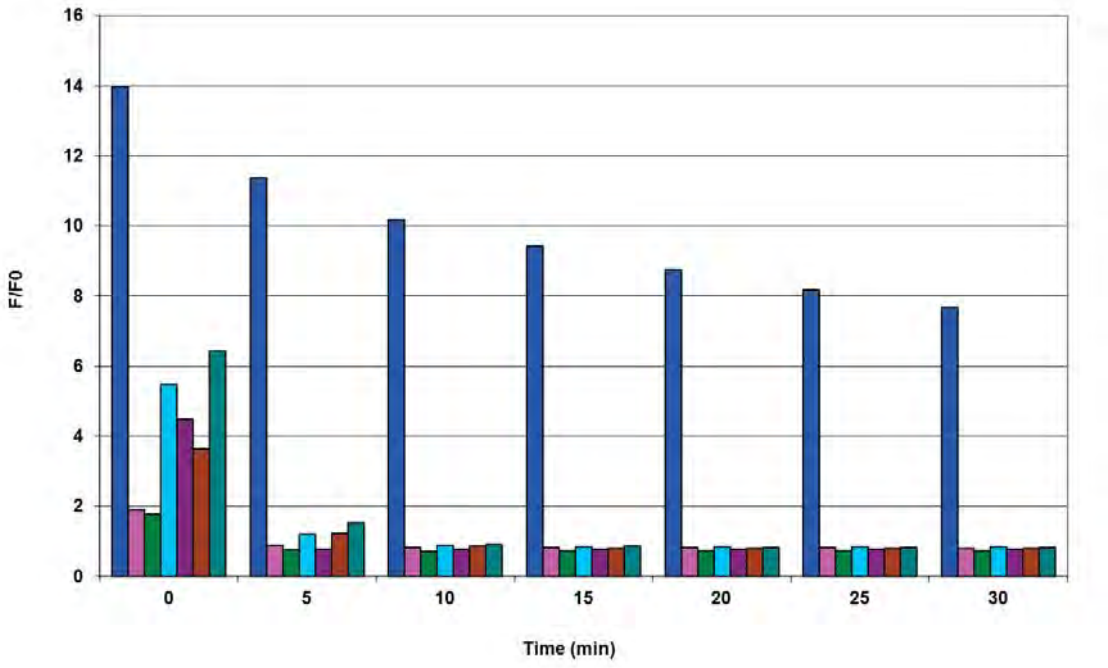

รูปที่ 41 อัตราส่วนของ F_{377} (ds/ss) ของ PyB-labeled acpcPNA CTAAATTCAGA ก่อน (time = 0 min) และหลังการย่อยด้วย S1 nuclease ที่เวลาต่างๆ (5–30 min). Conditions: [PNA] = 1 M; 30 mM sodium acetate buffer pH 4.6, 1 mM $Zn(OAc)_2$, 5% glycerol, 5 units/mL S1 nuclease, λ_{ex} 345 nm. Complementary DNA: ■ 3'-GATTTAAGTCT-5' (comp); mismatched DNA: ■ 3'-GATTTATGTCT-5', ■ 3'-GATTTAATTCT-5'; ■ 3'-GATTTTAGTCT-5'; ■ 3'-GATTAAAGTCT-5'; ■ 3'-GATTCAAGTCT-5'; ■ 3'-GATTGAAGTCT-5'

แม้การติดฉลากเรืองแสงแก่พีเอ็นเอโดยผ่านตัวเชื่อม APC โดยวิธีสร้างพันธะเอไมด์ดังที่ได้ศึกษามาทั้งหมดจะให้ผลเป็นที่น่าพอใจระดับหนึ่ง แต่ก็ยังมีปัญหาที่สำคัญได้แก่ 1. การติดฉลากด้วยพันธะเอไมด์จำเป็นจะต้องผ่านขั้นตอนการกำจัดหมู่ Tfa ออกจากตัวเชื่อม APC ภายใต้ภาวะ aqueous ammonia ที่ 60 °C ดังนั้นจึงทำให้หมู่ปกป้องอะมิโนของนิวคลีโอเบสหลุดออกไปด้วย การทำปฏิกิริยาเอซิลเลชันต่อจึงต้องควบคุมภาวะให้ดี

มิฉะนั้นจะเกิดปฏิกิริยาเอซิลเลชันที่ตำแหน่งของนิวคลีโอเบส โดยเฉพาะเบส C ซึ่งมีหมู่อะมิโนที่นิวคลีโอฟิลิกมากกว่าเบสอื่นเป็นปฏิกิริยาข้างเคียง 2. การติดฉลากผ่านพันธะเอไมด์จะทำให้ความเสถียรของพีเอ็นเอ-ดีเอ็นเอไฮบริดที่เกิดขึ้นลดลงอย่างมาก (ตารางที่ 19) คาดว่าน่าจะเกี่ยวกับ steric effect ของพันธะเอไมด์ 3. พันธะเอไมด์แบบเทอร์เชียรีที่เกิดขึ้นสามารถอยู่ได้ในสองคอนฟอร์เมชันที่เปลี่ยนกลับไปกลับมาได้ค่อนข้างช้า ดังนั้น พีเอ็นเอที่สังเคราะห์ได้จะเป็นของผสมของสองไอโซเมอร์ ซึ่งอาจส่งผลกระทบต่อการศึกษาสมบัติการจับยึดกับดีเอ็นเอ งานที่ได้ทำต่อมาคือการพัฒนาวิธีติดฉลากวิธีใหม่ที่ไม่ต้องอาศัยปฏิกิริยาเอซิลเลชัน โดยจะต่อหมู่แอลคิลเข้าไปโดยตรงที่ตำแหน่ง N ของตัวเชื่อม APC ที่ผ่านการกำจัดหมู่ปกป้องแล้ว เบื้องต้นได้ทดลองปฏิกิริยาแอลคิลเลชันด้วยแอลคิลเฮไลด์ แต่พบปัญหาคือ unactivated alkyl halide เช่น n-butyl bromide หรือ homopropargyl tosylate ไม่สามารถทำปฏิกิริยาได้ ในขณะที่ activated alkyl halide เช่น propargyl bromide ทำปฏิกิริยาได้เป็นของผสมระหว่างสารตั้งต้น และผลิตภัณฑ์ที่เกิดจากโมโนแอลคิลเลชันที่ต้องการ และผลิตภัณฑ์ที่เกิดจากไดแอลคิลเลชันได้เป็นหมู่ควอเทอร์นารีแอมโมเนียมในสัดส่วนที่ใกล้เคียงกัน วิธีการที่ได้ลองต่อมาคือการทำรีดักทีฟแอลคิลเลชัน ซึ่งเป็นปฏิกิริยาที่เกิดภายใต้ภาวะที่ไม่รุนแรง และมีประวัติการใช้งานกับการสังเคราะห์บนวัฏภาคของแข็งอยู่พอสมควร [Khan et al., 1996; Tourwé et al., 1993; Coy et al.; 1988; Balaji et al., 2006] อย่างไรก็ตาม เนื่องจากพีเอ็นเอจะมีหมู่อะมิโนของนิวคลีโอเบสอยู่ด้วย สิ่งแรกที่ต้องพิจารณาคือความจำเพาะเจาะจงของปฏิกิริยา ว่าจะเกิดเฉพาะที่ตำแหน่งของ N-APC ที่ต้องการหรือไม่ จึงได้ทดลองทำปฏิกิริยารีดักทีฟแอลคิลเลชันของพีเอ็นเอ Ac-GC(APC)TA-Lys ที่อยู่บนวัฏภาคของแข็งและผ่านการกำจัดหมู่ Tfa บน APC ออกไปแล้วด้วยบิวทีรัลดีไฮด์ (30 equiv) + กรดอะซิติก (60 equiv) และโซเดียมไซยาโนโบโรไฮไดรด์ (60 equiv) ในเมทานอล และติดตามผลโดยใช้ MALDI-TOF mass spectrometry พบว่าปฏิกิริยาเกิดสมบูรณ์หลังการทำปฏิกิริยาเป็นเวลา 12 ชั่วโมง และไม่พบปฏิกิริยาข้างเคียงอื่นเช่นการเกิดเกลือควอเทอร์นารีแอมโมเนียมหรือแอลคิลเลชันของหมู่อะมิโนของนิวคลีโอเบส (รูปที่ 42)

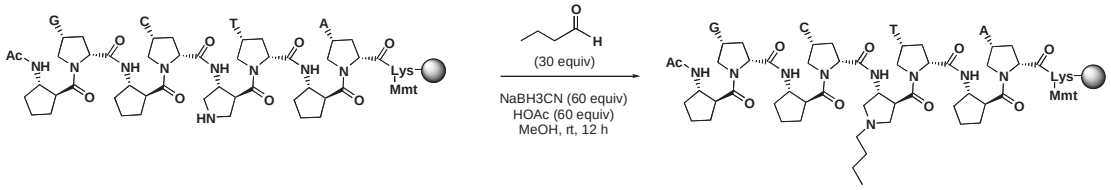

calcd *m/z* 1537.7 (after cleavage from the resin)

calcd *m/z* 1594.7 (after cleavage from the resin)

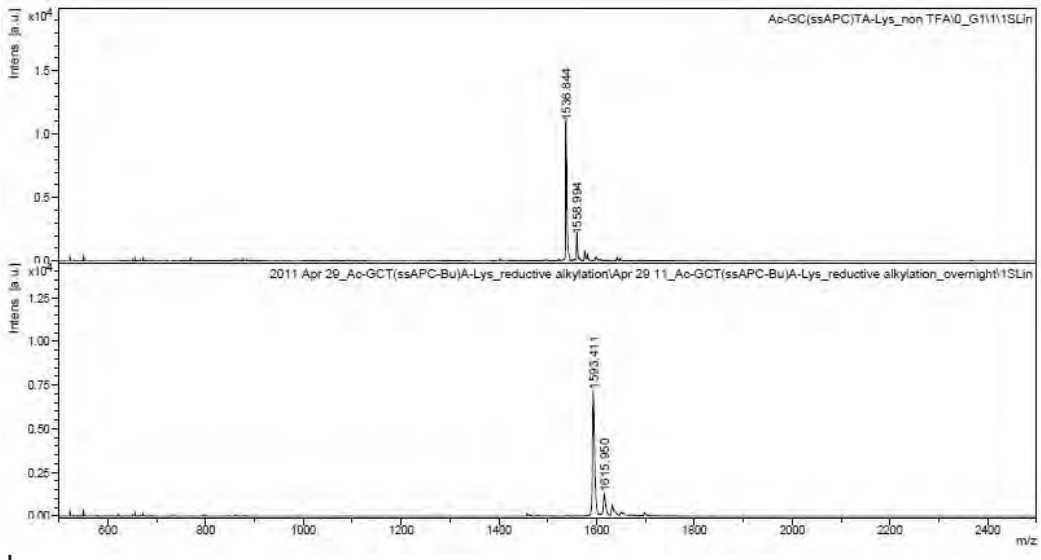

รูปที่ 42 ปฏิกิริยารีดักทีฟแอลคิลเลชันของ acpcPNA tetramer Ac-GCTA-Lys- บนวัฏภาคของแข็ง

จากผลเบื้องต้นนี้จึงได้ทดลองทำปฏิกิริยารีดักทีฟแอลคิลเลชันกับพีเอ็นเอที่มีลำดับเบสเป็น GTAGA(APC)TCACT บนวัฏภาคของแข็งกับแอลดีไฮด์ชนิดอื่นๆ พบว่าผลที่ได้เป็นที่น่าพอใจ กล่าวคือสามารถสังเคราะห์พีเอ็นเอที่ติดฉลากต่างๆ ได้ตามต้องการได้โดยวิธีนี้ (ตารางที่ 24) และพีเอ็นเอที่ได้มีความเสถียรไม่ลดลงมากนักเมื่อเทียบกับพีเอ็นเอที่ไม่ติดฉลาก โดยฉลากที่มีความเกะกะมากจะทำให้ T_m ลดลงมากกว่า ตัวอย่างเช่นพีเอ็นเอ **10mer-PyB** มี T_m 49.4 °C ซึ่งแม้จะลดต่ำลงมากเมื่อเทียบกับ unlabeled APC-modified PNA (61.4 °C) แต่ก็ยังสูงกว่าของพีเอ็นเอ ***RS*-mix(PyB)** ซึ่งมี T_m เพียง 45.7 °C ภายใต้ภาวะเดียวกัน (ตารางที่ 19) ในขณะที่พีเอ็นเอที่ติดฉลากขนาดเล็กเช่น methyl หรือ hydroxyethyl มีค่า T_m ต่ำกว่า unlabeled APC-modified PNA ภายใต้ภาวะเดียวกัน (59.3 °C) เพียงเล็กน้อยเท่านั้น และเนื่องจากฉลากที่มีหมู่แอลดีไฮด์มักไม่ค่อยเสถียร และเตรียมได้ไม่ง่ายนัก อีกทั้งยังไม่ค่อยมีจำหน่ายในเชิงการค้า จึงมีแนวคิดที่จะใช้วิธีรีดักทีฟแอลคิลเลชันในการติดฉลากที่มีหมู่ที่ว่องไวต่อปฏิกิริยาเข้าไป เช่นหมู่อะมิโนใน **10mer-AE** ซึ่งสามารถนำไปเพิ่มหมู่ฟังก์ชันต่อได้โดยปฏิกิริยาเอซิลเลชัน หรือหมู่เอไซด์และแอลไคน์ใน **10mer-N3** และ **10mer-alkyne** ซึ่งสามารถนำไปดัดแปลงต่อโดย Click chemistry โดยในทุกกรณีสามารถสังเคราะห์พีเอ็นเอที่มีหมู่ว่องไวเหล่านี้ได้ตามต้องการ และการดัดแปลงด้วยหมู่ที่ว่องไวดังกล่าวไม่มีผลกระทบในทางลบต่อความเสถียรของพีเอ็นเอ-ดีเอ็นเอไฮบริด (ตารางที่ 24)

ตารางที่ 24 ข้อมูล % yield, mass และ thermal stability ของ 10mer acpcPNA (sequence: GTAGATCACT) ที่ผ่านการติดฉลากโดยวิธี reductive alkylation

PNA	Aldehyde	Label	Yield	*m/z* (calcd)	*m/z* (found)	T_m (ºC)[a]
10mer-Me	HCHO	methyl	19.3	3574.8	3575.4	58.2[b]
10mer-HE	$HOCH_2CHO$ dimer	hydroxyethyl	1.6	3604.8	3604.0	58.7[b,c]
10mer-AE	$FmocNHCH_2CHO$	$H_2NCH_2CH_2$-	14.6	3604.7	3603.7	65.4[a]
10mer-PyB	pyrene-1-ylbutyraldehyde	pyrene-1-ylbutyl	2.9	3816.1	3816.9	49.4[d]
10mer-PyPm	4-(pyrene-1-yl)benzaldehyde	4-(pyrene-1-yl)phenylmethyl	7.2	3850.1	3852.5	46.4[d]
10mer-PyPn	(pyrene-1-yl)pentynal	(pyrene-1-yl)pentynyl	2.7	3828.2	3831.6	51.4[d]
10mer-N3	$N_3(CH_2)_3CHO$	$N_3(CH_2)_3$-	9.7	3657.8	3656.0	57.7[b]
10mer-alkyne	4-pentyn-1-al	$HC{\equiv}C(CH_2)_3$-	1.1	3626.8	3626.3	59.7[b]

[a] With complementary DNA (5'-AGTGATCTAC-3')

[b] Condition: 10 mM sodium phosphate buffer pH 7.0, [PNA] = 1.0 μM and [DNA] = 1.2 μM

[c] T_m with mismatched DNA (T) = 34.0 ºC

[d] Condition: 10 mM sodium phosphate buffer pH 7.0, [PNA] = 2.5 μM and [DNA] = 3.0 μM

จากนั้นจึงได้ทดลองติดฉลากเรืองแสงไพรีน (Py) และไทอะโซลออเรนจ์ (TO) โดยอาศัยปฏิกิริยาคลิกระหว่างฉลากเรืองแสงที่มีหมู่แอลไคน์หรือเอไซด์ กับพีเอ็นเอ **10mer-N3** หรือ **10mer-alkyne** ที่มี Cu(I)-TBTA complex เป็นตัวเร่งปฏิกิริยา ซึ่งพบว่าปฏิกิริยาเกิดได้ดีบนวัฏภาคของแข็ง โดยผลการวิเคราะห์ด้วย MALDI-TOF mass spectrometry แสดงว่าปฏิกิริยาเกิดได้อย่างสมบูรณ์และไม่พบปฏิกิริยาข้างเคียงอื่น ปฏิกิริยาคลิกนี้สามารถทำต่อเนื่องจากปฏิกิริยา reductive alkylation ได้เลยโดยไม่ต้องมีการแยกอินเทอร์มีเดียตออกมาก่อน ตัวอย่างดังแสดงในรูปที่ 43 ข้อมูลของพีเอ็นเอที่สังเคราะห์ได้เป็นดังแสดงในตารางที่ 25

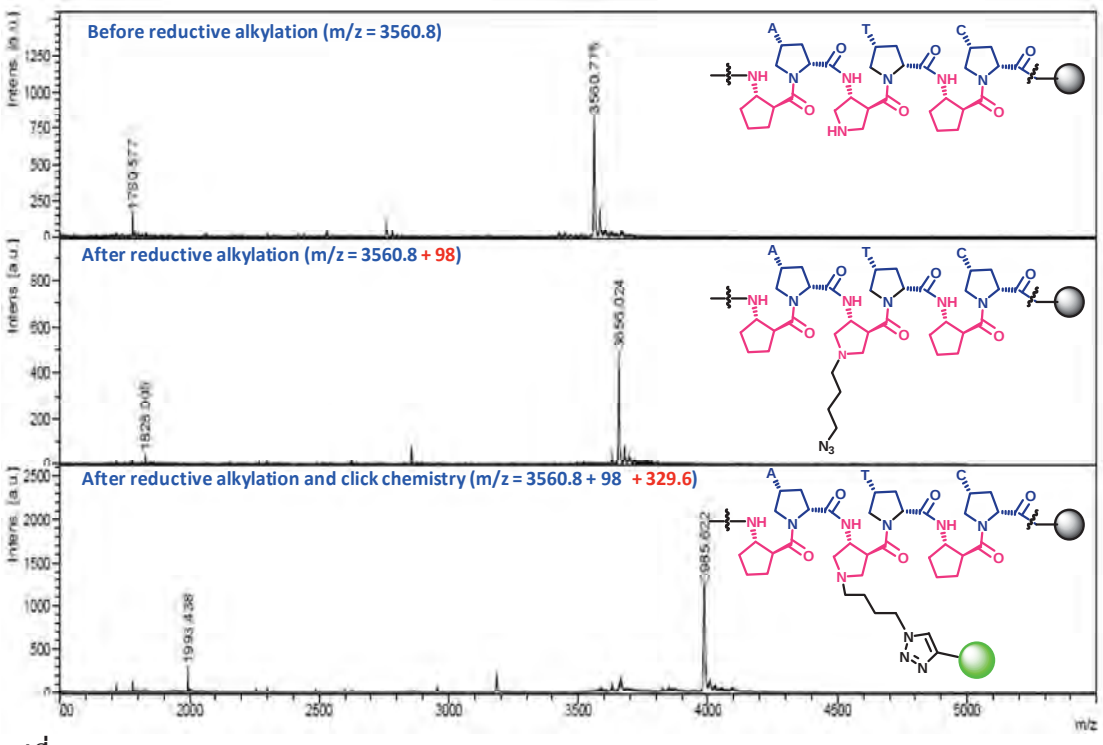

รูปที่ 43 Reductive alkylation-click chemistry of PNA **10mer-N3** -> **10mer-TzTO**

ตารางที่ 25 ข้อมูล sequence, % yield และ mass ของ 10mer acpcPNA ที่ผ่านการติดฉลากโดยวิธี sequential reductive alkylation/click

PNA	Sequence	Label	Yield	*m/z* (calcd)	*m/z* (found)
10mer-TzPy	GTAGATCACT	PyTz$(CH_2)_4$	4.6	3884.1	3883.3
10mer-TzTO	GTAGATCACT	TOTz$(CH_2)_4$	5.2	3987.4	3984.4
10mer-alkyne	GTAGATCACT	4-pentynyl	1.1	3626.8	3626.3
10mer-NTzPy	GTAGATCACT	*N*-PyTz$(CH_2)_3$	3.0	3870.1	3870.0
12mer-TzTO	AGTTATCCCTGC	TOTz$(CH_2)_4$	3.1	4613.1	4612.6

จากการศึกษาโดยเทคนิค UV-melting พบว่าพีเอ็นเอที่ติดฉลาก Py หรือ TO ผ่านปฏิกิริยาคลิกยังคงแสดงการจับยึดกับดีเอ็นเอที่แข็งแรงและจำเพาะเจาะจง (ตารางที่ 26) โดยพีเอ็นเอที่ติดฉลากด้วย TO จะมีความเสถียรของการจับยึดกับดีเอ็นเอที่ไม่แตกต่างจากพีเอ็นเอที่ไม่ได้ผ่านการติดฉลากมากเท่ากับพีเอ็นเอที่ติดฉลากด้วย Py

ตารางที่ 26 ข้อมูล thermal stability ของไฮบริดระหว่าง acpcPNA ที่ผ่านการติดฉลากโดยวิธี sequential reductive alkylation/click กับดีเอ็นเอที่เป็นคู่สมและไม่เป็นคู่สมต่าง ๆ

PNA	DNA[a]	T_m (ºC)[b]	ΔT_m (ºC)[c]	Note
T9-TzPy	**D9comp**	67.6	–12.4	Complementary
T9-TzTO	**D9comp**	75.8	–4.2	Complementary
T9-TzTO	**D9smT**	47.5	–32.5	Single mismatched
10mer-azide	**D10comp**	57.7	–2.5	Complementary
10mer-TzPy	**D10comp**	55.6	–3.7	Complementary
10mer-alkyne	**D10comp**	59.7	–0.5	Complementary
10mer-NTzPy	**D10comp**	51.1	–9.1	Complementary
10mer-TzTO	**D10comp**	60.3	+0.1	Complementary
10mer-TzTO	**D10smT**	38.0	–22.2	Complementary
10mer-TzTO	**D10smC**	37.2	–23.0	single mismatched
10mer-TzTO	**D10smG**	26.3	–33.9	single mismatched
12mer-TzTO	**D12comp**	74.5	–0.3	Complementary
12mer-TzTO	**D12smA**	58.6	–16.2	single mismatched
12mer-TzTO	**D12smC_3'**	59.8	–15.0	indirect single mismatched
12mer-TzTO	**D12smC_5'**	55.7	–19.1	indirect single mismatched

[a]DNA sequence (5'→3'): **D9comp** = dAAAAAAAAA; **D9smT** = dAAAAT<u>A</u>AAA; **D10comp** = dAGTGATCTAC; **D10smT** = dAGTG<u>T</u>TCTAC; **D10smC** = dAGTG<u>C</u>TCTAC; **D10smG** = dAGTG<u>G</u>TCTAC; **D12comp** = dGCAGGGATAACT; **D12smA** = GCAGG<u>A</u>ATAACT; **D12smC_3'** = GCAGGG<u>C</u>TAACT, **D12smC_5'** = GCAG<u>C</u>GATAACT.

[b]Condition: 10 mM sodium phosphate buffer pH 7.0, [PNA] = 1.0 μM and [DNA] = 1.2 μM

[c]Relative to unmodified acpcPNA under similar conditions. T_m of hybrids with complementary DNA; Ac-TTTTTTTTT-Lys (1.0:1.2 μM = 80.0 ºC, 2.5:3.0 μM = 81.8 ºC), Ac-GTAGATCACT-Lys (1.0:1.2 μM = 60.2 ºC, 2.5:3.0 μM = 62.4 ºC), Bz-GTAGA<u>T</u>CACT-Lys (1.0:1.2 μM = 59.3 ºC, 2.5:3.0 μM = 61.4 ºC), Ac-AGTTATCCCTGC-Lys (1.0:1.2 μM = 74.8 °C, 2.5:3.0 μM = 75.0°C)

จากนั้นจึงได้ศึกษาสมบัติการเรืองแสงของพีเอ็นเอที่ติดฉลาก Py และ TO ที่สังเคราะห์ได้ทั้งหมด ในสภาพที่เป็นสายเดี่ยว เปรียบเทียบกับเมื่อมีดีเอ็นเอคู่สมอยู่ด้วย (รูปที่ 44) ผลที่ได้แสดงให้เห็นอย่างชัดเจนว่าพีเอ็นเอที่ติดฉลากเหล่านี้แสดงการเรืองแสงที่ตอบสนองต่อการเกิดไฮบริดกับดีเอ็นเอ โดยบางชนิดก็เป็นการตอบสนองในลักษณะ fluorescence on กล่าวคือการเรืองแสงเพิ่มขึ้นเมื่อมีดีเอ็นเออยู่ด้วย ในขณะที่บางชนิดก็ลดลง โดยระบบที่แสดงการตอบสนองได้ชัดเจนที่สุดคือพีเอ็นเอ **10mer-TzTO** จึงเลือกเฉพาะพีเอ็นเอระบบนี้มาศึกษาต่อถึงความจำเพาะเจาะจงต่อไป ผลการทดลองเบื้องต้นไม่เป็นที่น่าพอใจนักเนื่องจากแม้ว่าการเติมดีเอ็นเอคู่สมจะทำให้การเรืองแสงเพิ่มขึ้นอย่างมาก แต่การเติมดีเอ็นเอที่เป็น single base mismatch หรือแม้แต่ non-complementary ก็ทำให้การเรืองแสงเพิ่มขึ้นค่อนข้างมากเช่นเดียวกัน ซึ่งคาดว่าเกิดจากการจับยึดระหว่างส่วนของฉลาก TO กับดีเอ็นเอโดยไม่เกี่ยวข้องกับพีเอ็นเอ

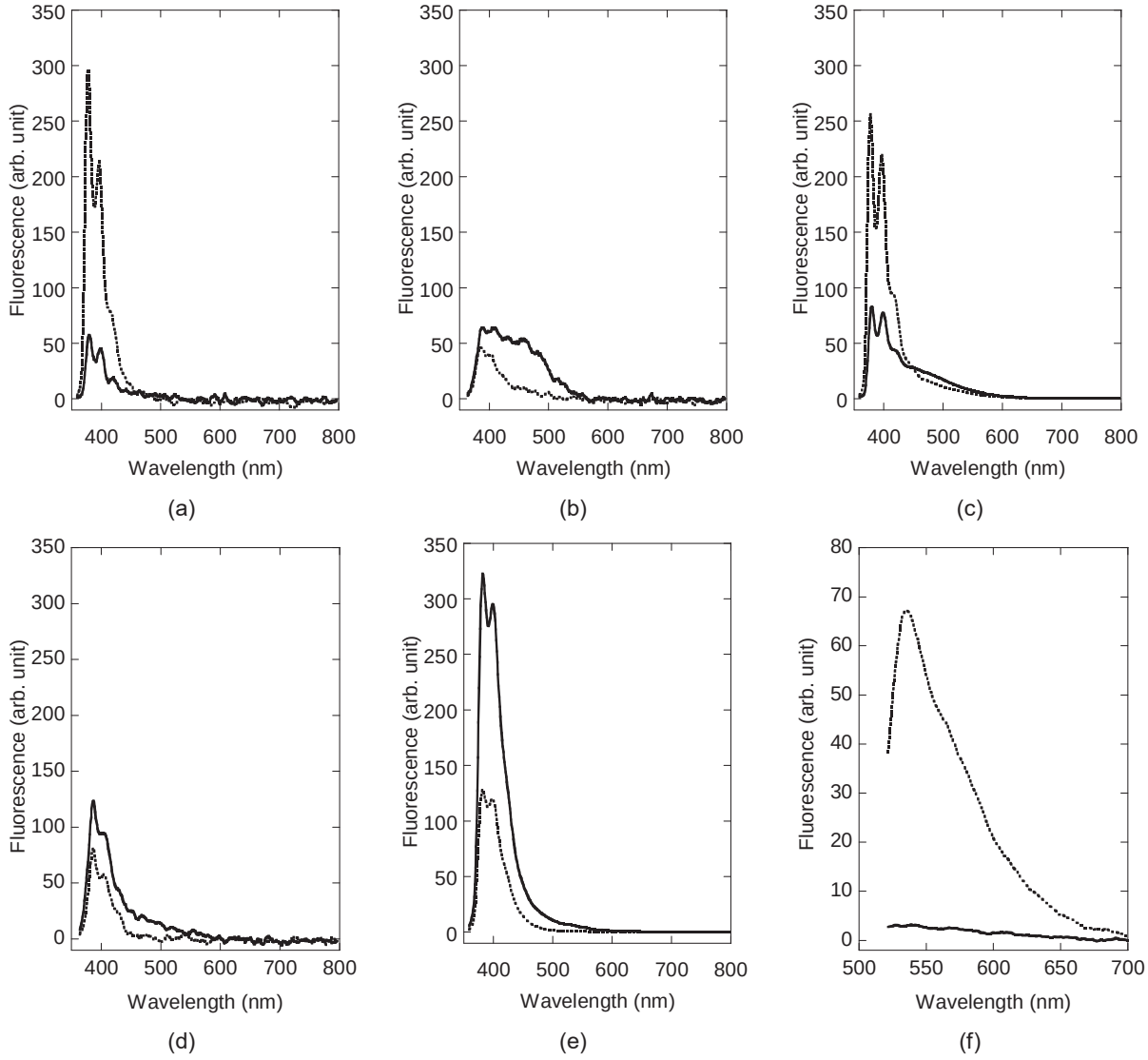

รูปที่ 44 Fluorescence spectra of **10mer-PyB** (a), **10mer-PyPm** (b), **10mer-PyPn** (c), **10mer-TzPy** (d), **10mer-NTzPy** (e) and **10mer-TzTO** (f) in the absence (–) and presence (--) of complementary DNA (**D10comp**). Conditions: 2.5 μM PNA, 3.0 μM DNA, 10 mM sodium phosphate buffer pH 7.0, λ_{excit} 345 nm (**10mer-PyB**, **10mer-PyPm**, **10mer-PyPn**, **10mer-TzPy** and **10mer-NTzPy**) or 508 nm (**10mer-TzTO**).

อย่างไรก็ตาม สามารถใช้การย่อยด้วยเอนไซม์ nuclease S1 เพื่อเพิ่มความจำเพาะเจาะจงได้ โดยระยะเวลาของการย่อยจะขึ้นกับความยาวของพีเอ็นเอที่เกี่ยวข้อง ตัวอย่างเช่น ในกรณีของ **12mer-TzTO** ระยะเวลาของการย่อยที่เหมาะสมคือ 60 นาที ซึ่งจะทำให้ได้สัญญาณ ของ mismatched hybrid ลดลงเหลือใกล้เคียงกับ single stranded PNA (F/F0 = 0.7–3.4) ในขณะที่สัญญาณของ complementary hybrid จะยังคงมีค่าสูงอยู่ (F/F0 = 49) (รูปที่ 45) พีเอ็นเอระบบอื่นจะใช้เวลาในการย่อยที่แตกต่างกัน แต่ในทุกกรณีสามารถบอกความแตกต่างระหว่าง complementary กับ non-complementary (รวมทั้ง single-base mismatched) DNA ได้

อย่างชัดเจน (ตารางที่ 27) ดังนั้นระบบพีเอ็นเอที่ติดฉลากด้วย TO ผ่านปฏิกิริยารีดักทีฟแอลคิลเลชัน-คลิกร่วมกับเทคนิคการย่อยเอนไซม์ในการตรวจสอบลำดับเบสของดีเอ็นเอได้ โดยให้การเปลี่ยนแปลงการเรืองแสงที่ชัดเจน

ตารางที่ 27 อัตราส่วนของการเรืองแสงที่ 528 nm ของพีเอ็นเอเมื่อมีดีเอ็นเออยู่ด้วยต่อพีเอ็นเอสายเดี่ยว (F/F_0) ก่อนและหลังการย่อยด้วย nuclease S1 conditions: 30 mM sodium acetate buffer pH 4.6, 1mM zinc acetate, 5% Glycerol, 5 units/mL S1 nuclease [PNA] = 1.0 μM and [DNA] = 1.0 μM, Excitation wavelength = 510 nm, PMT gain = high

PNA	DNA	F/F0 (at 528 nm) (before digestion)	F/F0 (at 528 nm) (after digestion)	Digestion time (min)
T9-TO	**D9comp**	25.7	20.3	15
	D9smT	34.6	1.6	15
	D9smC	45.5	2.9	15
	D9smG	30.7	1.5	15
10mer-TzTO	**D10comp**	39.2	10.1	10
	D10smT	22.3	1.6	10
	D10smC	16.1	1.4	10
	D10smG	11.3	1.2	10
	D11non	15.0	1.0	10
12mer-Tz TO	**D12comp**	83.6	49.0	60
	D12smA	53.6	3.4	60
	D12smC_3'	41.5	1.9	60
	D12smC_5'	83.8	2.0	60
	D11non	16.7	0.7	60

[a]DNA sequence (5'⟶3'): **D9comp** = dAAAAAAAAA; **D9smT** = dAAAA<u>T</u>AAAA; **D10comp** = dAGTGATCTAC; **D10smT** = dAGTG<u>T</u>TCTAC; **D10smC** = dAGTG<u>C</u>TCTAC; **D10smG** = dAGTG<u>G</u>TCTAC; **D11non** = TCTGCATTTAG ; **D12comp** = dGCAGGGATAACT; **D12smA** = GCAGG<u>A</u>ATAACT; **D12smC_3'** = GCAGGG<u>C</u>TAACT, **D12smC_5'** = GCAG<u>C</u>GATAACT.

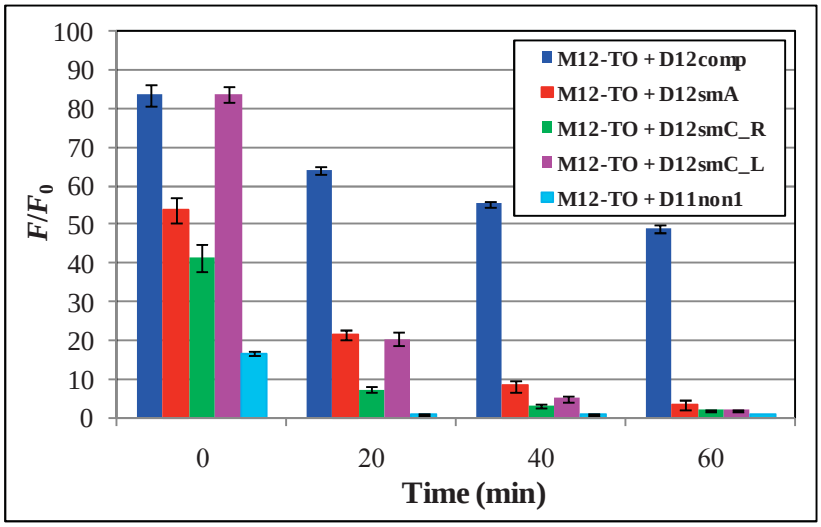

รูปที่ 45 อัตราส่วนของการเรืองแสงที่ 528 nm ของพีเอ็นเอ **12mer-TzTO** เมื่อมีดีเอ็นเออยู่ด้วยต่อพีเอ็นเอสายเดี่ยว (F/F_0) ก่อนและหลังการย่อยด้วย nuclease S1 ที่เวลาต่างๆ conditions: 30 mM sodium acetate buffer pH 4.6, 1mM zinc acetate, 5% Glycerol, 5 units/mL S1 nuclease [PNA] = 1.0 μM and [DNA] = 1.0 μM, Excitation wavelength = 510 nm, PMT gain = high

สรุปผลการดำเนินงาน

งานวิจัยที่ได้ดำเนินการภายใต้โครงการย่อยนี้แบ่งออกเป็น 3 ส่วนหลักๆ คือ 1) การสังเคราะห์และศึกษาสมบัติจับยึดของ acpcPNA 2) การสังเคราะห์และศึกษาสมบัติจับยึดของการสังเคราะห์และศึกษาสมบัติจับยึดของ acpcPNA ที่มี modified base และ 3) การสังเคราะห์และศึกษาสมบัติจับยึดของพีเอ็นเอที่มี modified backbone รายละเอียดของงานวิจัยโดยสรุปมีดังนี้

1. การสังเคราะห์และศึกษาสมบัติจับยึดของ acpcPNA

ได้สังเคราะห์ acpcPNA ที่มีความยาวเท่ากันคือ 10 เบส แต่มีสัดส่วนของเบส AT และ CG แตกต่างกันจำนวนทั้งสิ้น 9 ลำดับเบส และศึกษาสมบัติการจับยึดกับดีเอ็นเอ เปรียบเทียบกับอาร์เอ็นเอ และการจับยึดกับตัวเอง ผลการทดลองทั้งหมดยืนยันสมบัติที่เป็นเอกลักษณ์เฉพาะตัวของ acpcPNA 3 ประการ คือ 1. ความสามารถในการเลือกจับกับดีเอ็นเอได้ดีกว่าอาร์เอ็นเอ 2. ความเสถียรของโมเลกุลลูกผสมระหว่างพีเอ็นเอกับดีเอ็นเอที่ไม่ขึ้นกับสัดส่วนของเบสที่เป็นองค์ประกอบ และ 3. ไม่เกิดโมเลกุลลูกผสมกับตัวเองในทิศทางแอนติพาราเรล สมบัติประการแรกเป็นการบ่งชี้ข้อจำกัดของ acpcPNA ว่าน่าจะเหมาะกับงานที่เกี่ยวข้องกับเป้าหมายของการจับยึดที่เป็นดีเอ็นเอมากกว่าอาร์เอ็นเอ เช่นงานทางด้าน DNA-based diagnostics และ antigene therapeutics ส่วนสมบัติประการที่สองน่าจะเป็นประโยชน์ในการนำไปใช้เป็นโพรบสำหรับตรวจวินิจฉัยแบบ high throughput เช่นในการทำไมโครแอเรย์ เนื่องจากสามารถออกแบบพีเอ็นเอโพรบหลายๆ ชนิดเพื่อให้จับกับดีเอ็นเอเป้าหมายได้หลายๆ ตำแหน่งพร้อมกัน และสมบัติประการที่สามอาจนำไปประยุกต์ใช้ประโยชน์ได้ในการออกแบบพีเอ็นเอสองสายเพื่อให้จับกับดีเอ็นเอเป้าหมายที่เป็นโมเลกุลแบบเกลียวคู่โดยการเกิด double duplex invasion ซึ่งน่าจะช่วยเพิ่มประสิทธิภาพของการจับยึดระหว่างพีเอ็นเอกับดีเอ็นเอแบบเกลียวคู่(ซึ่งจะพบในสถานการณ์ของการใช้งานจริง)

2. การสังเคราะห์และศึกษาสมบัติจับยึดของ acpcPNA ที่มี modified base

ได้ศึกษา acpcPNA ที่มี modified base อยู่ 3 กลุ่ม กลุ่มแรกคือเบส hypoxanthine (H) ซึ่งพบว่า เบส H ใน acpcPNA แสดงการจับยึดอย่างจำเพาะเจาะจงกับเบส C ในดีเอ็นเอ การค้นพบนี้ได้เสนอแนะว่าสามารถแทนที่เบส G ใน acpcPNA ด้วยเบส H ได้โดยไม่มีผลกระทบต่อ specificity ในการจดจำเบส C ซึ่งมีความสำคัญอย่างยิ่งต่อการนำ acpcPNA ไปประยุกต์ใช้ประโยชน์ในด้านต่างๆ เนื่องจากโมโนเมอร์ของเบส H สามารถสังเคราะห์ได้ง่ายกว่าโมโนเมอร์ของ G นอกจากนี้ยังไม่มีปัญหาเรื่อง oxidation, quenching และการเกิด secondary structure เหมือนเบส G

งานในกลุ่มที่สองเป็นการพัฒนาวิธีการสังเคราะห์และศึกษาสมบัติการจับยึดกับดีเอ็นเอและสมบัติการเรืองแสงของ acpcPNA ที่มีฉลากเรืองแสง pyrene ติดอยู่ที่ตำแหน่ง 5 ของนิวคลีโอเบสยูเรซิล (U^{Py}) โดยพบว่าเบส U^{Py} ใน acpcPNA สามารถจดจำเบส A ในดีเอ็นเอได้อย่างจำเพาะเจาะจง และแสดงสมบัติ base discriminative fluorescence กล่าวคือการเรืองแสงจะเพิ่มขึ้นอย่างมากเมื่อมีการเข้าคู่ระหว่างเบส U^{Py} ใน acpcPNA กับเบส A ใน DNA ทำให้ acpcPNA ที่มีเบส UPy ทำตัวเป็น quencher free molecular beacon ได้ งานในกลุ่มที่ 3 เกี่ยวข้องกับการแทนที่นิวคลีโอเบสใน acpcPNA ด้วย polycyclic aromatic hydrocarbon เช่น pyrene และ anthracene ที่ต่อกับวงแหวนไตรอะโซล (Tz^{Py} และ Tz^{Ant}) โดยอาศัยปฏิกิริยาคลิกกับพีเอ็นเอที่มีหมู่เอไซด์ โดยพบว่าเบส Tz^{Py} ทำหน้าที่เป็น universal base กล่าวคือสามารถเข้าคู่กับเบสธรรมชาติได้ทุกตัวโดยมีความเสถียรไม่แตกต่างกันมากนัก จากนั้นจึงได้ศึกษาสมบัติการเรืองแสงของพีเอ็นเอที่ได้ในสภาพที่เป็นสายเดี่ยวเปรียบเทียบกับเมื่อเข้าคู่กับดีเอ็นเอ พบว่าพีเอ็นเอที่มีเบส Tz^{Py} เมื่อเข้าคู่กับดีเอ็นเอจะมีการเปลี่ยนแปลงการเรืองแสงจากพีเอ็นเอสายเดี่ยวอย่างชัดเจน กล่าวคือการเรืองแสงที่ 460 nm จะลดลง และการเรืองแสงที่ช่วง 390–430 nm จะเพิ่มขึ้น

3. การสังเคราะห์และศึกษาสมบัติจับยึดของพีเอ็นเอที่มี modified backbone

งานวิจัยที่ได้ดำเนินการไปแบ่งเป็น 3 ส่วน คือ 1. การสังเคราะห์และศึกษาสมบัติการจับยึดของพีเอ็นเอที่มีสเตอริเอเคมีของวงแหวนโพรลีนเป็น (2*R*′,4′*R*) 2. การสังเคราะห์และศึกษาสมบัติการจับยึดของพีเอ็นเอที่มีกรดเบต้าอะมิโนชนิดอื่นนอกเหนือจาก ACPC เป็นตัวเชื่อม และ 3. การสังเคราะห์ สมบัติการจับยึด และสมบัติการเรืองแสงของพีเอ็นเอที่ติดฉลากเรืองแสงผ่านตัวเชื่อม 3-aminopyrrolidine-4-carboxylic acid (APC)

งานวิจัยส่วนแรกเป็นการสังเคราะห์ acpcPNA ที่มีสเตอริโอเคมีของวงแหวนโพรลีนและ ACPC ที่ต่างไปจาก *RR*-Pro/*SS*-ACPC โดยแยกศึกษาแต่ละส่วนในพีเอ็นเอที่มีลำดับเบสเป็น T_5 พบว่าจากพีเอ็นเอทั้ง 7 ไดอะสเตอริโอเมอร์นั้น มีเพียงระบบ acpcPNA เดิม [(2′*R*,4′*R*)-Pro/(1*S*,2*S*)-ACPC] และอีพิเมอร์ของมันที่มีสเตอริโอเคมีของตำแหน่ง 4′ บนวงแหวนโพรลีนเปลี่ยนแปลงไป [(2′*R*,4′*S*)-Pro/(1*S*,2*S*)-ACPC] เท่านั้นที่แสดงการจับยึดกับดีเอ็นเอได้ จึงได้ศึกษาระบบใหม่ที่เรียกชื่อว่า *epi*-acpcPNA นี้ต่ออย่างละเอียดในพีเอ็นเอที่มีลำดับเบสที่ซับซ้อนขึ้น ผลการทดลองแสดงให้เห็นว่า *epi*-acpcPNA แสดงการจดจำดีเอ็นเอและอาร์เอ็นเอที่คล้ายคลึงกับ acpcPNA แต่ระบบ *epi*-acpcPNA สามารถเกิดไฮบริดที่ค่อนข้างเสถียรกับตัวเองได้ได้ในทิศทางแอนติพาราเรล ซึ่งแตกต่างจาก acpcPNA อย่างชัดเจน และอาจนำไปสู่การประยุกต์ใช้ที่แตกต่างกันของพีเอ็นเอทั้งสองระบบ โดย acpcPNA น่าจะเหมาะสำหรับ applications ที่เกี่ยวกับ DNA ที่ไม่ต้องการการเกิด self hybrid เช่น การ target cellular DNA ด้วย double duplex invasion mechanism ในขณะที่ *epi*-acpcPNA น่าจะเหมาะสมกับการนำไปใช้ทางด้านนาโนเทคโนโลยี/เครื่องมือระดับโมเลกุลที่อาศัยการจดจำระหว่างพีเอ็นเอสองสาย

งานวิจัยในส่วนที่สองเป็นการสังเคราะห์และศึกษาสมบัติการจับยึดของพีเอ็นเอที่มีการแทนที่ตัวเชื่อมที่เป็นกรดเบต้าอะมิโน 2-aminocyclopentancecarboxylic acid (ACPC) ซึ่งเป็น 5-membered ring ใน acpcPNA ด้วยไซคลิกเบต้าอะมิโนแอซิดที่มีวงแหวนขนาดเล็กลงและใหญ่ขึ้น ได้แก่ aminocyclopropanecarboxylic acid (ACC) (3-membered) /2-aminocyclobutanecarboxylic acid (ACBC) (4-membered) และ 2-

aminocyclohexanecarboxylic acid (ACHC) (5-membered) ทำให้ได้พีเอ็นเอชนิดใหม่คือ accPNA, acbcPNA และ achcPNA ผลการศึกษาการจับยึดของ acbcPNA กับ DNA และ RNA พบว่า acbcPNA เกิดไฮบริดกับ DNA และ RNA เฉพาะในทิศทางแอนติพาราเรล โดยไฮบริดที่เกิดขึ้นมีความเสถียรมากกว่าของ acpcPNA อยู่ประมาณ 9–15 °C สำหรับดีเอ็นเอ และ 15–18 °C สำหรับอาร์เอ็นเอ โดยที่ความจำเพาะเจาะจงของการจับยึดยังสูงอยู่ ในขณะที่ accPNA และ achcPNA ไม่แสดงการจับยึดกับดีเอ็นเอและอาร์เอ็นเอที่มีลำดับเบสคู่สม ซึ่งสามารถอธิบายได้จากค่า torsional angle (θ) ของไซคลิกเบต้าอะมิโนแอซิดที่เกี่ยวข้อง (ได้จากการคำนวณทางทฤษฎีและข้อมูลจากเอกสารอ้างอิง) โดย acbcPNA จะมีค่าใกล้เคียงกับค่าที่เหมาะสม (99 °)มากที่สุด ในขณะที่ accPNA และ achcPNA มีค่าต่างออกไปมากที่สุด ข้อมูลที่ได้จะนำไปสู่การออกแบบพีเอ็นเอระบบใหม่ที่มีความสามารถในการจับยึดกับดีเอ็นเอและ/หรืออาร์เอ็นเอที่ดีขึ้น

งานวิจัยในส่วนที่ 3 เป็นการสังเคราะห์ acpcPNA ที่มีการแทนที่ตัวเชื่อม ACPC ด้วย 3-aminopyrrolidine-4-carboxylic acid (APC) เพื่อให้มีหมู่อะมิโนที่สามารถดัดแปลงเพิ่มเติมได้ด้วยฉลากเรืองแสงที่บริเวณใดๆ ตามต้องการบนสายของพีเอ็นเอ โดยอาศัยการสร้างพันธะเอไมด์ ปฏิกิริยารีดักทีฟแอลคิลเลชัน หรือปฏิกิริยารีดักทีฟแอลคิลเลชัน-คลิก ได้ใช้วิธีการใหม่เหล่านี้ในการสังเคราะห์พีเอ็นเอที่ติดฉลากเรืองแสงที่สามารถเปลี่ยนแปลงการเรืองแสงได้ตามสภาพแวดล้อม ได้แก่ไพรีน และไทอะโซลออเรนจ์ และได้แสดงให้เห็นว่าพีเอ็นเอที่ติดฉลากเหล่านี้มีการเรืองแสงเพิ่มขึ้นเมื่อมีการเข้าคู่กับดีเอ็นเอ โดยพีเอ็นเอที่ติดฉลากไพรีนจะให้การเปลี่ยนแปลงการเรืองแสงประมาณ 4-14 เท่า ในขณะที่พีเอ็นเอที่ติดฉลากไทอะโซลออเรนจ์จะให้การเปลี่ยนแปลงการเรืองแสงที่ชัดเจนกว่า (10–50 เท่า) พีเอ็นเอที่ติดฉลากเหล่านี้แสดงการเรืองแสงที่เพิ่มขึ้นด้วยเมื่อมีดีเอ็นเอที่ไม่เป็นคู่สม อย่างไรก็ตาม สามารถใช้การย่อยด้วยเอนไซม์ nuclease S1 เพื่อช่วยเพิ่มความจำเพาะเจาะจงได้ โดยในทุกกรณีหลังการย่อย สัญญาณของไฮบริดคู่สมจะคงเดิม แต่สัญญาณของไฮบริดที่ไม่เป็นคู่สมจะลดลงเหลือเท่าสัญญาณของพีเอ็นเอสายเดี่ยว พีเอ็นเอที่ติดฉลากเหล่านี้จึงมีศักยภาพสูงในการนำไปใช้เป็น quencher free molecular beacon สำหรับการตรวจสอบลำดับเบสของดีเอ็นเอ

References

Aitken, D. J.; Gauzy, C.; Pereira, E. *Tetrahedron Lett.* **2004**, *45*, 2359–2361.

Amann, N.; Wagenknecht, H.-A. *Synlett* **2002**, 687–690.

Appella, D. H.; Christianson, L. A.; Karle, I. L.; Powell, D. R.; Gellman, S. H. *J. Am. Chem. Soc.* **1999**, *121*, 6206–6212.

Appella, D. H. ; Christianson, L. A.; Klein, D. A.; Richards, M. R.; Powell, D. R.; Gellman, S. H. *J. Am. Chem. Soc.* **1999**, *121*, 7574–7581.

Baker, B.R. Tanna, P.M. *J. Org. Chem.* **1965**, *30*, 3857–3858.

Balaji, B.S.; Gallazzi, F.; Jia, F.; Lewis, M.R. *Bioconjugate Chem.* **2006**, *17*, 551–558.

Bonger, K.M.; Kapoerchan, V.V.; Grotenberg, G.M.; van Koppen, C.J., Timmers, C.M.; van der Marel, G.A.; Overkleeft, H.S. *Org. Biomol. Chem.* **2010**, *8*, 1881–1884.

Boonlua, C.; Vilaivan, C.; Wagenknecht, H.-A.; Vilaivan, T. *Chem. Asian. J.* **2011**, *6*, 3251–3259.

Boontha B.; Nakkuntod, J.; Hirankarn, N.; Chaumpluk, P.;Vilaivan, T. *Anal. Chem.* **2008**, *80*, 8178–8186.

Case-Green, S.C.; Southern, E.M. *Nucleic Acids Res.* **1994**, *22*, 131–136.

Coy, D.H.; Hocart, S.J.; Sasaki, Y. *Tetrahedron* **1988**, *44*, 835–841.

Englund, E.A.; Appella, D.H. *Org. Lett.* **2005**, *7*, 3465–3467.

Fernandes, C.; Faure, S.; Pereira, E.; Théry, V.; Declerck, V.; Guillot, R.; Aitken, D. J. *Org. Lett.* **2010**, *12*, 3606–3609.

Fernandes, C.; Pereira, E.; Faure, S.; Aitken, D. J. *J. Org. Chem.* **2009**, *74*, 3217–3220.

Gothelf, K. V.; Thomas H. LaBean, T. H. *Org. Biomol. Chem.* **2005**, *3*, 4023–4037.

Kawai, K.; Wata, Y.; Hara, M.; Tojo, S.; Majima, T. *J. Am. Chem. Soc.* **2002**, *124*, 3586–3590.

Khan, N.; Arumukam, V.; Balasubramanian, S. *Tetrahedron Lett.* **1996**, *37*, 4819–4822.

Korkaew, P.; Vilaivan , T. *Nucleic Acids Symposium Series* **2008**, *52*, 251–252.

Lahoud, G.; Timoshchuk, V.; Lebedev, A.; Arar, K.; Hou, Y.-M.; Gamper, H. *Nucleic Acids Res.* **2008**, *36*, 6999–7008.

Lee, H.-S.; LePlae, P.R.; Porter, E.A.; Gellman, S.H. *J. Org. Chem.* **2001**, *66*, 3597–3599.

Lohse, J.; Dahl, O.; Nielsen, P.E. *Proc. Natl. Acad. Sci. USA* **1999**, *96*, 11804–11808.

MacKinnon, K.F.; Qualley, D.F.; Woski, S.A. *Tetrahedron Lett.* **2007**, *48*, 8074–8077.

Komiyama, M.; Ye, S.; Liang, X.; Yamamoto, Y.; Tomita, T.; Zhou, J.-M.; Aburatani, H. *J. Am. Chem. Soc.* **2003**, *125*, 3758–3762.

Manoharan, M.; Tivel, K.L., Zhao, M.; Nafisi, K.; Netzel, T.L. *J. Phys. Chem.* **1995**, *99*, 17461–17472.

Mansawat, W.; Boonlua, C.; Siriwong, K.; Vilaivan, T. *Tetrahedron* **2012**, *68*, 3988–3995.

Mansawat, W.; Vilaivan, C.; Balázs, Á.; Aitken, D.; Vilaivan, T. *Org. Lett.* **2012**, *14*, 1440–1443.

Marras, S.A.E. *Mol. Biotechnol.* **2008**, *38*, 247–255.

Mayer, E.; Valis, L.; Wagner, C.; Rist, M.; Amann, N.; Wagenknecht, H.-A. *Chem. Biochem.* **2004**, *5*, 865–868.

Morvan, F.; Rayner, B.; Imbach, J. L.; Lee, M.; Hartley, J. A.; Chang, D. K.; Lown, J. W. *Nucleic Acids Res.* **1987**, *15*, 7027–7044.

Reenabthue, N.; Boonlua, C.; Vilaivan C.; Vilaivan, T.; Suparpprom, C. *Bioorg. Med. Chem. Lett.* **2011**, *21*, 6465–6469.

Schweitzer, B.A.; Kool, E.T. *J. Am. Chem. Soc.* **1995**, *117*, 1863–1872.

Sezi, S.; Varghese, R.; Vilaivan, T.; Wagenknecht, H.-A. *ChemOpen* **2012**, in press.

Siriwong, K.; Chuichay, P.; Saen-oon, S.; Suparpprom, C.; Vilaivan, T.; Hannongbua, S. *Biochem. Biophys. Res. Commun.* **2008**, *372*, 765–771.

Sun, X.; Lee, J.K. *J. Org. Chem.* **2010**, *75*, 1848–1854.

Taechalertpaisarn, J.; Sriwarom, P.; Boonlua, C.; Yotapan, N.; Vilaivan, C.; Vilaivan, T. *Tetrahedron Lett* **2010**, *51*, 5822–5826.

Timár, Z.; Bottka, S.; Kovács, L.; Penke, B. *Nucleosides Nucleotides* **1999**, *18*, 1131–1133.

Tourwé, D.; Piron, J.; Defreyn, P.; Van Binst, G. *Tetrahedron Lett.* **1993**, *34*, 5499–5502

Varghese, R.; Wagenknecht, H.-A. *Chem Eur. J.* **2009**, *15*, 9307–9310.

Venkatesan, N.; Seo, Y. J.; Kim, B. H. *Chem. Soc. Rev.* **2008**, *37*, 648–663.

Vilaivan, T.; Srisuwannaket, C. *Org. Lett.* **2006**, *8*, 1879–1900.

Vilaivan, C.; Srisuwannaket, C.; Ananthanawat, C.; Suparpprom, C.; Kawakami, J.; Yamaguchi, Y.; Tanaka, Y.; Vilaivan, T. *Artificial DNA: PNA & XNA* **2011**, *2*, 50–59.

Wang, J.; Cai, X.; Wang, J.Y.; Johnsson, C.; Palecek, E. *Anal. Chem.* **1995**, *67*, 4065–4070.

Wang, J.; Rivas, G.; Fernandes, J.R.; Paz, J.L.L.; Jiang, M.; Waymire, R. *Anal. Chim. Acta.* **1998**, *375*, 197–203.

Wanninger-Weiss, C.; Wagenknecht, H.-A. *Eur. J. Org. Chem.* **2008**, 64–71.

Wilson, J. N.; Cho, Y.; Tan, S.; Cuppoletti, A.; Kool, E. T. *ChemBiochem.* **2008**, *9*, 279–285.

Woo, J.; Meyer, R.B.; Gamper, H.B. *Nucleic Acids Res.* **1996**, *24*, 2470–2475.

Yamana, K.; Iwase, R.; Furutani, S.; Tsuchida, H.; Zako, H.; Yamaoka, T.; Murakami, A. *Nucleic Acids Res.* **1999**, *27*, 2387–2392.

รายงานฉบับสมบูรณ์ของโครงการย่อยที่ 2

ชื่อโครงการ การตรวจวัดดีเอ็นเอด้วยเดนดริติกพอลิอิเล็กโทรไลต์เรืองแสงและเพพไทด์นิวคลีอิกแอซิด
Dencritic Fluorophores for Detection of DNA/PNA Hybridization

ชื่อหัวหน้าโครงการวิจัยย่อย รศ.ดร.มงคล สุขวัฒนาสินิทธิ์

รายงายในช่วงตั้งแต่วันที่ 1 มกราคม 2555 **ถึงวันที่** 30 มิถุนายน 2555

1. การดำเนินงาน

☑ ได้ดำเนินตามแผนที่วางไว้

☐ ได้ดำเนินล่าช้ากว่าแผนที่วางไว้

☐ ได้เปลี่ยนแผนงานที่วางไว้ดังนี้.....

2. รายละเอียดผลการดำเนินงานของโครงการ

2.1 กิจกรรมที่วางแผนไว้

- สังเคราะห์เดนดริติพอลิแคทไอออนฟลูออโรฟอร์ละลายน้ำได้
- พิสูจน์ทราบโครงสร้างของฟลูออโรฟอร์ที่สังเคราะห์ได้ด้วยเทคนิคต่อไปนี้ NMR, IR, MS, EA
- ศึกษาสมบัติเชิงแสงที่สำคัญของฟลูออโรฟอร์ เช่นการดูดกลืนแสง ความสามารถในการดูดกลืนแสง (extinction coefficient) การคายแสงประสิทธิภาพการคายแสง(quantum yield)อิทธิพลของสารลดแรงตึงผิว
- ศึกษาการตรวจวัดโดยใช้หลักการเข้าคู่กันของสาย DNA
- ศึกษาการตรวจวัดโดยใช้หลักการเข้าคู่กันระหว่างสายPNAและ DNA

2.2 กิจกรรมที่ได้ทำจริง

- สังเคราะห์เดนดริติพอลิแคทไอออนฟลูออโรฟอร์ละลายน้ำได้
- พิสูจน์ทราบโครงสร้างของฟลูออโรฟอร์ที่สังเคราะห์ได้ด้วยเทคนิคต่อไปนี้ NMR, IR, MS, EA
- ศึกษาสมบัติเชิงแสงที่สำคัญของฟลูออโรฟอร์ เช่นการดูดกลืนแสง ความสามารถในการดูดกลืนแสง (extinction coefficient) การคายแสงประสิทธิภาพการคายแสง (quantum yield) อิทธิพลของสารลดแรงตึงผิว
- ศึกษาการตรวจวัดไอออนโลหะโพแทสเซียมโดยใช้หลักการจับของ DNA aptamers
- ศึกษาการตรวจวัดลำดับเบสดีเอ็นเอโดยใช้หลักการเข้าคู่กันระหว่างสาย PNA และ DNA

3. ผลการดำเนินงาน

ผู้วิจัยได้สังเคราะห์เดนดริติกพอลิอิเล็กโทรไลต์เรืองแสงที่มีประจุบวก หรือเดนดริเมอร์ลำดับชั้นที่ศูนย์และหนึ่งที่มีโครงสร้างหลักเป็นหมู่ phenylene-ethynyleneและมีหมู่ปลายเป็นหมู่trimethylammonium โดยอาศัยปฏิกิริยาควบคู่แบบ Sonogashira reaction ดังแสดงตามขั้นตอนในกลไกที่ 1 และ 2

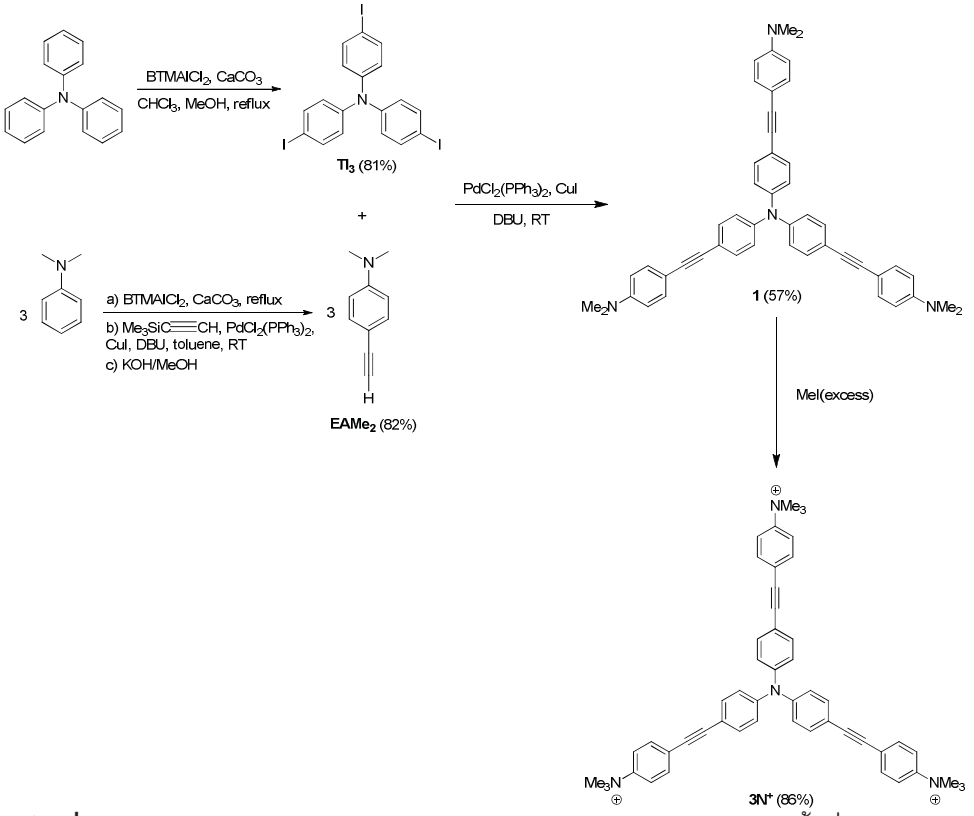

กลไกที่ 1 การสังเคราะห์เดนดริติกพอลิอิเล็กโทรไลต์เรืองแสง เดนดริเมอร์ลำดับชั้นที่ศูนย์ ($3N^{+}$)

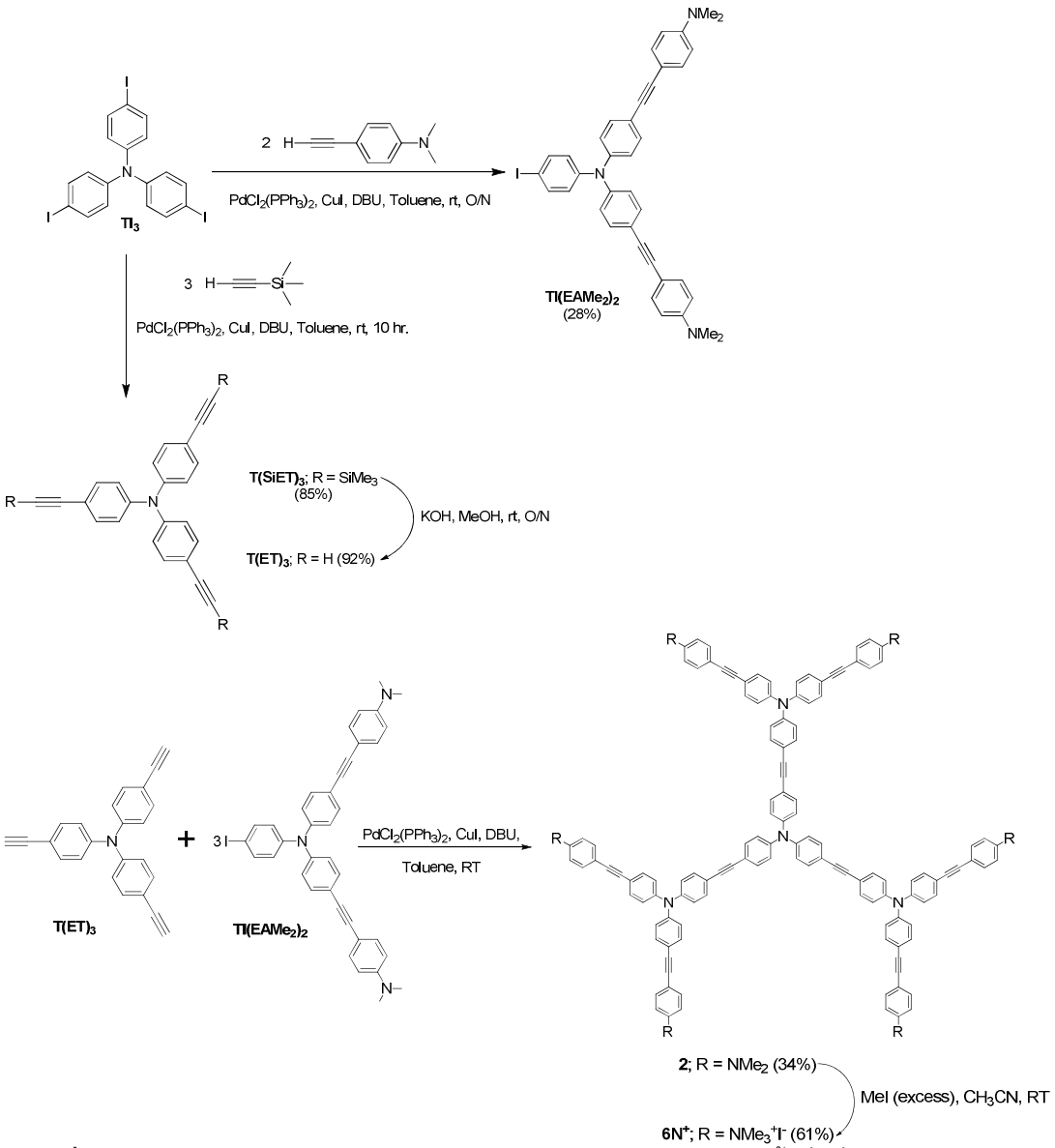

กลไกที่ 2 การสังเคราะห์เดนดริติกพอลิอิเล็กโทรไลต์เรืองแสง เดนดริเมอร์ลำดับชั้นที่หนึ่ง($6N^+$)

พบว่าเดนดริติกพอลิอิเล็กโทรไลต์เรืองแสงที่มีประจุบวกโครงสร้างดังรูปที่ 1 สามารถตอบสนองต่อ DNA ได้ โดยเดนดริเมอร์ลำดับชั้นที่ศูนย์ (G_0) ให้การตอบสนองโดยตรงในรูปของการเพิ่มสัญญาณฟลูออเรสเซนต์มากถึงสี่เท่าเมื่อในระบบมีสายดีเอ็นเอ (11 เบส)อยู่เป็นอัตราส่วน 1:1

ในขณะที่เดนดริเมอร์ลำดับชั้นที่หนึ่ง (G_1) จะไม่มีการเปลี่ยนแปลงสัญญาณฟลูออเรสเซนต์แต่อย่างใด เมื่อในระบบมีสายดีเอ็นเออยู่ อย่างไรก็ตามเราพบว่าหากทำการเติมสีย้อมฟลูออเรสเซนต์ (SyBrGreen II) ที่สามารถรับพลังงานจากเดนดริเมอร์ของเราได้ลงไปในระบบที่มีดีเอ็นเออยู่นั้น จะสังเกตุเห็นสัญญาณ FRET ที่เกิดขึ้นได้อย่างชัดเจน ซึ่งในระบบที่ไม่มีดีเอ็นเอเลยนั้น จะไม่เกิดการส่งผ่านพลังงานจากเดนดริเมอร์ไปสู่ SyBrGreen II แต่อย่างใด จากผลดังกล่าวทำให้เราสรุปถึงการมี interaction ต่อกันของเดนดริเมอร์ลำดับที่หนึ่งกับสายดีเอ็นเอ

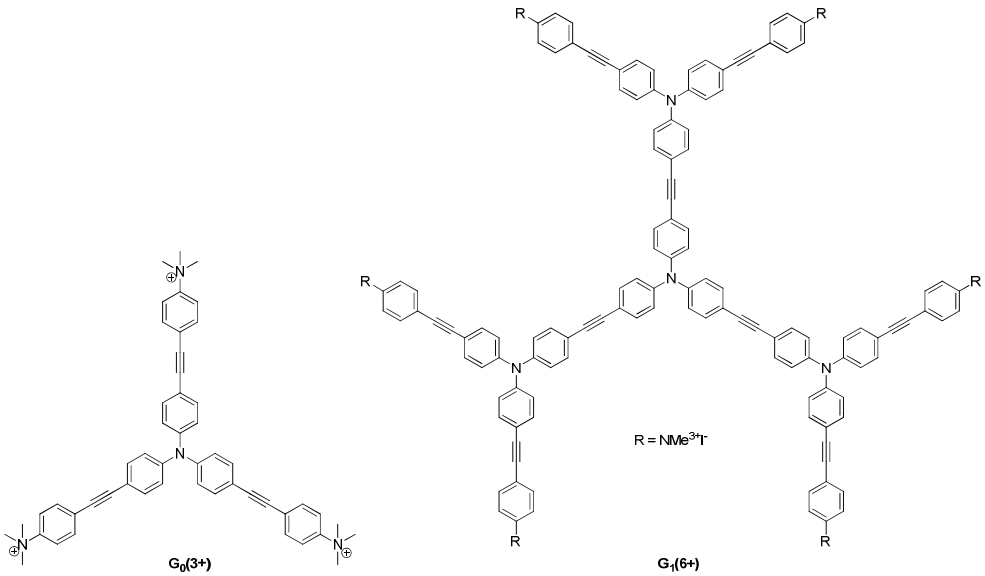

รูปที่ 1 โครงสร้างของเดนดริเมอร์ลำดับชั้นที่ศูนย์(G_0) และลำดับชั้นที่หนึ่ง (G_1)

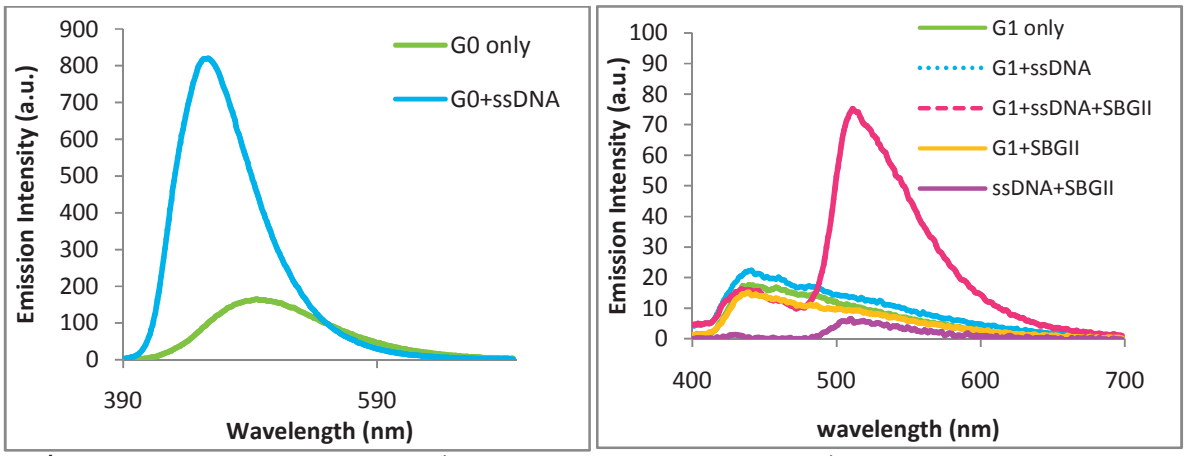

รูปที่ 2ซ้าย: กราฟฟลูออเรสเซนต์ในระบบที่ไม่มี (เส้นสีเขียว) และมีดีเอ็นเอสายเดี่ยว (5'TAGGCATATGC3') (เส้นสีฟ้า) ของเดนดริเมอร์ลำดับชั้นที่ศูนย์ขวา: กราฟฟลูออเรสเซนต์ในระบบที่ไม่มีดีเอ็นเอ (เส้นสีเขียว) ระบบที่มีดีเอ็นเอสายเดี่ยว (5'CCTATATAGGTGATGCCTTCTCCGGCGACG3') (เส้นสีฟ้า) และระบบที่มีสีย้อมฟลูออเรสเซนต์ (เส้นประสีชมพู) ของเดนดริเมอร์ลำดับชั้นที่หนึ่ง

1. จากผลการทดลองในเบื้องต้นโดยใช้ G_1เป็น fluorescence energy donor (รูปที่ 3) เติม complimentary DNA (N1A) จะเห็นสัญญาณการเรืองแสงของ fluorescein (สัญญาณ FRET) ได้ และเมื่อ mismatched DNA (N1) ก็เกิดสัญญาณ FRET เช่นกันแต่ในระดับที่ต่ำกว่า อย่างไรก็ตามผู้วิจัยยังพบว่ามีสัญญาณ FRET เกิดขึ้นก่อนการเติม DNA ด้วย ซึ่งจัดเป็น non-specific interaction ระหว่าง G_1และ PNA-Fl โดย lipophilic interaction ระหว่างโครงสร้างชั้นในของ G1 กับ peptide backbone ของ PNA เมื่อมีการเติม N1A และเกิด DNA/PNA duplex แล้ว อันตรกิริยาแบบcoulombic ระหว่าง duplex กับ G_1จึงเกิดขึ้น ซึ่งทำให้ไม่เห็นความแตกต่างระหว่างระบบที่มีและไม่มี DNA/PNA duplex แต่ในกรณีที่

เติม N1 ซึ่งไม่ทำให้เกิด DNA/PNA duplex แต่ N1 นั้นสามารถจับกับG1ได้ด้วยด้วยแรงระหว่างประจุ และอาจมีG1ที่เหลือบางส่วนเกิด lipophilic interaction กับ PNA ได้ จึงทำให้เห็นสัญญาณ FRET ที่น้อยลง

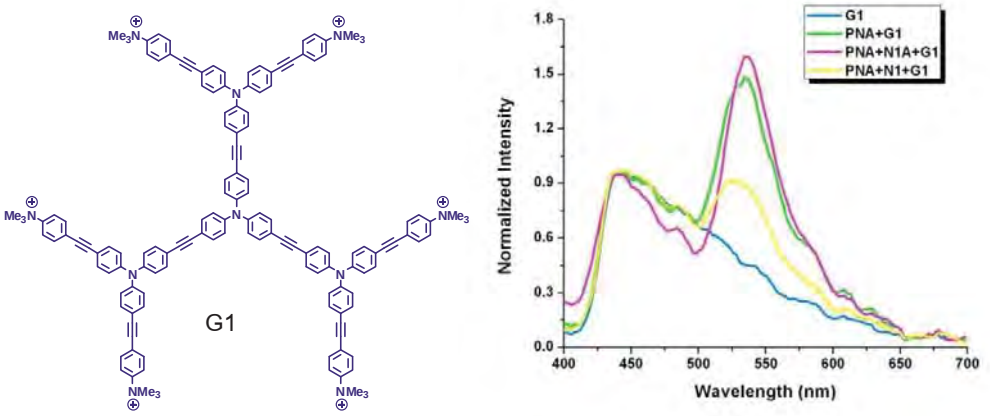

รูปที่ 1 ผลการทดลองกับ G_1

ผลการทดลองข้างต้นบ่งชี้ว่า G1 สามารถถ่ายเทพลังงานให้แก่ fluorescein ได้ แต่โครงสร้างชั้นในของ G1 ที่มีขั้วน้อยอาจเกิดอันตรกิริยากับส่วนที่มีขั้วน้อยใน PNA ได้ ดังนั้นผู้วิจัยจึงได้พยายามปรับลด non-specific interaction ระหว่าง PNA-Flกับ G1 โดยการเติมสารเติมแต่ง (additive) ต่างๆเช่น formamide 20%(v/v) ดังรูปที่ 4

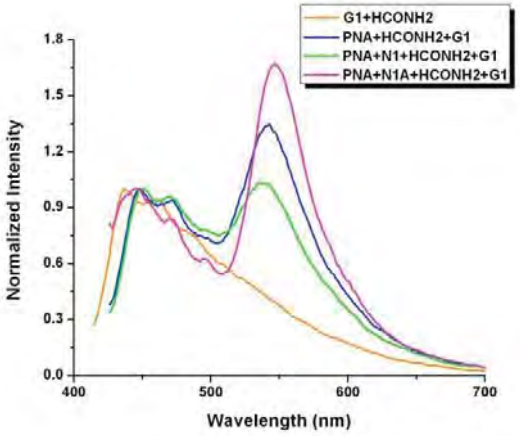

รูปที่ 4 ผลการทดลองเมื่อมีการเติม formamide 20% (v/v)

ซึ่งจากการทดลองจะเห็นว่าการเติม formamide ทั้งในปริมาณ 10%(v/v) และ 20% (v/v) นั้นพบว่าสามารถลด non-specific interaction ระหว่าง PNA-Flกับ G_1ได้บางส่วน สัญญาณ FRET ของระบบที่มี matched DNA(N1A) นั้นยังคงอยู่ในระดับที่สูงที่สุด และที่ 20% (v/v) ให้ FRET ratio ที่สูงกว่า

ต่อมาได้ทำการทดลองเติม N-methyl-pyrroridone (NMP) 10%(v/v) และ 20% (v/v) เพื่อพยายามปรับลด non-specific interaction ดังกล่าวเช่นเดียวกัน ซึ่งให้ผลการทดลองดังรูปที่ 5และยังได้ทำการทดลองเติม Polyvinylpyrrolidone เพื่อเปรียบเทียบผลการทดลอง (รูปที่ 6)

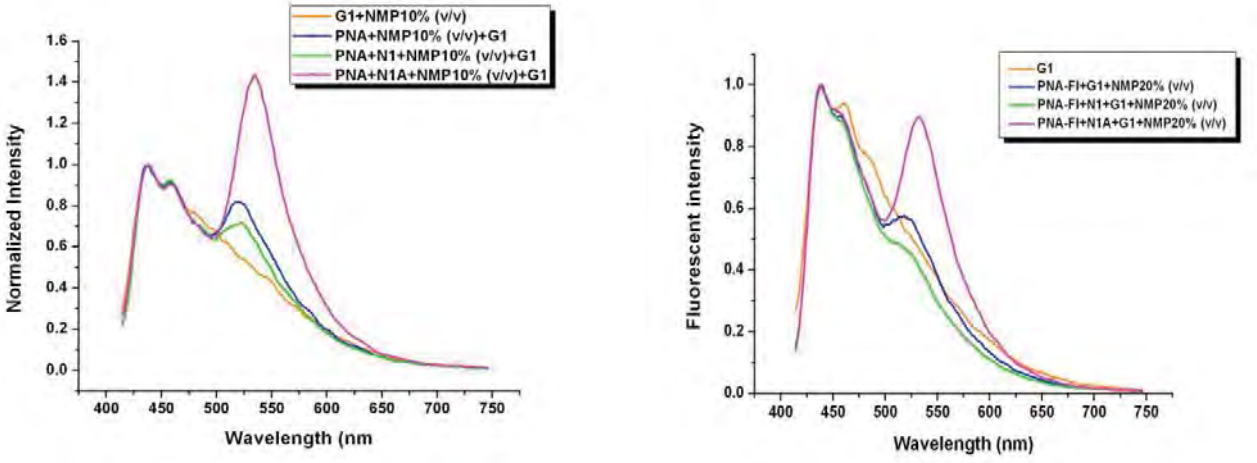

รูปที่5 ผลการทดลองกับ G_1เมื่อมีการเติม NMP 10 % (v/v)และ 20% (v/v) ตามลำดับ

ซึ่งจากการทดลองจะเห็นว่าการเติม NMP ในปริมาณทั้ง 10 %(v/v), 20% (v/v) และPolyvinylpyrrolidone นั้น พบว่าสามารถลด non-specific interaction ระหว่าง PNA-Flกับ G_1ได้บางส่วน และที่ปริมาณการเติม NMP 10%(v/v)ให้ FRET ratio ที่สูงที่สุด

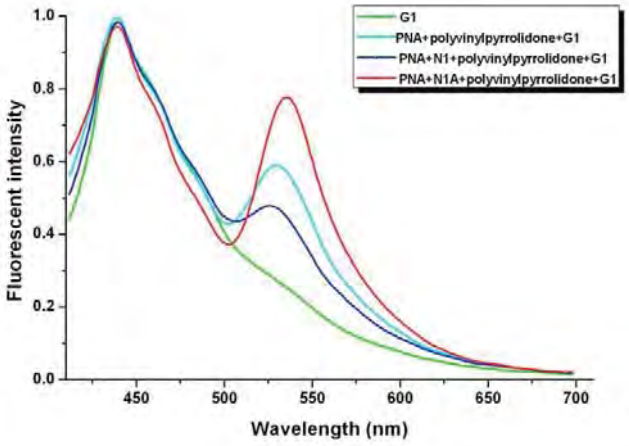

รูปที่ 6 ผลการทดลองกับ G_1 เมื่อมีการเติม Polyvinylpyrrolidone

และต่อมาได้ทำการทดลองเปลี่ยนแปลงความเข้มข้น G_1กับตัวอย่าง ssDNAใหม่ที่เพิ่มมา 3 สาย คือ single mismatched (**1**), Complimentary DNA +/- 5 bases (**2**) และ Complimentary DNA +/- 10 bases (**3**) และ ตัวอย่าง ssDNAเดิม คือ totally mismatched DNA (N1) กับ Complimentary DNA (N1A) ดังรูปที่ (5a-d) จากการทดลองพบว่า

ความเข้มข้นต่ำสุดของ G1 ที่สามารถแยกความแตกต่างของสัญญาณที่ได้จาก N1 และ N1A คือ 0.5 uMแต่ประสิทธิภาพในการถ่ายเทพลังงานแบบ FRET จะสูงที่สุดเมื่อความเข้มข้นของ G1 เท่ากับ 1.0 uM ดังรูปที่ 7

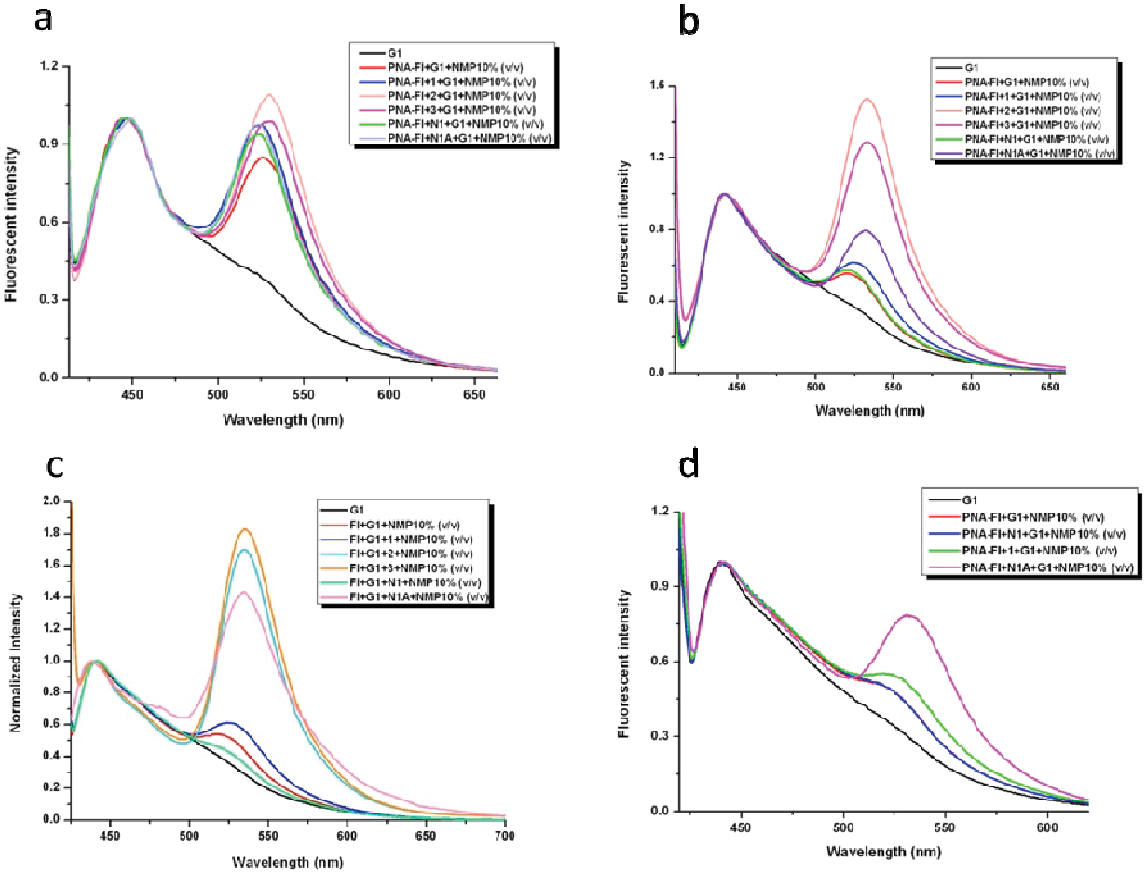

รูปที่ 7ผลการทดลองกับ G_1 เท่ากับ (a) 0.2 uM, (b) 0.5 uM, (c) 1.0 uMและ (d) 1.5 uM.

จากผลการทดลองข้างต้นเดนดริติกพอลิอิเล็กโทรไลต์ G_1 สามารถใช้เป็น energy donor ควบคู่กับ fluorescein-labelled PNA (PNA-FI) ในการตรวจหา DNA ที่มีลำดับเบสที่เป็นคู่สมกับ PNA ได้ โดยสัญญาณ FRET ของระบบที่มี complimentary DNA จะสูงกว่า 1.0 โดยผลงานวิจัยที่ผ่านมาได้ทำการทดลองกับ DNA ที่มีความยาวเท่ากับจำนวนเบสในสาย PNA (11 เบส)

ดังนั้นผู้วิจัยได้ทำการทำลองเพิ่มเติมกับตัวอย่าง complementary DNA (cDNA) และ single mismatch DNA (smDNA) ที่มีความยาวจาก 11 เบส เป็น 21, 31 และ 61 เบส เพื่อศึกษาเปรียบเทียบประสิทธิภาพของกระบวนการถ่ายเทพลังงานผลทดลองพบว่า ในกรณีของ cDNAเมื่อความยาวของสายเพิ่มขึ้นจาก 11 เป็น 21หรือ 31 เบส FRET ratio ที่ได้มีค่าเพิ่มขึ้นซึ่งเป็นผลมาจาก Coulombic interaction ระหว่าง residual base units ที่เพิ่มขึ้น แต่เมื่อเพิ่มความยาวไปเป็น 61 เบส พบว่า FRET ratio ที่ได้กลับมีค่าลดลงเล็กน้อย ซึ่งอาจจะอธิบายได้ว่าความยาวของสาย DNA ที่มากขึ้นนี้อาจไปลดโอกาสที่ G_1 จะเข้ามาอยู่ใกล้กับ fluorescein ในระยะที่เหมาะสมแต่ในกรณีของ smDNAเมื่อเพิ่มความยาวสาย DNA จาก

11 เป็น 21 และ 31 เบส FRET ratio ที่ได้เพิ่มขึ้นเพียงเล็กน้อยโดยจะไม่เห็นความแตกต่างที่ชัดเจนระหว่าง DNA ที่มี 21 และ 31 เบส ดังรูปที่ 8

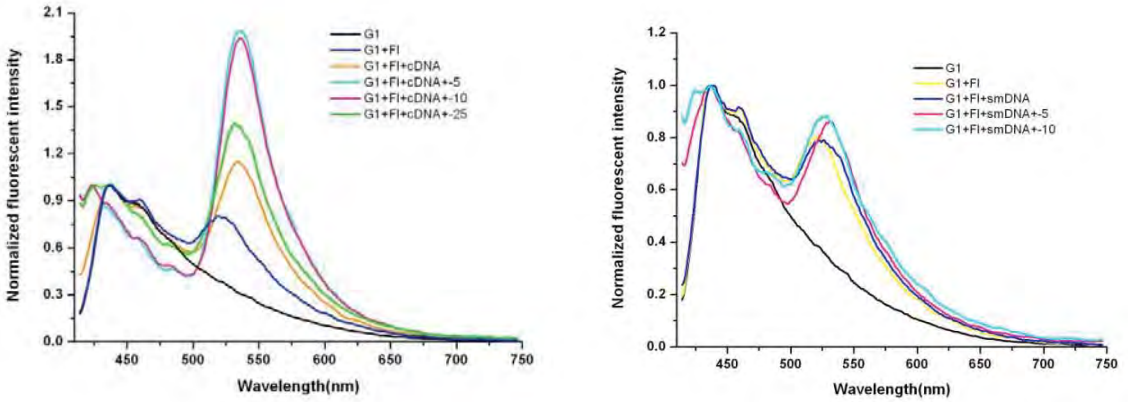

รูปที่ 8 Emission spectra ของการทดลองโดยใช้ complimentary (ซ้าย)และ single mismatched DNA (ขวา) ที่มีความยาวของสายแตกต่างกัน

ตารางที่ 1 เปรียบเทียบ FRET ratio ระหว่างผลการทดลองที่ผ่านมากับผลการทดลองใหม่

	FRET ratio (ผลที่เคยรายงานไว้)	FRET ratio (ผลการทดลองใหม่)
G1+Fl-acpcPNA	0.39	0.80
2+Fl-acpcPNA+cDNA(11bases)	1.42	1.15
2+Fl-acpcPNA+cDNA+/-5 (21bases)	1.72	1.99
2+Fl-acpcPNA+cDNA+/-10 (31bases)	1.86	1.94
2+Fl-acpcPNA+cDNA+/-25 (61bases)	-	1.40
2+Fl-acpcPNA+smDNA (11bases)	0.51	0.79
2+Fl-acpcPNA+smDNA+/-5 (21bases)	-	0.87
2+Fl-acpcPNA+smDNA+/-10 (31bases)	-	0.88

เนื่องจาก non-speciflc FRET signal ที่ได้จากการทดลองครั้งนี้มีค่าสูงกว่าผลการการทดลองก่อนหน้านี้แม้ว่าจะมีการเติม N-methyl-2-pyrrolidone แล้วก็ตาม จึงอาจเป็นไปได้ว่าความเข้มข้นของ PNA-Fl stock solution มีความคลาดเคลื่อน ซึ่งจะต้องตรวจสอบและทำการทดลองซ้ำอีกครั้ง อย่างไรก็ตามผลการทดลองส่วนใหญ่ยังคงเป็นไปในทิศทางเดิมและยังสามารถใช้บอกความแตกต่างระหว่าง cDNAกับ smDNAได้

ต่อมาผู้วิจัยได้ทำการทดลองซ้ำเพิ่มเติมโดยสามารถรวบรวมผลการทดลองดังกล่าวไปตีพิมพ์ในวารสารนานาชาติดังเอกสารข้อ 4 ซึ่งในสภาวะที่ดีที่สุด cDNAให้ค่าอัตราส่วน FRET สูงถึง 1.42 เมื่อเปรียบเทียบกับ ncDNAที่ให้ค่าเพียง 0.26 และ smDNAที่ให้ค่าเท่ากับ 0.51 เท่านั้น โดยการตอบสนองต่อความเข้มข้นของ DNA ในช่วงการตรวจวัดที่เป็นเส้นตรงให้ค่า detection limit ต่ำกว่า 1 nMซึ่งงานวิจัยนี้สามารถนำไปสู่การตรวจวัดลำดับเบสของดีเอ็นเอในการประยุกต์ใช้งานจริงได้ในอนาคตต่อไป

2. จากผลการทดลองเบื้องต้นพบว่าสารสังเคราะห์ G_0ที่มี counter ion เป็นไอโอไดด์ไอออน (R = $NMe_3^+I^-$) จะมีความสามารถในการละลายน้ำได้ลดลงเมื่อเก็บของแข็งไว้เป็นเวลานานหลายสัปดาห์ เนื่องจากเกิด demethylationของหมู่ ammonium ผู้วิจัยจึงได้เปลี่ยน counter ion เป็นคลอไรด์ไอออน (R = $NMe_3^+Cl^-$) ด้วยวิธี anionic ion exchange โดยใช้คอลัมน์เรซิน ซึ่งสารสังเคราะห์ใหม่เรียกว่า (N^{3+}) ที่ได้มีความเสถียรมากขึ้นดังแสดงรูปที่ 9

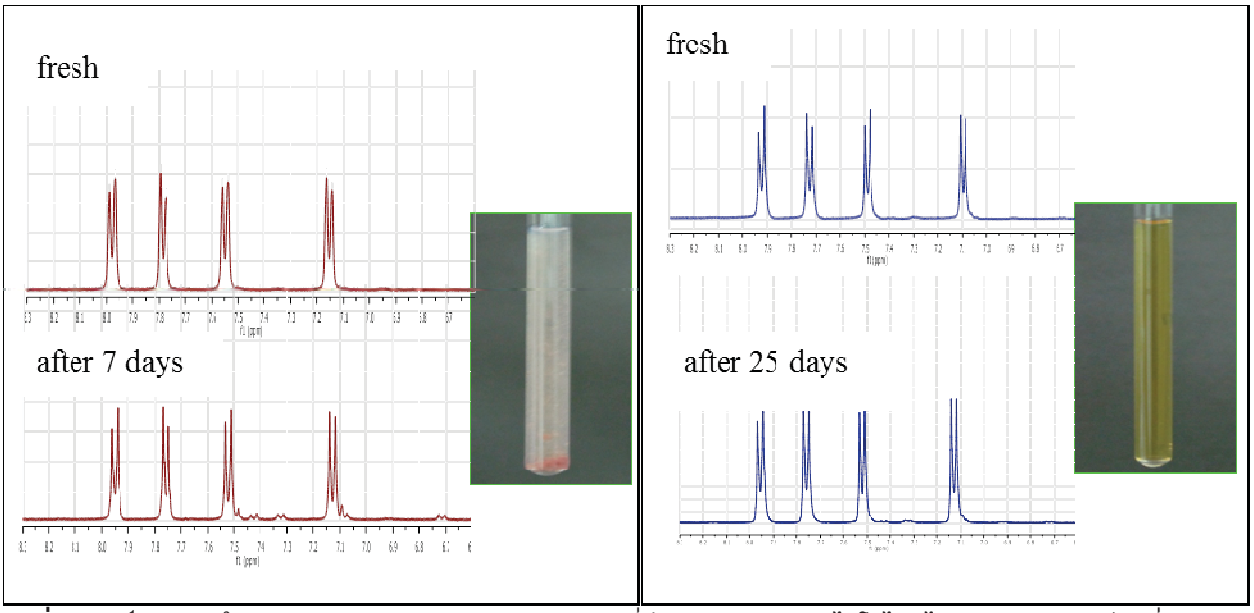

รูปที่ 9กราฟ ^{1}H NMR ในตัวทำละลาย CD_3OD ของ G_0 (ซ้าย) ที่มี counter ion เป็นไอโอไดด์ไอออน(R = $NMe_3^+I^-$) ที่เก็บไว้หลังจากสังเคราะห์ใหม่และผ่านไปเจ็ดวัน และ (ขวา)) ที่มี counter ion เป็นคลอไรด์ไอออน (R = $NMe_3^+Cl^-$) ที่เก็บไว้หลังจากสังเคราะห์ใหม่และผ่านไป 25 วันตามลำดับ

เมื่อทดสอบการจับกับดีเอ็นเอสายสั้น (Aptamer) พบว่ามีการขยายสัญญาณฟลูออเรสเซนต์ไปมากกว่า 5 เท่าและมีการเลื่อนของความยาวคลื่นไปทางสั้นลง (blue shift) และเมื่อในระบบมีโพแทสเซียมไอออนอยู่สามารถทำให้สัญญาณดังกล่าวลดลงได้ ดังแสดงในรูปที่ 10

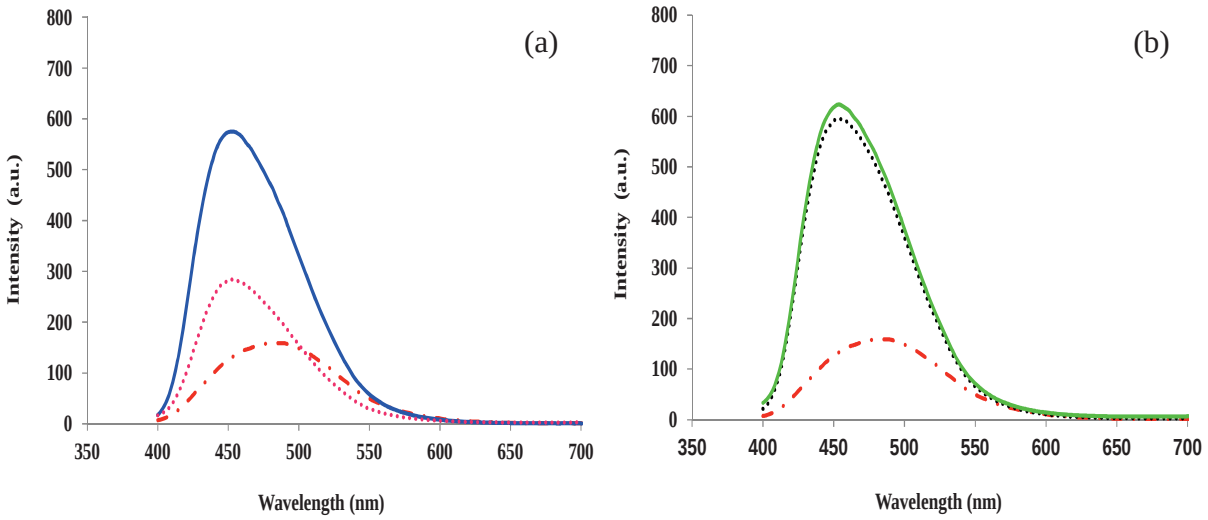

รูปที่ 10 (a)กราฟฟลูออเรสเซนต์ของ Aptamerเมื่อ N^{3+}(-·-·-), N^{3+}:Apt15, (——) and N^{3+}:Apt15:K^{+}, (·····) และ (b) กราฟฟลูออเรสเซนต์ของ Non-ptamerเมื่อ N^{3+}(-·-·-), N^{3+}:nApt15, (——) and N^{3+}:nApt15:K^{+}, (·····) ที่ความเข้มข้น [N^{3+}] = 0.20 μM; [Apt15] = [nApt15] = 0.02 μM; [K^{+}] = 1 mM

เมื่อทำการทดลองกับสายดีเอ็นเอที่ยาวแตกต่างกันคือ Apt12, Apt15 และ Apt21เปรียบเทียบกับ nApt15 พบว่าที่ความเข้มข้นเดียวกัน จะให้การขยายสัญญาณฟลูออเรสเซนต์ของฟลูออโรฟอร์ที่แตกต่างกันดังรูปที่ 11 ซึ่งผู้วิจัยเสนอว่าความสามารถในการจับกัน (binding affinity) กับฟลูออโรฟอร์ของดีเอ็นเอแต่ละสายมีไม่เท่ากัน

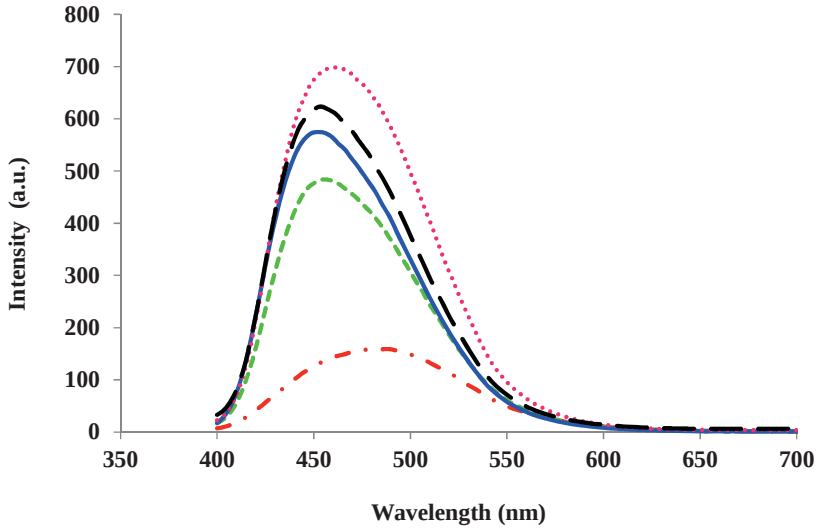

รูปที่ 11กราฟฟลูออเรสเซนต์ของสารละลาย N^{3+}(0.20 μM) ในสารละลายบัฟเฟอร์ (-·-·-) และในระบบที่มี aptamers (0.020 μM) ที่มีความยาวแตกต่างกันคือ Apt12 (----), Apt15 (——), Apt21 (·····)และ nApt15 (——)

ด้วยการสมมุติว่าการเกิด complexationของฟลูออโรฟอร์ต่อดีเอ็นเอเป็นสัดส่วนแบบ 1:1 ผู้วิจัยสามารถหาค่าคงที่ในการจับกัน (affinity constant, Ka) ด้วยสมการของ Benesi-Hildelbrandได้ดังแสดงในกราฟที่ 12 พบว่าค่าคงที่เพิ่มขึ้น

เมื่อสายดีเอ็นเอยาวขึ้น ในขณะที่ Apt15 และ nApt15 ให้ค่าคงที่ที่เท่ากัน แสดงให้เห็นถึงผลของ electrostatic interaction ที่เป็นปัจจัยหลัก

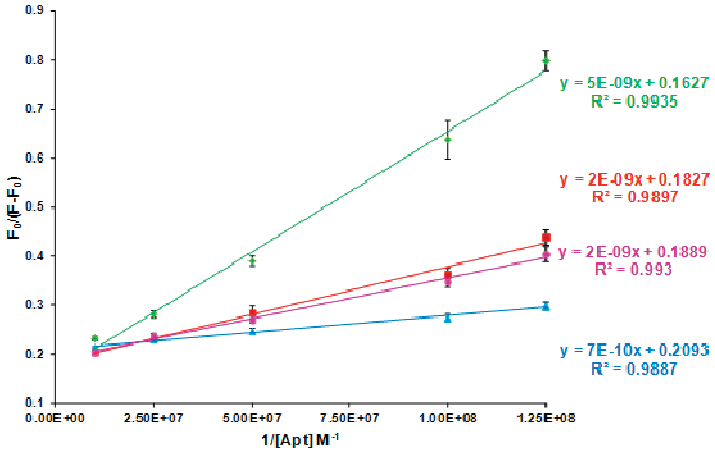

รูปที่ 11กราฟเส้นตรง Benesi-Hildelbrand จากการตอบสนองด้วยฟลูออเรสเซนต์ของ $\mathbf{N}^{3+}$(0.2 μM) ที่ความเข้มข้นของดีเอ็นเอต่างๆ (0.1 μM to 0.004 μM): Apt12 (——), Apt15 (——), nApt (——) and Apt21 (——) ให้ค่า K_a ซึ่งหาได้จาก intercept/slope = 3.25×10^7, 9.14×10^7, 2.99×10^8 and 9.45×10^7 M^{-1} ตามลำดับ

การวิเคราะห์ด้วย Job's plot พบว่า Apt12 จับกับฟลูออโรฟอร์ด้วยอัตราส่วน 2:1 แต่ดีเอ็นเอที่เหลือให้ค่า 1:1 ดังรูปที่ 12 และเมื่อคำนวณทางโปรแกรมคอมพิวเตอร์ (AM1 geometrical optimization) วัดระยะระหว่างหมู่ ammonium ได้เท่ากับ 21.7 Å เมื่อเปรียบเทียบกับความกว้างของเบสหนึ่งตัวเท่ากับ 3.3Å ทำให้ผู้วิจัยเสนอถึงการจับกันของฟลูออโรฟอร์และดีเอ็นเอโดยการโอบล้อมของดีเอ็นเอรอบๆหมู่ปลาย ammonium ของโครงสร้างฟลูออโรฟอร์

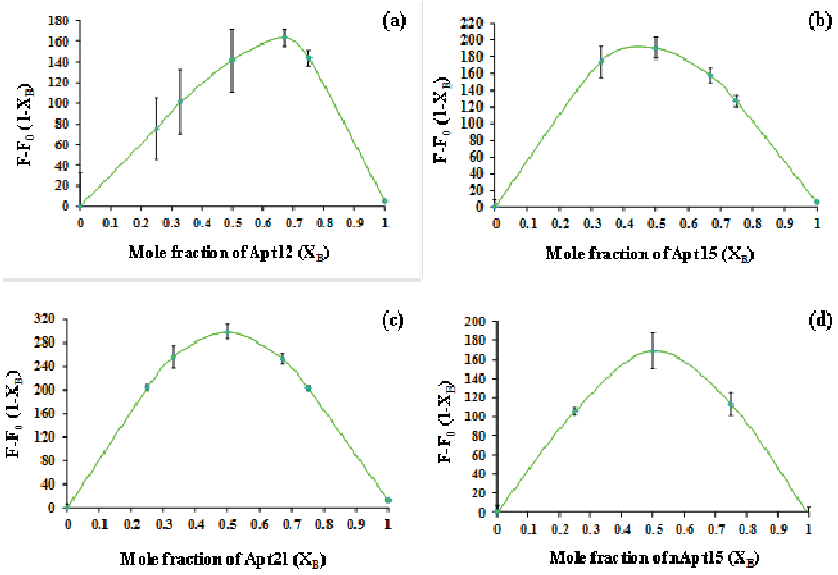

รูปที่ 12กราฟการตอบสนองของสัญญาณฟลูออเรสเซนต์แสดง Job's plot ของ $\mathbf{N}^{3+}$ต่อดีเอ็นเอที่ความยาวต่างๆ (a)Apt12 (b)Apt15 (c)Apt21 และ (d)nApt15

ต่อมาผู้วิจัยได้ทำการทดลองเพิ่มเติมสำหรับการตรวจวัดโพแทสเซียมไอออนเพื่อหาสภาวะที่ดีที่สุด ซึ่งเชื่อว่าถ้าให้ค่าการระงับสัญญาณฟลูออเรสเซนต์ (fluorescence quenching) สูงจะให้การตรวจวัดที่ดีพบว่าอัตราส่วนของ aptamer/fluorophore ที่เหมาะสมคือใช้ปริมาณดีเอ็นเอน้อยและให้ประสิทธิภาพดีคืออัตราส่วนเท่ากับ 1:10 ดังรูปที่ 13

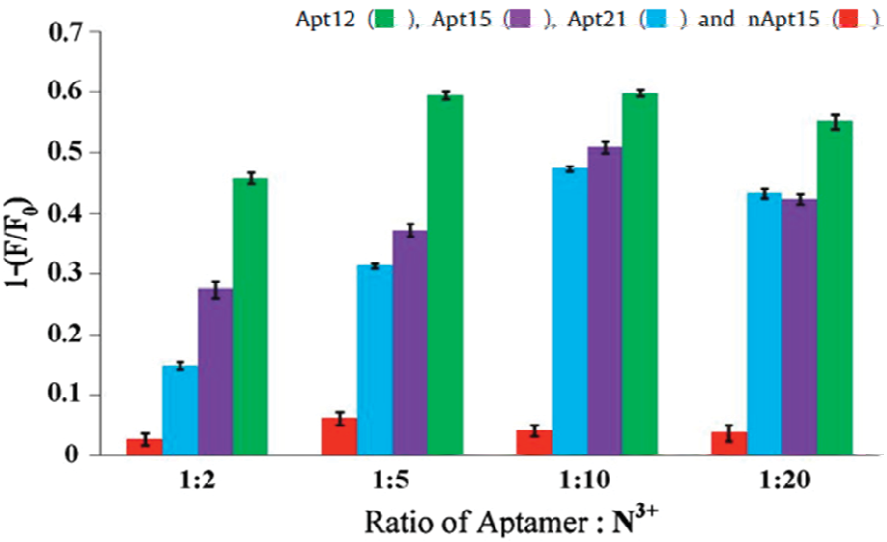

รูปที่ 13 กราฟแท่งแสดงประสิทธิภาพในการระงับสัญญาณฟลูออเรสเซนต์ของโพแทสเซียมไอออนในระบบที่ใช้ดีเอ็นเอความยาวต่างๆ

เมื่อทำการศึกษาผลการเลือกจำเพาะเจาะจง (selectivity) ต่อโพแทสเซียมไอออนเทียบกับแคทไอออนชนิดอื่นๆ พบว่าระบบของ aptamerให้การเลือกจำเพาะที่ดี ในขณะที่ระบบของ non-aptamerไม่มีการเลือกจำเพาะ ดังรูปที่ 14 นอกจากนี้ Apt12 ยังให้ selectivity ที่ต่ำที่สุดเมื่อเทียบกับaptamerตัวอื่นๆและพบว่า Apt15 เหมาะสมต่อการทดลองในขั้นต่อไป

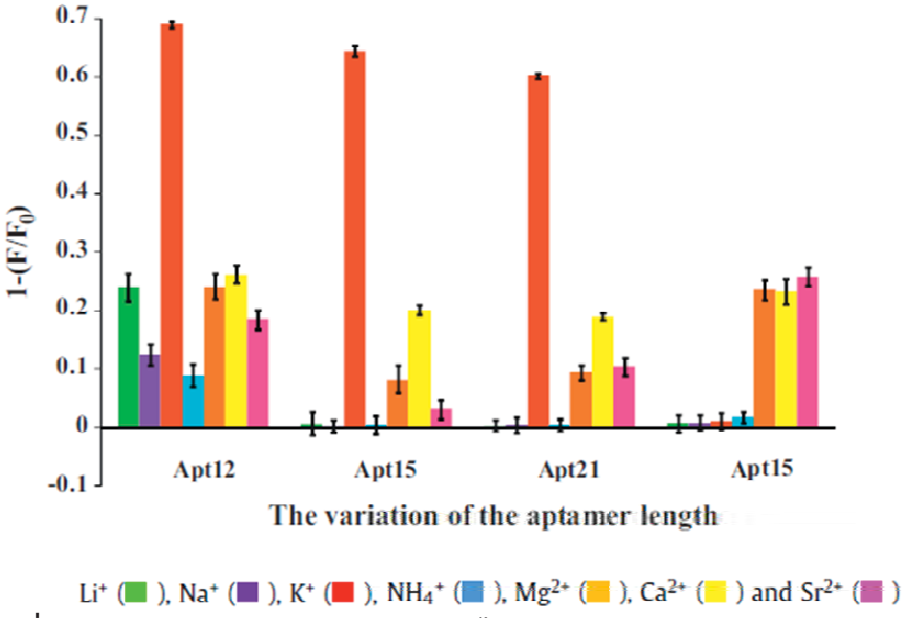

รูปที่ 14 กราฟแท่งแสดงการเลือกจำเพาะต่อแคทไอออนชนิดต่างๆ

หลังจากนั้นผู้วิจัยได้วิเคราะห์โพแทสเซียมไอออนความเข้มข้นต่างๆ พบว่าที่ความเข้มข้นต่ำ คือ ≤50 mM สัญญาณฟลูออเรสเซนต์ลดลงแต่ไม่เกิดการเลื่อนของความยาวคลื่น ในขณะที่ความเข้มข้นสูง คือ 100 mMสัญญาณฟลูออเรสเซนต์เกิดการเลื่อนของความยาวคลื่นกลับสู่สัญญาณเดิมเช่นเดียวกับสัญญาณฟลูออเรสเซนต์ของฟลูออโรฟอร์เริ่มต้น ผลการทดลองดังกล่าวสอดคล้องกับการเกิด complex ของ K^+/Aptแบบ 1:1 ที่ความเข้มข้นของโพแทสเซียมไอออนสูง และเป็นแบบ 2:1 ที่ความเข้มข้นต่ำ ซึ่งในช่วงความสัมพันธ์ที่เป็นเส้นตรงได้ค่าความเข้มข้นต่ำสุดที่สามารถตรวจวัดได้ (limit of detection)เท่ากับ 0.9 μMดังรูปที่ 15

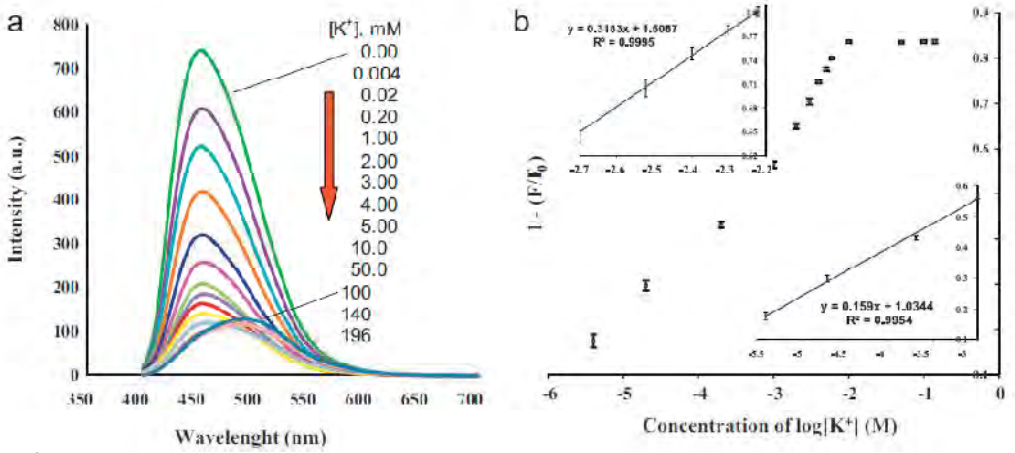

รูปที่ 15 กราฟแสดงความเข้มของสัญญาณฟลูออเรสเซนต์เมื่อในระบบมีโพแทสเซียมไอออนที่ความเข้มข้นต่างๆ

ผู้วิจัยยืนยันสมมุติฐานของการจับกันของฟลูออโรฟอร์และดีเอ็นเอด้วย circular dichroism (CD) ซึ่งผลการทดลองดังรูปที่ 16 แสดงให้เห็นชัดเจนว่าโพแทสเซียมไอออนสามารถแยกจับกับaptamerจากN^{3+}ได้

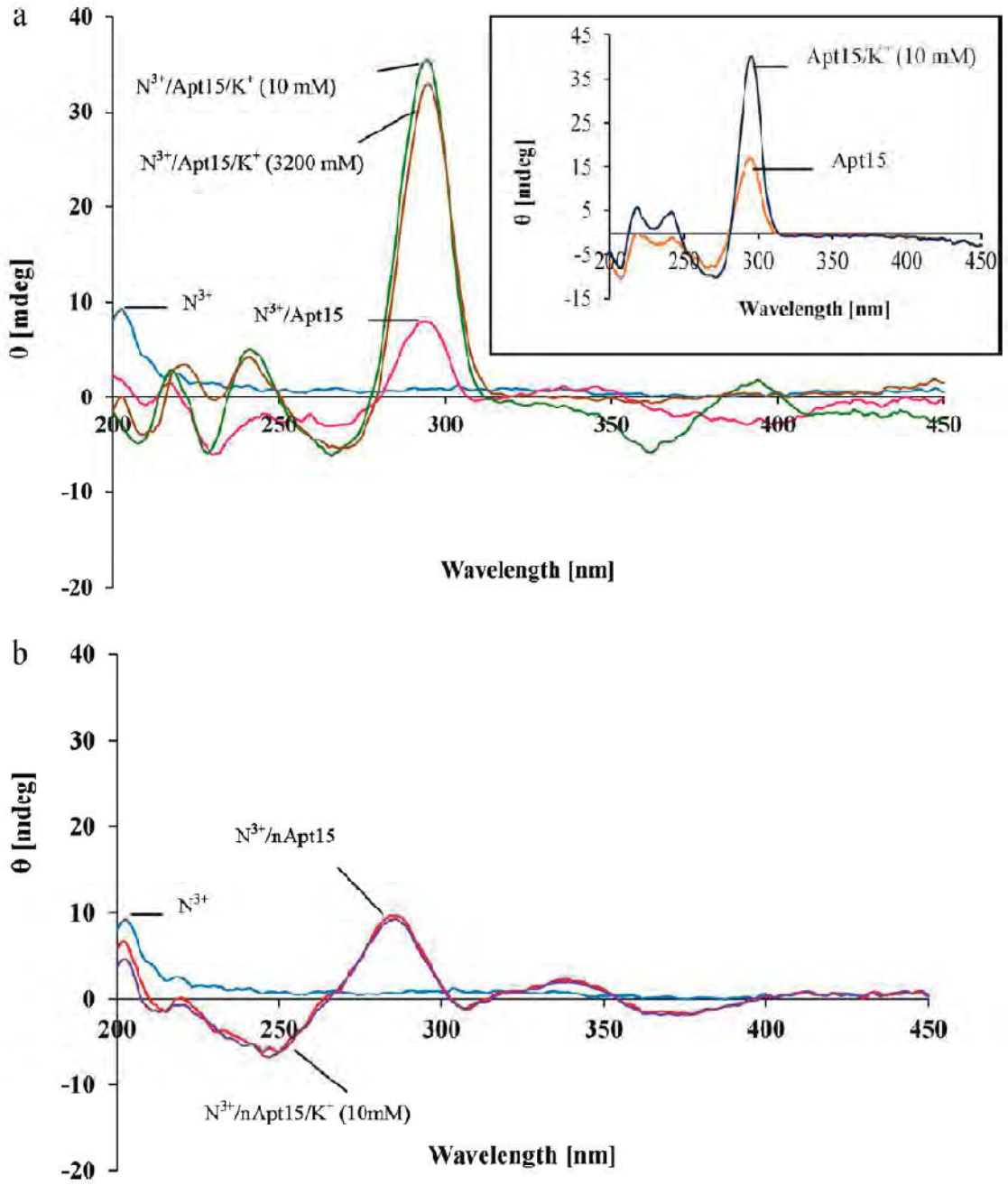

รูปที่ 16 กราฟ Circular dichroism (CD)ของ(a) ระบบที่มี Aptamerและ (b)ระบบที่เป็น non-aptamer, Insetเป็นระบบที่ไม่มี N^{3+}

และสุดท้ายผู้วิจัยได้ทำการวิเคราะห์โพแทสเซียมไอออนในตัวอย่างน้ำปัสสาวะจริง 4 ตัวอย่างให้ผลดังตารางที่ 2 ซึ่งแสดงให้เห็นถึงประสิทธิภาพการตรวจวัดที่ดีเหมาะสมต่อการนำไปใช้

ตารางที่ 2 ผลการวิเคราะห์โพแทสเซียมไอออนในตัวอย่างน้ำปัสสาวะจากอาสาสมัคร 4 คน

Sample	N^{3+}-Apt sensor Mean ± SD/mM (n = 5)	ICP-MS Mean ± SD/mM (n = 5)	F-Test between two methods[b]	Add K^+ (mM)	Found K^+ (mM)	Recovery (%)
Urine 1	4.20 ± 0.006	4.15 ± 0.033	S	10	9.875	98.8
Urine 2	11.17 ± 0.004	11.22 ± 0.152	3.15	10	9.952	99.5
Urine 3	14.58 ± 0.003	14.59 ± 0.063	2.30	10	9.753	97.5
Urine 4	23.21 ± 0.012	23.75 ± 0.091	3.67	10	9.741	97.4

[a] $[N^{3+}]/[Apt15] = 1/0.1\ \mu M$.
[b] The F-test value is 6.39 at a 95% confidence level.

สำหรับงานวิจัยในส่วนนี้นำไปสู่ผลงานตีพิมพ์ในวารสารนานาชาติดังข้อ 4

3. เมื่อทำการศึกษาเพิ่มเติมจากผลการทดลองเบื้องต้นในตอนแรกพบว่าสัญญาณฟลูออเรสเซนต์ที่ตอบสนองต่อ G_0จะเพิ่มขึ้นเมื่อสายดีเอ็นเอยาวขึ้นจนถึงความยาวเบสประมาณ 20 เบสจึงคงที่ ในขณะที่สัญญาณ FRET ในระบบที่มี SyBrGreen II เป็นตัวรับพลังงาน (Acceptor) จะเพิ่มขึ้นเรื่อย (ทำการทดลองถึงเพียง 30 เบส) เมื่อสายดีเอ็นเอยาวขึ้นดังกราฟที่แสดงข้างล่าง

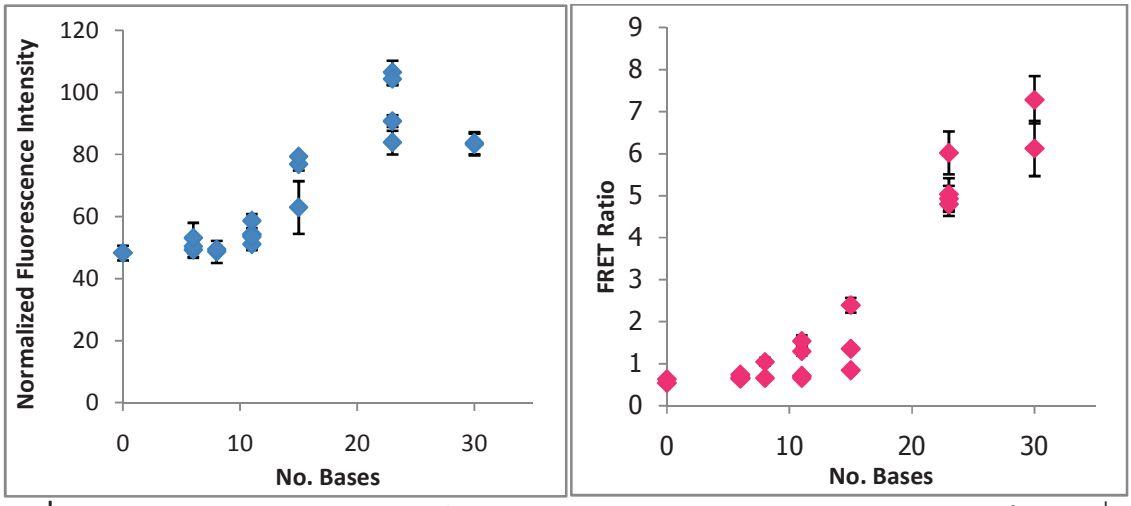

รูปที่ 17 กราฟแสดงสัญญาณฟลูออเรสเซนต์ของ G_0 (ซ้าย) และแสดงสัญญาณ FRET ของ G_1 (ขวา) ในระบบที่มีดีเอ็นเอสายเดี่ยวความยาวตั้งแต่ 0 ถึง 30 เบส (จำกัดความเข้มข้นของดีเอ็นเอให้มีค่า absorbance ที่ 260nm เท่ากับ 0.05)

และผู้วิจัยได้ศึกษาการจับกันของดีเอ็นเอรวมไปถึงสารชีวโมเลกุลอื่นๆกับเดนดริติกพอลิอิเล็กโทรไลต์เรืองแสงที่มีต่อการเปลี่ยนสัญญาณฟลูออเรสเซนต์ จึงได้ทำการทดลองเพิ่มเติมในระบบซึ่งจำกัดการเคลื่อนไหวของโมเลกุลขนาดเล็ก (nano-confined environments) ที่มีสารลดแรงตึงผิวชนิดต่างๆ (anionic, cationic, and non-ionic surfactants) cyclodextrins และโปรตีน BSA รวมทั้งพอลิเมอร์ชนิดประจุลบ (PVSK) โดยพบว่าในแต่ละสิ่งแวดล้อม มีผลทำให้สัญญาณฟลูออเรสเซนต์ของ G_0แตกต่างกันไป แต่แนวโน้มส่วนใหญ่มักเพิ่มสัญญาณฟลูออเรสเซนต์ (fluorescence enhancement) ไปทางความยาวคลื่นที่สั้นลง (blue shift) ดังรูปที่ 18 และ 19

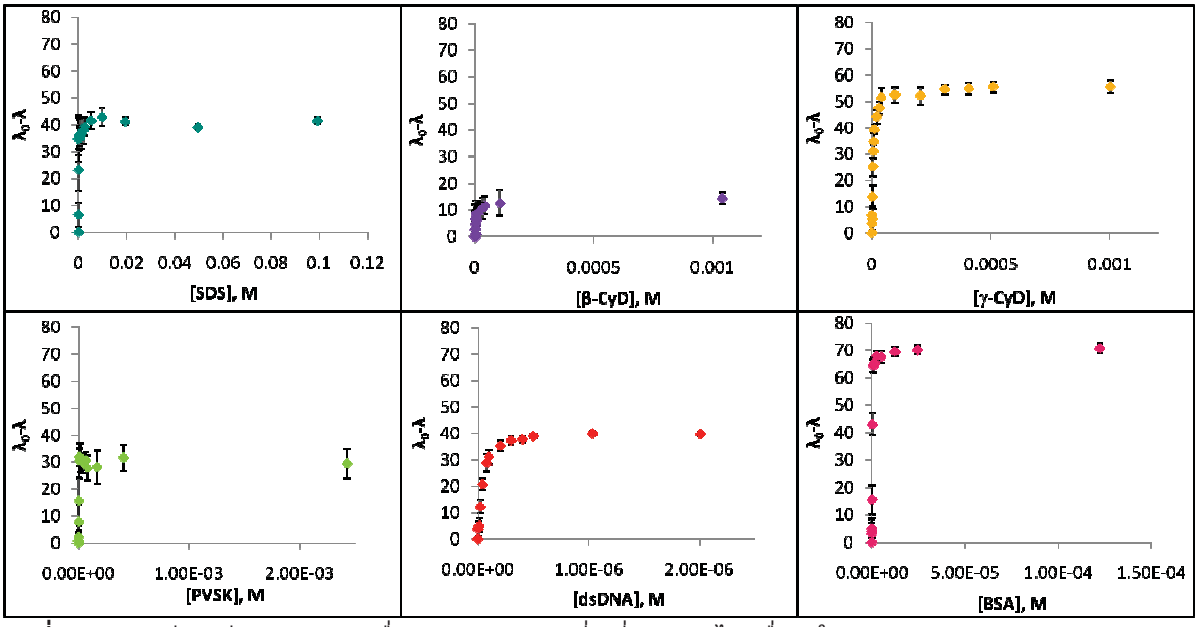

รูปที่ 18กราฟเปรียบเทียบความยาวคลื่นของ G_0 probes ที่เปลี่ยนแปลงไป เมื่ออยู่ในระบบต่างๆ

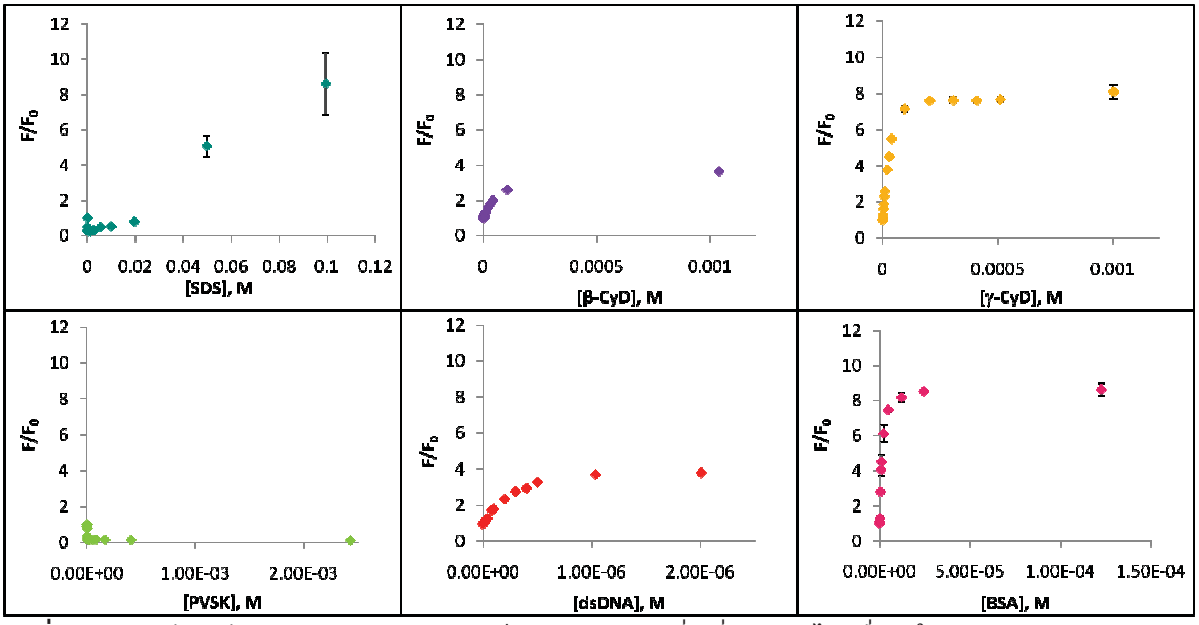

รูปที่ 19กราฟเปรียบเทียบสัญญาณฟลูออเรสเซนต์ของ G_0 probes ที่เปลี่ยนแปลงไป เมื่ออยู่ในระบบต่างๆ

ผู้วิจัยเลือกดีเอ็นเอสายเดี่ยว (ssDNA) ลำดับเบส 5´GCATATGCCTA3´ และสายคู่ซึ่งมีลำดับเบสคู่สม (dsDNA) มาเปรียบเทียบการเปลี่ยนแปลงสัญญาณฟลูออเรสเซนต์ของโมเลกุล G_0หรือเรียกว่า **3N**$^+$ ระหว่างดีเอ็นเอทั้งสองชนิดโดยควบคุมให้ความเข้มข้นของประจุของสายดีเอ็นเอเท่าๆกัน พบว่าดีเอ็นเอทั้งสองสามารถขยายสัญญาณฟลูออเรสเซนต์ของฟลูออโรฟอร์ขึ้นไปใกล้เคียงกันมาก คือประมาณ 5 เท่า และให้ absorption ที่เหมือนกัน ดังรูปที่ 20

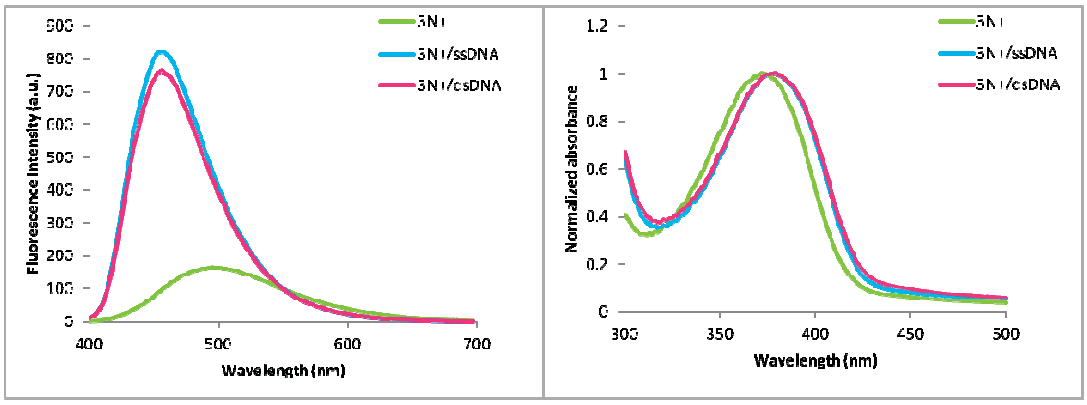

รูปที่ 20กราฟฟลูออเรสเซนต์ (ซ้าย) และการดูดกลืนแสง (ขวา) ของ **3N**$^{+}$ (5 μM) ที่มีssDNA (5′GCATATGCCTA3′, 10 μM) และdsDNA (5′GCATATGCCTA3′ + 5′TAGGCATATGC3′, 5 μM) ในสารละลายฟอสเฟตบัฟเฟอร์

นอกจากนี้ยังพบว่าการขยายสัญญาณฟลูออเรสเซนต์ด้วย dsDNAยังเพิ่มขึ้นตามความเข้มข้นของสายดีเอ็นเอดังรูปที่ 21 ซึ่งจะเริ่มคงที่ที่อัตราส่วนดีเอ็นเอต่อฟลูออโรฟอร์ที่ 1:1

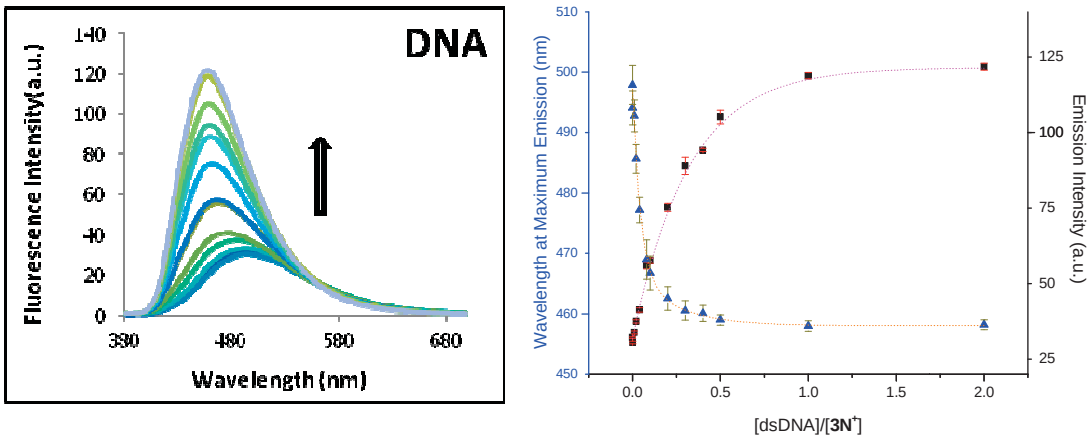

รูปที่ 21 กราฟฟลูออเรสเซนต์ (ซ้าย) และการเลื่อนของความยาวคลื่นของการคายแสงและความเข้มของสัญญาณฟลูออเรสเซนต์ (ขวา) ของ 3N^{+} (1 μM) ที่มี dsDNA (5′GCATATGCCTA3′ + 5′TAGGCA TATGC3′) ความเข้มข้นต่างๆ (0 — 2 μM)

จากการศึกษาด้วย Circular Dichroism (CD) พบว่าสัญญาณ CD ของ 3N^{+} ไม่มีความแตกต่างอย่างมีนัยสำคัญระหว่างในระบบที่มีและไม่มีดีเอ็นเอ เช่นเดียวกับระบบที่อุณหภูมิสูง สูงกว่า melting temperature(T_m) ของดีเอ็นเอคู่สม (รูปที่ 22) ทั้งนี้คาดว่าการเกิด interaction ของฟลูออโรฟอร์และดีเอ็นเอมีผลส่วนใหญ่มาจาก electrostatic forces โดยไม่น่าจะเกี่ยวข้องกับ hydrophobic part ของฟลูออโรฟอร์มากนัก

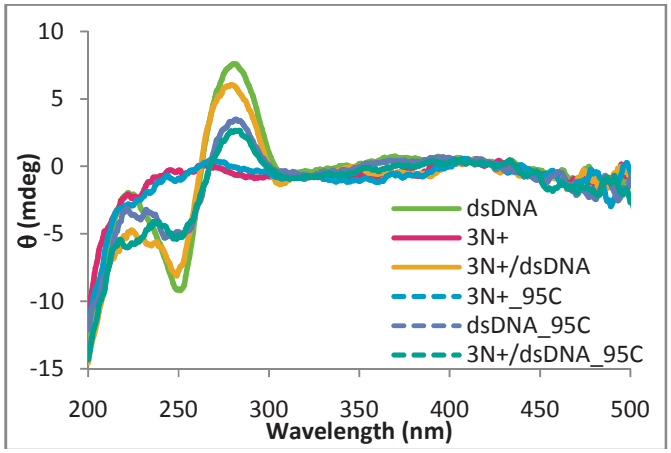

รูปที่ 22 กราฟ CD ของ $3N^+$ (1 μM) ที่มี dsDNA (5′GCATATGCCTA3′ + 5′TAGGCA TATGC3′) ณ อุณหภูมิ 20 และ 90°C

เนื่องจากภายหลังพบว่าลำดับเบสบนสายดีเอ็นเอที่เราเลือกใช้นั้น สามารถเกิดจับกันได้โดยลำพัง (self-hybridization) บนสายของมันเอง เราจึงเปลี่ยนมาใช้สายดีเอ็นเอที่มีลำดับเบสเป็นเบสเพียงชนิดเดียวกัน 4 แบบ คือ A, C, G, T ซึ่งมีเพียง 15 เบส โดยผลการทดลองแสดงให้เห็นว่ามีเพียงดีเอ็นเอสายคู่ (duplex) เท่านั้นที่ให้การขยายสัญญาณเท่ากัน ในขณะที่ดีเอ็นเอสายเดี่ยวหรือที่ไม่เข้าคู่กัน (non-complementary dsDNA) จะตอบสนองต่อฟลูออโรฟอร์ได้ไม่เหมือนกันคือมีทั้งระงับสัญญาณ ขยายสัญญาณมากน้อยขึ้นอยู่กับชนิดของเบสบนสายดีเอ็นเอ ดังรูปที่ 23 อย่างไรก็ดี ผลการทดลองนี้ชี้ให้เห็นว่าเราไม่สามารถนำฟลูออโรฟอร์ดังกล่าวมาใช้ตรวจวัดลำดับเบสของดีเอ็นเอได้โดยตรงเนื่องจากมีดีเอ็นเอสายเดี่ยวบางตัวสามารถขยายสัญญาณขึ้นไปสูงกว่าดีเอ็นเอสายคู่ที่มีเบสคู่สม

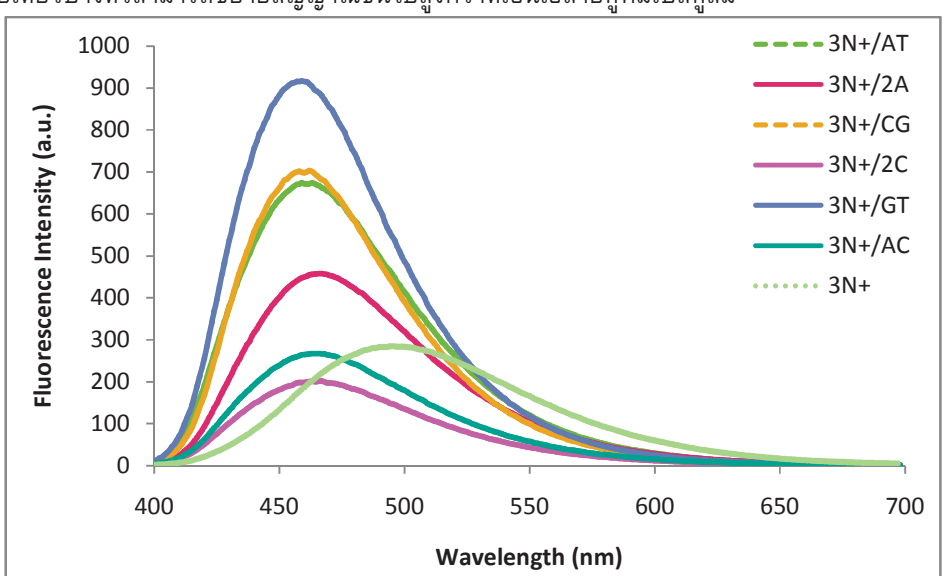

รูปที่ 23 กราฟฟลูออเรสเซนต์ของ $3N^+$ (5 μM) ที่มี ssDNA (2A และ 2C, 5 μM), dsDNA (AT และ CG, 5 μM) และ ncDNA (AC and GT, 5 μM) ในสารละลายบัฟเฟอร์ (A = 5′AAAAAAAAAAAAAAA3′, C = 5′CCCCCCCCCCCCCCC3′, T = 5′TTTTTTTTTTTTTTT3′ and G = 5′GGGGGGGGGGGGGGG3′)

จากการสังเกตข้างต้นทำให้เราทราบปัจจัยที่มีผลต่อการตอบสนองด้วยสัญญาณฟลูออเรสเซนต์ของฟลูออโรฟอร์ ได้แก่ ความยาว ชนิดของลำดับเบส ความเข้มข้น และโครงสร้างของดีเอ็นเอ ที่ใช้ในสภาวะที่ใช้ในการศึกษา

4.ผลงานวิจัยที่ตีพิมพ์ในวารสารวิชาการระดับนานาชาติ

1. ชื่อเรื่อง: FRET detection of DNA sequence via electrostatic interaction of polycationicphenyleneethynylenedendrimer with DNA/PNA hybrid
   ชื่อวารสารที่ส่งไปตีพิมพ์: Talanta
   เวลาที่ยื่นเพื่อตีพิมพ์:23 October2011
   สถานะของบทความ: published 15 January 2012
2. ชื่อเรื่อง: Phenylene-ethynylenetrication as an efficient fluorescent signal transducer in an aptasensor for potassium ion
   ชื่อวารสารที่ส่งไปตีพิมพ์: Biosensors and Bioelectronics
   เวลาที่ยื่นเพื่อตีพิมพ์:21 October2011
   สถานะของบทความ: published 15 March 2012

ภาคผนวก1
(ข้อเสนอโครงการย่อย 2)

Proposal for Subproject No. 2: Dencritic Fluorophores for Detection of DNA/PNA Hybridization

Fluorescence-based methodologies have attracted much interest due to their intrinsic sensitivity and selectivity. Water-soluble conjugated polymers exhibiting fluorescence quenching or enhancement in the presence of oppositely charged acceptors are of particular interest as the optical platforms of chemical and biological sensors.[1-8] Recently, fluorescent biosensors based on water-soluble cationic conjugated polymers (CCPs) to identify DNA and RNA in aqueous media.[9-13] DNA or RNA were labeled with fluorophore at the terminus and the distance controlled by the electrostatic interactions between the negatively charged phosphate groups of the DNA or RNA and the CCPs transduce the FRET signal. The enhancement of the FRET to fluorophore-tagged double-stranded DNA by increasing the cationic charge densities on the side-chain of CCPs has been reported.[14-15]Nonionic surfactant was also utilized for sensitivity enhancement of FRET and quenching in DNA sequence detection using CCPs.[16]Methods for strand-specific DNA detection with CCPs based on fluorophore-tagged peptide nucleic acid (PNA) have also been developed for DNA chips and microarray. [17] CCPs have been reported to be used for one-step fluorescent allele-specific PCR for single nucleotide polymorphisms genotyping assays. [18]

The CCPs used in the system previously described are all linear polymers .Despite offering the signal amplification due to a large number of fluorophores, the unpredictable secondary and tertiary structures in solution, due to polydipersity and random molecular conformations of linear conjugated polymers, can lead to inconsistent fluorescence quenching or enhancement effects as well as inexplicable behaviors. In comparison with linear polymers, the numbers of fluorophore units in dendrimers can be controlled by a stepwise synthesis. This should reflect in the more predictable fluorescence property and other structure-related behaviors of dendritic molecules. We thus decided to synthesize various cationic dendritic fluorophores (Figure 1) and study their fluorescent sensing for detection of PNA/DNA hybridization in comparision with DNA/DNA hybridization. The dendritic system also allows the ability to fine tune the positive charge on the molecular surface that may affect its selective binding to the PNA/DNA hybrids.

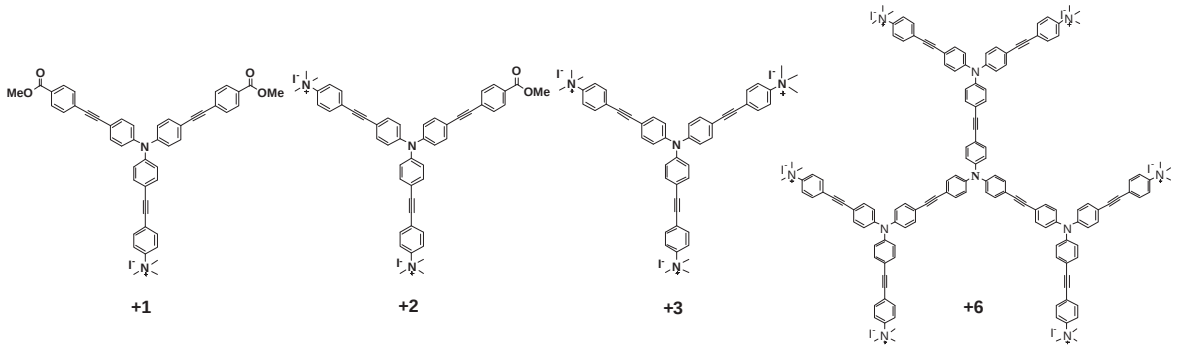

Figure 1. Molecular structuresof examples of cationic dendritic fluorophores with **+1**, +**2, +3,** and **+6** charges.

References

1. McQuade, D. T.; Pullen, A. E.; Swager,T. M. "Conjugated Polymer-Based Chemical Sensors" *Chem. Rev.***2000**, *100*, 2537-2574.
2. Bunz, U. H. F. "Poly(aryleneethynylene)s: Syntheses, Properties, Structures, and Applications" *Chem. Rev.***2000**, *100*, 1605-1644.
3. Fan, C.; Plaxco, K.W.; Heeger, A. J. "High-Efficiency Fluorescence Quenching of Conjugated Polymers by Proteins" *J. Am. Chem. Soc.***2002**, *124*(20), 5642-5643.
4. Nilsson, K. P.; Inganäs, R. O. "Chip and solution detection of DNA hybridization using a luminescent zwitterionic polythiophene derivative" *Nat. Mater.***2003**, *2*, 419-424.
5. Liu,B.; Bazan, G. C. "Homogeneous Fluorescence-Based DNA Detection with Water-Soluble Conjugated Polymers" *Chem. Mater.***2004**, *16*(23), 4467-4476.
6. Pinto, M. R.; Schanze, K. S. "Amplified fluorescence sensing of protease activity with conjugated polyelectrolytes" *Proc. Natl. Acad. Soc. USA***2004**, *101*, 7505-7510.
7. Kumaraswamy, S.; Bergstedt, T.; Shi, X.; Rininsland, F.; Kushon, S.; Xia, W.; Ley, K.; Achyuthan, K.; McBranch, D.; Whitten, D. "Fluorescent-conjugated polymer superquenching facilitates highly sensitive detection of proteases" *Proc. Natl. Acad. Soc. USA***2004**, *101*, 7511-7515
8. Wosnick, J. H.; Mello, C. M.; Swager, T. M. "Synthesis and Application of Poly(phenylene Ethynylene)s for Bioconjugation: A Conjugated Polymer-Based Fluorogenic Probe for Proteases" *J. Am. Chem. Soc.***2005**, *127*(10), 3400-3405.
9. Ho, H. A.; Be´ra-Abérem, M.; Leclerc, M. "Optical sensors based on hybrid DNA/conjugated polymer complexes" *Chem. Eur. J.***2005**, *11*, 1718-1724.

10. Gaylord, B. S.; Heeger, A. J.; Bazan, G. C. “DNA detection using water-soluble conjugated polymers and peptide nucleic acid probes” *Proc. Natl. Acad. Sci. USA***2002**, *99*, 10954-10957.
11. Gaylord, B. S.; Heeger, A. J.; Bazan, G. C. “DNA Hybridization Detection with Water-Soluble Conjugated Polymers and Chromophore-Labeled Single-Stranded DNA” *J. Am. Chem. Soc.***2003**, *125(4)*, 896-900.
12. Wang, S.; Bazan, G. C. “Optically amplified RNA-protein detection methods using light-harvesting conjugated polymers” *Adv. Mater.* **2003**, *15*,1425-1428.
13. He, F.; Tang, Y.; Wang, S.; Li, Y.; Zhu, D. “Fluorescent Amplifying Recognition for DNA G-Quadruplex Folding with a Cationic Conjugated Polymer: A Platform for Homogeneous Potassium Detection” *J. Am. Chem. Soc.* **2005**, *127* (35), 12343-12346.
14. Stork, M.; Gaylord, B.S.; Heeger, A. J.; Bazan, G. C. “Energy transfer in mixtures of water-soluble oligomers: Effect of charge, aggregation, and surfactant complexation” *Adv. Mater.***2002**, *14*, 361–366.
15. Yu, M.; Tang, Y.; He, F.; Wang, S.; Zheng, D.; Li, Y.; Zhu, D. “Synthesis of Water-Soluble Dendritic Conjugated Polymers for Fluorescent DNA Assays”*Macromol. Rapid Commun.***2006**, *27*, 1739–1745.
16. Al Attar, H. A.; Monkman, A. P. “Effect of Surfactant on FRET and Quenching in DNA Sequence Detection Using Conjugated Polymers” *Adv. Funct. Mater.***2008**, *18*, 2498–2509.
17. Liu, B.; Bazan, G. C. “Methods for strand-specific DNA detection with cationic conjugated polymers suitable for incorporation into DNA chips and microarrays” *Proc. Natl. Acad. Soc. USA***2005**, 102, 589–593.
18. Duan, X.; Liu, L.; Wang, S. “Homogeneous and one-step fluorescent allele-specific PCR for SNP genotyping assays using conjugated polyelectrolytes”*Biosens. Bioelectron.***2009***, 24, 2095–2099*.

Methodology

- Synthesis of water soluble dendritic polycationicfluorophores (DPFs)
- Characterization of the synthesized DPFs: NMR, IR, MS, EA
- Optical property study of synthesized DPFs: Absorption, Extinction Coefficient, Emission, Quantum Yield, Surfactant Effects
- Study of DNA/DNA hybrid detection
- Study of PNA/DNA hybrid detection

สัญญาเลขที่ RTA5280002

โครงการหลัก: การสังเคราะห์ สมบัติ และการประยุกต์ใช้เบต้าพิโรลิดินิลเพปไทด์นิวคลีอิกแอซิด ที่มีคอนฟอร์เมชันถูกจำกัด

รายงานฉบับสมบูรณ์

ชื่อโครงการย่อย Development of positively charged polymeric support for high throughput DNA sequence analysis using PNA probes

ระยะเวลาโครงการ 1 สิงหาคม 2552 – 31 กรกฎาคม 2555

ชื่อหัวหน้าโครงการย่อย รศ.ดร.วรวีร์ โฮเว่น

บทนำ

การตรวจสอบลำดับเบสของสารพันธุกรรม (ดีเอ็นเอและอาร์เอ็นเอ) มีบทบาทสำคัญต่อการพัฒนาเทคโนโลยีชีวภาพหลายแขนง เช่น ทางการแพทย์ใช้ในการตรวจคัดกรองความเสี่ยงต่อการเกิดโรคทางพันธุกรรม การบ่งชี้ชนิดและสายพันธุ์ของจุลชีพที่ก่อให้เกิดโรค ทางนิติวิทยาศาสตร์ใช้เป็นข้อมูลในการบ่งชี้บุคคลเพื่อเป็นหลักฐานประกอบการสืบสวนสอบสวนคดีต่างๆ ทางด้านอาหารและเกษตรกรรมใช้ในการตรวจสอบส่วนประกอบต้องห้ามในอาหาร สารก่อภูมิแพ้หรือการปนเปื้อนของสารปรับแต่งทางพันธุกรรม เป็นต้น เทคนิคที่ใช้ในการตรวจสอบสารพันธุกรรมถ้าไม่ใช่เป็นการหาลำดับเบสโดยตรง ก็มักจะเป็นการใช้เอนไซม์ตัดจำเพาะ หรือการใช้โพรบที่เหมาะสมในการจับยึดกับสารพันธุกรรม วิธีการทดสอบมาตรฐานที่ใช้ในปัจจุบันจะใช้เวลาในการวิเคราะห์นาน มีค่าใช้จ่ายสูงอันเนื่องมาจากเครื่องมือวิเคราะห์ที่มีราคาแพงและวัสดุสิ้นเปลืองที่ต้องนำเข้าจากต่างประเทศ เช่น เอนไซม์ สารเรืองแสง ทำให้ไม่สามารถนำไปใช้งานได้อย่างกว้างขวาง โดยเฉพาะอย่างยิ่งในพื้นที่ห่างไกลความเจริญหรือมีงบประมาณจำกัด ด้วยเหตุนี้คณะผู้วิจัยจึงมีแนวคิดที่จะพัฒนาเทคนิคการวิเคราะห์ที่นอกจากจะสามารถทำได้สะดวก รวดเร็ว ราคาไม่แพง มีความจำเพาะเจาะจงและความแม่นยำสูงแล้ว ยังสามารถดัดแปลงให้ทำการตรวจวิเคราะห์ในรูปแบบที่มีประสิทธิภาพสูง (high-throughput format) กล่าวคือสามารถตรวจสอบสารตัวอย่างหลายชนิดในเวลาเดียวกันได้อีกด้วย

<u>ตอนที่ 1</u> การตรวจลำดับเบสของดีเอ็นเอโดยใช้เพปไทด์นิวคลีอิกแอซิดร่วมกับอนุภาคไคโทซานด้วยมัลดิ-ทอฟแมสสเปกโทรเมทรี

จากความสำเร็จของ รศ.ดร.ธีรยุทธ วิไลวัลย์ และคณะในการตรวจลำดับเบสของดีเอ็นเอโดยอาศัยตัวแลกเปลี่ยนแอนไอออนทางการค้าคือ Q-sepharose ร่วมกับพิโรลิดินิลเพปไทด์นิวคลีอิกแอซิด (pyrrolidinyl peptide nucleic acid) หรือ acpcPNA และทำการวิเคราะห์ด้วยเทคนิคมัลดิ-ทอฟแมสสเปกโทรเมทรี (MALDI-TOF mass spectrometry) เป็นที่มาของงานวิจัยตอนที่ 1 ของโครงการวิจัยย่อยนี้ เนื่องจากทางคณะผู้วิจัยมีประสบการณ์ในการเตรียมอนุภาคขนาดเล็กที่มีประจุบวกของไคโทซาน ที่สามารถปรับเปลี่ยนหมู่ฟังก์ชันรวมทั้งความเป็นประจุของอนุภาคได้ จึงเล็งเห็นถึงศักยภาพในการใช้อนุภาคดังกล่าวเป็นตัวแลกเปลี่ยนแอนไอออนแทนการใช้ Q-sepharose ที่เป็นสารทางการค้าซึ่งอยู่ในรูปของอนุภาคที่แขวนลอยในน้ำ ซึ่งเสียสภาพได้หากทำให้แห้งจึงไม่ทราบน้ำหนักของตัวแลกเปลี่ยนไอออนที่แน่นอนเมื่อนำมาใช้งานในแต่ละครั้ง นอกจากนี้ความสามารถในการปรับเปลี่ยนหมู่ฟังก์ชันของไคโทซานยังอาจจะทำให้สามารถเพิ่มประสิทธิภาพในการตรวจวิเคราะห์ดีเอ็นเอซึ่งไม่สามารถทำได้ในกรณีของ Q-sepharose และหากสามารถนำอนุภาคไคโทซานมาใช้ประโยชน์ในการตรวจวิเคราะห์ลำดับเบสของสารพันธุกรรมได้ ก็นับว่าเป็นการเพิ่มมูลค่าให้กับไคโทซาน ซึ่งเป็นพอลิเมอร์ธรรมชาติที่ได้

จากการกำจัดหมู่แอซิทิลของไคทิน ที่เป็นสารสกัดได้จากเปลือกกุ้ง กระดองปู แกนหมึก รวมทั้งเห็ด และราบางชนิด งานวิจัยในส่วนนี้ได้รับการสนับสนุนงบประมาณในการทำวิจัยเบื้องต้น จากทุนสนับสนุนกลุ่มวิจัย สกว ที่มี ศ.ดร.สุดา เกียรติกำจรวงศ์ เป็นหัวหน้าโครงการ (RTA5080004) ภายใต้หัวข้อโครงการเรื่อง “การประยุกต์ทางชีวการแพทย์ของอนุภาคไคโทซานที่พื้นผิวมีประจุ”

อาศัยหลักการที่ว่าพีเอ็นเอเป็นโมเลกุลที่เป็นกลางทางประจุ ดังนั้นเมื่อมีการจับยึดกับดีเอ็นเอซึ่งมีประจุลบที่มีลำดับเบสคู่สมกัน จะทำให้เกิดโมเลกุลลูกผสมระหว่างพีเอ็นเอ-ดีเอ็นเอซึ่งมีประจุเป็นลบ และสามารถถูกจับยึดโดยตัวแลกเปลี่ยนแอนไอออนซึ่งมีประจุเป็นบวกได้ หากทำการแยกตัวแลกเปลี่ยนแอนไอออนซึ่งเป็นของแข็งออกจากสารละลาย และนำไปตรวจวิเคราะห์ด้วยมัลดิ-ทอฟแมสสเปกโทรเมทรี จะพบเพียงสัญญาณของพีเอ็นเอโดยไม่พบสัญญาณของดีเอ็นเอ ทั้งนี้เป็นผลเนื่องมาจากพีเอ็นเอถูกไอออไนซ์ได้อย่างมีประสิทธิภาพกว่าดีเอ็นเอภายใต้การวิเคราะห์ด้วย positive ion mode โดยหลักการแล้วการวิเคราะห์ดังกล่าวสามารถทำได้โดยไม่จำเป็นต้องคำนึงถึงการมีอยู่ของพีเอ็นเอที่ไม่จับยึดกับดีเอ็นเอ (unhybridized PNA) ซึ่งยังคงอยู่ในสารละลาย หรือดีเอ็นเอที่มีลำดับเบสที่ไม่เป็นคู่สมกับพีเอ็นเอ (noncomplementary DNA) เป็นการลดขั้นตอนและความยุ่งยากในการวิเคราะห์ วิธีการตรวจสอบลำดับเบสของดีเอ็นเอแสดงรายละเอียดพอสังเขปใน**รูปที่ 1.1**

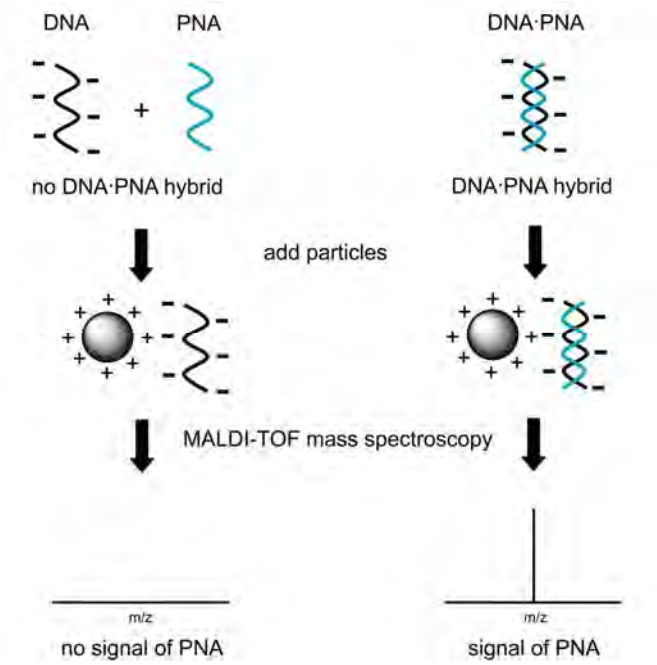

รูปที่ 1.1 แผนภาพแสดงแนวทางการวิเคราะห์ลำดับเบสของดีเอ็นเอโดยใช้อนุภาคไคโทซานเป็นตัวแลกเปลี่ยนแอนไอออนร่วมกับการใช้พีเอ็นเอโพรบและเทคนิคมัลดิ-ทอฟแมสสเปกโทรเมทรี

อนุภาคที่นำมาใช้เป็นตัวแลกเปลี่ยนแอนไอออนในงานวิจัยนี้มีทั้งหมด 5 ชนิด ซึ่งมีหมู่ฟังก์ชันแตกต่างกันดังแสดงรายละเอียดใน**ตารางที่ 1.1** อนุภาคไคโทซาน (CS) เตรียมได้จากการตกตะกอนสารละลายไคโทซานด้วยไทรพอลิฟอสเฟต (TPP) ส่วนอนุภาค MC เตรียมได้จากการทำปฏิกิริยาเมทิลเลชันอนุภาค CS ด้วยเมทิลไอโอไดด์แบบต่างวัฏภาค ในขณะที่อนุภาค MBzC เตรียมจากการทำปฏิกิริยารีดักทีฟแอลคิลเลชันด้วยเบนซาลดีไฮด์ตามด้วยเมทิลเลชันด้วยเมทิลไอโอไดด์แบบต่างวัฏภาคของอนุภาค CS สำหรับอนุภาค TMC และ HTACC เตรียมได้จากการตกตะกอนสารละลาย *N,N,N*-trimethylchitosan chloride และ *N*-[(2-hydroxyl-3-trimethylammonium)propyl]chitosan chloride ซึ่งเป็นอนุพันธ์ไคโทซานที่มีประจุบวกอยู่แล้วด้วย TPP ตามลำดับ ดังนั้นอนุภาค TMC และ HTACC จึงมีประจุบวกทั้งภายในและที่ผิวของอนุภาค ในขณะที่อนุภาค QAC

และ MBzC จะมีประจุบวกเฉพาะที่ผิวอนุภาคเท่านั้น ทั้งนี้สามารถวิเคราะห์ความเป็นประจุบวกของอนุภาคได้โดยใช้เทคนิค photon correlation spectroscopy (PCS) และจากการวิเคราะห์ด้วยเทคนิค transmission electron microscopy (TEM) พบว่าอนุภาคมีลักษณะเป็นทรงกลม มีขนาดอยู่ในช่วง ~0.13-0.40 ไมโครเมตร

ตารางที่ 1.1 ζ-potential (วิเคราะห์ด้วยเทคนิค PCS) และขนาดโดยเฉลี่ย (mean size) (วิเคราะห์ด้วยเทคนิค TEM) ของอนุภาคไคโทซานที่ใช้เป็นตัวแลกเปลี่ยนแอนไอออนในการทดลอง

Particles		ζ-potential (mV)	Mean size (μm)
CS	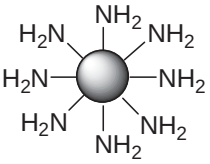	32.17±1.71	0.40±0.12
MC	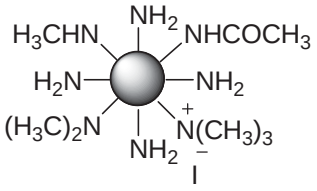	30.57±1.99	0.20±0.05
TMC	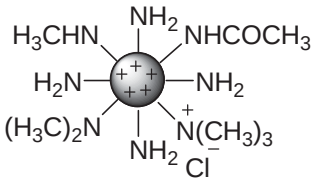	39.77±0.21	0.13±0.09
MBzC	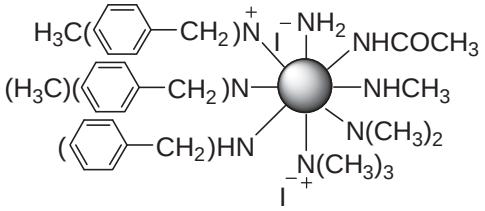	54.93±1.04	0.16±0.05
HTACC	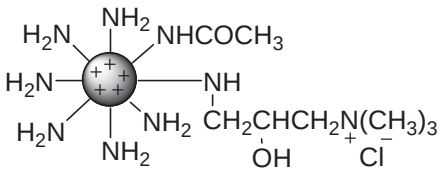	24.27±0.74	0.13±0.04

สำหรับดีเอ็นเอที่นำมาทำการตรวจวิเคราะห์มีลำดับเบสที่สัมพันธ์กับตำแหน่งที่แสดงความผิดปกติของยีนในผู้ป่วยโรคมะเร็ง (K-*ras* DNA) ดีเอ็นเอดังกล่าวมีความยาว 14 เมอร์ และมีเบสทุกชนิดเป็นองค์ประกอบ (A, T, C, G) โดยดีเอ็นเอที่เลือกใช้มีทั้งที่เป็น mutant (DNA mut) และ wild-type (DNA wt) ดีเอ็นเอและพีเอ็นเอโพรบที่ใช้ในการวิเคราะห์แสดงลำดับเบสใน**ตารางที่ 1.2**

ตารางที่ 1.2 ลำดับเบสของดีเอ็นเอและพีเอ็นเอที่ใช้ในการทดลอง

Code	Sequence	Note	*m/z*
PNA(mut)	Ac-Lys-O-CTACGCCAACAGCT-SerNH$_2$	-	5071.9
PNA(wt)	Ac-Lys-CTACGCCACCAGCT-SerNH$_2$		4902.8
DNA(mut)	d(5'-AGCTGTTGGCGTAG-3')	complementary to PNA(mut) single mismatch to PNA(wt)	-
DNA(wt)	d(5'-AGCTGGTGGCGTAG-3')	complementary to PNA(wt) single mismatch to PNA(mut)	-
DNA$_{3f}$ (J1)	d(5'-TAGTTGTACGTACA-3′)	full mismatch to both PNA(mut) and PNA(wt)	-

O = aminoethoxyethoxyacetyl linker

ผลการทดสอบการใช้อนุภาคไคโทซานทั้ง 5 ชนิด ได้แก่ CS, MC, TMC, MBzC และ HTACC เป็นตัวแลกเปลี่ยนแอนไอออนในการจับกับโมเลกุลลูกผสมระหว่างพีเอ็นเอและดีเอ็นเอและวิเคราะห์ด้วยมัลดิ-ทอฟแมสสเปกโทรเมทรีแสดงใน**รูปที่ 1.2** โดยผลการทดลองแบ่งออกเป็น 4 แถว หากพิจารณาจากบนลงล่าง แถวที่หนึ่งแสดงแมสสเปกตรัมของอนุภาคชนิดต่างๆหลังการสัมผัสกับ PNA (mut) ซึ่งจะเห็นว่าอนุภาค CS และ MBzC เท่านั้นที่แสดงสัญญาณของ PNA (mut) ปรากฏที่ตำแหน่งประมาณ m/z ~ 5,000 แสดงให้เห็นว่าอนุภาคทั้งสองเกิดแรงกระทำอย่างไม่จำเพาะเจาะจงกับ PNA (mut) ทั้งนี้คาดว่าเป็นผลเนื่องมาจากการที่ MBzC เป็นอนุภาคที่มีความชอบน้ำต่ำกว่าอนุภาคอื่นอีก 3 ชนิด เนื่องจากมีวงอะโรมาติกเป็นองค์ประกอบ จึงสามารถเกิด hydrophobic interaction กับ PNA (mut) ได้ง่าย ในขณะที่ CS ซึ่งมีลักษณะเป็นกลางทางประจุ เนื่องจากการทดลองทำในสารละลายบัฟเฟอร์ pH 7 (สูงกว่า pKa = 6.4 ของไคโทซาน) ดังนั้นจึงสามารถเกิดแรงกระทำกับ PNA (mut) ได้ทั้งผ่าน hydrophobic interaction และพันธะไฮโดรเจน

แถวที่สองแสดงแมสสเปกตรัมของอนุภาคชนิดต่างๆหลังการสัมผัสกับโมเลกุลลูกผสมระหว่าง PNA (mut) และ DNA (mut) ซึ่งมีลำดับเบสคู่สมกัน (complementary) จากการที่สามารถสังเกตเห็นสัญญาณของ PNA (mut) ในกรณีของอนุภาค MC, TMC และ HTACC แสดงให้เห็นว่าเกิดการดูดซับด้วยแรงระหว่างประจุบวกของอนุภาคกับประจุลบของโมเลกุลลูกผสม ส่วนในแถวที่สามเป็นแมสสเปกตรัมของอนุภาคชนิดต่างๆหลังการสัมผัสกับโมเลกุลลูกผสมระหว่าง PNA (mut) และ DNA (wt) ซึ่งมีลำดับเบสผิดไป 1 ตำแหน่ง (single mismatch) จากผลการทดลองพบว่ามีเพียงอนุภาค HTACC เท่านั้นที่ไม่ดูดซับโมเลกุลลูกผสมดังกล่าว ทั้งนี้สามารถอธิบายได้จากการที่อนุภาค HTACC มีความเป็นประจุสูงและมีความชอบน้ำสูง จึงไม่เกิดแรงกระทำอย่างไม่จำเพาะเจาะจงในขณะที่อนุภาคชนิดอื่นซึ่งมีความชอบน้ำไม่มากพอคือ MC, TMC และ MBzC จึงเกิดการดูดซับผ่านแรงกระทำอย่างไม่จำเพาะเจาะจงกับโมเลกุลลูกผสมดังกล่าวได้ ผลในแถวที่สี่ซึ่งเป็นแถวล่างสุดแสดงแมสสเปกตรัมของอนุภาคชนิดต่างๆหลังการสัมผัสกับโมเลกุลลูกผสมระหว่าง PNA (mut) และ DNA$_{3f}$ (J1) ซึ่งมีลำดับเบสไม่เข้าคู่กันทุกตำแหน่ง (full mismatch) โดยพบว่ามีเพียงอนุภาค CS เท่านั้นที่แสดงสัญญาณของ PNA (mut) จากผลการทดลองในส่วนนี้แสดงให้เห็นว่าอนุภาค HTACC เป็นตัวแลกเปลี่ยนแอนไอออนที่มีประสิทธภาพสูงที่สุดเนื่องจากสามารถบอกความแตกต่างระหว่างดีเอ็นเอที่มีลำดับเบสที่ผิดไปเพียงตำแหน่งเดียวได้ ส่วนอนุภาค MC และ TMC มีประสิทธิภาพรองลงมาเนื่องจากสามารถบอกความแตกต่างได้เฉพาะดีเอ็นเอที่มีลำดับเบสผิดไปทุกตำแหน่งเท่านั้น ในขณะที่อนุภาค MBzC ซึ่งถึงแม้จะบอกความแตกต่างในลักษณะเดียวกันได้ แต่ก็เกิดแรงกระทำอย่างไม่จำเพาะเจาะจงกับพีเอ็นเอเองด้วย ส่วนอนุภาค CS นั้นไม่เหมาะสมที่จะนำมาใช้ในการวิเคราะห์เนื่องจากไม่

สามารถบอกความแตกต่างระหว่างดีเอ็นเอที่มีลำดับเบสผิดไปทุกตำแหน่งและยังเกิดแรงกระทำอย่างไม่จำเพาะเจาะจงกับพีเอ็นเออีกด้วย

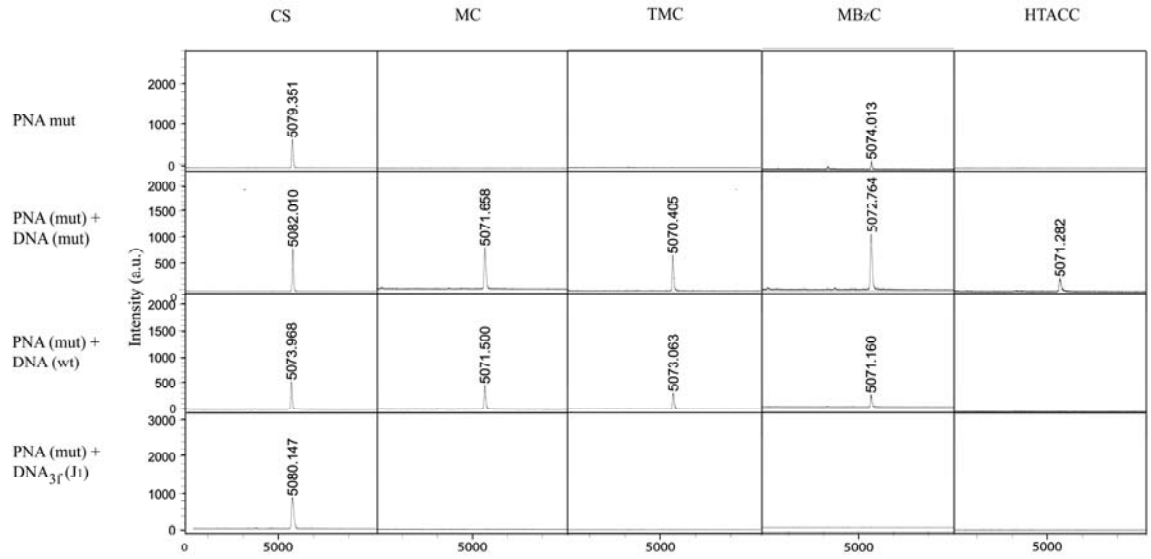

รูปที่ 1.2 MALDI-TOF แมสสเปกตรัมของอนุภาคไคโทซานชนิดต่าง ๆหลังจากที่นำไปจับยึดกับโมเลกุลลูกผสมระหว่างพีเอ็นเอและดีเอ็นเอ ที่อยู่ในสารละลาย 10 mM sodium phosphate buffer pH 7 ปริมาตร 30 µL (PNA 10 pmol, DNA 10 pmol) โดยใช้ PNA(mut) เป็นโพรบ

คณะผู้วิจัยได้ทำการทดสอบในลักษณะคล้ายคลึงกันกับอนุภาคไคโทซานทั้ง 5 ชนิดโดยเปลี่ยนพีเอ็นเอโพรบเป็น PNA (wt) ซึ่งมีลำดับเบสคู่สมกับ DNA (wt) และมีลำดับเบสผิดไปหนึ่งตำแหน่งและทุกตำแหน่งเมื่อเปรียบเทียบกับ DNA (mut) และ DNA_{3f} (J1) ตามลำดับ จากผลการทดลองที่แสดงใน**รูปที่ 1.3** มีแนวโน้มที่คล้ายคลึงกับที่แสดงใน**รูปที่ 1.2** เมื่อใช้ PNA (mut) เป็นโพรบ กล่าวคืออนุภาค HTACC มีประสิทธิภาพสูงสุด รองลงมาคืออนุภาค MC และ TMC ในขณะที่ทั้งอนุภาค CS และ MBzC ไม่เหมาะสมที่จะนำมาใช้ในการวิเคราะห์เนื่องจากไม่สามารถบอกความแตกต่างระหว่างดีเอ็นเอที่มีลำดับเบสผิดไปทุกตำแหน่งและยังเกิดแรงกระทำอย่างไม่จำเพาะเจาะจงกับ PNA (wt) อีกด้วย

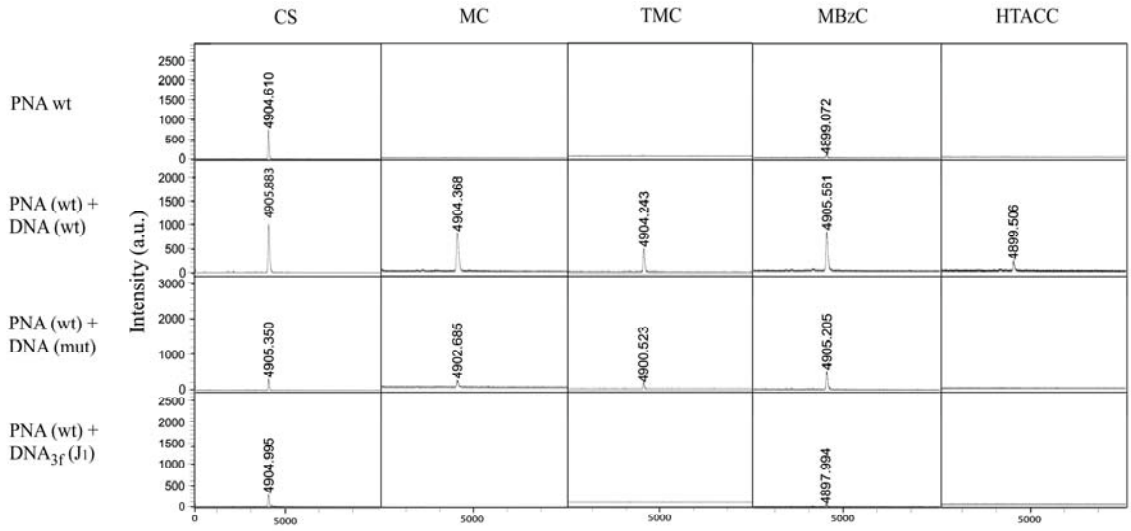

รูปที่ 1.3 MALDI-TOF แมสสเปกตรัมของอนุภาคไคโทซานชนิดต่างๆหลังจากที่นำไปจับยึดกับโมเลกุลลูกผสมระหว่างพีเอ็นเอและดีเอ็นเอ ที่อยู่ในสารละลาย 10 mM sodium phosphate buffer pH 7 ปริมาตร 30 µL (PNA 10 pmol, DNA 10 pmol) โดยใช้ PNA (wt) เป็นโพรบ

ถึงแม้ว่าอนุภาค HTACC มีสมบัติเหมาะสมในการทำหน้าที่เป็นตัวแลกเปลี่ยนแอนไอออนเนื่องจากสามารถบอกความแตกต่างระหว่างดีเอ็นเอที่มีลำดับเบสที่ผิดไปเพียงตำแหน่งเดียวได้และไม่เกิดแรงกระทำอย่างไม่จำเพาะเจาะจงกับพีเอ็นเอที่ใช้เป็นโพรบ แต่ก็มีข้อด้อยในเรื่องของสัญญาณที่ต่ำมากในกรณีที่จับยึดกับโมเลกุลลูกผสมระหว่างพีเอ็นเอและดีเอ็นเอที่มีลำดับเบสคู่สมกัน ทั้งนี้เป็นผลเนื่องมาจากสมบัติความชอบน้ำสูงมากของอนุภาค ซึ่งอาจส่งผลให้ HTACC บางส่วนที่ไม่เกิดการเชื่อมขวางละลายออกจากอนุภาคไปจับกับโมเลกุลลูกผสมในสารละลาย แทนที่จะยึดโมเลกุลลูกผสมไว้บนอนุภาคที่เป็นของแข็ง ด้วยเหตุนี้คณะผู้วิจัยจึงมีแนวคิดที่จะศึกษาความเป็นไปได้ในการเพิ่มประสิทธิภาพของอนุภาค MC และ TMC ซึ่งให้สัญญาณการจับกับโมเลกุลลูกผสมระหว่างพีเอ็นเอและดีเอ็นเอที่มีลำดับเบสคู่สมกันที่สูงกว่าอนุภาค HTACC โดยการล้างโมเลกุลของพีเอ็นเอโพรบที่ดูดซับอย่างไม่จำเพาะเจาะจงออกโดยใช้สารละลายที่เหมาะสม

รูปที่ 1.4 แสดงแมสสเปกตรัมของอนุภาค CS, MC, TMC และ MBzC หลังจากสัมผัสกับโมเลกุลลูกผสมระหว่าง PNA (mut) และ DNA (wt) และ PNA (wt) และ DNA (mut) ตามลำดับ และล้างอนุภาคด้วย 20% formamide ใน 10 mM sodium phosphate buffer pH 7 ตามด้วยน้ำ MilliQ 3 รอบ ซึ่งทั้งสองกรณีพีเอ็นเอโพรบมีลำดับเบสที่ผิดไปจากดีเอ็นเอเพียงตำแหน่งเดียว ผลปรากฏว่าสารละลายดังกล่าวสามารถกำจัดแรงกระทำอย่างไม่จำเพาะเจาะจงของโมเลกุลลูกผสมทั้ง 2 กรณีบนอนุภาค MC, TMC และ MBzC ได้ เนื่องจากไม่ปรากฏสัญญาณของพีเอ็นเอโพรบบนอนุภาคทั้ง 3 ชนิดหลังจากการล้าง แต่ไม่สามารถกำจัดแรงกระทำดังกล่าวบนอนุภาค CS ได้ เนื่องจากยังพบสัญญาณของ PNA (mut) ที่ m/z ~ 5,000 ใน**รูปที่ 1.4** (คอลัมน์ซ้าย) และสัญญาณของ PNA (wt) ที่ m/z ~ 4,900 ใน**รูปที่ 1.4** (คอลัมน์ขวา) หลังจากการล้างอนุภาค CS เพื่อเป็นการทดสอบว่าสภาวะในการล้างดังกล่าวสามารถใช้ในการวิเคราะห์โดยไม่มีผลกระทบกับโมเลกุลลูกผสมระหว่างพีเอ็นเอและดีเอ็นเอที่มีลำดับเบสคู่สมกัน คณะผู้วิจัยจึงได้ทดลองใช้วิธีการล้างเดียวกันกับอนุภาคชนิดต่างๆหลังจากการจับยึดกับโมเลกุลลูกผสมระหว่าง PNA (mut) และ DNA (mut) และ PNA (wt) และ DNA (wt) แมสสเปกตรัมของอนุภาคหลังจากการล้างแสดงใน**รูปที่ 1.5** ซึ่งพบว่ายังคงพบสัญญาณของพีเอ็นเอที่มีความเข้มสูงอยู่บนอนุภาค แสดงว่าการล้างดังกล่าวไม่ทำลายแรงยึดเหนี่ยวระหว่างโมเลกุลพีเอ็นเอและดีเอ็นเอที่มีลำดับเบสคู่สมกัน

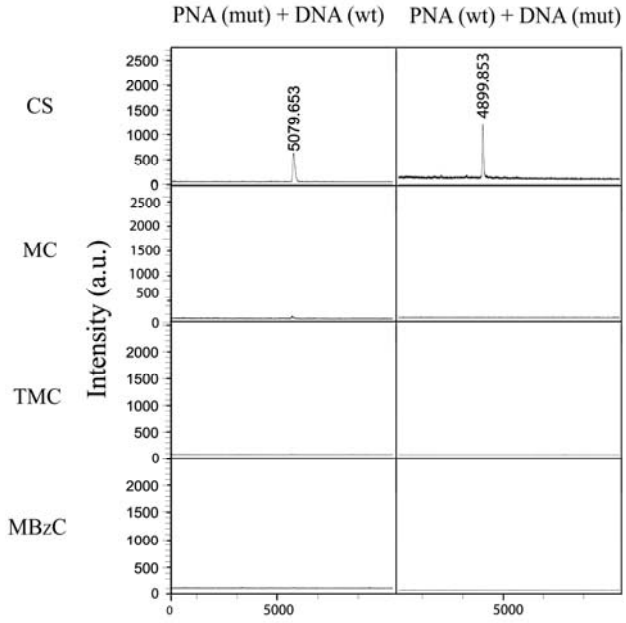

รูปที่ 1.4 MALDI-TOF แมสสเปกตรัมของอนุภาคไคโทซานชนิดต่างๆหลังจากที่นำไปจับยึดกับโมเลกุลลูกผสมระหว่าง PNA (mut) และ DNA (wt) หรือระหว่าง PNA (wt) และ DNA (mut) ที่อยู่ในสารละลาย 10 mM sodium phosphate buffer pH 7 ปริมาตร 30 µL (PNA 10 pmol, DNA 10 pmol) และล้างอนุภาคด้วย 20% formamide ใน 10 mM sodium phosphate buffer pH 7 และ น้ำ MilliQ 3 รอบ

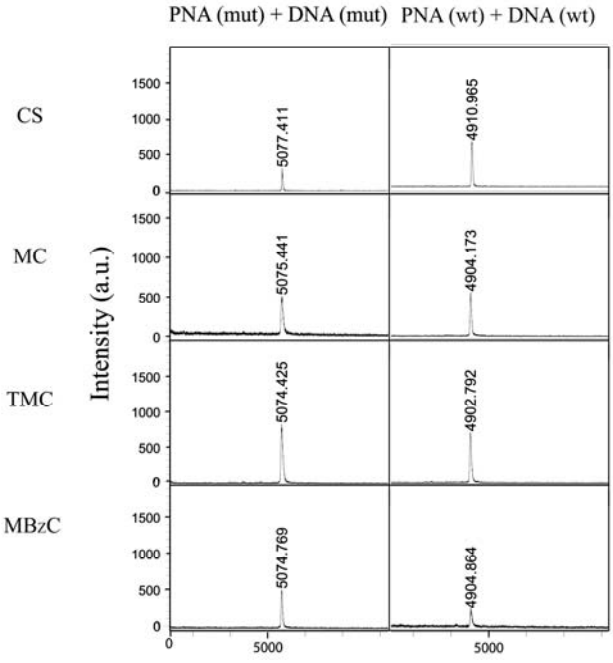

รูปที่ 1.5 MALDI-TOF แมสสเปกตรัมของอนุภาคไคโทซานชนิดต่างๆหลังจากที่นำไปจับยึดกับโมเลกุลลูกผสมระหว่าง PNA (mut) และ DNA (mut) หรือระหว่าง PNA (wt) และ DNA (wt) ที่อยู่ในสารละลาย 10 mM sodium phosphate buffer pH 7 ปริมาตร 30 µL (PNA 10 pmol, DNA 10 pmol) และล้างอนุภาคด้วย 20% formamide ใน 10 mM sodium phosphate buffer pH 7 และ น้ำ MilliQ 3 รอบ

นอกจากนี้คณะผู้วิจัยยังได้ศึกษาการเลือกจับดีเอ็นเอของอนุภาคชนิดต่างๆในกรณีที่มีพีเอ็นเอโพรบ 2 ชนิดผสมกัน ทั้งที่มีลำดับเบสเป็นคู่สมกันและมีลำดับเบสผิดไปหนึ่งตำแหน่ง (**รูปที่ 1.6**) จากผลการทดลองใน**รูปที่ 1.7** แสดงให้เห็นว่าทั้งอนุภาค MC, TMC และ HTACC แสดงความจำเพาะเจาะจงในการเลือกจับเฉพาะกับโมเลกุลลูกผสมระหว่างพีเอ็นเอและดีเอ็นเอที่มีลำดับเบสคู่สมกันเท่านั้น ในกรณีที่ผสม PNA (mut), PNA (wt) และ DNA (mut) จะสังเกตเห็นเฉพาะสัญญาณของ PNA (mut) ที่ m/z ~ 5,000 เท่านั้น โดยไม่ปรากฏสัญญาณของ PNA (wt) ที่ m/z ~ 4,900 บนอนุภาค ส่วนในกรณีที่ผสม PNA (mut), PNA (wt) และ DNA (wt) จะสังเกตเห็นเฉพาะสัญญาณของ PNA (wt) ที่ m/z ~ 4,900 เท่านั้น โดยไม่ปรากฏสัญญาณของ PNA (mut) ที่ m/z ~5,000 ผลการทดลองในส่วนนี้แสดงให้เห็นว่าอนุภาคดังกล่าวมีความจำเพาะเจาะจงในการเลือกจับสูง มีศักยภาพที่จะพัฒนาไปสู่การประยุกต์ในการวิเคราะห์สารตัวอย่างจริงซึ่งมีความซับซ้อนขององค์ประกอบมากขึ้นได้

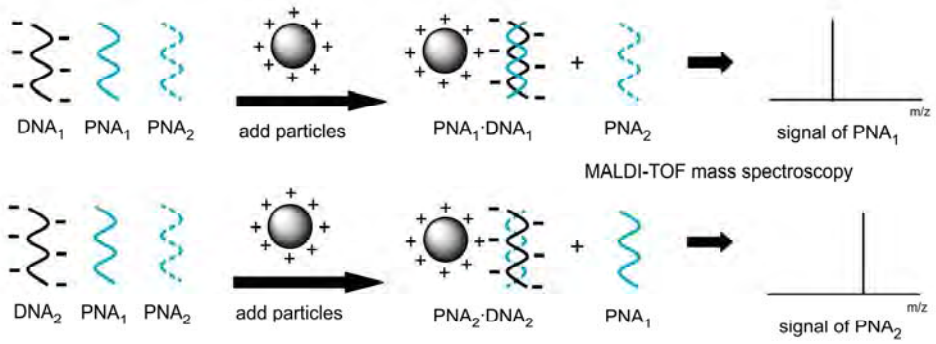

รูปที่ 1.6 แนวทางการตรวจลำดับเบสของดีเอ็นเอโดยใช้อนุภาคไคโทซานเป็นตัวแลกเปลี่ยนแอนไอออนซึ่งจะเลือกจับเฉพาะโมเลกุลลูกผสมระหว่างดีเอ็นเอและพีเอ็นเอที่มีลำดับเบสเป็นคู่สมกัน ในสภาวะที่มีการเติมพีเอ็นเอโพรบ 2 ชนิดผสมกัน และวิเคราะห์เทคนิคมัลดิ-ทอฟแมสสเปกโทรเมทรี

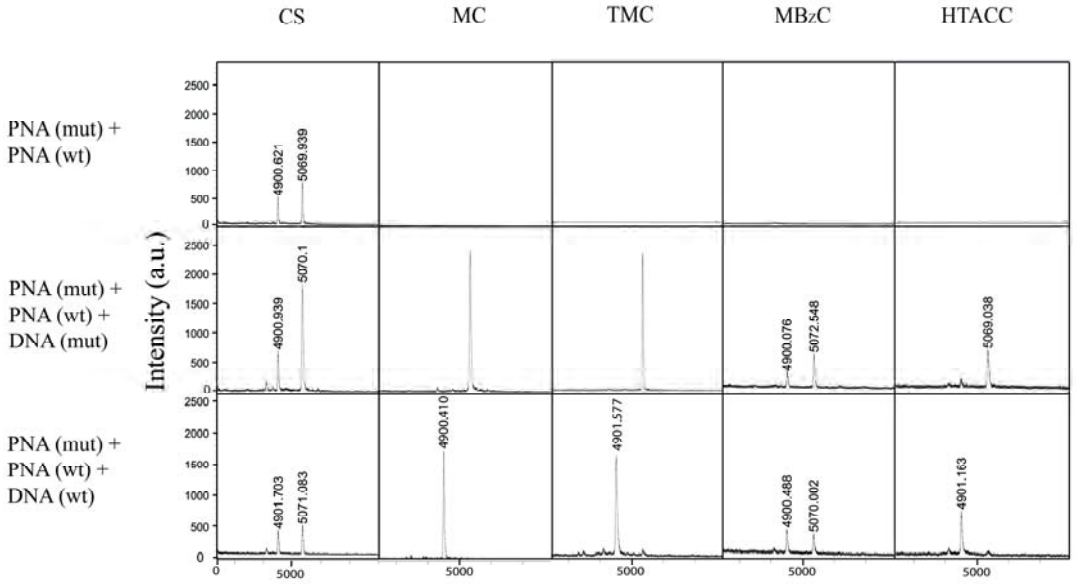

รูปที่ 1.7 MALDI-TOF แมสสเปกตรัมของอนุภาคไคโทซานชนิดต่างๆหลังจากที่นำไปจับยึดกับโมเลกุลลูกผสมที่อยู่ในสารละลายที่มีดีเอ็นเอและพีเอ็นเอโพรบทั้งชนิดที่มีลำดับเบสคู่สมกัน และมีลำดับเบสผิดไป 1 ตำแหน่ง ที่อยู่ในสารละลาย 10 mM sodium phosphate buffer pH 7 ปริมาตร 30 µL (PNA 10 pmol, DNA 10 pmol) และล้างอนุภาคด้วย 20% formamide ใน 10 mM sodium phosphate buffer pH 7 และ น้ำ MilliQ 3 รอบ

ถึงแม้จะสามารถใช้อนุภาคไคโทซานที่มีประจุบวกของหมู่ควอเทอร์นารีแอมโมเนียมในการวิเคราะห์ลำดับเบสของดีเอ็นเอได้ แต่ก็ยังมีข้อจำกัดในแง่ของวิธีการเตรียมที่ยังไม่เอื้ออำนวยต่อการนำไปประยุกต์ใช้ในการวิเคราะห์จริง ทั้งนี้เป็นผลเนื่องมาจากการที่วิธีการเตรียมที่ใช้ในปัจจุบันอาศัยการตกตะกอนอนุภาคด้วยสารเชื่อมขวาง ซึ่งมักจะได้อนุภาคในปริมาณน้อย ดังนั้นเป้าหมายต่อไปของงานวิจัยตอนที่ 1 นี้คือ การพัฒนาวิธีการเตรียมอนุภาคไคโทซานที่ผิวภายนอกมีประจุบวกของหมู่ควอเทอร์นารีแอมโมเนียมที่มีประสิทธิภาพมากขึ้น แนวทางที่ทางคณะผู้วิจัยสนใจคือ การใช้การประกอบตัวเอง (self assembly) ของพอลิเมอร์ที่มีองค์ประกอบทั้งส่วนที่ชอบน้ำ (hydrophilic) และไม่ชอบน้ำ (hydrophobic) หรือที่เรียกว่าแอมฟิฟิลิกพอลิเมอร์ (amphiphilic polymer) อาศัยหลักการที่ว่าพอลิเมอร์จะจัดตัวโดยหันด้านที่ไม่ชอบตัวทำละลายเข้าด้านในและด้านที่ชอบตัวทำละลายไว้ด้านนอก ดังนั้นหากนำไปใส่ในน้ำโมเลกุลของแอมฟิฟิลิกพอลิเมอร์จะเกิดการจัดเรียงตัวเป็นอนุภาคที่มีแกนกลาง (core) เป็นส่วนไม่ชอบน้ำ และมีเปลือกหรือผิวด้านนอก (shell) เป็นส่วนที่ชอบน้ำ ในที่นี้สนใจที่จะให้ผิวด้านนอกเป็นหมู่ควอเทอร์นารีแอมโมเนียมที่มีประจุบวก ซึ่งจะสามารถตอบสนองการใช้งานในการวิเคราะห์ลำดับเบสของดีเอ็นเอได้ จากการสืบค้นข้อมูลพบว่ามีนักวิจัยประสบความสำเร็จในการนำแนวทางดังกล่าวไปใช้ในการเตรียมอนุภาคเพื่อกักเก็บสารสำคัญชนิดต่างๆ เช่น ยา วิตามิน เพื่อประยุกต์ใช้งานทางด้านการแพทย์ เภสัชกรรม เครื่องสำอาง กันอย่างกว้างขวาง แต่ยังไม่พบการนำมาประยุกต์ใช้ในงานทางด้านการวิเคราะห์ในรูปแบบที่ทางคณะผู้วิจัยสนใจ

คณะผู้วิจัยได้ออกแบบวิธีการสังเคราะห์แอมฟิฟิลิกไคโทซานออกเป็น 2 แนวทาง แสดงรายละเอียดพอสังเขปตามแผนภาพใน**รูปที่ 1.8** ทั้ง 2 แนวทางใช้อนุพันธ์ของไคโทซานที่มีหมู่ไม่ชอบน้ำ ได้แก่ phthaloyl, hexyl, dodecyl เป็นสารตั้งต้น แนวทางแรกจะเติมหมู่ชอบน้ำของ poly(ethylene glycol) methyl ether (mPEG) น้ำหนักโมเลกุล 5,000 หลังจากการเกิดเป็นอนุภาคผ่านไดอะไลซิสในน้ำแล้ว จึงนำไปทำปฏิกิริยาเมทิลเลชันกับเมทิลไอโอไดด์เพื่อเปลี่ยนหมู่แอมิโนที่เหลือในโครงสร้างของไคโทซานเป็นหมู่ควอเทอร์นารีแอมโมเนียมของ *N,N,N*-trimethyl ในขณะที่แนวทางที่ 2 จะอาศัยการทำปฏิกิริยาเปิดวงของ glycidyltrimethylammonium chloride (GTMAC) โดยหมู่แอมิโนที่เหลือของอนุพันธ์ไคโทซานที่มีหมู่ไม่ชอบน้ำ ซึ่งจะทำให้ได้อนุภาคที่มีหมู่ควอเทอร์นารีของ *N*-[(2-hydroxyl-3-trimethylammonium)propyl] (HTAP) เมื่อเตรียมอนุภาคที่มีหมู่ควอเทอร์นารีแอมโมเนียมได้แล้ว จะใช้เทคนิค ^{1}H NMR ในการตรวจติดตามการเกิดปฏิกิริยา และใช้ข้อมูลที่ได้ในการคำนวณสัดส่วนของหมู่ไม่ชอบน้ำต่อหมู่ชอบน้ำในโครงสร้าง

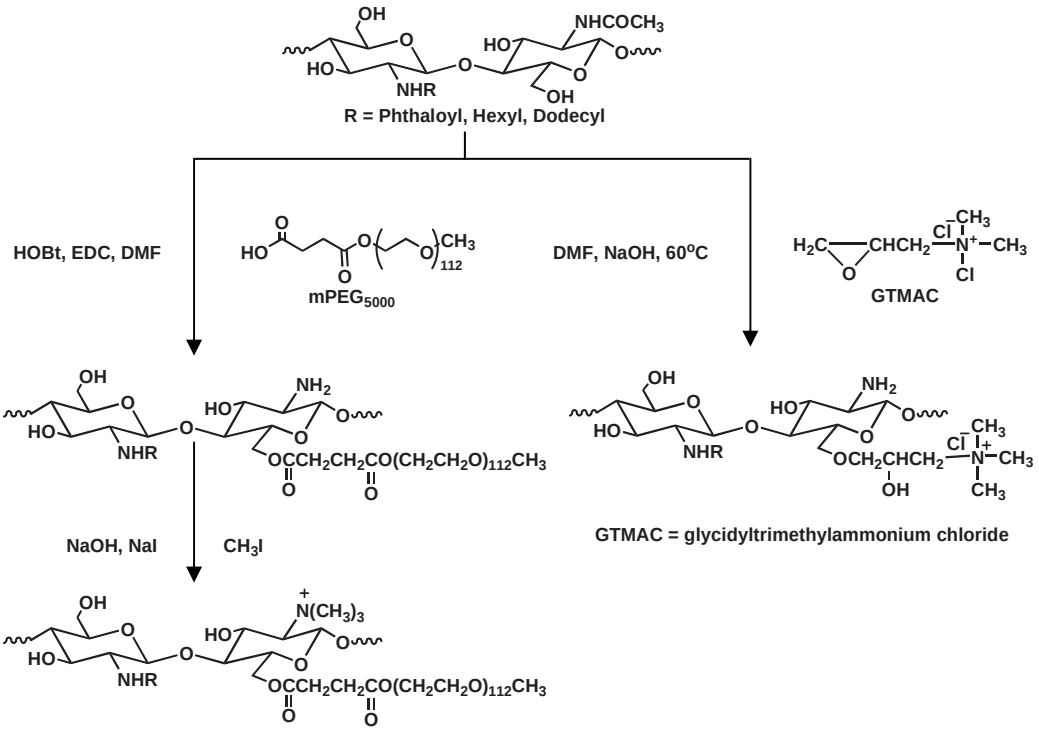

รูปที่ 1.8 แผนภาพแสดงการสังเคราะห์แอมฟิฟิลิกไคโทซาน

งานในส่วนแรกจะเป็นการสังเคราะห์และพิสูจน์เอกลักษณ์ของอนุพันธ์ไคโทซานที่ผ่านการตรึงด้วยหมู่ฟังก์ชันที่ไม่ชอบน้ำ ทั้งนี้เลือกศึกษาการตรึงหมู่ฟังก์ชันที่ไม่ชอบน้ำ 3 ชนิด ได้แก่ หมู่ทาโลอิล (phthaloyl group) หมู่เฮกซิล (hexyl group) และ หมู่โดเดคซิล (dodecyl group) การติดหมู่ทาโลอิลทำผ่านการทำปฏิกิริยาเปิดวงของ phthalic anhydride ด้วยหมู่แอมิโนและหมู่ไฮดรอกซิลของไคโทซาน ได้ผลิตภัณฑ์เป็น phthaloylchitosan (PhCS) ดังแสดงรายละเอียดใน**รูปที่ 1.9a** ส่วนการติดหมู่เฮกซิลและโดเดคซิลนั้นทำผ่านปฏิกิริยา *N*-reductive alkylation ของ *N*-hexanal (**รูปที่ 1.9b**) และ *N*-dodecanal (**รูปที่ 1.9c**) โดยหมู่แอมิโนของไคโทซาน ทำให้ได้ผลิตภัณฑ์เป็น hexylchitosan (HCS) และ dodecylchitosan (DCS) ตามลำดับ

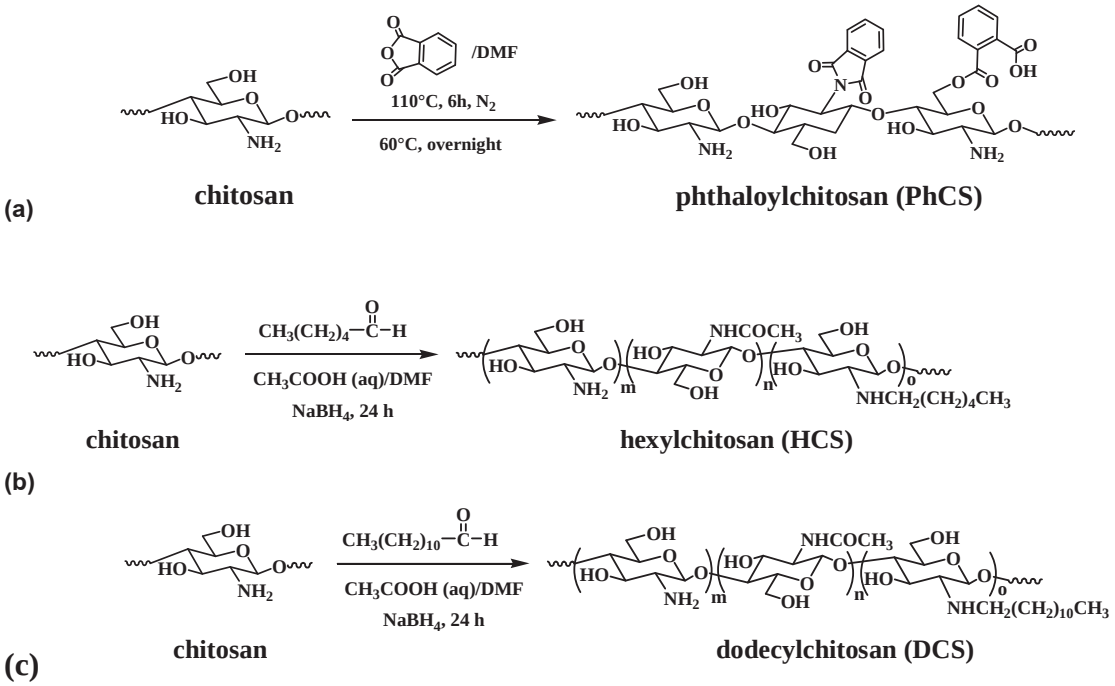

รูปที่ 1.9 แผนภาพแสดงการสังเคราะห์ (a) PhCS, (b) HCS และ (c) DCS

จากการวิเคราะห์ด้วยเทคนิค ^{1}H NMR จะพบสัญญาณแอโรมาติกโปรตอนของหมู่ทาโลอิลที่ chemical shift 7.2-8.2 ppm (ตำแหน่ง b ในรูปที่ 1.10b) ซึ่งไม่พบในสเปกตรัมของไคโทซาน ทั้งนี้สามารถคำนวณหาสัดส่วนการแทนที่ของหมู่ทาโลอิล (degree of phthaloyl group substitution; $\%DS_{Ph}$) ได้จากการนำอินทิเกรชันของโปรตอนตำแหน่งดังกล่าวเทียบกับอินทิเกรชันของโปรตอนที่ต่อกับคาร์บอนตำแหน่งที่ 2 ของไคโทซาน ซึ่งปรากฏที่ chemical shift 2.9 ppm โดยใช้สมการที่ 1

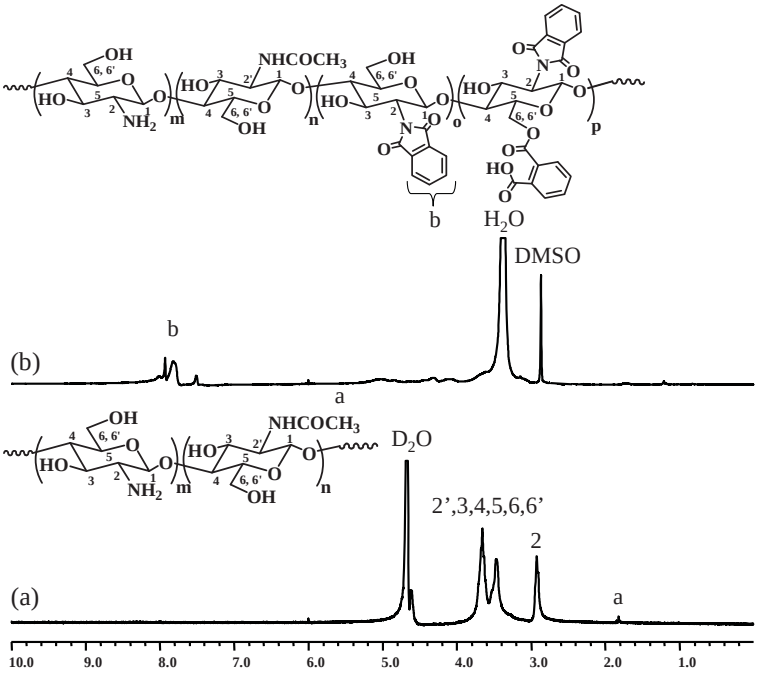

รูปที่ 1.10 ^{1}H NMR สเปกตรัมของ (a) ไคโทซาน และ (b) PhCS

$$\%\, DS_{Ph} = \left\{ \frac{\text{intergral of the } C_6H_4 / 4}{\text{integral of the H - 2 / 1}} \right\} \times 100 \quad (1)$$

สำหรับ HCS และ DCS (**รูปที่ 1.11**) นั้นจะพบสัญญาณโปรตอนของหมู่เมทิลและเมทิลีนที่ chemical shift 0.8 (ตำแหน่ง b) และ 1.2 ppm (ตำแหน่ง c) ตามลำดับ ทั้งนี้สามารถคำนวณหาสัดส่วนการแทนที่ของหมู่เฮก ซิล (degree of hexyl group substitution; $\%DS_{He}$) และโดเดกซิล (degree of dodecyl group substitution; $\%DS_{Do}$) ได้จากการนำอินทิเกรชันของโปรตอนของหมู่เมทิลเทียบกับอินทิเกรชันของโปรตอนที่ต่อกับคาร์บอนตำแหน่งที่ 2 ของไคโทซาน (2.9 ppm) โดยใช้สมการที่ 2

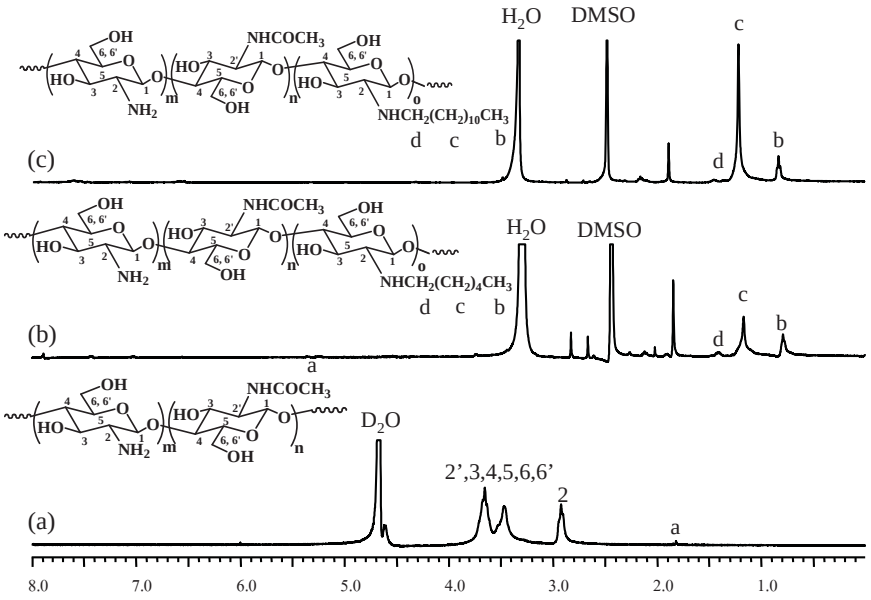

รูปที่ 1.11 ^{1}H NMR สเปกตรัมของ (a) ไคโทซาน, (b) HCS และ (c) DCS

$$\%\, DS_{HCS,DCS} = \left\{ \frac{\text{intergral of the } CH_3 / 3}{\text{integral of the H - 2 / 1}} \right\} \times 100 \quad (2)$$

นอกจากนี้ยังสามารถพิสูจน์เอกลักษณ์ของอนุพันธ์ที่ได้โดยการวิเคราะห์ด้วยเทคนิค FT-IR spectroscopy จาก**รูปที่ 1.12** จะพบพีกที่เลขคลื่น 721 cm^{-1} ซึ่งเป็นของ –CH deformation out of plane ของวงแอโรมาติกในสเปกตรัมของ PhCS และพีกของ C=O stretching ที่มาจาก cyclic imide ที่เลขคลื่น 1,710 cm^{-1} และ 1,770 cm^{-1} ซึ่งไม่ปรากฏในสเปกตรัมของไคโทซาน นอกจากนี้ยังพบการลดลงของพีก N-H bending ของ primary amine ที่เลขคลื่น 1,598 cm^{-1} แสดงว่าเกิดการแทนที่ที่หมู่แอมิโนของไคโทซาน ในส่วนของ HCS และ DCS นั้น จะพบสัญญาณของ C-H bending ที่มาจากหมู่เมทิลีน ที่เลขคลื่น 1,466 cm^{-1} และ C-H stretching ที่เลขคลื่น 2,950 cm^{-1} แสดงถึงการมีอยู่ของสายโซ่แอลคิลในโครงสร้างของทั้งสองอนุพันธ์ ซึ่งไม่พบในไคโทซาน นอกจากนี้ยังพบว่าไม่ปรากฏพีกของ N-H bending ที่เลขคลื่น 1,598 cm^{-1} แสดงถึงการแทนที่ของหมู่เฮกซิลและโดเดกซิลที่หมู่แอมิโนในโครงสร้างของ HCS และ DCS ตามลำดับ

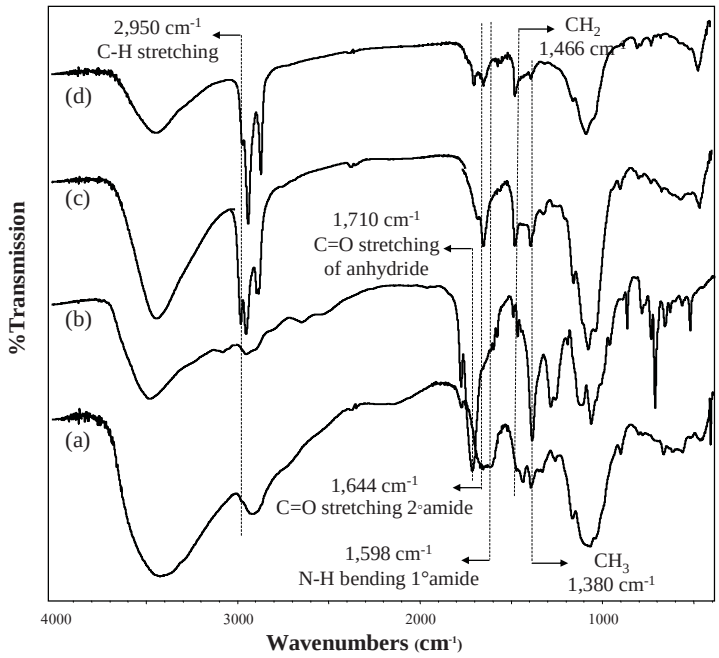

รูปที่ 1.12 FT-IR สเปกตรัมของ (a) ไคโทซาน, (b) PhCS, (c) HCS และ (d) DCS

จาก**ตารางที่ 1.3** การใช้ไคโทซานที่มีน้ำหนักโมเลกุลที่ $4.5x10^3$ Da และ $1.0x10^4$ Da ในการทำปฏิกิริยา พบว่าในกรณีของ PhCS ได้ $\%DS_{Ph}$ ที่มีค่าสูงสุดถึงประมาณ 80 และ 85% ตามลำดับ ทั้งนี้น่าจะเป็นผลเนื่องมาจาก phthalic anhydride เข้าทำปฏิกิริยาได้ทั้งกับหมู่แอมิโนและหมู่ไฮดรอกซิลของไคโทซาน ทำให้สัดส่วนการแทนที่สูง ในขณะที่ $\%DS_{He}$ ของHCS และ $\%DS_{Do}$ ของ DCS มีค่าเพิ่มขึ้นตามสัดส่วนโมลของรีเอเจนต์ที่ใช้ในการทำปฏิกิริยา *N*-reductive alkylation คือ *N*-hexanal และ *N*-dodecanal ตามลำดับ เมื่อเทียบกับจำนวนโมลของหมู่แอมิโนของไคโทซาน

ตารางที่ 1.3 เปอร์เซ็นต์การแทนที่ (%DS) ของหมู่ฟังก์ชันในโครงสร้างของ PhCS, HCS และ DCS คำนวณจากข้อมูลการวิเคราะห์ด้วยเทคนิค ^{1}H NMR

Sample	Mole equivalent of Reagent[a]	$\%DS_{Ph}$	
		$4.5x10^3$ Da	$1.0x10^4$ Da
PhCS	1	80.2±8.4	51.8±9.9
	3	73.4±5.0	85.5±4.0
	5	72.8±10.4	85.2±9.6
HCS	1	38.02±3.1	55.8±7.1
	3	46.32±4.5	51.0±5.8
	5	65.32±6.8	66.7±7.5
DCS	1	53.7±5.3	20.3±2.4
	3	72.3±6.8	41.0±3.0
	5	83.3±6.5	55.2±4.9

a- รีเอเจนต์ที่ใช้สำหรับสังเคราะห์ PhCS, HCS และ DCS คือ phthalic anhydride, *N*-hexanal และ *N*-dodecanal ตามลำดับ

สำหรับการตรึงหมู่ mPEG นั้น จำเป็นต้องมีการดัดแปรโครงสร้างของ mPEG ให้มีหมู่คาร์บอกซิลด้วยการทำปฏิกิริยากับ succinic anhydride (SA) เพื่อให้ได้ mPEG-COOH ก่อน ดังแสดงแผนภาพการทำปฏิกิริยาในรูปที่ 2 จากนั้นนำอนุพันธ์ที่ติดหมู่ที่ไม่ชอบน้ำทั้งสามชนิด (PhCS, HCS และDCS) มาทำปฏิกิริยากับ mPEG-COOH โดยใช้ EDC/NHS เป็นรีเอเจนต์คู่ควบ ต่อมาเป็นการเหนี่ยวนำให้เกิดเป็นอนุภาคด้วยการประกอบตัวเองผ่านไดอะไลซิสในน้ำ อนุภาคแอมฟิฟิลิกไคโทซานที่เตรียมจาก PhCS, HCS และ DCS และมีหมู่ที่ชอบน้ำเป็น mPEG จะเรียกว่า PgM, HgM และ DgM ตามลำดับ จากนั้นเมื่อนำอนุภาคข้างต้นดังกล่าวมาทำให้มีประจุบวกด้วยปฏิกิริยาเมทิลเลชันโดยใช้เมทิลไอโอไดด์ จะทำให้ได้ผลิตภัณฑ์เป็นอนุภาค QPgM, QHgM และ QDgM ตามลำดับ (**รูปที่ 1.8**)

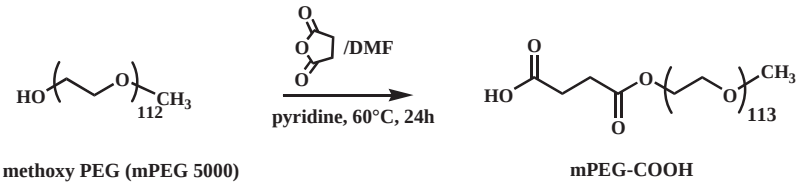

รูปที่ 1.13 แผนภาพแสดงการสังเคราะห์ mPEG-COOH

รูปที่ 1.14 แสดง ^{1}H NMR สเปกตรัมของอนุภาค QPgM, QHgM และQDgM เทียบกับไคโทซาน ทั้งนี้จะพบสัญญาณที่ตำแหน่ง 4.2-3.2 ppm ซึ่งเป็นของโปรตอนตำแหน่งที่ H 2', 3, 4, 5, 6 และ 6' บนโซ่หลักของไคโทซานในทุกสเปกตรัม นอกจากนี้ยังพบสัญญาณของอะโรมาติกโปรตอนของหมู่ทาโลอิล ที่ตำแหน่ง 7.2-8.0 ppm ในสเปกตรัมของ QPgM สัญญาณที่ตำแหน่ง 0.8 และ 1.2 ppm ซึ่งเป็นโปรตอนของหมู่เมทิล ($-CH_3$) และเมทิลีน ($-CH_2-$) ของ หมู่เฮกซิลและโดเดคซิล ในสเปกตรัมของ QHgM และ QDgM และสัญญาณที่ตำแหน่ง 2.6 ppm ซึ่งเป็นของเมทิลีนโปรตอนส่วนที่เชื่อมกับ mPEG

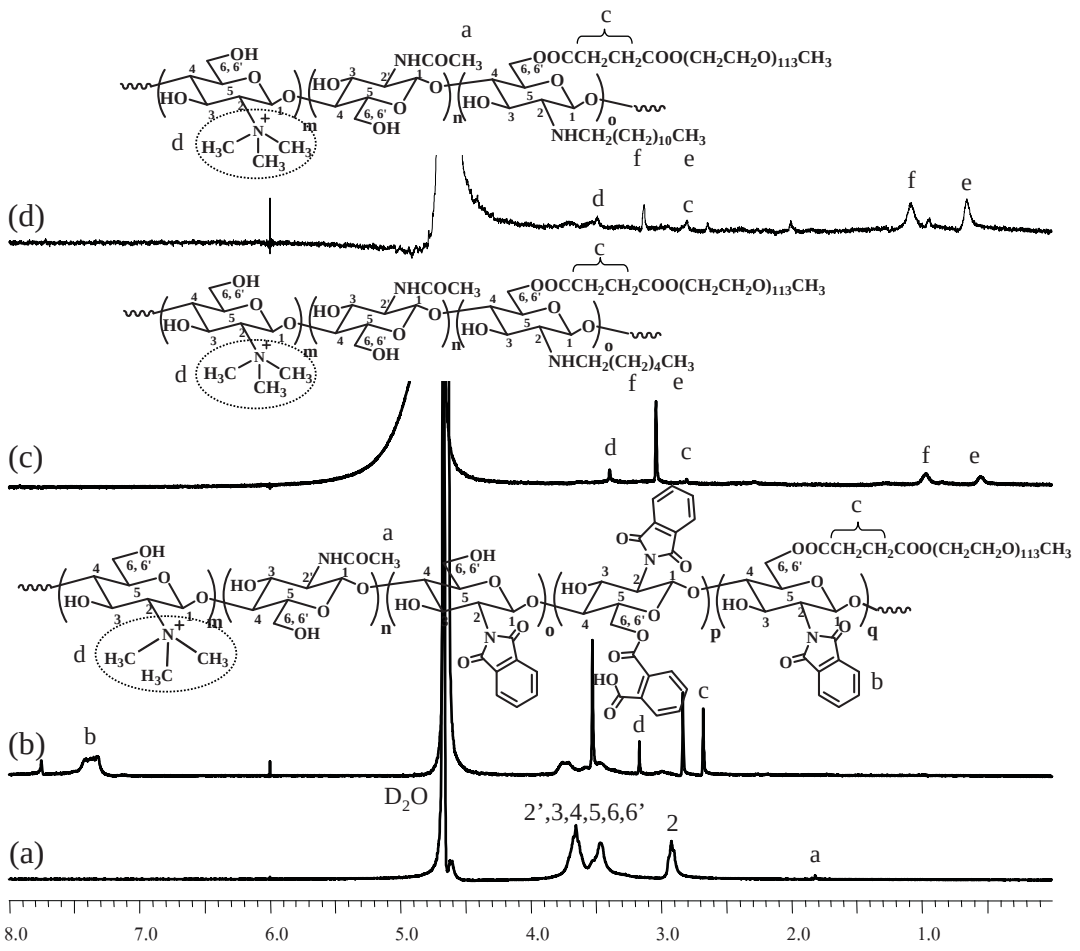

รูปที่ 1.14 ^{1}H NMR สเปกตรัมของ (a) chitosan (D_2O) และอนุภาคแอมฟิฟิลิกไคโทซานชนิดที่มีหมู่ mPEG เป็นหมู่ชอบน้ำหลังจากผ่านปฏิกิริยาเมทิลเลชัน (DMSO-d_6): (b) QPgM, (c) QHgM และ (d) QDgM

ทั้งนี้สามารถคำนวณหาเปอร์เซ็นต์การแทนที่ของหมู่ mPEG ($\%DS_{mPEG}$)ได้จากอัตราส่วนอินทิเกรชันของเมทิลีนโปรตอนส่วนที่เชื่อมกับ mPEG เทียบกับอินทิเกรชันของโปรตอนตำแหน่งที่ 2 (H-2) ที่ 2.9 ppm ของไคโทซาน ตามสมการที่ 3

$$\% DS_{mPEG} = \left\{ \frac{\text{intergral of the OOCC}\underline{\text{H}}_2\text{C}\underline{\text{H}}_2\text{COO}/4}{\text{integral of the H-2}/1} \right\} \times 100 \qquad (3)$$

นอกจากนี้จะพบสัญญาณที่ 3.2-3.4 ppm ซึ่งเป็นโปรตอนของหมู่ไทรเมทิลของหมู่ควอเทอร์นารีแอมโมเนียมในสเปกตรัมของ QPgM, QHgM และ QDgM ซึ่งสามารถใช้ในการคำนวณหาเปอร์เซ็นต์ของหมู่ที่เป็นควอเทอนารีแอมโมเนียม (%DQ) ได้จากอัตราส่วนอินทิเกรชันของโปรตอน 9 ตัวของหมู่ไทรเมทิลเทียบกับอินทิเกรชันของโปรตอนตำแหน่งที่ 2 (H-2) ที่ 2.9 ppm ของไคโทซาน ดังแสดงตามสมการที่ 4

$$\% DQ = \left\{ \frac{\text{intergral of the N}^{+}(\text{CH}_3)_3/9}{\text{integral of the H-2}/1} \right\} \times 100 \qquad (4)$$

เนื่องจากทาลิกแอนไฮไดร์ด (phthalic anhydride; PhA) ที่ใช้ในการตรึงหมู่ทาโลอิลของอนุภาค QPgM สามารถทำปฏิกิริยาได้กับทั้งหมู่แอมิโนและไฮดรอกซิลของไคโทซาน ด้วยเหตุนี้เปอร์เซ็นต์การแทนที่ของหมู่ทาโลอิล ($\%DS_{Ph}$) จึงมีค่าสูงอยู่ในช่วง 72.8-80.2% และจาก**ตารางที่ 1.4** พบว่าอนุภาคชนิด QPgM มีเปอร์เซ็นต์การแทนที่ของ mPEG ($\%DS_{mPEG}$) เพิ่มขึ้นตามอัตราส่วนโดยโมลของ mPEG-COOH เมื่อเทียบกับ PhA จาก 1 ไปเป็น 3 แต่อย่างไรก็ตามเมื่อเพิ่มอัตราส่วนเป็น 5 โมล จะพบว่ามีการแทนที่ลดลง ทั้งนี้คาดว่าน่าจะเป็นผลจากข้อจำกัดของ mPEG ซึ่งเป็นโมเลกุลใหญ่ในการเข้าถึงหมู่ไฮดรอกซิล ของไคโทซานที่ความเข้มข้นสูง เป็นที่น่าสังเกตว่า $\%DS_{mPEG}$ จะมีค่าไม่สูงมากนัก โดยอยู่ในช่วง 7.3-38.5% ซึ่งน่าจะสามารถอธิบายได้จากการที่หมู่ไฮดรอกซิลบางส่วนเกิดปฏิกิริยากับ PhA ในขั้นการติดหมู่ไม่ชอบน้ำชนิดทาโลอิล จึงทำให้มีเหลืออยู่ไม่มากนักที่จะทำปฏิกิริยากับ mPEG-COOH ในขั้นการติดหมู่ชอบน้ำชนิด mPEG และการได้ %DQ ค่อนข้างต่ำ (7.6-13.7%) ก็สามารถอธิบายได้ด้วยเหตุผลคล้ายคลึงกัน กล่าวคือหมู่แอมิโนของไคโทซานส่วนใหญ่เกิดการแทนที่ด้วยหมู่ทาโลอิล จึงมีจำนวนน้อยเท่านั้นที่จะเกิดปฏิกิริยาเมทิลเลชันกับเมทิลไอโอไดด์ได้เป็นหมู่ควอเทอร์นารีแอมโมเนียม

ตารางที่ 1.4 เปอร์เซ็นต์การแทนที่ของอนุภาค QPgM ที่อัตราส่วนต่างๆ

Sample	Mole equivalent of PhA:mPEG-COOH	$\%DS_{Ph}$	$\%DS_{mPEG}$	%DQ
QPgM	1:1	80.2±8.4	7.8±0.4	11.7±1.3
	1:3		38.5±1.7	7.6±2.1
	1:5		18.0±0.9	13.7±1.6
	3:1	73.4±5.0	7.3±0.7	11.4±0.2
	3:3		31.5±0.5	9.0±0.9
	3:5		13.3±0.5	10.6±1.6
	5:1	72.8±10.4	8.70±0.9	8.6±0.4
	5:3		23.3±1.5	9.3±0.9
	5:5		13.4±1.2	10.6±1.0

ในกรณีของอนุภาคชนิด QHgM (**ตารางที่ 1.5**) พบว่าเปอร์เซ็นต์การแทนที่ของ $\%DS_{He}$ เพิ่มขึ้นตามจำนวนโมลที่เพิ่มขึ้นของ *N*-hexanal (He) และพบว่ามีการแทนสูงสุดเป็น 65% ส่วน $\%DS_{mPEG}$ จะมีค่าเพิ่มขึ้นอัตราส่วนโดยโมลที่เพิ่มขึ้นของ mPEG-COOH เมื่อเทียบกับ He ถึงแม้ว่าการแทนที่ของหมู่ไม่ชอบน้ำชนิดเฮกซิล ($\%DS_{He}$) จะมีค่าไม่สูงมากนักหากเทียบกับการแทนที่ของหมู่ทาโลอิล ($\%DS_{Ph}$) ของอนุภาค QPgM ประกอบกับการแทนที่ของหมู่เฮกซิลจะเกิดขึ้นเฉพาะที่ตำแหน่งหมู่แอมิโนของไคโทซานเท่านั้น โดยไม่มีผลกับหมู่ไฮดรอกซิลที่จะทำปฏิกิริยาต่อกับ mPEG-COOH แต่ก็ยังพบว่า $\%DS_{mPEG}$ มีค่าไม่สูงมากนักหากเทียบกับของอนุภาค QPgM ซึ่งคาดว่าน่าจะเป็นผลของความเกะกะของโมเลกุล mPEG-COOH ทีมีน้ำหนักโมเลกุลสูงถึง 5,000 ในการเข้าทำปฏิกิริยากับหมู่ไฮดรอกซิลของไคโทซาน หลังจากผ่านการทำปฏิกิริยาเมทิลเลชันแล้ว พบว่า %DQ มีค่าค่อนข้างต่ำอยู่ในช่วง 7.4-14.6% ดังแสดงใน**ตารางที่ 1.5**

ตารางที่ 1.5 เปอร์เซ็นต์การแทนที่ของอนุภาค QHgM ที่อัตราส่วนต่าง ๆ

Sample	Mole equivalent of He:mPEG-COOH	$\%DS_{He}$	$\%DS_{mPEG}$	%DQ
QHgM	1:1	38.02±3.1	7.80±0.4	11.33±1.7
	1:3		27.5±0.4	12.3±1.9
	1:5		31.5±1.1	13.9±1.6
	3:1	46.32±4.5	17.0±1.0	12.7±1.3
	3:3		19.3±0.3	14.0±2.1
	3:5		23.3±1.0	7.4±1.1
	5:1	65.32±6.8	13.5±0.4	14.6±2.5
	5:3		19.0±1.2	13.1±1.6
	5:5		23.5±1.1	11.6±1.7

ส่วนอนุภาค QDgM ซึ่งแสดงผลการคำนวณเปอร์เซ็นต์การแทนที่ไว้ใน**ตารางที่ 1.6** พบว่ามีแนวโน้มของการแทนที่ของทั้งหมู่ไม่ชอบน้ำชนิดโดเดคซิล ($\%DS_{Do}$) และหมู่ชอบน้ำชนิด mPEG ($\%DS_{mPEG}$) เช่นเดียวกับของอนุภาค QHgM กล่าวคือ สามารถปรับเปลี่ยน $\%DS_{Do}$ ได้ตามจำนวนโมลที่เพิ่มขึ้นของรีเอเจนต์ที่ใช้คือ *N*-dodecanal (Do) ส่วน $\%DS_{mPEG}$ และ %DQ มีค่าไม่สูงมากนัก

ตารางที่ 1.6 เปอร์เซ็นต์การแทนที่ของอนุภาค QDgM ที่อัตราส่วนต่าง ๆ

Sample	Mole equivalent of Do:mPEG-COOH	$\%DS_{Do}$	$\%DS_{mPEG}$	%DQ
QDgM	1:1	53.7±5.3	12.3±0.7	8.1±3.2
	1:3		17.0±0.7	13.2±1.6
	1:5		18.3±1.2	9.3±2.7
	3:1	72.3±6.8	11.3±1.2	11.5±0.8
	3:3		13.0±0.4	8.3±1.3
	3:5		23.0±0.5	7.1±1.4
	5:1	83.3±6.5	28.0±1.2	8.3±0.5
	5:3		30.5±2.3	12.8±1.6
	5:5		22.3±0.5	10.7±2.0

สำหรับเส้นทางที่ 2 ซึ่งอาศัยการทำปฏิกิริยาเปิดวง GTMAC ของหมู่แอมิโนของไคโทซาน ซึ่งเป็นการติดหมู่ HTAP เข้าไปนั้น สามารถคำนวณสัดส่วนเปอร์เซ็นต์การแทนที่ของ HTAP (degree of HTAP group substitution; $\%DS_{HTAP}$) ได้จากการอินทิเกรชันของพีกที่เป็นโปรตอนของหมู่เมทิล 3 หมู่ ปรากฏที่ chemical shift 3.05-3.10 ppm ที่ตำแหน่ง f ในสเปกตรัมของ HgH และ DgH (**รูปที่ 1.15**) เทียบกับอินทิเกรชันของพีกที่ตำแหน่งที่ 2 (2.9 ppm) ของไคโทซาน ตามสมการที่ 5

$$\%DS_{HTAP} = \left(\frac{\int \frac{H - N^{+}(CH_3)_3}{9}}{\int \frac{H-2}{1}} \right) \times 100 \quad (5)$$

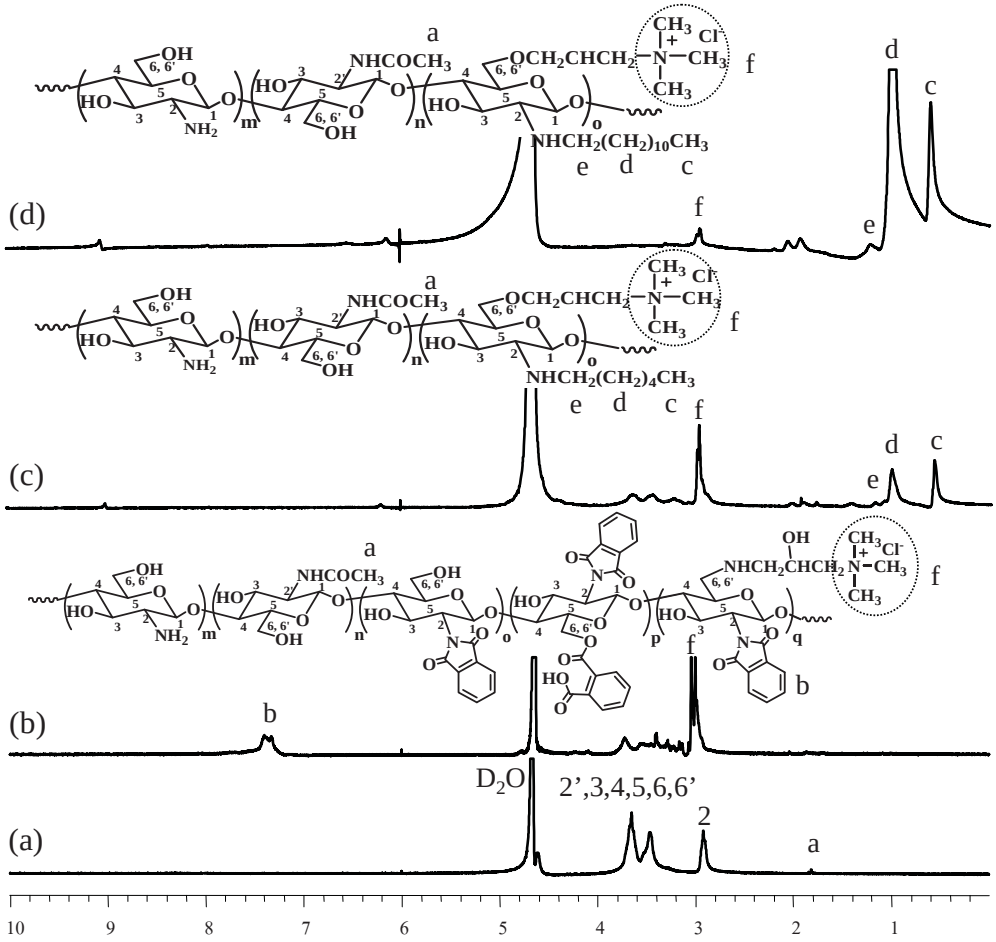

รูปที่ 1.15 ^{1}H NMR สเปกตรัมของ (a) chitosan (D_2O) และอนุภาคแอมฟิฟิลิกไคโทซานชนิดที่มีหมู่ HTAP เป็นหมู่ชอบน้ำ: (b) PgH, (c) HgH, and (d) DgH

จากการใช้ HCS และ DCS ที่มีหมู่เฮกซิลและโดเดคซิลเป็นหมู่ไม่ชอบน้ำไปทำปฏิกิริยากับ GTMAC เพื่อติดหมู่ชอบน้ำประเภท HTAP ได้เป็น HgH และ DgH ตามลำดับ พบว่า $\%DS_{HTAP}$ มีค่าเพิ่มขึ้นตามสัดส่วนโดยโมลของ GTMAC ที่เพิ่มขึ้น ในเกือบทุกสัดส่วนการแทนที่ของหมู่เฮกซิลและโดเดคซิล ดังแสดงผลการทดลองใน**ตารางที่ 1.7 และ 1.8** ทั้งนี้จะสังเกตเห็นได้ว่า $\%DS_{HTAP}$ ซึ่งเป็นค่าที่แสดงถึงการมีหมู่ควอเทอร์นารีแอมโมเนียม ที่เทียบเท่ากับ %DQ ในกรณีของแอมฟิฟิลิกไคโทซานที่เตรียมผ่านปฏิกิริยาตามเส้นทางที่แรกนั้น มีค่าสูงได้ถึงเกือบ 45% ซึ่งเป็นค่าที่สูงกว่า %DQ เป็นอย่างมาก ทั้งนี้น่าจะสามารถอธิบายได้จากที่การเปิดวงของ GTMAC นั้นเกิดได้ทั้งจากหมู่แอมิโนและหมู่ไฮดรอกซิลของไคโทซาน ในขณะที่ในกรณีของแอมฟิฟิลิกไคโทซานที่เตรียมผ่านปฏิกิริยาตามเส้นทางแรกนั้น การเกิดเป็นหมู่ควอเทอร์นารีแอมโมเนียมจะต้องผ่านปฏิกิริยาเมทิลเลชันของหมู่แอมิโนของไคโทซานเท่านั้น

ตารางที่ 1.7 สัดส่วนการแทนที่ของหมู่ฟังก์ชันต่าง ๆในโครงสร้างของแอมฟิฟิลิกไคโทซานที่มีหมู่เฮกซิลเป็นหมู่ไม่ชอบน้ำและ HTAP เป็นหมู่ชอบน้ำ ซึ่งคำนวณได้จากผลการวิเคราะห์ด้วยเทคนิค ^{1}H NMR

ชนิดของอนุพันธ์	hexanal : GTMAC by mol	%DS_{He}	%DS_{HTAP}
$HgH_{45,000}$	1:1	38.0	44.3
	1:3		30.8
	1:5		33.6
	3:1	46.3	7.1
	3:3		9.0
	3:5		13.6
	5:1	65.3	6.3
	5:3		7.8
	5:5		10.8
$HgH_{100,000}$	1:1	55.7	14.3
	1:3		31.8
	1:5		36.7
	3:1	51.0	17.7
	3:3		19.0
	3:5		26.9
	5:1	66.7	24.8
	5:3		29.6
	5:5		36.3

หมายเหตุ: ตัวเลขที่ปรากฏเป็นตัวห้อยในคอลัมน์แรกคือ 45,000 และ 100,000 เป็นน้ำหนักโมเลกุลของไคโทซานที่ใช้ในการสังเคราะห์

ตารางที่ 1.8 สัดส่วนการแทนที่ของหมู่ฟังก์ชันต่าง ๆในโครงสร้างของแอมฟิฟิลิกไคโทซานที่มีหมู่โดเดกซิลเป็นหมู่ไม่ชอบน้ำและ HTAP เป็นหมู่ชอบน้ำ ซึ่งคำนวณได้จากผลการวิเคราะห์ด้วยเทคนิค ^{1}H NMR

ชนิดของอนุพันธ์	hexanal : GTMAC by mol	$\%DS_{He}$	$\%DS_{HTAP}$
$DgH_{45,000}$	1:1	53.7	6.8
	1:3		9.2
	1:5		10.1
	3:1	72.3	11.9
	3:3		29.6
	3:5		22.9
	5:1	83.3	16.8
	5:3		21.4
	5:5		35.8
$DgH_{100,000}$	1:1	20.3	12.3
	1:3		20.1
	1:5		23.8
	3:1	41.0	8.6
	3:3		24.5
	3:5		23.1
	5:1	55.2	16.8
	5:3		21.4
	5:5		24.8

หมายเหตุ: ตัวเลขที่ปรากฏเป็นตัวห้อยในคอลัมน์แรกคือ 45,000 และ 100,000 เป็นน้ำหนักโมเลกุลของไคโทซานที่ใช้ในการสังเคราะห์

นอกจากนี้สามารถยืนยันความสำเร็จของการสังเคราะห์แอมฟิฟิลิกไคโทซานได้จากการวิเคราะห์ด้วยเทคนิค FT-IR (**รูปที่ 1.16-1.17**) โดยจะพบสัญญาณที่เด่นชัดของ C-H stretching ทั้งที่เป็นของหมู่เมทิลและเมทิลีน ในช่วง 2860-2930 cm^{-1}, การลดลงของสัญญาณที่แสดง N-H bending บริเวณ 1598 cm^{-1}และการปรากฏของสัญญาณ C-H deformation ที่ 1470 cm^{-1} เนื่องจากเกิดการแทนที่ของหมู่แอลคิลไปที่หมู่แอมิโนของไคโทซาน

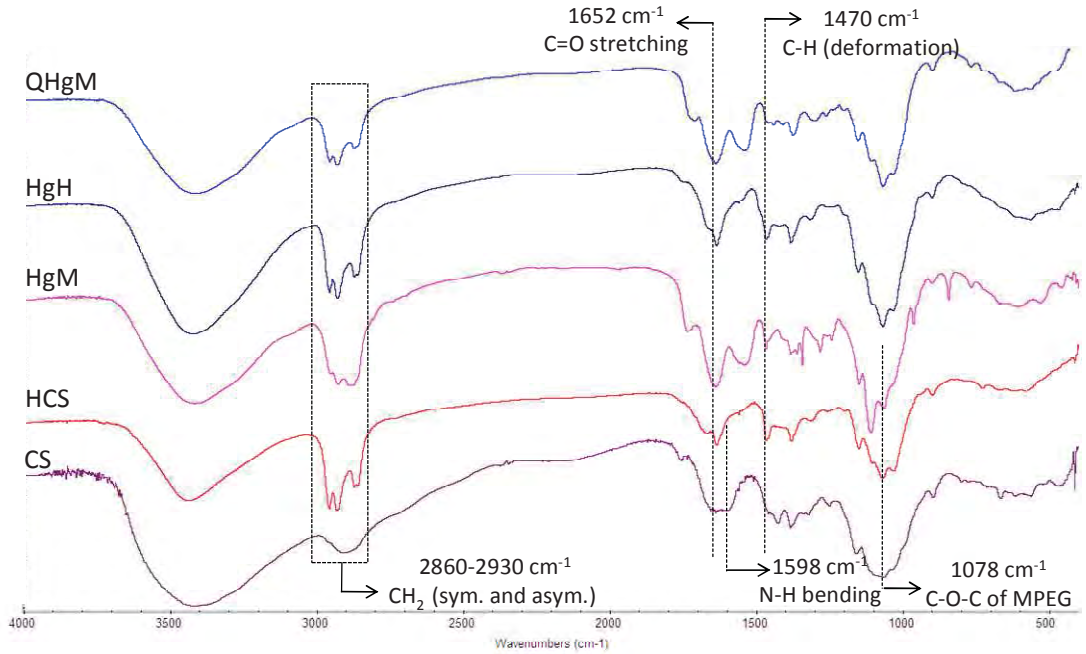

รูปที่ 1.16 FT-IR สเปกตรัมของ chitosan (CS), hexylchitosan (HCS), HCS ที่ติดหมู่ mPEG (HgM), HCS ที่ติดหมู่ HTAP (HgH) และ HgM หลังการทำปฏิกิริยาเมทิลเลชัน (QHgM) ที่เตรียมจากไคโทซานน้ำหนักโมเลกุล 45,000 Dalton, 85%DD

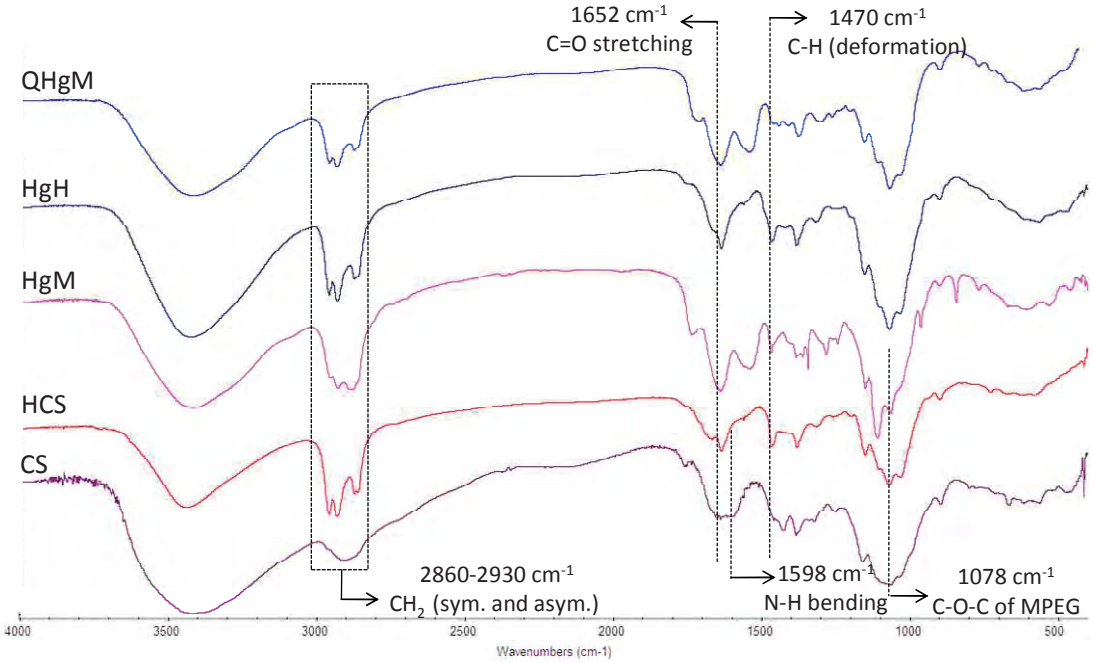

รูปที่ 1.17 FT-IR สเปกตรัมของ chitosan (CS), dodecyl chitosan (DCS), DCS ที่ติดหมู่ mPEG (DgM), DCS ที่ติดหมู่ HTAP (DgH) และ DgM หลังการทำปฏิกิริยาเมทิลเลชัน (QDgM) ที่เตรียมจากไคโทซานน้ำหนักโมเลกุล 45,000 Dalton, 85%DD

เพื่อเป็นการเพิ่มสัดส่วนการแทนที่ของหมู่ควอเทอร์นารีแอมโมเนียมหรือ %DQ ของอนุภาคที่มีหมู่ HTAP เป็นหมู่ชอบน้ำ ในงานวิจัยนี้ได้ทดลองเพิ่มความเป็นกรดของสารละลาย DMF ในขั้นการทำปฏิกิริยาเปิดวงของ GTMAC โดยการเติมสารละลายกรดแอซิติก (1.0% (v/v) เพื่อลด pH จาก 9 เป็น 5 ทั้งนี้คาดหวังว่าการเพิ่มความเป็นกรดเพียงเล็กน้อยจะลดโอกาสของการมีไอออนไฮดรอกไซด์ในระบบที่จะเข้าแข่งขันกับหมู่แอมิโนของไคโทซานในการเข้าทำปฏิกิริยาเปิดวงกับ GTMAC ข้อมูลใน**ตารางที่ 1.9** แสดงให้เห็นว่าแนวทางดังกล่าวประสบความสำเร็จในการช่วยเพิ่ม %DQ ของทุกอนุพันธ์เกือบทุกชนิดให้มีค่าสูงกว่า 50%

ตารางที่ 1.9 สัดส่วนการแทนที่ของหมู่ฟังก์ชันต่าง ๆในโครงสร้างของแอมฟิฟิลิกไคโทซานที่มีหมู่ HTAP เป็นหมู่ชอบน้ำ สังเคราะห์จากไคโทซานน้ำหนักโมเลกุล 45 kDa และมีการเติมสารละลายกรดแอซิติก (1.0% (v/v)) ซึ่งคำนวณได้จากผลการวิเคราะห์ด้วยเทคนิค ^{1}H NMR

Sample[a]	Mole equivalent of hydrophobic reagent: GTMAC[b]	$\%DS_{hydrophobic}$	$\%DQ_{HTAP}$
PgH	1:5	80.2	58.2
	3:5	73.4	52.6
	5:5	72.8	42.4
HgH	1:5	38.0	55.0
	3:5	46.3	59.1
	5:5	65.3	68.1
DgH	1:5	53.7	59.4
	3:5	72.3	65.4
	5:5	83.3	51.7

a- PgH, HgH และ DgH คืออนุภาคแอมฟิฟิลิกไคโทซานที่มีหมู่ชอบน้ำเป็น HTAP และหมู่ไม่ชอบน้ำเป็นทาโลอิล เฮกซิล และโดเดกซิล ตามลำดับ

b- Hydrophobic reagent คือ ทาลิกแอนไฮไดร์ด, เฮกซานาล และ โดเดกคานาล สำหรับการสังเคราะห์แอมฟิฟิลิกไคโทซานชนิด PgH, HgH และ DgH ตามลำดับ

ในงานวิจัยนี้วิเคราะห์ค่าความเป็นประจุของอนุภาคด้วยเทคนิค PCS จากผลการทดลองที่แสดงใน**ตารางที่ 1.10** จะเห็นได้ว่าอนุภาคแอมฟิฟิลิกไคโทซานที่เตรียมผ่านเส้นทางที่ 1 ซึ่งมี $mPEG_{5000}$ เป็นหมู่ชอบน้ำแสดงประจุเป็นลบ โดยมีอนุภาคชนิด QPgM ซึ่งมีหมู่ทาโลอิลเป็นหมู่ไม่ชอบน้ำแสดงความเป็นลบมากที่สุด คณะผู้วิจัยคาดว่าเป็นผลมาจากหลายปัจจัยดังนี้ ปัจจัยแรกเป็นผลจากการที่ %DQ ของทุกอนุภาคมีค่าต่ำกว่า 20% จึงส่งผลให้ค่าศักย์เซต้า (ζ-potential) มีค่าเป็นลบ ปัจจัยต่อมาเป็นผลมาจากการที่ $mPEG_{5000}$ ที่ประกอบด้วยหน่วยซ้ำของเอทิลีนไกลคอลซึ่งมีอิเล็กตรอนคู่โดดเดี่ยวเป็นจำนวนมากบนอะตอมของออกซิเจน ลักษณะดังกล่าวส่งผลให้อนุภาคมีประจุเป็นบวก ปัจจัยที่สามส่งผลโดยตรงต่ออนุภาคชนิด QPgM and PgH ที่มีหมู่ทาโลอิลเป็นหมู่ไม่ชอบน้ำ ซึ่งในการทำปฏิกิริยานอกจากจะมีการแทนที่ของหมู่ดังกล่าวที่ตำแหน่งของหมู่แอมิโนได้ผลิตภัณฑ์เป็นอิไมด์แบบวงแล้ว จะได้ผลิตภัณฑ์ที่มีการแทนที่ที่ตำแหน่งของหมู่ไฮดรอกซิลทำให้ได้ผลิตภัณฑ์เป็นแอนไฮไดร์ดแบบวงซึ่งไม่เสถียรและแตกออกเป็นหมู่คาร์บอกซิล (pKa 4.4) ที่สามารถแตกตัวเป็น

คาร์บอกซิเลตที่มีประจุเป็นลบ ผลของปัจจัยสุดท้ายนี้จะเห็นได้ชัดกับอนุภาค QPgM ที่มี $\%DS_{Ph}$ สูง และ %DQ ต่ำ ประจุบวกที่ให้กับอนุภาคผ่านปฏิกิริยาเมทิลเลชันมีไม่มากพอที่จะไปหักล้างความเป็นลบของหมู่คาร์บอกซิเลต ด้วยเหตุนี้อนุภาคชนิด QPgM จึงมีค่าศักย์เซต้าต่ำสุดถึง -44 mV

การเพิ่มสัดส่วนการแทนที่ของหมู่ควอเทอร์นารีแอมโมเนียมในอนุภาคชนิดที่มี HTAP เป็นหมู่ชอบน้ำที่สังเคราะห์ผ่านเส้นทางที่ 2 ให้สูงกว่า 50% ช่วยทำให้อนุภาคชนิด PgH ซึ่งมีหมู่ไม่ชอบน้ำเป็นหมู่ทาโลอิล เช่นเดียวกับ QPgM มีความเป็นประจุลบน้อยลง แสดงให้เห็นว่าประจุบวกเนื่องจากหมู่ควอเทอร์นารีแอมโมเนียมสามารถหักล้างความเป็นลบของหมู่คาร์บอกซิเลตได้ แต่ก็ยังไม่เพียงพอที่จะทำให้อนุภาค PgH มีประจุเป็นบวก ถึงแม้ว่าจะเป็นอนุภาคที่เตรียมโดยการเติมสารละลายกรดแอซิติก (1.0% (v/v)) ทำให้ได้ $\%DQ_{HTAP}$ สูงถึง 58.2% ก็ตาม การเติมกรดดังกล่าวส่งผลอย่างชัดเจนต่อการเพิ่มความเป็นประจุบวกให้กับอนุภาคชนิด HgH และ DgH ค่าพลังงานเซต้ามีค่าเพิ่มขึ้นจาก +22.5 เป็น +35.3 mV และจาก +15.5 เป็น +48.5 mV สำหรับอนุภาคชนิด HgH และ DgH ตามลำดับ หลังการเติมกรด ในที่นี้ไม่สามารถเปรียบเทียบค่าศักย์เซต้าของอนุภาคไคโทซานกับอนุภาคแอมฟิฟิลิกไคโทซานได้ เนื่องจากอนุภาคไคโทซานเตรียมจากการตกตะกอนด้วยไทรพอลิไทรฟอสเฟส ไม่ได้เตรียมจากการประกอบตัวเองซึ่งเป็นวิธีที่ใช้ในการเตรียมอนุภาคแอมฟิฟิลิกไคโทซาน

ตารางที่ 1.10 ค่าความเป็นประจุบวกซึ่งแสดงในรูปของศักย์เซต้าของอนุภาคแอมฟิฟิลิกไคโทซานซึ่งวิเคราะห์ด้วยเทคนิค PCS

Sample[a]	%DS of Hydrophobic:Hydrophilic[b]	%DQ	ζ-potential (mV)[c]	ζ-potential (mV)[d]
Chitosan	-	-	+27.1	+27.1
QPgM	73:13[c]	9	-44.3	-
QHgM	46:19[c]	14	-10.6	-
QDgM	72:13[c]	8	-6.5	-
PgH	73:46[c]/ 73:53[d]	-	-13.2	-10.4
HgH	46:31[c]/ 46:59[d]	-	+22.5	+35.3
DgH	72:29[c]/ 72:65[d]	-	+15.5	+48.5

a- QPgM, QHgM และ QPgM คือ อนุภาคแอมฟิฟิลิกไคโทซานที่มีหมู่ชอบน้ำเป็น $mPEG_{5000}$ และหมู่ไม่ชอบน้ำเป็นทาโลอิล เฮกซิล และโดเดกซิล ตามลำดับ ส่วน PgH, HgH และ DgH คืออนุภาคแอมฟิฟิลิกไคโทซานที่มีหมู่ชอบน้ำเป็น HTAP และหมู่ไม่ชอบน้ำเป็นทาโลอิล เฮกซิล และโดเดกซิล ตามลำดับ

b- หมู่ไม่ชอบน้ำมี 3 ชนิด ได้แก่ ทาโลอิล เฮกซิล และโดเดกซิล ส่วนหมู่ชอบน้ำมี 2 ชนิด ได้แก่ $mPEG_{5000}$ และ HTAP

c- อนุภาคเตรียมในสารละลาย DMF

d- อนุภาคเตรียมในสารละลาย DMF+ 1.0% (v/v) acetic acid

Critical micelle concentration (CMC) เป็นความเข้มข้นต่ำสุดที่ทำให้เกิดเป็นไมเซลล์. ในงานวิจัยนี้หาค่า CMC ของแอมฟิฟิลิกไคโทซานที่เตรียมได้โดยใช้เทคนิคฟลูออเรสเซนต์สเปกโทรสโกปีและไพรีนเป็นสีย้อม ทั้งนี้สามารถหาได้จากการเปลี่ยนแปลงของสัดส่วนระหว่าง vibrational peak ที่ 1 เปรียบเทียบกับ vibrational peak ที่ 3 ในสเปกตรัมเปล่งแสงฟลูออเรสเซนต์ (fluorescence emission spectrum) ของไพรีน (I_1/I_3) เมื่อความเข้มข้นต่ำกว่าค่า CMC จะยังไม่เกิดเป็นอนุภาค อัตราส่วน I_{373}/I_{384} จึงยังมีค่าสูงเนื่องจากไพรีนซึ่งเป็นสีย้อมที่มีสมบัติไม่

ชอบน้ำจะยังไม่สามารถกระจายตัวในน้ำที่เป็นตัวทำละลายได้ แต่เมื่อความเข้มข้นสูงเกินค่า CMC เกิดการประกอบเป็นอนุภาค ไพรีนจะถูกกักเก็บอยู่ภายในอนุภาค ส่งผลให้ อัตราส่วน I_{373}/I_{384} มีค่าลดลง กราฟแสดงความสัมพันธ์ระหว่าง I_{373}/I_{384} ของไพรีนและ log ความเข้มข้นของแอมฟิฟิลิกไคโทซาน (คัดเลือกเฉพาะที่มีค่าพลังงานเซต้าสูงสุดของอนุพันธ์แต่ละชนิด) แสดงไว้ใน**รูปที่ 1.18** เมื่อนำผลจากกราฟดังกล่าวไปคำนวณจะพบว่าค่า CMC ของแอมฟิฟิลิกไคโทซานอยู่ในช่วง 7-17 µg/mL ดังแสดงผลไว้ในตารางที่ 3 และเป็นที่น่าสังเกตว่าอนุภาคที่มีหมู่ชอบน้ำเป็น HTAP จะมีค่า CMC ต่ำกว่าอนุภาคที่มีหมู่ชอบน้ำเป็น $mPEG_{5000}$ ในกรณีที่มีหมู่ไม่ชอบน้ำชนิดเดียวกัน แสดงให้เห็นถึงประสิทธิภาพในการเกิดเป็นอนุภาคที่ดีกว่า

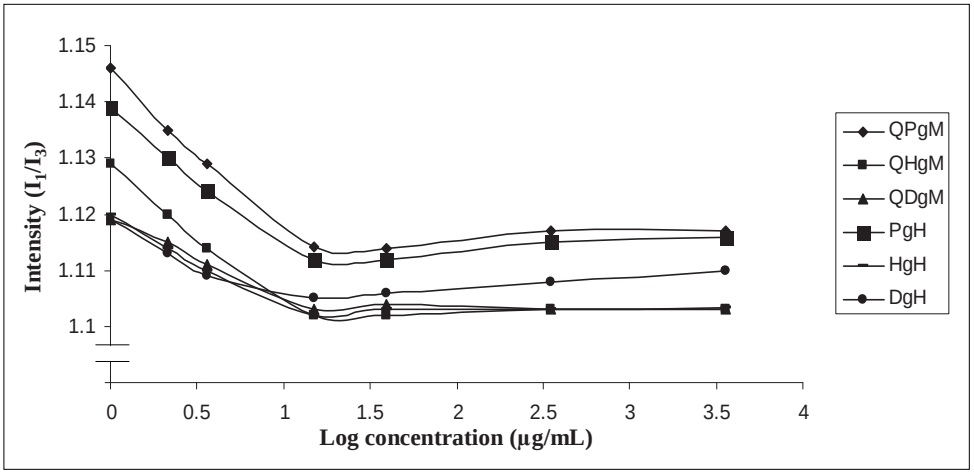

รูปที่ 1.18 กราฟแสดงความสัมพันธ์ระหว่าง I_{373}/I_{384} ของไพรีน และ log ความเข้มข้นของสารละลายแอมฟิฟิลิกไคโทซานชนิดต่างๆ

ตารางที่ 1.11 CMC ของแอมฟิฟิลิกไคโทซานชนิดต่างๆ

Sample	CMC (µg/mL)
QPgM	15.9
QHgM	16.9
QDgM	12.6
PgH	13.6
HgH	10.0
DgH	7.10

จากการวิเคราะห์ด้วยเทคนิค SEM พบว่าอนุภาคแอมฟิฟิลิกไคโทซานทุกชนิดมีลักษณะเป็นทรงกลม (**รูปที่ 1.19**) มีเส้นผ่าศูนย์กลางอยู่ในช่วง 0.11 ถึง 0.29 ไมโครเมตร (**ตารางที่ 1.12**) ซึ่งเป็นขนาดที่เล็กกว่าที่วิเคราะห์ได้ด้วยเทคนิค PCS ซึ่งอยู่ในช่วง 1.29 ถึง 3.10 ไมโครเมตร ทั้งนี้น่าจะเป็นสาเหตุจากที่การวิเคราะห์ด้วยเทคนิค PCS เป็นการวัด hydrodynamic size ที่วิเคราะห์ในสารละลายซึ่งมีผลของการบวมตัวเข้ามาเกี่ยวข้อง จึงทำให้ได้ขนาดของอนุภาคใหญ่กว่าที่ได้จากการวิเคราะห์ด้วยเทคนิค SEM ซึ่งทำในสภาวะแห้งภายใต้บรรยากาศลดความดัน นอกจากนี้ยังเป็นที่สังเกตเห็นได้ว่าอนุภาคที่มีหมู่ชอบน้ำเป็น $mPEG_{5000}$ มีขนาดเล็กกว่า

อนุภาคที่มีหมู่ชอบน้ำเป็น HTAP ทั้งนี้สันนิษฐานว่าน่าจะเป็นผลเนื่องมาจากพันธะไฮโดรเจนระหว่างโซ่ยาวของ $mPEG_{5000}$ ทำให้หมู่ไม่ชอบน้ำจัดตัวในแกนกลางได้มีประสิทธิภาพและแน่นกว่าหมู่ HTAP

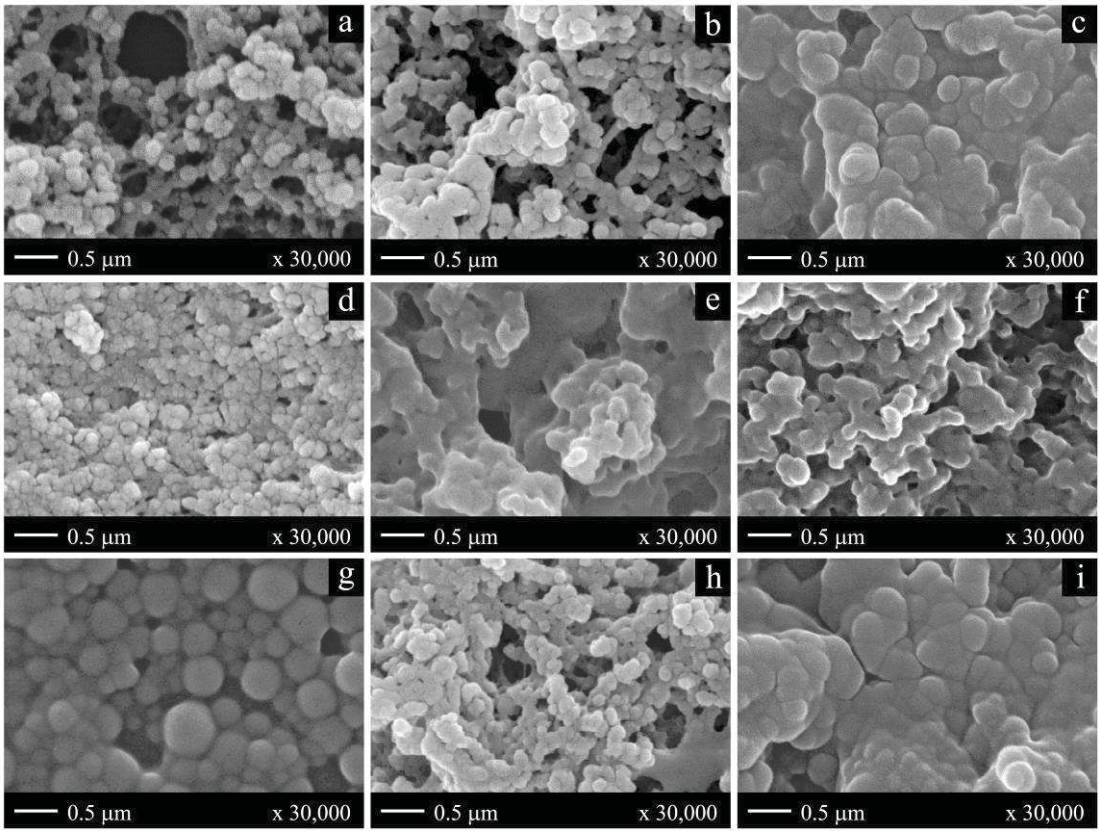

รูปที่ 1.19 เอสอีเอ็มไมโครกราฟของอนุภาคแอมฟิฟิลิกไคโทซานชนิดต่างๆ: (a) PgM, (b) HgM, (c) DgM, (d) QPgM, (e) QHgM, (f) QDgM, (g) PgH, (h) HgH และ (i) DgH

ตารางที่ 1.12 ขนาดของอนุภาคแอมฟิฟิลิกไคโทซานที่วิเคราะห์ด้วยเทคนิค SEM และ PCS

Particles	Size (μm)	
	SEM	PCS
PgM	0.11±0.03	2.24
HgM	0.14±0.03	2.67
DgM	0.25±0.05	2.89
QPgM	0.13±0.03	1.29
QHgM	0.17±0.05	1.78
QDgM	0.19±0.04	1.85
PgH	0.29±0.04	3.10
HgH	0.21±0.02	2.10
DgH	0.26±0.02	2.95

จากการศึกษาที่ผ่านมาพบว่ามีเพียงอนุภาคชนิดที่มีหมู่ชอบน้ำเป็น *N*-[(2-hydroxyl-3-trimethylammonium)propyl] (HTAP) และหมู่ไม่ชอบน้ำเป็นเฮกซิลและโดเดคซิลเท่านั้นที่แสดงประจุเป็นบวก โดยแทนด้วยสัญลักษณ์ของอนุภาคเป็น HgH และ DgH ตามลำดับ ดังนั้นจึงเลือกทดสอบการใช้อนุภาค HgH เป็นตัวแลกเปลี่ยนไอออนในการวิเคราะห์ลำดับเบสของดีเอ็นเอควบคู่กับพีเอ็นเอโพรบซึ่งในที่นี้เลือกศึกษากับระบบที่มีลำดับเบสไม่ซับซ้อนก่อนคือ พีเอ็นเอชนิด T9 และดีเอ็นเอชนิด A9 ทั้งนี้จะทำเปรียบเทียบกับอนุภาค PgH ซึ่งแสดงประจุเป็นลบ โดยอนุภาคชนิดนี้มีหมู่ชอบน้ำเป็น HTAP และหมู่ไม่ชอบน้ำชนิดทาโลอิล

จากการทดสอบพบว่าอนุภาคทั้งสองไม่เกิดการจับอย่างไม่จำเพาะเจาะจงกับพีเอ็นเอชนิด T9 จึงไม่ปรากฏสัญญาณของพีเอ็นเอชนิด T9 หลังจากวิเคราะห์ด้วยเทคนิคมัลดิทอฟแมสสเปกโทรเมทรี (**รูปที่ 1.20b และ 1.21b**) จากนั้นเมื่อทำการเติมดีเอ็นเอที่มีลำดับเบส A9 ซึ่งเป็นดีเอ็นเอคู่สมกับพีเอ็นเอชนิด T9 ซึ่งจากสมมติฐานที่ว่าเมื่อพีเอ็นเอและดีเอ็นเอมีลำดับเบสที่เป็นคู่สมเกิดการเข้าคู่อย่างสมบูรณ์แล้วนั้น อนุภาคควอเทอร์ไนซ์ไคโทซานซึ่งมีประจุบวกที่พื้นผิวจะสามารถจับกับประจุลบบนสายดีเอ็นเอคู่สมได้ และจะปรากฏสัญญาณของพีเอ็นเอชนิด T9 แต่จากการทดลองพบว่าไม่ปรากฏสัญญาณของพีเอ็นเอชนิด T9 บนอนุภาคชนิด PgH แต่จะพบสัญญาณต่ำมากในกรณีของอนุภาค HgH (**รูปที่ 1.20d และ 1.21d**) ในขณะที่ยังสามารถตรวจพบสัญญาณของพีเอ็นเอชนิด T9 ในสารละลายล้างอนุภาคทั้งในกรณีที่มีดีเอ็นเอคู่สม (**รูปที่ 1.20c และ 1.21c**) และดีเอ็นเอที่มีลำดับเบสผิดไป 1 ตำแหน่ง แสดงว่ายังคงมีพีเอ็นเอในสารละลาย (**รูปที่ 1.20e และ 1.21e**) ข้อมูลในส่วนนี้แสดงให้เห็นว่าอนุภาคควอเทอร์ไนซ์ไคโทซานไม่สามารถจับกับดีเอ็นเอได้ จึงไม่สามารถทำหน้าที่เป็นตัวแลกเปลี่ยนแอนไอออนในการวิเคราะห์ลำดับเบสของดีเอ็นเอได้ ทั้งนี้คาดว่าอาจเกิดจากการที่อนุภาคชนิด PgH มีส่วนไม่ชอบน้ำเป็นหมู่ทาโลอิลซึ่งจากผลการทดลองที่กล่าวมาข้างต้นพบว่าอนุภาคชนิดนี้มีประจุเป็นลบเนื่องจากการแทนที่ที่ตำแหน่งของหมู่ไฮดรอกซิลของไคโทซานทำให้ได้ผลิตภัณฑ์เป็นแอนไฮไดร์ดแบบวงซึ่งไม่เสถียรและแตกออกเป็นหมู่คาร์บอกซิล (pKa 4.4) ที่สามารถแตกตัวเป็นหมู่คาร์บอกซิเลตที่มีประจุเป็นลบ ส่งผลให้เกิดการผลักกันกับดีเอ็นเอที่มีประจุลบนั่นเอง ในขณะที่อนุภาคควอเทอร์ไนซ์ไคโทซานชนิด HgH ปรากฏสัญญาณเพียงเล็กน้อย คาดว่าอาจเป็นผลจากการที่อนุภาคดังกล่าวตกตะกอนกับเมทริกซ์คือ (*α*-cyano-4-hydroxycinnamic acid (CCA) ใน 0.1% TFA ในสารละลาย acetonitrile/water (1:1)) ได้ไม่สมบูรณ์ จึงส่งผลให้ได้ประสิทธิภาพของการวิเคราะห์ต่ำนั่นเอง

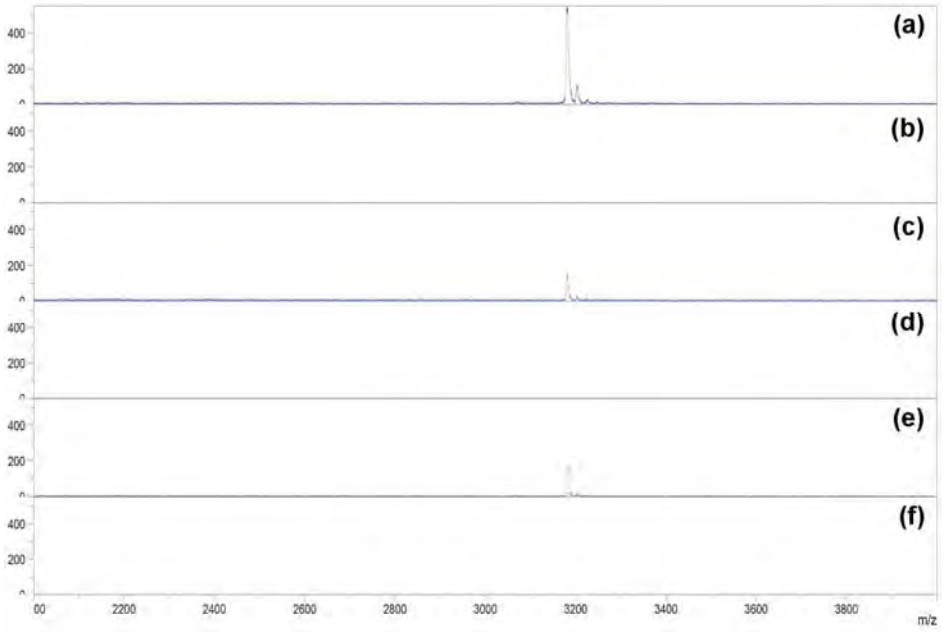

รูปที่ 1.20 แมสสเปกตรัมที่วิเคราะห์ด้วยเทคนิคมัลดิทอฟแมสสเปกโทรเมทรีของอนุภาค PgH, PNA_T9, DNA_A9 (ดีเอ็นเอคู่สม) และ DNA_A4CA4 (ดีเอ็นเอที่มีลำดับเบสผิดไป 1 ตำแหน่ง): (a) สารละลายล้างอนุภาคที่มีพีเอ็นเอแต่ปราศจากดีเอ็นเอคู่สม (control solution), (b) อนุภาคที่มีพีเอ็นเอแต่ปราศจากดีเอ็นเอคู่สม (control solid), (c) สารละลายล้างอนุภาคที่มีพีเอ็นเอและดีเอ็นเอคู่สม (PNA_T9+DNA_A9 solution), (d) อนุภาคที่มีพีเอ็นเอและดีเอ็นเอคู่สม (PNA_T9+DNA_A9 solid), (e) สารละลายล้างอนุภาคที่มีพีเอ็นเอและดีเอ็นเอที่มีลำดับเบสผิดไป 1 ตำแหน่ง (PNA_T9+DNA_A4CA4 solution), (f) อนุภาคที่มีพีเอ็นเอและดีเอ็นเอที่มีลำดับเบสผิดไป 1 ตำแหน่ง (PNA_T9+DNA_A4CA4 solid)

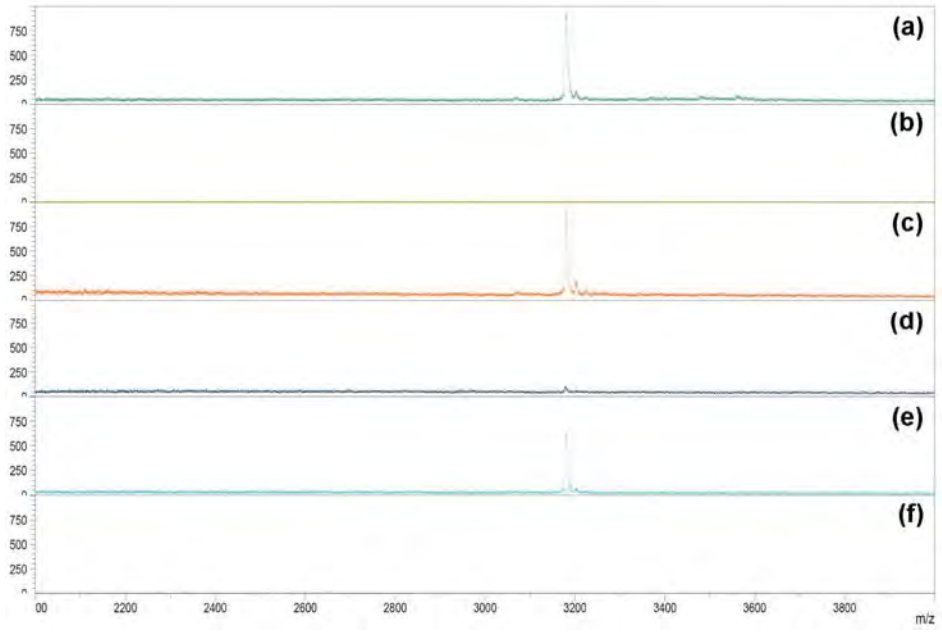

รูปที่ 1.21 แมสสเปกตรัมที่วิเคราะห์ด้วยเทคนิคมัลดิทอฟแมสสเปกโทรเมทรีของอนุภาค HgH, PNA_T9, DNA_A9 (ดีเอ็นเอคู่สม) และ DNA_A4CA4 (ดีเอ็นเอที่มีลำดับเบสผิดไป 1 ตำแหน่ง): (a) สารละลายล้างอนุภาคที่มีพีเอ็นเอแต่ปราศจากดีเอ็นเอคู่สม (control solution), (b) อนุภาคที่มีพีเอ็นเอแต่ปราศจากดีเอ็นเอคู่สม (control solid), (c) สารละลายล้างอนุภาคที่มีพีเอ็นเอและดีเอ็นเอคู่สม (PNA_T9+DNA_A9 solution), (d) อนุภาคที่มีพีเอ็นเอและดีเอ็นเอคู่สม (PNA_T9+DNA_A9 solid), (e) สารละลายล้างอนุภาคที่มีพีเอ็นเอและดีเอ็นเอที่มีลำดับเบสผิดไป 1 ตำแหน่ง (PNA_T9+DNA_A4CA4 solution), (f) อนุภาคที่มีพีเอ็นเอและดีเอ็นเอที่มีลำดับเบสผิดไป 1 ตำแหน่ง (PNA_T9+DNA_A4CA4 solid)

จากผลการทดลองข้างต้นพบว่าอนุภาคแอมฟิฟิลิกไคโทซานที่เตรียมได้ไม่มีประสิทธิภาพในการนำไปประยุกต์ใช้เป็นตัวแลกเปลี่ยนแอนไอออนสำหรับการตรวจลำดับเบสของดีเอ็นเอควบคู่กับพีเอ็นเอโพรบด้วยเทคนิคมัลติทอฟแมสสเปกโทรเมทรี แต่เพื่อเป็นการใช้ประโยชน์จากองค์ความรู้ที่ได้จากการศึกษาการเตรียมอนุภาคแอมฟิฟิลิกไคโทซานชนิดต่าง ๆที่กล่าวมาแล้ว คณะผู้วิจัยจึงเกิดแนวคิดที่จะนำอนุภาคที่เตรียมได้ไปประยุกต์ใช้กับงานวิจัยด้านอื่น เนื่องจากอนุภาคที่เตรียมได้โดยเฉพาะอย่างยิ่งชนิดที่มีหมู่ชอบน้ำเป็น HTAP มีประจุเป็นบวกและการที่แกนกลาง (core) ของอนุภาคเป็นหมู่ไม่ชอบน้ำ จึงอาจนำไปใช้เป็นวัสดุห่อหุ้มสารว่องไวทางชีวภาพ (bioactive compound) และนำส่งสารดังกล่าวเข้าสู่เซลล์เป้าหมายได้ ทั้งนี้คณะผู้วิจัยได้มีแนวคิดในการติดหมู่ฟังก์ชันที่เป็นสารเรืองแสงเพิ่มเติมเข้าไปที่อนุภาคแอมฟิฟิลิกไคโทซานที่มี HTAP เป็นหมู่ชอบน้ำเพื่อใช้ในการตรวจติดตามการนำเข้าสู่เซลล์เป้าหมาย ทั้งนี้ได้ออกแบบวิธีการเตรียมอนุภาคควอเทอร์ไนซ์ไคโทซานที่ติดฉลากเรืองแสงแสดงรายละเอียดตามแผนภาพใน**รูปที่ 1.22** โดยอาศัยโครงสร้างโมเลกุลของสารเรืองแสงชนิดไพรีน (pyrene) เป็นส่วนที่ไม่ชอบน้ำ ซึ่งตรึงบนโซ่หลักของไคโทซานผ่านปฏิกิริยาคลิก (click reaction) โดยปฏิกิริยาคลิกที่สนใจนำมาใช้คือ ปฏิกิริยาการปิดวงของฮุสเกนที่ใช้โลหะคอปเปอร์เป็นตัวเร่งปฏิกิริยา (copper-catalyzed Huisgen's 1,3-dipolar cycloaddition) ซึ่งในที่นี้จะเป็นการทำปฏิกิริยาระหว่างหมู่เอไซด์บนไคโทซานและแอลไคน์ที่ปลายของไพรีน ในที่นี้จะใช้อนุพันธ์ของไคโทซานที่มีหมู่ไม่ชอบน้ำ คือ phthaloyl เป็นสารตั้งต้นแล้วทำการดัดแปรหมู่หมู่ไฮดรอกซิลบนคาร์บอนตำแหน่งที่ 6 ของไคโทซานให้เป็นเอไซด์ ผ่านปฏิกิริยาโบรมิเนชัน (bromination) และ เอซิเดชัน (azidation) ตามลำดับ ซึ่งมีความเหมาะสมในการเกิดปฏิกิริยาคลิกกับสารเรืองแสงชนิดเอไทนิลไพรีน (1-ethynylpyrene) หลังจากนั้นจะทำปฏิกิริยาไฮโดรไลซิสเพื่อกำจัดหมู่ phthaloyl และได้หมู่แอมิโนกลับคืนมาพร้อมที่จะทำปฏิกิริยาเปิดวงของ GTMAC เพื่อให้ได้หมู่ควอเทอร์นารีชนิด HTAP ที่ผิวของอนุภาคหลังจากไดอะไลซิสในน้ำแล้ว

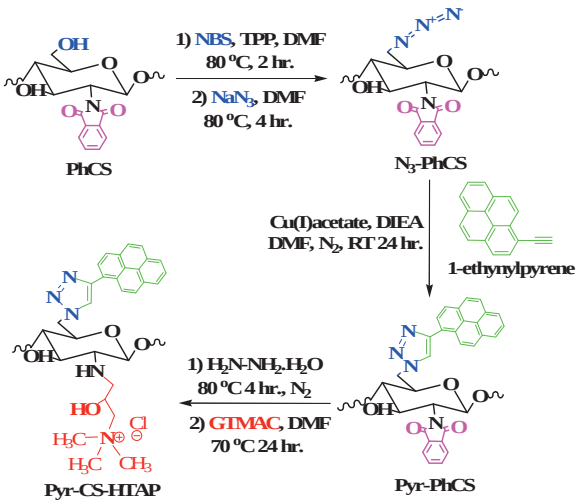

รูปที่ 1.22 สมการแสดงขั้นตอนการสังเคราะห์แอมฟิฟิลิกไคโทซานที่ติดฉลากเรืองแสง

จากการวิเคราะห์ด้วยเทคนิค FT-IR ดังแสดงผลใน**รูปที่ 1.23** พบสัญญาณที่เป็นลักษณะเฉพาะของหมู่เอไซด์ในโครงสร้างของไคโทซานที่ติดหมู่ทาโลอิลและดัดแปรให้มีหมู่เอไซด์ (N_3-PhCS) ที่เลขคลื่น 2100 cm^{-1} โดยสัญญาณดังกล่าวจะหายไปหลังจากการทำปฏิกิริยาคลิกกับเอไทนิลไพรีน ทำให้ได้อนุพันธ์ที่ติดฉลากด้วยสารเรืองแสงคือ Pyr-CS-HTAP การปรากฏของสัญญาณจาก C-H stretching ของหมู่ $-N(CH_3)_3$ ที่ 1480 cm^{-1} และการหายไปของ C=O stretching ที่ตำแหน่ง 1700 cm^{-1} ซึ่งพบในไคโทซานที่ติดหมู่ทาโลอิล (PhCS) ในสเปกตรัม

ของ Pyr-CS-HTAP ช่วยยืนยันความสำเร็จของการติดหมู่ HTAP และความสมบูรณ์ของการกำจัดหมู่ทาโลอิล ตามลำดับ

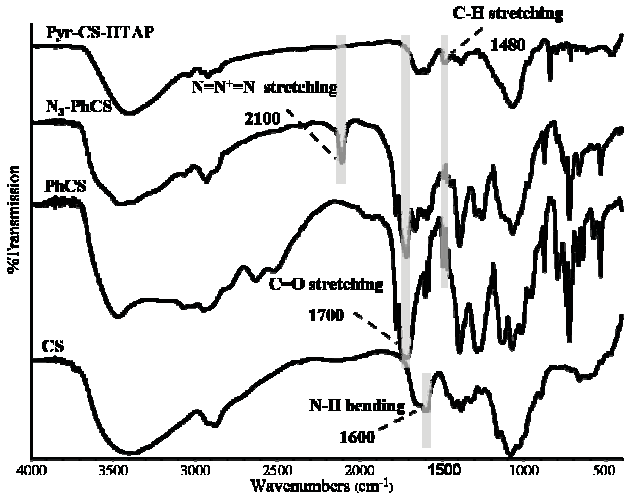

รูปที่ 1.23 เอฟทีไออาร์สเปกตรัมของ chitosan (CS), PhCS, N_3-PhCS และ Pyr-CS-HTAP

จากการวิเคราะห์ด้วยเทคนิค SEM พบว่าอนุภาคควอเทอร์ไนซ์ไคโทซานชนิด Pyr-CS-HTAP มีลักษณะคล้ายลูกแบล็คเบอร์รี่ (blackberry-like) มีเส้นผ่าศูนย์กลางขนาด 1.17±0.46 ไมโครเมตร (**รูปที่ 1.24a**) จากการวิเคราะห์ด้วยเทคนิค photon correlation spectroscopy พบว่าอนุภาคมีประจุเป็นบวก มีค่า zeta-potential เท่ากับ +49.6 mV และพบการเรืองแสงสีเขียวเมื่อส่องผ่านกล้องฟลูออเรสเซนต์ไมโครสโกป (**รูปที่ 1.24b**) แสดงว่ามีสารเรืองแสงอยู่ในอนุภาคจริง

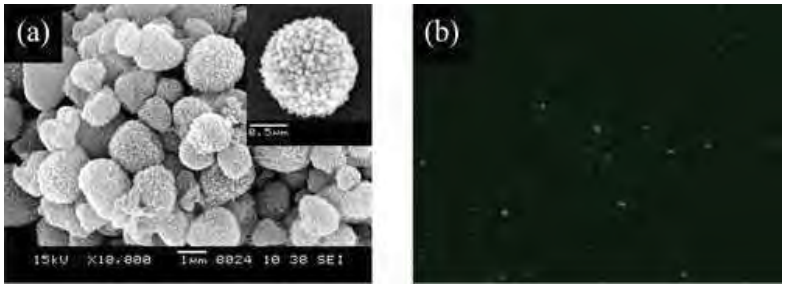

รูปที่ 1.24 เอสอีเอ็ม (a) และฟลูออเรสเซนต์ (b) ไมโครกราฟของอนุภาค Pyr-CS-HTAP

นอกจากนี้ยังพบว่าอนุภาค Pyr-CS-HTAP มีเสถียรภาพดี ไม่เกิดการเปลี่ยนแปลงสัณฐานวิทยาภายใต้การเปลี่ยนแปลงอุณหภูมิในช่วง 0 ถึง 100°C และการเปลี่ยนแปลงพีเอชจาก 1 เป็น 4, 10 และ 12 จะเกิดการแตกออกของอนุภาคเมื่ออยู่ในตัวทำละลายไม่มีขั้ว เช่น เฮกเซน แต่ก็จะได้อนุภาคที่มีลักษณะคล้ายลูกแบล็คเบอร์รี่กลับคืนมาเมื่อกำจัดเฮกเซนและเติมน้ำแสดงให้เห็นว่าการประกอบตัวเองเป็นกระบวนการที่ผันกลับได้ ดังแสดงผลใน**รูปที่ 1.25**

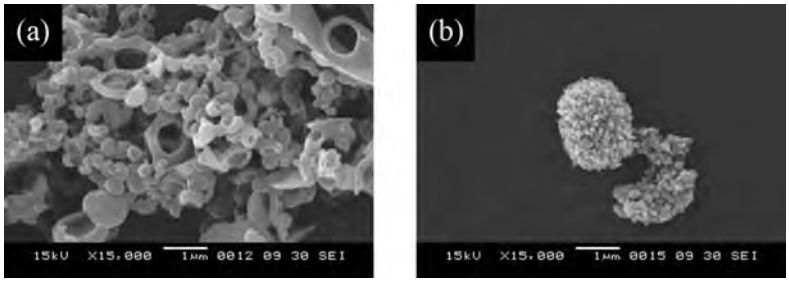

รูปที่ 1.25 เอสอีเอ็มไมโครกราฟของอนุภาค Pyr-CS-HTAP (a) หลังการเติมเฮกเซน และ (b) หลังการกำจัดเฮกเซนและเติมน้ำ

จากการทดสอบด้วย MTT assay พบว่าอนุภาค Pyr-CS-HTAP ไม่เป็นพิษต่อ mouse leukeamic monocyte macrophage cell line (RAW 264.7 cells) เซลล์ยังคงมีการเจริญเติบโตเป็นปกติในสภาวะที่มีความเข้มข้นสูงถึงประมาณ 10 μg/mL จากนั้นจึงตรวจติดตามการเข้าสู่เซลล์ชนิดเดียวกันของอนุภาคด้วยเทคนิค confocal laser scanning microscopy (CLSM) ทั้งนี้จะใช้การย้อมนิวเครียสของเซลล์ด้วย DAPI ซึ่งมีสีน้ำเงินจากภาพในคอลัมน์แรกใน**รูปที่ 1.26a** ซึ่งเป็นภาพถ่ายรวมหลังจากเติมอนุภาคเข้าไปในเซลล์เป็นเวลา 4 ชั่วโมง จะสังเกตเห็นสีน้ำเงินเป็นหลักซึ่งแสดงขอบเขตที่เป็นนิวเครียสของแต่ละเซลล์ เมื่อนำภาพดังกล่าวมาแยกเป็น DAPI channel และ pyrene channel จะเห็นการปรากฏสีเขียวซึ่งเป็นของไพรีนบริเวณเดียวกันกับที่ปรากฏสีน้ำเงิน แสดงให้เห็นว่าอนุภาคสามารถเข้าไปอยู่ภายในนิวเครียสของเซลล์ได้ อย่างไรก็ตามจะปรากฏจุดสีแดงซึ่งเป็นของไพรีนเช่นกันอยู่ภายนอกนิวเครียส ผลการทดลองปรากฏชัดมากขึ้นจากการใช้กำลังขยายสูงขึ้นหลังจากเวลาผ่านไป 24 ชั่วโมง (**รูปที่ 1.26b)** การปรากฏทั้งสีเขียวและแดงของไพรีนดังแสดง emission spectrum ใน**รูปที่ 1.27** คาดว่าเป็นผลจากการร่วมกลุ่มของอนุภาคซึ่งจะทำให้เกิดปรากฏการณ์ red shift ด้วยเหตุนี้ผู้วิจัยสันนิษฐานว่ามีเพียงอนุภาคที่มีขนาดเล็กซึ่งแสดงสีเขียวเท่านั้นที่สามารถเข้าสู่นิวเครียสได้ ส่วนอนุภาคที่เกิดการรวมกลุ่มและมีขนาดใหญ่กว่าซึ่งปรากฏเป็นสีแดงจะไม่สามารถเข้าสู่นิวเครียสได้ แต่จะอยู่ในบริเวณไซโตพลาสซึมของเซลล์ได้เท่านั้น

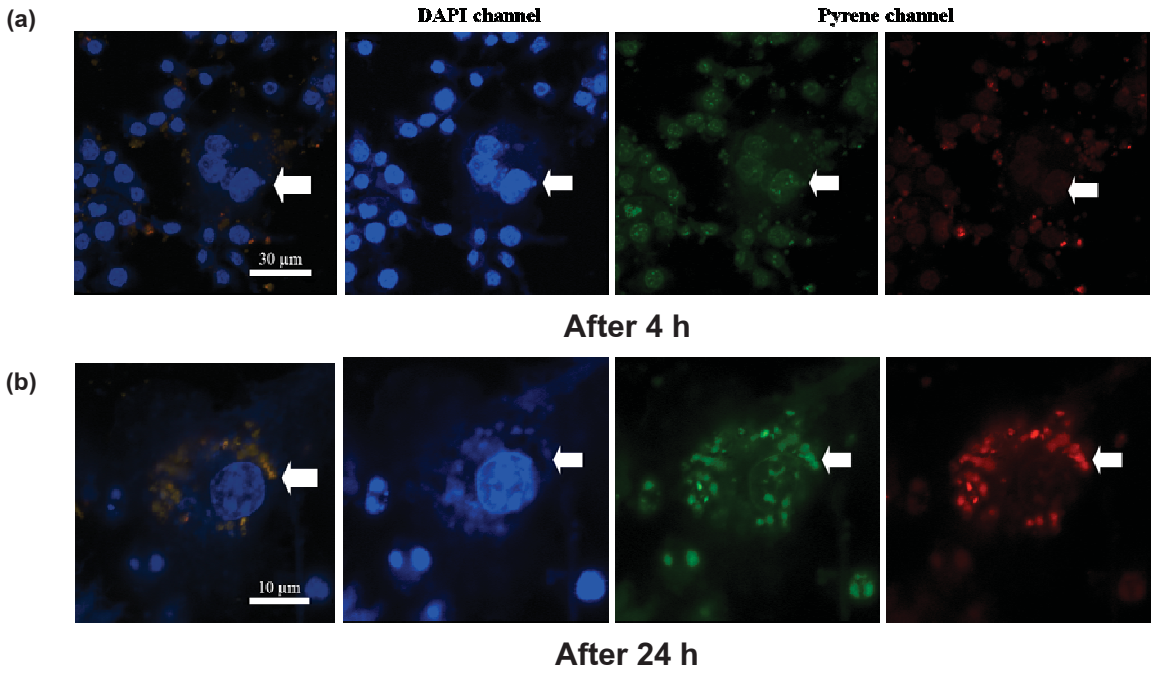

รูปที่ 1.26 Confocal fluorescence images ของอนุภาค Pyr-CS-HTAP และ RAW 264.7 cells หลังจากการผสมกันเป็นเวลา (a) 4 h และ (b) 8 h

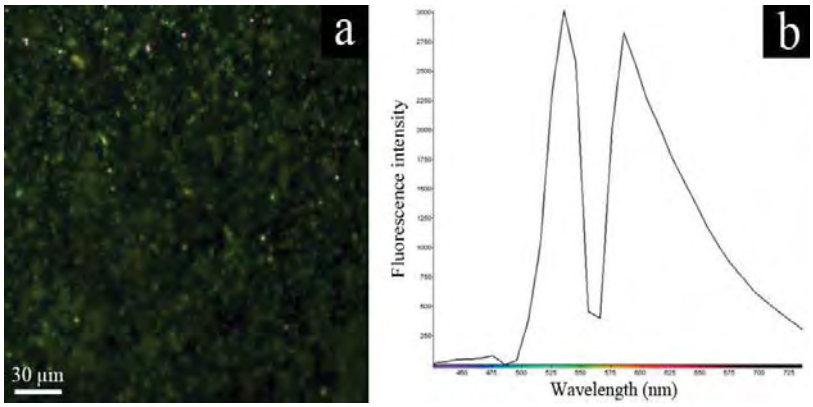

รูปที่ 1.27 Confocal fluorescence image (a) และ emission spectrum (b) ของอนุภาค Pyr-CS-HTAP ที่เป็นของแข็ง Scale bar = 30 µm at magnification 100x.

สรุปผลการดำเนินงานวิจัย

งานวิจัยที่ได้ดำเนินการศึกษาวิจัยในตอนที่ 1 นี้แสดงให้เห็นว่าสามารถใช้อนุภาคไคโทซานชนิด MC, TMC และ HTACC ร่วมกับโพรบที่เป็น acpc PNA ในการตรวจลำดับเบสของดีเอ็นเอที่มีลำดับเบสที่สัมพันธ์กับตำแหน่งที่แสดงความผิดปกติของยีนในผู้ป่วยโรคมะเร็ง ซึ่งมีความยาว 14 เมอร์ และมีเบสผสมได้ โดยอนุภาค MC และ TMC ให้ประสิทธิภาพในการวิเคราะห์ที่ดีกล่าวคือ ให้สัญญาณของพีเอ็นเอที่สูงในกรณีที่เป็นโมเลกุลลูกผสมที่มีลำดับเบสเป็นคู่สมกัน และสามารถกำจัดแรงกระทำอย่างไม่จำเพาะเจาะจงของโมเลกุลลูกผสมที่มีลำดับเบสผิดไปหนึ่งตำแหน่งได้ หลังจากการล้างด้วยสารละลาย 20% formamide ใน 10 mM sodium phosphate buffer pH 7 และ น้ำ MilliQ

นอกจากนี้ยังสามารถเตรียมอนุภาคไคโทซานโดยการประกอบตัวเองของแอมฟิฟิลิกไคโทซานที่มีหมู่ไม่ชอบน้ำชนิดทาโลอิล เฮกซิล และโดเดคซิล และมีหมู่ชอบน้ำเป็น $mPEG_{5000}$ และ HTAP ได้จากการพิสูจน์เอกลักษณ์ด้วยเทคนิค ^{1}H NMR และ IR โดยสัดส่วนการแทนที่ของหมู่ทั้งสองประเภทแปรเปลี่ยนได้ตามอัตราส่วนโดยโมลของรีเอเจนต์ที่ใช้ในการทำปฏิกิริยาแต่ละขั้นตอน ทั้งนี้พบว่าอนุภาคที่มี HTAP เป็นหมู่ชอบน้ำมีสัดส่วนของหมู่ควอเทอร์นารีแอมโมเนียมที่สูงกว่าอนุภาคที่มีหมู่ $mPEG_{5000}$ เป็นหมู่ชอบน้ำ แอมฟิฟิลิกไคโทซานที่เตรียมได้มีค่า CMC อยู่ในช่วง 7.1-16.9 µg/mL และอนุภาคที่มี HTAP เป็นหมู่ชอบน้ำจะมีค่า CMC ต่ำกว่าอนุภาคที่มีหมู่ชอบน้ำเป็น $mPEG_{5000}$ ในกรณีที่มีหมู่ไม่ชอบน้ำชนิดเดียวกัน จากการวิเคราะห์ด้วยเทคนิค SEM พบว่าอนุภาคแอมฟิฟิลิกไคโทซานทุกชนิดมีลักษณะเป็นทรงกลม มีเส้นผ่าศูนย์กลางอยู่ในช่วง 0.11 ถึง 0.29 และพบว่ามีเพียงอนุภาคชนิดที่มีหมู่ชอบน้ำเป็น HTAP และหมู่ไม่ชอบน้ำเป็นเฮกซิลและโดเดคซิลเท่านั้นที่แสดงประจุเป็นบวก จากการนำอนุภาคที่มีประจุบวกไปทดสอบพบว่าไม่มีประสิทธิภาพในการนำไปประยุกต์ใช้เป็นตัวแลกเปลี่ยนแอนไอออนสำหรับการตรวจลำดับเบสของดีเอ็นเอควบคู่กับพีเอ็นเอโพรบด้วยเทคนิคมัลดิทอฟแมสสเปกโทรเมทรี อย่างไรก็ตามคณะผู้วิจัยได้ต่อยอดองค์ความรู้ที่ได้จากการศึกษาที่ผ่านมาไปใช้ในการเตรียมอนุภาคแอมฟิฟิลิกไคโทซานที่ติดฉลากเรืองแสงของไพรีน ซึ่งให้ผลการทดลองที่น่าสนใจกล่าวคือ อนุภาคที่เตรียมได้มีลักษณะคล้ายลูกแบล็คเบอร์รี่ สามารถเรืองแสงฟลูออเรสเซนต์ มีประจุเป็นบวก และมีเสถียรภาพดี จากการศึกษาสมบัติการตอบสนองทางชีวภาพเบื้องต้นกับ mouse leukeamic monocyte macrophage cell line (RAW 264.7 cells) พบว่าอนุภาคไม่เป็นพิษต่อเซลล์ และสามารถนำเข้าสู่นิวเครียสของเซลล์ แสดงให้เห็นถึงศักยภาพในการนำไปประยุกต์ใช้เป็นพาหะในการนำส่งสารสำคัญทางชีวภาพ (bioactive carrier) เข้าสู่เซลล์หรือใช้ติดตามกระบวนการที่เกิดขึ้นภายในเซลล์ (bioimaging) ได้ต่อไป

<u>ตอนที่ 2</u> การตรวจลำดับเบสของดีเอ็นเอโดยใช้กระดาษกรองที่ตรึงด้วยพอลิเมอร์บรัชที่มีประจุบวกร่วมกับเพปไทด์นิวคลีอิกแอซิดอาศัยหลักการของ “Dot Blotting”

สำหรับงานวิจัยในตอนที่ 2 ได้รับแนวคิดมาจากวิธีการวิเคราะห์สารชีวโมเลกุลที่นิยมใช้ทางชีวเคมีและพันธุศาสตร์ที่เรียกว่า “Dot Blot” ซึ่งอาศัยการหยด (blotting) ดีเอ็นเอที่ต้องการวิเคราะห์ในลักษณะที่เป็นจุด (dot) ลงบนแผ่นเมมเบรนที่มีประจุเป็นบวกซึ่งทำจากแผ่นกระดาษหรือไนลอน จากนั้นจึงนำไปจับยึดกับดีเอ็นเอโพรบ (ในงานวิจัยนี้ใช้ acpc PNA เป็นโพรบ) ซึ่งส่วนใหญ่จะมีการติดฉลากด้วยสารที่สามารถให้สัญญาณในการตรวจวิเคราะห์ด้วยเทคนิคต่างๆได้ เนื่องจากสามารถหยดสารตัวอย่างหลายชนิดเป็นจุดลงบนแผ่นเมมเบรนเดียวกันได้ ทำให้กระบวนการ “Dot Blot” นี้สามารถพัฒนาไปสู่การตรวจวิเคราะห์ในรูปแบบที่มีประสิทธิภาพสูงได้โดยง่าย จากการที่ทางคณะผู้วิจัยมีประสบการณ์ในการดัดแปรพื้นผิววัสดุด้วยการตรึงพอลิเมอร์บรัชผ่านการริเริ่มปฏิกิริยาพอลิเมอไรเซชันจากพื้นผิว จึงมีแนวคิดที่จะใช้วิธีการดังกล่าวในการเตรียมแผ่นกระดาษสำหรับการทำ “Dot Blot” โดยการเลือกพอลิเมอร์ที่มีประจุบวก คือ ควอเทอไนซ์พอลิ(2-ไดเมทิลอะมิโน)เอทิลเมทาคริเลต หรือ quarternized poly(2-(dimethylamino)ethyl methacrylate) (QPDMAEMA) ซึ่งสามารถจับยึดกับดีเอ็นเอผ่านแรงกระทำระหว่างประจุได้ การนำเอาปฏิกิริยาพอลิเมอไรเซชันแบบอมตะมาใช้ในการเตรียมพอลิเมอร์บรัชทำให้สามารถควบคุมความหนาแน่นของประจุบวกที่ขึ้นกับความยาวของโซ่พอลิเมอร์ที่ตรึงบนพื้นผิวรวมทั้งความชอบน้ำ (hydrophilicity) ของแผ่นกระดาษ ที่เป็นปัจจัยสำคัญในการกำหนดประสิทธิภาพในการจับยึดกับดีเอ็นเอ รวมทั้งความสามารถในการป้องกันการดูดซับอย่างไม่จำเพาะเจาะจง (nonspecific adsorption) ขององค์ประกอบอื่นที่อาจปนมากับดีเอ็นเอโดยเฉพาะอย่างยิ่งที่สกัดมาจากสารตัวอย่างจริง ที่อาจจะไม่ได้ผ่านขั้นตอนการแยกให้บริสุทธิ์ด้วยเทคนิคทางโครมาโทกราฟีหรืออิเล็กโทรโฟริซิสก่อนนำมาวิเคราะห์

ปฏิกิริยาพอลิเมอไรเซชันที่เลือกนำมาใช้ในงานวิจัยนี้คือ Activator Regenerated by Electron Transfer-Atom Transfer Radical Polymerization (ARGET ATRP) ซึ่งเป็นปฏิกิริยาพอลิเมอไรเซชันที่มีกลไกเป็นแบบอมตะ สามารถเกิดขึ้นได้ภายใต้สภาวะที่มีออกซิเจน โดยมีการเติมตัวเร่งปฏิกิริยาที่เป็นสารประกอบประเภทคอปเปอร์ซึ่งมีราคาไม่แพง ทำให้การสังเคราะห์ทำได้สะดวกและไม่ยุ่งยาก สำหรับการวิเคราะห์นั้นคณะผู้วิจัยเลือกใช้การตรวจวัดการจับยึดระหว่างดีเอ็นเอและพีเอ็นเอโพรบจากการสังเกตสีด้วยตาเปล่าที่ทำให้เกิดได้โดยอาศัยเอนไซม์ ซึ่งในที่นี้จะใช้ สเตรปทาวิดินที่ติดฉลากด้วยเอนไซม์เอชอาร์พี (HRP-labeled streptavidin) หรือ SA-HRP ร่วมกับพีเอ็นเอโพรบที่มีไบโอติน (biotinylated PNA probe) หรือ b-PNA และสับสเตรท o-phenylenediamine dihydrochloride (OPD) และ Urea hydrogen peroxide (Urea-H_2O_2) หลักการในการวิเคราะห์แสดงดัง**รูปที่ 2.1**

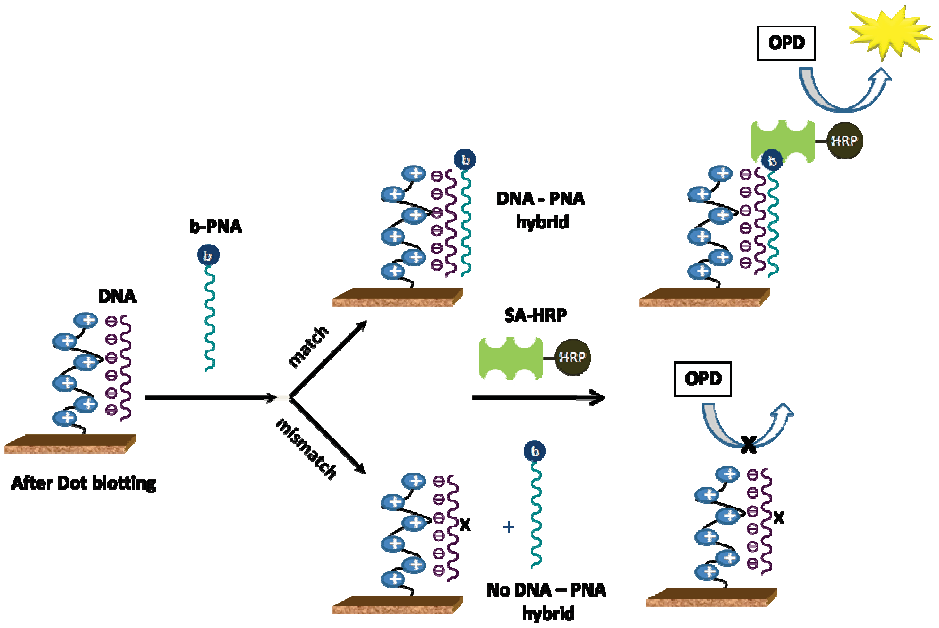

รูปที่ 2.1 แผนภาพแสดงแนวทางในการวิเคราะห์ลำดับเบสของดีเอ็นเอด้วย acpc PNA และการทำให้เกิดสีด้วยเอนไซม์

จากแนวทางการวิเคราะห์ที่แสดงใน**รูปที่ 2.1** ขั้นตอนแรกที่ต้องดำเนินการคือ การตรึงพอลิเมอร์บรัชที่มีประจุบวกคือ ควอเทอไนซ์พอลิ(2-ไดเมทิลอะมิโน)เอทิลเมทาคริเลต หรือ quarternized poly(2-(dimethylamino)ethyl methacrylate) (PQDMAEMA) ลงบนกระดาษกรอง โดยก่อนที่จะทำการตรึงพอลิเมอร์ดังกล่าวจำเป็นต้องศึกษาหาภาวะที่เหมาะสมในการทำปฏิกิริยาพอลิเมอไรเซชันของมอนอเมอร์คือ -dimethylamino) ethyl methacrylate (DMAEMA) ในสารละลายก่อน ปฏิกิริยาพอลิเมอไรเซชันที่ใช้ในงานวิจัยคือ Activator Regenerated by Electron Transfer-Atom Transfer Radical Polymerization (ARGET ATRP) ซึ่งมีกลไกแสดงดัง**รูปที่ 2.2** ปฏิกิริยา ARGET ATRP ได้รับการพัฒนามาจากปฏิกิริยาพอลิเมอไรเซชันแบบ ATRP ซึ่งระบบริเริ่มปฏิกิริยาประกอบด้วยสารประกอบเฮไลด์และโลหะแทรนซิชันทำหน้าที่เป็นพาหะให้กับอะตอมของธาตุแฮโลเจนในปฏิกิริยารีดอกซ์ กลไกดังกล่าวทำให้ปลายโซ่พอลิเมอร์ที่เกิดขึ้นเสถียรในรูปของสารประกอบแอลคิลเฮไลด์ แต่ว่องไวพอที่จะเกิดปฏิกิริยารีดอกซ์กับโลหะแทรนซิชัน โดยโลหะแทรนซิชันที่นิยมใช้มากที่สุดคือคอปเปอร์ ในปฏิกิริยาแบบ ARGET ATRP จะมีการเติมตัวรีดิวซ์ เช่น tin(II) 2-ethylhexanoate ($Sn(EH)_2$) กลูโคส หรือกรดแอสคอบิก เพื่อทำหน้าที่เปลี่ยนตัวเร่งปฏิกิริยาที่ไม่ว่องไวคือ Cu(II) ให้กลายเป็นตัวเร่งปฏิกิริยาที่ว่องไวคือ Cu(I) ซึ่งจะทำให้เกิดปฏิกิริยาพอลิเมอไรเซชันอย่างต่อเนื่อง เนื่องจากสามารถนำ Cu(II) มาใช้ได้ใหม่ ทำให้ไม่จำเป็นต้องใช้ตัวเร่งปฏิกิริยาในปริมาณมาก นอกจากนี้ยังไม่จำเป็นต้องทำปฏิกิริยาในระบบที่ปราศจากออกซิเจน เนื่องจากตัวรีดิวส์ที่เติมลงไปนอกจากจะทำหน้าที่เปลี่ยน Cu(II) เป็น Cu(I) แล้ว ยังสามารถเกิดปฏิกิริยาออกซิเดชันกับออกซิเจนในอากาศ จึงเป็นการกำจัดออกซิเจนที่มีอยู่ในระบบได้ ทำให้ปฏิกิริยาทำได้ง่ายและสะดวกมากยิ่งขึ้น

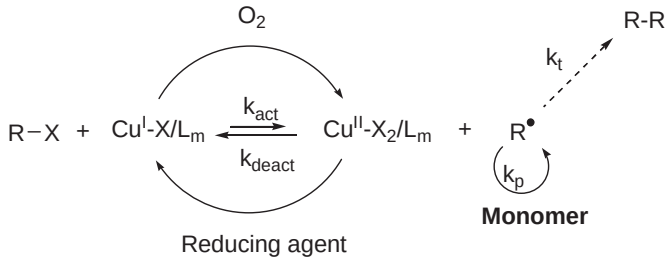

รูปที่ 2.2 กลไกการเกิดปฏิกิริยาพอลิเมอไรเซชันแบบ ARGET ATRP

การหาสภาวะที่เหมาะสมในการทำปฏิกิริยาพอลิเมอไรเซชันจำเป็นต้องศึกษาผลของตัวแปรสำคัญที่มีต่อการควบคุมน้ำหนักโมเลกุลและการกระจายน้ำหนักโมเลกุล (polydispersity; PDI) ของพอลิเมอร์ ได้แก่ เวลาในการทำปฏิกิริยา ปริมาณของตัวรีดิวซ์ ซึ่งในที่นี้ใช้ $Sn(EH)_2$ และ อัตราส่วนระหว่างมอนอเมอร์ต่อตัวริเริ่มปฏิกิริยาที่เป็นสารประกอบแอลคิลเฮไลด์ ซึ่งในที่นี้คือ DMAEMA:ethyl 2-bromoisobutyrate (EBIB) ลิแกนด์ที่ใช้ในปฏิกิริยาคือ tris[2-(dimethylamino)ethyl]amine (Me_6TREN)

ตารางที่ 2.1 แสดงน้ำหนักโมเลกุลของพอลิเมอร์ที่สังเคราะห์จาก DMAEMA โดยใช้แอซิโตนเป็นตัวทำละลาย จากการทดลองพบว่าอัตราส่วน $Sn(EH)_2$:$CuBr_2$: EBIB: Me_6TREN = 2.4:0.006:1:0.25 ใน entry ที่ 3 ให้น้ำหนักโมเลกุลที่วิเคราะห์ด้วยเทคนิค gel permeation chromatography (GPC) ที่ใกล้เคียงค่าน้ำหนักโมเลกุลเป้าหมายทางทฤษฎี (M_n, theo) มากที่สุด และให้ค่าการกระจายน้ำหนักโมเลกุลหรือ PDI (PDI = M_w/M_n) ที่แคบและมีค่าเข้าใกล้ 1 แสดงให้เห็นถึงความเป็นอมตะของปฏิกิริยาพอลิเมอไรเซชัน

ตารางที่ 2.1 M_n, %conversion และ PDI ของพอลิเมอร์ที่สังเคราะห์ได้โดยการปรับเปลี่ยนปริมาณตัวรีดิวซ์

entry	Mole ratio					% conv.	Mn, theo	Mn, GPC	PDI
	DMAEMA	EBIB	$CuBr_2$	Me_6TREN	$Sn(EH)_2$				
1	200	1	0.006	0.25	1.5	72	22,608	21,670	1.38
2	200	1	0.006	0.25	2.0	99	31,086	28,295	1.27
3	200	1	0.006	0.25	2.4	90	28,260	28,495	1.28
4	200	1	0.006	0.25	4.0	90	28,260	23,983	1.35

หมายเหตุ: %conversion คำนวณได้จากการวิเคราะห์ปริมาณ DMAEMA ที่เหลือหลังจากหยุดปฏิกิริยาพอลิเมอไรเซชันด้วยเทคนิค ^{1}H NMR

จากการศึกษาผลของเวลาในการทำปฏิกิริยาพบว่า การทำปฏิกิริยา 20 ชั่วโมงจะให้ผลการทดลองที่ดีที่สุดสำหรับอัตราส่วน DMAEMA:EBIB เป็น 200:1 ซึ่งได้ %conversion = 90% ปฏิกิริยายังเกิดไม่สมบูรณ์หากใช้เวลาสั้นกว่า 20 ชั่วโมง สังเกตได้จากการที่น้ำหนักโมเลกุลของพอลิเมอร์ยังมีค่าสูงไม่ถึงน้ำหนักโมเลกุลเป้าหมายตามทฤษฎี ในขณะที่การทำปฏิกิริยานานกว่า 20 ชั่วโมง จะส่งผลให้ค่า PDI มีค่าสูงขึ้นแสดงถึงการกระจายน้ำหนักโมเลกุลของพอลิเมอร์ที่กว้างขึ้น นอกจากนี้คณะผู้วิจัยได้ลองปรับเปลี่ยนชนิดของตัวรีดิวซ์เป็นกรดแอสคอบิกด้วย แต่ผลปรากฏว่าปฏิกิริยาพอลิเมอไรเซชันเกิดเร็วเกินไป จึงสูญเสียความเป็นอมตะและ

ความสามารถในการควบคุมน้ำหนักโมเลกุลของพอลิเมอร์ ส่งผลให้น้ำหนักโมเลกุลของพอลิเมอร์ที่ได้สูงกว่าน้ำหนักโมเลกุลเป้าหมายตามทฤษฎีมาก และได้ค่า PDI ที่สูงตามไปด้วย

เพื่อศึกษาความเป็นไปได้ในการควบคุมน้ำหนักโมเลกุลของพอลิเมอร์ คณะผู้วิจัยได้ทดลองปรับเปลี่ยนอัตราส่วน DMAEMA:EBIB ให้เป็น 100:1, 200:1 และ 400:1 ซึ่งจะได้จำนวนหน่วยซ้ำของมอนอเมอร์เป้าหมาย (targeted degree of polymerization; DP_{Target}) เป็น 100, 200 และ 400 จากผลการทดลองที่แสดงใน**ตารางที่ 2.2** พบว่าน้ำหนักโมเลกุลของพอลิเมอร์ที่วิเคราะห์ได้ด้วยเทคนิค GPC มีค่าสอดคล้องกับน้ำหนักโมเลกุลของพอลิเมอร์ที่คาดว่าจะได้ตามทฤษฎี นอกจากนี้ยังได้ค่า PDI ที่แคบ แสดงให้เห็นถึงความสามารถในการควบคุมน้ำหนักโมเลกุลของพอลิเมอร์ให้มีความยาวตามต้องการได้ เป็นที่สังเกตเห็นได้ว่าในการทำปฏิกิริยาแบบ ARGET ATRP นี้ จำเป็นต้องควบคุมไม่ให้ปฏิกิริยาพอลิเมอไรเซชันมี %conversion สูงจนเกินไป โดยเฉพาะอย่างยิ่งเมื่อมีการใช้ DMAEMA:EBIB ในอัตราส่วนที่สูง เนื่องจากจะมีผลในการลดความเป็นอมตะของปฏิกิริยา ทั้งนี้สามารถควบคุม %conversion ได้จากการควบคุมเวลาในการทำปฏิกิริยา

ตารางที่ 2.2 M_n, %conversion และ PDI ของพอลิเมอร์ที่สังเคราะห์ได้โดยการปรับเปลี่ยน DMAEMA:EBIB

Entry	DP_{Target}	% conversion	M_n, theo	M_n, GPC	PDI
1	100	85	13,345	21,010	1.24
2	200	90	28,260	28,495	1.28
3	400	69	43,332	42,650	1.18

ในการตรึงพอลิเมอร์บรัชที่มีประจุบวกของ quaternized poly(2-(dimethylaminoethyl) methacrylate) (QPDMAEMA) บนพื้นผิวกระดาษกรองประกอบด้วยขั้นตอนสำคัญ 3 ขั้นตอน แสดงดัง**รูปที่ 2.3** ในขั้นแรกเป็นการตรึงหมู่ริเริ่มปฏิกิริยาพอลิเมอไรเซชันบนกระดาษกรอง Whatman 1 ที่ตัดให้มีขนาด 3.5×8 cm^2 ผ่านการทำปฏิกิริยากับสารประกอบ 2-bromoisobutyryl bromide โดยมีไดคลอโรมีเทนเป็นตัวทำละลาย และ triethylamine, DMAP เป็นตัวเร่งปฏิกิริยา จากการติดตามการเกิดปฏิกิริยาด้วยการวัดมุมสัมผัสของน้ำพบว่า พื้นผิวของกระดาษกรองมีมุมสัมผัสน้ำสูงสุดคือ 130.21 ± 1.37° และเท่ากันทั่วทั้งแผ่น เมื่อใช้เวลาในการทำปฏิกิริยา 16 ชั่วโมง แสดงว่าปฏิกิริยาเกิดขึ้นอย่างสมบูรณ์แล้ว โดยค่ามุมสัมผัสของน้ำที่มากกว่า 90° แสดงให้เห็นว่าสามารถตรึงหมู่ 2-bromoisobutyryl ซึ่งเป็นหมู่ไม่ชอบน้ำบนพื้นผิวกระดาษกรองได้

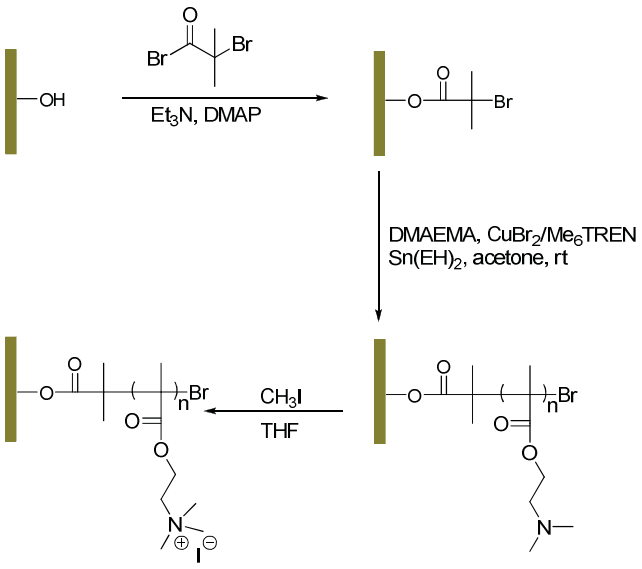

รูปที่ 2.3 ขั้นตอนการตรึงพอลิเมอร์บรัชของ QPDMAEMA บนกระดาษกรอง

ในขั้นที่ 2 เป็นการเตรียมพอลิเมอร์บรัชของ PDMAEMA ผ่านกลไกการเกิดปฏิกิริยาแบบ ARGET ATRP จากการศึกษาที่ผ่านมาพบว่า อัตราส่วน $Sn(EH)_2$:$CuBr_2$:EBiB:Me_6TREN = 2.4:0.006:1:0.25 เป็นอัตราส่วนเหมาะสมที่สุดที่ทำให้ได้น้ำหนักโมเลกุลของพอลิเมอร์ใกล้เคียงกับค่าทางทฤษฎี ให้ค่าการกระจายตัวของน้ำหนักโมเลกุลแคบ (PDI ~ 1) ในการเตรียมพอลิเมอร์บรัชเลือกใช้ DMAEMA:EBiB เป็น 200:1 ทำปฏิกิริยาเป็นเวลา 20 ชั่วโมง ทำให้ได้ 90% conversion, M_n = 28,495, PDI = 1.28 นอกจากนี้ยังสามารถพิสูจน์เอกลักษณ์ของกระดาษกรองที่ผ่านขั้นตอนในการทำปฏิกิริยาต่างๆได้จากการวิเคราะห์ด้วยเทคนิค ATR-FTIR (**รูปที่ 2.4**) โดยทำการเปรียบเทียบระหว่างกระดาษก่อนและหลังการติดหมู่ริเริ่ม หลังการทำปฏิกิริยาพอลิเมอไรเซชัน และหลังการทำปฏิกิริยาควอเทอร์ไนเซชัน จากสเปกตรัมสามารถยืนยันความแตกต่างของหมู่ฟังก์ชันบนพื้นผิวได้ดังนี้ คือ กระดาษกรองที่ติดหมู่ริเริ่ม (b) แสดงสัญญาณของ C=O stretching ที่ 1721 cm^{-1} ซึ่งไม่ปรากฏในกระดาษกรอง ก่อนทำปฏิกิริยา (a) เป็นการยืนยันว่าสามารถติดหมู่ริเริ่มปฏิกิริยาพอลิเมอไรเซชันซึ่งเป็นหมู่ฟังก์ชันประเภทเอสเทอร์ได้จริง โดยสัญญาณบริเวณเดียวกันปรากฏชัดมากขึ้นหลังจากการทำปฏิกิริยาพอลิเมอไรเซชัน (c) ที่ 1718 cm^{-1} ซึ่งแสดงถึง C=O stretching ในหน่วยซ้ำของ PDMAEMA และยังมีสัญญาณของ C-N stretching ปรากฏที่ 1449 cm^{-1} แสดงถึงพันธะ C-N ที่เชื่อมระหว่างหมู่แอมิโนและหมู่แอลคิล จึงเป็นการยืนยันว่าสามารถกราฟต์ PDMAEMA ลงบนกระดาษกรองได้ อย่างไรก็ตามหลังจากทำปฏิกิริยาควอเทอร์ไนเซชัน (d) แล้วไม่พบสัญญาณที่แตกต่างไปจากก่อนทำปฏิกิริยา

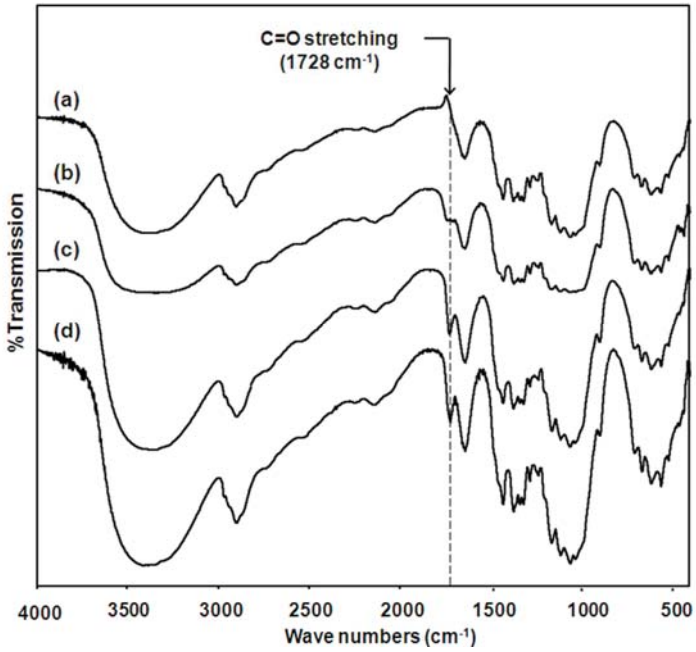

รูปที่ 2.4 อินฟราเรดสเปกตรัมของสารที่ขูดจากพื้นผิวของ (a) กระดาษกรอง, (b) กระดาษกรองหลังการติดหมู่ริเริ่ม, (c) กระดาษกรองกราฟต์ด้วย PDMAEMA และ (d) กระดาษกรองกราฟต์ด้วย QPDMAEMA

สามารถหาธาตุองค์ประกอบบนพื้นผิวของกระดาษกรองหลังจากการดัดแปรทางเคมีในขั้นตอนต่าง ๆ ได้ด้วยเทคนิค x-ray photoelectron spectroscopy (XPS) จากข้อมูลองค์ประกอบของธาตุที่แสดง**ในตารางที่ 2.3** จะพบธาตุโบรมีน 0.8% บนแผ่นกระดาษหลังจากการตรึงหมู่ริเริ่มแสดงให้เห็นว่ามีหมู่โบรโมเอสเทอร์ที่จะทำหน้าที่ริเริ่มปฏิกิริยาพอลิเมอไรเซชันบนแผ่นกระดาษ จะเหลือปริมาณธาตุโบรมีนในสัดส่วนต่ำ (~0.2%) บนแผ่นกระดาษที่ตรึงด้วยพอลิเมอร์บรัชของ PDMAEMA และ QPDMAEMA แสดงให้เห็นว่ายังมีหมู่โบรโมเอสเทอร์อยู่ที่ปลายโซ่พอลิเมอร์อยู่ การพบธาตุไนโตรเจนบนแผ่นกระดาษที่ตรึงด้วยพอลิเมอร์บรัชเป็นการยืนยันความสำเร็จของการติดพอลิเมอร์บนพื้นผิวของกระดาษด้วยปฏิกิริยาพอลิเมอไรเซชันริเริ่มจากพื้นผิว การที่อัตราส่วนของธาตุ C/N มีค่าเท่ากับ 8.1 ให้ผลสอดคล้องกับโครงสร้างของ PDMAEMA ตามทฤษฎี (C/N = 8.0). การเพิ่มขึ้นของอัตราส่วน C/N ratio เป็น11.9 ประกอบกับการปรากฏของพีก N_{1s} ที่ตำแหน่ง 402.0 eV บนพื้นผิวกระดาษกรองที่กราฟต์ด้วย QPDMAEMA (**รูปที่ 2.5**) แสดงให้เห็นว่ามีการเพิ่มขึ้นของคาร์บอนหลังจากการทำปฏิกิริยาควอเทอไนเซชันเพื่อเปลี่ยน PDMAEMA เป็น QPDMAEMA และธาตุไนโตรเจนส่วนใหญ่จะอยู่ในรูปของหมู่ควอเทอร์นารีแอมโมเนียม ทั้งนี้สามารถคำนวณหาเปอร์เซ็นต์ของหมู่ควอเทอร์นารีแอมโมเนียมบนพื้นผิวได้จากอัตราส่วนพื้นที่ใต้พีก N_{1s} ที่มาจากหมู่ควอเทอร์นารีแอมโมเนียมที่ตำแหน่ง 402.0 eV เทียบกับพื้นที่ใต้พีกทั้งหมด ซึ่งได้ค่าเท่ากับ 80% สัดส่วนที่ค่อนข้างสูงนี้แสดงให้เห็นถึงศักยภาพในการจับยึดกับสารที่มีประจุเป็นลบโดยเฉพาะอย่างยิ่งดีเอ็นเอด้วยแรงระหว่างประจุได้ ซึ่งในที่นี้ได้ทดสอบความสามารถในการดูดซับของแผ่นกระดาษที่เตรียมขึ้นกับดีเอ็นเอสังเคราะห์ที่มี 13 เบส ซึ่งเป็นส่วนหนึ่งของ human *IL-10* promoter gene (DNA SLE2) โดยใช้ 1 µL ของ 10 µM DNA ใน 0.4 M NaOH ที่มี 10 mM EDTA หยดบนกระดาษกรองที่ตรึงด้วย QPDMAEMA จากนั้นทำการล้างเพื่อกำจัดดีเด็นเอที่ไม่ดูดซับออก จากนั้นจึงนำไปวิเคราะห์ด้วยเทคนิค XPS จากตารางที่ 2.3 พบสัญญาณของธาตุฟอสฟอรัส 1.2 % ซึ่งมาจากหมู่ฟอสเฟตของดีเอ็นเอ แสดงให้เห็นว่าดีเอ็นเอถูกดูดซับบนกระดาษกรองที่พัฒนาขึ้นได้จริง และสามารถนำไปประยุกต์ใช้ในการตรวจวิเคราะห์ลำดับเบสของดีเอ็นเอตามแนวคิดที่เสนอไว้ข้างต้นได้

ตารางที่ 2.3 ธาตุองค์ประกอบของพื้นผิวแผ่นกระดาษกรองที่ถูกดัดแปรด้วยปฏิกิริยาเคมีในขั้นตอนต่าง ๆ

Sample	Atomic composition (%)						C/N
	C	O	Br	N	Cl	P	
Unmodified	58.2	41.7	N/D	N/D	N/D	N/D	-
Immobilized with initiator	57.7	41.5	0.8	N/D	N/D	N/D	-
Grafted with PDMAEMA	65.0	26.8	0.2	8.0	N/D	N/D	8.1
Grafted with QPDMAEMA[a]	69.2	24.9	0.2	5.8	<0.1	N/D	11.9
Grafted with QPDMAEMA after DNA adsorption	60.4	33.6	0.1	4.6	0.15	1.2	13.1

N/D = Not detected, [a] the analysis was done after chlorine exchange

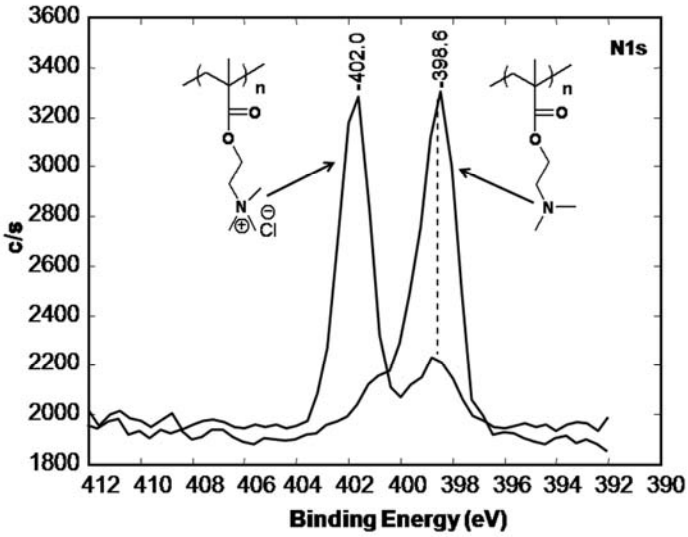

รูปที่ 2.5 N_{1s} XPS สเปกตรัมของกระดาษกรองที่ติดด้วย PDMAEMA (ขวา) และ QPDMAEMA (ซ้าย)

จากการตรวจสอบสมบัติความเปียก (wettability) ซึ่งอาศัยเทคนิคการวัดมุมสัมผัสของน้ำพบว่ากระดาษกรองกราฟต์ด้วย PDMAEMA แล้วนั้นไม่สามารถวัดค่ามุมสัมผัสของน้ำได้ หรือมีค่าเท่ากับ 0 ° ซึ่งมีค่าลดลงจาก 130.21 ± 1.37° ที่วัดได้จากกระดาษกรองที่ติดหมู่ริเริ่ม แสดงให้เห็นว่ากระดาษกรองที่กราฟต์ด้วย PDMAEMA มีสมบัติความชอบน้ำเพิ่มมากขึ้นจากกระดาษกรองที่ติดหมู่ริเริ่มอย่างมาก เมื่อวัดค่ามุมสัมผัสน้ำที่กราฟต์ด้วย QPDMAEMA ก็ให้ผลเช่นเดียวกันกับกระดาษกรองที่กราฟต์ด้วย PDMAEMA และจากการตรวจสอบสัณฐานวิทยาของพื้นผิวกระดาษกรองด้วยเทคนิคเอสอีเอ็ม (**รูปที่ 2.6**) พบว่าพื้นผิวของกระดาษกรองทั้งหมดไม่มีการเปลี่ยนแปลงไปในเชิงสัณฐานวิทยา จึงอาจกล่าวได้ว่าพอลิเมอร์ที่ทำการกราฟต์ลงไปนั้นมีลักษณะที่เป็นฟิล์มบางมากและการทำปฏิกิริยาเคมีในขั้นตอนต่าง ๆไม่มีผลต่อลักษณะทางกายภาพภายนอกของกระดาษกรองนั่นเอง

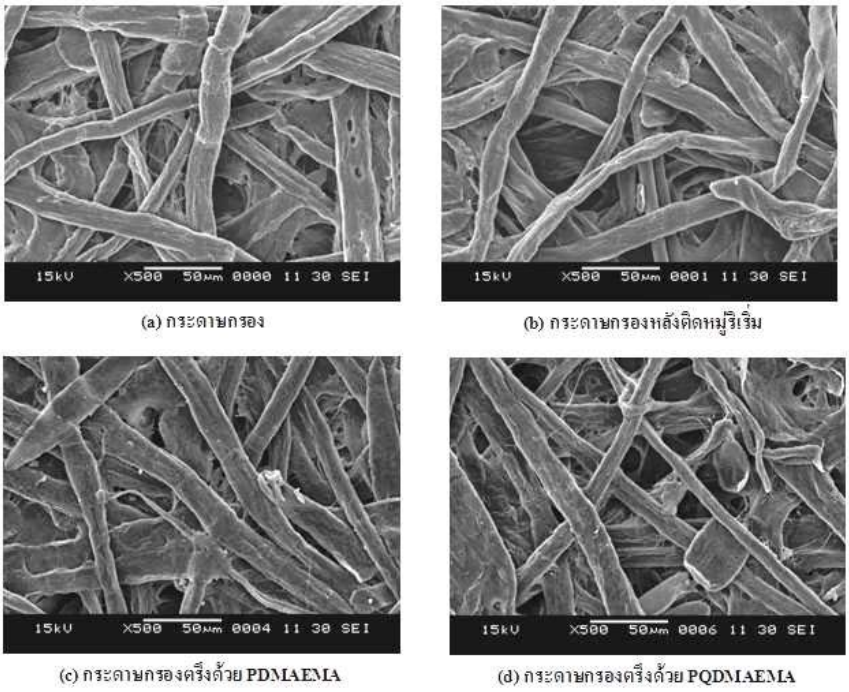

รูปที่ 2.6 เอสอีเอ็มไมโครกราฟของ (a) กระดาษกรอง, (b) กระดาษกรองหลังการติดหมู่รีเริ่ม, (c) กระดาษกรองกราฟต์ด้วย PDMAEMA และ (d) กระดาษกรองกราฟต์ด้วย QPDMAEMA

เมื่อได้กระดาษกรองที่ตรึงด้วยพอลิเมอร์บรัชของ QPDMAEMA แล้ว จึงนำไปทดสอบการตรวจวัดการจับยึดระหว่างดีเอ็นเอและพีเอ็นเอโพรบอาศัยการสังเกตสีด้วยตาเปล่าที่ทำให้เกิดได้โดยอาศัยเอนไซม์ ซึ่งในที่นี้ใช้สเตรปทาวิดินที่ติดฉลากด้วยเอนไซม์เอชอาร์พี (HRP-labeled streptavidin) หรือ SA-HRP ร่วมกันพีเอ็นเอโพรบที่มีไบโอติน (biotinylated PNA probe) หรือ b-PNA และสับสเตรท o-phenylenediamine dihydrochloride (OPD) และ Urea hydrogen peroxide (Urea-H_2O_2) ระบบดีเอ็นเอที่เลือกใช้ในการศึกษานี้มีลำดับเบสที่แสดงความผิดปกติของโรคภูมิคุ้มกันบกพร่องหรือ SLE ลำดับเบสของทั้งดีเอ็นเอและพีเอ็นเอที่ใช้ในการทดสอบแสดงใน**ตารางที่ 2.4**

ตารางที่ 2.4 ลำดับเบสของพีเอ็นเอและดีเอ็นเอที่ใช้ในการวิเคราะห์

สัญลักษณ์	ลำดับเบส	หมายเหตุ
b-DNA (SLE2)	b- dTTGGGAAGGGGAA	Full match to PNA (SLE2)
DNA (SLE1)	dTTGGGAGGGGGAA	Single mismatch to PNA (SLE2)
DNA (SLE2)	dTTGGGAAGGGGAA	Full match to PNA (SLE2)
b-PNA (SLE2)	b-O-O-TTCCCCTTCCCAA-Lys	

ในการทดลองแบ่งชุดการทดสอบออกเป็น 6 จุด ซึ่งมีการหยดพีเอ็นเอและ/หรือ ดีเอ็นเอ ในรูปแบบดังแสดงใน**ตารางที่ 2.5** จุดที่ 1 เป็น positive control ซึ่งจะให้ความเข้มของสีสูงสุด เนื่องจากดีเอ็นเอซึ่งมีประจุเป็นลบสามารถจับยึดกับกระดาษที่ตรึงด้วย QPDMAEMA และที่ปลายของดีเอ็นเอมีไบโอตินซึ่งสามารถจับยึดกับเอนไซม์ SA-HRP ซึ่งเมื่อเติม OPD และ Urea-H_2O_2 ก็จะเกิดสีเหลืองเข้มขึ้น จุดที่ 2 เป็น negative control เนื่องจาก b-PNA (SLE2) และ DNA (SLE1) มีลำดับเบสที่ต่างกัน 1 ตำแหน่ง (single mismatch) จุดที่ 3 เป็น negative control เพื่อพิสูจน์ให้เห็นว่าหากดีเอ็นเอไม่มีไบโอตินติดอยู่ก็ไม่ควรจะให้สีเมื่อมีการเติม SA-HRP/OPD/Urea-H_2O_2 ในขณะที่จุดที่ 4 ควรให้ผลทดสอบที่เป็นบวกเนื่องจาก b-PNA (SLE2) และ DNA (SLE2) มีลำดับเบสที่เป็นคู่สมกัน (full match) จุดที่ 5 เป็น negative control ทดสอบเพื่อพิสูจน์ให้เห็นว่า b-PNA (SLE2) ไม่ควรยึดติดบนพื้นผิวของกระดาษ หากไม่มีการเติมดีเอ็นเอที่มีลำดับเบสเป็นคู่สมกัน ส่วนจุดที่ 6 เป็น negative control เพื่อแสดงให้เห็นว่า SA-HRP ไม่เกิดแรงกระทำอย่างไม่จำเพาะเจาะจงกับกระดาษหากไม่มีการเติมทั้งดีเอ็นเอและพีเอ็นเอ

ตารางที่ 2.5 ดีเอ็นเอและพีเอ็นเอที่ใช้หยดบนแผ่นกระดาษกรองซึ่งตรึงด้วย QPDMAEMA ก่อนการเติมเอนไซม์ SA-HRP, สับสเตรท OPD และ Urea-H_2O_2

จุดที่	ดีเอ็นเอ	พีเอ็นเอ	หมายเหตุ
1	b-DNA (SLE2)	-	Positive control (+)
2	DNA (SLE1)	b-PNA (SLE2)	Negative control (-)
3	DNA (SLE2)	-	Negative control (-)
4	DNA (SLE2)	b-PNA (SLE2)	Positive result (+)
5	-	b-PNA (SLE2)	Negative control (-)
6	-	-	Negative control (-)

จากการทดสอบในเบื้องต้นพบว่าการล้างแผ่นกระดาษมีความสำคัญเป็นอย่างมากต่อความสำเร็จของการตรวจวิเคราะห์ โดยเฉพาะอย่างยิ่งขั้นการบล๊อคด้วยสารละลาย 0.1%BSA เป็นเวลา 30 นาที ก่อนการเติมเอนไซม์ SA-HRP ทั้งนี้สามารถสรุปเป็นลำดับของสารละลายที่ใช้ในการล้างและการบล๊อกได้ดัง**ตารางที่ 2.6** ในแต่ละขั้นจะทำการล้าง 3 ครั้ง โดยแต่ละครั้งต้องทำการแช่และเขย่าแผ่นกระดาษในสารละลายที่ล้างครั้งละ 1 นาที ยกเว้นขั้นการบล๊อกที่ต้องใช้เวลา 30 นาที

ตารางที่ 2.6 ชนิดของสารละลายที่ใช้ในการล้างและการบล๊อคแผ่นกระดาษในแต่ละขั้นตอน

Post hybridization	Blocking step (30 min) before SA-HRP addition	After SA-HRP addition
1)100 mM PBS pH 7.4, 100 mM NaCl 2) H_2O	0.1% BSA w/v	1) 100 mM PBS pH 7.4, 100 mM NaCl 2) 100 mM CTB pH 5 3) H_2O

รูปที่ 2.7 แสดงผลการทดสอบเปรียบเทียบระหว่างการใช้วัสดุต่างๆ ได้แก่ แผ่น Nylon 66 ที่มีประจุบวกซึ่งเป็นวัสดุที่มีจำหน่ายทางการค้า แผ่นกระดาษกรองที่ตรึงด้วยพอลิเมอร์บรัชของ PDMAEMA และ QPDMAEMA จากผลที่ปรากฏจะเห็นได้ว่าไม่สามารถบอกความแตกต่างของแต่ละสภาวะได้เมื่อใช้ แผ่น Nylon 66 แสดงให้เห็นถึงแรงกระทำที่ไม่จำเพาะเจาะจงเป็นอย่างมากระหว่างแผ่น Nylon 66 กับ เอนไซม์ SA-HRP ส่งผลให้เกิดสีเข้มปรากฏขึ้นทุกจุด ในขณะที่กระดาษกรองที่ตรึงด้วยพอลิเมอร์บรัชของ PDMAEMA แสดงสีที่ตำแหน่งที่ 4 เข้มกว่าจุดอื่นในระดับหนึ่ง แต่ก็ยังมีค่าไม่เข้มเท่ากับจุดที่ 1 ซึ่งเป็น positive control การได้ผลทดสอบที่ดีเมื่อใช้กระดาษกรองที่ตรึงด้วยพอลิเมอร์บรัชของ QPDMAEMA แสดงให้เห็นความสำคัญเป็นอย่างมากของการมีประจุบวกของหมู่ควอเทอร์นารีแอมโมเนียมในโครงสร้างของ QPDMAEMA ที่นอกจากจะช่วยเพิ่มประสิทธิภาพในการจับยึดกับดีเอ็นเอผ่านแรงระหว่างประจุแล้วยังช่วยลดแรงกระทำอย่างไม่จำเพาะเจาะจงของสารอื่นบนกระดาษกรองลงอีกด้วย

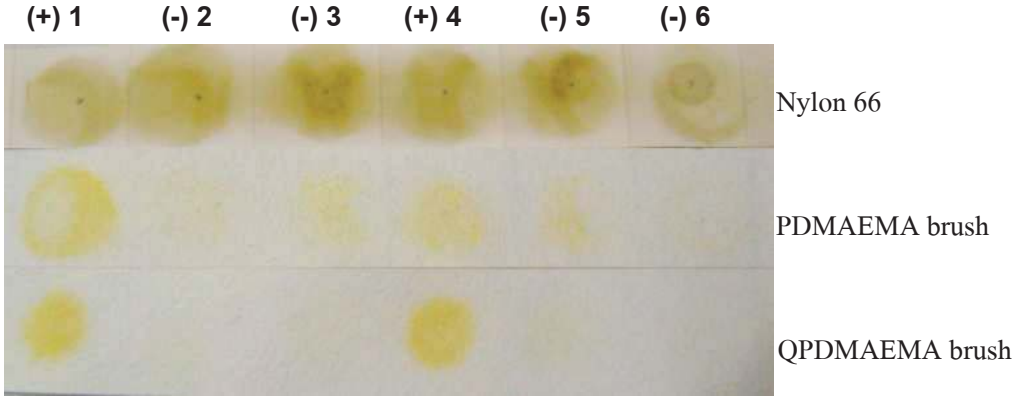

รูปที่ 2.7 ผลการตรวจสอบลำดับเบสของ DNA (SLE2) โดยใช้ b-PNA (SLE2) เป็นโพรบ บนแผ่น Nylon 66, กระดาษกรองที่ตรึงด้วยพอลิเมอร์บรัชของ PDMAEMA และ QPDMAEMA แล้วใช้ปฏิกิริยาการสร้างสีด้วยเอนไซม์ SA-HRP โดยใช้สับสเตรท OPD ร่วมกับ Urea-H_2O_2

เพื่อให้ผลการตรวจวัดที่มีประสิทธิภาพสูงที่สุด ทางคณะผู้วิจัยได้ทำการศึกษาผลของตัวแปรต่างๆที่มีต่อประสิทธิภาพในการวิเคราะห์ลำดับเบสของดีเอ็นเอดังต่อไปนี้

(1) การแลกเปลี่ยนแอนไอออนบนกระดาษกรองที่ถูกปรับปรุงพื้นผิวด้วย QPDMAEMA จากไอโอไดด์ไอออนเป็นคลอไรด์ไอออน

ตามปกติกระดาษกรองที่ถูกปรับปรุงพื้นผิวด้วย QPDMAEMA จะมีไอโอไดด์ไอออนเป็น counter ion ดังนั้นการทดลองนี้จะศึกษาผลของการเปลี่ยนไอโอไดด์ไอออนเป็นคลอไรด์ไอออน โดยการทดลองชุด d แช่กระดาษกรองในสารละลาย 0.1 M PBS, pH 7.4, 0.1M NaCl เป็นเวลา 2 ชั่วโมง ตามด้วยการล้างน้ำ 3 ครั้ง ทำให้แห้ง ก่อนนำไปใช้ในการวิเคราะห์ การทดลองชุด e แตกต่างจากชุด d ตรงที่ก่อนนำกระดาษกรองมาใช้ จะแช่ในสารละลาย 0.1M NaCl เป็นเวลา 2 ชั่วโมง แล้วล้างด้วยน้ำ 3 ครั้ง จากผลการทดลองที่แสดงใน**รูปที่ 2.8** พบว่าการเปลี่ยน counter ion จากไอโอไดด์ไอออนให้เป็นคลอไรด์ไอออน ช่วยเพิ่มประสิทธิภาพในการเกิด hybridization ของ PNA-DNA เนื่องจากจะพบว่าความเข้มสีของ positive test (4) มีความเข้มใกล้เคียงกับ positive control (1) นอกจากนี้ยังสามารถกำจัดการดูดซับแบบไม่จำเพาะเจาะจง (non-specific absorption) ออกจากกระดาษได้อีกด้วย การทดลองชุด f ทำการทดลองเช่นเดียวกับการทดลองชุด e แต่แตกต่างจากการทดลองชุด e ตรงที่ทำการเปลี่ยนสารละลายล้างในขั้น post hybridization และ post SA-HRP จาก 100 mM phosphate

buffer pH 7.4, 100 mM NaCl เป็น 50 mM phosphate buffer pH 7.4, 100 mM NaCl จากผลการทดลองที่ได้แสดงให้เห็นว่าการลดความเข้มข้นของสารละลายล้าง phosphate buffer pH 7.4 จาก 100 mM ให้เหลือเพียง 50 mM จะไม่สามารถกำจัดการดูดซับแบบไม่จำเพาะเจาะจง (non-specific absorption) ออกจากกระดาษได้หมด

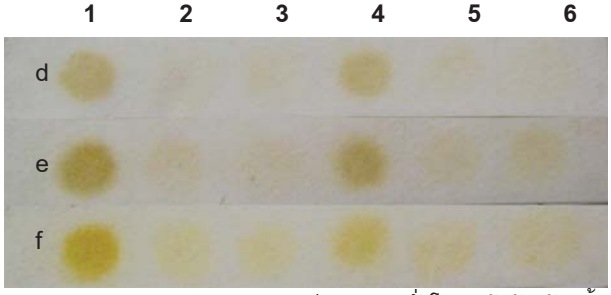

d: ก่อนใช้ แช่แผ่นในสารละลาย 0.1M PBS, pH 7.4, 0.1M NaCl เป็นเวลา 2 ชั่วโมง แล้วล้างด้วยน้ำ 3 ครั้ง

e: ก่อนใช้ แช่แผ่นในสารละลาย 0.1M NaCl เป็นเวลา 2 ชั่วโมง แล้วล้างด้วยน้ำ 3 ครั้ง

f: ก่อนใช้แผ่นทำเหมือน e แต่เปลี่ยนสารละลายล้าง ขั้น post hybridization และ post SA-HRP เป็น 50mM PBS, pH7.4, 100mM NaCl

รูปที่ 2.8 ผลการตรวจสอบลำดับเบสของ DNA (SLE2) โดยใช้ b-PNA (SLE2) เป็นโพรบ บนแผ่นกระดาษกรองที่ตรึงด้วยพอลิเมอร์บรัชของ QPDMAEMA โดยศึกษาการเปลี่ยนแอนไอออนบนกระดาษกรองจากไอโอไดด์ไอออนเป็นคลอไรด์ไอออน

(2) เวลาในขั้นตอนการย้อมสี

การทดสอบนี้ทำการทดลองเช่นเดียวกับการทดลองชุด e โดยนำกระดาษกรองที่ติด QPDMAEMA แล้วแช่ในสารละลาย 0.1M NaCl 2 ชั่วโมง จากนั้นล้างด้วยน้ำ 3 ครั้ง ก่อนนำไปใช้ในการทดสอบ โดยการทดลองชุด g และ h แตกต่างจากการทดลองชุด e ตรงที่ขั้นตอนสุดท้าย คือขั้นการจุ่มกระดาษกรองในสารละลายผสมของ 250 μL ของ Urea-H_2O_2 (1.6 mg/mL) และ 250 μL ของ OPD (o-phenylenediamine) (1.6 mg/mL) ซึ่งในการทดลองชุด e ใช้เวลาในขั้นนี้ 1 นาที ส่วนในการทดลองชุด g และ h ใช้เวลาในขั้นนี้ 5 และ 2 นาที ตามลำดับ จากผลการทดลองที่แสดงใน**รูปที่ 2.9** พบว่าการเพิ่มเวลาในขั้นตอนนี้ส่งผลทำให้สีในจุดที่ 1 (positive control) และจุดที่ 4 (positive test) มีความเข้มมากขึ้น แต่ในขณะเดียวกันก็ทำให้เกิดการดูดซับแบบไม่จำเพาะเจาะจง ในชุดการทดลองที่เป็น negative control (จุดที่ 3, 5 และ 6) และ negative test (จุดที่ 2) มากขึ้นด้วย ดังนั้นเวลาที่เหมาะสมในขั้นตอนการย้อมสีคือ 1 นาทีเพราะสีมีความเข้มมากเพียงพอ สามารถมองเห็นได้ชัดเจนและเกิดการดูดซับแบบไม่จำเพาะเจาะจงต่ำที่สุด

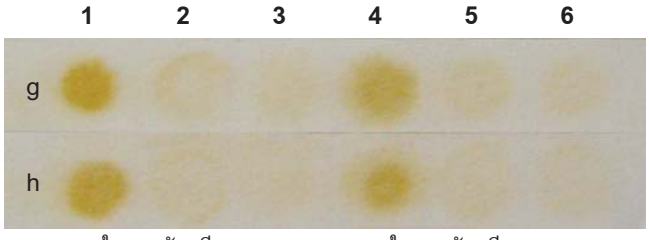

g: เวลาในการย้อมสี 5 min **h**: เวลาในการย้อมสี 2 min

รูปที่ 2.9 ผลการตรวจสอบลำดับเบสของ DNA (SLE2) โดยใช้ b-PNA (SLE2) เป็นโพรบ บนแผ่นกระดาษกรองที่ตรึงด้วยพอลิเมอร์บรัชของ QPDMAEMA โดยศึกษาผลของเวลาในการย้อมสี

(3) การเพิ่มความยืดหยุ่นและความชอบน้ำของพีเอ็นเอโพรบ

จากการทดลองก่อนหน้านี้ใช้ PNA (SLE2) เป็นโพรบโดยปลายสายของ PNA ที่ติดด้วย biotin โดยก่อนจะติด biotin จะติดหมู่ฟังก์ชัน [2-[2-(amino)ethoxy]ethoxy]acetic acid จำนวน 1 ยูนิตเพื่อเพิ่มความยืดหยุ่นให้โพรบ ซึ่งใช้สัญลักษณ์ว่า b-o-PNA(SLE1) แต่จากผลการทดลองก่อนหน้านี้จะพบว่า ณ จุดที่ 5 ซึ่งเป็น negative control พบการดูดซับแบบไม่จำเพาะเจาะจงระหว่างพื้นผิวของกระดาษกรองและ PNA อยู่เสมอ นอกจากนี้ยังพบว่าความเข้มสีของ positive test ในบางครั้งมีค่าต่ำกว่า positive control ดังนั้นจึงสนใจที่จะปรับเปลี่ยนโครงสร้างของพีเอ็นโพรบในส่วนหมู่ปลาย serine เป็น lysine และเพิ่มความยาวของ [2-[2-(amino)ethoxy]ethoxy]acetic acid เป็น 2 ยูนิต

การทดลองชุด i ทำเช่นเดียวกับการทดลองชุด c แต่แตกต่างตรงชนิดของ probe โดยเปลี่ยนจาก b-o-PNA(SLE2) เป็น b-o-o-PNA(SLE2) ผลการการทดลองที่ได้ปรากฏว่าสามารถกำจัดการดูดซับแบบไม่จำเพาะเจาะจงระหว่างของพีเอ็นเอโพรบบนพื้นผิวของกระดาษกรองได้ ส่งผลทำให้ประสิทธิภาพการเกิดโมเลกุลลูกผสมระหว่าง PNA-DNA เพิ่มขึ้น ดังนั้นจึงสังเกตเห็นสีที่ positive test (จุดที่ 4) มีความเข้มใกล้เคียงกับ positive control (จุดที่ 1) แสดงดัง**รูปที่ 2.10**

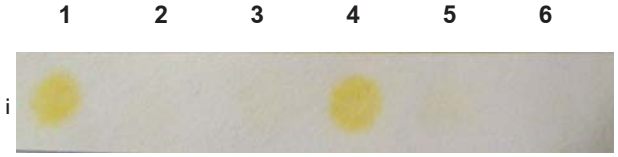

รูปที่ 2.10 ผลการตรวจสอบลำดับเบสของ DNA (SLE2) โดยใช้ b-PNA (SLE2) เป็นโพรบ บนแผ่นกระดาษกรองที่ตรึงด้วยพอลิเมอร์บรัชของ QPDMAEMA โดยศึกษาผลของการเปลี่ยนโครงสร้างของพีเอ็นเอโพรบ

(4) ความเข้มข้นของ SA-HRP และ substrate

การทดลองในส่วนนี้เป็นการศึกษาผลของความเข้มข้นของ SA-HRP และสารผสมของ substrate โดยพิจารณาเฉพาะผลการทดลองที่เป็น positive control (จุดที่ 1) และ negative control (จุดที่ 2) และทำการบันทึกสีของกระดาษโดยใช้ทั้งกล้องถ่ายรูปซึ่งเป็นรูปแบบที่ใช้อยู่เดิม เปรียบเทียบกับการใช้ scanner ด้วย จากผลการทดลองใน**รูปที่ 2.11** พบว่าปริมาณของ SA-HRP ที่น้อยที่สุดที่ให้ความเข้มของสีสูงสุดที่ตำแหน่ง positive control และเกิดสีที่ negative control ต่ำที่สุด คือ การทดลองชุด b การเพิ่มความเข้มข้นของ SA-HRP ในการทดลองชุด c ไม่ให้ผลที่แตกต่างกันอย่างมีนัยสำคัญ แต่เมื่อลดความเข้มข้นของ substrate ลงในชุดการทดลอง d จะส่งผลทำให้สีของจุดที่ 1 จางลง ดังนั้นปริมาณของ SA-HRP ที่เหมาะสมคือ 20 ng ความเข้มข้นของ substrate ที่เหมาะสมคือ 250 μL ของ 1.6 mg/mL OPD และ 250 μL ของ 1.6 mg/mL urea-H_2O_2

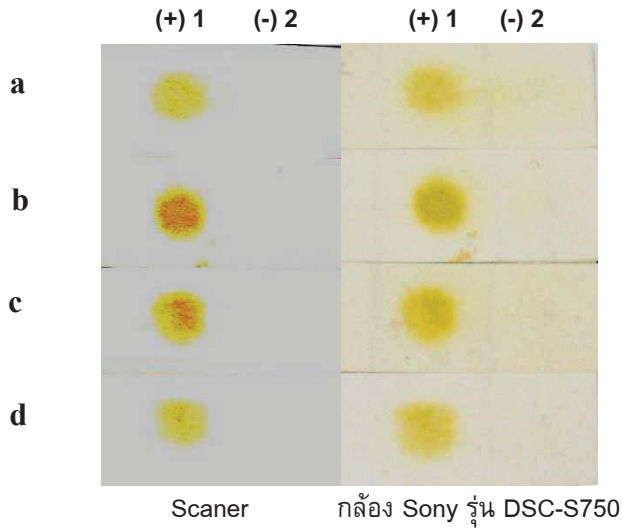

รูปที่ 2.11 ผลการตรวจสอบลำดับเบสของ DNA (SLE2) โดยใช้ b-PNA (SLE2) เป็นโพรบ บนแผ่นกระดาษกรองที่ตรึงด้วยพอลิเมอร์บรัชของ QPDMAEMA โดยศึกษาผลของความเข้มข้นของ SA-HRP และ substrate ต่อความเข้มของการเกิดสี โดยใช้สารละลายผสม substrate ในชุดการทดลอง a-c คือ 250 μL ของ 1.6 mg/mL OPD และ 250 μL ของ 1.6 mg/mL urea-H_2O_2 โดยมีการใช้ปริมาณสารที่แตกต่างกันดังนี้ a) 10 ng SA-HRP, b) 20 ng SA-HRP, c) 30 ng SA-HRP ในกรณีของ d) ใช้ 20 ng SA-HRP และ สารละลายผสม substrate คือ 250 μL OPD (0.8 mg/mL) และ 250 μL ของ urea-H_2O_2 (0.8 mg/mL)

(5) ตัวทำละลายของเอนไซม์ SA-HRP

การทดสอบในส่วนนี้ทำการทดลองเช่นเดียวกับชุดการทดลอง b แต่มีการปรับเปลี่ยนตัวทำละลายของ SA-HRP จากเดิมที่ใช้ PBS pH 7.4 เป็น น้ำ และ citrate buffer pH 5 (CTB) จากผลการทดลองที่แสดงใน**รูปที่ 2.12** พบว่าการใช้ CTB เป็นตัวทำละลาย ให้ความเข้มของสี ณ ตำแหน่ง positive control สูงที่สุด

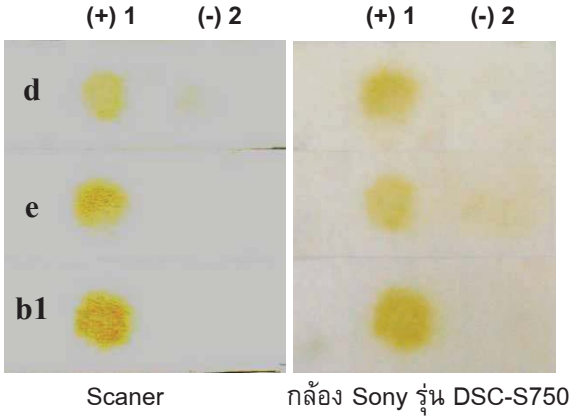

รูปที่ 2.12 ผลการตรวจสอบลำดับเบสของ DNA (SLE2) โดยใช้ b-PNA (SLE2) เป็นโพรบ บนแผ่นกระดาษกรองที่ตรึงด้วยพอลิเมอร์บรัชของ QPDMAEMA โดยศึกษาผลของตัวทำละลายของเอนไซม์ SA-HRP ต่อการเกิดสี: d) 0.1 M PBS pH 7.4, containing 0.1 M NaCl, e) water, b1) 0.1 M CTB

(6) สารละลาย blocking

การทดสอบในส่วนนี้ทำการทดลองเช่นเดียวกับชุดการทดลอง b แต่มีการปรับเปลี่ยนชนิดของสารละลายที่ใช้ในขั้นตอน blocking จากปกติที่ใช้ 1%BSA เป็น 1% skim milk เมื่อพิจารณาการทดลองที่แสดงใน**รูปที่ 2.13** พบว่าหากไม่ block แผ่นเมมเบรน จะมีการดูดซับแบบไม่จำเพาะเจาะจงกับ SA-HRP (การทดลองชุด g) เมื่อพิจารณาการทดลองชุด b2 และ f เปรียบเทียบชนิดของ blocking ระหว่าง BSA และ skim milk ที่ความเข้มข้นเดียวกัน พบว่าถึงแม้ skim milk จะป้องกันการดูดซับแบบไม่จำเพาะเจาะจงได้แต่ skim milk มีองค์ประกอบที่เป็นโปรตีนขนาดใหญ่กว่า BSA มาก จึงเกิดการดูดซับได้ดี ปกคลุมบริเวณที่มีไบโอติน ขัดขวางการทำปฏิกิริยาระหว่างไบโอตินและ SA-HRP ส่งผลทำให้เกิดสีเพียงเล็กน้อยที่ตำแหน่ง positive control ดังนั้น blocking solution ที่เหมาะสมที่สุดยังคงเป็น 1% BSA

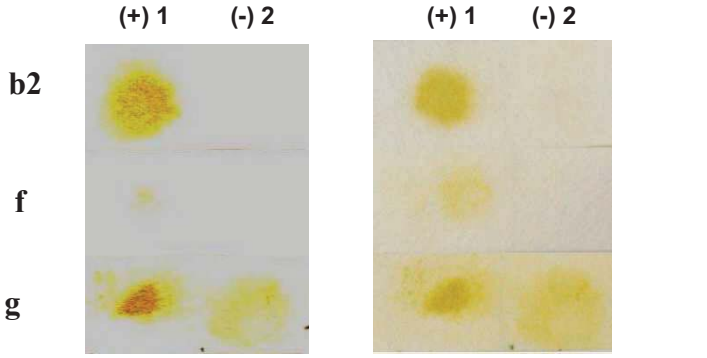

รูปที่ 2.13 ผลการตรวจสอบลำดับเบสของ DNA (SLE2) โดยใช้ b-PNA (SLE2) เป็นโพรบ บนแผ่นกระดาษกรองที่ตรึงด้วยพอลิเมอร์บรัชของ QPDMAEMA โดยศึกษาผลของสารละลาย blocking ต่อการป้องกันการดูดซับแบบไม่จำเพาะจงระหว่าง SA-HRP และ membrane : b2) 1% BSA in 0.1 M 0.1 M PBS pH 7.4, containing 0.1 M NaCl, f) 1% skim milk in 0.1 M PBS pH 7.4, containing 0.1 M NaCl และ g) ปราศจากขั้น blocking

(7) ชนิดของเอนไซม์

การทดสอบในส่วนนี้ทำการทดลองเช่นเดียวกับชุดการทดลอง b แต่มีการปรับเปลี่ยนชนิดของเอนไซม์จาก SA-HRP เป็น avidin-HRP ปริมาณ 20 และ 50 ng จากผลการทดลองแสดงใน**รูปที่ 2.14** พบว่า SA-HRP (การทดลองชุด **b3**) มีประสิทธิภาพในการให้สีที่เข้มกว่า avidin-HRP (การทดลองชุด **h-i**) ทั้ง 2 ความเข้มข้น ดังนั้น SA-HRP เป็นเอนไซม์ที่หมาะสมในการใช้ทดสอบมากกว่า avidin-HRP

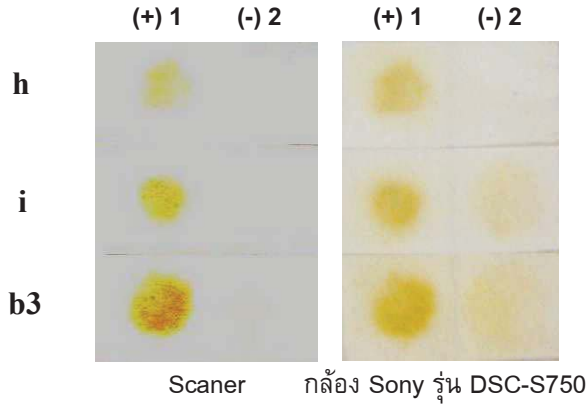

รูปที่ 2.14 ผลการตรวจสอบลำดับเบสของ DNA (SLE2) โดยใช้ b-PNA (SLE2) เป็นโพรบ บนแผ่นกระดาษกรองที่ตรึงด้วยพอลิเมอร์บรัชของ QPDMAEMA โดยศึกษาผลของชนิดของเอนไซม์: h) 20 ng avidin-HRP, i) 50 ng avidin-HRP และ b3) 20 ng SA-HRP

(8) เวลาในการกระตุ้นการเกิดสี

ในการทดลองนี้ได้ทำการแปรเปลี่ยนเวลาในการกระตุ้นการเกิดสีหลังจากการเติมสับสเตรท OPD และ Urea-H_2O_2 จาก 1 นาทีที่ใช้ในการทดลอง b5 เป็น 2 นาที (การทดลอง j) และ 5 min (การทดลอง k) จากผลการทดลองที่แสดงใน**รูปที่ 2.15** พบว่าการเพิ่มเวลาในการกระตุ้นการเกิดสี นอกจากจะทำให้สีบริเวณ positive control ((+) 1, มี b-DNA) เข้มขึ้นแล้วยังทำให้สีบริเวณ negative control ((-) 2, ไม่มี b-DNA) เข้มขึ้นเช่นกัน ดังนั้นเวลาเพียง 1 นาทีจึงเพียงพอที่จะให้ผลทดสอบชัดเจนโดยให้สีของ background น้อยที่สุด

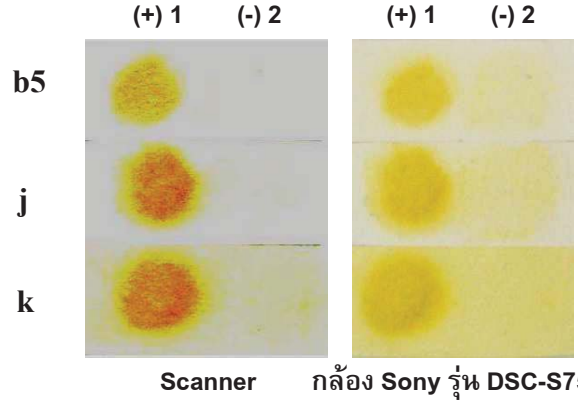

รูปที่ 2.15 ผลการตรวจสอบลำดับเบสของ DNA (SLE2) โดยใช้ b-PNA (SLE2) เป็นโพรบ บนแผ่นกระดาษกรองที่ตรึงด้วยพอลิเมอร์บรัชของ QPDMAEMA โดยศึกษาผลของของเวลาในการกระตุ้นการเกิดสี: b5) 1 นาที, j) 2 นาที และ k) 5 min

(9) ชนิดของสับสเตรท

การทดลองนี้สนใจศึกษาการเปลี่ยนชนิดของสับสเตรทจาก o-phenylenediamine (OPD) เป็น 3,3′,5,5′-tetramethylbenzidine (TMB) โดยใช้ความเข้มข้นเท่ากัน จากผลการทดลองที่แสดงใน**รูปที่ 2.16** พบว่า TMB เป็นสับสเตรทที่ให้สีฟ้า มีความว่องไวต่อการเกิดสีได้เร็วกว่า OPD แต่ให้ความเข้มของ background สูงกว่า OPD นอกจากนี้สีฟ้าที่เกิดขึ้นจะจางหายไปเมื่อทิ้งไว้เป็นเวลานานแสดงให้เห็นถึงความไม่เสถียรของผลิตภัณฑ์ที่เกิดขึ้น

ในขณะที่ลักษณะดังกล่าวไม่เกิดขึ้นเมื่อใช้ OPD เป็นสับสเตรท ดังนั้น OPD จึงเป็นสับสเตรทที่เหมาะสมกว่า TMB

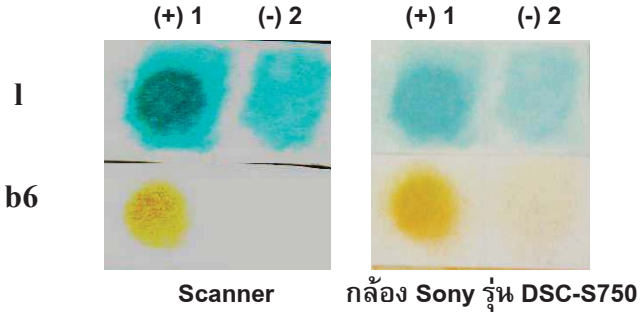

รูปที่ 2.16 ผลการตรวจสอบลำดับเบสของ DNA (SLE2) โดยใช้ b-PNA (SLE2) เป็นโพรบ บนแผ่นกระดาษกรองที่ตรึงด้วยพอลิเมอร์บรัชของ QPDMAEMA โดยศึกษาผลของชนิดของสับสเตรท: l) TMB (250 µL, 1.6 mg/mL ใน DMF/H_2O (1/9) และ 250 µL ของ 1.6 mg/mL urea-H_2O_2, b6) OPD (250 µL, 1.6 mg/mL และ 250 µL ของ 1.6 mg/mL urea-H_2O_2)

(10) ชนิดของรีเอเจนต์ที่ใช้หยุดปฏิกิริยาการเกิดสี

ในการทดลองนี้สนใจศึกษาผลของการใช้รีเอเจนต์ในการหยุดปฏิกิริยาการเกิดสี จากผลการทดลองที่แสดงใน**รูปที่ 2.17** พบว่าการใช้สารละลาย 1M HCl หลังจากการเติมสับสเตรทและทิ้งให้เกิดสีเป็นเวลา 1 นาที ช่วยทำให้ได้สีที่เข้มขึ้น แต่สีดังกล่าวจะหลุดออกจากกระดาษหลังจากทำการล้างเนื่องจากสารสีเหลืองที่เกิดขึ้นถูกเปลี่ยนให้อยู่ในรูปของเกลือซึ่งละลายน้ำและหลุดออกจากแผ่นกระดาษได้ นอกจากนี้กรดที่เติมจะไปโปรตอนเนตที่หมู่ฟอสเฟตของดีเอ็นเอ ส่งผลให้ดีเอ็นเอไม่สามารถยึดติดบนกระดาษด้วยแรงอิเล็กโทรสแตติก ดังนั้นการล้างแผ่นกระดาษด้วยน้ำประปาซึ่งเป็นวิธีที่ทำอยู่ตั้งแต่ต้นเป็นวิธีในการหยุดปฏิกิริยาการเกิดสีที่ดีกว่าการล้างด้วยกรด

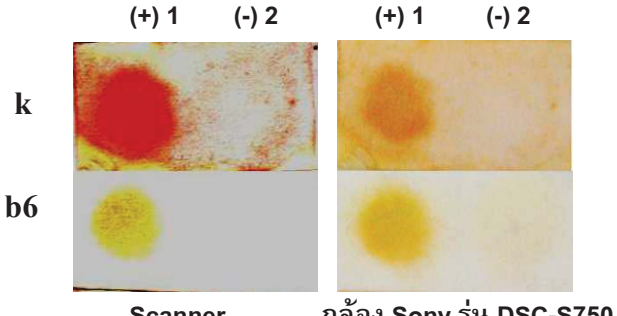

รูปที่ 2.17 ผลการตรวจสอบลำดับเบสของ DNA (SLE2) โดยใช้ b-PNA (SLE2) เป็นโพรบ บนแผ่นกระดาษกรองที่ตรึงด้วยพอลิเมอร์บรัชของ QPDMAEMA โดยศึกษาผลของรีเอเจนต์ที่ใช้หยุดปฏิกิริยาการเกิดสี: k) 0.1 M HCl และ b6) น้ำประปา

(11) ชนิดของสารละลายล้างหลังขั้นตอน SA-HRP binding

การทดลองในส่วนนี้สนใจการแปรเปลี่ยนสารละลายที่ใช้ล้างแผ่นกระดาษหลังขั้นตอนการหยด SA-HRP ผลการทดลองแสดงดัง**รูปที่ 2.18** ถึงแม้ว่าการใช้สารละลาย phosphate buffer pH 7.4 และ H_2O (การทดลอง l) เป็นสารละลายล้างจะสามารถกำจัดการดูดซับแบบไม่จำเพาะเจาะจงระหว่าง SA-HRP และแผ่นกระดาษได้ แต่แทบจะไม่ปรากฏสีเหลืองบนตำแหน่ง positive control ส่วนการใช้สารละลายล้างเป็น citrate buffer pH 5 และ

H_2O (การทดลอง m) เป็นสารละลายล้างสามารถกำจัดการดูดซับแบบไม่จำเพาะเจาะจงได้เช่นกัน และให้สีที่ตำแหน่ง positive control ได้อย่างชัดเจน แต่เมื่อใช้สารละลายล้างผสมทั้ง phosphate buffer pH 7.4 และ citrate buffer pH 5 หรือ CTB (การทดลอง b7) จะส่งผลทำให้สีที่ตำแหน่ง positive control เข้มกว่าการใช้สารละลายล้างที่มีเฉพาะ citrate buffer pH 5 (การทดลอง m) เนื่องจากสารละลายล้าง phosphate buffer pH 7.4 เป็นสภาวะที่ SA-HRP และ biotin สามารถเกิด hybridization กันได้ดี ส่วนสารละลาย citrate buffer pH 5 จะช่วยปรับ pH ทำให้เอนไซม์ทำงานได้ดีขึ้น ดังนั้นการใช้สภาวะในการล้างตามวิธีการทดลองที่ b7 จึงเป็นวิธีที่ให้ผลการทดสอบชัดเจนที่สุด

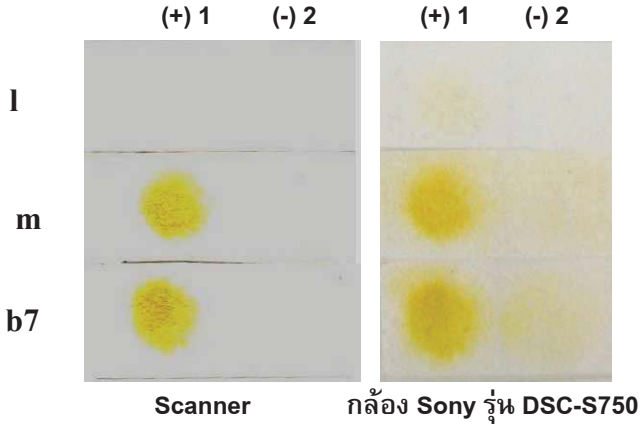

รูปที่ 2.18 ผลการตรวจสอบลำดับเบสของ DNA (SLE2) โดยใช้ b-PNA (SLE2) เป็นโพรบ บนแผ่นกระดาษกรองที่ตรึงด้วยพอลิเมอร์บรัชของ QPDMAEMA โดยศึกษาผลของสารละลายล้างหลังขั้นตอน SA-HRP hybridization ต่อการเกิดสี: l) 0.1 M PBS, 0.1 M NaCl และ H_2O, m) 0.1 M CTB pH 5 และ H_2O b7) 0.1 M PBS, ที่มี 0.1 M NaCl ตามด้วย H_2O และ 0.1 M CTB pH 5

(12) ชนิดของสารละลายล้างหลังขั้นตอน PNA hybridization

ลำดับเบสของดีเอ็นเอและพีเอ็นเอที่ใช้ในการศึกษาผลของตัวแปรในหัวข้อนี้แสดงใน**ตารางที่ 2.7**

ตารางที่ 2.7 ลำดับเบสของพีเอ็นเอและดีเอ็นเอที่ใช้ในการวิเคราะห์เพื่อศึกษาผลของชนิดของสารละลายล้างหลังขั้นตอน PNA hybridization

สัญลักษณ์	ลำดับเบส	หมายเหตุ
DNA (ATA)	dTGTGGATAGTGA	Full mismatch to PNA (AC)
DNA (GT)	dGTCATAGCATCA	Full match to PNA (AC)
b-PNA (AC)	b-O-O-TGATGCTATGAC-Lys	

ในการทดลองแบ่งชุดการทดสอบออกเป็น 6 จุด ซึ่งมีการหยดพีเอ็นเอและ/หรือดีเอ็นเอ ในรูปแบบดังแสดงใน**ตารางที่ 2.8** จุดที่ 1 เป็น positive control ซึ่งจะให้ความเข้มของสีสูงสุด เนื่องจากดีเอ็นเอซึ่งมีประจุเป็นลบสามารถจับยึดกับกระดาษที่ตรึงด้วย QPDMAEMA และที่ปลายของดีเอ็นเอมีไบโอตินซึ่งสามารถจับยึดกับเอนไซม์ SA-HRP เมื่อเติม OPD และ Urea-H_2O_2 ก็จะเกิดสีเหลืองเข้มขึ้น จุดที่ 2 เป็น negative control เนื่องจาก b-PNA (AC) และ DNA (ATA) มีลำดับเบสที่ต่างกันทุกตำแหน่ง (full mismatch) จุดที่ 3 เป็น negative control เพื่อพิสูจน์ให้เห็นว่าหากดีเอ็นเอไม่มีไบโอตินติดอยู่ก็ไม่ควรจะให้สีเมื่อมีการเติม SA-HRP/OPD/Urea-

H_2O_2 ในขณะที่จุดที่ 4 ควรให้ผลทดสอบที่เป็นบวกเนื่องจาก b-PNA (AC) และ DNA (GT) มีลำดับเบสที่เป็นคู่สมกัน (full match) จุดที่ 5 เป็น negative control ทดสอบเพื่อพิสูจน์ให้เห็นว่า b-PNA (AC) ไม่ควรยึดติดบนพื้นผิวของกระดาษ หากไม่มีการเติมดีเอ็นเอที่มีลำดับเบสเป็นคู่สมกัน ส่วนจุดที่ 6 เป็น negative control เพื่อแสดงให้เห็นว่า SA-HRP ไม่เกิดแรงกระทำอย่างไม่จำเพาะเจาะจงกับกระดาษหากไม่มีการเติมทั้งดีเอ็นเอและพีเอ็นเอ โดยหลังตรึงดีเอ็นเอแล้วปล่อยให้แห้ง จากนั้นหยดพีเอ็นเอลงตำแหน่งที่ 2 (mismatched DNA), 4 (matched DNA) และ 5 จากนั้นล้างด้วยสารละลายล้างดังตารางที่ 3 แล้ว block ด้วย 1% BSA w/v เป็นเวลา 30 นาที หลังจากนั้นหยด SA-HRP แล้วล้างด้วยสารละลายล้างดัง**ตารางที่ 2.9** ขั้นตอนสุดท้ายเป็นการจุ่มกระดาษกรองซึ่งตรึงด้วย QPDMAEMA ลงในสารละลายผสมของ OPD และ urea H_2O_2 เป็นเวลา 1 นาที

ตารางที่ 2.8 ดีเอ็นเอและพีเอ็นเอที่ใช้หยดบนแผ่นกระดาษกรองซึ่งตรึงด้วย QPDMAEMA ก่อนการเติมเอนไซม์ SA-HRP, สับสเตรท OPD และ Urea-H_2O_2 เพื่อศึกษาผลของตัวแปรในหัวข้อย่อย 2.5

จุดที่	ดีเอ็นเอ	พีเอ็นเอ	หมายเหตุ
1	b-DNA (SLE2)	-	Positive control (+)
2	DNA (ATA)	b-PNA (AC)	Negative control (-)
3	DNA (GT)	-	Negative control (-)
4	DNA (GT)	b-PNA (AC)	Positive result (+)
5	-	b-PNA (AC)	Negative control (-)
6	-	-	Negative control (-)

ผลการทดลองของการศึกษาในส่วนนี้แสดงใน**รูปที่ 2.19** เมื่อพิจารณาสารละลายล้างหลังจากขั้น PNA hybridization พบว่าการใช้ phosphate buffer pH 7.4 เป็นสารละลายล้างส่งผลทำให้การเกิด hybridization ระหว่างพีเอ็นเอโพรบและดีเอ็นเอตัวอย่างเกิดได้ดี อีกทั้งยังช่วยกำจัดการดูดซับแบบไม่จำเพาะเจาะจงได้อีกด้วย ดังแสดงผลในการทดสอบ n-q การใช้สารละลาย NaCl ร่วมกับ phosphate buffer (การทดลอง n) จะทำให้สีที่เกิดขึ้น ณ ตำแหน่งที่ 4 มีความเข้มลดลง แสดงให้เห็นว่าสารละลาย NaCl จะส่งผลทำให้ประสิทธิภาพการเกิด hybridization ระหว่างพีเอ็นเอและดีเอ็นเอลดลงหากเปรียบเทียบกับในกรณีที่ไม่มีการเติมเกลือ (การทดลอง o) การลดความเข้มข้นของ phosphate buffer ให้เหลือเพียง 0.05 M ช่วยทำให้เกิด hybridization ระหว่างพีเอ็นเอและดีเอ็นเอได้ดีขึ้น แต่จะพบปัญหาที่ว่าสารละลายดังกล่าวไม่สามารถกำจัดการดูดซับแบบไม่จำเพาะเจาะจงได้หมด ดังนั้นสารละลายล้างที่เหมาะสมคือ สารละลาย phosphate buffer pH 7.4 ดังการทดลอง o ส่วนการลดความเข้มข้นของ phosphate buffer ให้เหลือเพียง 0.05 M และไม่มีการเติม 0.1 M NaCl ในสารละลายล้าง ทั้งขั้นหลังPNA hybridization และหลัง SA-HRP binding (การทดลอง q) นอกจากจะทำให้การเกิด hybridization ระหว่างพีเอ็นเอและดีเอ็นเอลดลงแล้ว ยังส่งผลให้ไม่สามารถกำจัดการดูดซับแบบไม่จำเพาะเจาะจงได้

ตารางที่ 2.9 ชนิดของสารละลายที่ใช้ในการล้างแผ่นกระดาษกรองซึ่งตรึงด้วย QPDMAEMA ในแต่ละขั้นตอนของการทดสอบ

การทดลอง	Blocking step (30 min) before SA-HRP addition	Washing solution	
		After PNA hybridization	After SA-HRP binding
n	1% BSA w/v in 0.1 M PBS, 0.1 M NaCl	1) 0.1 M PBS, 0.1 M NaCl 2) H_2O	1) 0.1 M PBS pH 7.4, 0.1 M NaCl 2) H_2O 3) 0.1 M CTB pH 5
o	1% BSA w/v in 0.1 M PBS, 0.1 M NaCl	1) 0.1 M PBS 2) H_2O	1) 0.1 M PBS pH 7.4 2) H_2O 3) 0.1 M CTB pH 5
p	1% BSA w/v in 0.05 M PBS, 0.1 M NaCl	1) 0.05 M PBS, 0.1 M NaCl 2) H_2O	1) 0.05 M PBS pH 7.4, 0.1 M NaCl 2) H_2O 3) 0.1 M CTB pH 5
q	1% BSA w/v in 0.05 M PBS, 0.1 M NaCl	1) 0.05 M PBS 2) H_2O	1) 0.05 M PBS pH 7.4 2) H_2O 3) 0.1 M CTB pH 5

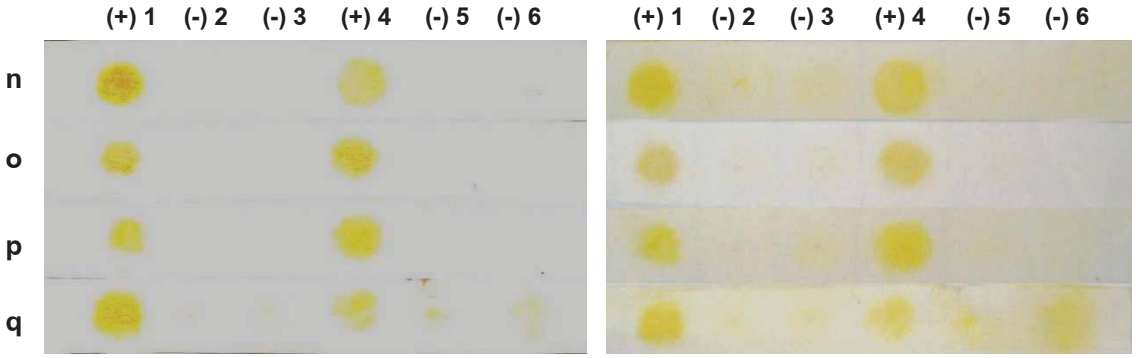

รูปที่ 2.19 ผลการตรวจสอบลำดับเบสของ DNA (GT) โดยใช้ b-PNA (AC) เป็นโพรบ บนแผ่นกระดาษกรองที่ตรึงด้วยพอลิเมอร์บรัชของ QPDMAEMA โดยศึกษาผลของสารละลายล้างหลังขั้น PNA hybridization และ SA-HRP binding

(13) ประสิทธิภาพในการตรวจวัดดีเอ็นเอตัวอย่างที่บ่งบอกความผิดปกติของโรคภูมิคุ้มกันบกพร่องหรือ SLE

การทดลองนี้จะศึกษาความหลากหลายและความมีประสิทธิภาพในการตรวจวัดดีเอ็นเอสังเคราะห์ที่บ่งบอกความผิดปกติของโรคภูมิคุ้มกันบกพร่องหรือ SLE โดยลำดับเบสของดีเอ็นเอและพีเอ็นเอที่ใช้ในการทดลองนี้

แสดงดัง**ตารางที่ 2.4 และ 2.7** ผลการทดลองที่ได้แสดงดัง**รูปที่ 2.20** จากการทดลองพบว่านอกจากกระดาษกรองที่ตรึง QPDMAEMA มีประสิทธิภาพและมีความหลากหลายในการตรวจวัดลำดับเบสของดีเอ็นเอแล้ว (การทดลอง t) เมื่อนำมาใช้ตรวจสอบลำดับเบสของดีเอ็นเอตัวอย่างที่บ่งบอกความผิดปกติของโรคภูมิคุ้มกันบกพร่องหรือ SLE ทั้ง SLE2 และ SLE1 ซึ่งมีลำดับเบสผิดไปเพียงหนึ่งตำแหน่งได้อย่างมีประสิทธิภาพ ดังผลในการทดลอง r และ s

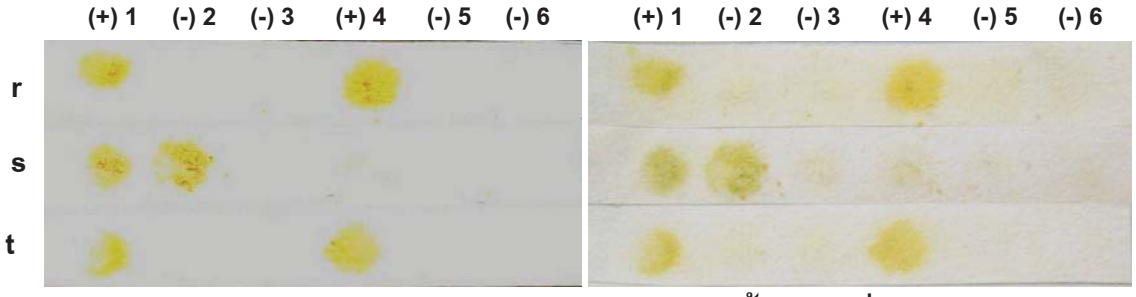

รูปที่ 2.20 ผลการตรวจสอบลำดับเบสของดีเอ็นเอบนแผ่นกระดาษกรองที่ตรึงด้วยพอลิเมอร์บรัชของ QPDMAEMA โดยใช้โพรบชนิดต่างๆ: r) b- PNA (SLE2), s) b-PNA (SLE1) และ t) b-PNA (AC)

(14) เสถียรภาพของกระดาษกรองที่ตรึงด้วย QPDMAEMA

ผลการทดลองที่แสดงใน**รูปที่ 2.21** แสดงถึงเสถียรภาพของกระดาษกรองที่ตรึง QPDMAEMA โดยเปรียบเทียบระหว่างกระดาษกรองที่นำมาใช้งานทันทีหลังจากการเตรียมเสร็จใหม่ๆ กับกระดาษกรองที่ตรึง QPDMAEMA แล้วเก็บไว้ที่อุณหภูมิห้อง (27-33 องศาเซลเซียส) เป็นเวลาหนึ่งเดือน จากผลการทดลองที่ได้พบว่าถึงแม้ว่าจะเก็บกระดาษกรองที่ตรึง QPDMAEMA ไว้นานถึงหนึ่งเดือนก็ไม่ทำให้ประสิทธิภาพของการเป็นแผ่นเมมเบรนในการตรวจสอบ DNA (SLE1) โดยใช้ b-PNA (SLE1) เป็นโพรบในการตรวจวัดลดลง

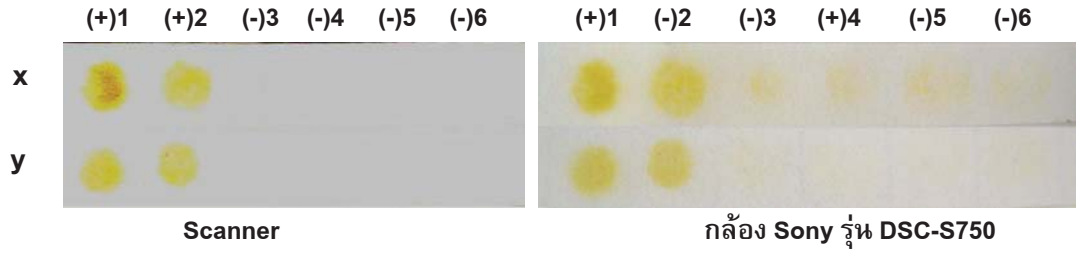

รูปที่ 2.21 ผลการตรวจสอบลำดับเบสของ DNA (SLE2) โดยใช้ b-PNA (SLE2) เป็นโพรบ บนแผ่นกระดาษกรองที่ตรึงด้วยพอลิเมอร์บรัชของ QPDMAEMA หลังจากที่เตรียมเสร็จทันที (x) เปรียบเทียบกับที่เก็บไว้ในช่วงอุณหภูมิ 27-33 $^{\circ}$C เป็นเวลา 1 เดือน (y)

***(15)* ขีดจำกัดการตรวจวัด**

เพื่อทดสอบประสิทธิภาพของแผ่นกระดาษที่พัฒนาขึ้นในการประยุกต์ใช้ในการตรวจวัดดีเอ็นเอที่มีอยู่ในสารตัวอย่างจริง คณะผู้วิจัยได้ทำการทดสอบเปรียบเทียบระหว่างดีเอ็นเอสังเคราะห์และดีเอ็นเอจากสารตัวอย่างจริงที่ผ่านการเพิ่มจำนวนด้วยเทคนิค polymerase chain reaction (PCR) ลำดับเบสของทั้งดีเอ็นเอและพีเอ็นเอที่ใช้ในการทดสอบแสดงใน**ตารางที่ 2.10** และแสดงผลการทดลองใน**รูปที่ 2.22**

ตารางที่ 2.10 ลำดับเบสของพีเอ็นเอและดีเอ็นเอที่ใช้ในการวิเคราะห์

สัญลักษณ์	ลำดับเบส	หมายเหตุ
b-PNA	b-o-o-CTACAAGCATAT-Lys	
DNA	5'- ATATGCTTGTAG -3'	Full match to PNA
b-DNA	5'-b-TTG GGA AGG GGA A-3'	

รูปที่ 2.22 ผลการตรวจสอบลำดับเบสของ DNA โดยใช้ b-PNA เป็นโพรบ (ลำดับเบสแสดงในตารางที่ 2.10) บนแผ่นกระดาษกรองที่ตรึงด้วยพอลิเมอร์บรัชของ QPDMAEMA

จากผลการทดลองพบว่าจะปรากฏสีชัดเจนในกรณีที่ใช้ดีเอ็นเอสังเคราะห์ (Syn.DNA) เมื่อเทียบกับตัวควบคุมบวกคือ b-DNA ในขณะที่จุดของสีจะจางมากในกรณีที่เป็นสารตัวอย่างจริงที่ผ่านการเพิ่มปริมาณด้วยเทคนิค PCR (0.74 µM, 60 µL) และเพิ่มความเข้มข้นด้วยการทำ speed dry และ denature ที่อุณหภูมิ 95 ºC ใน 5xSSC และทำให้เย็นอีกครั้ง ซึ่งจะทำให้ได้สารตัวอย่างที่มีความเข้มข้น 2 µM ใน 5xSSC, 0.5 M NaOH, 10 mM EDTA) ผลการทดลองในส่วนนี้แสดงให้เห็นว่าเทคนิคการวิเคราะห์ที่พัฒนาขึ้นยังมีข้อจำกัดในการนำไปใช้วิเคราะห์ดีเอ็นเอจากสารตัวอย่างจริงที่มีความเข้มข้นต่ำมาก

นอกจากนี้คณะผู้วิจัยได้พยายามเพิ่มขีดจำกัดในการตรวจวัด (detection limit) โดยการเปลี่ยนสับสเตรทของเอนไซม์ HRP จาก o-phenylenediamine และ urea-H_2O_2 เป็น 4-chloro-1-naphthol (CN), 3,3'-diaminobenzidine tetrahydrochloride (DAB) และ H_2O_2 จากผลการทดลองที่แสดงใน**รูปที่ 2.23** พบว่าสับสเตรททั้ง 2 ชนิด ให้ค่าขีดจำกัดในการตรวจวัดหรือความเข้มข้นของดีเอ็นเอต่ำสุดที่วัดได้ไม่แตกต่างกันคือ 10 fmol หรือ 1 µL จากสารละลายดีเอ็นเอความเข้มข้น 10 nM ในการทดลองนี้ใช้ DNA (SLE2) ซึ่งมีลำดับเบสเป็น dTTGGGAAGGGGAA และใช้ b-PNA (SLE2) เป็นโพรบซึ่งมีลำดับเบสเป็น b-O-O-TTCCCCTTCCCAA-Lys

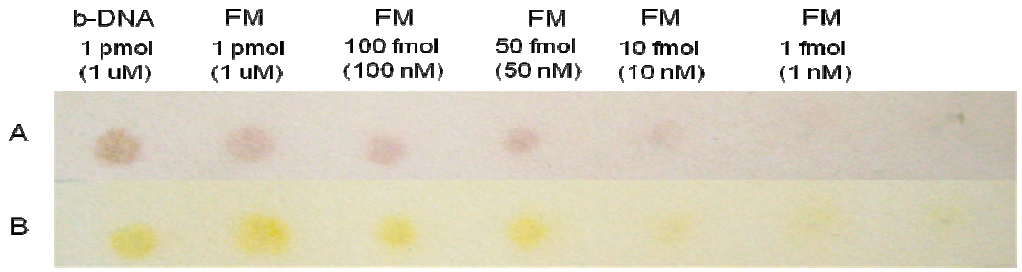

รูปที่ 2.23 ผลการตรวจสอบลำดับเบสของ DNA (SLE2) โดยใช้ b-PNA (SLE2) เป็นโพรบ บนแผ่นกระดาษกรองที่ตรึงด้วยพอลิเมอร์บรัชของ QPDMAEMA

สรุปผลการดำเนินงานวิจัย

งานวิจัยที่ได้ดำเนินการศึกษาวิจัยในตอนที่ 2 นี้แสดงให้เห็นว่าคณะผู้วิจัยประสบความสำเร็จในการตรึง QPDMAEMA บนกระดาษกรองด้วยปฏิกิริยาพอลิเมอไรเซชันริเริ่มจากพื้นผิวของมอนอเมอร์ DMAEMA ผ่านกลไกแบบ ARGET ATRP ตามด้วยการทำปฏิกิริยาควอเทอร์ไนเซชันด้วยเมทิลไอโอไดด์ โดยแผ่นกระดาษที่เตรียมได้แสดงประสิทธิภาพในการทำหน้าที่เป็นเมมเบรนสำหรับตรวจวัดลำดับเบสของดีเอ็นเอตามรูปแบบของ “Dot blot” โดยใช้ biotinylated acpcPNA เป็นโพรบ และขยายสัญญาณการเกิดสีด้วยเอนไซม์ ที่เหนือกว่าแผ่นเมมเบรนที่ใช้ทางการค้า แผ่นเมมเบรนที่พัฒนาขึ้นนี้แสดงการดูดซับอย่างไม่จำเพาะเจาะจงต่ำและมีประสิทธิภาพในการบ่งบอกลำดับเบสของดีเอ็นเอสังเคราะห์ที่ผิดไป 1 ตำแหน่งได้ที่มีปริมาณต่ำสุด 10 เฟมโตโมล อย่างไรก็ตามแผ่นเมมเบรนที่พัฒนาขึ้นยังไม่สามารถประยุกต์ใช้กับสารตัวอย่างดีเอ็นเอจริงที่มีความเข้มข้นต่ำมากได้ จำเป็นต้องมีการพัฒนารูปแบบการขยายสัญญาณที่มีประสิทธิภาพมากกว่านี้

อนุภาคนาโนแมกนีไทท์ที่มีการติดหมู่ฟังก์ชันบนพื้นผิวสำหรับการยึดติด PNA และ DNA

(Surface-functionalized magnetite nanoparticles for immobilization of PNA and DNA)

ที่มาและแนวคิดของงานวิจัย

ในปัจจุบันการสังเคราะห์และการประยุกต์ใช้อนุภาคนาโนแมกนีไทท์เพื่อประยุกต์ใช้ในทางการแพทย์กำลังได้รับความสนใจอย่างมาก ทั้งนี้เนื่องจากอนุภาคแมกนีไทท์มีขนาดเล็กระดับนาโนทำให้อนุภาคมีพื้นที่ผิวมากซึ่งเหมาะสำหรับการตรึงสารชีวโมเลกุลบนพื้นผิวอนุภาค นอกจากนี้ยังอาศัยประโยชน์จากสมบัติความเป็นแม่เหล็กของอนุภาคเพื่อใช้ในการแยกอนุภาคออกจากสารละลายได้ง่าย ดังนั้นงานวิจัยนี้จึงสนใจที่จะนำเอาข้อดีของอนุภาคนาโนแมกนีไทท์เพื่อใช้เป็น anion exchanger ในการวิเคราะห์ลำดับเบสของ DNA

ที่มาและแนวคิดของงานวิจัยนี้เกิดจากผลงานความสำเร็จของงานวิจัยของกลุ่มรองศาสตราจารย์ ดร. ธีรยุทธ วิไลวัลย์ ในการพัฒนาวิธีการวิเคราะห์ลำดับเบสในสายโซ่ DNA โดยการใช้ pyrrolidinyl PNA เป็นโพรบโดยใช้ anion exchanger ชนิดต่างๆเพื่อดูดซับสายเกลียวคู่ DNA.PNA ซึ่งอาศัยหลักการที่ว่าสายเกลียวคู่ PNA.DNA ซึ่งมีประจุลบสามารถดูดซับด้วยพันธะแบบไอออนิก (ionic interaction) กับตัวแลกเปลี่ยนไอออนที่มีประจุลบ (anion exchanger) ขณะที่ PNA ที่ไม่มีการเข้าคู่กับ DNA (unhybridized PNA) นั้นไม่มีประจุจึงไม่สามารถดูดซับบนพื้นผิวอนุภาคได้ อย่างไรก็ตาม การวิเคราะห์ด้วยวิธีนี้จะต้องมีขั้นตอนการกำจัด PNA ที่ไม่มีการเข้าคู่กับ DNA ออกโดยทำการล้างและเหวี่ยงแยกเป็นจำนวนหลายครั้ง ซึ่งเป็นข้อจำกัดในการวิเคราะห์หาลำดับเบสของ DNA ที่มีจำนวนตัวอย่างมากๆได้ ดังนั้นวัตถุประสงค์หลักของงานวิจัยนี้เป็นการดัดแปรพื้นผิวอนุภาคนาโนแมกนีไทท์ให้มีประจุบวกเพื่อใช้เป็น anion exchanger เพื่อใช้ในการแยกสายเกลียวคู่ PNA.DNA ที่มีประจุลบออกจาก PNA ที่ไม่มีการเข้าคู่กับ DNA โดยใช้สนามแม่เหล็กจากภายนอกแยกอนุภาคออกมาจากสารละลายและสามารถวิเคราะห์การยึดติดกันของสายเกลียวคู่ PNA.DNA กับอนุภาคนาโนแมกนีไทท์ได้ด้วยเทคนิค MALDI-TOF Mass Spectroscopy หรือเทคนิคอื่น ๆ ได้

<u>วิธีการทดลอง</u>

ขั้นตอนการสังเคราะห์และดัดแปรพื้นผิวอนุภาคนาโนแมกนีไทท์ แสดงดังภาพที่ 1 โดยแบ่งออกเป็น 3 ขั้นตอนดังนี้

1. การสังเคราะห์อนุภาคนาโนแมกนีไทท์ที่มีการตรึงสารเริ่มต้นปฏิกิริยาการพอลิเมอไรเซชันของอนุมูลอิสระแบบถ่ายโอนอะตอม (Atom Transfer Radical Polymerization, ATRP) (ATRP initiator) บนพื้นผิวอนุภาค

ขั้นตอนนี้แบ่งการทดลองออกเป็นสามส่วนย่อยดังนี้

1.1 การสังเคราะห์อนุภาคนาโนแมกนีไทท์ด้วยปฏิกิริยาการแตกสลายที่อุณหภูมิสูง (thermal decomposition)

ปฏิกิริยาการแตกสลาย iron acetyl acetonate ($Fe(acac)_3$) ในเบนซิลแอลกอฮอล์ ที่อุณหภูมิ 175 ^{o}C เป็นเวลา 48 ชั่วโมง ภายใต้สภาวะไนโตรเจน ขณะที่ปฏิกิริยากำลังดำเนินไปจะสังเกตเห็นการเปลี่ยนแปลงของสารจากสารละลายสีแดงเป็นสีดำ หลังสิ้นสุดปฏิกิริยานำสารละลายสีดำมาล้างด้วยเอทานอลและเมทิลีนคลอไรด์ 3-4 รอบ ทำให้แห้งและพิสูจน์เอกลักษณ์ของอนุภาคด้วยเทคนิค Fourier Transform Infrared Spectrometer (FTIR)

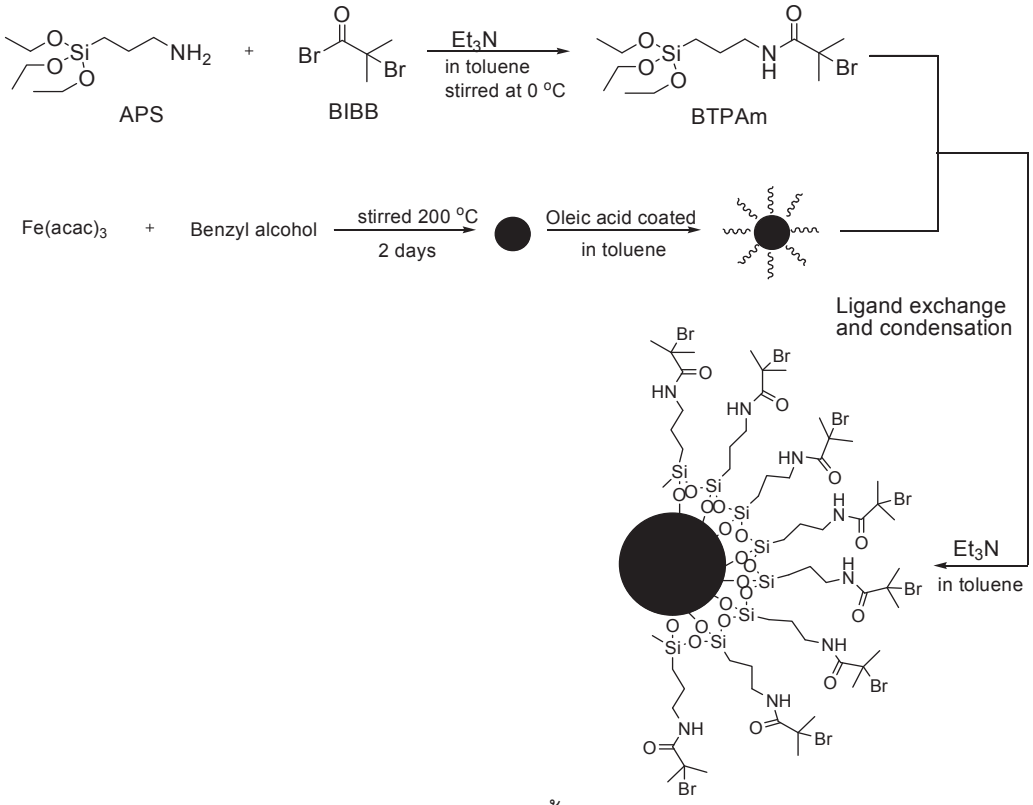

ภาพ 1 การสังเคราะห์และดัดแปรพื้นผิวอนุภาคนาโนแมกนีไทท์

1.2. การสังเคราะห์ 2-bromo-2-methyl-N-(3-(triethoxysilyl)propyl)propanamide (BTPAm) เพื่อเป็นสารเชื่อมต่อ (linker) (ภาพ 2)

ละลาย 2-bromoisobutyrylbromide (BIBB) ในโทลูอีน หยดช้าๆในสารละลายผสมระหว่าง triethoxylamine (TEA) 1และ 3-aminopropyl triethoxysilane (APS) ในโทลูอีน ทำปฏิกิริยาภายใต้สภาวะไนโตรเจนที่อุณหภูมิ 0 °C เป็นเวลา 2 ชั่วโมงและทำปฏิกิริยาต่อที่อุณหภูมิห้องตลอดคืน หลังสิ้นสุดปฏิกิริยากรองสารผสมเพื่อกำจัดเกลือและระเหยเอา TEA ที่ไม่ทำปฏิกิริยาออก ทำให้แห้งและพิสูจน์เอกลักษณ์ด้วยเทคนิค FTIR

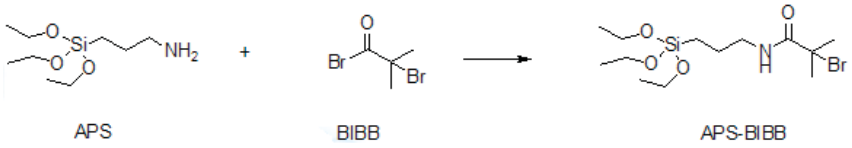

ภาพ 2 การสังเคราะห์สารเชื่อมต่อ BTPAm

1.3. การตรึงสารเชื่อมต่อ BTPAm ลงบนอนุภาคนาโนแมกนีไทท์ (ภาพ 3)

ทำการเคลือบกรดโอเลอิกบนอนุภาคเพื่อเสถียรอนุภาคไม่ให้เกิดเกาะกลุ่มเป็นตะกอนใหญ่ (aggregation) จากนั้นนำอนุภาคที่เคลือบด้วยกรดโอเลอิกมาผสมรวมกันกับ BTPAm, triethylamine (TEA) ในโทลูอีน โดยทำการปั่นกวนภายใต้สภาวะไนโตรเจนที่อุณหภูมิห้องเป็นเวลา 24 ชั่วโมง จากนั้นนำสารละลายอนุภาคนาโนแมกนีไทท์มาตกตะกอนใน เมธานอล และ re-disperse ในโทลูอีน จำนวน 3-4 ครั้ง เพื่อกำจัดสารที่ไม่ทำปฏิกิริยาออก จากนั้นจึงนำอนุภาคมาทำให้แห้งและพิสูจน์เอกลักษณ์ด้วยเทคนิค FTIR

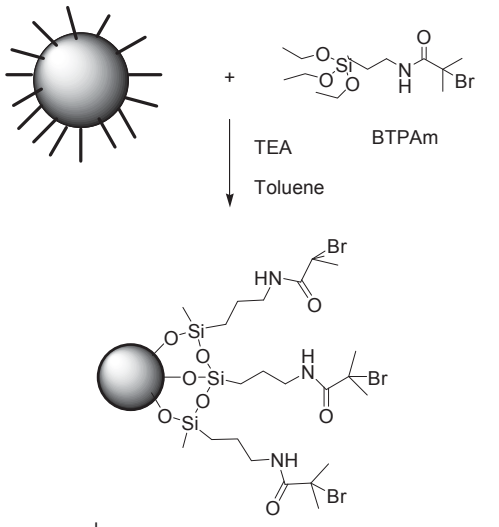

ภาพ 3 การตรึงสารเชื่อมต่อ BTPAm ลงบนอนุภาคนาโนแมกนีไทท์

2. การสังเคราะห์พอลิเมอร์ร่วมระหว่าง diethylamino ethyl methacrylate (DEAEMA) และ poly(ethyleneglycol) methacrylate (PEGMA) จากพื้นผิวอนุภาค โดยการปรับเปลี่ยนอัตราส่วนโดยโมลระหว่างพอลิเมอร์ทั้งสองเพื่อปรับเปลี่ยนความเป็นประจุบวกและระดับความเป็นขั้วบนพื้นผิวอนุภาค

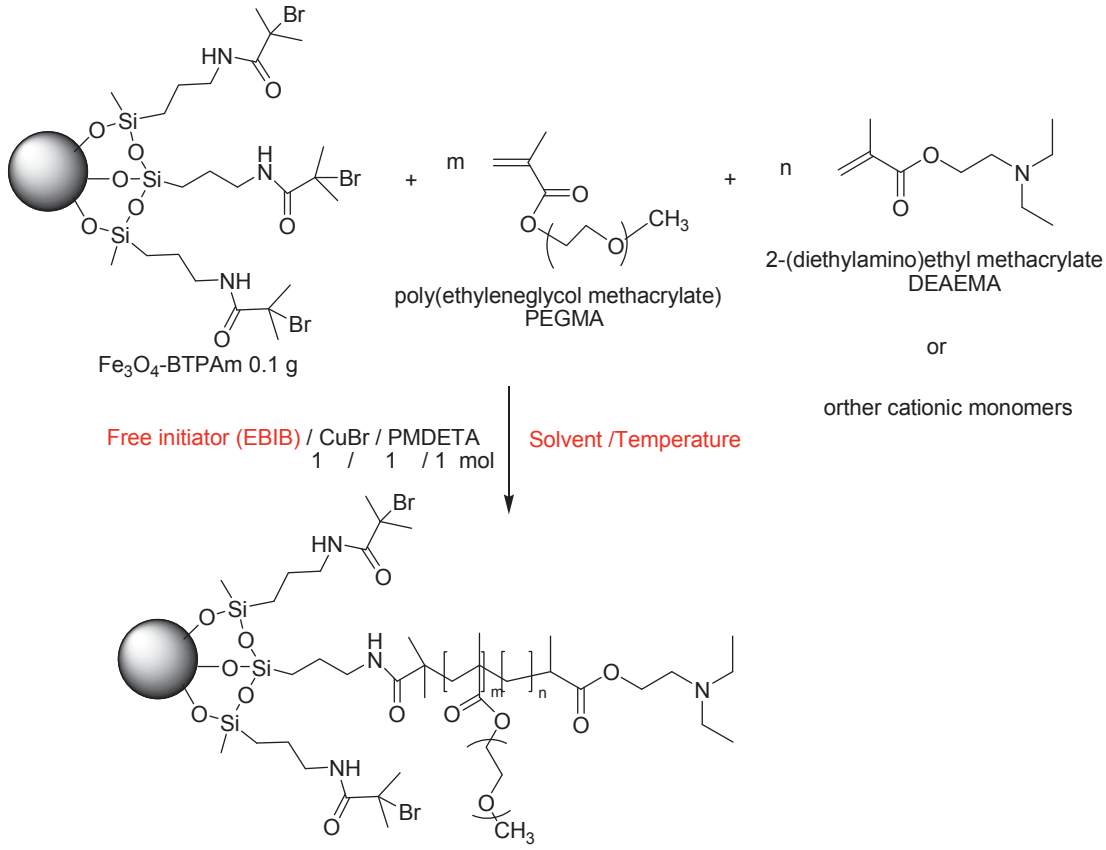

ภาพ 4 การดัดแปรพื้นผิวของอนุภาคนาโนแมกนีไทท์ด้วย PEGMA และ poly(DEAEMA) โดยใช้ปฏิกิริยา ATRP

การทดลองจะเริ่มจากการชั่งอนุภาคนาโนแมกนีไทท์ที่ติด BTPAm แล้ว 0.1 g ละลายในโทลูอีน 5.62 ml (60 %w/v) แล้วนำไป sonicate เป็นเวลา 1 ชั่วโมง จากนั้นจึงเติม PEGMA (poly(ethyleneglycol methacrylate)) (350 g/mol) 4.76 ml (50 mol) DEAEMA (2-(diethylamino) ethyl methacrylate) 3.34 ml (50 mol) EBIB (2-bromoisobutylate) 0.049 ml (1 mol) และ CuBr 0.048 g (1 mol) ลงในขวดสำหรับทำปฏิกิริยา ATRP (Atom transfer radical polymerization) จากนั้นนำของผสมไป freeze pump thaws 3-4 รอบ เพื่อกำจัดออกซิเจนในระบบ แล้วจึงทำการฉีด PMDETA (1,1,4,7,7-pentamethyldiethylenetri-amine) ลงไปอย่างรวดเร็ว แล้วนำไปทำปฏิกิริยาที่อุณหภูมิ 50 °C เป็นเวลา 24 ชั่วโมง โดยจะทำการ sampling สารทุกๆ 1 ชั่วโมง หลังสิ้นสุดปฏิกิริยาเติมสารละลาย BHT (ความเข้มข้น 9000 ppm) ลงไป 100 µL เพื่อ

ช่วยยับยั้งการดำเนินไปของปฏิกิริยา แล้วนำของผสมมาเหวี่ยงแยก (14,000 rpm) เป็นเวลา 15 นาที เพื่อทำการตกตะกอนอนุภาค นำส่วนของสารละลายไปศึกษาสมบัติทางจลศาสตร์ รวมถึงการดำเนินไปของปฏิกิริยาด้วยเทคนิค ^{1}H-NMR ต่อไป โดยได้ศึกษาที่อัตราส่วนโดยโมลเป็น 100:0, 50:50 และ 0:100 ของ PEGMA:DEAEMA ตามลำดับ

3. การประยุกต์ใช้อนุภาคที่มีประจุบวกเพื่อใช้เป็น anion exchanger เพื่อใช้ในการแยก PNA.DNA hybrid ซึ่งมีประจุลบออกจาก unhybridized PNA ซึ่งไม่มีประจุ (ภาพ 5)

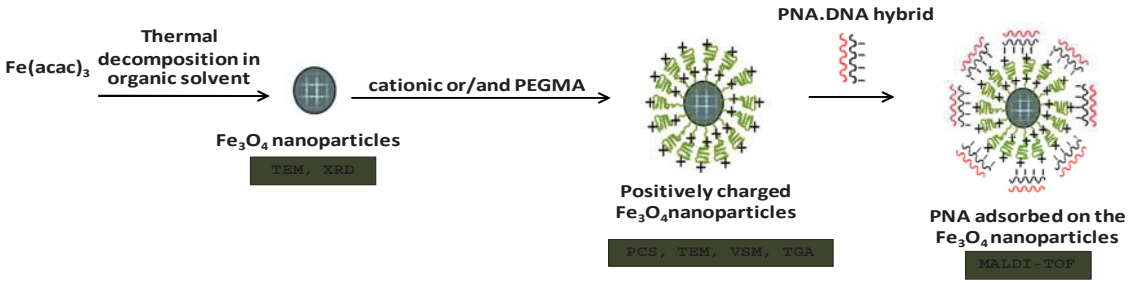

ภาพ 5 การประยุกต์ใช้อนุภาคนาโนแมกนีไทท์เพื่อใช้ในการดูดซับ PNA.DNA hybrid บนพื้นผิวอนุภาค

การทดลองจะเริ่มจากการนำเอาอนุภาคนาโนแมกนีไทท์แต่ละชนิดไปทำให้กระจายตัวในฟอสเฟตบัฟเฟอร์ pH=7 ประมาณ 20 µl จากนั้นเติมสารละลาย PNA · DNA ลงในอนุภาคที่กระจายตัวแล้ว และตั้งทิ้งไว้ 15 นาที หลังจากนั้นทำการแยกอนุภาคนาโนแมกนีไทท์ ออกจากสารละลาย PNA · DNA ด้วยแท่งแม่เหล็ก แล้วทำการล้างอนุภาคด้วยตัวทำละลายที่เหมาะสม จากนั้นนำส่วนของอนุภาคนาโนแมกนีไทท์ที่ทำการล้างแล้วไปทดสอบด้วยเทคนิค MALDI-TOF spectrometry

ผลการทดลองและอภิปรายผลการทดลอง

1. การสังเคราะห์อนุภาคนาโนแมกนีไทท์ที่มีการตรึง ATRP initiator บนพื้นผิวอนุภาค

1.1 การสังเคราะห์อนุภาคนาโนแมกนีไทท์ด้วยปฏิกิริยาการแตกสลายที่อุณหภูมิสูง (thermal decomposition)

เมื่อนำอนุภาคนาโนแมกนีไทท์ที่ได้ภายหลังจากปฏิกิริยาการแตกสลายของไอรอนอะซิติลอะซิโตเนต และผ่านการล้างตัวทำละลายที่มากเกินพอมาทำการพิสูจน์เอกลักษณ์ด้วยเทคนิค FTIR พบว่าสเปคตรัม FTIR ปรากฏเฉพาะสัญญาณ Fe-O ของสารประกอบเหล็กออกไซด์ที่ตำแหน่ง 578 cm^{-1} และจากการยืนยันโครงสร้างผลึกของอนุภาคนาโนแมกนีไทท์ด้วยเทคนิค XRD (ภาพ 7) พบสัญญาณตรงกันกับสัญญาณของอนุภาคนาโนแมกนีไทท์มาตรฐาน (2θ = 30.2° 35.6° 43.3° 53.7° 57.2° และ 62.7°)

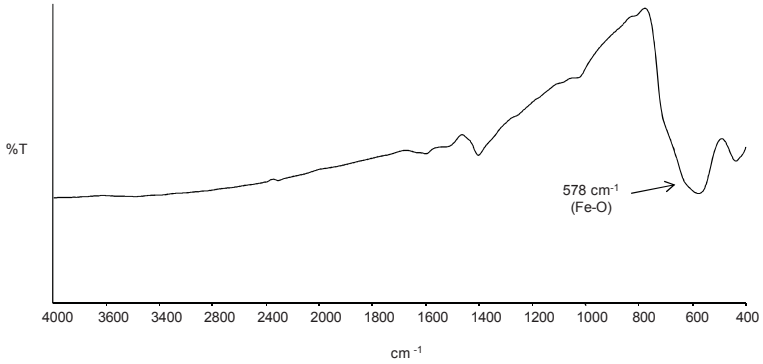

ภาพ 6 สเปคตรัม FTIR ของอนุภาคนาโนแมกนีไทท์

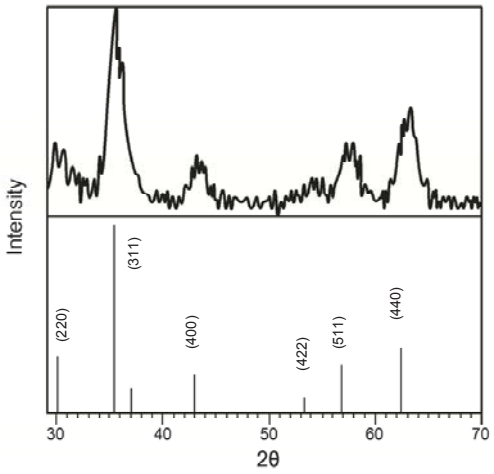

ภาพ 7 สเปคตรัม XRD ของอนุภาคแมกนีไทท์เทียบกับสารมาตรฐานแมกนีไทท์ (ICSD No. 01-075-0449)

อนุภาคแมกนีไทท์ที่ได้ภายหลังการทำให้แห้งจะมีลักษณะเป็นของแข็งสีดำ จากการศึกษาขนาดและการกระจายของขนาดอนุภาคด้วยเทคนิค TEM พบว่าอนุภาคมีขนาดเส้นผ่านศูนย์กลางอยู่ในช่วง 5-11 nm และมีขนาดเส้นผ่าศูนย์กลางเฉลี่ย 7.78 ± 1.58 nm (ภาพ 8)

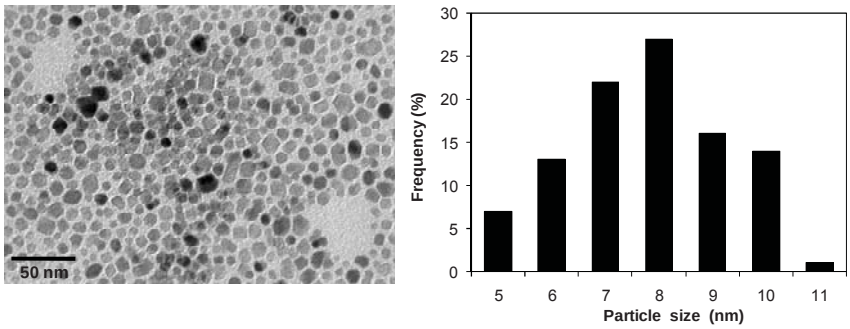

ภาพ 8 ขนาดและการกระจายของขนาดอนุภาคจากเทคนิค TEM

1.2 การสังเคราะห์ 2-bromo-2-methyl-N-(3-(triethoxysilyl)propyl)propanamide (BTPAm) เพื่อเป็นสารเชื่อมต่อ (linker)

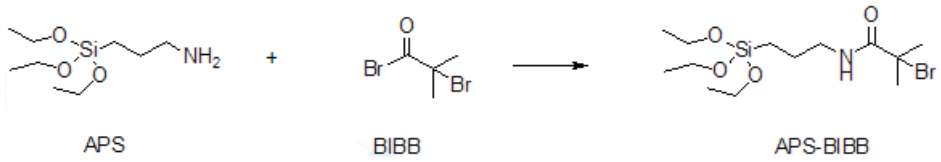

เมื่อทำการสังเคราะห์BTPAm พบว่า BTPAm จะมีลักษณะเป็นตะกอนสีขาวอมเหลือง และเมื่อนำเอา BTPAm มาทำการพิสูจน์เอกลักษณ์ด้วยเทคนิค FTIR พบว่าจากสเปคตรัม FTIR พบสัญญาณ -NH-CO- (1658 cm^{-1}) และสัญญาณ N-H (3345 cm^{-1}) ของหมู่เอไมด์ (ภาพ 9c) ซึ่งแสดงถึงการเกิดปฏิกิริยา coupling ระหว่างหมู่ฟังก์ชัน amine และ acid bromide นอกจากนี้ยังพบสัญญาณ-CO-Br (1738 cm^{-1}) ซึ่งแสดงถึงการเหลืออยู่ของ BIBB ที่ไม่ทำปฏิกิริยาเล็กน้อย จาก สเปคตรัม ^{1}H NMR ของ BTPAm (ภาพ 10c) พบสัญญาณเมทิลลีนโปรตอนของหมู่เอมีนตำแหน่ง 2.50 ppm (สัญญาณ *a*) ของ APS (ภาพ 10a) เกิดการเลื่อนตำแหน่ง (shift) ไปที่ตำแหน่ง 3.22 ppm (สัญญาณ *a'*) ของ BTPAm (ภาพ 9c) ซึ่งแสดงถึงการเกิดปฏิกิริยา coupling เกิดเป็น BTPAm ขึ้น นอกจากนี้ยังพบการเลื่อนตำแหน่ง (shift) ของสัญญาณเมทิลลีนโปรตอนตำแหน่ง 1.45 ppm (สัญญาณ *b*) เป็น 1.62 ppm (สัญญาณ *b'*) เล็กน้อย และการเลื่อนของสัญญาณเมทิลโปรตอนตำแหน่ง 2.50 ppm (สัญญาณ *f*) เป็น 2.40 ppm (สัญญาณ *f'*) ซึ่งแสดงถึงการเกิดขึ้นของ BTPAm เช่นกัน

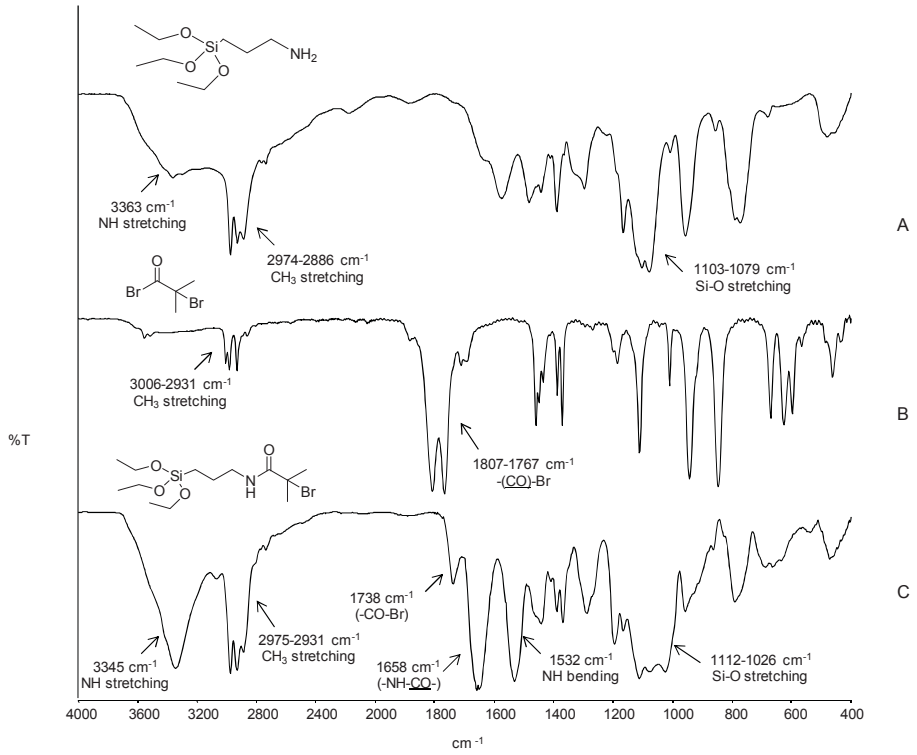

ภาพ 9 FTIR สเปคตราของ (A) APS (B) BIBB และ (C) BTPAm

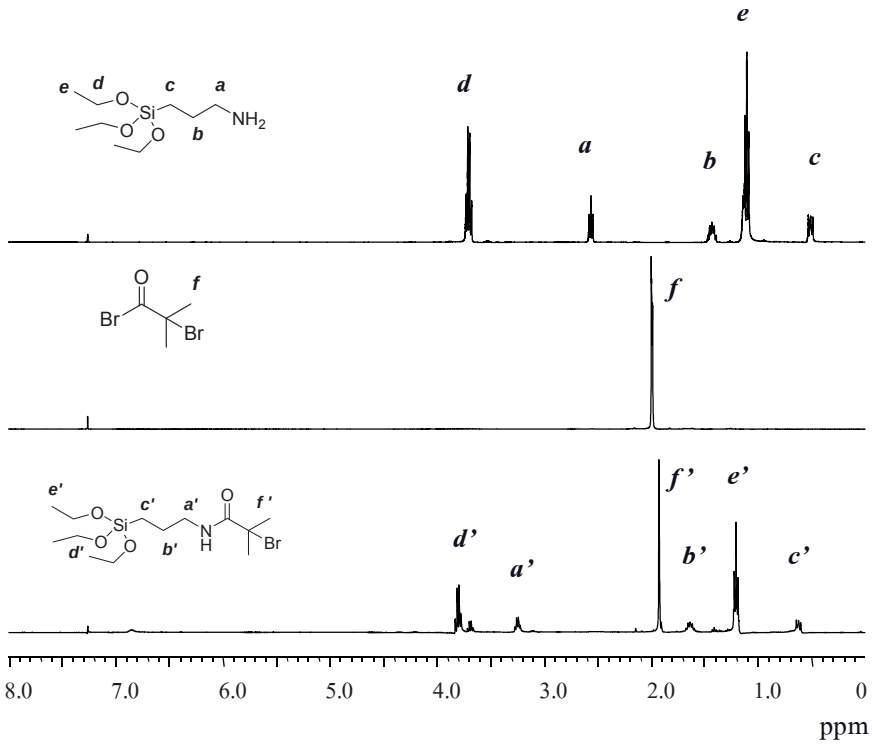

ภาพ 10 ^{1}H NMR สเปคตราของ (A) APS (B) BIBB และ (C) BTPAm

1.3. การตรึงสารเชื่อมต่อ BTPAm บนอนุภาคแมกนีไทท์ (BTPAm-coated magnetite nanoparticle, MNPs)

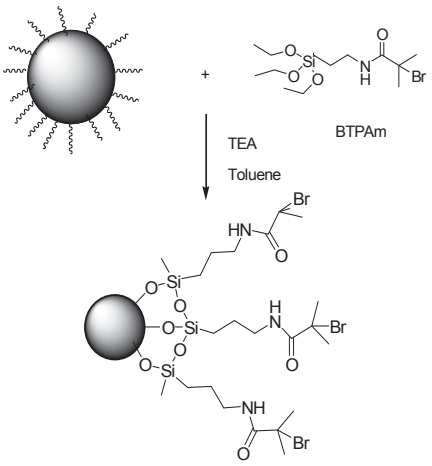

เมื่อนำเอาอนุภาคแมกนีไทท์ที่ทำการตรึงสารเชื่อมต่อ BTPAm มาพิสูจน์เอกลักษณ์ด้วยเทคนิค FTIR จากสเปกตรัม FTIR จะพบสัญญาณ Fe-O (586 cm^{-1}) ของสารประกอบเหล็กออกไซด์ (ภาพ 11) สัญญาณของหมู่ฟังก์ชันเอไมด์ ได้แก่ -NH-CO- stretching (1648 cm^{-1}) N-H bending (1529 cm-1) และ N-H stretching (3341 cm^{-1}) และสัญญาณ Si-O (1019-1111 cm^{-1}) แสดงถึงการมี BTPAm อยู่บนพื้นผิวอนุภาค

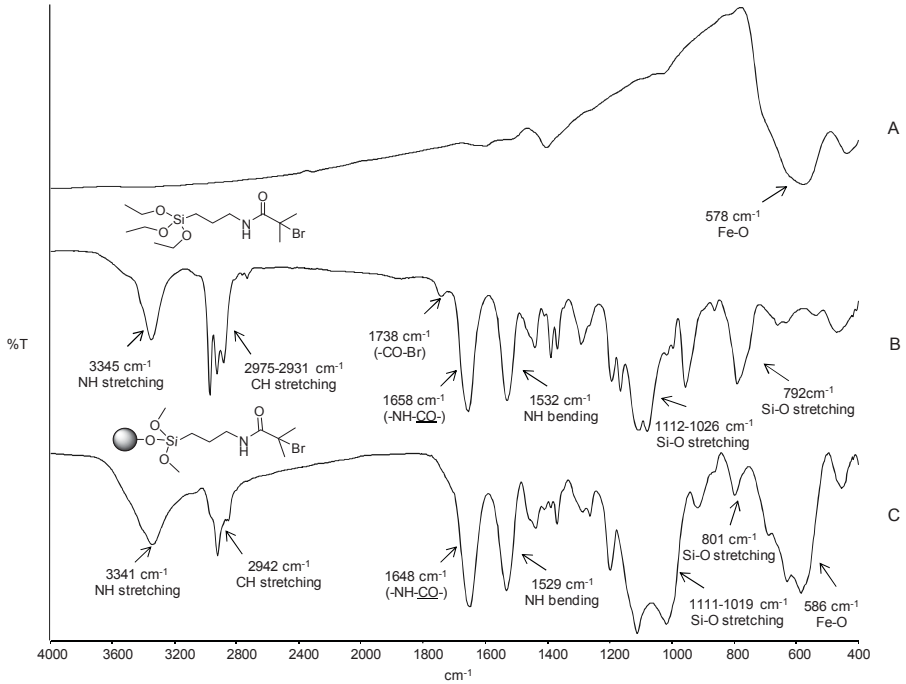

ภาพ 11 FTIR สเปคตราของ A) bare magnetite, B) BTPAm และ C) BTPAm-coated MNPs

2. การดัดแปรพื้นผิวของอนุภาคนาโนแมกนีไทท์ด้วย PEGMA และ DEAEMA โดยใช้ปฏิกิริยา ATRPโดยการปรับเปลี่ยนอัตราส่วนโดยโมลระหว่างพอลิเมอร์ทั้งสองเพื่อปรับเปลี่ยนความเป็นประจุบวกและระดับความเป็นขั้วบนพื้นผิวอนุภาค

ขั้นตอนนี้จะเป็นการนำอนุภาคนาโนแมกนีไทท์ที่สังเคราะห์ได้ในขั้นตอนที่ 1 เพื่อเป็น solid support สำหรับปฏิกิริยา ATRP (BTPAm) ระหว่าง poly(ethyleneglycol methacrylate) (PEGMA) และ diethylamino ethyl methacrylate (DEAEMA) โดยทำการศึกษาการดำเนินไปของปฏิกิริยา (% conversion) ของปฏิกิริยา ATRP น้ำหนักโมเลกุลของพอลิเมอร์ร่วมที่สังเคราะห์ได้โดยใชเทคนิคการใช้ “sacrificial” initiator ทั้งนี้เนื่องจากพอลิเมอร์ที่อยู่บนพื้นผิวอนุภาคนาโนไม่สามารถวิเคราะห์ด้วยเทคนิค 1H NMR ได้เนื่องจากอนุภาคนาโนมีสมบัติเป็นสารแม่เหล็ก จึงมีการเติม free initiator เพื่อให้เกิดปฏิกิริยา ATRP ไปพร้อมๆกับ initiator บนพื้นผิวอนุภาคนาโน โดยในการทดลองนี้ใช้ ethylbromoisobutyrate (EBIB) เป็น sacrificial initiator โดยในการทดลองได้ทำการแยกอนุภาคนาโนแมกนีไทท์ออกจากสารละลายด้วยแท่งแม่เหล็กถาวร และนำส่วนของสารละลายซึ่งมี free polymer ไปศึกษาโครงสร้างเคมีและน้ำหนักโมเลกุลของพอลิเมอร์ รวมถึงการดำเนินไปของปฏิกิริยาด้วยเทคนิค ^{1}H-NMRโดยได้ศึกษาที่อัตราส่วนโดยโมลเป็น 100:0, 50:50 และ 0:100 ของ PEGMA:DEAEMA ตามลำดับ

2.1 การศึกษา % conversion ของปฏิกิริยาการดัดแปรพื้นผิวของอนุภาคนาโนแมกนีไทท์ด้วย ด้วย PEGMA และ DEAEMA ที่มีอัตราส่วนที่แตกต่างกัน

2.1.1 การศึกษา % conversion ของปฏิกิริยาการดัดแปรพื้นผิวของอนุภาคนาโนแมกนีไทท์ด้วยด้วยPEGMA homopolymerโดยมีองค์ประกอบของพอลิเมอร์และสภาวะที่ใช้ดังตารางที่ 1

ตาราง 1 องค์ประกอบและสภาวะที่ใช้ในปฏิกิริยาการดัดแปรพื้นผิวของอนุภาคนาโนแมกนีไทท์ด้วย PEGMA homopolymer

PEGMA:DEAEMA:Catalyst (CuBr).:Ligand (PMDETA):Free initiator (EBIB)	ตัวทำละลาย	อุณหภูมิ
100:0:1:1:1	โทลูอีน	50 $^{\circ}$C

เมื่อทำการคำนวณ % conversion (ตามที่วิธีที่ได้เคยกล่าวไว้ในรายงานความก้าวหน้าครั้งก่อน) พบว่า เมื่อเวลาในการทำปฏิกิริยาเพิ่มมากขึ้น % conversion จะมีค่าเพิ่มขึ้นเรื่อยๆ จนเริ่มคงที่ ณ เวลา 16 ชั่วโมงซึ่งได้ %conversion ของพอลิเมอร์ประมาณ 90 % แต่เราจะเลือกพอลิเมอร์ที่มีค่า % conversion ไม่สูงมากนัก (40-50 % conversion) ไปใช้ในการทดลองขั้นต่อไป เพื่อให้ได้พอลิเมอร์ที่มีการกระจายของน้ำหนักโมเลกุลแคบ

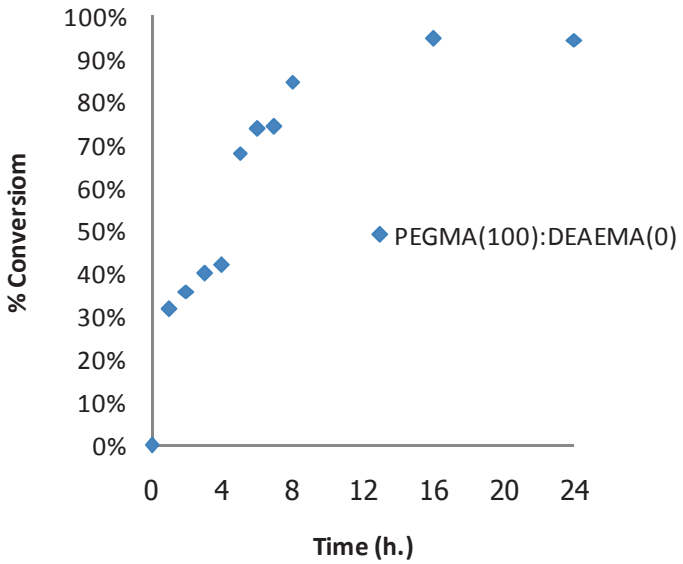

ภาพ 12 % conversion vs time plot ของ PEGMA โฮโมพอลิเมอร์

เมื่อนำมาศึกษาอันดับของปฏิกิริยาโดยพล็อตกราฟระหว่าง ln $[M_o]/[M]$ เทียบกับเวลาการเกิดปฏิกิริยา พบว่าในช่วงก่อนทำปฏิกิริยาจนถึงที่เวลา 8 ชั่วโมง ค่า ln $[M_o]/[M]$ จะอยู่ในแนวเส้นตรง แสดงว่าเป็นปฏิกิริยาอันดับหนึ่ง คือปฏิกิริยาจะดำเนินไปโดยขึ้นอยู่กับความเข้มข้นสารมอนอเมอร์เพียงชนิดเดียว จึงทำให้ปฏิกิริยาสามารถดำเนินไปในอัตราที่สม่ำเสมอ แต่เมื่อเวลาในการทำปฏิกิริยาเพิ่มมากขึ้นค่า ln $[M_o]/[M]$ มีค่าเบี่ยงเบนออกจากเส้นตรง ซึ่งอาจเนื่องมาจากการเกิดปฏิกิริยา termination เนื่องจากการ combination ของ active radical จึงทำให้ความเข้มข้นของ active radical ลดลง

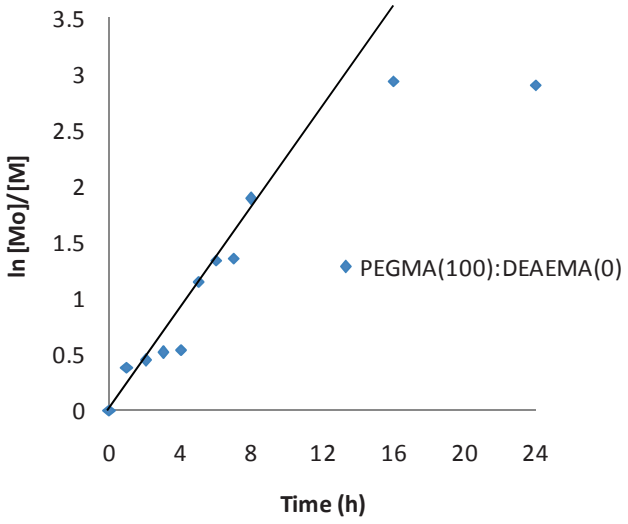

ภาพ 13 ln $[M_o]/[M]$ vs time plot ของ PEGMA homopolymer

2.1.2 การศึกษา % conversion ของปฏิกิริยาการดัดแปรพื้นผิวของอนุภาคนาโนแมกนีไทท์ด้วยด้วย PEGMA และ DEAEMAโดยมีองค์ประกอบของพอลิเมอร์และสภาวะที่ใช้ดังตารางที่ 2

ตาราง 2 องค์ประกอบและสภาวะที่ใช้ในปฏิกิริยาการดัดแปรพื้นผิวอนุภาคนาโนแมกนีไทท์ด้วย PEGMA และ DEAEMA

PEGMA:DEAEMA:Catalyst (CuBr).:Ligand (PMDETA):Free initiator (EBIB)	ตัวทำละลาย	อุณหภูมิ
50:50:1:1:1	โทลูอีน	50 °C

เมื่อทำการคำนวณ % conversion ของมอนอเมอร์ทั้งสองชนิดที่เวลาต่างๆ กันพบว่า % conversion ของมอนอเมอร์ทั้งสองชนิดเพิ่มขึ้นเรื่อยๆ เมื่อเวลาเพิ่มมากขึ้น และเมื่อพิจารณาอัตราการเกิดปฏิกิริยาของมอนอเมอร์ทั้งสองชนิดพบว่ามีอัตราการเกิดปฏิกิริยาใกล้เคียงกันโดย PEGMA มี reactivity สูงกว่าเล็กน้อย โดยพอลิเมอร์ที่จะนำไปใช้ในขั้นตอนต่อไป (quarternization) จะเลือกหยุดปฏิกิริยาที่พอลิเมอร์ทั้งสองชนิดมีค่า % conversion เป็น 40-50 %

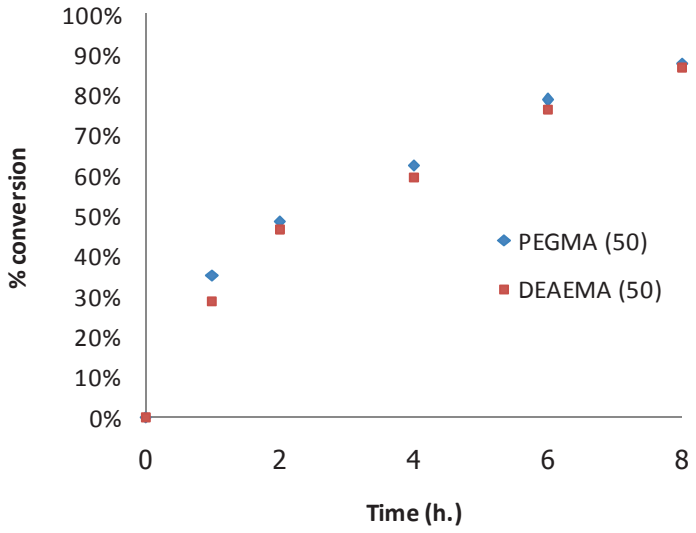

ภาพ 14 % conversion vs time plot ของพอลิเมอร์ร่วม PEGMA และ DEAEMA

2.1.3. การศึกษา % conversion ของปฏิกิริยาการดัดแปรพื้นผิวของอนุภาคนาโนแมกนีไทท์ด้วยด้วย DEAEMA homopolymer โดยมีองค์ประกอบของพอลิเมอร์และสภาวะที่ใช้ดังตารางที่ 3

ตาราง 3 องค์ประกอบและสภาวะที่ใช้ในปฏิกิริยาการดัดแปรพื้นผิวอนุภาคนาโนแมกนีไทท์ด้วย DEAEMA homopolymer

PEGMA:DEAEMA:Catalyst (CuBr).:Ligand (PMDETA):Free initiator (EBIB)	ตัวทำละลาย	อุณหภูมิ
0:100:1:1:1	โทลูอีน	50 °C

สามารถคำนวณ % conversion การเกิดเป็น poly(diethyl amino) ethyl methacrylate (PDEAEMA) ได้ในทำนองเดียวกันกับ PEGMA homopolymer และ PEGMA-DEAEMA copolymer จากกราฟในภาพที่ 4 พบว่าปฏิกิริยาดำเนินไปถึง 94% conversion ที่เวลา 24 ชั่วโมง และเมื่อนำมาพล็อตกราฟระหว่าง ln $[M_0]/[M]$ กับเวลา เพื่อศึกษาอันดับของปฏิกิริยา พบว่าเป็นปฏิกิริยาอันดับหนึ่งในช่วง 8 ชั่วโมงแรกของปฏิกิริยา

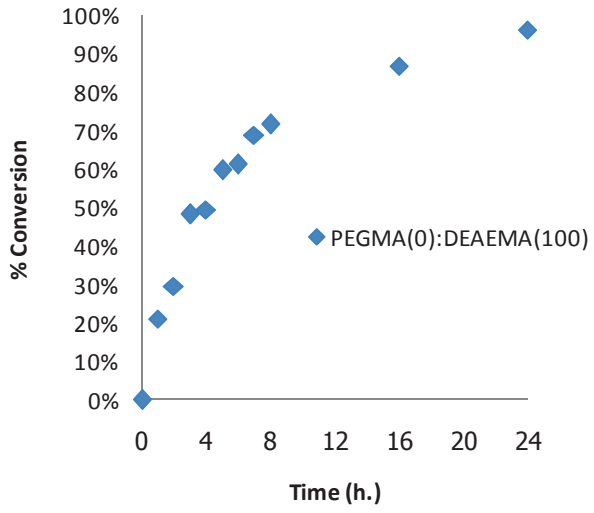

ภาพ 15 % conversion vs time plot ของ DEAEMA homopolymer

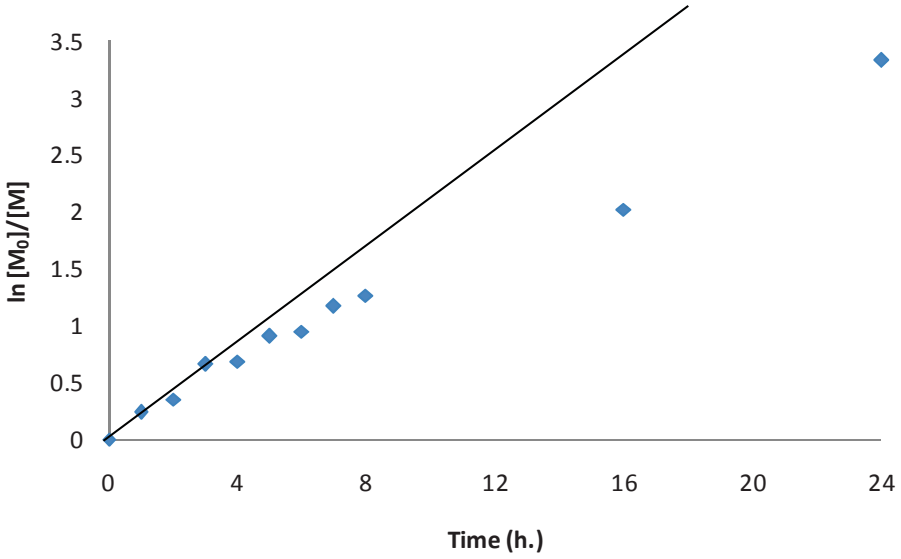

ภาพ 16 ln [M_o]/[M] vs time plot ของ DEAEMA homopolymer

2.2 การศึกษาน้ำหนักโมเลกุลและค่าการกระจายน้ำหนักโมเลกุลด้วยเทคนิค GPC

โดยทำการทดลองหาน้ำหนักโมลกลุของพอลิเมอร์ร่วมชนิด PEGMA:DEAEMA 50:50 เท่านั้น พอลิเมอร์จากชั้นสารละลาย (free polymer) ถูกนำมาผ่านคอลัมน์เพื่อกำจัดตัวเร่งปฏิกิริยา (CuBr) ที่มากเกินพอออก แล้วนำมาศึกษาน้ำหนักโมเลกุลด้วยเทคนิค GPC จากการศึกษาค่า Retention Volume ของพอลิเมอร์ที่เวลาในการทำปฏิกิริยา ATRP ต่างๆ กัน พบว่า เมื่อเวลาในการทำปฏิกิริยา ATRP เพิ่มขึ้นจาก 0, 1, 2 และ 4 ชั่วโมง จะได้ว่าพีค Retention Volume มีแนวโน้มเลื่อนมาทางซ้ายเพิ่มมากขึ้นตามลำดับ แสดงถึงการมีน้ำหนักโมเลกุลที่เพิ่มขึ้นของพอลิเมอร์ร่วม PEGMA:DEAEMA นอกจากนี้ยังพบว่าพอลิเมอร์ร่วมที่ทำปฏิกิริยาแล้วมีค่าการกระจายของน้ำหนักโมเลกุล (Polydisperse Index) อยู่ในช่วง 1.3 – 1.7 ดังแสดงในตาราง 4

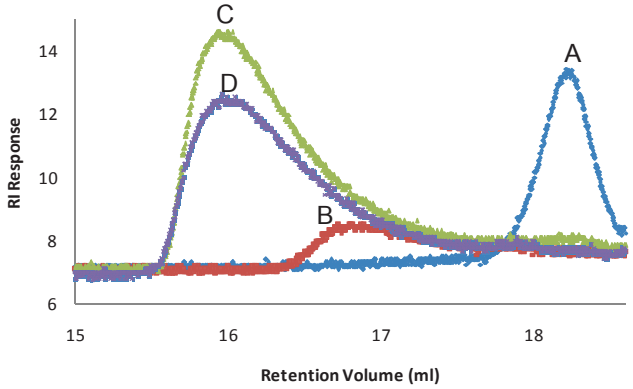

ภาพ 17 GPC Chromatogram ของพอลิเมอร์ร่วม PEGMA(50):DEAEMA(50) ที่ใช้เวลาในการทำปฏิกิริยา ATRP เป็นเวลา A) 0, B) 1, C) 2 และ D) 4 ชั่วโมง

ตาราง 4 น้ำหนักโมเลกุลและการกระจายของพอลิเมอร์ร่วม PEGMA(50):DEAEMA(50) ที่เวลาในการทำปฏิกิริยา ATRP ต่างๆ กันจากเทคนิค GPC

เวลาในการทำปฏิกิริยา (h)	M_w (Daltons)	M_n (Daltons)	PDI
0	403	388	1.04
1	1711	1254	1.36
2	4862	2946	1.65
4	4756	2846	1.67

2.3 การวิเคราะห์หมู่ฟังก์ชันของพอลิเมอร์ร่วมบนพื้นผิวอนุภาคนาโนแมกนีไทท์ด้วยเทคนิค FTIR

โดยการวิเคราะห์หมู่ฟังก์ชันด้วยเทคนิค FTIR จะแสดงผลเฉพาะอนุภาคนาโนที่เคลือบด้วย poly(DEAEMA)) homopolymer เท่านั้น โดยทำการเก็บสารที่เวลาในการทำปฏิกิริยา ATRP ต่างๆ จากนั้นนำมาล้างด้วยเอทานอล 3-4 ครั้งเพื่อกำจัดมอนอเมอร์ที่มากเกินพอออก แล้วเหวี่ยงแยกอนุภาคออกมา ทำให้แห้งก่อนนำสารไปวิเคราะห์ จากการวิเคราะห์โดยทำการเปรียบเทียบสเปคตรัม FTIR ของอนุภาคที่ผ่านการดัดแปรด้วย poly (DEAEMA) ที่เวลาในการทำปฏิกิริยา ATRP ต่างๆ กันเทียบกับอนุภาคก่อนการทำปฏิกิริยาและสารมอนอเมอร์เริ่มต้น พบว่า สเปคตรัมของอนุภาคหลังการทำปฏิกิริยาแล้วพบสัญญาณ Fe-O ของเหล็กออกไซด์ และยังพบสัญญาณ C-N และ C-Br ของ BTPAm ซึ่งใช้เป็นสารริเริ่มปฏิกิริยาบนพื้นผิวอนุภาค เมื่อเวลาการทำปฏิกิริยา ATRP เพิ่มมากขึ้นสัญญาณ C-N และ C-Br มีค่าลดลง แสดงอัตราส่วนที่ลดลงของสารริเริ่มปฏิกิริยาบนพื้นผิวอนุภาค

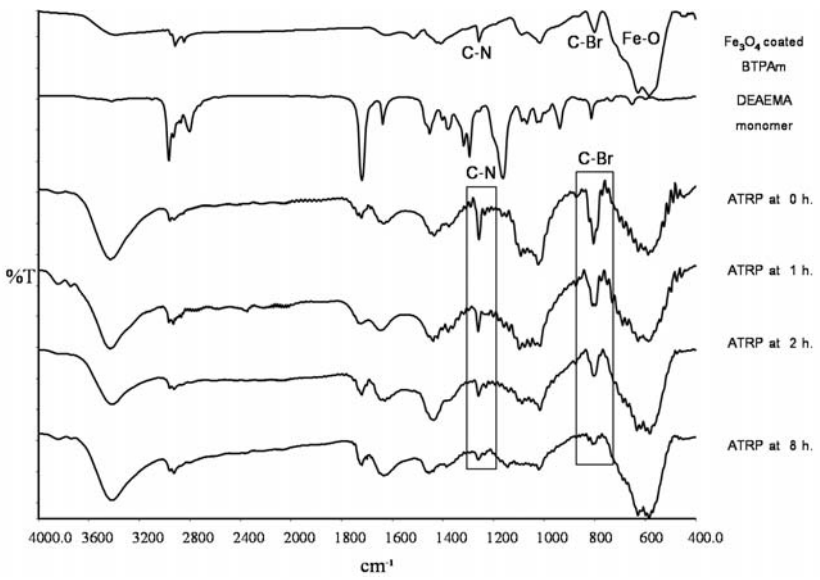

ภาพ 18 สเปคตรา FTIR ของอนุภาคนาโนแมกนีไทท์ที่ดัดแปรพื้นผิวด้วย poly (DEAEMA) homopolymer ที่เวลาในการทำปฏิกิริยา ATRP ต่างๆ กัน

อนุภาคแมกนีไทท์ที่ผ่านการดัดแปรพื้นผิวด้วยพอลิเมอร์ร่วม PEGMA และ DEAEMA จะถูกนำมาล้างเพื่อกำจัดตัวเร่งปฏิกิริยา ลิแกนด์ และสารมอนอเมอร์ที่มากเกินพอออกด้วยตัวทำละลายเอทานอล จากนั้นจึงนำอนุภาคมาทำการ quaternization กับเมทิลไอโอไดด์ในที่มืด เพื่อทำให้หมู่อะมิโนในหน่วยของ poly (DEAEMA) กลายเป็นประจุบวกของ quarternary amine จากนั้นจึงนำอนุภาคที่ผ่านการทำ quaternization แล้วมาละลายในสารละลายน้ำ DI ที่มี pH 7 เพื่อศึกษาขนาดปริมาตรไฮโดรไดนามิก (hydrodynamic volume) และความต่างศักย์ที่พื้นผิว (zetapotential) เปรียบเทียบกับอนุภาคแมกนีไทท์ก่อนการทำ quaternization

2.4. การศึกษาขนาดและการกระจายของขนาดอนุภาคด้วยเทคนิค TEM

2.4.1 การศึกษาขนาดและการกระจายตัวของขนาดอนุภาคนาโนแมกนีไทท์ที่เคลือบด้วยพอลิเมอร์ร่วมระหว่าง (poly (DEAEMA)-random-poly (PEGMA)) ที่มีอัตราส่วนโดยโมลเป็น 50:50 ก่อนและหลังการทำปฏิกิริยา quaternization

การเตรียมตัวอย่างสำหรับเทคนิค TEM นั้นจะนำอนุภาคแมกนีไทท์มาละลายในน้ำ DI แล้วนำไป sonicate เพื่อทำให้อนุภาคสามารถกระจายในตัวทำละลายได้ดีมากขึ้น จากนั้นจึงนำมาเหวี่ยงด้วยเครื่องเหวี่ยงอัตราเร็วสูง เพื่อกำจัดอนุภาคที่มีขนาดใหญ่หรือที่มีการรวมกลุ่มเป็นตะกอนออก แล้วดูดสารละลายส่วนบนหยดลงบน TEM grid ทิ้งไว้ให้แห้งในตู้อบความชื้นก่อนนำตัวอย่างไปวิเคราะห์

ภาพที่ 19A และ 19C แสดงขนาดและการกระจายของขนาดของอนุภาคนาโนแมกนีไทท์ที่ผ่านการดัดแปรพื้นผิวด้วยพอลิเมอร์ร่วม poly (DEAEMA) กับ poly (PEGMA) อัตราส่วน 50:50 โดยโมลก่อนการทำปฏิกิริยา quarternization พบว่าอนุภาคมีการเกาะกลุ่มกันบ้างเล็กน้อย และไม่แยกออกจากกันอย่างชัดเจน โดยมีขนาดเส้นผ่านศูนย์ของอนุภาคเท่ากับ 6.4 ± 1.3 nm และเมื่อทำการ quarternization แล้วดังรูป 8B และ 8D พบว่าอนุภาคมีแนวโน้มกระจายตัวแยกจากกันอย่างชัดเจน ทั้งนี้เนื่องมาจากพื้นผิวอนุภาคมีประเป็นบวกเพิ่มมากขึ้น ทำให้มีแรงผลักกันระหว่างประจุบวกของแต่ละอนุภาคมากขึ้น ส่วนขนาดอนุภาคจะมีค่าไม่แตกต่างอย่างมีนัยสำคัญเมื่อเทียบกับขนาดอนุภาคก่อนการทำ quarternization (ขนาดเส้นผ่านศูนย์กลางของอนุภาคโดยเฉลี่ยเป็น 6.1 ± 1.4 nm)

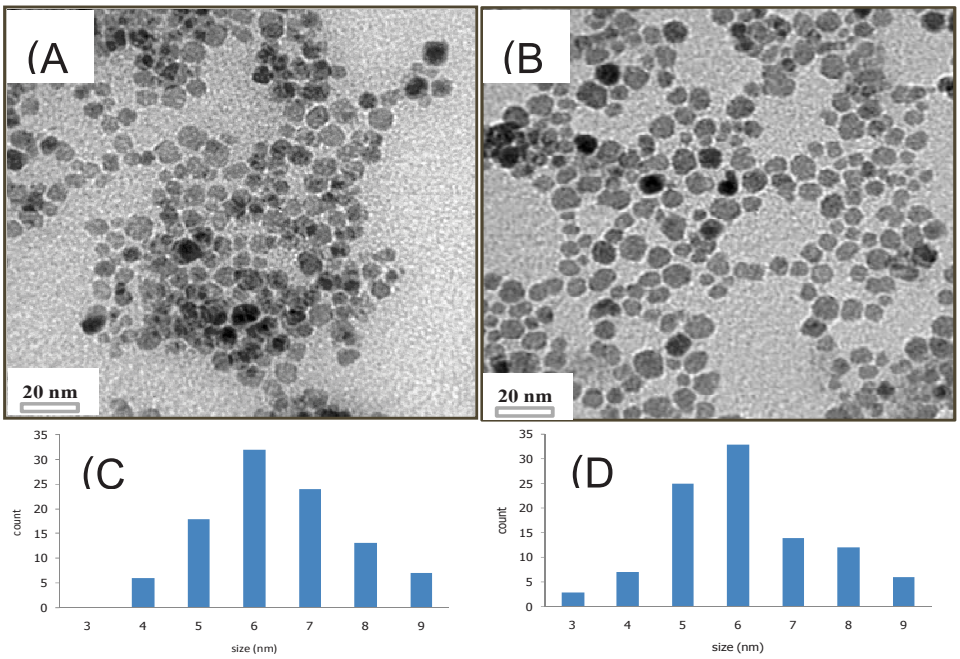

ภาพ 19 ขนาดและการกระจายของขนาดของอนุภาคนาโนแมกนีไทท์ที่เคลือบด้วยพอลิเมอร์ร่วม poly (DEAEMA)-random-PEGMA)) ก่อนและหลังการทำปฏิกิริยา quarternization โดยมีขนาดเส้นผ่านศูนย์กลางอนุภาคโดยเฉลี่ยเป็น 6.4 ± 1.3 nm และ 6.1 ± 1.4 nm ตามลำดับ

2.4.2 การศึกษาขนาดและการกระจายของขนาดอนุภาคนาโนแมกนีไทท์ที่ดัดแปรพื้นผิวด้วย poly (DEAEMA) ก่อนและหลังการทำปฏิกิริยา quarternization

ขนาดและการกระจายของขนาดอนุภาคนาโนแมกนีไทท์ที่ถูกดัดแปรด้วย poly(DEAEMA) homopolymer เปรียบเทียบระหว่างก่อนการทำ quarternization (ภาพ 20A และ 20C) และหลังการทำ quarternization (ภาพ 20B และ 20D) พบว่าก่อนการทำ quarternization มีการเกาะกลุ่มกัน แต่เมื่อทำการ quarternization แล้วพบว่าอนุภาคมีการกระจายตัวได้มากขึ้น ทั้งนี้เนื่องจากการมีประจุบวกบนพื้นผิว

ทำให้มีแรงผลักกันระหว่างอนุภาคเพิ่มมากขึ้นนั่นเอง ส่วนขนาดของอนุภาคก่อนและหลังการทำ quarternization นั้นมีขนาดใกล้เคียงกัน (ก่อนการทำ quaternization มีขนาดเส้นผ่านศูนย์กลางโดยเฉลี่ยเป็น 6.6 ± 1.2 nm และภายหลังการทำ quaternization มีขนาดเส้นผ่านศูนย์กลางโดยเฉลี่ยเป็น 6.5 ± 1.4 nm)

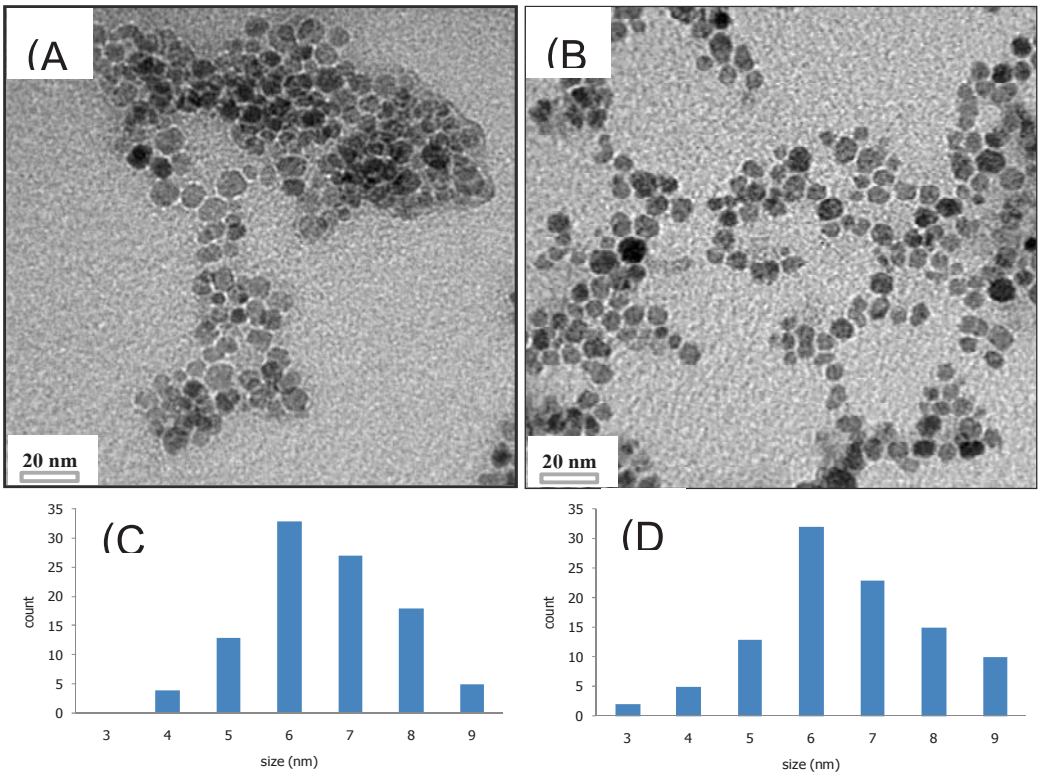

ภาพ 20 ขนาดและการกระจายของขนาดของอนุภาคนาโนแมกนีไทท์ที่เคลือบด้วย poly (DEAEMA) ก่อนและหลังการทำปฏิกิริยา quarternization โดยมีขนาดเส้นผ่านศูนย์กลางอนุภาคโดยเฉลี่ยเป็น 6.6 ± 1.2 nm และ 6.5 ± 1.4 nm ตามลำดับ

2.5 การศึกษาสมบัติทางแม่เหล็กของอนุภาคนาโนแมกนีไทท์ภายหลังการเคลือบด้วยพอลิเมอร์

ค่าสมบัติทางแม่เหล็กของสารสามารถพิจารณาได้จากค่าการตอบสนองต่อแม่เหล็กที่จุดอิ่มตัว (Saturation Magnetization, M_s) จากภาพ 21 และตาราง 5 แสดงสมบัติทางแม่เหล็กและค่าการตอบสนองต่อแม่เหล็กที่จุดอิ่มตัว (M_s) ของอนุภาคเปรียบเทียบกันระหว่างอนุภาคแมกนีไทท์เริ่มต้น (bare Fe_3O_4) กับอนุภาคแมกนีไทท์ที่ติดสารเชื่อมโยง (BTPAM-coated Fe_3O_4) และอนุภาคที่ถูกดัดแปรพื้นผิวด้วยพอลิเมอร์ร่วมแล้ว ซึ่งจากตาราง 5 พบว่าค่า M_s ของอนุภาคแมกนีไทท์เริ่มต้นที่ได้จากปฏิกิริยาการ

แตกสลายมีค่าเป็น 54.5 emu/g และค่า M_s จะมีค่าลดลงเล็กน้อยหลังจากทำการดัดแปรพื้นผิวด้วพอลิเมอร์แล้ว (40.1-44.6 emu/g) นอกจากนี้จากภาพ 10 พบว่ากราฟทุกเส้นจะตัดแกน x และ และแกน y ที่จุด 0,0 แสดงถึงสมบัติความเป็นซูเปอร์พาราแมกเนติก (superparamagnetic behavior) ที่อุณหภูมิห้อง

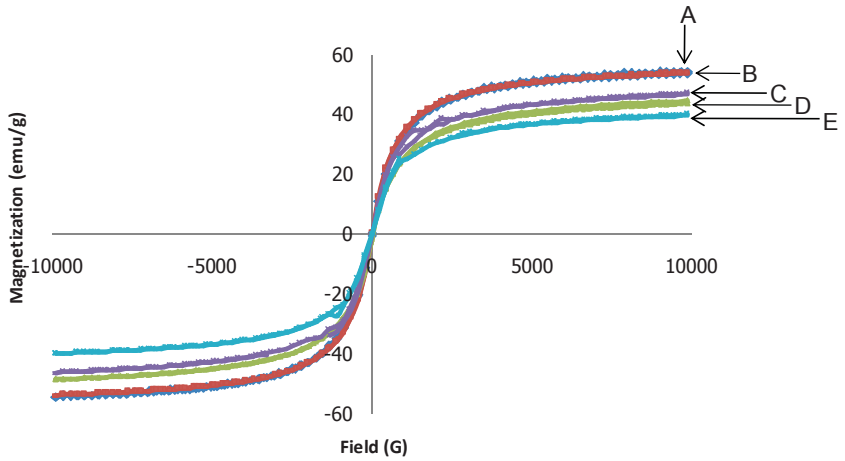

ภาพ 21 สมบัติทางแม่เหล็กของอนุภาคแมกนีไทท์ที่ได้จากขั้นตอน (A) หลังจากปฏิกิริยาการแตกสลาย (B) การติดสารเชื่อมโยง (C) หลังจากดัดแปรด้วย PEGMA(50) : poly(DEAEMA)(50) (D) หลังจากดัดแปรด้วย PEGMA(100) : poly(DEAEMA)(0) และ (E) หลังจากดัดแปรด้วย PEGMA(0) : poly(DEAEMA)(100)

ตาราง 5 ค่าการตอบสนองต่อแม่เหล็กที่จุดอิ่มตัวของอนุภาคนาโนแมกนีไทท์ที่ผ่านการทำปฏิกิริยาในขั้นตอนต่างๆ

ตัวอย่าง	ค่าการตอบสนองต่อแม่เหล็กที่จุดอิ่มตัว (emu/g)
Bare Fe_3O_4	54.5
BTPAM-coated Fe_3O_4	53.9
Fe_3O_4 coated PEGMA (100):DEAEMA (0)	44.6
Fe_3O_4 coated PEGMA (50):DEAEMA (50)	46.7
Fe_3O_4 coated PEGMA (0):DEAEMA (100)	40.1

2.6 การวิเคราะห์ค่าความต่างศักย์พื้นผิว (zeta potential) และขนาดเส้นผ่าศูนย์กลางไฮโดรไดนามิก (hydrodynamic diameter) ด้วยเทคนิค PCS (photo correlation spectroscopy)

การวิเคราะห์ค่าความต่างศักย์พื้นผิว (zeta potential) เป็นการศึกษาประจุบนพื้นผิวของอนุภาคนาโนแมกนีไทท์ โดยวิเคราะห์ค่าความต่างศักย์พื้นผิวของอนุภาคนาโนแมกนีไทท์ที่ผ่านการดัดแปรพื้นผิวด้วยปฏิกิริยา ATRP และอนุภาคหลังการเกิดปฏิกิริยา quarternization หมู่เอมีนใน poly(DEAEMA) ให้มีประจุบวก ซึ่งพอลิเมอร์ร่วมที่ใช้ในการทดลองนี้มีอัตราส่วนโดยโมลระหว่าง PEGMA:DEAEMA เป็น 0-100 25-75 50-50 และ 75-25 ตามลำดับ ซึ่งจากภาพ 22 จะพบว่าอนุภาคมีค่าความต่างศักย์พื้นผิวอยู่ในช่วง +22 ถึง +32 mV โดยค่าความต่างศักย์จะเป็นบวกเพิ่มมากขึ้นตามจำนวนโมลที่เพิ่มขึ้นของ DEAEMA และยังพบว่าหลังจากการทำ quarternization อนุภาคจะมีค่าความต่างศักย์พื้นผิวเพิ่มสูงขึ้นประมาณ 8 mV

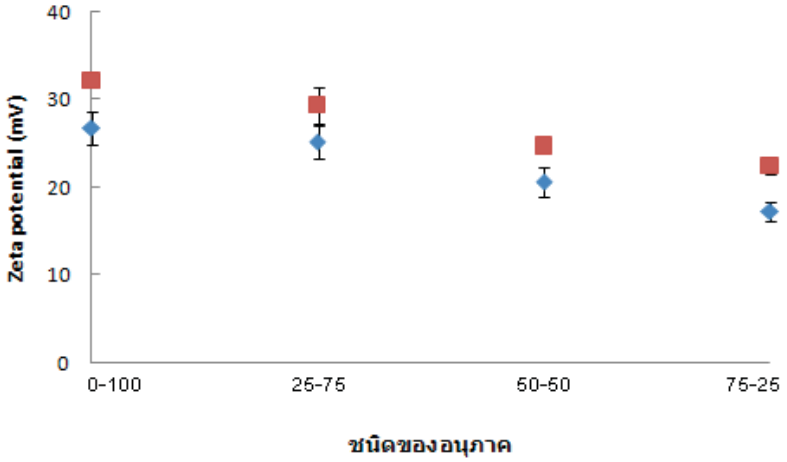

ภาพ 22 ค่าความต่างศักย์พื้นผิว (zeta potential) ของอนุภาคที่ดัดแปรด้วย PEGMA:DEAEMA อัตราส่วนโดยโมลต่างๆ เปรียบเทียบก่อนและหลังปฏิกิริยาการ quarternization

การศึกษาขนาดเสนผ่าศูนย์กลางไฮโดรไดนามิก (hydrodynamic diameter) ได้ทำการศึกษาในตัวทำละลายที่เป็นน้ำ ซึ่งเป็นตัวทำละลายที่สามารถละลาย PEGMA และ DEAEMA ได้ดี จากตารางที่ 6 พบว่าอนุภาคนาโนแมกนีไทท์ที่มีการดัดแปรพื้นผิวด้วยพอลิเมอร์ร่วมทั้ง 5 อัตราส่วนมีขนาดเส้นผ่าศูนย์กลางไฮโดรไดนามิกอยู่ในช่วง 302-461 นาโนเมตร และเมื่อผ่านปฏิกิริยาการ quarternization แล้วพบว่าขนาดปริมาตรไฮโดรไดนามิกมีขนาดเล็กลง (219-345 นาโนเมตร) ทั้งนี้อาจเนื่องมาจากการมีประจุบวกที่เพิ่มมากขึ้นในชั้นของพอลิเมอร์ ทำให้เกิดการผลักกันของกลุ่มอนุภาคมากขึ้น และทำให้มีขนาดของการรวมกลุ่มกันน้อยลง อย่างไรก็ตามขนาดเส้นผ่าศูนย์กลางไฮโดรไดนามิกที่วิเคราะห์จากเทคนิค PCS ยังมีขนาดใหญ่กว่าขนาดอนุภาคที่วิเคราะห์ได้จากเทคนิค TEM ทั้งนี้อาจเนื่องมาจากมีการ

เกิดการรวมกลุ่มขนาดนาโน (nanocluster) ของอนุภาคในน้ำ ทำให้ขนาดที่วัดได้จากเทคนิค PCS มีขนาดใหญ่กว่ามาก

ตาราง 6 ขนาดขนาดเส้นผ่าศูนย์กลางไฮโดรไดนามิกของอนุภาคชนิดต่างๆ ในน้ำที่ pH = 7.0

Fe_3O_4 ที่ดัดแปรด้วย PEGMA-DEAEMA อัตราส่วนโดยโมลต่างๆ	ขนาดเส้นผ่าศูนย์กลางไฮโดรไดนามิก (nm)	
	ก่อน quarternization	หลัง quarternization
0:100	328±8	219±2
25:75	316±10	284±5
50:50	302±6	251±9
75:25	461±10	345±6
100:0	457±8	-

3. การประยุกต์ใช้อนุภาคนาโนแมกนีไทท์ที่ได้จากการดัดแปรพื้นผิวให้มีประจุบวกเพื่อใช้การตรวจสอบลำดับเบสของดีเอ็นโดยใช้พีเอ็นเอเป็นโพรบ

หลักจากที่ทำการดัดแปรพื้นผิวของอนุภาคนาโนแมกนีไทท์ให้มีประจุบวกแล้ว อนุภาคนาโนแมกนีไทท์เหล่านี้ จะถูกนำมาประยุกต์ใช้ตรวจสอบลำดับเบสของดีเอ็นเอโดยใช้พิโรลิดินิลพีเอ็นเอ (*ss*-ACPC-PNA) เป็นโพรบร่วมกับเทคนิคมัลดิ-ทอฟแมสสเปกโทรเมตรีโดยอาศัยหลักการของ ion exchange capture ซึ่งอาศัยแรงยึดเหนี่ยวระหว่างประจุบวกของอนุภาคนาโนแมกนีไทท์กับประจุลบของสารเชิงซ้อนคู่ผสมระหว่างพีเอ็นเอกับดีเอ็นเอที่มีลำดับเบสคู่สมกันเท่านั้น ทั้งนี้เนื่องจากพีเอ็นเอไม่มีประจุจึงทำให้ไม่สามารถถูกดูดซับโดยอนุภาคนาโนแมกนีไทท์ที่มีประจุบวกได้ จากนั้นทำการแยกอนุภาคนาโนแมกนีไทท์ที่มีสารคู่ผสมระหว่างพีเอ็นเอกับดีเอ็นเอที่มีลำดับเบสคู่สมกันจับอยู่ที่ผิวด้วยแท่งแม่เหล็ก และล้างพีเอ็นเอที่ไม่ได้เกิดไฮบริดกับดีเอ็นเอออกจากอนุภาคนาโนแมกนีไทท์ที่แยกออกมาด้วยตัวทำละลายที่เหมาะสมหลังจากนั้นนำอนุภาคที่ล้างแล้วมาทำการวิเคราะห์ด้วยเทคนิคมัลดิ-ทอฟแมสสเปกโทรเมตรีซึ่งจะแสดงเฉพาะมวลโมเลกุลของพีเอ็นเอที่มีลำดับเบสคู่สมกับดีเอ็นเอเท่านั้น ดังแสดงในภาพ 23

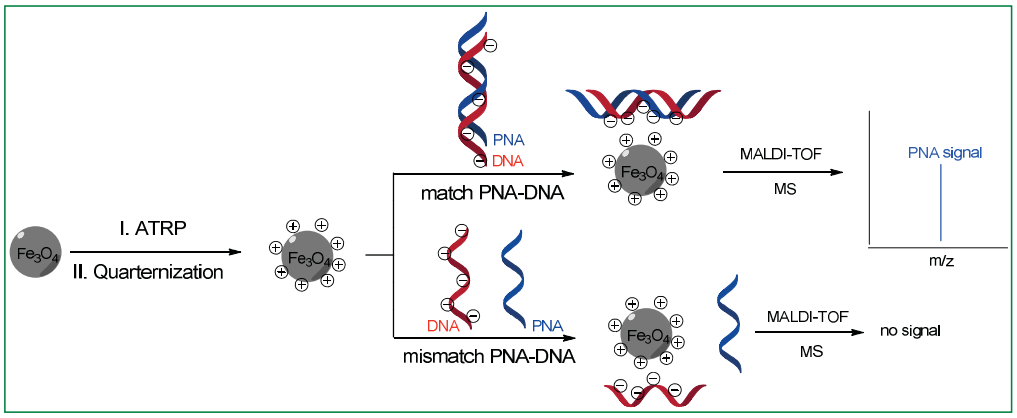

ภาพ 23 แผนภาพรวมของการประยุกต์ใช้อนุภาคนาโนแมกนีไทท์ที่ที่ดัดแปรพื้นผิวเป็นประจุบวกในการตรวจสอบลำดับเบสของดีเอ็นเอร่วมกับพิโรลิดินิลพีเอ็นเอ (*ss*-ACPC-PNA) และเทคนิค MALDI-TOF mass spectrometry

ในขั้นตอนแรกจะเป็นการทดสอบการเกิดแรงกระทำเฉพาะ (non-specificity) ระหว่างอนุภาคนาโนแมกนีไทท์ทั้ง 4 ชนิด กับ สารละลาย PNA อย่างเดียวเพื่อทดสอบว่าอนุภาคเหล่านั้น มีแรงกระทำใดๆ กับ PNA หรือไม่ โดยอนุภาคนาโนแมกนีไทท์ที่ทำการศึกษาคือ อนุภาคนาโนแมกนีไทท์ก่อน quarternization ที่มีอัตราส่วนของ PEGMA : DEAEMA มอนอเมอร์ เป็น 50:50 และ 0:100 และอนุภาคนาโนแมกนีไทท์ที่มีอัตราส่วนของ PEGMA : DEAEMA มอนอเมอร์ เป็น 50:50 และ 0:100 ที่ทำการ quarternization แล้ว และ PNA ที่ใช้ทำการศึกษามีลำดับเบสดังนี้ Ac-TTTTTTTTT-Lys-NH_2 (P1, m/z = 3179.404) โดยปริมาณของ PNA ที่ใช้คือ 100 pmole

ขั้นตอนการทดลองจะเริ่มจากการเติม PNA ลงไปในอนุภาคนาโนแมกนีไทท์แต่ละชนิดที่กระจายตัวในสารละลายฟอสเฟต บัฟเฟอร์ pH=7 และตั้งทิ้งไว้ 15 นาที หลังจากนั้นทำการแยกอนุภาคนาโนแมกนีไทท์ออกจากสารละลาย PNA ด้วยแท่งแม่เหล็ก แล้วทำการล้างอนุภาคด้วยน้ำกลั่น 3 ครั้ง จากนั้นนำส่วนของอนุภาคนาโนแมกนีไทท์ที่ทำการล้างแล้ว และส่วนของสารละลาย PNA ที่แยกอนุภาคนาโนแมกนีไทท์ออกแล้วไปทดสอบด้วยเทคนิค MALDI-TOF spectrometry พบว่าส่วนที่เป็นอนุภาคนาโนแมกนีไทท์ทั้ง 4 ชนิด จะไม่ปรากฏสัญญาณของ PNA (m/z = 3179.404) ในขณะที่สัญญาณของ PNA จะปรากฏในชั้นสารละลาย ซึ่งแสดงถึงอนุภาคทั้ง 4 ชนิดไม่มีแรงกระทำใดๆ กับ PNA (non-specificity) หรือไม่จับเอา PNA ไว้ที่ผิวของอนุภาคนั่นเอง ดังแสดงในภาพ 24

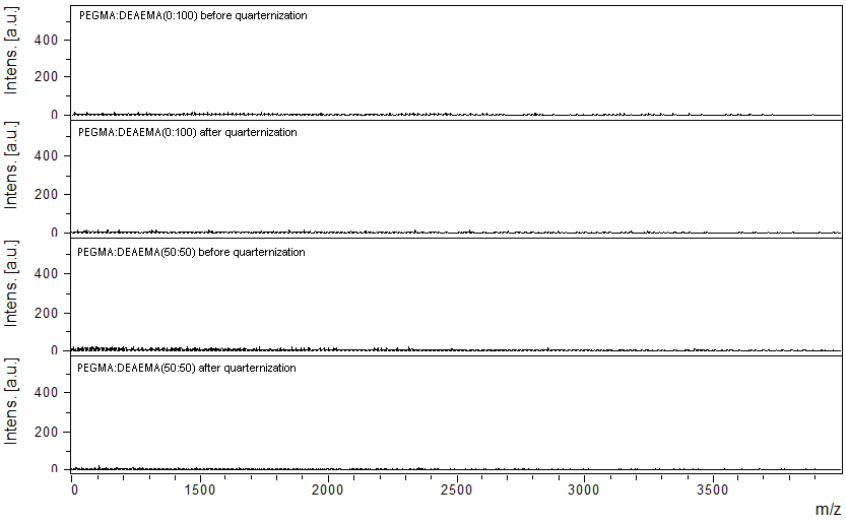

(ก.)

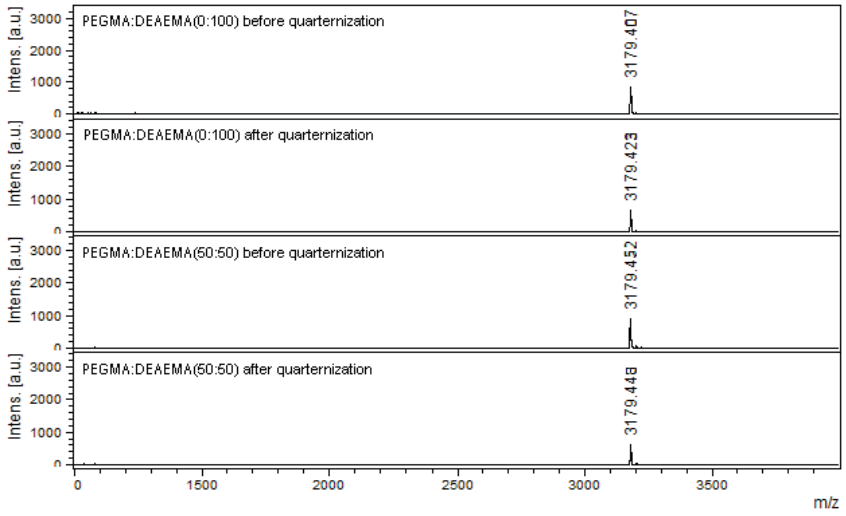

(ข)

ภาพ 24 การทดสอบ non-specificity ของอนุภาคนาโนแมกนีไทท์ทั้ง 4 ชนิด กับ *p*-PNA
(ก) = ส่วนของอนุภาคนาโนแมกนีไทท์ , (ข) = ส่วนของสารละลาย

ในขั้นตอนต่อไปจะเป็นการนำอนุภาคนาโนแมกนีไทท์ทั้ง 4 ชนิด มาทดสอบประสิทธิภาพในการดูดจับสารประกอบเชิงซ้อนลูกผสมระหว่าง PNA กับ DNA ที่มีลำดับเบสที่เป็นคู่สมกันเพื่อเปรียบเทียบประสิทธิภาพในการดูดจับสารประกอบเชิงซ้อนลูกผสมระหว่าง PNA กับ DNA ไว้ที่ผิวของอนุภาคนาโนแมกนีไทท์แต่ละชนิด โดย PNA และ DNA ที่ใช้มีลำดับเบสดังนี้

PNA (P1) : Ac-TTTTTTTTT-Lys-NH_2 (m/z = 3179.404)

DNA (D1) : 5'-AAAAAAAAA-3'

ปริมาณของ PNA และ DNA ที่ใช้ในการทดลองนี้คือ 100 pmole

การทดลองจะเริ่มจากการนำเอาอนุภาคนาโนแมกนีไทท์แต่ละชนิดไปทำให้กระจายตัวในฟอสเฟตบัฟเฟอร์ pH=7 ประมาณ 20 µl จากนั้นเติมสารละลาย PNA (P1) · DNA (D1) ลงในอนุภาคที่กระจายตัวแล้ว และตั้งทิ้งไว้ 15 นาที หลังจากนั้นทำการแยกอนุภาคนาโนแมกนีไทท์ ออกจากสารละลาย PNA (P1) · DNA (D1) ด้วยแท่งแม่เหล็ก แล้วทำการล้างอนุภาคด้วยน้ำกลั่น 3 ครั้ง จากนั้นนำส่วนของอนุภาคนาโนแมกนีไทท์ที่ทำการล้างแล้วไปทดสอบด้วยเทคนิค MALDI-TOF spectrometry พบว่าเมื่อทดสอบอนุภาคนาโนแมกนีไทท์ทั้ง 4 ชนิดด้วยเทคนิค MALDI-TOF spectrometry จะปรากฏสัญญาณของ PNA (P1) ดังภาพ 25

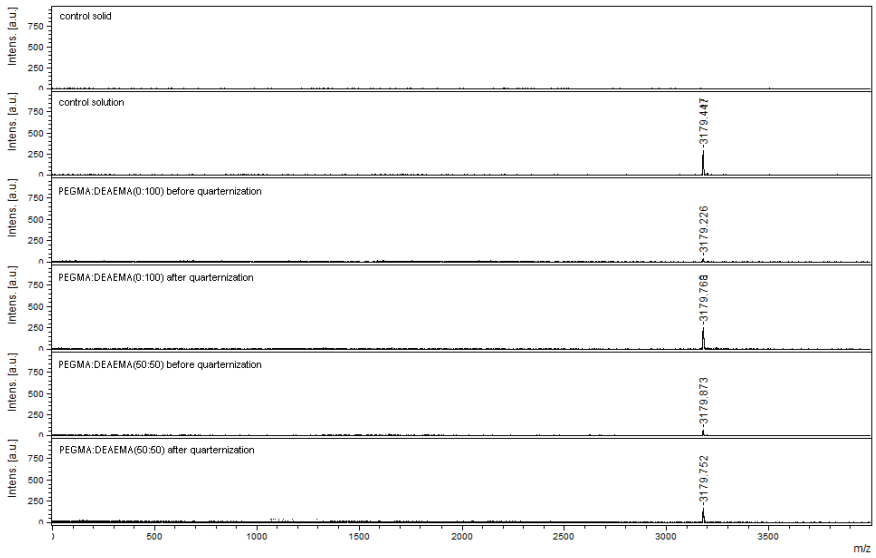

ภาพ 25 การเปรียบเทียบประสิทธิภาพในการยึดจับสารประกอบเชิงซ้อนลูกผสมระหว่าง PNA กับ DNA ของอนุภาคนาโนแมกนีไทท์แต่ละชนิด

จากภาพ 25 แสดงให้เห็นว่ามีการยึดจับกันด้วยพันธะไอออนิคระหว่างประจุลบของสารคู่ผสม PNA · DNA กับประจุบวกบนพื้นผิวอนุภาคนาโนแมกนีไทท์ นอกจากนี้ยังพบว่าสัญญาณของ PNA บนอนุภาคนาโนแมกนีไทท์หลังการทำ quarternization ที่มีอัตราส่วนของ PEGMA : DEAEMA มอนอเมอร์เป็น 0-100 และ 50-50 มีความเข้มของสัญญาณของ PNA ที่สูงกว่าสัญญาณของ PNA ที่พบบนอนุภาคนาโนแมกนีไทท์ก่อนการทำ quarternization ที่มีอัตราส่วนของ PEGMA : DEAEMA มอนอเมอร์เป็น 0-100 และ 50-50 ซึ่งแสดงให้เห็นว่าอนุภาคนาโนแมกนีไทท์หลังการทำ quarternization ทั้ง 2 อัตราส่วนมีประสิทธิภาพในการยึดจับกับสารคู่ผสมระหว่าง PNA · DNA ไว้ที่ผิวได้ดีกว่าอนุภาคนาโนแมกนีไทท์ก่อนการทำ quarternization ดังนั้นจึงเลือกเฉพาะอนุภาคนาโนแมกนีไทท์หลังการทำ quarternization ทั้ง 2 อัตราส่วนไปใช้ทดลองในขั้นตอนต่อไป

3.1 การศึกษาเบื้องต้นของประสิทธิภาพของอนุภาคนาโนแมกนีไทท์หลังการทำ quarternization ในการตรวจสอบลำดับของดีเอ็นเอ

การศึกษานี้ประกอบด้วย 2 การทดลอง โดยแต่ละการทดลองจะใช้PNA โพรบที่มีลำดับเบสที่ต่างกัน ดังนี้

3.1.1 การศึกษาประสิทธิภาพของอนุภาคนาโนแมกนีไทท์หลังการทำ quarternization ทั้ง 2 อัตราส่วน(PEGMA : DEAEMA เป็น 0-100 และ 50-50) ในการใช้เป็นตัวดูดจับ (solid support) เพื่อแยกความแตกต่างของลำดับเบสของดีเอ็นเอระหว่างดีเอ็นเอที่มีลำดับเบสที่เป็นคู่สม (complementary) และไม่เป็นคู่สม (non-complementary) ในการทดลองนี้จะใช้ PNA ที่มีลำดับเบสที่เป็นโฮโมเบสเป็นโพรบในการตรวจสอบ โดยลำดับเบสของของ PNA และ ดีเอ็นที่ใช้ในการทดลองของส่วนนี้เป็นดังนี้

PNA (P1) : Ac-TTTTTTTTT-Lys-NH_2 (m/z = 3179.404)

DNA (D1) : 5'-AAAAAAAAA-3' (complementary กับ P1)

DNA (D2) : 5’-TTTTTTTTT-3’ (non-complementary กับ P1)

DNA (D3) : 5'-AAAACAAAA-3' (single base mismatch กับ P1)

ปริมาณของ PNA และ DNA แต่ละชนิดที่ใช้ 100 pmole

โดยการทดลองจะเริ่มจากการนำเอาอนุภาคนาโนแมกนีไทท์แต่ละชนิดไปทำให้กระจายตัวในฟอสเฟต บัฟเฟอร์ pH=7 ประมาณ 20 µl จากนั้นเติมสารละลาย PNA (P1) · DNA (D1) ลงในอนุภาคที่กระจายตัวแล้ว และตั้งทิ้งไว้ 15 นาที หลังจากนั้นทำการแยกอนุภาคนาโนแมกนีไทท์ ออกจากสารละลาย PNA (P1) · DNA (D1) ด้วยแท่งแม่เหล็ก แล้วทำการล้างอนุภาคที่แยกได้ด้วยน้ำกลั่น 3 ครั้ง จากนั้นนำส่วนของอนุภาคนาโนแมกนีไทท์ที่ทำการล้างแล้วไปทดสอบด้วยเทคนิค MALDI-TOF spectrometry ในขณะที่ในกรณีของ DNA (D2) และ DNA (D3) การทดลองก็ทำเช่นเดียวกับ DNA (D1) ผลการทดลองแสดงดังภาพ 26

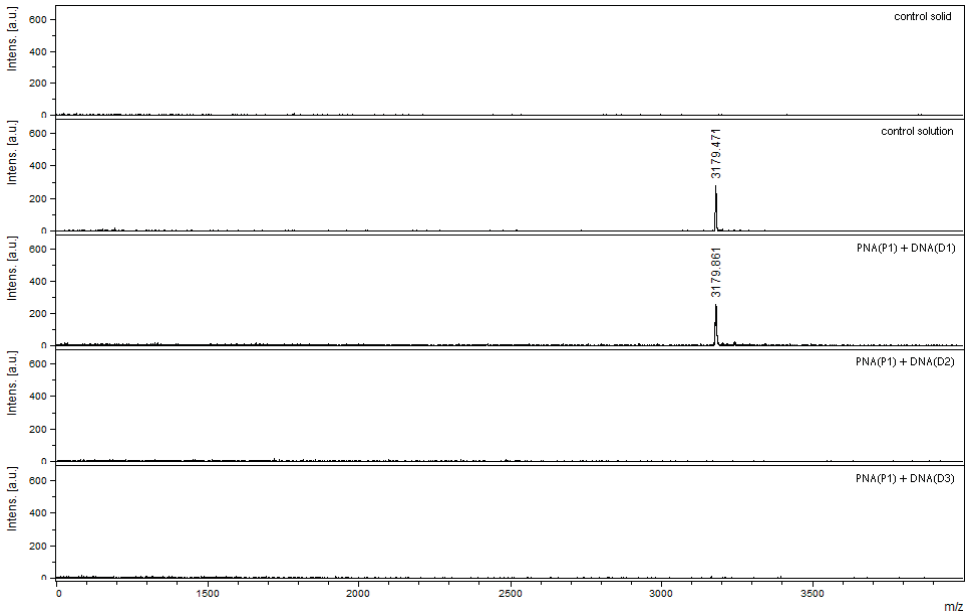

อนุภาคนาโนแมกนีไทท์ (PEGMA : DEAEMA, 0:100)

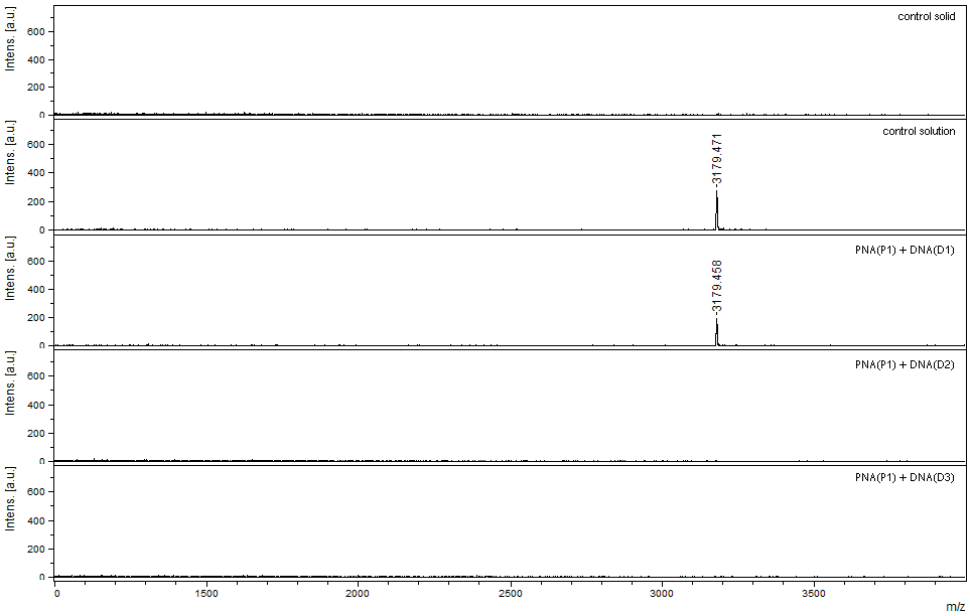

อนุภาคนาโนแมกนีไทท์ (PEGMA : DEAEMA, 50:50)

ภาพ 26 การศึกษาประสิทธิภาพของอนุภาคนาโนแมกนีไทท์หลังการทำ quarternizationในการใช้เป็นตัวดูดจับ (solid support) เพื่อใช้ตรวจสอบลำดับเบสของดีเอ็นเอ เมื่อใช้ PNA (P1) ที่เป็นโฮโมเบสเป็นโพรบ

จากภาพ 26 จะเห็นได้ว่าเมื่อทดสอบ non-specificity ระหว่างอนุภาคทั้ง 2 อัตราส่วนกับสารละลาย PNA อย่างเดียว พบว่าจะไม่ปรากฏสัญญาณของ PNA ดังแสดงในส่วนของ control solid ซึ่งแสดงถึงการ

ไม่มีแรงกระทำใดๆ ระหว่างอนุภาคนาโนแมกนีไทท์กับ PNA ในขณะที่ในส่วนของสารละลาย PNA ที่ทำการแยกเอาอนุภาคออกไปแล้ว ดังแสดงในส่วนของ control solution จะปรากฏสัญญาณของ PNA ขึ้น

เมื่อนำอนุภาคนาโนแมกนีไทท์ทั้ง 2 อัตราส่วนมาทดสอบกับสารละลาย PNA·DNA(D1), PNA·DNA (D2) และ PNA·DNA (D3) พบว่าอนุภาคที่ทดสอบกับสารละลาย p-PNA-DNA (D1) ที่มีลำดับเบสที่เป็นคู่สมกัน จะปรากฏสัญญาณของ PNA ที่ 3179.861 และ 3179.458 ซึ่งแสดงถึงเกิดการยึดจับกันระหว่าง PNA และ DNA(D1) แล้วจะถูกเหนี่ยวนำไปยังพื้นผิวของอนุภาคด้วยแรงทางไอออนิก ในขณะที่เมื่อทดสอบกับสารละลาย PNA·DNA (D2) และ PNA·DNA (D3) ที่มีลำดับเบสที่ไม่เป็นคู่สมกันและมีลำดับเบสต่างกันเพียง 1 เบส ตามลำดับ พบว่าจะไม่ปรากฏสัญญาณของ PNA ขึ้น ซึ่งแสดงถึงการยึดจับกันระหว่าง PNA กับ DNA(D1) และ DNA(D3) ไม่เกิดขึ้น จึงทำให้การเหนี่ยวนำสารคู่ผสม PNA ·DNA ไปยังพื้นผิวของอนุภาคไม่เกิดขึ้นเช่นเดียวกัน

จากผลการทดลองข้างต้นจะเห็นได้ว่าอนุภาคนาโนแมกนีไทท์ทั้ง 2 อัตราส่วนสามารถนำมาใช้เป็นอนุภาคดูดจับ (solid support) เพื่อใช้ในการตรวจสอบลำดับเบสของดีเอ็นเอได้และนอกจากนี้ยังสามารถแยกความแตกต่างของลำดับเบสของดีเอ็นเอระหว่างเบสที่เป็นคู่สมกันและลำดับเบสที่มีเบสต่างกันเพียงแค่ 1 ตำแหน่งได้

3.1.2 การศึกษาประสิทธิภาพของอนุภาคนาโนแมกนีไทท์หลังการทำ quarternization ทั้ง 2 อัตราส่วนในการใช้เป็นตัวดูดจับ (solid support) เพื่อใช้ตรวจสอบลำดับเบสของดีเอ็นเอ ในการทดลองนี้จะใช้ PNA ที่มีลำดับเบสที่เป็นเฮทเทอโรเบสหรือมีชนิดของเบสที่แตกต่างกันเป็นโพรบในการตรวจสอบโดย PNA โพรบที่ใช้จะทำการติดหมู่ phosphonium ไว้ที่ปลายด้าน N ของสายไว้ด้วยทั้งนี้เพื่อเพิ่มความไว (sensitivity) ของเทคนิค MALDI-TOF spectrometry ให้ดีขึ้น โดยลำดับเบสของของ PNA และ DNA ที่ใช้ในการทดลองของส่วนนี้เป็นดังนี้

PNA (P3) : $^{+}PPh_3$-TTTTAC<u>A</u>CAACCC-Ser-NH_2 (m/z = 4732.117)

PNA (P4) : $^{+}PPh_3$-TTTTAC<u>G</u>CAACCC-Ser-NH_2 (m/z = 4748.116)

DNA (D4): 5’-GGGTTG<u>T</u>GTAAAA-3’ (complementary กับ P3, single base mismatch กับ P4)

DNA (D5): 5’-AATGGAATTTTGT-3’ (full mismatch กับ P3 และ P4)

DNA (D6) : 5’-GGGTTG<u>C</u>GTAAAA-3’ (complementary กับ P4, single base mismatch กับ P3)

ปริมาณของ p-PNA และ DNA แต่ละชนิดที่ใช้ 100 pmole

ขั้นตอนในการทดลองจะทำคล้ายกับส่วนแรก และผลการทดลองแสดงดังรูปที่ 27 และ 28

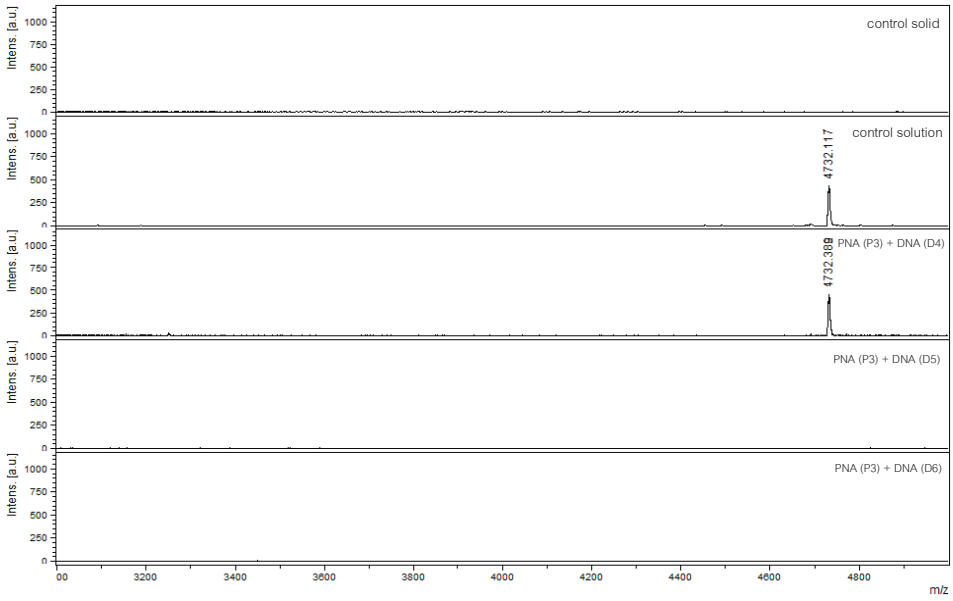

อนุภาคนาโนแมกนีไทท์ (PEGMA : DEAEMA, 0:100)

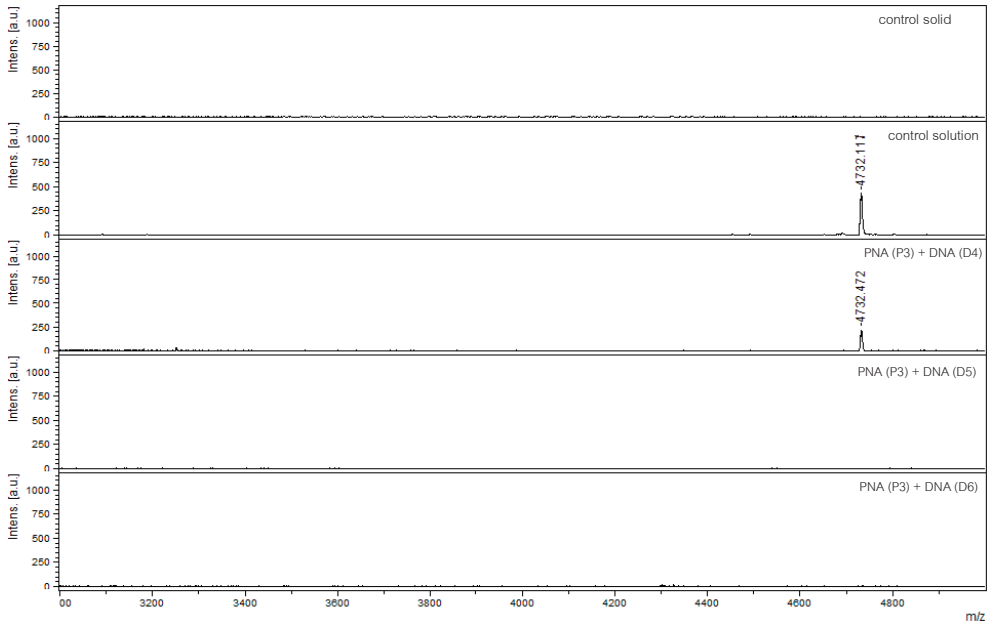

อนุภาคนาโนแมกนีไทท์ (PEGMA : DEAEMA, 50:50)

ภาพ 27 การศึกษาประสิทธิภาพของอนุภาคนาโนแมกนีไทท์หลังการทำ quarternizationในการใช้เป็นตัวดูดจับ (solid support) เพื่อใช้ตรวจสอบลำดับเบสของดีเอ็นเอ เมื่อใช้ PNA (P3) ที่เป็นเฮทเทอโรเบสเป็นโพรบ

จากภาพ 27 จะเห็นได้ว่าเมื่อทดสอบแรงกระทำหรือ non-specificity ระหว่างอนุภาคนาโนแมกนีไทท์ทั้ง 2 อัตราส่วนกับสารละลาย PNA (P3) เพียงอย่างเดียว พบว่าไม่เกิดแรงกระทำขึ้นเนื่องจากไม่ปรากฏสัญญาณของ PNA (P3) ขึ้น ดังแสดงในส่วนของ control solid ของทั้ง 2 สเปคตรัม เมื่อนำเอาอนุภาคแต่

ละชนิดมาทดสอบกับสารละลาย PNA (P3) · DNA (D4) ซึ่งมีลำดับเบสที่เป็นคู่สมกันพบว่าสเปคตรัมจะแสดงสัญญาณของ PNA (P3) ที่ *m/z* = 4732.472 ขึ้น ซึ่งแสดงถึงสารประกอบคู่ผสม PNA (P3) · DNA (D4) ถูกเหนี่ยวนำไปยังพื้นผิวของอนุภาคด้วยแรงทางไอออนิก ในขณะที่เมื่อทดสอบกับสารละลาย PNA (P3) ·DNA (D5) ซึ่งมีลำดับเบสที่ไม่เป็นคู่สมและสารละลาย PNA (P3) ·DNA (D6) ซึ่งลำดับเบสต่างกันเพียง 1 เบส พบว่าจะไม่ปรากฏสัญญาณของ PNA เกิดขึ้นทั้งคู่ ซึ่งแสดงให้เห็นถึงการยึดจับกันระหว่าง PNA (P3) กับ DNA (D5) และ DNA(D6) จะไม่เกิดขึ้น จึงทำให้ไม่เกิดการเหนี่ยวนำสารคู่ผสม PNA ·DNA ไปยังพื้นผิวของอนุภาค

เช่นเดียวกันเมื่อเปลี่ยน PNA (P3) โพรบ เป็น PNA (P4) โพรบ ผลการทดลองที่ได้แสดงดังภาพ 28

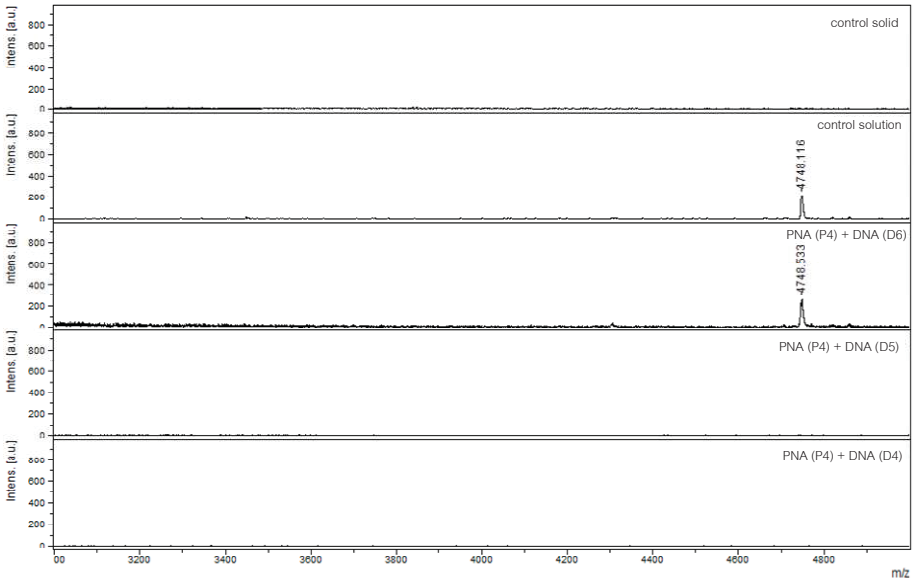

อนุภาคนาโนแมกนีไทท์ (PEGMA : DEAEMA, 0:100)

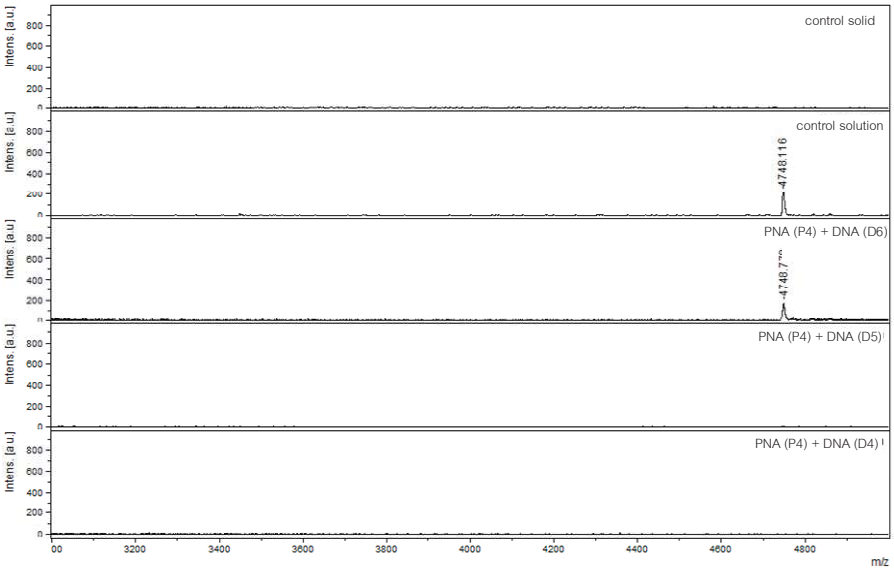

อนุภาคนาโนแมกนีไทท์ (PEGMA : DEAEMA, 50:50)

ภาพ 28 ศึกษาประสิทธิภาพของอนุภาคนาโนแมกนีไทท์หลังการทำ quarternizationในการใช้เป็นตัวดูดจับ (solid support) เพื่อใช้ตรวจสอบลำดับเบสของดีเอ็นเอ เมื่อใช้ PNA (P4) ที่เป็นเฮทเทอโรเบสเป็นโพรบ

จากภาพ 28 จะเห็นได้ว่าแรงกระทำหรือ non-specificity ระหว่างอนุภาคนาโนแมกนีไทท์แต่ละชนิดกับสารละลาย PNA (P4) เพียงอย่างเดียว ไม่เกิดขึ้นเช่นเดียวกับ PNA (P3) เนื่องจากไม่ปรากฏสัญญาณของ PNA (P4) ขึ้น ดังแสดงในส่วนของ control solid ของทั้ง 2 สเปคตรัม เมื่อนำเอาอนุภาคแต่ละชนิดมาทดสอบกับสารละลาย PNA (P4) · DNA (D6) ซึ่งมีลำดับเบสที่เป็นคู่สมกันพบว่าสเปคตรัมจะปรากฏสัญญาณของ PNA (P4) ขึ้นที่ *m/z* = 4748.778 ในขณะที่เมื่อทดสอบกับสารละลาย PNA (P4)

·DNA (D5) ซึ่งมีลำดับเบสที่ไม่เป็นคู่สมและสารละลาย PNA (P4) ·DNA (D4) ซึ่งลำดับเบสต่างกันเพียง 1 เบส พบว่าสัญญาณของ PNA จะไม่ปรากฏเกิดขึ้นทั้งคู่ ซึ่งแสดงให้เห็นถึงการยึดจับกันระหว่าง PNA (P4) กับ DNA(D5) และ DNA(D4) ไม่เกิดขึ้น จึงทำให้การเหนี่ยวนำสารคู่ผสม PNA ·DNA ไปยังพื้นผิวของอนุภาคไม่เกิดขึ้น

จากผลการทดลองของส่วนที่ 2 ข้างต้นพบว่าอนุภาคนาโนแมกนีไทท์ทั้ง 2 อัตราส่วนสามารถนำมาใช้เป็นอนุภาคดูดจับ (solid support) เพื่อใช้ในการตรวจสอบลำดับเบสของดีเอ็นเอที่เป็นเฮทเทอโรเบสได้โดยการใช้ PNA จำนวนโพรบเดียวตรวจสอบและนอกจากนี้ยังสามารถแยกความแตกต่างของลำดับเบสของดีเอ็นเอระหว่างเบสที่เป็นคู่สมกันและลำดับเบสที่มีเบสต่างกันเพียงแค่ 1 ตำแหน่งได้

ดังนั้นเพื่อเป็นการยืนยันประสิทธิภาพของอนุภาคนาโนแมกนีไทท์ในการนำมาใช้เป็นอนุภาคดูดจับ (solid support) เพื่อใช้ตรวจสอบลำดับเบสของดีเอ็นเอโดยใช้ร่วมกับเทคนิค MALDI-TOF mass spectrometryได้นั้น จึงทำการศึกษาถึงประสิทธิภาพของอนุภาคนาโนแมกนีไทท์ที่ทำการ quaternization แล้วทั้ง 2 อัตราส่วน (PEGMA : DEAEMA เป็น 0:100 และ 50:50) ในการนำมาใช้เป็นอนุภาคดูดจับ (solid support) เพื่อใช้ตรวจสอบลำดับเบสของดีเอ็นเอโดยการใช้ PNA จำนวน 2 โพรบเป็นโพรบในการตรวจสอบ

3.2 การยืนยันประสิทธิภาพของอนุภาคนาโนแมกนีไทท์ในการนำมาใช้เป็นอนุภาคดูดจับ (solid support) เพื่อใช้ตรวจสอบลำดับเบสของดีเอ็นเอโดยการใช้ PNA จำนวน 2 โพรบเป็นโพรบในการตรวจสอบ

การศึกษานี้ประกอบด้วย 2 การทดลอง โดยแต่ละการทดลองจะใช้ PNA โพรบที่มีลำดับเบสที่ต่างกันดังนี้

3.2.1 การศึกษาประสิทธิภาพของอนุภาคนาโนแมกนีไทท์ มาใช้เป็นอนุภาคดูดจับ (solid support) เพื่อแยกความแตกต่างของลำดับเบสของดีเอ็นเอระหว่างดีเอ็นเอที่มีลำดับเบสที่เป็นคู่สม (complementary) และ ไม่เป็นคู่สม (non-complementary) ในการทดลองนี้จะใช้ PNA จำนวน 2 โพรบ ที่มีลำดับเบสที่เป็นโฮโมเบสที่แตกต่างกันอย่างสิ้นเชิง มาเป็นโพรบในการตรวจสอบ โดยลำดับเบสของของ PNA และ ดีเอ็นที่ใช้ในการทดลองของส่วนนี้เป็นดังนี้

PNA (P1) : Ac-TTTTTTTTT-Lys-NH_2 (m/z = 3179.404)

PNA (P2) : Ac-AAAAAAAAA -Lys-NH_2 (m/z = 3260.561)

DNA (D1) : 5'-AAAAAAAAA-3' (complementary กับ P1 และ non-complementary กับ P2)

DNA (D2) : 5'-TTTTTTTTT-3' (complementary กับ P2 และ non-complementary กับ P1)

ปริมาณของ PNA และ DNA แต่ละชนิดที่ใช้ 100 pmole

ในขั้นตอนแรกจะเป็นการทดสอบการเกิดแรงกระทำเฉพาะ (non-specificity) ระหว่างอนุภาคนาโนแมกนีไทท์ทั้ง 2 ชนิด กับ สารละลาย PNA ทั้ง 2 โพรบ เพื่อทดสอบว่าอนุภาคเหล่านั้น มีแรงกระทำใดๆ กับ PNA เหล่านี้หรือไม่ ผลการทดสอบแสดงในภาพ 29

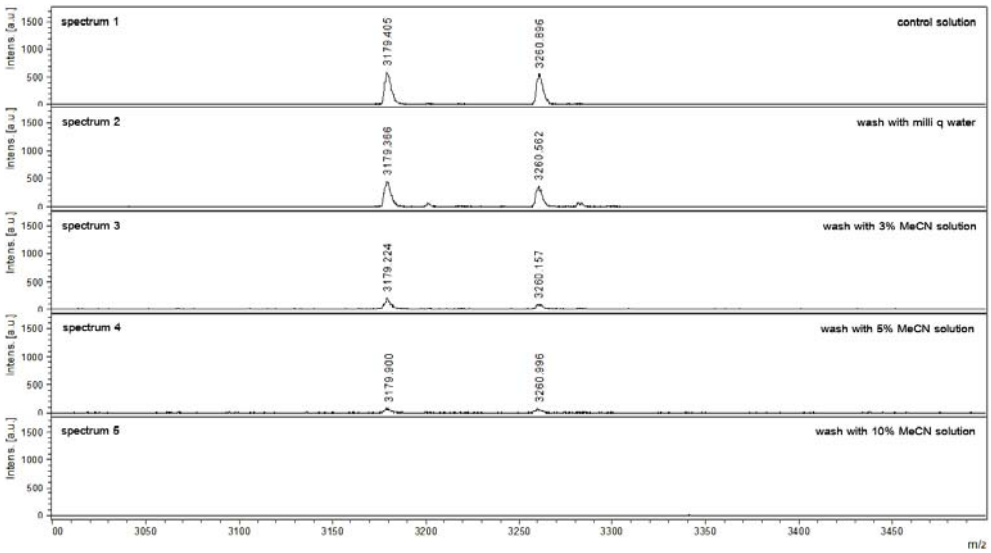

A. อนุภาคนาโนแมกนีไทท์ (PEGMA : DEAEMA, 0:100)

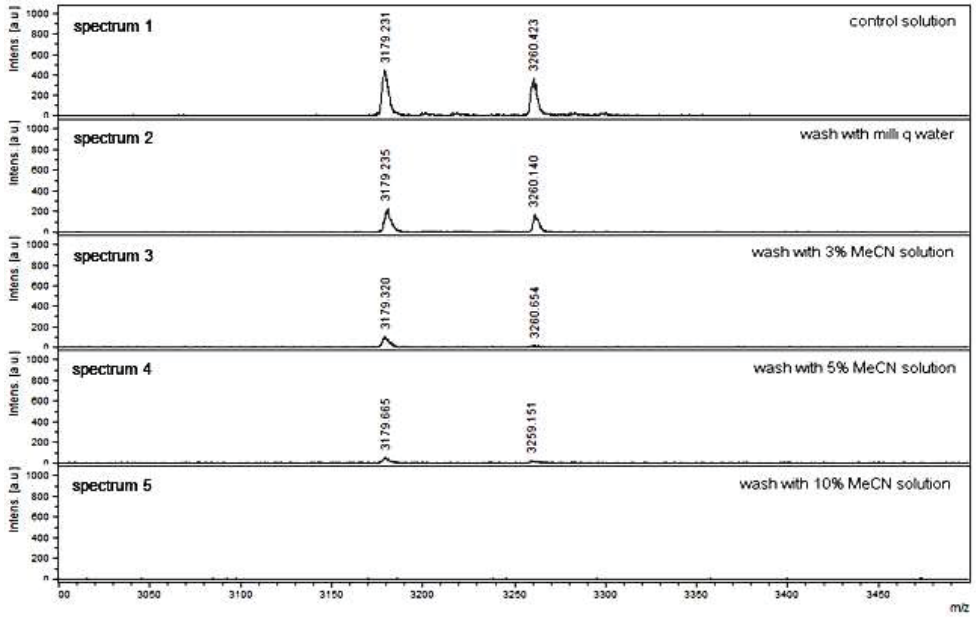

B. อนุภาคนาโนแมกนีไทท์ (PEGMA : DEAEMA, 50:50)

ภาพ 29 การทดสอบ non-specific และการศึกษาปริมาณของอะซิโตรไนไตล์ที่แตกต่างกันในการกำจัด non-specific ของอนุภาคนาโนแมกนีไทท์ทั้ง 2 ชนิด กับ PNA (P1) และ PNA (P2)

จากภาพ 29 จะเห็นได้ว่าเมื่อทำการล้างอนุภาคแต่ละชนิดด้วยน้ำกลั่นและนำไปตรวจสอบด้วยเทคนิค MALDI-TOF spectrometry พบว่าส่วนที่เป็นอนุภาคนาโนแมกนีไทท์ทั้ง 2 ชนิดจะปรากฏสัญญาณของ PNA ทั้ง 2 โพรบ (spectrum 2A, 2B) ในขณะที่สัญญาณของ PNA ทั้ง 2 โพรบก็ปรากฏในชั้นสารละลาย (control solution) เช่นเดียวกัน (spectrum 1A, 1B) ซึ่งแสดงถึงอนุภาคทั้ง 2 ชนิดมีแรงกระทำใดๆ (non-specificity) กับ PNA หรือจับเอา PNA ไว้ที่ผิวของอนุภาคไว้บางส่วนนั่นเองดังนั้นเพื่อเป็นการกำจัด non-specificity ระหว่าง PNA ทั้ง 2 โพรบกับอนุภาคทั้ง 2 ชนิดที่เกิดขึ้นนี้จึงได้เปลี่ยนสารสะลายที่ใช้ล้างอนุภาคจากน้ำกลั่นเป็นสารละลายอะซิโตรไนไตล์ในน้ำที่มีปริมาณของอะซิโตรไนไตล์ที่แตกต่างกันไป ดังนี้ 3%, 5% และ 10% ในน้ำ จากรูปที่ 1 พบว่าเมื่อใช้สารละลาย 10% อะซิโตรไนไตล์ในน้ำล้างอนุภาคนาโนแมกนีไทท์ทั้ง 2 ชนิดพบว่าสัญญาณของ PNA ทั้ง 2 โพรบไม่ปรากฏขึ้นมา (spectrum 5A, 5B) ในขณะที่เมื่อใช้สารละลายอะซิโตรไนไตล์อัตราส่วนอื่นพบว่าจะปรากฏสัญญาณของ PNA โพรบอยู่ (spectrum 3A,4A,3B,4B) ดังนั้นการทดลองในขั้นตอนต่อไปจึงเลือกใช้สารสะลายที่ใช้ล้างอนุภาคเป็น10% อะซิโตรไนไตล์ในน้ำ

ในขั้นตอนต่อไปจะเป็นการนำอนุภาคนาโนแมกนีไทท์ทั้ง 2 ชนิด มาทดสอบประสิทธิภาพในการใช้เป็นตัวดูดจับ (solid support) เพื่อแยกความแตกต่างของลำดับเบสของดีเอ็นเอระหว่างดีเอ็นเอที่มีลำดับเบสที่เป็นคู่สม (complementary) และ ไม่เป็นคู่สม (non-complementary) ผลการทดลองแสดงดังภาพ 30

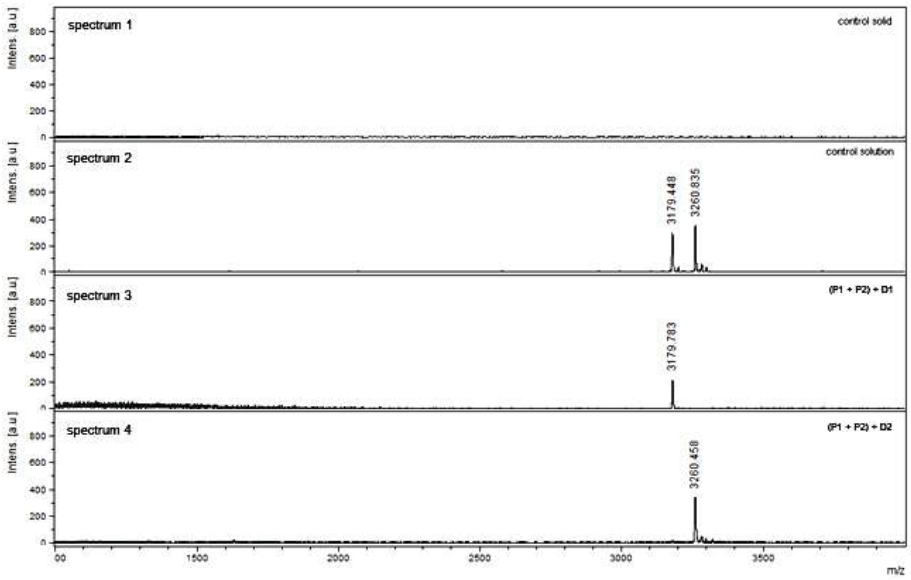

A. อนุภาคนาโนแมกนีไทท์ (PEGMA : DEAEMA, 0:100)

B.

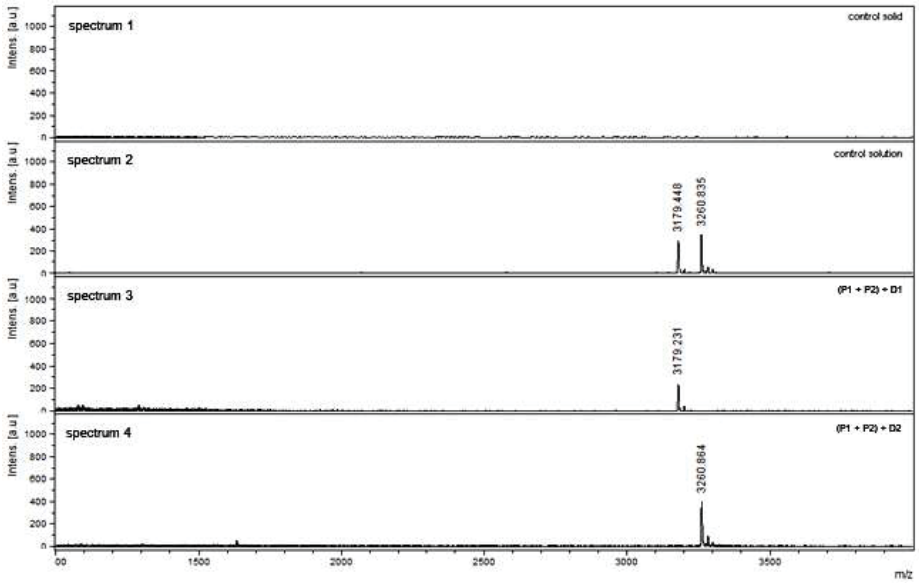

B. อนุภาคนาโนแมกนีไทท์ (PEGMA : DEAEMA, 50:50)

ภาพ 30 การศึกษาประสิทธิภาพของอนุภาคนาโนแมกนีไทท์หลังการทำ quarternizationในการใช้เป็นตัวดูดจับ (solid support) เพื่อใช้ตรวจสอบลำดับเบสของดีเอ็นเอ เมื่อใช้ PNA (P1) และ PNA (P2) ที่เป็นโฮโมเบสเป็นโพรบ

จากภาพ 30 จะเห็นได้ว่าเมื่อทดสอบ non-specificity ระหว่างอนุภาคทั้ง 2 อัตราส่วนกับสารละลาย PNA อย่างเดียว โดยการใช้ 10% อะซิโตรไนไตล์ในน้ำล้างอนุภาคออกจากสารละลาย PNA พบว่าจะไม่ปรากฏสัญญาณของ PNA ทั้ง 2 โพรบดังแสดงในส่วนของ control solid ของทั้ง 2 สเปกตรัม ในขณะที่ใน

ส่วนของสารละลาย PNA ที่ทำการแยกเอาอนุภาคออกไปแล้ว ดังแสดงในส่วนของ control solution ของทั้ง 2 สเปกตรัมจะปรากฏสัญญาณของ PNA ทั้ง 2 โพรบขึ้น

หลังจากนั้นเมื่อทำการเติม DNA (D1) ลงในสารละลาย PNA (P1+P2) ที่มีอนุภาคนาโนแมกนีไทท์กระจายตัวอยู่แล้วทำการแยกเอาอนุภาคมาตรวจสอบด้วยเทคนิค MALDI-TOF spectrometry พบว่าจะปรากฏสัญญาณของ PNA (P1) ที่ 3179.783 และ 3179.231 ดังแสดงใน spectrum 3A และ 3B ตามลำดับ ซึ่งแสดงถึงเกิดการยึดจับกันระหว่าง PNA (P1) และ DNA (D1) ที่มีลำดับเบสที่เป็นคู่สมกันเท่านั้น ซึ่งจะถูกเหนี่ยวนำไปยังพื้นผิวของอนุภาคด้วยแรงทางไอออนิก ในขณะที่ PNA (P2) ไม่สามารถยึดจับกับ DNA (D1) ได้ทั้งนี้เนื่องจากมีลำดับเบสที่ไม่เป็นคู่สมกันนั่นเองจึงมีผลทำให้ไม่ปรากฏสัญญาณของ PNA (P2) ขึ้น

ในขณะเดียวกันเมื่อนำสารละลาย PNA (P1+P2) ที่มีอนุภาคนาโนแมกนีไทท์อยู่มาทำการเติมด้วย DNA (D2) ที่มีลำดับเบสที่เป็นคู่สมกับ PNA (P2) เท่านั้น ผลการทดสอบพบว่าจะปรากฏเฉพาะสัญญาณของ PNA (P2) ที่ 3260.458 และ 3260.864 เท่านั้นดังแสดงใน spectrum 4A และ 4B ตามลำดับ ในขณะที่สัญญาณของ PNA (P1) จะไม่ปรากฏซึ่งแสดงให้เห็นถึงการยึดจับกันระหว่าง PNA (P1) กับ DNA(D2) ไม่เกิดขึ้น จึงทำให้การเหนี่ยวนำสารคู่ผสม PNA (P1) ·DNA (D2) ไปยังพื้นผิวของอนุภาคไม่เกิดขึ้นนั่นเอง

จากผลการทดลองข้างต้นจะเห็นได้ว่าอนุภาคนาโนแมกนีไทท์ทั้ง 2 อัตราส่วนสามารถนำมาใช้เป็นอนุภาคดูดจับ (solid support) เพื่อใช้ในการตรวจสอบลำดับเบสของดีเอ็นเอได้เมื่อใช้ PNA 2 โพรบที่มีลำดับเบสที่เป็นโฮโมเบสที่ต่างกันโดยสิ้นเชิงเป็นโพรบในการตรวจสอบ ซึ่งสามารถแยกความแตกต่างของลำดับเบสของดีเอ็นเอระหว่างเบสที่เป็นคู่สมกันกับไม่เป็นคู่สมกันได้

3.2.2 การศึกษาประสิทธิภาพของอนุภาคนาโนแมกนีไทท์ มาใช้เป็นอนุภาคดูดจับ (solid support) เพื่อใช้ตรวจสอบลำดับเบสของดีเอ็นเอ ในการทดลองนี้จะใช้ PNA จำนวน 2 โพรบ ที่มีลำดับเบสที่เป็นเฮทเทอโรเบสที่มีลำดับเบสต่างกันเพียงแค่ตำแหน่งเดียวมาเป็นโพรบในการตรวจสอบ โดยลำดับเบสของของ PNA และ ดีเอ็นที่ใช้ในการทดลองของส่วนนี้เป็นดังนี้

PNA (P3) : $^{+}PPh_3$-TTTTAC<u>A</u>CAACCC-Ser-NH_2 (m/z = 4732.117)

PNA (P4) : $^{+}PPh_3$-TTTTAC<u>G</u>CAACCC-Ser-NH_2 (m/z = 4748.116)

DNA (D3): 5’-GGGTTG<u>T</u>GTAAAA-3’ (complementary กับ P3, single base mismatch กับ P4)

DNA (D4) : 5’-GGGTTG<u>C</u>GTAAAA-3’ (complementary กับ P4, single base mismatch กับ P3)

ปริมาณของ PNA และ DNA แต่ละชนิดที่ใช้ 100 pmole

ในขั้นแรกจะทำการศึกษาการเกิดแรงกระทำเฉพาะ (non-specificity) ระหว่างอนุภาคนาโนแมกนีไทท์ทั้ง 2 ชนิด กับ สารละลาย PNA ทั้ง 2 โพรบ เพื่อทดสอบว่าอนุภาคเหล่านั้น มีแรงกระทำใดๆ กับ PNA เหล่านี้หรือไม่ ซึ่งผลการทดลองแสดงดังภาพ 31

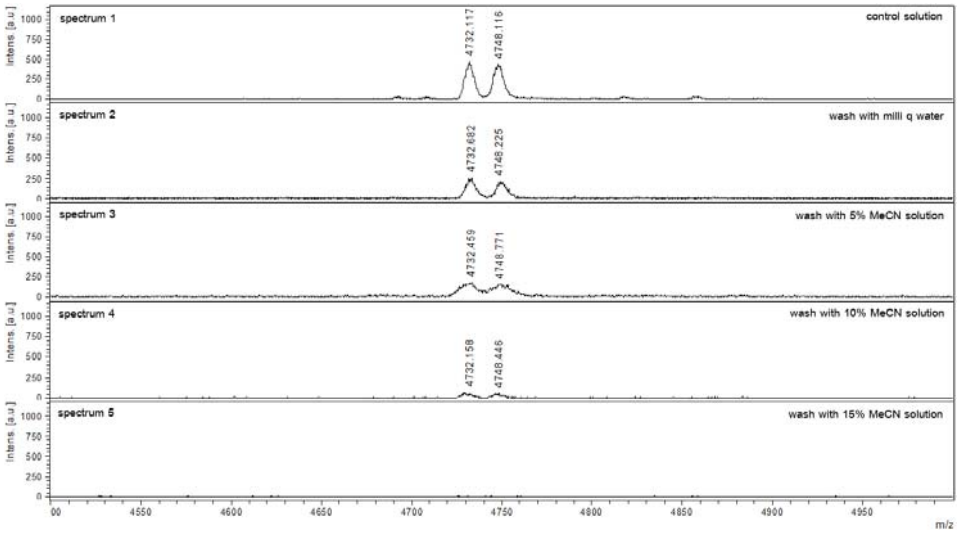

A. อนุภาคนาโนแมกนีไทท์ (PEGMA : DEAEMA, 0:100)

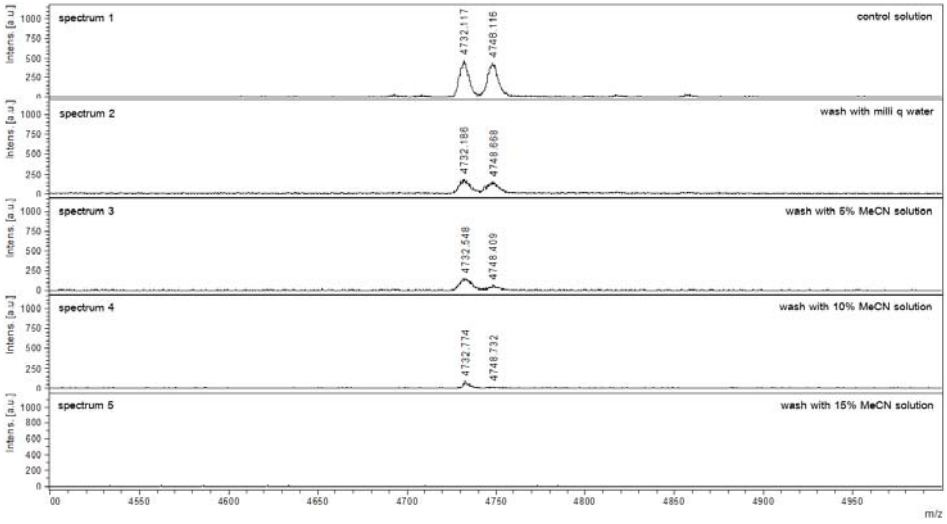

B. อนุภาคนาโนแมกนีไทท์ (PEGMA : DEAEMA, 50:50)

ภาพ 31 การทดสอบ non-specific และการศึกษาปริมาณของอะซิโตรไนไตล์ที่แตกต่างกันในการกำจัด non-specific ของอนุภาคนาโนแมกนีไทท์ที่ 2 ชนิด กับ PNA (P3) และ PNA (P4)

จากภาพ 31 เมื่อใช้สารละลายที่ใช้ล้างอนุภาคที่แตกต่างกันคือ น้ำกลั่น , 5%, 10% และ 15% อะซิโตรไนไตล์ในน้ำ พบว่าเมื่อใช้สารละลาย 15% อะซิโตรไนไตล์ในน้ำล้างอนุภาคนาโนแมกนีไทท์ทั้ง 2 ชนิด พบว่าสัญญาณของ PNA ทั้ง 2 โพรบไม่ปรากฏขึ้นมา (spectrum 5A, 5B) ซึ่งแสดงให้เห็นว่าสารละลายนี้สามารถกำจัด non-specificity ระหว่าง PNA ทั้ง 2 โพรบกับอนุภาคทั้ง 2 ชนิดที่เกิดขึ้นได้ในขณะที่เมื่อน้ำกลั่นและสารละลายอะซิโตรไนไตล์อัตราส่วนอื่นพบว่าจะปรากฏสัญญาณของ PNA โพรบอยู่ (spectrum 3A,4A,3B,4B) ดังนั้นการทดลองในขั้นตอนต่อไปจึงเลือกใช้ สารสะลายที่ใช้ล้างอนุภาคเป็น15% อะซิโตรไนไตล์ในน้ำ

ในขั้นตอนต่อไปจะเป็นการนำอนุภาคนาโนแมกนีไทท์ทั้ง 2 ชนิด มาทดสอบประสิทธิภาพในการใช้เป็นตัวดูดจับ (solid support) เพื่อแยกความแตกต่างของลำดับเบสของดีเอ็นเอระหว่างดีเอ็นเอที่มีลำดับเบสต่างกันเพียงตำแหน่งเดียวโดยใช้ PNA (P3) และ PNA (P4) เป็นโพรบ ซึ่งผลการทดลองแสดงดังภาพ 32

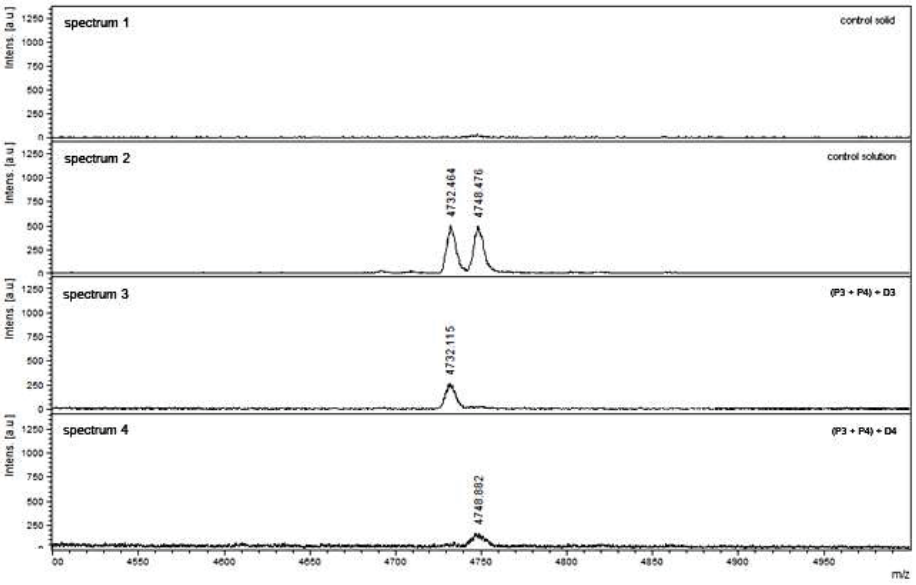

A. อนุภาคนาโนแมกนีไทท์ (PEGMA : DEAEMA, 0:100)

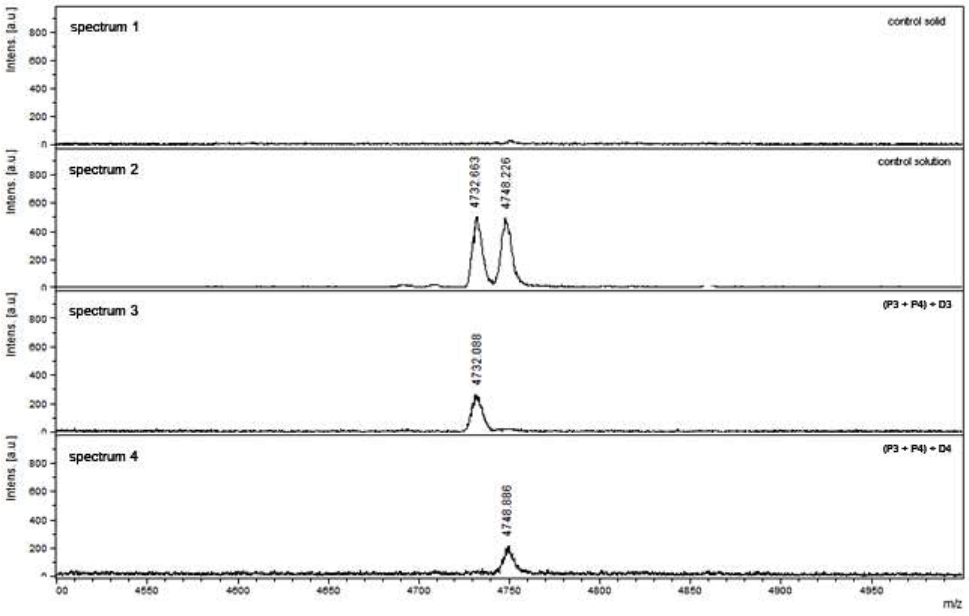

B. อนุภาคนาโนแมกนีไทท์ (PEGMA : DEAEMA, 50:50)

ภาพ 32 การศึกษาประสิทธิภาพของอนุภาคนาโนแมกนีไทท์หลังการทำ quarternizationในการใช้เป็นตัวดูดจับ (solid support) เพื่อใช้ตรวจสอบลำดับเบสของดีเอ็นเอ เมื่อใช้ PNA (P3) และ PNA (P4) ที่เป็นเฮทเทอโรเบสเบสเป็นโพรบ

จากภาพ 32 จะเห็นได้ว่าเมื่อใช้ 15% อะซิโตรไนไตล์ในน้ำล้างอนุภาคออกจากสารละลาย PNA จะไม่เกิด non-specificity ระหว่างอนุภาคทั้ง 2 อัตราส่วนกับสารละลาย PNA ซึ่งจะไม่ปรากฏสัญญาณของ PNA ทั้ง 2 โพรบดังแสดงในส่วนของ control solid ของทั้ง 2 สเปกตรัม ในขณะที่ในส่วนของสารละลาย PNA ที่ทำการแยกเอาอนุภาคออกไปแล้ว ดังแสดงในส่วนของ control solution ของทั้ง 2 สเปกตรัมจะปรากฏสัญญาณของ PNA ทั้ง 2 โพรบขึ้น

หลังจากนั้นเมื่อนำสารละลาย PNA (P3+P4) ที่มีอนุภาคนาโนแมกนีไทท์กระจายตัวอยู่มาทำการเติมด้วย DNA (D3) ที่มีลำดับเบสที่เป็นคู่สมกับ PNA (P3) เท่านั้น และล้างอนุภาคด้วย 15% อะซิโตรไนไตล์ในน้ำ แล้วทำการแยกเอาอนุภาคมาตรวจสอบด้วยเทคนิค MALDI-TOF spectrometry ผลการทดสอบพบว่าจะปรากฏเฉพาะสัญญาณของ PNA (P3) ที่ 4732.115 และ 4732.088 เท่านั้นดังแสดงใน spectrum 3A และ 3B ตามลำดับ ซึ่งแสดงถึงสารประกอบคู่ผสม PNA (P3) · DNA (D3) ที่เกิดขึ้นจะถูกเหนี่ยวนำไปยังพื้นผิวของอนุภาคด้วยแรงทางไอออนิก ในขณะที่สัญญาณของ PNA (P4) จะไม่ปรากฏซึ่งแสดงให้เห็นถึงการยึดจับกันระหว่าง PNA (P4) กับ DNA(D3) ไม่เกิดขึ้น จึงทำให้การเหนี่ยวนำสารคู่ผสม PNA (P4) ·DNA (D3) ไปยังพื้นผิวของอนุภาคไม่เกิดขึ้นนั่นเอง

ในทางกลับกันเมื่อทำการเติม DNA (D4) ลงในสารละลาย PNA (P3+P4) ที่มีอนุภาคนาโนแมกนีไทท์กระจายตัวอยู่แล้วทำการแยกเอาอนุภาคมาตรวจสอบด้วยเทคนิค MALDI-TOF พบว่าจะปรากฏสัญญาณของ PNA (P4) ที่ 4748.882 และ 4748.886 ดังแสดงใน spectrum 4A และ 4B ตามลำดับ ซึ่งแสดงถึงเกิดการยึดจับกันระหว่าง PNA (P4) และ DNA (D4) ที่มีลำดับเบสที่เป็นคู่สมกันเท่านั้นจึงทำให้ถูกเหนี่ยวนำไปยังพื้นผิวของอนุภาคด้วยแรงทางไอออนิก ในขณะที่ PNA (P3) ไม่สามารถยึดจับกับ DNA (D4) ได้ทั้งนี้เนื่องจากมีลำดับเบสที่ไม่เป็นคู่สมกันนั่นเองจึงมีผลทำให้ไม่ปรากฏสัญญาณของ PNA (P3) ขึ้น

จากผลการทดลองของส่วนที่ 2 ข้างต้นพบว่าอนุภาคนาโนแมกนีไทท์ทั้ง 2 อัตราส่วนสามารถนำมาใช้เป็นอนุภาคดูดจับ (solid support) เพื่อใช้ในการตรวจสอบลำดับเบสของดีเอ็นเอที่เป็นเฮทเทอโรเบสได้เมื่อใช้ PNA 2 โพรบที่มีลำดับเบสที่เป็นเฮทเทอโรเบสที่มีลำดับเบสแตกต่างกันเพียงตำแหน่งเดียวเป็นโพรบในการตรวจสอบและนอกจากนี้ยังสามารถแยกความแตกต่างของลำดับเบสของดีเอ็นเอระหว่างเบสที่เป็นคู่สมกันและลำดับเบสที่มีเบสต่างกันเพียงแค่ 1 ตำแหน่งได้

อย่างไรก็ตามปริมาณของ PNA และ DNA ที่ใช้นั้นยังคงจัดว่าใช้ปริมาณที่มาก ดังนั้นในการทดลองขั้นต่อไปจะเป็นการศึกษาหาปริมาณของ PNA และ DNA ที่เหมาะสมที่สามารถใช้ร่วมกับอนุภาคนาโนแมกนีไทท์นี้ต่อไป

4. การศึกษาหาปริมาณของ PNA และ DNA ที่น้อยที่สุดที่สามารถใช้ร่วมกับอนุภาคนาโนแมกนีไทท์

โดย PNA และ DNA ที่เลือกใช้เป็นโมเดลของการทดลองเป็นดังนี้

PNA (P3) : $^{+}PPh_3$-TTTTACACAACCC-Ser-NH_2 (m/z = 4732.117)

DNA (D3): 5'-GGGTTGTGTAAAA-3' (complementary กับ P3)

อนุภาคนาโนแมกมีไทด์ที่เลือกใช้ คืออนุภาคนาโนแมกนีไทท์ ที่มีอัตราส่วนของ PEGMA : DEAEMA เป็น 0:100

โดยการทดลองจะใช้อัตราส่วนของปริมาณของ PNA และ DNA เป็น 1:1 และปริมาณ ของ PNA และ DNA ที่ใช้แตกต่างกันออกไป ดังนี้ 10, 30, 70 และ 100 pmole ตามลำดับ ผลการทดลองดังแสดงในภาพ 33

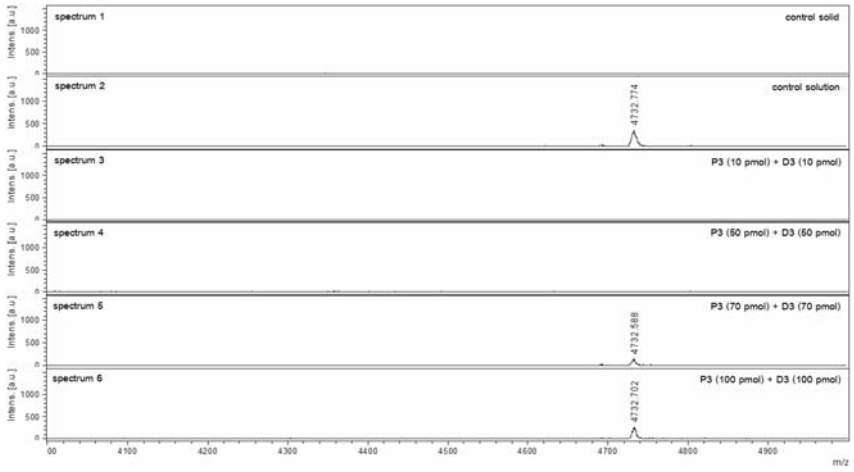

ภาพ 33 การศึกษาหาปริมาณของ PNA และ DNA ที่น้อยที่สุดที่สามารถใช้ร่วมกับอนุภาคนาโนแมกนีไทท์

จากภาพ 33 พบว่าปริมาณของ PNA และ DNA ที่น้อยที่สุดที่ทำให้สัญญาณของ PNA (m/z = 4732.111) ปรากฏคือ 70 pmole ดังแสดงใน spectrum 5 ในขณะที่เมื่อปริมาณของ PNA และ DNA น้อยกว่า 70 pmol พบว่าไม่สามารถตรวจสอบสัญญาณของ PNA ได้

จากปริมาณของ PNA และ DNA ที่น้อยที่สุดที่ทำการศึกษาข้างต้นในขั้นตอนต่อไปจึงนำเอาปริมาณที่ศึกษาได้มาลองใช้ในการตรวจสอบลำดับเบสของ *K-ras* DNA 2 ชนิดคือ *K-ras* (mutation) และ *K-ras* (wild-type allele) ที่มีลำดับเบสที่สอดคล้องกับลำดับเบสของ DNA จริง โดยใช้อนุภาคนาโนแมกนีไทท์แต่ละอัตราส่วนเป็นอนุภาคในการดูดจับ ซึ่งลำดับเบสของ PNA และ DNA ที่ใช้เป็นดังนี้

PNA (P5) = Ac-Lys-O-CTA CGC CAA CAG CT-Ser-NH_2 (m/z = 5069.459)

PNA (P6) = Ac-Lys-CTA CGC CAC CAG CT-ser NH_2 (m/z = 4900.277)

DNA (D5) = 5'-AGC TGT TGG CGT AG-3' (*K-ras* (mutation), complementary กับ P5, single base mismatch กับ P6)

DNA (D6) = 5'-AGC TGG TGG CGT AG-3' (*K-ras* (wild-type allele), complementary กับ P6 single base mismatch กับ P5)

โดยใช้ปริมาณ PNA และ DNA 70 pmole ผลการทดลองแสดงดังภาพ 34 และ ภาพ 35

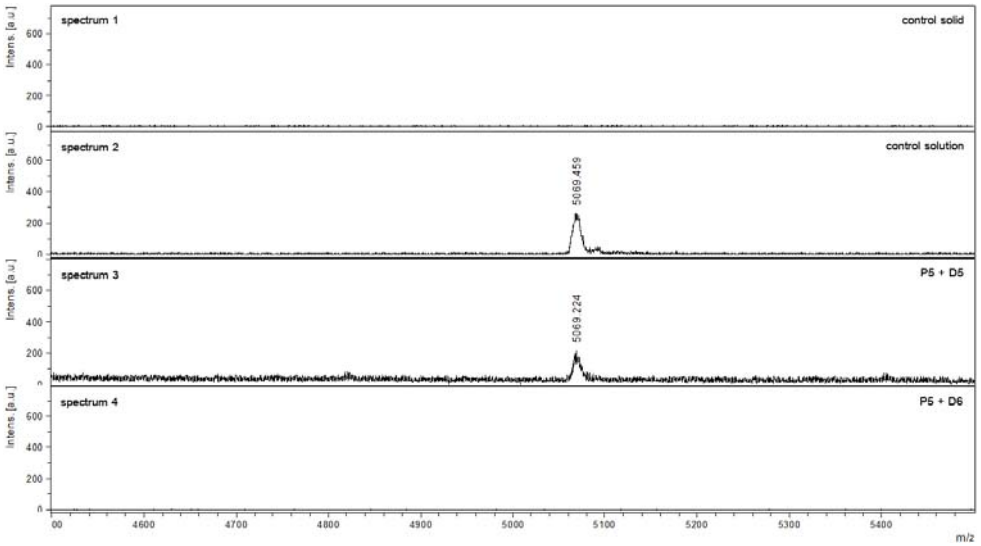

A. อนุภาคนาโนแมกนีไทท์ (PEGMA : DEAEMA, 0:100)

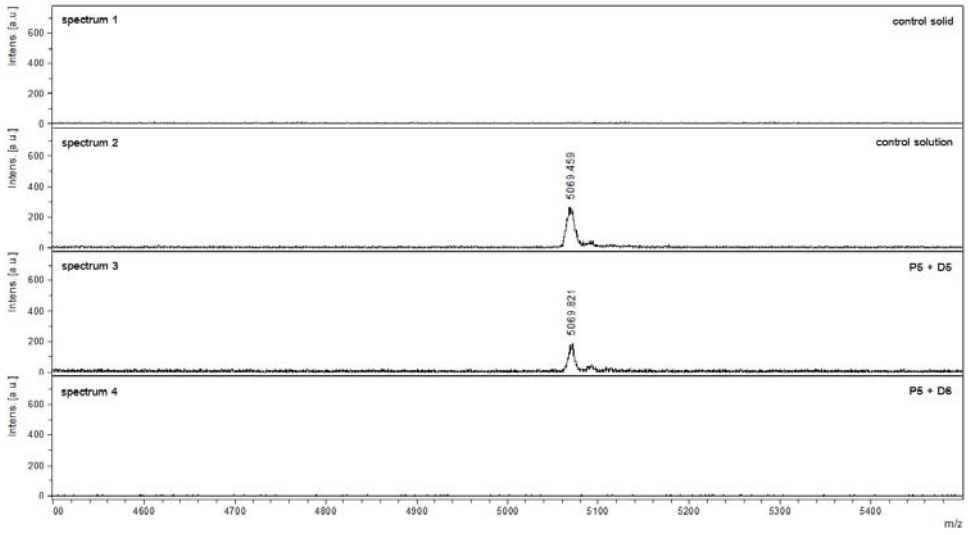

B. อนุภาคนาโนแมกนีไทท์ (PEGMA : DEAEMA, 50:50)

ภาพ 34 การศึกษาประสิทธิภาพของอนุภาคนาโนแมกนีไทท์หลังการทำ quarternizationในการใช้เป็นตัวดูดจับ (solid support) เพื่อใช้ตรวจสอบลำดับเบสของดีเอ็นเอ *K-ras* (mutation) เมื่อใช้ PNA (P5) เป็นโพรบ

จากภาพ 34 จะเห็นได้ว่าเมื่อใช้ 15% อะซิโตรไนไตล์ในน้ำล้างอนุภาคออกจากสารละลาย PNA จะไม่เกิด non-specificity ระหว่างอนุภาคทั้ง 2 อัตราส่วนกับสารละลาย PNA ซึ่งจะไม่ปรากฏสัญญาณของ PNA ทั้ง 2 โพรบดังแสดงในส่วนของ control solid ของทั้ง 2 สเปกตรัม ในขณะที่ในส่วนของสารละลาย PNA ที่ทำการแยกเอาอนุภาคออกไปแล้ว ดังแสดงในส่วนของ control solution ของทั้ง 2 สเปกตรัมจะปรากฏสัญญาณของ PNA ทั้ง 2 โพรบขึ้น

เมื่อนำเอาสารละลาย PNA (P5) · DNA (D5) ซึ่งมีลำดับเบสที่เป็นคู่สมกันเติมลงในอนุภาคแต่ละชนิดที่กระจายตัวอยู่ในฟอสเฟตบัฟเฟอร์ หลังจากนั้นทำการแยกอนุภาคนาโนแมกนีไทท์ออกจากสารละลาย PNA (P5) · DNA (D5) ด้วยแท่งแม่เหล็ก แล้วทำการล้างอนุภาคด้วย 15% อะซิโตรไนไตล์ในน้ำ จากนั้นนำส่วนของอนุภาคนาโนแมกนีไทท์ที่ทำการล้างแล้วไปทดสอบด้วยเทคนิค MALDI-TOF spectrometry พบว่าจะแสดงสัญญาณของ PNA (P5) ที่ *m/z* = 5069.224 และ 5069.821 ขึ้น ดังแสดงใน spectrum 3A และ 3B ซึ่งแสดงให้เห็นถึงการเกิดสารประกอบคู่ผสม PNA (P5) · DNA (D5) ขึ้นแล้วถูกเหนี่ยวนำไปยังพื้นผิวของอนุภาคด้วยแรงทางไอออนิก

ในทางกลับกันเมื่อทำการเติมสารละลาย PNA (P5) · DNA (D6) ซึ่งมีลำดับเบสที่ต่างกันเพียงตำแหน่งเดียวเติมลงในอนุภาคแต่ละชนิดที่กระจายตัวอยู่ในฟอสเฟตบัฟเฟอร์ พบว่าจะไม่แสดงสัญญาณของ PNA (P5) ดังแสดงใน spectrum 4A และ 4B ตามลำดับ ซึ่งแสดงให้เห็นว่าการยึดจับกันระหว่าง PNA (P5) และ DNA (D6) ไม่เกิดขึ้นนั่นเอง ดังแสดงในภาพ 35

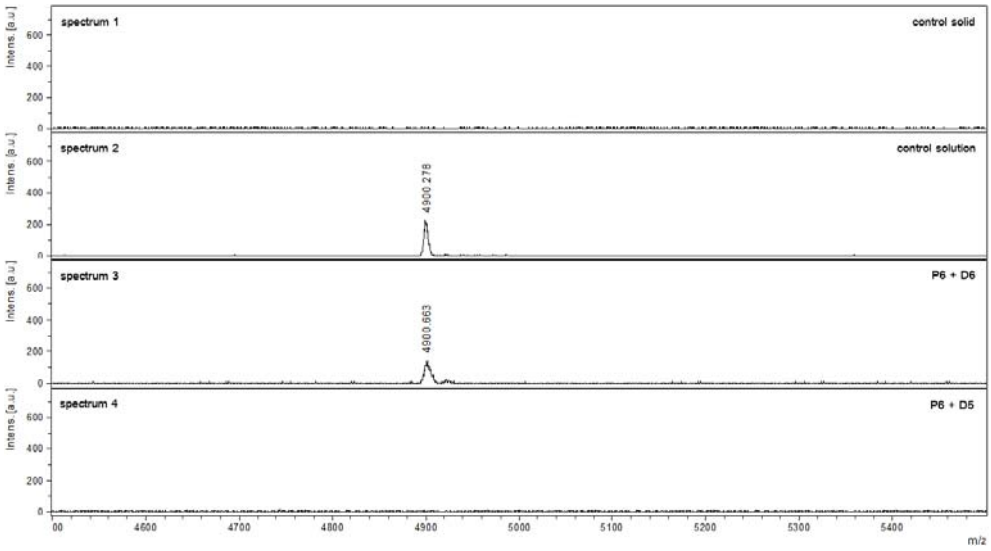

A. อนุภาคนาโนแมกนีไทท์ (PEGMA : DEAEMA, 0:100)

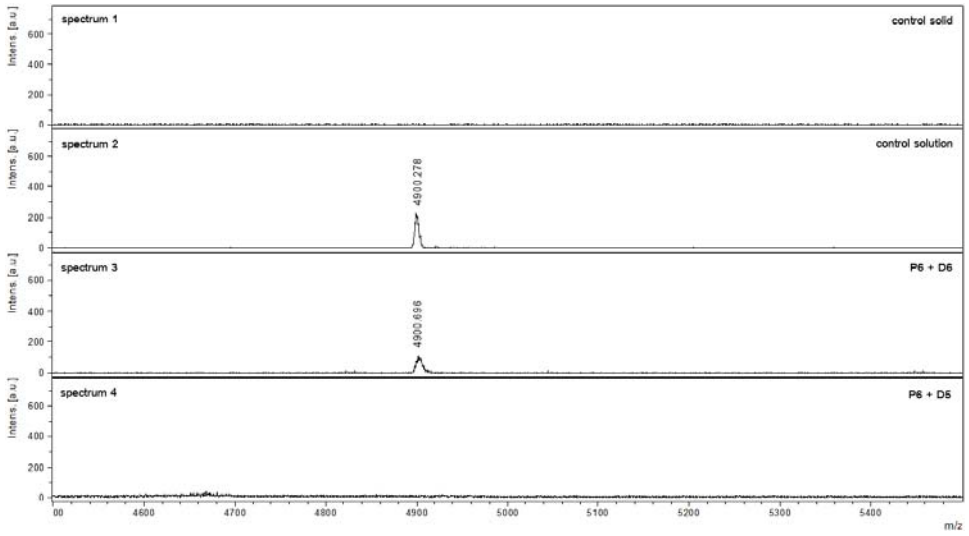

B. อนุภาคนาโนแมกนีไทท์ (PEGMA : DEAEMA, 50:50)

ภาพ 35 การศึกษาประสิทธิภาพของอนุภาคนาโนแมกนีไทท์หลังการทำ quarternizationในการใช้เป็นตัวดูดจับ (solid support) เพื่อใช้ตรวจสอบลำดับเบสของดีเอ็นเอ *K-ras* (wild-type allele) เมื่อใช้ PNA (P6) เป็นโพรบ

จากภาพ 35 จะเห็นได้ว่า จะไม่เกิด non-specificity ระหว่างอนุภาคทั้ง 2 อัตราส่วนกับสารละลาย PNA เมื่อใช้ 15% อะซิโตรไนไตล์ในน้ำล้างอนุภาคออกจากสารละลายPNAโดยจะเห็นได้จากสัญญาณของ PNA ทั้ง 2 โพรบจะไม่ปรากฏขึ้นมา ดังแสดงในส่วนของ control solid ของทั้ง 2 สเปกตรัม ในขณะที่ในส่วนของสารละลาย PNA ที่ทำการแยกเอาอนุภาคออกไปแล้ว จะปรากฏสัญญาณของ PNA ทั้ง 2 โพรบขึ้นดังแสดงในส่วนของ control solution ของทั้ง 2 สเปกตรัม

เมื่อนำเอาอนุภาคแต่ละชนิดที่กระจายตัวอยู่ในฟอสเฟตบัฟเฟอร์มาถูกเติมด้วยสารละลาย PNA (P6) · DNA (D6) ซึ่งมีลำดับเบสที่เป็นคู่สมกัน หลังจากนั้นทำการแยกอนุภาคนาโนแมกนีไทท์ออกจากสารละลาย PNA (P6) · DNA (D6) ด้วยแท่งแม่เหล็ก แล้วทำการล้างอนุภาคด้วย 15% อะซิโตรไนไตล์ในน้ำ จากนั้นนำส่วนของอนุภาคนาโนแมกนีไทท์ที่ทำการล้างแล้วไปทดสอบด้วยเทคนิค MALDI-TOF spectrometry พบว่าจะแสดงสัญญาณของ PNA (P6) ที่ *m/z* = 4900.663 และ 4900.696 ขึ้น ดังแสดงใน spectrum 3A และ 3B ซึ่งแสดงให้เห็นถึงการเกิดการยึดจับกันระหว่าง PNA (P6) กับ DNA (D6) ขึ้นแล้วถูกเหนี่ยวนำไปยังพื้นผิวของอนุภาคด้วยแรงทางไอออนิกจึงมีผลทำให้เกิดสัญญาณของ PNA (P6) บนอนุภาคขึ้นนั่นเอง

ในขณะเดียวกันเมื่อทำการเติมสารละลาย PNA (P6) · DNA (D5) ลงในอนุภาคแต่ละชนิด พบว่าจะไม่ปรากฏสัญญาณของ PNA (P6) ดังแสดงใน spectrum 4A และ 4B ตามลำดับ ซึ่งแสดงให้เห็นว่าการยึดจับกันระหว่าง PNA (P6) และ DNA (D5) ไม่เกิดขึ้นทั้งนี้เนื่องจาก PNA (P6) และ DNA (D5) มีลำดับเบสที่ต่างกันเพียงตำแหน่งเดียวนั่นเอง

เมื่อศึกษาหาปริมาณของ PNA และ DNA ที่เหมาะสมที่สามารถใช้ร่วมกับอนุภาคนาโนแมกนีไทท์ พบว่าปริมาณ PNA และ DNA ที่น้อยที่สุด ที่สามารถนำมาใช้ร่วมกับอนุภาคนาโนแมกนีไทท์ทั้ง 2 อัตราส่วนในการตรวจสอบลำดับของเบสของ DNA ได้และสามารถทำให้สัญญาณของ PNA ปรากฏขึ้นคือ 70 pmole อย่างไรก็ตามปริมาณของ PNA และ DNA ที่ศึกษาได้นี้ยังคงจัดว่าเป็นปริมาณที่มากอยู่ ทั้งนี้อาจเนื่องมาจากความสามารถในการกระจายตัวของอนุภาคเองและความเป็นบวกที่ผิวค่อนข้างน้อย ดังนั้นเพื่อเป็นการยืนยันถึงความสามารถในการจับ PNA-DNA complex ของอนุภาคทั้ง 2 อัตราส่วน การทดลองต่อไปจึงทำการศึกษาถึงความสามารถในการจับ DNA ของอนุภาคแม่เหล็กทั้ง 2 อัตราส่วน โดยในการทดลองได้เลือกใช้ DNA ที่มีหมู่ฟลูออเรสซีนติดที่ตำแหน่ง 5' เป็นโมเดลในการทดสอบ

5. การศึกษาความสามารถในการจับ DNAของอนุภาคนาโนแมกนีไทท์

โดย DNA ที่เลือกใช้เป็นโมเดลของการทดลองเป็นดังนี้

DNA: FAM-AAAAAAAAA -3'

โดยในการทดลองได้ทำการเตรียมสารละลาย FAM-DNA ให้มีความเข้มข้น 30 nM ปริมาตร 1000 µL จากนั้นนำสารละลาย DNA ที่เตรียมไปวัดค่าการให้สัญญาณ ฟลูออเรสเซนส์ที่ความยาวคลื่น 516.86 nm หลังจากนั้นทำการเติมสารละลายอนุภาคนาโนแมกนีไทท์ (อนุภาค1.5 mg : TE บัฟเฟอร์ 2 ml) แต่ละชนิดลงในสารละลาย DNA 100 µL แล้วนำการคนสารละลายเป็นเวลา 30 นาที จากนั้นนำสารละลาย DNA ที่มีอนุภาคภนาโนแทมกนีไทท์ไปวัดค่าการให้สัญญาณฟลูออเรสเซนส์ ทุกๆ 5 นาทีจนครบ 100 นาที จากนั้นนำค่าสัญญาณที่วัดได้มาทำการคำณวนหาความสามารถการจับ DNA ของอนุภาค ผลการทดลองแสดงดังภาพ 36

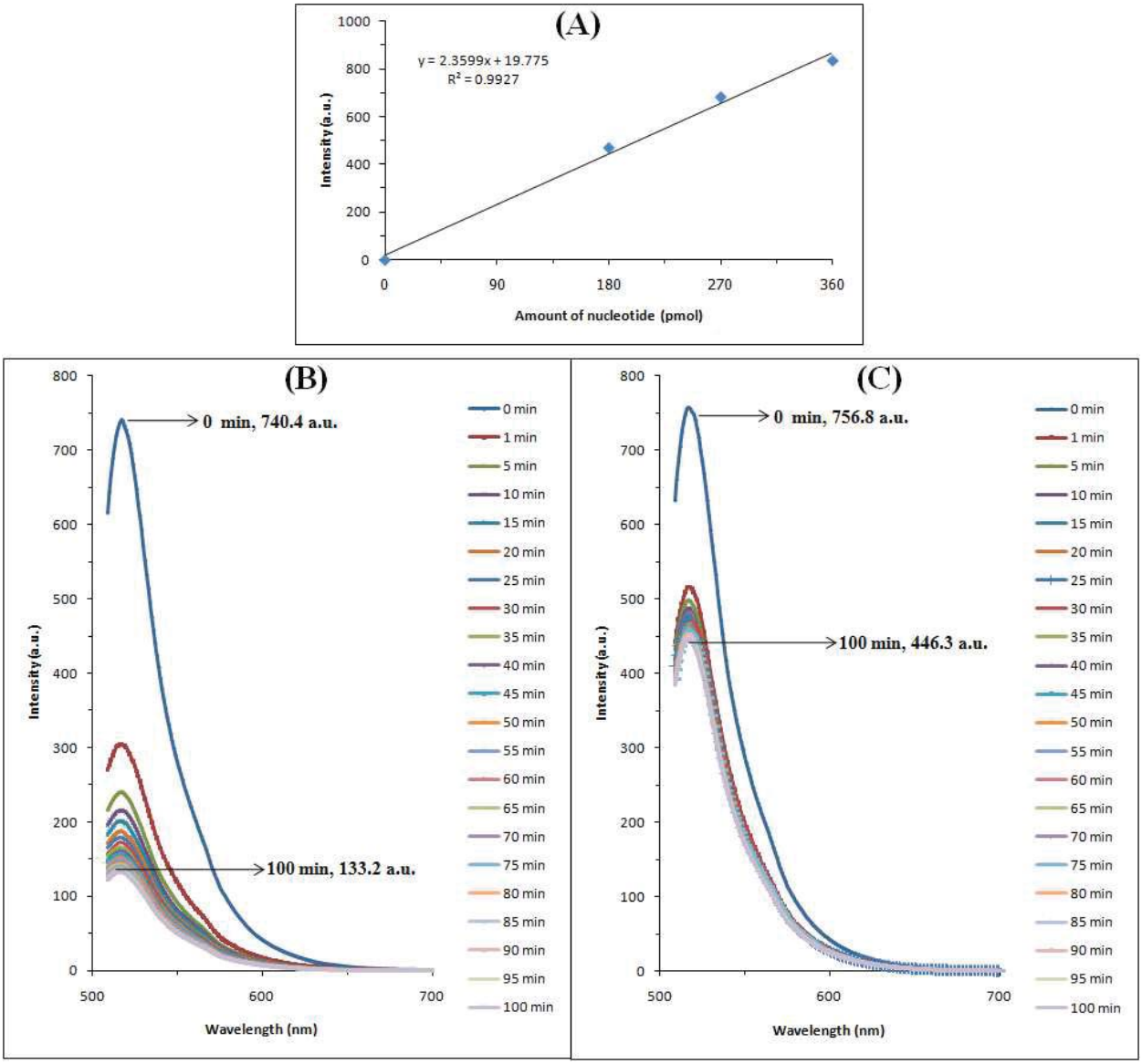

ภาพ 36 (A) Calibration curve

(B) Fluorescence spectra ของ อนุภาคนาโนแมกนีไทท์ที่ประกอบด้วย อัตราส่วนของ PEGMA:DEAEMA เป็น 0 : 100

(C) Fluorescence spectra ของ อนุภาคนาโนแมกนีไทท์ที่ประกอบด้วย อัตราส่วนของ PEGMA:DEAEMA เป็น 50 : 50

จากผลการทดลองในกรณีที่ทดสอบกับอนุภาคนาโนแมกนีไทท์ที่ประกอบด้วย อัตราส่วนของ PEGMA:DEAEMA เป็น 0 : 100 พบว่าเมื่อเวลาผ่านไป 100 นาทีค่าการให้สัญญาณฟลูออเรสเซนต์ของ FAM-DNA อยู่ที่ 133.2 a.u. ในขณะที่ค่าการให้สัญญาณฟลูออเรสเซนต์ของ FAM-DNA เมื่อไม่ได้เติมอนุภาคนาโนแมกนีไทท์อยู่ที่ 740.4 a.u. และเมื่อทำการคำณวนความสามารถในการจับ DNA ของอนุภาคนาโนแมกนีไทท์ชนิดนี้พบว่าอยู่ที่ 171 pmol ของนิวคลีโอไทด์ต่ออนุภาค 1 mg โดยการคำณวนแสดงดังนี้

จากการทำ calibration curve พบว่า linear equation เป็น

(Intensity; a.u.) = 2.36 x (amount of nucleotide; pmol) + 19.77

จากการคำณวนพบว่าค่าการให้สัญญาณฟลูออเรสเซนต์ของ FAM-DNA เมื่อไม่ได้เติมอนุภาคนาโนแมกนีไทท์อยู่ที่ 740.4 a.u. คิดเป็นปริมาณของนิวคลีโอไทด์ 305 pmol

เมื่อเวลาผ่านไป 100 นาทีค่าการให้สัญญาณฟลูออเรสเซนต์ของ FAM-DNA อยู่ที่ 133.2 a.u.คิดเป็นปริมาณของนิวคลีโอไทด์ 48 pmol ดังนั้น

ปริมาณของนิวคลีโอไทท์ที่ถูกอนุภาคจับ = 305 pmol – 48 pmol

= 257 pmol/ 1.5 mg ของอนุภาค

= 171 pmol/ mg ของอนุภาค

ในขณะที่เมื่อทดสอบกับอนุภาคนาโนแมกนีไทท์ที่ประกอบด้วย อัตราส่วนของ PEGMA:DEAEMA เป็น 50 : 50 พบว่าค่าการให้สัญญาณฟลูออเรสเซนต์ของ FAM-DNA เมื่อไม่ได้เติมอนุภาคนาโนแมกนีไทท์อยู่ที่ 756.8 a.u.เมื่อเติมอนุภาคนาโนแมกนีไทท์ค่าการให้สัญญาณฟลูออเรสเซนต์ของ FAM-DNA อยู่ที่ 446.3 a.u. เวลาผ่านไป 100 นาที และเมื่อทำการคำณวนความสามารถในการจับ DNA ของอนุภาคนาโนแมกนีไทท์ชนิดนี้โดยใช้วิธีเดียวกับการคำณวนข้างบนพบว่าอยู่ที่ 88 pmol ของนิวคลีโอไทด์ต่ออนุภาค 1 mg

จะเห็นได้ว่าจากการศึกษาความสามารถในการจับ DNA ของอนุภาคทั้ง 2 อัตราส่วนพบว่าอนุภาคนาโนแมกนีไทท์ที่ประกอบด้วย อัตราส่วนของ PEGMA:DEAEMA เป็น 0 : 100 สามารภดูดจับ DNA ได้ดีกว่าอนุภาคนาโนแมกนีไทท์ที่ประกอบด้วย อัตราส่วนของ PEGMA:DEAEMA เป็น 50 : 50 แต่อย่างไรก็ตามปริมาณของ DNA ที่ศึกษาได้นี้ยังคงจัดว่าเป็นปริมาณที่น้อยอยู่ ทั้งนี้อาจเนื่องมาจากความสามารถในการกระจายตัวของอนุภาคเองและความเป็นบวกที่ผิวค่อนข้างน้อย

สรุปผลการทดลอง

การดัดแปรพื้นผิวอนุภาคนาโนแมกนีไทท์ให้มีประจุเป็นบวกของ พอลิเมอร์ร่วมระหว่าง PEGMA:DEAEMA ที่มีอัตราส่วนเป็น 0 :100 และ 50:50 ด้วยปฏิกิริยา ATRP พบว่าอนุภาคที่ได้มีค่าความต่างศักย์พื้นผิวอยู่ในช่วง +22 ถึง +32 mV โดยค่าความต่างศักย์จะเป็นบวกเพิ่มขึ้นตามอัตราส่วนของ DEAEMA ที่เพิ่มขึ้น และเมื่อทำควอเทอร์ไนซ์ด้วยเมทิลไอโอไดด์เพื่อเพิ่มค่าความต่างศักย์พื้นผิวพบว่าที่พื้นผิวของอนุภาคมีความต่างศักย์เพิ่มขึ้นอีกประมาณ 8 mV นอกจากนี้อนุภาคที่ทำการควอเทอร์ไนท์แล้วยังมีความสามารถกระจายตัวในน้ำได้ดีอีกด้วยและเมื่อนำเอาอนุภาคที่ทำการควอเทอร์ไนท์แล้วมาใช้เป็นวัสดุดูดซับโดยใช้ร่วมกับ acpcPNA และเทคนิคแมสสเปกโตรเมตรีในการตรวจสอบลำดับเบสของดีเอ็นเอ โดยอาศัยหลักการ ion-exchange capture พบว่าสามารถบอกความแตกต่างของดีเอ็นเอเป้าหมายที่มีลำดับเบสต่างกันเพียงตำแหน่งเดียว และเมื่อศึกษาหาปริมาณของ PNA และ DNA ที่เหมาะสมที่ใช้ร่วมกับอนุภาคพบว่าปริมาณ PNA และ DNA ที่น้อยที่สุด ที่สามารถนำมาใช้ร่วมกับอนุภาคทั้ง 2 อัตราส่วนในการตรวจสอบลำดับของเบสของ DNA ได้คือ 70 pmol จากการศึกษาความสามารถในการจับ DNA ของอนุภาคทั้ง 2 อัตราส่วนพบว่าอนุภาคนาโนแมกนีไทท์ที่ประกอบด้วย อัตราส่วนของ PEGMA:DEAEMA เป็น 0 : 100 สามารถดูดจับดีเอ็นเอคิดเป็น171 pmole ของนิวคลีโอไทด์ ต่อ อนุภาค 1 mgในขณะที่อนุภาคนาโนแมกนีไทท์ที่ประกอบด้วย อัตราส่วนของ PEGMA:DEAEMA เป็น 50 : 50 สามารถดูดจับดีเอ็นเอคิดเป็น 88 pmole ของนิวคลีโอไทด์ ต่อ อนุภาค 1 mg

โครงการย่อย 4: อนุภาคนาโนแมกนีไทท์ที่มีการติดหมู่ฟังก์ชันบนพื้นผิวสำหรับการยึดติด PNA และ DNA (Surface-functionalized magnetite nanoparticles for immobilization of PNA and DNA)

หัวหน้าโครงการ: รศ.ดร.เมธา รัตนากรพิทักษ์

กิจกรรมที่ได้ทำเพิ่มเติมในช่วงขยายระยะเวลาโครงการ (1 สิงหาคม 2555 - 31 มกราคม 2556)

การตรวจสอบลำดับเบสของ *K-ras* DNA 2 ชนิดคือ *K-ras* (mutation) และ *K-ras* (wild-type allele) ที่มีลำดับเบสที่สอดคล้องกับลำดับเบสของ DNA จริง โดย ใช้ PNA 2 โพรบที่มีลำดับเบสที่สอดคล้องกับ *K-ras* gene เป็นโพรบในการตรวจสอบและ ใช้อนุภาคนาโนแมกนีไทท์แต่ละอัตราส่วนเป็นอนุภาคในการดูดจับ ซึ่งลำดับเบสของ PNA และ DNA ที่ใช้เป็นดังนี้

PNA (P5) = Ac-Lys-O-CTA CGC CAA CAG CT-Ser-NH_2 (m/z = 5069.459)

PNA (P6) = Ac-Lys-CTA CGC CAC CAG CT-ser NH_2 (m/z = 4900.277)

DNA (D5) = 5'-AGC TGT TGG CGT AG-3' (*K-ras* (mutation), complementary กับ P5, single base mismatch กับ P6)

DNA (D6) = 5'-AGC TGG TGG CGT AG-3' (*K-ras* (wild-type allele), complementary กับ P6 single base mismatch กับ P5)

โดยใช้ปริมาณ PNA และ DNA 70 pmole

ผลการทดลองพบว่า 15% อะซิโตไนไตรล์ในน้ำเป็นสารละลายที่เหมาะสมในการล้างอนุภาคออกจากสารละลาย PNA เพื่อกำจัด non-specificity ระหว่างอนุภาคทั้ง 2 อัตราส่วนกับสารละลาย PNA ได้ หลังจากนั้นเมื่อเติม DNA (D5) ที่มีลำดับเบสที่เป็นคู่สมกับ PNA (P5) ลงในสารละลาย PNA (P5+P6) ที่มีอนุภาคนาโนแมกนีไทท์กระจายตัวอยู่ และล้างอนุภาคแล้วทำการแยกเอาอนุภาคมาตรวจสอบด้วยเทคนิค MALDI-TOF spectrometry ผลการทดสอบพบว่าจะปรากฏเฉพาะสัญญาณของ PNA (P5) เท่านั้น ในทางกลับกันเมื่อทำการเติม DNA (D6) ลงในสารละลาย PNA (P5+P6) ที่มีอนุภาคนาโนแมกนีไทท์กระจายตัวอยู่แล้วทำการแยกเอาอนุภาคมาตรวจสอบพบว่าจะปรากฏสัญญาณของ PNA (P4) เท่านั้น

จากผลการทดลองนี้พบว่าอนุภาคนาโนแมกนีไทท์ทั้ง 2 อัตราส่วนสามารถนำมาใช้เป็นอนุภาคดูดจับ (solid support) เพื่อใช้ในการตรวจสอบลำดับเบสของดีเอ็นเอที่สอดคล้องกับลำดับเบสของ DNA จริงได้เมื่อใช้ PNA 2 โพรบเป็นโพรบในการตรวจสอบและนอกจากนี้ยังสามารถแยกความแตกต่างของลำดับเบสของดีเอ็นเอระหว่างเบสที่เป็นคู่สมกันและลำดับเบสที่มีเบสต่างกันเพียงแค่ 1 ตำแหน่งได้อย่างชัดเจน

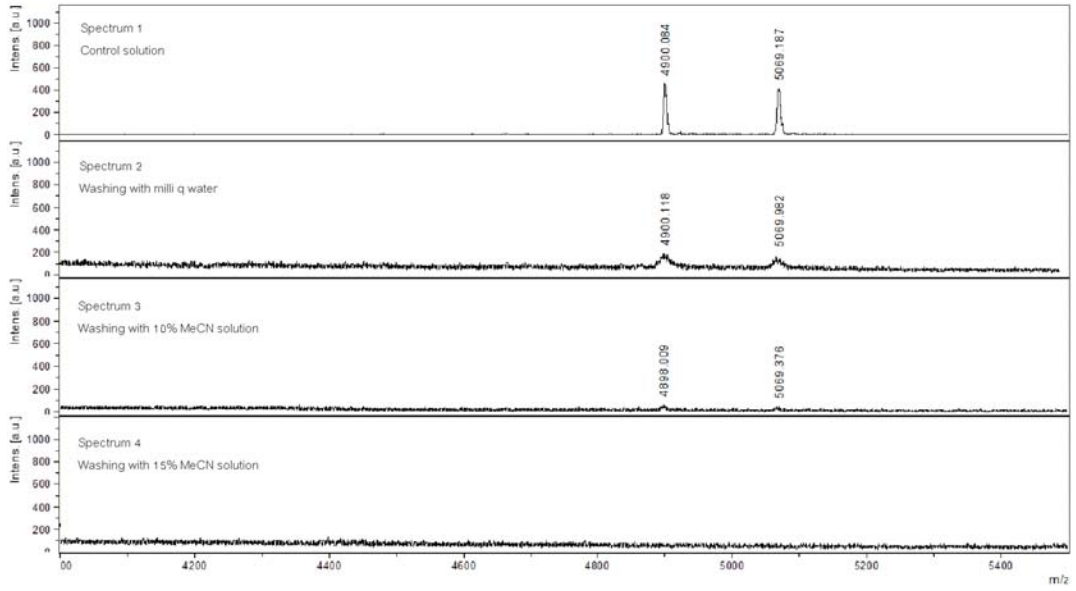

ก. อนุภาคนาโนแมกนีไทท์ (PEGMA : DEAEMA, 50:50)

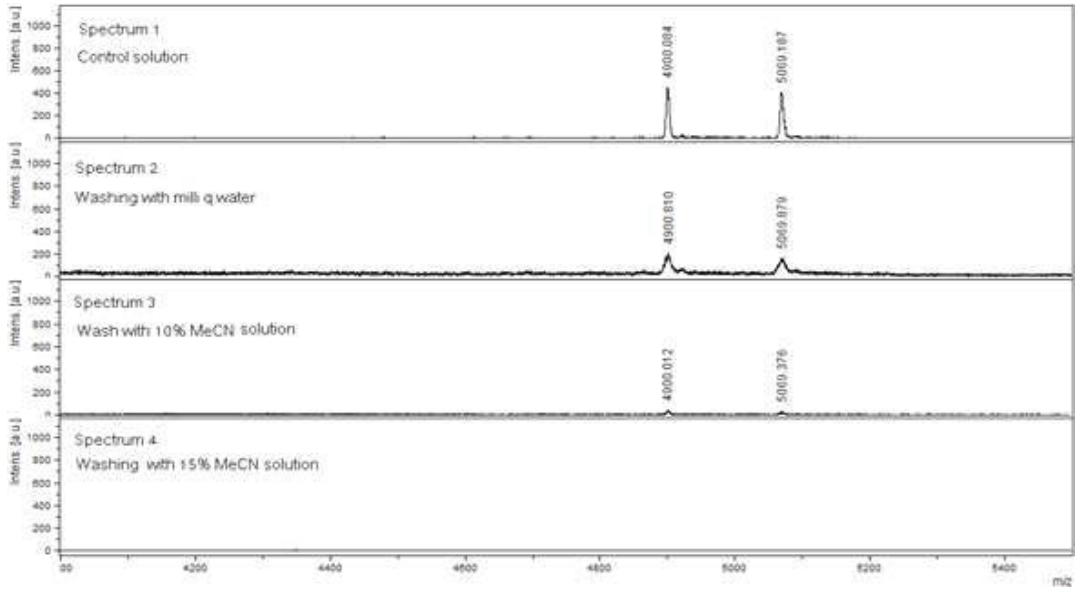

ข. อนุภาคนาโนแมกนีไทท์ (PEGMA : DEAEMA, 0:100)

รูปที่ 1.การทดสอบ non-specific และการศึกษาปริมาณของอะซิโตรไนไตล์ที่แตกต่างกันในการกำจัด non-specific ของอนุภาคนาโนแมกนีไทท์ทั้ง 2 ชนิด กับ PNA (P5) และ PNA (P6)

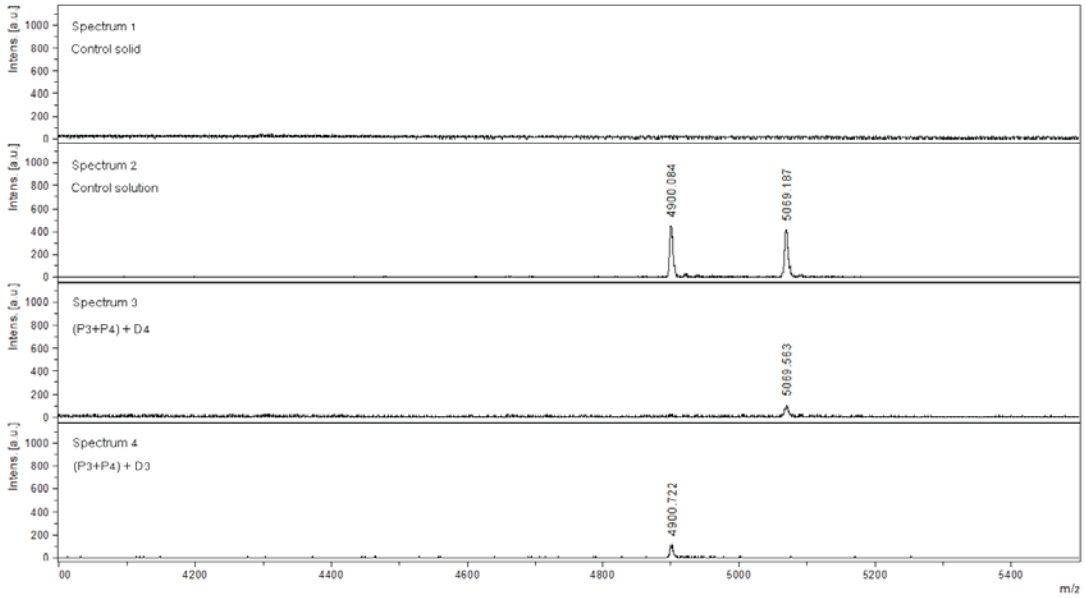

ก. อนุภาคนาโนแมกนีไทท์ (PEGMA : DEAEMA, 50:50)

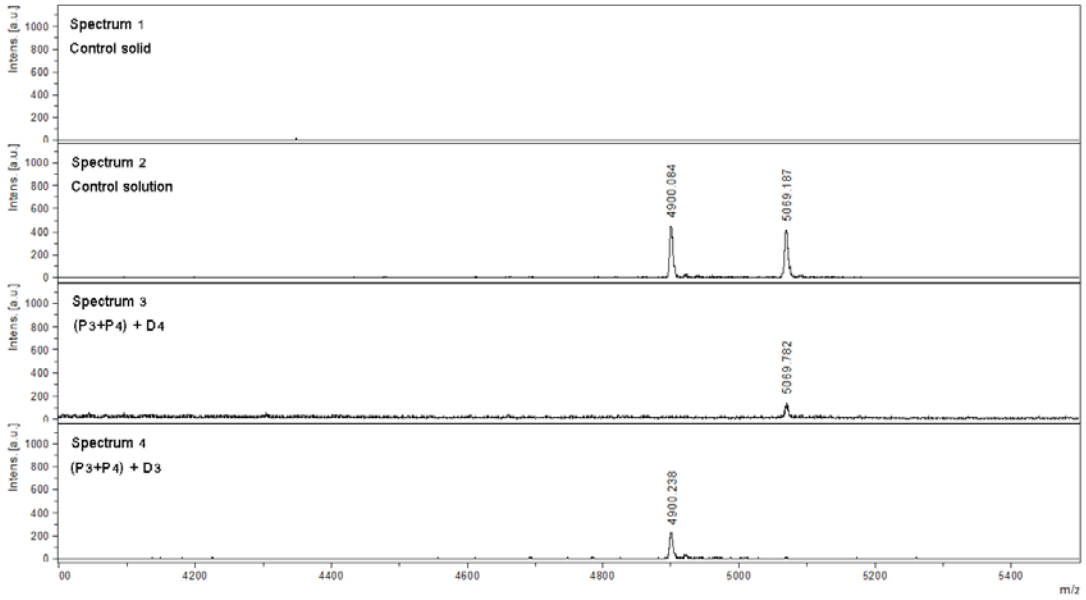

ข.อนุภาคนาโนแมกนีไทท์ (PEGMA : DEAEMA, 0:100)

รูปที่ 2. การศึกษาประสิทธิภาพของอนุภาคนาโนแมกนีไทท์ทั้ง 2 อัตราส่วน ในการใช้เป็นตัวดูดจับ (solid support) เพื่อใช้ตรวจสอบลำดับเบสของดีเอ็นเอ *K-ras* เมื่อใช้ PNA (P5) และ PNA (P6) เป็นโพรบ

รายงานความก้าวหน้าของโครงการ

โครงการ การสังเคราะห์ สมบัติ และการประยุกต์ใช้เบต้าพิโรลิดินิลเพปไทด์นิวคลีอิกแอซิดที่มีคอนฟอร์เมชันถูกจำกัด

โครงการ 5; Development of label-free electrochemical DNA biosensor based on immobilized PNA probes

หัวหน้าโครงการวิจัยย่อย

รองศาสตราจารย์ ดร.ปณต ถาวรังกูร มหาวิทยาลัยสงขลานครินทร์

ผู้ร่วมวิจัย

รองศาสตราจารย์ ดร.เพริศพิชญ์ คณาธารณา มหาวิทยาลัยสงขลานครินทร์

ดร.วรากร ลิ่มบุตร มหาวิทยาลัยสงขลานครินทร์

ดร.อาภรณ์ นุ่มน่วม มหาวิทยาลัยสงขลานครินทร์

วัตถุประสงค์ของโครงการ

1. ศึกษาการตรึง Peptide Nucleic Acid (PNA) บนผิวหน้าอิเล็กโทรด
2. พัฒนาอิเล็กโทรเคมิคัลไบโอเซนเซอร์สำหรับตรวจวัด DNA

รายงานในช่วงตั้งแต่วันที่ 1 เดือนสิงหาคม พ.ศ. 2552 ถึงวันที่ 31 เดือนกรกฎาคม พ.ศ. 2555

รายละเอียดผลการดำเนินงานของโครงการ

- *กิจกรรมที่วางแผนไว้*

แผนการดำเนินงานตลอดโครงการในแต่ละช่วง เดือน 6

กิจกรรม/ขั้นตอนการดำเนินงาน	เดือน					
	1-6	7-12	13-18	19-24	25-30	31-36
1. ศึกษาการตรึง PNA บนผิวหน้าอิเล็กโทรด	←→	←→	←→	←→		
	←- -	- -	- -	- -		
1.1 ศึกษาสภาวะที่เหมาะสมสำหรับการตรึง PNA บนอิเล็กโทรดโดยตรง และบนอิเล็กโทรดที่มีการโมดิไฟด์ด้วย SAM และ พอลิเมอร์	←→	←→	←→			
	←- -	- -	- -			
1.2 ศึกษาการทดสอบและการเปรียบเทียบประสิทธิภาพของ PNA สภาวะตรึง			←→	←→		
			←- -	- -		
2. พัฒนาระบบตรวจวัดอิเล็กโตรเคมิคัลไบโอเซนเซอร์สำหรับ DNA			←→	←→	←→	←→
			←- -	- -	- -	- -
2.1 ศึกษาสภาวะที่เหมาะสมของระบบตรวจวัดอิเล็กโตรเคมิคัลไบโอเซนเซอร์			←→	←→	←→	
			←- -	- -	- -	
2.2 ศึกษาการทดสอบประสิทธิภาพของระบบตรวจวัดอิเล็กโตรเคมิคัลไบโอเซนเซอร์					←→	←→
					←- -	- -
2.3 ศึกษาการวิเคราะห์หาปริมาณ DNA ในตัวอย่างและเปรียบเทียบผลการวิเคราะห์โดยเทคนิคมาตรฐาน						←→

←→ กิจกรรมขั้นตอนการดำเนินงานที่วางแผนไว้/

←- - → กิจกรรมขั้นตอนการดำเนินงานที่ทำแล้ว/

การดำเนินงาน

ล่าช้ากว่าแผนที่วางไว้โดยข้อที่ 2.2 อยู่ระหว่างการดำเนินการ และ 2.3 ยังไม่ได้ดำเนินการ

งานวิจัยที่ได้ดำเนินการเป็นการพัฒนาอิเล็กโทรเคมิคัลดีเอ็นเอเซนเซอร์แบบไม่ติดฉลากโดยการตรึง Peptide nucleic acid (PNA)

งานวิจัยที่ 1 ศึกษาการตรึง Peptide Nucleic Acid (PNA) บนผิวหน้าอิเล็กโทรด

งานวิจัยนี้เป็นการพัฒนาคาพาซิทีฟดีเอ็นเอเซนเซอร์แบบไม่ติดฉลาก (label-free) โดยใช้วัสดุชีวภาพ คือ Pyrrolidinyl Peptide nucleic acid ที่มีแกนเป็น D-prolyl-2-aminocyclopentanecarboxylic acid (acpcPNA) ร่วมกับอุปกรณ์ตรวจวัดทางไฟฟ้าเคมีชนิดคาพาซิทีฟ เพื่อตรวจวัดค่าความจุไฟฟ้าที่เปลี่ยนแปลงเมื่อ PNA probe จับกับ target DNA โดยปัจจัยที่สำคัญของการตรวจวัดด้วยเทคนิคคาพาซิทีฟ คือ สภาพความเป็นฉนวนของพื้นผิวอิเล็กโทรด (Berggren et al., 1999) ดังนั้น จึงจำเป็นต้องปรับผิวหน้าอิเล็กโทรดด้วยวัสดุที่ไม่นำไฟฟ้า เช่น สารประกอบ อัลเคนไธออนเพื่อเกิดเป็นชั้นเซลฟแอสเซมเบิลโมโนเลเยอร์ (self-assembled monolayer, SAM) (Limbut et al., 2006; Loyprasert et al., 2008; Samanman et al., 2011) หรือพอลิเมอร์ (Chen et al., 2001; Teeparuksapun et al., 2009; Zhou et al., 2010; Loyprasert et al., 2010) ในงานวิจัยนี้จึงประกอบด้วย 2 งานวิจัยย่อย ดังนี้

1.1 พัฒนาคาพาซิทีฟดีเอ็นเอเซนเซอร์แบบไม่ติดฉลากโดยตรึง Pyrrolidinyl acpcPNA probe ผ่านชั้น Self-assemble monolayer เพื่อศึกษาผลของความยาวและหมู่ฟังก์ชันของ blocking thiols

1.2 ศึกษาเปรียบเทียบการตรึง Pyrrolidinyl acpcPNA probe บนพอลิเมอร์ไม่นำไฟฟ้าสำหรับการวัด DNA ปริมาณน้อยด้วยเทคนิคคาพาซิทีฟแอฟฟินิตีไบโอเซนเซอร์

1.1 พัฒนาคาพาซิทีฟดีเอ็นเอเซนเซอร์แบบไม่ติดฉลากโดยตรึง Pyrrolidinyl acpcPNA probe ผ่านชั้น Self-assemble monolayer เพื่อศึกษาผลของความยาวและหมู่ฟังก์ชันของ blocking thiol

ปัจจุบันดีเอ็นเอเซนเซอร์ได้รับความสนใจและพัฒนาอย่างกว้างขวางเพื่อให้ได้ดีเอ็นเอเซนเซอร์ที่มีความไววิเคราะห์และความสามารถในการเลือกจับกับดีเอ็นเอเป้าหมายสูง ปัจจัยที่มีผลอย่างมาก คือ การตรึง probe บนตัวตรวจวัด (Lucarelli et al., 2004, 2008; Tichoniuk et al., 2008) ซึ่งการตรึงผ่านชั้น SAM เป็นวิธีหนึ่งที่น่าสนใจ สามารถทำได้ง่าย และสามารถใช้ blocking thiol เพื่อช่วยผลักให้ probe ขึ้นจากผิวอิเล็กโทรดมาอยู่ในสารละลายเพื่อเพิ่มประสิทธิภาพในการ hybridization ของ probe กับ target DNA (Herne and Tarlov, 1997) ดังนั้น จึงมีความจำเป็นอย่างยิ่งที่จะต้องศึกษาความยาวและหมู่ฟังก์ชันของ blocking thiol ที่นำมาใช้ร่วมกับ SAM ในขั้นของการตรึง probe

งานวิจัยนี้ได้ตรึง 9-mer lysine-modified acpcPNA (Ac-TTT TTT TTT-LysNH_2), PNA-T9 probe บน SAM 4 ชนิด คือ mercaptosuccinic acid (MSA) 3-mercaptopropionic acid (MPA) thioctic acid (TA) และ thiourea (TU) พร้อมทั้งศึกษาผลของความยาวและหมู่ฟังก์ชันของ blocking thiol ที่เหมาะสมสำหรับการ

ดัดแปลงผิวอิเล็กโทรดแต่ละชนิด ผลของความเข้มข้นของ PNA probe รวมทั้งศึกษาประสิทธิภาพของเซนเซอร์ ได้แก่ การนำกลับมาใช้ใหม่ได้ของอิเล็กโทรด ความสามารถในการทำซ้ำ ความสามารถในการเลือก ช่วงการตอบสนองเชิงเส้นและขีดจำกัดต่ำสุดของการตรวจวัด

งานวิจัยนี้ได้รับการตีพิมพ์จากวารสาร Biosensors and Bioelectronics

Orawan Thipmanee, Saluma Samanman, Supannee Sankoh, Apon Numnuam, Warakorn Limbut, Proespichaya Kanatharana, Tirayut Vilaivan and Panote Thavarungkul. 2012. Label-free capacitive DNA sensor using immobilized pyrrolidinyl PNA probe: Effect of the length and terminating head group of the blocking thiols. *Biosensors and Bioelectronics*. Inpress (impact factor 2011: 5.361)

1.1.1 ศึกษาการตรึง PNA-T9 บนผิวหน้าอิเล็กโทรดที่มีการโมดิฟายด์ด้วย SAM 4 ชนิด ซึ่งประกอบด้วย 3 ขั้นตอนดังนี้

ขั้นที่ 1 เตรียมชั้น SAM บนอิเล็กโทรดทอง

ขั้นที่ 2 ตรึง PNA-T9 บนชั้น SAM

ขั้นที่ 3 ปิดช่องว่าง (pinholes) ของผิวหน้าอิเล็กโทรดโดยใช้ blocking thiol

โดยทดสอบผิวอิเล็กโทรดแต่ละขั้นตอนด้วยเทคนิคไซคลิกโวลแทมเมทรี (cyclic voltammetry) ในสารละลาย 5 mM $K_3[Fe(CN)_6]$) ใน 0.1 M KCl ในช่วงศักย์ไฟฟ้า -0.30 ถึง 0.70 V เพื่อยืนยันผลการเตรียมอิเล็กโทรดแต่ละขั้นตอน (รูปที่ 1)

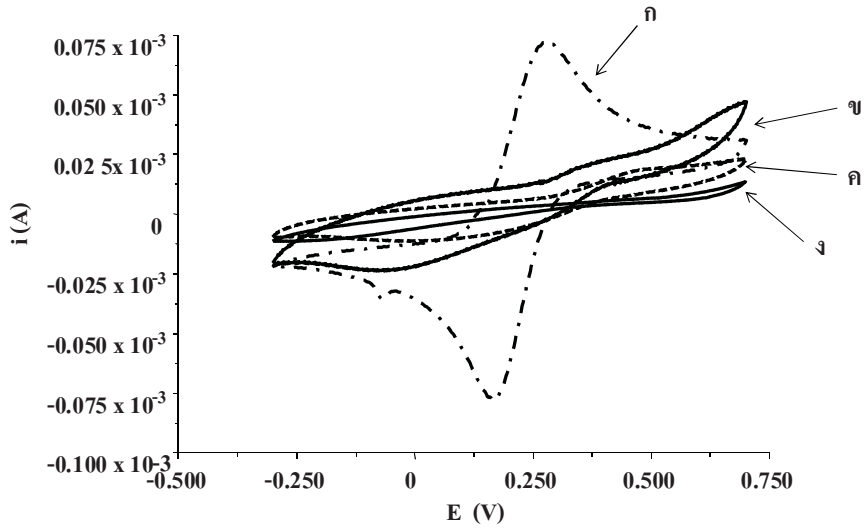

รูปที่ 1 ไซคลิกโวลแทมโมแกรมของอิเล็กโทรดทองในสารละลาย $K_3[Fe(CN)_6]$ (ก) อิเล็กโทรดทอง (ข) อิเล็กโทรดทองหลังโมดิฟายด์ด้วย SAM อิเล็กโทรดทองหลัง (ค) ตรึง PNA-T9 บนชั้น SAM และ (ง) หลังปิดช่องว่างด้วย blocking thiol

จากไซคลิกโวลแทมโมแกรม พบว่าหลังจากผิวอิเล็กโทรดถูกปกคลุมด้วยชั้น SAM PNA-T9 และ blocking thiol รีดอกซ์พีค (redox peak) ของ 5 mM $K_3[Fe(CN)_6]$ ใน 0.1 M KCl ลดลงตามลำดับ แสดงว่า PNA-T9 ถูกตรึงอยู่บนชั้น SAM แล้ว และในขั้นสุดท้ายหลังจากการบล็อกด้วย blocking thiol แล้วไม่มีรีดอกซ์พีคแสดงว่าอิเล็กโทรดที่เตรียมขึ้นมีสภาพความเป็นฉนวนเหมาะสำหรับการนำไปใช้ในระบบคาพาซิทีฟ

1.1.2. ทดสอบอิเล็กโทรดที่เตรียมได้ในระบบคาพาซิทีฟแอฟฟินิตีไบโอเซนเซอร์

คาพาซิทีฟไบโอเซนเซอร์ เป็นเทคนิคที่อาศัยหลักการวัดค่าความจุไฟฟ้า (Capacitance, C) ที่เปลี่ยนแปลงเมื่อเกิดการจับกันระหว่างวัสดุชีวภาพกับสารตัวอย่าง โดยค่าความจุไฟฟ้าจะเกิดขึ้นระหว่างผิวอิเล็กโทรดที่มีการปรับปรุงพื้นผิวให้เป็นฉนวนด้วยวัสดุที่เป็นฉนวน เมื่อวัสดุชีวภาพจับกับสารตัวอย่างจะเปรียบเสมือนมีตัวเก็บประจุมาต่อกันแบบอนุกรมทำให้ค่าความจุไฟฟ้ารวมลดลง ซึ่งค่าค่าความจุไฟฟ้าที่เปลี่ยนแปลงไปคือสัญญาณการตรวจวัด (Berggren et al., 1999)

โดยงานวิจัยนี้วัดการเปลี่ยนแปลงของค่าความจุไฟฟ้าระหว่างผิวอิเล็กโทรดกับสารละลายเมื่อมีการจับกันอย่างจำเพาะเจาะจงระหว่าง target DNA กับ PNA-T9 อิเล็กโทรดที่โมดิฟายด์แล้วสามารถใช้วิเคราะห์ซ้ำได้โดยการฉีดสารละลายทำลายพันธะ (regeneration solution, 50 mM NaOH) (Ananthanawat et al., 2009) ระหว่าง target DNA กับ PNA-T9 probe เพื่อให้ DNA หลุดออกจาก probe จากนั้นจะได้เบสไลน์อีกครั้งก็สามารถเริ่มตรวจวัดครั้งถัดไปได้ และจากช่วงความเป็นเส้นตรงของความสัมพันธ์ระหว่างค่าความจุไฟฟ้าและความเข้มข้นของ DNA พบว่าสัญญาณของค่าความจุไฟฟ้าที่วัดได้จะแปรผันตามความเข้มข้นของ DNA รูปที่ 2)

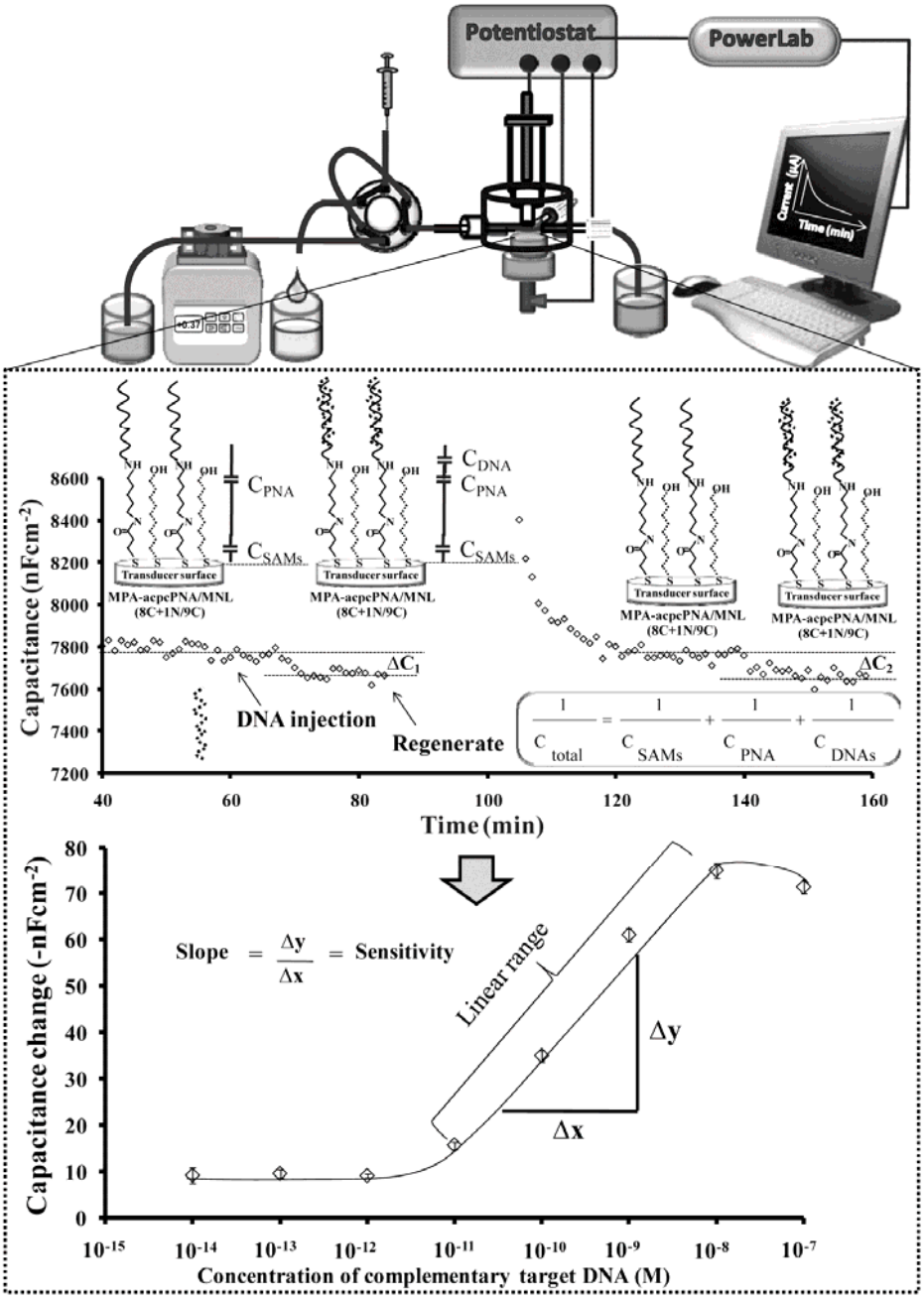

รูปที่ 2 ระบบตรวจวัด DNA ด้วยเทคนิคคาซิทีฟไบโอเซนเซอร์ร่วมกับระบบไหลผ่าน ลักษณะของสัญญาณเมื่อ probe จับกับ target DNA และกราฟความสัมพันธ์ระหว่างค่าความจุไฟฟ้าที่เปลี่ยนแปลงกับความเข้มข้นของ target DNA

1.1.3. ศึกษาผลของความยาวของ blocking thiol

ทดสอบความสามารถในการจับกันของ PNA-T9 และ target DNA ที่มีลำดับเบสที่เป็นคู่สมของอิเล็กโทรดที่ตรึง PNA-T9 บน SAM ของ 3-mercaptopropionic acid (3-MPA) mercaptosuccinic acid (MSA) thioctic acid (TA) และ thiourea (TU) โดยใช้ blocking thiol ที่มีความยาวและหมู่ฟังก์ชันต่างกัน 6 ชนิด คือ mercaptopropanol (3-MPL) mercaptohexanol (6-MHL) mercaptooctanol (8-MOL) mercaptononanol (9-MNL) 11-mercaptoundecanol (11-MUL) และ 1-dodecanethiol (DDT) โดยพิจารณาจากค่าความไววิเคราะห์ของค่าความจุไฟฟ้าที่เปลี่ยนแปลงไป พบว่าถ้า blocking thiol มีความยาวเท่ากับ spacer ของอัลเคนไธออลรวมกับ lysine (รูปที่ 3) จะให้ค่าความไววิเคราะห์สูงสุด ดังรูปที่ 4 และตารางที่ 1 เนื่องจาก blocking thiol ที่มีความยาวเท่ากับ spacer จะช่วยให้ PNA probe อยู่ในตำแหน่งที่เหมาะแก่การ hybridization กับ target DNA ส่วนกรณีที่ blocking thiol มีความยาวน้อยกว่า spacer ของ probe จะทำให้หมู่ปลาย (–OH group) ของตัวบล็อกอยู่ไกลจาก PNA probe จึงไม่ช่วยให้ PNA probe อยู่ในตำแหน่งที่เหมาะสมกับการ hybridization กับ target DNA และกรณีที่ blocking thiol มีความยาวมากกว่า spacer ของ PNA probe จะได้ความไววิเคราะห์ต่ำ เนื่องจากมีบางส่วนของ blocking thiol ไปซ้อนทับกับ PNA probe ทำให้ยากแก่การ hybridization กับ target DNA (Wong et al., 2005)

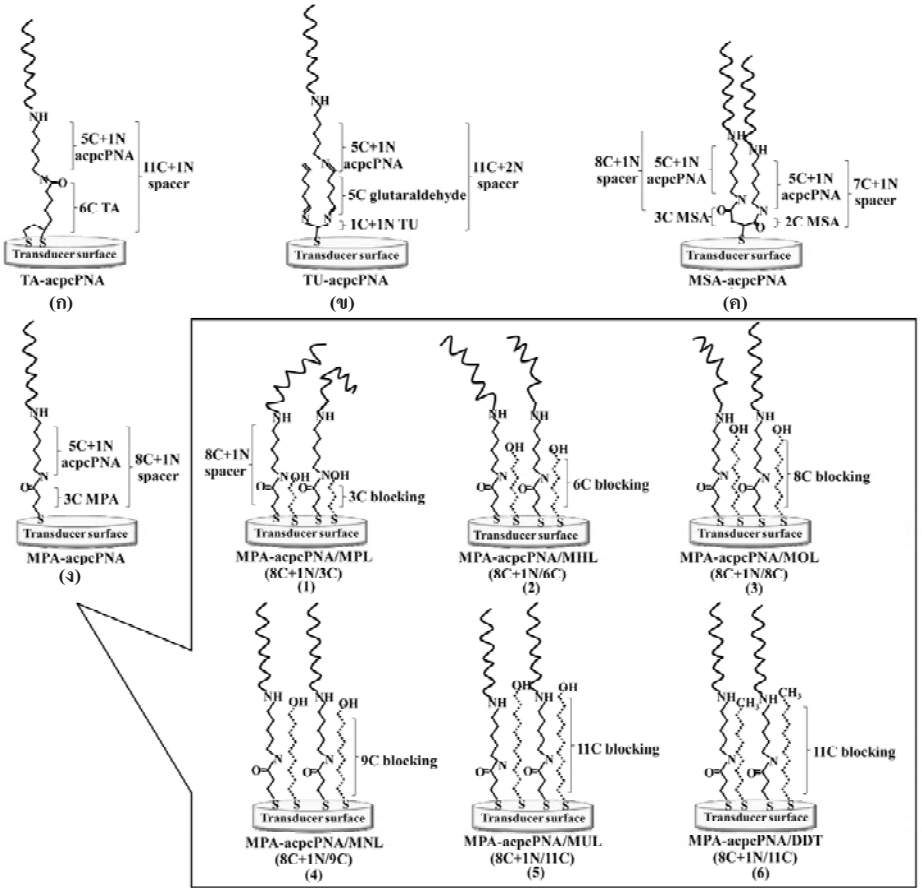

รูปที่ 3 แสดง spacer รวมของ PNA-T9 ที่โมดิฟายด์บน SAM 4 ชนิด (ก) TA (ข) TU (ค) MSA และ (ง) MPA และรูปขยายของ MPA ที่โมดิฟายด์บนผิวอิเล็กโทรดทอง (spacer รวมเท่ากับ 8C + 1N) กับ blocking thiols ที่ยาวต่างกัน (ง1) 3-MPL(3C) (ง2) 6-MHL(6C) (ง3) 8-MOL(8C) (ง4) 9-MNL (9C) (ง5) 11-MUL(11C) ที่มีหมู่ฟังก์ชัน –OH group และ (ง6) 1-DDT(11C) ที่มีหมู่ฟังก์ชัน $–CH_3$ group

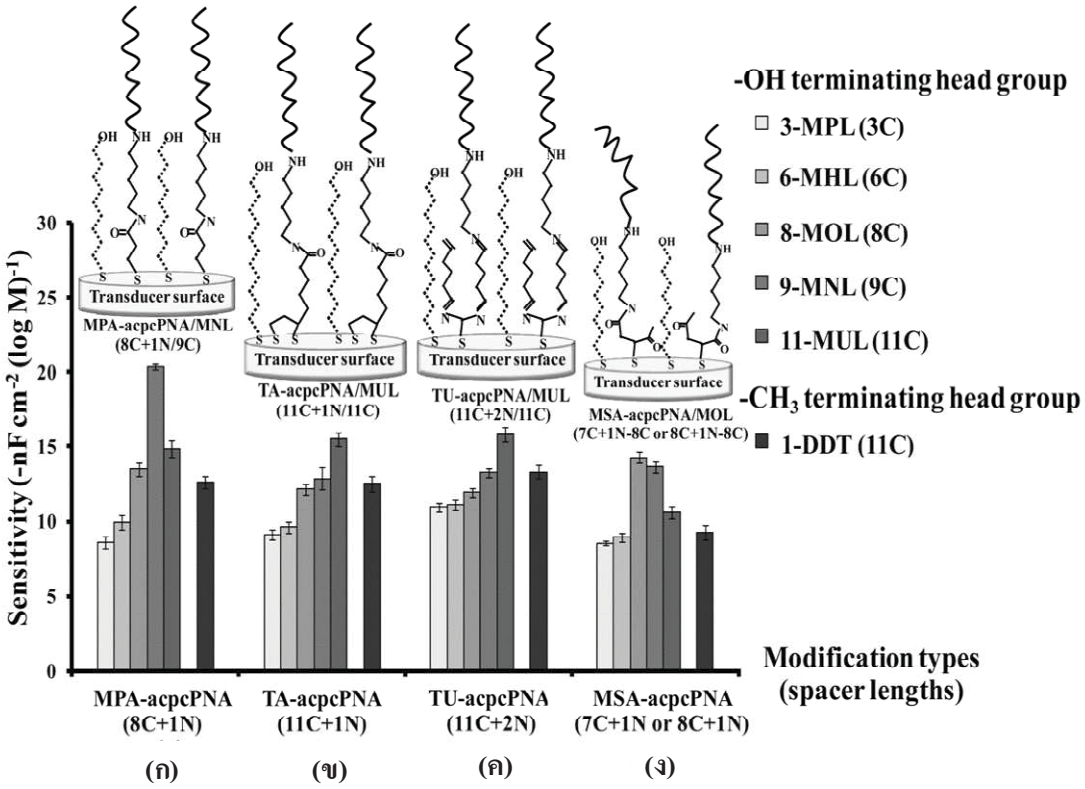

รูปที่4 ผลของความยาวและหมู่ฟังก์ชันของ blocking thiol ต่อค่าความไววิเคราะห์ของดีเอ็นเอเซนเซอร์ที่โมดิฟายด์ PNA-T9 บน SAM 4 ชนิด (ก) MPA (ข) TA (ค) TU และ (ง) MSA

ตารางที่ 1 เปรียบเทียบค่าความไววิเคราะห์ของอิเล็กโทรดทองที่โมดิฟายด์ผิวหน้าด้วย SAM ชนิดต่างๆ กับ blocking thiol ที่เหมาะสม

ชนิดของ SAM	Spacer รวม	ชนิดของ blocking thiol ที่เหมาะสม	ค่าความไววิเคราะห์ ($-nFcm^{-2}(\log M^{-1})$)
3-MPA	8C + 1N	9-MNL	20.4 ± 0.7
MSA	8C + 1N หรือ 7C + 1N	8-MOL หรือ 9-MNL	14.3 ± 0.5 และ 13.6 ± 0.3
TA	11C + 1N	11-MUL	15.5 ± 0.5
TU	11C + 2N	11-MUL	15.8 ± 0.4

1.1.4. ศึกษาผลของหมู่ฟังก์ชันของ blocking thiol

ทดสอบผลของหมู่ฟังก์ชันของ blocking thiol 2 ชนิด ที่มีความยาวเท่ากัน คือ 11-MUL ที่มีหมู่ –OH group และ 1-DDT ที่มีหมู่ $–CH_3$ group พบว่าการบล็อกด้วย blocking thiol ที่มี –OH group ซึ่งมีอิเล็กตรอนคู่โดดเดี่ยวจะให้ความไววิเคราะห์สูงกว่า blocking thiol ที่มี $–CH_3$ group (รูปที่ 4) เพราะ –OH group มีความชอบน้ำมากกว่า $–CH_3$ group (Dharuman and Hahn, 2007) ทำให้ target DNA เข้าใกล้ probe ได้มากกว่า (Gillmor et al., 2000) จึงทำให้เกิดการไฮบริไดเซชันได้มากกว่า แต่อย่างไรก็ตามผลของหมู่ฟังก์ชันมีผลต่อการไฮบริไดเซชันน้อยกว่าผลของความยาวของ blocking thiol

1.1.5. ศึกษาผลของความเข้มข้นของ probe

ความเข้มข้นของ probe มีผลต่อประสิทธิภาพของการไฮบริไดเซชัน (Keighley et al., 2008; Liu et al., 2005) จากการศึกษาเบื้องต้นพบว่าเมื่อใช้ความเข้มข้นของ probe 3.0 μM จะให้ความไววิเคราะห์น้อย เนื่องจากมีปริมาณของ probe จำนวนน้อยที่จะเกิดไฮบริไดเซชันกับ target DNA ได้ แต่เมื่อเพิ่มความเข้มข้นของ probe เป็น 5.0 และ 7.0 μM จะได้ค่าความไววิเคราะห์เพิ่มขึ้นแต่ไม่ต่างกันมากนัก (รูปที่ 5) เนื่องจากที่ความเข้มข้นของ probe 5.0 μM ก็เพียงพอสำหรับพื้นผิวอิเล็กโทรดแล้ว ดังนั้นจึงเลือกความเข้มข้นของ probe เท่ากับ 5.0 μM เพื่อใช้ในสภาวะตรึง

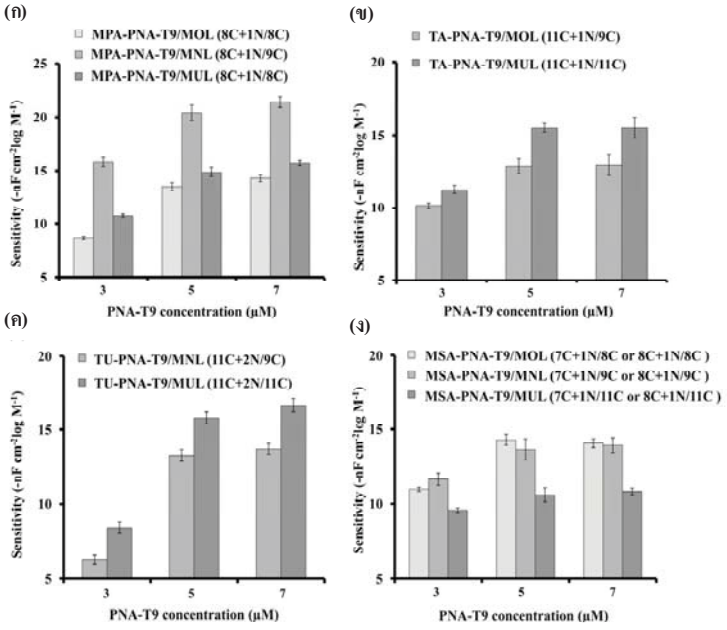

รูปที่ 5 ผลของความเข้มข้นของ probe ต่อค่าความไววิเคราะห์ของเซนเซอร์ เมื่อตรึง PNA-T9 บน SAM ชนิดต่างๆ (ก) MPA (ข) TA (ค) TU และ (ง) MSA ที่บล็อกด้วย blocking thiol ชนิด 8-MOL 9-MNL และ 11-MUL ที่มีความยาวต่างกัน

1.1.6. ศึกษาการนำกลับมาใช้ใหม่ได้ของอิเล็กโทรด (Reuseability)

การทดสอบการนำกลับมาใช้ใหม่ได้ของ PNA-T9 ที่ตรึงบน SAM 4 ชนิด ด้วยระบบคาพาซิทีฟแอฟฟินิตีไบโอเซนเซอร์ทำได้โดยหลังการวิเคราะห์แต่ละครั้งจะฉีดสารละลายทำลายพันธะเข้าสู่ระบบ เพื่อทำลายพันธะไฮโดรเจนระหว่าง probe กับ DNA target และ probe พร้อมที่จะจับกับ DNA ในการวิเคราะห์ครั้งถัดไป พบว่าจำนวนการนำกลับมาใช้ได้ใหม่อยู่ในช่วงตั้งแต่ 58 - 73 ครั้งต่อการเตรียมอิเล็กโทรดหนึ่งครั้ง (ตารางที่ 2) แสดงว่า PNA probe สภาวะตรึงนี้สามารถนำกลับมาใช้ใหม่ได้ เนื่องจาก PNA เป็น DNA สังเคราะห์ที่มีคุณสมบัติทนต่อสารเคมีและความร้อน

1.1.7. ศึกษาความสามารถในการทำซ้ำ (Reproducibility)

ทดสอบความสามารถในการทำซ้ำของ PNA-T9 ที่ตรึงบน SAM ชนิด MPA TU และ TA ชนิดละ 2 อิเล็กโทรด ซึ่งเตรียมในเวลาต่างกัน โดยเปรียบเทียบจากค่าความไววิเคราะห์ พบว่า probe ที่ตรึงบน MPA มีค่าความไววิเคราะห์เท่ากับ 20.4 ± 0.7 20.6 ± 0.5 -nFcm^{-2}(log M)$^{-1}$ probe ที่ตรึงบน TU มีค่าความไววิเคราะห์เท่ากับ 15.8 ± 0.4 16.3 ± 0.5 -nFcm^{-2}(log M)$^{-1}$ และ probe ที่ตรึงบน TA มีค่าความไววิเคราะห์เท่ากับ 13.3 ± 0.5 13.5 ± 0.4 -nFcm^{-2}(log M)$^{-1}$ พบว่าค่าความไววิเคราะห์มีค่าไม่แตกต่างกันระหว่างการเตรียมแต่ละครั้ง แสดงว่าอิเล็กโทรดที่สภาวะตรึงมีความสามารถในการทำซ้ำได้

1.1.8. ศึกษาความสามารถในการเลือก (Selectivity)

ทดสอบความสามารถในการเลือกของอิเล็กโทรดที่ตรึง PNA-T9 และ PNA-M12 บน SAM ชนิด MPA กับ DNA ที่มีลำดับเบสที่เป็นคู่สม DNA ที่มีลำดับเบสที่ไม่เป็นคู่สมจำนวนหนึ่งตำแหน่ง DNA ที่มีลำดับเบสที่ไม่เป็นคู่สมจำนวนสองตำแหน่ง และ DNA ที่มีลำดับเบสที่ไม่เป็นคู่สมมากกว่าสองตำแหน่ง ที่ความเข้มข้นเท่ากับ 1.0×10^{-8} M โดยมีลำดับเบสดังนี้

สำหรับ PNA-T9 probe

DNA ที่มีลำดับเบสที่เป็นคู่สม

D6comp:5'-AAAAAA-3'

D9comp:5'-AAAAAAAAA-3'

D12comp:5'-AAAAAAAAAAAA-3'

D15comp:5'-AAAAAAAAAAAAAAA-3'

D27comp:5'-AAAAAAAAAAAAAAAAAAAAAAAAAAA-3'

D27compM18a:5'-*TTTTTTTTT*AAAAAAAAA*TTTTTTTTT*-3'

D27compM18b:5'-*TGCTCAGCT*AAAAAAAAA*TGCTCAGCT*-3'

DNA ที่มีลำดับเบสที่ไม่เป็นคู่สมจำนวนหนึ่งตำแหน่ง

D9M1G:5'-AAAA*G*AAAA-3'

D9M1C:5'-AAAA*C*AAAA-3'

D9M1T:5'-AAAA*T*AAAA-3'

DNA ที่มีลำดับเบสที่ไม่เป็นคู่สมจำนวนสองตำแหน่ง

D9M2G:5'-AAA*G*AGAAA-3'

D9M2C:5'-AAA*C*ACAAA-3'

D9M2T:5'-AAA*T*A*T*AAA-3'

DNA ที่มีลำดับเบสที่ไม่เป็นคู่สมมากกว่าสองตำแหน่ง

D9non-compa:5'-*TTTTTTTTT*-3'

D9non-compb:5'-*TATTATTAT*-3'

สำหรับ PNA-M12 probe

DNA ที่มีลำดับเบสที่เป็นคู่สม

D9comp:5'-CAGTTGACA-3'

D12comp:5'-AGTCAGTTGACA-3'

D15compM3:5'-*GCT*AGTCAGTTGACA-3'

D30compM18:5'-*GACTGCACC*AGTCAGTTGACA*TGTTGCGAC*-3'

DNA ที่มีลำดับเบสที่ไม่เป็นคู่สมจำนวนหนึ่งตำแหน่ง

D12M1T:5'-AGTCA*T*TTGACA-3'

D12M1C:5'-AGTCA*C*TTGACA-3'

D12M1A:5'-AGTCA*A*TTGACA-3'

DNA ที่มีลำดับเบสที่ไม่เป็นคู่สมจำนวนสองตำแหน่ง

D12M2T:5'-AGT*T*A*T*TTGACA-3'

D12M2CG:5'-AGT*G*A*C*TTGACA-3'

D12M2A:5'-AGT*A*A*A*TTGACA-3'

DNA ที่มีลำดับเบสที่ไม่เป็นคู่สมมากกว่าสองตำแหน่ง

D12non-comp:5’-*TCAGTCAACTGT*-3’

จากงานวิจัยพบว่า DNA ที่มีลำดับเบสที่เป็นคู่สมให้สัญญาณการเปลี่ยนแปลงของค่าความจุไฟฟ้าสูงกว่า DNA ที่มีลำดับเบสที่ไม่เป็นคู่สมจำนวนหนึ่งและสองตำแหน่ง โดยพิจารณาจากค่า % signal suppression (%SS) ซึ่งเป็นค่าที่บ่งบอกว่าสัญญาณการ hybridization ของ PNA probe กับ DNA ที่มีลำดับเบสที่ไม่เป็นคู่สมมีความแตกต่างจากสัญญาณการ hybridization ของ PNA probe กับ DNA ที่มีลำดับเบสที่เป็นคู่สมมากน้อยเพียงใด ดังสมการที่ 1

$$\%SS = \frac{\Delta C_{complementary\ DNA} - \Delta C_{mismatched\ DNA}}{\Delta C_{complementary\ DNA}} \times 100 \qquad (1)$$

ถ้า %SS มีค่ามากแสดงว่า PNA probe มีความสามารถในการเลือกสูง โดย %SS ของ DNA ที่มีลำดับเบสที่ไม่เป็นคู่สมจำนวนหนึ่งตำแหน่ง ในกรณีที่ใช้ blocking thiol ที่มีความยาวเท่ากับ spacer (9C) มีค่าสูงที่สุดอยู่ในช่วงตั้งแต่ 76-79% ในกรณีที่มีความยาวสั้นกว่า (8C) จะอยู่ในช่วงตั้งแต่ 70-74% และกรณีที่ blocking thiol มีความยาวมากกว่า spacer (11C) มีค่าจะอยู่ในช่วง 68-69% และพบว่า %SS ของ DNA ที่มีลำดับเบสที่ไม่เป็นคู่สมสองตำแหน่ง มีค่ามากกว่า DNA ที่มีลำดับเบสที่ไม่เป็นคู่สมหนึ่งตำแหน่ง ส่วน DNA ที่มีลำดับเบสที่ไม่เป็นคู่สมมากกว่าสองตำแหน่งจะให้ %SS สูงสุด (99-100%) ดังรูปที่ 6 แสดงว่าเซนเซอร์ที่พัฒนาขึ้นมีความสามารถในการเลือก

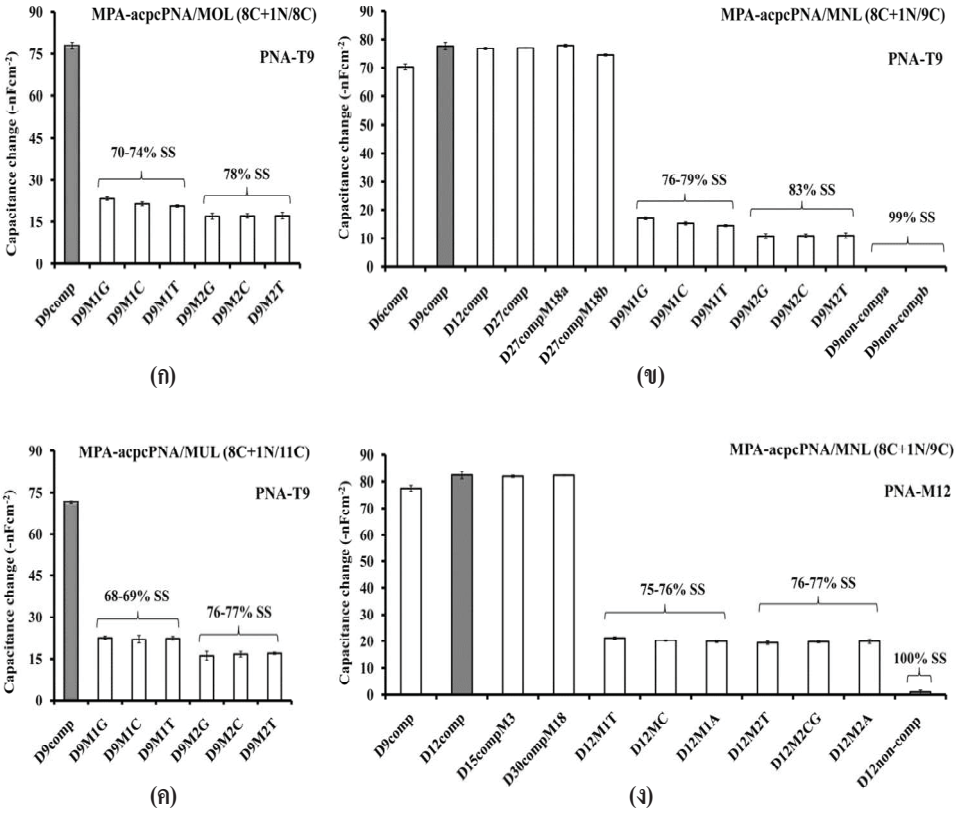

รูปที่ 6 สัญญาณการเปลี่ยนแปลงค่าความจุไฟฟ้า เมื่อฉีด DNA ที่มีลำดับเบสที่เป็นคู่สม DNA ที่มีลำดับเบสที่ไม่เป็นคู่สมจำนวนหนึ่งตำแหน่ง DNA ที่มีลำดับเบสที่ไม่เป็นคู่สมจำนวนสองตำแหน่งและ DNA ที่มีลำดับเบสที่ไม่เป็นคู่สมมากกว่าสองตำแหน่ง ที่ความเข้มข้น 1.0×10^{-8} M เข้าสู่ระบบที่มี acpcPNA probe (PNA-T9 และ PNA-M12) ตรึงอยู่บนชั้นของ MPA (8C+1N spacer) และบล็อกด้วย blocking thiol ที่มีความยาวต่างกัน (ก) 8-MOL(8C) (ข) และ (ง) 9-MNL(9C) และ (ค) 11-MUL (11C) โดยพิจารณาความสามารถในการเลือกจากค่า %SS

1.1.9. ศึกษาช่วงความเป็นเส้นตรงและขีดจำกัดต่ำสุดในการตรวจวัด (Linear range and detection limit)

ศึกษาช่วงความเป็นเส้นตรงและขีดจำกัดต่ำสุดในการตรวจวัดของ DNA sensor ที่พัฒนาขึ้นของอิเล็กโทรดทองที่ตรึง PNA-T9 (5.0 μM) ผ่านชั้น SAM ชนิดต่างๆ และบล็อกด้วย blocking thiol ที่เหมาะสม คือ MPA บล็อกด้วย MNL TA บล็อกด้วย MUL TU บล็อกด้วย MUL และ MSA บล็อกด้วย MOL โดยศึกษาสัญญาณการเปลี่ยนแปลงของค่าความจุไฟฟ้าเมื่อฉีด target DNA ที่มีความเข้มข้นตั้งแต่ 1.0×10^{-14} ถึง 1.0×10^{-7} M พบว่าช่วงความเป็นเส้นตรงอยู่ในช่วง 1.0×10^{-11} ถึง 1.0×10^{-8} M และมีขีดจำกัดต่ำสุดในการตรวจวัดอยู่ในช่วง 6-10 pM ดังตารางที่ 2 แสดงให้เห็นว่าเทคนิคที่พัฒนาขึ้นมีขีดจำกัดต่ำสุดในการตรวจวัด

ต่ำกว่าวิธีอื่น เช่น QCM (5μM) SPR (2 μM) นั่นคือเทคนิคคาพาซิทีฟดีเอ็นเอเซนเซอร์จึงเป็นอีกทางเลือกหนึ่งในการตรวจวัดดีเอ็นเอปริมาณน้อยมาก

ตารางที่ 2 ประสิทธิภาพของคาพาซิทีฟดีเอ็นเอเซนเซอร์แบบไม่ติดฉลาก โดยตรึง PNA-T9 probe เมื่อใช้ blocking thiol ที่มีความยาวเท่ากับ spacer

Performances	Type of SAM/ blocking thiol			
	MPA/ 9-MNL	**TA/ 11-MUL**	**TU/ 11-MUL**	**MSA/ 8-MOL**
Linear range (M)	1.0×10^{-11}–1.0×10^{-8}	1.0×10^{-11}–1.0×10^{-8}	1.0×10^{-11}–1.0×10^{-8}	1.0×10^{-11}–1.0×10^{-8}
Correlation coefficient -r	0.9984	0.9977	0.9960	0.9934
Sensitivities ($-nF\ cm^{-2}\ (logM)^{-1}$)	20.6±0.5	16.3±0.5	14.3±0.5	14.3±0.5
Limit of detection (pM)	6	8	10	8
Reusability				
- Number of cycle	70	69	73	58
- Average residual activity (%)	98.9±1.3	98.9±1.3	99.6±1.3	98.0±1.4
- % RSD	1.3	1.3	1.3	1.4

สรุป

งานวิจัยนี้เป็นการพัฒนาคาพาซิทีฟดีเอ็นเอเซนเซอร์แบบไม่ติดฉลากโดยตรึง Pyrrolidinyl acpcPNA probe (PNA-T9) ผ่านชั้น SAM 4 ชนิด โดยศึกษาผลของความยาวและหมู่ฟังก์ชันของ blocking thiol พบว่า blocking thiol ที่มีความยาวเท่ากับ spacer ของอัลเคนไธออลรวมกับ lysine และมีหมู่ฟังก์ชันเป็น -OH จะให้ความไววิเคราะห์สูงที่สุด เนื่องจาก blocking thiol ช่วยให้ probe อยู่ในตำแหน่งที่เหมาะสมต่อการ hybridization นอกจากนี้เซนเซอร์ที่พัฒนาขึ้นนี้ยังมีความสามารถในการเลือกสูง มีช่วงการตอบสนองเชิงเส้นที่กว้าง (1.0×10^{-11} ถึง 1.0×10^{-8} M) และขีดจำกัดการตรวจวัดต่ำถึงระดับพิโคโมลาร์ (pM)

1.2 ศึกษาเปรียบเทียบการตรึง Pyrrolidinyl PNA probe บนพอลิเมอร์ไม่นำไฟฟ้าสำหรับการวัด DNA ปริมาณน้อยด้วยเทคนิคคาพาซิทีฟแอฟฟินิตีไบโอเซนเซอร์

การโมดิฟายด์พื้นผิวอิเล็กโทรดด้วย SAM เพื่อเพิ่มสภาพความเป็นฉนวนในเทคนิคคาพาซิทีฟแอฟฟินิตีไบโอเซนเซอร์มีข้อด้อย คือ ใช้เวลานานในการเกิดชั้น SAM (12-24 ชั่วโมง) และพื้นผิวอิเล็กโทรดทองต้องเรียบเพื่อให้เกิดชั้น SAM (Loyprasert et al., 2010; Teeparuksapun et al., 2009) งานวิจัยนี้จึงใช้พอลิเมอร์ชนิดไม่นำไฟฟ้าสำหรับโมดิฟายด์ผิวอิเล็กโทรดสำหรับตรึง probe เนื่องจากใช้เวลาน้อย (8 นาที) ดังนั้นจึงได้ศึกษาเปรียบเทียบประสิทธิภาพและพัฒนาคาพาซิทีฟดีเอ็นเอเซนเซอร์โดยการโมดิฟายด์พื้นผิวอิเล็กโทรดด้วยพอลิเมอร์ไม่นำไฟฟ้า 3 ชนิด ได้แก่ poly-*o*-phenylenediamine (P*o*PD) (Cheng et al.,2001; Teeparuksapun et al., 2009) poly-*p*-phenylenediamine (P*p*PD) (Zhou et al., 2010) และ polytyramine (Pty) (Loyprasert et al., 2010)

งานวิจัยนี้ได้ศึกษาการตรึง PNA probe (PNA-T9) บนพอลิเมอร์ชนิด P*o*PD P*p*PD และ Pty การเกิดฟิล์มบางพอลิเมอร์ชนิดไม่นำไฟฟ้า การตรึง PNA-T9 บนพอลิเมอร์ทั้ง 3 ชนิด และปัจจัยที่เหมาะสมในการเกิด electropolymerization จากนั้นจึงศึกษาพื้นผิวอิเล็กโทรดทองที่โมดิฟายด์ด้วยฟิล์มบางพอลิเมอร์ ผลของความเข้มข้นของ PNA probe ปริมาณการตรึงติดของ probe และได้ศึกษาเปรียบเทียบช่วงการตอบสนองเชิงเส้นและขีดจำกัดต่ำสุดของการตรวจวัด การนำกลับมาใช้ใหม่ได้ของอิเล็กโทรด ความสามารถในการทำซ้ำ ความสามารถในการเลือก และผลของความยาวของ target DNA

1.2.1. ศึกษาการเกิดฟิล์มบางพอลิเมอร์ชนิดไม่นำไฟฟ้า

การศึกษาเปรียบเทียบไซคลิกโวลแทมโมแกรมของการโมดิฟายด์ผิวอิเล็กโทรดทองด้วยฟิล์มบางของพอลิเมอร์ 3 ชนิด คือ P*o*PD P*p*PD และ Pty ที่เป็นพอลิเมอร์ชนิดไม่นำไฟฟ้า โดยใช้เทคนิค electropolymerization ในการเกิดฟิล์มบางในช่วงค่าศักย์ไฟฟ้า 0.0 – 0.8 V จากรูปที่ 7(ก ข และ ค) แสดงถึงรีดอกซ์พีคของพอลิเมอร์แต่ละชนิดที่ลดลงเมื่อจำนวนสแกนเพิ่มขึ้นเนื่องจากสภาพความเป็นฉนวนเพิ่มขึ้น และเมื่อเปรียบเทียบสภาพความเป็นฉนวนของฟิล์มพิลิเมอร์ทั้ง 3 ชนิด พบว่า ไซคลิกโวลแทมโมแกรมของ Pty มีค่ากระแสไฟฟ้าต่ำสุด ตามด้วย P*p*PD และ P*o*PD (รูปที่ 7(ง)) แสดงว่าฟิล์มของ Pty P*p*PD และ P*o*PD มีความเป็นฉนวนเหมาะกับการประยุกต์ใช้ในระบบคาพาซิทีฟ

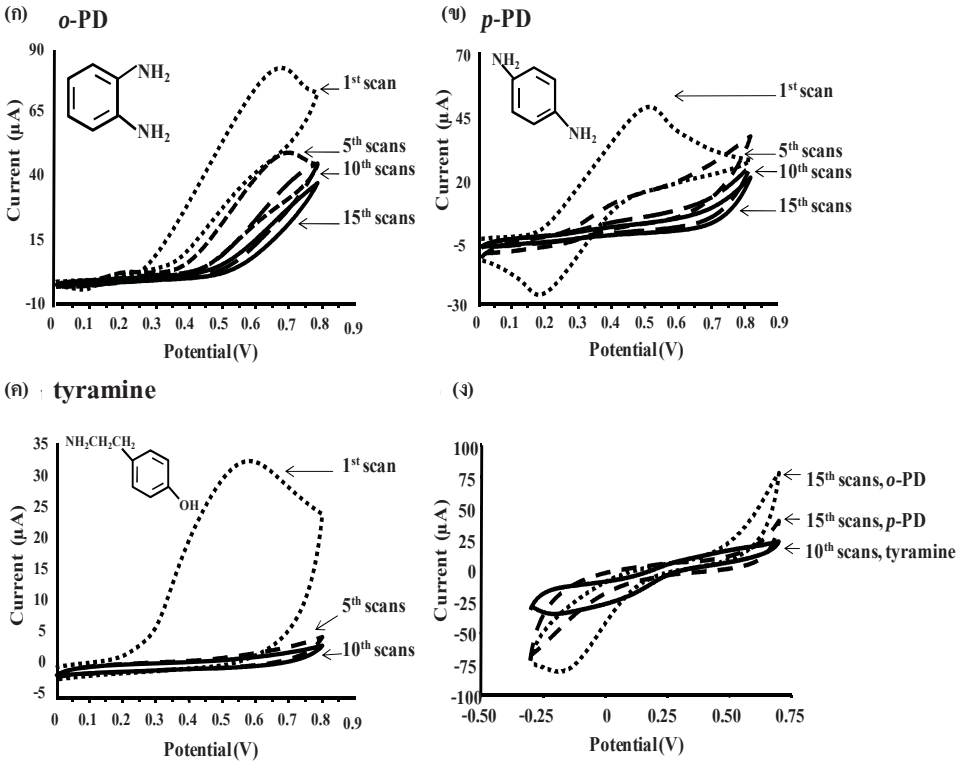

รูปที่ 7 ไซคลิกโวลแทมโมแกรมของการ electropolymerization ของมอนอเมอร์ 3 ชนิด คือ (ก) *o*-PD (ข) *p*-PD (ค) tyramine และ (ง) เปรียบเทียบไซคลิกโวลแทมโมแกรมของแต่ละพอลิเมอร์ใน สารละลาย 5 mM $K_3[Fe(CN)_6]$ ใน 0.1 M KCl

1.2.2. ศึกษาการตรึง PNA-T9 บนผิวหน้าอิเล็กโทรดโมดิฟายด์ด้วยพอลิเมอร์ 3 ชนิด

ประกอบด้วย 3 ขั้นตอนดังนี้

ขั้นที่ 1 เตรียมชั้นพอลิเมอร์บนอิเล็กโทรดทอง

ขั้นที่ 2 แอคติเวตพื้นผิวของชั้นพอลิเมอร์ให้มีหมู่ฟังก์ชันเหมาะต่อการตรึง PNA-T9

ขั้นที่ 3 ตรึง PNA-T9 บนชั้นพอลิเมอร์

ขั้นที่ 4 ปิดช่องว่างของผิวหน้าอิเล็กโทรดโดยใช้ blocking thiol

ทดสอบผิวอิเล็กโทรดแต่ละขั้นตอนของการตรึงด้วยเทคนิคไซคลิกโวลแทมเมทรี (รูปที่ 8) ใน สารละลาย 5 mM $K_3[Fe(CN)_6]$ ใน 0.1 M KCl เพื่อยืนยันผลการเตรียมอิเล็กโทรดแต่ละขั้นตอน

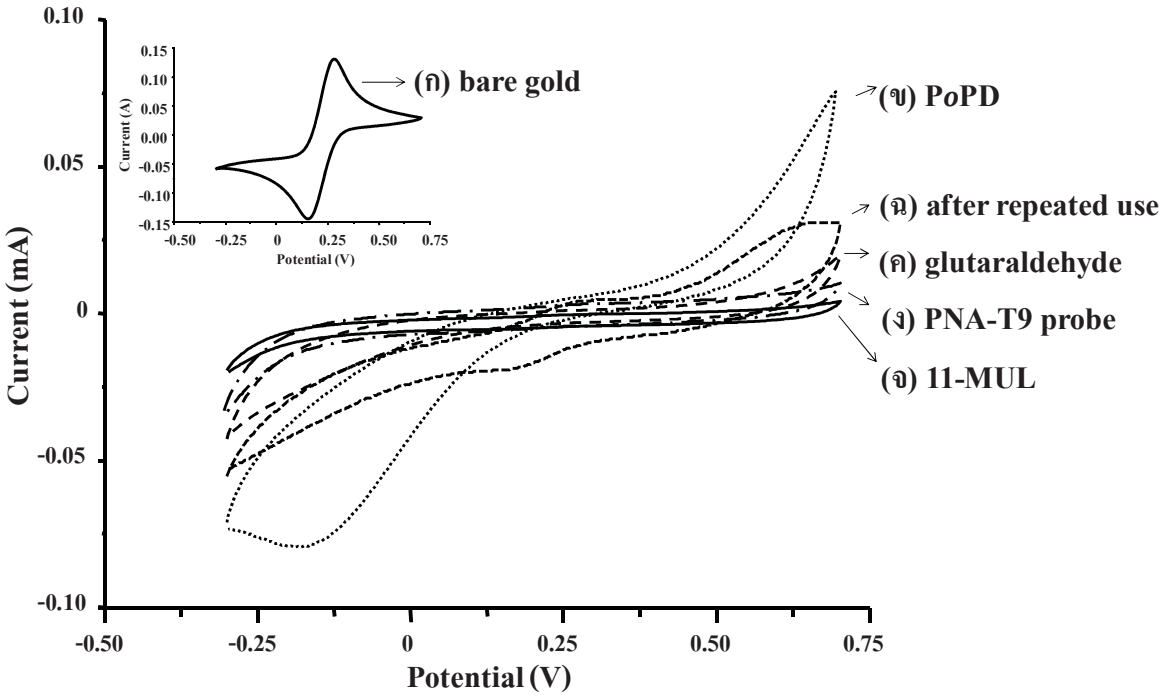

รูปที่ 8 ไซคลิกโวลแทมโมแกรมของอิเล็กโทรดทองในสารละลาย 5 mM $K_3[Fe(CN)_6]$ ใน 0.1 M KCl (ก) อิเล็กโทรดทอง (ข) อิเล็กโทรดทองหลังโมดิฟายด์ด้วยพอลิเมอร์ อิเล็กโทรดทองหลัง (ค) แอคติเวตพื้นผิวพอลิเมอร์ (ง) ตรึง PNA-T9 บนชั้นพอลิเมอร์ และ (ง) หลังปิดช่องว่างด้วย 11-MUL

จากไซคลิกโวลแทมโมแกรม พบว่าหลังจากแต่ละขั้นตอนในการเตรียมอิเล็กโทรดรีดอกซ์พีคของ $K_3[Fe(CN)_6]$ ลดลงตามลำดับเมื่อผิวอิเล็กโทรดถูกปกคลุมด้วยชั้นพอลิเมอร์ PNA-T9 และ blocking thiol แสดงว่า PNA-T9 ถูกตรึงอยู่บนอิเล็กโทรดแล้ว และในขั้นสุดท้ายหลังจากการบล็อกด้วย blocking thiol แล้วไม่มีรีดอกซ์พีคแสดงว่าอิเล็กโทรดที่เตรียมขึ้นมีความเป็นฉนวนเหมาะสำหรับการนำไปใช้ในระบบคาพาซิทีฟ

1.2.3. ศึกษาปัจจัยที่เหมาะสมในการเกิด electropolymerization

ปัจจัยที่มีผลต่อการเกิดปฏิกิริยา electropolymerization ของมอนอเมอร์ ได้แก่ ความเข้มข้นของสารละลายมอนอเมอร์ (5 10 15 20 mM สำหรับ *o*PD และ *p*PD 5 15 35 50 และ 60 mM สำหรับ tyramine) และจำนวนสแกน (5 10 15 และ 20 scans) เพื่อให้ได้ฟิล์มบางพอลิเมอร์ที่มีหมู่ฟังก์ชันเหมาะสมสำหรับการตรึง PNA probe และความเป็นฉนวนเหมาะสำหรับการประยุกต์ใช้ในเทคนิคคาพาซิทีฟ จากรูปที่ 9 พบว่าความเข้มข้นของสารละลายมอนอเมอร์และจำนวนสแกนที่เหมาะสมของ *o*PD และ *p*PD เท่ากับ 5 mM และ 15 scans ตามลำดับ และ 50 mM 10 scans สำหรับ tyramine โดยพิจารณาจากค่าความจุไฟฟ้าที่เปลี่ยนแปลง

ไปเมื่อฉีด target DNA เข้าสู่ระบบ พบว่า สำหรับ *o*PD และ *p*PD ที่ทุกความเข้มข้น ค่าสัญญาณจะเพิ่มขึ้นตามจำนวนสแกนจนถึง 15 scans จากนั้นจึงลดลงเนื่องจากที่จำนวนสแกนน้อย (5 และ 10 scans) จะมีพอลิเมอร์จำนวนน้อยอยู่บนผิวอิเล็กโทรด ทำให้มีหมู่เอมีนน้อยจึงตรึง PNA probe ได้น้อย ส่วนที่จำนวนสแกนมากเกินไป (20 scans) จะให้สัญญาณน้อยเช่นกัน เนื่องจากพอลิเมอร์ที่เกิดขึ้นจะเป็นก้อนบนผิวอิเล็กโทรด (รูปที่ 10) ส่วนในกรณีของ Pty ก็ได้ผลในลักษณะเดียวกัน คือ ที่ทุกความเข้มข้นค่าสัญญาณจะเพิ่มขึ้นตามจำนวนสแกนจนถึง 10 scans แต่เมื่อจำนวนสแกนมากเกินไป (15 และ 20 scans) พอลิเมอร์ที่เกิดขึ้นจะเป็นก้อนบนผิวอิเล็กโทรด ทำให้พื้นผิวขรุขระซึ่งไม่เหมาะกับการตรวจวัดด้วยเทคนิคคาพาซิทีฟ ส่งผลให้สัญญาณลดลง

เมื่อเปรียบเทียบสัญญาณที่ตรวจวัดระหว่างอิเล็กโทรดที่โมดิฟายด์ด้วย P*o*PD และ P*p*PD ภายใต้สภาวะที่เหมาะสม พบว่าอิเล็กโทรดที่โมดิฟายด์ด้วย P*p*PD จะให้สัญญาณที่สูงกว่า อาจเป็นเพราะหลังจากเกิดฟิล์มพอลิเมอร์ที่สภาวะที่เหมาะสมแล้วจะให้ฟิล์มที่มีลักษณะเรียบ แน่น และปกคลุมอย่างสม่ำเสมอ และในกรณีของอิเล็กโทรดที่โมดิฟายด์ด้วย Pty มีลักษณะฟิล์มที่เรียบน้อยกว่า (รูปที่ 11) แต่สภาพความเป็นฉนวนของฟิล์มหลัง electropolymerization ซึ่งเหมาะกับการตรวจวัดด้วยเทคนิคคาพาซีทีฟดีกว่า จึงทำให้สัญญาณที่ตรวจวัดมีค่าไม่แตกต่างจาก P*p*PD

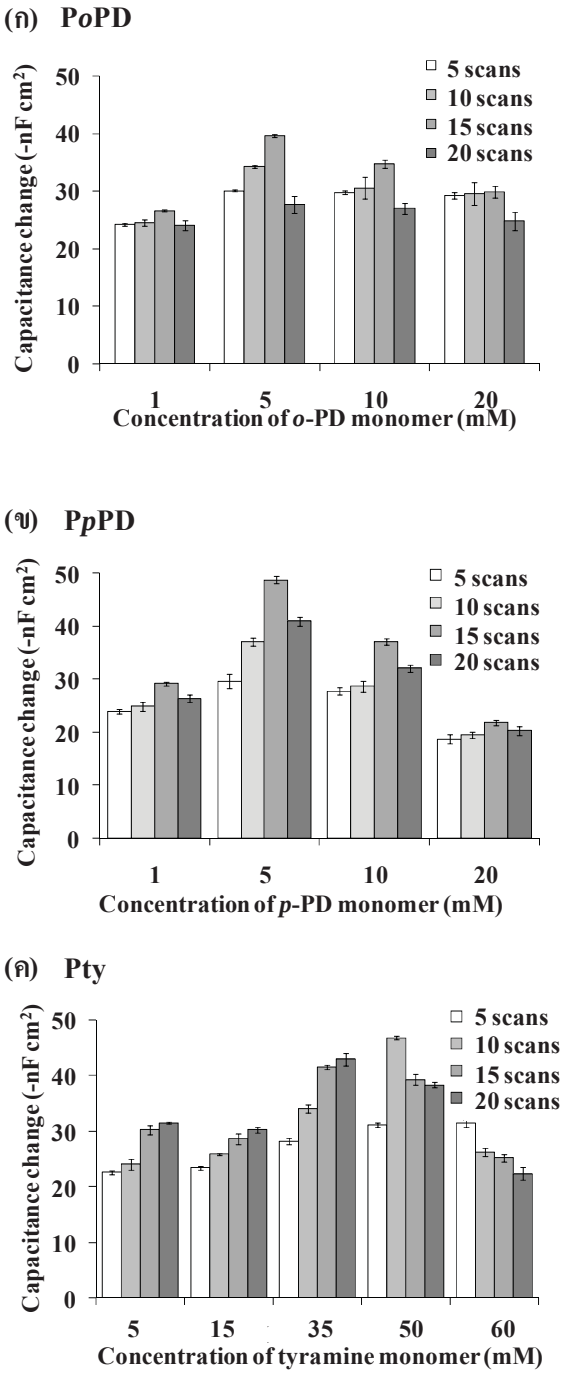

รูปที่ 9 ผลของความเข้มข้นของมอนอเมอร์และจำนวนสแกนในการเกิด electropolymerization ของ (ก) P*o*PD (ข) P*p*PD และ (ค) Pty

1.2.4. ศึกษาพื้นผิวอิเล็กโทรดทองที่โมดิฟายด์ด้วยฟิล์มบางพอลิเมอร์

การศึกษาลักษณะพื้นผิวของพอลิเมอร์ 3 ชนิด ที่โมดิฟายด์บนอิเล็กโทรดทองโดยใช้เทคนิค Scanning electron microscopy (SEM) เพื่อดูลักษณะการเคลือบของฟิล์มพอลิเมอร์แต่ละชนิดที่จำนวนสแกนต่างกัน (5 10 15 และ 20 scans) จากภาพ SEM (รูปที่ 10) ที่จำนวนสแกนน้อย (5 และ 10 scans สำหรับ P*o*PD และ P*p*PD และ Pty ที่ 5 scans) จะมีฟิล์มบางพอลิเมอร์ปกคลุมพื้นผิวอิเล็กโทรดทองไม่สมบูรณ์ แต่ที่จำนวนสแกนที่เหมาะสมของพอลิเมอร์แต่ละชนิด (15 scans สำหรับ P*o*PD และ P*p*PD และ Pty ที่ 10 scans) พบว่าพื้นผิวของอิเล็กโทรดจะมีฟิล์มบางพอลิเมอร์ปกคลุมอย่างสม่ำเสมออย่างสมบูรณ์ สำหรับที่จำนวนสแกนมากเกินไป (20 scans สำหรับ P*o*PD และ P*p*PD และ Pty ที่ 15 และ 20 scans) พบว่าพอลิเมอร์จะเกาะเป็นก้อนอยู่บนพื้นผิวของอิเล็กโทรด เมื่อเปรียบเทียบภาพ SEM ของ P*o*PD และ P*p*PD จะเห็นได้ว่าฟิล์มบางของ P*p*PD บนอิเล็กโทรดมีลักษณะที่เรียบมากกว่าฟิล์มบางของ P*o*PD

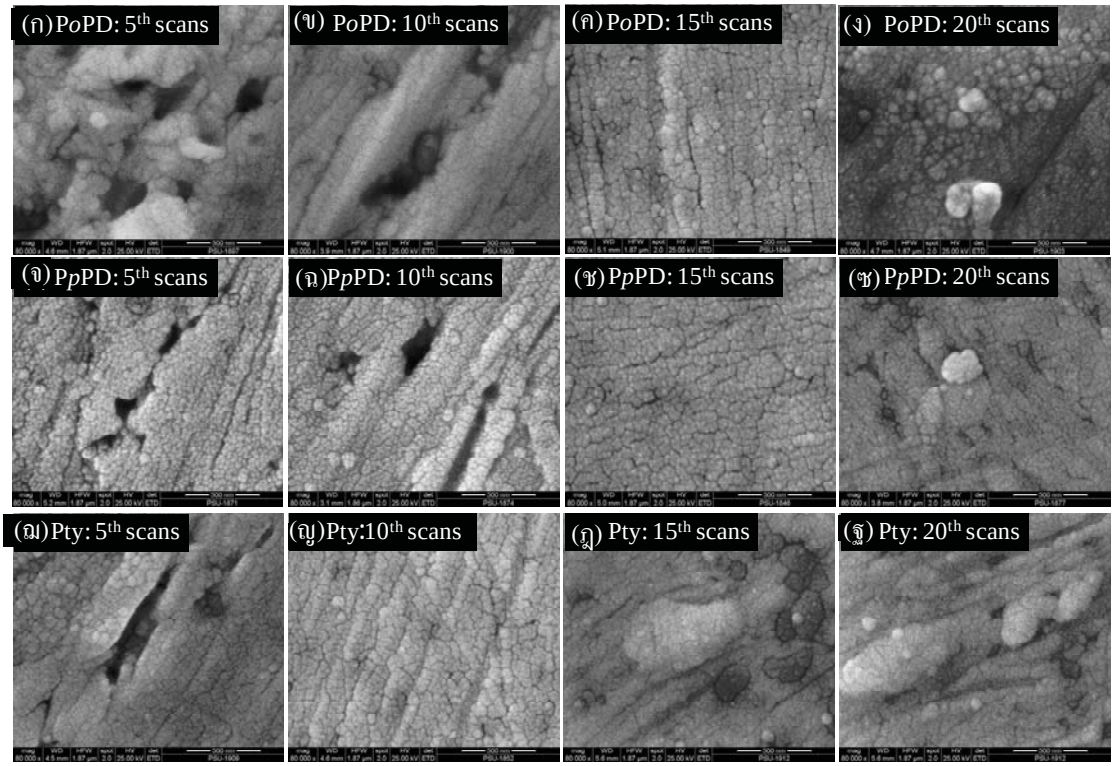

รูปที่ 10 ภาพ SEM ของอิเล็กโทรดที่ electropolymerization ด้วย P*o*PD 5 scans (ก) 5 scans (ข) 10 scans (ค) 15 scans (ง) 20 scans P*p*PD 5 mM (จ) 5 scans (ฉ) 10 scans (ช) 15 scans (ซ) 20 scans และ Pty 50 mM (ฌ) 5 scans (ญ) 10 scans (ฎ) 15 scans (ฐ) 20 scans

1.2.5. ศึกษาผลของความเข้มข้นของ probe

ความเข้มข้นของ probe มีผลต่อประสิทธิภาพของการไฮบริไดเซชัน จากการศึกษาเบื้องต้นพบว่าที่ความเข้มข้นของ 3.0 μM จะให้ความไววิเคราะห์น้อยเมื่อเทียบกับที่ความเข้มข้น 5.0 และ 7.0 μM เนื่องจากมีปริมาณของ probe จำนวนน้อยที่จะเกิดไฮบริไดเซชันกับ target ได้ และที่ความเข้มข้น 5.0 และ 7.0 μM จะได้ค่าความไววิเคราะห์เพิ่มขึ้นแต่ไม่ต่างกัน ดังรูปที่ 11 ดังนั้นจึงเลือกความเข้มข้นของ probe เท่ากับ 5.0 μM เพื่อใช้ในการตรึง

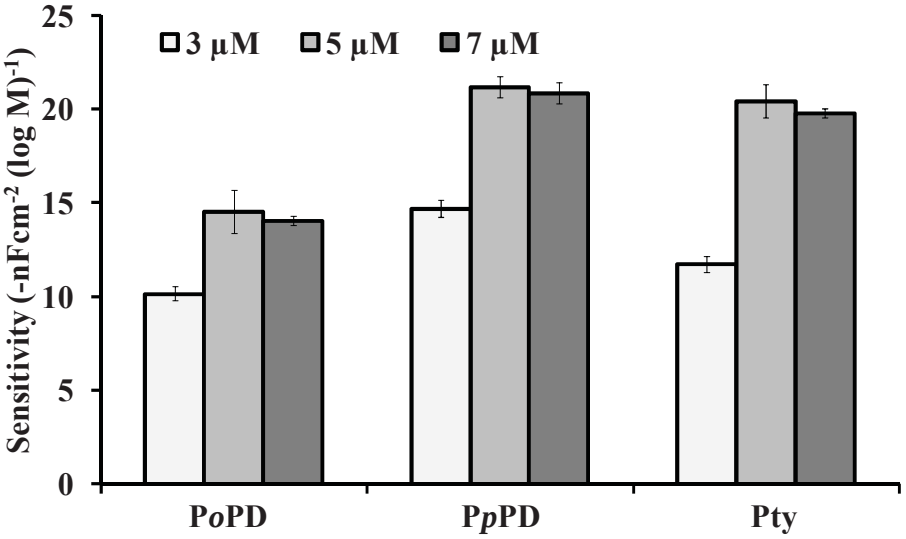

รูปที่ 11 ผลของความเข้มข้นของ PNA probe ต่อค่าความไววิเคราะห์ ในสภาวะที่ตรึง PNA-T9 บนพอลิเมอร์ชนิด P*o*PD P*p*PD และ Pty

1.2.6. ปริมาณการตรึงติดของ probe

ปัจจัยหนึ่งที่มีผลต่อสัญญาณที่ตรวจวัดคือปริมาณของ probe ที่ตรึงติดบนผิวอิเล็กโทรด (Keighley et al., 2008; Liu et al., 2005) ดังนั้นจึงได้หาปริมาณของ probe ที่ตรึงบนพอลิเมอร์ทั้ง 3 ชนิด ที่ 5 μM จำนวนสแกนต่างๆ (5 10 15 และ 20 scans) จากตารางที่ 3 พบว่า สำหรับ P*o*PD และ P*p*PD ที่ 15 scans และ Pty ที่ 10 scans มีปริมาณการตรึงติดของ probe มากที่สุด เท่ากับ 38 ± 0.8 **56** ± 1.2 **และ** **57** ± 0.3 pmol ตามลำดับ และที่ความเข้มข้น 5 μM ของ probe ที่โมดิฟายด์บนพอลิเมอร์ทั้ง 3 ชนิด ให้ค่าปริมาณการตรึงติดของ probe สูงที่สุด ซึ่งสอดคล้องกับสัญญาณการตรวจวัดที่ได้

ตารางที่ 3 ผลของจำนวนสแกนในการเกิด electropolymerization ต่อปริมาณการตรึงติดของ PNA-T9 (5 μM) ของสารละลายมอนอเมอร์ทั้ง 3 ชนิด และผลของความเข้มข้นของ PNA-T9 (3.0 5.0 and 7.0 μM) ที่จำนวนสแกนที่เหมาะสมต่อปริมาณการตรึงติดของ probe

The number of scans (scans)	**Amount of immobilized PNA-T9 probe on the modified electrode surface using 5 μM PNA-T9 probe (pmol)**		
	***Po*PD**	***Pp*PD**	**Pty**
5	20.1±1.2	25.9±1.2	27.8±0.6
10	32.6±1.1	34.7±1.2	56.6±0.3
15	38.3±0.8	55.6±1.2	41.2±1.1
20	20.1±1.2	37.4±1.1	35.5±1.2
Probe concentration	**Amount of immobilized PNA-T9 probe on the modified electrode surface (pmol)**		
	3 μM PNA-T9	**5 μM PNA-T9**	**7 μM PNA-T9**
P*o*PD	32.5±0.6	40.6±1.7	39.3±1.0
P*p*PD	39.9±0.4	55.6±1.4	54.9±1.1
Pty	35.2±0.5	55.0±0.9	54.5±0.7

1.2.7. ศึกษาช่วงความเป็นเส้นตรงและขีดจำกัดต่ำสุดในการตรวจวัด (Linear range and detection limit)

ศึกษาช่วงความเป็นเส้นตรงและขีดจำกัดต่ำสุดในการตรวจวัดของเซนเซอร์ที่พัฒนาขึ้น โดยตรึง PNA-T9 (5.0 μM) ผ่านฟิล์มบางของพอลิเมอร์ชนิดต่างๆ พบว่าสำหรับอิเล็กโทรดที่โมดิฟายด์ด้วย P*o*PD มีความเป็นเส้นตรงอยู่ในช่วง 1.0×10^{-11} ถึง 1.0×10^{-8} M และมีขีดจำกัดต่ำสุดในการตรวจวัดเท่ากับ 10 pM สำหรับอิเล็กโทรดที่โมดิฟายด์ด้วย P*p*PD และ Pty มีความเป็นเส้นตรงอยู่ในช่วง 1.0×10^{-12} ถึง 1.0×10^{-8} M และมีขีดจำกัดต่ำสุดในการตรวจวัดเท่ากับ 0.2 และ 0.8 pM ตามลำดับ ดังตารางที่ 4

ตารางที่ 4 ประสิทธิภาพของคาพาซิทีฟดีเอ็นเอเซนเซอร์แบบไม่ติดฉลากที่ตรึง PNA-T9 บนพอลิเมอร์ไม่นำไฟฟ้า **3** ชนิด

Modification	**Linear range (M)**	**Sensitivity (-nF cm^{-2} ($logM^{-1}$))**	**Limit of Detection**	**Reusability**
polymer types	**correlation coefficient (r)**		**(pM)**	**(cycles)**
P*o*PD	$1.0\times10^{-11} - 1.0\times10^{-8}$, 0.9984	14.5±1.2	10	68
P*p*PD	$1.0\times10^{-12} - 1.0\times10^{-8}$, 0.9934	20.9±0.6	0.2	74
Pty	$1.0\times10^{-12} - 1.0\times10^{-8}$, 0.9986	19.1±1.1	0.8	77

1.2.8. ศึกษาการนำกลับมาใช้ใหม่ได้ของอิเล็กโทรด (Reuseability)

จากการทดสอบการนำกลับมาใช้ใหม่ได้ของ probe ที่ตรึงบนฟิล์มบางของพอลิเมอร์ชนิด P*o*PD P*p*PD และ Pty ด้วยระบบคาพาซิทีฟแอฟฟินิตีไบโอเซนเซอร์ ให้จำนวนการนำกลับมาใช้ได้ใหม่เท่ากับ 68 74 และ 77 ครั้ง ตามลำดับ แสดงว่า PNA probe สภาวะตรึงนี้สามารถนำกลับมาใช้ใหม่ได้

1.2.9. ศึกษาความสามารถในการทำซ้ำ (Reproducibility)

ทดสอบความสามารถในการทำซ้ำของอิเล็กโทรดที่โมดิฟายด์ด้วยฟิล์ม Pty จำนวน 3 อิเล็กโทรด ที่เตรียมในเวลาต่างกัน โดยเปรียบเทียบจากค่าความไววิเคราะห์ พบว่ามีค่าเท่ากับ 19.1 ± 1.1 19.0 ± 1.2 และ 18.7 ± 1.5 $-nFcm^{-2}(\log M)^{-1}$ โดยค่าความไววิเคราะห์มีค่าไม่แตกต่างกันระหว่างการเตรียมแต่ละครั้ง แสดงว่าอิเล็กโทรดที่สภาวะตรึงมีความสามารถในการทำซ้ำได้

1.2.10. ศึกษาความสามารถในการเลือก (Selectivity)

จากการทดสอบความสามารถในการเลือกจับกันของ PNA probe 2 ชนิด คือ PNA-T9 ที่ตรึงบนฟิล์มบางของพอลิเมอร์ทั้ง 3 ชนิด (P*o*PD P*p*PD และ Pty) กับ DNA ที่มีลำดับเบสที่ไม่เป็นคู่สมจำนวนหนึ่งตำแหน่ง และ DNA ที่มีลำดับเบสที่ไม่เป็นคู่สมจำนวนสองตำแหน่ง ที่ความเข้มข้น 10^{-10} M โดยมีค่า %SS ในช่วง 69 – 74 และ 87 – 89 % 59 – 68 และ 77 – 83 % 67 – 75 และ 85 – 88 % ตามลำดับ และสำหรับ

PNA-M12 ที่ตรึงบนฟิล์มบางของ P*p*PD มีค่าในช่วง 71 – 72 และ 85 – 88 % ตามลำดับ (รูปที่ 12) แสดงว่าเซนเซอร์นี้มีความสามารถในการเลือก

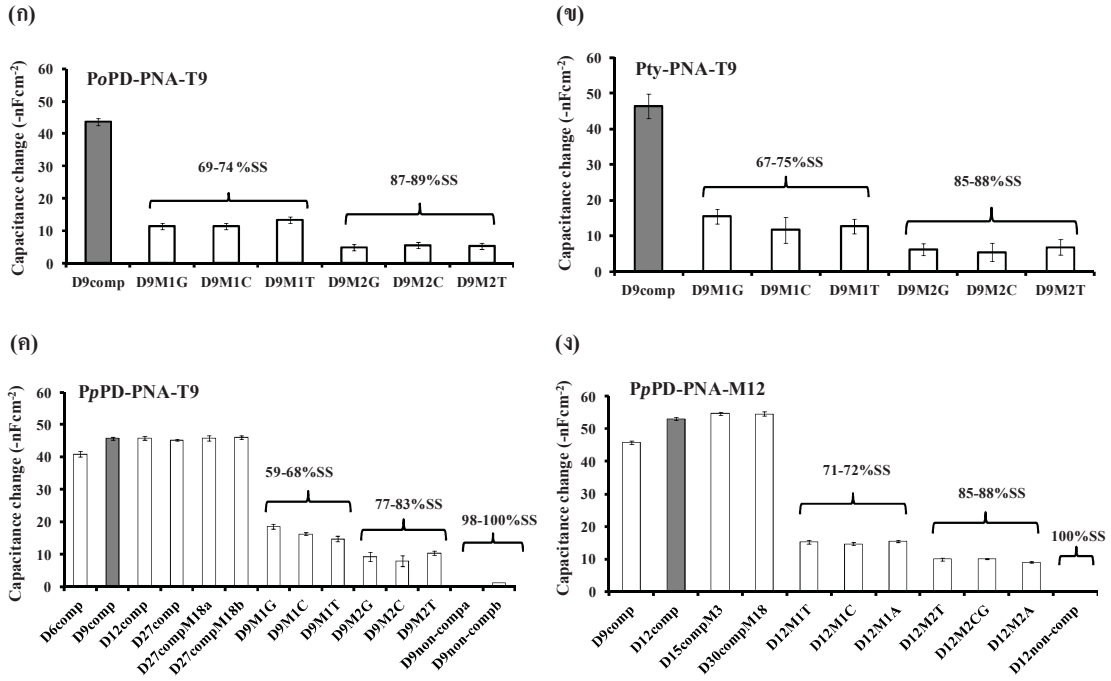

รูปที่ 12 ค่าความจุไฟฟ้าที่เปลี่ยนแปลงของเซนเซอร์ที่ตรึง PNA-T9 บนพอลิเมอร์ชนิด P*o*PD (ก) Pty (ข) และ P*p*PD (ค) และ PNA-M12 บน P*p*PD (ง) เมื่อฉีด DNA ความเข้มข้น 1.0×10^{-10} M ที่มีลำดับเบสที่เป็นคู่สม และ DNA ที่มีลำดับเบสที่ไม่เป็นคู่สม

1.2.11. ผลของความยาวของ target DNA

การไฮบริไดเซชันระหว่าง probe กับ target DNA จะทำให้โมเลกุลของน้ำและอิเล็กโตรไลต์ถูกแทนที่ด้วย DNA ทำให้ค่าความจุไฟฟ้าเปลี่ยนแปลงไป ในกรณีที่ DNA สั้นกว่า probe จะให้สัญญาณน้อยกว่ากรณีที่ DNA ยาวเท่ากับ probe แต่ในกรณีที่ DNA ยาวกว่า probe จะไม่มีผลต่อค่าความจุไฟฟ้า เนื่องจากส่วนของสาย DNA ที่ไม่เกิดไฮบริไดเซชันจะอยู่ในสารละลายซึ่งไม่มีผลต่อการเปลี่ยนแปลงค่าความจุไฟฟ้า ดังรูปที่ 12 (ค และ ง)

สรุป

งานวิจัยนี้ได้ศึกษาเปรียบเทียบประสิทธิภาพการตรวจวัด DNA ด้วยเทคนิคคาพาซิทีฟ โดยตรึง acpcPNA probe บนชั้นฟิล์มพอลิเมอร์ไม่นำไฟฟ้า 3 ชนิด พบว่า P*p*PD และ Pty ให้ช่วงการตอบสนองเชิงเส้นในช่วง 1.0×10^{-12} ถึง 1.0×10^{-8} M และขีดจำกัดการตรวจวัดต่ำถึง 0.2 และ 0.8 พิโคโมลาร์ ตามลำดับ ในขณะที่ P*o*PD มีช่วงการตอบสนองเชิงเส้นในช่วง 1.0×10^{-11} ถึง 1.0×10^{-8} M และขีดจำกัดการตรวจวัด 10 พิโคโมลาร์ เซนเซอร์ที่พัฒนาขึ้นมีความสามารถในการเลือก และอิเล็กโทรดสามารถใช้ซ้ำได้อย่างน้อย 68 ครั้งต่อหนึ่งครั้งของการเตรียม

งานวิจัยที่ 2 อิเล็กโทรเคมิคัลไบโอเซนเซอร์สำหรับตรวจวัด DNA

เป็นการพัฒนาคาพาซิทีฟดีเอ็นเอเซนเซอร์แบบไม่ติดฉลากเพื่อตรวจวัด DNA โดยตรึง Pyrolidinyl acpcPNA probe ชนิด 11-mixed bases (Ac-GCT CCG TCC TC-LysNH_2) บนชั้นพอลิเมอร์ชนิด poly-*p*-phenylenediamine (P*p*PD) เนื่องจากเป็นพอลิเมอร์ชนิดไม่นำไฟฟ้าที่ทำให้เกิดสภาพเป็นฉนวนบนผิวอิเล็กโทรดซึ่งเหมาะกับการตรวจวัดด้วยเทคนิคคาพาซิทีฟ และจากงานวิจัยที่ 1.2 พบว่าอิเล็กโทรดที่โมดิฟายด์ P*p*PD จะให้สัญญาณการตรวจวัดและความไววิเคราะห์สูงมากกว่าพอลิเมอร์อีกสองชนิดที่ศึกษา (P*o*PD Pty) โดยเบื้องต้นได้ศึกษาสภาวะการตรึง PNA probe บนผิวหน้าอิเล็กโทรดที่มีการโมดิฟายด์ด้วย P*p*PD จากนั้นจึงศึกษาประสิทธิภาพของระบบ ได้แก่ ช่วงการตอบสนองเชิงเส้นและขีดจำกัดต่ำสุดของการตรวจวัด การจับกันของ PNA probe กับ target DNA ที่เป็น single strand และ double strand ความสามารถในการทำซ้ำ การนำกลับมาใช้ใหม่ได้ของอิเล็กโทรด ความสามารถในการทำซ้ำ อายุการเก็บอิเล็กโทรดในสภาวะตรึง และความสามารถในการเลือก

2.1. ศึกษาสภาวะการตรึง PNA probe บนผิวหน้าอิเล็กโทรดที่มีการโมดิฟายด์ด้วยพอลิเมอร์

ตรึง 11-mixed bases acpcPNA probe (Ac-GCT CCG TCC TC-LysNH_2) บนชั้นพอลิเมอร์ชนิดไม่นำไฟฟ้า P*p*PD ในระบบคาพาซิทีฟแอฟฟินิตีไบโอเซนเซอร์ ประกอบด้วย 4 ขั้นตอนดังนี้

ขั้นที่ 1 เตรียมชั้น P*p*PD บนอิเล็กโทรดทอง

ขั้นที่ 2 แอคติเวตหมู่ฟังก์ชันด้วยกลูตารัลดีไฮด์ (glutaraldehyde; GA)

ขั้นที่ 3 ตรึง PNA probe บนชั้นพอลิเมอร์

ขั้นที่ 4 ปิดช่องว่าง (pinholes) ของผิวหน้าอิเล็กโทรดโดยใช้ blocking thiol

โดยทดสอบผิวอิเล็กโทรดแต่ละขั้นตอนด้วยเทคนิคไซคลิกโวลแทมเมทรีในสารละลาย 5 mM $K_3[Fe(CN)_6]$ ใน 0.1 M KCl เพื่อยืนยันผลการเตรียมอิเล็กโทรดแต่ละขั้นตอน

จากไซคลิกโวลแทมโมแกรม (รูปที่ 13) พบว่า หลังจากแต่ละขั้นตอนในการเตรียมอิเล็กโทรดทองรีดอกซ์พีคของ $K_3[Fe(CN)_6]$ จะลดลงตามลำดับ นั่นคือ เมื่อผิวอิเล็กโทรดถูกปกคลุมด้วยชั้นฟิล์มบางของ P*p*PD กลูตารัลดีไฮด์ PNA probe และ blocking thiol แสดงว่าผิวอิเล็กโทรดที่โมดิฟายด์มีสภาพเป็นฉนวนและเหมาะสำหรับระบบตรวจวัดด้วยเทคนิคคาพาซิทีฟ

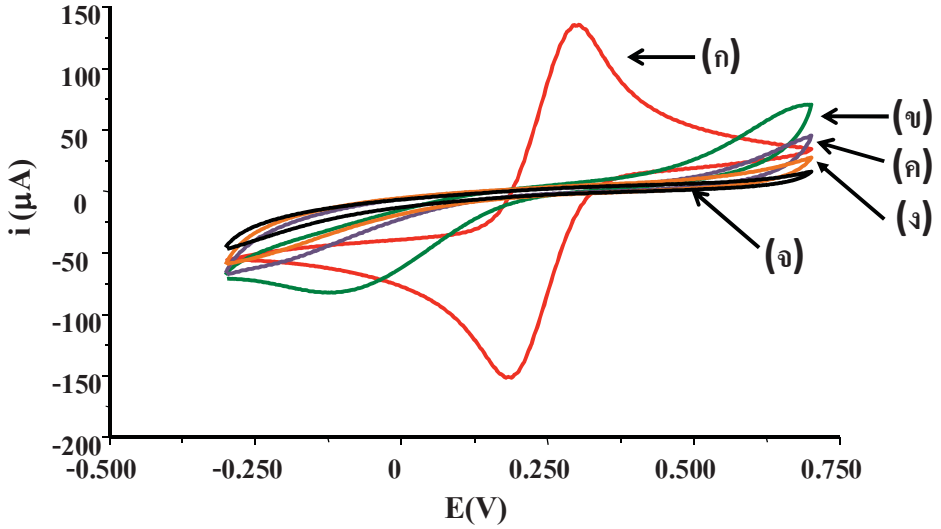

รูปที่ 13 ไซคลิกโวลแทมโมแกรมของอิเล็กโทรดทองในสารละลาย 5 mM $K_3[Fe(CN)_6]$) ใน 0.1 M KCl
(ก) อิเล็กโทรดทอง (ข) อิเล็กโทรดทองหลังโมดิฟายด์ด้วย P*p*PD อิเล็กโทรดทองหลัง
(ค) แอคติเวตหมู่เอมีนด้วยกลูตารัลดีไฮด์ (ง) ตรึง PNA probe บนชั้นพอลิเมอร์ และ
(จ) หลังปิดช่องว่างด้วย blocking thiol

2.2. ทดสอบการตรวจวัด DNA ในระบบคาพาซิทีฟแอฟฟินิตีไบโอเซนเซอร์

วัดการเปลี่ยนแปลงค่าความจุไฟฟ้าระหว่างผิวหน้าอิเล็กโทรดกับสารละลายที่เกิดจากการจับกันอย่างจำเพาะเจาะจงระหว่าง target DNA กับ PNA probe จากสภาวะที่เหมาะสม และเมื่อเขียนกราฟแสดงความสัมพันธ์ระหว่างค่าความจุไฟฟ้าที่วัดได้กับล็อกของความเข้มข้นของ DNA พบว่ามีค่าการตอบสนองเชิงเส้นที่ดีในช่วง 10^{-11} ถึง 10^{-8} โมลาร์ และสามารถตรวจวัด DNA ได้ในระดับพิโคโมลาร์ (pM) ดังรูปที่ 14

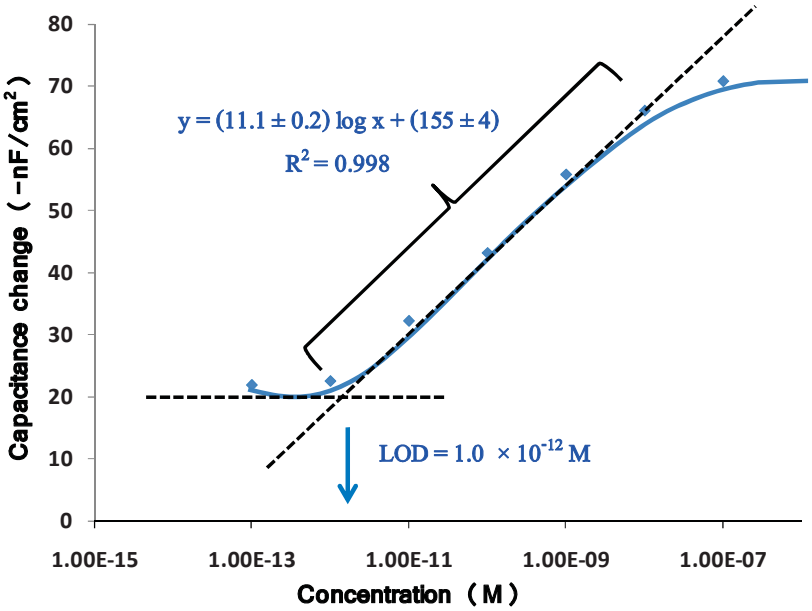

รูปที่ 14 กราฟมาตรฐานระหว่างค่าความจุไฟฟ้าที่เปลี่ยนแปลงกับความเข้มข้นของ target DNA

2.3. ศึกษาความสามารถในการทำซ้ำ (Reproducibility)

ทดสอบความสามารถในการทำซ้ำของอิเล็กโทรดจำนวน 3 อิเล็กโทรด ที่เตรียมในเวลาต่างกัน โดยเปรียบเทียบจากค่าความไววิเคราะห์ พบว่ามีค่าเท่ากับ 11.1 ± 0.2 11.5 ± 0.6 และ 11.0 ± 0.5 $-nFcm^{-2}(\log M)^{-1}$ โดยค่าความไววิเคราะห์มีค่าไม่แตกต่างกันระหว่างการเตรียมแต่ละครั้ง แสดงว่าอิเล็กโทรดที่สภาวะตรึงมีความสามารถในการทำซ้ำได้

2.4. ศึกษาอายุการเก็บอิเล็กโทรดสภาวะตรึง (Storage stability)

ทดสอบความสามารถในการใช้ซ้ำของอิเล็กโทรดเดียวจำนวน 4 ครั้ง ภายในเวลา 1 เดือน โดยเปรียบเทียบจากค่าความไววิเคราะห์มีค่าเท่ากับ 11.1 ± 0.2 11.5 ± 0.2 11.4 ± 0.1 และ 11.2 ± 0.3 $-nFcm^{-2}(\log M)^{-1}$ พบว่าค่าความไววิเคราะห์มีค่าไม่แตกต่างกัน และเมื่อทดสอบต่อภายในเวลา 3 เดือน (เดือนละ 1 ครั้ง) พบว่าความไววิเคราะห์ยังคงมีค่าไม่แตกต่างกัน นั่นคือเท่ากับ 11.1 ± 0.2 11.1 ± 0.2 และ 10.8 ± 0.3 $-nFcm^{-2}(\log M)^{-1}$ และเมื่อทดสอบความสามารถในการใช้ซ้ำในระยะเวลา 3 เดือนของ 3 อิเล็กโทรดที่เตรียมในครั้งเดียวกันซึ่งมีค่าความไววิเคราะห์ไม่ต่างกันเช่นกัน เท่ากับ 11.1 ± 0.2 11.1 ± 0.1 และ 10.9 ± 0.2 $-nFcm^{-2}(\log M)^{-1}$ ตามลำดับ แสดงว่าอิเล็กโทรดในสภาวะตรึงสามารถเก็บได้อย่างน้อย 3 เดือน

2.5. ศึกษาการนำกลับมาใช้ใหม่ได้ของอิเล็กโทรด (Reuseability)

จากการทดสอบการนำกลับมาใช้ใหม่ได้ของ acpcPNA probe ที่ตรึงบนชั้นพอลิเมอร์ poly-*p*-phenylenediamine ด้วยระบบคาพาซิทีฟแอฟฟินิตีไบโอเซนเซอร์ ให้จำนวนการนำกลับมาใช้ได้ใหม่เท่ากับ 85 ครั้ง ดังรูปที่ 15 แสดงว่า acpcPNA probe สภาวะตรึงนี้สามารถนำกลับมาใช้ใหม่ได้

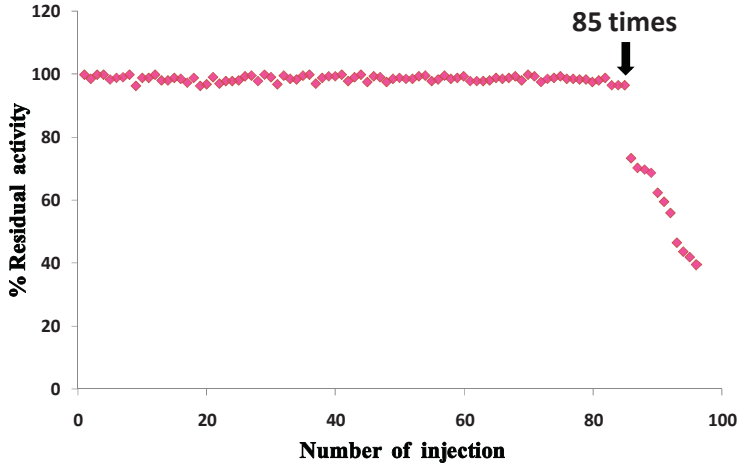

รูปที่ 15 ความสัมพันธ์ระหว่าง % Residual activity และจำนวนครั้งของการใช้อิเล็กโทรดซ้ำ

2.6. ศึกษาความสามารถในการเลือก (Selectivity)

จากการทดสอบความสามารถในการเลือกจับกันของ PNA probe ที่ตรึงบนฟิล์มบางของ P*p*PD กับ DNA ที่มีลำดับเบสที่เป็นคู่สม DNA ที่มีลำดับเบสที่ไม่เป็นคู่สมจำนวนหนึ่งตำแหน่ง และ DNA ที่มีลำดับเบสที่ไม่เป็นคู่สมจำนวนสองตำแหน่ง ที่ความเข้มข้น 1.0×10^{-10} และ 1.0×10^{-10} M (ตารางที่ 5) พบว่าค่า %SS มีค่าอยู่ในช่วง 53 – 68 และ 60 – 73 % ตามลำดับ แสดงว่าเซนเซอร์ที่พัฒนาขึ้นมีความสามารถในการเลือก เพราะสามารถแยกความแตกต่างของสัญญาณระหว่าง DNA ที่เป็นคู่สมกับที่ไม่เป็นคู่สมได้

ตารางที่ 5 เปอร์เซ็นต์ของสัญญาณที่ลดลงเมื่อเทียบกับสัญญาณของ target DNA ที่เป็นคู่สม

เปอร์เซ็นต์ของสัญญาณที่ลดลงเมื่อเทียบกับสัญญาณของ target DNA ที่เป็นคู่สม			
single mismatched DNA		**double mismatched DNA**	
ความเข้มข้น 1.0×10^{-8} M	**ความเข้มข้น 1.0×10^{-10} M**	**ความเข้มข้น 1.0×10^{-8} M**	**ความเข้มข้น 1.0×10^{-10} M**
53 - 68		60 - 73	

2.7. ศึกษาการไฮบริไดเซชันของ acpcPNA probe กับ target DNA ที่เป็น single strand และ double strand

จากการศึกษาความสามารถของการไฮบริไดเซชันระหว่าง acpcPNA probe กับ target DNA ที่เป็น single strand (ใช้ความร้อนในการเตรียมตัวอย่าง, Heat) และ double strand (ไม่ใช้ความร้อนในการเตรียมตัวอย่าง, W/O Heat) พบว่าดีเอ็นเอเซนเซอร์ที่พัฒนาขึ้นสามารถจับกับ DNA ได้ทั้งชนิด ss-DNA และ ds-DNA โดยในงานวิจัยได้ทดลองกับ DNA ที่มีลำดับเบสที่เป็นคู่สมที่มีความยาวจำนวน 41 และ 61 เบส พบว่าค่าความไววิเคราะห์ของระบบจากการเตรียมตัวอย่างทั้ง 2 วิธี มีค่าต่างกันไม่เกิน 5% (รูปที่ 16) ทั้งนี้เนื่องจาก acpaPNA probe มีความแรงของการเข้าจับคู่กับเบสที่เป็นคู่สมในสภาพที่เป็นสายคู่ได้ จึงสามารถเกิดการไฮบริไดเซชันกับ ds-DNA ได้

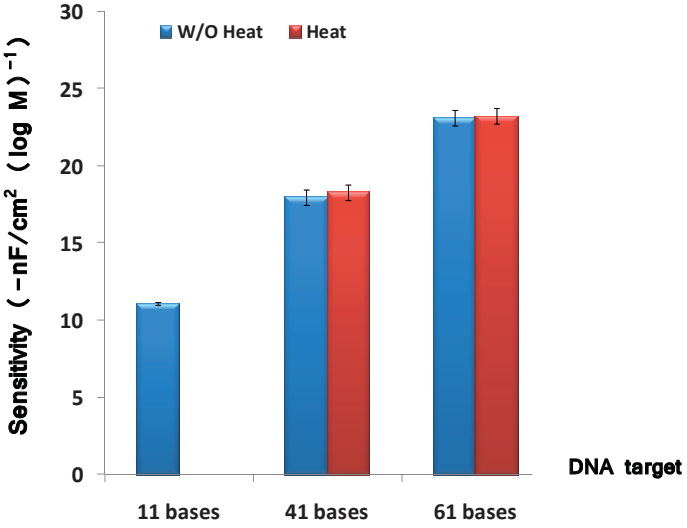

รูปที่ 16 ความสัมพันธ์ระหว่างความไววิเคราะห์และ target DNA ทั้งชนิด ss-DNA และ ds-DNA

สรุป

งานวิจัยนี้ได้พัฒนาระบบตรวจวัดอิเล็กโตรเคมิคัลไบโอเซนเซอร์สำหรับตรวจวัด DNA ด้วยเทคนิคคาพาซิทีฟ โดยตรึง 11 – mixed bases acpcPNA probe บนชั้นฟิล์มบางของ P*p*PD ซึ่งให้ช่วงการตอบสนองเชิงเส้นตั้งแต่ 1.0×10^{-12} ถึง 1.0×10^{-8} M และมีขีดจำกัดการตรวจวัดต่ำถึงระดับพิโคโมลาร์ อิเล็กโทรดที่สภาวะตรึงมีความสามารถในการทำซ้ำ สามารถเก็บได้อย่างน้อย 3 เดือน อิเล็กโทรดสามารถใช้ซ้ำได้อย่างน้อย 85 ครั้งต่อหนึ่งครั้งของการเตรียม และดีเอ็นเอเซนเซอร์ที่พัฒนาขึ้นมีความสามารถในการเลือกและสามารถจับได้ทั้ง ss-DNA และ ds-DNA

สรุปผลการดำเนินงานของโครงการ

จากผลการดำเนินงานของโครงการ Development of label-free electrochemical DNA biosensor based on immobilized PNA probes ในช่วง 3 ปี ประกอบด้วยงานวิจัยที่ 1 และ 2 ในงานวิจัยที่ 1 ได้ศึกษาการตรึง acpcPNA probe บนผิวหน้าอิเล็กโทรดผ่านชั้น SAM จากงานวิจัยนี้ได้ทราบถึงสภาวะที่เหมาะสมสำหรับการตรึง acpcPNA probe บนอิเล็กโทรดที่โมดิฟายด์ด้วย SAM 4 ชนิดคือ MPA MSA TA และ TU และความยาวและหมู่ฟังก์ชันของ blocking thiol ที่เหมาะสม เพื่อช่วยให้ probe อยู่ในตำแหน่งที่เหมาะสมต่อการไฮบริไดเซชันกับ target DNA นอกจากนี้ยังได้ศึกษาการตรึง acpcPNA probe บนอิเล็กโทรดที่โมดิฟายด์ด้วยฟิล์มพอลิเมอร์ไม่นำไฟฟ้า 3 ชนิด ได้แก่ P*o*PD P*p*PD และ Pty และได้ทดสอบเปรียบเทียบประสิทธิภาพของ PNA สภาวะตรึง สำหรับงานวิจัยที่ 2 ได้พัฒนาระบบตรวจวัดอิเล็กโตรเคมิคัลไบโอเซนเซอร์สำหรับ DNA โดยได้ศึกษาสภาวะการตรึงที่เหมาะสมและทดสอบประสิทธิภาพของระบบตรวจวัด

ผลงานตีพิมพ์

Orawan Thipmanee, Saluma Samanman, Supannee Sankoh, Apon Numnuam, Warakorn Limbut, Proespichaya Kanatharana, Tirayut Vilaivan and Panote Thavarungkul. 2012. Label-free capacitive DNA sensor using immobilized pyrrolidinyl PNA probe: Effect of the length and terminating head group of the blocking thiols. *Biosensors and Bioelectronics*. Inpress (impact factor 2011: 5.361)

ผลงานที่เสนอในที่ประชุมระดับชาติผลงานตีพิมพ์ที่เกิดขึ้นในระหว่างช่วงของการรายงาน/นานาชาติ-

ได้เสนอผลงานระดับชาติแบบบรรยาย 1 เรื่อง และแบบโปสเตอร์ 2 เรื่อง (ดังแสดงในเอกสารแนบ)

การนำเสนอแบบบรรยาย 1 เรื่อง

1. Orawan Thipmanee, Saluma Samanman, Supannee Sankoh, Apon Numnuam, Warakorn Limbut, Proespichaya Kanatharana, Tirayut Vilaivan and Panote Thavarungkul *"Effect of the Length and Terminating Head group of Blocking Thiols on the Label-free Capacitive Detection of DNA using Immobilized Pyrrolidinyl acpcPNA Probe"* การประชุมประจำปี ครั้งที่ 2 ทุนส่งเสริมการวิจัยปี 2552 , 9 December 2011, Faculty of Science, Naresuan University, Pitsanulok, Thailand.

การนำเสนอแบบโปสเตอร์ 3 เรื่อง

1. Orawan Thipmanee, Saluma Samanman, Supannee Sankoh, Apon Numnuam, Warakorn Limbut, Proespichaya Kanatharana, Tirayut Vilaivan and Panote Thavarungkul

" *Effect of Blocking reagents on the Capacitive Detection of PNA-DNA Hybridization"*

(Poster Presentation) 14th Asian Chemical Congress 2011, 5-8 September 2011, Bangkok, Thailand.

2. Supannee Sankoh, Saluma Samanman, Orawan Thipmanee, Apon Numnuam, Warakorn Limbut, Proespichaya Kanatharana, Tirayut Vilaivan and Panote Thavarungkul
"Label-free Capacitive DNA Sensor Based on Tyramine Modified Pyrrolidinyl PNA Probe"
(Poster Presentation) การประชุมประจำปี ครั้งที่ 2 ทุนส่งเสริมการวิจัยปี 2552 , 9 December 2011, Faculty of Science, Naresuan University, Pitsanulok, Thailand.

3. Supannee Sankoh, Orawan Thipmanee, Saluma Samanman, Warakorn Limbut, Apon Numnuam, Proespichaya Kanatharana, Tirayut Vilaivan, and Panote Thavarungkul, "*THE CHAIN LENGTH EFFECT OF BLOCKING REAGENT ON THE CAPACITIVE DETECTION OF PNA-DNA HYBRIDIZATION*" (Poster Presentation) Pure and Applied Chemistry International Conference 2012 (PACCON 2012) 11-13 January 2012, Chiang Mai, Thailand.

แผนงานของโครงการที่จะศึกษาต่อไปในอนาคต

สำหรับแผนงานที่จะศึกษาต่อไปในอนาคตในงานวิจัยที่ 1.2 คือ ดำเนินการเตรียมต้นฉบับเพื่อการตีพิมพ์ สำหรับงานวิจัยที่ 2 ศึกษาผลของความยาวของ target DNA ตรวจวัดดีเอ็นเอจากตัวอย่างจริงและเตรียมต้นฉบับเพื่อการตีพิมพ์

เอกสารอ้างอิง

Ananthanawat, C., Vilaivan, T., Mekboonsonglarp, W., Hoven, V. P., 2009. Biosens. Bioelectron. 24, 3544-3549.

Berggren, C., Stalhandske, P., Brundell, J., Johansson, G., 1999. Electroanalysis. 11, 156-160.

Dharuman, V., Hahn, J. H., 2007. Sensor Actuator B: Chemical. 127, 536-544.

Gillmor, S. D., Thiel, T. C., Strother, T. C., Smith, L. M., Lagally, M. G., 2000. Langmuir. 16, 7223-7228.

Herne, T. M., Tarlov, M. J., 1997. J. Am. Chem. Soc. 119, 8916-8920.

Keighley, T.D., Estrela, P., Li, P., Migliorato, P., 2008. Biosens. Bioelectron. 24, 906-911.

Limbut, W., Kanatharana, P., Mattiasson, B., Asawatreratanakul, P., Thavarungkul, P., 2006. Biosens. Bioelectron. 22, 233-240.

Liu, J., Tian, S., Nielsen, P. E., Knoll, W., 2005. Chem. Commun. 2969–2971.

Loyprasert, S., Thavarungkul, P., Asawatreratanakul, P., Wongkittisuksa, B., Limsakul, C., Kanatharana, P., 2008. Biosens. Bioelectron. 24, 78-86.

Loyprasert, S., Hedström, M., Thavarungkul, P., Kanatharana, P., Mattiasson, B., 2010 Biosens. Bioelectron. 25, 1977-1983.

Lucarelli, F., Marrazza, G., Turner, A. P. F., Mascini, M., 2004. Biosens. Bioelectron. 19, 515-530.

Lucarelli, F., Tombelli, S., Minunni, M., Marrazza, G., Mascini, M., 2008. Anal Chim Acta. 609, 139-159.

Samanman, S., Kanatharana, P., Chotigeat, W., Decahmag, P., Thavarungkul, P., 2011. J. Virol. Methods. 173, 75-84.

Teeparuksapun, K., Kanatharana, P., Limbut, W., Thammakhet, C., Asawatreratanakul, P., Mattiasson, B., Wongkittisuksa, B., Limsakul, C., Thavarungkul, P., 2009. Electroanalysis. 21, 1066-1074.

Tichoniuk, M., Ligaj, M., Filipak, M., 2008. Sensors. 8, 2118-2135.

Wong, E. L. S., Chow, E., Gooding, J. J., 2005. Langmuir. 21, 6957-6965.

รายงานฉบับสมบูรณ์

โครงการย่อยที่ 6 การประยุกต์โมเลกุล PNA สำหรับการตรวจวินิจฉัยทางการแพทย์ เกษตร และอาหาร

ส่วนที่ 1 บทสรุปสำหรับผู้บริหาร

การตรวจวิเคราะห์ทางพันธุกรรม เป็นหัวใจสำคัญการตรวจวิเคราะห์ทางชีวเคมีที่ประยุกต์ใช้ตอบโจทย์ทางการการแพทย์ทางการเกษตรและอาหาร และเป็นที่ยอมรับในทางนิติวิทยาศาสตร์ เนื่องจากการตรวจสารพันธุกรรมให้ข้อมูลที่จำเพาะของลำดับทางพันธุกรรมทั้งในรูปโมเลกุลดีเอ็นเอหรืออาร์เอ็นเอ ในอดีตการตรวจวิเคราะห์ทางพันธุกรรมดำเนินการโดยอาศัยความจำเพาะของลำดับนิวคลิโอไทด์ระหว่างคู่ไพรเมอร์และสารพันธุกรรมเป้าหมายผ่านเทคนิค PCR หรือการเชื่อมโยงกับเอนไซม์จำเพาะ (restriction enzyme) ที่จับตัวแบบจำเพาะต่อลำดับนิวคลิโอไทด์ตำแหน่งจดจำ หรือ การตรวจสอบลำดับนิวคลิโอไทด์โดยการทำ nucleic acid hybridization หรือ microsequencing เทคนิคเหล่านี้แม้ให้ผลที่มีความจำเพาะและแม่นยำแต่การดำเนินการมีกระบวนการที่ซับซ้อน ใช้เวลา และที่สำคัญต้องพึ่งพาห้องปฏิบัติการและความชำนาญการ ทำให้เกิดข้อจำกัดในกรณีที่ต้องตอบโจทย์การวิเคราห์ในรูปแบบ point of care test

เพปไทด์นิวคลีอิกแอซิด (peptide nucleic acid, PNA) แสดงสมบัติจำเพาะต่อลำดับนิวคลิโอไทด์ ไม่ต่างจากดีเอ็นเอทั่วไปแต่กลับมีแรงยึดจับ (affinity) สูงกว่า ให้ความจำเพาะมากกว่า และเกิดปฏิกิริยาที่จำเพาะแม้ที่อุณหภูมิห้อง เปิดโอกาสให้เกิดการพัฒนาเทคนิคการตรวจวิเคราะห์ทางพันธุกรรม ทำได้ด้วยความรวดเร็ว แม่นยำ ลดขั้นตอนที่ยุ่งยากและการพึ่งห้องปฏิบัติการลง

โครงการย่อยนี้ได้พัฒนาวิธีการตรวจวิเคราะห์ โดยเชื่อมโยงเทคนิคการเพิ่มปริมาณสารพันธุกรรมแบบลูบอุณหภูมิเดียวในการเพิ่มสัญญาณทางพันธุกรรม และพัฒนาระบบการตรวจสัญญาณสารพันธุกรรมโดยใช้เบต้าพิโรลิดินิลเพปไทด์นิวคลีอิกแอซิดเป็นโพรบและตรวจสัญญาณผ่านการเรืองแสง (fluorescence) หรือการเปลี่ยนสีทางแสง (colorimetry) อาศัยข้อได้เปรียบทางเทคนิค LAMP สำหรับเพิ่มปริมาณสารพันธุกรรมภายในเวลาน้อยกว่า 40 นาที ที่อุณหภูมิคงที่ โดยให้ความจำเพาะสูงเนื่องจากอาศัยชุดของไพร์เมอร์ที่จับตัวกับดีเอ็นเอเป้าหมายมากถึง 6 บริเวณและการยืนยันผลโดยเบต้าไพโรริดินิลเพพไทด์นิวคลิอิคเป็นโพรบ เข้าทำปฏิกิริยาhybridization ที่อุณหภูมิห้อง

ในระบบการตรวจแบบเรืองแสง การจับตัวของโพรบและการแสดงผลดำเนินการโดยการติดฉลากบริเวณ N’ ของเพพไทด์นิวคลิอิค ด้วยฟูโอโรฟอร์ชนิด FAM ร่วมกับโมเลกุลแข่งขันที่ได้จากการสังเคราะห์โอลิโกนิวคลิโอไทด์ ขนาด 5-6 นิวคลิโอไทด์ที่ติดฉลากบริเวณ 3’ ด้วยฟูโอโรฟอร์ชนิด BHQ เนื่องจากโครงสร้างของPNA ไม่มีประจุ โพรบเมื่อจับกับดีเอ็นเอเป้าหมายแล้วจึงไม่เกิดแรงผลัก ทำให้ปรากฏการณ์ hybridization เกิดขึ้นด้วยความจำเพาะสูง การจับตัวเริ่มจาก การนำโมเลกุลเควนเชอร์ไปจับกับโพรบก่อน ยังผลให้ไม่เกิดการเรืองแสง และเมื่อใดที่มีดีเอ็นเอเป้าหมาย จะเกิดการจับตัวของโพรบกับดีเอ็นเอเป้าหมายที่มีเสถียรภาพมากกว่า ส่งผลให้โพรบแยกออกจากเควนเซอร์ จึงทำให้ FAM group ที่ใช้เป็นฟูโอโรฟอร์หลุดออกเป็นอิสระ ไม่เกิดปรากฏการณ์ fluorescence resonance energy transfer (FRET) ขึ้น จึงเกิดการเรืองแสงที่ชัดเจนและช่วยให้การตรวจ ทำได้นอกห้องปฏิบัติการ

สำหรับระบบการเปลี่ยนสีทางแสงของสารละลายอนุภาคนาโนของโลหะ การจับตัวของโพรบบนอนุภาค กระตุ้นให้เกิดการเปลี่ยนแปลงของอนุภาค ทำให้อนุภาคเข้าใกล้ชิดกันมากขึ้นเนื่องจากโพรบทำหน้าที่เป็น coagulant เกิดการเปลี่ยนแปลงคลื่นแม่เหล็กไฟฟ้าของแสง ทำให้เกิดการหักเหด้วยแนวระนาบและความยาวคลื่นที่เปลี่ยนแปลงไป แต่ในภาวะที่มีดีเอ็นเอเป้าหมาย ดีเอ็นเอเป้าหมายจะจับตัวกับโพรบส่งผลให้เกิด hybridization complex ที่เป็น double stand helix จึงทำให้เกิดการปกป้องอนุภาคไม่ให้มาเกาะตัวกันในยามที่มีเกลือเป็นตัวกระตุ้นจึงทำให้อนุภาคไม่เกิดการเปลี่ยนสี ในกรณีอนุภาคนาโนทองคำตัวอย่างที่แสดงผลบวกให้สีแดงขณะที่ตัวอย่างให้ผลลบให้สีม่วง

ด้วยระบบดังกล่าวได้พัฒนาองค์ความรู้สำหรับการตรวจตรวจยีน neuraminidase ของ 2009 H1N1 human influenza A virus ดื้อยา oseltamivir และ ระบบการตรวจไวรัสซิคุนกุนยาสำหรับการประยุกต์ทางการแพทย์และการตรวจยีนจำเพาะต่อไวรัสกุ้ง white spot syndrome virus (WSSV) infectious hypodermal and hematopoietic necrosis virus (IHHNV) ระบบการตรวจยีนจำเพาะต่อไวรัส pineapple mealybug wilt associated virus (PMWaV) สายพันธุ์ 1 และ 2 และการตรวจการสุกแก่ทางสรีระวิทยาผ่านการแสดงออกของยีน *AcSUT1*สำหรับการประยุกต์ทางการเกษตร ให้สามารถดำเนินการได้ในเวลาน้อยกว่า 1 ชั่งโมง ด้วยความแม่นยำ และลดระดับการพึ่งพาห้องปฏิบัติการลง

<u>ส่วนที่ 2</u> เนื้อหากิจกรรมที่ได้ดำเนินการ

กิจกรรมเป้าหมายตามแผนงาน	กิจกรรมที่ได้ดำเนินการ	ผลสัมฤทธิ์
1. การศึกษาเปรียบเทียบลำดับนิวคลิโอไทด์และยีนที่ใช้ในการจำแนกเป้าหมายเพื่อการตรวจวินิจฉัยทางการแพทย์ เกษตร และอาหาร โดยการวิเคราะห์ผ่านโปรแกรมการวิเคราะห์ดีเอ็นเอด้วยคอมพิวเตอร์	ได้ดำเนินการศึกษายีนที่คาดว่าจะใช้เป็นเป้าหมายเปรียบเทียบและค้นหา domain ของยีนที่ต้องการ *'** ได้ออกแบบ และคัดเลือกและตรวจสอบ ไพรเมอร์สำหรับตรวจวิเคราะห์และสังเคราะห์ไพรเมอร์สำหรับระบบการเพิ่มปริมาณดีเอ็นเอ*'**	เป็นไปตามแผน โดยได้ระบบที่ต้องการพัฒนา 5 ระบบ หากเทียบเป็นผลสัมฤทธิ์ให้ผลลัพท์ที่มากกว่าที่เสนอในแผนงาน
2.การโคลนยีนและตรวจสอบลำดับนิวคลิโอไทด์	ได้เพิ่มปริมาณสารพันธุกรรมด้วยวิธี PCR และโคลนยีนสำหรับการพัฒนาระบบการเพิ่มปริมาณดีเอ็นเอ	เป็นไปตามแผน
3. การเก็บตัวอย่างและการสกัดสารพันธุกรรม	ได้ดำเนินการเก็บรวบรวมตัวอย่างและสกัดสารพันธุกรรมที่สอดคล้องกับระบบ	เป็นไปตามแผน
4. การพัฒนาระบบการเพิ่มปริมาณสารพันธุกรรม บนหลักการเพิ่มปริมาณดีเอ็นเออุณหภูมิเดียว	ได้ดำเนินการพัฒนาระบบการเพิ่มปริมาณสารพันธุกรรม	เป็นไปตามแผน
5. การพัฒนาโมเลกุลดีเอ็นเอเพื่อใช้เป็นดีเอ็นเออ้างอิง	ได้ดำเนินการเพิ่มปริมาณโมเลกุลดีเอ็นเอเพื่อใช้เป็นดีเอ็นเออ้างอิง*'**	เป็นไปตามแผน
6. การออกแบบ PNA โพรบและการพัฒนาระบบการตรวจสัญญาณดีเอ็นเอ	ได้ออกแบบ DNA/PNA โพรบสำหรับการตรวจและได้พัฒนาระบบการตรวจสอบสัญญาณผ่านการเรืองแสงของ PNA และการเปลี่ยนสีของตะกอนอนุภาคนาโนของโลหะผ่านการเชื่อมโยงระบบและทดสอบปฏิกิริยา nucleic acid hybridization*'**	เป็นไปตามแผน โดยได้ระบบที่ต้องการพัฒนา 5 ระบบ หากเทียบเป็นผลสัมฤทธิ์ให้ผลลัพท์ที่มากกว่าที่เสนอในแผนงาน
7. การเชื่อมโยงและประเมินระบบการตรวจผ่านการเพิ่มปริมาณสารพันธุกรรมและการตรวจสัญญาณสารพันธุกรรม	ได้ระบบที่เป็นพื้นฐานในการต่อยอดเป็นชุดตรวจสำเร็จรูป*'**	เป็นไปตามแผน
8. การทดสอบปฏิกิริยาและการทดสอบการใช้งาน	ได้ดำเนินการตรวจสอบการใช้งานจากตัวอย่างจริง	เป็นไปตามแผน

หมายเหตุ * สำหรับการประยุกต์ทางการแพทย์ใช้ระบบการตรวจยีน neuraminidase ของ 2009 H1N1 human influenza A virus ดื้อยา oseltamivir และ ระบบการตรวจไวรัสซิคุนกุนยา

** สำหรับการประยุกต์ทางการเกษตรใช้ระบบการตรวจยีนจำเพาะต่อไวรัสกุ้ง white spot syndrome virus (WSSV) infectious hypodermal and hematopoietic necrosis virus (IHHNV) ระบบการตรวจยีนจำเพาะต่อไวรัส pineapple mealybug wilt associated virus (PMWaV) สายพันธุ์ 1 และ 2 และการตรวจการสุกแก่ทางสรีระวิทยาผ่านการแสดงออกของยีน *AcSUT*1

ส่วนที่ 3 รายงานผลการดำเนินงาน

1. บทนำ

การตรวจสารพันธุกรรมเป็นกุญแจสำคัญในเทคโนโลยีการตรวจวิเคราะห์ที่ประยุกต์ใช้ในทางการเกษตรและทางการแพทย์ เนื่องจากการตรวจสารพันธุกรรมให้ข้อมูลที่จำเพาะไปยังลำดับทางพันธุกรรมทั้งในรูปโมเลกุลดีเอ็นเอหรืออาร์เอ็นเอ ที่เชื่อมโยงกับประเด็นปัญหาไม่ว่าจะเป็นเรื่องโรคหรือเรื่องการเปลี่ยนแปลงทางปัจจัยพันธุกรรม

นับตั้งแต่การค้นพบโครงสร้างดีเอ็นเอเกลียวคู่โดย Watson และ Click ในปี 1953 เทคนิคการตรวจวิเคราะห์ทางพันธุกรรมได้รับการพัฒนาอย่างต่อเนื่องเริ่มจาก การพัฒนาเทคนิค PCR ที่อาศัยความจำเพาะของลำดับนิวคลิโอไทด์ระหว่างคู่ไพรเมอร์และสารพันธุกรรมเป้าหมาย ไปจนถึงการเชื่อมโยงกับเอนไซม์จำเพาะ (restriction enzyme) ที่การจับตัวเป็นแบบจำเพาะต่อลำดับนิวคลิโอไทด์ที่เป็นตำแหน่งจดจำ หรือการตรวจสอบลำดับนิวคลิโอไทด์โดยการทำ nucleic acid hybridization เหล่านี้ทำให้การตรวจความจำเพาะ หรือแม้กระทั่งการหาลำดับนิวคลิโอไทด์ โดยการทำ micro sequencing โดยตรง เทคนิคเหล่านี้แม้ให้ผลที่มีความจำเพาะและแม่นยำแต่อย่างไรก็ดี การดำเนินการมีกระบวนการที่ซับซ้อน ใช้เวลา

การค้นพบดีเอ็นเอสังเคราะห์ (DNA analog) ในรูปเพปไทด์นิวคลีอิกแอซิด (peptide nucleic acid, PNA) ที่มีคุณสมบัติการจับตัวล้อตามการจับตัวแบบคู่สมของสารพันธุกรรมโดยทั่วไปแต่กลับมีแรงยึดจับ (affinity) สูงกว่า ให้ความจำเพาะมากกว่า ทำให้เปิดโอกาสให้การพัฒนาเทคนิคการตรวจวิเคราะห์ทางพันธุกรรม ทำได้ด้วยความแม่นยำ จำเพาะสูง และลดขั้นตอนที่ยุ่งยากลง

โครงการย่อยที่ 6a เน้นการนำเพปไทด์นิวคลีอิกแอซิด ในรูปเบต้าพิโรลิดินิลเพปไทด์นิวคลีอิกแอซิด มาประยุกต์ใช้ในการพัฒนาระบบการตรวจวิเคราะห์ทางพันธุกรรม โดยเชื่อมโยงกับหลักการทางไบโอเซ็นเซอร์ โดยเฉพาะอย่างยิ่งการนำหลักการมาประยุกต์เพื่อตอบปัญหาการตรวจในระบบที่ง่ายและรวดเร็ว

อาศัยความจำเพาะในการจับตัวระหว่าง PNA และสารพันธุกรรมเป้าหมาย บนหลักการ nucleic acid hybridization technology ที่ PNA มีความโดดเด่นกว่าในแง่ความแน่นในการจับตัว และความจำเพาะในระดับยิ่งยวด ในภาวะการทดสอบที่ควบคุมได้ง่ายและรวดเร็ว อย่างไรก็ดี แม้ในการศึกษาจะครอบคลุมการศึกษาหลายระดับตั้งแต่การเปรียบเทียบลำดับนิวคลิโอไทด์ของยีนที่เกี่ยวข้องกับการตรวจวิเคราะห์ในทางการแพทย์ และปัญหาในภาคการเกษตรและอาหาร การเพิ่มปริมาณดีเอ็นเอเพื่อโคลนยีนและตรวจสอบลำดับนิวคลิโอไทด์ สัญญาณดีเอ็นเอ การเก็บตัวอย่าง เพื่อการทดสอบ การพัฒนาระบบการเพิ่มปริมาณสัญญาณดีเอ็นเอ การพัฒนาโมเลกุลดีเอ็นเอเพื่อใช้อ้างอิง การพัฒนาระบบการตรวจสอบสัญญาณดีเอ็นเอในรูปแบบต่างๆ การเชื่อมโยงระบบเพิ่มปริมาณดีเอ็นเอเข้ากับระบบการตรวจสอบสัญญาณ และการปรับปฏิกิริยาและการประเมินการใช้งาน แต่เนื่องจากการพัฒนาองค์ความรู้สำหรับการตรวจ

วิเคราะห์ อยู่บนพื้นฐานของการตอบโจทย์ปัญหาประยุกต์ ทั้งในด้านการแพทย์ และการเกษตรและอาหาร ดังนั้น ในรายงานจึงได้สรุปเนื้อหา เป็น 3 ส่วน โดยนำทั้งหมดมารายงานรวมกันในแต่ละระบบได้แก่

1) การพัฒนาระบบการเพิ่มปริมาณสารพันธุกรรมอุณหภูมิระนาบเดียว ในส่วนนี้ ครอบคลุมการสืบค้นข้อมูลเพื่อตอบโจทย์ปัญหา การวิเคราะห์ข้อมูลลำดับนิวคลิโอไทด์ และการออกแบบไพรเมอร์สำหรับการพัฒนาระบบการเพิ่มปริมาณดีเอ็นเอ การโคลนยีนเพื่อใช้เป็นโมเลกุลอ้างอิงการพัฒนาระบบการเพิ่มปริมาณสารพันธุกรรม ที่สนองตอบโจทย์ปัญหาทางการแพทย์และการเกษตร

2) การพัฒนาระบบการตรวจสอบสัญญาณดีเอ็นเอ เน้นการแสดงในรูปการเรืองแสง บนพื้นฐาน fluorescence resonance energy transfer (FRET) หรือการเปลี่ยนแปลงสีทางแสง colorimetric measurement ของอนุภาคนาโนของโลหะ

3) การเชื่อมโยงระบบ ข้อ 1 และ 2 เข้าด้วยกัน และการทดสอบประเมินผลปฏิกิริยา

โดยรายงานทั้งสามส่วนพร้อมกันเป็นแต่ละกรณีตามประเด็นปัญหาวิจัยที่ปรากฏ

2. วัตถุประสงค์

เพื่อพัฒนาระบบการตรวจวิเคราะห์ โดยการออกแบบระบบการเพิ่มปริมาณสารพันธุกรรมอย่างง่ายและรวดเร็ว และระบบการตรวจสอบสัญญาณดีเอ็นเอโดยการใช้โพรบในรูปอนาลอกดีเอ็นเอที่เป็นเบต้าพิโรลิดินิลเพปไทด์นิวคลีอิกแอซิด เพื่อตอบสนองการตรวจแบบ point of care สำหรับการตรวจวิเคราะห์ทางการแพทย์และด้านอาหารและการเกษตร

3. วิธีการทดลอง

3.1รวบรวมข้อมูล

สำรวจประเด็นปัญหาทางการแพทย์รวบรวมข้อมูลของลำดับนิวคลิโอไทด์จากธนาคารข้อมูลนิวคลิโอไทด์ GenBankและเปรียบเทียบด้วยการทำ alignment ด้วย Clustal และ Blastn

3.2 ออกแบบไพรเมอร์ที่ใช้ในการตรวจสอบและการเพิ่มปริมาณยีนเป้าหมายด้วยเทคนิคการเพิ่มปริมาณดีเอ็นเอแบบลูปด้วยอุณหภูมิเดี่ยว

เงื่อนไขวิธีการดำเนินการทดลองออกแบบไพรเมอร์เพื่อใช้ในการเพิ่มปริมาณดีเอ็นเอหรืออาร์เอ็นเอแบบลูปด้วยอุณหภูมิเดี่ยวเพื่อให้จำเพาะกับยีนเป้าหมายโดยใช้ข้อมูลของลำดับนิวคลิโอไทด์จากธนาคารข้อมูลนิวคลิโอไทด์ GenBank เพื่อนำไปออกแบบไพรเมอร์โดยโปรแกรม Explorer V4 (Fujitsu, Japan) ประกอบปฏิกิริยาด้วยปริมาตร 10 ไมโครลิตร โดยใช้ไพร์เมอร์คู่ใน 5-10 พิโครโมล, ไพรเมอร์คู่นอก 40-80 พิโครโมล, เอ็นไซม์ *Bst* DNA

polymerase 6-12 ยูนิต, $MgSO_4$ 2-8 มิลลิโมล, betaine 0.8-1.2 โมล, dNTP 1-1.4 มิลลิโมล และดีเอ็นเอต้นแบบ ในช่วง 50 – 100 นาโนกรัม หรือร่วมกับ AMV reverse transcriptase40-200 ยูนิต จากนั้นนำไปบ่มที่อุณหภูมิ 63 องศาเซลเซียส เป็นเวลา 40 นาที และนำดีเอ็นเอที่ได้จากการเพิ่มปริมาณแล้วมาตรวจสอบผลโดยเจลอิเล็กโทรโฟเรซิส

3. 3 การตรวจสอบยืนยันเปรียบเทียบด้วยวิธี PCR

สำหรับการเปรียบเทียบผลการเพิ่มปริมาณดีเอ็นเอดำเนินการเพิ่มปริมาณดีเอ็นเอด้วยเทคนิค PCR อ้างอิงจากรายงานการศึกษาที่มีมาก่อนหน้า ควบคู่กับผลที่ได้จากการเพิ่มปริมาณดีเอ็นเอนำดีเอ็นเอแบบลูปด้วยอุณหภูมิเดี่ยวที่ได้จากการเพิ่มปริมาณมาตรวจสอบผลโดยเจลอิเล็กโทรโฟเรซิส

3.4 การโคลนชิ้นส่วนดีเอ็นเอเพื่อสร้างโมเลกุลอ้างอิง

โคลนชิ้นส่วนดีเอ็นเอที่เพิ่มปริมาณในข้อ 3. 3 ได้ด้วยวิธี TA cloning ตามวิธีที่รายงานในเอกสารประกอบชุดตรวจสำเร็จรูป pGEM ®- T Easy vector system I โดยทำปฏิกิริยาที่อุณหภูมิ 16 องศาเซลเซียส เป็นเวลา 12 ชั่วโมง แล้วนำดีเอ็นเอลูกผสมที่ได้ถ่ายเข้าสู่เซลล์ของแบคทีเรีย *E. coli* สายพันธ์ TOP 10 ด้วยวิธี heat shock (Sambrook *et al.*, 1989) และนำแบคทีเรียไปเลี้ยงในอาหารเลี้ยงแบคทีเรียเหลว LB broth เป็นเวลา 2 ชั่วโมง แล้วนำเชื้อที่ได้มาเกลี่ยในอาหารแบคทีเรียแข็งที่เติมยาปฏิชีวนะแอมพิซิลินเข้มข้น 25 มิลลิกรัมต่อมิลลิลิตร บ่มที่อุณหภูมิ 37 องศาเซลเซียสเป็นเวลา 18 ชั่วโมง ตรวจสอบคัดเลือกโคลนที่ได้โดยการทำ colony direction PCR (Grunenwald, 2001) ตรวจสอบขนาดของดีเอ็นเอที่มีขนาดใกล้เคียงกับขนาดที่ต้องการและเพิ่มปริมาณดีเอ็นเอที่ได้ด้วยวิธี large scale plasmid preparation ตามที่รายงานใน Sambrook *et al.* (1989) นำพลาสมิดที่ได้ไปหาลำดับนิวคลิโอไทด์และตรวจสอบเปรียบเทียบลำดับนิวคลิโอไทด์ที่ได้กับลำดับนิวคลิโอไทด์ของยีน *Pen m 2* ในครัสเตเชียน

3.5 การพัฒนาเทคนิคการตรวจสอบด้วยวิธีการเพิ่มปริมาณดีเอ็นเอแบบลูปด้วยอุณหภูมิเดี่ยว

นำดีเอ็นเอที่สกัดได้จากข้อ 3.2 มาเพิ่มปริมาณด้วยเทคนิคการเพิ่มปริมาณดีเอ็นเอแบบลูปด้วยอุณหภูมิเดี่ยว โดยใช้ชุดไพร์เมอร์เป้าหมายที่ออกแบบไว้ข้างต้น ดำเนินการโดยปฏิกิริยาและ ขั้นตอนเป็นข้อ 3.2 แล้วจึงประเมินศักยภาพของวิธีการเพิ่มปริมาณดีเอ็นเอแบบลูปด้วยอุณหภูมิเดี่ยวเปรียบเทียบกับวิธีมาตรฐานที่มีผู้รายงานไว้

- การตรวจสอบความจำเพาะ (specificity) ของปฏิกิริยาเมื่อใช้ตัวอย่างเป็นตัวอย่างดีเอ็นเอชุดทดสอบ ตรวจสอบแถบดีเอ็นเอที่เพิ่มปริมาณได้แล้วนำไปเปรียบเทียบผลกับผลที่ได้จากวิธีมาตรฐานที่ใช้ PCR

- การตรวจสอบความไวของปฏิกิริยา (sensitivity) โดยใช้ดีเอ็นเอแม่แบบจากพลาสมิดที่ใช้ในข้อ 3.4 โดยแปรผันพลาสมิดที่ทราบจำนวนชุดของดีเอ็นเอจากมากไปหาน้อย (10^6 - 1 ชุด) ตามลำดับ (Anthony, 2000) ตรวจสอบแถบดีเอ็นเอที่เพิ่มปริมาณได้และเปรียบเทียบผลกับผลที่ได้จากวิธีมาตรฐาน

3.6 การตรวจสอบสัญญาณดีเอ็นเอโดยวัดการเปลี่ยนแปลงทางสีของแสงด้วยการตรวจสอบการเรืองแสง

ในการตรวจจับสัญญาณดีเอ็นเอเป้าหมายจากการเพิ่มปริมาณสัญญาณด้วยวิธีเพิ่มปริมาณดีเอ็นเอแบบลูปด้วยอุณหภูมิเดียว จะใช้ดีเอ็นเออนาลอกโพรบชนิดเบต้าพิโรลิดินิลเพปไทด์นิวคลีอิกแอซิดจากวิธีการสังเคราะห์ทางเคมี ที่มีลำดับนิวคลิโอไทด์คู่สมกับดีเอ็นเอเป้าหมายของแต่ละระบบ โพรบสังเคราะห์โดยวิธีการสังเคราะห์แบบ Fmoc solid-phase peptide synthesis (Suparpprom *et al*., 2005, Vilaivan and Srisuwannaket, 2006) และติดฉลากโพรบด้วยฟูออโรฟอร์ FAM โมเลกุลเควนเชอร์ได้จากการสังเคราะห์โดยบริษัท (Biobasic, Canada) หลักการของการแสดงผลการเรืองแสงของการเกิดปฏิกิริยาระหว่างโมเลกุลเควนเชอร์กับดีเอ็นเอเป้าหมายอยู่บนพื้นฐานหลักการ FRET (fluorescence resonance energy transferred) ดีเอ็นเอเป้าหมาย จะถูกตรวจจับสัญญาณได้จากปฏิกิริยาการเรืองแสง โดยชนิดปริมาตรและความเข้มข้นของสารเคมีในปฏิกิริยา ประกอบไปด้วยดีเอ็นเออนาลอกโพรบความเข้มข้น 1 ไมโครโมลาร์ เควนเชอร์ 3 ไมโครโมลาร์ ผลิตภัณฑ์ดีเอ็นเอจากปฏิกิริยาเพิ่มปริมาณดีเอ็นเอแบบลูปด้วยอุณหภูมิเดียว 1 ไมโครลิตร ละลายในสารละลาย PBS ความเข้มข้น 10 มิลลิโมลาร์ ที่อุณหภูมิห้อง แล้วสังเกตการณ์เรืองแสงภายใต้รังสีอัลตร้าไวโอเลต

3.7 การตรวจสอบสัญญาณดีเอ็นเอโดยวัดการเปลี่ยนแปลงทางสีของแสงด้วยอนุภาคทองคำนาโน

การตรวจสอบสัญญาณดีเอ็นเออยู่บนพื้นฐานของการทำ nucleic acid hybridization ระหว่าง DNA-DNA analog probe complex ชนิดเบต้าพิโรลิดินิลเพปไทด์นิวคลีอิกแอซิดโดยในปฏิกิริยาประกอบด้วย อนุภาคทองคำนาโน ขนาด 30 นาโนเมตร ความเข้มข้น 1,200 ppm 5-10 ไมโครลิตร Pienpinijtham *et al*. (2010) ดีเอ็นเอที่ได้จากการเพิ่มปริมาณด้วยเทคนิคลูปอุณหภูมิเดียวในข้อ 3.2 ปริมาตร 1 ไมโครลิตร ดีเอ็นเออนาลอกโพรบ 1 ไมโครลิตร ภายใต้การควบคุมปริมาณเกลือความเข้มข้น 10 มิลลิโมล ปริมาตร 0.2 ไมโครลิตร สังเกตเห็นการเปลี่ยนแปลงของการตกตะกอนของอนุภาคทองคำนาโนภายใน 5 นาที พร้อมทั้งดำเนินการหาความจำเพาะของปฏิกิริยา ความไวของปฏิกิริยา และ การตรวจหายีนเป้าหมายโดยใช้ตัวอย่างดีเอ็นเอที่ได้ในข้อ 3.2

4. ผลการวิจัย

4.1 การประยุกต์ใช้เบต้าพิโรลิดินิลเพปไทด์นิวคลีอิกแอซิดในทางการแพทย์

ในปัจจุบัน ปัญหาของโรคอุบัติใหม่ และโรคอุบัติซ้ำ กลายเป็นปัญหาที่สำคัญที่ส่งผลกระทบต่อสุขภาพและความมั่นคงทางสุขภาพของประชากรโลก โดยเฉพาะการเกิดขึ้นของโรคไข้หวัดใหญ่สายพันธุ์ใหม่ 2009 การระบาดของเชื้อ human influenza A virus 2009 อย่างรวดเร็วและในบางรายที่พบการติดเชื้อเข้าสู่ระบบทางเดินหายใจส่วนล่าง (WHO, 2009a) ส่งผลให้เกิดการระบาดรุนแรงถึงขั้นเสียชีวิตได้ การกลับมาระบาดอีกครั้งของโรคชิคุนกุนยา (chikun gunya) การระบาดของเชื้อ enterovirus ในหลายประเทศ การกลายพันธุ์ของไวรัสหวัดนกไปสู่สายพันธุ์ที่รุนแรงและระบาดไปทั่ว การกลับมาของการระบาดของกลุ่มเชื้อวัณโรค เหล่านี้สะท้อนให้เห็นถึงความจำเป็นในการพัฒนาการตรวจวินิจฉัยเชื้อให้ได้อย่างรวดเร็ว

ในปัจจุบัน การดำเนินการทางการแพทย์ต่อการพัฒนาการตรวจวินิจฉัยเชื้อมักเน้นการตรวจวิเคราะห์เชื้อโดยเทคนิค PCR โดยเฉพาะด้วยเทคนิค Real time PCR ซึ่งเป็นเทคนิคที่ต้องพึ่งพาเครื่องมือและความชำนาญการทางเทคนิค และเป็นเทคนิคที่การใช้งานจำกัดอยู่เฉพาะในห้องปฏิบัติการที่มีความพร้อมเท่านั้น (Centers for Disease Control and Prevention, 2009) การตรวจสอบสายพันธุ์จำเพาะด้วยแนวคิดใหม่ที่ลดการพึ่งพาห้องปฏิบัติการและการพึ่งพาเครื่องมือและความชำนาญการทางเทคนิคจึงมีความสำคัญ

การตรวจสารพันธุกรรมบนพื้นฐานโมเลกุลในทางปฏิบัติจะประกอบด้วยขั้นตอน 3 ขั้น ได้แก่ การสกัดกรดนิวคลิอิคจากเนื้อตัวอย่าง การเพิ่มปริมาณสัญญาณของกรดนิวคลิอิคผ่านการเพิ่มปริมาณกรดนิวคลิอิคเป้าหมาย และการตรวจสอบสัญญาณของกรดนิวคลิอิคเพื่อการแสดงผล การสกัดกรดนิวคลิอิคจากเนื้อตัวอย่างเป็นขั้นตอนที่ได้รับการพัฒนาไปมาก วิธีการการสกัดดีเอ็นเอหรืออาร์เอ็นเอ และขั้นตอนการสกัดดีเอ็นเอหรืออาร์เอ็นเอที่ใช้มักอ้างอิงตามวิธีการวิเคราะห์ที่ได้รายงานไว้ในแหล่งข้อมูลต่างๆเช่น CDC หรือตามที่ปรากฏในวิธีการวิเคราะห์มาตรฐานตามเอกสารแนะนำของแต่ละประเทศ ส่วนใหญ่มักจะพบว่าสามารถนำหลักการและวิธีมาปรับแต่งให้มีความสะดวก เหมาะสม ให้ง่าย และมีประสิทธิภาพ สอดคล้องไปกับตัวอย่างที่ส่งมาตรวจวิเคราะห์ได้ไม่ยากนัก หากมีความรู้ความเข้าใจก็จะสามารถปรับแต่งวิธีการสกัดดีเอ็นเอที่เหมาะสมกับเนื้อตัวอย่างแต่ละชนิดได้ ดังนั้นการพัฒนาการตรวจจึงเน้นไปที่การเพิ่มปริมาณสัญญาณของกรดนิวคลิอิคผ่านการเพิ่มปริมาณกรดนิวคลิอิคเป้าหมาย และการตรวจสอบสัญญาณของกรดนิวคลิอิคเพื่อการแสดงผลแทน

การเพิ่มปริมาณสัญญาณของกรดนิวคลิอิค ผ่านการเพิ่มปริมาณกรดนิวคลิอิคเป้าหมายให้มีจำนวนมาก (amplification) นั้นในช่วงทศวรรษที่ผ่านมาได้มีการนำเทคนิคการเพิ่มปริมาณดีเอ็นเอด้วยปฏิกิริยาลูกโซ่พอลิเมอร์เรสหรือ PCR (Polymerase Chain Reaction) มาใช้ ตัวเทคนิคมีบทบาทอย่างมากในงานวิจัยสาขาต่างๆ ช่วยในการเพิ่มปริมาณดีเอ็นเอเป้าหมายใดๆที่นักวิทยาศาสตร์สนใจได้อย่างมีประสิทธิภาพอย่างที่ไม่เคยมีมาก่อน

โดยหลักการ เทคนิคPCRนี้เลียนแบบการจำลองดีเอ็นเอในธรรมชาติ โดยอาศัยเอนไซม์ DNA polymerase ทนร้อน กลไกเริ่มจากการคลายเกลียวของดีเอ็นเอแม่แบบด้วยความร้อนทดแทนการทำหน้าที่ของเอนไซม์ helicase และ topoisomerase จนได้ดีเอ็นเอแม่แบบที่เป็นสายเดี่ยว ssDNA จากนั้นอาศัยความจำเพาะของดีเอ็นเอสายสั้นๆ ที่เป็น oligonucleotide primer แทนการสังเคราะห์ RNA primerในธรรมชาติโดยเอนไซม์ primase ช่วยให้เกิดการจับตัวระหว่าง oligonucleotide primer กับดีเอ็นเอแม่แบบภายหลังการลดอุณหภูมิลง เมื่อไพร์เมอร์มาจับตัวกับดีเอ็นเอแม่แบบที่เป็นสายเดี่ยวที่ได้จากขั้นตอนแรก บริเวณปลาย 3’ ของ primer จะใช้เป็นเป็นจุดเริ่มต้นในการต่อสายดีเอ็นเอให้ยาวออกไปด้วยปฏิกิริยา polymerization โดยพอลิเมอร์เรสทนร้อนที่เรียกว่า thermophilic DNA polymerase โดยใช้ dNTP เป็นวัตถุดิบ ทั้ง 3 ขั้นตอนมีอุณหภูมิที่เหมาะสมต่างกัน การคลายเกลียวที่เรียกว่า denaturation จะดำเนินการที่ 50-53°C การชักนำให้ไพรเมอร์จับตัวกับดีเอ็นเอแม่แบบเรียกว่า annealing จะดำเนินการที่ 50-55°C และท้ายสุดการต่อสายดีเอ็นเอให้ยาวขึ้นเรียกว่า extention จะดำเนินการที่อุณหภูมิ 70-73 °C ในหนึ่งรอบดีเอ็นเอจะเพิ่มจาก 1 เป็น 2 และเมื่อครบ 30 รอบ จะเพิ่มดีเอ็นเอได้ในระดับ 1030 ล้านโมเลกุล ด้วยเหตุนี้จึงทำให้การเพิ่มปริมาณดีเอ็นเอด้วยเทคนิค PCR ต้องขึ้นกับระบบการควบคุมอุณหภูมิต่างกัน 3 ระดับให้แม่นยำอยู่ตลอดเวลา การควบคุมอุณหภูมิอยู่นี้ดำเนินการในรูปอุปกรณ์เฉพาะที่รู้จักในนาม thermo cycler (Saiki, 1988)

การที่ระบบการเพิ่มปริมาณดีเอ็นเอต้องผูกติดกับระบบควบคุมอุณหภูมิ ทำให้การดำเนินการต้องลงทุนด้านเครื่องมือ ซึ่งปัจจุบันมีราคาไม่น้อยกว่า 3-4 แสนบาทสำหรับตัวมาตรฐาน และต้องใช้ระยะเวลาในการทำปฏิกิริยาที่อาจนานถึง 3-4 ชั่วโมง ต้องใช้บุคลากรที่มีทักษะความชำนาญ และต้องเสริมด้วยเทคนิคบางเทคนิคในการวิเคราะห์ วินิจฉัยและสรุปผล เหล่านี้ทำให้ไม่สามารถตอบสนองหลักการ point of care ที่เน้นการตรวจวิเคราะห์ที่ดำเนินการได้ในทุกที่ แม้ในคลินิกเล็กๆ ในโรงงานอุตสาหกรรม ในสถานที่เกิดเหตุ หรือในไร่นา เป็นต้น

แม้ในปัจจุบัน เทคนิค PCR ได้รับการยอมรับเป็นวิธีมาตรฐานในการตรวจเชื้อหลายชนิดในทางการแพทย์ ซึ่งพิสูจน์แล้วว่าใช้งานได้เป็นอย่างดี (Lockley and Bardsley, 2000) แต่ด้วยข้อจำกัดในการนำไปใช้ข้างต้น ทำให้จำเป็นต้องพัฒนาวิธีการตรวจรูปแบบใหม่ๆ เพื่อเป็นทางเลือก

นวัตกรรมทางเทคโนโลยีในปัจจุบันส่งผลให้วิธีการตรวจมีความหลากหลายมากขึ้น ตัวอย่างที่สำคัญได้แก่ การเพิ่มปริมาณโดยอาศัยลำดับนิวคลิโอไทด์เป็นพื้นฐาน (sequence-based amplification) (Compton, 1991) การเพิ่มปริมาณจากการจำลองตัวเอง (self-sustained replication) (Guatelli *et al.*, 1990) การเพิ่มปริมาณโดยการใช้ปฏิกิริยาแทนที่สายดีเอ็นเอ (strand displacement amplification) และการเพิ่มปริมาณอุณหภูมิระนาบเดียว (Walker *et al.,* 1992) โดยการชักนำในระบบห่วง (Loop mediated isothermal amplification) (Notomi, 2000) นอกเหนือจากนี้ยังพบว่ามีผู้คิดค้นวิธีการเพิ่มปริมาณสัญญาณที่เป็นดีเอ็นเอขนาดสั้นๆ ได้แก่

branched DNA amplification (bDNA) invader และ rolling circle amplification (Lyamichev *et al*., 1999 และ Lizardi *et al*., 1998) ซึ่งเทคนิคในกลุ่มหลังจัดเป็นวิธีการเพิ่มปริมาณดีเอ็นเอตรงบริเวณเป้าหมาย

จากการเปรียบเทียบข้อดีข้อเสียทางเทคนิคพบว่า นอกจากเทคนิค PCR แล้ว การเพิ่มปริมาณดีเอ็นเอด้วยหลักการชักนำให้เพิ่มปริมาณดีเอ็นเออุณหภูมิระนาบเดียวโดยการชักนำในระบบห่วง (LAMP) มีข้อเด่นกว่าเทคนิคอื่นโดยเฉพาะการใช้อุณหภูมิระนาบเดียว(Notomi, 2000) โดยที่ไม่มีกระบวนการทางความร้อนต่างระดับอุณหภูมิ มาคลายสายดีเอ็นเอจากเกลียวคู่ให้กลายเป็นสายเดียวมาเกี่ยวข้อง จึงสามารถประยุกต์ใช้ในการเพิ่มปริมาณกรดนิวคลีอิกทั้งดีเอ็นเอและอาร์เอ็นเอได้ในระดับที่ใกล้เคียงกัน ปฏิกิริยา LAMP อาศัยเอนไซม์ DNA polymersase ที่มีกิจกรรมแทนที่สายดีเอ็นเอในตัว โดยการผลักสายดีเอ็นเอเดิมให้หลุดออกและแทนที่ด้วยการสังเคราะห์สายใหม่ การใช้ไพรเมอร์ 2-3 คู่ ทำให้ความเฉพาะเจาะจงของปฏิกริยาสูงมาก มากกว่าเทคนิค PCR ที่เคยทำได้ถึง1000 เท่าในเวลาที่น้อยกว่า นำให้เทคนิคนี้เหมาะที่จะใช้เพิ่มปริมาณสารพันธุกรรมจากตัวอย่างทางการแพทย์ หรือแม้กระทั่งตัวอย่างอาหารหลากวัตถุดิบที่มักมีดีเอ็นเอหลากชนิดปนกัน การที่อุณหภูมิเป็นระนาบเดียวที่ 63-65^{0}C จึงทำให้การตรวจสอบไม่จำเป็นต้องใช้เครื่องมือควบคุมอุณหภูมิอัตโนมัติที่ใช้สำหรับPCR ซึ่งมีข้อจำกัด จึงเหมาะอย่างยิ่งในการนำมาประยุกต์ใช้ในการออกแบบระบบตรวจสอบให้สามารถดำเนินการได้ แม้ในสถานที่ที่ขาดความพร้อมของเครื่องมือ

การวิจัยในครั้งนี้จึงมุ่งพัฒนาวิธีการตรวจสอบโรคโดยการวิเคราะห์ทางพันธุกรรม ที่ใช้งานง่ายและมีประสิทธิภาพโดยพื้นฐานการวิเคราะห์โมเลกุลดีเอ็นเอหรืออาร์เอ็นเอ เพื่อเชื่อมโยงกับเทคนิคการตรวจสัญญาณดีเอ็นเอที่ประยุกต์ใช้เบต้าพิโรลิดินิลเพปไทด์นิวคลีอิกแอซิดเป็นโพรบ โดยบูรณาการเทคนิคการเพิ่มปริมาณดีเอ็นเอด้วยอุณหภูมิระนาบเดียวที่เรียกว่า LAMP พร้อมทั้งพัฒนาดีเอ็นเอที่ใช้ตรวจสอบในรูปโคลนดีเอ็นเอ เน้นการตอบโจทย์ทางการแพทย์ที่สำคัญดังนี้

4.1.1 พัฒนาวิธีการตรวจสอบไข้หวัดชนิด 2009 human influenza A virus สายพันธุ์ดื้อยา Oseltamivir

การตรวจสอบเอกสารเบื้องต้นพบว่าไข้หวัดชนิด 2009 human influenza A virus มีแนวโน้มจะกลายพันธุ์ในยีน Neuraminidase ทำให้เกิดการดื้อต่อยา oseltamivir ได้ และเมื่อ WHO ได้รายงานการพบการกลายพันธุ์ของเชื้อไวรัสไข้หวัดใหญ่สายพันธุ์ใหม่ 2009 ที่ดื้อต่อยา oseltamivir ในฮ่องกง เดนมาร์ก และญี่ปุ่น ทำให้ทั่วโลกตระหนักถึงความสำคัญ และมุ่งเน้นศึกษารูปแบบการกลายและลำดับนิวคลิโอไทด์ของไวรัสพันธุ์กลายเหล่านี้ (WHO, 2009b)

การกลายของเชื้อไข้หวัดที่ยีน Neuraminidase (N) ของไวรัสในกลุ่ม 1 จะพบเป็น H275Y/ N294S และในกลุ่ม 2 (N2) เป็น R292K ส่งผลต่อการดื้อยา 80 เท่าและ 700-1700 เท่า ตามลำดับ (Collin *et al*., 2008)

การศึกษาโดย Rungrotmonglol *et al*., (2009) ได้ทำนายทิศทางการกลายพันธุ์ที่มีประสิทธิภาพของไวรัสผ่านการสร้างโมเดลทำนายค่า ΔG binding หรือ free energy พบว่าการกลายที่ตำแหน่ง N294S H275Y และ R292K เป็นตำแหน่งที่ทำใช้เกิดความสามารถในการต้านทานยา oseltamivir ได้ดีตามลำดับ

การพัฒนาการตรวจสายพันธุ์กลายเน้นการพัฒนาเทคนิคที่มีความแตกต่างในเรื่องประสิทธิภาพและการใช้งานไปจาก real time PCR ที่ใช้ในปัจจุบัน เริ่มจากได้ดำเนินการสำรวจข้อมูลลำดับนิวคลิโอไทด์ของสายพันธุ์ 2009 human influenza A virus จากหลายแหล่งเทียบกับสายพันธุ์กลายจาก ฮ่องกงและเดนมาร์ก สหรัฐอเมริกา(WHO, 2009b)

ผลการเปรียบเทียบลำดับนิวคลิโอไทด์ของยีน neuraminidase ของสายพันธุ์ไข้หวัดใหญ่สายพันธุ์ใหม่ (H1N1) ทั้งหมดจากจำนวนตัวอย่างตัวแทนที่รายงานในธนาคารข้อมูล CDC 25 ชนิดจาก 120 ชนิด พบว่า สายพันธุ์ 2009 H1N1 human influenza A virus เป็นไวรัสสายพันธุ์ใหม่ มียีน neuraminidase ต่างไปจาก H1N1 human influenza A virus เล็กน้อย แต่ภายในกลุ่ม 2009 H1N1 human influenza A virus มีลำดับนิวคลิโอไทด์คล้ายกัน (similarlity) ในระดับสูงถึง 99-100 % similarity (ภาพที่ 1.) ความคล้ายกันของสารพันธุกรรม จัดอยู่ในระดับเรียกได้ว่าเป็นสายพันธุ์เดียวกันทั้งหมด ความแตกต่างในระดับ 1% เป็นเพียงความแตกต่างเพียง 1-2 นิวคลิโอไทด์ ซึ่งเป็นเพียงการกลายในรูปแบบ transition ที่มักพบโดยทั่วไปกับยีนของไวรัส

SeqA	Name	Lenght(nt)	SeqB	Name	Lenght(nt)	Score (% similarity)
1	CY039988	1410	2	GQ179931	1382	99
1	CY039988	1410	3	GQ179932	1382	100
1	CY039988	1410	4	GQ150343	1438	99
1	CY039988	1410	5	GQ169381	1410	99
1	CY039988	1410	6	A/Hong	1410	99
2	GQ179931	1382	3	GQ179932	1382	99
2	GQ179931	1382	4	GQ150343	1438	99
2	GQ179931	1382	5	GQ169381	1410	99
2	GQ179931	1382	6	A/Hong	1410	99
3	GQ179932	1382	4	GQ150343	1438	99
3	GQ179932	1382	5	GQ169381	1410	99
3	GQ179932	1382	6	A/Hong	1410	99
4	GQ150343	1438	5	GQ169381	1410	100
4	GQ150343	1438	6	A/Hong	1410	99
5	GQ169381	1410	6	A/Hong	1410	99

ภาพที่ 1 การเปรียบเทียบความคล้ายของลำดับนิวคลิโอไทด์ของยีน neuraminidase ระหว่างสายพันธุ์ของไวรัสไข้หวัดใหญ่สายพันธุ์ใหม่ 2009 โดยไวรัสตัวแทนแต่ละสายพันธ์ระบุด้วยหมายเลข accession number ในส่วนสายพันธุ์กลาย (ฮ่องกง) ที่ต้านทาน oseltamivir ระบุเป็น A/Hong

อย่างไรก็ดีหากการเปรียบเทียบลำดับนิวคลิโอไทด์กับไวรัสสายพันธุ์ที่ต้านทานยา oseltamivir พบว่าลำดับนิวคลิโอไทด์ส่วนใหญ่มีความคล้ายกัน ยกเว้นการเปลี่ยนแปลงของลำดับนิวคลิโอไทด์จาก C เป็น T ที่ตำแหน่ง 825 (ภาพที่ 2.)

```
GQ179931        AACAATATATTGAGAACACAAGAGTCTGAATGTGCATGTGTAAATGGTTCTTGCTTTACT 720
GQ179932        AACAATATATTGAGAACACAAGAGTCTGAATGTGCATGTGTAAATGGTTCTTGCTTTACT 720
CY039988        AACAATATATTGAGAACACAAGAGTCTGAATGTGCATGTGTAAATGGTTCTTGCTTTACT 720
GQ150343        AACAATATATTGAGAACACAAGAGTCTGAATGTGCATGTGTAAATGGTTCTTGCTTTACT 720
GQ169381        AACAATATATTGAGAACACAAGAGTCTGAATGTGCATGTGTAAATGGTTCTTGCTTTACT 720
A/Hong          AACAATATATTGAGAACACAAGAGTCTGAATGTGCATGTGTAAATGGTTCTTGCTTTACT 720
                ************************************************************

GQ179931        GTAATGACCGATGGACCAAGTGATGAACAGGCCTCATACAAGATCTTCAGAATAGAAAAG 780
GQ179932        GTAATGACCGATGGACCAAGTGATGAACAGGCCTCATACAAGATCTTCAGAATAGAAAAG 780
CY039988        GTAATGACCGATGGACCAAGTGATGAACAGGCCTCATACAAGATCTTCAGAATAGAAAAG 780
GQ150343        GTAATGACCGATGGACCAAGTGATGGACAGGCCTCATACAAGATCTTCAGAATAGAAAAG 780
GQ169381        GTAATGACCGATGGACCAAGTGATGGACAGGCCTCATACAAGATCTTCAGAATAGAAAAG 780
A/Hong          GTAATGACCGATGGACCAAGTGATGGACAGGCCTCATACAAGATCTTCAGAATAGAAAAG 780
                ************************* ********************************

                                                  275 mutation
GQ179931        GGAAAGATAGTCAAATCAGTCGAAATGAATGCCCCTAATTATCACTATGAGGAATGCTCC 840
GQ179932        GGAAAGATAGTCAAATCAGTCGAAATGAATGCCCCTAATTATCACTATGAGGAATGCTCC 840
CY039988        GGAAAGATAGTCAAATCAGTCGAAATGAATGCCCCTAATTATCACTATGAGGAATGCTCC 840
GQ150343        GGAAAGATAGTCAAATCAGTCGAAATGAATGCCCCTAATTATCACTATGAGGAATGCTCC 840
GQ169381        GGAAAGATAGTCAAATCAGTCGAAATGAATGCCCCTAATTATCACTATGAGGAATGCTCC 840
A/Hong          GGAAAGATAGTCAAATCAGTCGAAATGAATGCCCCTAATTATTACTATGAGGAATGCTCC 840
                *************************************************************

GQ179931        TGTTATCCTGATTCTAGTGAAATCACATGTGTGTGCAGGGATAACTGGCATGGCTCGAAT 900
GQ179932        TGTTATCCTGATTCTAGTGAAATCACATGTGTGTGCAGGGATAACTGGCATGGCTCGAAT 900
CY039988        TGTTATCCTGATTCTAGTGAAATCACATGTGTGTGCAGGGATAACTGGCATGGCTCGAAT 900
GQ150343        TGTTATCCTGATTCTAGTGAAATCACATGTGTGTGCAGGGATAACTGGCATGGCTCGAAT 900
GQ169381        TGTTATCCTGATTCTAGTGAAATCACATGTGTGTGCAGGGATAACTGGCATGGCTCGAAT 900
A/Hong          TGTTATCCTGATTCTAGTGAAATCACATGTGTATGCAGGGATAACTGGCATGGCTCGAAT 900
                ******************************** ***************************

GQ179931        CGACCGTGGGTGTCTTTCAACCAGAATCTGGAATATCAGATAGGATACATATGCAGTGGG 960
GQ179932        CGACCGTGGGTGTCTTTCAACCAGAATCTGGAATATCAGATAGGATACATATGCAGTGGG 960
CY039988        CGACCGTGGGTGTCTTTCAACCAGAATCTGGAATATCAGATAGGATACATATGCAGTGGG 960
GQ150343        CGACCGTGGGTGTCTTTCAACCAGAATCTGGAATATCAGATAGGATACATATGCAGTGGG 960
GQ169381        CGACCGTGGGTGTCTTTCAACCAGAATCTGGAATATCAGATAGGATACATATGCAGTGGG 960
A/Hong          CGACCGTGGGTGTCTTTCAACCAGAATCTGGAATATCAGATAGGATACATATGCAGTGGG 960
                ************************************************************
```

ภาพที่ 2 การเปรียบเทียบความคล้ายของลำดับนิวคลิโอไทด์ของยีน neuraminidase ระหว่างสายพันธุ์ของไวรัสไข้หวัดใหญ่สายพันธุ์ใหม่ 2009 ระหว่างสายพันธุ์ของไวรัสไข้หวัดใหญ่สายพันธุ์ใหม่ 2009 กับสายพันธุ์กลาย (ฮ่องกง) ที่ต้านทาน oseltamivir โดยไวรัสตัวแทนแต่ละสายพันธ์ระบุด้วยหมายเลข accession number ในส่วนสายพันธุ์กลาย (ฮ่องกง ระบุเป็น A/Hong และตำแหน่งการกลายที่ 275 ระบุด้วยตัวเลข

ผลดังกล่าวจะสอดคล้องกับผลการเปลี่ยนแปลงของลำดับนิวคลิโอไทด์ของกรดอะมิโนตำแหน่งที่ 275 จาก H เป็น Y ในตำแหน่งที่เทียบเคียงได้กับการเปลี่ยนแปลงที่ต้านทานยา oseltamivir ในไข้หวัดใหญ่สายพันธุ์ปกติ H1N1 ที่พบในแถบทวีปยุโรป และแคนาดาในหลายปีที่ผ่านมา (Meijer, *et al.*, 2009)

ความคล้ายกันของลำดับนิวคลิโอไทด์ของยีน Neuraminidase ในไข้หวัดใหญ่สายพันธุ์ใหม่ 2009 และความต่างของลำดับนิวคลิโอไทด์ ทำให้สามารถนำลำดับนิวคลิโอไทด์มาใช้เป็นแม่แบบในการออกแบบไพรเมอร์ โครงการได้ดำเนินการออกแบบไพร์เมอร์โดยการกลายเน้นการเพิ่มสัญญาณดีเอ็นเอ (cDNA) ผ่านการเพิ่มปริมาณดีเอ็นเอด้วยปฏิกิริยาอุณหภูมิเดียว เน้นการออกแบบที่ครอบคลุมบริเวณที่เกิดการกลาย เพื่อจะได้ใช้ระบบการเพิ่มปริมาณดีเอ็นเอร่วม

ไปกับระบบตรวจสอบลำดับนิวคลิโอไทด์ด้วยโพรบที่เป็นตัวตรวจจับที่เป็นเบต้าพิโรลิดินิลเพปไทด์นิวคลีอิกแอซิดในภายหลัง

การออกแบบและคัดเลือกไพรเมอร์ด้วยไปรแกรม Primer Explorer Ver 4.0 (Fujitsu, Japan) และคัดเลือกผ่านเงื่อนไขเสถียรภาพทางอุณหภูมิ ตำแหน่งการจับตัว และโอกาสในการเพิ่มปริมาณดีเอ็นเอที่จำเพาะ ทำให้ได้ไพรเมอร์ 4 ชนิดครอบคลุม 6 บริเวณของยีน neuraminidase ดังตารางที่ 1. โดยแต่ละไพรเมอร์ มีตำแหน่งสอดคล้องกับลำดับนิวคลิโอไทด์ของยีน neuraminidase ตำแหน่ง 718-731 752-818 904-929 และ 930-953 ตามลำดับ

ตารางที่ 1. ชุดของไพรเมอร์ที่ใช้ตรวจวิเคราะห์ยีน neuraminidase และลำดับนิวคลิโอไทด์ที่เกี่ยวข้อง

Primer name	Corresponding sequence (5'-3')	Position
09NeuraF3	ACTGTAATGACCGATGGA	718-731
09NeuraF2	TACAAGATCTTCAGAATAGAAAAGG	756-781
09Neura F1c	TTAGGGGCATTCATTTCGACT	797-818
09Neura B1c	TTCTAGTGAAATCACATGTGTGT	852-875
09NeuraB2	GTTGAAAGACACCCACGG	904-921
09NeuraB3	CATATGTATCCTATCTGATATTCCA	930-953

การตรวจสอบความเฉพาะเจาะจงโดยการทำ Basic Local Alignment Search พบว่าไพรเมอร์ที่ออกแบบได้มีทั้ง 6 บริเวณ จำเพาะต่อ N1 ยีน โดยมีความสัมพันธ์ชนิด 100% กับเฉพาะ 2009 H1N1 human influenza A virus มีค่า E value 0.0002-0.10

ความสัมพันธ์ของไพร์เมอร์และลำดับนิวคลิโอไทด์ปันดังภาพที่ 3.

```
GQ179931        AACAATATATTGAGAACACAAGAGTCTGAATGTGCATGTGTAAATGGTTCTTGCTTTACT 720
GQ179932        AACAATATATTGAGAACACAAGAGTCTGAATGTGCATGTGTAAATGGTTCTTGCTTTACT 720
CY039988        AACAATATATTGAGAACACAAGAGTCTGAATGTGCATGTGTAAATGGTTCTTGCTTTACT 720
GQ150343        AACAATATATTGAGAACACAAGAGTCTGAATGTGCATGTGTAAATGGTTCTTGCTTTACT 720
GQ169381        AACAATATATTGAGAACACAAGAGTCTGAATGTGCATGTGTAAATGGTTCTTGCTTTACT 720
A/Hong          AACAATATATTGAGAACACAAGAGTCTGAATGTGCATGTGTAAATGGTTCTTGCTTTACT 720
                ************************************************************

                     F3                                          F2
GQ179931        GTAATGACCGATGGACCAAGTGATGAACAGGCCTCATACAAGATCTTCAGAATAGAAAAG 780
GQ179932        GTAATGACCGATGGACCAAGTGATGAACAGGCCTCATACAAGATCTTCAGAATAGAAAAG 780
CY039988        GTAATGACCGATGGACCAAGTGATGAACAGGCCTCATACAAGATCTTCAGAATAGAAAAG 780
GQ150343        GTAATGACCGATGGACCAAGTGATGGACAGGCCTCATACAAGATCTTCAGAATAGAAAAG 780
GQ169381        GTAATGACCGATGGACCAAGTGATGGACAGGCCTCATACAAGATCTTCAGAATAGAAAAG 780
A/Hong          GTAATGACCGATGGACCAAGTGATGGACAGGCCTCATACAAGATCTTCAGAATAGAAAAG 780
                ************************ ***********************************

                                      F1c          275 mutation
GQ179931        GGAAAGATAGTCAAATCAGTCGAAATGAATGCCCCTAATTATCACTATGAGGAATGCTCC 840
GQ179932        GGAAAGATAGTCAAATCAGTCGAAATGAATGCCCCTAATTATCACTATGAGGAATGCTCC 840
CY039988        GGAAAGATAGTCAAATCAGTCGAAATGAATGCCCCTAATTATCACTATGAGGAATGCTCC 840
GQ150343        GGAAAGATAGTCAAATCAGTCGAAATGAATGCCCCTAATTATCACTATGAGGAATGCTCC 840
GQ169381        GGAAAGATAGTCAAATCAGTCGAAATGAATGCCCCTAATTATCACTATGAGGAATGCTCC 840
A/Hong          GGAAAGATAGTCAAATCAGTCGAAATGAATGCCCCTAATTATTACTATGAGGAATGCTCC 840
                ******************************************************************

                                  B1c
GQ179931        TGTTATCCTGATTCTAGTGAAATCACATGTGTGTGCAGGGATAACTGGCATGGCTCGAAT 900
GQ179932        TGTTATCCTGATTCTAGTGAAATCACATGTGTGTGCAGGGATAACTGGCATGGCTCGAAT 900
CY039988        TGTTATCCTGATTCTAGTGAAATCACATGTGTGTGCAGGGATAACTGGCATGGCTCGAAT 900
```

```
GQ150343        TGTTATCCTGATTCTAGTGAAATCACATGTGTGTGCAGGGATAACTGGCATGGCTCGAAT 900
GQ169381        TGTTATCCTGATTCTAGTGAAATCACATGTGTGTGCAGGGATAACTGGCATGGCTCGAAT 900
A/Hong          TGTTATCCTGATTCTAGTGAAATCACATGTGTATGCAGGGATAACTGGCATGGCTCGAAT 900
                ****************************** ************************

                      B2                          B3
GQ179931        CGACCGTGGGTGTCTTTCAACCAGAATCTGGAATATCAGATAGGATACATATGCAGTGGG 960
GQ179932        CGACCGTGGGTGTCTTTCAACCAGAATCTGGAATATCAGATAGGATACATATGCAGTGGG 960
CY039988        CGACCGTGGGTGTCTTTCAACCAGAATCTGGAATATCAGATAGGATACATATGCAGTGGG 960
GQ150343        CGACCGTGGGTGTCTTTCAACCAGAATCTGGAATATCAGATAGGATACATATGCAGTGGG 960
GQ169381        CGACCGTGGGTGTCTTTCAACCAGAATCTGGAATATCAGATAGGATACATATGCAGTGGG 960
A/Hong          CGACCGTGGGTGTCTTTCAACCAGAATCTGGAATATCAGATAGGATACATATGCAGTGGG 960
                ************************************************************
```

ภาพที่ 3 ความสัมพันธ์ระหว่างไพรเมอร์ทุกตำแหน่งที่ออกแบบได้และบริเวณกลายของอะมิโนตำแหน่ง 275 (ตำแหน่ง 825 บนนิวคลิโอไทด์)

.

การทดสอบการเพิ่มจำนวนเบื้องต้นด้วยเงื่อนไขของปฏิกิริยาที่ 63 °C 20mM Tris-HCl (pH 8.8) 10 mM KCl 10mM $(NH_4)_2SO_4$ 0.1% Triton X-100 ไพรเมอร์ F3 B3 ความเข้มข้น 5 pmol /ปฏิกิริยา ไพรเมอร์ FIP และ BIP ความเข้มข้น 40 pmol /ปฏิกิริยา พบว่าชุดไพรเมอร์ที่ออกแบบได้สามารถเพิ่มปริมาณดีเอ็นเอของยีน neuraminidase ได้โดยจะได้แถบดีเอ็นเอขนาด เทียบเท่าผลคูณของ ช่วงคู่ไพรเมอร์ 180 nt (ภาพที่ 4.)

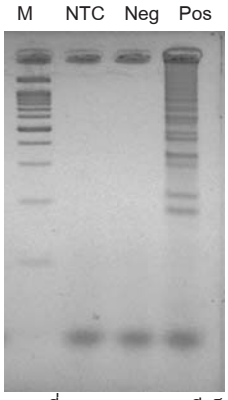

ภาพที่ 4 รูปแบบของดีเอ็นเอผลิตภัณฑ์ที่ได้ภายหลังการเพิ่มปริมาณดีเอ็นเอของยีน neuraminidase ด้วยชุดไพรเมอร์ เลน M , มาร์กเกอร์ ขนาด 100 นิวคลิโอไทด์ เลน NTC non template control เลน Neg เป็นชุดควบคุม (ยีนอื่น) และ Pos เป็นชุดควบคุมบวก (ยีน neuraminidase ของไข้หวัดสายพันธุ์ใหม่)

การตรวจสอบความจำเพาะต่อสายพันธุ์ของไวรัส 9 ชนิด รวมทั้งไข้หวัดใหญ่สายพันธุ์ใหม่ 2009 2 ชนิด และไข้หวัดใหญ่ สายพันธุ์อื่น เช่น H1N1 H3N2 และไข้หวัดนก H5N1 ด้วยเงื่อนไขของปฏิกิริยาเดิม พบว่าคู่ไพรเมอร์ที่ใช้มีความจำเพาะต่อยีน neuraminidase ของหวัดสายพันธุ์ใหม่เท่านั้น (ภาพที่ 5.)

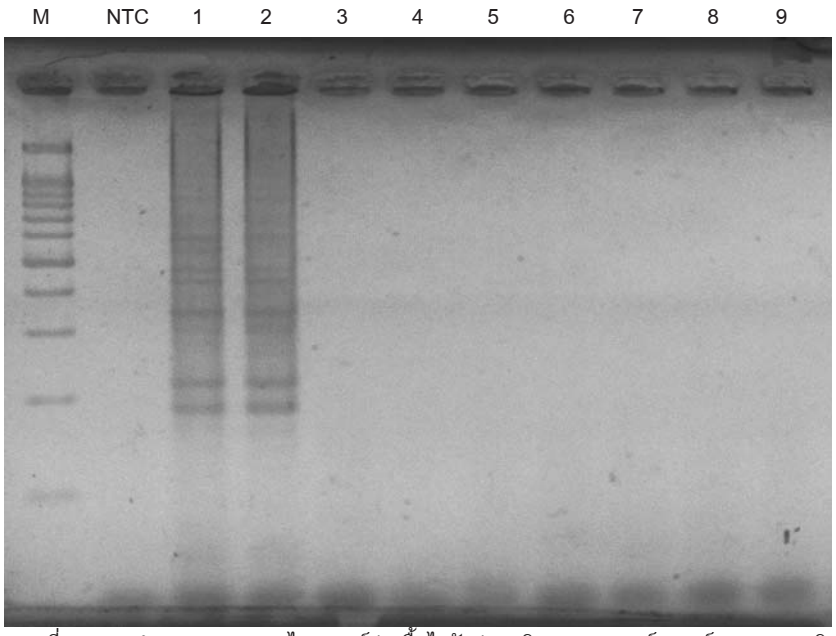

1. Ca H1N1 2009
2. Th H1N1 2009
3. H5N1 Avian Influenza
4. H5N1 Human Influenza
5. H1N1 Swine Influenza
6. H3N2 Swine Influenza
7. H1N1 Human Influenza
8. H3N2 Human Influenza
9. Flu A (H1+H3) + Flu B

ภาพที่ 5 ความจำเพาะจงของชุดไพรเมอร์ต่อเชื้อไวรัสต่างชนิด เลน M มาร์กเกอร์ขนาด 100 นิวคลิโอไทด์ เลน NTC non template control เลน 1-9 ไวรัสไข้หวัดใหญ่สายพันธุ์ใหม่ Ca H1N1 2009 Thailand H1N1 2009 H5N1 Avian influenza H5N1 Human Influenza H1N1 Swine Influenza H3N2 Swine Influenza H1N1 Human Influenza H3N2 Human Influenza และ Flu A (H1+H3) + Flu B ตามลำดับ

การทดสอบความไวของปฏิกิริยาของชุดไพรเมอร์ต่อจำนวนความเข้มข้นของดีเอ็นเอที่ทราบจำนวนชุด(กอปปี้)เจือจางลงระดับละ 10 พบว่าชุดไพรเมอร์มีความไวในการตรวจสอบดีเอ็นเอในระดับ 10^{-7} เทียบเท่าความเข้มข้นของดีเอ็นเอที่ 20 ชุด/ปฏิกิริยา (ภาพที่ 6.)

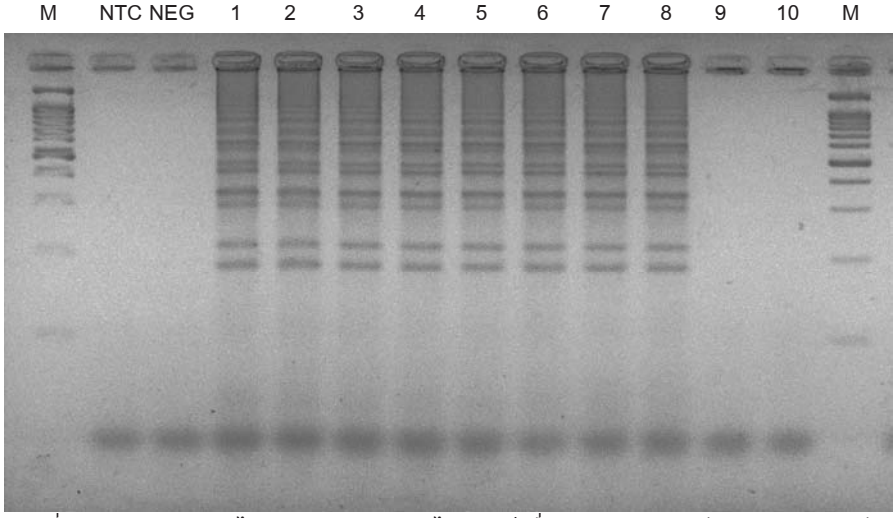

ภาพที่ 6 การทดสอบความไวของปฏิกิริยาของชุดไพรเมอร์ เมื่อลดระดับปริมาณดีเอ็นเอแม่แบบลงทีละ 10 เท่าจาก เลน 1 10000000 ชุด เลนที่ 2 1000000 ชุด เลนที่ 3 100000 เลนที่ 4 10000ชุด เลนที่ 5 1000 ชุด เลนที่ 6 500 ชุด เลนที่ 7 100 ชุด เลนที่ 8 20 ชุด เลนที่ 9 10 ชุด และเลนที่ 10 0 ชุด

จากผลการทดลองที่ได้ดำเนินการพบว่าระบบการเพิ่มปริมาณดีเอ็นเอของยีน neuraminidase มีประสิทธิภาพ และสามารถเพิ่มปริมาณสัญญาณดีเอ็นเอคร่อมบริเวณนิวคลิโอไทด์ตำแหน่ง 825 ได้เป็นอย่างดี

การพัฒนาการตรวจสอบสัญญาณดีเอ็นเอต่อยอด ได้นำหลักการ FRET (fluoresense Resonance Energy Transfer) ระหว่าง donor กับ acceptor ในรูป PNA ที่เป็นเบต้าพิโรลิดินิลเพปไทด์นิวคลีอิกแอซิด

การออกแบบ Probe ที่สามารถเปลี่ยนแปลงสัญญาณการเรืองแสงขณะจับตัวกับดีเอ็นเอเป้าหมาย การเปลี่ยนแปลงอยู่ในรูป การปลดปล่อยแสง emission wavelength ในขณะที่จับตัวในรูปแบบ hybridization กับดีเอ็นเอเป้าหมายภายหลังการเกิด excitation ในที่นี้เลือกใช้ปฏิกิริยาระหว่างโมเลกุลที่เป็น reporter และ quencher ในรูปโอลิโกเมอร์ของ PNA และ DNA ที่ติดฉลากด้วย fluorophore ในกรณีที่การจับตัวประสบความสำเร็จ quencher จะเป็นอิสระและไม่สามารถรบกวนการเรืองแสงของ reporter ได้ และหากการจับตัวไม่ประสบความสำเร็จ quencher ที่เกาะอยู่กับ reporter จะรับพลังงานของ reporter ไว้ทำให้ไม่สามารถปลดปล่อยแสงออกมาได้

การทำงานของโพรบจะได้รับการออกแบบให้จับตัวที่ตำแหน่ง 825 ซึ่งครอบคลุมบริเวณสำคัญ รอบตำแหน่งรหัสดีเอ็นเอที่ถอดรหัสเป็น H275Y การออกแบบโพรบ PNA ได้โพรบ PNA 2 ชนิด และ quencher 2 ชนิด ดังภาพที่ 7.

ภาพที่ 7 ความสัมพันธ์ระหว่าง PNA โพรบและ quencher และปริมาณลำดับนิวคลิโอไทด์ภายในยีน neuraminidase ของทั้ง 2 ระบบ

โพรบ PNA และquencher ชนิดแรกใช้สำหรับการตรวจสอบไปที่ยีน neuraminidase ของตัวอย่าง โดยโพรบได้รับการออกแบบให้จับตัวกับยีน neuraminidase และมี FAM fluorophore ที่ตำแหน่ง 5‘ ขณะที่ quencherได้รับการออกแบบให้จับตัวกับโพรบและมี BHQ เป็นโมเลกุลรับพลังงาน โดยทุกตัวอย่างที่เป็นเชื้อไข้หวัดใหญ่สายพันธ์ใหม่จะให้ผลิตภัณฑ์ดีเอ็นเอที่จับได้กับโพรบ PNA และทุกครั้งที่การจับตัวประสบความสำเร็จ quencher ของโพรบดังกล่าวจะหลุดเป็นอิสระ ไม่สามารถรับพลังงานจากโพรบได้อีดต่อไป ส่งผลให้เกิดการเรืองแสง เรียกโพรบ PNA และquencher ชนิดแรกว่า internal control probe and quencher

โพรบ PNA และquencher ชนิดที่สองใช้สำหรับการตรวจสอบไปที่ตำแหน่งการกลายของยีน neuraminidase ของตัวอย่างที่ตำแหน่ง 275 โดยโพรบได้รับการออกแบบให้จับตัวกับบริเวณนิวคลิโอไทด์ที่ 818-830 และมี FAM fluorophore ที่ตำแหน่ง 5‘ ขณะที่ quencherได้รับการออกแบบให้จับตัวกับโพรบและมี BHQ เป็นโมเลกุลรับพลังงานเช่นเดียวกัน

รายละเอียดของโพรบและ quencher เป็นดังตารางที่ 2. การจับตัวกันของ quencher # 1 กับ internal control probe จะทำให้ไม่เกิดการเรืองแสง ทำนองเดียวกัน การจับตัวของ quencher#2 กับ target 275 mutation ไม่ทำให้เกิดการเรืองแสง และเมื่อ internal control probe จับตัวกับ target internal DNA การจับตัวจะทำให้ quencher หลุดออกเป็นอิสระ จึงทำให้ internal probe เรืองแสงได้ในที่สุด

ตารางที่ 2. PNA โพรบ และ quencher สำหรับการตรวจสอบยีน neuraminidase และลำดับนิวคลิโอไทด์ที่เกี่ยวข้อง

Element	detail sequence	binding position
PNA internal control	Flu-O-CTGTTATCCTG-LysNH_2	839-851
Quencher # 1 internal control	5’-ATAACAG-3’-BHQ	839-846
PNA 275 mutation	Flu-O-TTATCACTATGA-LysNH_2	818-830
Quencher# 2 275 mutation	5’-GTGATAA-3’-BHQ	818-825

ในการทดลองได้ทดสอบการเรืองแสงโดยจับตัวระหว่าง probe ที่เป็น internal โดยทำปฏิกิริยาระหว่าง probe ความเข้มข้น 10 μM ปริมาตร 3 μl จับ DNA products ที่เพิ่มปริมาณได้ โดยให้ความร้อนกับดีเอ็นเอที่ 85 $^{\circ}$C เป็นเวลา 5 นาที และปล่อยให้จับตัวที่ 50°C เป็นเวลา 15 นาที ก่อนนำมาทดสอบโดยการส่องดูด้วยแสง UV ความยาวคลื่น ● 312 nm พบว่าเฉพาะหลอดที่ให้ดีเอ็นเอเป้าหมายเท่านั้นที่พบการเรืองแสง (ภาพที่ 8. ซ้าย) และเมื่อนำ probe และ quencher เดียวกันมาทดสอบกับตัวอย่างทั้งตัวอย่างปกติ (wild type) และตัวอย่างที่กลายพันธุ์ดื้อต่อยา oseltamivir (mutant) ซึ่งทั้ง ดีเอ็นเอจากทั้ง 2 ทำปฏิกิริยาโดยตรงกับ probe จึงทำให้เกิดการเรืองแสงขึ้น ดังภาพที่ 8. ขวา

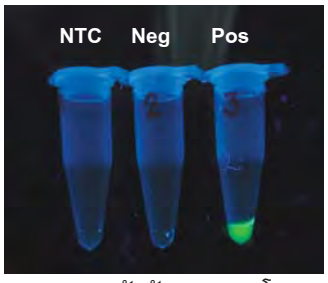

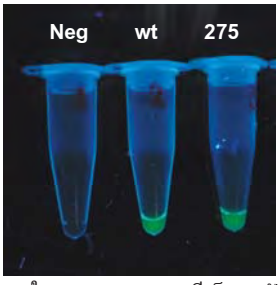

ภาพที่ 8 แสดงผลการจับตัวของ PNA โพรบ ชนิด intermal control การตรวจในชุดควบคุม และดีเอ็นเอเป้าหมายโดยภาพซ้าย ; แสดงการจับตัวกับชุดควบคุมบวก (Pos)และลบ (Neg) และภาพขวา; แสดงการจับตัวของโพรบกับตัวอย่างยีนโดยทุกตัวอย่างแสดงการจับตัวชัดเจนและเรืองแสง

เนื่องจากบริเวณที่ใช้เป็น internal control ไม่พบการกลายพันธุ์ใดๆ ดังนั้น จากภาพชุดโพรบและquencher ที่ใช้สำหรับ internal control จึงให้ผลการเรืองแสงกับตัวอย่างที่มียีน neuraminidase

การทดสอบกับ probe ที่จำเพาะต่อตำแหน่งกลาย 275 ด้วยหลักการเดียวกัน พบว่าเฉพาะสายพันธุ์ที่เป็น 275 wild type ที่ไม่เกิดการกลายเท่านั้นที่ probe จับได้และจะสามารถตรวจสอบการเรืองแสงได้ชัดเจน และหากดีเอ็นเอของบริเวณตำแหน่งกลาย 275 เกิดการกลายพันธุ์หรือเป็น mutant จะพบว่าการเรืองที่เกิดขึ้นจะไม่เกิดขึ้นอีกต่อไป (ภาพที่.9.)

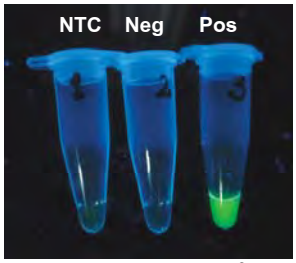

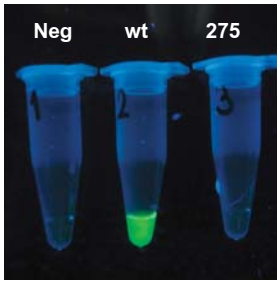

ภาพที่ 9 แสดงผลการจับตัวของ PNA โพรบชนิดตรวจการกลายกับดีเอ็นเอเป้าหมาย ภายซ้าย แสดงการจับตัวได้ของโพรบในชุดควบคุมบวก (Pos) ที่เรืองแสง เมื่อเปรียบเทียบกับชุดควบคุมลบ (Neg) และภาพขวา แสดงการตรวจตัวอย่างจริงโดย wt แสดงสายพันธุ์ไวรัสปกติและ 275 แสดงตัวอย่างดีเอ็นเอกลายพันธุ์ ทำให้โพรบไม่จับตัว จึงไม่เกิดการเรืองแสง

จากผลการทดลองทั้งหมด ทำให้ได้ระบบการตรวจสอบไวรัสไข้หวัดสายพันธุ์ใหม่ที่กลายพันธุ์ในตำแหน่ง 275-275 ได้ภายในเวลา 60 นาที โดยระบบไม่พึ่งพาเครื่องมือราคาแพง สามารถปรับประยุกต์ไปใช้ในภาคสนามได้ และที่สำคัญไม่ต้องอาศัยความชำนาญการของผู้ปฏิบัติงานเหมือนเทคนิค real-time PCR ที่ใช้งานอยู่ในปัจจุบัน

นอกจากนี้ยังได้เพิ่มเติมผลการพัฒนาระบบการตรวจสอบการกลายพันธุ์ของไวรัส โดยนำอนุภาคนาโนเงินชนิดสีน้ำเงิน (blue silver nanoparticle) มาต่อยอด ซึ่งเป็นการพัฒนาระบบการตรวจที่อาศัยการประยุกต์ใช้ silver nanoparticles สีน้ำเงินเป็นครั้งแรก

ในการตรวจวิเคราะห์โดยใช้ nanoparticles เริ่มเป็นระบบขึ้นจากการเริ่มค้นคว้าของ Mirkin *et al*., 1996 โดยนำปรากฏการณ์จับตัว (conjugate) ระหว่างอนุภาคนาโนกับดีเอ็นเอ เป็นหลักในการพัฒนารูปแบบการตรวจ และต่อมา Li and Rothberg, (2004) ได้พัฒนาระบบ unmodified nanoparticles ขึ้นบนพื้นฐานการตอบสนองของอนุภาคในภาวะ ionic strength ที่ต่างกัน ในภาวะที่มี single strand DNA (ssDNA) หรือ double strand DNA (ssDNA) ซึ่งให้ผลการตอบสนองของอนุภาค nanoparticles ต่างกันอย่างสิ้นเชิง

โดยปกติในภาวะที่มีความเข้มข้นของ DNA ไม่สูงมาก ทั้ง ssDNA จะป้องกันไม่ให้อนุภาคทองตกตะกอนในภาวะที่มีเกลือต่ำ ขณะที่ dsDNA จะกระตุ้นให้เกิดการตกตะกอน

คุณสมบัติที่ต่างกันนี้เกิดจากความต่างกันของ ssDNA และ dsDNA ในด้าน hydrophobicity โดย ssDNA มี hydrophobicity สูงกว่า การเปลี่ยนไปของสมบัติ hydrophobicity หลังทำปฏิกิริยามีผลต่อผลกระทบต่อคุณสมบัติ electrostatic ของอนุภาคที่มีอิทธิพลเหนือกว่า ทำให้นำไปสู่การตกตะกอนของอนุภาค

ที่ผ่านมามีผู้ใช้อนุภาคทองคำในการพัฒนาระบบค่อนข้างมาก แต่สำหรับการพัฒนาระบบโดยใช้อนุภาคเงิน กลับมีน้อยกว่า ทั้งๆ ที่เงินมีคุณสมบัติในเรื่อง molar extinction coefficient ที่ดีกว่าทอง ผลดังกล่าวทำให้เพิ่มความไวของปฏิกิริยา ส่งผลต่อการสังเกตุผลที่เห็นได้ชัด และอนุภาคเงินผงกระตุ้นให้เกิด Raman scattering ได้ดีกว่าอนุภาคทองคำ

Thomson *et al*., (2008) ได้สาธิตแนวคิดการนำ sandwich assay ในการใช้อนุภาคนาโน ที่เชื่อมโยงกับโพรบที่เป็นโอลิโกดีเอ็นเอในการเชื่อมโดยให้ เกิดการจับตัวยามที่มีดีเอ็นเอเป้าหมาย ทำให้เกิดการเปลี่ยนแปลงของอนุภาคเงินนาโนจากสีเหลืองอ่อนเป็นสีชมพู เนื่องจากการเลื่อนไปของสเปคตรัมแสง เป็นสีแดง (518 nm เป็น 523 nm) ปฏิกิริยาดังกล่าวเกิดจากการ hybridization ของดีเอ็นเอที่เชื่อมโยงอยู่กับอนุภาค การเปลี่ยนไปของสีของอนุภาค สามารถมองเห็นได้ด้วยตาเปล่า หรือตรวจวัดโดยใช้ UV-Vis spectroscopy

อย่างไรก็ดี การเปลี่ยนสีจากเหลืองเป็นชมพู ของคอลลอยด์เงิน ในระบบ colorimetric เป็นการเปลี่ยนสีจากสีจางไปเป็นสีจาง ทำให้การสังเกตผลด้วยตาเปล่าอาจไม่ชัดเจน ดังนั้นในโครงการวิจัยที่ดำเนินการนี้ จึงได้นำเอาอนุภาคเงินนาโนสีน้ำเงิน (blue silver nano) ซึ่งให้สีเข้มกว่ามาประยุกต์ใช้

อนุภาคเงินนาโนที่ใช้ในครั้งนี้ เกิดจากการสังเคราะห์โดยวิธีที่ปลอดภัยต่อสิ่งแวดล้อม อนุภาคเป็นผลิต lattice ขนาด 200 นาโนเมตร อนุภาคเงินนาโนสีน้ำเงินดังกล่าวเมื่อกระตุ้นให้เกิดการจับตัวและตกตะกอน จะได้ผลึกเงินขนาดเล็กที่resonance แสงที่ความยาวคลื่น near inflared ซึ่งที่ความยาวคลื่นนี้ อยู่ในช่วงคลื่นที่มองไม่เห็น จึงทำให้เห็นสารละลายเงินเปลี่ยนสีจากน้ำเงินเป็นใสไม่มีสี

ในการทดลองได้ใช้โพรบในรูป β-pyrolidinyl peptide nucleic acid ที่ จำเพาะต่อบริเวณของยีนในจุดกลายพันธุ์ 2 ตัวได้แก่ PNA internal control Flu-O-CTGTTATCCTG-LysNH_2 และ PNA 275 mutation Flu-O-TTATCACTATGA-LysNH_2 เช่น เดียวกัน

ในทางทฤษฎี การออกแบบโพรบบริเวณตำแหน่ง 275 กลายพันธุ์ ดื้อต่อยา oseltamivia ทำให้การจับตัวเกิดความจำเพาะ ด้วยคุณสมบัติสำคัญของ β-pyrolidinyl peptide nucleic acid ที่จับตัวกับบริเวณดีเอ็นเอเป้าหมายเฉพาะในกรณีที่โพรบจับอย่างจำเพาะ 100% กับtarget sequence เท่านั้น โพรบที่ออกแบบขึ้นในครั้งนี้จะจับตัวกับบริเวณของยีนเป้าหมาย โดยโพรบจะจับเฉพาะกับไวรัสสายพันธุ์ 2009 ที่เป็น wild type (ไม่ดื้อยา oseltamivir) แต่จะไม่จับกับ mutant ที่เป็นสายพันธุ์ ดื้อยา oseltamivir ในชุดควบคุมอาศัยโพรบอีกหนึ่งชนิดได้แก่ internal control probe ซึ่งจะจับตัวกับบริเวณของยีนเป้าหมายได้ไม่ว่าเป้าหมายนั้นจะเป็นไวรัสสายพันธุ์ ดื้อยา oseltamivir หรือ ไม่ดื้อยา oseltamivir ก็ตาม (ภาพที่ 10.)

ในการทดลอง ได้นำระบบการเพิ่มปริมาณดีเอ็นเอของยีน NA ที่ได้ดำเนินการในช่วงเดือนที่ 1-6 มาประยุกต์ใช้โดยนำโพรบที่ออกแบบได้ มาทำปฏิกิริยากับอนุภาคเงิน โดยใช้ความเข้มข้นโพรบที่ 100 μM ในสารละลาย 10mM PBS pH 7.6

อย่างไรก็ดี จากการทดลองพบว่าดีเอ็นเอเป้าหมายสามารถเป็นได้ทั้งผลิตภัณฑ์ดีเอ็นเอที่ได้จากการเพิ่มปริมาณดีเอ็นเอด้วยปฏิกิริยาลูกโซ่พอลิเมอเรสที่เป็นที่นิยมในปัจจุบัน หรือ ดีเอ็นเอผลิตภัณฑ์ที่ได้จากการเพิ่มปริมาณดีเอ็นเอด้วยปฏิกิริยาอุณหภูมิระนาบเดี่ยวที่ได้กล่าวไว้ การจับตัวเป็นไปตามหลักการ Southern hybridization และใช้เวลาเพียง 10 นาที

ภาพที่ 10 ความสัมพันธ์ระหว่าง PNA โพรบกับลำดับนิวคลีโอไทด์ภายในยีน neuraminidase ที่ได้จากไวรัสไข้หวัดใหญ่สายพันธุ์ 2009 สายพันธุ์ย่อยต่างๆ ตามหมายเลข accession number ที่ปรากฏ เทียบกับสายพันธุ์ดื้อยา oseltamivir (A/Hong)

ผลการตรวจวิเคราะห์เมื่อใช้อนุภาคนาโนเป็นระบบตรวจสัญญาณ พบการจับตัวของอนุภาคทำให้เกิดการตกตะกอนเป็นสารละลายใสไม่มีสี มองเห็นได้ด้วยตาเปล่าในตัวอย่างที่เป็นลบ และตัวอย่างที่เป็นดีเอ็นเอที่ไม่ใช่ดีเอ็นเอเป้าหมาย ขณะที่ในตัวอย่างที่เป็นบวกจะไม่ตกตะกอน (ภาพที่ 11.)

ภาพที่ 11 การเปลี่ยนสีของตะกอนอนุภาคเงินนาโน ก่อน (before) และหลัง (after) ปฏิกิริยา พบการตกตะกอนในชุดควบคุมลบ และในชุดควบคุมที่ไม่มีดีเอ็นเอเป้าหมาย ขณะที่อนุภาคเงินนาโนไม่ตกตะกอนในตัวอย่างที่มีดีเอ็นเอเป้าหมาย

การเปลี่ยนแปลงดังกล่าวจะทำให้คุณสมบัติพลาสมอนของอนุภาคนาโนเงินเปลี่ยนไป ทำให้เกิดการเปลี่ยนแปลงทางแสงไปสู่ความยาวคลื่น near infrared ซึ่งที่ความยาวคลื่นนี้ อยู่ในช่วงคลื่นที่มองไม่เห็นด้วยตาเปล่า จึงทำให้เห็นสารละลายเงินเปลี่ยนสีจากน้ำเงินเป็นใสไม่มีสี

ในการทดลองสามารถตรวจสอบการเปลี่ยนแปลงทางสีของแสงที่วัดด้วยเครื่อง UV-Vis spectrophotometer ได้ดังภาพที่ 12.

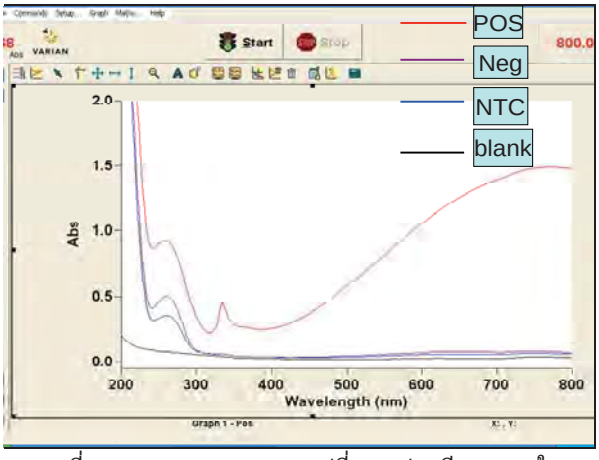

ภาพที่ 12 การตรวจสอบการเปลี่ยนแปลงสีทางแสงในระหว่างการตรวจสอบเปรียบเทียบระหว่างตัวอย่างชุดควบคุมลบ (เส้นกราฟสีม่วง) และในชุดควบคุมที่ไม่มีดีเอ็นเอเป้าหมาย(เส้นกราฟน้ำเงิน)ซึ่งพบการตกพะกอนจนสารละลายเงินเปลี่ยนเป็นใสไม่มีสี ขณะที่อนุภาคเงินนาโนไม่ตกตะกอนในตัวอย่างที่มีดีเอ็นเอเป้าหมาย (เส้นกราฟแดง) และ cuvette ที่ใช้เป็น blank ไม่เปลี่ยนแปลง (เส้นกราฟสีดำ)

ในตัวอย่างที่เป็นบวก (เส้นกราฟสีแดง) จะพบว่า resonance ทางแสงที่วัดได้มีความยาวคลื่นในช่วง 550-800 nm ซึ่งเป็นช่วงสีน้ำเงิน-น้ำเงิน-ม่วง ขณะที่ตัวอย่างที่ไม่มีดีเอ็นเอเป้าหมาย หรือตัวอย่างที่เป็นลบ (มีดีเอ็นเออื่นที่ไม่ใช่เป้าหมาย) จะตกตะกอนทิ้งไว้แต่เพียง peak ของความยาวคลื่น ประมาณ 270 nm ไว้และไม่พบช่วงแสงความยาวคลื่นในช่วง 550-800 nm ซึ่งเป็นช่วงสีน้ำเงิน-น้ำเงิน-ม่วงแต่อย่างใด

การเปลี่ยนสีของสารละลายปฏิกิริยาเกิดการจับตัวตกตะกอนของอนุภาค ไม่ได้เกิดจากการเกิดปฏิกิริยา oxidation ของอนุภาค เนื่องจากการตรวจสอบด้วย sodium borohydride ไม่พบการเปลี่ยนแปลงของสารละลายเป็นสีเหลือง (ภาพที่ 13.)

ภาพที่ 13 ผลการทดสอบตัวอย่างที่พบการตกตะกอนของอนุภาคเงินนาโนด้วย sodium boro hydrideไม่พบการเปลี่ยนแปลงของสารละลายเป็นสีเหลือง

นอกจากนี้การตกตะกอนเกิดจากการจับตัวของอนุภาค ทั้งนี้โดยเมื่อตรวจสอบภายใต้กล้องจุลทรรศน์อิเล็คตรอน (SEM) ที่กำลังขยาย 10000 เท่า จะพบว่าเฉพาะตัวอย่างที่ตกตะกอนจะพบปฏิกิริยาของอนุภาคเงินที่จับตัวกันอยู่ (ภาพที่ 14. และ 15.)

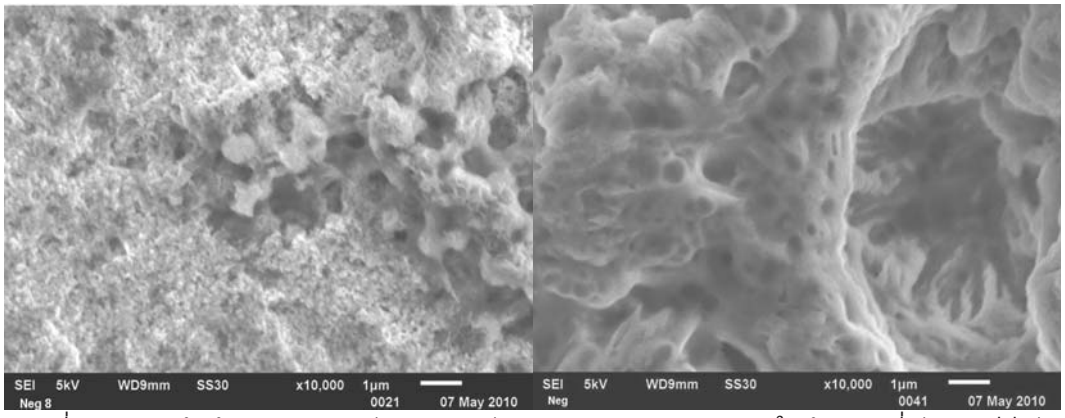

ภาพที่ 14 การจับตัวของอนุภาคเป็นตะกอนเล็กจากส่วนตะกอน (ซ้าย) ในตัวอย่างที่เป็นลบ(มีดีเอ็นเอแต่ไม่ใช่เป้าหมาย) หรือไม่มีดีเอ็นเอ และส่วนใสที่ได้ซึ่งไม่พบตะกอนของอนุภาค

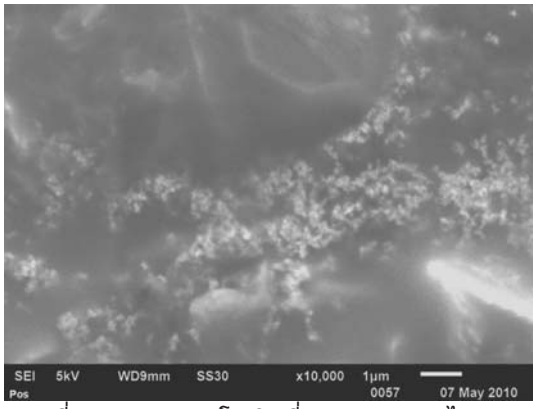

ภาพที่ 15 อนุภาคนาโนเงินที่แขวนลอยและไม่ตกตะกอนในตัวอย่างที่เป็นบวก

จากผลการทดลองที่ได้ดำเนินการพบว่าระบบการตรวจที่อาศัย β-pyrolidinyl peptide nucleic acid สามารถเปลี่ยนแปลงสัญญาณ ในรูปแบบการเปลี่ยนของพลาสมอนทางแสง โดยในภาวะที่ไม่มีดีเอ็นเอเป้าหมาย โพรบจะจับตัวบนผิวอนุภาคโดยอาศัยด้าน hydrophobic ไปที่ผิวอนุภาค เกลือในระบบจะกระตุ้นให้เกิดการจับตัวของอนุภาค แต่ในภาวะที่มีดีเอ็นเอเป้าหมาย โพรบจะกับดีเอ็นเอเป้าหมาย ช่วยให้อนุภาคกระจายตัวไม่เกาะกัน จึงไม่เกิดการเปลี่ยนแปลงอยู่ในรูปการตกตะกอน

การแสดงผลในรูปการตกตะกอนดังกล่าวล้อไปกับผลการตรวจการเรืองแสงตามวิธีที่ใช้ β-pyrolidinyl peptide nucleic acid ที่ติดโมเลกุล fluorophore ไปที่ตำแหน่ง 5’ ที่ได้ดำเนินการในช่วง 6 เดือนแรก

โดยสรุป การดำเนินการทำให้ได้ระบบการตรวจด้วยอนุภาคเงินนาโนสีน้ำเงิน ซึ่งยังไม่เคยมีรายงานมาก่อน ระบบดังกล่าวใช้งานง่ายและมีต้นทุนต่ำ

4.1.2 พัฒนาวิธีการตรวจสอบไวรัสชิคุนกุนยา

ได้พัฒนาเทคนิคตรวจโรคอุบัติซ้ำเพิ่มเติมจากโรคอุบัติใหม่ โดยการดำเนินงานเน้นการใช้รูปแบบตรวจสัญญาณดีเอ็นเอจากการเปลี่ยนแปลงของสีทางแสงของสารละลายเงินนาโนสีน้ำเงิน โดยการใช้ peptide nucleic acid (PNA) ในรูป β-pyrrolidinyl peptide nucleic acid เป็นโพรบ ในรูปแบบ nucleic acid hybridization โดยระบบการตรวจโรคอุบัติซ้ำที่พัฒนาขึ้นในครั้งนี้ เน้นการตรวจโรคชิคุนกุนยา (Chikungunya)

โรคชิคุนกุนยาเป็นโรคที่เกิดจากเชื้อไวรัสชิคุนกุนยา(CKK) เดิมไวรัสดังกล่าวเริ่มแพร่ระบาดครั้งแรกในทวีปแอฟริกา สำหรับในประทศไทย โรคดังกล่าวตรวจพบครั้งแรกในปี พ.ศ. 2501 พร้อมๆ กันกับการระบาดประเทศในเอเชียอื่น

การแพร่ระบาดมีทั้งด้วยวงจร primate cycle ได้แก่จาก ลิง ยุง สู่คน โดยมีลิง barboon เป็นเจ้าเรือน และมียุงลาย *Aedes aegypti* เป็นพาหะ และด้วยวงจรที่สอง urban cycle จากคน ยุง สู่คน โดยเฉพาะเมื่อยุงลายไปกัดและดูดเลือดผู้ป่วยในขณะไข้สูง ซึ่งเป็นระยะ

ที่พบเชื้อไวรัสอยู่ในกระแสเลือดสูง เชื้อจะเข้าสู่กระเพาะของยุง เพิ่มจำนวน และเคลื่อนเข้าสู่ต่อมน้ำลายของยุงและเมื่อยุงไปกัดคนอื่นต่อก็จะแพร่เชื้อต่อไปได้ (Chevillon *et al*., 2008)

อาการของโรคที่แสดงได้แก่ ภาวะไข้สูงเฉียบพลัน มีผื่นแดงตามตัว พบตาแดง ในผู้ใหญ่อาการเด่นชัดคือ ปวดตามข้อเนื่องจากข้ออักเสบ (Power *et. al.,* 2000) ในประเทศไทยโรคดังกล่าวกลับมาระบาดซ้ำตั้งแต่ปี 2552 เริ่มที่จังหวัดยะลาและขยายต่อไปสู่จังหวัดอื่นๆในภาคใต้ของประเทศไทย (Rianthavorn *et al*., 2010)

ลักษณะทางอณูชีววิทยา พบว่าไวรัสอยู่ในจีนัส Alphavirus มีจีโนมเป็น ssRNA ขนาด 12000 นิวคลิโอไทด์ ที่มีปลาย 5’ เป็น 7-methylated guanosine และปลาย 3’ เป็น Poly A (Khan *et. al*., 2003)

การวินิจฉัยโรคโดยการแยกเชื้อแม้จะเป็นวิธีที่แม่นยำแต่อาจต้องใช้เวลาถึง 2 สัปดาห์ และต้องใช้ห้องปฏิบัติการระดับ P3 จึงทำให้การตรวจมีข้อจำกัด การตรวจด้วยเทคนิคชีวโมเลกุลจึงเป็นที่นิยมมากกว่า ในปัจจุบันเทคนิคชีวโมเลกุลที่นิยมนำมาใช้ได้แก่ เทคนิคเทคนิคเซรั่มวิทยา ในรูปแบบ ELISA และเทคนิค RT-PCR ซึ่งใช้เป็นหลักและเป็นที่นิยมมากกว่าเทคนิคอื่นๆ (Carletti *et al*., 2007, WHO, 2008) เทคนิค ELISA ตรวจโดยใช้เซรั่มจากคนไข้อาศัยกลไกการจับตัวกับ Ig M ที่เรียกว่า Immunoglobulin M Antibody Capture Enzyme-linked Immunosorbent Assay (MAC-ELISA) อย่างไรก็ดี เนื่องจากเทคนิคนี้ต้องใช้เวลาตรวจ 2-3 วันและมีโอกาสcross กับ o’nyong o’nyong virus จึงเป็นข้อจำกัดทำให้การใช้งานจำกัดอยู่เฉพาะในห้องปฏิบัติการ สำหรับอีกเทคนิคหนึ่งได้แก่ RT-PCR ซึ่งอาศัยการเพิ่มจำนวนยีนซึ่งในปัจจุบันมีทั้งยีนเป้าหมายในรูป structural gene capsid protein gene และ envelope E1 และ E2 โดยเทคนิค Nested RT-PCR (Pfeffer *et al*., 2002)

แม้ว่าการตรวจจะได้รับการพัฒนาให้สามารถตรวจไวรัสชนิดนี้ได้ดีแต่การตรวจในรูปแบบ Nested RT-PCR ดังกล่าวยังคงติดกับเงื่อนไขในการใช้ห้องปฏิบัติการและใช้เวลาในการตรวจนานอย่างน้อย 1 วัน และแม้ว่าในปัจจุบันจะมีผู้พัฒนาเทคนิค real-time RT-PCR (Smith *et al*., 2007) แต่ตัวเทคนิคฯ ยังคงพึ่งพาเครื่องมือและน้ำยาราคาแพงและต้องใช้ผู้ชำนาญการเฉพาะทาง

การพัฒนาการตรวจสอบไวรัสของโครงการในครั้งนี้ ได้นำหลักการเพิ่มปริมาณดีเอ็นเอแบบอุณหภูมิเดียวมาใช้ร่วมกับการตรวจสัญญาณดีเอ็นเอแบบเรืองแสงที่ใช้ peptide nucleic acid (PNA) ในรูป β-pyrrolidinyl peptide nucleic acid เป็นโพรบร่วมกับ quencher ในรูปแบบ competitive hybridization

การดำเนินการเริ่มจากการสืบค้นข้อมูลลำดับนิวคลีโอไทด์ของยีน E1 ของไวรัสชิคุนกุนยา ซึ่งเป็นส่วนของenvelop protein ซึ่งแสดงคุณสมบัติความรุนแรงของโรคของไวรัส เนื่องจากใน E1 มีผลต่อการสร้างโปรตีนในการห่อหุ้มอนุภาคภายนอก

การศึกษาลำดับนิวคลีโอไทด์ ของยีน E1 สายพันธุ์ต่างๆ พบว่าสายพันธุ์ของไวรัสทั้ง 3 กลุ่ม ได้แก่ เอเชีย อเมริกาและแอฟฟริกา มีส่วนของยีน E1 ที่คล้ายกัน (ภาพที่ 16.)

```
CLUSTAL 2.0.12 multiple sequence alignment

AM397006        TGCTTCTGCGACACCGAAAATACGCAATTGAGCGAAGCACATGTGGAGAAGTCCGAATCA 60
AM397005        TGCTTCTGCGACACCGAAAATACGCAATTGAGCGAAGCACATGTGGAGAAGTCCGAATCA 60
AM397007        TGCTTCTGCGACACCGAAAATACGCAATTGAGCGAAGCACATGTGGAGAAGTCCGAATCA 60
AM397009        TGCTTCTGCGACACCGAAAATACGCAATTGAGCGAAGCACATGTGGAGAAGTCCGAATCA 60
AM397008        TGCTTCTGCGACACCGAAAATACGCAATTGAGCGAAGCACATGTGGAGAAGTCCGAATCA 60
AF394211        TGCTTCTGCGACACCGAAAATACGCAATTGAGCGAAGCACATGTGGAGAAGTCCGAATCA 60
AF394210        TGCTTCTGCGACACCGAAAATACGCAATTGAGCGAAGCACATGTGGAGAAGTCCGAATCA 60
EU192143        TGCTTCTGCGACACCGAAAATACGCAATTGAGCGAAGCACATGTGGAGAAGTCCGAATCA 60
DQ520746        TGCTTCTGCGACACTGAAAATACGCAATTGAGCGAAGCACATGTGGAGAAGTCCGAATCA 60
DQ520748        TGCTTCTGCGACACTGAAAATACGCAATTGAGCGAAGCACATGTGGAGAAGTCCGAATCA 60
DQ520754        TGCTTCTGCGACACTGAAAATACGCAATTGAGCGAAGCACATGTGGAGAAGTCCGAATCA 60
AF192899        TGCTTCTGCGACACTGAAAATACGCAATTGAGCGAAGCACATGTGGAGAAGTCCGAATCA 60
AF192900        TGCTTCTGCGACACTGAAAATACGCAATTGAGCGAAGCACATGTGGAGAAGTCTGAATCA 60
AF192897        TGCTCCTGCGACACTGAAAATACGCAATTGAGCGAAGCACATGTGGAGAAGTCTGAATCA 60
AF192895        TGCTTCTGCGACACTGAAAATACGCAATTGAGCGAAGCACATGTGGAGAAGTCCGAATCA 60
AF192894        TGCTTCTGCGACACTGAAAATACGCAATTGAGCGAAGCACATGTGGAGAAGTCCGAATCA 60
FJ457636        CCCCTCTGCGACGCTGAAAATACGCAGTTGAGCGAAGCACATGTGGAGAAGTCCGAATCA 60
FJ882922        TGCTTCTGCGACGCTGAAAATACGCAGTTGAGCGAAGCACATGTGGAGAAGTCCGAATCA 60
FJ457640        TGCTTCTGCGACGCTGAAAATACGCAGTTGAGCGAAGCACATGTGGAGAAGTCCGAATCA 60
FJ457639        TGCTTCTGCGACGCTGAAAATACGCAGTTGAGCGAAGCACATGTGGAGAAGTCCGAATCA 60
FJ457638        TGCTTCTGCGACGCTGAAAATACGCAGTTGAGCGAAGCACATGTGGAGAAGTCCGAATCA 60
FJ457637        TGCTTCTGCGACGCTGAAAATACGCAGTTGAGCGAAGCACATGTGGAGAAGTCCGAATCA 60
AY549581        TGCTTCTGCGACGCTGAAAACACGCAATTGAGCGAAGCACATGTGGAGAAGTCCGAATCA 60
AY549582        TGCTTCTGCGACGCTGAAAACACGCAATTGAGCGAAGCACATGTGGAGAAGTCCGAATCA 60
EF051584        TGCTTCTGCGACGCTGAAAACACGCAATTGAGCGAAGCACATGTGGAGAAGTCCGAATCA 60
                  *  ******* * ***** ***** ************************** ******


AM397006        TGCAAAACAGAATTTGCATCAGCATACAGGGCTCATACCGCATCCGCATCAGCTAAGCTC 120
AM397005        TGCAAAACAGAATTTGCATCAGCATACAGGGCTCATACCGCATCCGCATCAGCTAAGCTC 120
AM397007        TGCAAAACAGAATTTGCATCAGCATACAGGGCTCATACCGCATCCGCATCAGCTAAGCTC 120
AM397009        TGCAAAACAGAATTTGCATCAGCATACAGGGCTCATACCGCATCCGCATCAGCTAAGCTC 120
AM397008        TGCAAAACAGAATTTGCATCAGCATACAGGGCTCATACCGCATCCGCATCAGCTAAGCTC 120
AF394211        TGCAAAACAGAATTTGCATCAGCATACAGGGCTCATACCGCATCCGCATCAGCTAAGCTC 120
AF394210        TGCAAAACAGAATTTGCATCAGCATACAGGGCTCATACCGCATCCGCATCAGCTAAGCTC 120
EU192143        TGCAAAACAGAATTTGCATCAGCATACAGGGCTCATACCGCATCCGCATCAGCTAAGCTC 120
DQ520746        TGCAAAACAGAATTTGCATCAGCATATAGGGCTCATACCGCATCCGCATCAGCTAAGCTC 120
DQ520748        TGCAAAACAGAATTTGCATCAGCATATAGGGCTCATACCGCATCCGCATCAGCTAAGCTC 120
DQ520754        TGCAAAACAGAATTTGCATCAGCATATAGGGCTCATACCGCATCCGCATCAGCTAAGCTC 120
AF192899        TGCAAAACAGAATTTGCATCAGCATATAGGGCTCATACCGCATCCGCATCAGCTAAGCTC 120
AF192900        TGCAAAACGGAATTTGCATCAGCATACAGGGCCCATACCGCATCCGCATCAGCTAAGCTC 120
AF192897        TGCAAAACGGAATTTGCATCAGCATACAGGGCCCATACCGCATCCGCATCAGCTAAGCTC 120
AF192895        TGCAAAACAGAATTTGCATCAGCATACAGGGCCCATACCGCATCCGCATCAGCTAAGCTC 120
AF192894        TGCAAAACAGAATTTGCATCAGCATACAGGGCCCATACCGCATCCGCATCAGCCAAGCTC 120
FJ457636        TGCAAAACAGAATTTGCATCAGCGTACAGGGCTCATACCGCATCTGCATCAGCTAAGCTC 120
FJ882922        TGCAAAACAGAATTTGCATCAGCGTACAGGGCTCATACCGCATCTGCATCAGCTAAGCTC 120
FJ457640        TGCAAAACAGAATTTGCATCAGCGTACAGGGCTCATACCGCATCTGCATCAGCTAAGCTC 120
FJ457639        TGCAAAACAGAATTTGCATCAGCGTACAGGGCTCATACCGCATCTGCATCAGCTAAGCTC 120
FJ457638        TGCAAAACAGAATTTGCATCAGCGTACAGGGCTCATACCGCATCTGCATCAGCTAAGCTC 120
FJ457637        TGCAAAACAGAATTTGCATCAGCGTACAGGGCTCATACCGCATCTGCATCAGCTAAGCTC 120
AY549581        TGCAAAACAGAATTTGCATCAGCACACAGGGCTCATACAGCATCCGCATCAGCTAAGCTC 120
AY549582        TGCAAAACAGAATTTGCATCAGCACACAGGGCTCATACAGCATCCGCATCAGCTAAGCTC 120
EF051584        TGCAAAACAGAATTTGCATCAGCATACAGGGCTAATACAGCATCCGCATCAGCTAAGCTC 120
                ******** ***************  * *****  **** ***** ******** ******


AM397006        CGCGTCCTTTACCAAGGAAATAATATCACTGTAGCTGCTTATGCAAACGGCGACCATGCC 180
AM397005        CGCGTCCTTTACCAAGGAAATAATATCACTGTAGCTGCTTATGCAAACGGCGACCATGCC 180
AM397007        CGCGTCCTTTACCAAGGAAATAATATCACTGTAGCTGCTTATGCAAACGGCGACCATGCC 180
AM397009        CGCGTCCTTTACCAAGGAAATAATATCACTGTAGCTGCTTATGCAAACGGCGACCATGCC 180
AM397008        CGCGTCCTTTACCAAGGAAATAATATCACTGTAGCTGCTTATGCAAACGGCGACCATGCC 180
AF394211        CGCGTCCTTTACCAAGGAAATAATATCACTGTAGCTGCTTATGCAAACGGCGACCATGCC 180
AF394210        CGCGTCCTTTACCAAGGAAATAATATCACTGTAGCTGCTTATGCAAACGGCGACCATGCC 180
EU192143        CGCGTCCTTTACCAAGGAAGTAATATCACTGTTGCTGCTTATGCAAACGGCGACCATGCC 180
DQ520746        CGCGTCCTTTACCAAGGAAATAATGTTACTGTATCTGCCTATGCAAACGGCGACCATGCC 180
DQ520748        CGCGTCCTTTACCAAGGAAATAATGTTACTGTATCTGCCTATGCAAACGGCGACCATGCC 180
DQ520754        CGCGTCCTTTACCAAGGAAATAATGTTACTGTATCTGCCTATGCAAACGGCGACCATGCC 180
AF192899        CGCGTCCTTTACCAAGGAAATAGTGTTACTGTATCTGCTTATGCAAACGGCGACCATGCC 180
AF192900        CGCGTCCTTTACCAAGGAAATAATGTCACTGTATCTGCTTATGCAAACGGCGACCATGCC 180
AF192897        CGCGTCCTTTACCAAGGAAATAATGTCACTGTATCTGCTTATGCAAACGGCGACCATGCC 180
AF192895        CGCGTCCTTTACCAAGGAAATAATGTCACTGTATCTGCTTATGCAAACGGCGACCATGCC 180
AF192894        CGCGTCCTTTACCAAGGAAATAATGTCACTGTATCTGCTTATGCAAACGGCGACCATGCC 180
FJ457636        CGCGTCCTTTACCAAGGAAATAACATCACTGTAACTGCCTATGCAAACGGCGACCATGCC 180
FJ882922        CGCGTCCTTTACCAAGGAAATAACATCACTGTAACTGCCTATGCAAACGGCGACCATGCC 180
FJ457640        CGCGTCCTTTACCAAGGAAATAACATCACTGTAACTGCCTATGCAAACGGCGACCATGCC 180
FJ457639        CGCGTCCTTTACCAAGGAAATAACATCACTGTAACTGCCTATGCAAACGGCGACCATGCC 180
FJ457638        CGCGTCCTTTACCAAGGAAATAACATCACTGTAACTGCCTATGCAAACGGCGACCATGCC 180
FJ457637        CGCGTCCTTTACCAAGGAAATAACATCACTGTAACTGCCTATGCAAACGGCGACCATGCC 180
AY549581        CGCGTCCTTTACCAAGGAAATAACATCACTGTAACTGCCTATGCAAACGGCGACCATGCC 180
AY549582        CGCGTCCTTTACCAAGGAAATAACATCACTGTAACTGCCTATGCAAACGGCGACCATGCC 180
EF051584        CGCGTCCTTTACCAAGGAAATAACATCACTGTAACTGCCTATGCAAACGGCGACCATGCC 180
                ******************* **   * *****  **** **********************


AM397006        GTCACAGTTAAGGACGCCAAATTCATAGTGGGGCCAATGTCTTCAGCCTGGACACCTTTC 240
AM397005        GTCACAGTTAAGGACGCCAAATTCATAGTGGGGCCAATGTCTTCAGCCTGGACACCTTTC 240
AM397007        GTCACAGTTAAGGACGCCAAATTCATAGTGGGGCCAATGTCTTCAGCCTGGACACCTTTC 240
AM397009        GTCACAGTTAAGGACGCCAAATTCATAGTGGGGCCAATGTCTTCAGCCTGGACACCTTTC 240
AM397008        GTCACAGTTAAGGACGCCAAATTCATAGTGGGGCCAATGTCTTCAGCCTGGACACCTTTC 240
AF394211        GTCACAGTTAAGGACGCTAAATTCATAGTGGGGCCAATGTCTTCAGCCTGGACACCTTTC 240
AF394210        GTCACAGTTAAGGACGCTAAATTCATAGTGGGGCCAATGTCTTCAGCCTGGACACCTTTC 240
EU192143        GTCACAGTTAAGGACGCTAAATTCATAGTGGGGCCAATGTCTTCAGCCTGGACACCTTTC 240
DQ520746        GTCACAGTTAAGGACGCTAAATTCATTGTGGGGCCAATGTCTTCAGCCTGGACACCTTTC 240
DQ520748        GTCACAGTTAAGGACGCTAAATTCATTGTGGGGCCAATGTCTTCAGCCTGGACACCTTTC 240
DQ520754        GTCACAGTTAAGGACGCTAAATTCATTGTGGGGCCAATGTCTTCAGCCTGGACACCTTTC 240
AF192899        GTCACAGTTAAGGACGCTAAATTCATAGTGGGGCCAATGTCTTCAGCCTGGACACCTTTC 240
AF192900        GTCACAGTTAAGGACGCTAAATTCATAGTGGGGCCAATGTCTTCAGCCTGGACACCTTTC 240
AF192897        GTCACAGTTAAGGACGCTAAATTCATAGTGGGGCCAATGTCTTCAGCCTGGACACCTTTC 240
AF192895        GTCACAGTTAAGGACGCTAAATTCATAGTGGGGCCAATGTCTTCAGCCTGGACACCTTTC 240
AF192894        GTCACAGTTAAGGACGCTAAATTCATAGTGGGGCCAATGTCTTCAGCCTGGACACCTTTC 240
FJ457636        GTCACAGTTAAGGACGCCAAATTCATTGTGGGGCCAATGTCTTCAGCCTGGACACCTTTC 240
FJ882922        GTCACAGTTAAGGACGCCAAATTCATTGTGGGGCCAATGTCTTCAGCCTGGACACCTTTC 240
FJ457640        GTCACAGTTAAGGACGCCAAATTCATTGTGGGGCCAATGTCTTCAGCCTGGACACCTTTC 240
FJ457639        GTCACAGTTAAGGACGCCAAATTCATTGTGGGGCCAATGTCTTCAGCCTGGACACCTTTC 240
FJ457638        GTCACAGTTAAGGACGCCAAATTCATTGTGGGGCCAATGTCTTCAGCCTGGACACCTTTC 240
FJ457637        GTCACAGTTAAGGACGCCAAATTCATTGTGGGGCCAATGTCTTCAGCCTGGACACCTTTC 240
AY549581        GTCACAGTCAAGGACGCCAAATTCATTGTGGGGCCAATGTCTTCAGCCTGGACACCTTTC 240
AY549582        GTCACAGTCAAGGACGCCAAATTCATTGTGGGGCCAATGTCTTCAGCCTGGACACCTTTC 240
EF051584        GTCACAGTCAAGGACGCCAAATTCATTGTGGGGCCAATGTCTTCAGCCTGGACACCTTTC 240
                ******** ******** ******** **********************************
```

ภาพที่ 16 เปรียบเทียบลำดับนิวคลิโอไทด์ของไวรัสชิคุนกุนยาสายพันธุ์ต่างๆตามที่ระบุด้วย accession number

อย่างไรก็ดีมีรายงานจากการสัมภาษณ์ ศ.นพ.ยง ภู่วรวรรณ พบบางตำแหน่งของลำดับนิวคลีโอไทด์ที่ระบาดในขณะนี้อาจต่างจากสายพันธุ์ที่ระบาดในประเทศไทยอยู่แล้ว จึงได้ดำเนินการศึกษาลำดับนิวคลิโอไทด์เพิ่มเติมโดยดำเนินการโคลนชิ้นส่วนของยีน E1 จากตัวอย่างที่ได้มา และเปรียบเทียบระหว่างเชื้อที่ระบาดในประเทศกับเชื้ออื่น การศึกษาเปรียบเทียบความแตกต่างระหว่างลำดับนิวคลีโอไทด์ พบการกลายพันธุ์ในบางตำแหน่ง อย่างไรก็ดียังคงมีตำแหน่งที่ให้ความเหมือนกันของลำดับนิวคลีโอไทด์มากพอ ที่จะใช้ออกแบบไพรเมอร์ สำหรับการเพิ่มปริมาณชิ้นส่วนของดีเอ็นเอ บนหลักการของการเพิ่มปริมาณดีเอ็นเออุณหภูมิระนาบเดียว (ภาพที่ 17.)

```
CLUSTAL W (1.83) multiple sequence alignment

FJ457640        ------------------------------------------------------TGCTTCTG 8
AF192894        ---------------------------------------------GGCGCCTACTGCTTCTG 17
thCKK           GGTACTTATATAGGGGCGATTGGGCCCGACGTCGCATGCTCCCGGCCGCCATGGCGGCCG 60
                                                              **  * *

FJ457640        CGACGCTGAAAATACGCAGTTGAGCGAAGCACATGTGGAGAAGTCCGAATCATGCAAAAC 68
AF192894        CGACACTGAAAATACGCAATTGAGCGAAGCACATGTGGAGAAGTCCGAATCATGCAAAAC 77
thCKK           CGGGAATTCGATTACGCAATTGAGCGAAGCACATGTGGAGAAGTCCGAATCATGCAAAAC 120
                **    *   * ****** **************************************

FJ457640        AGAATTTGCATCAGCGTACAGGGCTCATACCGCATCTGCATCAGCTAAGCTCCGCGTCCT 128
AF192894        AGAATTTGCATCAGCATACAGGGCCCATACCGCATCCGCATCAGCCAAGCTCCGCGTCCT 137
thCKK           AGAATTTGCATCAGCGTACAGGGCTCATACCGCATCTGCATCAGCTAAGCTCCGCGTCCT 180
                *************** ******** *********** ******** **************

FJ457640        TTACCAAGGAAATAACATCACTGTAACTGCCTATGCAAACGGCGACCATGCCGTCACAGT 188
AF192894        TTACCAAGGAAATAATGTCACTGTATCTGCTTATGCAAACGGCGACCATGCCGTCACAGT 197
CKK             TTACCAAGGAAATAATATCACTGTAACTGCCTATGCAAACGGCGACCATGCCGTCACAGT 240
                ***************  ******** **** ******************************

FJ457640        TAAGGACGCCAAATTCATTGTGGGGCCAATGTCTTCAGCCTGGACACCTTTCGACAACAA 248
AF192894        TAAGGACGCTAAATTCATAGTGGGGCCAATGTCTTCAGCCTGGACACCTTTCGACAACAA 257
thCKK           TAAGGACGCCAAATTCATTGTGGGGCCAATGTCTTCAG---------------------- 278
                ********* ******** ********************

FJ457640        AATTGTGGTGTACAAAGG 266
AF192894        AATCGTGG---------- 265
thCKK           ------------------
```

ภาพที่ 17 ลำดับนิวคลิโอไทด์ของตัวแทนไวรัสทั้ง 3 กลุ่มได้แก่ เอเชีย FJ457640 แอฟฟริกา AF192894และสายพันธุ์ที่พบในประเทศไทย(thCKK)

การออกแบบไพรเมอร์ด้วยโปรแกรม Primer Explorer Ver 4 (Fujitsu, Japan) ได้ ไพรเมอร์ตัวแทน 1 ชุด ที่มีความจำเพาะต่อยีน E1 ทั้ง 6 บริเวณ และเมื่อนำไปตรวจสอบความจำเพาะโดยการทำ Blastn พบว่ามีความจำเพาะกับ ยีน E1ของ ไวรัสดังกล่าวไม่ทำปฏิกิริยากับสารพันธุกรรมของไวรัสอื่น

ในการพัฒนาวิธีการเพิ่มปริมาณอาร์เอ็นเอของไวรัส เริ่มจากการสกัดอาร์เอ็นเอของไวรัสและทดสอบการเพิ่มปริมาณด้วยเทคนิค RT-PCR ได้ดำเนินการสกัด RNA จาก Serum ตัวอย่างที่มีเชื้อไวรัส (CKK) 5 ตัวอย่าง และเพิ่มปริมาณ cDNA ด้วยเทคนิค RT-PCR 2 ขั้นตอน เริ่มจากทำปฏิกิริยา reverse transcription ในสารละลายที่ประกอบไปด้วย 50mM Tris HCl(pH. 8.3) 8mM MgCl2 10mM DTT 100pM 3’ primer (5’-GAAGACATTGGCCCCAC-3’) 20U AMV reverse transcriptase บ่มปฏิกิริยาที่ 42^{0}C เป็นเวลา 60 นาที จากนั้นนำไปทำปฏิกิริยาเพิ่มปริมาณดีเอ็นเอในขั้นที่สองประกอบด้วย 10mM Tris.HCl (pH. 8.3) 1.5mM MgCl2 50mM KCl 1mM DTT 0.5% Tween 0.5% Nonidet P-40 2.5mM dNTP each และ 10pM primer each บ่มปฏิกิริยาที่ 93^{0}C 40 วินาที 55^{0}C 1 นาที และ 73 ^{0}C 1 นาที เป็นจำนวน 40 รอบ ภายหลังบ่มปฏิกิริยา cDNA ที่เพิ่มปริมาณได้มาแยกใน

สนามไฟฟ้า พบว่า cDNA ที่ได้มีขนาดประมาณ 220 นิวคลีโอไทด์สอดคล้องกับขนาดคาดหวังทางทฤษฎี เมื่อคำนวนขนาดจากไพรเมอร์(ภาพที่ 18.) cDNAที่ได้จะนำมาโคลนเข้าสู่พาหะ pGEM เพื่อใช้เป็นดีเอ็นเอควบคุมบวกต่อไป

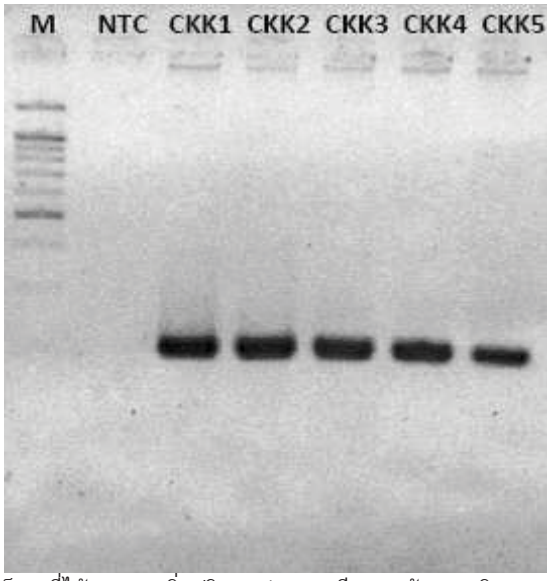

ภาพที่ 18 ผลิตภัณฑ์ดีเอ็นเอที่ได้จากการเพิ่มปริมาณส่วนของยีน E1 ด้วยเทคนิค RT-PCR เลน M 100 นิวคลีโอไทด์มาร์เกอร์ เลน NTC ชุดควบคุมที่ไม่มีดีเอ็นเอแม่แบบและ เลน CKK1-5 ตัวอย่างไวรัสที่ผ่านการทดสอบด้วยเทคนิค ELISA แล้ว แถบดีเอ็นเอดังกล่าวใช้เป็นแม่แบบในการโคลนยีนเพื่อใช้เป็นดีเอ็นเอควบคุมบวกต่อไป

การทดสอบการเพิ่มปริมาณRNA ด้วยเทคนิค การเพิ่มปริมาณดีเอ็นเอ อุณหภูมิเดียวด้วย เทคนิค RT-LAMPในสารละลายของปฏิกิริยาที่ประกอบไปด้วย40 mM Tris pH 8.8 20 mM KCl 16mM $MgSO_4$ 20 mM $(NH_4)_2SO_4$ 0.2% Tween 20 1.6 M Betaine 2.8 mM dNTP และ 8 U. *Bst* DNA polymerase ตามที่ระบุไว้โดย Notomi *et al*., (2000) โดยปฏิกิริยาประกอบด้วยไพรเมอร์ผสม ที่ประกอบด้วย 10 pmole each ของ F3B3 และ 40 pmole ของ FIP และ BIP การทดสอบสภาวะที่เหมาะสมในการบ่มปฏิกิริยาโดยใช้ชุดไพรเมอร์ที่ออกแบบได้ ได้ผลิตภัณฑ์ดีเอ็นเอจาก cDNA โดยเมื่อบ่มปฏิกิริยาในอุณหภูมิ 63 ^{0}C 40 นาที พบว่าสามารถเพิ่มปริมาณ cDNA ด้วยเทคนิค LAMP ทำให้ได้ผลิตภัณฑ์ดีเอ็นเอรูปขั้นบันได (ladder)ในทั้ง 5 ตัวอย่างที่ดำเนินการ ผลิตภัณฑ์ดีเอ็นเอขนาดเท่ากับผลคูณของขนาดดีเอ็นเอ 175 นิวคลิโอไทด์ ในทุกตัวอย่างแสดงให้เห็นถึงประสิทธิภาพในการเพิ่มปริมาณดีเอ็นเอ(ภาพที่ 19.)

การตรวจสอบความไวของปฏิกิริยา โดยใช้ดีเอ็นเอแม่แบบจากพลาสมิดที่ทราบจำนวนชุดของดีเอ็นเอ จาก 10^{+6}-1 copy และใช้องค์ประกอบของปฏิกิริยาเช่นเดียวกับการเพิ่มปริมาณด้วย RT-LAMP พบว่าชุดไพรเมอร์ที่ออกแบบได้สามารถเพิ่มปริมาณยีน E1 ได้แม้จะมีระดับความเข้มข้นของแม่แบบต่ำเพียง 100 copies หรือสรุปได้ว่า ไพรเมอร์มีมากกว่า ใช้ Limit of detection (LOD) ที่ 100 copies (ภาพที่ 20.)

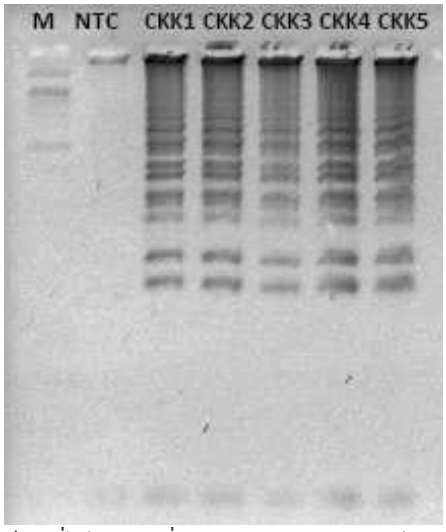

ภาพที่ 19 ผลิตภัณฑ์ดีเอ็นเอที่ได้จากการเพิ่มปริมาณส่วนของยีน E1 ด้วยเทคนิค RT-LAMP เลน M 100 นิวคลิโอไทด์มาร์เกอร์ เลน NTC ชุดควบคุมที่ไม่มีดีเอ็นเอแม่แบบและ เลน CKK1-5 ตัวอย่างไวรัสที่ผ่านการทดสอบด้วยเทคนิค ELISA แล้ว

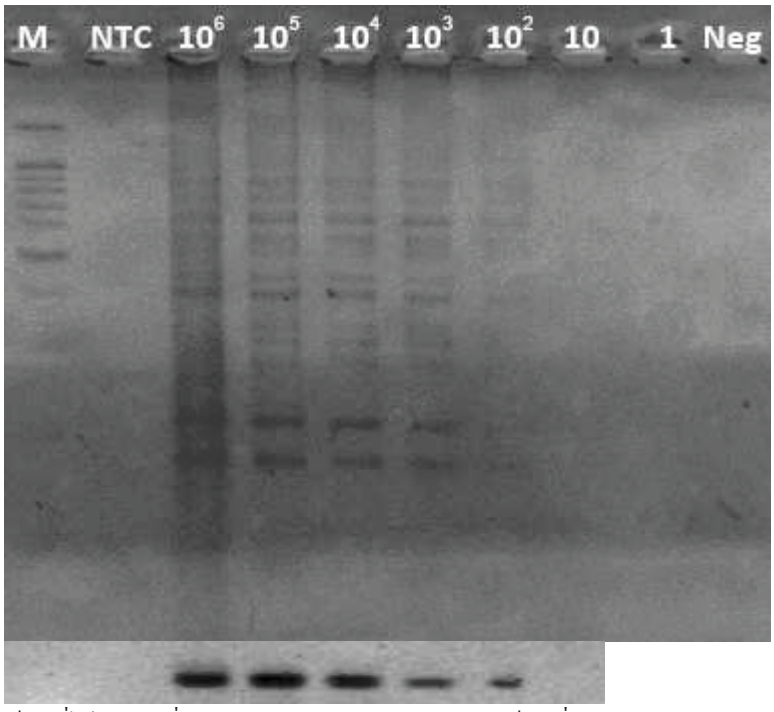

ภาพที่ 20 ผลิตภัณฑ์ดีเอ็นเอที่ได้จากการเพิ่มปริมาณส่วนของยีน E1 กับแม่แบบดีเอ็นเอที่ทราบปริมาณในรูปจำนวนชุดหรือ ก็อปปี้ จาก 10^6-1 ก็อปปี้ ด้วยเทคนิค RT-LAMP เลน M 100 นิวคลิโอไทด์มาร์เกอร์ เลน NTC ชุดควบคุมที่ไม่มีดีเอ็นเอแม่แบบและ เลน ตัวอย่างยีน E1 ของไวรัสที่ทราบจำนวน และเลน Neg เมื่อใช้แม่แบบเป็นอาร์เอ็นเอจาก influenza virus ด้านล่างเป็นผลเปรียบเทียบเมื่อทดสอบด้วยเทคนิค RT-PCR

การตรวจสอบความจำเพาะของปฏิกิริยา เมื่อใช้ไวรัสเดงกี่ ชนิดต่างๆ เป็นตัวทดสอบ พบว่าชุดไพรเมอร์ที่ออกแบบได้มีความจำเพาะตัวไวรัสชิคุนกุนยา แต่ไม่ทำปฏิกิริยากับอาร์เอ็นเอของไวรัสเดงกี่ แต่อย่างใด (ภาพที่ 21.)

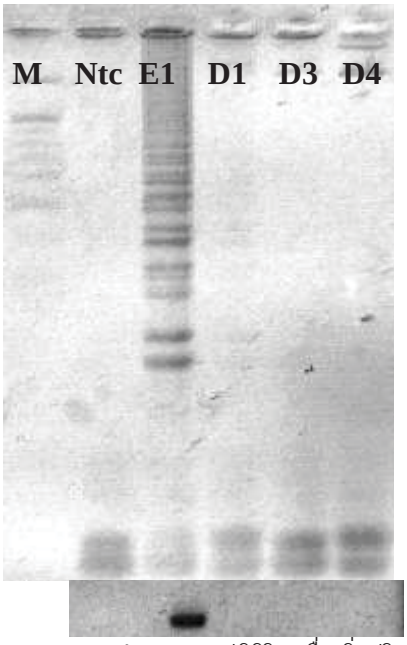

ภาพที่ 21 การทดสอบความจำเพาะของปฏิกิริยาเมื่อเพิ่มปริมาณส่วนของยีน E1 ด้วยเทคนิค RT-LAMP เปรียบเทียบกับเมื่อทดสอบกับไวรัสเดนกี่ สายพันธุ์ 1 3 และ4 เลน M 100 นิวคลิโอไทด์มาร์เกอร์ เลน Ntc ชุดควบคุมที่ไม่มีดีเอ็นเอแม่แบบ เลน E1 ชิคุนกุนยาไวรัส และ เลนD1-4 ตัวอย่างเดนกี่ไวรัส สายพันธุ์ D1 3 และ 5 ด้านล่างเป็นผลเปรียบเทียบเมื่อทดสอบด้วยเทคนิค RT-PCR

โครงการยังได้พัฒนาระบบการตรวจสอบสัญญาณดีเอ็นเอโดยใช้วิธี colorimetric โดยการทำปฏิกิริยากับอนุภาคนาโนเงิน สีน้ำเงินโดยใช้เงื่อนไขเช่นเดียวกับที่ได้รายงานผลในรอบ 1 ปี ผลการตรวจวิเคราะห์เมื่อใช้อนุภาคนาโนเป็นระบบตรวจสัญญาณ พบการจับตัวของอนุภาคทำให้เกิดการตกตะกอนเป็นสารละลายใสไม่มีสี มองเห็นได้ด้วยตาเปล่าในตัวอย่างที่เป็นลบ และตัวอย่างที่เป็นดีเอ็นเอที่ไม่ใช่ดีเอ็นเอเป้าหมาย ขณะที่ในตัวอย่างที่เป็นบวกจะไม่ตกตะกอน (ภาพที่ 22.)

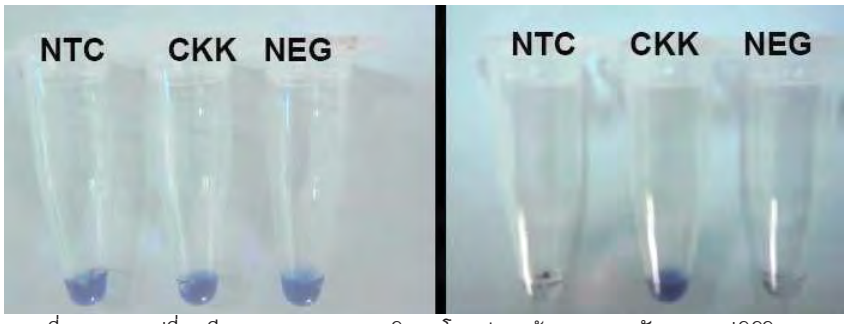

ภาพที่ 22 การเปลี่ยนสีของตะกอนอนุภาคเงินนาโน ก่อน(ซ้าย) และหลัง(ขวา) ปฏิกิริยา พบการตกตะกอนในชุดควบคุมลบ (NEG) และในชุดควบคุมที่ไม่มีดีเอ็นเอเป้าหมาย (NTC) ขณะที่อนุภาคเงินนาโนไม่ตกตะกอนในตัวอย่างที่มีดีเอ็นเอเป้าหมาย (CKK)

จากผลการทดลองที่ได้ดำเนินการพบว่าระบบการตรวจที่อาศัย β-pyrolidinyl peptide nucleic acid สามารถเปลี่ยนแปลงสัญญาณ ในรูปแบบการเปลี่ยนของพลาสมอนทางแสง โดยในภาวะที่ไม่มีดีเอ็นเอเป้าหมาย โพลบจะจับตัวบนผิวอนุภาคโดยอาศัยด้าน hydrophobic ไปที่ผิวอนุภาค เกลือในระบบจะกระตุ้นให้เกิดการจับตัวของอนุภาค แต่ในภาวะที่มีดีเอ็นเอเป้าหมาย โพลบจะกับดีเอ็นเอเป้าหมาย ช่วยให้อนุภาคกระจายตัวไม่เกาะกัน จึงไม่เกิดการเปลี่ยนแปลงอยู่ในรูปการตกตะกอน โดยสรุป การดำเนินการทำให้ได้ระบบการตรวจชิคุนกุนยาไวรัสด้วยอนุภาคเงินนาโนสีน้ำเงิน ซึ่งยังไม่เคยมีรายงานมาก่อน ระบบดังกล่าวใช้งานง่ายและมีต้นทุนต่ำ

4.2 การประยุกต์ใช้เบต้าพิโรลิดินิลเพปไทด์นิวคลีอิกแอซิดในทางการเกษตรและอาหาร

สำหรับการประยุกต์ใช้เบต้าพิโรลิดินิลเพปไทด์นิวคลีอิกแอซิดในทางการเกษตรนั้น ได้นำหลักการเดียวกันกับที่ประสบความสำเร็จกับยีน neuraminidase ข้างต้น มาปรับใช้สำหรับการตรวจสอบโรคในกุ้งที่ผลิตเพื่อการส่งออก โดยนำระบบการเพิ่มปริมาณดีเอ็นเอที่ทางห้องปฏิบัติการได้พัฒนาขึ้นมาพัฒนาต่อยอด (ณัฐพร อุดมพงษ์ และปิยะศักดิ์ ชอุ่มพฤกษ์, 2551) นอกจากนี้ยังได้พัฒนาเทคนิคการตรวจเพื่อตอบโจทย์การตรวจสอบไวรัสที่ก่อให้เกิดโรคในสับปะรด และ การตรวจสอบการสุกแก่ทางสรีรวิทยาแบบไม่ทำลายผลในสับปะรด

4.2.1 พัฒนาวิธีการตรวจสอบไวรัสที่ก่อให้เกิดโรคในกุ้ง

สำหรับประเทศไทยแล้ว อุตสาหกรรมการเพาะเลี้ยงกุ้งเป็นอุตสาหกรรมที่มีขนาดใหญ่เกี่ยวข้องกับเกษตรกรหลายแสนราย และเกี่ยวกับโรงงานแปรรูปต่อเนื่องที่มีคนงานเป็นจำนวนมากจึงมีความสำคัญในเชิงเศรษฐกิจมาก ส่วนหนึ่งเป็นเพราะประเทศไทยส่งกุ้งแช่แข็งเป็นอันดับต้นๆของโลก โดยแต่ละปีประเทศไทยส่งออกกุ้งคิดเป็นมูลค่าสูงถึง 53,000 ล้านบาท ความสามารถในการรักษาศักยภาพในการแข่งขันนี้ ขึ้นกับความสามารถในการจัดการทางด้านคุณภาพในการผลิต

ในการผลิตกุ้งเชิงพาณิชย์มีโรคสำคัญได้แก่โรคไวรัส โรคดังกล่าวส่งผลกระทบโดยตรงในระหว่างการผลิต การติดเชื้อไวรัสในกุ้งส่งผลต่อการเจริญเติบโต และอัตตราการตายของกุ้งในบ่อ โดยปกติในการผลิตกุ้ง ปัญหาโรคกุ้งมีความสำคัญยิ่ง โดยปกติกุ้งที่เลี้ยงมักพบปัญหาโรคติดเชื้อจากไวรัส โดยเฉพาะอย่างยิ่ง white spot syndrome virus (WSSV) infectious hypodermal and hematopoietic necrosis virus (IHHNV)

การตรวจหาเชื้อจึงมีความสำคัญยิ่งสำหรับอุตสาหกรรมการเลี้ยงกุ้ง โดยที่ผ่านมาเทคนิคการตรวจทางอณูชีววิทยาได้เข้ามามีบทบาท เช่น การตรวจโดยเทคนิค dot blot hybridization และเทคนิคบนพื้นฐานของหลักการ PCR ทั้ง PCR มาตรฐาน RT-PCR RT-

nested PCR multiplex RT-PCR และ real-time PCR (Lightner, 1996, Flegel et al., 1995) การตรวจเชื้อไวรัส WSSV ใช้ไพรเมอร์ที่ออกแบบมาเป็นพิเศษให้เฉพาะเจาะจงกับส่วนยีน Transmembrane signal peptide ของไวรัส WSSV ขณะที่การตรวจเชื้อไวรัส IHHNV ใช้ไพรเมอร์ที่ออกแบบมาเป็นพิเศษให้เฉพาะเจาะจงกับส่วนยีน NS-1 ของไวรัส IHHNV

การเพิ่มปริมาณดีเอ็นเอ การตรวจสอบความจำเพาะของปฏิกิริยาและการทดสอบความไวของปฏิกิริยาได้ดำเนินการและรายงานมาก่อนหน้าแล้ว (ณัฐพร อุดมพงษ์ และปิยะศักดิ์ ชอุ่มพฤกษ์, 2551)

การพัฒนาระบบตรวจสอบในครั้งนี้ได้ออกแบบ PNAโพรบและquencher ได้โพรบ PNA 2 ชนิด และquencher 2 ชนิดแต่ละชนิดมีความจำเพาะต่อยีน Transmembrane signal peptide ของไวรัส WSSV และยีน NS-1 ของไวรัส IHHNV ดังตารางที่ 3

ตารางที่ 3. PNA โพรบ และ quencher สำหรับการตรวจสอบไวรัส wssv และ IHHNV และนิวคลีโอไทด์ที่เกี่ยวข้อง

Element	detail sequence	binding position
PNA WSSV	Flu-O-ctaaattcaga-LysNH_2	258835-258845
Quencher # 1	5'-aatttag-3'-BHQ	258835-258841
PNA IHHNV	TMR-O-gaaccaacaga-LysNH_2	281-291
Quencher# 2	5'-ttggttc-3'-BHQ	281-287

กลไกการจับตัวระหว่าง PNAโพรบและquencher ยังคงเป็นไปตามหลักการเดียวกันกับที่ใช้ตรวจไวรัสไข้หวัดใหญ่ 2009 neuraminidase ยีน ยกเว้นในการตรวจไวรัส WSSV ใช้ FAM fluorophore ติดที่ตำแหน่ง 5' ของPNAโพรบและในการตรวจไวรัส IHHNV ใช้ TAMRA fluorophore ติดที่ตำแหน่ง 5' ของPNAโพรบ(ดูตารางที่ 3 ประกอบ) ในทางทฤษฎีการจับตัวของPNAโพรบกับกรดนิวคลิอิกของไวรัสที่ประสบความสำเร็จจะทำให้เกิดการเรืองแสงที่ต่างกัน โดยผลการตรวจ WSSV เรืองแสงสีเขียวและผลการตรวจ IHHNV เรืองแสงสีชมพู

ผลการทดสอบการเรืองแสงโดยจับตัวระหว่าง probe ทั้งที่จำเพาะต่อ WSSV และต่อ IHHNV โดยทำปฏิกิริยาระหว่าง probe ความเข้มข้น 10 µM ปริมาตร 3 µl จับ DNA products ที่เพิ่มปริมาณได้ โดยให้ความร้อนกับดีเอ็นเอที่ 80 $^{\circ}$C เป็นเวลา 5 นาที และปล่อยให้จับตัวที่ 50°C เป็นเวลา 15 นาที ก่อนนำมาทดสอบโดยการส่องดูด้วยแสง UV ความยาวคลื่น ● 312 nm พบว่า เฉพาะหลอดที่ให้ดีเอ็นเอเป้าหมายเท่านั้นที่พบการเรืองแสง (ภาพที่ 23.)

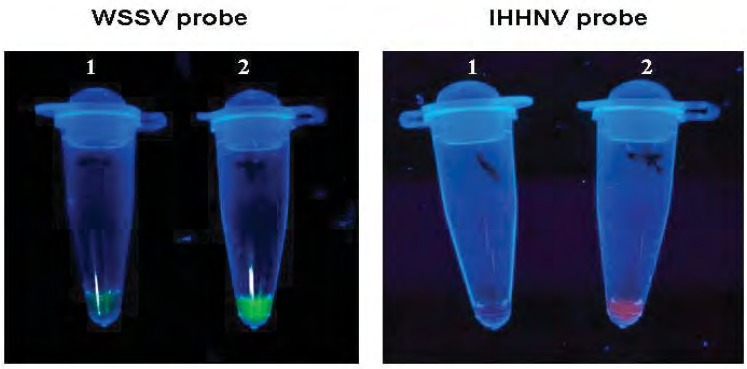

ภาพที่ 23 แสดงผลการจับตัวของ PNA โพรบต่อเป้าหมายกรดนิวคลีอิกของไวรัส WSSV (ซ้าย) และ IHHNV (ขวา) โดยตัวอย่างที่เป็นลบ (Negative) แสดงด้วยหมายเลย (1) และตัวอย่างที่เป็นบวกแสดงด้วยหมายเลข 2

ผลดังกล่าวแสดงให้เห็นว่าระบบการทดสอบปฏิกิริยา hybridization ด้วยเบต้าพิโรลิดินิลเพปไทด์นิวคลีอิกแอซิดสามารถใช้ตรวจวิเคราะห์โรคไวรัสที่เกิดขึ้นกับกุ้งได้พร้อมๆ กัน (แยกหลอด)

นอกจากนี้ได้พัฒนาระบบการตรวจต่อยอดให้สามารถเพิ่มปริมาณสารพันธุกรรมของไวรัสภายในหลอดเดียวกันที่เรียกว่า multiplex LAMP ทั้งนี้จากการศึกษาเบื้องต้น ไวรัสทั้ง 2 ชนิดเป็นไวรัสที่มีสารพันธุกรรมเป็นดีเอ็นเอ และไวรัสทั้งสองชนิดเป็นไวรัส คนละวงศ์กัน จึงมีลำดับนิวคลีโอไทด์แตกต่างกันอย่างสิ้นเชิง ดังนั้นจึงได้พัฒนาเทคนิคการตรวจสอบในรูป multiplex LAMP ขึ้น ซึ่งที่ผ่านมาไม่เคยมีรายงานการพัฒนาเทคนิค LAMP ในรูป multiplex มาก่อน เนื่องจากในปฏิกิริยาการเพิ่มปริมาณดีเอ็นเอ เกี่ยวพันกับไพรเมอร์หลายคู่ และจำเพาะต่อหลายบริเวณของยีนเป้าหมาย

การพัฒนาเทคนิคการเพิ่มปริมาณดีเอ็นเอจึงเริ่มต้นจาก การตรวจแต่ละปฏิกิริยาไม่ให้สามารถทำปฏิกิริยาข้ามกัน ซึ่งดำเนินการโดยการโปรแกรม Blastn (Altschul, *et al.,* 1990) สำหรับ WSSV ได้ออกแบบไพรเมอร์โดยใช้ยีน transmembrane signal peptide ของไวรัส wssv และสำหรับ IHHNV ใช้ยีน NS-1

ไพรเมอร์ที่ได้จะนำมาปรับให้เป็นสัดส่วนของไพรเมอร์ F3 B3 ต่อสัดส่วนของไพรเมอร์ที่เหลือ (F1cF2) (B1c B2) เป็น 1:8 และใช้ชุดของไพรเมอร์สำหรับ WSSV และชุดไพรเมอร์สำหรับ IHHNV ในสัดส่วน 1:1 ในการทำปฏิกิริยาแบบ multiplex LAMP สำหรับการตรวจโรคไวรัสกุ้ง 2 ชนิดในครั้งนี้ได้ปรับตัวปฏิกิริยารวมของไพรเมอร์ให้อยู่ในระดับไม่เกิน 40 pmole ของ F3B3 และ 5 pmole ของชุดไพรเมอร์ที่เหลือและชดเชยปฏิกิริยาในเฉพาะส่วนของสารเคมีมากกว่าปกติได้แก่ dNTP ชดเชย 1.5 เท่า $MgSO_4$ เพิ่มเป็น 2 เท่าของปกติ Betain เพิ่มเป็น 1.25 เท่าของปกติ และเอนไซม์ *Bst* DNA polymerase เพิ่มเป็น 1.2 เท่าของปกติ

multiplex ของปฏิกิริยามาตรฐานของไวรัสโรคกุ้งสามารถดำเนินการได้ในหลอดเดียวและให้ผลิตภัณฑ์ในรูปขั้นบันได ที่เป็นลักษณะเฉพาะของผลิตภัณฑ์ดีเอ็นเอที่ได้จากปฏิกิริยา LAMP โดยเป็นผลคูณของขนาดดีเอ็นเอ 180/210 นิวคลีโอไทด์สำหรับ WSSV และ 160/180

นิวคลีโอไทด์สำหรับ IHHNV และในกรณีที่เป็น mix virus จะได้ผลิตภัณฑ์ดีเอ็นเอขนาดเท่ากับผลคูณของขนาดดีเอ็นเอที่ 160/180 นิวคลีโอไทด์ โดยผลการตรวจสอบสอดคล้องกับวิธีการตรวจสอบปกติที่ดำเนินการด้วยเทคนิค PCR (Kono et al, 2004, Sun et al, 2006) (ภาพที่ 24.)

สำหรับการตรวจสอบสัญญาณดีเอ็นเอดำเนินการโดยระบบตรวจการเปลี่ยนแปลงทางสีของแสงอันเป็นผลจาก plasmon resonance ของอนุภาคนาโนของทองคำตามหลักการที่อธิบายไว้ (Kanchanawarut et al, 2009) ในปฏิกิริยาประกอบด้วยทองคำขนาด 20 nm 5000 ppm 10 µl ผลิตภัณฑ์ดีเอ็นเอที่ได้จากปฏิกิริยา LAMP 1 µl PNA probe ที่จำเพาะต่อไวรัสแต่ละชนิด 1 µM และ 1 µl เกลือในรูปสารละลาย PBS บัฟเฟอร์ (100mM PBS) โดยปฏิกิริยา hybridization เกิดขึ้นที่อุณหภูมิห้อง ผลการตกตะกอนของอนุภาคทองคำนั้นจะเกิดขึ้นในเวลา 30 วินาทีถึง 1 นาที โดย PNA probe จะแสดงพฤติกรรมเป็น coagulant โดย PNA probe จะจับตัวอยู่ที่ผิวของอนุภาคทองคำการจับตัวนี้เกิดได้จากส่วนของ nitrogen/oxygen ในเบสและจากโครงสร้างของ PNA เองที่เป็น hydrophobic neutral structure โดยในขณะที่ไม่มีดีเอ็นเอเป้าหมาย ในภาวะที่มีเกลือเข้มข้นต่ำ PNA จะช่วยกระตุ้นให้เกิดการจับตัวของอนุภาคทำให้เกิดการตกตะกอนเปลี่ยนสีของสารละลายอนุภาคทองคำจากสีแดงอมชมพูไปเป็นสีม่วงเข้ม ขณะที่ในภาวะที่มีดีเอ็นเอเป้าหมาย การจับตัวระหว่าง PNA probe กับ ดีเอ็นเอเป้าหมายจะก่อให้เกิด hybridization complex ซึ่งเป็นโครงสร้างที่คล้ายกับ double stand DNA ทำหน้าที่ป้องกันการจับตัวของอนุภาคทองคำ จึงทำให้เกิดการตกตะกอนและไม่เกิดการเปลี่ยนสีของสารละลายอนุภาคทองคำ

ผลการทดลองแสดงให้เห็นการตะกอนหรือการเปลี่ยนสีของสารละลายอนุภาคทองคำเป็นสีม่วงเข้มในหลอดที่เป็นผลลบ ขณะที่ในหลอดที่เป็นผลบวกจะไม่ตกตะกอนจึงยังคงเห็นสีของสารละลายอนุภาคทองคำเป็นสีแดงอมชมพูเหมือนเดิม (ภาพที่ 24 ล่าง)

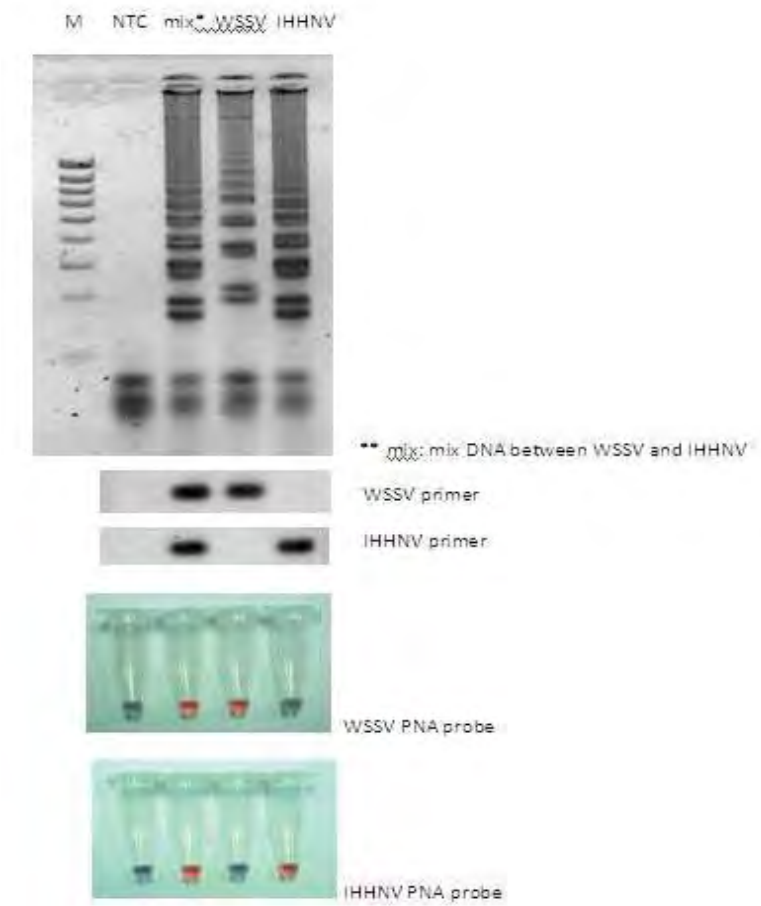

ภาพที่ 24 ผลการเพิ่มปริมาณดีเอ็นเอของไวรัส WSSV และ IHHNV ด้วยปฏิกิริยา multiplex LAMP เมื่อตรวจจากผลิตภัณฑ์ดีเอ็นเอที่ได้จากการแยกด้วยสนามไฟฟ้า(บน) เปรียบเทียบกับการเพิ่มปริมาณดีเอ็นเอของไวรัส WSSV และ IHHNV ด้วยปฏิกิริยา PCR (กลาง) และผลการตรวจด้วยวิธี colorimetric detection บนพื้นฐานของการตกตะกอนของอนุภาคทองคำนาโนตามหลักการไบโอเซ็นเซอร์ เมื่อใช้โพรบ PNA ที่จำเพาะต่างกัน (ล่าง) เลน M 100 nucleotide ladder เลน ntc nontemplate control เลน mix ดีเอ็นเอผสมจาก WSSV IHHNV เลน WSSV ดีเอ็นเอจาก WSSV เลนIHHNV ดีเอ็นเอจาก IHHNV WSSV primer หมายถึงผลิตภัณฑ์ดีเอ็นเอที่ได้จากการเพิ่มปริมาณโดยวิธี PCR ด้วยWSSV primer และ IHHNV IHHNV primer หมายถึงผลิตภัณฑ์ดีเอ็นเอที่ได้จากการเพิ่มปริมาณโดยวิธี PCR ด้วย IHHNV primer

การทดสอบความจำเพาะของคู่ไพรเมอร์ทั้ง 2 ชุดในรูปแบบ multiplex กับไวรัสเป้าหมายทั้งสองชนิดร่วมกับไวรัส TSV (Taura symdrome virus) YHV (Yellow head virus) ซึ่งทั้งสองเป็น อาร์เอ็นเอไวรัสที่ติดเชื้อในกุ้ง รวมถึงไวรัสที่พบในสัตว์ในฟาร์มเช่น PCV (Porcine circo virus) PRRSV (porcine reproductive and respiratory syndrome virus) ทั้งสายพันธุ์ US En และ China รวมถึงกับสารพันธุกรรมจากเชื้ออื่นเช่น *Escherichia canis* *Aspergillus flavus* และเชื้อ Swine virus (HA)

พบว่าชุดไพรเมอร์ multiplex ยังคงมีความจำเพาะต่อไวรัสทั้งสองชนิด และไม่ทำปฏิกิริยากับสารพันธุกรรมของไวรัสและของเชื้อของสัตว์ในฟาร์มแต่อย่างใด ผลดังกล่าวแสดงให้เห็นถึงประสิทธิภาพของภาพรวมชุดไพรเมอร์ทั้ง 2 ในการตรวจสอบชนิดของไวรัสโรคกุ้ง (ภาพที่ 25.) นอกจากนี้ผลการตรวจด้วย PNA ร่วมกับอนุภาคนาโนทองคำยังสอดคล้องกับผลการตรวจสอบโดยการแยกผลิตภัณฑ์ดีเอ็นเอด้วยสนามไฟฟ้า (ภาพที่ 25 ล่าง) และผลดังกล่าวสอดคล้องกับการตรวจด้วยวิธี PCR

ทำนองเดียวกัน การทดสอบความไวของปฏิกิริยาพบว่าการใช้คู่ไพรเมอร์ทั้ง 2 ชุด ผสมเป็น multiplex ยังคงให้ผลการเพิ่มปริมาณดีเอ็นเอได้เป็นอย่างดีและสามารถตรวจสอบแม่แบบที่เป็นดีเอ็นเอของยีน transmembrane signal peptide และ NS-1 ได้ในระดับ 10 copies ซึ่งอยู่ในระดับเดียวกับการตรวจด้วยวิธี PCR ที่สำคัญสามารถดำเนินการได้ในหลอดเดียว ซึ่งถือว่าเป็นข้อได้เปรียบอย่างมาก (ภาพที่ 26A. และ 26B.) การตรวจสอบความไวของปฏิกิริยาโดย PNA probe ร่วมกับสารละลายอนุภาคทองคำนาโน ต่างก็ให้ผลสอดคล้องกับผลการตรวจด้วยวิธี PCR

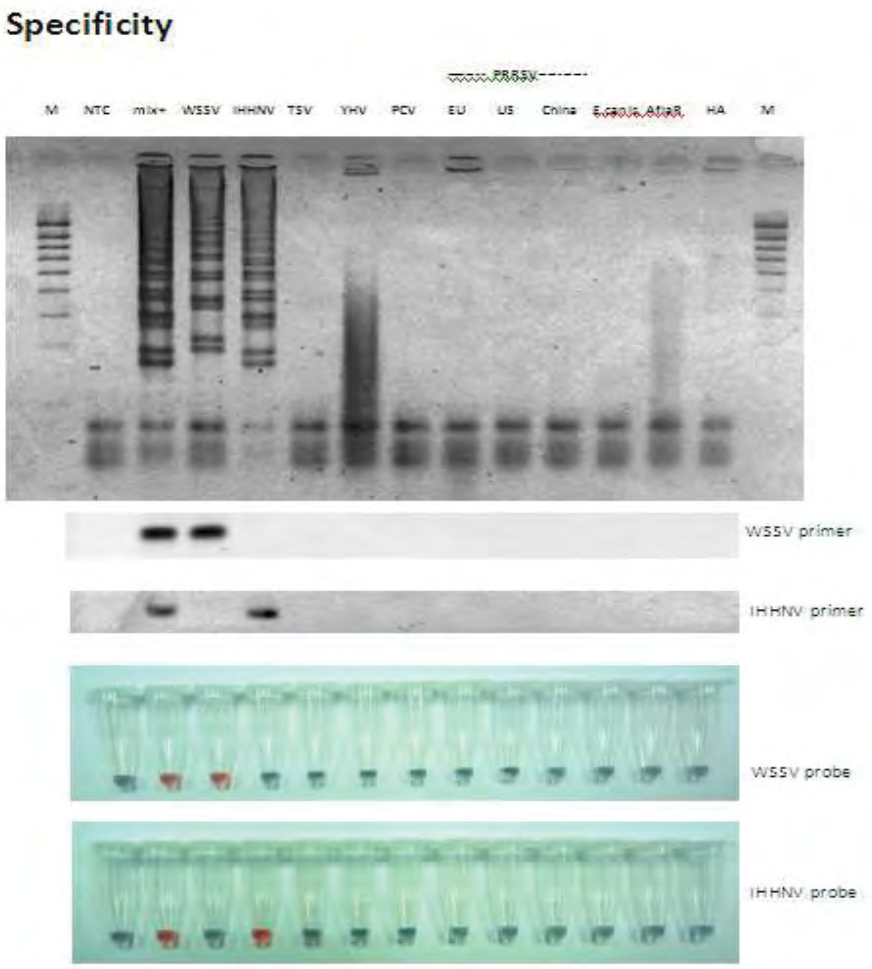

ภาพที่ 25 ความจำเพาะของปฏิกิริยาสำหรับการตรวจไวรัสทั้งสองชนิด เมื่อตรวจจากผลิตภัณฑ์ดีเอ็นเอจากปฏิกิริยา LAMP ที่ได้จากการแยกด้วยสนามไฟฟ้า(บน) จากผลิตภัณฑ์ดีเอ็นเอจากปฏิกิริยา PCR ที่ได้จากการแยกด้วยสนามไฟฟ้า (กลาง) และผลการตรวจด้วยวิธี colorimetric detection บนพื้นฐานของการตกตะกอนของอนุภาคทองคำนาโนตามหลักการไบโอเซ็นเซอร์ เมื่อใช้โพลบ PNA ที่จำเพาะต่างกัน (ล่าง) เลน M 100 nucleotide ladder เลน ntc non template control เลน mix เป็นดีเอ็นเอผสมของ WSSV IHHNV เลน WSSV ดีเอ็นเอจาก WSSV เลน IHHNV ดีเอ็นเอจาก IHHNV WSSV primer หมายถึงผลิตภัณฑ์ดีเอ็นเอที่ได้จากการเพิ่มปริมาณโดยวิธี PCR ด้วยWSSV primer และ IHHNV IHHNV primer หมายถึงผลิตภัณฑ์ดีเอ็นเอที่ได้จากการเพิ่มปริมาณโดยวิธี PCR ด้วย IHHNV primer

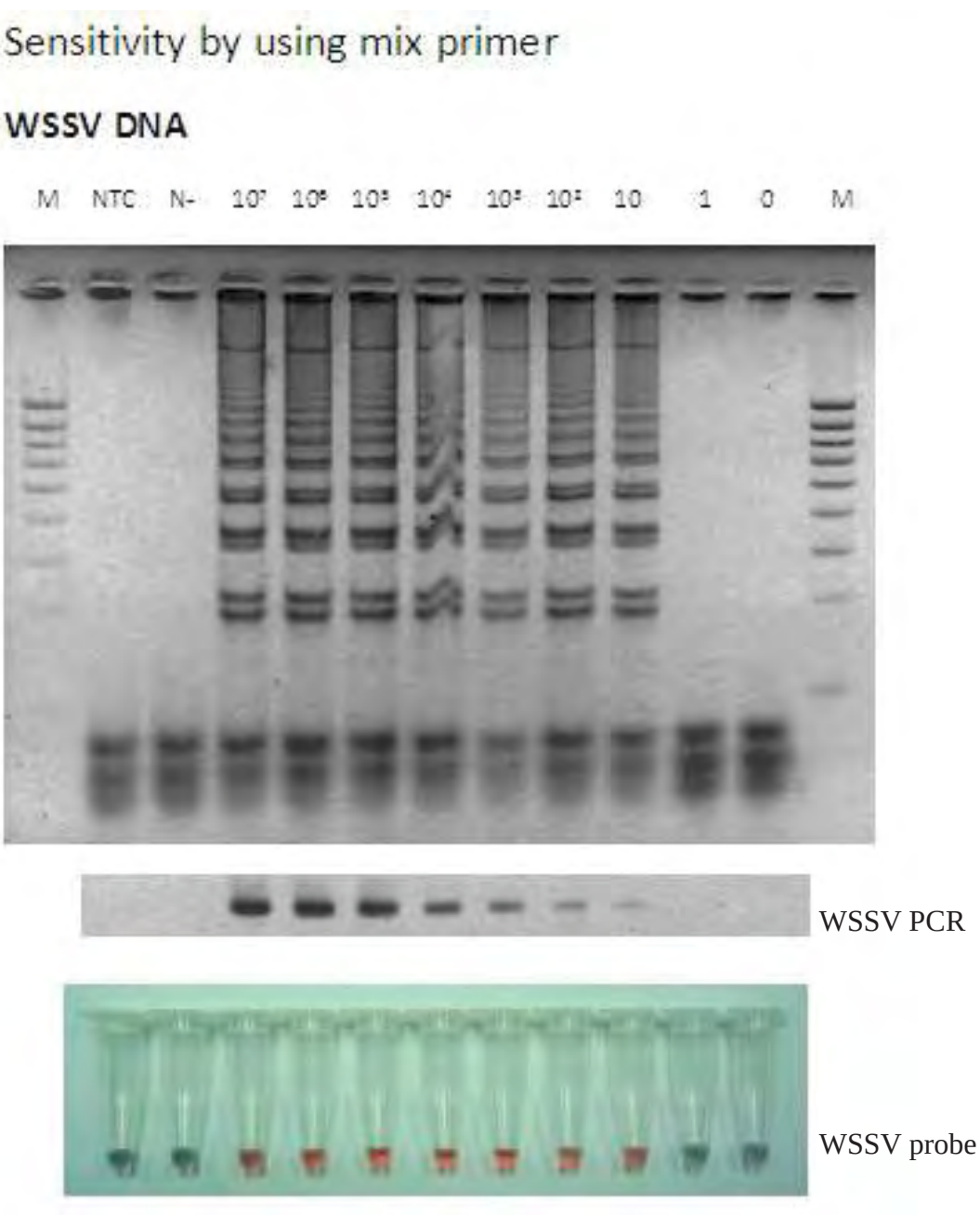

ภาพที่ 26A ความไวของปฏิกิริยาของชุดไพรเมอร์ในการเพิ่มปริมาณดีเอ็นเอไวรัส WSSV เมื่อตรวจจากผลิตภัณฑ์ดีเอ็นเอจากปฏิกิริยา LAMP ที่ได้จากการแยกด้วยสนามไฟฟ้า(บน) เปรียบเทียบกับผลิตภัณฑ์ดีเอ็นเอจากปฏิกิริยา PCR ที่ได้จากการแยกด้วยสนามไฟฟ้า (กลาง) และผลการตรวจด้วยวิธี colorimetric detection บนพื้นฐานของการตกตะกอนของอนุภาคทองคำนาโนตามหลักการไบโอเซ็นเซอร์ เมื่อใช้โพลบ PNA ที่จำเพาะ (ล่าง) เลน M 100 nucleotide ladder เลน ntc non template control เลน N– ตัวอย่างควบคุมลบ PCV เลน10^7 ถึง 10^2 10 1 แสดงจำนวนก๊อปปี้ของดีเอ็นเอแม่แบบจากไวรัส WSSV

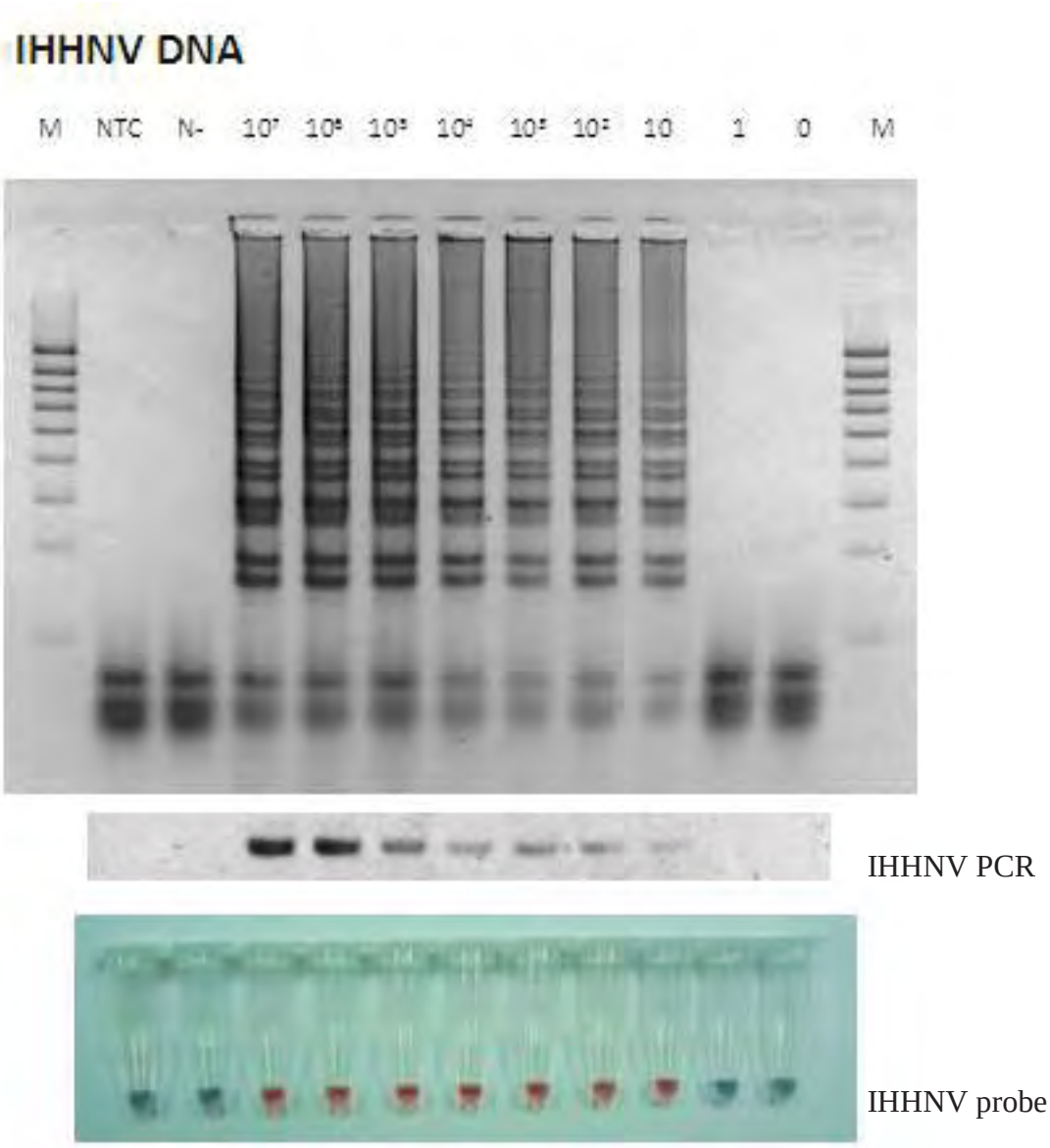

ภาพที่ 26B ความไวของปฏิกิริยาของชุดไพรเมอร์ในการเพิ่มปริมาณดีเอ็นเอไวรัส IHHNV เมื่อตรวจจากผลิตภัณฑ์ดีเอ็นเอจากปฏิกิริยา LAMP ที่ได้จากการแยกด้วยสนามไฟฟ้า(บน) เปรียบเทียบกับผลิตภัณฑ์ดีเอ็นเอจากปฏิกิริยา PCR ที่ได้จากการแยกด้วยสนามไฟฟ้า (กลาง) และผลการตรวจด้วยวิธี colorimetric detection บนพื้นฐานของการตกตะกอนของอนุภาคทองคำนาโนตามหลักการไบโอเซ็นเซอร์ เมื่อใช้โพลบ PNA ที่จำเพาะ (ล่าง) เลน M 100 nucleotide ladder เลน ntc non template control เลน N– ตัวอย่างควบคุมลบ PCV เลน10^7 ถึง 10^2 10 1 แสดงจำนวนก๊อปปี้ของดีเอ็นเอแม่แบบจากไวรัส IHHNV

การพัฒนาปฏิกิริยาในรูปแบบ multiplex LAMP เพื่อการตรวจไวรัสทั้ง 2 ชนิดพร้อมกัน ดังกล่าวนี้ร่วมกับการพัฒนาระบบการตรวจสัญญาณดีเอ็นเอโดยใช้ PNA probe ร่วมกับการตกตะกอนของอนุภาคทองคำนาโน สะท้อนให้เห็นถึงความจำเพาะของ probe แต่ละนิดในการแสดงผลการจำแนกชนิดของไวรัส ซึ่งเป็นหัวใจของความสำเร็จในการพัฒนาเทคนิคสำหรับการตรวจซึ่งจะใช้เป็นรากฐานสำหรับการต่อยอดไปสู่การควบคุมป้องกันและจัดการโรคให้กับอุตสาหกรรมกุ้งของประเทศในระยะยาวต่อไป

เนื่องจากระบบ multiplex เป็นระบบที่ไม่เคยมีรายงานมาก่อน นอกจากนี้การนำปฏิกิริยา LAMP มาใช้รวมกับการตรวจโดย PNA และอนุภาคทองคำนาโนยังเป็นของใหม่ ผลการดำเนินการในครั้งนี้จึงช่วยให้สามารถช่วงชิงความเป็นผู้นำในการพัฒนาวิธีการตรวจที่รวดเร็วในระดับโลกได้ต่อไป

4.2.2 พัฒนาวิธีการตรวจสอบไวรัสโรคเหี่ยวในสับปะรด

อุตสาหกรรมแปรรูปสับปะรดกระป๋อง จัดเป็นอุตสาหกรรมสินค้าเกษตรที่สามารถทำรายได้เข้าประเทศจำนวนมาก ดังนั้นจึงถือได้ว่าสับปะรดเป็นผลไม้เศรษฐกิจที่สำคัญชนิดหนึ่งที่ได้รับความนิยมปลูกและการส่งเสริมให้ปลูกกันมากขึ้น อย่างไรก็ตามการเพาะปลูกสับปะรดพันธุ์ดังกล่าวรวมถึงพันธุ์อื่น ๆที่ปลูกในประเทศไทย มักประสบปัญหาสำคัญโดยเฉพาะปัญหาของโรคเหี่ยวที่เกิดจากไวรัสโรคเหี่ยวของสับปะรด (Pineapple Mealy Bug Wilt: PMW) ซึ่งมีสาเหตุจากไวรัสพืช *pineapple mealybug wilt-associated viruses* (PMWaVs) โรคไวรัสนี้มีการระบาดรุนแรงและทำให้เกิดความเสียหายแก่พื้นที่ปลูกเป็นจำนวนมาก เนื่องจากโรคเหี่ยวของสับปะรดมีการถ่ายทอดโรคโดยแมลงพาหะ คือ เพลี้ยแป้ง {(*Pseudococcus brevipes* หรือชนิด *Dysmicoccus brevipes* (Cockerell)} และมดหัวโต (*Solenopsis gemnata* และ *Pheidole megacephala*) เป็นตัวนำพาเพลี้ยแป้ง (ชำนาญ และคณะ, 2542; Beardsley, 1993) ทำให้โรคเหี่ยวของสับปะรดแพร่ระบาดได้อย่างรวดเร็ว และมีความรุนแรงมากยิ่งขึ้นในทุกพื้นที่ปลูก นอกจากนี้การปลูกสับปะรดโดยทั่วไปและในประเทศไทยนิยมใช้หน่อ ตะเกียง และจุกเป็นส่วนขยายพันธุ์ ซึ่งไวรัสสาเหตุโรคเหี่ยวของสับปะรดสามารถติดไปกับส่วนขยายพันธุ์ได้ทำให้การแพร่ระบาดของโรคเป็นไปอย่างกว้างขวางและรวดเร็วมากในปัจจุบัน

ดังนั้นการตรวจสอบและการวินิจฉัยโรคไวรัสสาเหตุโรคเหี่ยวของสับปะรดอย่างมีประสิทธิภาพด้วยวิธีการที่รวดเร็วและแม่นยำ ทั้งการตรวจสอบลักษณะอาการของโรคในสภาพแปลงปลูกของเกษตรกรหรือแปลงปลูกเพื่ออุตสาหกรรมในระยะแรกเริ่มของการปลูก การตรวจสอบชิ้นส่วนของพืชที่จะนำไปขยายพันธุ์เพื่อการเพาะปลูก ตลอดจนการวางแผนงานเพื่อบริหารจัดการโรค การควบคุมโรคและการแพร่ระบาดของโรคอย่างมีประสิทธิภาพ จึงจะทำให้สามารถควบคุมโรคและสามารถลดความเสียหายที่จะเกิดขึ้นต่ออาชีพของเกษตรกรและอุตสาหกรรมสับปะรดของประเทศ

ที่ผ่านมาการตรวจวินิจฉัยไวรัสโรคเหี่ยวสับปะรดมีวิธีการต่าง ๆ ดังนี้

1) ตรวจสอบด้วยวิธี Tissue blot immunoassays (TBIA) Hu *et al.*, (1997)ทดลองใช้โมโนโคลนนอลแอนติบอดี (MAb) ที่จำเพาะต่อ PMWaVs แต่ละชนิด ได้แก่ โมโนโคลนนอลแอนติบอดี 35-6-5 มีความจำเพาะต่อ PMWaV-1 และ 63-2-2 มีความจำเพาะต่อ PMWaV-2 และอีก 5 ปีถัดมา Sether and Hu (2002a, 2002b) ได้นำโมโนโคลนนอลแอนติบอดีที่จำเพาะต่อไวรัสทั้งสองชนิดมาใช้ในการตรวจสอบไวรัสโรคเหี่ยวของสับปะรด ด้วยวิธี Tissue blot immunoassays (TBIA) เช่นเดียวกัน และพบว่าโมโนโคลนนอลแอนติบอดี 35-6-5 มีความจำเพาะต่อ PMWaV-1 ส่วนโมโนโคลนนอลแอนติบอดี 63-2-2 มีความจำเพาะต่อ PMWaV-2
2) การตรวจอนุภาคด้วยกล้องจุลทรรศน์อิเล็กตรอนร่วมกับการตกแต่งอนุภาคด้วยแอนติซีรั่ม (Immuosorbent electron microscope: ISEM) วิธีการนี้ตรวจอนุภาคไวรัสภายใต้กล้องจุลทรรศน์อิเล็กตรอนจากการพบอนุภาคไวรัสโรคเหี่ยวของสับปะรด อนุภาคไวรัสมีรูปร่างท่อนยาว ขนาด 1,200-1,500 นาโนเมตร มักพบอยู่ท่อลำเลียงอาหาร (phloem) ของสับปะรดที่แสดงอาการโรคเหี่ยว และพบว่า PiWV มีความสัมพันธ์ทางซีรั่มวิทยากับแอนติซีรั่ม จากประเทศออสเตรเลีย ที่ความเข้มข้นเจือจางของซีรั่มของโรคเหี่ยวของสับปะรด PiWV อัตรา 1:100
3) วิธี reverse transcription polymerase chain reaction (RT-PCR) ตรวจสอบไวรัสในห้องปฏิบัติการโดยวิธี รีเวิร์สทรานสคริปชั่นและโพลีเมอเรสเชนรีเอคชั่น โดยใช้คู่ไพรเมอร์ที่เฉพาะกับยีน HSP 70 ของเชื้อไวรัส PMWaV-1 และ PMWaV-2 คู่ไพรเมอร์สำหรับ PMWaV-1HSP70

ในทั้ง 3 วิธี RT-PCR เป็นวิธีที่นิยมมากสุด อย่างไรก็ดีแม้ว่าการตรวจด้วยวิธีดังกล่าวเป็นที่ยอมรับแต่การตรวจจำเป็นต้องพึ่งห้องปฏิบัติการ ต้องใช้ความชำนาญการทางเทคนิค เนื่องจากเป็นงาน RNA และใช้เวลาตรวจนานในระดับ 2-5 วัน ทำให้มีความจำเป็นในการพัฒนาวิธีการตรวจทางเลือก นอกจากนี้ในช่วง 2-3 ปีที่ผ่านมา การตรวจไวรัสทั้ง 2 ทำโดยเทคนิค RT-RCR โดยใช้ไพรเมอร์ที่จำเพาะกับ PMWaV-1 และ PMWaV-2 (Sether and Hu, 2002 a,b) ยังไม่มีรายงานการตรวจในรูปการตรวจที่เกิดขึ้นในหลอดเดียว (single tube) มาก่อน การพัฒนารูปแบบการตรวจให้เกิดขึ้นในหลอดเดียวจึงเป็นสิ่งท้าทาย

การตรวจสอบข้อมูลเบื้องต้น พบว่าเนื่องจากไวรัสทั้ง 2 ชนิด แม้มีชื่อเดียวกันแต่ในความเป็นจริงแล้ว ไวรัสทั้ง 2 เป็นไวรัสคนละชนิด แม้ว่าจะอยู่ในจีนัส Ampero virus เดียวกันก็ตาม แต่ PMWaV-1 มีความใกล้เคียงกับ GLRaV (grapevine leafroll associated virus) 4และ 5 มากกว่า PMWaV-2 ขณะที่ PMWaV-2 สัมพันธ์หรือใกล้เคียงกับไวรัส LChV-2 (Little Cherry Virus 2) (Melzer *et. al.*, 2001) (ภาพที่ 27.)

การเปรียบเทียบลำดับนิวคลีโอไทด์รวม พบว่าแม้ไวรัสทั้ง 2 จะมีโครงสร้างของยีนคล้ายกันแต่ในระดับนิวคลีโอไทด์กลับมีลำดับนิวคลิโอไทด์คล้ายกัน(similarity) ต่ำกว่า 60 % โดยเฉพาะกับยีน CP ซึ่งใช้เป็นยีนอ้างอิงในการพัฒนาการตรวจโรคนี้ ซึ่งพบว่า CP ยีนของไวรัสทั้ง 2 มีความยาวต่างกันอย่างสิ้นเชิง (774 กับ 909 นิวคลีโอไทด์) (ภาพที่ 28.) และมีความคล้ายกันในระดับนิวคลีโอไทด์ ต่ำกว่า 42 %

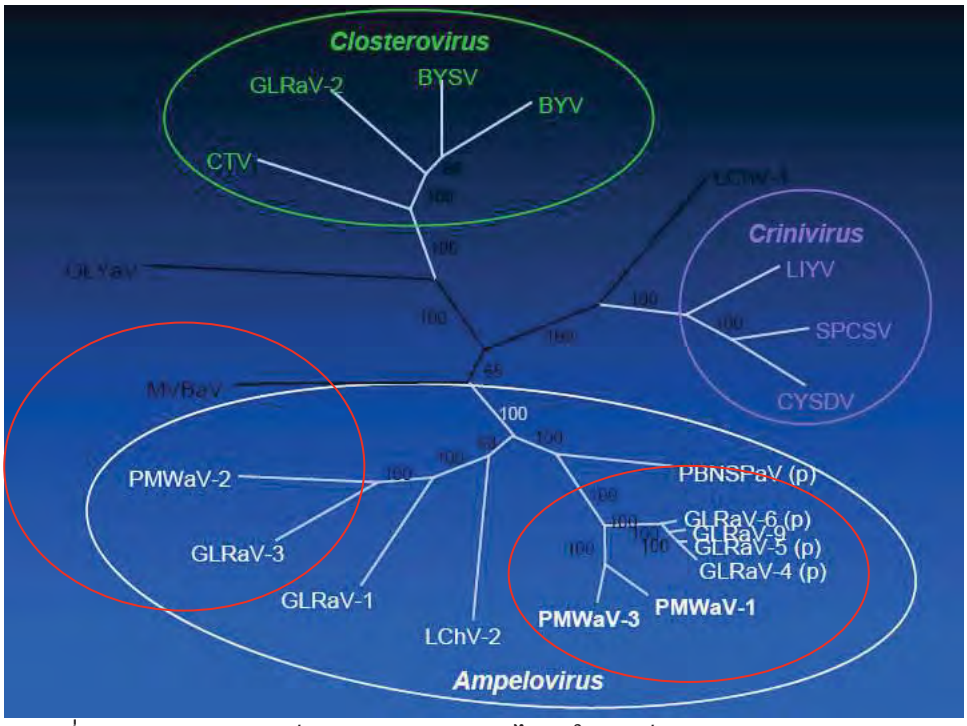

ภาพที่ 27 ความสัมพันธ์ทางพันธุกรรมของไวรัสในวงศ์ Closteroviridae และความใกล้ชิดของสมาชิกในจีนัส ampelovirus วงกลมแสดงความสัมพันธ์ระหว่าง PMWaV-1 3 และ GLRaV และ PMWaV-2 และ LChV-2

```
CLUSTAL 2.0.12 multiple sequence alignment

EU769114.11virus      ------------------------------------ATGGCT--GATTCGAGCAAACAA 21
FJ209048.13virus      ------------------------------------ATGAGTACGATTCCAGTAC-CAC 22
EU769116.12virus      CCTAAACGATTTAGAGTGGCGACGTCTGATGTGGGGAAATATTACGATAGTAGCAAATAC 120
                                                          *    *  ***   ** *   *

EU769114.11virus      AAACAACC--TGAACAT-GCTGACTCTGG------------GCCTAAGACAGCGGAC-- 63
FJ209048.13virus      CTCCTCCC--TCTGCACCATCGACTCCGGTACAACCGCAGCTGCCCAAAGCTGATGAG-- 78
EU769116.12virus      CGCTCTGTAACGGGCGTAGCTACAGCCGAGAGGGAT-CGGTTACCAGCGATAGAGGAAAC 179
                                 *          * *                ***       *  **

EU769114.11virus      -GACCAAGTCAAGGAAATACTGAACCTGCCTGTGCCGGGAGGTAGGACTACTGTGTCGAC 122
FJ209048.13virus      -GAACAATTACAGGAGATTGAAAATCTGCCTCTACCTGGAGGTAGGACTACAGTGAACAC 137
EU769116.12virus      TGAACTATTGGCAACAATCCCAACGGAAGCTTCGACAGATAAGGGTGTTATTCCTGAGAC 239
                       ** * * *       **    *      **    * *      *   **         **

EU769114.11virus      GTTTGAAGATTTGAT--AGCAGCTGAAAATGCTATAATTGATTTCACCAAGGTTGATGTA 180
FJ209048.13virus      TTTCACTGATCTGAT--ATCGTCGAATAACGCGGTATTGGATTTCACTAAAGTGGAAGTA 195
EU769116.12virus      TGTTACGAGGTCGAGTAATAAACCAGAAATAGTAGATGATGTATCAACGTTGCTGTTAAA 299
                        *         **   *    *    **       *     * ***     *  *    *

EU769114.11virus      CCAC-GCATGATTAACGTTCCGATCCCAGGAATAGTTACTAATGCACACAAGGTGATAGG 239
FJ209048.13virus      CCGC-GGATGATCAACATCACCATACCTGGGATAGTGGCGAAAGAACATCGAGTGAAGGG 254
EU769116.12virus      TCCTAGAAAGAACGTTGTACTAAATATTGGATCGGTTAAAACCGTGCCAAAGGTAGTTAA 359
                       *   * * **       *    *      **    **     *  *  *     **

EU769114.11virus      --ATCCAAA----GCTCTGTGGGAGTTGGGTAA--ATCGAAGGGTATATCAGAATCGGC- 290
FJ209048.13virus      --AGCCAAA----GCATTATGGGAACTAGGTAA--ATCTAAAGGAATCTCTGAAAGTGA- 305
EU769116.12virus      TCAGCCGGGTTTGATATCCCGGGAGATTGCTATCCGTATAGGGGAGGCTCTGAAGGAACA 419
                        * **                ****  * * **    *  *  **    ** ***

EU769114.11virus      ---GAAACACAT----GATCCAATTTCTGATGCAATCTT---TCCAAGATATGTGCACCT 340
FJ209048.13virus      ---CAAACACAT----GATACAGTTTCTGATGCAGAGTT---TCCAAAGTTTCGTCACTC 355
EU769116.12virus      TTGCAAACAAGTTATGGGTTCGGATAGTAGTACTGACTTAGCTACATACTTTATACATTT 479
                         *****  *    * * *   *  *  * *    **   * **   * *   **

EU769114.11virus      TTTCTACATCACC-GAAAGTTTCGGCGACTCAGAACTACTCCACC---ACAGCTAAG--- 393
FJ209048.13virus      ATTCGACATCACC-TAAGGTTTCAGGTGCATCGAACCGTACAATA---ACTGCTAAG--- 408
EU769116.12virus      GATTCAACTCGCTATTACGTTTTCTACATCCAAAAATAGCGAATACAAAGAGTTTGACTA 539
                        *  *  ** *    * ****           **       *     *  * *

EU769114.11virus      TATGATGGTAAAGATGTTAACG----TCACGCACGAGGAGATCAGAATTGCTTTGAGCAA 449
FJ209048.13virus      TACGACAACAAAGATGTTCCGG----TGTCTCATGAAGAGTTAAAGACTACTTTAGATAA 464
EU769116.12virus      TATAGAAACAGAGACGCAAAAGAAAATATACATCAAGGACGTGAGTGAGGTGGTTGAGAG 599
                      **       * *** *     *    *        * **  * *         *    *

EU769114.11virus      CTCACTATCCAATTTGGGATACGATAATCCTATGAGACAGTTTGGGAGAGGTTTTACTTC 509
FJ209048.13virus      TTCACTAGCCAGTTACGGCTATGAAATTACCATGAGACAATTTGGGAGGGCATTCACAAC 524
EU769116.12virus      AGCGGCGATGAATTCGGGGTACGAAAACCCGTTTAGGCAATATATGCGTTATTTTACAAG 659
                        *       * **  ** ** ** *   *  * ** ** * *  * *    ** **

EU769114.11virus      CACAA---TTGTTCAAGGACTGAGTTCTGGGAAGTTGGTGGTTAACACTAGGATATGTAC 566
FJ209048.13virus      TGCAA---TAGTTCAGGGTTTAAGGTCGGGTAAAATGGAGGTAAATACTCGAATTTGCTC 581
EU769116.12virus      CTCGAGTATAACACTAACTTTAAAT---GGTAAAATAACACCTAACGAGAGAACTATGGC 716
                        * *   *    *     * *     ** **  *       **     * *      *

EU769114.11virus      TAAGAACGGAGTACCGAGGAATTATTACTCGTTCTATCCAGATTGCTTACACGTGGAAGC 626
FJ209048.13virus      TTCTCACGGTATACCTCCTAACTACTATCCCTACTCTCCAGACTGCTTACATGTAGACGC 641
EU769116.12virus      TCATCACGGAGTACCCAAGCAGTTCTTTGCGTATACTTACGATTTTATTGACCCCGACTA 776
                      *    ****  ****     * *  *   * *    *   ** *   *  *    **

EU769114.11virus      CAGAGTACACGGTGATGATGCAGCGTTGGTAAGTGAGTTAGCCAGAATGGTAGCCGTAAA 686
FJ209048.13virus      ACGCATACAAGGATATGATGCCGCTTTAGCAAACGAGTTAGGGAAGATGGTAGCACTCAA 701
EU769116.12virus      TAGCCTCATGAACCATTCGGCGATTAATGCTTACAACTTAGCGAGGATTCAAGCATTTAA 836
                        *  *          **   **         *      * ****  *  **   ***  * **

EU769114.11virus      CAGAGCAAACTCGAGTGGTTCTGGCGAACACAACGTCTTTGAGAAGACGGCTGTGTCCCC 746
FJ209048.13virus      CAAAAACGCTGGAGGTAAGCGTACGCAACATAACTTGTTTCAGGAGACTGACATATCTCC 761
EU769116.12virus      GAATAAGAT----AGCTTCAGTGAACAATACTATGCATAACACATACCAGCTG-AACCAG 891
                       *            *      *    ** *  *    *   *    *     * *      *

EU769114.11virus      GCACATCTTTATGGGTGGACGCAAATAA 774
FJ209048.13virus      TCAAATATTTACAGGTAATCGCAGATGA 789
EU769116.12virus      GGAGCTGTTTCAGGGTAG---------- 909
                        *  * ***   ***
```

ภาพที่ 28 ลำดับนิวคลิโอไทด์ของยีนโปรตีนเปลือกหุ้มเปรียบเทียบระหว่าง PMWaV-1 และ PMWaV-2 และความคล้ายกันในระดับที่ต่ำ

ผลดังกล่าวทำให้ชุดของไพรเมอร์ ที่ออกแบบใหม่เหมาะสมกับไวรัส PMWaV ชนิดที่ 1 และชุดของไพรเมอร์ที่ออกแบบให้เหมาะสมกับไวรัส PMWaV ชนิดที่ 2 มีลำดับนิวคลีโอไทด์ต่างกันอย่างสิ้นเชิงและผลการตรวจสอบความน่าจะเป็นของไพรเมอร์ในการทำปฏิกิริยากับดีเอ็นเอหรืออาร์เอ็นเอเป้าหมายด้วยการ Blast (Altschul *et. al*., 1990) พบว่า มีความต่างกันให้ค่า E value มากกว่า 1000 เท่า การพัฒนาวิธีตรวจสอบไวรัสทั้ง 2 จึงออกแบบให้อยู่ในรูป Multiplex LAMP

นับจนถึงปัจจุบันแม้ Notomi *et. al*., (2000) จะได้รายงานการพัฒนาเทคนิคการเพิ่มปริมาณดีเอ็นเอแบบใหม่ แต่ในช่วง 10 ปีที่ผ่านมา ยังไม่เคยมีรายงานการเพิ่มปริมาณดีเอ็นเอโดยใช้ไพรเมอร์ LAMPมากกว่า 1 ชุด ในรูป Multiplex แต่อย่างใด ที่เป็นเช่นนี้เนื่องจากในแต่ละระบบการเพิ่มปริมาณดีเอ็นเอของ LAMP มีไพรเมอร์เกี่ยวข้องกับบริเวณดีเอ็นเอหรืออาร์เอ็น

เอถึง 6 บริเวณหรือต้องมี 4 ไพรเมอร์เป็นอย่างน้อย เมื่อนำมาคิดเป็นจำนวนนิวคลีโอไทด์ที่เกี่ยวข้อง จะพบว่ากินบริเวณมากถึง 120 นิวคลิโอไทด์ คิดเป็นความน่าจะเป็นได้ถึง$(1/4)^{120}$ ซึ่งสูงกว่า PCR ที่เกี่ยวข้องกับไพรเมอร์เพียงคู่เดียว ความน่าจะเป็น $(1/4)^{40}$ มากถึง $(1/4)^{80}$ หรือ $1.461x10^{48}$ เท่า

ดังนั้นในระบบ Multiplex LAMP 2 ยีนใดๆ ซึ่งมีไพรเมอร์เกี่ยวข้องกับบริเวณ 12 บริเวณ (8 ไพรเมอร์) และหากระบบยีนเป็นระบบที่ไกล้หรือมีความสัมพันธ์กัน โอกาสที่จะเกิดการผิดพลาดและเพิ่มจำนวนแบบ primer dimmer กับไพรเมอร์ด้วยกันจะสูงมาก

อย่างไรก็ตามเนื่องจากระบบการตรวจไวรัสโรคเหี่ยวในสับปะรดในครั้งนี้ แม้จะมีเป้าหมายในการเพิ่มปริมาณสารพันธุกรรมส่วนของยีนโปรตีนเปลือกหุ้มที่เหมือนกัน แต่ตัวยีนเป้าหมายเป็นไวรัสคนละชนิด ดังนั้น จึงได้ทดลองทำ Multiplex LAMP ขึ้นเป็นครั้งแรก การทดลองปรับสภาวะของปฏิกิริยาทำให้พบว่าการเพิ่มปริมาณในระบบ Multiplex จะประสบความสำเร็จ เมื่อมีการปรับสัดส่วนโมลของไพรเมอร์เป็น โมลของไพรเมอร์ F3 B3 FIP และ BIP ของคู่แรก ต่อ คู่ที่สอง เป็น 1:1 โดยปรับตัวปฏิกิริยารวมของไพรเมอร์ไม่เกิน 40 pmol F3 B3 และ 5 pmol FIP BIP ของทั้ง 2 ชุดไพรเมอร์และในปฏิกิริยาจะต้องชดเชยสารเคมีมากกว่าปฏิกิริยาปกติที่รายงานโดย Notomi *et. al*., (2000) เป็น dNTP เพิ่ม 1.5 เท่าของ dNTP ปกติ $MgSO_4$ เพิ่มปริมาณเป็น 2 เท่าของปกติ และเพิ่มปริมาณเอ็นไซม์เป็น 1.2 เท่าของปกติ

Multiplex ของปฏิกิริยามาตรฐานของไวรัสโรคเหี่ยวสับปะรดสามารถดำเนินการได้ในหลอดเดียวและให้ผลิตภัณฑ์ดีเอ็นเอในรูปแบบขั้นบันได ที่เป็นลักษณะเฉพาะของผลิตภัณฑ์ดีเอ็นเอที่ได้จากปฏิกิริยา LAMP นอกจากนี้เมื่อดำเนินการตรวจสัญญาณดีเอ็นเอด้วยระบบเรืองแสงโดยใช้เบต้าพิโรลิดินิวเปปไทด์นิวคลีอิกแอซิด ที่ติดฉลากด้วยโมเลกุลเรืองแสงทำปฏิกิริยา competitive hybridization เป็นโพลบทำปฏิกิริยา hybridization ในภาวะอุณหภูมิห้องโดยใช้ PNA โพลบ 5μM quencher 4 μM LAMP products 1 μLใน 10 mM PBS ให้ผลการเรืองแสงเป็นดังภาพที่ 29.

การทดสอบความจำเพาะของคู่ไพรเมอร์ในรุปแบบ Multiplex กับไวรัสเป้าหมายทั้งสองชนิด PMWaV-1 และ 2 และไวรัสอื่นที่พบในประเทศไทย พบว่าชุดไพรเมอร์ Multiplex ยังคงมีความจำเพาะต่อไวรัสทั้ง 2 ชนิด และไม่ทำปฏิกิริยากับสารพันธุกรรมของไวรัสพืชหลักชนิดอื่นที่พบในประเทศแต่อย่างใด

ผลดังกล่าวแสดงให้เห็นถึงประสิทธิภาพของภาพรวมชุดไพรเมอร์ทั้งสองในการตรวจสอบชนิดของไวรัส โรคเหี่ยว (ภาพที่ 30.)

ทำนองเดียวกันการทดสอบ ความไวของปฏิกิริยา พบว่าการใช้คู่ไพรเมอร์ผสมที่เป็น Multiplex ยังคงให้ผลการเพิ่มปริมาณชิ้นยีนโปรตีนเปลือกหุ้มได้เป็นอย่างดี สามารถตรวจสอบแม่แบบที่เป็นดีเอ็นเอของยีนเปลือกหุ้มได้ในระดับ 100 ชุด (ก๊อปปี้) ของยีน แม้จะต่างจากการแยกตรวจ 10 เท่าแต่สามารถดำเนินการได้ในหลอดเดียวซึ่งเป็นข้อได้เปรียบอย่างมาก (ภาพที่ 31.)

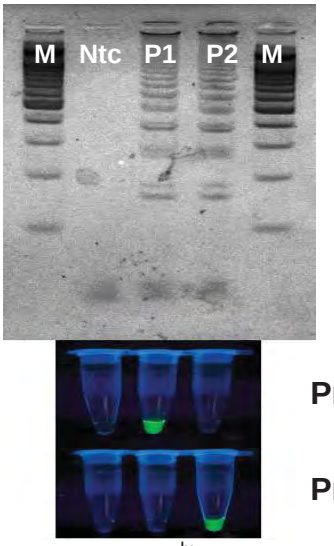

ภาพที่ 29 ผลิตภัณฑ์ดีเอ็นเอที่ได้จาก multiplex RT-LAMP ของไพรเมอร์ผสม(บน)และการตรวจสัญญาณดีเอ็นเอโดยใช้ PNA probe จำเพาะต่อ PMWaV-1 และ 2 บนพื้นฐานการทำ competitive hybridization (ล่าง) เลน M 100 นิวคลิโอไทด์มาร์เกอร์ เลน NTC ชุดควบคุมที่ไม่มีดีเอ็นเอแม่แบบและ เลนตัวอย่าง PMWaV-1 และ 2 ตามลำดับ

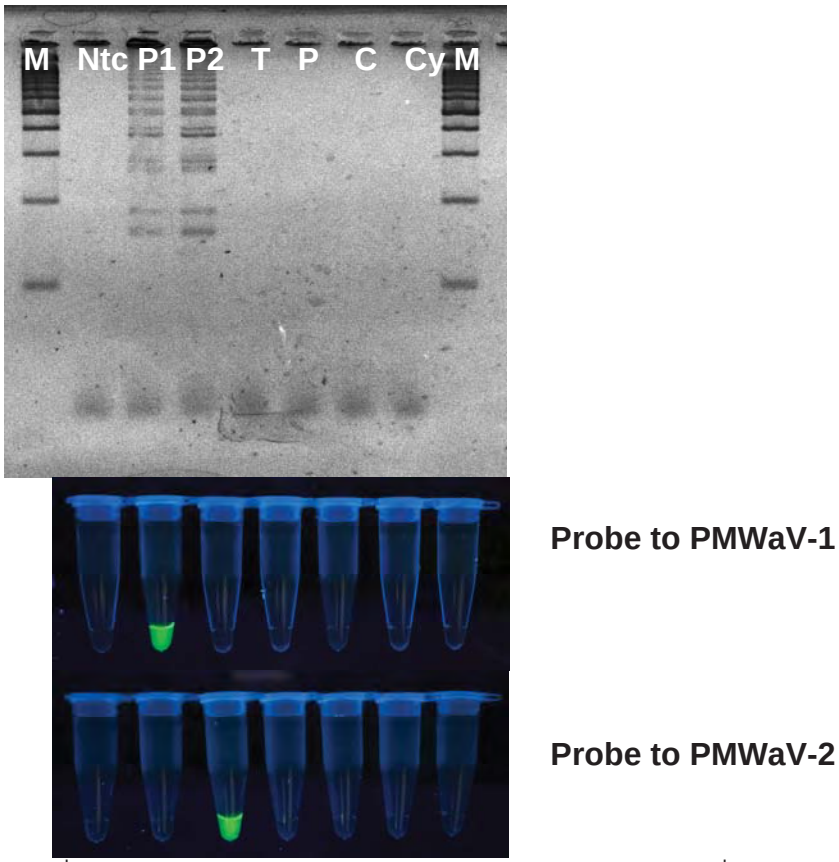

ภาพที่ 30 ความจำเพาะของปฏิกิริยาตรวจสอบจากผลิตภัณฑ์ดีเอ็นเอที่ได้จาก multiplex RT-LAMP ของไพรเมอร์ผสม(บน)และการตรวจสัญญาณดีเอ็นเอโดยใช้ PNA probe จำเพาะต่อ PMWaV-1 และ 2 บนพื้นฐานการทำ competitive hybridization (ล่าง) เลน M 100 นิวคลิโอไทด์มาร์เกอร์ เลน NTC ชุดควบคุมที่ไม่มีดีเอ็น

เอแม่แบบและ เลนตัวอย่าง P1 PMWaV-1 และP2 PMWaV-2 เลน T Tobacco mosaic virus เลน P Papaya ringspot virus เลน C cucumber mosaic virus และ เลน Cy Cymbidium mosaic virus ตามลำดับ

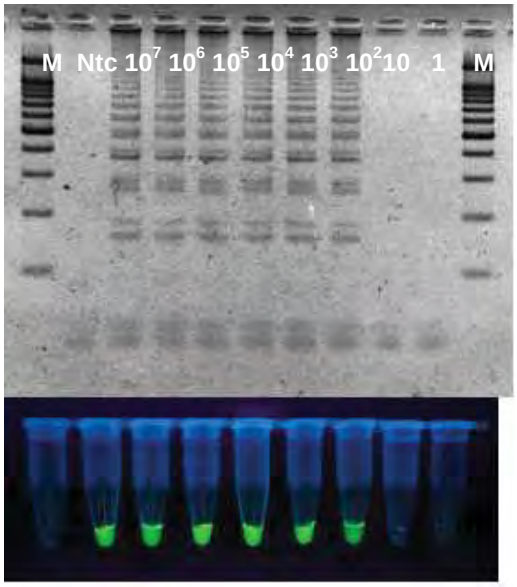

ภาพที่ 31 ความไวของปฏิกิริยาตรวจสอบจากผลิตภัณฑ์ดีเอ็นเอที่ได้จาก multiplex RT-LAMP ของไพรเมอร์ผสม และการตรวจสัญญาณดีเอ็นเอโดยใช้ PNA probe จำเพาะต่อ PMWaV-1 และ 2 บนพื้นฐานการทำ competitive hybridization เลน M 100 นิวคลิโอไทด์มาร์เกอร์ เลน NTC ชุดควบคุมที่ไม่มีดีเอ็นเอแม่แบบและ เลนตัวอย่าง PMWaV ที่ทราบจำนวนชุดของดีเอ็นเอหรือ ก็อปปี้ จาก 10^7-1 ก็อปปี้ ตามลำดับ ภาพชุดบนแสดงผลความไวของปฏิกิริยาต่อ PMWaV-1 และภาพชุดล่างแสดงผลความไวของปฏิกิริยาต่อ PMWaV-2 ตามลำดับ

ผลการพัฒนาปฏิกิริยาเพื่อตรวจไวรัสสายพันธุ์ทั้งสองพร้อมกันดังกล่าวนี้ ร่วมกับการตรวจสัญญาณดีเอ็นเอโดยอาศัยโพลบที่ทำจากเบต้าพิโรลิดินิลเพปไทด์นิวคลีอิกแอซิด สะท้อนให้เห็นความสำเร็จในการพัฒนาปฏิกิริยาสำหรับการตรวจ ซึ่งจะใช้เป็นฐานสำหรับการต่อยอดไปสู่การควบคุมและป้องกันโรคไวรัสเหี่ยวในสับปะรดในระยาวต่อไป

เนื่องจากระบบดังกล่าวไม่เคยมีรายงานมาก่อน แม้แต่กลุ่มนักวิจัยนำที่เป็นห้องปฏิบัติการระดับโลกอย่างเช่น Dr. John Hu แห่ง University of Hawaii ที่ศึกษาไวรัสในระดับต้นๆ และการทำ multiplex LAMP ยังเป็นครั้งแรกนับตั้งแต่ Notomi *et al*., 2000 ได้คิดค้นเทคนิคขึ้น ดังนั้นผลการดำเนินการในครั้งนี้จะช่วยให้สามารถช่วงชิงความเป็นผู้นำในการพัฒนาวิธีการตรวจที่รวดเร็วในต่อไป

นอกจากการตรวจสัญญาณจากการเรืองแสงแล้ว โครงการย่อย ยังได้นำระบบการตรวจสัญญาณดีเอ็นเอด้วยการเปลี่ยนสีทางแสงในรูปแบบเดียวกันกับที่รายงานใน ข้อ 4.2.1 โดยใช้อนุภาคนาโนทองคำและนาโนเงินสีน้ำเงิน โดยใช้เงื่อนไขปฏิกิริยาที่ในปฏิกิริยาประกอบด้วยทองคำขนาด 20 nm 5000 ppm 10 µl หรือเงิน 200 nm 5 µl ผลิตภัณฑ์ดีเอ็นเอที่ได้จากปฏิกิริยา LAMP 1 µl PNA probe ที่จำเพาะต่อไวรัสแต่ละชนิด 1 µM และ 1 µl เกลือในรูปสารละลาย PBS บัฟเฟอร์ (100mM PBS) โดยปฏิกิริยา hybridization เกิดขึ้นที่อุณหภูมิห้อง ผลการตกตะกอนของอนุภาคทองคำนั้นจะเกิดขึ้นในเวลา 30 วินาทีถึง 1 นาที และผลการตกตะกอนของอนุภาคเงินนาโนสีน้ำเงินจะเกิดขึ้นในเวลา 15 นาที ดังภาพที่ 32.

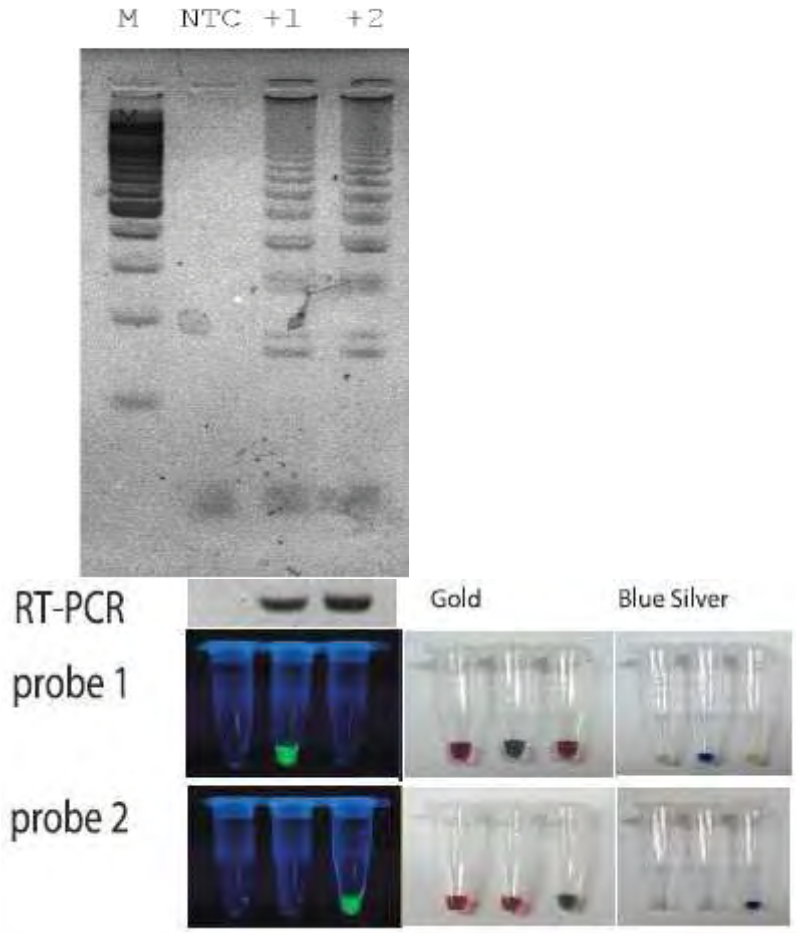

ภาพที่ 32 ผลการทดสอบการเปลี่ยนสีผ่านรูปแบบการตรวจสอบสัญญาณบนพื้นฐานการเปลี่ยนสีทางแสงของอนุภาคนาโนทองคำ (Gold) และนาโนเงินสีน้ำเงิน (Blue silver) เปรียบเทียบกับผลการตรวจด้วยการเรืองแสงและ PCR +1 ตัวอย่างให้ผลบวกของ PMWaV-1 +2 ตัวอย่างให้ผลบวกของ PMWaV-2 ตามลำดับ

การพัฒนาระบบการตรวจสัญญาณดีเอ็นเอโดยใช้ PNA probe ร่วมกับการตกตะกอนของอนุภาคทองคำนาโน สะท้อนให้เห็นถึงความจำเพาะของ probe แต่ละนิดในการแสดงผลการจำแนกชนิดของไวรัส PMWaV-1 และ PMWaV-2 ออกจากกันโดยทำการทดลองเพิ่มปริมาณในหลอดเดียว ซึ่งเป็นหัวใจของความสำเร็จในการพัฒนาเทคนิคสำหรับการตรวจซึ่งจะใช้เป็นรากฐานสำหรับการต่อยอดไปสู่การตรวจติดตามตามหลัก point of care การควบคุมป้องกันและจัดการโรคให้กับภาคอุตสาหกรรมของประเทศในระยะยาวต่อไป

4.2.3 พัฒนาวิธีการตรวจสอบการสุกแก่ทางสรีรวิทยาแบบไม่ทำลายผลในสับปะรด

การสุกแก่ทางสรีรวิทยาของผลไม้มีผลต่อคุณภาพของผล ในผลไม้บางชนิดการเก็บเกี่ยวในภาวะที่ยังไม่สุกนำไปสู่การด้อยคุณภาพ ทั้งในแง่รสชาติ สี กลิ่น และการเปลี่ยนแปลง

ทางสรีรวิทยาในทิศทางที่ไม่พึงประสงค์ ซึ่งโดยรวมจะมีผลต่ออายุการเก็บรักษา และคุณภาพหลังการเก็บเกี่ยวได้ (Kader, 1999)

โดยทั่วไป คุณภาพของผลไม้จะสูงสุดเมื่อปล่อยให้สุกแก่เต็มที่คาต้น แต่ในทางปฏิบัติเกษตรกรไม่สามารถรอจนถึงภาวะดังกล่าวแล้วค่อยเก็บเกี่ยวผลผลิตได้ การทำนายการสุกแก่ได้อย่างแม่นยำก่อนหน้าจะช่วยให้เกษตรกรสามารถกำหนดระยะเวลาการเก็บและกำกับดูแลคุณภาพของผลผลิตได้ดียิ่งขึ้น

ในอดีต ดัชนีชี้วัดการสุกของผลไม้ที่นิยมใช้มีทั้งลักษณะภายนอกเช่น การเปลี่ยนแปลงทางสีของผล ความแน่นเนื้อ ต่อมาเริ่มมีการตรวจสอบไปถึงการเปลี่ยนแปลงทางสรีรวิทยาภายในผล ซึ่งมีหลายดัชนีที่เกี่ยวข้อง เช่น total soluble solid titratable acidity ฯลฯ แต่การวัดการสุกแก่ยังคงมีความคลาดเคลื่อนได้ นอกจากนี้ ในทุกครั้งที่วัดค่าดัชนียังมีความเสี่ยงในการทำลายผลให้เกิดความเสียหาย (Pattee, 1985)

โดยปกติ การสุกแก่ของผลเป็นผลจากการเปลี่ยนแปลงลักษณะ (phenotype) ซึ่งเกี่ยวข้องกับการเปลี่ยนแปลงทางสรีรวิทยา การเปลี่ยนแปลงดังกล่าวเป็นผลจากการเปลี่ยนระดับและชนิดของการแสดงออกของยีนภายในผลไม้นั้น

ในการทดลองได้ใช้สับปะรดเป็นโมเดลในการศึกษาเนื่องจากเป็นพืชเศรษฐกิจที่สำคัญ สับปะรดเป็น non-climacteric fruit หากเก็บเกี่ยวพัฒนาการของผลหลังการเก็บเกี่ยวจะไม่เด่นชัด ผลจะผลิตก๊าซเอทิลีนน้อยมากและไม่ตอบสนองต่อก๊าซนี้ ดังนั้นการเปลี่ยนแปลงของผลภายหลังการสุกจึงไม่เกี่ยวข้องกับก๊าซเอทิลีน เฉกเช่นกับที่พบใน climacteric fruit

การศึกษาการแสดงออกของยีนหลังผลสุก พบว่า ภายหลังการเก็บเกี่ยว ในผลจะพบการแสดงออกของยีนในกลุ่ม chitinase แต่การแสดงออกของยีนในกลุ่มดังกล่าว ไม่มีสอดคล้องกับระยะการสุกแก่ นอกจากนี้ ยังพบการแสดงออกของยีน ribosomal RNA L10 และ ยีนสังเคราะห์โปรตีนที่เกี่ยวข้องในกลุ่มเดียวกัน มีการแสดงออกสอดคล้องกับการสุกและการเปลี่ยนสีของผล แต่การเปลี่ยนแปลงดังกล่าวเกิดขึ้นอย่างต่อเนื่องในแต่ละระยะจึงไม่สามารถนำมาใช้เป็นมาร์คเกอร์ ในการทำนายการสุกของผลได้ (Taira *et al*., 2005, Moyle et al., 2005)

อย่างไรก็ดี ในระหว่างการสุก พบว่า มีความแตกต่างอย่างชัดเจนในการแสดงออกของยีนในกลุ่มการกระจายและเปลี่ยนแปลงคาร์โบไฮเดรตภายในผล โดยเฉพาะยีน *AcSUT* 1 ซึ่งเกี่ยวข้องกับการเคลื่อนย้ายน้ำตาลซูโครสภายในผลจากแหล่งผลิตน้ำตาล (source) จากลำต้นไปยังภายในผล (sink) เป็นอีกยีนหนึ่งที่มีการแสดงออกและหยุดการแสดงออกเด่นชัดในแต่ละระยะ ระหว่างที่ผลมีพัฒนาการการสุกแก่ทางสรีรวิทยา โดยพบว่า ขณะที่ผลสุกเต็มที่จะหยุดการเคลื่อนย้ายน้ำตาลทำให้การแสดงออกของยีนจะหยุดลง และไม่เกิดการเคลื่อนย้ายน้ำตาลชนิดดังกล่าวไปยังผลอีก ดังนั้นจึงได้นำการแสดงออกของยีนนี้มาใช้เป็นดัชนีในการทำนายการสุกแก่

การวิจัยนี้ได้พัฒนาระบบการสุกแก่ของผลสับปะรด โดยการสร้างระบบการตรวจผ่านการเพิ่มปริมาณดีเอนเอจากการแสดงออกของยีน *AcSUT* 1 เพื่อตรวจสอบการแสดงออกบนพื้นฐานทางเทคนิค RT-LAMP และตรวจสอบการเปลี่ยนแปลงสัญญาณดีเอนเอที่ได้ควบคู่ไปกับการสุกแก่ที่เกิดขึ้น และตรวจสอบสัญญาณดีเอนเอผ่านการเปลี่ยนแปลงทางสีของสารละลายอนุภาคนาโนทองคำที่สกัดได้จากใบย่อยของจุกสับปะรดเป็นตัวอย่างในการทดสอบ

การทดลองเริ่มจากการออกแบบและคัดเลือกไพรเมอร์ด้วยไปรแกรม Primer Explorer Ver 4.0 (Fujitsu, Japan) และคัดเลือกผ่านเงื่อนไขเสถียรภาพทางอุณหภูมิ ตำแหน่งการจับตัวและโอกาสในการเพิ่มปริมาณดีเอ็นเอที่จำเพาะ ทำให้ได้ไพรเมอร์ 4 ชนิดครอบคลุม 6 บริเวณของยีน

การตรวจสอบความเฉพาะเจาะจงโดยการทำ Basic Local Alignment Search พบว่าไพรเมอร์ที่ออกแบบได้มีทั้ง 6 บริเวณ จำเพาะต่อยีน *AcSUT* 1 โดยมีความสัมพันธ์ชนิด 100% และมีค่า E value 0.00005

การทดสอบการเพิ่มจำนวนเบื้องต้นด้วยเงื่อนไขของปฏิกิริยาที่ 63 $^{\circ}$C 20mM Tris-HCl (pH 8.8) 10 mM KCl 10mM $(NH_4)_2SO_4$ 0.1% Triton X-100 ไพรเมอร์ F3 B3 ความเข้มข้น 5 pmol /ปฏิกิริยา ไพรเมอร์ FIP และ BIP ความเข้มข้น 40 pmol /ปฏิกิริยา พบว่าชุดไพรเมอร์ที่ออกแบบได้สามารถเพิ่มปริมาณดีเอ็นเอของยีน *AcSUT* 1 ได้โดยจะได้แถบดีเอ็นเอขนาดเทียบเท่าผลคูณของ ช่วงคู่ไพรเมอร์ 180/210 nt (ภาพที่ 33.) สอดคล้องกับการตรวจสอบด้วยเทคนิค RT-PCR ที่นิยมใช้

สำหรับระบบการตรวจสัญญาณดีเอ็นเอ ดำเนินการด้วยการเปลี่ยนสีทางแสงในรูปแบบเดียวกันกับที่รายงานใน ข้อ 4.2.1 โดยใช้อนุภาคนาโนทองคำ โดยใช้เงื่อนไขปฏิกิริยาที่ในปฏิกิริยาประกอบด้วยทองคำขนาด 20 nm 5000 ppm 10 µl หรือเงิน 200 nm 5 µl ผลิตภัณฑ์ดีเอ็นเอที่ได้จากปฏิกิริยา LAMP 1 µl PNA probe ที่จำเพาะต่อยีน *AcSUT* 1 1 µM และ 1 µl เกลือในรูปสารละลาย PBS บัฟเฟอร์ (100mM PBS) โดยปฏิกิริยา hybridization เกิดขึ้นที่อุณหภูมิห้อง ผลการตกตะกอนของอนุภาคทองคำนั้นจะเกิดขึ้นในเวลา 30 วินาทีถึง 1 นาที

ภาพที่ 33. การตรวจสอบการแสดงออกของยีน *AcSut* 1 จากใบจุกของสับปะรด โดยเทคนิค RT-LAMP กับชุดของไพร์เมอร์ที่ออกแบบและการตรวจสอบสัญญาณดีเอ็นเอที่ได้ผ่านการเปลี่ยนแปลงของสีทางแสงของสารละลายอนุภาคนาโนทองคำ

การทดสอบความไวของปฏิกิริยาของชุดไพรเมอร์ต่อจำนวนความเข้มข้นของดีเอ็นเอที่ทราบจำนวนชุด(กอปปี้)เจือจางลงระดับละ 10 พบว่าชุดไพรเมอร์มีความไวในการตรวจสอบดีเอ็นเอในระดับ 10^{-7} เทียบเท่าความเข้มข้นของดีเอ็นเอที่ 10 ชุด/ปฏิกิริยา (ภาพที่ 34.)

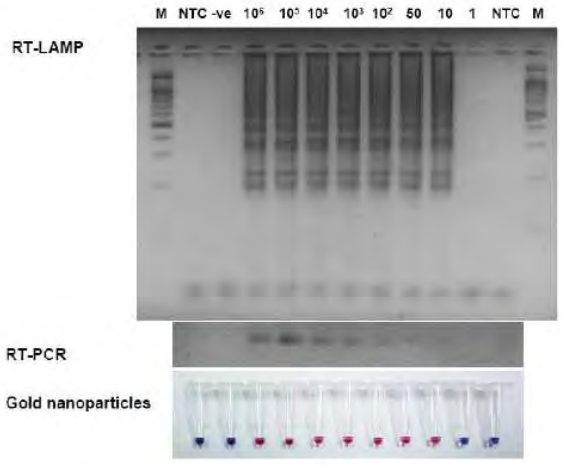

ภาพที่ 34. การทดสอบความไวของปฏิกิริยาของชุดไพรเมอร์ เมื่อลดระดับปริมาณดีเอ็นเอแม่แบบลงทีละ 10 เท่า NTC non template control -ve negative M 100 nt ladder และการตรวจสอบสัญญาณดีเอ็นเอที่ได้ผ่านการเปลี่ยนแปลงของสีทางแสงของสารละลายอนุภาคนาโนทองคำ เปรียบเทียบกับผลที่ได้จาก RT-PCR

และเมื่อนำวิธีการตรวจสอบที่พัฒนาขึ้นไปตรวจสอบการสุกแก่ของผลสับปะรด พบว่าในผลที่ยังไม่สุกแก่ยีน *AcSUT*1ยังคงแสดงออกอย่างต่อเนื่อง ทำให้สามารถเพิ่มระดับปริมาณดีเอ็นเอด้วยเทคนิค RT-LAMP และตรวจสอบการตกตะกอนและการเปลี่ยนสีของอนุภาคนาโนทองคำโดยใช้โพรบ พบว่าการจับตัวของโพรบกับดีเอ็นเอทำให้ไม่เกิดการตกตะกอนและการ

เปลี่ยนสีของอนุภาคนาโนทองคำ อย่างไรก็ดีในผลที่สุกแก่ทางสรีรวิทยา การแสดงออกของยีน *AcSUT*1 ที่หยุดลง มีผลทำให้ไม่สามารถเพิ่มระดับปริมาณดีเอ็นเอด้วยเทคนิค RT-LAMP จึงทำให้ผลการตรวจอนุภาคนาโนทองคำเกิดการเปลี่ยนแปลงทางสีจากแดงเป็นม่วงได้

วิธีการดังกล่าวทำให้ สามารถตรวจสอบการสุกแก่ทางสรีรวิทยาของผลโดยไม่เป็นการทำลายผลให้เกิดความเสียหายแต่อย่างใด

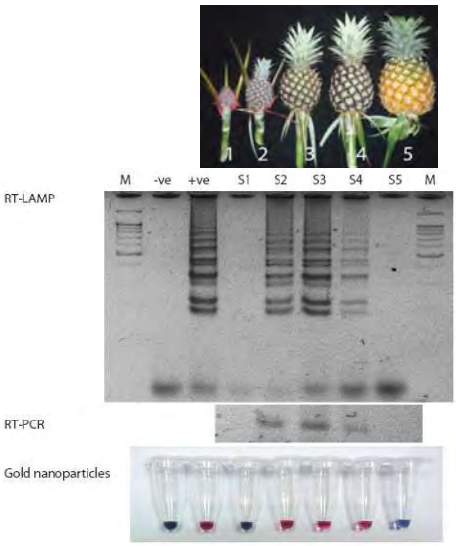

ภาพที่ 35. การตรวจสอบการสุกแก่ของผลสับปะรดในแต่ระยะในการพัฒนาการของผล จาก Stage1(S1) anthesis (2 months after flowering treatment), Stage2 (S2) late anthesis stage (2.5 months after stage1), Stage3 (S3) small fruit stage (3.5 months after flowering treatment), Stage 4 (S4) medium fruit stage (4-4.5months after flowering treatment), and Stage 5 (S5) mature fruit (5 months after flowering treatment) NTC non template control -ve negative M 100 nt ladder และการตรวจสอบสัญญาณดีเอ็นเอที่ได้ผ่านการเปลี่ยนแปลงของสีทางแสงของสารละลายอนุภาคนาโนทองคำเปรียบเทียบกับผลที่ได้จาก RT-PCR

5. อภิปรายผล

การพัฒนาการตรวจวิเคราะห์ในครั้งนี้ อาศัยการนำข้อดีทางเทคนิคของการเพิ่มปริมาณสารพันธุกรรมแบบลูบอุณหภูมิเดียวมาเชื่อมโยงกับการทำ nucleic acid hybridization โดย PNA ข้อได้เปรียบที่สำคัญได้แก่ 1. การที่เทคนิคการเพิ่มปริมาณสารพันธุกรรมแบบลูบอุณหภูมิเดียวทำปฏิกิริยาที่อุณหภูมิคงที่ ที่60-65°C ทำให้ลดความจำเป็นที่ต้องพึ่งพาเครื่อง thermocycler ลง 2. การทำปฏิกิริยาที่ไม่เป็นรอบ ทำให้อัตราการเพิ่มปริมาณสารพันธุกรรมสูงกว่าของ PCR 3-8 ออเดอร์ (1000-100000000เท่า) จึงมีปริมาณสัญญาณสูงกว่าแม้ที่ near limit of detection 3. รูปแบบปฏิกิริยาที่ใช้ไพร์เมอร์ จำเพาะต่อ 6 บริเวณทำให้เทคนิคการเพิ่มปริมาณสารพันธุกรรมแบบลูบอุณหภูมิเดียวโด่ดเด่นเหนือกว่า PCR ในด้านความจำเพาะ

(Notomi *et al.,* 2000) ด้วยเหตุดังกล่าวทำให้รายงานส่วนใหญ่เน้นการแสดงผลด้วยตัวเทคนิคโดยไม่เชื่อมโยงกับเทคนิค nucleic acid hybridization มากนัก

อย่างไรก็ดีหากการพัฒนาเทคนิคยังต้องเน้นการตอบโจทย์ point of care เทคนิคการเพิ่มปริมาณสารพันธุกรรมแบบลูบอุณหภูมิเดียวเป็นเทคนิคเดียวที่เหนือกว่า เทคนิคการเพิ่มปริมาณโดยอาศัยลำดับนิวคลีโอไทด์เป็นพื้นฐาน (sequence-based amplification) (Compton, 1991) การเพิ่มปริมาณจากการจำลองตัวเอง (self-sustained replication) (Guatelli *et al*., 1990) การเพิ่มปริมาณโดยการใช้ปฏิกิริยาแทนที่สายดีเอ็นเอ (strand displacement amplification) และการเพิ่มปริมาณอุณหภูมิระนาบเดียว (Walker *et al.,* 1992) การเพิ่มปริมาณสัญญาณที่เป็นดีเอ็นเอขนาดสั้นๆ branched DNA amplification (bDNA) invader และ rolling circle amplification (Lyamichev *et al*., 1999 และ Lizardi *et al*., 1998) ซึ่งเทคนิคในกลุ่มหลังส่วนใหญ่ ไม่เป็น isothermal จริง หรือไม่ได้สารพันธุกรรมเป้าหมายแต่เป็นการเพิ่มสัญญาณจากโพรบแทน หรือให้ความจำเพาะที่ไม่เทียบเท่า ดังนั้นในทุกโมเดลที่ได้พัฒนาขึ้นจึงอยู่บนพื้นฐานทางเทคนิคการเพิ่มปริมาณสารพันธุกรรมแบบลูบอุณหภูมิเดียวทั้งสิ้น

อย่างไรก็ดี เพื่อให้เห็นศักยภาพในการตรวจสัญญาณดีเอ็นเอจึงได้วางระบบให้การเพิ่มปริมาณสารพันธุกรรมแบบลูบอุณหภูมิเดียวให้ดีเอ็นเอมากกว่า 1 เป้าหมาย โดยการทำ multiplex LAMP การทดลอง multiplex LAMP เช่นนี้ไม่เคยมีรายงานมาก่อน โดยหลักการจะใช้ไพร์เมอร์จำเพาะต่อบริเวณของยีนต่างกัน 2 ยีน 8 บริเวณ และเนื่องจากมีการปรับปฏิกิริยาให้ดำเนินการได้ในหลอดเดียว จึงทำให้ต้องปรับเงื่อนไขของปฏิกิริยาซึ่งต่างไปจากปกติ

ในที่นี้ ได้ดำเนินการพัฒนาระบบการเพิ่มปริมาณสารพันธุกรรมแบบลูบอุณหภูมิเดียวสำหรับการตรวจไวรัสโรคกุ้งต่างชนิดซึ่งได้แก่ WSSV และ IHHNV ได้พร้อมกัน และพัฒนาระบบการเพิ่มปริมาณสารพันธุกรรมแบบลูบอุณหภูมิเดียว สำหรับการตรวจไวรัสโรคใบเหี่ยวในสับปะรดทั้งชนิดที่ 1 และ 2 ได้พร้อมกัน รูปแบบการตรวจดังกล่าวจึงเป็นนวัตกรรม

สำหรับการเทคนิคการตรวจสอบสัญญาณดีเอ็นเอในครั้งนี้อาศัยการจับตัวของโพรบกับสารพันธุกรรมเป้าหมายในรูปแบบ nucleic acid hybridization เน้นการแสดงผลเป็น 2 ลักษณะ ได้แก่การเชื่อมโยง nucleic acid hybridization กับการเรืองแสงโดยโมเลกุลฟูโอโรฟอร์และการตรวจสอบการเปลี่ยนแปลงทางสีทางแสงของอนุภาคนาโนของโลหะ เน้นคุณลักษณะของโพรบ PNA ที่ใช้ ได้แก่ ความจำเพาะในระดับ single nucleotide การจับตัวด้วย affinity ที่สูงกว่าและความสามารถในการทำหน้าที่ที่อุณหภูมิห้อง (Vilaivan and Srisuwannaket, 2006)

การแสดงผลระบบแรกอาศัยโพรบและquencher โพรบจะได้รับการออกแบบให้ทำหน้าที่จับตัวกับยีนเป้าหมาย โดยต้องมีการติดฉลาก ในที่นี้ได้แก่ FAM fluorophore ที่ตำแหน่ง 5‘ ขณะที่ quencherได้รับการออกแบบให้จับตัวกับโพรบและมีโมเลกุลที่เป็นคู่รับพลังงาน ในที่นี้ได้แก่ BHQ เป็นโมเลกุลรับพลังงาน ในขั้นต้นต้องนำโพรบและquencher มาจับตัวกันก่อนเพื่อให้แสงจาก fluorophore ที่ตำแหน่ง 5‘ ดับลง จากนั้นหากในทุกตัวอย่างที่มียีนเป้าหมายตัวอย่างเหล่านั้นก็จะให้ผลิตภัณฑ์ดีเอ็นเอหลังการเพิ่มปริมาณอย่างแม่นยำ ดีเอ็นเอที่ได้จะจับ

ได้กับโพรบ PNA และทุกครั้งที่การจับตัวประสบความสำเร็จ quencher ของโพรบดังกล่าวจะหลุดเป็นอิสระ ไม่สามารถรับพลังงานจากโพรบได้อีกต่อไป ส่งผลให้เกิดการเรืองแสง

การแสดงผลในส่วนที่สอง อาศัยคุณลักษณะของ PNA ทั้งในแง่ที่ไม่มีประจุ ในแง่การจับตัวด้วย affinity ที่สูงกว่า DNA และจำเพาะมากกว่าแม้เพียง single mismatch ก็ไม่จับตัว และความสามารถในการทำงานที่อุณหภูมิห้อง โดย PNA probe จะแสดงพฤติกรรมเป็น coagulant โดย PNA probe จะจับตัวอยู่ที่ผิวของอนุภาคทองคำการจับตัวนี้เกิดได้จากส่วนของ nitrogen/oxygen ในเบสและจากโครงสร้างของ PNA เองที่เป็น hydrophobic neutral structure โดยในขณะที่ในตัวอย่างไม่มีดีเอ็นเอเป้าหมาย ในภาวะที่มีเกลือเข้มข้นต่ำ PNA จะช่วยกระตุ้นให้เกิดการจับตัวของอนุภาคทำให้เกิดการตกตะกอน เปลี่ยนสีของสารละลายอนุภาคทองคำจากสีแดงอมชมพูไปเป็นสีม่วงเข้ม แต่ในขณะที่ตัวอย่างมีดีเอ็นเอเป้าหมาย การจับตัวระหว่าง PNA probe กับ ดีเอ็นเอเป้าหมายจะก่อให้เกิด hybridization complex ซึ่งเป็นโครงสร้างที่คล้ายกับ double stand DNA ทำหน้าที่ป้องกันการจับตัวของอนุภาคทองคำ จึงทำให้เกิดการตกตะกอนและไม่เกิดการเปลี่ยนสีของสารละลายอนุภาคทองคำ (Kanjanawarut and Xu, 2009)

โมเดลที่ดำเนินการประกอบไปด้วย การตรวจตรวจยีน neuraminidase ของ 2009 H1N1 human influenza A virus ดื้อยา oseltamivir และ ระบบการตรวจไวรัสซิคุนกุนยาสำหรับการประยุกต์ทางการแพทย์ และการตรวจยีนจำเพาะต่อไวรัสกุ้ง WSSV และ IHHNV ระบบการตรวจยีนจำเพาะต่อไวรัส PMWaV สายพันธุ์ 1 และ 2 และการตรวจการสุกแก่ทางสรีระวิทยาผ่านการแสดงออกของยีน *AcSUT*1สำหรับการประยุกต์ทางการเกษตร โดยแต่ละระบบ ได้นำการตรวจสัญญาณในแต่ละระบบมาใช้ ขั้นตอนการพัฒนาได้รวมการสืบค้นข้อมูลเพื่อตอบโจทย์ปัญหา การวิเคราะห์ข้อมูลลำดับนิวคลิโอไทด์ และการออกแบบไพรเมอร์สำหรับการพัฒนาระบบการเพิ่มปริมาณดีเอ็นเอ การโคลนยีนเพื่อใช้เป็นโมเลกุลอ้างอิง การพัฒนาระบบการเพิ่มปริมาณสารพันธุกรรม การพัฒนาระบบการตรวจสอบสัญญาณดีเอ็นเอ การเชื่อมโยงระบบเข้าด้วยกัน และการทดสอบประเมินผลปฏิกิริยา โดยแต่ละโมเดลที่ได้ดำเนินการสามารถตรวจสอบทางพันธุกรรมเสร็จสิ้นได้ในเวลาน้อยกว่า 1 ชั่งโมง ด้วยความแม่นยำโดยดูจากปฏิกิริยาที่เฉพาะตัว ความไวของปฏิกิริยาที่อยู่ในระดับ มากกว่า 100 ก๊อปปี้ของยีนแม่แบบที่ปรากฏในตัวอย่าง และที่สำคัญลดระดับการพึ่งพาห้องปฏิบัติการเนื่องจากตลอดขั้นตอนใช้เพียง heat block incubator หรือ water bath เท่านั้น

ความสามารถลดการพึ่งพาห้องปฏิบัติการนี้เป็นเพราะการเลือกรูปแบบการเพิ่มปริมาณแบบ isothermal platform และการตรวจสัญญาณโดย PNA ที่ทั้งสองช่วยให้การดำเนินการได้ที่อุณหภูมิห้อง ทำนองเดียวกันการเลือกรูปแบบการเพิ่มปริมาณดีเอ็นเอที่ใช้ไพร์เมอร์จำเพาะถึง 6 บริเวณ ทำให้เกิดความโด่งเด่นในการสร้างความจำเพาะของปฏิกิริยาอย่างน้อย 4^{-100} (จากความต่างกันของไพร์เมอร์รวมในระบบ 160-180 nt เมื่อเทียบกับของ PCRที่มีเพียง 50-60 nt) platform นี้เป็น platform เดียวที่ให้ความจำเพาะสูงกว่า platform ใดๆ และจากความจำเพาะของ PNA ที่โดดเด่นในเรื่อง error prone hybridization

ในระบบเรืองแสงเมื่อทำปฏิกิริยา การแข่งขันระหว่างเป้าหมายจะทำให้ quencher หลุดออก จึงทำให้คู่ โพรบ/quencher ที่ดับลงกลับส่งสัญญาณขึ้น ทำให้เห็นกลไกการจับตัวได้โดยตรง อย่างไรก็ดีระบบการตรวจสัญญาณดังกล่าวใช้ความเข้มข้นของโพรบสูง ใช้โพรบมาก ซึ่งการสังเคราะห์โพรบมีต้นทุนเชิงพาณิชย์ 50-100 ng ประมาณ 25000-30000 บาท (รวมติดฉลาก FAM) ทำให้มีต้นทุนในการดำเนินการสูงตามไปด้วย นอกจากนี้ระบบการตรวจการเรืองแสงจำเป็นต้องใช้ แหล่งกำเนิดแสง UV ความยาวคลื่น 312-350 nm ซึ่งเกี่ยวข้องกับความยาวคลื่นที่อาจก่อให้เกิดอันตรายขณะใช้งานได้ ขณะที่ในระบบการเปลี่ยนแปลงทางสีของแสงผ่านการจับตัวแบบ hybridization ที่เชื่อมโยงกับการตกตะกอนของอนุภาคนาโนของโลหะ มีข้อดีที่เห็นการเปลี่ยนแปลงได้ด้วยตาเปล่า ไม่จำเป็นต้องมีอุปกรณ์เสริมอื่น และมีต้นทุนต่ำกว่า เนื่องจากระบบการตรวจสัญญาณดังกล่าวใช้ความเข้มข้นของโพรบต่ำกว่า 10-20 เท่า ขณะที่ต้นทุนของสารละลายทองคำนาโน/ปฏิกิริยา ไม่เกิด 1 บาท/ปฏิกิริยา อย่างไรก็ดีการตรวจสัญญาณการเปลี่ยนแปลงทางสีทางแสงของอนุภาคนาโน ยังมีข้อจำกัดในแง่ของอายุการเก็บรักษาของอนุภาคนาโนที่ใช้ที่จะเสื่อมลงเนื่องจากการตกตะกอนในเวลา 1 เดือนสำหรับทองคำ และ 6 เดือนสำหรับเงินสีน้ำเงิน

เทคนิคที่ได้ดำเนินการในครั้งนี้ตอบโจทย์เฉพาะการตรวจเชิงคุณภาพ สำหรับการตรวจสอบสัญญาณเชิงปริมาณ จำเป็นต้องพัฒนาระบบการเพิ่มปริมาณสัญญาณที่สอดล้อกับปริมาณสารพันธุกรรมแม่แบบ และการตรวจวัดสัญญาณอย่างง่ายที่ตอบโจทย์การวัดระดับสัญญาณตามปริมาณจริง ซึ่งสามารถดำเนินการได้ผ่านการปรับวิธีการทางเทคนิคต่อไป

อย่างไรก็ดี หากพิจารณาภาพรวมพบว่าการพัฒนาระบบการตรวจวิเคราะห์โดยเชื่อมโยงเทคนิคการเพิ่มปริมาณสารพันธุกรรมแบบลูบอุณหภูมิเดียว ในการเพิ่มสัญญาณทางพันธุกรรม และพัฒนาระบบการตรวจสัญญาณสารพันธุกรรมโดยใช้เบต้าพิโรลิดินิลเพปไทด์นิวคลีอิกแอซิดเป็นโพรบและตรวจสัญญาณผ่านการเรืองแสง (fluorescence) หรือการเปลี่ยนสีทางแสง (colorimetry)ในภาพรวม สรุปได้ว่าเทคนิคที่พัฒนาขึ้นมีข้อได้เปรียบเหนือกว่าเทคนิคที่มีรายงานในปัจจุบัน ช่วยให้การตรวจสารพันธุกรรมทำได้ภายในเวลาน้อยกว่า 60 นาที ที่อุณหภูมิคงที่ โดยลดการพึ่งพาห้องปฏิบัติการ และให้ความจำเพาะสูงเนื่องจากอาศัยทั้งชุดของไพร์เมอร์ที่จับตัวกับดีเอ็นเอเป้าหมายและการยืนยันผลโดยเบต้าไพโรริดินิลเพพไทด์นิวคลิอิคโพรบ โดยกระบวนการโดยรวมสามารถปรับประยุกต์ให้อยู่ในรูปแบบชุดตรวจสำเร็จได้ง่าย

6. ผลลัพธ์ของโครงการ

ได้องค์ความรู้ที่สามารถพัฒนาต่อยอด ไปสู่การสร้างชุดตรวจสำเร็จสำหรับการตรวจยีน neuraminidase ของ 2009 H1N1 human influenza A virus ดื้อยา oseltamivir และ ระบบการตรวจไวรัสชิคุนกุนยาสำหรับการประยุกต์ทางการแพทย์และการตรวจยีนจำเพาะต่อไวรัสกุ้ง

white spot syndrome virus (WSSV) infectious hypodermal and hematopoietic necrosis virus (IHHNV) ระบบการตรวจยีนจำเพาะต่อไวรัส pineapple mealybug wilt associated virus (PMWaV) สายพันธุ์ 1 และ 2 และการตรวจการสุกแก่ทางสรีระวิทยาผ่านการแสดงออกของยีน *AcSUT1*สำหรับการประยุกต์ทางการเกษตร ทั้งหมด 5 องค์ความรู้

วิทยานิพนธ์วิทยาศาสตร์มหาบัณฑิต

Nussara Donraman. 2012. Genosensor Based on Colorimetric Detection Using Silver Nanoparticles for Chikungunya Disease Assay. Master Thesis, Faculty of Science, Chulalongkorn University.

นุสรา ดลระหมาน. จีโนเซนเซอร์ด้วยการตรวจสอบสีของอนุภาคเงินนาโนเพื่อใช้ในการสอบวิเคราะห์โรคชิคุนกุนยา

Najwa Yanya. 2012. Simple and Rapid Technique for Detection of Virus Causing Pineapple Wilt-Disease. Master Thesis, Faculty of Science, Chulalongkorn University.

นัจวา ยานยา. เทคนิคอย่างง่ายและรวดเร็วในการตรวจหาไวรัสที่เป็นสาเหตุก่อให้เกิดโรคเหี่ยวในสับปะรด

Proceeding

Chaumpluk, P. Chaiprasart, P. Vilaivan, T. 2012. Postharvest Non-destructive Determination of Fruits: a Model on Fruit Maturity Assay via Biosensor Based on Colorimetric Change of Gold Nanoparticles. Acta Horticulture 945:205-211.

เอกสารยื่นขอสิทธิบัตร 2 รายการ

อานาล็อกดีเอ็นเอสังเคราะห์และโอลิโกนิวคลีโอไทด์สังเคราะห์เพื่อการตรวจสารพันธุกรรมของไวรัสโรคเหี่ยวสับปะรดชนิด พีเอ็มดับเบิลยูเอวี (PMWaV)1 และ 2 และวิธีตรวจสอบสารพันธุกรรม

โอลิโกนิวคลีโอไทด์สังเคราะห์และอานาล็อกดีเอ็นเอเพื่อการตรวจสารพันธุกรรมของไวรัสโรคกุ้งชนิด ดับเบิ้ลยูเอสเอสวี (WSSV) และ ไอเฮชเฮชเอ็นวี และวิธีตรวจสอบสารพันธุกรรม **(กำลังเตรียมดราฟ)**

7. เอกสารอ้างอิง

ชำนาญ พิทักษ์ อนุวัฒน์ จันทรสุวรรณ และ อรนุช กองกาญจนะ. 2542. การป้องกันและกำจัดมดในไร่สับปะรด. กลุ่มงานวิจัยแมลงศัตรูข้าวโพดและพืชไร่อื่น ๆ กองกีฏและสัตววิทยา. 3 น กรุงเทพฯ.

ณัฐพร อุดมพงษ์ และปิยะศักดิ์ ชอุ่มพฤกษ์, 2551. การตรวจวิเคราะห์เชื้อตัวแดงดวงขาวในกุ้งใน 45 นาที. การประชุมวิชาการเกษตรแห่งชาติ. มหาวิทยาลัยนเรศวร 5-14 กันยายน 2551.

Altschul, S.F., Gish, W., Miller, W., Myers, E.W. & Lipman, D.J. 1990. Basic local alignment search tool. J. Mol. Biol. 215:403-410.

Anthony, P. F. T. 2000. Biosensors-Sense and Sensitivity. Biochemistry 290:1315-1317.

Beardsley, J.W. 1993. The pineapple mealybug complex; taxonomy, distribution and host relationships. Acta Horticulture 334: 383-386.

Carletti F, Bordi L, Chiappini R, Ippolito G, Sciarrone MR, Capobianchi MR, Di Caro A, Castilletti C. 2007.Rapid detection and quantification of Chikungunya virus by a one-step reverse transcription polymerase chain reaction real-time assay. Am J Trop Med Hyg. 77:521-4.

Centers for Disease Control and Prevention (CDC), 2009. Swine influenza A (H1N1) infection in two children-Southern California, March-April 2009. MMWR. Morb. Mortal. Wkly. Rep. 58, 400-402.

Chevillon C., Briant L., Renaud F., Devaux C. 2008. The Chikungunya threat: an ecological and evolutionary perspective. Trends in Microbiology 16: 80-88.

Collins, P. J.; Haire, L. F.; Lin, Y. P.; Liu, J.; Russell, R. J.; Walker, P. A.; Skehel, J. J. , Martin, S. R.; Hay, A. J.; Gamblin, S. J. 2008. Crystal structures of oseltamivir-resistant influenza virus neuraminidase mutants. Nature 453:1258-1261.

Compton, J.1991. Nucleic acid sequence-based amplification. Nature 350:91-92.

Flegel, T.W., Sriurairtana, S., Wongteerasupaya, C., Boonsaeng, V., Panyim, S. and Withyachumnarnkul, B. 1995. Progress in characterization and control of yellow-head virus of *Penaeus monodon*. Pp. 76-83 *In:* C.L. Browdy and J.S. Hopkins, editors. Swimming Through Troubled Water, Proceedings of the Special Session on Shrimp Farming, Aquaculture '95. World Aquaculture Society, Baton Rouge, LA, USA.

Grunenwald, H. 2009. Direct PCR from a Single Bacterial Colony Without DNA

Extraction Using the FailSafe™ PCR System. [Online]. Available from: http://www.epibio.com/ newsletter/8_3fail_safe.pdf [2010, May 15]

Guatelli, J.C., Whitefield, K.M., Kwoh, D.Y., Barringer, K.J., Richman, D.D. and Gingeras, T.R.1990.Isothermal, in vitro amplification of nucleic acids by a multienzyme reaction modeled after retro viral replication. Proc.Nat. Acad. Sci., USA 87:392-396.

Hu, J.S., D.M. Sether, X.P. Liu and M. Wang. 1997. Use of a tissue blotting immunoassay to examine the distribution of pineapple Closterovirus in Hawaii. Plant Disease. 81: 1150-1154.

Kader, A.A. 1999. Fruit maturity, ripening and quality relationships. Acta Hort 485:203-208.

Kanjanawarut, R., and Su, X. D. 2009. Colorimetric detection of DNA using unmodified metallic nanoparticles and peptide nucleic acid probes. Anal. Chem. 81:6122–6129.

Khan A.H., Marita K., Parquet M.C., Hasebe F., Mathenge E.G.M., Igarashi A. 2002. Complete nucleotide Sequence of chikugunya virus and evidence for an internal poly adenylation site. J. Gen. Virol. 83:3075-3084.

Kono, T., Savan, R., Sakai, M., and Itami, T. 2004. Detection of white spot syndrome virus in shrimp by loop-mediated isothermal amplification. J. of Virol Methods 115:59-65.

Lightner, D.V., Pantoja, C.R., Poulos, B.T., Tang, K.F.J., Redman, R.M, Andrade, T.P.D., Bonami, J.R., 2004. Infectious Myonecrosis: New Disease in Pacific White Shrimp. The Advocate. Global Aquaculture Alliance. October 2004.

Lizardi, P.M., Huang, X., Zhu, Z., Bray-Ward, P., Thomas, D.C. and Ward, D.C. 1998. Mutation detection and single-molecule counting using isothermal rolling-circle amplification Nature Genetics 19:225-232.

Lockley, A.K. and Bardsley, R.G., 2000. DNA-based methods for food authentication. *Trends in Food Sci. and Technol.* 11: 6777-9.

Lyamichev, V., Mast, A.L., Hall, J.G., Prudent, J.R., Kaiser, M.W., Takova, T., Kwiatkowski, R.W., Sander, T. J., de Arruda, M., Arco, D.A., Neri, B.P. and Brow, M.A. 1999. Polymorphism identification and quantitative detection of genomic DNA by invasive cleavage of oligonucleotide probes. Nature Biotech. 17:929-926.

Meijer, A., Lackenby, A., Hungnes, O., Lina, B., van der Werf, S., Schweiger, B., Opp, M., Paget, J., van de Kassteele, J., Hay, A., Zambon, M. 2009. Oseltamivir-resistant influenza virus A (H1N1), Europe, 2007-08 season. Emerg Infect Dis DOI: 10.3201/eid1504.081280.

Melzer, M.J., A.V. Karasev, D.M. Sether and J.S. Hu. 2001. Nucleocapside sequence, genome organization and phylogenetic analysis of pineapple mealybug wilt associate virus-2. J. Gen. Viro. 82:1-7.

Mirkin, C. A., Letsinger, R.L., Mucic, R.C., Storhoff, J.J. 1996. DNA-based method for rationally assembling nanoparticles into macroscopic materials. Nature 382: 607–609.

Moyle, R., Fairbairn, D.J., Ripi, J., Crowe, M. and Botella, J.R. 2005. Developing pineapple fruit has a small transcriptome dominated by metallothionein. J. Experimental Botany 56:101-112.

Notomi, T., Okayama, H., Masubuchi, H., Yonekawa, T., Watanabe, K., Amino, N. and Hase, T. 2000. Loop-mediated isothermal amplification of DNA. Nucleic Acids Research 28:e63.

Pattee, H.E.(ed,).1985. Evaluation of quality of Fruits and vegetables. AVI Publishing Co. Inc. Westport, CT.p. 410.

Pienpinijtham, P., Thammacharoen, C., and Ekgasit S. 2010. Enhacement of reducing efficiency of soluble starch for green synthesis of gold nanoparticles. Pure and Applied Chemistry International Conference 21-23 January 2010 Sunee Grand Hotel Ubon Ratchathani, Thailand. p. 366.

Pfeffer M, Linssen B, Park M.D., Kinney R.M. 2002. Specific detection of chikugunya virus using RT-PCR/nested.PCR combination. J. Vet. Med. B Infect. Dis. Vet. Public Health 49:49-54.

Powers A.M., Bravlt, A.C., Tesh R.B., Weawer S.C. 2000, Reemerged of Chikungunya and onyong-nyong virus: evidence for distinct geographical lineage and distance evoutionany reation ship J. Gm V.101 81: 417-479.

Rianthavorn P, Prianantathavorn K, Wuttirattanakowit N, Theamboonlers A, Poovorawan Y. 2010. An outbreak of chikungunya in southern Thailand from 2008 to 2009 caused by African strains with A226V mutation.. Int J Infect Dis. 2010 Sep;14 Suppl 3:e161-5.

Rungrotmongkol, T., Malaisree, M., Nunthaboot, N.,• Sompornpisut, P., Hannongbua, S. 2009. Molecular prediction of oseltamivir efficiency against probable influenza A (H1N1-2009) mutants: molecular modeling approach.Amino Acids DOI 10.1007/s00726-009-0452-3.

Saiki, R.K., Gelfand, D.H., Stoffel, S., Scharf, S.J., Higuchi, R., Horn, G.T., Mullis, K.B. and Erlich, H.A. 1988. Primer-directed enzymatic amplification of DNA with a thermostable DNA polymerase. Science 239:487-491.

Sambrook, J., Fritsch, E.F., and Maniatis, J. 1989. Molecular cloning: A laboratory manual, 2nd edition. Cold Spring Harbor Laboratory Press, New York, USA.

Sether, D.M., and J.S. Hu. 2002a. Closterovirus infection and mealybug exposure are ecessary for the development of mealybug wilt of pineapple disease. Phytopathology 92: 928-935.

Sether, D.M., and J.S. Hu. 2002b. Yield impact and spread of pineapple mealybug wilt associated virus-2 and Mealybug Wilt of pineapple in Hawaii. Plant Dis. 86: 867-874.

Smith D. R., Lee J. S, Development of Field-based real-time reverse transciption-polymerase chain reaction assays for detection of chikungunya and o'nyung o'nyung viruses in mosquitoes. Am J. Trop Med. Hyg. 81:679-684.

Sun, Z.F., Hu, C.Q., Ren, C.H., and Shen, Q. 2006. Sensitive and rapid detection of infectious hypodermal and hematopoitic necrosis virus (IHHNV) in shrimps by loop-mediated isothermal amplification. J. of Virol. Methods 131:41-46.

Suparpprom, C., Srisuwannaket, C., Sangvanich, P., Vilaivan, T. 2005. Synthesis and oligodeoxynucleotide binding properties of pyrrolidinyl peptide nucleic acids bearing prolyl-2-aminocyclopentanecarboxylic acid (ACPC) backbones. Tetrahedron Lett. 46: 2833-2837.

Taira, T., Toma, N., Ichi, M., Takeuchi, M., and Ishihara, M. 2005. Tissue distribution, synthesis stage and ethylene induction of pineapple (*Ananus comosus*) chitinase. Biosci. Biotechnol. Biochem. 69:852-854.

Thomson, D.G., Enright, A., Faulds, K., Smith, W.E. and Graham, D. 2008. Ultrasensitive DNA detection using oligonucleotide silver nanoparticle conjugates. Analytical Chemistry 80: 2805-2810.

Vilaivan, T., Srisuwannaket, C. 2006. Hybridization of pyrrolidinyl peptide nucleic acids and DNA: Selectivity, base-pairing specificity, and direction of binding. Org. Lett. 8:1897-1900.

Walker, G.T., Little, M.C., Nadeau, J.C. and Shank, D.D. 1992. Strand displacement amplification- isothermal, in vitro DNA amplification technique. Nucleic Acids Research 20:1691-1696.

WHO. Laboratory Diagnosis of Chikungunya Fevers. http://www.searo.who.int/EN/Section10/Section2246_12902.htm. (Retrieved 2008-07-11.)

WHO, 2009a. Pandemic H1N1 2009–Update 58 Laboratory-confirmed cases of pandemic (H1N1) 2009 as officially reported to WHO by States Parties to the International Health Regulations (2005) available online on 6 July 2009 at http://www.who.int/csr/don/2009_07_06/en/index.html

WHO, 2009b. Pandemic (H1N1) 2009 news brief: no. 1 Viruses resistant to oseltamivir (Tamiflu) identified. available online on 8 July 2009 at http:// www.who.int/csr/disease/ swineflu/newsbriefs/h1n1_antiviral_resistance_ 20090708/ en/index.html

Project 6a: Applications of PNA based diagnostics in medical, food and agricultural sciences

หัวหน้าโครงการ ผศ.ดร. ปิยะศักดิ์ ชอุ่มพฤกษ์

กิจกรรมที่ได้ทำเพิ่มเติมในช่วงขยายระยะเวลาโครงการ (1 สิงหาคม 2555 - 31 มกราคม 2556)

โครงการย่อยที่ 6a เน้นการนำเบต้าพิโรลิดินิลเพปไทด์นิวคลีอิกแอซิด มาประยุกต์ใช้ในการพัฒนารูปแบบการตรวจวิเคราะห์ทางพันธุกรรม โดยเชื่อมโยงกับความสำเร็จในการตรวจสัญญาณดีเอ็นเอกับการพัฒนาชิปในระบบกระดาษที่ห้องปฏิบัติการดำเนินการอยู่แล้ว เน้นการตรวจสอบสัญญาณดีเอ็นเอที่มองเห็นได้ด้วยตาเปล่า

การดำเนินการอาศัยความจำเพาะในการจับตัวระหว่าง PNA กับสารพันธุกรรมเป้าหมาย บนหลักการ nucleic acid hybridization ที่ PNA มีความโดดเด่นกว่าในแง่ความแน่นในการจับตัว ความจำเพาะในระดับยิ่งยวด และการตรวจสอบสัญญาณดีเอ็นเอโดยวัดการเปลี่ยนแปลงทางสีของแสงด้วยเงินนาโนเพลทสีฟ้าน้ำเงิน

วัตถุประสงค์

พัฒนาระบบการตรวจสัญญาณดีเอ็นเอโดยการนำเบต้าพิโรลิดินิลเพปไทด์นิวคลีอิกแอซิด มาประยุกต์ใช้เป็นโพรบบนชิปที่ทำด้วยกระดาษเซลลูโลส

วิธีการทดลอง

การดำเนินการอาศัยการทำปฏิกิริยา nucleic acid hybridization ระหว่างดีเอ็นเอเป้าหมาย โพรบ ในสารละลายของนาโนเงินสีฟ้า ในปฏิกิริยาประกอบด้วย เงินนาโนเพลทขนาด 120 นาโนเมตร ความเข้มข้น 1,200 ppm 10 ไมโครลิตร (Pakdeenard *et al*., 2010) ดีเอ็นเอตัวอย่างได้จากการเพิ่มปริมาณดีเอ็นเอของยีน ฮีแมกกลูตินิน (HA) ด้วยเทคนิคลูปอุณหภูมิเดี่ยวตามที่เคยรายงานมาก่อนหน้า โดยใช้ปริมาตร 1 ไมโครลิตร ในสารละลายที่ประกอบไปด้วย 20 mM Tris-HCl (pH 8.8) 10 mM KCl 10mM $(NH_4)_2SO_4$ 0.1% Triton X-100 ไพรเมอร์ F3 B3 ความเข้มข้น 5 pmol /ปฏิกิริยา ไพรเมอร์ FIP และ BIP ความเข้มข้น 40 pmol/ปฏิกิริยา ดีเอ็นเออนาลอกโพรบปริมาณ 1 นาโนโมล โดยรายละเอียดของไพรเมอร์และดีเอ็นเอ อนาลอกโพรบที่เป็นเบต้าพิโรลิดินิลเพปไทด์นิวคลีอิกแอซิด เป็นดังรายงานที่ได้ดำเนินการมาก่อนหน้านี้ ในการควบคุมการตกตะกอนของนาโนเงิน ดำเนินการโดยใช้เกลือความเข้มข้น 10 มิลลิโมล ปริมาตร 0.2 ไมโครลิตร และสังเกตเห็นการเปลี่ยนแปลงของการตกตะกอนของเงินนาโนเพลทหลังทำปฏิกิริยา 15 นาที

การนำสารในปฏิกิริยาทั้งหมดมาปรับใช้กับชิปที่ทำด้วยกระดาษเซลลูโลส ใช้ชิปส่วนแสดงผลที่ผ่านการขึ้นรูปชิปจากกระดาษกรอง Whatman No. 1 และลวดเสตนเลส SUS 304 เส้นผ่านศูนย์กลาง 0.4 mm โดยกระบวนการ plastic lamination ที่อุณหภูมิ 130°C ด้วย

pouch film ขนาด 125 mm และ pouch laminator (LMR-220) (Lamirel, France) การแสดงผลทำด้วยกระดาษรูปสี่เหลี่ยมผืนผ้า (square pad) ขนาด 2x2 mm โดยประมาณ ที่ได้ดูดซับสารละลายเกลือ 20 นาโนโมล (detection pad) บริเวณโพรบทำจาก Polystyrene พลาสติกขนาด 1x2 มิลลิเมตรโดยประมาณ (probe pad) ที่มีโพรบแห้งตัวเกาะอยู่

ตัวชิปเต็มมีขนาด 2.5x3 ตารางเซนติเมตร ประกอบด้วย 2 ส่วน ส่วนแรกสำหรับการทำปฏิกิริยาในการเพิ่มสัญญาณดีเอ็นเอซึ่งไม่เกี่ยวกับการทดลองในครั้งนี้ ส่วนที่สองเกี่ยวข้องกับการตรวจสัญญาณดีเอ็นเอ ทั้งสองส่วนเชื่อมด้วยโครงสร้างที่เกิดจากการเคลือบพลาสติกกับลวดเสตนเลส SUS 304 ให้เป็นรูป W shape การเคลื่อนตัวของสารละลายดำเนินการโดยใช้แรงดันจากมือในการบีบตัวชิปเป็นหลัก

การตรวจสัญญาณในชิป สังเกตจากการเคลื่อนตัวของสารละลายในปฏิกิริยา nucleic acid hybridization ระหว่างดีเอ็นเอเป้าหมาย ไปผสมกับสารละลายของนาโนเงินสีฟ้า โพรบ (probe pad)และแสดงผลบนแผ่นกระดาษ (detection pad) ที่สามารถสังเกตได้ด้วยตาเปล่า

ผลการทดลอง

การดำเนินการอาศัยการทำปฏิกิริยา nucleic acid hybridization ระหว่างดีเอ็นเอเป้าหมาย โพรบ ในสารละลายของเงินนาโนเพลทสีฟ้าในสภาพหลอดทดลองพบว่า ในกรณีที่ไม่มีดีเอ็นเอเป้าหมาย สารละลายเงินนาโนเพลทสีฟ้าจะตกตะกอนได้เป็นสารละลายสีเหลืองอ่อน-ใส เมื่อเทียบกับสีของสารละลายเดิม อย่างไรก็ดีในภาวะที่มีดีเอ็นเอเป้าหมายสารละลายเงินนาโนเพลทสีฟ้าจะไม่ตกตะกอน ทำให้ยังคงเห็นสีของสารละลายเงินนาโนเพลทสีฟ้าเช่นเดิม ผลการทดลองแสดงให้เห็นว่าการใช้ β-pyrrolidinyl peptide nucleic acid โพรบ และทำปฏิกิริยากับดีเอ็นเอที่เพิ่มปริมาณได้ ช่วยให้สามารถบ่งบอกความแตกต่างของดีเอ็นเอเป้าหมายที่สามารถมองเห็นได้ด้วยตาเปล่าได้ (ภาพที่ 1) การตรวจด้วยวิธีดังกล่าวอยู่บนพื้นฐานของการทำปฏิกิริยา nucleic acid hybridization โดยใช้ PNA (Kanjanawarut and Su, 2009)

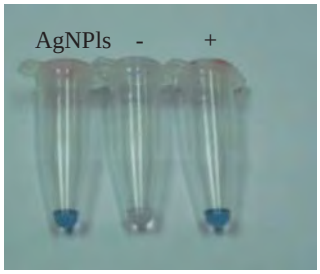

ภาพที่ 1 ผลการทดสอบการเกิดปฏิกิริยา nucleic acid hybridization ในสารละลายของเงินนาโนเพลทสีฟ้าเมื่อใช้ β-pyrrolidinyl peptide nucleic acid เป็นโพรบ เมื่อตัวอย่างเป็นดีเอ็นเอเป้าหมาย + ดีเอ็นเออื่น – เปรียบเทียบกับสารละลายของเงินนาโนเพลทสีฟ้า AgNPls

การตรวจที่อาศัย β-pyrrolidinyl peptide nucleic acid เป็นโพรบ สามารถเปลี่ยนแปลงสัญญาณในรูปแบบการเปลี่ยนของพลาสมอนทางแสง โดยในภาวะที่ไม่มีดีเอ็นเอเป้าหมาย โพรบจะจับตัวบนผิวอนุภาคโดยอาศัยด้าน hydrophobic ไปที่ผิวอนุภาค เกลือในระบบจะกระตุ้นให้เกิดการจับตัวของอนุภาค แต่ในภาวะที่มีดีเอ็นเอเป้าหมาย โพรบจะกับดีเอ็นเอเป้าหมาย ช่วยให้อนุภาคกระจายตัวไม่เกาะกัน จึงไม่เกิดการเปลี่ยนแปลงอยู่ในรูปการตกตะกอน

อย่างไรก็ดี การตรวจในสภาพหลอดทดลอง จำเป็นต้องเคลื่อนย้ายสารละลายจากหลอดหนึ่งไปยังอีกหลอดหนึ่ง ซึ่งอาจก่อให้เกิดการปนเปื้อนของโมเลกุลในลักษณะแคริโอเวอร์ได้ นอกจากนี้การตรวจในสภาพหลอดทดลองยังเกี่ยวข้องกับปริมาตรของสารละลายที่มาก ไม่สะดวกในการเก็บรักษา ดังนั้นการปรับประยุกต์ตัวเทคนิคการตรวจสอบจึงเน้นการเชื่อมโยงกับเทคนิคการตรวจวิเคราะห์ในรูปแบบห้องปฏิบัติการบนชิป

การทดสอบระบบการตรวจสัญญาณดีเอ็นเอบนชิป ในขั้นต้นอยู่บนพื้นฐานหลักการที่ Li and Rothberg, (2004) ได้พัฒนาขึ้น โดยใช้ unmodified gold nanoparticles ผลการตรวจอยู่บนพื้นฐานการตอบสนองของอนุภาคในภาวะ ionic strength ที่ต่างกัน ในภาวะที่มี single strand DNA (ssDNA) หรือ double strand DNA (dsDNA) ซึ่งให้ผลการตอบสนองของอนุภาค nanoparticles ต่างกัน การทดลองในครั้งนี้เริ่มจากการทดสอบหลักการเดียวกันร่วมกับสารละลายเงินนาโนเพลทสีฟ้า พบว่าในชิปที่ขึ้นรูปด้วยโครงสร้างอย่างง่ายที่ประกอบด้วยส่วนของ detection pad ที่มีเกลือในปริมาณเหมาะสมและทำให้แห้งอยู่ เชื่อมโยงอยู่กับท่อส่งที่เกิดจากวัสดุเคลือบพลาสติกและลวดเสตนเลส SUS 304 เส้นผ่านศูนย์กลาง 0.4 mm (ภาพที่ 2บน) เมื่อนำดีเอ็นเอตัวอย่างมาผสมร่วมกับสารละลายเงินนาโนเพลทสีฟ้า แล้วบังคับให้เกิดการเคลื่อนตัวในลักษณะบีบ ผสมและบีบดันสารละลายไปยัง detection pad (ภาพที่ 2 ล่าง)

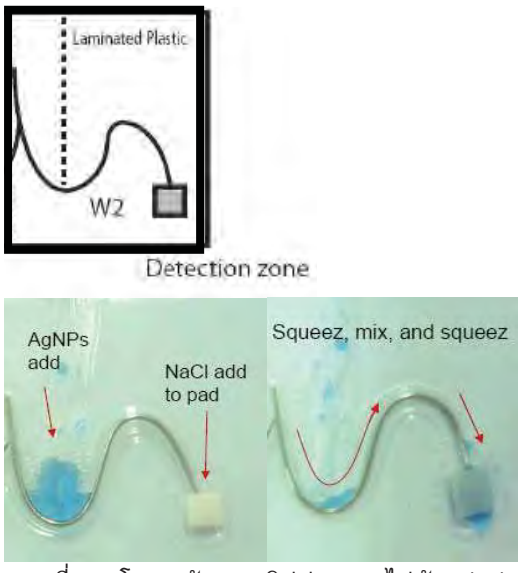

ภาพที่ 2 โครงสร้างของชิปประกอบไปด้วยท่อส่งที่เกิดจากวัสดุเคลือบพลาสติกและลวดเสตนเลส เชื่อมโยงไปสู่บริเวณที่เป็น detection pad (บน) และรูปแบบการใช้งานผ่านการบังคับให้เกิดการเคลื่อนตัวของสารละลายในลักษณะบีบ ผสมและบีบ ดันสารละลายไปยัง detection pad เพื่อการแสดงผล

ในกรณีที่มีดีเอ็นเอเป้าหมาย ปฏิกิริยาเพิ่มปริมาณดีเอ็นเออย่างจำเพาะจะทำให้ได้ผลิตภัณฑ์ดีเอ็นเอที่เป็น double strand DNA ส่งผลให้เมื่อทำปฏิกิริยากับสารละลายเงินนาโนเพลทสีฟ้าบน detection pad ที่มีเกลือในปริมาณเหมาะสมจะกระตุ้นให้เกิดการตกตะกอนเป็นสารละลายสีเหลืองอ่อน-ใส มีความแตกต่างอย่างชัดเจนเมื่อเทียบกับสีของสารละลายเดิม และเมื่อสังเกตุบน detection pad จะเห็นสีของ detection pad เป็นสีขาวขาวหม่น (ภาพที่ 3)
ในกรณีที่ไม่มีดีเอ็นเอเป้าหมาย ปฏิกิริยาเพิ่มปริมาณดีเอ็นเออย่างจำเพาะจะไม่เกิดขึ้น ทำให้ไม่มีผลิตภัณฑ์ดีเอ็นเอที่เป็นdouble strand DNA คงเหลือแต่ไพร์เมอร์ในรูป single strand DNA (ssDNA) เมื่อทำปฏิกิริยากับสารละลายเงินนาโนเพลทสีฟ้าบน detection pad ที่มีเกลือในปริมาณเหมาะสมจะไม่กระตุ้นให้เกิดการตกตะกอน ดังนั้นเมื่อสังเกตุบน detection pad จะเห็นสีของ detection pad ยังคงเป็นสีฟ้าของสารละลายเงินนาโนเพลทชัดเจน

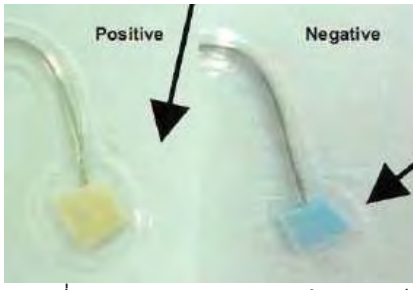

ภาพที่ 3 ผลการตรวจสัญญาณดีเอ็นเอเปรียบเทียบกรณีมีผลิตภัณฑ์ดีเอ็นเอที่เพิ่มปริมาณจากดีเอ็นเอเป้าหมาย (positive) กับกรณีที่ไม่มีผลิตภัณฑ์ดีเอ็นเอที่เพิ่มปริมาณจากดีเอ็นเอเป้าหมาย (negative) ให้ผลของสีบนกระดาษในส่วนของ detection pad ต่างกัน (ศรชี้)

แม้ว่าการตรวจสัญญาณดีเอ็นเอบนพื้นฐานหลักการที่ Li and Rothberg, (2004) จะไม่ใช่การตรวจดีเอ็นเอด้วยปฏิกิริยา nucleic acid hybridization ระหว่างดีเอ็นเอเป้าหมาย กับโพรบ ที่ได้รับการยอมรับว่าเป็นวิธีที่ได้มาตรฐาน อย่างไรก็ดีความรู้ที่ได้จากการนำหลักการของ Li and Rothberg, (2004) มาใช้ร่วมกับการตรวจบนชิป ทำให้เห็นได้ว่าการนำสารละลายเงินนาโนเพลทสีฟ้ามาใช้กับรูปแบบของชิปที่พัฒนาขึ้นในครั้งนี้ สามารถแสดงสัญญาณของดีเอ็นเอได้ และรูปแบบของชิปที่พัฒนาขึ้นยังสอดคล้องกับรูปแบบและขั้นตอนการทำปฏิกิริยาในขณะตรวจดีเอ็นเออีกด้วย

เพื่อเป็นการพัฒนาต่อยอดให้การตรวจสัญญาณดีเอ็นเอเป็นไปตามหลักการ nucleic acid hybridization ขณะที่ยังคงใช้ประโยชน์จากปรากฏการณ์ plasmon resonance ของนาโนของโลหะ จึงได้ประยุกต์ผลการทดลองที่รายงานในภาพที่ 1 มาต่อยอด

ผลการทดลองที่รายงานในภาพที่ 1 ใช้ β-pyrrolidinyl peptide nucleic acid เป็นโพรบทำปฏิกิริยากับดีเอ็นเอที่เพิ่มปริมาณได้ ในสภาพแวดล้อมที่มีสารละลายเงินนาโนเพลทสีฟ้า โพรบจะจับตัวบนผิวอนุภาค โดยปกติ peptide nucleic acid โพรบจะแสดงพฤติกรรมเป็น co-agglulator พร้อมจะกระตุ้นให้เงินนาโนเพลทสีฟ้าตกตะกอนเมื่อมีระดับของเกลือเหมาะสม ในยามที่มีดีเอ็นเอเป้าหมาย การจับตัวของดีเอ็นเอเป้าหมายจะทำให้ peptide nucleic acid ที่จับ

บนผิวของแผ่นเงินนาโนเพลทสีฟ้าลดปริมาณลง ส่งผลต่อพฤติกรรมเป็น co-agglulatorให้เปลี่ยนแปลงไป จึงทำให้แผ่นเงินนาโนเพลทสีฟ้าไม่ตกตะกอน การต่อยอดระบบตรวจจึงทำโดยการเพิ่ม probe pad ก่อนการทำปฏิกิริยากับเกลือ และเพื่อไม่ให้เกิดการสูญเสียของโพลบอันเนื่องจากการจับตัวกับเนื้อกระดาษเซลลูโลส จึงได้เลือกใช้วัสดุ PS พลาสติกทำเป็น probe pad แทนเนื้อกระดาษเซลลูโลส

โครงสร้างของส่วนตรวจสัญญาณดีเอ็นเอบนชิปที่พัฒนาขึ้นและชิปที่สร้างขึ้นเป็นดังภาพที่ 4 ส่วนของ probe pad ที่วางอยู่หน้า detection pad ช่วยให้การตรวจดีเอ็นเอเป็นไปตามปฏิกิริยา nucleic acid hybridization

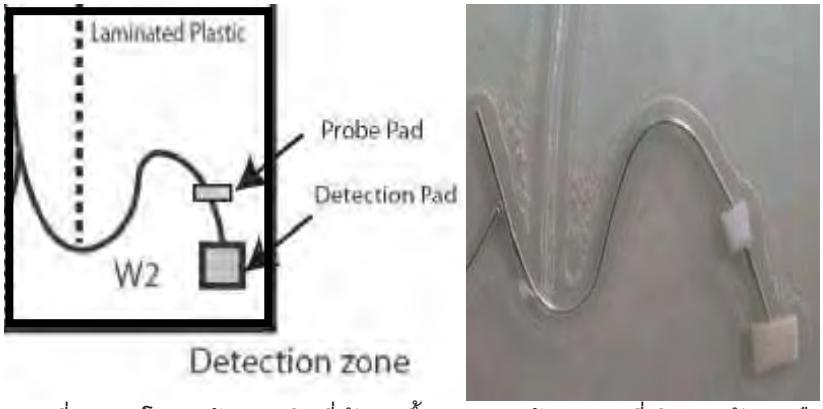

ภาพที่ 4 โครงสร้างของชิปที่พัฒนาขึ้นประกอบด้วยท่อส่งที่เกิดจากวัสดุเคลือบพลาสติกและลวดเสตนเลสเชื่อมโยงจากบริเวณ probe pad สู่บริเวณที่เป็น detection pad

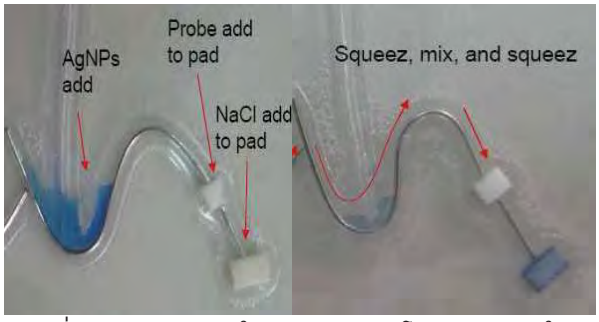

ภาพที่ 5 รูปแบบการใช้งานบนชิปทำโดยการบังคับให้เกิดการเคลื่อนตัวของสารละลายในลักษณะบีบ ผสม และบีบ ดันสารละลายเงินนาโนเพลทสีฟ้าและดีเอ็นเอให้เลื่อนตัวไปยัง probe pad และสิ้นสุดลงที่ detection pad เพื่อตรวจสอบผล

รูปแบบการใช้งานบนชิปยังคงรูปแบบเช่นเดิม โดยการบังคับการเคลื่อนตัวของสารละลายเงินนาโนเพลทสีฟ้า ทำผ่านการบีบ ผสมและบีบ ดันสารละลายไปยัง probe pad และ สิ้นสุดลงที่detection pad เพื่อการแสดงผล (ภาพที่ 5)

ผลการตรวจบนชิปในกรณีที่ใช้ β-pyrrolidinyl peptide nucleic acid เป็นโพรบ จะต่างไปจากผลการตรวจตามหลักการของ Li and Rothberg, (2004) โดยการตกตะกอนจะพบใน

กรณีที่ไม่มีดีเอ็นเอเป้าหมายหรือไม่มีดีเอ็นเอ ทำให้โพรบแสดงสถานะเป็น co-agglulator ขณะที่เงินนาโนเพลทสีฟ้ายังคงกระจายตัวไม่ต่างไปจากสารละลายเงินนาโนเพลทสีฟ้าปกติ เฉพาะในกรณีที่มีดีเอ็นเอเป้าหมาย จึงส่งผลให้สามารถบ่งบอกความแตกต่างระหว่างตัวอย่างที่มีดีเอ็นเอเป้าหมายและไม่มีดีเอ็นเอเป้าหมายจากสีของกระดาษบริเวณ detection pad ที่เป็นไปตามหลัก nucleic acid hybridization และสามารถมองเห็นได้ด้วยตาเปล่า (ภาพที่ 6)

ภาพที่ 6 ผลการตรวจบนชิปแสดงการตกตะกอนของสารละลายเงินนาโนเพลทสีฟ้าเป็นสารละลายสีเหลืองอ่อน-ใสบนกระดาษในส่วน detection pad ในกรณีที่ไม่มีดีเอ็นเอเป้าหมาย (ซ้าย) เปรียบเทียบกับการไม่ตกตะกอนและคงสีฟ้าในกรณีที่มีดีเอ็นเอเป้าหมาย (ขวา)

การตรวจตามหลักการ nucleic acid hybridization ร่วมกับ β-pytrrolidinyl peptide nucleic acid และสารละลายเงินนาโนเพลทสีฟ้า จะช่วยลดความผิดพลาดของการตรวจอันเกิดจากการเพิ่มปริมาณดีเอ็นเออย่างไม่จำเพาะ (non target specific) หรือการปนเปื้อนดีเอ็นเออื่นซึ่งมักพบในกรณีที่การตรวจพึ่งระบบการเพิ่มปริมาณดีเอ็นเอเพียงอย่างเดียว

การตรวจสอบประสิทธิภาพของวิธี (validation) โดยการสุ่มตัวอย่างดีเอ็นเอ (blind test) ที่จำนวนตัวอย่างเป็น 29 (N=29) แสดงเบื้องต้นว่าการตรวจด้วยชิปเมื่อเปรียบเทียบกับวิธี RT-PCR ให้ผลความไวของปฏิกิริยาเป็น 100% และความจำเพาะเป็น 92.3% (ตารางที่ 1) อย่างไรก็ดีผลการตรวจยังคงพบ false positive 1 ตัวอย่าง ซึ่งอาจสื่อให้เห็นถึงคุณภาพในการประกอบชิปที่ใช้มือประกอบที่ยังต้องปรับปรุง

ตารางที่ 1 การประเมินประสิทธิภาพของการตรวจด้วยชิปเมื่อเปรียบเทียบกับวิธี RT-PCR

Specimens	RT-PCR	RT-LAMP with AgNPls Chip
positive	16	16
negative	13	12
False positive	0	1
False negative	0	0
Sensitivity[a]		100
Specificity[b]		92.3

a = true positive/(true positive + false negative)

b = true negative/(true positive + false negative)

ผลการดำเนินการข้างต้นชี้ให้เห็นถึงศักยภาพของการนำ β-pyrrolidinyl peptide nucleic acid ไปประยุกต์ใช้ร่วมกับสารละลายเงินนาโนเพลทสีฟ้าเพื่อเอื้ออำนวยให้การตรวจดีเอ็นเอมีความสะดวกมากยิ่งขึ้น เข้าไกล้อุดมคติของการตรวจในรูปแบบ point of care มากขึ้นอีกด้วย

เอกสารอ้างอิง

Kanjanawarut, R. and Su, X. 2009. Colorimetric detection of DNA using unmodified metallic nanoparticles and peptide nucleic acid probes. Anal. Chem. 81:6122-6129.

Pakdeenard, S., Thammacharoen, C., and Ekgasith, S. 2010. PACCON, 21-23, January 2010, Sunee Grand Hotel Convention Center, Ubon Ratchathani. pp. 362.

รายงานความก้าวหน้าของโครงการในรอบ 3 ปี

โครงการ การสังเคราะห์ สมบัติ และการประยุกต์ใช้เบต้าพิโรลิดินิลเพปไทด์นิวคลีอิกแอซิดที่มีคอนฟอร์เมชันถูกจำกัด

โครงการ 6: Applications of PNA based diagnostics in medical, food and agricultural sciences

ชื่อหัวหน้าโครงการวิจัยย่อย

รศ.พญ.ดร.ณัฏฐิยา หิรัญกาญจน์ จุฬาลงกรณ์มหาวิทยาลัย

ชื่อนักวิจัย

น.ส.ศิตา วีรกุล จุฬาลงกรณ์มหาวิทยาลัย

วัตถุประสงค์ของโครงการ

เนื่องจากมีการรายงานความสัมพันธ์ระหว่างยีนเอชแอลเอบี 1502 กับการแพ้ยาคาร์บามาซินพีน ยีนเอชแอลเอบี 5701 กับยาอะบาคาเวีย และเอชแอลเอบี 5801 กับยาอัลโลพูรินอลอย่างรุนแรง ซึ่งพบอัตราการเสียชีวิตสูงถึงประมาณ 30% จึงมีความสำคัญในการตรวจหาชนิดของเอชแอลเอให้ได้อย่างรวดเร็ว และแม่นยำก่อนการจ่ายยา เพื่อไม่ให้คนไข้ได้รับผลข้างเคียงจากยา จึงนำมาสู่การวิเคราะห์ลำดับเบสของยีนเอชแอลเอบีซึ่งมีความหลากหลายมากเพื่อหาบริเวณที่จำเพาะต่อยีนเอชแอลเอบี 1502 เอชแอลเอบี 5701 และ 5801 และใช้เป็นบริเวณในการสร้างไพร์เมอร์ โดยการเพิ่มจำนวนยีนเอชแอลเอสามารถทำได้ด้วยวิธีเอสเอสพีพีซีอาร์ (SSP-PCR: sequence-specific primer PCR) ที่เป็นวิธีมาตรฐานในการหาชนิดของเอชแอลเอ โดยได้เคยมีการรายงานไพร์เมอร์ของเอชแอลเอบี 1502 ซึ่งจะต้องอาศัยไพร์เมอร์อย่างน้อย 6 คู่ ส่วนเอชแอลเอบี 5801 นั้นจะต้องอาศัยไพร์เมอร์อย่างน้อย 2 คู่ ในการวิจัยครั้งนี้จะทำการพัฒนาวิธีเอสเอสพีพีซีอาร์ให้มีการใช้ไพร์เมอร์ลดลงเพื่อลดจำนวนปฏิกิริยาและค่าใช้จ่ายลง

เนื่องจากวิธีพีซีอาร์เป็นวิธีที่ใช้เวลานานและมีค่าใช้จ่ายสูง จึงได้พัฒนาวิธีทางเลือกคือ แลมพ์ (LAMP: Loop-mediated isothermal amplification) ซึ่งเป็นการเพิ่มจำนวนดีเอนเอด้วยอุณหภูมิเดียวที่ใช้เวลาวิเคราะห์ที่สั้นกว่าและมีค่าใช้จ่ายที่ถูกกว่า เนื่องจากไม่ต้องอาศัยเครื่องพีซีอาร์ที่มีราคาแพง อย่างไรก็ตามวิธีแลมพ์นั้นเป็นวิธีที่เพิ่มจำนวนดีเอนเอได้ไม่จำเพาะเท่าวิธีเอสเอสพีพีซีอาร์ จึงต้องอาศัยการใช้พีเอนเอร่วมกับการตรวจผลของแลมพ์เพื่อเพิ่มความจำเพาะด้วย เนื่องจากพีเอนเอมีความสามารถในการจับดีเอนเออย่างแน่นและมีความจำเพาะสูง

การนำพีเอนเอมาใช้ร่วมกับพีซีอาร์และแลมพ์นั้นสามารถทำได้หลายวิธีตามการติดฉลากสาร เช่น การติดสารเรืองแสง จะอาศัยหลักการการแทนที่สายดีเอนเอสายสั้นที่ติดสารดูดกลืนแสง (Quencher) ด้วยดีเอนเอที่เป็นผลจากการเพิ่มจำนวน (Strand displacement probe) ดังนั้นเมื่อสายพีเอนเอไปจับกับดีเอนเอที่ถูกเพิ่มจำนวน จะเห็นการเรืองแสงภายใต้แสงยูวี อีกวิธีคือการติดไบโอติน เป็นสารที่ถูกกว่าสารเรืองแสง และสามารถดูผลได้ง่ายโดยไม่ต้องอาศัยรังสียูวี โดยเทคนิคที่ใช้ตรวจสอบปฏิกิริยา ได้แก่การทำ dot blot ด้วย Strepavidine ที่ติดฉลากด้วยเอ็นไซม์แล้วดูการเปลี่ยนสีแทน

อย่างไรก็ตามการใช้พีเอนเอในการจับแลมพ์เพื่อแปลผลด้วยการใช้เป็น strand displacement probe และใช้พีเอนเอจับพีซีอาร์เพื่อแปลผลด้วยวิธี dot blot ยังคงไม่ประสบความสำเร็จเนื่องจากไม่พบสัญาณหรือมีความไวต่ำมาก จึงมีความสำคัญที่จะต้องศึกษาพฤติกรรมของพีเอนเอในการเข้าจับดีเอนเอสายคู่เพื่อหาคำอธิบายถึงสาเหตุที่เกิดขึ้น โดยการศึกษานี้จะใช้วิธี gel electrophoresis เพื่อดูประสิทธิภาพและความจำเพาะของพีเอนเอในการเข้าจับดีเอนเอสายคู่ โดยจะอาศัยคุณสมบัติของพีเอนเอที่ไม่มีประจุซึ่งจะไม่เดินทางในเจลเมื่อให้กระแสไฟฟ้าและคงอยู่บริเวณต้นทาง ดังนั้นเมื่อให้กระแสไฟฟ้า พีเอนเอที่เข้าจับกับดีเอนเอได้จะสามารถเดินทางผ่านเจลไปได้ ในทางกลับกันหากพีเอนเอไม่สามารถเข้าจับดีเอนเอสายคู่ได้ก็จะยังคงอยู่ในบริเวณต้นทาง เมื่อทำการศึกษาดังกล่าวแล้วพบว่าพีเอนเอสามารถเข้าจับดีเอนเอสายคู่ที่เป็นผลจากการทำพีซีอาร์ได้ แต่เนื่องจากพีเอนเอมีขนาดเล็กมากเมื่อเปรียบเทียบกับดีเอนเอสายคู่ จึงได้ตั้งสมมติฐานไว้ว่าพีเอนเอจะถูกผลักออกจากการเข้าคู่ของดีเอนเอสายคู่ เนื่องจากดีเอนเอสายคู่สามารถจับกันเองได้เสถียรกว่าดีเอนเอกับพีเอนเอ ดังนั้นจึงได้พัฒนาการทำพีซีอาร์แบบไม่สมมาตร (Asymmetric PCR) เพื่อให้เกิดผลผลิตจากพีซีอาร์เป็นดีเอนเอสายหนึ่งมากกว่าอีกสายหนึ่ง ซึ่งทำได้โดยการใส่ไพร์เมอร์ฝั่งที่ต้องการใช้สร้างเป็นดีเอนเอสายคู่สมกับพีเอนเอมากกว่าไพร์เมอร์อีกฝั่งหนึ่ง เพื่อให้เกิดสายดีเอนเอสายเดี่ยว (Single-stranded DNA) สำหรับพีเอนเอให้เข้าจับได้อย่างเสถียร

นอกจากการนำพีเอนเอมาใช้เพื่อแปลผลชนิดของดีเอนเอแล้ว ยังมีอีกวิธีหนึ่งที่อาศัยความจำเพาะของพีเอนเอเพื่อเพิ่มความจำเพาะให้กับพีซีอาร์ วิธีนี้เรียกว่า พีซีอาร์แคลมพ์ (PCR clamp) หลักการในการเกิดพีซีอาร์แคลมพ์คือ ในการทำพีซีอาร์ตามปกตินั้น หลังจากขั้นตอนการแยกดีเอนเอต้นฉบับสายคู่ที่ 95 องศาเซลเซียส (Denaturing step) จะเพิ่มขั้นตอนให้สายพีเอนเอเข้าจับอย่างจำเพาะ (PNA annealing step) แล้วจึงจะตามมาด้วยขั้นตอนการเข้าจับของไพร์เมอร์อย่างจำเพาะ (Primer annealing step) ดังนั้นเมื่อถึงขึ้นตอนการต่อสายไพร์เมอร์ (Extension step) สายดีเอนเอที่ถูกพีเอนเอจับได้ จะไม่สามารถถูกเพิ่มจำนวนได้ จึงจะไม่มีผลผลิตจากพีซีอาร์เกิดขึ้น วิธีดังกล่าวจะสามารถช่วยให้สามารถทำพีซีอาร์สำหรับเอชแอลเอได้อย่างจำเพาะมากยิ่งขึ้นโดยไม่ต้องอาศัยการใช้ไพร์เมอร์จำนวนมากหรือการทำพีซีอาร์หลายๆ ปฏิกิริยาเพื่อให้สามารถแปลผลได้อย่างถูกต้อง

รายงานในช่วงตั้งแต่วันที่ 1 เดือน สิงหาคม พ.ศ. 2552 ถึงวันที่ 31 เดือน กรกฎาคม พ.ศ. 2555

การดำเนินงาน

ได้ดำเนินงานตามแผนที่วางไว้

รายละเอียดผลการดำเนินงานของโครงการ

- *กิจกรรมที่วางแผนไว้*

แผนการดำเนินงานตลอดโครงการในแต่ละช่วง 6 เดือน

กิจกรรมการดำเนินงาน	เดือน					
ช่วงที่ 1	1-6	7-12	13-18	19-24	25-30	31-36
1. เลือกบริเวณที่เหมาะสมเพื่อใช้สร้างไพร์เมอร์ในการหายีนเอช แอลเอบี 1502 และ 5801 โดยอาศัยลำดับเบสจากฐานข้อมูล						
2. รวบรวมเลือดของผู้บริจาคโลหิตจากสภากาชาดไทยเพื่อทำการสกัดดีเอนเอ						
3. สร้างไพร์เมอร์ในการหายีนเอช แอลเอบี 5801 สำหรับวิธีแลมพ์						
4. สร้างพีเอนเอเพื่อใช้ในการตรวจผลแลมพ์						
5. ทดสอบพีเอนเอกับดีเอนเอคู่สมที่สังเคราะห์ขึ้น						
6. หาสภาวะที่เหมาะสมในการใช้พีเอนเอกับพีซีอาร์และแลมพ์						
7. หาสภาวะที่เหมาะสมกับการทำพีซีอาร์แบบไม่สมมาตรและทดสอบการจับกับพีเอนเอ						

8. หาสภาวะที่เหมาะสมกับการทำพีซีอาร์แคลมพ์						

- *กิจกรรมที่ทำได้จริง*

1. ได้ส่งวิทยานิพนธ์ฉบับสมบูรณ์ของ น.ส.ศิตา วีรกุล ในชื่อเรื่อง **การพัฒนาวิธีการตรวจหาเอชแอลเอบี 1502 และ 5801 ด้วยวิธีเอสเอสพีพีซีอาร์ และแลมพ์โดยใช้พีเอนเอ** ในภาคการศึกษาตอนปลาย ปีการศึกษา 2552

2. ได้นำเสนอผลงานเป็นรายงานฉบับสมบูรณ์ในหัวข้อ **วิธีการตรวจหาเอชแอลเอบี 5801 ด้วยวิธีพีซีอาร์เอสเอสพี** ในงานประชุมวิชาการเสนอผลงานวิจัย ระดับบัณฑิตศึกษา ครั้งที่ 11 มหาวิทยาลัยขอนแก่น เมื่อวันที่ 12 กุมภาพันธ์ 2553

3. ได้รับรางวัล Travel Grant ให้นำเสนอผลงานในหัวข้อ **A Simple Nested Sequence Specific Primer-Polymerase Chain Reaction for HLA-B*1502** ในงาน The 14th International Congress of Immunology ณ เมืองโกเบ ประเทศญี่ปุ่น ระหว่างวันที่ 22 – 27 สิงหาคม 2553

4. ได้รับการตอบรับตีพิมพ์บทความเรื่อง **A Nested Sequence Specific Primer-Polymerase Chain Reaction for the detection of HLA-B*15:02** เมื่อวันที่ 4 มกราคม 2555 ในวรสาร **Tissue Antigens**

5. หาสภาวะของพีเอนเอที่เหมาะสมในการดูผลด้วย gel electrophoresis โดยใช้ดีเอนเอสายเดี่ยวที่เข้าคู่กันและจำนวนเบสเท่ากันในการทดลอง (Single-stranded synthetic DNA)

6. ศึกษาการเข้าจับของพีเอนเอกับดีเอนเอสายคู่ที่เกิดจากการทำพีซีอาร์ยีนอินเตอเฟียรอนแกมมา (IFN-g) และหาสภาวะที่เหมาะสมให้เกิดการเข้าจับระหว่างพีเอนเอและดีเอนเอ และดูผลด้วย gel electrophoresis

7. ได้นำเสนอผลงานในหัวข้อ **Loop-mediated isothermal amplification as a screening test for HLA-B*57:01 and 58:01 in drug hypersensitivity prediction** ในงาน The Joint 16th International HLA and Immunogenetics Conference / 26th European Immunogenetics

and Histocompatibility Conference / 23rd British Society of Histocompatibilty and Immunogenetics Conference ณ เมืองลิเวอร์พู ประเทศอังกฤษ ระหว่างวันที่ 31 พฤษภาคม ถึง 3 มิถุนายน 2555

8. หาสภาวะที่เหมาะสมสำหรับการทำพีซีอาร์แบบไม่สมมาตร (Asymmetric PCR) และทดสอบการจับกับพีเอนเอด้วย gel electrophoresis ในยีนอินเตอร์เฟียรอนแอลฟา และเอชแอลเอบี 1502

9. หาสภาวะที่เหมาะสมสำหรับการทำพีซีอาร์แคลมพ์ (PCR clamp) ในยีนอินเตอร์เฟียรอนแอลฟา และเอชแอลเอบี 1502

วิธีการทดลอง

<u>การทำเอสเอสพีพีซีอาร์กับดีเอนเอจากอาสาสมัคร</u>

1. ทำการรวบรวมเลือดจากอาสาสมัครที่เป็นผู้บริจาคเลือดจากสภากาชาดไทยประมาณ 3 ml.

2. ทำการสกัดดีเอนเอด้วยวิธีการตกตะกอนด้วยเกลือ

3. ทำการหาชนิดของเอชแอลเอบีด้วยวิธีเอสเอสพีพีซีอาร์ต่อยีนเอชแอลเอบี 1502 และ 5801

4. คำนวณหาค่าความไวและความจำเพาะของวิธีเอสเอสพีพีซีอาร์ต่อยีนเอชแอลเอบี 1502 และ 5801 โดยเทียบผลที่ได้จากวิธีมาตรฐานกับวิธีที่ได้พัฒนาขึ้นใหม่ทั้งเมื่อทำการเพิ่มจำนวนจากดีเอนเอและเลือดโดยตรง

<u>การหาไพร์เมอร์สำหรับเอชแอลเอบี 5801</u>

1. นำข้อมูลลำดับเบสของเอชแอลเอบี 5801 จากฐานข้อมูลเอชแอลเอ (http://www.ebi.ac.uk/imgt/hla) มาหาบริเวณที่จำเพาะเพื่อสร้างไพร์เมอร์สำหรับการทำแลมพ์ด้วยโปรแกม Primer Explorer 4 (http://primerexplorer.jp/e/)

2. หาสภาวะที่เหมาะสมของไพรเมอร์ต่อเอชแอลเอบี 5801 ในการทำแลมพ์โดยหาอุณหภูมิและปริมาณ $MgSO_4$ ที่เหมาะสม

3. ทำการทดสอบความจำเพาะในเอชแอลเอบีหลายๆชนิด

<u>การหาบริเวณที่จำเพาะต่อการสร้างพีเอนเอ 2 เส้น</u>

1. การแยกเอชแอลเอบี 1502 จากเอชแอลเอบี 1513 (HLA-B*1502 probe)

ทำการเทียบลำดับเบส (Alignment) ของเอชแอลเอบี 1502 และ 1513 ในช่วงไพร์เมอร์ของปฏิกิริยาพีซีอาร์แล้วหาบริเวณที่จำเพาะต่อเอชแอลเอบี 1502 เพื่อใช้ในการสร้างพีเอนเอ

2. การทดสอบการเกิดปฏิกิริยาพีซีอาร์ (Internal control probe)

เนื่องยีนอินเตอร์เฟียรอนแอลฟา (IFN-a) ที่ใช้เป็นตัวควบคุมการเกิดปฏิกิริยาพีซีอาร์เป็นยีนที่มีความหลายหลายทางพันธุกรรม จึงจะเลือกบริเวณที่ไม่มีความหลากหลายทางพันธุกรรมในการสร้างพีเอนเอ เพื่อให้พีเอนเอดังกล่าวสามารถจับผลจากการเกิดพีซีอาร์ได้ในทุกคน

<u>การหาสภาวะที่เหมาะสมในการใช้พีเอนตรวจผลจากพีซีอาร์ด้วยวิธี Dot blot</u>

1. การหา Membrane ที่ใช้ทำ Dot blot
2. การหา Denaturing solution เพื่อแยกสายคู่ของพีซีอาร์
3. การหา Blocking solution เพื่อลดปฏิกิริยาที่ไม่จำเพาะที่รบกวนการแปลผล (Background)

<u>การเตรียมพีซีอาร์และแลมพ์สำหรับการจับพีเอนเอด้วยวิธีต่างๆ</u>

1. เตรียมพีซีอาร์ของระบบเอชแอลเอบี 1502 แยกหลอดการเกิดพีซีอาร์ระหว่างยีนเอชแอลเอ และยีนอินเตอร์เฟียรอนแอลฟา โดยเริ่มทดสอบพีเอนเอต่อยีนอินเตอร์เฟียรอนแอลฟาที่ทำให้บริสุทธิ์โดยการผ่านคอลัมน์ เพื่อลดการรบกวนการจับของพีเอนเอกับผลจากพีซีอาร์ด้วยวิธี Dot blot บน membrane ที่มีประจุบวกที่พัฒนาขึ้น
2. เตรียมพีซีอาร์และแลมพ์ของเอชแอลเอบี 5801 โดยเริ่มทดสอบพีเอนเอต่อพีซีอาร์และทำให้บริสุทธิ์โดยการผ่านคอลัมน์ เนื่องจากผลของพีซีอาร์มีความซับซ้อนของดีเอนเอน้อยกว่าแลมพ์ และการทำให้บริสุทธิ์จะช่วยลดการรบกวนการจับของพีเอนเอ จากนั้นนึงนำไปทดสอบด้วยวิธี Capacitive biosensor

การหาปริมาณความเข้มข้นพีเอนเอที่เหมาะสมในการดูผลจาก gel electrophoresis

ใช้พีเอนเอความเข้นข้น 100, 50, 20, 10 และ 1 pmol กับดีเอนเอสายเดี่ยวความเข้มข้น 100 pmol เพื่อหาความเข้นข้นพีเอนเอที่เหมาะสมในการดูผลบน 2% agarose gel เมื่อให้กระแสไฟฟ้า 100 V เวลา 30 นาทีแล้วจึงดูผลด้วย UV จากนั้นจะย้อมเจลด้วย ethidium bromide เพื่อดูดีเอนเอคงเหลือ จากนั้นจึงใช้ค่าความเข้มข้นพีเอนเอที่เหมาะสมไปทดสอบกับพีซีอาร์ในสภาวะต่างๆต่อไป

การหาสภาวะที่เหมาะสมในการเกิดการเข้าคู่ของพีเอนเอกับพีซีอาร์

1. การใช้พีซีอาร์ที่ผ่านการทำให้บริสุทธิ์กับพีซีอาร์ที่อยู่ในบัฟเฟอร์

   เปรียบเทียบการเข้าจับของพีเอนเอเมื่อใช้พีซีอาร์ที่ผ่านและไม่ผ่านการทำให้บริสุทธิ์ก่อนด้วยวิธี column-based purification

2. อุณหภูมิและเวลาที่ใช้ในการแยกดีเอนเอสายคู่

   เปรียบเทียบการเข้าจับของพีเอนเอเมื่อให้ความร้อน 95°C, 99°C และไม่ให้ความร้อนก่อนและหลังใส่พีเอนเอ

3. ระยะเวลาในการเกิดปฏิกิริยา

   เมื่อทำการแยกดีเอนเอสายคู่แล้วรอให้เย็นแล้วจึงใส่พีเอนเอและทิ้งไว้เป็นเวลา 1, 10, 35, 60 นาทีก่อนทำ gel electrophoresis

4. การใช้พีเอนเอ 2 สายที่ไม่เข้าคู่กัน (pseudocomplementary PNA)

   เนื่องจากพีเอนเอที่ใช้ในการทดลองมีคุณสมบัติพิเศษคือ ไม่จับกันเองแม้มีลำดับเบสที่เข้าคู่กัน จึงสามารถนำมาใช้ช่วยในการแยกดีเอนเอหลังจากการใช้ความร้อนแยกดีเอนเอสายคู่

การหาสภาวะที่เหมาะสมสำหรับการทำพีซีอาร์แบบไม่สมมาตร (Asymmetric PCR)

ทำการหาอัตราส่วนของไพร์เมอร์ที่เหมาะสมเพื่อให้เกิดดีเอนเอสายเดี่ยวฝั่งที่ต้องการมากกว่าอีกสายหนึ่งแล้วทำการดูผลจากพีซีอาร์ด้วย Gel electrophoresis ว่ามีผลผลิตเพียงพอต่อการดูผลด้วยพีเอนเอที่ติดสารเรืองแสงไว้ด้วย Gel electrophoresis เช่นกัน โดยเริ่มทำในยีนอินเตอร์เฟียรอนแอลฟา (IFN-a)

ก่อนทำกับยีนเอชแอลเอบี 1502 เพื่อลดการทำปฏิกิริยาจาก Nested SSP-PCR

การหาความจำเพาะของพีเอนเอเมื่อนำไปทดสอบกับพีซีอาร์แบบไม่สมมาตร (Asymmetric PCR)

ในการทำพีซีอาร์เพียงปฏิกิริยาเดียวในยีนเอชแอลเอบี 1502 เพื่อให้มีผลผลิตจากพีซีอาร์มากพอต่อการทดสอบการจับด้วยพีเอนเอ จะมีเอชแอลเอบี 1301 1513 1525 และ 4402 ขึ้นเป็นผลบวกปลอม ดังนั้นเพื่อจำทดสอบความจำเพาะของพีเอนเอเพื่อใช้ในช่วยในการแปลผล พีเอนเอจะต้องจับเพียงเอชแอลเอบี 1502 และ 1525 ซึ่งมีลำดับเบสตรงกับพีเอนเอเท่านั้น

การหาสภาวะที่เหมาะสมสำหรับการทำพีซีอาร์แคลมพ์ (PCR clamp)

ทำการหาปริมาณและอุณหภูมิที่เหมาะสมที่พีเอนเอสามารถขัดขวางการเกิดปฏิกิริยาพีซีอาร์ได้ โดยจะเริ่มต้นจากการใช้สภาวะพีซีอาร์ที่สามารถเพิ่มจำนวนได้อย่างสมบูรณ์แล้วเปรียบเทียบเมื่อใส่พีเอนเอเข้าไปในปฏิกิริยา

ผลการทดลอง

การทำเอสเอสพีพีซีอาร์กับดีเอนเอและเลือดจากอาสาสมัคร

ทำการรวบรวมดีเอนเอสำหรับการตรวจหาเอชแอลเอบี 1502 ได้ทั้งหมด 200 ราย พบว่าวิธีเอสเอสพีพีซีอาร์ที่พัฒนาขึ้นใหม่สามารถให้ค่าความไวและความจำเพาะเท่าเทียมกับวิธีมาตรฐาน 100% ทั้งเมื่อทำพีซีอาร์จากดีเอนเอที่ได้สกัดแล้วและจากการเพิ่มจำนวนโดยตรงจากเลือด

		Commercial SSP-PCR		
		Positive	Negative	
In-house SSP-PCR HLA-B*1502	Positive	24	0	PPV = 24/24 = 100.0%
	Negative	0	80	NPV = 80/80 = 100.0%
		Sensitivity = 24/24 = 100.0%	Specificity = 80/80 = 100.0%	

สำหรับการตรวจหาเอชแอลเอบี 5801 ได้ทั้งหมด 95 ราย พบว่าวิธีเอสเอสพีพีซีอาร์ที่พัฒนาขึ้นใหม่สามารถให้ค่าความไวและความจำเพาะเท่าเทียมกับวิธีมาตรฐาน 100% เมื่อทำพีซีอาร์กับดีเอนเอที่สกัดแล้ว แต่หากทำพีซีอาร์จากเลือดโดยตรงจะพบว่า เอชแอลเอบี 5701 นั้นจะเป็นผลบวกปลอมด้วย

		Commercial SSP-PCR		
		Positive	Negative	
In-house SSP-PCR HLA-B*5801	Positive	13	0	PPV = 13/13 = 100.0%
	Negative	0	82	NPV = 82/82 = 100.0%
		Sensitivity = 13/13 = 100.0%	Specificity = 82/82 = 100.0%	

<u>การทำแลมพ์กับดีเอนเอจากอาสาสมัคร</u>

เอชแอลเอบี 5710 และ 5801 สามารถถูกเพิ่มจำนวนได้ด้วยไพร์เมอร์จากวิธีแลมพ์ ทำให้สามารถใช้วิธีแลมพ์นี้ทำนายการแพ้ยาได้สองชนิดคือ เอชแอลเอบี 5701 กับยาต้านไวรัสเอชไอวี (อะบาคาเวีย) และเอชแอลเอบี 5801 กับยารักษาโรคเกาต์ (อัลโลพูรินอล) โดยจากผลการทดลองจะเห็นว่า จะมีเพียงเอชแอลเอบี 1517 เป็นผลบวกปลอมเพียงชนิดเดียว ทั้งนี้เนื่องจากเป็นยีนที่มีความถี่ที่ต่ำมากในประชากรไทย (0.7%) จึงไม่เป็นปัญหาในการทำนายการแพ้ยา

เมื่อทำการเพิ่มจำนวนทดสอบกับดีเอนเอจากอาสาสมัครทั้งหมด 99 ราย พบว่ามีความไว 100 % และความจำเพาะ 98.99 % โดยมี 4 รายเป็น HLA-B*57:01 12 รายเป็น 58:01 และอีก 82 รายเป็นเอชแอลเอชนิดอื่นๆ โดยจะมี 1 รายเป็นผลบวกปลอม

		Commercial SSP-PCR		
		Positive	Negative	
In-house LAMP HLA-B*5701 and 5801	Positive	16	1	PPV = 16/17 = 94.12%
	Negative	0	82	NPV = 82/82 = 100.0%
		Sensitivity = 16/16 = 100.0%	Specificity = 82/83 = 98.8%	

<u>การหาบริเวณที่จำเพาะต่อการสร้างพีเอนเอ 2 เส้น</u>

พบว่าได้บริเวณที่จำเพาะในการสร้างพีเอนเอต่อทั้งยีนเอชแอลเอบี 1502 และอินเตอร์เฟียรอนแอลฟา และเมื่อนำไปทดสอบกับดีเอนเอคู่สมที่สังเคราะห์ขึ้น พบว่าสามารถจับกับดีเอนเอคู่สมได้อย่างจำเพาะด้วยวิธี Dot blot จึงนำไปทดสอบกับผลจากพีซีอาร์ต่อไป

การหาสภาวะที่เหมาะสมในการใช้พีเอนตรวจผลจากพีซีอาร์ด้วยวิธี Dot blot

1. การหา Membrane ที่ใช้ทำ Dot blot

เมื่อเปรียบเทียบชนิดของ Membrane ที่มีการใช้แพร่หลาย พบว่าพีเอนเอจะจับกับ Nylon membrane จะทำให้เห็นเป็นผลบวกปลอม จึงเลือกทดสอบระหว่าง membrane ที่มีประจุบวกที่ที่พัฒนาขึ้น Nitrocellulose membrane และ PVDF membrane พบว่าทั้งดีเอนเอและพีเอนเอไม่สามารถซึมลงบน PVDF membrane ได้ ส่วน Nitrocellulose membrane จะเห็นผลบวกรบกวน (Background) มากกว่า membrane ที่มีประจุบวกที่พัฒนาขึ้น จึงเลือกใช้ membrane นี้ในการใช้จริง

2. การหา Denaturing solution เพื่อแยกสายคู่ของพีซีอาร์

พบว่าเมื่อใช้บัฟเฟอร์ที่มี NaOH และ EDTA จะให้ผลดีในดีเอนเอสายเดี่ยวที่สังเคราะห์ขึ้น และเป็นสารเคมีที่ไม่รบกวนการจับของพีเอนเอและดีเอนเอ แต่เมื่อทดสอบกับผลของพีซีอาร์พบว่า ไม่สามารถเห็นผลได้ จึงต้องใช้การให้ความร้อน 95°C เป็นเวลา 10 นาที ร่วมกับการใช้บัฟเฟอร์ด้วย เพื่อช่วยการเข้าจับของพีเอนเอแบบ Duplex invasion

3. การหา Blocking solution เพื่อลดปฏิกิริยาที่ไม่จำเพาะที่รบกวนการแปลผล (Background)

เมื่อเปรียบเทียบการใช้ BSA และ Skim milk พบว่า Skim milk สามารถใช้ได้ดีเท่าเทียมกับ BSA จึงเลือกใช้ Skim milk ซึ่งมีราคาถูกกว่า

การทดสอบพีเอนเอต่อผลของพีซีอาร์จากยีนอินเตอร์เฟียรอนแอลฟา

สามารถเห็นสัญญาณจาก Dot blot บน membrane ที่มีประจุบวกที่พัฒนาขึ้นได้เมื่อทำการแยกสายพีซีอาร์ที่เป็นดีเอนเอสายคู่ด้วยการให้ความร้อน 95°C เป็นเวลา 10 นาที ร่วมกับการใช้บัฟเฟอร์เพื่อช่วยการเข้าจับของพีเอนเอแบบ Duplex invasion

การทดสอบพีเอนเอต่อผลของพีซีอาร์จากยีนเอชแอลเอบี 5801

สามารถเห็นสัญญาณจาก Capacitive biosensor ได้เมื่อทำการแยกสายพีซีอาร์ที่เป็นดีเอนเอสายคู่ด้วยการให้ความร้อน 95°C เป็นเวลา 10 นาที ก่อนนำเข้าทดสอบในระบบ อีกทั้งยังเห็นค่าความต่าง

ที่ชัดเจนระหว่างพีเอนเอที่จับกับบเอชแอลเอบี 5801 และ 5701

<u>การหาปริมาณความเข้มข้นพีเอนเอที่เหมาะสมในการดูผลจาก gel electrophoresis</u>

พีเอนเอความเข้มข้น 10 pmol เป็นความเข้มข้นที่ต่ำที่สุดที่สามารถเห็นการเรืองแสงได้ชัดเจนบนเจล และพีเอนเอสามารถเข้าจับกับดีเอนเอสายเดี่ยวได้ 100% เมื่อความเข้มข้นพีเอนเอต่อดีเอนเอเป็น 1:1

<u>การหาสภาวะที่เหมาะสมในการเกิดการเข้าคู่ของพีเอนเอกับพีซีอาร์</u>

1. การใช้พีซีอาร์ที่ผ่านการทำให้บริสุทธิ์กับพีซีอาร์ที่อยู่ในบัฟเฟอร์

   พบว่าพีซีอาร์ที่อยู่ในบัฟเฟอร์พบสัญญาณการเข้าคู่ของพีเอนเอมากกว่าพีซีอาร์ที่ไม่ผ่านการทำให้บริสุทธิ์

2. อุณหภูมิและเวลาที่ใช้ในการแยกดีเอนเอสายคู่

   พบว่าที่อุณหภูมิ 99°C 10 นาที สามารถช่วยแยกดีเอนเอสายคู่ได้ดีกว่าที่ 95°C 10 นาที และเมื่อไม่ใช้ความร้อนช่วยแม้ทิ้งเวลาให้เกิดปฏิกิริยาข้ามขึ้น

3. ระยะเวลาในการเกิดปฏิกิริยา

   พบว่าเมื่อปล่อยเวลาให้ผ่านไป สัญญาณการเข้าคู่ของพีเอนเอกับพีซีอาร์จะลดลงเรื่อยๆ ซึ่งคาดว่าจะเกิดจากการกลับเข้าคู่ของดีเอนเอสายคู่ที่มีความเสถียรมากกว่า ดีเอนเอสายยาวจึงดันพีเอนเอซึ่งเป็นสายสั้นๆออก

4. การใช้พีเอนเอ 2 สายที่ไม่เข้าคู่กัน (pseudocomplementary PNA)

   พบว่าการใช้พีเอนเอ 2 สายจะช่วยให้การจับของพีเอนเอกับดีเอนเอสายคู่มีความเสถียรมากขึ้น เมื่อปล่อยให้เกิดปฏิกิริยา 2 ชั่วโมง แต่ไม่ทำให้พีเอนเอเข้าจับดีเอนเอสายคู่ได้มากขึ้น

<u>การหาสภาวะที่เหมาะสมสำหรับการทำพีซีอาร์แบบไม่สมมาตร (Asymmetric PCR)</u>

เมื่อทำการทดสอบหลักการของพีซีอาร์แบบไม่สมมาตรในยีนอินเตอร์เฟียรอนแอลฟ่าพบว่าพีเอนเอสามารถเข้าจับได้หมดอย่างสมบูรณ์ และจับได้อย่างเสถียรแม้เวลาผ่านไปถึง 2 ชั่วโมง โดยดูได้จากบริเวณเริ่มต้นของเจลว่าไม่มีพีเอนเอเหลืออยู่เมื่อเปรียบเทียบกับพีซีอาร์สภาวะปกติที่ยังพบการเรืองแสง

ของพีเอนเออยู่และมีอยู่มากที่สุดที่เวลา 2 ชั่วโมง

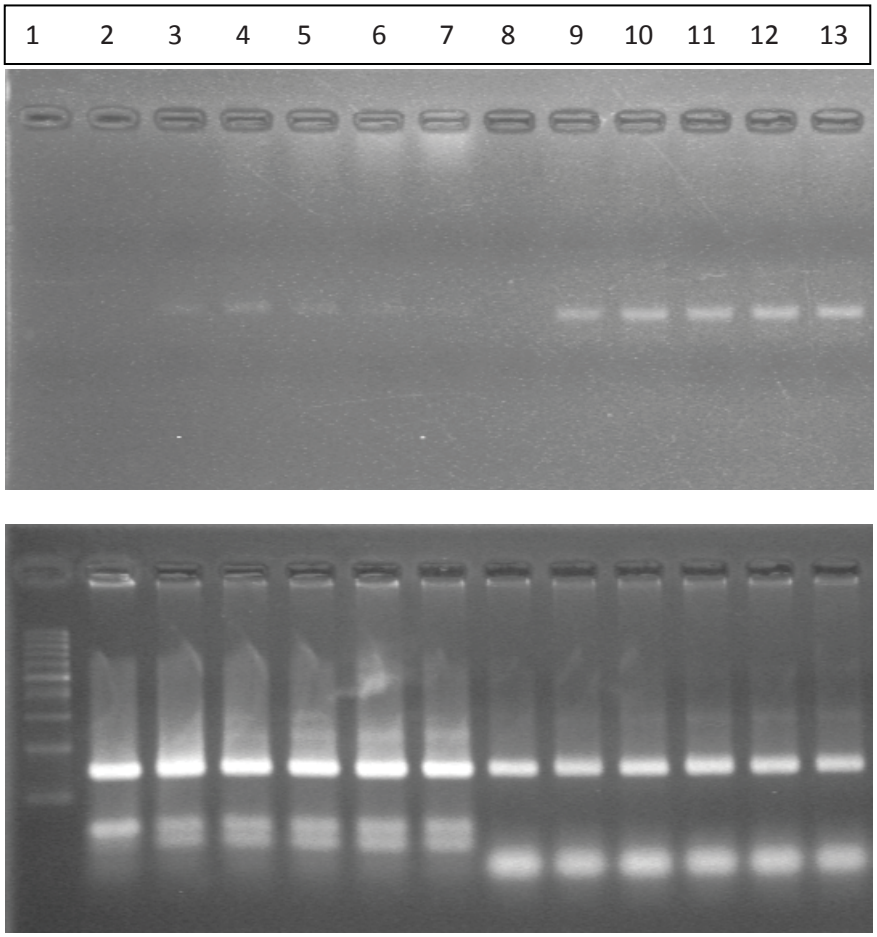

หมายเหตุ หลุมที่ 1 ดีเอนเอที่ใช้เพื่อบอกขนาด (DNA ladder) พีซีอาร์ในสภาวะปกติ หลุมที่ 2 – 7 (ไม่มีพีเอนเอ, ที่เวลา 1 นาที, ที่เวลา 10 นาที, ที่เวลา 30 นาที, ที่เวลา 1 ชั่วโมง และ ที่เวลา 2 ชั่วโมง) และพีซีอาร์แบบไม่สมมาตร หลุมที่ 8 - 13 (ไม่มีพีเอนเอ, ที่เวลา 1 นาที, ที่เวลา 10 นาที, ที่เวลา 30 นาที, ที่เวลา 1 ชั่วโมง และ ที่เวลา 2 ชั่วโมง)

จากนั้นจึงได้ทดสอบการทำพีซีอาร์แบบไม่สมมาตรกับเอชแอลเอบี 1502 พบว่าพีเอนเอไม่สามารถเข้าจับได้อย่างสมบูรณ์เหมือนกับยีนอินเตอร์เฟียรอนแอลฟ่า และไม่เห็นความแตกต่างระหว่างพีซีอาร์ในสภาะปกติและในสภาะที่ไม่สมมาตร ทั้งนี้ได้ตั้งสมมติฐานไว้ว่าเอชแอลเอมีผลผลิตจากพีซีอาร์ที่ขนาดใหญ่กว่า ทำให้การแยกดีเอนเอสายคู่อาจทำได้ไม่สมบูรณ์เท่า และอาจจะเป็นเพราะพีเอนเอนี้เองไม่สามารถจับดีเอนเอได้อย่างเสถียร ซึ่งเป็นคุณสมบัติเฉพาะตัวของพีเอนเอแต่ละเส้นที่ความลำดับเบสต่างกันทำให้ไม่สามารถนำสภาวะของการจับของคนละยีนมาปรับใช้ได้ อีกทั้งเมื่อได้เพิ่มปริมาณพีเอนเอจนถึง 100 pmol ก็ยังไม่สามารถหยุดปฏิกิริยาพีซีอาร์ได้ จึงสรุปได้ว่า ริมาณพีเอนเอที่มากขึ้นไม่สามารถช่วยขัดขวางการ

เกิดพีซีอาร์ได้มากขึ้นตามไปด้วย

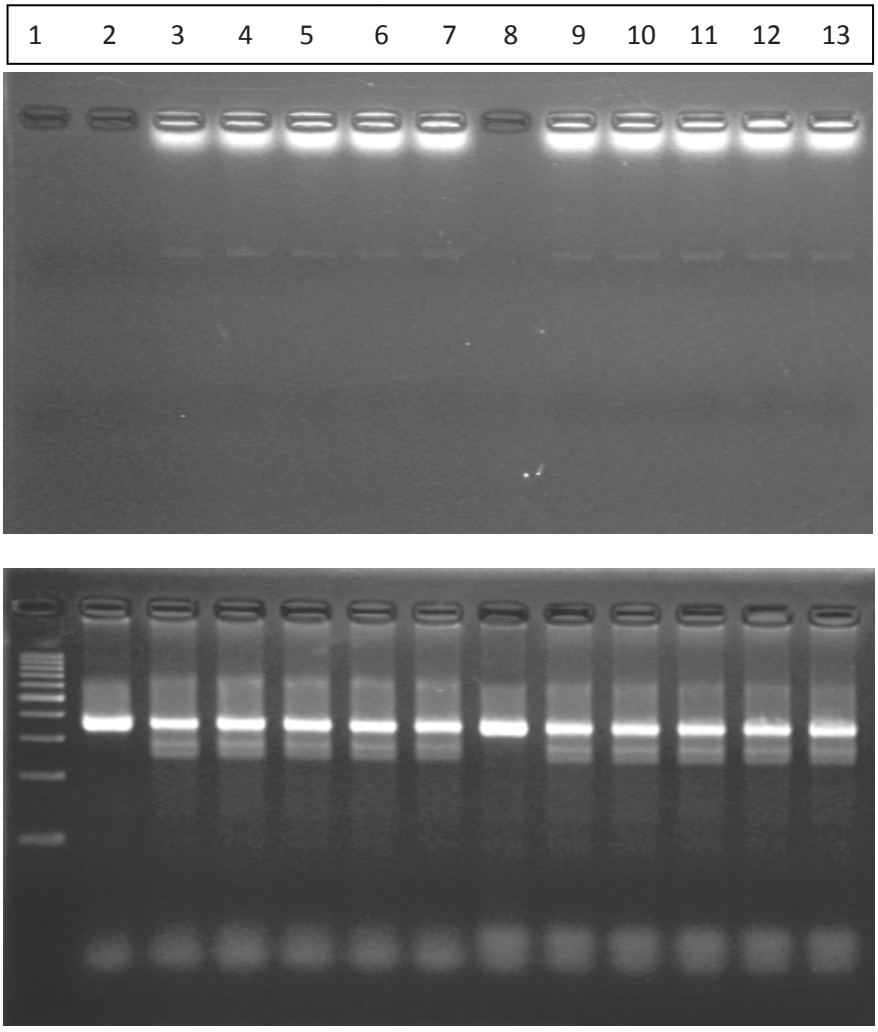

หมายเหตุ หลุมที่ 1 ดีเอนเอที่ใช้เพื่อบอกขนาด (DNA ladder) พีซีอาร์ในสภาวะปกติ หลุมที่ 2 – 7 (ไม่มีพีเอนเอ, ที่เวลา 1 นาที, ที่เวลา 10 นาที, ที่เวลา 30 นาที, ที่เวลา 1 ชั่วโมง และ ที่เวลา 2 ชั่วโมง) และพีซีอาร์แบบไม่สมมาตร หลุมที่ 8 - 13 (ไม่มีพีเอนเอ, ที่เวลา 1 นาที, ที่เวลา 10 นาที, ที่เวลา 30 นาที, ที่เวลา 1 ชั่วโมง และ ที่เวลา 2 ชั่วโมง)

<u>การหาความจำเพาะของพีเอนเอเมื่อนำไปทดสอบกับพีซีอาร์แบบไม่สมมาตร (Asymmetric PCR)</u>

แม้ปฏิกิริยาพีซีอาร์ที่จำเพาะต่อเอชแอลเอบี 1502 จะไม่สามารถเพิ่มจำนวนดีเอนเอให้มากพอที่พีเอนเอจะจับและแสดงสัญญาณได้ จึงได้ทำการลดความจำเพาะของปฏิกิริยาเพื่อให้ได้ปริมาณดีเอนเอมากพอเพื่อจะทดสอบความจำเพาะของพีเอนเอ จากการทดสอบพบว่า พีเอนเอสามารถจับดีเอนเอได้อย่างจำเพาะ โดยจะจับเฉพาะเอชแอลเอบี 1502 และ 1525 เท่านั้น

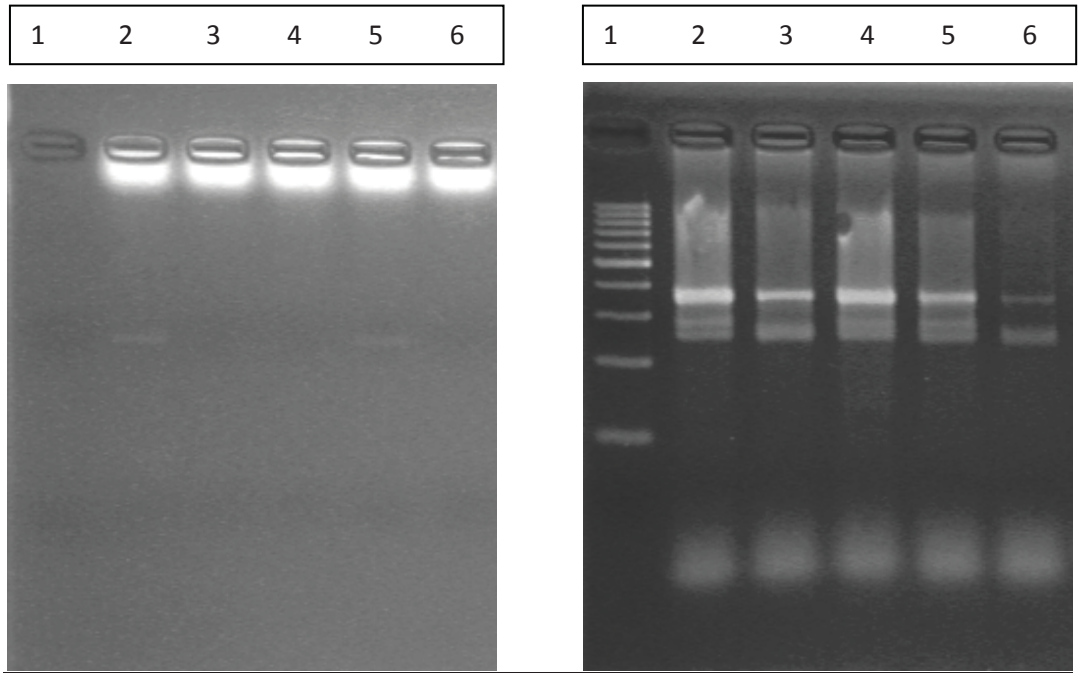

หมายเหตุ หลุมที่ 1 ดีเอนเอที่ใช้เพื่อบอกขนาด (DNA ladder) หลุมที่ 2 เอชแอลเอบี 1502 หลุมที่ 3 เอชแอลเอบี 1301 หลุมที่ 4 เอชแอลเอบี 1513 หลุมที่ 5 เอชแอลเอบี 1525 หลุมที่ 6 เอชแอลเอบี 4402

การหาสภาวะที่เหมาะสมสำหรับการทำพีซีอาร์แคลมพ์ (PCR clamp)

เมื่อทำการทดสอบพีซีอาร์แคลมพ์กับยีนอินเตอร์เฟียรอนแอลฟ่าพบว่าพีเอนเอสามารถขัดขวางการเกิดปฏิกิริยาพีซีอาร์ได้มากในทุกอุณหภูมิ แต่ยังคงเห็นผลผลิตจากพีซีอาร์อยู่ จึงได้ตั้งสมมติฐานไว้ว่าปริมาณของพีเอนเอไม่เพียงพอต่อการขัดขวางปฏิกิริยาพีซีอาร์ ดังนั้นจึงได้ทำการเพิ่มปริมาณพีเอนเอจนถึง 100 pmol ก็ยังไม่สามารถขัดขวางปฏิกิริยาพีซีอาร์ได้อย่างสมบูรณ์ จึงต้องทำการศึกษาต่อไปว่ามีปัจจัยใดที่ส่งผลให้การเกิดพีซีอาร์แคลมพ์เป็นไปได้อย่างสมบูรณ์มากยิ่งขึ้น

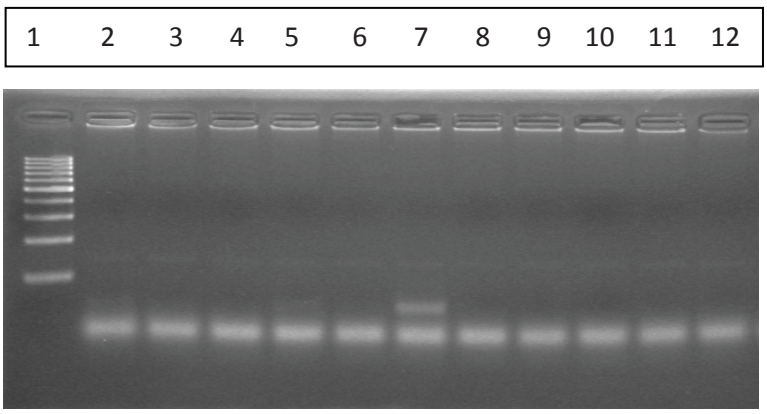

หมายเหตุ หลุมที่ 1 ดีเอนเอที่ใช้เพื่อบอกขนาด (DNA ladder) หลุมที่ 2 – 12 60.0, 60.4, 61.6, 63.4, 65.6, 68.2, 70.9, 73.6, 76.0, 78.1, และ 79.6 องศาเซลเซียส

จากนั้นจึงทำการทดสอบพีซีอาร์แคลมพ์กับเอชแอลเอบี 1502 โดยใช้พีเอนเอสองสายที่มีลำดับเบสคู่สมกันมาเปรียบเทียบความสามารถในการเกิดพีซีอาร์แคลมพ์พบว่า แม้พีเอนเอทั้งสองสายจะจับดีเอนเอบริเวณเดียวกันแต่คนละเส้นดีเอนเอก็ไม่สามารถขัดขวางปฏิกิริยาการเกิดพีซีอาร์ได้เท่ากัน โดยจะเห็นได้ว่าพีเอนเอสายฝั่งตรงข้ามกับดีเอนเอ (รูปบน) สามารถขัดขวางปฏิกิริยาได้ดีกว่าพีเอนเอฝั่งเดียวกับดีเอนเอ จึงสรุปได้ว่าการเกิดพีซีอาร์แคลมพ์ได้มีประสิทธิภาพหรือไม่นั้นขึ้นกับลำดับเบสของพีเอนเอนั้นๆ

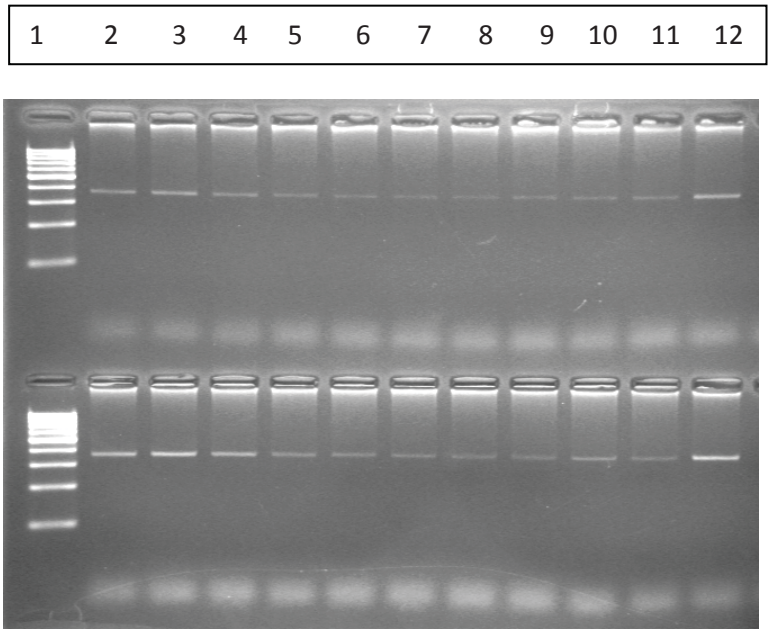

หมายเหตุ รูปบนแสดงการเกิดพีซีอาร์แคมพ์กับพีเอนเอสายฝั่งตรงข้ามกับดีเอนเอ ส่วนรูปล่างแสดงการเกิดพีซีอาร์แคลมพ์กับพีเอนเอสายฝั่งเดียวกับดีเอนเอ โดยหลุมที่ 1 ดีเอนเอที่ใช้เพื่อบอกขนาด (DNA ladder) หลุมที่ 2 – 12 60.0, 60.4, 61.6, 63.4, 65.6, 68.2, 70.9, 73.6, 76.0, 78.1, และ 79.6 องศาเซลเซียส

สรุปผลการดำเนินงานของโครงการ

จากการดำเนินงานเป็นเวลา 3 ปี สามารถพัฒนาวิธีการตรวจหาเอชแอลเออย่างจำเพาะและมีราคาถูกได้ทั้งวิธีพีซีอาร์และแลมพ์เพื่อให้บริการแก่คนไข้ ณ โรงพยาบาลจุฬาลงกรณ์ อีกทั้งการนำพีเอนเอ

มาช่วยเพื่อการแปลผลให้จำเพาะมากขึ้นและหยุดปฏิกิริยาพีซีอาร์ หรือการทำพีซีอาร์แคลมพ์ก็ได้หลักการในการที่จะต่อยอดพัฒนาวิธีดังกล่าวต่อไป

แผนงานของโครงการที่จะศึกษาต่อไปในอนาคต

ในส่วนของการนำพีเอนเอมาช่วยเพื่อการแปลผลให้จำเพาะมากขึ้นนั้นจะยังคงต้องพัฒนาวิธีพีซีอาร์ให้เหลือเพียงเอชแอลเอที่สามารถแยกด้วยพีเอนเอได้ และมีปริมาณพีซีอาร์ที่มากพอที่จะเห็นผลการจับของพีเอนเอได้ อีกทั้งจะยังศึกษาการใช้สารเรืองแสงใหม่ๆมาติดพีเอนเอเพื่อช่วยในการแปลผลพีซีอาร์ได้โดยตรงจากสารละลายโดยไม่ต้องทำ Gel electrophoresis นอกจากนี้การใช้พีเอนเอเพื่อหยุดปฏิกิริยาพีซีอาร์ หรือการทำพีซีอาร์แคลมพ์ก็มีการศึกษาหาปัจจัยที่มีผลต่อการขัดขวาปฏิกิริยาต่อไปเพื่อใช้แปลผลการหาเอชแอลเอโดยไม่ต้องอาศัยสารเรืองแสงที่มีราคาแพง

หัวข้อการวิจัย

พิสูจน์ประสิทธิภาพของชุดตรวจกรอง Hemoglobin E ที่ใช้เทคนิคทางนาโนเทคโนโลยีมาใช้ร่วมกับตัวตรวจจับที่เป็น PNA ในชุดตรวจวินิจฉัยโรค

มูลเหตุจูงใจ

โรคธาลัสซีเมียและฮีโมโกลบินผิดปกตินั้นเป็นโรคทางพันธุกรรมที่ทำให้เกิดภาวะโลหิตจาง สามารถถ่ายทอดสู่ลูกหลานได้ และพบได้บ่อยในประเทศไทย ซึ่งมีผู้ป่วยที่เป็นโรคนี้ประมาณ 6 แสนคน และผู้ที่เป็นพาหะของโรคนี้มากกว่า 20 ล้านคน ในปัจจุบันทารกเกิดใหม่ในทุกๆ 1000 คนจะเป็นโรคนี้ประมาณ 12 คน[1] โดยผู้ที่มียีนผิดปกติของธาลัสซีเมียมีทั้งผู้ที่เป็นโรคและเป็นพาหะซึ่งจะมีอาการโลหิตจาง อาจมีความรุนแรงแตกต่างกันขึ้นกับชนิดของยีนที่ผิดปกติ ผู้ป่วยธาลัสซีเมียที่มีอาการหนักจะมีความทุกข์ทรมานมากจากการมีโลหิตจางเรื้อรัง ความผิดปกติในส่วนต่างๆ ของร่างกาย ความพิการ ความป่วย ความเจ็บ ทั้งสุขภาพกาย สุขภาพใจ ทั้งของตนเองและครอบครัว รวมทั้งเป็นภาระหนักทางการแพทย์ สังคมและมีผลต่อเนื่องกับสภาวะเศรษฐกิจของประเทศ

สาเหตุของโรคนี้เกี่ยวกับความผิดปกติของยีนที่ควบคุมการสร้างฮีโมโกลบินในเม็ดเลือดแดง ฮีโมโกลบินชนิดที่สำคัญคือ Hb A (hemoglobin A) ซึ่งประกอบไปด้วยสายโกลบินชนิดแอลฟา(α-globin chain) 2 สาย อยู่บนโครโมโซมที่ 16 และสายโกลบินชนิดบีต้า (β-globin chain) 2 สาย อยู่บนโครโมโซมที่ 11 การสร้างสายโกลบินดังกล่าวควบคุมโดยยีนโกลบินแอลฟา (α-globin chain) และยีนโกลบินบีต้า (β-globin chain) ยีนธาลัสซีเมียแบ่งตามมิวเตชันของยีนโกลบินที่เป็นชนิดต่างๆได้ดังนี้ 1 ยีนกลุ่ม α-thalassemia ได้แก่ α-thalassemia 1 ,α-thalassemia 2 และ Hb Constant Spring (Hb CS) 2 ยีนกลุ่ม β-thalassemia ได้แก่ β-thalassemia และ Hb E ทำให้มีปริมาณน้อยหรือไม่สร้างเลย เกิดการกลายพันธุ์ (mutation) ของยีนโกลบินที่ควบคุมการสร้างสายโกลบินนั้นๆ ความไม่สมดุลของปริมาณสายโกลบินและเกิดความผิดปกติของเม็ดเลือดแดงและความผิดปกติต่างๆตามมา[2] ซึ่งเป็นปัญหาสาธารณสุขที่พบอุบัติการณ์สูงและมีแนวโน้มจะเพิ่มขึ้น สำหรับประเทศไทยมีคนที่เป็นพาหะของธาลัสซีเมียประมาณ 30-40 %[2] ซึ่งนับได้ว่าเป็นภาวะที่พบบ่อยและควรตระหนักอย่างยิ่ง ดังนั้นการตรวจวินิจฉัยที่มีประสิทธิภาพและถูกต้องแม่นยำจึงเป็นผลดีต่อการป้องกันโรคที่จะถ่ายทอดต่อไปในลูกหลาน

การตรวจวินิจฉัยโรคธาลัสซีเมีย มีการตรวจได้หลายระดับ เริ่มตั้งแต่ระบบการตรวจกรองหาบุคคลที่มีความเสี่ยงต่อการเป็นโรค (Screening Test) ปัจจุบันสามารถตรวจกรองได้ด้วย 3 วิธีหลักคือ

1. MCV (Mean Corpuscular Volume) เป็นการวัดขนาดของเม็ดเลือดแดง
2. OF (Osmotic Fragility) เป็นการตรวจความเปราะของเม็ดเลือดแดง
3. DCIP (Dichrolophenol Indophenol Precipitation) เป็นการตรวจการตกตะกอนของ Hemoglobin ที่ไม่อยู่ตัว คือ Hb E ,Hb Bart's , Hb H

เมื่อตรวจพบบุคคลที่มีความเสี่ยงของโรคนี้ จะทำการตรวจเพิ่มเติมด้วยวิธีการหาชนิดและปริมาณของฮีโมโกลบิน Hemoglobin-typing (Hb-typing) โดยใช้การตรวจวิเคราะห์ด้วยเครื่องมือพิเศษ คือ High Perfermance Liquid Chromatography (HPLC) หรือวิธี Capillary Electrophoresis (CE) รวมทั้งการตรวจดีเอ็นเอเพื่อเป็นการยืนยันการวินิจฉัย (Confirm Test) โดยวิธี Polymerase Chain Reaction (PCR) [3]

ความผิดปกติในกลุ่มบีต้า-ธาลัสซีเมีย ชนิด ฮีโมโกลบิน อี เป็นภาวะที่พบได้บ่อยประมาณร้อยละ 13 ของประชากรไทย โดยในจำนวนนี้พบว่าประชากรในภาคตะวันออกเฉียงเหนือมีความผิดปกติแบบ Hemoglobin E มากที่สุด เช่น ในจังหวัดสุรินทร์ สกลนครพบได้ถึงร้อยละ 50-60 ของประชากร และจากการตรวจหญิงตั้งครรภ์ที่มาฝากครรภ์ที่โรงพยาบาลศิริราชพบพาหะชนิดฮีโมโกลบิน อี ร้อยละ 25 [4]

การตรวจกรอง Hemoglobin E ในปัจจุบันจึงมีเพียงการตรวจ DCIP เป็นส่วนใหญ่ แต่เนื่องจากการตรวจกรอง DCIP ยังมีปัญหาถึงความชัดเจนของผลที่ได้ ซึ่งเป็นปัญหาใหญ่ของผู้ปฏิบัติการ คือต้องใช้ผู้ที่มีประสบการณ์ ความชำนาญในการทำสูงและทำตามขั้นตอนของกระบวนการวิเคราะห์อย่างเคร่งครัด จึงได้ผลที่แม่นยำและมีความถูกต้อง หากเกิดความคลาดเคลื่อนในเรื่องของเวลา และอุณหภูมิที่เปลี่ยนไปเพียงเล็กน้อย อาจส่งผลให้เกิดการแตกของเม็ดเลือดแดงซึ่งส่วนใหญ่ผู้ที่เป็นโรคนี้ก็มีความเปราะของเม็ดเลือดอยู่แล้ว จนในที่สุดทำให้เกิดปัญหาผลบวกปลอม (Fale Positive) ซึ่งมักเป็นปัญหาที่เกิดขึ้นบ่อย ในกรณีที่ผู้ป่วยซีดมากอาจทำให้เกิดผลลบลวงได้ (False Negative) อีกทั้งการทำจะต้องทำควบคู่กับตัวอย่างควบคุมผลบวกและผลลบเสมอ[5] นอกจากขั้นตอนในการตรวจที่ค่อนข้างยุ่งยาก เวลาที่ใช้ในการตรวจประมาณ 20 นาที อีกทั้งค่าใช้จ่ายที่ค่อนข้างสูง ดังนั้นหากมีวิถีการตรวจใหม่ๆที่สามารถเข้ามาแก้ไขปัญหาต่างๆ เหล่านี้ได้ก็จะส่งผลประโยชน์อย่างยิ่งต่อการวินิจฉัย และเพื่อเป็นประโยชน์สูงสุดแก่คนไข้เอง

<u>นาโนเทคโนโลยี</u> <u>(Nanotechnology)</u>

นาโนเทคโนโลยี (Nanotechnology) เป็นเทคโนโลยีประยุกต์ที่เกี่ยวข้องกับกระบวนการจัดการการสร้างวัสดุที่มีขนาดเล็กในระดับนาโนเมตร และการจัดเรียงอะตอม/โมเลกุลในตำแหน่งที่ต้องการได้อย่างถูกต้องแม่นยำ[6] รวมถึงการออกแบบหรือการใช้เครื่องมือสร้างวัสดุที่มีขนาดเล็กมาก ทำให้ได้วัสดุนาโน (ท่อนาโน เส้นใยนาโน และอนุภาคนาโน) ซึ่งเป็นวัสดุที่มีคุณสมบัติพิเศษ ทั้งทางด้านฟิสิกส์ เคมีและชีวภาพ ต่างไปจากสารเดิมที่มีขนาดใหญ่ ดังนั้นในปัจจุบันจึงมีการนำวัสดุนาโนมาประยุกต์ใช้ประโยชน์ในหลายสาขาวงการ เช่น ด้านอุตสาหกรรม เทคโนโลยีคอมพิวเตอร์ เทคโนโลยีชีวภาพ และทางการแพทย์ เป็นต้น

อนุภาคทองคำระดับนาโนเมตร (gold nanoparticles, AuNPs) เป็นอนุภาคของโลหะในระดับนาโนเมตรที่มีความเสถียรสูงสุดชนิดหนึ่ง[7] ซึ่งถูกสังเคราะห์ได้เป็นคอลลอยด์ การสังเคราะห์ AuNPs ในน้ำนั้นสามารถทำได้โดยอาศัยสารช่วยทำให้เสถียร (nanoparticle stabilizer) ซึ่งสารช่วยทำให้เสถียรที่นิยมใช้กันมากก็คือ sodium citrate ข้อดีประการหนึ่งคือ sodium citrate จะทำหน้าที่เป็นได้ทั้งสารช่วยทำให้

เสถียร และเป็นตัวรีดิวซ์ไปด้วย[8] เมื่อมีสารช่วยทำให้เสถียรเข้ามาล้อมรอบ จะทำให้ AuNPs ไม่รวมตัวกันหรือเกาะตัวกันจนตกตะกอน เพราะสารช่วยทำให้เสถียรจะเกาะที่ผิวของ AuNPs และทำให้ผิวของ AuNPs แต่ละอนุภาคไม่สามารถเชื่อมต่อกันได้

รูปที่ 1 การสังเคราะห์ gold nanoparticles จากสารตั้งต้น [สารละลายทองคำและสารช่วยทำให้เสถียร (nanoparticle stabilizer)] โดยอาศัยปฏิกิริยา reduction และอุณหภูมิที่เหมาะสม

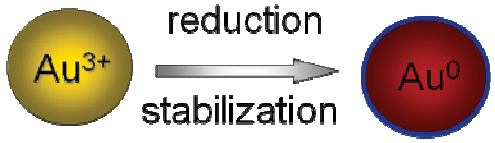

$HAuCl_4.3H_2O$ + Citrate ———> AuNPs-Citrate

ที่มา: Pal T. (2002) [7]

อย่างไรก็ตามสามารถที่จะปรับปรุงพื้นผิวของ AuNPs ให้มีโมเลกุลที่ต้องการมาเคลือบผิวได้ โดยเฉพาะอย่างยิ่งการใช้อนุภาคทองคำระดับนาโนเมตรมาปรับปรุงพื้นผิวให้เกาะยึดกับสารชีวโมเลกุลเป้าหมาย เช่น DNA[9] หรือ โปรตีน[10]หรือสายคาร์โบไฮเดรต [11] หรือยา สี Fluorescent[12] ด้วยเหตุนี้เองจึงสามารถนำ AuNPs มาสร้างเป็นอุปกรณ์ตรวจวัดสารทางชีวภาพ (biosensor) ที่มีความจำเพาะเจาะจงได้อย่างหลากหลาย[13] โดยการปรับปรุงจากพื้นผิวของ AuNPs ด้วยสารที่มีความสามารถในการจำเพาะกับสารตัวอย่างที่ต้องการจะวิเคราะห์ตรวจหาโดยคอลลอยด์ของ AuNPs สามารถเปลี่ยนสีได้ง่ายเมื่อถูกกระตุ้นด้วยสิ่งเร้าภายนอก จึงเปรียบได้ว่า AuNPs ทำหน้าที่เป็นหน่วยรายงานผล(reporter)สำหรับอุปกรณ์ตรวจวัดระดับโมเลกุล

รูปที่ 2 การเปลี่ยนแปลงของสี เมื่อขนาดของ AuNPs เปลี่ยนแปลงไป

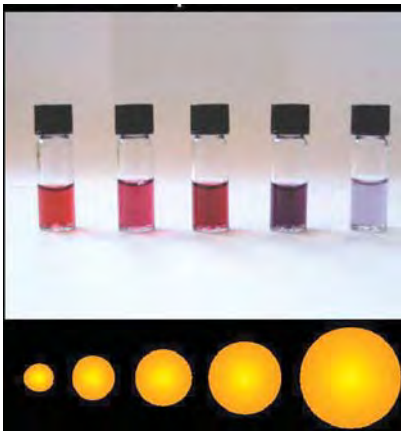

ที่มา: Liu J, and Lu Y. (2003) [13]

พีเอ็นเอ เทคโนโลยี (PNA Technology)

เพปไทด์นิวคลีอิกแอซิด (peptide nucleic acid) หรือพีเอ็นเอเป็นโมเลกุลสังเคราะห์ที่มีโครงสร้างเลียนแบบดีเอ็นเอโดยแทนที่ส่วนของดีออกซีไรโบสฟอสเฟตในดีเอ็นเอด้วยเพปไทด์หรือพอลิเอไมด์ ในปี ค.ศ. 1991 การสังเคราะห์และสมบัติการจับยึดกับดีเอ็นเอของพีเอ็นเอได้ถูกรายงานเป็นครั้งแรก โดย Nielsen และคณะ [14] จากรายงานการวิจัยพบว่าพีเอ็นเอของ Nielsen สามารถจับยึดกับดีเอ็นเอที่มีลำดับเบสคู่สม (A เป็นเบสคู่สมกับ T และ C เป็นเบสคู่สมกับ G) เกิดเป็นไฮบริดเช่นเดียวกันกับดีเอ็นเอโดยไฮบริดที่ได้มีเสถียรภาพสูงกว่าไฮบริดที่เกิดระหว่างดีเอ็นเอกับดีเอ็นเอเอง และการจับยึดของพีเอ็นเอยังมีการเลือกจำเพาะที่ดีกว่าดีเอ็นเอโดยสามารถบอกความแตกต่างของการจับยึดกับดีเอ็นเอที่ไม่เข้าคู่กันอย่างสมบูรณ์ได้ชัดเจนกว่าดีเอ็นเอ [15] จากข้อดีของพีเอ็นเอนี้ทำให้มีการพัฒนาและสังเคราะห์พีเอ็นเอระบบใหม่ๆ ขึ้นมาอย่างต่อเนื่อง[16-20]นอกจากนี้พีเอ็นเอยังเริ่มเข้ามามีบทบาทในด้านเทคโนโลยีทางชีวภาพมากขึ้นโดยการนำมาประยุกต์ใช้ในการตรวจวินิจฉัยโรคและการวิเคราะห์การกลายพันธุ์ เป็นต้น โดยมีการนำพีเอ็นเอโพรบมาใช้ในการตรวจลำดับเบสของดีเอ็นเอแทนที่ดีเอ็นเอโพรบมากขึ้น โดยงานวิจัยที่มีรายงานแล้วส่วนใหญ่ยังคงใช้พีเอ็นเอของ Nielsen [21]

ระบบพีเอ็นเอชนิดใหม่ซึ่งพัฒนาขึ้นโดย Vilaivan และคณะที่เรียกว่า พิร์โรลิดินิลพีเอ็นเอ (pyrrolidinyl PNA) แสดงสมบัติในการจับยึดกับดีเอ็นเอได้ดีกว่าดีเอ็นเอและพีเอ็นเอของ Nielsen ทั้งในด้านของความแข็งแรงของการจับยึด (affinity) และการเลือกจำเพาะทั้งลำดับเบสและทิศทางของการจับยึด [17]

จึงได้เล็งเห็นถึงศักยภาพของการพัฒนาพิร์โรลิดินิลพีเอ็นเอดังกล่าวเป็นอุปกรณ์ตรวจลำดับเบสของดีเอ็นเอและพัฒนาวิธีการวิเคราะห์ที่สามารถทำได้อย่างสะดวกและรวดเร็วยิ่งขึ้น ในงานวิจัยนี้จึงมุ่งเน้นพัฒนาพิร์โรลิดินิลพีเอ็นเอเรืองแสงเพื่อใช้เป็นโพรบในการตรวจลำดับเบสของดีเอ็นเอด้วยเทคนิคทางสเปกโทรฟลูออริเมตรี โดยอาศัยหลักการ Fluorescence Resonance Energy Transfer (FRET) ซึ่งเกี่ยวข้องกับถ่ายทอดพลังงานระหว่างโมเลกุลทำให้มีความจำเพาะ (selectivity) และมีความแม่นยำสูง (sensitivity)

วัตถุประสงค์

เพื่อพัฒนาชุดตรวจโดยการนำนาโนเทคโนโลยีมาประยุกต์ใช้ในการทำชุดตรวจกรอง Hemoglobin E โดยใช้ synthetic DNA ในการศึกษาการพัฒนาชุดตรวจนี้ขึ้น

วิธีดำเนินงานวิจัย

1. **การสังเคราะห์อนุภาคทองคำระดับนาโนเมตรความเข้มข้น** 1 g/ml

สังเคราะห์อนุภาคทองคำระดับนาโนเมตรจากปฏิกิริยา reduction ของสารละลาย (O2H4.3uClH) hydrogen tetratetrihydrate(III) acholoaurate โดยใช้สารละลาย trisodium citrate (O2H7.2O5H6C3Na)dihydrate ขั้นแรกปิเปตสารละลาย 1% (O2H4.3uClH) hydrogen tetratetrihydrate(III) acholoaurate ปริมาณ 0.5mL ใส่ใน flask ที่มี DI water อยู่ 24.5 mL นำไปต้ม บน stirrer hot plate โดยมี magnetic bar กวนสารจนมีอุณหภูมิถึง 100° C จึงเติมสารละลาย 38.8 mM (O2H7.2O5H6C3Na)trisodium citrate dihydrate ลงไป 0.94 mL สีของสารละลายจะเริ่มเปลี่ยนจากสีเหลืองอ่อน เป็นสีเทา สีม่วงและสีแดงตามลำดับ จากนั้นต้มต่อที่อุณหภูมิ 100° C เป็นเวลา 20 น าที แล้วจึงปล่อยให้เย็นที่อุณหภูมิห้อง เก็บสารละลายอนุภาคทองคำระดับนาโนที่ได้ในที่มืดและเย็น

2. Characterization **ของ** AuNPs

นำอนุภาคทองคำระดับนาโนที่ได้ไปตรวจสอบสมบัติการดูดกลืนแสงโดยใช้ UV-visible absorption

3. **จัดเตรียม** PNA Probe **และ** DNA Probe **สำหรับ** Hemoglobin E

PNA Probe ได้รับความร่วมมือจาก รศ.ดร.ธีรยุทธ วิไลวัลย์ ภาควิชาเคมี คณะวิทยาศาสตร์ จุฬาลงกรณ์มหาวิทยาลัย

1 PNA Probe ที่ตรึงบริเวณ Test Line

PNA Probe (A) 5’ TGGTAAGGCC-Lys(biotins) 3’

PNA Probe (G) 5’ TGGTGAGGCC-Lys(biotins) 3’

ส่วน DNA Probe ทำการสั่งซื้อจากบริษัทเอกชนในการสังเคราะห์ตามลำดับดังนี้

1 DNA Probe(1) ที่ตรึงบริเวณ Control Line

DNA (1) 5’-biotin-CTTCATCCACGTTCACCTTG-3’

2 DNA Probe(2) For Conjugate AuNPs ใช้ใน Conjugate pad

DNA (2) 5’-Thiol-CAAGGTGAACG-3’

3.Synthetic Target A 5’ CAACCTGCCCAGGGCCTTACCACCACCTTC ATCCACGTTCACCTTGCCCCACAGGGCAGT 3’

Synthetic Target G 5’ CAACCTGCCCAGGGCCTCACCACCACCTTC ATCCACGTTCACCTTGCCCCACAGGGCAGT 3’

4. **การติด** DNA Probe(2) For Conjugate **ลงบนอนุภาคทองคำระดับนาโนเมตร** (AuNPs)

การติด DNA probe ลงบนผิวอนุภาคทองคำระดับนาโนเมตร ทำได้โดยนำ DNA probe(2) ที่ต่อกับหมู่ thiol (1.0 OD) ปริมาณ 98 uL มาผสมกับ triethylamine ปริมาณ 2 uL และ เติม DDT ปริมาณ 7.7 mg วางทิ้งไว้ที่อุณหภูมิห้อง ประมาณ 30 นาที จากนั้นล้างด้วย ethylacetrate ปริมาณ 400uL 4 ครั้ง หลังจากนั้นเติม DNA probe(2) ลงใน AuNPs 1 mL นำไปแช่ที่อุณหภูมิ 4oC เป็นเวลา 20 ชั่วโมง เติม NaCl โดยให้สารละลาย AuNPs มี NaCl เข้มข้นสุดท้ายเป็น 150mM แช่ที่อุณหภูมิ 4oC เป็นเวลา 20 ชั่วโมง นำไปcentrifuge ที่ 12,000 rpm 12 นาที ดูดส่วนของเหลวใสทิ้งและละลายตะกอนด้วยสารละลาย eluent buffer (20 mM Na3PO4, 5% BSA, 0.25% Tween และ 10% sucrose) ปริมาณ 1 mL

5. **การเตรียม** PNA Probe (A),(G) **และ** DNA Probe (1) **สำหรับตรึงอยู่บน** Lateral flow strip

ทำการเติม 1 mM ของ PNA Probe (A),(G) และ DNA Probe (1) ซึ่งต่อกับ biotin ทำเป็น3 ชุด แยกกัน ปริมาณอย่างละ 60uL และ PBS 140 uL ลงใน 1.67mg/ml ของสารละลาย streptavidin ปริมาณ 30 uL ผสมให้เข้ากัน วางไว้ที่อุณหภูมิห้องเป็นเวลา 1ชั่วโมง

6. **การเตรียม** Simple pad

นำ glass fiber (4 mm x 17 mm) ไปจุ่มในสารละลาย buffer (ประกอบด้วย 0.25% Triton X 100, 0.05 M Tris-HCl, และ 0.15M NaCl) ตากให้แห้งและเก็บไว้ใน desiccator ที่อุณหภูมิห้อง

7. **การเตรียม** Conjugate pad

นำ glass fiber (4 mm x 8 mm) มาจุ่มในสารละลาย AuNPs ที่ต่อกับ DNA porbe จากนั้นนำมาตากให้แห้งที่อุณหภูมิห้อง เก็บไว้ใน desiccator ที่อุณหภูมิ 4oC

8. **การเตรียม** Nitrocellulose membrane

นำ Probe PNA และ DNA Probe มาหยดลงบนกระดาษ Nitrocellulose membrane (4 mm x 25 mm) .ให้มีความกว้างขนาด 2mmโดย หยดบริเวณที่เป็น test zone ส่วน control หยดบริเวณที่เป็น control zone จากนั้นตากให้แห้งที่อุณหภูมิห้องเป็นเวลา 4 ชั่วโมง และเก็บที่อุณหภูมิ 1oC

9. **การประกอบชุด** Lateral flow strip

นำส่วนของ Simple pad Conjugate pad Nitrocellulose membrane และ Absorption pad มาประกอบบนแผ่นพลาสติก (Backing) ขนาด 4 mm x 60 mm โดยแต่ละส่วนจะมีบริเวณที่วางซ้อนทับกันยาว 2mm แล้วเก็บไว้ที่แห้งและมืดเพื่อเก็บไว้ทำการทดลองต่อไป

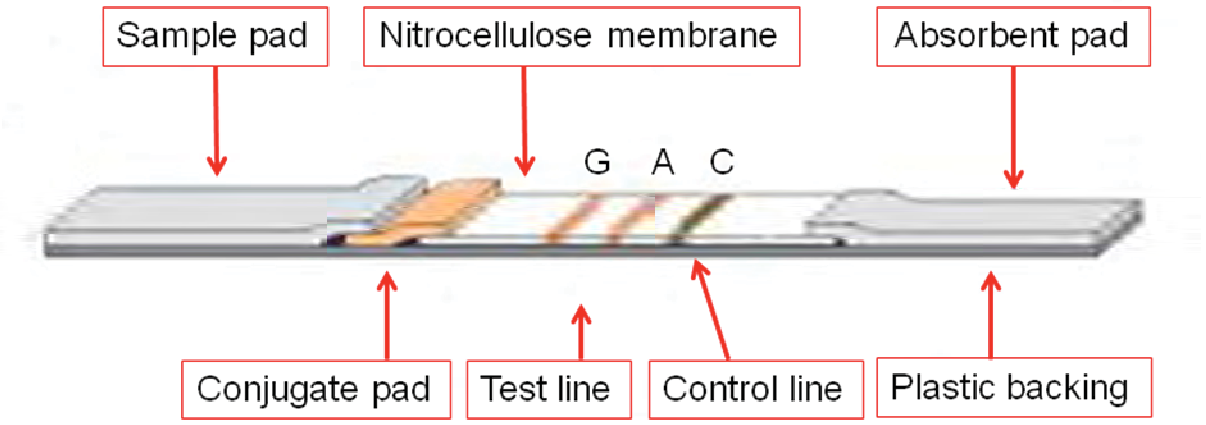

รูปที่ 3 Model แสดงส่วนประกอบของ Lateral flow Hb E strip test

ผลการวิจัย

ผลจากการสังเคราะห์ Gold Nanopartical

รูปที่ 4 ผลที่ได้จากการสังเคราะห์ Gold Nanopartical

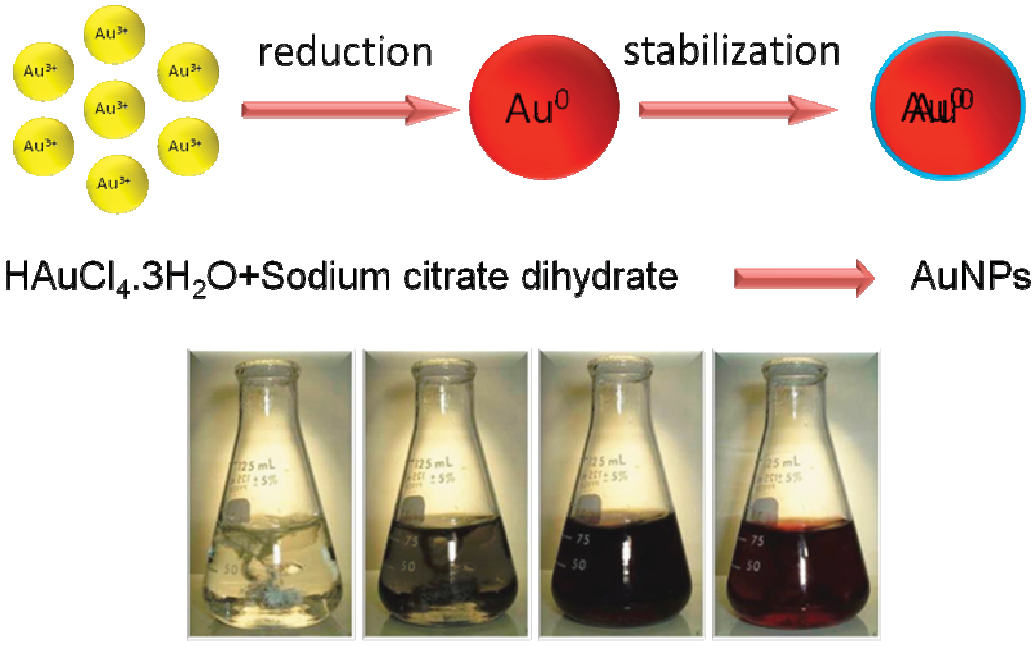

สีของGold nanopartical ที่ได้จะมีลักษณะสีแดง จากนั้นนำอนุภาคทองคำระดับนาโนที่ได้ไปตรวจสอบสมบัติการดูดกลืนแสงโดยใช้ UV-visible absorption

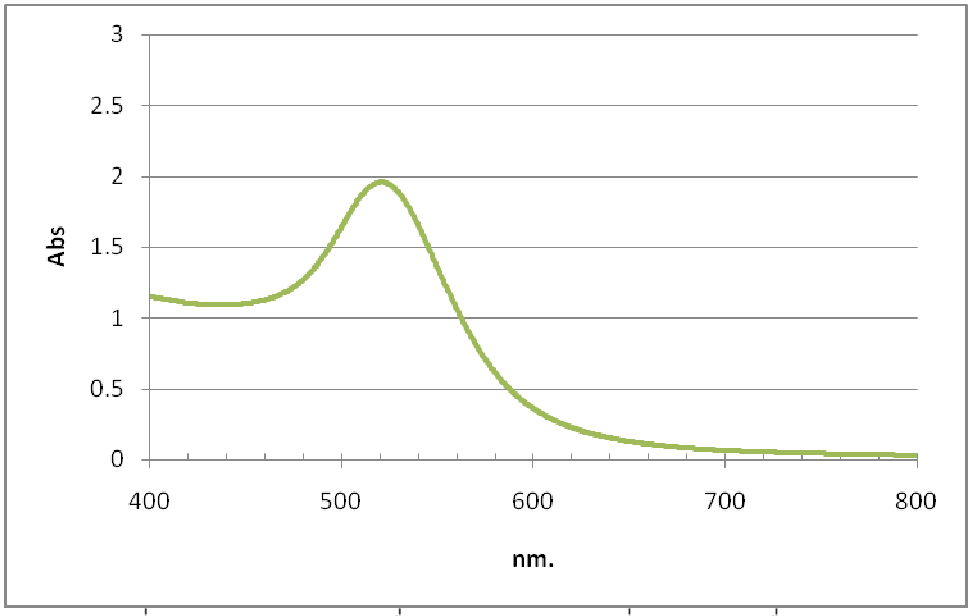

รูปที่ 5 การวัดค่าการดูดกลืนแสงของ AuNPs ที่ความยาวคลื่น 520 nm

การแปลผล

Hemoglobin E เป็นฮีโมโกลบินผิดปกติ เกิดจากการกลายพันธุ์ของยีนบีต้าอี ที่ตำแหน่งโครโมโซมคู่ที่ 11 โดยเกิดการแทนที่(Point Mutation)ของนิวคลีโอไทด์เบส (single nucleotide base substitution) ที่ตำแหน่งที่ 26 ในสาย บีต้า จากรหัส GAG เปลี่ยนเป็น AAG ดังนั้น Hb E Strip นี้จึงเป็นการตรวจกรองในระดับพันธุกรรม โดยใช้หลักการของ PNA Probe ที่สามารถจับกับลำดับ DNA ในตัวอย่างเลือดได้ในตำแหน่งที่เกิดการแทนที่(Point Mutation)ดังกล่าว จึงสามารถรายงานผลได้ใน 3 ลักษณะ ดังนี้หากผลเป็น Positive จะเห็นแถบสีเกิดขึ้นมี 2 กรณีคือ กรณีแรกหากเป็นความผิดปกติชนิด EA จะขึ้นในตำแหน่ง G,A,Control ส่วนกรณีที่สองเกิดความผิดปกติชนิด EE จะขึ้นแถบสีในตำแหน่ง A , Control ตามลำดับ ส่วนในกรณีที่สามเทียบกับ Negative Control จะเห็นแถบสีเกิดขึ้นในตำแหน่ง G , Control ดังแสดงได้ในรูป 6

รูปที่ 6 แสดงแสดงตัวอย่างการแปลผล Lateral flow Hb E strip test

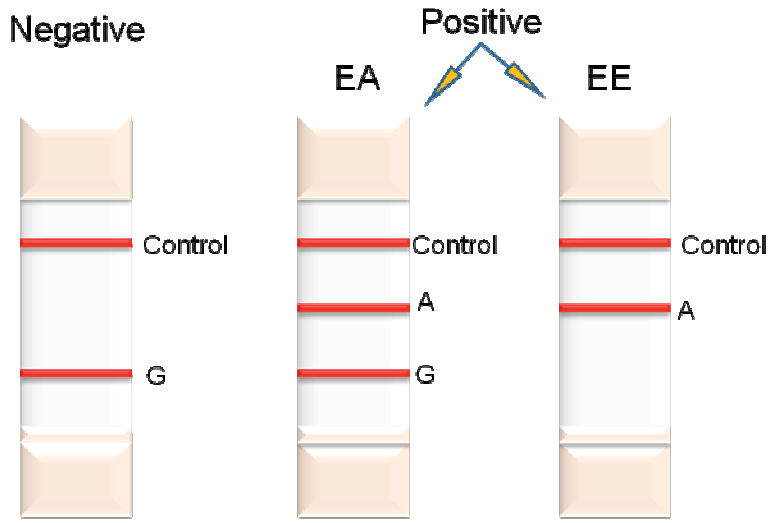

ซึ่งผลที่ได้จากการทดลองนี้จะเป็นผลที่ได้จากการอ่านได้ด้วยสายตาในการเกิดแถบสีในตำแหน่งที่ได้ทำสัญลักษณ์เอาไว้ โดยใช้หลักการแปลผลในลักษณะต่างๆดังที่ได้กล่าวมาในด้านต้นหลังจากนั้นจะทำการบันทึกผล โดยการถ่ายภาพ

ผลจากการทดลองจริงโดยใช้ DNA Target ที่ออกแบบมาเฉพาะในการทดลองได้ผลดังต่อไปนี้

การทดลองที่ 1

• Streptavidin-biotin	• PNA : test line • Probe DNA : control line
• Concentration probe	• 100 µM
• Target	• Synthetic target (100 fM) type A,G
• Buffer	• PBS

ผลของการทดลอง

G A C

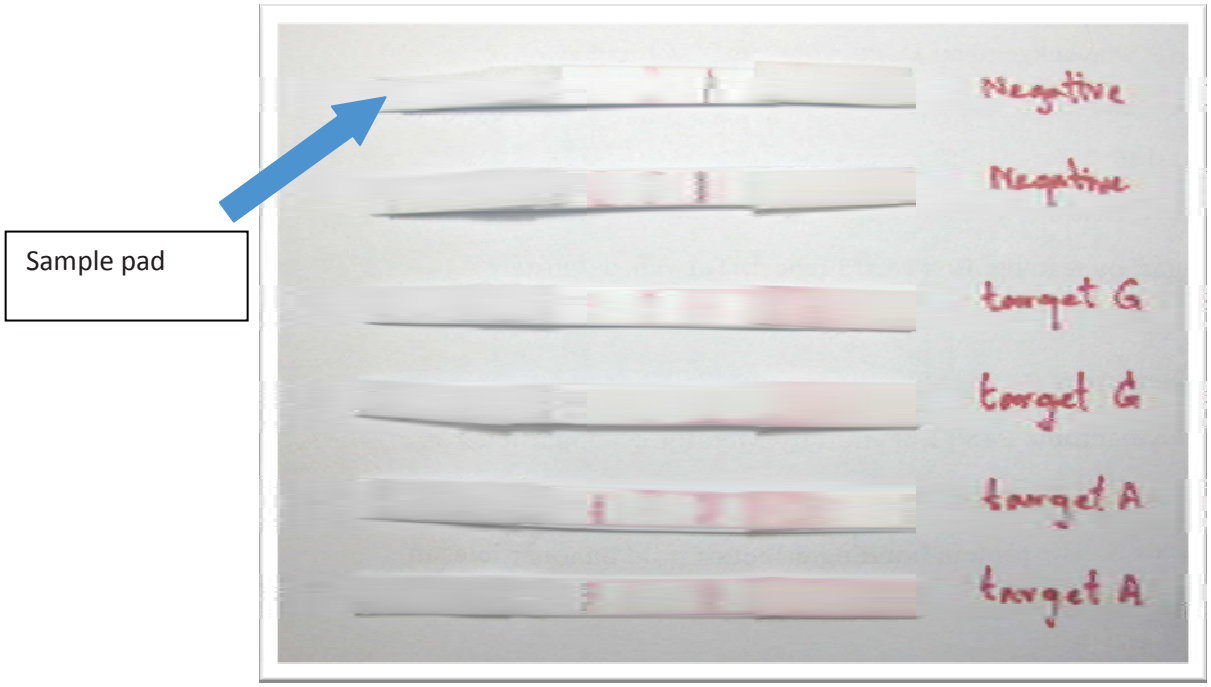

จากการทดลองครั้งที่ 1 ใช้ PBS เป็นตัว run ผลคือจะพบการขึ้นของทั้งสามแถบของ test line และ control line ซึ่งไม่น่าเป็นไปได้ เพราะว่าเราใช้ synthetic target ที่ออกแบบมาให้เหมือนกับ Hb E ที่เบสเป็น CTC ซึ่งน่าจะขึ้นแถบได้เฉพาะที่ test line ที่เบสคู่สมกับตัวตรวจจับ PNA ที่เป็น 5' TGGTGAGGCC 3' จะขึ้นแถบที่ test line ที่เป็นแถบ G ได้เท่านั้นแต่กับขึ้นได้หมดแสดงว่าไม่มีความจำเพาะเจาะจง และใช้ synthetic target ที่ออกแบบมาให้เหมือนกับ Hb E ที่เบสเป็น CTT ที่เบสคู่สมกับตัวตรวจจับ PNA ที่เป็น 5' TGGTAAGGCC 3' จะต้องขึ้นแถบที่ test line ที่เป็นแถบ A ก็ให้ผลการทดลองที่คล้ายกันกับแถบ G พบการขึ้นของแถบทุกแถบ ซึ่งไม่น่าเป็นไปได้ จึงจะทำการทดลองต่อไปโดยจะใช้ dH_2O แทน PBS และดูการขึ้นของแถบแบน

การทดลองที่ 2

• Streptavidin-biotin	• PNA : test line • Probe DNA : control line
• Concentration probe	• 100 µM
• Target	• Synthetic target (100 fM) type G,A
• Buffer	• dH_2O

ผลของการทดลอง

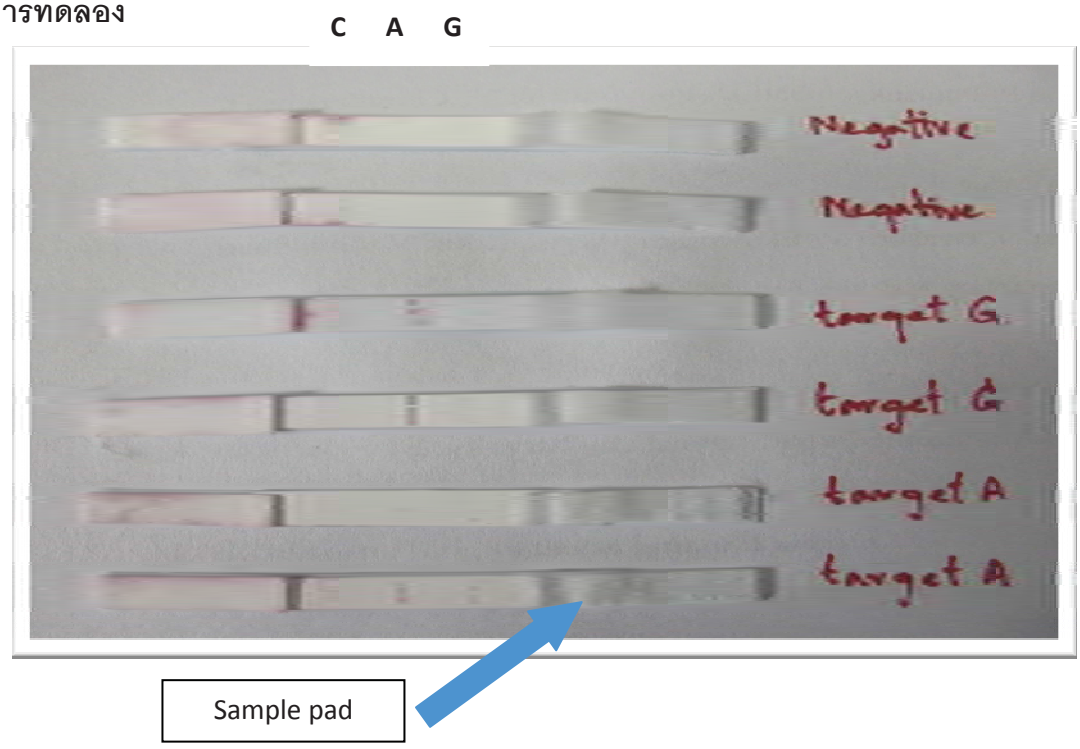

ส่วนการทดลองที่ 2 พบปัญหาการขึ้นของแบนทั้งสามแถบ และขึ้นแถบ control line บางๆ ในครั้งที่สอง โดยครั้งนี้ใช้ dH_2o เป็นตัว run แต่ signal ของแต่ละแถบไม่ดีนัก

จากการทดลองข้างต้นที่ผ่านจึงตั้งข้อสันนิษฐานว่าน่าจะเกิดมาการที่ความเข้มข้นของเกลือที่มากเกินไปซึ่งอาจทำให้เกิดผลดังกล่าวขึ้น และจะทำการทดลองต่อไป

การทดลองที่ 3

• Streptavidin-biotin	• PNA : test line • Probe DNA : control line
• Concentration probe	• 100 µM
• Target	• Synthetic target (100 fM) Type G
• Buffer	• dH2O, 1x PBS, o.1x PBS

ผลของการทดลอง

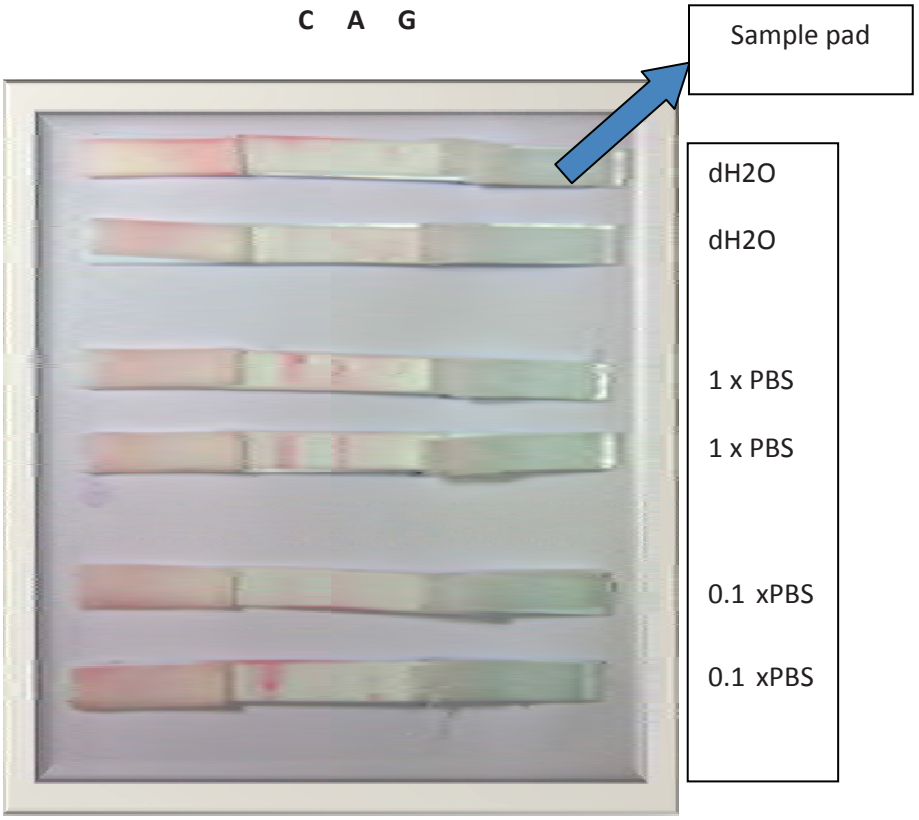

จากข้อสันนิษฐานจากการทดลองครั้งก่อนจึงทำให้การทดลองครั้งนี้จะออกแบบให้ปริมาณความเข้มข้นของปริมาณเกลือน้อยลงโดยการเจือจางลงเป็น 1 ใน 10 เท่าจากความเข้มข้นเดิม และเปรียบเทียบกับความเข้มข้นเดิม แต่ผลที่ออกมาก็คือ แถบที่ใช้ความเข้มข้นของเกลือที่ถูกเจือจางไป 10 เท่า นั้นให้ผล signal ค่อนข้างแย่กว่าแบนที่ใช้ PBS ซึ่งเป็นไปตามข้อสันนิษฐานของเรา แต่ผลของการขึ้นของทดสอบ synthetic target นั้นยังค่อนข้างไม่แน่นนอนและยังขึ้นแถบที่ไม่จำเพาะเจาะจงอยู่

การทดลองที่ 4

• Streptavidin-biotin	• PNA : test line • Probe DNA : control line
• Concentration probe	• 100 µM
• Target	• Synthetic target (100 fM) type G
• Buffer	• 10mM phosphate buffer + 2M Nacl • Dilute 0.1x ,0.01x ,0.001x

ผลของการทดลอง

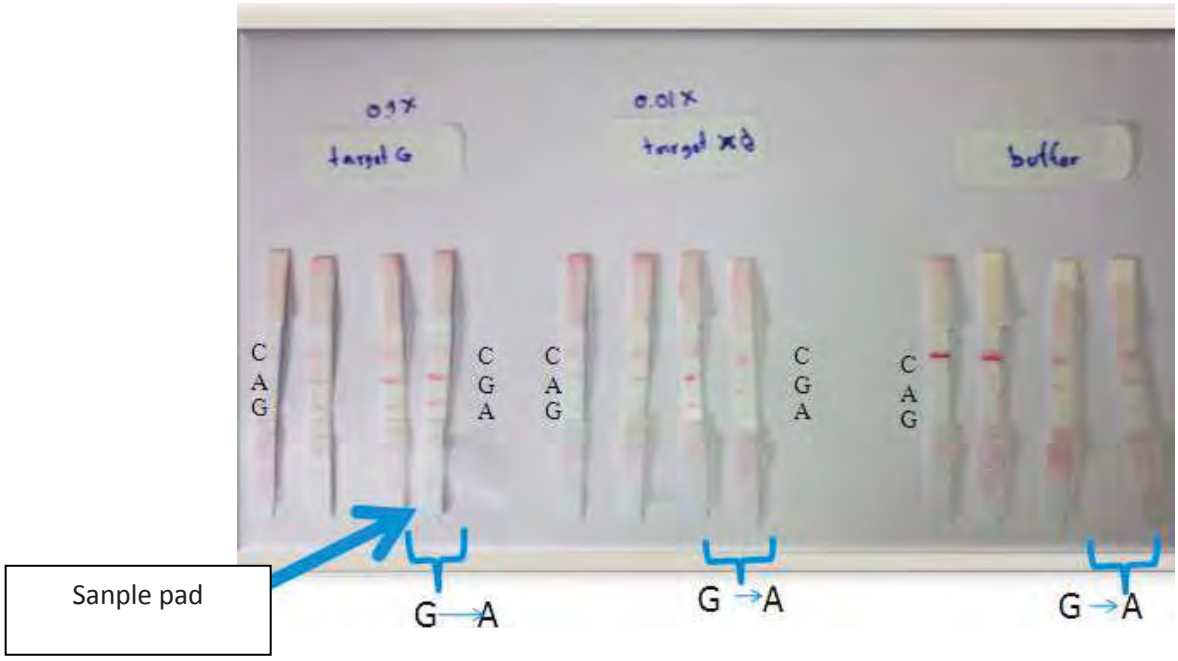

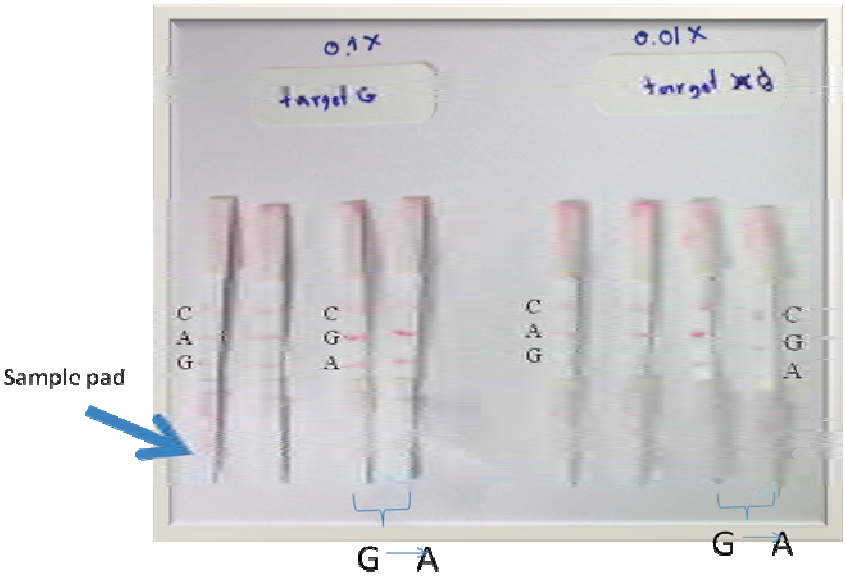

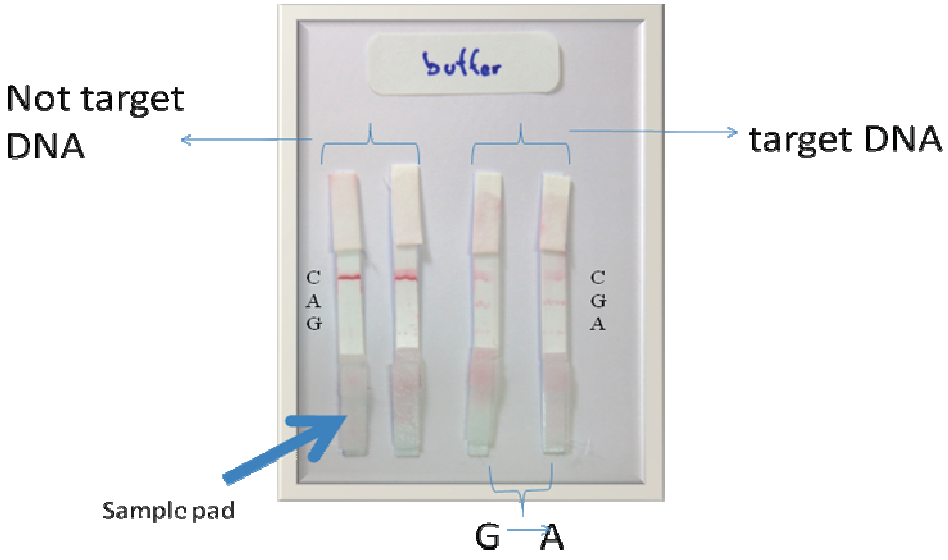

ผลจากการทดลอง

การทดลองนี้ที่จะใช้ในการตรวจสอบ DNA ของคนที่ต้องการตรวจสอบว่าเป็นโรคธาลัสซีเมียหรือไม่ โดยการใช้วิธีตรวจแบบ strip test ยังไม่สามารถทำได้ เนื่องจากการทดลองโดยใช้ Synthetic target แล้วลองทดสอบใน strip test ยังให้ผลไม่แน่นอนและไม่ได้มาตรฐาน แต่มีข้อสันนิษฐานหนึ่งเชื่อว่าที่การขึ้นของแถบอย่างไม่แน่นอนอาจจะเกิดมาจากการที่ความเข้มข้นของ probe ที่ test line และ control line มีความเข้มข้นมากเกินไปจึงจะทำการทดลองต่อไปในการลองเจือจางความเข้มข้นของ probe ให้ลดลง

การทดลองที่ 5

• Streptavidin-biotin	• PNA : test line • Probe DNA : control line
• Concentration probe	• 100 µM
• Target	• Synthetic target (100 fM) type G
• Buffer	• 10mM phosphate buffer + 2M Nacl • Dilute 0.1 x

ผลการทดลอง

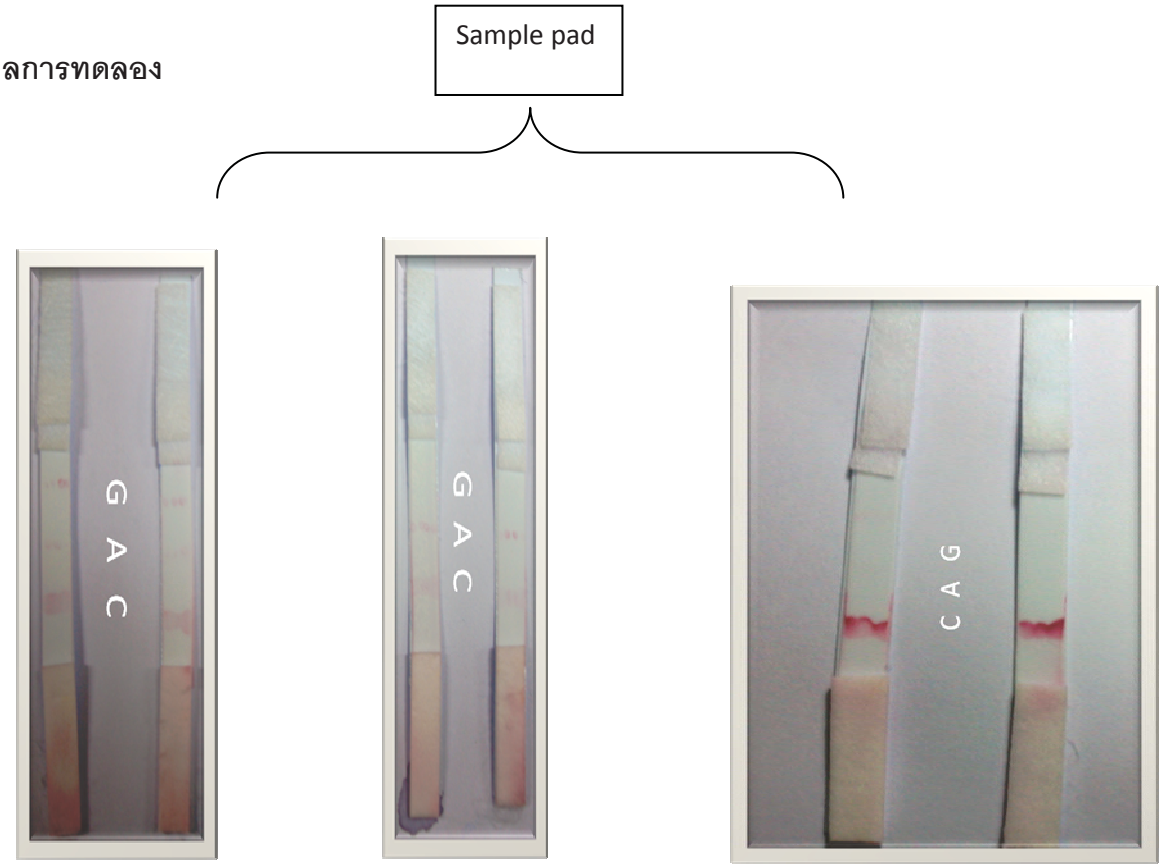

จากการทดลองที่ทำการเจือจางความเข้มข้นของ probe ให้ลดลง ผลที่ได้คือแถบที่เกิดขึ้นยังคงขึ้นอย่างไม่แน่นอนอยู่ดี เมื่อเปรียบเทียบกับ control ที่ใส่ Synthetic target จึงทำการสรุปว่าการทดลองทำชุดตรวจกรอง Hemoglobin E ที่ใช้ตัวตรวจจับเป็น PNA ยังให้ผลไม่แน่นอนและยังคงไม่จำเพาะเจาะจงแล้ว ความที่ไม่จำเพาะเจาะจงน่าจะเกิดมาจากที่ PNA จับกับ Synthetic target

ผลการทดลองเพื่อลดความเกิดการจับกันของ PNA กับ พื้นที่ผิวรอบอนุภาคทองคำระดับนาโนเมตร โดยการใช้โปรตีน BSA ตามความเข้มข้นต่างๆ

การทดลองที่ 6

• Streptavidin-biotin	• PNA : test line • Probe DNA : control line
• Concentration probe	• 1 μM
• Conjugate probe	• AuNPs+5% BSA
• Target	• No target
• Buffer	• 4x ssc 10 % SDS

ผลของการทดลอง

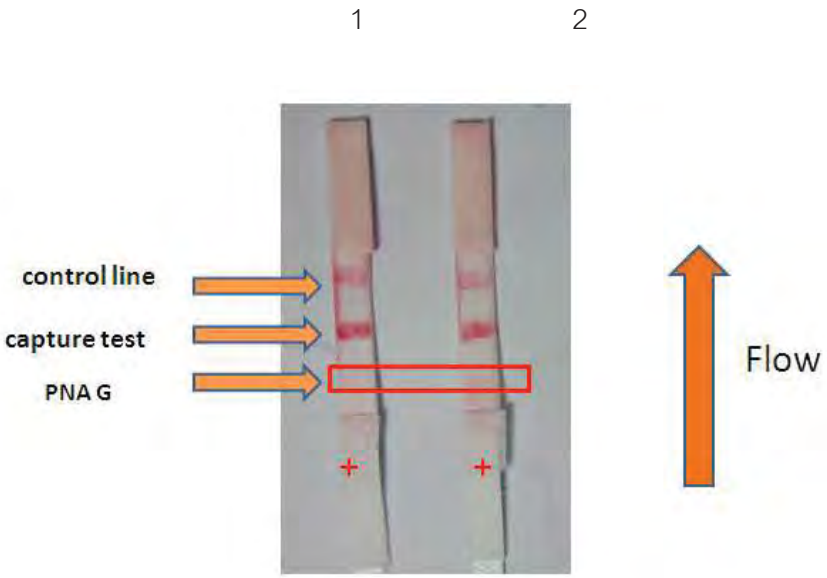

จากผลการทดลองที่ได้พบว่ามีการเกิดขึ้นของแถบแบนเกิดการจับกันของ PNA ชนิดG กับ พื้นที่ผิวรอบอนุภาคทองคำ ทำให้เกิดแถบแบนที่ผิดปกติขึ้น เพราะเนื่องมาจากยังทำการล้อมโปรตีน BSA กับพื้นที่ผิวรอบอนุภาคทองคำ ไม่ได้สัดส่วนที่พอเหมาะหรือหมายความว่ายังล้อมไม่หมดทำให้เกิดการจับขึ้น เพื่อสนับสนุนเหตุผลดังกล่าวจึงจะลองสลับตำแหน่งของ probe PNA ชนิด G และสังเกตุแถบแบนที่เกิดขึ้น

การทดลองที่ 7

• Streptavidin-biotin	• PNA : test line • Probe DNA : control line
• Concentration probe	• 1 μM
• Conjugate probe	• AuNPs+5% BSA
• Target	• No target
• Buffer	• 4x ssc 10 % SDS

ผลของการทดลอง

1 2

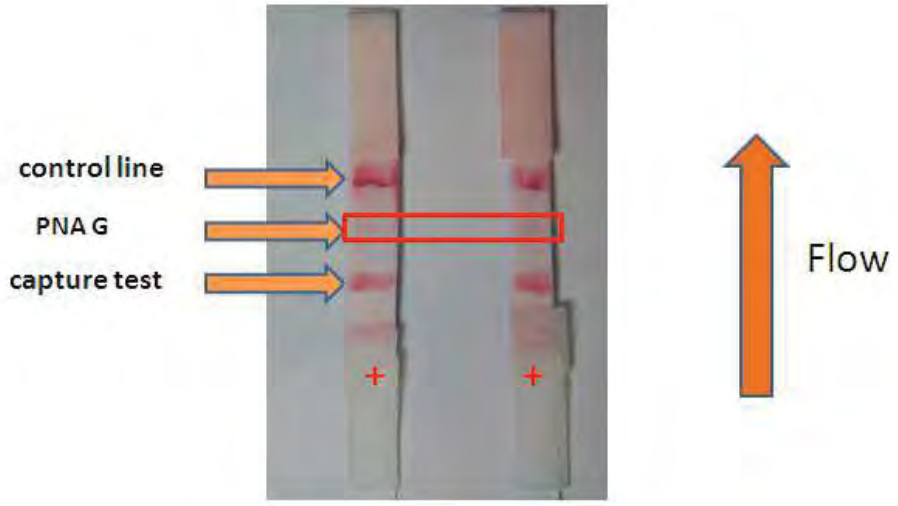

จากผลการทดลองดังกล่าวพบว่าเป็นไปตามเหตุผลที่คิดไว้ พบการเกิดแถบแบนเกิดการจับกันของ PNA ชนิดG กับ พื้นที่ผิวรอบอนุภาคทองคำ ถึงแม้จะทำการสลับตำแหน่งดังกล่าวแล้ว จากผลที่ได้เรายังล้อมไม่ได้สัดส่วนที่พอเหมาะ จะทำการเพิ่มปริมาณของโปรตีน BSA ให้มากขึ้น และระยะทางในการเครื่องของสารไม่มีผลต่อการเกิดแถบแบนดังกล่าว

การทดลองที่ 8

• Streptavidin-biotin	• PNA : test line • Probe DNA : control line
• Concentration probe	• 1 μM
• Conjugate probe	• AuNPs+10% BSA, 15% BSA
• Target	• No target
• Buffer	• 4x ssc

ผลของการทดลอง

10% 15%

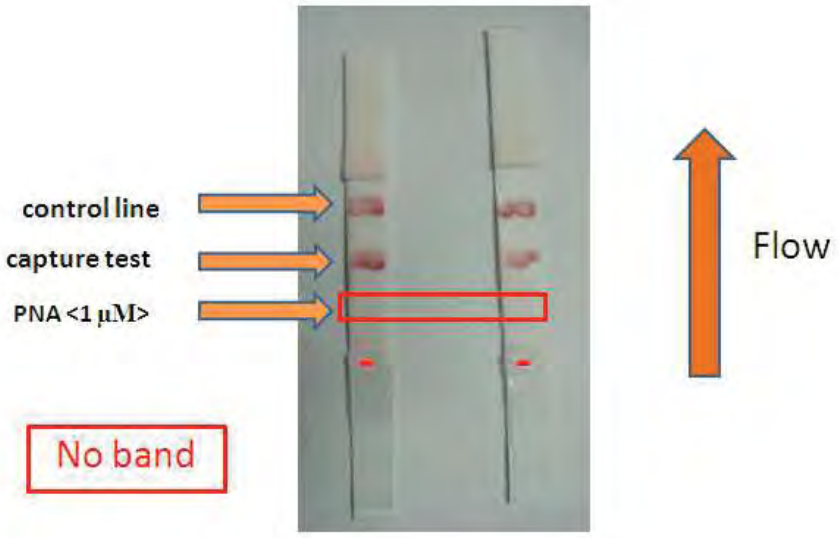

จากการทดลองโดยการเพิ่มปริมาณความเข้มข้นของโปรตีน BSA จาก 5 % เป็น 10 % และ 15% เพื่อทำการล้อมพื้นที่ผิวรอบอนุภาคทองคำไม่ให้จับกับ PNA ผลที่ได้ ปริมาณของ BSA 10 % และ 15% ให้ผลเหมือนกันคือขึ้นแถบแบนจางๆของPNA ถือว่าให้ผลดีมาก และเราเลือกความเข้มข้นที่ 10% เพราะว่าที่ความเข้มข้นที่ 15% ก็ให้ผลเหมือนกัน จะทำการทดลองต่อไปโดยใช้ปริมาณของ BSA ที่ 10%

การทดลองที่ 9

• Streptavidin-biotin	• PNA : test line • Probe DNA : control line
• Concentration probe	• 1 μM
• Conjugate probe	• AuNPs+10% BSA
• Target	• No target
• Buffer	• 4x ssc

ผลของการทดลอง

ทำการทดลองนำ PNA ชนิด G และ PNA ชนิด A มาลองทำกับ strip test ที่มี conjugate probe ที่ถูกล้อมด้วยโปรตีน BSA 10% และไม่ได้ใส่ target DNA ได้ผลดังนี้

1 2 3

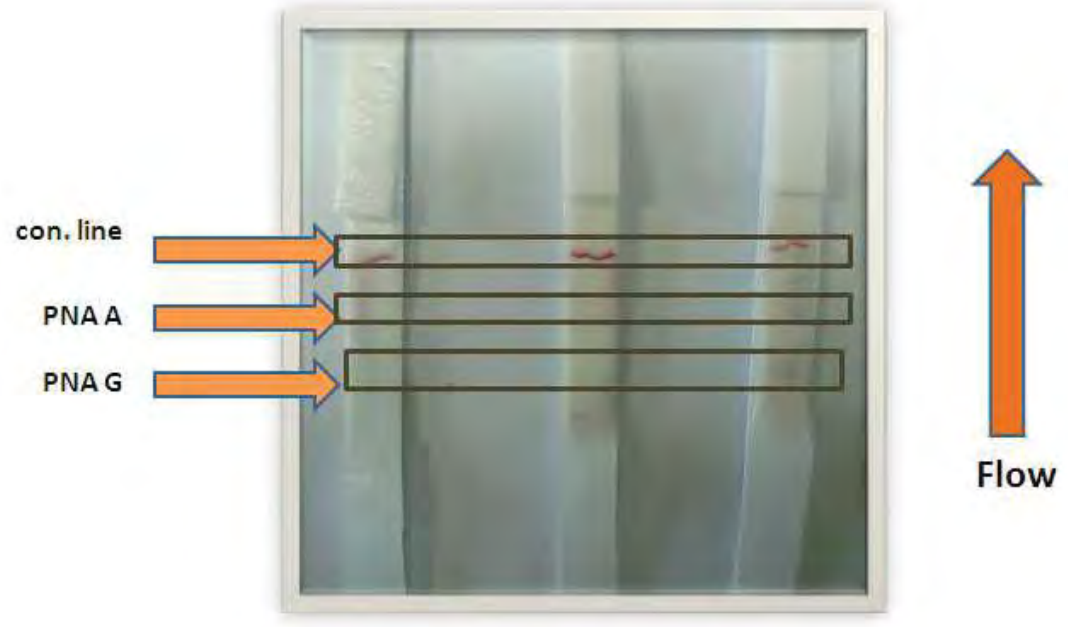

จากการทดลองได้ผลคือ ไม่พบแถบแบนของการจับกันของ PNA กับ พื้นที่ผิวรอบอนุภาคทองคำ โดยทำการทั้งหมด 3 ซ้ำ และได้ผลเหมือนกัน การทดลองต่อไปในอนาคตจะทำการทดลองใช้ target DNA

ต่อไปในการทดลองข้างหน้า และทำการทดลองสนับสนุนผลว่าโปรตีน BSA ไม่ได้ทำให้ AuNPs เกิดการจับกันขึ้น

การทดลองที่ 10

• Conjugate probe	• AuNPs+10% BSA
• Time	• 0,1,2,4,8 Hrs.
• UV-visible absorption	• 520 nm

ทำการทดลองเพื่อดูผลของโปรตีน BSA ว่าสามารถทำให้ AuNPs เกิดการจับกันได้หรือเปล่า โดยได้ผสม AuNPs และ โปรตีน BSA เข้าไว้ด้วยกัน โดยทำการศึกษาตามเวลาดังนี้ 0,1,2,4,8 ชั่วโมง จากนั้นนำไปวัดค่าการดูดกลืนแสง UV-visible absorption โดยที่ AuNPs ปกติจะดูดกลืนที่ 520 nm ถ้าหากเกิดการจับกันเกิดขึ้นจะได้ค่าการดูดกลืนแสงที่มากกว่า 520 nm

ผลของการทดลอง

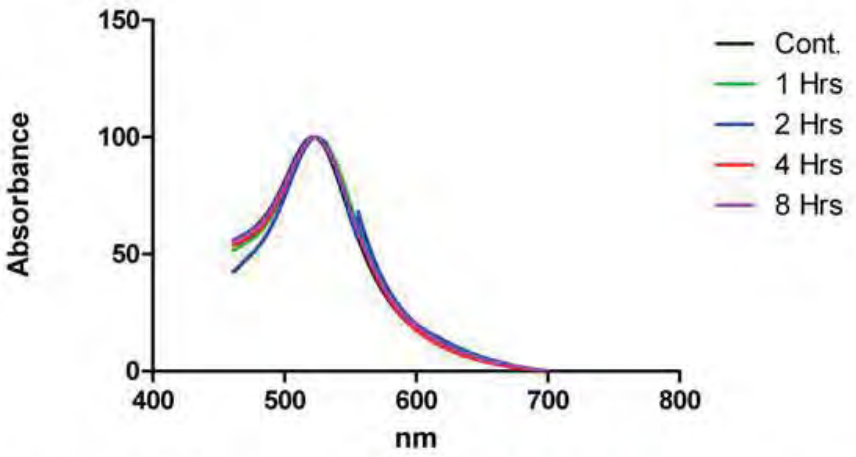

รูปที่ 1 กราฟแสดงความสัมพันธ์ระหว่างเวลาในการบ่ม BSA กับ AuNPs โดยทำการเทียบกับค่าการดูดกลืนแสงที่ความยาวคลื่น 520 nM

ผลที่ได้คือ โปรตีน BSA ไม่ได้ทำให้ AuNPs เกิดการจับตัวกันขึ้นโดยดูผลได้จากกราฟข้างต้น ซึ่งสังเกตเห็นได้ว่า ยิ่งเพิ่มชั่วโมงไปในการผสมของ AuNPs และโปรตีน BSA ก็ไม่ให้เกิดการจับกันของ AuNPs เพราะค่าการดูดกลืนแสงขึ้นที่ 520 nm ซึ่งแสดงว่า AuNPs ยังแสดงความเป็นอนุภาคขนาดนาโนเมตรอยู่ และไม่เกิดการจับกัน

การทดลองที่ 11

• Streptavidin-biotin	• PNA : test line • Probe DNA : control line
• Concentration probe	• 1 μM
• Conjugate probe	• AuNPs(New)+10% BSA, AuNPs(Old)+10% BSA
• Target	• No target
• Buffer	• 2x ssc

เนื่องจากได้ AuNPs มาใหม่จึงทำการทดลองเทียบกับ AuNPs อันเดิมว่าอันไหนก่อให้เกิด non specific น้อยกว่ากัน

ผลของการทดลอง

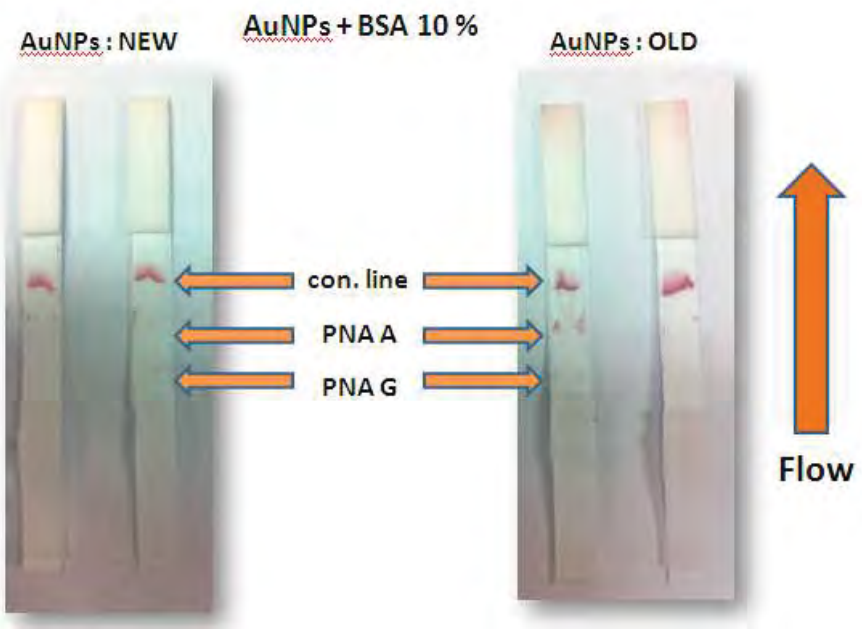

ผลการทดลองที่ได้ AuNPs อันใหม่จะก่อเกิด non specific น้อยกว่าAuNPs อันเดิม เพราะอาจจะเกิดจากการสังเคราะห์ที่แตกต่างของ AuNPs ซึ่งอันใหม่จะค่อนข้างมีการกระจายตัวของ AuNPs ที่ขนาดใกล้เคียงกันมากกว่าของอันเดิมจึงทำให้โปรตีน BSA ล้อมได้ดีกว่า และเกิด non specific น้อยกว่า จากศึกาและทดลองต่อไปจะใช้ AuNPs อันนี้

การทดลองที่ 12

• Streptavidin-biotin	• PNA : test line • Probe DNA : control line
• Concentration probe	• 1 μM
• Conjugate probe	• AuNPs+10% BSA
• Target	• Synthetic G,A
• Buffer	• 2x ssc

ทำการทดลองโดยใช้ synthetic DNA และดูผลการทดลองที่เกิดขึ้น

ผลของการทดลอง

ตัวควบคุมการทดลองที่ไม่ได้ใส่ synthetic DNA

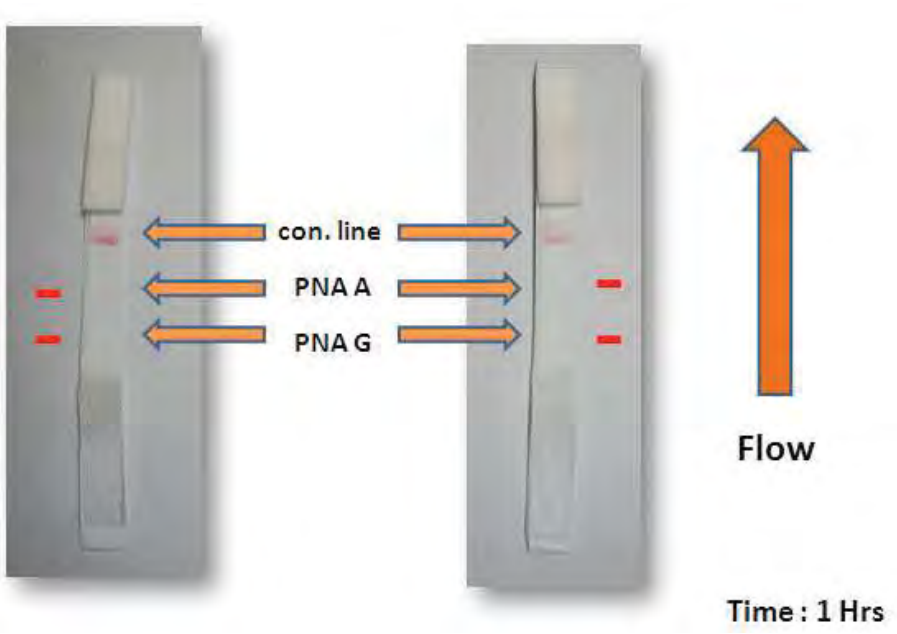

ตัวการทดลองที่ใส่ synthetic DNA

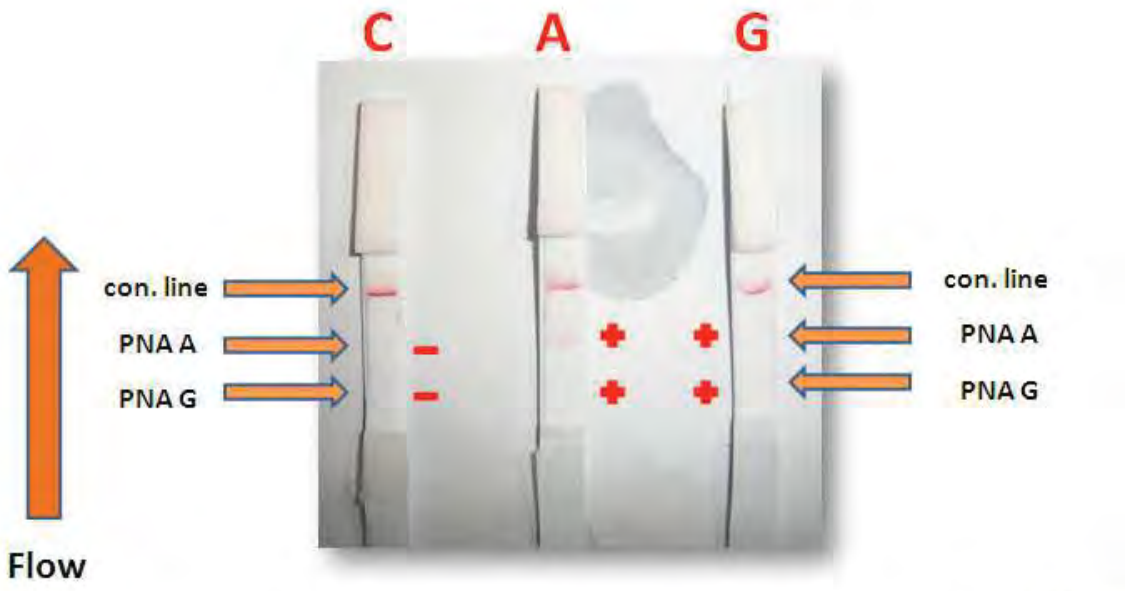

ทำการทดลองเปรียบเทียบใน strip test ที่ทำการใส่กับไม่ใส่ synthetic DNA ผลปรากฏว่าที่ไม่ใส่ synthetic DNA ไม่ขึ้นแถบแบน non specific แสดงว่าระบบที่เราทำมาสามารถทำงานได้ ต่อมา strip test ที่ทำการใส่ synthetic DNA กับขึ้นแถบแบนของ non specific ทั้ง Synthetic G , A ที่เวลา 1 ชั่วโมง แสดงว่า PNA Probe ทั้งสองตัวไม่มีความจำเพาะเจาะจง แต่ยังไม่แน่ใจแต่ทำการทดลองซ้ำเพื่อยืนยันผลอีกครั้ง โดยจะใช้ synthetic DNA ตัวอื่น ที่ไม่เกี่ยวกับงานในการศึกษาผล

การทดลองที่ 13

• Streptavidin-biotin	• PNA : test line • Probe DNA : control line
• Concentration probe	• 1 μM
• Conjugate probe	• AuNPs+10% BSA
• Target	• Synthetic A , 47 kDA , 56 kDA
• Buffer	• 2x ssc

ศึกษาผลความไม่จำเพาะเจาะจงของ probe PNA โดยใช้ synthetic DNA ที่ไม่เกี่ยวข้องกับงานในการศึกษาและทำการวิเคราะห์ผล โดยเลือกใช้ synthetic DNA ของ bacteria

ผลของการทดลอง

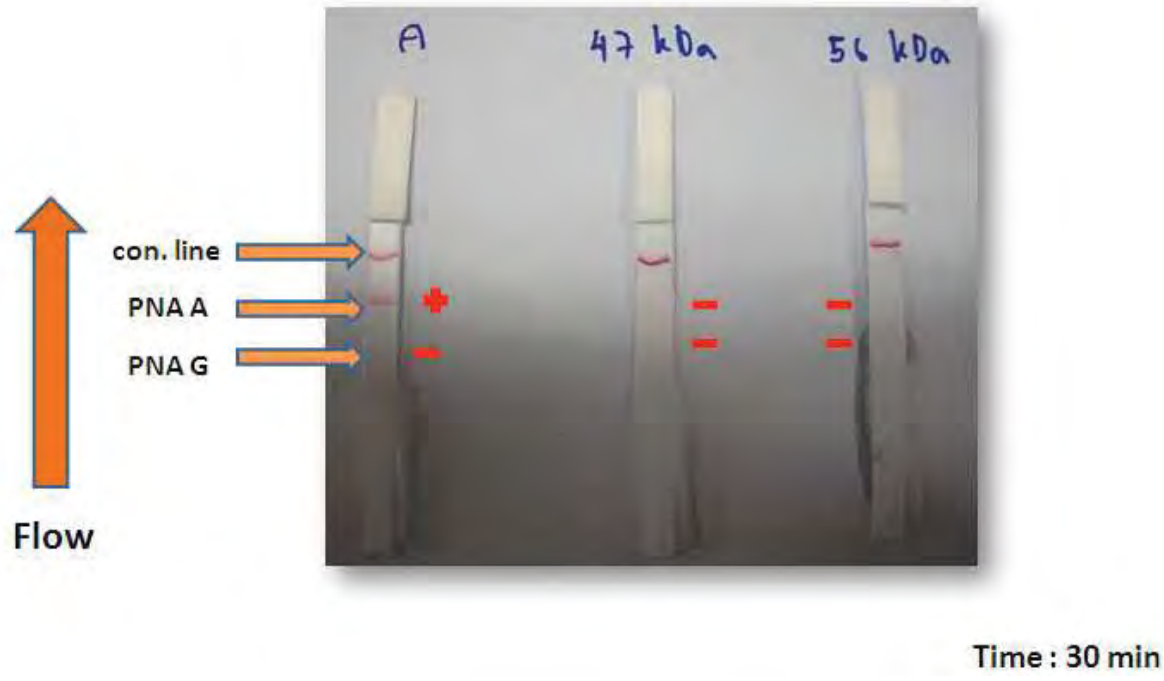

เมื่อเวลาผ่าน 30 นาที หลังจากใส่ synthetic DNA

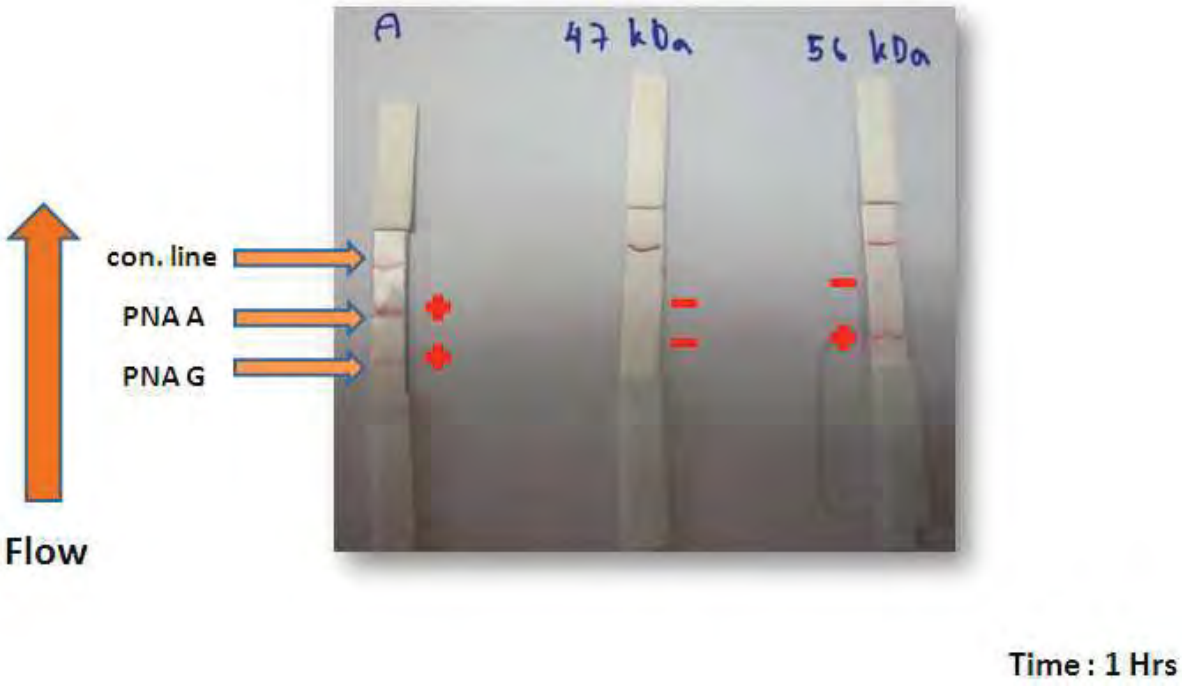

เมื่อเวลาผ่าน 60 นาที หลังจากใส่ synthetic DNA

ผลการศึกษาที่ได้ เมื่อนำ synthetic DNA ของ bacteria ใส่ลงไปใน strip test ผลปรากฏว่าที่เวลา 30 นาที ยังไม่พบการขึ้นของแถบแบน non specific แต่เมื่อเวลาผ่านไป 60 นาที กลับพบว่ามีแถบแบนเกิดขึ้น ที่ synthetic DNA 56kDa

การทดลองที่ 14

• Streptavidin-biotin	• PNA : test line • Probe DNA : control line
• Concentration probe	• 1 μM
• Conjugate probe	• AuNPs+10% BSA
• Target	• Synthetic A, G
• Buffer	• 2x ssc + 10% fermamide + 0.05%SDS

ศึกษาผลของความจำเพาะเจาะจงของ probe PNA โดยใช้ synthetic DNA โดยใช้ 2x ssc + 10 % fermamide + 0.05% sds เป็น Buffer ที่ใช้ในการศึกษา

ผลของการทดลอง

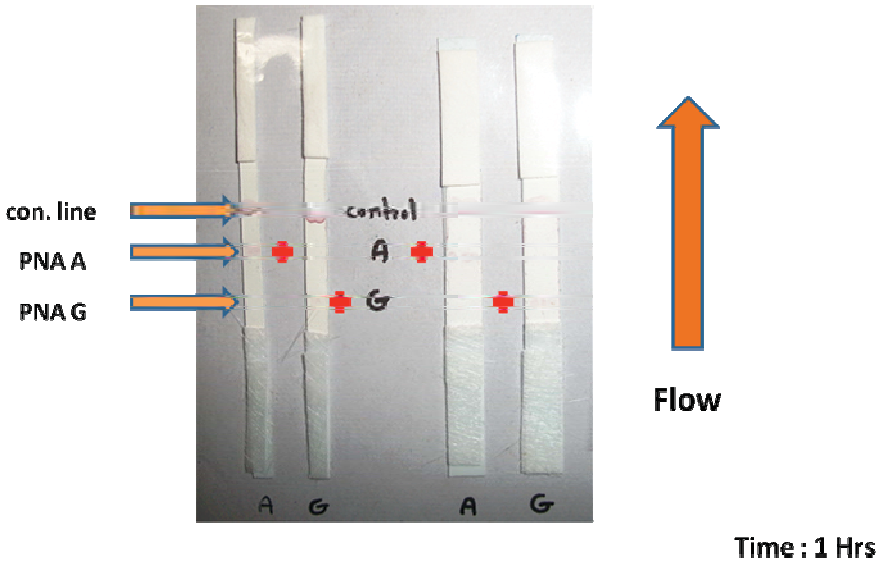

เมื่อเวลาผ่านไปหลังจากใส่ synthetic DNA ประมาณ 60 นาที

ผลที่ได้ปรากฏว่าหลังจากใส่ synthetic DNA ไป พบการขึ้นของแถบแบนที่ test line และ control line โดยที่ test line พบว่าการขึ้นของแถบแบนนั้นตรงกับ synthetic ที่ใส่ลงไป อย่างจำพะเจาะจง ผลที่ได้น่าจะเกิดจาการที่ fermamide เข้าไปทำให้การเกิด non specific ระหว่าง ผิว AuNPs และ PNA ลดลง จะทำการทดลองใน sample ผู้ป่วยต่อไป

การทดลองที่ 15

• Streptavidin-biotin	• PNA : test line • Probe DNA : control line
• Concentration probe	• 1 μM
• Conjugate probe	• AuNPs+10% BSA
• Target	• sample
• Buffer	• 2x ssc + 10% fermamide + 0.05%SDS

ศึกษาผลของความจำเพาะเจาะจงของ probe PNA โดยใช้ sample ผู้ป่วย โดยใช้ 2x ssc + 10 % fermamide + 0.05% sds เป็น Buffer ที่ใช้ในการศึกษา ทำการทดลองใน sample ผู้ป่วย

ผลของการทดลอง

Time : 1 Hrs

เมื่อเวลาผ่านไปหลังจากใส่ sample ผู้ป่วย ประมาณ 60 นาที

ผลที่ได้จากการทดลอง พบว่าใน sample ผู้ป่วยบาง sample ขึ้นแถบแบนที่จำเพาะเจาะจง และในบาง sample พบการขึ้นของแถบแบนจางมาก ผลที่เกิดขึ้นน่าจะเกิดมาจากที่ปริมาณของ fermamide มากเกินไป จนทำให้ไปรบกวนการจับกันของ sample กับ Probe pna จะทำการแก้ไขโดยการลดปริมาณของ fermamide ลง

การทดลองที่ 16

• Streptavidin-biotin	• PNA : test line • Probe DNA : control line
• Concentration probe	• 1 μM
• Conjugate probe	• AuNPs+10% BSA
• Target	• sample
• Buffer	• 2x ssc + 9% fermamide, 7% fermamide + 0.05%SDS

ศึกษาผลของความจำเพาะเจาะจงของ probe PNA โดยใช้ sample ผู้ป่วย โดยการลดปริมาณของเปอร์เซ็นต์ fermamide ลง เป็น 7 และ 9 เปอร์เซ็นต์ ตามลำดับ สังเกตุผลที่ได้จากการทดลอง

ผลของการทดลอง

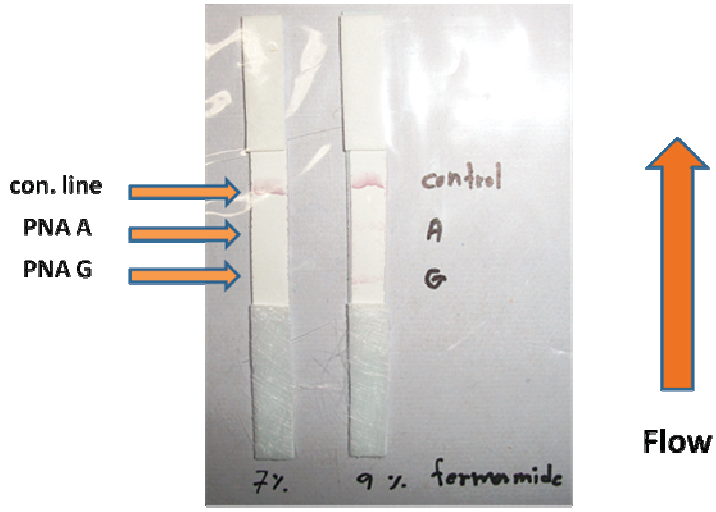

Time : 1 Hrs

ผลที่ได้จากการทดลองพบว่าที่ 9 เปอร์เซ็นต์ พบการขึ้นของแถบแบนที่จำเพาะเจาะจง แต่ที่ 7 เปอร์เซ็นต์ ไม่พบการขึ้นของแถบแบนที่ต้องการ น่าจะเกิดจากปริมาณของ fermamide มีผลต่อการทดลองที่เกิดขึ้น ความมากหรือน้อยไปก็อาจจะมีผลต่อการจับกันของแถบแบนที่เกิดขึ้น และปริมาณที่พอเหมาะคือ 7 % fermamide

การทดลองที่ 17

• Streptavidin-biotin	• PNA : test line • Probe DNA : control line
• Concentration probe	• 1 μM
• Conjugate probe	• AuNPs+10% BSA
• Target	• sample(purify PCR)
• Buffer	• 2x ssc +9 % fermamide + 0.05%SDS

ศึกษาผลของปริมาณเกลือ MgCl2 ในชุดน้ำยา PCR ที่อาจจะมีผลต่อการจับกันของ sample และ probe PNA โดยการทำผ่านชุด purify pcr kit และนำผลิตภัณฑ์ที่ได้ไปทำ strip test ต่อไป

ผลของการทดลอง

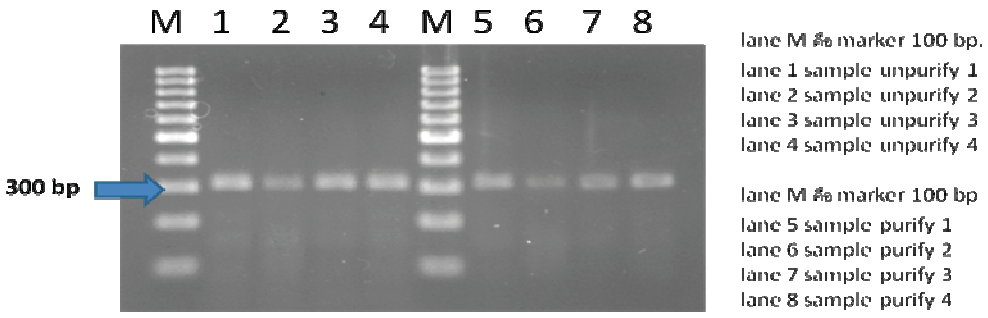

รูปภาพแสดงการทำ Gel electrophoresis ระหว่างตัวอย่างที่ purify PCR กับที่ไม่ได้ purify PCR มีการขึ้นของชิ้นผลิตภัณฑ์ที่ 312 bp.

ผลที่ได้จากการทดลองในการ purify pcr โดยทำการ run gel electrophoresis เทียบกันระหว่าง sample ก่อนถูก purify กับหลังจากที่ทำการ purify แล้วพบว่ามีการสูญหายไปของผลิตภัณฑ์ pcr น้อยมากประมาณ 5 – 10 % มี marker 100 bp. เป็นตัวใช้ในการดูแถบแบนที่เกิดขึ้น ซึ่งจะทำการนำไปลงใน strip test ต่อไป เพื่อดูผลของ Mgcl2 ต่อการจับกันของ sample และ probe PNA

ผลของการทดลอง

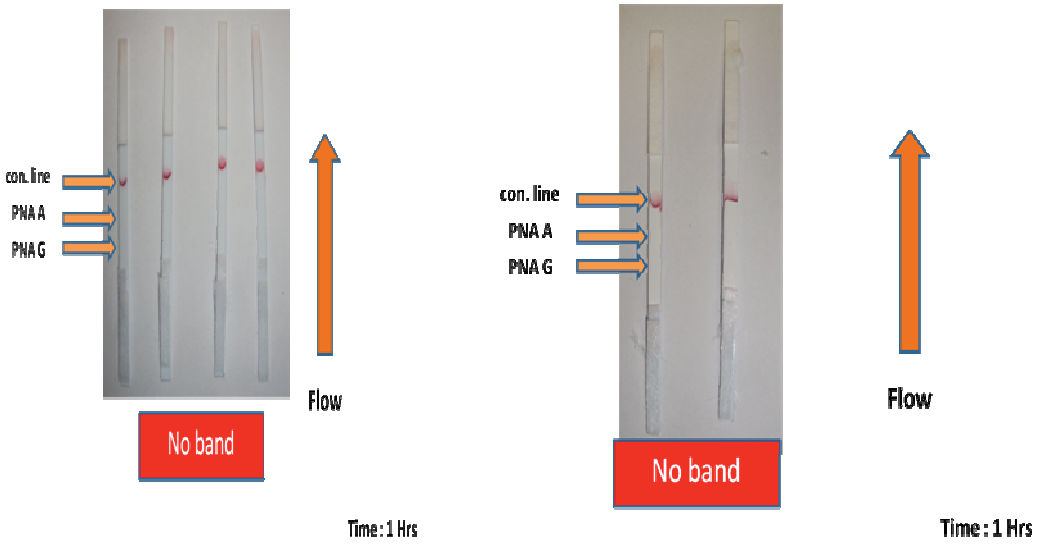

ผลที่ได้จากการทดลองโดยทำการสุ่ม sample ที่ทำการ purify มา 3 sample ผลที่พบปรากฏว่าไม่พบการขึ้นของแถบแบนที่ต้องการในทุก sample ใช้เวลาในการทดลอง 1 ชั่วโมง

การทดลองที่ 18

• Streptavidin-biotin	• PNA : test line • Probe DNA : control line
• Concentration probe	• 1 μM
• Conjugate probe	• AuNPs+10% BSA
• Target	• Synthetic A, G
• Buffer	• 2x ssc + 7 % fermamide + 0.05%SDS

ศึกษาผลของ strip test ที่ได้ โดยทำการหาความเข้มข้นที่ต่ำที่สุดที่ strip test สามารถทำได้ เพื่อบอกถึงขอบเขตจำกัดที่สุดที่ strip test มีความสามารถตรวจสอบได้

ผลของการทดลอง

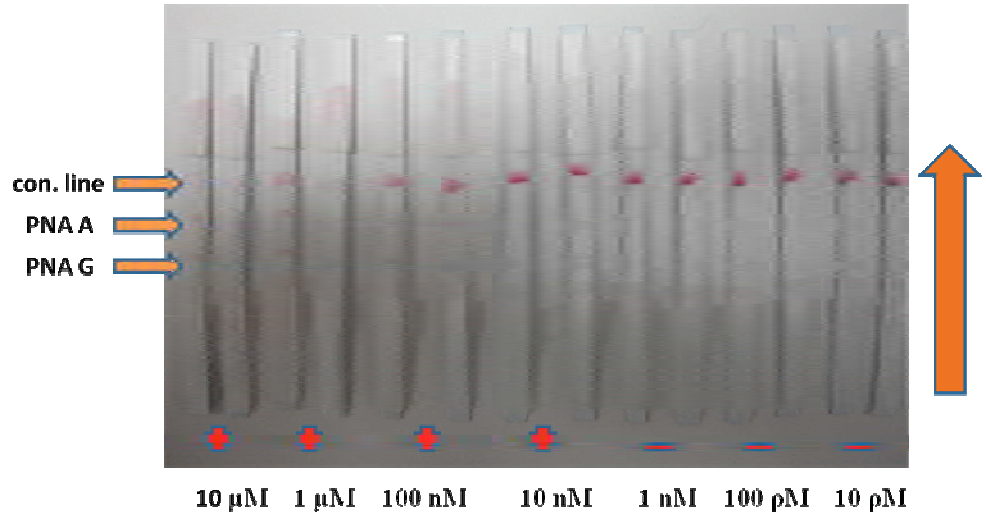

ผลที่ได้จากการทดลองพบว่า ความสามารถในการตรวจสอบที่ต่ำที่สุดที่ strip test ทำได้ คือ 10 nM ถ้าน้อยไปกว่านั้นไม่สามารถตรวจสอบได้ ซึ่งการทดลองนี้นั้นทำการทดลองใน synthetic dna และจะนำไปใช้อ้างอิงในการทดลองใน sample ผู้ป่วยต่อไป

การทดลองที่ 19

• Streptavidin-biotin	• PNA : test line • Probe DNA : control line
• Concentration probe	• 1 μM
• Conjugate probe	• AuNPs+10% BSA
• Target	• Sample (Asymmetric PCR)
• Buffer	• 2x ssc +7% fermamide + 0.05%SDS

ศึกษาผลของ probe PNA กับการจับกับ sample โดยใช้หลักการของ Asymmetric PCR ในการทดลอง เพื่อทำให้ผลิตภัณฑ์ที่ได้มีลักษะเป็น single strand เพื่อลดปัญหาในการที่ไม่เกิดการจับกันของ sample กับ probe PNA ที่เกิดขึ้น

ผลของการทดลอง

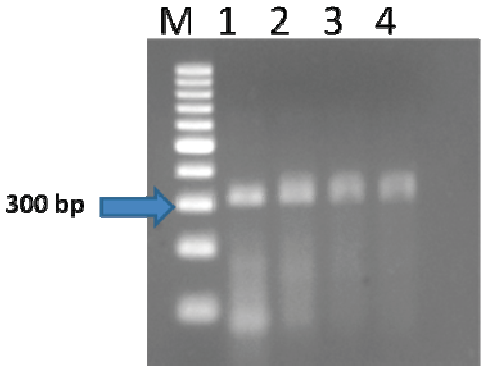

lane M คือ marker 100 bp.
lane 1 sample 1:1
lane 2 sample 1:10
lane 3 sample 1:100
lane 4 sample 1:1000

รูปภาพแสดงการทำ Gel electrophoresis โดยใช้เทคนิค asymmethic PCR
พบว่ามีการขึ้นของชิ้นผลิตภัณฑ์ที่ 312 bp.

ผลที่ได้จากการทดลอง พบว่าเมื่อทำการเจือจางปริมาณของไพร์เมอร์ PCR ให้แตกต่างกันเป็น 1:1 1:10 1:100 1:1000 หลังจากนั้นนำไป PCR พบการเลื่อนขึ้นของแถบแบนยิ่งเจือจางยิ่งเลื่อนขึ้นสูง น่าจะเกิดมาจากรูปร่างของผลิตภัณฑ์ที่เปลี่ยนแปลงไปในรูป single strand มากขึ้นทำให้พบการเลื่อนขึ้นของแถบแบนใน gel electrophoresis และจะนำทั้งหมดไปทดลองต่อใน strip test ต่อไป

ผลของการทดลอง

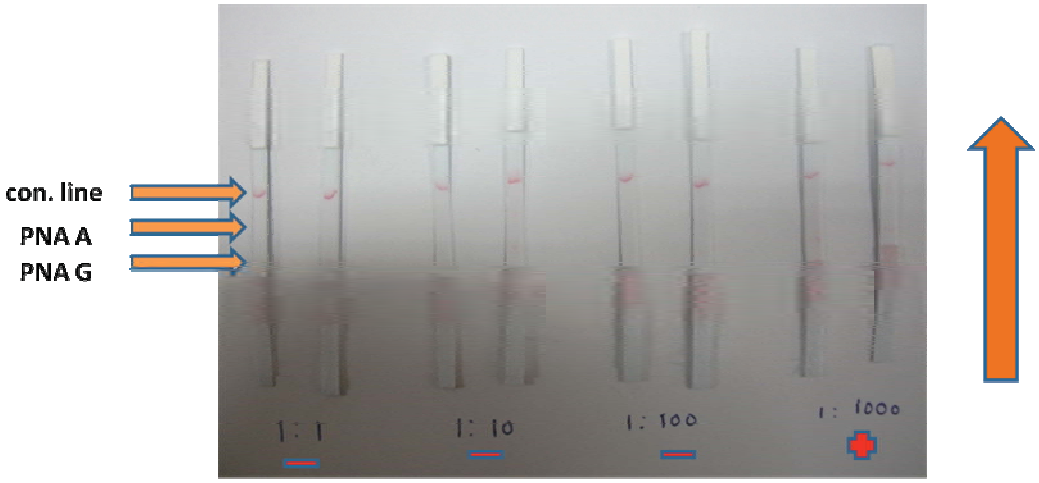

Time : 1 Hrs

ผลที่ได้จากการทดลอง พบว่าชุดของ strip test ที่ทำการเจือจาง 1: 1000 ให้ผลของแถบแบนที่ต้องการ แต่ในทางกลับกันชุด strip test ที่ทำการเจือจางที่น้อยกว่ากลับไม่ให้ผลของแถบแบนที่ต้องการ สาเหตุน่าจะมาจาก ผลของ single strand ที่เกิดขึ้นเนื่องจากการทำ Asymmetric PCR โดยการเจือจางที่ 1:1000 น่าจะเกิด single strand มากกว่าการเจือจางแบบอื่น จึงจะนำความเจือจาง 1 :1000 ไปใช้ในการทำ PCR กับ sample จริงต่อไป

การทดลองที่ 20

• Streptavidin-biotin	• PNA : test line • Probe DNA : control line
• Concentration probe	• 1 μM
• Conjugate probe	• AuNPs+10% BSA
• Target	• Sample (Asymmetric PCR) 1 : 1000
• Buffer	• 2x ssc +7 % fermamide + 0.05%SDS

ศึกษาผลของ strip test ที่ใช้ probe PNA ในการตรวจจับ sample ผู้ป่วย Hemoglobin E โดยการนำเทคนิค Asymmetric PCR มาช่วยในการศึกษา ใช้อัตราส่วนของการเจือจางไพร์เมอร์ 1:1000

ผลของการทดลอง

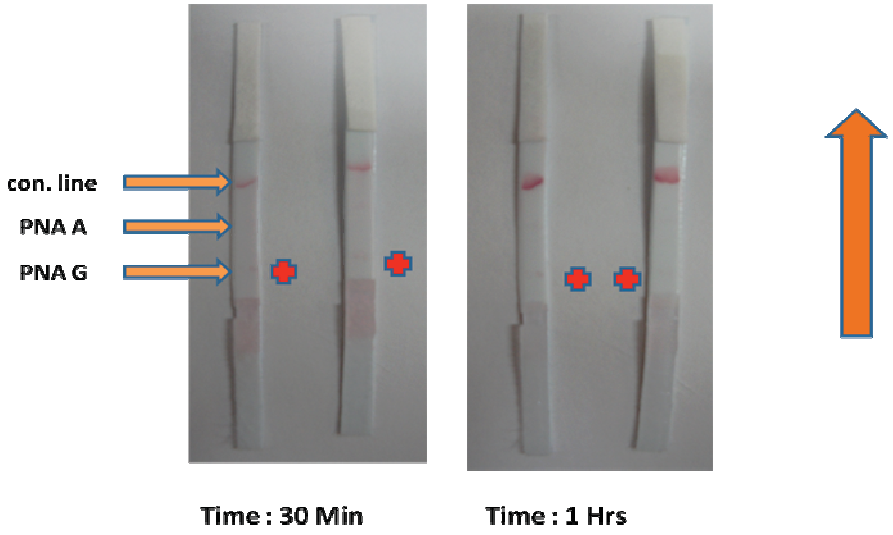

ผลที่ได้จากการทดลองกับ sample จริง พบว่าที่ 30 นาทีหลังจากใส่ sample ลงไป พบการขึ้นของแถบแบนที่ test line แต่เมื่อเวลาผ่านไปเป็น 1 ชั่วโมง พบว่าแถบแบนที่ test line เริ่มจางลง ยังไม่ทราบสาเหตุที่แน่ชัด จะต้องรอทำการศึกษาต่อไปในอนาคต

สรุปผลการทดลอง

จากการทำการสังเคราะห์อนุภาคทองคำโดยใช้ tratetrisodium ci เป็นตัว stabilizer แล้วทำการวัดค่าการดูดกลืนแสง โดยใช้เครื่อง UV spectrum ผลที่ได้นั้นพบว่ามีการดูดกลืนแสงที่ความยาวคลื่น 520 nm ของอนุภาคทองคำโดยสังเกตได้จากกราฟที่ 5 แต่เรายังพบการจับกันของ AuNPs กับ probe PNA ทำให้เกิดแถบแบนที่ไม่จำเพาะเจาะจงขึ้น เราจึงนำโปรตีน BSA มาทำการล้อมรอบพื้นที่ผิวของ AuNPs โดยใช้เวลาในการล้อมประมาณ 1 ชั่วโมง เพราะถ้ามากกว่านี้ก็ไม่มีผลที่แตกต่างกันอย่างมีนัยสำคัญทางสถิติ หรือถ้าน้อยไปโปรตีน BSA อาจจะยังล้อมไม่ดี และปริมาณที่ใช้คือ 10 % BSA หลังจากนั้นทำการเปลี่ยนตัว AuNPs เป็นตัวใหม่ ผลที่ได้พบว่าแถบแบนที่ไม่จำเพาะเจาะจงลดลง แต่ยังไม่ดีนัก การลดการเกิดแถบแบนที่ไม่จำเพาะเจาะจงอีกอย่างที่เราทำคือ การนำสาร fermamide เข้ามาช่วยในการทดลอง ผลที่ได้ปริมาณ 7% fermamide เหมาะสมที่สุดที่นำมาใช้ในการทดลองเพื่อลดแถบแบนที่ไม่จำเพาะเจาะจงที่เกิดขึ้น เราทำการทดสอบความไวของตัว strip test โดยใช้ synthetic DNA พบว่ามีค่าเท่ากับ 10 nM ที่ strip test สามารถทำได้

การทำความสะอาดตัวผลิตภัณฑ์จาก PCR หรือการทำ purify PCR products และพร้อมทั้งนำไปทำ Asymmetric PCR ที่ทำการเจือจางไพร์เมอร์ให้มีความเข้มข้นลดลง ผลที่ได้การเจือจางที่ 1: 1000 ให้ผลในการทำการทดลองกับตัว sample จริง ดีที่สุดขึ้นตรงตามแถบแบนที่เราสนใจ แต่การนำไปทดลองกับ sample จริงนั้นพบว่าที่เวลา 30 นาที ตัว strip test ขึ้นแถบแบนที่ชัดเจนพอสังเกตได้ด้วยตาเปล่า แต่พอที่เวลา 1 ชั่วโมงพบว่าแถบแบนมีการจางลงจนสังเกตผลได้แต่ลางๆ ยังไม่ทราบสาเหตุที่แน่ชัดนักจะต้องรอการศึกษาต่อไปในอนาคต

การตรวจคัดกรองโรค Hemoglobin E ในปัจจุบัน ยังมีปัญหาอยู่มากมายในการวิเคราะห์ผล รวมถึงขาดผู้เชี่ยวชาญ งานวิจัยชิ้นนี้จึงมีวัตถุประสงค์เพื่อพัฒนาชุดตรวจโดยการนำนาโนเทคโนโลยีมาประยุกต์ใช้ในการทำชุดตรวจกรอง Hemoglobin E โดยใช้ตัว pyrrolidinyl PNA มาเป็นตัวตรวจจับความผิดปกติที่เกิดขึ้น จากการทดลองทั้งหมดผลที่ได้คือเราสามารถพัฒนาชุดตรวจคัดกรองโรค Hemoglobin E ได้ สามารถตรวจจับกับ sample ได้ อีกทั้งยังมีความไว 10 nM รวมถึงยังมีการนำเทคนิค Asymmetric PCR มาใช้ควบคู่ในการทดลองอีกด้วย แต่อย่างไรก็ตามต้องรอการพัฒนาชุดตรวจให้มีความสมบูรณ์ต่อไปในอนาคต

เอกสารอ้างอิง

1. วิชัย เหล่าสมบัติ . ธาลัสซีเมีย(Thalassemia) กรุงเทพ: โอเอส พรินติ้งเฮ้าส์; 2541
2. จินตนา ศิรินาวินชล. พรพิมล เรืองวุฒิเลิศ, เสถียร สุขพณิชนันท์, วันชัย วนะชิวะนาวิน, วรวรรณ ตันไพจิตร. ความรู้พื้นฐานธาลัสซีเมีย เพื่อการป้องกันและควบคุมโรค. กรุงเทพฯ: หมอชาวบ้าน; 2547
3. สุทัศน์ ฟู่เจริญ. ธาลัสซีเมีย การตรวจวิเคราะห์ยีนด้วยเทคนิค PCR: โครงการวิจัยธาลัสซีเมีย สถาบันวิจัยและพัฒนาวิทยาศาสตร์และเทคโนโลยีมหาวิทยาลัยมหิดล.; 2541
4. วรวรรณ ตันไพจิตร. พาหะของธาลัสซีเมียโรคเลือดจางธาลัสซีเมีย: โครงการพัฒนาระบบสุขภาพสำหรับธาลัสซีเมีย คณะแพทยศาสตร์ศิริราชพยาบาล .2546
5. รัตนา สินธุภัค. คู่มือการตรวจคัดกรองเลือดธาลัสซีเมียเบื้องต้น ภาวะพร่องเอ็นไซม์ จี**6**พีดี การให้ความรู้และให้คำปรึกษา สำหรับเจ้าหน้าที่อนามัย: สถาบันวิจัยวิทยาศาสตร์การแพทย์ จุฬาลงกรณ์มหาวิทยาลัย; 2546
6. Roco MC. Nanotechnology: Convergence with Modern Biology and Medicine. Current Opinion in Biotechnology 2003; 14: 337-346
7. Pal T. Nucleophile-Induced Dissolution of Gold and Silver in Micelle. Cur. Sci. 2002; 83 (5): 627-628.
8. Zhong X, Yuan R, Chai Y, Lui Y, Dai J, Tang D. Glucose Biosensor Based on Self-Assembled Gold Nanoparticles and Double-Layer 2D-Network (3-Mercaptopropyl) -Trimethoxysilane Polymer onto Gold Substrate. Sensors and Actuators B 2005; 104: 191-198.
9. Ackerson CJ, Sykes MT, Kornberg RD. Defined DNA/Nanoparticle Conjugates. PNAS 2005; 102(38): 13383-13385.
10. Storhoff JJ, Elghanian R, Mucic RC, Mirkin CA, Letsinger RL. One-Pot Colorimetric Differentiation of Polynucleotides with Single Base Imperfections Using Gold Nanoparticle Probes. J. Am. Chem. Soc. 1998; 120: 1959-1964.
11. Reynolds AJ, Haines AH, Russell DA. Gold Glyconanoparticles for Mimics and Measurement of Metal Ion-Mediated Carbohydrate-Carbohydrate Interactions. Langmuir 2006; 22: 1156-1163.

12. Salata OV. Applications of Nanoparticles in Biology and Medicine. Journal of Nanobiotechnology 2004 March; 2.

13. Liu J, Lu Y. A Colorimetric Lead Biosensor using DNAzyme─Directed Assembly of Gold Nanoparticles. J. Am. Chem. Soc. 2003; 125: 6642-6643.

14. Weatherall DJ,Clegg JB.The Thalassemia Syndromes.Oxford:Blackwell Scientific Publication 1981:296

15. ธาลัสซีเมีย.สถานการณ์ปัจจุบันและกลวิธีในการป้องกันและควบคุมโรคเลือดในประเทศไทย(พศ. 2532-2533).กรุงเทพฯ: นำอักษรการพิมพ์ 2533:1-43

16. ลักษณา มกรแก้วเกยูรและคณะ.การสร้างไฮบริโดม่าหนูที่สามารถหลั่งโมโนโคลนอลแอนติบอดีที่จำเพาะต่อสายเบต้าอีโกลบินเพื่อใช้คัดกรองฮีโมโกลบินอี.เชียงใหม่เวชสาร 2549;45(1):1-10.)

17. บุษบา เตชาชัยนิรันดร์ . การตรวจกรองฮีโมโกลบินอีด้วยชุดน้ำยาสำเร็จรูป KKU-DCIP-Clear โดยใช้ Heating block,คณะแพทยศาสตร์ จุฬาลงกรณ์มหาวิทยาลัย.2547

18. Catherine JM, Anand MG, John WS, Patrick NS, Alaaldin MA, Edie CG et al. Gold Nanoparticles in Biology: Beyond Toxicity to Cellular Imaging. Acc. Chem. Res 2008; 41 (12):1721-1730

19. Li, Q., et al., Gold Nanoparticle-Based Immunochromatographic Assay for The Detection of 7-Aminoclonazepam in Urine. International Journal of Environmental Analytical Chemistry, 2009. 89(4): p. 261-268.

20. Kalogianni, D.P., et al., Dry-reagent Disposable Dipstick Test for Visual Screening of Seven Leukemia-Related Chromosomal Translocations. Nucleic Acids Research, 2007. 35(4): p. 1-12.

21. Litos, I.K., et al., Multianalyte, Dipstick-type, Nanoparticle-Based DNA Biosensor for Visual Genotyping of Single-Nucleotide Polymorphisms. Biosensors and Bioelectronics, 2009. 24(10): p. 3135-3139.